CONTINENTAL MAGMATISM
ABSTRACTS

I A V C E I

International Association of Volcanology and Chemistry of the Earth's Interior

GENERAL ASSEMBLY Santa Fe, New Mexico, USA June 25–July 1, 1989

BULLETIN 131 New Mexico Bureau of Mines & Mineral Resources 1989

A DIVISION OF
NEW MEXICO INSTITUTE OF MINING & TECHNOLOGY

Bulletin 131

New Mexico Bureau of Mines & Mineral Resources

A DIVISION OF
NEW MEXICO INSTITUTE OF MINING & TECHNOLOGY

CONTINENTAL MAGMATISM

ABSTRACTS

International Association of Volcanology and Chemistry of the Earth's Interior

GENERAL ASSEMBLY
Santa Fe, New Mexico, USA
June 25–July 1, 1989

SOCORRO, 1989

Original Printing

Published by Authority of State of New Mexico, NMSA 1953 Sec. 63–1–4
Printed by University of New Mexico Printing Services, April 1989

Available from New Mexico Bureau of Mines & Mineral Resources, Socorro, NM 87801

Contents

(see front cover for details of Valles caldera)

STRATIGRAPHY AND DEPOSITIONAL FEATURES OF THE PERALTA TUFF, JEMEZ MOUNTAINS, NEW MEXICO

ABITZ, R.J., and SMITH, G.A., Department of Geology, University of New Mexico, Albuquerque, NM 87131, USA

The late Miocene Peralta Tuff Member of the Bearhead Rhyolite consists of interbedded deposits of pyroclastic flows, fallout tephra, surges, braided streams and debris flows. These deposits form constructional landforms around the principal vents and have accumulated to a thickness of at least 275 m in the study area. Pyroclastic eruptions preceded extrusion of rhyolite domes and coulees within a 150 km^2 area adjacent to and within the study area. A minimum of 30 rhyolitic eruptive episodes are documented in measured sections. Small-volume pyroclastic-flow and surge deposits were emplaced in 14 of these episodes and remaining episodes are recorded by fall deposits. Seven pyroclastic packages of pyroclastic flow, surge and fallout were mapped on the basis of lithic content and composition, distinct fallout and surge units and compound fallout beds. Lobate morphology, flow-direction indicators and bomb-trajectory geometry suggest that at least three pyroclastic flows originated from the Bearhead Peak area. At least 30 m of pumiceous surge beds were deposited prior to emplacement of a dome in lower Peralta Canyon.

Proximal facies consist mainly of pyroclastic flows and surges and grade to distal facies dominated by products of braided streams and debris flows. Upward decrease in primary pyroclastic units indicates waning of Bearhead Rhyolite volcanism, supported by an upward increase in the ratio of epiclasts to pyroclasts in ephemeral braided-stream deposits and a decrease in the spacing of paleosols.

Structural and compositional features of primary pyroclastic deposits include: (1) lobate morphologies of pyroclastic flows and pyroclastic packages; (2) inverse- and normal-graded lithic and pumice zones in pyroclastic flows and fallout; (3) pumice stringers and lithic concentration zones in the center and top of pyroclastic-flow units; (4) ash- and lapilli-filled, gas-escape diapirs in fallout deposited on hot pyroclastic-flow deposits; (5) erosion of pyroclastic flow surfaces by subsequent pyroclastic flows in multievent packages; (6) common antidune and chute-and-pool structures within surge units; (7) topographically induced, abrupt flow transformations in pyroclastic flows producing lateral transitions from massive to cross-bedded pyroclastic-flow deposits and surge beds. The latter feature is demonstrated by deposits of surge and cross-bedded pyroclastic flows that are proximal to and downslope from preexisting coulees and domes. Therefore, these deposits represent surges and turbulent flows generated by irregular landscape, rather than processes at the vent.

MAGMA MIXING AND CRUSTAL CONTAMINATION IN THE MIOCENE VOLCANISM OF NORTH CENTRAL ALGERIA: THEIR IMPLICATION IN THE NORTH AFRICAN CONTINENTAL MARGIN

AIT-HAMOU, F. and CHIKHAOUI, M., Institute of Earth Sciences, Department of Geology, U.S.T.H.B. BP. 32 El-Alia Bab-Ezzouar (Algiers, Algeria)

The Miocene volcanism (16 to 9 m.a.) occurs in the southwestern subsiding part of Mitidja's basin and belongs to the Tertiary magmatism related to the post-tectonic evolution of northern Algeria.

Rocks are mainly silicic andesite with tuff deposits. These rocks have typical calc-alkaline character of continental-margin volcanics. Petrological and geochemical evidence indicates the presence of heterogeneous magmas and suggests an origin by magma-mixing process and minor fractional crystallization.

The hybrid magmas implicated in the mixing are both of basaltic melt, mantle origin, and crustal-derived rhyodacitic melt. The abundance of the REE suggests that the mixing took place in a magma reservoir situated in the lower continental crust.

Magmas undergo a crustal contamination during their ascent through the continental crust. This is attested to by the high and variable isotopic values (87SR/86Sr ratios ranging between 0.7064 and 0.7104) and by the presence of granulitic xenoliths of Disth-An-Cor-Spin and Gt-Pl-Opx-Spin $\pm$ biot.

GEobarometry of these infra-crustal xenoliths indicates low-pression conditions and compatibility with intermediate continental crust (<25 km thick).

The high values of the 87Sr/86Sr ratios are attributed not only to crustal contamination, but probably also to an important fraction of silicic magma in the mixing mechanism. The role and the proportion of each process in the genesis of lavas are difficult to determine.

The calc-alkaline volcanism of the studied area, as all the magmatism of northern Algeria, are related to the active continental margin of North Africa. The relation between orogenic magma and subduction in the occidental mediterranean basin is still being discussed.

MID-TERTIARY SILICEOUS IGNEOUS ACTIVITY ABOVE CRATONIC AND ACCRETED BASEMENT IN NORTHERN MEXICO; COMPARISON OF TWO TYPE LOCALITIES

ALBRECHT, A. and BROOKINS, D.G., Department of Geology, The University of New Mexico, Albuquerque, NM 87131

The southern edge of the North American craton is located in northern Mexico, but its location can not be exactly plotted due to lack of basement outcrops. This paper investigates the use of the 1000 m thick cover of Tertiary igneous rocks dominating the Mexican Sierra Madre Occidental as a tracer of variations in basement composition. For this purpose two type localities have been studied. San Buenaventura, located in north-western Chihuahua, represents igneous activity above Precambrian cratonic basement. The Copper Canyon section at El Divisadero in south-western Chihuahua represents igneous activity above accreted terranes with unknown basement. Both areas are dominated by siliceous lava flows and ignimbrites. In the Buenaventura area a section of 600 m has been sampled and mapped. It is characterized by an 11km large caldera structure associated with a resurgent granite intrusion. The area adjacent to the caldera structure is formed by 5 major ignimbrites and intermediate lava flows of basaltic andesitic to rhyolitic composition. The entire suite plots in the field of high K calc-alkaline rocks. The siliceous rocks are characterized by K-feldspar, plagioclase, biotite, amphibole, opaque phases and rare clinopyroxene. The Rb/Sr whole rock isochron age is 33.2 Ma with an initial $^{87}Sr/^{86}Sr$ ratio of 0.706577 +/-0.000425 at a 95% confidence interval. As all siliceous rocks plot on the isochron they are interpreted as being derived from a common magmatic source, probably a large composite pluton. The existence of cumulative rocks within the granite complex suggest that the final stage of differentiation did not occur at greater depth. Whole rock major and trace element composition of 16 samples were measured using INAA and XRF. A linear increase of LIL element abundance with SiO_2 exists and has to be taken into account when comparing the Buenaventura suite with other suites.

The Copper Canyon section at El Divisadero is characterized entirely by siliceous rocks of dacitic to rhyolitic composition. The entire section of 1400 m consists of horizontal layers of siliceous lava flows and ignimbrites. The section has been subdivided into a lower and upper unit, where the lower part has dacitic to rhyodacitic composition, while the upper part is rhyolitic. The lower part has a Rb/Sr age of 40 Ma with an initial $^{87}Sr/^{86}Sr$ of 0.70484 +/-0.001247, whereas the upper unit is 28.9 Ma old with an initial of 0.70572 +/-0.000341. Mineralogically the siliceous rocks are similar to the Buenaventura rocks, suggesting similar petrographic evolution. Comparison of geochemical data of 24 samples from El Divisadero with the Buenaventura suite show that besides the difference in Sr-isotopic composition a significant difference exists in the K-, Ti-, and Th-group elements, the REE abundances and inter element group ratios. The Tertiary igneous rocks can therefore be used as indicators of basement variations.

THE MECHANISM OF DEVELOPMENT OF THE MOUNT ST. HELENS BLAST OF MAY 18, 1980.

ALIDIBIROV, Michail, Institute of Volcanology, Petropavlovsk-Kamchatsky, 683006, USSR

The May 18, 1980 directed blast at Mount St.Helens is among the most studied. A wealth of data were obtained on its parameters which enabled us to reconstruct the chronology of events during the blast. But the suggested models somehow do not explain the large ($\sim$150 s) duration of the blast process, its multiactness and the distribution of the explosion sources in space at a distance of a few kilometers.

The present study considers the mechanism of the blast development and explains its characteristic features. Herein we consider a process of fragmentation of a magma body (cryptodome) located in the volcanic edifice prior to the blast. It is proposed that the cryptodome had a store of potential energy of compressed gas which depended on porosity (vesiculation) and gas pressure in pores (bubbles) of the cryptodome material. Interbubble partitions were assumed to be solid. Decompression caused by landslide led to fragmentation of the cryptodome by propagation of the disruption wave from the free surface inside the cryptodome. The calculations indicate that the velocity of disruption wave front movement N is usually less than 10 m/s. For the diameter of cryptodome D$\approx$700-800 m and N$\approx$5 m/s the duration of the blast $\tau \sim D/N$ turns out to be close to that obtained from observations. Origination of a few explosive episodes during the blast can be explained by cessation of cryptodome fragmentation because of disruption wave stops which occur as a result of pressure increase behind the wave front. Such pressure increase could result from overlaying of the destroying cryptodome with rockslide material in the course of their joint movement. Therefore, the suggested mechanism of origination of secondary explosions is explained by the character of cryptodome destruction and thereby it is not necessary to attract the "phreatic" hypothesis. Discrete destruction of cryptodome as it moves with the rockslide down the slope explains the stretched character of explosion source distribution in space.

The suggested mechanism of the May 18, 1980 Mount St.Helens directed blast development explains some typical features of the event and may be useful in studying analogous blasts. Additional experiments and theoretical studies on the process of fragmentation of gaseous magma during decompression are needed.

DIFFUSE SOIL DEGASSING FROM VOLCANOES: GEOCHEMICAL AND VOLCANOLOGICAL IMPLICATIONS.

ALLARD, P., Centre des Faibles Radioactivités, CNRS-CEA, 91190 Gif/Yvette, France, BAUBRON, J.C., Bureau de Recherches Géologiques et Minières, B.P. 6009, Orléans, France, CARBONNELLE, J., DAJLEVIC, D., LE BRONEC, J., ROBE, M.C., ZETTWOOG, P., Comm. à l'Energie Atomique, SPIN/DPT, 91190 Gif/Yvette, France, TOUTAIN, J.P., Osservatorio Vesuviano, via A. Manzoni 249, 80123 Napoli, Italy.

Airborne and field measurements carried out since 1976 on Mt. Etna, Sicily, have revealed that this very active strato-volcano releases huge amounts of gas, not only as visible exhalations from its summit craters (plume), but also as diffuse soil emanations from its flanks*(1-3)*. Recent investigations on two other Italian volcanoes, Vulcano and Vesuvius, demonstrate that diffuse lateral degassing also occurs from these sites *(3-5)* and suggest it may be a general phenomenon on active volcanoes. From the results obtained several interesting features can be outlined.

1) Volcanic soil emanations are essentially composed of carbon dioxide, variably enriched in helium and other rare gases (Ar, Rn) and variably diluted by air. Air dilution depends on the gas flow and on the ground porosity.

2) The concentration range of soil gases is related to the intensity of volcanic activity: CO_2 concentrations thus reach up to 50-100% (with up to 18 ppm He) in the ground of Etna and Vulcano, but reach only 1% at most on a dormant volcano such as Vesuvius.

3) A magmatic origin of the gases can be evidenced from both their chemical and isotopic ratios. On Etna, the soil CO_2 in the summit area thus has a similar $\partial^{13}C$ (-3.5‰) as the eruptive exhalations *(2,6)*. Preliminary results for helium indicate a $^3He/^4He$ ratio of 8 times the air ratio ($1.4x10^{-6}$), typical of MORBs. At Vulcano, soil emanations from the base of the active cone have similar He/CO_2 ratios and $\partial^{13}C$ as the crater fumaroles, whereas those from other areas clearly derive from a distinct source *(5)*.

4) Soil gas anomalies are preferentially concentrated in permeable zones or along active faults and thus provide information upon the structure of volcanic edifices. Lava flows usually act as impermeable barriers. The proportions of the species allow to distinguish sub-surface thermal anomalies from deeper and cooler gas leaks.

5) The whole output of soil CO_2 from Etna is nearly equivalent to the CO_2 output from the summit craters. At Vulcano, soil degassing accounts for about 20% of the crater fumarolic discharge*(5)*.

Three major implications thus arise from these results. First, diffuse lateral degassing from volcanoes must be considered when evaluating the volatile budget of subaerial volcanism and might significantly increase the figures. Second, once demonstrated their connection with magma degassing at depth, soil emanations may prove very useful for continuous geochemical volcano monitoring at safe distance from active craters. Such a monitoring was underwent in 1987 at Vesuvius*(4)*. Finally, mapping these emanations may help to identify the active structural features of volcanic piles and potential sites of future eruptions.

(1) Carbonnelle et al., Bull. PIRPSEV-CNRS, 108, 64 pp., 1985.
(2) Allard et al., Terra Cognita 7, G17-52, 407, 1987.
(3) Baubron, BRGM int. reports, DT-ANA, 1986, 1987, 1988.
(4) Allard et al., Kagoshima Inter. Conference proceedings, 47, 1988.
(5) Allard, Baubron, Toutain, (submitted to Nature).
(6) Allard, XVIII IUGG Assembly, Hamburg, proceedings, 42, 1983.

FALSE PYROCLASTIC TEXTURES IN SILICIC LAVAS

ALLEN, R.L., Dept. of Earth Sciences, Monash University, Clayton, Victoria, Australia 3168

Apparent welded and non-welded pyroclastic flow deposits form a major component of a regionally altered Silurian silicic volcanic complex in south-eastern Australia (Cowombat Rift). However, critical evaluation of rock textures and contact relationships indicates that most of the rocks are silicic lavas rather than pyroclastics. The lavas have remarkably deceptive false pyroclastic textures, including apparent pumice fiamme and glass shards. Research on analogous Neogene sequences in Japan and other Palaeozoic and Precambrian sequences in Australia has identified lavas with similar false pyroclastic textures, suggesting that such rocks may be more common than generally recognized.

Five major primary facies are recognized within the lavas: (1) massive coherent, (2) flow banded, (3) nodular devitrified, (4) autobreccia, (5) hyaloclastite. Original glassy composition, perlitic fracture networks, and style of devitrification and alteration, are important features in generating the false pyroclastic textures. Apparent fiamme textures formed where nodular devitrification or silicification fronts progressed outward through glassy lava from scattered nuclei, and coalesced to form an interconnected continuous domain. Remnant glassy patches isolated by these domains were subsequently altered to dark phyllosilicate compositions and appear like pumice clasts in a siliceous matrix. These apparent clasts have irregular non-welded shapes where formed in massive lava, and have lenticular welded shapes where flow banding caused a preferred orientation in the devitrification or silicification domains. Shard-like textures result from alteration obscuring the continuity of perlitic networks, leaving many isolated shard-shaped segments of the perlitic texture. Cuspate non-welded shard shapes were formed from alteration of classical concentric perlite, whereas welded shard shapes formed from elongate banded perlite fabrics. Abundant broken crystals in some hyaloclastites, and dismembering of phenocrysts and groundmass fabrics in strongly foliated rocks, have further enhanced pyroclastic appearance.

Euhedral unbroken phenocrysts in coherent lava facies, calc-alkaline rather than alkaline composition, and moderate rather than high eruption temperatures (indicated by phenocryst types and contents) suggest these rocks are true silicic lavas rather than rheomorphic pyroclastics.

To date this research has been focussed on sequences of largely subaqueous volcanic rocks hosting Zn-Cu-Pb massive sulphides. Subaqueous settings appear conducive to extensive textural modification, by promoting quenching to glassy compositions and circulation of large volumes of fluid. However, originally glassy lavas with pervasive devitrification and alteration effects (and false pyroclastic textures) might also be expected within hydrothermally active subaerial volcanic centres.

SUBMARINE SILICIC VOLCANOES ASSOCIATED WITH MIOCENE KUROKO MINERALIZATION, NORTHERN JAPAN

ALLEN, R.L., CAS, R.A.F., Department of Earth Sciences, Monash University, Clayton, Victoria, 3168, Australia.
YAMAGISHI, H., Geological Survey Hokkaido, Sapporo, Japan.
ISHIKAWA, Y., OHGUCHI, T., Mining College, Akita University, Akita, Japan.

The Kuroko Zn-Cu-Pb-Ag-Au massive sulphide deposits in northern Japan are one of the main type examples of volcanic-associated massive sulphide ores. These deposits occur in the Green Tuff Belt, a province of regionally altered, mainly submarine volcanic rocks of Tertiary age. The Green Tuff Belt is dominated by volcaniclastic rocks with subordinate coherent lava and intrusives. Several previous workers have interpreted many of the submarine volcaniclastic rocks as subaqueously erupted pyroclastic flow, fall and explosion breccia deposits, culminating in recent models of deep marine pyroclastic caldera volcanoes. We suggest that most of the volcaniclastics are hyaloclastites, autobreccias, and pyroclastic debris that has been resedimented from shallow water and subaerial basin margins and intra-basin highs.

Extensive mapping of superb coastal exposures in Hokkaido (by H.Y.) shows that the voluminous submarine volcaniclastic deposits overlying the ore deposits in this region mainly represent numerous, small to moderate volume, hyaloclastite-lava volcanoes. These volcanoes comprise dyke swarms feeding in situ hyaloclastite breccias, flow lobes, domes or pillow lavas, and flanking aprons of resedimented hyaloclastite. The poorly exposed volcanics hosting the kuroko deposits in Hokkaido also appear to be lava-hyaloclastite-dominant volcanoes.

In the Hokuroku District of Honshu, most kuroko deposits lie at the top of a thick (up to 1000m), laterally extensive massive rhyolitic complex, composed of lava domes, intrusive domes, possible sheet flows and volcaniclastics. The volcaniclastics are mainly autoclastics (autobreccias, hyaloclastites) and resedimented autoclastics. True pyroclastic debris is volumetrically minor and we consider insufficient to invoke large scale deep submarine pyroclastic volcanism and classical caldera subsidence as precursors to ore formation. Most pyroclastic debris in the Hokuroku District occurs in the post-ore succession, and consists of mass flow deposits of reworked and juvenile pyroclastic debris, interbedded with mudstone. Much of this pyroclastic debris could be sourced from subaerial or shallow water pyroclastic centres at the basin margins. Extensive work around the Fukazawa and Ezuri ore deposits (by Y.I.) suggests that these deposits occur on the flanks of a moderate volume, possibly conical, silicic lava volcano. On a broader scale, the extensive rhyolitic complex underlying the Hokuroku ore deposits, could be interpreted as a large volume, tabular, multivent lava complex.

ERUPTIVES RELATING TO A c. 22.5 Ka B.P. DEBRIS AVALANCHE AT EGMONT VOLCANO, NEW ZEALAND

ALLOWAY, B.V., STEWART, R.B., and NEALL, V.E., Soil Science Department, Massey University, Palmerston North, New Zealand.

Egmont Volcano is a 2518 m high andesitic strato-volcano situated in Taranaki Region, New Zealand. This volcano has been the site of repetitive, large volume edifice collapses over the last c. 130 kyrs. Four discrete pre-historic debris avalanche deposits (Okawa, Pungarehu, Warea and Opua Formations) have so far been mapped on its surrounding lower flanks but no eruptives directly relating to these collapse events have been recognised.

Another debris avalanche deposit (Ngaere Formation) has been recently identified extending over a >350 km² area to the east and south-east of Egmont Volcano. This deposit relates to a flank failure event at c. 22.5 kyrs B.P. and is associated with pre- and post-avalanche eruptives. There is no evidence for a directed-blast deposit relating to the debris avalanche.

Immediately underlying Ngaere Formation at sites between c. 15 and 23 km south-east of the Egmont Volcano summit is a fine to coarse sandy textured air-fall tephra, which is strongly leptokurtic and reverse graded. The mineralogy of this tephra comprises plagioclase, clinopyroxene, titanomagnetite, hornblende and minor olivine, typical of many Egmont eruptives. Particles are predominantly holohyaline, ranging to holocrystalline, and silica contents of glass fall in a narrow range of 57-60 wt %, suggesting derivation from a magma rather than fragmentation of pre-existing lavas during an explosive eruption. This tephra probably represents a pulse of new magma entering the volcano and leading to a new cycle of activity.

Immediately overlying Ngaere Formation in the same vicinity is a sequence of thirteen, very closely spaced air-fall tephra units. These units represent a post-avalanche phase of high frequency eruptive activity and active reconstruction of a lava dome or central cone and is consistent with Bezymianny-type eruptive activity.

The emplacement of Ngaere Formation in a wide eastern arc closely preceded that of the c. 7.5 km³ Pungarehu Formation in western Taranaki. It appears that these similar but chronologically distinct deposits relate to the same eruptive episode.

MAFIC MAGMATISM WITHIN INTRACRATONIC BASINS: THE IMPACT CONNECTION

ALT, D., SEARS, J.W., and HYNDMAN, D.W.
Department of Geology, University of Montana, Missoula, Montana 59812

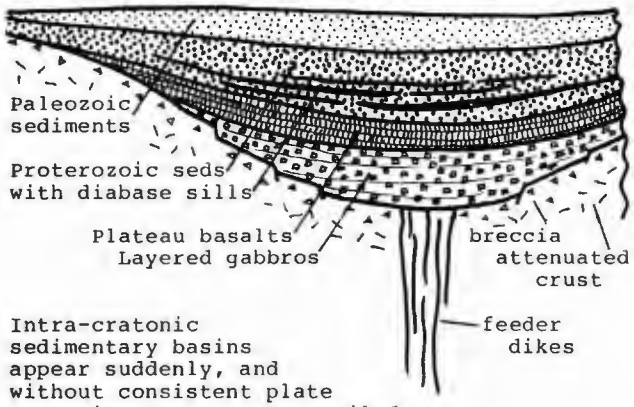

Intra-cratonic sedimentary basins appear suddenly, and without consistent plate tectonic context. A compiled composite section through a typical intra-cratonic sedimentary basin reveals Paleozoic formations resting on a deep fill of Proterozoic sediments interlayered with basalt flows and diabase sills. The Proterozoic section rests on a flood basalt plateau, which in turn lies on a lopolithic gabbroic layered intrusion with a granophyre cap.

We earlier showed that flood basalt plateaus develop from very large impact sites. The association of intra-cratonic basins with flood basalts and large layered gabbro and granophyre complexes suggests that they also evolve from very large impact sites. Bedrock beneath the Sudbury lopolith is brecciated and shock metamorphosed.

We propose a model in which a very large impact opens a crater that first floods with basalt to form a lava plateau resting on a layered gabbro and granophyre complex, then begins to sink as the heated lithosphere beneath cools. The sagging surface ultimately collects thick sediments, which contribute to further subsidence as thermal contraction continues. Inversion of gabbro to eclogite may also contribute.

Meanwhile, rising basalt magma erupts within the basin, or injects the accumulating basin fill sediments to form diabase sills. Magmatic activity within basins may continue for hundreds of millions of years.

Very large impacts may also fracture the crust. In some cases, the result is a large basement dike swarm such as the Mackenzie dikes of the Canadian shield, which radiate from the Amundsen basin. Crustal fractures originating at impact sites may also open into rift basins, even into oceanic rift systems.

MONITORING AND VOLCANIC HAZARD OF ARENAL VOLCANO (COSTA RICA): 20 YEARS OF CONTINUOUS ACTIVITY (1968-1988)

ALVARADO, G.E., Sección de Sismología, Depto Geología, ICE, Apdo. 10032-1000 San José, Costa Rica. Observatorio Vulcanológico del Arenal (OVA), Red Sismológica Nacional (RSN:ICE-UCR).
MATUMOTO, T., Institute for Geophysics, University of Texas at Austin.
BORGIA, A., Dept. of Geological and Geophysical Sciences, Princeton University, N.J. 08544, USA.
BARQUERO, R.A, Sección de Sismología e Ing Sísmica, Obs. Vulcan. del Arenal (OVA) and RSN, Apdo. 10032-1000 San José.

Arenal is a small (12.5 km^3, 1.1km height) stratovolcano that began an intensive explosive phase on July 29, 1968 after several centuries of calm. Arenal is between the Central and Guanacaste volcanic chains of Costa Rica and shares geologic characteristics with both. The main activity consisted of 6 phases: a) Premonitory (before 1968), b) Pelean explosion (July 29-31, 1968), c) Lateral effusion (September 19, 1968 to 1973), d) Terminal effusion (1974 to present), e) Important lateral blocky and glowing avalanches of Merapi and Soufriére types (June 17-21, 1975), f) Strombolian explotion alternating with lava flows and local debris and ash flows (June 1984 to present). A new lateral cone was formed after 1978. An area of the 7 Km^2 is now covered by the recent composite block flows, of low K, high alumina basaltic andesite.

In 1965, the Instituto Costarricense de Electricidad (ICE) began geological studies for the Arenal Hydroelectric Project. During 1974-1978 was established a seismic network around Arenal lake and the volcano. Four kinds of seismic signals were identified: 1) Volcano-tectonic earthquakes (A-type), premonitory to the most intense explosive phases, 2) Volcanic earthquakes (B-type) wich take place at shallow levels in the proximity of the cone, 3) Explosive earthquake (E-type) sometimes with an associated acoustic shock wave, 4) Volcanic tremor of different frequencies originated by degassing, blocky avalanches (high) or magma column fluctuations (interm. to low). The frequency and magnitud of earthquakes and tremor usually correlate well with the monthly earthtides with maxima around the full moon phase. In 1976 ICE began geodetic monitoring with four dry tilt stations. At the beginning of the strombolian activity in 1984, the monitoring systems were increased: 9 dry tiltmeters, 2 EDM lines, 10 water chemical sampling sites, and geophysical control (magnetic, gravimetric and geoelectric profiles).

At this moment, we have a good knowledge of the volcanological, neotectonic and risk aspects of the Arenal volcano area. Assuming that the actual eruptive activity type does not change, we divided the volcanic hazard in three periods: a) **Short term (1974 to present)**: principally within a radius of 4 Km in west and northward flanks with ash falls and small "lahars", b) **Intermediate term (next 250 years)**: 10 Km around the cone will probably have strong strombolian "basaltic" and lateral explosions with pyroclastic and base surge flows, lateral lava flows and normal activity similar to present type. c) **Long term (next 600 years)**: Probably will have a plinian explosion and associated volcanic phenomenons.

Within 7 Km around the Arenal are located the Sangregado Dam (2 Km^3 of reservoir, 60% of the electric power of Costa Rica), the Tempisque-Arenal Irrigation Project and La Fortuna, a prosperous town with more o less 3000 inhabitants.

PREERUPTIVE CO_2 IN KILAUEAN GLASS INCLUSIONS

ANDERSON, A.T., Jr. and SKIRIUS, C.M. Dept. Geophys. Sci., Univ. Chicago., Chicago, Illinois 60637

Inclusions of glass in phenocrysts of olivine that were erupted and collected in 1959 from Kilauea Iki have been spectroscopically analysed for CO_2 and H_2O. CO_2 is present as CO_3^{-2} groups. Four inclusions in four crystals erupted on Nov. 18 have 0.08, 0.02, 0.02 and <0.01 wt % CO_2. Two inclusions erupted on Nov. 21 have <0.01 wt % CO_2. Large gas bubbles occur in two of the inclusions analysed and are common in other inclusions indicating that the melts were gas saturated. The low concentrations of CO_2 in all but one of the melt inclusions indicate that the inclusions formed within or above the level of Kilauea's summit reservoir of magma and after parental CO_2 had effervesced from the melt, consistent with current concepts of Kilauea's outgassing behavior deduced from volcanological studies. Primary CO_2-rich gas bubbles in olivines from Kilauea, Mauna Loa and Loihi documented by Roedder indicate that concentrations of CO_2 as great as about 0.2 wt % may be expected in melt inclusions formed from CO_2 saturated magmas beneath Hawaii. Published volcanological estimates of parental CO_2 are as high as 0.6 wt % and suggest that even greater concentrations might be encountered, but these have not yet been found. The later erupted inclusions have significantly greater H_2O. The concentrations of H_2O that we have measured in inclusions are substantially larger than values reported for submarine basaltic glasses from Kilauea's east rift. These results, although fragmentary, suggest that the 1959 picritic eruption of Kilauea sampled some magma that had not completely equilibrated with the low pressure in the summit reservoir. Submarine Kilauean lavas, on the other hand, may generally have first equilibrated in a near surface body of magma and subsequently migrated down rift to higher pressure vents as suggested by volcanological studies.

VOLCANIC HAZARD MITIGATION THROUGH TRAINING IN VOLCANO MONITORING

ANDERSON, J.L., and DECKER, R.W., Geology Department, University of Hawaii at Hilo, Hilo, Hawaii 96720-4091

A center for the study of active volcanoes (CSAV) has been established at the University of Hawaii at Hilo in cooperation with the United States Geological Survey's Hawaiian Volcano Observatory. A main objective of CSAV is to assist in the mitigation of volcanic hazards worldwide, with special emphasis on the circum-Pacific area. A training program has been designed and will soon be implemented to assist developing nations in attaining self-sufficiency in the area of applied volcanology. The program will involve an integrated course of study containing both field and classroom/laboratory elements. Field training will emphasize volcano monitoring methods, both data collection and interpretation, currently in use by the U. S. Geological Survey. Participants will be taught the use and maintenance of volcano monitoring instruments. In addition, the training program will also address the assessment of volcanic hazards and the interrelationship of scientists, governing officials, and the news media during volcanic crises. Completion of the overall course of study will result in certification in the field of volcanology.

This program will contribute to accomplishing a long-standing goal of the IAVCEI Working Group on Mitigation of Volcanic Disasters. It will help decrease volcanic risk in developing countries by providing local scientists with a training opportunity in applied volcanology. These individuals, after completion of the program, will be capable of collecting baseline geologic, geophysical, and geochemical data on high-risk volcanoes for which such data is currently unavailable or inadequate. It is anticipated that the CSAV training program will improve international cooperation in the area of volcano monitoring and help make it possible for quick and effective international response to emergency situations.

AN EVALUATION OF ERUPTION TRIGGERING MECHANISMS AT THE MOUNT ST. HELENS DOME

Anderson, S.W., and Fink, J.H., Department of Geology, Arizona State University, Tempe, Arizona 85287

Hydrogen isotopic and water content data for lava samples from the Mount St. Helens dome have been used to evaluate four possible triggering mechanisms: local dilation of the conduit induced by earth tides, periodic influx of deep seated volatiles into the magma reservoir, over-pressurization caused by crystallization of anhydrous minerals, and interaction between magma and snowmelt during the spring. These data have been used to determine the movement of volatiles in magmas and are a potentially useful tool for evaluating various eruption triggering mechanisms.

Within each lobe, the highest delta D values are generally found in the samples with the lowest water content, suggesting deuterium preferentially accumulates in the solid phase during degassing. Scoriaceous samples generally have lower water contents and higher delta D values than smooth samples from the flow front and vent regions. Although the accumulation of deuterium in the solid phase contradicts what is generally observed in more water-rich lavas, Taylor (Reviews in Mineralogy, vol. 16, 1986) has also suggested that deuterium will prefer the solid phase during degassing of silicic lavas with very low water contents.

We have compared the delta D values of similar texture types for several different lobes. For each texture type there are large variations in delta D (up to 40 per mil) for a given texture type with time, although water content values for these textures vary little (less the 0.1 wt. %). We feel this trend is best explained as follows. Volatiles from the deep portions of the magma chamber are steadily added to the eruptible cap. As this process proceeds, water continually escapes from the cap through fractures in the conduit and dome, as demonstrated by the gas plume emitted from the dome during periods of quiescence. Pressure accumulation will thus be controlled by the water escape rate - if gas loss is high, which may happen following extrusions which generate large amounts of deformation, then pressure will build more slowly, and the length of hiatus between extrusions will increase. If gas loss from the chamber releases isotopically lighter water species, as occurs during degassing of the dome lava samples, then with time the top of the magma chamber will become isotopically heavier than the rest of the chamber. This model is supported by the fact that the lavas erupted after longer periods of repose are isotopically heavier than those erupted after relatively short repose periods, although their water contents remain the same.

The lava samples from the spring do not show any evidence of meteoric water contamination, and variations in the isotopic composition of lava samples with time can be explained by this model of volatile replenishment/degassing. The earth tide and crystallization models cannot account for the large isotopic variations in the eruptive products. Removal of a thick snowpack from the crater floor and dome could lead to additional overpressurization of the underlying magma chamber. We calculate that removal of a 50 meter thick snow layer will result in 0.6% overpressurization within the Mount St. Helens magma chamber. Removal of snow during the spring is probably not capable of triggering a dome eruption by itself, although it may provide the extra impetus needed to start the extrusive process.

SULFUR DIOXIDE AND PARTICLE EMISSIONS OF MOUNT ETNA, ITALY FROM JUNE TO AUGUST 1987

ANDRES, R.J.* and KYLE, P.R., Geoscience Dept., NM Tech, Socorro, New Mexico 87801 USA
CHUAN, R.L., Brunswick Corporation, Costa Mesa, California 92626 USA
*Currently at Geol. Engrg. Dept., Michigan Tech. Univ., Houghton, Michigan 49931 USA

The sulfur dioxide (SO_2) and particle emissions of Mount Etna, Italy were sampled from June to August 1987. Only two of the four summit craters were active at that time; Southeast Crater (SC) was degassing constantly by a puffing mechanism with no emission of ash or lava and Bocca Nuova (BN) was undergoing strombolian eruptions.

SO_2 emissions were monitored with a Barringer correlation spectrometer (COSPEC). SO_2 fluxes for the entire system averaged 1056 $\pm$ 921 tonnes per day (tpd) from a total of 126 measurements. The large standard deviation in system fluxes resulted from a 300 percent increase in SO_2 emissions on 19 July with no apparent change in eruptive activity. These measurements highlight the uncertainty of predicting eruptions based solely on SO_2 flux data. The increased SO_2 fluxes observed are postulated to be due to rising magma and/or an influx of undegassed magma into the SC vent.

The individual contributions from BN and SC to the total SO_2 flux were measured on 19, 20, and 22 July. BN emitted 278 to 3898 tpd (averaged 1166 tpd from 64 measurements) and SC emitted 165 to 5229 tpd (averaged 629 tpd from 49 measurements). Differing volumes of magma degassing beneath each crater is postulated to account for the emission of almost twice as much SO_2 from BN as from SC.

Separation of the nearly transparent SO_2 plume from the visible steam plume was observed. High winds cause the SO_2 to separate because of its lower heat capacity than steam and higher density than air. The existence of SO_2-plume separation can have severe consequences for COSPEC-obtained SO_2 flux data.

A quartz crystal microbalance cascade impactor was used to collect particles >0.07 μm in diameter emitted from BN and SC. Most of BN particles were >2 μm in diameter while most of SC particles were <2 μm in diameter. Particles identified include silicates, chlorides, chlorates, sulfites, and sulfides. Chlorine was a constituent of SC's particles only. Differences observed in size distributions and particle compositions for each crater were likely due to the differing eruption style of each crater. Chlorine compounds were likely missing from BN-sampled particles because their sublimation or crystallization onto ash caused the particles to fall back into the crater.

Particle and acid gas samples were collected using LiOH-treated filters from BN and SC and analyzed by INAA for 30 elements. Chlorine, bromine, and sulfur were the most enriched elements in the sampled fume. Both BN and SC have similar element enrichment factors testifying to the homogeneous composition of the magma source beneath each crater.

Atmospheric implications of Etnean emissions were negligible compared to the region's anthropogenic emissions for all elements except fluorine and chlorine.

A COMPARISON OF FLOW BEHAVIORS OF ERUPTION- AND POST-ERUPTIVE LAHARIC DEBRIS FLOWS OF MAYON VOLCANO, PHILIPPINES AS INFERRED FROM THEIR DEPOSITS

ARGUDEN, A.T., RODOLFO, K.S.
Department of Geological Sciences, University of Illinois at Chicago, P.O. Box 4348, Chicago, IL, 60680 U.S.A.

Numerous hot lahars produced during and immediately after the 1984 eruption of Mayon Volcano, and frequent cold lahars that occurred during the succeeding two wet-monsoon seasons, have left widespread deposits. Fresh eruption-lahar debris-flow deposits are distinguished by scalded vegetation; thin crusts that are remarkably resistant to erosion and to vegetal growth; thin, baked, erosion-resistant rims around surface clasts; and rare soft-sediment deformation structures and gas-escape tubes. Deposits of unchannelized debris flows of eruption- and post-eruptive lahars both have sheetlike or lobate geometry, non-erosional or insignificantly erosional bases, poor sorting, basal inverse grading, and relatively minor silt and clay contents. Both may display matrix or clast support, and out-sized clasts are common at their tops. Although it is very difficult to distinguish between the deposits after burial, they have subtle, significant textural differences. Deposits of eruption debris flows have more variable grain-size distributions and generally smaller median diameters.

Steep gradients, coupled with buoyancy due to high clast concentrations in the matrix, may account for the high mobility and competence of lahars with very low clay content. The inversely graded basal portions of eruption debris-flow deposits (a) are thick, suggesting the considerable rheologic role of dispersive pressure and, to a lesser extent, of pore pressure; (b) have long clast axes aligned parallel to bedding, suggesting strongly sheared laminar flow conditions; and (c) usually are succeeded by gradual normal grading that indicates waning-flow conditions. In post-eruptive debris-flow beds only the basal few centimeters or decimeters are inversely graded, and the major, upper portions are commonly ungraded or are composed of one or more inverse-to-normal sequences, indicating a non-sheared plug and the major role of frictional strength in supporting the larger particles.

Bed thickness/maximum particle size correlations suggest significant differences in the clast-support mechanisms of hot and cold debris flows. Clasts in hot debris flows are supported mainly by dispersive pressure resulting from clast collisions, possibly augmented by pore-fluid pressures, whereas those in cold debris flows are supported primarily by frictional and cohesive strength. In hot flows, the decrease in viscosity as a consequence of water temperature may be relatively minor; however, conversion of water to vapor may facilitate mobility by decreasing internal friction.

Indirect velocity calculations indicate that the hot debris flows are faster (3.1 m/sec on 3.2° slopes to 5.6 m/sec on 5.4° slopes) than cold post-eruptive flows (2.4 m/sec on 3° slopes to 4.7 m/sec on 4.8° slopes). All but two of the hot debris flows analyzed were super-critical, and all the cold flows were sub-critical. Reconstituted shear strengths of the deposits of both types had similar values. The hot debris flows of the 1984 eruption were more mobile, some reaching the coast 11 km from the summit. In contrast, none of the cold post-eruptive debris flows had runout distances exceeding 8 km.

TIME-SPACE PATTERNS OF MESOZOIC-CENOZOIC MAGMATISM IN WESTERN U. S. AND CANADA

RICHARD LEE ARMSTRONG, Department of Geological Sciences, University of B. C., Vancouver, B. C., V6T 2B4
PETER WARD, United States Geological Survey, Menlo Park, CA, 94025

Late Triassic to Early Jurassic and Middle to early Late Jurassic magmatic culminations, widespread in exotic terranes and affecting the outer parts of the Cordilleran miogeosyncline, were largely unrecorded in the continental interior of N America. These early magmatic arcs developed on the craton only in the Southwest. The Jurassic magmatic culmination was accompanied by regional metamorphism and deformation in the area of the Mesocordilleran Geanticline.

In Early Cretaceous time, following a wide- spread lull of magmatic activity, an Andean continental-margin magmatic belt, continuous from Mexico to Alaska, became established: A high temperature batholith belt existed in accreted terranes. An inland magmatic belt , parallel to the B-subduction-related arc, but chemically and isotopically distinct, was created by melting or bulk assimilation of tectonically thickened crust.

About 80 Ma ago a dramatic cessation of magmatic activity began between latitude 32° and 45° - forming the Laramide magmatic gap. At the same time the earlier Cretaceous magmatic-tectonic patterns persisted to the N and S of the magmatic gap, although magmatism in those areas was somewhat reduced in volume and extent.

Beginning about 58 Ma ago the Mesozoic magmatic-tectonic patterns were suddenly extinguished and replaced by a new regime: magmatic quiescence and waning Laramide uplift and basin subsidence S of 42°, volcanism and crustal extension across the deformed belt N of 42°.

During the Early and Middle Eocene the Kamloops-Challis-Absaroka magmatic belt existed N of 42°. Its southern end curved into cratonic parts of Montana, mimicking a Late Cretaceous-Paleocene magmatic trend. Along the continent margin an oceanic basaltic island chain formed and was accreted in Oregon, Washington and southern B. C. and continent-edge magmatism occurred from Vancouver Island to Alaska. In Colorado and the Black Hills region and in southern Arizona Laramide magmatic belts waned and shifted eastward.

During Late Eocene to Late Oligocene time (40 to 25 Ma) magmatic activity in the N was concentrated into Cascade arc and Great Basin fields. Several continent-margin magmatic fields persisted from Vancouver Island northwards, and inland there was scattered basaltic magmatism. Magmatic fields in Arizona-New Mexico and the San Juan Mountains regions expanded and merged along the future trend of the Rio Grande Rift. The large southern and northern magmatic fields were weakly linked by scattered magmatic centers on the Colorado Plateau.

In latest Oligocene through most of Miocene time the most notable magmatic development was merging of the northern and southern fields into one continuous and vigorous magmatic belt extending from Mexico to Canada. Farther N magmatism occurred in scattered fields of hot spot or within-plate character and in the Wrangell arc. The flood basalt episode of the Columbia Plateau occurred, less voluminous basalts were erupted over southern Intermontane Belt in British Columbia, the Snake River Plain magmatic transgression began, and the Cascade arc persisted in place. Magmatism rapidly spread over much of California southwest of the San Andreas fault, Colorado Plateau activity declined and Rio Grande Rift activity became more focused on modern patterns. After the merger of the two major magmatic fields, about 22 Ma ago, there has been both a general decline in the amount of magmatic activity and a change in most areas to the bimodal, predominantly basaltic petrochemical association.

Since Late Miocene time magmatism has followed modern patterns. In the N, the Wrangell Arc has shrunk into Alaska. Several continent-margin and within plate fields have waxed and waned. Small- volume hot spot and back-arc plateau magmatism have occurred over much of southern British Columbia. The Cascade Arc persisted from Canada to northern California, while back-arc activity has diminished to little more than the eastern plateaus of Oregon. The Snake River Plain continued to expand eastward. Magmatic activity has persisted on the margins of the Basin and Range and Colorado Plateau provinces. In southwestern California a continent-margin magmatic belt has moved northwestward to the Geysers-Clear Lake area.

The merging of two large magmatic fields in early Miocene time, explains the time and place of the metamorphic core complex hyperextension episode of the Colorado River corridor, the sudden reorientation of stress patterns across much of western N America, and many subsequent tectonic events in California.

SMALL-VOLUME ANDESITES INTERLAYERED WITH LARGE-VOLUME ASH-FLOW TUFFS IN THE SAN JUAN (CO), INDIAN PEAK (UT-NV), AND CENTRAL NEVADA VOLCANIC COMPLEXES

ASKREN, D.R.R., RODEN, M.F., and WHITNEY, J.A., Dept. Geology, University of Georgia, Athens, GA 30602

Small volumes of andesite are interlayered with voluminous ash-flow tuffs in the San Juan (SJ), Indian Peak (IP), and Central Nevada (CN) caldera complexes of CO, UT, and NV. These three areas are along an east-west transect perpendicular to the Tertiary N. America-Pacific plate boundary. In all three areas, tuffs and interlayered andesites were erupted 32-25 Ma, and bimodal eruptions of basalt and rhyolite followed. In the SJ area, this package is preceded by an extensive period of andesitic volcanism (Lipman, 1976; Dungan, 1988), but the IP and CN areas have no such mafic precursor (Best, 1986). In each area, andesite is the most mafic composition associated with felsic caldera complexes.

Most of the andesitic units are dominantly pyroxene andesite, and a few units are olivine andesite (present in SJ and IP areas) or hornblende andesite. All of the andesitic units contain pl + cpx + mt, and different stratigraphic units contain $\pm$ ol $\pm$ opx $\pm$ hb $\pm$ bio $\pm$ ap. Samples from the SJ field are at least as potassic as high-K andesite, and those from the IP and CN complexes range from medium- to high-K andesite. Although high K contents are more common in samples from the SJ field, incompatible trace element abundances are broadly similar in samples from all areas.

For most of the units, phenocryst compositions are typical for andesitic bulk compositions. However in two units from the IP complex, phenocryst compositions are unusual for bulk SiO2 contents even though the rocks display apparent equilibrium textures. Some samples from one unit contain Mg-rich olivine and Cr spinel, and some samples from another unit contain extremely calcic plagioclase (up to An90). Pressures of magmatic equilibrium have been estimated by comparison of mineral and rock compositions to experimental phase equilibria. Although some pressure variations may exist between certain units, all units appear to have equilibrated from 2 to 8 kb.

The interlayered, small-volume andesites were erupted from volcanic centers within and peripheral to established ash-flow tuff calderas. Olivine andesites occur only at centers peripheral to calderas, and hornblende andesites occur only at centers within these calderas. Pyroxene andesites occur at centers both peripheral to and within calderas. The intracaldera hornblende andesites are generally more silicic and have higher abundances of incompatible trace elements than the peripheral olivine andesites. These mineralogic and compositional correlations suggest that evolution of andesitic magmas may be modified if ponded beneath ash-flow calderas. The andesites may represent mantle input via basaltic parents, and perhaps greater differentiation or interaction with felsic materials modifies those mafic magmas trapped beneath calderas. Further documentation of these differences may reveal the relative importance of interlayered andesites in the development of these large, felsic caldera complexes.

EARLY PROTEROZOIC (1890 MA), BASALTIC VOLCANICLASTIC UNITS IN THE FLIN FLON-SNOW LAKE GREENSTONE BELT, CANADA

AYRES, L. D., Department of Geological Sciences, Sciences, University of Manitoba, Winnipeg, Manitoba, R3T 2N2, Van Wagoner, N.A., Department of Geology, Acadia University, Wolfville, Nova Scotia, B0P 1X0, and DOLOZI, M.B., Department of Geography and Earth Sciences, University of Malawi, Zomba, Malawi

Basaltic volcaniclastic units ranging from sandstone to coarse breccia are a common component of the western part of the greenstone belt. At Amisk Lake the volcano is characterized by a vertical and lateral transition from near-shore, subaerial basaltic sandstone through flow-foot breccias produced at the shoreline to relatively shallow-water, storm-generated basaltic turbidites. Although occurring in several different depositional environments, all deposits exhibit a limited amount of reworking, and are composed largely of rounded to angular, originally vitric, non-vesicular, basaltic granules with minor scoriaceous basaltic clasts, basaltic lithic clasts, broken plagioclase and clinopyroxene grains, and rare accretionary lapilli. The subaerial deposits, which are up to 1 km thick and have a lateral extent of more than 13 km, comprise very thin to medium-bedded, locally normally graded sandstone interbedded with less abundant, very thick bedded, pebble conglomerate of debris flow origin and local basaltic lava flows; bed contacts are sharp but are only locally erosive. This sequence appears to be an apron of reworked phreatomagmatic tuff. The subaqueous turbidites are up to 500 m thick and comprise thinly bedded Bouma AB beds and interbedded graded laminated layers. They represent further reworking of both the phreatomagmatic tuff and flow-foot breccias. The huge volume of explosively generated, hydroclastic tuff represented by these deposits and the limited amount of reworking imply extensive interaction of magma and water in the near-shore zone of a rapidly subsiding, basaltic island.

East of Flin Flon the basaltic volcaniclastic units are coarser. They are typified by a 380-m thick, lenticular sequence of very thick bedded tuff-breccia and intercalated pillowed basalt flows, capped by thin to medium-bedded turbiditic sandstone. Tuff-breccia beds have sharp, non-erosive contacts and are ungraded to graded. Fragments are commonly amygdaloidal (range 5-55%; mean 31%), with amygdules commonly uniformly distributed through fragments, angular to subangular, and 0.5-100 cm in size with partial chilled rims. The sandstone and the matrix of the tuff-breccia are largely blocky, vitric to holocrystalline, vesicular to non-vesicular ash and fine lapilli. The intercalated pillowed flows have a lower amygdule content (range 0-35%; mean 19%) with amygdules concentrated near pillow margins. The tuff-breccias were deposited by debris flows that were apparently generated by slumping of pre-existing fragmental material explosively erupted in shallow water by a combination of magmatic and steam explosions. The prevalence of the basaltic volcaniclastic rocks in this part of the greenstone belt apparently reflects the shallow water to subaerial nature of much of the basaltic volcanism.

LEAD ISOTOPIC DIVERSITY IN THE BANDELIER TUFF, VALLES CALDERA, AND RELATED ROCKS OF THE JEMEZ MOUNTAINS, NEW MEXICO

AYUSO, Robert A., U.S.G.S., Reston, VA 22092, and
SMITH, Robert L., U.S.G.S., Sacramento, CA 95821

The Jemez Mountains are located in north-central New Mexico at the intersection of the Rio Grande rift and the Jemez lineament. Following a long history of complex volcanism, two Pleistocene pyroclastic outbursts, approximately 350,000 years apart, deposited the Otowi and the Tshirege members of the Bandelier Tuff. Each member was associated with caldera collapse, Toledo and Valles Calderas respectively, and each caldera had a complex history of rhyolitic volcanism, the Cerro Toledo and Valles rhyolites, respectively. Pb-U-Th determinations of 45 HF-leached rocks and feldspars in the Bandelier Tuff and associated rocks indicate that the Otowi is less radiogenic than the Tshirege. The range in $^{206}Pb/^{204}Pb$ for the Otowi is 17.811 to 17.853 and in the Tshirege is 17.938 to 18.003; $^{207}Pb/^{204}Pb$ values range from 15.497 to 15.534 and from 15.538 to 15.577, respectively. $^{208}Pb/^{204}Pb$ values range from 37.560 to 37.699 in the Otowi and 37.798 to 37.930 in the Tshirege. Lead isotope variations in the Bandelier Tuff are directly correlated with minor-element gradients in the Bandelier magma chamber (e.g., Nb, Ta, and Th), however aberrations occur. Cerro Toledo rhyolites have compositions overlapping those in the Otowi. Early Valles Caldera rhyolites overlap the Tshirege but later Valles rhyolites are the least radiogenic of the system. Pre-Bandelier basalts, intermediate rocks, and rhyolites, including potential parental magmas, have lead isotopic compositions that bracket the entire Bandelier system.

Our results do not identify clearly the isotopic reservoirs required to produce the Bandelier system. Precambrian granites in the vicinity of the Valles Caldera are significantly less radiogenic than the Bandelier Tuff. Thus, it is unlikely that Bandelier magmas were derived primarily by anatexis of Precambrian granitic rocks. Local xenoliths from eruptions within the caldera are also far less radiogenic than any volcanic rock from the Jemez Mountains. Source regions for Bandelier magmas may include mixtures of mafic melts (e.g., olivine basalt) from the subcontinental lithosphere or mantle and more felsic melts produced from more sialic rocks in the middle and lower continental crust. Melts obtained from such a mixing are expected to fractionate rock-forming and accessory minerals and change the contents of major- and trace-elements, including U, Th, and Pb. Crystal-liquid fractionation alone, however, cannot explain the observed lead isotopic heterogeneity within the magmatic system.

We present two alternatives to explain the isotopic variability in the Bandelier magma system. One requires crystal-liquid differentiation processes and mixing of isotopically distinct magmas by a process of incremental replenishment. The second also involves crystal-liquid fractionation but depends on assimilation of roof rocks to produce minor-element and isotopic heterogeneity. Other processes of fractionation are not ruled out. In the second alternative, minor element gradients and isotopic differences reflect gradients in volatile distribution between the Bandelier magmatic system and the roof rocks. However, in either case, periodically discharged volcanic systems may remove from the roof of the magma chamber upper volcanic members whose isotopic signatures differ greatly from those in lower members from the volcanic depths. Plutonic rocks crystallized after substantial removal of the upper volcanic members may in such cases provide no evidence of isotopic heterogeneity in the magma chamber during earlier stages of evolution.

EVIDENCE AND CONSTRAINTS FOR THE PRESENCE OF A SHALLOW RESERVOIR AT PITON DE LA FOURNAISE (REUNION)

P. Bachelery* and J-F Lénat **
* LAB. GEOL., UNIV. REUNION, BP 5 Le chaudron, 97490 Ste Clotilde FRANCE.
** OPGC (CRV-CNRS), UNIV. CLERMONT II, 5 rue kessler, 63038 CLERMONT-FERRAND, FRANCE.

The average magma output of Piton de la Fournaise, as determined for the last 60 years, is 0.34 m^3/s. Recent geological and geophysical studies show that this magma is usually buffered in a shallow reservoir complex beneath the summit area.

The presence of this complex in the past may be inferred from surface volcanotectonic features ; the inprint of a series of collapse-and-refilling episodes of the summit area is obvious in the topography. The centers of these paleo collapse-craters have drifted over a restricted area (few hundreds of meters), with a pronounced E-W elongation that may reflect a slight tendency to an eastward migration. The present main summit crater, Dolomieu crater, resulted from an episode of collapse that took place in the early 30's, following a noticeable inflation of the whole summit zone since 1927, and the eruption of a large volume of lava ($135x10^6$ m^3) along a fissure which openned along the NE rift zone in the caldera. The deflation of the summit and the formation of a small pit crater inside Dolomieu, during the eruption of March 1986 at low altitude along the SE rift zone, have recently provided further tangible proof of the existence of magma storage at shallow depth beneath the summit.

This model is fully supported by the available structural geophysical data. Aeromagnetic data suggest the presence of a weakly magnetized volume of rock beneath the summit, which can be attributed to the presence of rocks above the Curie temperature and to hydrothermally altered rocks. The same geological situation, in addition to the presence of water impounded in the intrusion network, would fit with the low resistivities revealed by DC and AMT soundings. The very large (1.5 volt) SP anomaly of the summit can be related to hydrothermal convection cells surrounding the reservoir complex.

With the data collected by the volcanological observatory since 1980, it has been possible to refine the model of the reservoir for both geometrical and dynamical aspects. From the pattern of seismicity and deformation, it can be inferred that the storage complex is composed of discrete pockets separated by rigid walls.These storage units can be permanently or intermitently connected. They are distributed over an area that corresponds approximately to that of Dolomieu crater. The shallowest ones can be located at only a few hundreds of meters below the surface, but the main storage zone lies between 1km and at least 2.5 km (there are no definitive arguments to characterize it below).

Magma transfer between the deep zones and the shallow reservoir is thought to be discontinuous or irregular. The larger episodes of transfer may be associated with the major oceanite eruptions (last one in 1977). Petrologically, the lavas erupted during the recent years are supposed to be tapped from batches of magma residing in the shallow reservoir complex.

SHALLOW AND DEEP PROCESSES AT CRATER LAKE, OREGON: A MODEL SYSTEM FOR MAGMATISM IN A YOUNG CONTINENTAL ARC

BACON, C.R., U.S. Geological Survey, 345 Middlefield Road, Menlo Park, CA 94025

Mount Mazama erupted ~50 km^3 of magma ~6850 yr B.P., providing samples of the contents and walls of a shallow, zoned magma chamber. Compositionally uniform rhyodacite pumice erupted first from a Plinian column, next as pyroclastic flows derived from the collapsed column, and finally (along with crystal-rich andesitic and mafic-cumulate scoriae) as highly mobile pyroclastic flows generated from many columns during collapse of Crater Lake caldera. Preeruptive temperature increased from 880°C in rhyodacite and early andesite to >940°C in late-erupted scoria; residual glass ranged from rhyolite to andesite. Melt inclusions in plagioclase in pumice contain ~4.5 wt% H_2O, implying depth to the magma chamber was 6 km, more if magma was H_2O-undersaturated. At least two scoria trace-element and Sr-isotopic compositions require that multiple parental liquids entered the chamber. Compositions of magmatic inclusions in preclimactic rhyodacite flows suggest addition of high $^{87}Sr/^{86}Sr$ andesite, followed by low $^{87}Sr/^{86}Sr$ andesite as the chamber grew during ~30,000 yr. Each injection of andesitic liquid formed a hot lens between plagioclase-rich cumulates and overlying convecting rhyodacitic magma; crystallization of this liquid during thermal equilibration produced buoyant differentiated melt that mixed into the rhyodacitic magma while complementary crystal mush formed a new cumulate layer. Denser basaltic inputs lodged deeper in the cumulate pile.

Lack of increase in $\delta^{18}O$ of rhyodacite over less evolved magmas reflects assimilation of low-^{18}O material represented by partially fused granitoid blocks ejected in the climactic eruption. The granitoids were derived from a pluton of Mazama-like chemistry that had exchanged with hydrothermal fluids before reequilibrating at as much as 970°C. Maximum melt fraction of ~0.35 among the granitoids suggests more extensively fused material was assimilated. Had the climactic eruption not occurred, crystallization would have formed a granodiorite pluton with underlying dioritic to gabbroic cumulates, emplaced within the older plutonic source of the granitoid blocks. If the chamber had solidified after the climactic eruption, the only record of the rhyodacite would be the complementary cumulates, which must have been disturbed by caldera collapse.

Mount Mazama consists of dominantly andesitic stratocones built on a foundation of earlier rhyodacite. Shallow chambers that support hydrothermal systems and produce catastrophic eruptions are associated with such volcanic foci where evolved magmas have erupted at various times over a long period. Crystallization of these chambers results in epizonal plutons that punctuate the dominantly volcanic upper crust of arc terranes.

In contrast to the upper crustal evolution of the climactic chamber, lavas of monogenetic vents acquired their trace-element and isotopic compositions largely in the lower crust and upper mantle. Tholeiitic basalt, calc-alkaline basaltic andesite and andesite, and minor shoshonitic basaltic andesite were erupted from vents near Mount Mazama, commonly along north-south alignments parallel to regional normal faults. These lavas possess a range of $^{87}Sr/^{86}Sr$ similar to that of the climactic ejecta. Their O and Sr compositions may reflect interaction with deep crustal material of low $^{87}Sr/^{86}Sr$ and comparatively high $\delta^{18}O$, such as pre-Cenozoic rocks of the Klamath terrane, which may extend northeast beneath Crater Lake. Primitive tholeiites and magnesian basaltic andesites have variable LILE abundances that suggest primary liquids, derived from the mantle wedge, contained different amounts of a subduction-related component before fractionating in and interacting with the deep crust. Such a model may apply to the Cascades south of the northern Washington crystalline basement and seems to be common to intraoceanic and primitive continental arcs.

MAAR DEPOSITS AT KILBOURNE HOLE: IMPLICATIONS FOR BASE SURGE PROCESSES

BAHAR, D., Department of Earth Sciences, New Mexico State University, NM 88003, and
MCCURRY, M., Department of Earth Sciences, New Mexico State University, NM 88003

Kilbourne Hole maar formed in the late Pleistocene as a result of explosive phreatomagmatic eruptions. It is one of the three Afton Craters located in the southern Rio Grande rift of New Mexico. The rim deposits of Kilbourne Hole were emplaced by base surges. The deposits exhibit a wide variety of classic base surge structures. These include: low angle sandwaves, anti-dunes, planar beds, massive beds, and chute-and-pool structures. Some of these beds are mantled by thin, continuous, well sorted fallout beds. Additional features include: splash-like deformation of beds around bombs, stream-wise deflection of soft sediment structures, intact, yet highly friable bombs of siltstone and fine sandstone, and interbeds of well sorted accretionary lapilli and essential basalt lapilli. First, these structures help constrain certain dynamic processes within the base surges including characteristics of turbulence and boundary shear stress. Second, they reflect the varying intensities of particle emplacement mechanisms such as surge and fall. Third, they indicate the importance of liquid H_2O in the cloud. In addition, stratigraphically vertical variations of bedforms, structures, and composition suggest that the amount of liquid H_2O increased within the surge cloud as the eruption progressed. These variations include an upward increase in the abundance of accretionary lapilli, soft sediment structures, and massive beds.

PETROCHEMICAL FEATURES OF THE RIPHEAN (LATE PROTEROZOIC) DYKE SWARM IN MONGOLIA (AN EXAMPLE OF THE GASHUNNUR COMPLEX)

BAIKOVA, V. S., Institute of Precambrian Geology & Geochronology, the USSR Academy of Sciences, 199034, nab. Makarova 2, Leningrad, USSR

A NW-trending mafic dyke swarm is revealed in Mongolia to be traced via China within the USSR (Kazakhstan). It has about 700 km long and 20 km wide. The studied subparallel dykes of diabase porphyrites confined to the Gashunnur complex present a part of this major swarm (Fig. 1). They mark a boundary between the Early and Late Proterozoic. Their emplacement was preceded by formation of slightly differentiated mafic-ultramafic rocks of the Buren-Kharkan massif.

The dykes have been sheared, deformed and metamorphosed (at low grade epidote-amphibolite facies) together with the enclosing rocks; however, they retain chilled margins and relics of primary diabase textures and zonal plagioclases with anorthite content up to 95% (average 80%).

The dykes show major and REE (Rb, Sr, Y, Yb, Zr) distribution patterns similar to those of the mafic-ultramafic rocks that suggests a single magma source for them. Both the diabase porphyrites and massif diabases correspond in chemical composition to low-K tholeiitic basalts.

The comparison of the Gashunnur dykes with other dyke and ophiolite suites as well as dykes of continental basalts of different age showed that the former have higher contents of Al_2O_3, total Fe, CaO, K_2O and lower MgO and Na_2O contents. This suggests that the Gashunnur dykes were emplaced at an earlier rifting stage--transitional from the continental to oceanic crust.

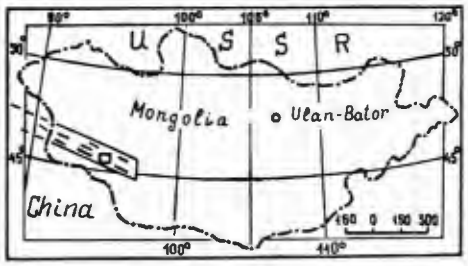

CALC-ALKALINE VOLCANISM ASSOCIATED WITH CRUSTAL EXTENSION IN NORTHEASTERN OREGON

Bailey, David G., Dept. of Geology, Washington State Univ., Pullman, WA, 99164

Calc-alkaline magmatic activity is most commonly associated with convergent plate boundaries. During the Late Tertiary in northeastern Oregon, calc-alkaline andesites and dacites erupted from small vents, and flowed unconformably over widespread tholeiitic basalt sheet flows. This region of calc-alkaline volcanic activity was situated nearly 400 km behind the main Cascade arc, and over 550 km from the trench. Thus, it appears unlikely that this activity was directly related to plate subduction. Instead, the inception of calc-alkaline volcanism in northeastern Oregon was associated with widespread WSW crustal extension that generated many small grabens. The association of calc-alkaline volcanism with the initiation of crustal extension is also observed in the Rio Grande Rift and throughout the Basin and Range Province.

The chemical and mineralogical features of these rocks require a complex, and unusual petrogenetic history. One of the most striking features of the rocks is their virtual lack of phenocrysts; hypersthene is the only phenocryst phase of common occurrence, and it is present only as microphenocrysts. The vast majority of over 200 whole-rock samples analyzed are low-K, calc-alkaline andesites and dacites. They are characterized by steep rare-earth profiles with no europium anomalies: chondrite normalized La/Yb ratios range from 7-10 for the andesites, and from 9-12 for the dacites. Strontium 87/86 ratios range from .7035 to .7040 for the entire group, with the lowest values observed in the dacites.

A compositionally diverse group of basaltic rocks is spatially and temporally associated with these intermediate rocks. The vast majority are olivine-phyric, tholeiitic basalts. Primitive, high-Mg basalts and moderately alkaline basalts (6-7 wt % Na2O+K2O) also occur in the area. All of these basalts have higher strontium 87/86 ratios (.7040-.7045) than do the intermediate rocks of calc-alkaline affinity discussed above.

It is proposed that the generation of calc-alkaline magmas in northeastern Oregon was the result of: 1) intrusion of large volumes of basaltic magma into, or beneath, the lower crust causing an increased ductility of the lower crust; 2) propagation of a WSW oriented extensional stess regime causing crustal thinning and enhancing the interaction of mafic magmas with the lower crust; 3) partial melting of the lower crust to produce a rhyodacite magma with a low strontium 87/86 ratio; and 4) mixing of this silicic melt with variably evolved mafic magmas.

LONG VALLEY CALDERA AND MONO-INYO CRATERS VOLCANIC CHAIN, EASTERN CALIFORNIA: PETROLOGIC INTERRELATIONS

BAILEY, ROY A., U.S. Geological Survey, Menlo Park, California 94025

Long Valley caldera (LVC) and the Mono-Inyo Craters volcanic chain (MIVC) are spatially and temporally overlapping volcanic complexes on the eastern Sierra Nevada front, at the western edge of the Basin-Range province. Both complexes are trachybasalt-trachyandesite/rhyodacite/rhyolite sequences but in different stages of structural and magmatic evolution. LVC, the older (3.6 - 0.1 Ma), has evolved through a caldera stage, successively erupting precaldera trachybasalt-trachyandesite, rhyodacite, and high-silica rhyolite, the syncaldera rhyolitic Bishop Tuff, and postcaldera low- and high-silica central and moat rhyolite. MIVC, a N-trending, 50-km-long chain transecting the western part of LVC, is younger (0.3 Ma to present) and has erupted trachybasalt-trachyandesite, rhyodacite, and rhyolite analogous to that of the LVC precaldera stage but has not evolved further. During its shorter life span, MIVC has erupted more frequently and evolved chemically more rapidly than the LVC precaldera stage, and chemical differences between LVC and MIVC trachybasalts-trachyandesites suggest greater involvement of crustal contamination in the latter. These aspects of MIVC evolution may be due to thermal conditioning of the crust by the preceding long-lived LVC magmatism.

While LVC magmatism may have preconditioned MIVC magmatism, MIVC also affected subsequent LVC evolution. Initiation of MIVC trachybasaltic magmatism thermally and chemically perturbed the residual LVC rhyolite chamber. At 0.3 Ma postcaldera coarsely porphyritic low-silica moat rhyolite was succeeded by finely porphyritic high-silica rhyolite with higher FeTi-oxide temperature and a fractionation pattern similar to that of the Bishop Tuff; the sequence suggests rejuvenation of convection within the residual crystal-rich LVC chamber by MIVC trachybasalt magmatism and development of a more fractionated crystal-poor cap. Sporadic occurrence of liquid basaltic inclusions in postcaldera rhyolites suggests that all LVC postcaldera rhyolite eruptive episodes (at 0.5, 0.3, and 0.1 Ma) may have been accompanied and possibly triggered by basaltic magmatism at depth. Structural and stratigraphic evidence in the caldera fill suggests that the 0.3- and 0.1-Ma eruptive episodes were accompanied by renewed uplift of the resurgent dome. These relations, considered in the light of recent (1980 - present) seismicity and uplift within LVC, suggest that LVC currently could be exhibiting the early effects of basalt injection at depth, which, depending on future frequency and intensity of such root-zone intrusion, may or may not lead to another episode of rhyolitic volcanism.

The common association of finely and coarsely porphyritic rhyolites in LVC and MIVC, as well as in other caldera sequences, is reminiscent of the association of aplites and porphyritic granites in igneous ring complexes and suggests that they are volcanic/plutonic analogs; possibly both are linked genetically to thermal rejuvenation of their reservoirs by episodic basaltic recharge at their roots.

ELUCIDATING THE TIME OF INITIATION AND DURATION OF VOLCANISM FOR VARIOUS MESOZOIC-TERTIARY FLOOD BASALT PROVINCES.

BAKSI, Ajoy K., Department of Geology & Geophysics, Louisiana State University, Baton Rouge, LA 70803-4101.

A considerable amount of interest in the formation of flood basalt provinces has been created by the hypothesis linking their extrusion to global faunal extinctions. A necessarY, but not sufficient, prerequisite in this regard, is to show that voluminous, episodic, flood basalt volcanism took place at various times, coincident, within experimental error, with the time of various global faunal extinctions. In light of the composition and age of the Provinces under consideration, only the argon dating techniques can supply radiometric data of the required precision and accuracy. I have earlier shown that the K-Ar dates for such material are often in substantial error in determining crystallization ages. In effect, only the 40Ar-39Ar incremental heating technique can yield crystallization ages and help eliminate incorrect K-Ar dates resulting from loss of radiogenic 40Ar or the presence of excess 40Ar. Herein, I summarise what is currently known regarding the timing and duration of extrusion of various flood basalt provinces.

Columbia River Basalts, USA. Evaluation of all available results suggests the bulk of this Province, ~150,000 km^3 (the Imnaha, Picture Gorge and Grane Ronde Basalt), were formed between ~17.0 and 15.5 Ma. The peak value for lava extrusion was ~275 km^3/ka for a period of ~0.5 m.y. around 15.8 Ma.

Deccan Traps, India. K-Ar dates for this province with over 500,000 km^3 of extrusive material, span the range 112-32 Ma, and are, in large measure, unreliable for determination of crystallization ages. 40Ar-39Ar dating experiments suggest that the Western Ghats section, representing ~80% of the total volume of material, was formed within 1 m.y. at ~65 Ma, with an average lava extrusion rate >400km^3/ka. Estimates for the age of the K/T boundary fall in the range ~66.5-64.5 Ma, and hence the time of the Deccan volcanic episode is currently indistinguishable from that of the K/T boundary.

Rajmahal Province, India. K-Ar dates span the range ~122-70 Ma and are, in general, not reliable for determination of the timing and duration of volcanism. A limited number of 40Ar-39Ar results suggest that this Province, initially covering >200,000 km^2, was formed <2 m.y. at ~117 Ma.

Serra Geral Province, South America. Over 80 K-Ar dates have been reported, spanning the range 165-100 Ma, with a clustering of dates around 135-125 Ma. Scrutiny of these results suggests that the initiation of the main phase of volcanism probably occurred >135 Ma. Currently, there are no 40Ar-39Ar data for this Province and it is not possible to accurately estimate the duration of volcanism.

Karoo Province, South Africa. About 100 K-Ar dates and the results of thirteen 40Ar-39Ar dating experiments are available in the literature. Other authors have utilized these data to suggest two main periods of volcanism, around 193 and 178 Ma. If this is borne out by further careful experiments, it would represent the first case of protracted, voluminous volcanism for a Phanerozoic Province.

Siberian Traps, USSR. K-Ar dates spanning the range 280-180 Ma have been reported for this Province; the accompanying petrographic reports indicate the material dated was badly altered, and hence all K-Ar results are suspect. Since these Traps form the largest Phanerozoic flood basalt province, careful determination of their age with respect to the Permo-Triassic boundary is essential to evaluation of the hypothesis linking flood basalt volcanism to global faunal extinctions.

Current attempts in these direction are seriously hampered by (a) lack of 40Ar-39Ar dating results and (b) the accuracy of the "accepted" ages of the various Period/Epoch boundaries. The latter have undergone considerable revision over the last decade (e.g. the age of the Permo-Triassic boundary has been revised from ~225 Ma in 1977 to ~245 Ma in 1986). Efforts are currently under way to obtain 40Ar-39Ar ages on the other Provinces mentioned above and to attempt close resolution of the time of the Deccan Volcanic Episode and the K/T boundary. In the interim, I urge restraint in utilizing imperfect geochronological data sets to seek periodicity in various global phenomena .

MAGMATISM ASSOCIATED WITH LITHOSPHERIC EXTENSION: MIDDLE TO LATE CENOZOIC MAGMATISM OF THE SOUTHEASTERN COLORADO PLATEAU AND CENTRAL RIO GRANDE RIFT, NEW MEXICO AND ARIZONA

W. S. Baldridge,[1] F. V. Perry,[2] D. T. Vaniman,[1] L. D. Nealey,[3] B. D. Leavy,[4] A. W. Laughlin,[1] P. Kyle,[5] Y. Bartov,[6] G. Steinitz,[6] and E. S. Gladney[7]

[1] Earth and Space Sciences Division, Los Alamos National Laboratory, Los Alamos, NM 87545

[2] Department of Geology, University of New Mexico, Albuquerque, NM 87131

[3] U.S. Geological Survey, 2255 North Gemini Drive, Flagstaff, AZ 86001

[4] P.O. Box 1052, Los Alamos, NM 87544

[5] Geoscience Department, New Mexico Institute of Mining and Technology, Socorro, NM 87801

[6] Geological Survey of Israel, 30 Malkhei Yisrael, Jerusalem, Israel 95501

[7] Health, Safety, and Environment Division, Los Alamos National Laboratory, Los Alamos, NM 87545

The region of the present Rio Grande rift and southeastern Colorado Plateau underwent lithospheric extension during middle to late Cenozoic deformation affecting the entire southwestern U.S. Igneous rocks erupted or intruded during this deformation yield insights into processes of magmatism associated with extension of continental lithosphere.

Magmatic rocks associated with an early (late Oligocene- early Miocene), ductile phase of extension are dominantly basaltic andesites and related, intermediate to silicic derivative rocks. Mafic magmas may have been derived from lithospheric mantle; high 87Sr/86Sr suggests that these rocks interacted strongly with upper crust. Igneous rocks associated with a later (middle Miocene-Holocene), more brittle phase of extension include widespread basaltic rocks and localized central volcanoes of intermediate to silicic composition. Isotopic compositions of mafic rocks, which include both tholeiitic and alkalic basalts, correlate strongly with tectonic setting and lithospheric structure. Basalts erupted in areas of greatest crustal extension, such as the central and southern rift and Basin and Range province, were derived from isotopically "depleted" (correlated with "asthenospheric") mantle. In addition, isotopic compositions of Pliocene to Holocene basalts are slightly more depleted than those of Miocene basalts, suggesting that subcrustal lithospheric mantle was thinned during late Miocene extension. Intermediate rocks of the central volcanoes evolved by a complex combination of processes, probably dominated by fractional crystallization and by assimilation of upper and lower crust in isolated, small magma chambers.

The petrologic, geochemical, and isotopic data are compatible with a model, derived first from geophysical data, whereby lithosphere is thinned beneath the central rift and southeastern Colorado Plateau, with greatest thinning centered beneath the axis of the rift. A lithospheric model involving uniform-sense simple shear does not appear compatible with the data as presently understood.

THE MIDDLE TUFF OF THE TREASURE MOUNTAIN TUFF: A UNIQUE PYROCLASTIC SEQUENCE IN THE SAN JUAN VOLCANIC FIELD, SOUTH-CENTRAL COLORADO

BALSLEY, S.D., DUNGAN, M.A., Dept. Geological Sciences, Southern Methodist University, Dallas, TX 75275, LIPMAN, P.W., U.S. Geological Survey, MS903, Denver, CO 80225, and BROWN, L., Dept. of Geology and Geography, Univ. of Massachusetts, Amherst, MA 01003

The middle tuff member of the Treasure Mountain Tuff comprises an assemblage of densely welded to nonwelded ash-flow tuffs and pumice fall units that make up a volumetrically minor (30-50 km^3 cumulative) but petrologically important contribution to the volcanic stratigraphy of the Oligocene age southeastern San Juan volcanic field. The middle tuff is uniquely distinguished from other ash-flow tuffs of the San Juans in three important ways: (1) it is composed of a collection of relatively small-volume units that erupted between much larger caldera-forming eruptions, (2) it is made up of mostly nonwelded ash-flow units, and (3) it contains compositional components from the three caldera-related regional ash-flow sheets that surround it.

The three regional sheets that bracket the middle tuff (La Jara Canyon tuff below and Ojito Creek and Ra Jadero tuffs above) formed in association with collapse of the Platoro and Summitville calderas, respectively, and are zoned from dacite to hornblende andesite. The oldest middle tuff flow units are densely welded vitrophyres that have chemical compositions identical to the underlying La Jara Canyon tuff. Stratigraphically higher middle tuff flow units are generally nonwelded to only incipiently welded and have chemical affinities to the overlying Ojito Creek and Ra Jadero tuffs. The Zr versus SiO_2 plot below illustrates the close compositional similarites of the middle tuff to the regional Treasure Mountain units (La Jara Canyon tuff shown by the lower shaded field; Ra Jadero tuff shown by the upper subvertical shaded field; Ojito Creek tuff shown as the narrow open field within the La Jara Canyon field). The regional tuff fields are based on bulk-tuff analyses of lithic-free welded samples; the middle tuff data is based on analyses of pumice clasts.

The Ra Jadero component of the middle tuff defines a steep array that may represent a mixing trend between high-Zr Ra Jadero type magma and a either a La Jara Canyon or Ojito Creek magma. Two additional subparallel trends (shown in open triangles and solid squares for La Jara Canyon and Ojito Creek components, respectively) define the remaining two components. Low SiO_2 samples to the left of the La Jara Canyon field represent compositions tapped from the lower, more mafic portions of the La Jara Canyon magma chamber following collapse of the Platoro caldera. The low SiO_2 extension of the Ojito Creek component is compositionally similar to mafic andesitic fiamme within the Ojito Creek tuff.

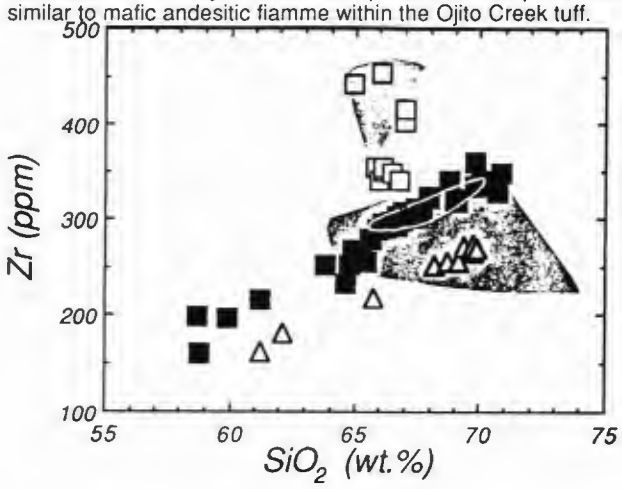

EVALUATION OF VOLCANIC HAZARD BASED ON PAST BEHAVIOR AND NUMERICAL MODELS FOR GUAGUA PICHINCHA (ECUADOR)

F.Barberi(1), G.Macedonio(2), M.T.Pareschi(3), M.Rosi(1)
(1) Dipartimento di Scienze della Terra, via Santa Maria 53, I-56100, Pisa, Italy
(2) Centro di Geologia Strutturale dell'Appennino, CNR, via Santa Maria 53, I-56100, Pisa, Italy
(3) Centro Ricerca IBM, Via Santa Maria 67, I-56100, Pisa, Italy

Volcanic hazard maps have been elaborated for volcano Guagua Pichincha, whose crater is located only about ten kilometer west of Quito, the capital city of Ecuador. The volcano is constituted by two edifices. The oldest, Rucu Pichincha, ended its activity about 1Ma ago and it is now deeply dissected by fluvial and glacial erosion; the younger, Guagua Pichincha, was built on the western flank of Rucu Pichincha and is characterized by a large amphitheater formed by gravitational failure of the cone. Archeological and historical evidences confirm that in the last millennia, human communities were affected by volcanic eruptions in this region. The most recent event of Guagua Pichincha was that of 1660, characterized by tephra fall and pyroclastic flowages. The reconstruction of the eruptive history of Pichincha of the last 30,000 years has been obtained by means of sound tefrostratigraphic studies and about new 25 14C datings. Results indicate that activity has been characterized by mostly explosive eruptions with an average frequency of one event every few centuries. Eruptions emitted relatively small volumes of dacitic pumice fall and pyroclastic surge and flow. Eruptions of the last 10,000 years BP also included lava dome growth and dome explosions with lateral blasts. Explosive activity was extensively accompanied by lahars that flowed along the main drainage.

On the basis of the volcanic history, the expected eruption has been evaluated and its main parameters assumed. These data have been then elaborated by means of physical-numerical models in order to simulate eruption behavior and consequently to evaluate hazardous areas.

The following models have been used:

1) Column behavior (CB) model (Wilson and Walker, 1987). This model, based on mass, momentum and energy balance plus the equation of state for gases, describes column behavior and in particular predicts collapse or sustained column.
2) Tephra fall (TF) model (Armienti et al., 1988; Macedonio et al., 1988; Macedonio et al, 1988bis), based on a mass balance.
3) Pyroclastic surge (PS) or flow (PF) model (Malin and Sheridan, 1983), based on a simplified balance of energy.

As expected, the reliability of the results depends, on one side, on the capacity of the stated models to appropriately describe the physical behavior of the volcanic phenomena and, on the other side, on the correct choice of the input parameters. The estimation of these parameters are based on historical considerations and experimental data (total mass available for eruption, gas weight percent, granulometric and density spectra, etc.), others are computed by models (for example one of the input datum to TF model: the height of the column, or the height of collapse in PF or PS models are computed by the CB model). A discussion of the range of validity of the input parameters is presented. Some of these can be assigned with a certain reliability (for example wind profile and vent position), others can assume different values, but the results are slightly affected by them (coefficients of diffusions); others are very important (for example erupted mass), and for these, extreme cases are presented.

PHREATOMAGMATIC PHASES IN EXPLOSIVE ERUPTIONS OF VESUVIUS.

BARBERI F., CIONI R., SANTACROCE R., SBRANA A., VECCI R. - Dipartimento di Scienze della Terra, University of Pisa, Italy

Grain-size and component analyses have been carried out on pyroclastic deposits of three explosive eruptions of Vesuvius: (79 A.D., 1631 and 1906). These eruptions cover a wide energy spectrum, from Plinian to Strombolian, and each includes a transition from a magmatic to a well-documented and clearly distinguishable phreatomagmatic phase of activity. The chronicles of the eruptions are revisited in light of the data obtained from the study of the deposits and interpretation of the dynamics of the main episodes is provided for each eruption. The phreatomagmatic products (originated from explosive interaction of magma with groundwater) have characteristic grain-size and component distribution patterns distinct from associated purely magmatic pyroclastic products: in any eruption phreatomagmatic products exhibit: i) a marked increase in both the lithic/juvenile and the crystal/total juvenile ratios, and ii) a preferential fragmentation of the juvenile fraction. Moreover eruption energy, degree of evolution of erupted magma, lithic content and depth of provenance are all clearly correlated. The abundance of lithics and crystals in phreatomagmatic deposits can be ascribed to (i) preferential fragmentation of the aquifer-hosting rocks due to explosive vaporization of ground water; (ii) vent flaring and craterization possibly related to overpressure conditions following the entrance of large quantities of steam in the conduit; (iii) indirect enrichment in both crystal and lithic fractions by removal of juvenile fines from the eruptive cloud. In each eruption some of the deposits with "phreatomagmatic" component distribution patterns also exhibit evidence of steam condensation (accretionary lapilli, vesiculated tuff, mud coating, soft deformations) and some do not: these are therefore to be considered sufficient but not necessary diagnostic features for a hydromagmatic origin of the deposit ("wet" in the sense of Sheridan and Wohletz, 1983). "Dry" phreatomagmatic products correspond to higher energy conditions allowing production and maintenance of overheated steam.

The magma/water ratio in terms of heat exchange surface is certainly the main factor controlling the efficiency and the energy balance of the interaction. A series of observations suggest that a primarily fragmented magma is a basic requisite for the explosive magma/water interaction: i) occurrence of short phreatomagmatic episodes interrupting lava fountains activity (1906 eruption) in connection with drawdown of the magma column in the conduit, ii) parallel increase in depth of magma fragmentation level and magma/water interaction level (as deduced by the nature of lithics), and iii) preferential occurrence of phreatomagmatic activity at the end of explosive eruptions (when juvenile gas pressure declines and water from the confining aquifer more easily enters the conduit).

BIDIMENSIONAL CELLULLAR MODEL FOR LAVA FLOW SIMULATION

BARCA, D., CRISCI, G.M., DI GREGORIO, S., NICOLETTA, F.P., Universita' della Calabria 87030 Arcavacata (Cs) Italy

We present further developments of our project in order to simulate lava flows by the formal support of Cellular Automata (C.A.), overcaming the "classic" approach of fluid dynamics equations, involving severe problems of tractability by the phenomenon complexity and the morphology representation.

We agree with the epistemological principles of Computational Physics, which permit to simulate complex phenomena by arbitrary algorithms with internally coherent structure.

C.A. are the first model of parallel computation, their specifications involve only discrete quantities; so the time is a sequence of intervals called steps, the space or plane is tesselled in squares, cubes, exagons etc. of uniform size, which are the cells.

A C.A. for lava flow can be seen as a bidimensional space, partitioned in squares, each one corresponding to a piece of surface and embedding an identical elementary automaton, whose states describe the physical characters of that surface piece.

Variations in the cell state at the next step is determined by its state and the states of the neighbouring cells with common sides, according to a state transition function, which simulate the lava physical processes.

The cell state is specified by the following parameters: a) average quote, b) average lava thickness, c) average temperature, d) lava flows toward the four neighbouring cells.

We implemented the model, choicing a simple transition function, whose main mechanisms concern computing the possible "lava flow down" from the single cells toward the neighbouring cells and updating the single cell "temperature". Such a transition function is based on physical laws, which are applied contemporary to all the cells individually.

Our model is very flexible and can be used for the simulations of different types of lava, the morphology is updated considering the lava solidification, so that multiple lava flows can be managed.

We tared our model considering real different lava flows and obtained for the most cases a good fitting between real morphology and results of simulated lava flows.
A simulation example of Pantelleria's (Sicily) lava flow is showed in the following figures.

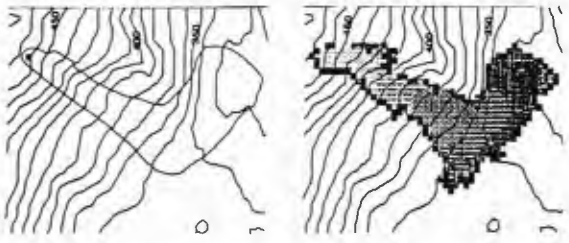

In the left one is represented the preeruptive digitalized morphology with real lava flow shape; in the right one is given the simulation of lava flow at the last stage according to the temperature variation (darker tonality corresponds to higher cooling).

KOS ISLAND (GREECE): RECENT EXPLOSIVE VOLCANISM, HYDROTHERMAL PARAGENESES AND GEOTHERMAL AREA OF VOLCANIA.

BARDINTZEFF, J.M.*, DALABAKIS, P., TRAINEAU, H.*** and BROUSSE, R.*.**

Kos Island (Dodecanese, Greece) is covered by several pyroclastic deposits. During the youthful < 2.7 Ma. old episode two major explosive events are recorded. First, a 0.55 Ma. old pumice tuff-ring is associated to the Kefalos caldera. A second generation is made up of the 0.25-0.12 Ma. old non-welded ignimbrites of Kos.

These deposits contain abundant xenoliths torn out from the sedimentary and metamorphic rocks of the basement, and from co-magmatic granite intrusions. (1) The granite xenoliths had gone through a hydrothermal stage which produced a diopside-titanite-biotite paragenesis (PH2O = 0.9-1.2 kb; T = 650-680°C). (2) The metamorphic and sedimentary xenoliths exhibit secondary mineralisations: (a) muscovite + adularia + chlorite + talc (PH2O < 0.6 kb, T< 500 °C), (b) actinolite + epidote + biotite, (c) pyrite + bornite + haematite (T> 300 °C).

Important heat retention at shallow levels in the island bedrock is provoked by long time-duration granite crystallization processes until recently. Intense fracturing by active seismo-tectonics favours the percolation of marine waters at depths, increasing the geothermal potential. Since the Antiquity, numerous hot springs have been used for medical purposes, especially by the famous physician Hippocrates.

Volcania area is located 1 km N.E. far from the rim of Kefalos caldera. Inhabitants relate that up to 30 years ago thermal waters sprung out and now remains a strong sulphur smell. This area is a 1 km-wide basin with 14 small circular hydrothermalized zones forming two cross-alignments. These zones, 5-20 m-large, constitute minute 1 m-high reliefs covered by whitish strongly altered products and native sulphur. The 70 m-large main central zone, located at the crossing of the two alignments, contains subaqueous fumarolitic 1 m-thick organic matter-enriched layered deposits.

The water emergence temperatures recorded from 7 wells near the Volcania basin are low (19.3 and 20.5°C) and similar to surface water temperatures. They have a pH value between 5.7 and 7.6 (anal. 1). Another well, located in one alignment 200 m far from the central zone, contains sulfate calcic water (pH = 2.8, 20.3°C; anal. 2) which regularly releases gas. At 60 m far from the well, a spring produces 20.0°C-hot and 7.7 pH water. Near the coastal line, an old Artesian drill produces 23.4°C-hot and 6.5 pH water. At 1 km S.E., gas bubbles escape safely from the bottom of the sea as alignments near the so-called "Paradise bubble beach"!

Water chemical analyses show mild mineralizations. SiO2 contents (65-110 mg.l-1) are comparatively high for waters yielding not so hot temperatures. High Ca and Mg contents as well as Na/Cl ratios (0.65) a little higher than in the sea (0.55) can be attributed to rock-water interactions. Na/K and Na/K/Ca geothermometers applied to these waters yield unrealistically high temperatures ranging from 145 to 250°C. Lower temperatures of 85-140°C obtained by the silica geothermometer seem more likely.

These surface geothermal manifestations could be regarded as a zone of lateral leakage from a hydrothermal convection system, which developed above the cooling ignimbritic chamber.

	Ca++	Mg++	Na+	K+	NH4+	Cl-	SO4--	TAC	NO3-	SiO2
1	189.5	29.9	135.4	11.5	-	215	260	5.75	2	105
2	131.4	16.2	136.2	15.5	2.2	245	435		3	110

HAMBLIN-CLEOPATRA VOLCANO, NEVADA: GENESIS OF A SHOSHONITE-LATITE-TRACHYDACITE-TRACHYTE SUITE

BARKER, D. S., and THOMPSON, K. G., Department of Geological Sciences, The University of Texas at Austin, Austin TX 78713-7909

The Hamblin-Cleopatra volcano (HCV), Lake Mead National Recreational Area, is a 60km^3 stratovolcano built of lava flows (30%), tephra (15%), epiclastic debris (40%), and intrusions (15%). HCV lavas are bracketed by others with K-Ar ages of 14.2 $\pm$ 0.5 and 11.5 $\pm$ 0.5 Ma. Faulting (concurrent with HCV growth) cut the volcano into three segments and tapped reservoirs of diverse magma compositions. HCV comprises two sequences separated by an unconformity. The earlier sequence contains shoshonite and high-K latite through trachydacite to trachyte lavas (as classified by the IUGS system using total alkalis versus silica). The second sequence contains the same lava types, but toward the top the proportion of trachytic tephra increases. Minor mugearite and subalkaline basalt occur in the HCV section. Analyses of 24 lavas of known relative position in the HCV succession show no consistent trends with time; instead, all magma types were available throughout the eruptive history. Within each rock type, there are no discernible differences between lavas of the first and second sequences.

Post-HCV hawaiite, the only nepheline-normative lava, is the most primitive ($mg^{\#}$ = 66, Ni = 244 ppm), and was not comagmatic with the rest of the suite, although hawaiite and subalkaline basalt were both derived from lithospheric mantle enriched in incompatible elements. HCV lavas yield $^{87}Sr/^{86}Sr$ ratios of 0.70455 to 0.70548, and the younger hawaiite, 0.70536. Major and trace element data show that high-K magmas of HCV could be derived from subalkaline basalt by removal of plagioclase, clinopyroxene, and minor olivine and orthopyroxene, without assimilation or magma mixing. However, kaersutite occurs in shoshonite, latite, and trachydacite, as do two kinds of clinopyroxene; the less abundant, present in nearly every sample, is richer in Al and Ti. These phases appear to be xenocrystic, derived from mafic alkalic magma.

THE PRE-ERUPTIVE CHARACTERISTICS OF MAYON VOLCANO, PHILIPPINES

BAUTISTA, M.L.P., Philippine Institute of Volcanology and Seismology, 29 Quezon Ave., Quezon City, Philippines.

This paper aims to establish the pre-eruptive characteristics of Mayon Volcano. Mayon, the most active volcano in the Philippines, had been exhibiting moderate seismic levels since August 1988, slight tilting since March 1988 and occasional presence of crater glow, bluish fumes and moderate emission of white steam, which rarely changes to dirty white or brown in color, from its crater. New steaming grounds are apparent around its vent.

Mayon's more recent eruptions occurred in 1968, 1978 and 1984. Although there was no direct casualty during these eruptions, the risk to people living within its slopes remains high as Mayon is known to extrude lava, pyroclastic and ashfall. There is even the possibility of a sector collapse considering that triggering factors for such phenomenon exists for the volcano.

The results of the analysis of available volcanological data implies that Mayon's eruptions are preceded by manifestations such as increase in seismic level, ground tilting, presence of crater glow, rumbling sounds, increase in volume and change in color of steam being emitted. After some time, the volcano's condition may return to normal or culminate in a major eruption or to just a minor ash puff. Otherwise, the volcano's condition may worsen as seismic unrest continues, occurrence of harmonic tremors intensifies, rockfalls along the slopes become evident and wild animals may be observed behaving abnormally.

Based on these, the present manifestations of Mayon could either:

1. Return to normal
2. Culminate in an ash puff
3. Cease for a few months but will ultimately culminate in a major eruption

THE CHALUPAS IGNIMBRITE

BEATE, B., Instituto Ecuatoriano de Electrificación - Proyecto Geotérmico, P.O. Box 565-A, Quito, Ecuador.

The N-S oriented interandean valley of the northern Ecuadorean Andes was buried along a distance of 200 km by the largest known Pleistocene ignimbrite in the northern Andes. The deposit covers an area of about 3000 square kilometers, and its volume is estimated at 90 cubic kilometers, considering an average thickness of 30 m. The massive and paroxismal ejection of the ignimbrite formed the approximately circular Chalupas collapse caldera, which has an average diameter of 18 km and a depth of 400 m. Thus, the actual collapse volume is 100 cubic kilometers, which agrees with the ejected one.

The Chalupas ignimbrite is a single flow unit showing the typical sequence of an ash flow deposit: a basal plinian white pumice and lithic lapilli deposit; a central massive part consisting mainly of non-welded fine light gray ash with rounded pumice clasts concentrated on top and base; the top of this part is reddish in color and shows gas pipes. The third and upper section is a very fine ash with accretionary lapilli and, in most cases, reworked or absent due to erosion. The pumice fragments total about 10% of the deposit and are highly vesiculated and fibrous, contain few plagioclase, quartz and biotite crystals, as well as magnetite. All these crystals are also present in the bulk part (80-90%) of the deposit. The lithic fragments are similar to rock types found in the vent are prior to the collapse. First geochemical data of the pumice indicate highly differentiated magmas of rhyolitic composition with 72.5% of SiO2.

The absolute age of the Chalupas event is unknown, but its stratigraphic position intercalated in the late Pleistocene "Cangahua Formation" gives a rough limit. Presumably, NE and NW tectonic trends played an important role in the caldera formation and its final shape.

Given its recent age, as well as the volume of the ejected rhyolitic ignimbrite, the Chalupas Caldera seems suitable as an economically exploitable geothermal system. On the other hand, more studies are required to establish its magmatic evolution and periods of recurrence, since the occurrence of an event of similar characteristics would constitute a disaster with unprecedented consequences.

PLIO-QUATERNARY VOLCANOES FROM S.W. COLOMBIA

BECHON, F. and DELALOYE, M., Département de minéralogie, Faculté des Sciences, Rue des Maraîchers 13, 1211 Genève 4, Suisse

Volcanoes from the Central and Occidental Colombian Andes Cordilleras result from the subduction of the Nazca plate under the South-American continental crust. They belong to a calcoalkaline serie, typical of an active continental margin, and have a Plio-Quaternary age. Their effusive formations are associated to important volcano-sedimentary deposits.

Six volcanoes (Puracé, Doña Juana, Galeras, Azufral, Cumbal and Chiles) located in the Cauca and Nariño departments, between 2.37°N and 0.80°N, have been studied. They are situated on active fault zones (principaly the Romeral fault system).

The composition of their lavas range from basaltic andesites, andesites to dacites. The glass (when present) is of rhyolitic or dacitic composition. The petrographic assemblages are: ol - opx - cpx - pl -(Ti)mg - (chr) for basaltic andesite, ol - opx - cpx -pl - (amph) - (Ti)mg - (chr) for andesite, (ol) -(opx) - (cpx) - pl - amph - qtz - bio - K feldspar - (Ti)mg - (chr) for dacite with, often, abundant glass. Particularly in the last group, different minerals (especially olivine and quartz) show reaction rims and reverse zonings can be seen in particular plagioclases and orthopyroxenes. These features suggest magma mixing which importance changes between the volcanoes. Various stages of this magma mixing can be deduced according to the more or less complete homogeneization of the rocks.

CUMULUS AND POST-CUMULUS PROCESSES IN MONTEREGIAN AND WHITE MOUNTAIN COMPLEXES

Bédard, J.H., Geological Survey of Canada, 588 Booth St., Ott., Ont., Canada, K1A0E4.

Monteregian and White Mountain intrusions display a wide range of structures and textures that provide information about cumulus and post-cumulus processes. Granite and quartz syenite of crustal derivation dominate White Mountain complexes. Heat for anatexis was provided by crystallization of Coombs-trend, hynormative alkali basalts, which differentiate to hawaiite by fractionating Ol + Cpx + Plag. Hawaiites differentiate to residual cpx-quartz-syenite and riebeckite granite by fractionating Hornblende + Plag + Oxides + Apatite $\pm$ Cpx $\pm$ Ol. Contamination leads to Opx saturation.

Widespread Camptonites and monchiquites are potential parental magmas for Monteregian intrusions. Both lamprophyre types have different incompatible element ratios and cannot be related by fractionation, but contain similar phenocryst assemblages: Cpx + Amp $\pm$ Ol $\pm$ Oxides. Cpx phenocrysts are oscillatory- and sector-zoned, with increasing Fe, Ti, Aliv, and decreasing Mg & Alvi outward. Green Cpx cores rich in Fe, Na & Alvi are common. Kaersutite phenocrysts may contain Ti-pargasite cores. The zoning of Cpx and Amp phenocrysts implies polybaric crystallization. Ultramafic and mafic cumulates may contain Cpxs like those of the dykes, implying mechanical sorting and accumulation of phenocrysts entrained from depth. Plag joined the fractionation assemblage in the shallow chambers. Fractionation of gabbroic cumulates and minor crustal contamination yield varied residual magmas: peralkaline tinguaite, feldspathoidal syenite, and rare quartz-bearing syenites.

Cumulates in the White Mountains and Monteregians occur as: 1) massive adcumulus textured rocks, 2) breccia and dyke complexes, 3) cm-scale rhythmic layers defined by alternating concentrations of mafic and felsic minerals, 4) 10cm to m-scale layering defined by variations of phenocryst mode and grain size. The layered rocks are typically vertically-dipping. Cm-scale layers occur near contacts and are interpreted as in-situ growth phenomenon caused by transient thermo-chemical instabilities. Imbrication structures and mineral zonations imply that the cm to m-scale layers formed by mechanical accretion of phenocrysts with pre-cumulus histories onto vertical magma chamber walls from convecting magmas. The larger complexes cooled slowly and early textures are absent. Cumulus Cpx typically lacks inherited zoning, but is commonly stuffed with Ti-oxide lamellae. The temperature dependence of Ti-solubility in Cpx suggest that Ti-oxide lamellae exsolve during thermal re-equilibration. Amp and Biot typically occur as replacements of earlier phases, but chemical data (e.g. high Ba) imply that they are "cumulus" phases formed by reactions with residual melts. The reactions require addition of K, Fe, Na and loss of Mg and Ca. Evidence from layered intrusions (Rhum, Muskox) also implies large-scale igneous metasomatic transformation of cumulates during post-cumulus compaction-recrystallization. Flow of nutrients to reaction sites was partly through percolation flow, partly through channelized flow. Experimental simulations (Kerr & Bedard in prep.) suggest that channels develop in sloping or vertical cumulate mushes.

POSTGLACIAL ERUPTION HISTORY OF MT. ST. AUGUSTINE, SOUTHERN COOK INLET, ALASKA

BEGET, J. E., Dept. of Geology and Geophysics, University of Alaska, Fairbanks, Alaska 99775-0760

Mt. St. Augustine has erupted frequently in the 200 years since its discovery, and an eruption in 1883 produced a large debris avalanche and a tsunami (Kienle and others, 1987). Stratigraphic studies and radiocarbon dating of prehistoric volcanic deposits on Augustine Island suggest that eruptions of tephra and pyroclastic flows, and the generation of debris avalanches large enough to reach the sea and form tsunamis have occurred repeatedly during the last two thousand years.

The oldest volcanic deposits, first recognized by D. Johnston (1978), consist of hyaloclastites and pumice sands that may reflect sub-glacial eruptions. Newly discovered sites expose hyaloclastites, pyroclastic flows, and tephra intercalated with Pleistocene till, and record construction of the proto-Augustine cone in late Pleistocene time.

Mt. St. Augustine may have been dormant for extended periods during the early and middle Holocene. Extensive wave-eroded cliffs are largely buried by late Holocene deposits and fans.

During the last two millenia Mt. St. Augustine has been very active, with an early cycle of eruptions lasting from 2000-1000 yr B.P., while the current cycle began approximately 500 years ago. One large debris avalanche occurred more than 1830±80 years ago, and constitutes the oldest Holocene event which can be dated on the island. At least six thick pumiceous tephra layers record plinian eruptions between 1830±80 and 330±145 yr B.P. These tephra layers can be used to subdivide and date other deposits on the island. At least seven debris avalanches occurred since 1830 yr B.P. suggesting that tsunamagenic events have an average recurrence interval of approximately 250-300 years. Dramatic erosion of debris avalanche hummocks indicates recent (1883?) tsunami waves were approximately 10-15 m high.

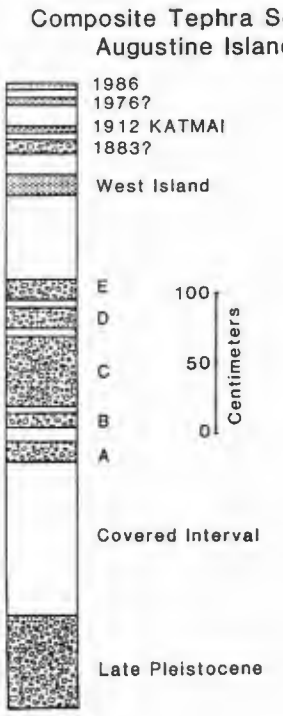

GLASS, PHLOGOPITE, AND APATITE IN SPINEL PERIDOTITE XENOLITHS FROM SARDINIA (ITALY):EVIDENCE FOR MANTLE METASOMATISM.

BELKIN, Harvey E., 959 National Center, U.S. Geological Survey, Reston, VA 22092 and,
DE VIVO, Benedetto, Dipartimento di Geofisica e Vulcanologia, Largo S. Marcellino 10, 80138 Napoli, Italy

Spinel peridotite xenoliths hosted by Pliocene to Quaternary alkaline to subalkaline volcanic rocks have been studied from the Lugodoro and the Dorgali areas in west and east central Sardinia, respectively. The occurrence of glass, phlogopite, apatite, and CO_2 fluid inclusions are evidence that metasomatic processes operated in the lower crust/upper mantle region of the Sardinian/Corsican microcontinent prior to xenolith entrainment and ascent in the host magmas.

The studied xenoliths are spinel lherzolites, spinel harzburgites and augite megacrysts. The harzburgites and lherzolites are characterized by a protogranular texture, a large and variable grain size (1 mm to 1 cm), and a typical four-phase assemblage: olivine (70 to 80 vol.%, Fo~90, unzoned), orthopyroxene (15 to 20 vol.%, En~90, unzoned), clinopyroxene (4 to 10 vol.%, emerald green color, Wo 45-50 En 46-50 Fs 3.5-5, zoned with rims higher in Mg and Ca and lower in Al and Na) and chromian spinel (1 to 2 vol.%, Cr/(Cr+Al) = 0.14-0.46). Olivine and orthopyroxene contain kink bands. The application of various geothermometers based on mineral composition give values that indicate that the four-phase assemblage last equilibrated in the range of 920 to 1050°C. The augite megacrysts are more Fe-rich and have lower Cr/Al ratios than clinopyroxenes in the peridotites, and are interpreted to have crystallized from mafic magmas at upper mantle conditions.

Phlogopite and apatite have been found in one lherzolite (A422). The phlogopite occurs as clusters of anhedral crystals, 200 to 800μm in size, and is relatively uniform in composition: Mg/(Mg+FeT) ~ 0.88; TiO_2 = 4.4 ; BaO = 0.35; Cr_2O_3 = 0.44; F = 0.35; Cl = 0.12 (wt.%, microprobe). The apatites are small (100μm) anhedral crystals that occur at triple junctions in textural equilibrium with the silicate assemblage and appear to have formed before or during the last silicate equilibration. The apatites contain F = 1.3, Cl = 1.7, SrO = 1.3, REE ≥ 1.0, SO_3 = 0.2, and MgO = 1.0 (wt%, microprobe) and trails of secondary CO_2 fluid inclusions.

Glasses occur as thin, irregular veins between phases or associated with CO_2 fluid inclusions along healed fractures in both peridotites and megacrysts. Some glasses in the megacrysts contain a distinctive rapid quench texture of skeletal clinopyroxenes. Microprobe analyses (>100) show two different populations. The augite megacrysts contain a relatively low silica, high iron glass, whereas the spinel peridotites contain a higher silica, lower iron glass. The glass compositions are:[avg.wt%(1σ)]

Spinel peridotites; SiO_2 = 57.81 (4.50), TiO_2 = 0.35 (0.29), Al_2O_3 = 25.66 (3.45), FeOT = 0.74 (0.55), MnO = nd, MgO = 0.30 (0.49), CaO = 6.93 (3.62), Na_2O = 5.30 (1.07), K_2O = 2.57 (3.05), P_2O_5 = 0.14 (0.17).

Augite megacrysts; SiO_2 = 48.19 (2.03), TiO_2 = 1.93 (0.39), Al_2O_3 = 19.88 (0.93), FeOT = 11.24 (2.87), MnO = 0.22 (0.07), MgO = 2.12 (0.94), CaO = 6.28 (2.11), Na_2O = 4.66 (1.69), K_2O = 3.14 (1.28), P_2O_5 = 0.87 (0.22).

The highest value of K_2O (13.06 wt%) measured in a glass was not from the phlogopite-bearing xenolith.

The xenoliths are hosted in alkali basalt, basanite, hawaiite, and trachybasalt. The glass in the augite megacrysts can be attributed to remnants of its host magma. However, the glasses in the spinel peridotites are unrelated to the host magma. There is also no compositional or textural evidence that these glasses were generated by simple decompressional melting of phases now observed in the xenoliths. We suggest that mantle metasomatism, operating in the spinel peridotite stability field, introduced CO_2-rich silicate fluids. Furthermore, multiple metasomatic stages are indicated by the textural relationships among the modal phases, glass, and CO_2 fluid inclusions.

THERMO-MECHANICAL CONSTRAINTS ON MELT GENERATION AND ASCENT: THE ROLE OF DEEP CRUSTAL CHEMICAL HETEROGENEITY AND THE PHYSICS OF PARTIAL MELTING

BERGANTZ, G.W., Department of Geological Sciences, AJ-20, University of Washington, Seattle, WA 98195

One of the outstanding questions in the physical and chemical characterization of continental magmatism is the degree and manner in which chemical heterogeneity in continental lithosphere influences both the physical and chemical character of magmatism. It is clear that magmatic systems display open system behavior, however the physical constraints on the time and length scales over which chemical signatures are generated and sustained in igneous rocks remains to be elucidated. These issues take on particular importance in light of a growing body of isotopic and structural work on plutonic rocks that suggests that the crustal locus for magmatism (a magma chamber) is perhaps best conceptualized as a *crustal scale* region of repeated intrusion, and penetrative mixing. It is not difficult to appreciate that the compositional and thermal state and tectonic regime of continental lithosphere acts as a "filter", determining the size and timing of magma parcels that can successfully ascend, even if not far, to ultimately yield a magmatic complex.

The task then is to identify the thermo-mechanical constraints on such a process, particularly as revealed by the structural and isotopic histories of deep seated plutonic suites. I submit that there are two first order influences on these histories: the length scales (directional) of chemical heterogeneity of deep crust, particularly the hydrous phases, and the inherent length scales associated with the physics of the fusion event. To this end, I have completed analytical and numerical studies of partial melting which explicitly includes the presence and influence of a region of crystals and liquid, i.e. a mush and a liquid region. No a priori assumptions are made about convective state, simple parameterizations and estimates of cooling time that result from invoking a Rayleigh number are inappropriate for geological systems where the enthalpy change and physical properties are dominated by the presence of crystals and liquid.

The results from my study predicts the conditions for the onset of melting, the disposition of the melt and mush regions, in both the lower crust and upper mantle, relative to one another at early times during generation and ascent, critical Rayleigh numbers, styles of convection and the concomitant mixing (or lack thereof) in the mush and melt pile, and the large scale thermal regime. For a variety of physical conditions thought to exist in the lower and mid-crust, the under-plating of mafic material can lead to large regions of crystal mush which facilitates crystal-liquid fractionation and mixing. These processes do not require turbulent mixing or rapid cooling

Of particular interest here is the ongoing fusion process in regions where the deep crust is chemically heterogeneous. Local variations in composition can lead to focussing of heat and mass flux by virtue of the strong compositional dependence of solid fraction, and hence rheological state, during fusion and the large thermal melting interval for hydrous mafic phases. Preliminary results from the modelling suggest that *much of the petrologic diversity ultimately manifested in continental magmatism is generated in the deep crust where elevated geotherms and a concomitant reduction in rheological contrast serve to optimize dynamic processes.*

GIANT MAFIC DYKE SWARMS OF THE EAST EUROPEAN CRATON

BERKOVSKY, A.N., PLATUNOVA, A.P. Institute of Precambrian Geology & Geochronology, the USSR Academy of Sciences, 199034, nab.Makarova 2, Leningrad, USSR.

Major mafic dyke swarms of the East European craton are dominated by those showing broadly N-S trends. They include the Hyperite, Blekinge-Dalarna, Karelian, Kola-Onegan and Timan-Donian swarms ranging in age from Late Proterozoic to Devonian (Fig.1). The Hyperite and Blakinge-Dalarna swarms are co-linear, rather narrow dyke sets extended for some hundreds km. The Karelian swarm (700x300 km) is confined to the Karelian Province and is defined by NW- and N-trending gabbro-diabase dykes some 10-20 km long associated with extensive coeval sills and volcanics. The Kola-Onegan swarm composed of gabbroid dykes (30-50 km long) and associated volcanics has a total width about 500 km and fans southwards from the Barentz sea with the eastern branch being traced for 600 km. The Timan-Donian swarm has a persistent NS-trend and is defined by diabase dykes up to 40-50 km long and associated Devonian volcanics revealed by geological and aeromagnetic data within the Timan fold area where the swarm is about 250 km wide and 700--800 km long. Devonian volcanics and NS-dykes are also found in the south of the platform (middle course of Don river) suggesting the continuation of the Timan dykes to form a single swarm. Upper Devonian rocks are at 1-2 km depth within the platform, so probable dykes cannont be detected by aeromagnetic surveys; although the late Devonian volcanics and diabases are known from numerous boreholes. This suggests the existence of a vast magmatic province in late Devonian times to cover an area of 300-500x2500 km to include a giant transcontinental mafic dyke swarm.

The study of the giant swarms may greatly contribute to understanding of mechanism magma propagation, to global correlations and palaeoreconstructions.

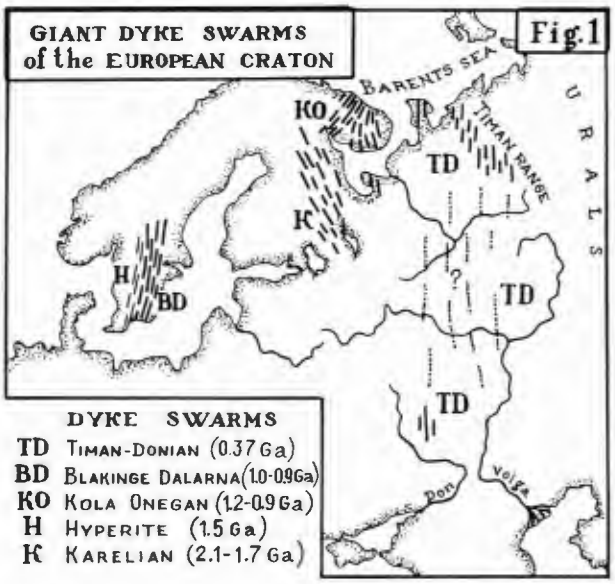

THE 1906 ERUPTION OF VESUVIUS: FROM MAGMATIC TO PHREATOMAGMATIC ACTIVITY THROUGH THE FLASHING OF THE SHALLOW DEPTH HYDROTHERMAL SYSTEM

BERTAGNINI, A., LANDI, P., SANTACROCE, R. (1), SBRANA, A., Dipartimento di Scienze della Terra, University of Pisa, Italy, and (1) Istituto Internazionale di Vulcanologia, CNR, Catania, Italy.

The April 1906 eruption of Vesuvius is the type-example of the "final eruptions" that close the short cycles of semi-persistent activity having characterized the volcano in the 1637-1694 period. The eruption had a marked explosive character that accompanied the emission of lava from several vents on the southern slopes of the volcano. The observed sequence of events was characterized by repeated fluctuations of the magma level within the conduit, by large lava fountains, by conduit partial collapses and by the final explosive decapitation of the summit cone. Contemporary chronicles, although frequently contradictory, allow to depict a rather reliable picture of the eruption which can be divided into four main phases: 1. Lateral lava effusions; 2. Lava fountains; 3. Sustained gas column; 4. Low dense clouds. Pyroclastic deposits of the Monte Somma ridge and northeastern slope can be related to observed and described events and refer to the 2nd and 3rd phases. The increase of the degree of fragmentation of the juvenile component together with the marked increase of the lithic component emphasize the repeated occurrence of magma-water interaction, whose most spectacular example was the 3rd phase of the eruption in which, after the decapitation of the cone, a high gas eruption column was formed. The solid material ejected during this phase was relatively scarce if compared with the height (up to 13 Km) and the duration (about 30 hours) of the sustained column. Rough calculations lead to an estimation of the amount of steam involved at several tens of millions tons. This fact together with the high lithic/juvenile ratio (about 1:1) makes it unlikely that the largest part of the energy in play be related to the contact between magma and cold phreatic water. As also suggested by the nature of the lithic fragments (mainly hydrothermalized and metasomatic rocks), we conclude that most of the steam involved in this phase of the eruption come from the flashing of the hydrothermal system connected to the very shallow feeding system of the volcano and left open by the lowering of the magmatic column.

EARLY PRECAMBRIAN METABASIC DYKES OF THE OLEKMA AREA, ALDAN SHIELD

Beryozkin V.I., Institute of Geology, Yakut Branch, Siberian department, USSR Academy of Sciences, Yakutsk, 677891, USSR

The basement complex of the Aldan shield is composed of Early Archean rocks of amphibolite and granulite facies with migmatites and granites. Small outcrops are composed of Late Archean and Early Proterozoic rocks of greenschist and amphibolite facies without migmatites. Sills, dykes and intrusives can be discerned in the basement.

Late Archean and Early Proterozoic dykes and sills have been studied in the Olekma River basin. There are three dyke suites there: Sarylyr, Tasmiele, Kuranakh.

The Late Archean Sarylyr dykes reach 50 m in thickness and 100 m in length. The dykes are composed of amphibolites, sometimes blastoophitic. The amphibolites represent subalkalic rocks with wide FeO /MgO variations characteristic of tholeiitic trend. In comparison with other dykes suites, these dykes are poorer in Al_2O_3, richer in Cr, Co, V, and show least fractionated REE patterns (Ce^N/Yb^N = 1.2 - 2.0, sometimes up tp 3.0).

The Tasmiele dykes, also Late Archean, but somewhat younger and smaller than the Sarylyr ones are composed of actinolite and hornblende amphibolites of basic and more rarely intermediate composition. Plagioclase blades characteristic of diabases have been preserved in them. The rocks are also subalkalic, but have higher SiO_2, Al_2O_3, lower FeO*, TiO_2, MnO and REE patterns (Ce^N/Yb^N = 2.8 - 4.0) different from the Sarylyr ones.

The Lower Proterozoic Kuranakh sills and dykes up to 200 m in thickness are also made up of actinolite and hornblende amphibolites, the rocks, however, show more frequent relicts of ophitic texture and rare magmatic clinopyroxene. The amphibolites are chemically similar to the Sarylyr ones differing from the later by highly variable Al_2O_3, higher P_2O_5 and alkalies, lower MnO, different REE patterns (Ce^N/Yb^N = 2.8 - 3.5).

Compositional diversity of rocks in each dyke suites is mainly due to differentiation of primary mantle melts.

EOCENE THROUGH MIOCENE VOLCANISM IN THE GREAT BASIN OF THE WESTERN UNITED STATES

BEST, Myron G. and CHRISTIANSEN, Eric H., Brigham Young University, Provo, UT. 84602, DEINO, Alan L., Berkeley Geochronology Center, Berkeley, CA. 94709, GROMME, C. Sherman and MCKEE, Edwin H., U.S. Geological Survey, Menlo Park, CA. 94025, and NOBLE, Donald C., University of Nevada, Reno, NV. 89557

The area that is now the Great Basin of Nevada and western Utah experienced profound volcanic activity in the middle Tertiary while oceanic lithosphere was being subducted in a northeasterly direction off the continental margin. Cenozoic volcanism first began in the northern part of the province in the middle Eocene about 43 Ma, after earlier activity to the north, and subsequently swept southward, decelerating and finally stagnating in the southern Great Basin after about 35-30 Ma. In the western Great Basin, west of the edge of the Precambrian basement, east-west isochrons marking the sweep bend northward, indicating a west to southwest migration of activity. From the Eocene through the Miocene (43-6 Ma), more than 50,000 km^3 of ash-flow tuff--represented in well over 100 cooling units--was deposited around and within 70 recognized or inferred source calderas in the Great Basin. Some units cover several tens of thousands of square kilometers and have volumes of thousands of cubic kilometers. Roughly three-fourths of these ash flows were erupted in the late Oligocene-early Miocene (31 to 20 Ma) in the central and southern Great Basin where the southward transgression of volcanism was slowest. Based on preserved deposits, the rate of lava extrusion remained approximately constant before and during this peak ash-flow activity and the volume of lava is less than a fifth of the total volume of volcanic deposits. In contrast, in the Marysvale, Utah, and San Juan, Colorado, volcanic fields east of the Great Basin and bordering the Colorado Plateaus nearly contemporaneous (about 35-20 Ma) activity produced large coalesced composite volcanoes chiefly before pyroclastic activity and proportions of tuff to lava and debris flow deposits are reversed to that in the Great Basin. After roughly 17 Ma, volcanic activity in the Great Basin was concentrated along the northern, western, and southern margins and produced mostly lava and debris flows.

Great Basin volcanic rocks are potassic like continental-margin volcanic-arc rocks worldwide; although still potassic, they became more sodic during the Miocene as subduction along the continental margin was replaced by transform plate motion. Rhyolite tuff is the most common Cenozoic volcanic rock in the Great Basin. However, at least 12,000 km^3 of crystal-rich dacite ash flows was extruded chiefly from only five sources about 31 to 27 Ma; these deposits belong to what we call the "Monotony compositional type." This earlier eruptive episode was succeeded from about 27 to 23 Ma by more numerous but smaller eruptions of calc-alkaline plagioclase-pyroxene trachyte and trachydacite ash flows (IUGS classification); resulting deposits belong to the "Isom compositional type." Oligocene lavas, like their pyroclastic counterparts, are calc-alkaline but include mostly andesite and dacite and minor rhyolite. Miocene lavas tend to have higher sodium concentrations and include more rhyolite and basaltic compositions, but the spectrum of compositions is more continuous than bimodal. Some Miocene rhyolite lavas in the eastern Great Basin are topaz-bearing and some ash-flow tuffs are peralkaline and associated with calderas near the southern and northern margins of the province.

ALLUVIAL ARCHITECTURE AND ERUPTION EPISODICITY OF THE MIOCENE KISINGIRI VOLCANO, KAVIRONDO RIFT, KENYA

BESTLAND, E.A., Dept. of Geological Sciences, Univ. of Oregon, Eugene, OR 97403

Paleosols and volcaniclastic deposits exposed in the dissected flanks of the Miocene Kisingiri volcano reveal a detailed history of eruption episodicity and volcanic tectonism. The Kisingiri volcano was a large and long-lived (24 to 16 My) carbonatite-nephelinite volcano. The denuded remains of the central vent volcano now sit in a down dropped graben of the Kavirondo Rift and make up the Gwasi Hills and Rusinga and Mfangano islands in Lake Victoria, western Kenya.

Rusinga Island, an uplifted segment of the rifted block, contains badland exposures of the volcanoes alluvial apron facies. Fossil excavations in these alluvial deposits have uncovered an abundant fossil record including Hominoid fossils of Louis Leakey fame. The fossils owe their preservation to the extreme alkalinity of the carbonatite-nephelinite deposits and to rapid, volcanically induced burial.

The four formations on Rusinga island (total thickness of 250 m) record four major doming events of the Kisingiri volcano. Each formation contains a basal section of coarse-grained Precambrian detritus. These granitic and gneissic conglomerates are interpreted to originate from volcanic doming of the basement complex in the central vent area. Subsequent carbonatite-nephelinite volcanism supplied large quantities of lapilli and ash-sized detritus to the aggrading alluvial aprons. During volcanic hiatus, calcareous soils developed on the alkaline deposits.

Fining-upward sequences of grits and sands followed by overbank silts and sands, pyroclastic airfall beds, and paleosols are common in two of the three alluvial formations and are between 10 and 30 m thick. The grits and sands contain nephelinite rock fragments and ash and were deposited by migrating braided channels and by hyperconcentrated floods. Up-section from the lower "nephelinite rock fragment facies" are carbonatite-nephelinite arifall beds, moderate to well developed paleosols, and alluvial sands and silts, all of the "pyroclastic and pedogenic facies." The lower, nephelinite rock fragment facies is interpreted as alluvial aggradation in response to intense volcanism and the upper pyroclastic and pedogenic facies is interpreted as pyroclastic aggradation and pedogenic alteration during relative volcanic hiatus.

Time estimates of Rusinga paleosol development are made by comparison with modern calcareous soils forming on carbonatite-nelphelinte ash on the Serengeti Plain of northern Tanzania. K-Ar age estimates in the Rusinga formations provide a calibration of paleosol estimates. The duration of a typical fining-upward sequence is approximately 50,000 to 100,000 years using paleosol duration estimates. Basement doming events occurred every one to two million years.

PB ISOTOPIC EVIDENCE FOR SUBOCEANIC VERSUS SUBCONTINENTAL MANTLE SOURCES FOR LATE CENOZOIC VOLCANIC ROCKS, STIKINE VOLCANIC BELT, BRITISH COLUMBIA AND YUKON TERRITORY, CANADA

BEVIER, Mary Lou, Geological Survey of Canada, 601 Booth Street, Ottawa, Ontario, Canada K1A 0E8

Pb isotopic signatures for Late Cenozoic alkali basalts, basanites, nephelinites, and peralkaline differentiates from the Stikine volcanic belt help constrain the nature and composition of the mantle in the magmatic source region beneath the northern Canadian Cordillera. Many of these volcanic rocks erupted through crustal terranes (Stikinia, Cache Creek, Yukon-Tanana, Cassiar, and Slide Mountain) that accreted to the North American craton during Phanerozoic time. Alkali basalt flows near Watson Lake, Yukon, are of particular interest because they erupted at or close to the inferred edge of the North American craton, and their isotopic values may reflect the presence of old, enriched subcontinental mantle.

Stikine volcanic belt is approximately 550 km long and contains >100 eruptive centers. The volcanoes are localized within the North American plate along a zone of extension at an acute angle to the right-lateral Queen Charlotte transform fault boundary between the Pacific and North American plates. Two types of centers dominate: large volume shield volcanoes or differentiated volcanic piles, and small isolated volcanoes or cinder cones. The larger centers (e.g. Mt. Edziza) were active for millions of years (Miocene to Holocene) and the eruptive products range in composition from alkali basalts to peralkaline differentiates. Smaller volcanic centers (e.g., Volcano Mountain, Aiyansh) are isolated cones, mostly Quaternary, with one or more associated flows or ice-contact features; the rock types are alkali basalt, basanite, and nephelinite, and ultramafic xenoliths are common.

Pb isotopic results indicate that a suboceanic mantle source is present beneath Stikine volcanic centers that erupted through Phanerozoic accreted terranes. This mantle source is characterized by $^{206}Pb/^{204}Pb$=18.68-19.29, $^{207}Pb/^{204}Pb$=15.52-15.66, and $^{208}Pb/^{204}Pb$= 38.09-38.78 ($^{87}Sr/^{86}Sr$=.7028; Souther et al., 1984), and is like that for northeast Pacific seamounts, i.e. more radiogenic than the northeast Pacific MORB source. Based on a comparison with Anahim and Chilcotin basalts from southern British Columbia, this mantle source is likely continuous throughout the Canadian Cordillera. Data for Watson Lake basalts, erupted through Cassiar and Slide Mountain terranes, indicate a more radiogenic source component with high time-integrated Th/U ($^{208}Pb/^{204}Pb$ up to 39.38 for $^{206}Pb/^{204}Pb$= 19.48). Further isotopic and petrogenetic data are needed to distinguish between derivation of Watson Lake basalts from a subcontinental mantle source versus contamination of a depleted mantle melt by an old, radiogenic crustal component.

MAFIC DIKES AND DIKE SWARMS AROUND PROTEROZOIC CUDDAPAH BASIN, SOUTH INDIA: THEIR MODE OF EMPLACEMENT AND GEODYNAMIC SIGNIFICANCE

S. BHATTACHARJI, Department of Geology, Brooklyn College and Graduate Center, City University of New York, New York, U.S.A.
J.M. RAO, National Geophysical Research Institute, Hyderabad, India

Extensive mafic dikes and dike swarms are concentrated around the mid-Proterozoic, crescent-shaped Cuddapah Basin. Studies of several hundred of these dikes of various trends and frequencies show periodic crustal dilation of the Precambrian shield around the basin between Ca 2400 and 650 Ma. $Ar^{39/40}$ and K-Ar age dates and petrological studies show that early crustal dilation occurred between Ca 2400 and 2200 Ma mainly N-S and E-W with tholeiitic mafic dike formation. This was followed by episodic crustal dilation radially around the convex margin of the basin with alkaline and tholeiitic dike activitite between Ca 1800 and 650 Ma. The youngest dikes, mainly granophyres, were emplaced Ca 700-650 Ma. Ca 1600-1100 Ma, several intense episodes of mafic dike activity occurred, with peak activity Ca 1300-1100 Ma; these are characterized by basaltic komatiite, kimberlite and lamproiite dikes of deep mantle origin. The tholeiite and alkaline dikes show differentiation trends in iron, magnesium, alkalies and silica. Immobile trace and other major element data show continental type magma for exterior dikes and interior sills and flows, and suggest a common source for them. K, Rb, and Ba contents of these mafic suites show minimal crustal contamination and magma mixing. Tectonic analyses of the mafic dikes and dike swarms show that the locus of the radiating dikes is within the basin. It coincides with the center of a large positive gravity anomaly (+60 mgals) covering an area of ~80x50 km. This high-density mass is interpreted as a lopolithic magma cupola of peridotite-picritic gabbro, emplaced at a depth of 4-7 km in the crust. This is the immediate source for the radiating mafic dikes and dike swarms, sills and flows where magma was tapped periodically with mantle thermal pulses. Simulation experiments and analytic stress models of fracture propagation show that episodic radial dikes and dike swarms and semi-concentric sills and flows can originate from an upper crustal lopolithic magma chamber with periodic thermal stress release and crustal dilation. This is most probable when such a body evolves over a rising asthenospheric diapir. The lherzolite nodules in dolerite-picrite sills give a depth estimate of an origin at ~140 km. From a depth of ~70 km, the nodules were transported by a picrite magma which developed into a magma cupola at a shallower depth before being emplaced as sills. The rise of asthenospheric diapirs, crustal magma cupola development and periodic thermal dilation resulting in dike swarm activities, periodic thermal cooling and basin evolution on the south Indian shield are shown to be interrelated. They are connected with the evolution of the eastern Ghat mobile belt, E-W compression, continental collision and underplating.

COMPOSITION AND PROVENANCE OF MARINE TEPHRA FROM THE VØRING PLATEAU AND THE QUESTION OF MAGMATIC EPISODICITY IN THE NORTH ATLANTIC

P. R. BITSCHENE and H.-U. SCHMINCKE (Institut für Mineralogie, RUB, 4630 BOCHUM, FRG)

The opening of the Norwegian-Greenland sea and emerging Iceland are recorded by submarine tephra layers resulting from major explosive eruptions. Oligocene to Recent ash layers from the North Atlantic (north of 63° N) were recovered during DSDP-Leg 38 and especially ODP-Leg 104 (Vøring Plateau). Five glass compositions, accompanied by distinct mineral assemblages, are revealed by microprobe analysis of fresh glasses. Based on their major element compositions, and confirmed by trace element compositions, the ash layers can be divided into a) tholeiitic MPT-basalts (medium P- and Ti-concentrations), b) tholeiitic HPT-basalts (high P- and Ti-concentrations, c) high-K rhyodacites (stratigraphically younger), d) low-K rhyolites, and e) high-K rhyolites. Basaltic ash layers may contain shards with rhyolitic and also intermediate compositions. Plinian to Ultra-Plinian eruptions are inferred as the most likely mechanism for ash distribution. A co-ignimbrite origin of some rhyolitic ashes, however, cannot be ruled out.

Sources for the basaltic and rhyolitic ashes are volcanoes on Iceland where both MPT- and HPT-basalts and rhyolitic volcanic centers occur. The Oligocene and Late Miocene to Pliocene high K-rhyolites, however, are probably not derived from Icelandic sources, because no Oligocene to Pliocene high-K rhyolitic rocks are yet known from Iceland. High-K rhyolitic provinces on and off the Greenlandic continental margin and from Jan Mayen island are the most likely sources. A compilation of available chemical data from North Atlantic ash layers indicates the overall evolution of explosive volcanism at divergent North Atlantic plate boundaries from LPT-basalts to HPT-basalts and from low-K to high-K rhyolites.

Volcanic episodicity in the North Atlantic has been inferred previously for various Cenozoic epochs. The outstanding good core recovery of ODP-Leg 104 and near complete Oligocene to Recent stratigraphic sequences have revealed average ash layer frequencies of 6 to 10 layers per Ma from the Miocene to Recent. No significant peak in explosive magmatic activity reflecting episodic changes in magma production rates or spreading rate was found. Age resolutions better than 1 Ma, however, are required to test episodicity within certain epochs (e.g. Middle and Late Miocene).

EMBAYED QUARTZ, SILICA DIFFUSIVITY AND PTt PATHS OF RHYOLITES

BLAKE, S., Department of Earth Sciences, The Open University, Walton Hall, Milton Keynes, MK7 6AA, England and HAMILTON, D.L., Department of Geology, University of Manchester, Manchester, M13 9PL, England.

Embayed quartz crystals are often reported from rhyolites. In these instances, the process of dissolution has been interrupted by the magma being quenched on eruption. The positive dP/dT of the quartz in/out boundary on a rhyolite's phase diagram means that several paths of magmatic evolution can yield embayed quartz crystals. These paths include (1) decompression during magma rise either to the surface or to a sufficiently shallow chamber, (2) heating due to the arrival of hotter magma in the chamber, and (3) anatexis of quartz-bearing protolith. Each of these paths last for a particular time scale ranging from minutes for magma eruption to perhaps hundreds of years for anatexis. For a given crystal to have avoided being completely resorbed the duration of disequilibrium conditions must have been less than some critical time dependent on the crystal's initial size and dissolution rate.

We have started to calculate dissolution rates and times in order to test the idea that resorbed quartz crystals are typically formed during the rapid decompression of rhyolite rising from a deep crustal chamber. The calculation of dissolution rate, dX/dt, is complex but the important controls emerge from the basic physical relationship $dX/dt \sim D \Delta C/\Delta x$. D is the diffusivity of silica in rhyolite, ΔC the difference in SiO_2 between contaminated rhyolite and the quartz-saturated melt at the solid/liquid interface. The width of the compositional boundary layer is Δx. The buoyancy of the boundary layer drives compositional convection such that Δx is kept smaller than if solely diffusive transport of silica took place. Thus compositional convection increases the dissolution rate. In order to make the relevant calculations all physical and chemical properties apart from D are known. It has therefore been necessary to measure D experimentally over a range of P, T and water content.

The experimental charge consists of a vertical cylinder of rhyolite sandwiched between quartz rods. Run conditions have covered $750 \leq T \leq 1100°C$, $1 \leq P \leq 2$ Kbar, 2 days $\leq t \leq 3$ months, $^1/_2 \leq H_2O \leq 6$ wt%. In the absence of compositional convection, microprobe traverses across the glass/crystal interfaces show identical compositional profiles in a single run. The analyses give the amount of dissolution and the saturation concentration which together with run duration allow D to be calculated. Our first results showed 10μm dissolution in 55 days at 850°C into rhyolite with ca. 4% water. This gave $D \approx 6 \times 10^{-12}$ cm^2s^{-1}, which when compared with results by Baker (1988, EOS 69, 511) confirms that D increases with water content.

HOMOGENEITY VERSUS HETEROGENEITY IN TEPHRA CRYSTAL POPULATIONS

BOGAARD, P.v.d., SCHMINCKE, H.-U., Institut für Mineralogie, Ruhr-Universität, Postfach 102148, D-4630 Bochum 1, and HALL, C.M., YORK, D., Dept. of Physics, University of Toronto, Toronto, Ontario M5S 1A7

There is now general agreement that crystal disequilibria in magma columns are the rule, caused by magma mixing, convection and related processes. It has also been recognized for some time that eolian fractionation can lead to drastic changes in the crystal/crystal as well as crystal/glass shard ratios in tephra fall deposits. Here we report on two different types of xenocrysts that can dominate the crystal populations of both essential clasts and the matrix ash of tephra layers.

(A) Xenocrystic heavy minerals in Laacher See ash are derived from basanitic and tephritic scoria cones and tuff rings that were intersected by the crater, and fragmented and admixed to Laacher See tephra during the eruption. Ca 50 heavy mineral analyses of matrix ash samples yield xenocryst contents up to > 90 % in near-vent surge and fallout deposits.

(B) Single crystal $^{40}Ar/^{39}Ar$ laser studies are presently revolutionizing the precise dating of tephra layers. One of the significant and largely unexpected results of our study of East Eifel tephras is that in some tephra layers the feldspar population of essential lapilli is dominated by crystals whose apparent ages are many-fold that of the eruption. These are interpreted to be xenocrysts derived from older subvolcanic/plutonic rock bodies, which were not sufficiently heated to reset their argon clock.

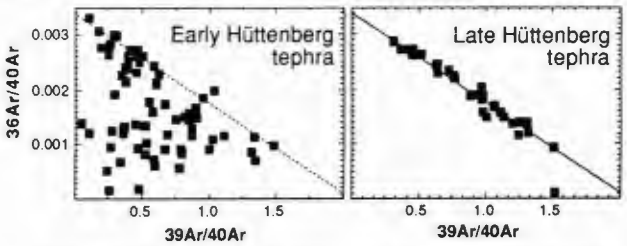

In compositionally zoned tephras, the problem of xenocrystic contamination is most pronounced in the early erupted fall and surge units, because the initial tephras are commonly very crystal-poor due to eruption from nearly phenocryst-free, highly evolved magma cupolas. Foreign crystals incorporated from the magma chamber and conduit walls prior to and during the eruption therefore dominate the mineral assemblages. Later magma batches are usually more crystal-rich, resulting in a strong dilution of the xenocrysts. The Ar isotope correlation diagrams (Fig.) show the composition of anorthoclase feldspar phenocrysts from Hüttenberg tephra; Wehr volcano. Analyses plotting below the 214,000 ± 3,000 a isochron lines (eruption age) yield apparent ages up to ca 5 Ma.

We conclude that petrologic analyses and age studies on bulk crystal separates from Plinian eruptions, especially their earliest crystal-poor magma batches, are highly unreliable.

DIRECTED-BLAST DEPOSITS AT BEZYMIANNY VOLCANO

BOGOYAVLENSKAYA, G.E. and BELOUSOV, A.B., Institute of Volcanology, Petropavlovsk-Kamchatsky,683006,USSR

The directed blast was the main event of the 1956 catastrophic eruption at Bezymianny volcano. Studies conducted during the last few years allowed us to specify the character of deposits related to this event.

1. Debris avalanche deposits formed as a result of destruction of the volcanic edifice, have a typical hummocky surface (the hummocks are 2-18 m high). The deposits form three branches with the total area of 36 km^2, and the volume of 0.5 km^3. They are composed predominantly of old rocks of the volcanic edifice. The maximum way traveled by the avalanche is 22 km. The velocity of their movement at a distance of 10-15 km from the volcano was estimated as 60 m/s.

2. The directed-blast deposits studied along the blast axis at a distance of 10-20 km are represented by loose material: from gravel close to the volcano to sand in the marginal zones. Dense juvenile andesites (40-72%) predominate among debris, porous juvenile andesites are less abundant (13-39%) and the old rock debris constitute 5-33%. Bread-crust bombs have been found.

At a distance of 10-15 km from the volcano three layers have been identified. The lower, widely spread layer contains a large shlieren of soil, shattered volcanic fragments and considerable quantity of organic material; the middle layer is friable massive and poorer in fines; and the upper layer which has the smallest area of distribution, contains predominantly fine fractions; occasionally rough-wavy lamination is observed. The layers vary in thickness from a few cm to one meter. At a distance of 15 km and more the deposits form a uniform layer of fine-grained material with a thickness of 20 cm and less.

Separate small hills (typical hummocks) lying together with the directed-blast deposits are observed on a high-lying ground beyond the zone of distribution of debris avalanche. Displacement and deposition of these hummocks occurred presumedly with the directed-blast deposits.

3. Directed-blast pyroclastic flow deposits. Pyroclastic flow deposits have been identified which differ from the Plinian phase classic pyroclastic flows (Sparks, 1976) by smaller amount of porous juvenile andesites and by greater amounts of finer matrix.

The directed-blast deposits proper represent a complex of facies which have the features of both pyroclastic surges and pyroclastic flows and form from a density current.

Thus, the formation of debris avalanche, directed-blast deposits proper and directed-blast pyroclastic flows is associated with the directed-blast phase at Bezymianny volcano.

REFERENCE

Sparks, R.S.J., 1976. Grain size variations in ignimbrites and implications for the transport of pyroclastic flows, Sedimentology,23, 147-188.

TEMPERATURE MAPPING OF ACTIVE VOLCANIC AREAS USING SATELLITE THERMAL INFRARED DATA.

Alain BONNEVILLE, C.N.R.S. Centre Géologique et Géophysique, U.S.T.L., Pl. Bataillon, 34060 Montpellier cedex FRANCE.

Magmatic activity may result in short term surface temperature anomalies that can be recorded by satellite thermal infrared surveys. Consequently such surveys may provide an unique and cheap tool for volcanic activity monitoring. However things are not so straightforward, and many questions need to be answered before such data can be extensively used:

(I) first, we have to accurately link the measured radiance to the actual soil temperature. In remote sensing and specially with thermal infra-red data, processing is important; in our case the final aim is to obtain surface ground absolute temperature maps. In order to do this, we try to answer in more details the following questions: how could we discriminate between real temperature anomalies and emissivity variations (vegetation effects)? What is the atmospheric contribution to the recorded signal? Due to the extreme altitudes of the studied areas, is it necessary to use a digital terrain model for correcting the large thermal effects which are mainly altitude dependent? What is the importance of the spectral ranges and spatial resolutions of satellite radiometers? The feasability of the method depends on the answers to these questions.

(II) second, we have to relate the surface temperature to the underlying thermal phenomena in connection with the volcanic activity. After a brief review of the existing works, we present the main terms of the heat budget at the ground surface and discuss the role of each of them. We present the conditions on which it is possible to link volcanic events to surface thermal anomalies and a few simple convective and conductive thermal models are discussed.

The results obtained during two surveys in 1981 (after an eruption) and 1983 (before an eruption) over Mt ETNA with the AVHRR radiometer on board NOAA meteorological satellites, illustrate the problems and offer some answers. New results obtained with higher spatial resolution data of Landsat TM satellite are also presented. For this last survey (october 1986), we have tried an original method for correcting atmospheric effects, that it is based on the simultaneous use of several satellites working in different spectral ranges and with various spatial resolutions (Landsat, Meteosat and NOAA 9).

THE NATURE OF THE SILICIC VOLCANISM IN THE SNAKE RIVER PLAIN, IDAHO, U.S.A.

BONNICHSEN, Bill, Idaho Geological Survey, University of Idaho, Moscow, Idaho 83843

The Snake River Plain (SRP) volcanic province extends northeastward for 700 km from near the Idaho-Oregon-Nevada junction, across southern Idaho, to include the Yellowstone Plateau in NW Wyoming. This elongate zone has been the site of extensive basalt-rhyolite volcanism for the past 14 Ma, as the volcanic focus has shifted from SW to NE. At most places in the province the pattern of volcanism has followed the sequence: (1) silicic ignimbrites, (2) rhyolite lava flows, and (3) basalt lava flows, with large-volume, high-temperature, silicic ignimbrite eruptions as the dominant component. This has resulted in a series of calderas buried along the topographically-depressed trend of the SRP province.

The silicic ignimbrites and associated rhyolite lava flows contain plagioclase, pyroxenes, and Fe-Ti oxides as phenocrysts, and many have quartz and sanidine. Biotite and hornblende are rare. Textures suggest that many phenocrysts are unmelted residue from the magma-source region. Pyroxene geothermometry suggests eruption temperatures of 850-1050 degrees C for many units. The rocks are mainly calc-alkaline rhyolites with 68-75 percent silica. High initial Sr isotope ratios suggest large quantities of older crustal material were melted. Periodic influxes of basaltic magmas into the crust probably melted quartz- and Kspar-bearing material to form the rhyolitic magmas that rose and erupted. Where sufficient water was available, ignimbrite-forming eruptions occurred, and where not, rhyolite lava flows resulted.

The SRP silicic ignimbrites are mainly densely-welded sheets that cover hundreds to thousands of sq. km. Many of the sheets show evidence of liquid-state, rheomorphic flowage, whereas others show little or none, and some small units are not even welded. The wide range observed in physical characteristics is largely the result of varying emplacement temperatures, with low-temperature (type L) sheets not being welded and showing only modest amounts of compaction; medium-temperature (type M) sheets being welded and densely compacted but lacking liquid-state flowage features; high-temperature (type H) sheets being thoroughly welded and compacted and having restricted-size, liquid-state flowage features; and the very high-temperature (type V) sheets showing evidence that the entire sheet may have undergone en masse, liquid-state flowage after pyroclastic emplacement. Large, type H, ignimbrite sheets are the dominant type in the SRP province.

Many rhyolite lava flows occur in the SRP province and some are as voluminous as 200 cu. km. These lava flows are subordinate to the ignimbrite sheets in number and size, and tend to fill in the interiors of the calderas. The rhyolite lava flows closely resemble the type H, and especially the type V, ignimbrite sheets. Detailed examination of physical features in these contrasting types of units has shown that they can be distinguished from one another in well-exposed situations, however.

VOLCANOLOGICAL EFFECTS OF SECTOR COLLAPSES AT COMPOSITE VOLCANOES OF THE LESSER ANTILLES ARC

Georges BOUDON, Michel P. SEMET, and Pierre M. VINCENT, Observatoires Volcanologiques, Institut de Physique du Globe de Paris, 75252 Paris Cedex 05, France

Since the May 18, 1980 catastrophic failure of Mount St. Helens (MSH), we have shown that several eruptive events that involve sector collapses of a composite volcano occur on la Grande Découverte volcano (GDV), Guadeloupe. The two most recent ones may be compared to MSH-type (3,100 BP), and Bandaï-san - type (11,500 BP) events, respectively. These last events, that represent failure of the western then the southern flank of the volcano have km-size craters and km^3-size associated debris avalanches. Work in progress in Guadeloupe and on other islands of the Lesser Antilles arc shows that GDV is by no means an isolated case and that sector collapse structures and their deposits are present at a number of volcanic edifices either active or extinct. Most are events of the same kindred as at GDV. However, some collapse structures present on composite volanoes similar to GDV, that is ca. 1,500 m elevation and 15 km in diameter, show much larger sizes (5-10 km). Volumes that are mobilized are on the order of tens of km^3. For example, Vincent et al. (in press, 1989) argue that collapse of the WSW sector of Mount Pelée, Martinique formed an amphitheater crater some 3.5 x 6.5 km within which all activity more recent than ca. 25,000 BP took place. An older example of yet larger size (7.2 x 10.5 km) may be given by the Vieux-Habitants structure in Guadeloupe. For some of the larger structures, superposed large volume debris avalanche point out to an origin by repetitive failure along a single strike and at a time scale much longer than seconds.

Collapse structures are evidently due to the same general physical phenomenon of gravitative failure but we attribute their occurence at varying scales to different triggering mechanisms. (1) Relatively small MSH-type features are caused by mechanical instability resulting from over- or assymetrical loading of the edifice. (2) Sector collapses occuring after a prolonged period of magmatic inactivity but showing evidence of protracted hydrothermal activity (as in the 11,500 BP event of GDV) apparently take place by reduction of friction along argillized slip surfaces. (3) We tentatively attribute the formation of some of the large structures to gradual loading of the edifice by continuous volcanic activity and the steep slopes of the edifices.

The collapse structures we have observed are major volcanological events of the edifices on which they occur; they must involve substantial unloading of crustal reservoirs were they to be active. Type 1 structures are accompanied and/or followed by magmatic activity that rebuilds the edifice. In type 3, entire composite volcanoes generally grow in the upper parts of the structure. Gradual sliding of the loaded edifice may be a prerequisite for magmas to reach the surface.

Given the number of cases of sector collapses we have recorded in the Lesser Antilles, we stress that their probable reccurrence has strong hazard implications.

PB-ISOTOPIC DATA FOR MIOCENE-QUATERNARY BASALTS FROM THE BAIKAL RIFT, U.S.S.R.

BOWRING, S.A., HOUSH, T., LUHR, J.F., and PODOSEK, F.A., Department of Earth and Planetary Sciences, Washington University, St. Louis, MO 63130, RASSKAZOV, S.V., Institute for the Earth's Crust, Irkutsk, U.S.S.R., DUNGAN, M.A., Department of Geological Sciences, Southern Methodist University, Dallas, TX 75275, and LIPMAN, P.W., U.S.G.S., Denver Federal Center, Denver, CO 80225.

The Baikal Rift, in central Siberia, follows a NE-SW trend for over 1200 km along the boundary between the Archean Siberian-Aldan Shield to the northwest and the late-Proterozoic to Paleozoic fold belts to the southeast. Extension within the rift is related to the India-Eurasian collision, beginning about 30 Ma.

We present Pb isotopic data for a suite of basaltic samples from the southwest end of the Baikal Rift. These are the first reported isotopic data for volcanic rocks from one of the greatest continental rift zones on Earth. This study marks the initial phase of a major collaborative investigation to compare and contrast the evolution of the Baikal Rift of the U.S.S.R. and the Rio Grande Rift of the U.S.

The analyzed samples range in age from Miocene to Quaternary, and in composition from basalts (normative hy) through basanites (>5% normative ne). Many samples contain crustal and mantle xenoliths/xenocrysts. $^{206}Pb/^{204}Pb$ varies from 17.406 to 18.266, $^{207}Pb/^{204}Pb$ from 15.405 to 15.517, and $^{208}Pb/^{204}Pb$ from 37.528 to 38.306. The data define a linear array parallel to the unradiogenic end of the Atlantic-Pacific MORB array, but are slightly elevated in $^{207}Pb/^{204}Pb$ and $^{208}Pb/^{204}Pb$. Pb isotopic ratios do not correlate with degree of silica-saturation, but there is a slight trend towards higher $^{207}Pb/^{204}Pb$ with increasing Mg#. The most-radiogenic sample is a 9.7 Ma basanite which contains pyroxenite and spinel lherzolite xenoliths; conversely, the least-radiogenic sample is a Quaternary basanite containing crustal xenoliths.

A preliminary interpretation of the isotopic, petrographic, and geochemical data is that the spread in Pb isotopic ratios reflects interaction of mantle-derived melts with an unradiogenic source (lower crust?). The limited range in $^{207}Pb/^{204}Pb$ suggests that the unradiogenic component has a uniform Pb isotopic composition.

ERUPTION, DEPOSITION AND SOFT-SEDIMENT DEFORMATION OF THE WHORNEYSIDE TUFF, AN ANCIENT PHREATOPLINIAN DEPOSIT IN THE ENGLISH LAKE DISTRICT.

BRANNEY, M.J. Department of Earth Sciences, University of Liverpool, P.O. Box 147, Liverpool, L69 3BX, U.K.

The Whorneyside Tuff is an extensive pyroclastic deposit within the Ordovician Borrowdale Volcanic Group of the English Lake District. It marks a change in the eruptive style of a calc-alkaline continental arc volcano from multicentred eruptions producing mostly basic to intermediate lavas, to violent explosive activity associated with the development of a subaerial dacite-rhyolite caldera complex.

The lower part of the Whorneyside Tuff consists of welded lapilli-tuffs, up to 120 m thick. These were emplaced from hot pyroclastic flows which inundated the early formed shield-like lava piles. Resultant onset of volcanotectonic subsidence possibly allowed access of large volumes of surface water to the magma, as the pyroclastic flow deposits pass up into a laterally extensive, nonwelded, shower-bedded phreatomagmatic tuff (WBT), ca. 20 m thick. The WBT is characterised by parallel bedding and lamination, defined by variations of grain size and abundance of crystal fragments. Several fine-grained tuff beds contain abundant accretionary lapilli, and some of the coarser grained beds contain lithic lapilli which occupy impact depressions. The fine stratification records fallout of damp ash in rapidly successive localised showers, which resulted from a vast umbrella cloud. The grainsize distribution and morphology of the original pyroclasts of the WBT are not completely known, but a phreatoplinian eruption is indicated by the available data. However, the WBT is considerably thicker than previously documented phreatoplinian deposits elsewhere and the eruption may have been far more voluminous.

The WBT was mainly deposited onto a subaerial plain and was subjected to only minor gullying and redistribution by surface run-off water during the eruption. However, in proximal areas the ash fell into shallow ephemeral lakes, where it was reworked by wave action and in ash-rich turbidity currents and debris flows.

Before its lithification, and whilst the volcano subsided following the evacuation of over 15 km^3 andesitic magma, the WBT was extensively disrupted by seismic activity and ground tilting. Remarkable preservation of subaerially slumped WBT was achieved by rapid burial beneath succeeding welded ignimbrites, which were emplaced before the WBT could be eroded away

LATE PALEOZOIC TO TRIASSIC CONTINENTAL-ARC VOLCANISM IN THE NORTH CHILEAN ANDES

BREITKREUZ, Chr., Institut für Geologie und Paläontologie, Technische Universität, Ernst-Reuter-Platz 1, 1000 Berlin 10, Federal Republic Germany.

A prominent chain of outcrops of thick Late Carboniferous to Triassic volcanic successions can be traced from 19° to 40°S in the High Andes of Chile and Argentina. The predominantly siliceous tuffs and flows are associated with calc-alkaline to slightly alkaline high level intrusions and continental volcanigenic sediments.

In the north Chilean Precordillera between 19° and 25°S numerous sections of these terrestrial volcanosedimentary successions have been studied. In the area of the Sierra de Almeida, south of the Salar de Atacama, volcanic activity started during the very Late Carboniferous. The minimum age of the volcanism is documented by sections in the Precordillera south of 23°30'S where terrestrial volcanic deposits are overlain by Late Triassic (Norian) marine sediments. The lithology of the volcanosedimentary successions comprises siliceous lapilli and breccia flow tuffs, basic lavas and tuffs, obsidian flows and airfall ash tuffs. Among the epiclastic deposits there are red conglomerates, pebbly sandstones and well-sorted sandstones to mudstones. Although basic volcanic deposits are subordinate within the successions, clasts of basic volcanic rocks are the main component of the epiclastic intercalations, whereas reworked clasts of siliceous tuffs seem to be scarce. Local erosional and angular unconformities within the volcanic successions are abundant. These features fit the facies model of relatively siliceous 'continental stratovolcanoes' quite well.

The volcanic rocks are of a bimodal calc-alkaline composition (47% to 80% wt. SiO_2, with emphasis on siliceous compositions). Trace element and REE patterns are consistent with the formation of the volcanic rocks in an active continental margin setting. Compared to modern volcanic rocks of northern Chile, the samples are characterized by high Ba, Sr and low K, Rb values. Relatively high Ti and P contents in the basic to intermediate rocks and a trend towards Rb- as well as Y+Nb enrichments with the siliceous rocks point to a within-plate tendency of the geotectonic setting.

The results favor the assumption that the north Chilean Late Carboniferous to Triassic magmatic rocks formed in a tensional active continental margin setting. Volcanic activity seems to have produced high amounts of siliceous tuff nappes and bimodally composed stratovolcanoes. It was genetically connected to calc-alkaline high level intrusions. In places both can be seen to constitute relictic caldera systems. The intrusive rocks in the area under consideration also display a within-plate affinity.

The north Chilean Late Paleozoic to Triassic magmatic arc can be regarded as the northern continuation of the subduction setting active in the Southern Andes during that time (Choiyoi Group). The geotectonic relation of the north Chilean magmatism to the Late Permian-Early Triassic continental rift magmatism in the Peruvian Eastern Cordillera (Mitu Group) is little known so far.

PETROLOGY OF THE ALEXANDRA VOLCANICS, NEW ZEALAND: COEXISTING CALC-ALKALINE, ALKALINE, AND POTASSIC MAGMATISM.

BRIGGS, R.M., Department of Earth Sciences, University of Waikato, Hamilton, New Zealand, and
McDONOUGH, W.F., Research School of Earth Sciences, The Australian National University, Canberra, Australia, and Max-Planck-Institut fur Chemie, Mainz, West Germany.

The Alexandra Volcanics consist of a calc-alkaline, alkaline and K-rich mafic lava series, and occur in a back-arc setting, 200-250 km above the Benioff Zone. Each magma series is intercalated stratigraphically and has overlapping K-Ar radiometric ages (1.60-2.74 Ma).

The calc-alkaline series forms a linear chain of stratovolcanoes aligned at right angles to the presently active Taupo Volcanic Zone. They are composed of ankaramites, transitional olivine basalts, tholeiitic basalts, high-Al basalts, and medium and high-K andesites. Mass balance models suggest that the range in rock types is compatible with closed-system polybaric fractional crystallization. The most primitive calc-alkaline ankaramites and transitional olivine basalts have geochemical features (high LIL/LREE and LIL/HFS element ratios, low Nb and Ta abundances) and Sr, Nd and Pb isotopic compositions typical of convergent margin magmas, and show no evidence of crustal contamination. Calculated source compositions for the calc-alkaline lavas suggest that three components are involved: a MORB-like component, a component derived from subducted oceanic crust, and a contribution from subducted sediments.

The alkalic series (Okete Volcanics) consist of small volume monogenetic basaltic volcanoes distributed around the flanks of the larger calc-alkaline stratovolcanoes. These basalts have enriched LILE, LREE, Nb and Ta concentrations, and low Ba/Nb and Ba/La ratios, all of which are characteristic of intraplate alkalic basalts. Their relatively high ϵ_{Nd} (+5.5) and low $^{87}Sr/^{86}Sr$ (0.7031 - 0.7036) are similar to other OIB's. We prefer a model where these alkalic magmas were derived from a MORB-like source region within the mantle wedge which has been metasomatically enriched by upward migrating silica undersaturated melts from the low velocity zone. A subducted slab component is not required to account for their LILE and LREE enrichment.

The K-rich mafic lava series consist of basanites and phlogopite absarokites that are volumetrically minor and occur as capping lavas on the flanks of Pirongia, the largest of the calc-alkaline stratovolcanoes. The origin of K and Rb enrichment in the absarokites is uncertain but may be derived from open system crustal assimilation, AFC or source enrichment processes. The basanites have Sr, Nd and Pb isotopic compositions which suggest mixing between a calc-alkaline and alkaline component, although simple two component mixing cannot explain all of their chemical characteristics. It also indicates that Pirongia magmas required at least two mantle sources.

THE MONTS-DORE MASSIF (FRENCH MASSIF CENTRAL): CHRONOSTRATIGRAPHY AND GEOCHEMISTRY OF TWO CONTINENTAL ALKALINE VOLCANOES

D. BRIOT and J.M. CANTAGREL. Univ. Clermont. CNRS and CRV. 5 rue Kessler. 63000 Clermont-Ferrand (France).

The Monts Dore massif (500 km2. 200 km3) is part of the Tertiary and Quaternary volcanism of the French Massif Central. It consists of two distinct volcanic centres (Guery volcano in the north and Sancy volcano in the south) where both silica saturated (basalt to rhyolite) and undersaturated (basalt to phonolite) series are present. However. 70% of the erupted lavas are trachyandesites containing abundant comagmatic inclusions and reaction xenocrysts. These heterogeneities reflect repeated and incomplete magma mixing.

1) Stratigraphical and chronological (K-Ar) studies can be summarised as follows:

6-3Ma : Lower basalts with minor quartz-bearing trachytes and phonolites scattered on the Hercynian basement.

3-1.4Ma : Centralisation of volcanic activity with rhyolitic pumice flows (9 km3) related to a C1 caldera collapse. Successive eruptive cycles of heterogeneous trachyandesites build the Guery volcano. Minor pyroclastic eruptions recorded at 2.25. 2.0 and 1.45 Ma. Episodic tephritic and phonolitic eruptions at 2.6 and 1.95 Ma.

1.4-0.9 Ma : Scarce basaltic eruptions.

0.9-0.2 Ma : Successive eruptive cycles of heterogeneous trachyandesites build the Sancy volcano. Trachytic pyroclastites and C2 caldera collapse dated at 0.78 Ma.

In both volcanoes this stratigraphy has been obscured by cataclysmic debris avalanches and large debris flows which carried shattered lava blocks as far as 35 km from their source region. These events occurred at 2 Ma and 1 Ma in the Guery volcano and at younger ages. which are not yet well constrained. in the Sancy volcano.

2) Geochemical data on the over- and under-saturated series indicate that they both evolved through fractional crystallization involving olivine. clinopyroxene. plagioclase. amphibole. and alkali feldspar as well as sphene. zircon. ano apatite. For saturated and oversaturated lavas. initial 87Sr/86Sr and 143Nd/144Nd range from 0.70350 to 0.70537 and from 0.51287 to 0.51260 respectively and these correlate with SiO_2 contents. 18_O values range from +5.6 to +8.1 per mil and are correlated with 87Sr/86Sr. These co-variations are interpreted in terms of 12-15% assimilation of granitic materials for rhyolites and 6-10% assimilation for less evolved trachyandesites and trachytes. both coupled with fractional crystallization. This AFC process occurred in upper crustal magmatic reservoirs which were periodically refilled. mingled and tapped. Tephrites and phonolites display similar Sr and Nd isotopic ratios to basalts (0.70363-0.51285) suggesting that this assimilation did not occur for these lavas. either because they were generated at greater depth. or in an ancient inactive reservoir after exhaustion of the potential contaminants.

O-ISOTOPE RATIOS OF PRIMITIVE FRENCH MASSIF CENTRAL (FMC) LAVAS AND THE ^{18}O CHARACTER OF MANTLE SOURCES FOR CONTINENTAL BASALTS.

BRIOT D. and HARMON R.S., NERC Isotope Geology Centre, 64, Gray's Inn Road, London WC1X 8NG, UK.

$^{18}O/^{16}O$ ratios have been measured for primitive Plio-Pleistocene basanites from FMC volcanic centres which exhibit distinct radiogenic isotope variations. The samples analyzed, with 43-46% SiO_2, Mg#'s of 64-55, 197-90 ppm Ni, and <0.6% H_2O^+, are from Devès (5.4-0.8 Ma), Monts Dore (4.3-0.4 Ma), and Chaîne des Puys (0.41-0.08 Ma). On a standard Nd-Sr isotope variation diagram, these FMC suites plot between the PREMA focal point for continental intraplate lavas and Bulk Earth in distinct fields that are subparallel to the reference mantle array. Respective $^{87}Sr/^{86}Sr$ and $^{143}Nd/^{144}Nd$ ranges are : Devès: 0.70327-0.70350 and 0.512900-0.512844, Monts Dore: 0.70353-0.70369 and 0.512873-0.512848, and Chaîne des Puys: 0.70370-0.70400 and 0.512773-0.512750. Values of $\partial^{18}O$ (‰ SMOW) for the FMC centres exhibit similar systematic spatial variations : for the southeast Devès basalts $\partial^{18}O$=5.5 to 5.8 (x=5.6±0.1), for Monts Dore $\partial^{18}O$=5.4 to 6.0 (x=5.8±0.2), and for the youngest and northern Chaîne des Puys basalts $\partial^{18}O$=5.4-6.5 (x=6.0±0.4). Striking is the fact that the Devès $\partial^{18}O$ values fall just within the 5.3 to 5.8 range for protogranular spinel lherzolite xenoliths from the same region of the FMC, whereas Chaîne des Puys O-isotopes ratios extend to only slightly higher values than those for deformed and trace element enriched peridotite xenoliths obtained localy from the Puy Beaunit centre. The common base level $\partial^{18}O$ value for lavas at each centre and the correspondence of lava and xenolith ^{18}O compositions imply a common mantle source on a regional scale; the sympathetic covariation of O-, Sr-, and Nd- isotope ratios among volcanic centres indicates that a common process is responsible for the stable and radiogenic isotope features. Thus, we suggest an origin for primitive FMC basalts through partial melting of an OIB-type mantle source that is isotopically heterogeneous on the scale of individual volcanic centres or less. In the case of Chaîne des Puys lavas, the ^{18}O data also suggest the possibility of up to 5% crustally derived oxygen having been added during their transit through the crust.

Worldwide, primitive Pleistocene continental intraplate basalts, many of which are akin to those erupted in the FMC with Mg#'s>58, Ni>100 ppm, and H_2O^+<0.6 wt%, and which bear mantle peridotite xenoliths, have $^{18}O/^{16}O$ ratios which are equivalent to the Devès and Monts Dore lavas. The average $\partial^{18}O$ value for 45 such basalts we have analyzed is 5.7±0.3‰ (Geronimo, SW USA : 5.7±0.3 ; Pali Aike, S.Chili : 5.6±0.2 ; Mt Melbourne, Antarctica : 5.8±0.3 ; Tariat and Dariganga, Mongolia : 5.4±0.2 ; Karasu Valley, Turkey : 5.8±0.1; Eifel, W.Germany : 5.9±0.3). This $^{18}O/^{16}O$ ratio is identical to that of MORB and to the worldwide average for garnet and spinel mantle peridotite xenoliths contained in continental alkalic basalts, implying that the upper mantle source for basaltic magmas is of essentially uniform ^{18}O content on a regional scale. From our studies of primitive continental intraplate basalts and their mantle xenoliths, we see no evidence for $\partial^{18}O$ values in excess of c.6‰. Therefore, we consider that parental (but not primitive) intraplate basalts, and their evolved derivatives, with significantly higher $^{18}O/^{16}O$ ratios have acquired this characteristic through some process of magma-crust interaction subsequent to partial melting and equilibration in the mantle.

AN EMPLACEMENT AND PETROGENETIC MODEL FOR THE HIGH TEMPERATURE ASH FLOWS OF THE JOZINI FORMATION, SOUTH AFRICA

BRISTOW, J.W. DBCM Geology Dept, Box 47, Kimberley, 8300, and ARMSTRONG, R.A. Geochemistry Dept, UCT, Rondebosch, 7700, RSA

Comparative field studies in the Canary Islands, south western U.S.A. and southern Africa of flow banded felsic flow units support a model of high-temperature pyroclastic emplacement for the Jurassic Jozini Rhyolites of the Lebombo Mountain belt.

The Jozini Rhyolites form a major succession (~4.5 km thick) consisting of numerous extensive and voluminous flows showing characteristics of both rhyolite lavas (senso stricto) and major ash-flow tuffs. Individual flows are sheet-like, columnar jointed, vary from 85-340m in thickness and can be traced along strike for up to 60km. Lateral extent typically exceeds 10km but erosion and monoclinal tilting prevent determination of original east-west dimensions. The flows are characterised by well defined gradational zones. These (from bottom) include a Streaky or Eutaxitic basal zone in which flattened and highly stretched fiamme may be recognisable, a thick Massive Central zone, a Contorted Flow Banded zone, a Breccia zone and an uppermost Sandy-Tuffaceous zone consisting of reworked tuffs and palaeosoils. Evidence for fumerolic activity is apparent at the tops of flows.

These flows represent high temperature ash flows erupted from elongate depression cauldrons. Mineral temperatures calculated using 5 thermodynamic methods suggest equilibration temperatures in excess of 800degC, possibly as high as 1200degC. Emplacement involved turbulent outwelling, rather than column collapse, giving way to laminar flow and annealing of pyroclastic particles to the point where the flows assumed a lava-like character. Flow banding developed during laminar and later more viscous lava-like flow; brecciation reflects late fragmentation of congealing flow tops assisted by explosive release of entrapped volatiles. Intense welding and devitrification led to overprinting of most original pyroclastic textures.

Geochemical and isotopic data, eg. low initial-Sr ratios, and U-Pb (conventional and Ion Microprobe) studies of zircon xenocrysts (which yield Proterozoic ages) suggest the rhyolites represent partial melts derived from mafic lower crustal granulites. Heat supply was provided by the basaltic event which saw some 5km of Lebombo basalts erupted immediately prior to rhyolitic volcanism. A model involving partial melting of underplated basaltic material was tested but is considered less plausible. Emplacement of the rhyolite flows occurred during a period of strong rifting. Partial melting to produce rhyolitic magmas occurred in response to high heat flow, crustal attenuation and upwarping of the crust mantle interface with associated decompression.

Rocks showing broadly similar features to the Jozini rhyolites occur elsewhere in southern Africa eg. Rooiberg, Ventersdorp, Soutpansberg, Sinclair and Etendeka, Brazil, West Australia, and the U.S.A. Nearly all occur in major bimodal basic-felsic provinces. High heat flow associated with basaltic magmatism appears to be a controlling factor in their formation.

Galunggung 1982-83 high-Mg basalts : Quaternary Indonesian arc primary magma

S. Bronto
Department of Geology, University of Canterbury, New Zealand

Galunggung volcano, West Java, Indonesia, erupted from April 1982 to January 1983. The eruption began with the production of pyroclastic flow and fall deposits leading to Vulcanian eruptions in which pyroclastic flows became less frequent and smaller in volume, but pyroclastic falls became more frequent. Paroxysmal eruptions occurred from June to August 1982 when the eruption column reached 20,000 m in height. Eruptions changed to Strombolian type in September 1982, after which activity decreased and ended in January 1983 when a lava flow was extruded.

During the eruption sequence, compositions became more basic, until the final products were high-Mg basalts having 49 % SiO_2, 12 % MgO, 190 ppm Ni and 710 ppm Cr. Phenocrysts in these rocks are euhedral, with normally-zoned olivine (Fo_{90-80}) containing Cr-spinel inclusions (up to 48 % Cr_2O_3 but < 20 % Al_2O_3), diopsidic pyroxene ($Ca_{48-45}Mg_{47-46}Fe_{9-5}$) and calcic plagioclase (An_{95-80}).

In Indonesia, the 1982-83 Galunggung high-Mg basalts are the most primitive rocks (Mg# = 69-74) recorded the volcano's history and have a similar composition to basalts from New Britain.

The textural and compositional temporal changes in the 1982-83 Galunggung eruption suggest a compositionally stratified magma chamber in which crystal fractionation is the main mechanism of differentiation. Least square mixing suggests that the Galunggung high-Mg basalts represent a parental magma derived from the upper mantle beneath the volcanic arc.

VOLCANO POWER AND THE ROLE OF CRATER LAKES

BROWN, G.C., RYMER, H., and STEVENSON, D.,
Department of Earth Sciences, The Open
University, Milton Keynes, MK7 6AA, UK

The world's most energetic eruptions require 10^{18}-10^{20}J, mainly through the kinetic and thermal energy of short-term plinian explosions, and several recent eruptions produced 10^{12}-10^{15}W over the short-term, for hours to days. In their normal quiescent state, highly explosive volcanoes transfer relatively little heat to the surface. However, many volcanoes maintain *long-term* efficient cooling systems, through fumarolic activity, boiling mud pools etc. which generate 10^{6}-10^{8} W. Occasionally, especially if the cooling meteoric water supply is low a lava lake may rise within a crater and radiate 10^{8}-10^{9}W continuously for years to decades. Alternatively, in regions of high rainfall or extensive snow melt, potentially explosive volcanoes with craters develop hot, acid water lakes. In such cases, the dominant mode of heat transfer to the atmosphere is by evaporation, again yielding a steady-state 10^{8}-10^{9}W. If maintained for 10^{2}-10^{3}years, typical water and lava lake energy losses are equivalent to and may replace short-term highly energetic explosions. Nevertheless, short-term power output increases are recorded from lava lakes in the form of fire fountaining and from water lakes as phreatomagmatic eruptions.

Here we examine the detailed energy budget for stratovolcanoes with hot water lakes of which three (at Poas, Ruapehu and Soufriere) have well-documented histories. It is argued that the sub-surface magma column develops a frozen cap, cooled by the meteoric hydrothermal system which transfers heat to the crater lake. Thus the equilibrium position of the magma-rock interface is strongly influenced by the meteoric water supply and the efficiency of the cooling system. We postulate that such steam-water systems, through their high latent and specific heat capacity, are capable of absorbing short-term energy fluctuations of more than an order of magnitude. Thus the hydrothermal system buffers the surface expression of natural high heat flow and perpetuates an unstable equilibrium. Longer-term increases in power output may change the style of activity as water is rapidly vaporised and the system dries. Thus the probability of phreatomagmatic eruptions may be monitored using simple observations of crater lake characteristics.

Systematic monitoring of the energy budget from Poas (Costa Rica) crater lake and fumaroles indicates an increasing power output from early 1985 (1.6×10^{8}W) to early 1988 (2.6×10^{8}W) to late 1988 (2.9×10^{8}W minimum). We propose that the capacity of the buffer system has been exceeded by this long-term power increase, perhaps due to renewed ascent of magma or cracking of the magma chamber roof. A rapid lake volume reduction (mid-1986 to late-1988 from 3×10^{6} to 2×10^{5} m^{3}) was accompanied by lake temperature increases from 45 to 90°C, and in 1988 by occasional 200 m high phreatic eruptions each generating 10^{10}-10^{11}J (a short-term power of 10^{8}-10^{9}W). Either the increased power output from the crater lake and fumaroles has compensated for source changes, or the trend will continue, possibly culminating in magmatic activity. The local consequences in terms of ash fall and sulphurous acid rain in this populated agricultural region are already serious. However, returning to the earlier theme, thermal emission of ca. 1.2×10^{17}J from Poas in the 24 years since the present crater lake was established may well have prevented, or at least postponed the production of a globally-significant explosive eruption.

THICKNESS AND FLOW DYNAMICS AS FACTORS CONTROLING WELDING VARIATIONS IN IGNIMBRITES

BUESCH, D.C., Department of Geological Sciences, University of California, Santa Barbara, CA 93106, and
VALENTINE, G.A., Geoanalysis Group, ESS-5, Los Alamos National Laboratory, Los Alamos, NM 87545

Welding in ignimbrites has historically been attributed to post depositional processes governed by the temperature of emplacement, viscosity of the glassy fragments, and thickness of the deposits. According to this "classical" view of welding, the welding features of an ignimbrite deposited upon a hill should vary in a relatively symmetrical fashion according to the deposit thickness, assuming temperature and glass rheology are constant. Where welding shows asymmetrical variations around a hill (e.g., ignimbrite is more intensely welded on the stoss side of a hill than on the lee side at equivalent elevations) another factor must be called on in addition to the classical ones; we infer that this factor results from the the dynamics of the moving pyroclastic flow. Here we summarize results on asymmetric welding observed in the 18.6 Ma Peach Springs Tuff, a laterally extensive, large-volume ignimbrite exposed in southwestern U.S.A.

The Peach Springs Tuff (PST) can be divided into two local facies. Open-valley facies occur where the ignimbrite was deposited in broad, open valleys to thickness of 40 to 100 m. In open-valley facies dense welding typically begins about 10 to 20 m above the base of the deposit and is characterized by brown devitrified and vapor-phase-altered material; vitrophyre is very rare in open-valley facies. Edge facies occur where the tuff was deposited against or over paleohills and valley edges, and the tuff is 0 to 25 m thick. Edge facies deposits, although relatively thin, commonly have densely welded zones that begin at 2 to 10 m above the base; they are characterized by black vitrophyre in the densely welded zones. Locally, the upper part of the edge facies deposits exhibits the brown devitrification and vapor-phase-alteration that thickens toward the adjacent open-valley facies. The variation between edge and open-valley facies welding patterns can be attributed to the differences in thickness of the deposits in each facies. In edge facies the interstitial gas just after deposition remained near atmospheric pressure during cooling because it was able to flow easily through the relatively thin deposits; thus the gas did not hinder compaction and welding of the deposit. Open-valley deposits, being much thicker, hindered flow of the gas out of the deposit; thus higher pore pressures developed during cooling which acted against compaction and welding.

Asymmetric welding within edge facies is also observed in the PST. On stoss sides of paleohills dense welding occurs close to the base of the deposits (< 5 m), whereas on the lee sides at the same elevations dense welding is > 5 m above the base (commonly about 10 m). We attribute this asymmetric welding to increased compaction of the pyroclastic flow material when it impinged upon the stoss side of paleohills. In this highly compacted state, the shards shared greater contact areas which resulted in better welding efficiency on stoss than on lee sides. After cresting the hills, the pyroclastic flow presumably expanded to its unperturbed state and may have even been slightly more inflated on the lee side slopes.

As the pyroclastic material compacted on the stoss side of a hill to form an asymmetric welding facies, the interstitial gas was either trapped within the deposit and compressed into to a smaller volume, or transferred from the lower part to the upper part of the flow by a process similar to filter pressing. Trapped gas may form ovoid vesicles within the densely welded tuff (this has been described in other ignimbrites) and vapor phase alteration of the upper parts of the deposit may be extensive. If gas was expelled , no vesicles form and vapor phase alteration in the upper parts of the deposit may be minimal (as is the case for the Peach Springs Tuff).

COUPLED SPATIAL, CHEMICAL, AND ISOTOPIC CHARACTERISTICS OF PRIMITIVE LAVAS FROM THE LASSEN REGION, CALIFORNIA

BULLEN, T.D. AND CLYNNE, M.A., U.S Geological Survey, Menlo Park, CA 94025 USA

During the past 3 Ma, a spectrum of chemically and isotopically diverse lavas have erupted from numerous diffuse, monogenetic vents in the Lassen region of the southernmost Cascades. These lavas range from low-K olivine tholeiite (LKOT) through calc-alkaline basalt (CAB) to andesite (CAA). LKOT's are remarkably uniform in major- and trace-element composition, have low SiO_2 (48-49.5 wt.%), K_2O (< 0.40 wt.%), and Sr (< 400 ppm), and have nearly flat REE-patterns that display positive Eu-anomalies. Straight Gd-Yb distributions are particularly diagnostic of LKOT. In contrast, at given SiO_2-content, calc-alkaline lavas have highly variable abundances of incompatible elements; for example, at 53 wt.% SiO_2, K_2O ranges from 0.25 to 2.0 wt.%, and Sr ranges from 400 to 1200 ppm. A few lower-K_2O CAA lavas have as much as 1500 ppm Sr. La/Sm and Sm/Yb in all calc-alkaline lavas are greater than in chondrites, and REE-patterns range in shape from concave-upward to sigmoidal (i.e., concave-downward from La to Sm, concave-upward from Gd to Yb).

Many of the lavas erupted in the Lassen region are primitive (i.e., they have not changed appreciably in composition since segregation from their source region). Most LKOT and many CAB lavas have not attained multiple-phase saturation, contain high compatible element abundances (Mg# > 65, Ni > 100 ppm, Cr > 150 ppm) without having accumulated phenocrysts, and thus are primitive magmas. Of the primitive mafic samples we have analyzed, all LKOT and the higher-K_2O CAB lavas are "continental" in isotopic affinity (e.g., have $^{87}Sr/^{86}Sr > 0.7036$). K_2O-rich CAB lavas have geochemical characteristics (e.g., high Nb/Y) that suggest affinities to alkalic within-plate magmatism. In contrast, the primitive lower-K_2O CAB lavas we have analyzed are "oceanic" (MORB-like) in isotopic affinity (e.g., have $^{87}Sr/^{86}Sr < 0.7034$). Moreover, although typically impoverished in compatible elements, the lower-K_2O, high-Sr CAA lavas likewise represent primitive compositions. These particular andesites are isotopically the most MORB-like of Lassen region magmas, and cannot be derived from potential LKOT and CAB parents by geologically reasonable crustal-level processes. Modeling based on petrographic, geochemical, and isotopic data reveals that the compositional array of primitive magmas in the Lassen region cannot be derived from either a single primary magma-type, or from diverse primary magmas produced by variable degrees of melting of a chemically homogeneous source region.

In the Lassen region, we observe a systematic across-arc variation of chemistry and isotopic composition of the primitive lavas. The majority of lower-K_2O calc-alkaline lavas have erupted within and to the west of the Cascade axis. In contrast, LKOT's and the majority of higher-K_2O calc-alkaline lavas have erupted within and to the east of the Cascade axis. Consideration of the isotopic variability with major- and trace-element compositon (e.g., $^{87}Sr/^{86}Sr$ vs. SiO_2- and Sr-content), as well as the coupled isotopic systematics (e.g., Pb-Pb, Pb-Sr, Pb-Nd, Sr-Nd) in light of field relations leads us to propose the existence of a chemically and isotopically heterogeneous upper mantle source region for the primitive magmas. We interpret the various coupled isotopic arrays to reflect mixing of components derived from two distinct reservoirs: isotopically heterogeneous sub-continental lithosphere (the "continental" component) and subducted oceanic lithosphere (the "oceanic" component). Steepening of the subducted oceanic lithosphere beneath northern California since the late-Miocene has allowed for the concentration of slab-derived fluids at and to the west of the present Cascade axis.

TECTONIC FRAMEWORK OF THE CORDILLERAN OROGNEIC BELT OF WESTERN NORTH AMERICA

BURCHFIEL, B. C., 54-1010, MIT, Cambridge, MA, 02139, USA

The Cordilleran Orogen can be divided into two parts; an eastern part formed on older North American Precambrian craton and a western part formed by fragments from Phanerozoic oceanic, island arc and continental environments accreted to the craton from mid-Paleozoic to Cenozoic time. The northern part of the North American craton consists at least 6 Archean fragments sutured together during a short period of early Proterozoic time, and its southern part consists of largely primitive tectonic elements accreted progressively southward from about 2.3 to 1.0Ga. The southern part of the craton was affected by anorogenic granite/rhyolite magmatism from 1.5 to 1.34 Ga. Mafic magmatism affecterd the craton at about 1.4, 1.0-1.2, and 0.7-0.8Ga during periods of extension.

Cordilleran paleogeographic elements trend north-south across the westward projected tends of cratonal tectonic elements truncated by diachronous rifting in latest Proterozoic time with the establishment of a well developed passive margin that persisted throughout early Paleozoic time. Early Paleozoic island arc rocks are present within the accreted crustal fragments in the western Cordillera, but their position relative to North America in early Paleozoic time remains uncertain. The arcs were intruded by Devonian plutons and locally metamorphosed, but rocks of the passive margin, intruded locally by mafic rocks and very local alkaline plutons, show no evidence of convergent activity until the Late Devonain to Mississippian Antler orogeny. During the Antler event continental slope and rise rocks were thrust eastward onto Cordilleran shelf rocks with little associated magmatism or metamorphism and created an orogenic highlands. During late Paleozoic time magmatism continued in the offshore arcs, some of which may have been separated from North America only by marginal seas, and the Cordilleran passive margin was reestablished as the Antler highlands were worn away. The continental interior and the eastern part of the Cordillera was affected by the amagmatic foreland Ancestral Rocky deformation during Pennsylvanian-Permian time at the same time that the southwestern part of the Cordillera was truncated along a left-slip transform boundary. This trucation established a new margin along which Mesozoic tectonic and magmatic units trend almost at right angles across all older units whereas farther north early and late Paleozoic tectonic and magmatic units are subparallel. Amalgamation of some offshore arcs took place during late Paleozoic time. During Permo-Triassic time within the southern and central Cordillera arc and associated marginal basin rocks were accreted to North America in the Sonoma orogeny, and granitic plutons and associated deformation affected North American rocks along part of the truncated continental margin in the southernmost part of the Cordillera.

In the early Mesozoic an Andean margin developed along much of the Cordillera constructed across both North American rocks and accreted fragments. Subduction related rocks were developed west of the arc and pulses of intracontinental deformation affected the back arc region. Arc magmatism continued in island arcs that remained off shore. In late Mesozoic time the Andean margin and its related subduction and back arc convergent deformation became broader and more well developed; thick and broad zones of subduction melange, blueschist and ophiolitic rocks were accreted west of the magmatic arc and a wide east-vergent thin-skinned thrust belt formed east of the arc. In the northern part of the Cordillera at least two large fragments dominated by arc magmatic rocks were accreted from early Jurassic to mid-Cretaceous time. During accretion the zone of eastward subduction of paleo-Pacific oceanic lithosphere and the Andean magmatic arc migrated westward intruding into previously accreted fragments. Although transcurrent faults were active early Mesozoic time, evidence for such structures is clear only during late Mesozoic time. Transcurrent faults, mainly right lateral, disrupted older subduction zone, magmatic and North American tectonic and paleogeographic elements producing both duplication and truncation of these elements and locally opened and closed small regions floored by oceanic crust along the western part of the margin.

During latest Cretaceous and early Cenozoic time a gap developed in the Andean magmatic arc within the U. S. part of the Cordillera and east of this gap large basement cored thrust plates accompanied by local magmatism formed the Laramide Rocky Mountains within the North American craton. Both to the north and south the Andean arc and related structures continued to develop. These relations suggest the area of the magmatic gap and the Laramide Rocky Mountains formed above a subhorizontal segment of the subducted oceanic slab, whereas normal slab dips continued north and south. Plate reconstructions indicate a rapid increase in the convergence rate across the plate boundary at this time. In Eocene time extension began within parts of the Cordillera and even though arc magmatism, with a continued magmatic gap, is wide spread, transcurrent movement along the western parts of the Cordilleran margin continued. During Oligocene and Miocene time extension affected most of the southern Cordillera and the magmatic arc swept west and the magmatic gap was closed. During late Cenozoic time extension became more widespread and diachronous subduction of the oceanic spreading ridge caused diachronous lengthening of transform boundaries, cesession of arc volcanism, and gradual shortening of the subduction boundaries along the margin. Basalt/rhyolite volcanism became widespread within the region of extension. Back arc extension was accompanied by local voluminous basaltic volcanism forming the Columbia plateau. During the past 15 Ma basaltic and bimodal volcanic rocks have been extruded progressively eastward along the Snake River plain currently reaching the active calderas at Yellowstone. The present high elevation of the Colorado Plateau and the Cordilleran region occurred in late Cenozoic time. The Basin and Range is underlain by extended and thin crust but stands at an average elevation of 1.5-2 km because of thin mantle lithosphere and an elevated asthenosphere.

MODELS OF CLAST DISPERSAL FROM EXPLOSIVE VOLCANIC ERUPTIONS

BURSIK, Marcus, Dept. of Earth Sciences, University of Cambridge, Cambridge CB2 3EQ, United Kingdom; WOODS, Andrew, Dept. of Applied Maths. and Theor. Phys., University of Cambridge, CB3 9EW, United Kingdom

The clast-dispersal models of Carey and Sparks (1986) (CS) and Wilson and Walker (1987) (WW), and clast-dispersal patterns calculated from the plume model of Woods (1988) (W) provide estimates of maximum radii of clast support in maintained volcanic eruption columns. We have investigated the relationship between clast-support radii, column height and mass-eruption rate predicted by each of these models, and compared the results with field data. To calculate clast-support envelopes, CS uses time-mean gaussian profiles for velocity and density at each height in the column, and vertical velocity and density variations based on the simple plume model of Morton *et al.* (1956). W and WW assume that clast support extends to the characteristic radial distance of top-hat velocity and density profiles, and also use vertical velocity and density gradients based on more complete thermodynamic modeling. These differences in plume structure and dynamics assumed by the clast-support models affect interpretation of field data. For example, in comparing model predictions with dispersal patterns from eruptions for which cloud heights are known, we have found that for a given degree of dispersal CS seems to systematically overestimate cloud height, while W and WW tend to underestimate heights of larger eruptions.

We have identified further differences between the models and data, and among the models themselves. All three models differ systematically from data in that they predict clast-support radii for large particles that are anomalously large in comparison with those for small particles. The models also differ in their prediction of the relationship between mass-eruption rate and cloud height. CS and W predict higher columns than WW for any mass-eruption rate. Woods (1988) investigated these model differences using a plume model based on the dusty-gas approximation, which did not include particle fallout. To characterize the model differences more thoroughly and to improve our understanding of the variables controlling clast support, we are developing and investigating new models that take into account fallout of clasts from columns containing particles with different total-size distributions, incomplete transfer of heat from large particles to plume gas before fallout, and release of heat by condensation of plume steam.

Carey S and Sparks RSJ (1986) *Bull Volc 48*: 109–125. Morton B, Taylor GI and Turner JS (1956) *Proc Roy Soc A234*: 1–23. Wilson L and Walker GPL (1987) *Geophys J Roy astr Soc 89*: 651–679. Woods A (1988) *Bull Volc 50*: 169–193.

VOLCANO-TECTONIC CONTROLS ON SEDIMENTATION IN AN EXTENSIONAL CONTINENTAL ARC: A JURASSIC EXAMPLE FROM THE EASTERN MOJAVE DESERT, CALIFORNIA

BUSBY-SPERA, Cathy J, SCHERMER, Elizabeth R., and MATTINSON, James, Department of Geological Sciences,University of California, Santa Barbara, CA 93106

The early Mesozoic continental arc of California, Arizona and western Nevada has been postulated to have occupied a graben-depression more than 1000 km long, similar to the modern extensional arc of Central America (Busby-Spera, Geology, December 1988). Late Mesozoic intra-arc compressive deformation and voluminous plutonism overprinted structural and sedimentological features of the earlier extensional arc in many places, but non-deformed, weakly metamorphosed domains occur locally, including excellent exposures of middle Jurassic strata in the Cowhole Mountains. Volcano-tectonic processes controlled sedimentation in this part of the arc graben-depression in two major ways: (1) due to rapid intra-arc subsidence, cration-derived quartz sands were trapped and preserved in vent-proximal areas; and (2) syndepositional faults provided control on the distribution of volcaniclastic and epiclastic rocks, and shed landslide blocks into the basin.

Eolian quartz sandstone over 800 m thick in the Cowhole Mountains contains interbeds of dacite lava flow and lapilli tuff 10-30 m thick in its upper part and is overlain by over 575 m of ignimbrites, lava flows and minor sedimentary rocks, divided into four units. The lowest two units include a quartz latite ignimbrite 120 m thick overlain by a dacite lava flow 200 m thick; these are each capped by fluvial sandstones that contain a mixture of eolian quartz and pyroclastic debris. The third unit is a rhyodacite ignimbrite. The fourth and highest exposed unit is a latite lithic-rich ignimbrite, greater than 200 m thick, that contains a megabreccia with slabs up to 0.5 km long derived from subjacent units.

U-Pb zircon dates on a dacite lava flow within the thick eolianite section and on units 1 and 3 show that the Cowhole Mountains section ranges from 172 to 167 Ma in age. These data support the interpretation that the quartz sands were supplied by coastal dunes associated with the Carmel seaway and/or by the areally extensive Entrada dune field, both of the present-day Colorado Plateau. Interstratification of these quartz sands with very thick, stubby silicic lava flows suggests burial of a vent-proximal region of the arc. Admixing of the quartz sands with shards, pyrogenic crystals, pumice and volcanic rock fragments occured in very shallow ephemeral streams in interdune areas and on pumice plains.

Syndepositional faulting resulted in erosional stripping of more than 125 meters of ignimbrite (unit 3) from the upthrown side of a high-angle fault, leaving behind a horizon of ignimbrite cobbles that overlaps the fault and was deposited above the ignimbrite on the downthrown block. The immediately overlying megabreccia contains slabs of the two subjacent volcanic units that were shed from an inferred fault beyond the limits of present-day exposures. The megabreccia is encased within an ignimbrite that is non-welded and thus probably does not represent an intracaldera accumulation. An alternative explanation is that catastrophic landslides, similar to those associated with mid-Tertiary extensional basins of the S.W. Cordillera, were triggered along a graben boundary fault by seismicity during the ignimbrite eruption.

EVOLUTION OF THE EARLY OLIGOCENE ORGAN CAULDRON, SOUTH CENTRAL NEW MEXICO

BUTCHER, D. P., New Mexico State University, Las Cruces, New Mexico 88003, and
MCCURRY, M., New Mexico State University, Las Cruces, New Mexico 88003, and
FARMER, G. L., University of Colorado, Boulder, Colorado 80309

The early Oligocene Organ Cauldron of south central New Mexico consists of large volume silicic ash-flow tuffs and a subjacent comagmatic batholith. The volumetrically dominant phase of the batholith is the compositionally zoned Organ Needle pluton (55% to 75% SiO_2). The most mafic part of pluton is a monzodiorite with preliminary ϵ_{Nd} and $(^{87}Sr/^{86}Sr)_m$ values of -2.96 and 0.7053, respectively. These values are consistent with a parental magma source in the subcontinental mantle lithosphere. Mass balance calculations suggest that compositional variation within the pluton is primarily a result of fractional crystallization.

Chemical and isotopic data as well as field relationships suggest that the tuff of Squaw Mountain, a 1.4 km thick ash flow unit located at the top of the cauldron tuff stratigraphy, represents magma extruded from the same magma chamber that formed the Organ needle pluton. Rapid solidification of the Organ Needle pluton was the result of degassing of the magma chamber during the eruption which produced the Tuff of Squaw Mountain. Relicts of the degassing event include numerous and widespread miarolitic cavities.

Detailed chemical studies of the tuff of Squaw Mountain show that the bulk of the ash flow is virtually identical in whole rock chemistry to the most silicic part of the Organ Needle pluton, an alkali feldspar granite (75% SiO_2). Strong stratigraphically vertical gradients in major and trace element chemistry at the top of the tuff are probably genetically related to the gradational contact between the quartz syenite and alkali feldspar granite facies of the organ Needle pluton.

The 32 Ma Organ Cauldron is located in the southern Rio Grande rift, an Oligocene to recent continental rift system. The apparent mantle origin for parental magma, north trending syn-cauldron normal faults, and outcrop patterns of plutons and dikes suggest that the cauldron evolved in a WSW extensional stress field, perhaps offering a constraint for the age of earliest rifting of the southern Rio Grande rift.

FACTORS INFLUENCING SEISMOVOLCANIC ACTIVITY AT VULCANO (SOUTHERN ITALY)

CACCAMO, D.,Istituto Geofisico e Geodetico, Università di Messina, via Osservatorio 4, Messina, Italy, MONTALTO, A., NERI, G., PRIVITERA, E., Istituto Internazionale di Vulcanologia, CNR, viale R. Margherita 6, Catania, Italy.

Seismicity of Vulcano volcano is monitored by an 8-station short-period network covering the whole area of the Aeolian Island Archipelago (Southern Tyrrhenian Sea). Data collected in more than 10 years (January 1978 - June 1988) are used in the present work in order to investigate (1) the temporal pattern of shocks of purely volcanic origin (in our case mainly associated with gas dynamics within the volcano), (2) possible relationships betwwen these events and regional tectonic seismicity, and (3) periodic trends in their occurrence features, which could help us to identify factors producing some influence on the phenomena in question.

During the period investigated, volcanic activity was essentially limited to fumarolic emission, even if swarms of small shocks (magnitude < 2.5) episodically occurred in the upper structures of the volcano, often accompanied by remarkable changes in gas temperature and composition at the fumaroles.

The autocorrelation approach reveals a main periodicity in the seismic sequence submitted to the investigation for $T \sim 420$ days. A smaller peak in the autocorrelation function is obtained for $T \sim 1$ year. On the basis of these findings, we are led to suppose that "external" factors, and in particular, Chandler wobble and seasonal phenomena play some role in the occurrence of shallow volcanic shocks at Vulcano.

Also tectonic earthquakes occurring in the area of the archipelago seem to influence the evolution of volcanic seismicity. In a significant number of cases, the most energetic tectonic earthquakes were in fact followed, in a very short lapse of time (few days), by remarkable increases in both rate and energy of volcanic shocks. A strict correlation between tectonic and volcanic seismic events must, however, be excluded on the basis of available information. It is reasonnable to suppose that factors other than regional events contribute to the evolution of volcanic seismicity. Apart from the already discussed factors, the most obvious one is that of physico-chemical equilibria patterns inside the volcano.

THE DECCAN TRAPS AND ATMOSPHERIC CO_2

CALDEIRA, K.G., and RAMPINO, M.R., Earth Systems Group, Dept. of Applied Science, New York University, 26 Stuyvesant St., New York, NY 10003.

We have developed a carbon-cycle model and have used it to assess the climatological consequences of volatile emissions from the Deccan Traps. The Deccan Traps emitted significant amounts of CO_2, HCl, and H_2SO_4, each of which would increase the atmospheric partial pressure of CO_2. CO_2 emissions increase atmospheric pCO_2 through increasing the ocean-atmosphere total carbon reservoir. Emissions of HCl and H_2SO_4 increase atmospheric pCO_2 by decreasing ocean alkalinity, resulting in partial degassing of the ocean carbon reservoir to the atmosphere. A primary sink for this excess atmospheric CO_2 is the weathering of terrestrial silicate rocks. The weathering rate of silicate rocks is an increasing function of soil pCO_2, which increases with atmospheric pCO_2, therefore elevated CO_2 levels lead to elevated rates of atmospheric CO_2 removal. Model results indicate that emissions from the Deccan Traps may have significantly increased Paleocene atmospheric pCO_2, and that this excess CO_2 would have been removed through increased weathering over a period lasting on the order of a million years.

As there is uncertainty in the timing and magnitude of Deccan Traps volatile emissions, a number of scenarios are examined. Model results for an unrealistic "worst-case" scenario of instantaneous emission of the high-end estimates for Deccan Traps volatiles indicate pCO_2 increase of about 3000 ppm. However, if these emissions are spread out over 500,000 year, the resulting pCO_2 increase is on the order of 300 ppm. The resulting temperature increases depend non-linearly upon the amount of CO_2 in the atmosphere near the Cretaceous/Tertiary boundary. Plausible estimates for Deccan Traps induced temperature increases range from near zero for very slow releases and low volatile volume estimates, up to about 4°C for releases of maximum predicted volatiles over a 500,000 year release time into an atmosphere similar to that of today. Reconstructions of early-Paleocene atmospheric CO_2 fluctuations are complicated by the end-Cretaceous fall-off in pelagic biological productivity, which affected the distribution of carbon within the ocean-atmosphere system and may have altered carbonate deposition rates.

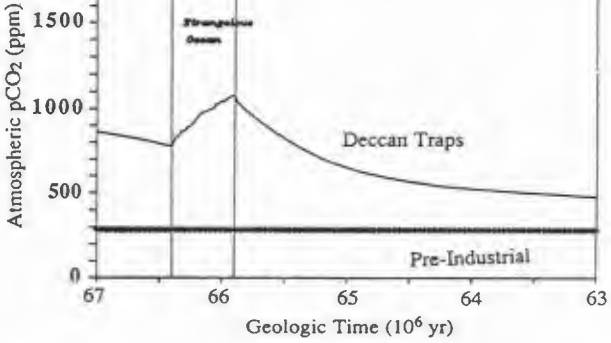

Model results based on Deccan Traps emissions of 10^{12} moles CO_2 yr^{-1}, 0.69 x 10^{12} moles H_2SO_4 yr^{-1}, and 0.015 x 10^{12} moles HCl yr^{-1}, during the period from 66.4 mybp to 65.9 mybp. The transient increase in atmospheric pCO_2 of about 300 ppm occurs against a background of a model-computed secular pCO_2 decrease. A pre-industrial pCO_2 level of 285 ppm is presented for comparison.

COMPOSITIONS OF 1972-1986 VOLCANIC EJECTA FROM MT. EREBUS, ANTARCTICA: IMPLICATIONS FOR THE 1984 ERUPTIVE ACTIVITY

CALDWELL, D.A., Geoscience, N.M. Inst. Mining & Tech., Socorro, N.M. 87801
KYLE, P.R. and MCINTOSH, W.C.

Mt. Erebus (77°32'S, 167°9'E, 3794 m) Ross Island, Antarctica, is an active intra-plate volcano. A persistent convecting anorthoclase phonolite lava lake discovered in 1972 grew until it was 60 m in diameter by 1980. Volcanic activity from 1972 until 1984 consisted of 2-6 strombolian eruptions per day from the lake and nearby vents. Eruptions often ejected bombs onto the Main Crater rim, 200 m above the lake. Starting Sept 13, 1984 strombolian eruptions increased in frequency and size. An estimated 0.3X10^6 m^3 of ejecta was erupted and this buried the lava lake and built a 1 m thick blanket on the crater rim. Bombs up to 10 m long were thrown 1 km from the vent. Older bombs show a similar size range and distribution pattern to those erupted in late 84, suggesting that similar eruptive activity occured in the recent past. In Jan 85, eruptive activity declined to pre-Sept 84 or lower levels. Since Jan 85 collapse has enlarged the Inner Crater and the lava lake has been exhumed. Several small convecting lava pools grew from 1985 through 1987.

A geochemical study was made of bombs erupted between 1972 and 1987 to search for changes in composition which may coincide with the 1984 increase in eruptive activity. Electron microprobe analyses of olivine ($Fa_{46}Te_3Fo_{51}$), pyroxene ($Wo_{47}En_{36}Fs_{17}$) and weakly zoned anorthoclase ($An_{12-23}Ab_{68-69}Or_{10-21}$) show no significant changes through time. Microprobe transects across anorthoclase and pyroxene from 1986 bombs show no discontinuities. Analyses of glass from bombs erupted from 1972 through 1986 are similar, indicating no change in the magma composition or its degree of crystallization.

The increase in magnitude and violence of eruptions in 1984, as compared with other years, is consistent with a higher volatile content of the magma. The volatiles may have been introduced into the magma chamber by a batch of volatile-rich (non-degassed, relative to the convecting magma already present in the lake and underlying chamber) magma, or by addition of a fluid phase. Our analytical data show that if new magma was introduced it was mineralogically and compositionally identical to that already present in the magma system. Frequent microearthquakes swarms preceding the eruptions in 1984 may have been related to magma injection. There was also a slight inflation of the summit area of Erebus between 1983 and 1985 consistent with magma injection. On the otherhand if volatiles were enriched in the form of a fluid it was probably CO_2-rich, because the H_2O content of the magma is low and thus saturation and separation would only occur at shallow depths. The CO_2 could have been evolved from basanite and intermediate composition magmas which undergo fractional crystallization to form the anorthoclase phonolite.

SO_2 FLUX MEASUREMENTS DURING A PERSISTENT SUMMIT CRATERS ACTIVITY ON MOUNT ETNA (SICILY)

CALTABIANO, T., BUDETTA, G. and ROMANO, R.,
Istituto Internazionale di Vulcanologia
C.N.R. - Catania - Italy.

After the last flank eruption of October 1986 - February 1987, persistent eruptive activity was noted only at the Summit Craters of Mt. Etna, and without paroxysmal eruptive events.

Since June 1987 some periodic measurements of the SO_2 flux coming out of the Summit Craters have been made with a MINI-COSPEC correlation spectrometer.

This paper reports the data obtained, relating them with other parameters connected to the Etnean area dynamics. In particular, the correlations apparently possible with seismic and summit crater eruptive activity are discussed.

The period of measurements considered coincides with a state which is relatively steady and of less eruptive activity. This allowed us to obtain information about SO_2 flux that, as far as Mt. Etna is concerned, can be considered a baseline.

On the basis of this we have hypothesized a steady state behavior useful for surveillance purposes of the volcano.

ESTIMATION OF SEISMIC AND VOLUMETRIC MOMENTS FOR THE MARCH 1981 ERUPTION AT ETNA VOLCANO

CALTABIANO, T., NUNNARI, G., PUGLISI, G.
Istituto Internazionale di Vulcanologia - CNR - Catania, Italy, CRISTOFOLINI, R., GRESTA, S., and PATANE', G., Istituto di Scienze della Terra, Catania University, Italy.

The March 17-23, 1981 flank eruption is one of the most interesting among the recent eruptive episodes occurred at Etna volcano.

An estimate of the cumulative seismic moment (ΣMo) for the earthquakes related to the swarm which preceded and accompanied the eruption has been made, giving a value of about $1.3*10^{22}$ dyne*cm.

From the volume of the erupted lavas ($30*10^6$ m^3) the relative volumetric moment ($M_v=K\mu\Delta V$, as proposed by Mc Garr (1976)) resulted about $6*10^{24}$ dyne*cm).

The ratio between the two values is two order of magnitude, confirming previous results based on the comparison between seismic and potential energy for this and other etnean eruptions (Cristofolini et al., 1987).

This fact can be explained by a magma transport mechanism that, at Etna, should occur mainly aseismically, also for flank eruptions.

Furthermore, the analysis of both trilateration and leveling data allows us to estimate the energy associated with ground deformations accompanying the eruption.

The value of seismic efficiency η, defined as the ratio between ground deformation energy and seismic energy, is also computed of about 2+3 %.

In this work the obtained results will be discussed in view of a better definition of the eruptive mechanism at Etna volcano.

PYROCLASTIC DEPOSITS OF THE NOVEMBER 13, 1985 ERUPTION OF NEVADO DEL RUIZ, COLOMBIA

CALVACHE V., Marta Lucia Department of Geology and Geophysics, Louisiana State University, Baton Rouge, LA 70803 USA

The November 13, 1985 eruption of Nevado del Ruiz produced a series of pyroclastic flows and surges that eroded channels on the surface of the summit glacier and generated lahars which descended most of the rivers that drain the volcano. The stratigraphy of the proximal pyroclastic deposits indicates that there were at least four episodes during the eruption. Episode I, deposited an unusual surge consisting of small pieces of ice mixed with ash and exhibiting planar stratification. Ballistically emplaced fragments are also intercalated with this unit. During Episode II, at least 2 pyroclastic flows were generated. These flows contain the most evolved pumice of the entire eruption with the SiO_2 content of matrix glass between 74.5 and 74.9 percent. High K_2O content (above 5 percent) may indicate the high degree of evolution reached by a magma undergoing fractional crystallization. The fractionation process may have set up a pre-eruption chemical gradient in the chamber which began with a dacitic cap and progressed downwards into an andesitic composition. As the eruption continued, magma was tapped from increasingly deeper levels. Episode III is marked by the emplacement of welded tuff with an average SiO_2 content of about 66 percent in the matrix glass. The final Episode (IV), was characterized by the development of a high-altitude eruption column and the emplacement of several non-welded pyroclastic flows. Banded pumice is common in the pyroclastic flows as well as in the pumice fall. Co-existing dark and light pumice bands differ in SiO_2 content by 3.5 percent and are in general similar to the composition of welded pumices from episode III. The compositional zonation of the pyroclastic deposits from episode I to IV suggests that a near-surface compositionally-stratified magma body was tapped during episode II. During episodes III and IV the main body of magma was involved, although the coexistence of compositionally distinct pumice clasts at similar stratigraphic levels argues for mixing of magma from different levels in the chamber during the eruptive process.

STRONTIUM ISOTOPE AND TRACE ELEMENT GEOCHEMISTRY OF PICO DE ORIZABA, TRANS MEXICAN VOLCANIC BELT, MEXICO: COMPARISON OF PHASES II AND III.

CALVIN, E.M., KUDO, A.M., BROOKINS, D.G., WARD, D.B. (all at Department of Geology, University of New Mexico, Albuquerque, NM 87131)

The Trans Mexican Volcanic Belt (TMVB) is unique relative to other continental volcanic arcs in that the strike of the arc trends obliquely to the Middle American trench. At 5700 m, Pico de Orizaba is the largest stratovolcanic complex of the TMVB, lying 450 Km N.E. of the convergent margin between the Cocos and North American plates.

Pleistocene to Recent lavas comprising Orizaba are a compositionally diverse suite of calc-alkaline basaltic andesite, andesite and dacite. Previous investigators (1) proposed a three-phase construction for Orizaba; this study concentrates on the second and third (middle and youngest) phases. Investigations of phase III volcanics (2) revealed an SiO2 range of 55% to 66% and an 87Sr/86Sr range of 0.7039 to .7050. This diversity, in conjunction with common diorite and calc-silicate xenoliths, attest to some degree of crustal contamination. Trace element and Sr-isotopic compositions of phase III volcanics appear to be inconsistent with genesis of Orizaba lavas via any simple fractional crystallization mechanism (2). Phase II volcanics collected from three eruptive centers on Orizaba's S.W. flank (Cerra La Negra, Cerro Colorado and Tres Cruces) are compositionally more uniform; two pyroxene andesites yield SiO2 from 56% to 63% and 87Sr/86Sr from .703759 to .704543 (+/- 4.9 ppm). Phase II chemistry also shows inconsistencies with simple crystal fractionation and appears to preclude simple two-component mixing for genesis of Orizaba lavas. However, plots of 87Sr/86Sr vs. 1/Sr and Sr suggest that magma mixing and/or crustal contamination may have played some role in the formation of phase II rocks. This is further substantiated by a pseudoisochron (corresponding to approximately 231 Ma) obtained for phase II andesites.
Additionally, Pearce element ratios of (2Ca+Na)/K vs. Al/K indicate that crystal fractionation, dominated by plagioclase with minor pyroxene, also contributed to petrogenesis.

Relative abundance of xenoliths and greater petrologic diversity of phase III material suggest more extensive crustal interaction and perhaps increasingly diverse source magmas compared to phase II. This may account for a general paucity of correlation between major and trace element compositions with Sr-isotopic abundances of phase III volcanics and a more cohesive correlation among phase II material. This may be facilitated by protracted residence times for phase III magmas, in turn allowing prolonged wallrock assimilation and fractional crystallization.

(1) Robin, C., and Cantagrel, J. (1982), Bull. Volcanol., vol. 45, p. 299.
(2) Singer, B., et al., (1987), G.S.A. (abstract), Fall Meeting, 1987.

ORIGIN OF THE VOLUMINOUS MID-CENOZOIC IGNIMBRITES OF WESTERN MEXICO: IMPLICATIONS OF Sr-Nd-Pb ISOTOPIC COMPOSITIONS OF CENOZOIC BASALTS, DEEP CRUSTAL GRANULITES, AND MANTLE PYROXENITES

CAMERON, K.L. (1), NIMZ,G.J. (1,2), NIEMEYER,S. (2); and ROBINSON, J.V. (1); (1) Earth Sciences, University of California, Santa Cruz, CA, 95064; (2) Lawrence Livermore National Laboratory, Livermore, CA, 94550

The most conspicuous mid-Cenozoic volcanic rocks of western Mexico are rhyolitic ignimbrites; however, some intermediate lavas are interlayered with the ignimbrites and abundant intermediate lavas, at least in part mid-Cenozoic in age, underlie the rhyolites. Interlayered basaltic lavas, although rare, are potentially important because most models for the origin of voluminous rhyolites require a major pulse of basaltic magmatism. Depending on the model, the mafic magmas serve either as the heat source for crustal anatexis or as parental melts that evolve into silicic magmas by AFC or MASH. In Chihua-hua, the basalt-andesite-rhyolite series has "baseline" Sr and Nd isotopic values that scatter significantly but are mainly independent of silica and are near Bulk Earth ($^{87}Sr/^{86}Sr$ between 0.7043 and 0.7050; ϵNd between +2 and -2). Rising above the baseline values are some andesites and rhyolites with $^{87}Sr/^{86}Sr$ as high as 0.7070, but even these have $\epsilon Nd > -2$. Pb isotopic data on the rhyolites are limited to Batopilas in the Sierra Madre Occidental. Here a basalt to rhyolite series is virtually identical in Pb isotopic ratios (Barreiro et al., 1982, CIW Yearbook; Nimz, unpub.). In order to assess the relative contributions of mantle and crustal components to the silicic rocks, the following are vital to determine: (1) the isotopic compositions of deep crustal lithologies, and (2) the sub-crustal isotopic compositions of mid-Cenozoic basaltic magmas. Samples from the La Olivina xenolith locality in the Chihuahuan Basin and Range provide data bearing on both of these issues.

Granulite-facies deep crustal xenoliths at La Olivina are of two main classes: those that have isotopic compositions appropriate for LREE-enriched Proterozoic rocks (e.g. $\epsilon Nd \approx -10$), and those that have ϵNd near Bulk Earth ($\epsilon Nd \approx 0$). The latter are dominantly two-pyroxene mafic granulites containing about 50% plagioclase. Three mafic granulites have $^{87}Sr/^{86}Sr = 0.7045$ to 0.7057, $\epsilon Nd = +1.6$ to -0.4, and $^{206}Pb/^{204}Pb = 18.62$ to 18.78. Although undated, their isotopic compositions are so similar to those of the volcanic rocks that they seem related. For example, mid-Cenozoic basaltic rocks from the area have $^{87}Sr/^{86}Sr = 0.7042$ to 0.7047, $\epsilon Nd = +0.7$ to -1.7, and $^{206}Pb/^{204}Pb = 18.23$ to 18.68. Positive Eu anomalies, high concentrations of compatible elements, high Mg-numbers in some, and model calculations establish that most if not all of the mafic granulites are cumulates, and their $^{147}Sm/^{144}Nd$ (≈ 0.17) is that expected for cumulates from mid-Cenozoic basalts. Although the mafic granulites have Nd depleted-mantle model ages of 1100 to 1400 Ma, these ages are irrelevant if the mafic granulites crystallized from melts with $\epsilon Nd \approx 0$. The Nd budget of the deep crust beneath La Olivina is dominated by the LREE-enriched Proterozoic rocks (24-60ppm Nd) because the Nd concentrations of the mafic granulites are so low (3-14 ppm).

As basaltic magmas rise through the mantle they vein lherzolite wall-rock with pyroxenite. These pyroxenites provide information on the sub-crustal isotopic compositions of the basaltic magmas before the magmas have an opportunity to interact with overlying continental lithosphere. At La Olivina, equigranular metapyroxenites are found that are similar in isotopic compositions to the mid-Cenozoic basalts. Seven metapyroxenites have $^{87}Sr/^{86}Sr = 0.7038$ to 0.7043, $\epsilon Nd = +3$ to +1, and $^{206}Pb/^{204}Pb = 18.55$ to 18.80. These rocks are plagioclase-free websterites and olivine websterites with relatively high Mg numbers (0.81 to 0.85). One is found in a composite xenolith with lherzolite establishing a mantle origin for that one, if not all the metapyroxenites. These metapyroxenites are interpreted to be mid-Cenozoic in age, and if that is true, they demonstrate that "baseline" Sr and Nd isotopic compositions of the mid-Cenozoic volcanic rocks could be mostly mantle in origin.

The isotopic data on the deep crustal and mantle samples are consistent with the interpretation that the intermediate to silicic magmas evolved from basaltic magmas with ϵNd and $^{87}Sr/^{86}Sr$ near Bulk Earth. If the primary role of the basaltic magmas was that of a heat source (underplating) for crustal anatexis, then the isotopic compositions of the silicic rocks should reflect a significant contribution from the most fusible, Nd-rich Proterozoic rocks. Little Proterozoic crustal component is needed to model the isotopic compositions of most intermediate and silicic rocks, but "contamination" with crust similar in isotopic composition to the volcanic rocks cannot be ruled out. Nevertheless, the eruption of the voluminous ignimbrites apparently marked a major crust-forming event, and the mafic granulites may be samples of young, mid-Cenozoic crust that underlies much of western Mexico.

INTRAPLATE ALKALIC VOLCANISM AND MAGMATIC PROCESSES ALONG THE 600-KM-LONG MAKKAH-MADINAH-NAFUD VOLCANIC LINE, WESTERN SAUDI ARABIA

CAMP, Victor.E., Department of Geological Sciences, San Diego State University, San Diego, CA 92182; ROOBOL, M.John., Directorate General of Mineral Resources, P.O. Box 345, Jeddah, Saudi Arabia; HOOPER, Peter.R., Department of Geology, Washington State University, Pullman, WA 99163

Miocene-to-Recent continental volcanism on the western Arabian plate has produced 180,000 km² of well-preserved alkali basalt lava fields. Known locally as the **harrats**, these large volcanic plateaus were extruded from linear vent systems. The longest vent system is the Makkah-Madinah-Nafud volcanic line (MMN) in western Saudi Arabia. The MMN extends for 600 km along a N-S strike, and it is segmented into smaller, slightly en echelon, vent systems from which Harrats Rahat (19,830 km²), Khaybar (14,063 km²) and Ithnayn (3,988 km²) were extruded over a period of 10 million years.

The loci of volcanism along the MMN migrated to the north with time; the three harrats are thus only partly contemporaneous. However, the stratigraphic sequence in each harrat is broadly similar. Early eruptions produced extensive lava flows which were primarily composed of olivine transitional basalt (OTB). Later, less voluminous eruptions were composed of OTB, alkali olivine basalt (AOB), and hawaiite. The most recent eruptions were composed of minor OTB, abundant AOB and hawaiite, and significant amounts of mugearite, benmoreite, and trachyte. Restricted comendite, also a product of the most recent eruptions, occurs as domes and tuff rings in the scenic, high central vent area of Harrat Khaybar.

Over the past 5 m.y., continental OTB-to-trachyte volcanism along the MMN has been contemporaneous with (1) oceanic tholeiitic volcanism along the Red Sea axial trough, and (2) continental basanitic-to-phonolitic volcanism on some harrats not associated with the MMN; these more undersaturated harrats commonly contain abundant ultramafic nodules. The evidence suggests that the three magma series evolved from a common source in the asthenosphere, but that the resulting magma types differ by the degree of partial melting, and by the subsequent magmatic processes in effect during magma ascent.

We suggest a model in which the mantle beneath the MMN underwent 15-20% partial melting of garnet lherzolite to produce a primary magma which rose and accumulated at the crust-mantle boundary. Varying degrees of picotite-bearing olivine fractionation then produced OTB magmas which rose quickly through the crust and were extruded in massive outpourings along the entire MMN. Some OTB magma became trapped in crustal magma chambers; here, AOB and hawaiite magmas developed as the result of open-system fractionation in concert with magma mixing as the chambers were continuously replenished by rising OTB. On central Harrat Khaybar, a concentric distribution of increasingly differentiated vents suggests that at least one of these reservoirs developed as a large, high-level, zoned magma chamber. Peralkaline comenditic liquids at the top of this chamber were derived from a combination of advanced fractionation of trachytic magma, crustal assimilation, and volatile complexing.

THE JUNE 1984 ERUPTION OF MERAPI (JAVA, INDONESIA)

CAMUS, G., BERTHOMMIER, P., GOURGAUD, A., Centre de Recherches Volcanologiques, Clermont-Ferrand, France.
BAHAR, I., Merapi Volcano Observatory, Jogjakarta, Indonesia.
BOUDON, G., Observatoire de la Montagne Pelée, St Pierre de la Martinique, France.
LAJOIE, J., Département de Géologie, Université de Montréal, Canada.

During historic times (<2 centuries), St Vincent-type and Merapi-type eruptions occurred at Merapi : the 1984 one was typically of the Merapi-type. The nuées ardentes were emplaced on june 13 and15 (after five days of increasing sismicity), along the Batang, Blongkeng and Krasak rivers : the major phase occurred between 2h15 and 6h00, on june 15.

The deposits : Two nuées ardentes deposits were found in Blongkeng river just after the eruption :

U1, the lower (2h15 explosion), 7 km long, the surface of which was characterized by abundant vesiculated blocks of juvenile magma, and charcoal (in situ temperature 280°C)

U4, the upper (channellized in the axial furrow of U1 or in the lateral gullies) 6.5 km long, the surface of which was characterized by fragments of the dome and uncarbonized wood.

By september 1988 the deposits were cut from the top to the bottom by the Blongkeng river.

U1, 2.7 to 12 m thick, is a reversely graded tuff breccia made of blocks up to 40 cm derived from the fragmentation of the dome in a matrix of ash and lapilli, capped by a veneer of highly vesiculated blocks.

U4 is 0 to 3.5 m thick, made up of coarse lapilli and ash, and more rarely of blocks up to 37 cm ; it exhibits several sub-units, and is normally graded, with long-wave (>20 m) antidune like undulations.

Two intermediate units (U2 and U3), thin, lens-shaped bodies, were also found ; they are made up of coarse to fine ash, normally graded and exhibit wavy structures and cross bedding.

Magmatology

The juvenile magma is heterogeneous (mixed).

The acid and basic members of the mixing are characterized by their mineralogy and the composition of the glasses :

	Basic	Acid
Glass	70% SiO_2	75% SiO_2
Plagioclase	Reverse zoning (An 45-An 70)	Normal zoning (An 90-An 70)

Interpretation

The june 1984 eruption of Merapi can be interpreted as follows

(i) mixing of two magmas, slightly contrasted, after a short break in the magma supply (3 months) : triggering of the eruption after several days.

(ii) explosive destruction of the 1979-1984 dome (june 13 to june 15, 2h15) and emission of a small quantity of juvenile magma : emplacement of U1 flow, Merapi-type (a typical grain-flow).

(iii) hydromagmatic phase when the regional aquifer gained access to the conduit : emplacement of numerous, surge-like, nuées (ex U2-U3, typical dilute turbulent flows and U4, typical turbulent flow of high concentration).

Such a succession : magmatic-hydromagmatic activity is common (Vesuvius, 79 ; Galunggung, 1982-83, and has widespread implications with regards to volcanic hazard evaluation.

EXPERIMENTAL AND THEORETICAL STUDIES OF THE MAGMATIC VAPOR EVOLUTION PROCESS

CANDELA, PHILIP A., Laboratory for Mineral Deposits Research, Department of Geology, University of Maryland, College Park, Maryland 20742

The generation and testing of specific magmatic-hydrothermal hypotheses for the origin of porphyry, skarn, and other types of ore deposits can be accomplished by the forward modeling of magmatic-aqueous fluid evolution. Algorithms (Candela, Rev. Econ. Geol. v. 4, 1989) yield the concentrations of elements of interest in the magmatic aqueous fluid (and in other magmatic phases), and the efficiency with which the aqueous phase can remove elements from the melt. In addition to the calculation of model ore-fluid compositions, some characteristics of volcanic gases can be explored by these methods.

The modeling requires the input of a large amount of experimental data on the partitioning of the elements of interest among the melt, vapor and crystalline phases. The pertinent data have been collected under a rather restricted range of conditions (750-900C and 1-2kb); however, general trends can be obtained under other conditions. Fluid compositions and efficiencies of removal can be calculated (for either first or second boiling) as a function of the initial water concentration in the melt, $C_w^{l,o}$, the saturation water concentration $C_w^{l,s}$ (which is a function of depth), the Cl/H_2O ratio of the melt, and the bulk mineral/melt partition coefficients. The general composition range of fluid inclusions from porphyry deposits can now be reproduced by this model.

Modeling and recent experimental data suggest that pressure exerts a rather strong control on the composition of the magmatic aqueous phase and on the efficiency of removal of metals from melts. Urabe (Econ. Geol., 1987) has shown that some vapor/melt partition coefficients decrease with increasing pressure. Modeling of the second boiling process has shown that as depth increases (for a given $C_w^{l,o}$), the efficiency of removal of compatible elements decreases relative to the efficiency of removal of incompatible elements. Recent experiments in my laboratory indicate that the crystal/melt partitioning of W and Mo is a function of oxygen fugacity. These data suggest that the efficiency of removal of Mo, relative to W, increases with increasing oxygen fugacity. It is also possible to contrast the results of first and second boiling. First boiling favors the removal of elements with high vapor/melt partition coefficients, whereas second boiling favors the removal of crystal-incompatible elements. Aqueous phase evolution from decompressing, subvolcanic permeable magmatic foams (first boiling) at high Cl/H_2O ratios (~ 1/10 by wt.) can result in the infiltration of Cu, Zn,Mn-rich, Mo-poor fluids into permeable wall rocks. Surfaces of ash particles coated by precipitates from such fluids should be rich in Cu,Zn, and Mn and comparatively poor in B and Mo.

VOLCAN DE COLIMA: PRESENT ACTIVITY INFERRED FROM STRATIGRAPHIC RECORDS AND GEOCHEMICAL DATA.

CAPACCIONI B., Istituto di Mineralogia e Petrografia, Via M.Oddi 14, Urbino, Italy.
RODRIGUEZ S., Istituto di Geologia, U.N.A.M., Coyoacan, Mexico D.F., Mexico.

In the last 0.5 m.y. the Colima Volcanic Complex (Colima state, Mexico), which is composed by two huge stratovolcanoes (Nevado and Fuego), have experienced different kinds of eruptions from plinian to almost effusive type, with recurrent Merapi and/or St.Vincent events. These different activities lead to the building of an high (several meters above the base) and steep cone (more than 30°deg, as determined at the present Volcan de Fuego). These conditions make the edifice instable and susceptible to produce a rockslide-debris avalanche. On the stratigraphic base, three different avalanche events referring to the Nevado de Colima and two referring to the active Volcan de Fuego have been recognized.

A detailed field work concerning the areal distributions and textural features of these two debris avalanche deposits from Volcan de Colima (or Volcan de Fuego), together with a series of geochemical analyses on several samples of surficial waters from the southern flank of the volcano and gases from the summit dome, have been carried out.

The older avalanche deposit appear to cover more than 1000 Km2, with a volume not less than 12 Km3 and to be distributed towards the south, as already suggested by other authors (Robin et al., 1986). Charcoal samples, emballed in the deposits itself, have been collected in order to obtain 14C datations. The younger avalanche deposit shows again a southward distribution but a quite smaller volume, probably not exceeding 1-2 Km3. Its flow direction appear to be influenced by the asymmetric hummocks distribution of the older one. The geometry of the debris avalanche deposits, together with the following fluvial erosion, resulted into the present topography of the southern flank of Volcan de Colima. Several recent "block and ash flow" deposits, probably referring to Merapi-type activity, appear to be channelized towards the village of S.Marcos, which, therefore, can represent an area of high volcanic hazard.

With reference to geochemical features of natural fluids (waters from streams, lakes and springs), the compositions of waters from the southern flank of Volcan de Colima appear absolutely not influenced by uprising magmatic fluids, so minimizing the possibility of the opening of parasitic vents along the N-S main fracture. On the contrary, the composition of gaseous phases from the summit dome seem to represent a mixing between magmatic gases (HCl and SO2) and air, with a clear predominance of the latter. This mixing could be the typical products from an active growing dome,as observed from M.St.Helens.

EMPLACEMENT MECHANISMS OF DOME-LIKE STRUCTURES INSIDE THE LATERA CALDERA (VULSINI VOLCANOES, ITALY).

CAPACCIONI B., NAPPI G., RENZULLI A., SANTI P.
Istituto di Mineralogia e Petrografia,
Via M. Oddi 14, University of Urbino, Italy.

The last explosive phase of the Latera Caldera (Central Italy) was characterized by volcanic products belonging to the High Potassium Series. These cover approximatively an area of 120 Km^2, distributed both inside and outside the north-western sector of Latera Caldera ("Vulcanite Complessa di Pitigliano", Auct.). During this event the present north-western side of the Caldera collapsed, outlining a distinct structure, called Vepe Caldera.

The depositional units of such an eruptive phase, seem to refer to a rapid succession of different kinds of eruptive events. Beyond the Latera Caldera, the initial activity is represented by several white pumice flow units, composed of leucite-free pumices in micropomiceous matrix. After a short pause, the activity resumes with the emplacement of a pumice flow, constituted of grey pumices with leucite phenocrysts. In the following phase, strongly welded flow units took place; the lower shows a typical "pipernoid" facies with brown collapsed pumices in a fluidal texture. In the overlying unit the "pyroclastic" character becomes progressively less evident. In the final "foam lava" facies, it tends to be replaced by a lava-like feature.

Inside the Caldera depression such lava-like rocks give rise to a series of dome-like structures along the Vepe ring fracture. They show a conical shape with a high/diameter ratio of 0.17 and a flank steepness of about 18°. Their development results from the superposition of a successive flows, which can be related to lava flow-like units with a different vesciculation.

Let us consider now the eruptive styles of the "Vulcanite Complessa di Pitigliano" units. First, an evolved melt of phonolitic composition erupts as pyroclastic flow. Since the initial rapid emission of the phonolitic melt leaves a partially depleted magma chamber, a roof collapse occurs. The consequent piston-like effect produces a squeezing out of the degassed residual melt. In the final phase the piston-like effect represents the only active mechanism, when an outpouring of an almost completely degassed melt determine a series of dome-like structures ("Monte Calveglio di Latera", "Poggio Montione", "Poggio Pilato" and "Monte Calveglio").

RADON AS A PRECURSOR OF ERUPTIONS: A PROGRESS REPORT

CAPALDI, G., Department of Geofisica e Vulcanologia, University of Naples, Italy
GASPARINI, P., Department of Geofisica e Vulcanologia, University of Naples, Italy
PECE, R., Department of Geofisica e Vulcanologia, University of Naples, Italy.

In the last decade many laboratory data concerning the effect of temperature and pressure on Radon emission from rocks and minerals have been collected by our and other laboratories. We have also determined how pH can effect Radon solubility in groundwaters. All the available data show that Rn emission increases when the applied stress triggers fracture propagation and when rocks are heated at temperature between 100 and 200 C. Rn gas/water distribution coefficient is strongly dependent on pH. All these informations are used to build models of Radon degassing and propagation in volcanic areas.

Field data relative to some volcanic areas of Southern Italy show some degree of correlation with the volcano dynamics of these areas. Space distribution of Rn emission seem to be related to stress concentration.

A model relating Radon circulation to magma uplifting and fracture propagation is presented.

LATERAL COMPOSITIONAL VARIATION IN FLOW UNITS IN THE BANDELIER TUFF, NEW MEXICO

Caress, M.E., Department of Geological Sciences, University of California, Santa Barbara, CA 93106

The Tshirege Member of the Bandelier Tuff (1.12 Ma) is an ignimbrite composed of multiple flow units in which vertical compositional variation has been previously described. In this study, the lowermost, most voluminous flow unit of the Tshirege Member and two overlying flow units of lesser volume were correlated and sampled in Pueblo canyon, oriented radially to the caldera. Samples have been analyzed from several levels at 4 localities in the lowermost flow unit (8 to 22 km from the caldera rim), and from two localities in the upper flow units (13 and 22 km from the rim). Microprobe analyses of sodic sanidines from the matrices of all three flow units show similar, subtle but distinct geochemical trends From distal to more proximal localities, the average Or content decreases, while the compositional range of feldspar increases. Minor vertical stratification is present in the most proximal locality of the lower flow unit, indicated by an upward increase in Or component, but is less pronounced than the observed lateral changes. The base of the flow unit at the most proximal locality has a lower Or component than those at any of the distal sites. The trend of decreasing Or content towards the source is the same trend observed upward within a stratigraphic section through all three flow units, and is consistent with eruption from a magma chamber which decreases in Or content downwards.

The lateral preservation of compositional trends derived from progressive tapping of deeper levels within a zoned magma chamber indicates that the material in the flow moved laterally and was deposited as a unit, with a minimal degree of turbulence or mixing. The first material to be erupted traveled farthest, and the more subtle vertical variation may be the result of partial overriding of earlier erupted material by later segments of the flow. The existence of identifiable compositional variation within flow units has the potential of providing information on the manner by which material is transported and deposited in pyroclastic flows, and has implications for the interpretation of compositional variation and mixing in magma chambers.

INTENSITY AND MAGNITUDE OF POST-GLACIAL PLINIAN ERUPTIONS AT MOUNT ST. HELENS.

Carey, S., Gardner, J. and H. Sigurdsson,
University of Rhode Island, Graduate School of Oceanography, Narragansett, R.I. 02882

During post-glacial times Mount St. Helens has been the site of numerous plinian eruptions which have produced widespread tephra fall deposits over large areas of the NW United States and Canada. Maximum pumice and lithic clasts have now been measured at 51 sites for the 18 May 1980, T, We, Wn, and Yn layers in order to construct isopleth distribution maps for each deposit. Isopleth geometries are used to calculate peak eruption column heights and intensities (magma discharge rates) based on a theoretical model of tephra dispersal. Excellent agreement is found between the model-derived column height of the 18 May 1980 eruption and radar observations of the actual column. New proximal thickness measurements are combined with a general distal extrapolation, based on examination of many plinian deposits, to calculate the magnitude (erupted volume) of each eruption.

Layer Yn (3,510 Ybp) corresponds to the eruption with the highest intensity and largest magnitude at Mount St. Helens in post-glacial times. It began with a column height of 22 km and grew to a peak of 31 km before gradually declining at the end of the plinian phase (~26 hours). At sites close to the volcano several intraplinian surge deposits are present in the upper part of the fall layer. These have been traced to a distance of 40 km to the NE of Mount St. Helens and indicate a larger flowage hazard zone than has previously been proposed. Peak intensity of the plinian phase was $1x10^8$ kg/s and the total erupted volume was 4.0 km^3 (DRE of magma). For comparsion, the eruption of Yn is virtually identical to the 79 AD eruption of Vesuvius based on 1) area enclosed by lithic isopleths, 2) peak intensity and column height, 3) temporal evolution of column height, 4) total erupted volume, and 5) the late stage development of intraplinian surges.

Layers Wn and We of the Kalama episode were deposited within two years of each other (1480 and 1482 AD) from eruptions intermediate in scale between the 18 May 1980 and Yn event. Peak column height during the larger, Wn eruption was 24 km, corresponding to an intensity of $5x10^7$ kg/s. Eruption column height during the We was lower than during the Wn and attained a maximum elevation of 21 km with an intensity of $2.5x10^7$ kg/s. The magnitude of the Wn deposit is about one half of Yn layer, or 2 km^3 DRE of magma whereas the We was only 0.4 km^3. Durations of the events are estimated to be 26 and 10 hours respectively. Minor intraplinian surges are also present in the upper part of both the Wn and We fall deposits.

The most recent plinian eruption prior to the 18 May 1980 activity was a small event which produced the T fall deposit in 1800 AD. It forms a highly elongated, yet relatively thin depositional lobe northeast of the volcano. Peak column height was only 16 km with an intensity of $8x10^6$ kg/s, or similar to the average column height of the 18 May 1980 eruption. Isopleth shapes indicate strong tropospheric wind velocities suggesting that the eruption may have occurred in the winter months. The magnitude of the T eruption was 0.5 km^3.

When compared with plinian eruptions from other volcanoes the post-glacial eruptions of Mount St. Helens span from the lower to the middle part of the known range in intensity and magnitude. The eruptions follow the previously-documented positive correlation between eruption intensity (column height) and magnitude (total erupted volume), reflecting the control of progressive vent erosion and initial overpressures on magma discharge rate.

ARC – BACK-ARC BOUNDARY CONTROLS ON THE COMPOSITION OF CENOZOIC MAFIC LAVAS IN THE NORTHWESTERN U.S.

CARLSON, R.W., Dept. of Terrestrial Magnetism, Carnegie Institution of Washington, 5241 Broad Branch Rd., Washington, DC, 20015 and HART, W.K., Geology Dept., Miami University, Oxford, OH, 45056, U.S.A.

Mafic volcanism in the northwestern United States was most voluminous roughly 15 Ma ago during the flood basalt volcanism at Steens Mountain in south-central Oregon (Oregon Plateau) and in the Columbia River Province of Oregon and Washington. Following a hiatus of nearly 5 million years, the high-Fe, low-Mg tholeiitic volcanism that characterized the flood basalt episode was replaced by sporadic eruptions of relatively undifferentiated high-Al olivine tholeiites (HAOT) throughout the Oregon Plateau and extending into the Snake River Plain to the east and the Cascades to the west, but not into the Columbia Plateau to the north nor the more typical Basin and Range Province to the south.

We have characterized the Oregon Plateau previously (Carlson and Hart, JGR, 1987) as a developing back-arc basin behind the Cascade volcanic arc. A dramatic change primarily in isotopic composition of the HAOT occurs along the eastern border of the Oregon Plateau, roughly coinciding with the Oregon-Idaho border, that reflects a change in basalt source composition from relatively young mantle to the west to a 2.5 Ga old subcontinental lithospheric mantle beneath the Wyoming craton to the east (Hart, GCA, 1985). Through the center of the Oregon Plateau, however, there are only limited, if any, geographically related trends in basalt chemistry or isotopic composition. The major variability in basalt characteristics within the Oregon Plateau itself is the compositional difference between the two age groups outlined above.

At the western boundary of the extensional plateau, along the eastern edge of the Cascades, circa 15 Ma old tholeiitic lavas show many similarities to the central Oregon Plateau lavas, in particular in degree of fractionation and incompatible element enrichment and in Sr and Nd isotopic composition. The western lavas, however, do have some important chemical differences compared to their counterparts from the eastern and central Oregon Plateau. The 14 to 16 Ma tholeiites from the west follow more calc-alkaline differentiation trends compared to the Fe-enrichment typical of central Oregon Plateau lavas: e.g. at a MgO content of 4 wt%, western boundary samples have between 7 to 10 % FeO* (total Fe as FeO) versus 10 to 15% FeO* for the typical Steens Mountain type basalt. This difference in Fe is accompanied by higher Al_2O_3 (16 to 18% vs 14 to 16%), lower TiO_2 (0.9 to 1.6% vs 1.6 to 3.2%) and lower Zr/Ba (0.18 vs 0.3 to 0.9) in the western compared to central Oregon Plateau samples. These differences, however, are not accompanied by variation in Sr or Nd isotopic composition or in other indicators of crustal contamination such as K/P.

In general, the chemical differences between the western and central Oregon Plateau basalts are those expected between "arc" (western) and back-arc or intraplate lavas (central); i.e. calc-alkaline, high-field strength element depletion vs Fe-enrichment. The "arc – back-arc" transition occurs about 200 km east of the present locus of Cascade volcanism. Because of the similarity of the western and central Oregon Plateau basalts in Sr and Nd isotopic composition and in other indicators of crustal contamination, the differences between the lava types appear to indicate differences in the processes of their formation as opposed to chemically distinct sources or disparate degrees of crustal contamination from either crustal wallrocks or crustal material introduced into the mantle by subduction in the arc. This conclusion is supported by the characteristics of the younger HAOT that show little, if any, variation in composition across the Cascade-Oregon Plateau boundary. Many of the first-order distinctions between the two groups of circa 15 Ma old lavas can be explained if the western lavas fractionated a phase assemblage richer in pyroxene and relatively deficient in plagioclase compared to the central Oregon Plateau lavas. The details of the chemical variation across this province border zone, thus, may serve to illuminate the mechanism responsible for the distinct characteristics of arc and back-arc basalts.

GENESIS AND EVOLUTION OF CALC-ALKALINE MAGMAS IN THE ISLAND OF ALICUDI, AEOLIAN ARC (SOUTHERN TYRRHENIAN SEA)

CARNESECCHI F., PECCERILLO A., WU C.

Istituto di Scienze della Terra, University of Messina, Messina (Italy), and Department of Geology, University of Western Ontario, London (Canada)

Alicudi is the westernmost island of the Aeolian Archipelago, an island arc developed on a thin continental crust. The island consists entirely of volcanic rocks which range in composition from calcalkaline basalts (CAB), basaltic andesites (BA) to high-K andesites (HKA). The age of the outcropping volcanics range from less than 100 ka to about 30 ka. The most mafic basaltic lavas have Mg-v=72, Ni=120 ppm, which represent the highest values found in rocks from the whole Aeolian Arc. CaO, MgO, FeO, Ni and Sc decrease more or less regularly with increasing SiO2%. Alkalies, Al2O3, P2O5, LREE and other incompatible elements are positively correlated with silica. Sr displays scattered values. Sr isotope ratios range from 0.70379 to 0.70538 in CAB and BA, displaying a positive correlation with silica and Rb/Sr ratio. Interestingly, the more evolved HKA have poorly variable and lower Sr isotope ratios which range from 0.70352 to 0.70369. These are the lowest Sr isotope values found over the entire Aeolian Arc.

Geochemical and isotopic data rule out that the Alicudi volcanics represent one single comagmatic series derived by crystal fractionation from one parental magma. The simplest, and most likely, petrogenetic hypothesis is that the CAB-BA suite was formed by AFC processes, whereas the HKA derived by simple crystal fractionation processes starting from a common parental magma. The primary melt(s) were characterized by Sr isotope ratios as those of HKA and by a major and trace element composition more primitive than that of the analyzed CAB. Accordingly, the Alicudi basalts appear to have suffered significant interaction with crustal material, in spite of their high degree of primitivity. Since the Alicudi basalts display by far the most primitive compositions over the entire Aeolian Arc, the hypothesis that the mafic magmas from other islands also have been affected by crustal contamination appears very likely. This casts doubts on petrogenetic hypotheses that are based on the assumption that the mafic Aeolian Arc volcanics represent near-primary liquids whose isotopic composition closely matches that of the source.

VARIATIONS OF INCOMPATIBLE ELEMENT AND ISOTOPIC RATIOS ALONG THE CENTRAL AMERICAN ARC: EVIDENCE FOR MULTIPLE SOURCES

CARR, M.J., FEIGENSON, M.D., BENNETT, E.A.
Geological Sciences, Rutgers University, New Brunswick, New Jersey 08903

Large variations in LIL element ratios and isotopic ratios correlate with changes in regional geologic and tectonic parameters. The geochemical variations can be described by the mixing of four components in proportions that vary with crustal age and thickness and the depth and dip of the subducted slab.

Central Costa Rican magmas are a distinct group with high P, La, Ba, K at high MgO contents. Spidergrams show a smooth OIB-like pattern except for Nb depletion at some volcanoes. Isotopic ratios of Sr and Nd are along the mantle array at 0.7036 and 0.5129.

In western and central Nicaragua magmas appear to have a strong slab signature with high Ba/La (100 to 120) and isotopic ratios of 0.7041 and 0.5131. Spidergrams are almost flat in REEs, Ti, Zr and P but have positive Ba, K, Rb, Sr and negative Nb.

Low Ba/La ratios (10 to 30) characterize magmas that appear to be asthenospheric melts with minimal input from the slab. They have relatively smooth spidergrams with variable slopes suggesting changes in the extent of melting between the basalts of southeast Guatemala and those of central Nicaragua. Isotopically, these basalts plot on or near the mantle array intermediate between MORB and bulk earth values.

The Sr and Nd isotopic ratios of Guatemalan samples progress toward higher Sr (0.7046) and lower Nd (0.5127),indicating involvement of the Mesozoic and Paleozoic crust present there. This could occur either by incorporating locally derived sediment, recycled through subduction, or by AFC processes operating within the crust.

Crustal thickness is least in Nicaragua and increases toward both Guatemala and Costa Rica. Depth to the seismic zone and its dip are greatest in Nicaragua and decrease toward both Guatemala and northern Costa Rica. However, the slab abruptly shallows in central Costa Rica, adjacent to the subducting Cocos Ridge. The distinct magmas of central Costa Rica may be related to this perturbation in subduction geometry and may receive a contribution from the subducting hot spot trace.

From central Nicaragua to Guatemala there is a progression from high percent melts dominated by slab signature to lower percent melts dominated by asthenosphere signature. This progression accompanies a decrease in distance between the top of slab and the base of the crust, suggesting that the apparent change in melt fraction results from different extents of diapiric rise. The dip of the slab also decreases toward Guatemala. This may allow a greater amount of asthenospheric melt to be pulled into the volcanic front. Finally, the increase in crustal thickness toward Guatemala leads to more fractionated magmas, allowing a greater extent of AFC modification.

THE SIGNIFICANCE OF SEDIMENTS IN VOLCANIC SUCCESSIONS

CAS, R.A.F., Department of Earth Sciences, Monash University, Clayton, Victoria, 3168, Australia.

Surface processes operate at generally greater rates in volcanic terrains than in other surface environments. In areas of high relief, erosion produces stratigraphic discordances, and loss of stratigraphic record and of the record of the eruptive events. In depositional areas within and peripheral to volcanic terrains, depositional processes operate at two levels, and by the same range of mechanisms as in normal surface environments.

First, they operate at ambient levels and rates. The resultant sediments reflect the paleoenvironment and the physical conditions under which eruption and/or sedimentation took place. In particular relative ambient pressure and water presence both of which have fundamental effects on the style of volcanism can be inferred. Ambient sediments show normal sedimentary structures, and frequently have heightened levels of maturity and provenance diversity.

Secondly, surface processes are activated in direct response to volcanic eruptions, which increase topography and often liberate huge volumes of unconsolidated debris. Resultant surface processes operate at orders of magnitude rates greater than normal ambient processes. Such processes severely overload the ambient environment and produce deposits which are atypical of the ambient environment. These deposits however, being direct derivatives of primary eruptive products most clearly, reflect the style of volcanism. Mass-flow and/or high flow regime depositional processes are common, and the sediments are texturally immature and compositionally monomictic. Deposits resulting as a direct consequence of eruption may be difficult to distinguish from primary eruptive products, especially pyroclastic deposits. This is particularly the case where primary transportation modes translate into epiclastic analogues through interaction with surface water.

Tectonically induced sedimentation may also be evident and produces sediments of volcanic and/or basement derivation.

Provenance, facies characteristics, facies associations and position in stratigraphy may assist in interpreting the origins of sedimentary units in volcanic successions.

A representative range of examples from the rock record are considered.

TRANSPORTATION AND DEPOSITION OF PYROCLASTICS OF HYDROVOLCANIC TEPHRA.

CAS, R.A.F., Department of Earth Sciences, Monash University, Clayton, Victoria, 3168, Australia.

Pyroclastics of hydrovolcanic origin are dispersed/transported by a variety of processes:

1. Ballistic blasts disperse individual blocks and bombs, producing directed sag structures in wet, cohesive substrate, or minor or no disturbance in cohesionless substrate. Directed blasts of aggregates of blocks may produce fines depleted horizons consisting of continuous to discontinuous lenses, implying a fluid dynamic control.
2. Airfall, under both simple gravitational control and/or rain flushing.
3. Surge (base). Depositional processes, bedforms, structures and textures will depend on grainsize, surge velocity, and moisture content of the surge and substrate, but generally this is an area of poor understanding. Substrate adhesion and clumping of ash and moisture droplets in transit are likely to complicate concepts of depositional processes. Flow regime concepts and levels for cohesionless sediments in aqueous systems are inappropriate because of the foregoing and because the driving medium is gaseous, velocity levels and bed shear stresses are higher, and particle density variations due to vesicularity are significant. Because of variations in physical properties surges are not likely to produce consistent sequences of bedforms/structures downstream. There is also a lack of experimental/modelling data. A significant problem exists in distinguishing massive surge deposits from small volume pyroclastic flow deposits, if in fact there is a distinction.
4. Surge-modified fall deposits. Where both fall and surge activity occur in near-vent settings, the rain of fall tephra is affected by the turbulence of ground hugging surges. Where the rain of fall material is heavy, the deposits will have fall characteristics (planar layering, ballistics) with superimposed evidence of lateral turbulent eddies (ripples, discontinuous lensoidal layers). Low rates of airfall will result in deposits with normal surge characteristics. Co-surge ashes may also accumulate.
6. Pyroclastic flows. Characteristics of large volume deposits are well documented. Problems exist in distinguishing small volume flow deposits from the massive facies of deflated, overloaded surges.

THE 1988 ERUPTION OF ANAK KRAKATAU, INDONESIA: A RETURN TO PRE-1981 COMPOSITIONS

CASADEVALL, T.J., U.S. Geological Survey, Vancouver, WA, 98661, deNEVE, G., KASWANDA, O. and MacLEOD, N.S., Direktorat Vulkanologi, Bandung, INDONESIA

The cataclysmic eruption of Krakatau in August 1883 produced at least 18 km^3 of dacitic ejecta and created a large submarine caldera. In December 1927, a small volcanic cone appeared above sea level that by August 1930 had become a permanent island volcano, Anak Krakatau (1988 surface area, 3.2 km^2; subaerial volume, 0.20 km^3). Analyses of lava bombs collected from Anak Krakatau in 1929, 1930, and 1935 indicate that the erupted rock types ranged from basalt through dacite to rhyolite [SiO_2 = 52-69%], but the dominant rock type was basaltic andesite [SiO_2 = 52-55%]. From 1960 through 1979, vents on the southwestern part of Anak Krakatau erupted approximately 5 million m^3 of basaltic andesite lava flows.

An eruption in October 1981 produced a small volume (<1,000 m^3) of dacite ejecta [SiO_2 = 61-62%] containing significantly more silica than the 1960-79 products. Recently, Camus and others (1987, JVGR, v.33, p.299-316) interpreted this 1981 ejecta as the product of fractional crystallization that had occurred between 1979 and 1981 and warned that future activity would probably include explosive eruptions followed by emplacement of domes.

After a repose period of nearly 7 years, Anak Krakatau erupted basaltic andesite lava (Table) between February and April 1988, to cast doubt on the existence of a volumetrically significant body of fractionated magma beneath the vent. The eruption began in mid-February with about 2 weeks of intermittent explosions from a fissure on the south side of the 1960-79 cone. In late February and March, two small aa lava flows were extruded, while the explosions continued. By mid-March, approximately 50,000 m^3 of lava had been erupted in the two lava flows. Activity ended in early April. Because the Krakatau Islands are uninhabited, no protective measures were necessary during this small eruption.

The basaltic andesite lava flows of 1988 are chemically and petrographically similar to those of 1963-79. Reappearance of mafic lava suggests that the small-volume dacite ejecta erupted in 1981 is not simply the product of fractional crystallization. Furthermore, we detected no significant compositional variation among 1963-79 lava flows from Anak Krakatau. Thus, most of the magma beneath Anak Krakatau is probably basaltic andesite in composition, and any eruption of large volumes of fractionated magma is unlikely at present. The small volumes of dacite magma erupted in 1929-30 and 1981 may represent unerupted remnants of stored 1883 magma, or remelting of wallrock or previously erupted material. We believe that future activity is more likely to consist of relatively nonexplosive eruptions of basaltic andesite, rather than explosive eruptions of dacite. Additional studies are underway to document the growth of Anak Krakatau.

TABLE: COMPOSITION OF 1981 AND 1988 PRODUCTS (wt%, normalized to 100% water-free)

[1981] - SiO_2 60.8, TiO_2 1.0, Al_2O_3 16.9, FeO_t 6.7, MnO .15, MgO 2.3, CaO 6.0, Na_2O 4.3, K_2O 1.45, P_2O_5 .35.

[1988] - SiO_2 54.8, TiO_2 1.1, Al_2O_3 17.6, FeO_t 9.1, MnO .17, MgO 4.1, CaO 8.5, Na_2O 3.5, K_2O .91, P_2O_5 .33.

DEVELOPING AN OBSERVATIONAL FOUNDATION FOR MODELING CRYSTALLIZATION IN NATURAL SYSTEMS

CASHMAN, Katharine V. Dept. of Geol. and Geophys. Sci. Princeton U. Princeton NJ 08544-1003

Models of crystallization in multicomponent silicate systems are complicated not only by the difficulty in predicting nucleation and growth kinetics at a single point in time, but also by our incomplete understanding of their evolution through episodes of magma transport and cooling. Detailed studies of the products of active volcanic systems provide a phenomenological foundation for such modeling. I have measured the textural and chemical changes involved in the crystallization of groundmass plagioclase of 1980-1986 Mount St. Helens dacite and have interpreted these changes in light of both crystallization kinetics and the physical development of the Mount St. Helens system.

Textural measurements provide estimates of the growth rates of groundmass plagioclase microphenocrysts. Areal increases in crystal size are approximately constant through 1981, with rates decreasing slightly from 1981-1986; calculated linear growth rates are approximately 10um/yr. During the same period, measured number densities of crystals decrease from 1500 to 500/mm2. Measured plagioclase crystallinity of the same samples increases rapidly from June, 1980 to October, 1981, followed by a much slower increase in crystallinity through 1986.

Crystallinity changes may also be estimated from changes in the groundmass glass composition with time. If Na2O is used as a measure of plagioclase crystallization alone and an average composition of An40 is assumed, calculated changes in crystallinity match measured changes almost exactly. Both crystallinity and Na2O content change approximately linearly with time through 1981, suggesting that kinetically plagioclase crystallization follows a first-order rate law. The dramatic decrease in the rate of change after late 1981 may be the result of reaching plagioclase saturation; changes from 1981-1986 would then be the result of slow cooling of the shallow magmatic system.

The average anorthite content of plagioclase microphenocryst rims decreases with time (from An45 to An32), with the rate of change again somewhat more rapid through 1981. In any one sample, the An content of microphenocryst cores is approximately a linear function of crystal size, with more An-rich cores in larger microphenocrysts; linear trends project to measured rim compositions at small size. All plagioclase crystals show pronounced zoning patterns; interior zonations commonly have rounded corners and other evidence of resorption, even in very small crystals (20-30um). These observations suggest 1) continuous nucleation of plagioclase, 2) evolution of the equilibrium plagioclase toward more albitic compositions, and 3) the importance of non-equilibrium conditions in the development of the groundmass plagioclase.

Thus chemical and textural changes of Mount St. Helens lavas can be explained by 1) relatively rapid crystallization through 1981 resulting from a May 18, 1980 intrusion of material into a shallow (2-3km) reservoir on and the subsequent attainment of equilibrium plagioclase saturation for those P,T conditions, and 2) continued crystallization from 1981-1986 at a much reduced rate. Late 1981 also marks the time that the average the magma eruption rate decreased (Swanson et al., 1987) and the bulk chemistry of the lava reached its most mafic (Cashman and Taggart, 1983). The most unexpected observation is the decreasing number density of crystals with time despite evidence for continuous plagioclase nucleation; an explanation is the sytem's approach with time toward textural as well as thermodynamic equilibrium.

MONITORING SEISMICITY AND VOLCANIC ACTIVITY AT MT. ETNA VOLCANO (SOUTHERN ITALY) BY MEANS OF THREE-COMPONENT TEMPORARY ARRAYS.

CASTELLANO, M. and F. FERRUCCI, Osservatorio Vesuviano;249,Via Manzoni 80123 Naples (Italy)
PATANE', G. and S. IMPOSA, Dipt. Scienze della Terra, Università di Catania; 55, Corso Italia 95129 Catania (Italy).
HIRN, A., Institut de Physique du Globe; 4, Place Jussieu 75252 Paris Cedex05 (France).
DOREL, J., Institut de Physique du Globe; 73000 Clermont-Ferrand (France).

In late 1984, a 41 stations temporary seismic array run by I.P.G.-Paris and spread on the higher part (above 1,000 m. a.s.l.) of Mt. Etna volcano, allowed to draw a close picture of the final phase of a long-lasting eruption and of the associated intense central and peripheral seismicity.

By simultaneous P-S traveltimes inversion, evidence was supplied of a high velocity body underlying the Central-Eastern part of the volcano: relocation of the seismic sequences in the 3-D heterogeneous structure allowed to constrain strong spatial coherence of the events, not detectable without use of S-waves nor by ordinary location in a horizontally-layered model.

The information obtained by this field experiment was taken into account for planning a longer-term experiment: since April 1988 a three-component digital array is constantly operated on Mt. Etna by Osservatorio Vesuviano.

Centered on the Eastern, more densely inhabited, flank of the volcano, it is based on a PCM telemetered principal array (12 channels) and on some signal-triggered three-component recording units, routinely displaced for following the spatial variations of the seismicity. The array has been integrated, during shorter periods, by similar equipment of IPG-P and IPG-CF: a maximum total amount of 23 stations was run in the field during June 1988, when the most significant events of the whole year 1988 were recorded.

Location of the seismicity in the 3-D heterogeneous structure (as obtained by the 1984 survey) and time-space relationships between seismic peripheral and central volcanic activities are here illustrated.

Particular attention is given to the extremely shallow and strong events occurring on the lower eastern flank of the volcano, as well as to the grouping into "families" of the intermediate depth ($10 < z < 25$ km) earthquakes.

THERMAL OUTPUT OF MAJOR ERUPTIONS OF MAYON VOLCANO

CATANE, J.P.C., Philippine Institute of Volcanology, 5th & 6th Flrs. Hizon Bldg., 29 Quezon Ave., Quezon City, Philippines

The thermal energy released during the September 1984 eruption of Mayon Volcano is estimated from volumetric data of erupted magmatic products and their observed physical properties. The lava extrusion during the first phase and the ejection of pyroclastic material during the second phase are eruption of intermediate magnitude, intensity V+ on the Herdervari scale. The total energy yield for both eruptive phases is computed to be 8.5×10^{23} ergs. Cumulative volume and energy curves for major eruptions are constructed to correlate the amount of erupted solids as a function of time as well as identify the trend of the energy budget. The linear relationship of these curves tests the validity of Wadge's concept for steady state behavior, wherein the gradient defines the magma output rate during a given period. The average rate of magma supply of Mayon Volcano over the past 200 years of eruption history is approximately 0.001 cu.m./sec.

THERMAL WATERS AND NATURAL GASES IN THE VOLCANIC AREA OF Mt. AMIATA (CENTRAL ITALY)

CECCARELLI, A., ENEL-UNG, Via A. Pisano,120,Pisa,Italy
CORAZZA, E., and MAGRO, G., Istituto di Geocronologia e Geochimica Isotopica, Via Maffi, 36, Pisa, Italy,
PIERI, S., ENEL-UNG/P.C. Laboratorio Larderello,Italy,
and RIDOLFI, A., SCANDIFFIO, G., and VALENTI, M.,ENEL-UNG, Via A. Pisano, 120, Pisa, Italy

In the region of Mt. Amiata volcano, where geothermal systems are present and exploited, 44 thermal waters and 16 natural gases were sampled. The hydrothermal system is known from the wells tapping two main geothermal fields, their pressure being regulated by a hydrostatic load of 250 m a.s.l.. All sampled sites lie below this level.

Waters can be classified into the following types:

- calcium bicarbonate (shallow, in volcanics, flysch and carbonates);
- calcium sulfate (evaporite leaching, H_2S oxidation);
- alkali chloride (leaching of marine neogenic terrains);
- alkali bicarbonate (slow circulation in clay sediments).

Among gases CO_2 is the main component (>90%); CH_4 too is present in all samples at a few %, while H_2S is present in some samples at trace levels; H_2 is always in the range of ppm. The atmospheric components (O_2, Ar, N_2) are low and not derived from air such but from air-saturated groundwater, as shown by the Ne/Ar ratio. The ratios He/Ne and $^{40}Ar/^{36}Ar$ (and N_2/Ar) put into evidence that excesses of He and Ar do exist (radiogenic origin) as well as of N_2 (decomposition of sedimentary organic matter).

Even though application of chemical geothermometers is influenced by many factors, an agreement was found between Na/Li in waters and CO/CO_2 in gases. A hot area outside the known geothermal fields was spotted in this way and needs further investigation.

The water chemistry and the height of the sampling sites rule out a direct water contribution from the deep geothermal system; the only contribution can take place in the gas phase as shown by the gas chemistry. A preliminary investigation and comparison between deep gases from wells and free gases from springs pointed out that the deep component contribution is modified by the low-temperature re-equilibration and reaction with shallow waters.

WHY ARE THERE CIRCUMFERENTIAL ERUPTIVE FISSURES ON THE GALAPAGOS VOLCANOES?

CHADWICK, W.W., Jr., HOWARD, K.A., and DIETERICH, J.H. (all at: U.S. Geological Survey, 345 Middlefield Rd, Menlo Park, CA 94025, USA)

Most volcanic eruptions on the Galapagos islands of Fernandina and Isabela occur along linear eruptive fissures marked by rows of spatter and scoria cones. The eruptive fissures form a distinctive pattern consisting of circumferential fissures around the summit calderas and radial fissures lower on the flanks: this pattern is virtually unique to the Galapagos. It is not yet understood why this pattern is common on Galapagos volcanoes but rare elsewhere. The eruptive fissures are fed by dikes that propagate from magma reservoirs beneath the calderas to the surface. We have mapped fissures on Fernandina (see figure) and Isabela from aerial photos taken in 1946 and 1960, and are conducting numerical modeling to try to explain the mechanical reasons for this unusual pattern of diking.

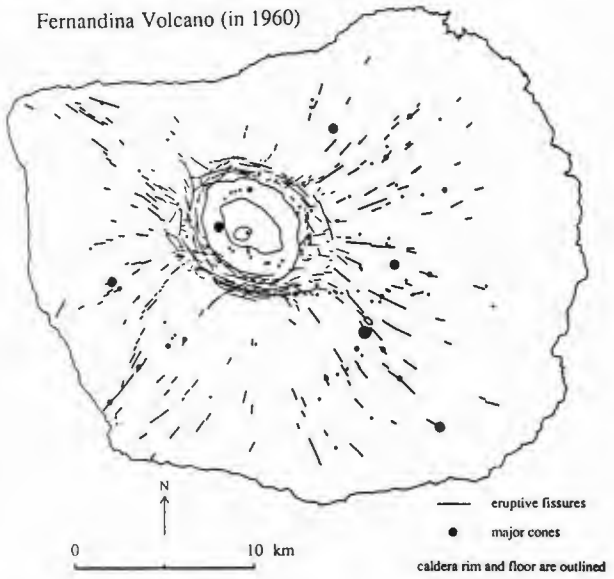

Recent field work on the island of Fernandina yielded the following observations: 1) The circumferential vents lie within 1-1.5 km of the caldera rim, but within this zone are mainly concentrated farthest from the rim. Near the rim, normal faults which downdrop blocks into the caldera are common but the location of the circumferential vents appears to be independent of these faults. This indicates that the circumferential fissures are not simply leaky faults, but are distinct structures in themselves, and require specific mechanical conditions for their emplacement. 2) Many circumferential dikes are exposed in the caldera walls. They are consistently vertical or nearly so, and about 1 m thick. No vertical offset was observed in the layers adjacent to the dikes, indicating that dip slip faulting does not commonly accompany dike emplacement. 3) Within the zone of circumferential vents, structures showing extension perpendicular to the caldera rim were found, including open tension cracks and fault grabens (particularly south of the caldera). This suggests that there may be some mechanism leading to extension which allows dike intrusion to continue in the long term. Otherwise, repeated dike intrusion in this area would eventually alter the stress field and prevent further circumferential intrustions. How this extension is accommodated is not known, but it is interesting to speculate that the series of unusually large earthquakes (M 4-5) during the six months preceding an intra-caldera avalanche and eruption in September 1988 may represent infrequent but necessary tectonic adjustment within the volcano.

To investigate the mechanical reasons for the pattern of diking in the Galapagos, we are conducting finite element computer modeling to investigate how stresses suitable for the pattern of dike intrusion can be produced, what tectonic adjustments might be necessary to maintain these stresses over the long term, and how these considerations might relate to the unusual shape of the Galapagos volcanoes.

PETROLOGICAL EVOLUTION OF THE ITCHA MT. SHIELD VOLCANO, CENTRAL BRITISH COLUMBIA: IMPLICATIONS FOR ALKALINE VOLCANISM IN THE ANAHIM BELT.

CHARLAND, A., and **FRANCIS, D. M.**, Dept. of Geological Sciences, McGill University, Montréal, Québec, H3A 2A7.
LUDDEN, J., Dépt. de Géologie, Université de Montréal, Québec, H3C 3J7.

The Anahim Volcanic Belt is a suite of easterly younging late Tertiary alkaline complexes aligned along lat. 52° N in west-central B.C.. The belt comprises a number of centers characterized by a bimodal population of alkaline basalts and alkaline and peralkaline felsic lavas. The Itcha Mountain Range is the youngest and easternmost shield volcano of the Anahim Belt, and is composed of an early (3.5-2.6 Ma) felsic shield and more recent (~ 1 Ma) basaltic capping lavas. The early felsic shield is dominated by ne-trachytes and trachytes, and displays a wide range of incompatible element (IE) contents (300-2000 ppm Zr; 30-340 ppm Nb). This IE variation is positively correlated with Si-undersaturation and is inconsistent with extensive K-feldspar fractionation. The mafic lavas range from primitive (10 wt% MgO) alkaline olivine basalts and basanites to hawaiites and ne-hawaiites. A number of independent fractionation trends exist within the mafic lavas; each being characterized by a different degree of Si-undersaturation and IE content. The occurrence of highly alkaline felsic and mafic magmas, and the presence of basaltic xenocrysts in some trachytes, strongly favors a petrogenetic link between the two lava types. Fractionation models suggest that the most Si-undersaturated basalts are parental to the IE-enriched trachytes and that the more Si-saturated mafic melts are parental to the IE-poor trachytes. The detailed study of the Itcha shield can be extrapolated to define regional variations in the Anahim belt: 1) trachytic and basaltic lavas show increasingly Si-undersaturated compositions easterly across the belt (see fig.). The greater Si-saturation of the western Anahim shields probably reflects fractionation from more Si-saturated parental magmas; 2) the volume of primitive basalt relative to felsic lavas is largest in the Itcha shield. This may be consistent with geophysical models which indicate lithospheric thinning in central B.C..

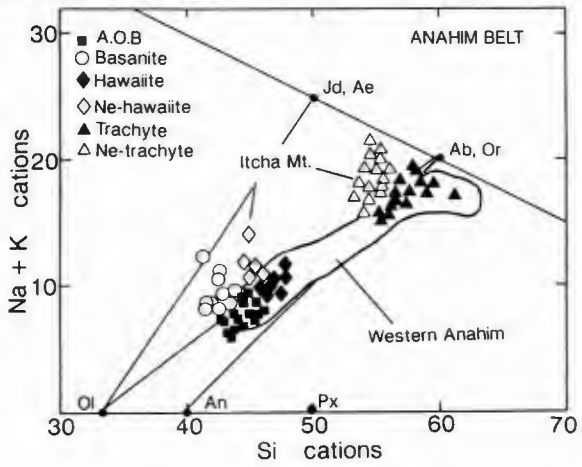

SPATIAL AND TEMPORAL VARIATIONS OF NEOGENE CONTINENTAL BASALTS IN TAIWAN: Nd AND Sr ISOTOPE AND TRACE ELEMENT CONSTRAINTS

CHEN Cheng-Hong, CHEN Sujin, CHUNG S. L., HUANG H. H., LEE Chi-yu, Department of Geology, National Taiwan University, and LEE Typhoon, Institute of Earth Sciences, Academia Sinica, Taipei

Neogene continental basalts in the Taiwan area occurred mainly in Penghu Islands and northern Taiwan, the latter can be further subdivided into Kungkuan and Kuanhsi-Chutung (K-C) volcanics by NE-SW thrust systems. Both alkali basalt and tholeiite, often intercalated with sediments of variable thickness, have been found in these three volcanics. A striking feature is that tholeiites have younger eruption ages (late Miocene) than the alkali basalts (early to late Miocene).

Mineralogically, alkali basalts contain K-feldspar ± analcime in addition to olivine, clinopyroxene and plagioclase, and are either Ne- or Hy-normative, whereas tholeiites are distinguished by the lack of K-feldspar and the presence of low-Ca pyroxene, and are generally Q-normative. Major element data in terms of normative compositions of basaltic tetrahedron show an obvious distinction between alkali basalt and tholeiite in Penghu volcanics, but in northern Taiwan especially the K-C volcanics, a continuous relationship from alkali basalt to tholeiite was seen, indicating progressive transition from one type to the other.

Although these two types of basalts in all volcanics show LREE enriched pattern with $(La/Yb)n = 9-23$ in alkali basalts and 5-9 in tholeiites, their isotopic compositions are different. Sr- and Nd-isotope ratios for Penghu and Kungkuan volcanics are rather clustered and indistinguishable to each other, i.e. $^{87}Sr/^{86}Sr$ = 0.70361-0.70386 and $^{143}Nd/^{144}Nd$ = 0.51285-0.51296 in alkali basalts; 0.70359-0.70385 and 0.51291-0.51294 in tholeiites. They are very much similar to the values of many alkali basalts in the continental rifting systems. On the other hand, those in K-C volcanics display a larger spread with $^{87}Sr/^{86}Sr$ = 0.70406-0.70507 and $^{143}Nd/^{144}Nd$ = 0.51264-0.51282 in alkali basalts, 0.70500-0.70669 and 0.51255-0.51270 in tholeiites, covering the range for many island arc rocks. Interestingly, Al-augite and kaersutite megacrysts in the alkali basalts have Sr- and Nd-isotope ratios close to Penghu and Kungkusn volcanics irrespective to the province where they occurred. Thus they may represent fragments of high pressure cumulates for pre-Miocene continental rifting volcanism in northern Taiwan.

Trace element spidergrams of Neogene volcanics in Taiwan seem to reveal that the K-C tholeiites contain less Ta than in those from Penghu Islands and Kungkuan area. Since Ta depletion is a well-known feature in rocks derived from arc volcanism, such a result and the accompanying isotopic differences can be explained by spatial and temporal tectonism. Penghu Islands are far away from the Ryukyu arc-trench system in the western Pacific and should not involve island arc component since Cenozoic, so the Sr- and Nd-isotope ratios reflect its subcontinental mantle values. At early Miocene time when the Ryukyu subduction volcanics were further south than their present position and the fold-and-thrust belt had not yet been developed in Taiwan region, the mantle giving rise to melts for Kungkuan volcanics remained unaffected by the Ryukyu subducting plate, but melts responsible for the late Miocene K-C volcanics had already been contaminated by the same subducting system to some extents. It is the post-Miocene reactivated germano type of thrust fault that brought the arc-contaminated low-Ta tholeiites of K-C volcanics close to the Kungkuan volcanics and resulted in the present-day distribution of continental volcanics in northern Taiwan.

QUATERNARY VOLCANISM ON THE NORTHERN SECTORS OF THE WONJI FAULT BELT

Tadiwos Chernet, Ethiopian Institute of Geological Surveys (Geothermal Exploration Project), P.O.Box 2302, Addis Ababa, Ethiopia.

The Main Ethiopian Rift (MER) is a large scale tectonic feature in the form of a graben which shows intensive tensional tectonism and related implacement of volcanic products. This tectonic structure belongs to the Afro-Arabian rift system and is part of the continental East African Rift Valley.

Six dominantly rhyolitic volcanic centers which lie on three sectors of the active spreading axis of the MER (Wonji Fault Belt) are studied to asses the structural and petrological relations between individual centers and the sectors of the Wonji Fault Belt they are located on. Each segment of the fault belt is disposed en-echelon fashion in the center of the rift. The southern most segment contains the volcanoes Tullu Moye and Gadamsa. The middle segment contains volcanoes Bosetti and Kone and the northern most segment contains Fantale and Doffane. Each segment of the fault belt is characterized by intensive normal faults and fissures. These tectonic events are accompanied by fissural basalt eruptions which produced basaltic fields and spatter cones on each segment. The teconism was more dynamic on the Northern segment of the Wonji Fault Belt to the extent that it has formed a major graben on the Doffane volcanic complex.

The latest volcanic activity some of which are historic even on the central silicic volcanoes are fissural basalts. Evidences of hydrothermal activity (hot springs, fumaroles and solfatara activity) are wide spread, particularly associated with the silicic centers. These geothermal manifestations and other petrologic evidences indicate the presence of shallow (4-6 km deep) rhyolitic magma chambers under the silicic centers. The injection of the less viscous basaltic magma from the mantle into these rhyolitic magma chambers must have induced some of the silicic eruptions.

Major elements chemical analyses of samples from the silicic volcanic complexes shows that the rhyolites are dominantly pantellerites and comendites both with normative acmite and sodium metasilicate. The proportion of comendites is very low in the studied area and particularly diminishes on the northern segment where the rift is more evolved and crustal attenuation is more pronounced. The basalts are mildly alkaline with normative nepline and olivine (> 10 wt %). The basalts range in composition to Hawaittes and mugearites. Intermediate rocks are mainly pantelleritic trachytes.

INFLUENCE OF THE SHAPE OF MAGMA CHAMBERS ON THE TECTONIC AND MECHANICAL BEHAVIOR OF VOLCANOES: A NUMERICAL APPROACH.

CHEVALLIER, L., Department of Geology, University of Stellenbosch 7600, South Africa.

The dynamics of a volcano is directly connected with the dynamics of its magma chamber. The most important factor that determines the stress field inside a volcanic edifice is the geometry of this magma chamber. Many of the differences observed between intraplate volcanoes can be ascribed to differences in shape between chambers. Three different axisymmetric models (1, a laccolith; 2, a spheriod and 3, a prolate shape with a central column) have been tested mechanically by numerical simulation using the finite element method. From the stress fields obtained, three different tectonic patterns are predicted (see fig.) which are then compared with existing volcanoes. Possible applications of this approach are: structural classification of volcanoes, dynamic evolution of a single volcano and the interpretation of pictures obtained by remote sensing eg. on other planets.

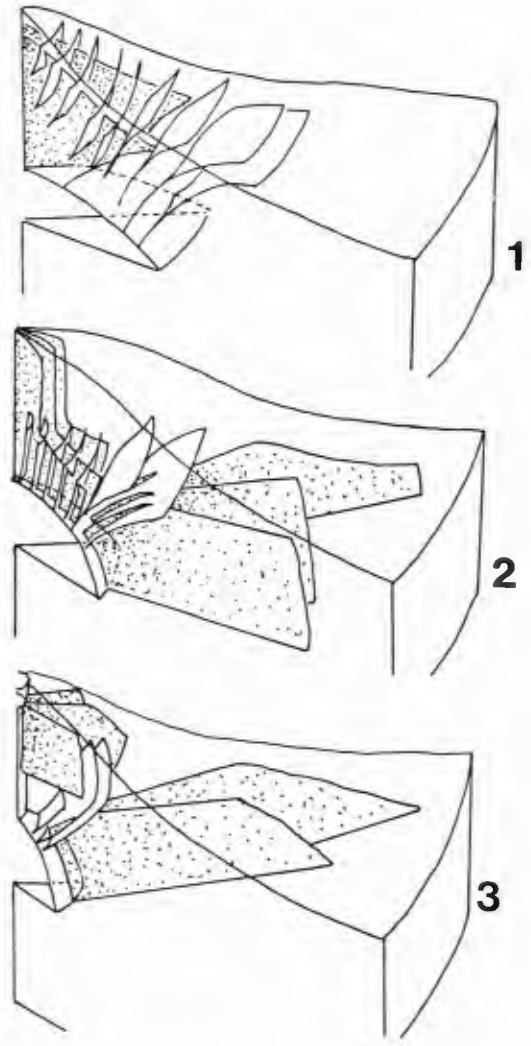

COMPOSITIONAL CONTRASTS AMONG MIDDLE CENOZOIC ASH-FLOW TUFFS OF THE GREAT BASIN, WESTERN UNITED STATES

CHRISTIANSEN, Eric H, and BEST, Myron G., Department of Geology, Brigham Young University, Provo, Utah 84604

Although most ash flows erupted during the 31-20 Ma peak of Cenozoic magmatism in the Great Basin are rhyolitic, two widespread types of non-rhyolitic tuff have been identified. These distinctive compositional types are significant because they demonstrate that similar processes of magma generation and/or evolution were reproduced in several magma systems over a wide region. Moreover, the eruption of both types from single volcanic centers may elucidate the nature of the interaction between mantle-derived magmas and continental crust.

The Monotony compositional type, named for the Monotony Tuff of southeastern Nevada, includes at least 12 stratigraphic units that are generally of large volume (ranging up to 4000 km3) and variably welded. With one exception they have ages of 31 to 20 Ma. Over 104 km3 of Monotony-type dacites--about 20% of the total ash-flow volume in the Great Basin--were erupted from just four sources 31-27 Ma, immediately preceding the peak of the Isom-type (see below) eruptions. The Monotony types are crystal-rich dacitic tuffs, containing 25-50% phenocrysts of plag>biot,hb>qtz>mt, ilm; apatite and zircon are ubiquitous accessories. Cpx, opx, san, and titanite are accessories in some units. Groundmass glass in vitrophyres is rhyolitic and the dacitic bulk compositions result from their phenocryst-rich character. Mineral compositions indicate that relative to the Isom-type trachydacites, Monotony-type dacites crystallized at lower temperatures (<880°C), higher water and oxygen fugacities (2-3 log units above QFM), and moderate pressures (about 3 kb). In the Indian Peak volcanic field astride the Nevada-Utah stateline, Monotony-type dacites have high Sr isotope ratios and lie on linear trends between andesites and rhyolites, suggesting that combination of crustal material and mantle-derived magma played an important role in the generation of these large volume dacites.

The Isom compositional type, named after the voluminous Isom Formation of the Indian Peak volcanic field, includes at least 12 stratigraphic units erupted chiefly 27 to 23 Ma. They generally form relatively thin (10-20 m thick) densely welded sheets up to 1000 km3 in volume. In IUGS terms, Isom-type tuffs range from trachyte to trachydacite in composition. However, none of the tuffs are peralkaline and their relatively low Fe/Mg ratios show they are calc-alkaline like contemporary tuffs in the region. Members of this group contain less than 20% phenocrysts of plag>>cpx> opx> mt,ilm; apatite and zircon are common accessories. Sparse qtz, san, biot, and hb are present in some units, but may be partly xenocrystic. Compared to other Great Basin volcanic rocks of similar SiO_2 content, Isom-type tuffs have low CaO concentrations and high concentrations of TiO_2, Al_2O_3, K_2O, Zr (up to 600 ppm), and other incompatible trace elements. Notably, Isom-type rocks have high Al/Ca ratios, consistent with an important role for cpx fractionation. Low Al in cpx and projections in Ol-Di-Plag-SiOr indicate that they crystallized at relatively low pressures (about 2 kb). Mineral compositions show that eruption temperatures were relatively high (about 950°C) and that oxygen fugacities were moderate (1 log unit above QFM). Within some volcanic fields, Isom-type tuffs were erupted a few million years after eruptions of Monotony-type tuffs. In the Indian Peak volcanic field, Isom-type tuffs appear to be derived from high Zr (and other incompatible element) andesites by fractional crystallization. Small changes in incompatible element ratios across this differentiation series are consistent with some sort of open system behavior.

The compositional contrasts between these two distinct types of ash-flow tuffs may result from different parent magmas. Alternatively, time-varying processes, such as changes in depth of crystallization or the nature of crustal interaction in evolving magma systems, produced divergent magma series in single magma systems within the Great Basin.

VOLCANISM ASSOCIATED WITH POST-LARAMIDE TECTONIC EXTENSION IN THE WESTERN U.S.

CHRISTIANSEN, Robert L., U.S. Geological Survey, 345 Middlefield Road, Menlo Park, CA 94025, USA.

Post-Laramide continental volcanic rocks in the Western U.S. occur in 3 tectonomagmatic associations: (1) predominant calc-alkalic basalt to andesite and subordinate dacite to rhyolite erupted along continental-margin arcs parallel to active subduction zones; (2) volcanic suites with little or no basalt but abundant andesite to rhyolite, broadly calc-alkalic but more potassic than the arc suites, erupted in belts spanning from the ends of the arcs across interior regions of active extension (and in areas near migrating triple junctions at the ends of a coastal transform system); and (3) basaltic, alkalic, and bimodal rhyolite-basalt suites erupted in rifted regions and in cratonic forelands adjacent to the interior andesite-rhyolite belts.

Contractional deformation, mainly Mesozoic, culminated in the Laramide and ended by 55-50 Ma. From 55 to 43 Ma, an arc reached from coastal Canada to W-central Oregon. (Coeval oceanic basalt in coastal Washington and Oregon accreted later). In the adjacent Challis belt, andesite-rhyolite magmatism accompanied extension between the N Cascades and the Rocky Mountain front, producing large ash-flow calderas in Idaho. Contemporaneous alkalic centers evolved on the foreland to the E. Another arc was active concurrently in W Mexico, and an extensional andesite-rhyolite belt reached N into W Texas and S New Mexico.

From 43 to 37 Ma, the NW arc widened and lengthened into NE California. Extension and major andesite-rhyolite volcanism stepped S to the Tuscarora belt, from central Oregon to NW Utah. In the S, andesite erupted N from the end of the Mexican arc through SE Arizona to central Colorado, with voluminous rhyolite in S New Mexico.

From 37 to 21 Ma, the Cascades arc ran from coastal Canada to NW Nevada. To the E, the John Day-Lewis & Clark belt produced local trachyandesite and rhyolite. The belt of andesite to rhyolite and associated extension jumped S across central Nevada and split into two branches in W Utah. Major activity, including ash-flow calderas, expanded S after 34 Ma and again at 28 Ma. Until 21 Ma, however, some activity continued in the older part of the belt to the N. The S arc remained in Mexico. In the adjoining interior belt, ash-flow calderas erupted in Colorado and SW New Mexico between 34 and 27 Ma, and less voluminous andesite and rhyolite reached SE California; by 26-21 Ma inland of the arc, andesite to rhyolite erupted from Sonora to the S Coast Ranges (now offset by the San Andreas fault), rhyolite was voluminous in SE Arizona, and mafic andesite and basalt accompanied extension in New Mexico and Colorado. Alkalic centers formed on the adjacent Great Plains and Colorado Plateau between at least 43 and 21 Ma.

At 21-17 Ma, the Cascades arc, which formerly had ended in N California and Nevada, became virtually continuous with the Mexican arc except for a gap of a few hundred km in SE California where subduction had ceased; part was later disrupted by translation and rotation in S California. Interior volcanism waned during a transition from local to regional extension.

Since 17 Ma, the gap in the arc has widened as the coastal transform system lengthens; volcanism near the N-migrating Mendocino triple junction has erupted predominantly andesite and rhyolite. Basalt to bimodal rhyolite-basalt suites accompany regionally distributed extension to the E. At 17-14 Ma, a rift from central Nevada to W Idaho and E Washington erupted basalt, more voluminous and less alkalic N-ward. Ash-flow calderas of 21-6 Ma formed an E-W belt across S Nevada. During basin-range extension since 14-10 Ma, volcanism has concentrated toward the margins of the extending region.

These events since 55 Ma are consistent with basaltic magma generation beneath the thinning lithosphere of extending regions; basaltic intrusion induces lower-crustal melting and rhyolitic magmatism. During local extension, ponded basaltic magma fractionates and assimilates crust to produce potassic andesite; during distributed extension, basaltic magma rises more readily with less assimilation and fractionation, enhancing crustal melting in zones of especially high basaltic magma production to yield basaltic and bimodal rhyolite-basalt suites.

VOLUMINOUS RHYOLITIC LAVAS OF BROAD EXTENT ON THE YELLOWSTONE PLATEAU

CHRISTIANSEN, Robert L., and HILDRETH, Wes,
U.S. Geological Survey, 345 Middlefield Road,
Menlo Park, CA 94025, USA.

The overall size and morphologic characteristics of silicic volcanic bodies, including aggregate volume, extent, and aspect ratio, are sometimes taken as criteria for distinguishing rheomorphic tuffs from lava flows. Rhyolitic lavas that partly fill and locally overflow the 600-ka Yellowstone caldera demonstrate that such criteria are insufficient. The Madison, Central, and Pitchstone Plateaus cover an area of 70x50 km ($\sim$2,800 km^2) that is underlain by high-silica rhyolitic lava flows extruded in 3 pulses at about 155, 110, and 75 ka--18 of them exposed at the surface. Many of these flows are quite large; each of 5 of them has maximum dimensions in the range of 25-32 km, an area of 275-350 km^2, and a volume of 30-60 km^3. The exposed flows are unambiguously lavas. Their margins are steep lobate scarps, commonly 75-200 m high, they are enveloped by characteristic flow breccias, and they have homogeneous textures, few broken phenocrysts, and virtually no lithic inclusions; they also have well developed internal flow layering --parallel to the base and margins but steep and commonly contorted in the upper parts and concentric around the vents. Although the flows are locally >300 m thick, their surface profiles are gently convex or nearly flat. The locations of the vents were controlled by regional tectonic faults that intersect the caldera and its large and still active magma chamber.

All of the known flows are geochemically similar, having SiO_2=76.3-77.2%, FeO*=1.35-1.6%, K/Na=1.6-2.1, Rb=180-230 ppm, Ce=160-200 ppm, Ce/Yb=22-28, $^{87}Sr/^{86}Sr$ $\sim$0.710, ϵNd $\sim$-7, and notably low Sr (<5 ppm), Mg, and Ca (each <0.5%). They all have 3-10 wt% euhedral phenocrysts, mostly sodic sanidine ($Ab_{42-54}An_{2-3}$), quartz, ferroaugite, and titanomagnetite. Fayalite (Fo_{5-9}) occurs in several of the younger flows; ilmenite, zircon, apatite, and chevkinite are sparse. Mt-ilm geothermometry gives $\sim$850°C. The absence of hydrous phases indicates low preeruptive H_2O; magmatic halogen contents also were modest, with Cl<800 ppm and F=800-1800 ppm still retained in the vitrophyres.

The compositions of these flows, not unusual for high-silica rhyolites, should not have produced exceptionally low viscosities. High stress accumulation and displacement along the length of faults that localized the eruptions probably allowed these fractures to tap large high-level aphophyses of the Yellowstone magma chamber directly, thus favoring large effusive volumes. The unusually large areal coverage and high ratio of breadth to thickness of these lavas probably reflect efficient heat retention and low volatile loss that would have been favored by large effusive volumes and high discharge rates, sustained by an enormous shallow magmatic reservoir.

Similar lavas in older volcanic fields might easily be regarded as rheomorphic tuffs if judged mainly by their ratios of maximum dimension to average thickness, $\sim$200, especially if eroded remnants of the whole field (with ratios of 300-500) were mistakenly taken to represent only one or a few eruptive units.

PETROGENESIS OF NA-ALKALINE ROCKS IN BACK-ARC AREAS: EVIDENCE FROM THE USTICA ISLAND, SOUTHERN TYRRHENIAN SEA

CIVETTA, L., Department of Geofisica e Vulcanologia, University of Naples, Italy
ORSI, G., Department of Geofisica e Vulcanologia, University of Naples, Italy
PECCERILLO, A., Institute of Scienze della Terra, University of Messina, Italy.

The island of Ustica, southern Tyrrhenian Sea, is a typical example of Na-alkaline volcanism in a back-arc structural setting. Widespread on the island are the products of effusive submarine activity such as pillow-lavas and pillow-breccias. Subaerial activity produced either domes and lava flows or pyroclastic deposits. Most of the explosive eruptions were triggered by efficient water-melt interaction. The island has been deeply affected by tectonics, as testified by the many faults recognizable in the field. It also has many level surfaces at different heights above sea level, which were produced by variations in sea-level determined either by glacial-eustatic movements or by tectonics and volcano-tectonics.

The volcanic rocks of Ustica have a Na-alkaline affinity with composition ranging from alkali-basalt to trachyte with a SiO_2 gap between 55 and 60%.

The basic rocks are characterized by different contents of P_2O_5, different LILE versus HFSE ratios, and different Sr-isotope composition (0.7030-0.7034) for the same MgO content. Furthermore, all the rocks display negative anomalies of Hf, Ti, K and Rb when normalized to primordial mantle values. Their geochemical characteristics are interpreted in light of experimental results on the genesis of Na-alkaline magmas.

The Na-alkaline basaltic magmas of Ustica were generated within the mantle wedge above the subducted slab, where metasomatic agents are rich in Na, having lost their K and Rb at greater depths by reaction with peridotite to give phlogopite. This model explains the close spatial and temporal association, in the southern Tyrrhenian sea, of calc-alkaline, K-alkaline and Na-alkaline rocks, being related to the degree of interaction of slab-components with peridotite, to the degree of hydratation of the mantle and to the depth of magma generation.

GEOCHEMISTRY OF UNGARAN VOLCANO, CENTRAL JAVA

CLAPROTH, Richard, and CARR, Paul F., Department of Geology, University of Wollongong, P.O. Box 1144, Wollongong, NSW, 2500, Australia

The development of Java in the Sunda Arc is due to subduction of the northward-moving Indian-Australian Plate beneath the Eurasian Plate. Ungaran volcano is situated 200 km above the Benioff Zone and forms part of the second of three cycles of Tertiary to Recent volcanism recognized on Java. The volcano, which was active between the Late Pliocene and Late Pleistocene, is characterized by three stages of growth, interrupted by two episodes of cone collapse. Eruption products can be grouped into four major units comprising Oldest Ungaran, Old Ungaran, Parasitic Cones and Young Ungaran.

Lavas from Ungaran exhibit a continuum of compositions which range from 48.95% to 60.80% SiO_2. On the basis of K_2O and SiO_2 contents, most of the basalts are shoshonites whereas most of the basaltic andesites and all andesites are high-K calcalkaline. Shoshonitic rocks dominated the early stages of magmatic activity whereas high-K calcalkaline rocks were produced during later stages. Compared with most volcanic rocks of similar SiO_2 content, the lavas from Ungaran are characterized by high contents of Al_2O_3, total alkalis and incompatible elements, high ferric/ferrous ratios, and low MgO contents. Basalts from Ungaran range from Ne-normative to Q-normative depending on the ferric/ferrous ratio used in the calculation. Low Mg-numbers (maximum value = 0.55) indicate that these basalts crystallized from derivative melts and do not represent primary, mantle-derived magmas.

Trace element modelling on the basis of published distribution coefficients and possible source compositions suggests that the rocks from Ungaran were generated by 5 to 10% partial melting of spinel lherzolite or amphibole lherzolite which had been previously enriched in incompatible elements. Subsequent to magma generation, fractionation of early formed olivine and clinopyroxene produced the most mafic rocks in Ungaran.

Ungaran basalts have a wider range and higher mean $^{87}Sr/^{86}Sr$ ratio than associated basaltic andesites and andesites and the available isotopic data are consistent with derivation of Ungaran lavas from a heterogeneous OIB-type source. Depletion of Ta, Nb and Ti relative to large ion lithophile elements (LILE) cannot be attributed to a residual Ti-rich phase in the source. Geochemical data are consistent with enrichment of LILE in the mantle wedge by the processes of mantle metasomatism or zone refining, or from a fluid derived from the subducted slab. Comparison between Sr isotopic ratios and contents of high field strength elements and LILE in Ungaran basalts and the crust of the eastern Indian Ocean suggests that a model involving derivation of Ungaran lavas from a mantle wedge contaminated by fluid from the subducted slab is plausible.

GRANITIC MAGMATISM IN THE TRANSITION FROM A COMPRESSIONAL TO AN EXTENSIONAL REGIME,TIIE IDAHO BATHOLITH.

CLARKE, C.B., IIAWKESWORTH, C.J., Dept. Earth Science, Open University, Milton Keynes, MK76AA, England.
LEEMAN, W.P., Earth Sciences Division, NSF, Washington DC20550.

Continental margin magmatism reflects the complex interaction of compressional and extensional tectonic regimes, but the relationship between petrogenetic and tectonic processes remains poorly understood. Results are presented from a detailed study of 95-40 Ma granitoids in the Idaho batholith, emplaced as the tectonic environment changed from continent/arc collision in the mid Cretaceous, to within plate extension as the subduction zone migrated westwards. The main phase (K) are 95-56Ma old, they range from diorite to leucogranite, and are both met- and peraluminous. The Tertiary rocks comprise an older (50-45 Ma) metaluminous, quartz-monzodiorite suite (Tgd), and a younger (49-42 Ma) peraluminous suite of Eocene granites (Tg), which are the intrusive equivalents of the Challis volcanics.

Rb and K increase, but Sr, Ba, and Zr decrease with increasing SiO_2 in the K and Tgd suites. Ba/Zr and Ba/Nb ratios are high in the less evolved magmas, consistent with a contribution from subduction related material. The younger Tg suite exhibits significant Eu anomalies and a more restricted range in major elements. Overall there is a progressive increase in the Y + Nb contents of the K to the Tg suites reflecting a change from magmas with more subduction-related to more within-plate characteristics. ε_{Sr} ranges from 20 to 160 (average =50) and ε_{Nd} ranges from -3 to -14, with large heterogeneities in ε_{Sr} and no isochron relationships preserved. The Tgd suite have the least evolved isotopic compositions (ε_{Sr} =27 to 40, ε_{Nd} =-4 to -12), whereas the Tg suite show the most evolved isotopic compositions, (ε_{Sr}=40 to 70 , ε_{Nd}=-7 to -15.5).

A striking feature of many of the less evolved rocks is that Rb/Sr in their source, as inferred from T^{DM}_{Nd} and $^{87}Sr/^{86}Sr_i$, is greater than that in the rocks themselves. This is contrary to what is typically observed in crustal rocks, and it is best developed in granitoids with exeptional HREE depletion. It is argued that the main phase of the Idaho batholith was generated by partial melting of garnet-plagioclase bearing rocks in the lower crust, and that this resulted in exceptional Sm/Nd fractionation. It is proposed that progressive increases in Sm/Nd (0.174-0.227) and related decreases in Nd/Yb (29-16) from the K, through the Tgd, to the Tg suite reflects partial melting at progressively shallower levels of the crust. The older rocks were generated near the base of a tectonically thickened crust with a higher pressure eclogitic (or garnet amphibolitic) residual source assemblage, and as extension attenuated the crust, partial melting occurred at shallower levels with a lower pressure gabbroic or amphibolitic residual source assemblage. Partial melting calculations indicate that for 30% melting in equillibrium with residual eclogite, the source Sm/Nd yields $T^{DM}_{Nd} \geq 2.5$Ga, consistent with the Wyoming Archean craton.

PROGRESS ON INTERPRETATION OF NEW CHEMICAL STUDIES OF VOLCANIC ROCKS OF THE SUPERSTITION MOUNTAINS, ARIZONA

CLIFFORD, Paul M., McMaster University, 1280 Main Street W., Hamilton, Ontario L8S 4M1, Canada, and PETERSON, Donald W. U.S. Geological Survey, MS-910, Menlo Park, California 94025, USA

New major- and minor-element analyses have been made for several Miocene volcanic units from the Superstition Mountains. The units are here designated, from older to younger, lower ash-flow tuff (LAT), middle rhyodacite and rhyolite lava (MRL), upper ash-flow tuff (UAT), and upper rhyolite lava (URL). Field relations and geochemical characteristics both suggest that the rocks have been derived from a single evolving magma chamber. Available radiometric dates, however, are equivocal and have not been utilized in the current studies.

All the units are calc-alkaline, and they contain from 69.3% to 75.2% SiO_2 (water-free). As SiO_2 increases, the Al_2O_3, TiO_2, and Zr decline. REE patterns for LAT and UAT are virtually identical, but some for MRL are relatively slightly depleted. With increasing SiO_2, the Eu anomalies become increasingly negative. These characteristics are compatible with fractionation of feldspar and sphene. Samples of the youngest lavas, URL, are relatively depleted in Al_2O_3, TiO_2, Ba, La, La/Lu, Eu, Sr, and Zr and enriched in Nb and SiO_2 relative to most samples of the older rocks. URL thus represents the most extreme fractions erupted from the magma chamber. On discrimination diagrams, some rocks plot in the within-plate field, whereas others plot in the volcanic-arc field. This dichotomy suggests that tectonic discrimination diagrams may be applied only with difficulty to evolved silicic volcanic rocks.

Isotopic studies by others have suggested that the magma may be derived by partial melting of the amphibolitic lower crust, and this is compatible with the current whole-rock chemistry. The rocks are metaluminous, suggesting little assimilation of the schistose rocks (metapelite) widely exposed in the upper crust of the region.

DISAGGREGATION OF QUENCHED MAGMATIC INCLUSIONS CONTRIBUTES TO CHEMICAL DIVERSITY IN SILICIC LAVAS OF LASSEN PEAK, CALIFORNIA

CLYNNE, M.A., U.S. Geological Survey, Menlo Park, CA, 94025 USA

At the Lassen volcanic center, most silicic lavas contain variable amounts (up to 20%) of fine-grained andesitic inclusions. Magmatic compositions and textural features indicative of quenching lead to the conclusion that the inclusions are quenched blobs of mafic magma (cf. Bacon, 1986). Commonly, phenocrysts from the host silicic magma are mixed into the magmatic inclusions (cf. Heiken and Eichelberger, 1980) and are partially melted, devolatilized, or resorbed by reaction with the hot mafic liquid (cf. Glazner and others, 1988). Field and petrographic evidence shows that quenched inclusions in many of the silicic lavas disaggregated into their silicic host magmas. Features such as multiple and disequilibrium phenocryst populations and compositional variations within flow units in these and some other calc-alkaline lavas can be explained in part by disaggregation of inclusions. The dacite of Lassen Peak dome and the 1915 lava of Lassen Peak both show especially clear examples that illustrate this process.

The eruptions of Lassen Peak in 1915 produced porphyritic lavas with 62-68 wt.% SiO_2 and abundant quenched inclusions. The host lavas contain phenocrysts of plagioclase (An_{30-40}), hornblende, biotite, quartz, and Fe-Ti oxides that crystallized from a felsic magma. These phenocrysts occur in two populations, one that is in textural equilibrium with the host lava and one that is strongly resorbed. In addition there are crystals of olivine (Fo_{84}), plagioclase (An_{50-70}), augite, and bronzite that crystallized from a mafic magma. The quenched inclusions contain sparse olivine phenocrysts (Fo_{84}) in a vesicular network of acicular plagioclase (An_{50-70}), augite, and bronzite, with abundant glass. The inclusions also contain resorbed phenocrysts derived from the host magma. Details of mineral compositions, textures, and zoning patterns demonstrate that disaggregation of quenched inclusions is the process by which the multiple phenocryst population originated.

Lavas of the Lassen Peak dome range from 63.5 to 70 wt.% SiO_2. On variation diagrams, samples plot as a linear array between inclusions, which contain 55-56 wt.% SiO_2, and the most silicic lava. The inclusions are commonly rounded and have apparently lost much of their chilled primary outer surfaces through disaggregation. Lavas of the Lassen Peak dome also contain abundant mm-sized fragments of mafic inclusions, individual groundmass crystals from inclusions, and magnesian olivine and clinopyroxene crystals identical to phenocrysts found in the inclusions. The abundance of fragments increases with decreasing SiO_2 in the lavas of Lassen Peak. Chemical heterogeneity in the Lassen Peak dome originated, at least in part, through addition of mafic material by disaggregation of quenched magmatic inclusions.

Disaggregation of magmatic inclusions into small fragments and individual crystals can be an efficient magmatic mixing process. Disaggregation of inclusions is enhanced if a substantial part of the inclusion is still liquid upon thermal equilibration with the host magma. Disaggregation of quenched inclusions carrying resorbed host magma phenocrysts can produce coexisting resorbed and equilibrium phenocryst populations. These coupled processes are responsible for much of the chemical heterogeneity in silicic rocks of the Lassen volcanic center and may be more important elsewhere than previously recognized.

Bacon, 1986, JGR 91:6091-6122
Glazner and others, 1988, EOS 69:1504
Heiken and Eichelberger, 1980, JVGR 7:443-481

CERRO TUZGLE - QUATERNARY ANDEAN VOLCANISM IN THE EASTERN PUNA-ALTIPLANO PLATEAU, ARGENTINA

COIRA, B., CONICET - Univ. Nacional de Jujuy, C. Correo 258, 4600 Jujuy, Argentina, and KAY, S. Mahlburg, INSTOC, Snee Hall, Cornell Univ., Ithaca, NY, 14853, USA

Cerro Tuzgle (24°S, 66°W) on the eastern margin of the Puna-Altiplano plateau is one of the easternmost volcanoes (0.5 Ma to Recent) in the central Andes. The volcano is 500 km east of the trench and 220 km above the seismic zone. Tuzgle rocks consist of older dacitic ignimbrites and younger andesitic to dacitic lava flows and domes, which all have a within-plate geochemical signature. Different units cannot be related by closed system fractional crystallization, suggesting a complicated evolution involving mixing between melts of an inhomogeneous garnet peridotite mantle and a crustal component.

Tuzgle andesites and dacites (57-70% SiO_2) have relatively high trace element abundances (i.e., Ba = 420-690 ppm) and little to no depletion of the high field strength elements (Ta, Nb) (La/Ta = 12-18) and little to no enrichment of Ba relative to the light REE (Ba/La = 10-12), features of within-plate lavas. Th, U and K contents are high relative to Ba (K/Ba = 38-61; Ba/Th = 25-42). Plagioclase-bearing xenoliths and quartz xenocrysts rimmed with pyroxene attest to interaction with the crust. A decrease in $^{87}Sr/^{86}Sr$ from older ignimbrites (0.70922) and dacites (0.70762) to andesites (0.70911-0.79762) to the youngest andesite (0.70640) suggests progressively less crustal contamination with decreasing age and SiO_2 content. All Tuzgle rocks have some degree of crustal contamination. Non-equilibrium mineral assemblages and reversely zoned minerals indicate magma mixing. Distinct mineral populations suggest mixing of a basaltic end member with a more radiogenic dacitic end member. La/Yb ratios vary with the older dacites and andesites having ratios from 15-28 and the younger andesites having ratios from 30-39.

Contemporaneous Quaternary basaltic andesites (52-55% SiO_2) from monogenetic Cerro Negro de Chorrillos and San Jerónimo along the El Toro lineament to the south have higher K content and incompatible trace element concentrations (i.e., Sr = 730-970 ppm; Ba 970-2400 ppm) and higher La/Ta (20-29), Ba/La (16-29), Ba/Th (67-123), and Ba/Ta (320-840) ratios. La/Yb ratios range from 31-44 and initial $^{87}Sr/^{86}Sr$ ratios (from the literature) from 0.70676 to 0.70755. These arc-like shonshonitic volcanic rocks suggest small degrees of melting of a garnet-bearing mantle with trace element characteristics distinct from that of the parent of the Tuzgle lavas.

Spatially associated interplate and arc volcanic rocks have been reported in other arcs. In the Puna, Tuzgle rocks could be related to a recently recognized Plio-Quaternary extensional event, while the shoshonitic volcanism shows the influence of a component from the subducted slab. Miocene ignimbrites from the Tuzgle region have arc-like geochemical signatures (Ba/La ratios = 15-18, Ba/Ta = 407-506) indicating the recent development of the within-plate signature.

CRUSTAL STRUCTURE AND VOLCANISM IN THE TAUPO VOLCANIC ZONE, NEW ZEALAND

COLE, J.W. Department of Geology, University of Canterbury, Private Bag, Christchurch, New Zealand.

Taupo Volcanic Zone (TVZ) is the currently active volcanic arc and marginal basin associated with the Hikurangi Subduction Zone, New Zealand. The volcanic arc, on the eastern side of TVZ, comprises andesite and dacite volcanoes with minor tholeiitic basalt. The marginal basin, which is best developed in the central part of TVZ between Rotorua and Taupo, comprises bimodal rhyolite - high-alumina basalt. Widespread ignimbrite eruptions have occurred from this area during the past 0.6Ma.

Geophysical data suggests that the crust is approximately 15km thick under TVZ (compared to 25-35km on either side) overlying a relatively low seismic velocity (7.4-7.5km/s) upper mantle. Seismic, borehole and experimental data suggest the lower crust under TVZ is igneous and probably metaluminous granitoids. Upper crust is predominantly sedimentary or volcanogenic with silicic or diorite intrusions, and has a high heat flow ($\sim 800 mW/m^2$).

All known surface faults in TVZ are normal, and fault zones are en echelon. High-alumina basalts are generally fissure-controlled and at Tarawera dikes within the fissure are en echelon. Historic earthquakes have resulted in the formation of open fissures (e.g. 1866, 1886, 1895, 1922, 1987), indicative of extension and this is confirmed by geodetic measurements of at least 7 $\pm$ 3 m/ka. In March 1987 an ML 6.3 earthquake occurred with the main surface expression at Edgecumbe in the northeastern part of TVZ. Focal depth of the earthquake was approximately 8km on the opposite side of TVZ indicating a dip on the main fault plane of 45 $\pm$ 10° towards the NW. It is thus typical of normal faults generated in brittle crust.

To the east of TVZ is the North Island Shear Belt, a series of dextral-reverse strike slip faults, surface expression of which terminates at the eastern margin of TVZ. Similar trending faults occur offshore in the western Bay of Plenty. If the two sets of faults are associated, strike slip movement must extend under TVZ and a combination of strike-slip movement in the basement together with marginal basin extension could account for the en echelon arrangement of faulting and basalt dikes, and provide a suitable tectonic environment for caldera formation and voluminous ignimbrite eruptions. The association is typical of many areas where there is oblique subduction and could account for the voluminous ignimbrites in places like Sumatra (Indonesia), Kyushu (Japan) and Central America.

HISTORY OF CALDERA FORMATION ON ROCCAMONFINA VOLCANO (SOUTHERN ITALY) AND ASSOCIATED EXPLOSIVE ERUPTIONS

COLE, P.D. and DUNCAN, A.M., School of Earth Sciences, Luton College of Higher Education, LU1 3JU,
GUEST, J.E., University of London Observatory, Mill Hill Park, NW7 2QS,
CHESTER, D.K., Department of Geography, University of Liverpool, L69 3BX.

Roccamonfina volcano, about 50 km north of Vesuvius, is part of the Quaternary Roman co-magmatic province. The summit is truncated by two calderas, a central caldera some 6 by 5 km in size with a low eastern rim, and a 3 km wide amphitheatre-shaped caldera which cuts the northern flank.

The low eastern rim of the central caldera is draped by a heterogeneous proximal facies of the Campagnola Tuff (previously known as the Brown Leucitic Tuff), a compound ignimbrite which postdates caldera formation. In the caldera the Campagnola Tuff is concealed beneath ignimbrites of the Galluccio Tuff (previously known as the White Trachytic Tuff), which forms the base of the exposed caldera-fill. Interbedded with and overlying the Galluccio Tuff of the caldera-fill are lacustrine horizons including giant pumice beds. Hydromagmatic and magmatic pyroclastics are intercalated with the lacustrine beds. These caldera lakes were ephemeral and probably provided the water source for the hydromagmatic eruptions. Deposits above the lacustrine beds show progressively less evidence upwards of water/magma interaction. Younger pyroclastic surge and flow deposits are tentatively linked to the formation of large lava domes which represent the last major eruptive activity within the central caldera.

The northern caldera is developed on an edifice which is considered to predate the main construct. The Galluccio Tuff crops out widely within this caldera overlying fluvial volcaniclastics, older ignimbrites and lavas. Younger debris flow and fluviatile volcaniclastic deposits which overlie the Galluccio Tuff suggest continued active erosion of this caldera feature. In addition, the presence of intercalated hydromagmatic beds indicates periods of extensive water/magma interaction. The youngest event in the caldera is a period of explosive activity associated with the formation of the Conca Crater, which lies at the back of the amphitheatre of the northern caldera. It is a circular depression some 1.5 km in diameter which cuts southwards into the northern wall of the main caldera. This crater activity generated plinian airfall, pyroclastic surges and a relatively substantial ignimbrite, the Conca Ignimbrite (previuosly known as the Yellow Trachytic Tuff), which extends for over 7 km. Activity from the Conca Crater ended with a phase of phreatomagmatism.

NATURE OF MANTLE AND CRUSTAL SOURCES AND KINEMATICS OF EXTENSION INFERRED FROM GEOCHEMISTRY OF MIO-PLIOCENE VOLCANIC ROCKS IN THE DEATH VALLEY AREA

COLEMAN, D.S., and WALKER, J.D., Department of Geology, University of Kansas, Lawrence KS 66045 USA

Synextensional Mio-Pliocene volcanic rocks in the Panamint Mountains west of Death Valley, range in composition from basalt to rhyolite. Rocks of intermediate composition (SiO_2>50%) dominate the sequence and exhibit a variety of disequilibrium textures, including sieved and glass-bearing plagioclase, and quartz and sanidine xenocrysts. These features are interpreted to have resulted from mixing of mafic and silicic magmas and/or assimilation of older crust by mafic magmas. Major-, trace-, and rare-earth-element data are consistent with this interpretation, and indicate that minor fractional crystallization also occurred.

U-Pb, Rb-Sr, and Sm-Nd isotopic compositions support a three component mixing system of mafic parent magmas with two distinct crustal silicic or intermediate components. The mafic source is characterized by 208Pb/204Pb = 38.2-38.4, $(87Sr/86Sr)_{initial}$ = 0.706, and Epsilon Nd(t_0,CHUR) (E_{Nd}) = 0. One of the silicic components is rather radiogenic and has 208Pb/204Pb > 39, $(87Sr/86Sr)_i$ = 0.716, and E_{Nd} = -10. The other silicic source is less radiogenic and is characterized by 208Pb/204Pb = 38.7, $(87Sr/86Sr)_i$ = 0.704, and E_{Nd} = +5. The three component system is shown well on a plot of 208Pb/204Pb vs. E_{Nd}. Variation of E_{Nd} vs. $(87Sr/86Sr)_i$ is more complicated, but consistent with three component mixing. Mafic lavas plot around E_{Nd} = 0 with intermediate lavas trending toward positive and negative E_{Nd} values, supporting both more and less radiogenic silicic contaminants.

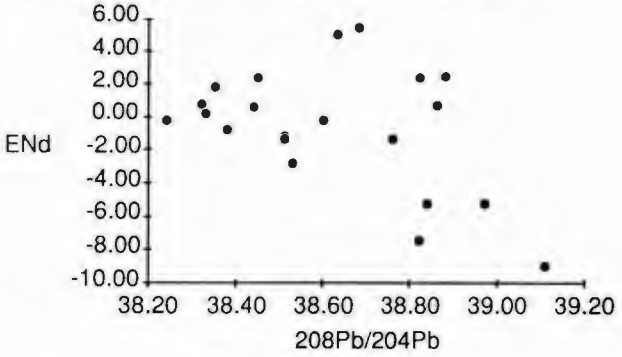

Geochemical data indicate that the mafic component was derived from the mantle characteristic of this part of the Basin and Range Province. This source is distinguished by low Rb/Sr ratios (<0.01) which leave its relatively high $(87Sr/86Sr)_i$ unsupported. We interpret this to indicate recent Rb depletion of an enriched mantle source. Data for the radiogenic silicic component indicate that it is derived from Precambrian crust typical of this region.

The source of the less radiogenic silicic component is problematical. It is unlike Precambrian upper or lower crustal rocks in the Basin and Range, but rather resembles Mesozoic rocks of the Sierra Nevada Batholith. We interpret this component to be lower crustal rocks of the Sierra Nevada structurally emplaced beneath the Death Valley area by low-angle simple-shear deformation. This implies that extensional deformation in the Death Valley area is accommodated by west-dipping shear zones that have dismembered the entire crust, placing Mesozoic age lower crust under Precambrian age upper and middle crust. This indicates that the $(87Sr/86Sr)_i$ = 0.706 line is still west of the Death Valley area in the upper crust (as supported by studies of now upper crustal Mesozoic plutonic rocks), but is under or east of Death Valley in the lower crust. Tertiary volcanic rocks record the passage of this feature, in the lower crust, under the Basin and Range. Understanding such deformation is critical in determining the overall crustal evolution and geochemical structure of the continents.

COMPOSITION AND EVOLUTION OF LOWER CONTINENTAL CRUST: EVIDENCE FROM XENOLITHS IN EOCENE LAVAS FROM THE BEARPAW MOUNTAINS, MONTANA

COLLERSON, K.D., Earth Sciences, UCSC, Santa Cruz, CA. 95064 USA, Hearn, B.C., USGS, Reston, VA. 22093 USA, MACDONALD, R.A., Envir. Sci. Univ. Lancaster, UK. UPTON, B.G.J., Grant Inst. Geol. Univ. Edinburgh, U.K. and HARMON, R.S. NERC, Keyworth, UK.

Abundant granulite facies, amphibolite facies and ultramafic xenoliths occur in middle Eocene mafic phonolite pyroclastic deposits in the Bearpaw Mountains, north central Montana. Ultramafic xenoliths include garnet pyroxenites, biotite (phlogopite) pyroxenites and two groups of peridotites - cumulate textured dunites and wehrlites, and porphyroclastic spinel dunites and harzburgites (Hearn *et al.*, 1989). Seismic studies in the region indicate a crustal thickness of >45 km. The xenolith assemblage affords an excellent opportunity to evaluate: (1) the character and evolution of lower crust in Montana, (2) the crust - mantle lithospheric boundary, and (3) the extent of Archean and early Proterozoic (1.7 - 1.9 Ga) crustal growth in the buried extension of the Wyoming craton.

Granulite xenoliths are dominated by mafic compositions (66.5%). They include high-pressure assemblages (HPG: - grt-cpx-pl-rt±hb±qtz) transitional to eclogite (Jd/Ts >0.95 - 10.8) and intermediate pressure granulites (IPG:-grt-pl-opx-cpx±hb and opx-cpx-pl±hb). A large proportion of the xenoliths belong to a differentiated mafic - anorthosite - leuconorite - norite - pyroxenite and hornblendite) suite (ANPH). Felsic granulites (12.4%), and metasedimentary lithologies (10.6%) that include ky-, sill-, and sapph- bearing gneisses are minor members of the crustal suite. Amphibolite facies gneisses are relatively rare (10.5%). Thermobarometric data for the high pressure granulites record metamorphic temperatures of 650-800°C and minimum pressures of 9 to >16 kbar.

Major and trace element data indicates that Montana lower crust is dominantly basaltic in character. Relatively uniform Rb/Sr ratios and generally low K/Rb ratios (ANPH: 0.028-0.159 & 113-367; HPG: 0.026-0.164 & 115-425; IPG: 0.038 - 0.075 & 91-361) indicate that the lower crust did not experience the degree of LILE depletion reported from many exposed granulite facies terranes. REE patterns reflect the effect of crystal fractionation processes and in general do not show the pronounced negative Eu anomalies hypothesized for the lower continental crust. $^{87}Sr/^{86}Sr$ ratios for different members of the mafic suites show relatively little variation (HPG: - 0.70698 - 0.709032; IPG: - 0.70816 - 0.70855; ANPH: 0.70751 - 0.70758). εNd(0) vary between -8 and -28. O-isotope ratios (as $\delta^{18}O$ values permil SMOW) for the main rock units are: HPG = +6.6 to +8.6, IPG = +7.4 to +8.5 and ANPH = +6.6 to +7.3. Such normal $^{18}O/^{16}O$ ratios, but relatively large variations, indicate that the "deep"-lower continental crust in this cratonic setting has not been affected by pervasive interaction or equilibration with fluids of either internal or external derivation that would be expected to equilibrate O-isotope ratios on a regional scale. These O-isotopic characteristics are unlike those seen in regional granulite facies terranes.

Although some of the felsic and supracrustal xenoliths are clearly derived from the Wyoming craton, the data indicate that the lower continental crust is dominated by chemically distinctive mafic lithologies probably added by magmatic underplating. The crust - mantle boundary is believed to be dominated by ultramafic, mafic and felsic cumulates that crystallized under high pressure granulite to eclogite facies conditions.

PETROLOGY AND ISOTOPE GEOCHEMSITRY OF THE CONEJOS FORMATION, SE SAN JUAN VOLCANIC FIELD: IMPLICATIONS FOR MULTIPLE PARENT MAGMAS AND CRUSTAL INTERACTIONS.

COLUCCI, M.T., DUNGAN, M.A., Dept. Geological Sciences, SMU, Dallas, TX 75275, LIPMAN, P.W., U.S.G.S., Federal Center, Denver, CO 80225, MOORBATH, S., Univ. of Oxford, Parks Road OX1 3PR, Oxford, UK

The Oligocene Conejos Formation of the southeastern San Juan Volcanic Field (SJVF), southern Colorado, comprises all intermediate lava flows and minor ash-flow tuffs erupted prior to collapse of the Platoro caldera complex. Conejos volcanism ensued from at least 7 stratovolcanoes peripheral to the caldera, and preceded eruption of the Treasure Mountain Tuff during multiple collapse events. All lavas are high-K in character ranging from 53-70% SiO_2.

Three stratigraphic members of the Conejos Formation are distinctive in their mineralogy and mineral chemistry, major and trace element compositions, and isotopic character. The Horseshoe Mountain member (HMM) (33.3 to 31.9 Ma) exhibits dominantly hydrous mineralogies (hornblende-phyric andesites and dacites) and is generally characterized by lower total alkali, TiO_2, and incompatible element contents (e.g. Zr = 120-155 & Rb = 25-105 ppm) than other Conejos lavas. These lavas are exposed primarily along the northern periphery of the caldera and represent the most voluminous outpouring of Conejos material (approx. 2500 km^3). A later, more alkaline and incompatible element enriched series, the Rock Creek member (RCM) (Zr = 325-600 & Rb = 80 - 260 ppm), is characterized by anhydrous mineralogies (plag + opx + cpx) up to trachydacitic compositions (63% SiO_2). Eruption of RCM lavas represent a short-lived and relatively low-volume (<100 km^3) event localized along the northern and NE peripheries of the caldera. Willow Mountain member (WMM) (31.8 to 29.0 Ma) lavas are intermediate in alkali and trace element abundances between HMM and RCM, and are preserved as widespread exposures (approx. 1500 km^3) along the southern and SE peripheries of the Platoro Caldera.

Basaltic andesites of the HM and RC members evolved from genetically distinct mantle-derived basaltic parents differing primarily in their trace element abundances. Lavas of the WMM represent late-stage hybrids of the two compositionally extreme (HMM and RCM) Conejos magma series. Radiogenic isotope and trace element relations suggest the evolution from parent basalt to basaltic andesite was accompanied by assimilation of a locally heterogeneous crust. Pb isotope compositions of all members ($^{206}Pb/^{204}Pb$ = 17.3-17.7) are markedly unradiogenic, and ε_{Nd} is significantly radiogenic (-6 to -8), compared to plausible mantle ratios ($^{206}Pb/^{204}Pb$ > 18.2, ε_{Nd} = +8 to -1). HMM basaltic andesites exhibit high Ba abundances and negative Th anomalies compared to low Ba and positive Th-anomalies displayed by RCM trachybasaltic andesites. Ba and Th concentrations, and Pb and Nd isotope compositions of the least evolved lavas within each magma series establish baseline trace element and isotopic signatures indicative of extensive assimilation of a heterogeneous and relatively unradiogenic (in Pb) Proterozoic lower crust during deep crustal residence in large-volume reservoirs (MASH process of Hildreth and Moorbath, 1988). The evolution of basaltic andesites to silicic compositions was accompanied by increasing trace element concentrations and Rb/Th ratios and more radiogenic Pb- and Sr-isotope compositions reflecting additional contamination in higher level, second-stage reservoirs. Diverging evolutionary trends among Conejos magma series in isotope-isotope plots suggest that the second-stage contaminant was also locally heterogeneous.

These results highlight the importance of detailed stratigraphic sampling when attempting to decipher the fine-scale history of crust-magma interactions in a large-volume magmatic system.

SR-RICH BASALTIC ANDESITE VOLCANOES OF THE MT. JEFFERSON AREA, HIGH CASCADE RANGE, OREGON

CONREY, Richard M., Department of Geology, Washington State University, Pullman, WA 99164

The Quaternary High Cascade Range in Oregon is composed of a "mafic platform" of overlapping basaltic andesite shield volcanoes with localized, long-lived centers of andesite-dacite volcanism. The Mt. Jefferson area is one of these centers, and is underlain by an approximately 200 square km field of andesite and dacite volcanoes. This field has probably been active for the past 3 Ma, and has been interpreted as the surface expression of a small granodiorite batholith (Conrey, 1988 - GSA Abs. w. Prog. v.20, A196).

Three basaltic andesite volcanoes mapped at the margins of the Mt. Jefferson field are composed of lavas with from 1000 to 2000 ppm Sr. All three are considerably eroded and of modest volume (< 2-3 km^3). Ages range from 0.65 Ma (K-Ar) for East Park Ridge (EPR) volcano NE of Mt. Jefferson, to an estimated 0.4 Ma and 0.2 Ma for Lower Skyline Trail (LST) and North Cinder Peak (NCP) volcanoes, respectively, south of Mt. Jefferson. The Sr-rich lavas have rather high contents of augite phenocrysts (to 6-7 vol%) and rare orthopyroxene. In contrast, Sr contents of typical Cascade basaltic andesites are rarely in excess of 900 ppm, orthopyroxene phenocrysts are common, and augite is sparse.

Chemical patterns in the three volcanoes are remarkably similar. Initially, each erupted Sr (≤2040 ppm), K_2O (≤1.8 wt%), Ba (≤900 ppm), Rb (≤18 ppm), P_2O_5 (≤0.6 wt%), La (≤43 ppm), Zr (≤215 ppm)-rich and SiO_2-poor lavas, followed by more SiO_2-rich and incompatible element (IE)-poor lavas. The best available stratigraphy is from NCP volcano; 10 samples from a stack of 18 successive flows there show an essentially linear decrease upsection in IE content, and an increase in SiO_2. EPR has the widest range in SiO_2, from 55.1-58.5 wt%; the range is much more restricted at NCP (55.5-56.5) and LST (54.2-54.9) volcanoes. Variations in all other major elements are small, even at EPR. TiO_2 is less than 1.3 wt% at all three volcanoes, and Nb is less than 12 ppm. Nb correlates with Sr at EPR, but at NCP and LST Nb contents are constant.

Plagioclase (20-40 vol%) is the major phenocryst mineral in all of the rocks, accompanied by lesser augite, olivine (Fo82-76; with rare Cr-spinel inclusions), orthopyroxene (En80-65), magnetite, and resorbed amphibole. Plagioclase is oscillatory zoned, with wide compositional jumps between zones. Oscillatory mantles (An68-51) are grown on either more sodic (to An50) or more calcic (to An84) cores. NCP has oscillatory cores (An74-55) overgrown by more calcic (An82-65) "fritted" zones. Augite is both sector and oscillatory zoned; Wo content is as high as 47 at EPR, but is 38-43 at the other volcanoes. Resorbed, reverse zoned orthopyroxene is present in some EPR augites.

The decrease in SiO_2 with increasing IE contents in the volcanoes eliminates fractionation as a possible means of explaining the chemical variations. The linear chemical patterns and evidence for mineralogic disequilibrium support a mixing model instead. It appears that SiO_2-poor, IE-rich magmas were mixed with fairly normal andesite magmas to create the Sr-rich lavas. At depth this mixing may take the form of synplutonic lamprophyre dikes injected into the tonalite margin of a small batholith. The ultimate genesis of the lamprophyre magmas remains uncertain. Rare basalts and basaltic andesites found throughout the length of the Cascade Range in Oregon have similar chemistry and mineralogy to the Sr-rich basaltic andesites. The high La/Yb ratios (ca. 25-30 chondrite normalized) of these lavas imply residual garnet in their source, probably sediment in the subducted slab.

PETROLOGICAL SIGNIFICANCE OF HIGH-PRESSURE ULTRAMAFIC XENOLITHS FROM ULTRAPOTASSIC ROCKS OF CENTRAL ITALY

Sandro CONTICELLI & Angelo PECCERILLO

Dipartimento di Scienze della Terra, Firenze & Istituto di Scienze della Terra, Messina, Italy

In this study we describe for the first time high pressure ultramafic xenoliths occurring in ultrapotassic rocks of the Roman province. The studied xenoliths have been found enclosed in lavas outpoured from the Torre Alfina volcano, a 0.8 ma old apparatus sited on the northern border of the Vulsinian district, Central Italy. The ultramafic xenoliths have a maximum size of 4-5 cm and are represented by spinel lherzolites, spinel harzburgites with minor wehrlites and dunites. Some samples contain discrete laths of phlogopite. The absence of alteration products as well as textural and compositional evidence exclude that this inclusion are fragments of ultramafic ophiolitic rocks. The same lines of evidence rule out a cumulitic origin. Textural characteristics such as triple points, deformed olivine with well developed kink banding and porphyroclastic textures indicate equilibration at high pressure. Pressure estimate gave minimum values of about 1.5 GPa, corresponding to upper mantle in the studied area. Equilibration temperatures have been estimated around 950-1030 degree C. Accordingly, the Torre Alfina ultramafic inclusions represent the only samples of upper mantle material brought to the surface by ultrapotassic magmas in Central-Southern Italy. The chemical composition of these phases, especially the very high Fo contents (up to Fo94%) of olivines, Mg# of orthopyroxenes, and Cr/Al relationship in spinels and clinopyroxenes suggest that the investigated xenoliths represent residual peridotites that have suffered different degrees of partial melting before being incorporated into the Torre Alfina magma. On the other hand, the presence of phlogopite also suggests the occurrence of a metasomatic event. The host lavas have an intermediate composition between high-silica lamproites and Roman-type ultrapotassic rocks. They have high abundance of incompatible elements (Rb = 450 ppm; Th = 62 ppm; La = 100 ppm) and radiogenic Sr ($^{87}Sr/^{86}Sr$) coupled with high Mg# (77), Ni (350 ppm) and Cr (840), that support a genesis in a residual upper mantle, enriched in incompatible elements by metasomatic processes.

KALAUPAPA, MOLOKAI AND OTHER HAWAIIAN LAVA CHANNELS: TERRESTRIAL ANALOGS TO LUNAR SINUOUS RILLES

COOMBS, C.R., Johnson Space Center, SN 15, Houston, Tx, 77058

Introduction: Lava channels and tubes associated with both recent and historic Hawaiian lava flows are morphologically very similar to lunar sinuous rilles. This study investigated the basic processes responsible for the formation of several Hawaiian lava channels and tubes (i.e.: Kauhako Crater, Kalaupapa, Molokai; Makapu'u, Oahu; Kupaianaha and Mauna Ulu, Kilauea, Hawaii) and related them to the formation of lunar sinuous rilles. Both the terrestrial and lunar features formed as a result of basaltic volcanism, have deep source craters, exhibit some degree of tube formation, follow sinuous paths, and show evidence of some thermal erosion.

Kauhako Crater, Kalaupapa, Molokai, Hawaii: Kalaupapa is a 10 km^2 shield volcano that rises 135 m above sea at Pu'u 'Uao. The Kalaupapa shield is capped by Kauhako Crater (diameter: 500 m x 650 m). The crater forms a funnel-like pit with a circum-crater terrace and lake at the bottom. The terrace is at 40 m elevation and is ~150 m wide. Kauhako Lake, at the bottom of the crater, is 50 m wide and 248 m deep. A sinuous lava channel/tube extends northward from the northeast side of Kauhako crater. This discontinuous channel is 1.0 km long, up to 30 m deep and ranges in width from 100 m to 150 m. Tumuli at the distal end of this channel mark the location of the underlying tube system and extend the channel another 1.3 km to the N-NE. Thermal erosion downcut portions of this channel at a rate of 10.5 μms^{-1}.

Mauna Ulu/Kupaianaha, Kilauea, Hawaii, Hawaii: Both of these mini-shields are located along the southeast rift zone of Kilauea. Observations made during both eruptions indicate that the channels and tubes formed along their flanks developed in a similar manner. The sinuousity and presence of ledges or small terraces within the main channels/tubes suggest that some thermal erosion occurred during their formation. At present, thermal erosion appears to be occurring in the active Kupaianaha conduit system as it transports lava from the main vent to the Kalapana coast 3.0 km away.

Whittington lava tube, Mauna Loa, Hawaii, Hawaii/Makapu'u lava tube, Oahu, Hawaii: Both of these lava tubes show evidence of thermal erosive activity in their formational histories. The Makapu'u tube, now completely filled in, was formed in several stages. The first stage cut the main channel, and is the conduit by which all others flowed. The Whittington lava tube on Hawaii cut through two older, successive flows adjacent to it. These two flows are separated by a thin, weathered paleosol. Several tree molds also present within these two layers suggest that some time interval occurred between the eruption and deposition of the two flows. Field evidence strongly suggests that the lava tube did not form contemporaneously with the adjacent lava flows, and supports a thermal erosion model for the downcutting of the tube into the previously formed stratigraphic layers.

Rima Mozart, a lunar analog: Rima Mozart is a 40 km-long lunar sinuous rille located 100 km southwest of the Apollo 15 landing site. The rille originates at a deep source crater, is basaltic in composition, and exhibits evidence for thermal erosion along the main channel, analogous to the terrestrial conduit systems mentioned above. An explosive phase is thought to have been associated with the formation of this rille. Likewise, minor explosive activity is thought to have been associated with the Hawaiian analogs. Thermal erosion downcut the main channel of this bifurcated rille at a rate of 1.55 μms^{-1}.

Conclusion: The morphology and apparent eruptive history of the Hawaiian lava channels discussed above make them good analogs to lunar sinuous rilles (e.g., Rima Mozart). Thermal erosion does occur in terrestrial basaltic lava channels/tubes and appears to be an important factor in their formation. Similarly, thermal erosion is thought to be an important process involved in the formation of lunar sinuous rilles.

ON THE RUIZ VOLCANO SEISMIC ACTIVITY

CORAL G., Carlos E., Universidad Nacional de Colombia, Departamento de Geosciencias, Apartado Aereo No. 14490, Bogota, Colombia

The Ruiz volcano seismic activity prior to and after the November 13, 1985 eruption which killed nearly 25,000 people, is described. Before the September 11th and November 13th (1985) eruptions, a high micro-earthquake frequency was followed by a decrease in seismic activity and energy release, as well as, variations of the b-value in the magnitude-frequency relation.

The spatial distribution of volcanic microearthquakes shows a region "free" of seismicity at depths of 5 to 9 km which could be associated with a volume of melt material. Earthquakes with M greater than or equal to 4.5 observed at intermediate depths in the Caldas region seem to be related to the volcanic activity in that zone.

Total energy released on the November 13, 1985 eruption of the Ruiz volcano is estimated. Its amount, on the order of 10^{23} erg., appears to be equivalent to only 1% of the total energy released on May 19, 1980 by the Mount St. Helen's eruption.

FREE GASES IN Mt. EUGANEI (NORTHERN ITALY): He AND Rn AS TRACERS OF HYDROLOGICAL PATHS

CORAZZA, E., and MAGRO, G., Istituto di Geocronologia e Geochimica Isotopica, Via Maffi, 36, Pisa, Italy,
CECCARELLI, A., ENEL-UNG, Via A. Pisano,120,Pisa,Italy,
PANICHI, C., Istituto Internazionale Ricerche Geotermiche, P.za Solferino, Pisa, Italy, and
ANTONELLI, R., Dipartimento Scienze della Terra, Via Giotto, 20, Padova, Italy

A number of samples of free gases were collected in the Mt. Euganei (northern Italy) volcanic area. This is a thermal area of economic interest because of its exploitation for spa and recreation. This work was carried out in cooperation with the University of Padova (Department of Earth Science) under a contract with the Veneto regional administration (P.U.R.T.) with the purpose of investigating if a high-enthalpy geothermal system exists at depth.

The main component of gases is N_2 (69 to 96%) with CO_2 1 to 20%; CH_4 reaches several percent in most samples, with minor amounts of C_2H_6 and of C_3H_8. H_2S was revealed at low concentrations in few samples, while H_2 is generally at the ppm level. The He concentrations are remarkable, reaching several hundreds of ppm; Ar instead is always close to the air concentration. A high Rn activity was also measured in gases.

The presence of CH_4 and higher hydrocarbons, low H_2 and high atmospheric components indicate that if a deep contribution does exist it must have had long residence times in shallow systems where its composition was greatly changed.

A positive correlation was found between He and Rn, both from radioactive decay of U and Th of the rocks: He increases up to an asymptotic value of 1500 ppm He, while Rn keeps increasing. The two elements have a common origin , but He is a stable element while Rn decays fast (3.8 days half-life), so that its activity at the surface is related to the upwelling time of fluids; high Rn concentrations with high and constant He are found in areas of fast circulation (hundreds of wells) while low He and Rn correspond to natural springs.

Stable isotope compositions of thermal waters, anomalous with respect to the local meteoric waters of the area, are exhibited by the same springs as the ones mentioned for He and Rn anomalies.

The ^{18}O vs. D relationship for some samples demonstrates a strong water-rock exchange at high temperature. These anomalies are not general all over the area, but the processes producing them are masked by the local shallow water circulation which alters the isotopic and chemical characteristics of the deep geotherml fluids.

CAENOZOIC EXTENSIONAL TECTONICS AND EXTRANDEAN VOLCANISM IN SOUTHERN SOUTH AMERICA, PATAGONIA, ARGENTINA

CORBELLA, H., CONICET-CIRGEO, BAires. FAX:(541)345437.

On the atlantic slope of southern South America, caenozoic volcanism is associated with extensional tectonics. The main continental structures and the magnetic anomalies and transform faults of the neighbouring Pacific Ocean (shown in the map) allow to remark:

-) The split and extension of the continental crust occurred mainly in a back-arc setting.

-) The direction of the main fractures and alignments in the extrandean region is perpendicular to the trend of the subduction zone. In the South area the dominant continental structures and the normal to the subduction trend have a NNE direction. In the North area instead, the NW direction of the megalignments and structures corresponds remarkably with the change of direction of the Pacific subduced belt-segment N of the Valdivia fault zone.These facts indicate that the continental structures are linked with the subduction phenomena, which can generate tensional stresses behind the orogenic area.

-) In the extrandean continental region, the pattern of gravitational fractures shows a block type tectonics. Cyclical compression-relaxation periods in the Andean orogen (Incaic II, Quechuan I and II) pushed the contiguous back-arc basement producing tilt, shift, lift and sink of large blocks. Long rhomboidal trenches of "pull-apart" origin and parallel fault clusters of well developed rift geometry are also observed.

-) The voluminous effusions of predominantly basaltic composition and the perfectly radial dike patterns in some highly differentiated centers point out the extensional or atectonic state of the lithosphere during the extrandean igneous events.

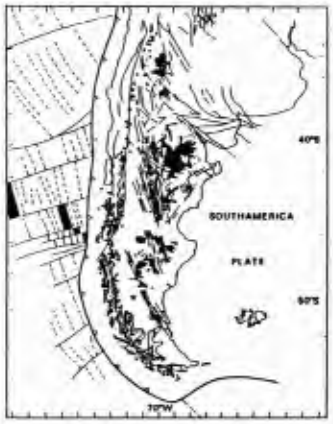

Among the Caenozoic extrandean volcanics, 300 age determinations allow to recognize:

-) Oligocene alkali-basaltic rocks (now gently folded) associated with a tight parallel NNW fault system of rift geometry (SW Chubut).

-) Miocene volcanics poured out as large floods of alkaline to transitional basalts (the Somuncura and Cuadrada plateaus among the biggest) with differentiated effusive centers of trachite-commenditic nature (Sierra de Somuncura, Apas, Telsen, Chacays and Talagapa). Small post plateau volcanic cones of basaltic, basanitic, nephelinitic or phoiditic nature. The eroded roots of some volcanic bodies outcrop as subvolcanic annular complexes of zonal composition (alkali gabbro, essexite, nepheline syenite). Finally, late Miocene subvolcanic and volcanic rocks of potassic (latites) and ultrapotassic (orendites) nature also occur (Sierra Chacays).

-) Important Plio-pleistocene stratovolcanoes and widespreaded outcrops of basaltic composition in the Northwest; whereas in the South large basaltic floods and numerouos basaltic cones, some aligned along a rift fault system (SE Santa Cruz), are found.

BASALT TO ANDESITE, EASTERN GALAPAGOS RIFT: STABLE ISOTOPE, VOLATILE, AND HALOGEN TRACERS AND AFC PROCESSES IN SPREADING CENTER MAGMAS

CORNELL, W. C., TAYLOR, B. E., Geological Survey of Canada, 601 Booth Street, Ottawa, Ontario, Canada K1A0E8, and PERFIT, M. R., Department of Geology, University of Florida, Gainesville, Florida, U.S.A. 32611

Oxygen and hydrogen isotope compositions, and concentrations of H_2O, Cl, F, and S in fresh, hand-picked MORB, ferrobasalt, FeTi basalt, basaltic andesite, and andesite glasses from the eastern Galapagos rift (85°W) indicate that magmas were modified by assimilation-fractional crystallization (AFC) processes along the Galapagos ridge axis. Relationships among these tracers, and between them and MgO and SiO_2, indicate that assimilation of Cl-enriched (and F-enriched ?), S-depleted, sea-water-hydrated (high-T) oceanic crust has lead to modification of basalt magma.

The water content of fresh basaltic to andesitic glass (wt. % MgO >7.5 to nearly 1.0), varies from 0.17 to 1.35 wt. % H_2O, but is as much as 0.6 wt.% in excess of that expected from enrichment during fractional crystallization (FC) Galapagos basalt has δD = -80 to -67 (one sample: -95), whereas the δD of andesite varies from -66 to -51. Increases in δD, Cl (85 to 4245 ppm), and F (68 to 903 ppm) with wt. % H_2O suggest the assimilation of crust with Cl/H_2O of ca. 0.3, (perhaps a high-Cl amphibolite: Vanko, 1986; cf., Cl/H = 0.5 found elsewhere by Michael and Schilling, 1988). The narrow range (1 °/oo) and the primary signature of $\delta^{18}O$ (5.2 to 6.2; most have $\delta^{18}O$ = 5.7 ± 0.2) support contamination of the magmas by stoping of crust previously altered at high temperature and low water/rock ratio rather than by direct interaction with an aqueous fluid. The hydrogen isotope composition of andesitic magmatic water thus differs from that of MORB, ferrobasalt, and FeTi basalt (δD ≈ -78 ± 5), and is determined, in this case, by the composition of the assimilated crust. However, the $^{87}Sr/^{86}Sr$ ratio increases only slightly from fresh basalt (0.7025) to andesite (0.7030).

FC and AFC paths are distinguished on plots of ppm S vs wt. % MgO, and ppm S vs δD. Reversals in enrichment/depletion trends are apparent at ca. 2000 ppm S on both plots. S increases to ca. 2000 ppm at 5 wt. % MgO, then decreases with further increase in MgO. δD is constant as S increases in the basalts, then increases to -50 as S decreases in the andesites. Similarly, a plot of wt. % MgO vs δD indicates an FC path (decrease in MgO at constant δD) for the basalts, but an AFC path (decrease in MgO with increasing δD) for the andesites. The wt.% SiO_2 and δD do not covary for basalt, whereas the positive correlation for andesites (wt. % SiO_2 = 55.1 to 61; δD= -67 to -50) further supports AFC processes.

This study suggests that assimilation of altered oceanic crust is an important process associated with extensive fractional crystallization in small magma chambers. Large magma chambers can be less readily modified. They reqire less crystallization (which accentuates chemical variability) to provide heat for assimilation of equivalent amounts of altered crust which readily contaminate smaller magmas.

TOPOGRAPHIC CONTROLS ON SMALL-VOLUME PYROCLASTIC FLOWS: AN EXAMPLE FROM HIBOK-HIBOK VOLCANO, PHILIPPINES

CORPUZ, E.G. and SOLIDUM, R.U. Philippine Institute of Volcanology and Seismology, 29 Quezon Ave. Quezon City, Philippines.

Recent destructive eruptions from 1948-53 at Hibok-Hibok Volcano in the Philippines show that changes in topography during the course of an eruption can adversely affect directions of descent and subsequent areas of emplacement of small-volume pyroclastic flows. Small lateral explosions and disruption of a growing dome during the 1951 eruption of Hibok-Hibok produced pyroclastic flows which swept the northeastern valley with velocities in excess of 55 m/s and emplaced at temperatures of at least 700 degrees celsius. Initial blasts of 4 December 1951 produced fine-grained and gas-charged pyroclastics which flowed east-northeast. Blocky lava which flowed from 1948-49 as well as lava ridges from the adjacent northern slopes of Mt. Mambajao diverted the pyroclastic flows northeastward and fanned across Mambajao Town, killing 500 persons. Subsequent flows on 6 December 1951 were relatively coarser grained and less inflated, consequently being more or less channeled. Other pyroclastic flows rode the previously formed blocky lava flow along a northeast track but were diverted northwestward by an oblique pressure ridge and by ancient deposits. Rapid aggradation of channel floors led to overtopping. Pre-eruption topographic models showed projected azimuths through an east-northeast track across scarcely populated areas. Because of newly emplaced deposits combined with previous surfaces, flowage paths were significantly modified. Thus, in preparing hazard maps for future volcanic eruptions, studies must therefore account for probable topographic changes during eruption in addition to pre-eruption geomorphology as an approximation for qualifying high risk areas for flowage phenomena.

GEOCHEMICAL AND ISOTOPIC EVOLUTION OF A THREE-COMPONENT VOLCANOLOGICAL SYSTEM : THE ISLAND OF LIPARI, AEOLIAN ARC, ITALY

CRISCI, G.M.; DE ROSA, R.; MAZZUOLI, R., Dipto. Scienze della Terra, Universita della Calabria, 87030 Castiglione Scalo, CS, Italy, and ESPERANÇA, S., Dept. Geological Sciences, Old Dominion University, Norfolk, VA 23529

The history of volcanism in Lipari, characterized by lavas of calc-alkalic to shoshonitic compositions, has been described in terms of time of eruption and geographic distribution in the island. In the emerged part of the island, volcanic activity can be subdivided in two periods. The first period, from 223 to 42 Ka, is characterized by flows of basalt-andesitic composition with progressive increase in both SiO_2 and K_2O content with time. The second period, post-42 Ka, is marked by an apparent rejuvenation of the geochemical system and the appearance of the first rhyolitic compositions. Models using fractional crystallization, assimilation and mixing indicate that the Lipari lavas have geochemical characteristics derived from a complex petrogenetic process involving three heterogeneous end-members. Two end-members are primarily mantle-derived and have distinct chemical and isotopic compositions and the third end-member is a composite crustal end-member.

Isotopic composition of the early volcanic products (Pre-Tyrrhenian cycle) of the first period show $\epsilon Nd=3$ to 4, $^{87}Sr/^{86}Sr=0.704-0.7045$ and OIB-like Pb. The end of the first period (San Angelo cycle II) is marked by the eruption of cordierite-bearing lavas that exhibit $\epsilon Nd \sim -4$ and the most radiogenic Sr isotopic composition (0.706 to 0.7068) of the lavas analysed. The second period of activity (M.Guardia cycles) is characterized by lavas with $\epsilon Nd \sim 0$ to -1 and 0.705 to 0.706. In Pb-Sr and Pb-Nd space, departure from the OIB field takes place at $^{206}Pb/^{204}Pb \sim 19.1$ to 19.3, in the direction of the Roman Campanian Province.

The combined petrologic and chemical evidence suggest that there is a variation in the input ratio of the different components through time. The sub-alkaline end-member is the main component in the early stages of volcanism in the island. This end-member has Pb-Sr-Nd isotopic characteristics of an OIB-like mantle source. The second mantle component, the alkaline end-member, is characterized by large concentrations of incompatibles such as K, Sr, Ba, Rb and LREE and is exemplified by the shoshonites from Vulcano. This alkaline component increases its contribution to the system with time and tends to overwhelm the geochemical character of the sub-alkaline end-member specially during the second period of activity. This end-member appears to be the continental mantle responsible for the unusual isotopic characteristics of volcanics from the Roman Campanian Province. The input of the crustal end-member becomes dominant during the last stages of volcanic activity in the island. This input is a mixture of crustal materials derived from the Calabrian arc (Serre) and primarily crustal melts (rhyolites).

The model suggested for the evolution of volcanism in Lipari is one where melting is initiated at depth due to the subduction process and/or opening of the Tyrrhenian Sea. In time, the thermal input rises causing the progressive melting of the deeper sub-alkaline mantle, the intermediate alkaline continental mantle and involving the crust during the late stages of volcanism. Because of the almost simultaneous melting of the different sources, the volcanic products present geochemical and petrologic evidence of complex mixing. The compositional gaps and the mixing evidence suggest the existence of a series of small chambers at different depths instead of a wide-staging area of magmas. Interaction between the different levels of this system may be controlled by changes in the tectonic behaviour of the W. Mediterranean.

VOLUMES AND COMPOSITIONAL VARIATIONS OF THE MAY 18, 1980 ERUPTION OF MOUNT ST. HELENS: IMPLICATIONS FOR ERUPTION FORECASTS

Criswell, C.W., Department of Geology, Univ. New Mexico, Albuquerque, New Mexico 87131

The Plinian phase of the May 18, 1980 eruption of Mount St. Helens is estimated to have vented about 0.33 (0.12 - pyroclastic flows and 0.213 tephra) km^3 dense-rock-equivalent magma. The May 18 Pumice Plain deposits contain 76% hornblende dacite (64% SiO_2), 23% hornblende andesite (62% SiO_2) and about 1% pyroxene andesite (60% SiO_2). Considering the estimated volumes of the lateral blast, subsequent small pyroclastic flows and tephras, and dome lavas, total volume was about 0.5 km^3 of compositionally zoned magma. Post-May 18 activity records a general decline in erupted volumes and proportions of hornblende dacite, interpreted by others as the progressive tapping of a zoned magma chamber 7-12 km deep. As these compositional trends were apparent on May 18, the initial mobilization of these magmas occurred during the climactic phases of May 18.

It is well documented that the dome lavas originated from a shallow (1-2 km) reservoir and not the deep (7-12 km) magma chamber tapped during the May 18 eruption. Considering that (1) the estimated volume of magmatic gases released on May 18 indicate that 1-5 km^3 of magma degassed; and (2) the nonexplosive products are chemically identical to their explosive counterparts vented during the post-May 18 events, it is possible that the post-May 18 explosive products were also fed by a shallow magma body that I interpret to have been emplaced during the climactic phases of May 18. The greatest seismic energy release of May 18 occurred during the climactic phase at 3-6 km depth, a zone that is now, in part, aseismic. Although slightly deeper than the accepted depth of origin of the dome lavas, the 3-6 km depths are consistent with the seismic trends that accompanied the small post-May 18 eruptions; deeper earthquakes followed each eruptive pulse, but appeared to be related to fault movements and mechanical adjustments.

If post-May 18 explosive eruptions originated from an intrusion or magma body shallower than the deep chamber, then the observed trends of decreasing volatile content (i.e., hornblende/ hornblende + pyroxene ratios) and increased crystallinity represent only the conditions within the shallow intrusion. These successive products cannot then be used as a basis for forecasting the future explosive activity of Mount St. Helens. The climactic phase of May 18 may have tapped crystal-rich portions of the deep chamber and moved these into shallower parts of the crust. These crystal-rich materials may represent the viscosity barrier that inhibited further magma withdrawal, and hence may have stopped the eruption. Whether this deep chamber was completely evacuated of its most volatile-rich materials is actually unknown, and, therefore, its capacity for future explosive eruption is also unknown. The deep chamber may have been exhausted of its most differentiated materials during the climactic phase of May 18, but the less-evolved nature of subsequent products may not be the evidence. Deep (12-20 km) seismicity of late May 18 may have been fresh influx, so that regeneration may have begun.

POLYCYCLIC VOLCANISM: A COMMON ERUPTION MECHANISM OF SMALL VOLUME BASALTIC VOLCANIC CENTERS OF THE SOUTHERN GREAT BASIN, USA

B. CROWE[1], B. TURRIN[2], S. WELLS[3], L. McFADDEN[3], C. RENAULT[3], F. PERRY[3], C. HARRINGTON[1], and D. CHAMPION[2]
[1]Los Alamos National Laboratory, Los Alamos, NM 87545;
[2]U.S. Geological Survey, Menlo Park, CA 94025
[3]University of New Mexico, Albuquerque, NM 87131

Small volume (<1 km^3) basaltic volcanic centers consisting of scoria cones and associated lava flows are inferred traditionally to form during a short duration (months to years) eruptive episode (monogenetic centers). Detailed studies of alkali basalt (hawaiite) centers in the southern Great Basin indicate that eruptions of these centers are much more complex. These studies are based on field mapping (scale 1:4000), analysis of progressive degradation, the degree of soil formation and the development of rock varnish on cone and lava surfaces, measurement of the paleomagnetic pole position of volcanic units, and conventional K-Ar age determinations. Examination of basalt centers of the southern Great Basin using these techniques shows that: (1) many, perhaps most, of the centers exhibit brief periods of eruptive activity separated by longer periods of inactivity; (2) small volume basalt centers may erupt intermittently over time spans of 10^3 to 10^5 yrs; and (3) there is a general decline in volume and increase in the ratio of scoria/lava in succeeding eruptions.

We classify the basalt centers as polycyclic and distinguish them from polygenetic centers. Polygenetic volcanoes are characterized by eruptions over time spans of 10^5 to 10^6 yrs, with eruption volumes of >1 to <10 km^3. There may be significant variation in the composition of magma of polygenetic centers. These centers are inferred to develop above a maintained, shallow sub-volcanic reservoir. Polycyclic behavior, in contrast, is associated with small volume (<1 km^3) basalt centers that exhibit intermittent eruptive activity separated by long periods of inactivity. The magma eruption rates of these centers are low (<10^6 m^3 yr^{-1}) and the erupted magmas are of uniform composition. The magma supply rate is too small to maintain a chamber in the shallow crust for the lifetime of the volcano. The repeated eruptions must be derived from ascent of individual pulses of magma from a deep crustal chamber or mantle source.

The frequency of occurrence of polycyclic volcanic centers is being investigated. Polycyclic eruptive patterns have been documented at Quaternary volcanic centers in the Crater Flat and Cima volcanic fields (Turrin and Renne, 1987; Renault et al., 1988); it has been recognized, based on preliminary studies, at other Quaternary centers (Lunar Crater and Sleeping Butte volcanic fields). We infer that it may be a common eruption mechanism of other basaltic centers of the southern Great Basin. The recognition of polycyclic volcanism has three significant impacts. (1) Past petrological studies of these centers are incomplete. They are based on sampling lavas which represent only part of the eruptive units. (2) The ascent of an initial pulse of basalt magma may create a preferential pathway through the shallow crust. This pathway controls the site of ascent of future magma until it is sealed by the regional stress field. (3) Polycyclic eruption patterns of basalt centers must be considered for volcanic hazard studies.

SPECTRAL AND MORPHOLOGIC CHARACTERISTICS OF IGNIMBRITES: THE FRAILES FORMATION, BOLIVIA

CROWN, D.A., R. GREELEY, and M.F. SHERIDAN, *Department of Geology, Arizona State University, Tempe, AZ 85287*
CARRASCO, R., *Servicio Geologica de Bolivia, La Paz Bolivia*

The Frailes Formation, an extensive ignimbrite plateau (>100 km in diameter) located along the western margin of the Eastern Cordillera of the Andes in southern Bolivia, is among the largest ignimbrite deposits in the world. The ash-flow sheets comprising the 5 - 8 Ma Frailes Formation display various degrees of welding with exposures averaging 100 m in thickness and reaching a maximum of ~1 km. A remote sensing and field reconnaissance study of this region has been initiated to develop morphologic and spectral criteria for the identification of ash deposits. A primary objective is the assessment of LANDSAT Thematic Mapper (TM) data in mapping volcanic materials in order to make interpretations regarding the eruption and emplacement processes leading to their formation.

The spatial resolution and spectral variations of TM data allow mapping of the units and identification of sub-units within the ignimbrite plateau. Volcanic materials are easily distinguished from the surrounding sedimentary rocks in the fold belts of the Eastern Cordillera and on the surface of the Altiplano. Extrusive volcanic materials associated with the Frailes Formation can also be differentiated from the ash deposits. The majority of the exposed horizontal rock surfaces are of the partially-welded, columnar-jointed interior of the tuffs (the upper non-welded zone presumably has been stripped off). In areas where the non-welded base of the flows are exposed, they can easily be identified and distinguished from outcrops of partially-welded ash.

Discrimination of probable ignimbrite source areas from other eruptive centers is based upon examination of TM images and field observations. Five major eruptive centers and their associated flow materials can be identified. To the north in the Frailes Formation are two quasi-circular regions, which appear spectrally different than the main part of the plateau due to the presence of a well-developed glacial deposit. These areas (Cerro Livicucho and Cerro Condor Nasa/Cerro Chokkota) are apparently older, self-contained eruptive centers with the extrusions at their summits representing post-Frailes eruptions at the locations of ignimbrite source vents. The main part of the plateau consists of 2 overlapping ash shields with sources represented by Cerro Villacollo, a cone of lava with a prominent summit crater, and Cerro Pascual Canaviri, a large, high-standing dome complex. A fifth and the youngest eruptive center is the Nuevo Mundo Province, a complex of large rhyolite domes and related ash deposits at the southern margin of the Frailes Formation. Wind-blown, weathered ash from this area blankets much of the SE part of the plateau. Identification of the units within the Frailes Formation and interpretations of the age relationships on the plateau using TM data are generally in agreement with previous remote sensing and geochemical studies.

Interpretations made from the spectral information of the TM data are supported by laboratory, visible and near-infrared, bidirectional reflectance measurements of samples collected in the field. Spectra of Frailes ash are relatively featureless, exhibiting bands due only to water and hydroxyl. A progression in brightness from welded to windblown to non-welded ash, as seen in the TM image, is attributed to a decrease in the effective particle size. Spectra of lavas found in the plateau can be easily distinguished from those of the ash and exhibit a 0.9 micron band due to ferrous iron as well as water and hydroxyl absorptions.

From examination of the Frailes Formation, several distinctive morphologic properties of large ignimbrites erupted from central vents are evident. Ash-flow sheets form low-relief shields around their eruptive centers which are identified by post-ignimbrite domes and cones. In addition to their steeper slopes, these extrusions are more resistant to erosion than the surrounding ash. On the western margin of the plateau a prominent radial drainage pattern is observed reflecting the topography associated with an eruptive center. The partially-welded interiors of the ash flows create cliff-forming exposures, whereas the non-welded bases are slope-forming units. Distinctive erosional outliers of tuff, which are capped by partially-welded ash, are found on the surface of the Altiplano.

INFLUENCE OF QUATERNARY TECTONIC DEFORMATION ON VOLCANISM IN THE SPRINGERVILLE VOLCANIC FIELD, COLORADO PLATEAU, USA

CRUMPLER, L.S., and **AUBELE, Jayne C.**, *Department of Geological Sciences, Brown Univeristy, Providence, RI, 02912* , and **CONDIT, C.D**, *Department of Geology and Geography, University of Massachusetts, Amherst, MA 01003*

The Springerville volcanic field is the southern-most of several predominantly basaltic late Cenozoic volcanic fields on the margins of the Colorado Plateau. The Springerville volcanic field is noted both for its size and volume (about half that of the San Francisco volcanic field 300 km to the northeast), and for its "classic" cinder cone field morphology, including over 380 vents and lava flows ranging in age from 2.1 Ma to 0.3 Ma and clustered together at an altitude of 2000 to 3000 m. The occurrence of Quaternary structural features within the field offers the potential for evaluating in detail the interaction between tectonic stresses and regional volcanism.

Detailed mapping and K-Ar dating of individual flow units demonstrates that many of the flows in the Springerville field have undergone complex tilting and faulting in the last million years, primarily along a series of tectonic steps or deformation zones, and that locally the field appears warped into a few elongate structural lows as well. The surface descends over one kilometer to the northeast across at least two regional northwesterly-trending arcuate topographic steps or scarps, each of which is characterized by disparate types of deformation (folds, strike-slip, pull-apart basins, and linear graben). The presence of different deformational types, and the amplitude of deformation changes along strike, suggest that the steps and the deformation are not the result of simple normal faulting. The orientation of folds and pull-apart basins implys that the local sense of shear along the steps is left-lateral, but structural relief and displacements are frequently subtle, so that many of the deformations may best be described as being of an incipient nature. The altimetric steps and structural zones are narrow (<1 km), continuous, parallel, and linear to arcuate, changing in strike from WNW in the southern part of the field to NW in the northern field. The occurrence of this variety of characteristics along a long and relatively narrow linear to arcuate trend implies that the steps have experienced complex strain histories. The location of the field at the intersection of the Rio Grande Rift structural trend (NE) and the NW-SE Transition Zone between the Basin and Range-Colorado Plateau suggests that these structural patterns may be a result of the potentially complex changes in regional structural trends and associated tectonic stresses at this intersection.

Although these structural features imply the interaction of tectonic stresses of complex but limited amplitude with volcanism, corresponding linear fissure-type vent structures, indicative of strong trends in extension, are uncommon in the Springerville field. In this respect the field differs from the Mount Taylor field, 200 km to the northeast, where extension along the eastern margin of the Colorado Plateau and and the Rio Grande rift occurs and fissure-type vents are common. In the Springerville field, the location and orientation of the few observed fissure-type vents and the location and displacement of the structural trends suggest that the field has experienced step-like down-faulting and small amounts of left-lateral strike slip movement accompanying the clockwise rotation of (possibly detached) upper crustal blocks. This sense of tectonic transport could occur if nearly east-west striking regional tectonic shear has been active along the southern margin of the Colorado Plateau for the last million years.

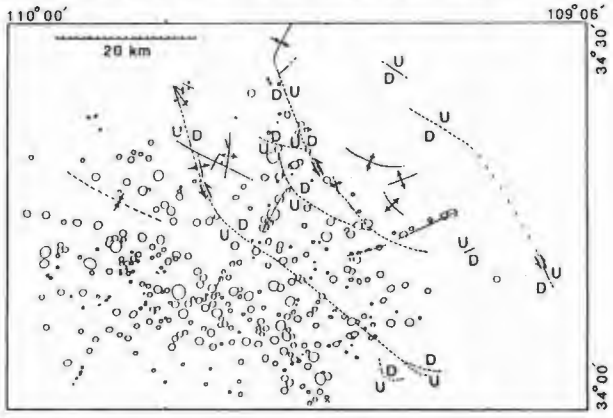

Springerville volcanic field. Dotted line, fissure type vents. Open circles, vents. Dashed lines, major deformation zones. Arrows, standard structural map symbols.

BASALT HYDROVOLCANIC DEPOSITS: GUIDES TO STRUCTURAL AND STRATIGRAPHIC EVOLUTION IN THE OWYHEE REGION OF OREGON, U.S.A

Cummings, Michael L., Department of Geology, Portland State University, Portland, Oregon, 97207

The Deer Butte Formation of Miocene age crops out west of the Owyhee Reservoir in Mahleur County, Oregon. The Deer Butte Formation accumulated within an extensional setting and was deposited after eruption of the Mahogany Mountain and Three Fingers calderas at 15.5 m.y. and 15.4 m.y. respectively from areas east of the Owyhee Reservoir (Rytuba, 1988).

Geologic mapping in the Twin Springs 7.5 minute quadrangle and parts of neighboring quadrangles, indicates that volcanism, sedimentation and basin formation, structural development, and hydrothermal activity occured simultaneously. Basalt hydrovolcanic deposits are interbedded with felsic volcaniclastic sediments and arkose and occur in three of the seven stratigraphic packages exposed in the mapped area. The hydrovolcanic deposits allow reconstruction of the paleohydrology and the stratigraphic and structural evolution of the area.

Stratigraphic relations indicate changes in the size, shape, and location of sedimentary basins during accumulation of the Deer Butte Formation. The sediments associated with the basalt hydrovolcanic deposits were deposited in fluvial, paludal, and lacustrine environments. Fluvial sediments are dominated by backswamp facies and contain minor channel and levee facies. Lacustrine sediments include diatomite, silts, and clay-rich beds; fish scales and skeletons, pelycepods, gastropods, and aquatic vegetation are also present. The sedimentary basins are developed between fault zones or within fault zones. The width of individual basins ranges from 4.5 to 13 km and their locations are controlled by concurrently developing north-south fault zones.

The north-south fault zones are composed of many closely spaced faults. The normal sense of throw on individual faults is generally less than 15 m, but a fault with throws of 30 m or more is commonly present within each zone. The distance between the zones is approximately 4.8 km and each zone is approximately 3.2 km wide.

The time of deformation along the structural zones, development of sedimentary basins, volcanic activity, and hydrothermal activity are closely linked. The fault zones provided conduits along which basalt and rhyolite rose to the surface. In the near-surface environment, the basalt magmas encountered water-saturated sediment in flood plains and deltas, or shallow lake basins. The violent interaction of the lava and the external water produced the basalt hydrovolcanic deposits. At least eleven eruption centers for basalt tuff cones, tuff rings, and maars are exposed in the map area. In the craters of maars and tuff rings, flows of basalt are interbedded with palagonite and, in some centers, the flows breached the tephra ring and flowed up to 2.4 km from the vent.

The distribution of basalt hydrovolcanic deposits provides a means to determine when the fault zones acted as the conduits by which magma rose to the surface. Distribution of basalt hydrovolcanic deposits indicates that individual fault zones became inactive and new zones developed at different times during evolution of the stratigraphic section.

Since the fault zones also controlled the location of hydrothermal activity and emplacement of silicic volcanic centers, the basalt hydrovolcanic deposits are a valuable tool in determining the history of volcanism, structural development, sedimentary basin formation, and hydrothermal activity.

Rytuba, J. J., 1988, Volcanism, extensional tectonics, and epithermal mineralization in the northern Basin and Range Province, California, Nevada, Oregon, and Idaho: U.S.Geological Survey Circular 1035, p. 59-61.

LIQUID LINES OF DESCENT IN ALKALIC CONTINENTAL RIFT MAGMAS: PETROLOGIC, GEOCHEMICAL, AND EXPERIMENTAL CONSTRAINTS FROM THE EAST AFRICAN RIFT

CURTIS, PC, MEEN, JK, and GLAZNER, AF, Dept. of Geology, Univ. of North Carolina, Chapel Hill, NC 27599

Basaltic magmas erupted in continental settings may be derived from source regions that include depleted asthenospheric mantle, enriched asthenospheric mantle such as that feeding some ocean islands, subcontinental lithospheric mantle, and continental crust. One object of petrologic studies is to distinguish between the relative contributions of different sources and their relationship to the eruption of alkalic versus subalkalic basaltic suites. A major obstacle to characterization of source compositions and melting history of continental alkalic magmas is the ubiquity of overprinting by low pressure fractional crystallization and crustal contamination processes.

The East African Rift has erupted ≈500,000 km^3 of volcanic rocks of both tholeiitic and alkalic affinities. Common associations in different parts of the rift are strongly *ne*-normative phonolites with nephelinites and basanites, trachytes and/or peralkaline rhyolites with alkalic basalts, and subalkalic rhyolites with subalkalic basalts. The subalkalic rocks are largely restricted to the Ethiopian Rift. We present data from a series of evenly spaced volcanos in the Turkana Rift of northern Kenya. Despite the proximity and virtually identical tectonic setting of the volcanos they erupted suites of different composition. Two of the volcanos erupted alkalic basalt, hawaiite, mugearite and trachyte with a significant Daly Gap between mugearite and trachyte. Two other volcanos erupted predominantly alkalic basalt with sparse flows of compositions ranging toward phonolite with no Daly Gap. A fifth volcano has erupted all the mentioned rock types. The proportion of more evolved rock types relative to alkalic basalt varies widely from volcano to volcano.

The Mg#s of the alkalic basalts range as high as 71. Many of the rocks with the highest Mg# are, however, porphyritic and may be olivine cumulophyric. The presence of populations of magnesian olivine (Fo_{86}) and augite (Mg# 85) and calcic plagioclase (An_{86}) both as phenocrysts and in the groundmass of some rocks attests to the presence of liquids little evolved from *ne*-normative primary mantle melts. Experimentally determined liquid lines of descent at QFM+0.5 log units due to crystallization of observed phenocryst phases (olivine, augite, plagioclase and Fe-Ti oxide) are toward more *ne*-normative compositions. This results in evolution from basalts through hawaiites and tephritic phonolites to phonolites. The most *ne*-normative rocks (phonolites) have phenocryst assemblages indicating that simple anhydrous phase relations may satisfactorily model the behavior of even the most evolved melts.

Trachytes have a few percent *hy* in the norm. Although the position of the thermal divide olivine-plagioclase-augite is difficult to determine accurately because of the wide range of compositions exhibited by natural clinopyroxenes, the thermal divide must lie between the compositions of the basalt-to-phonolite suite and the trachytes. In the absence of strongly *ne*-normative phenocryst assemblages (e.g. amphibole) in *ne*-normative rocks, trachytes cannot have developed by closed-system fractional crystallization from the alkalic basalts. Experimental study of alkalic basalts at 1 atm. indicates no new ways of evolving across the thermal divide and substantiates a liquid line of descent with increasing *ne* with crystallization. Trachytes apparently formed by open-system evolution with incorporation of felsic melts of the continental crust into the more mafic melts.

Despite similarities in major-element chemistry between alkalic basalts, the least evolved rocks have trace element enrichment patterns that are distinctive for each eruptive center. Whereas one volcano has high Nb/Zr ratios and low Ba/La, the neighboring volcano 50 km away has low Nb/Zr and high Ba/La. These differences cannot be due to crustal contamination as they are found in the most mafic rocks that can contain only minor amounts of crustal contaminants. Rather, they are thought to represent source-region heterogeneities.

EVIDENCE OF REDUCTION AND THE EVOLUTION OF METALUMINOUS TO PERALKALINE MAGMA, QUESTA, NEW MEXICO, U.S.A.

CZAMANSKE, G.K., U.S. Geological Survey, 345 Middlefield Rd., Menlo Park, CA 94025

Structural and topographic relief along the east margin of the Rio Grande Rift provide a remarkable cross section through 26-Ma Questa caldera (15 km across) and cogenetic, intrinsically oxidized volcanic and plutonic rocks. The caldera-forming eruption produced the weakly peralkaline Amalia Tuff (high-silica rhyolite, >500 km^3). During the interval 25-19 Ma, nine subvolcanic granitoid intrusions were emplaced above an inferred magma body of batholithic dimensions (20x35 km). Weakly peralkaline porphyry (75.2-77.0 wt% SiO_2; molar Na_2O+K_2O/Al_2O_3 (a.i.) <1.03; 2-4 modal % acmite+arfvedsonite) forms a partial ring dike and the northern margins of two plutons intrusive into the caldera floor. Along the northern margins of the Virgin Canyon and Canada Pinabete plutons, where peralkaline rocks are >30 m thick, peralkaline porphyry becomes seriate toward metaluminous granite (a.i., 0.82-0.88). The compositionally uniform porphyry, geochemically and mineralogically transitional between Amalia Tuff and the dominant metaluminous parts of the two plutons, is interpreted to represent unerupted portions of the tuff-forming magma.

Replacement of sphene by ilmenite, in both the porphyry and parts of the metaluminous granite, indicates that the highest unerupted components of the magma chamber underwent a period of magmatic reduction. Moreover, parts of the Canada Pinabete pluton are magnetite-free; they are also uniquely characterized by iron-rich biotite and amphibole and REE-poor sphene. In contrast, an oxidation trend, postulated to reflect vapor saturation and preferential hydrogen loss, is recorded by Mg-enrichment from core-to-rim in zoned biotite in the metaluminous interiors of the plutons. These two subvolcanic plutons at Questa provide the first known tangible evidence of this fugitive, H_2-rich reducing fluid.

At least seven mineralogic features of the intrusive peralkaline porphyry suggest that the weakly peralkaline magma evolved in the uppermost part of a metaluminous magma chamber after crystallization had commenced. 1) Both rock types were intrinsically oxidized, as indicated by early sphene crystallization, and sphene reacted to ilmenite in some rocks of each type. 2) Sphene of low Al and high Na, Fe, and Mn contents, characteristic of peralkaline porphyry, is found as cores of some grains in metaluminous granite. 3) Sphene in peralkaline and metaluminous rocks is indistinguishable in terms of La/Nd (0.2-0.6), average total REE concentration, and range in total REE concentration (27,000-42,000 ppm). 4) Ilmenite containing 15-68 mol% pyrophanite characterizes both peralkaline and metaluminous rocks. 5) Only peralkaline rocks contain amphiboles, zoned from katophoritic or richteritic (calcic) cores to arfvedsonitic (sodic) rims. 6) Biotite of identical composition is found in metaluminous granite and as partly replaced, relic grains in peralkaline porphyry. 7) In peralkaline porphyry, tetrasilicic mica (3.30-3.35 Si cations) partly replaces biotite and amphibole cores.

Removal of melt from alkali feldspar (containing as much as 3 wt% BaO) must have helped to promote peralkalinity because Ba and Sr contents drop from 630-1,680 and 22-225 ppm, respectively, in metaluminous rocks to 82-150 and 1.5-23 ppm in peralkaline porphyry. Average Na/K for whole rocks is 1.61 in peralkaline porphyry and 1.24 in metaluminous granite; albite component of sanidine (<0.03 wt% SrO and BaO) increased downward in the magma sampled by the Amalia Tuff, from $Ab_{49}Or_{51}$ to $Ab_{59}Or_{41}$. The role of F and Cl in promoting peralkalinity at Questa is speculative. Fluorite, fully fluorinated apatite, and biotite containing 4-5 wt% F (as much as 7.9 wt% in tetrasilicic mica) show that the system was characterized by relatively high a_F. (Cl contents of apatite and biotite are below 0.08 wt%.) Contents of Cs (0.62-1.59 ppm), Nb (30-50), Rb (116-161), Ta (3.73-5.35), Th (13.8-18.3), U (2.64-4.61), and Y (30-82) are comparable in metaluminous and peralkaline rocks.

Eruption of peralkaline and metaluminous silicic volcanic rocks from a common center has been reported previously (e.g. Mahood, 1981). However, the subtle mineralogic relations preserved in peralkaline porphyry at Questa, and the spatial relations of the porphyry, provide rare insight into the still controversal origin of peralkaline magma.

THE GEOLOGY AND GEOCHEMISTRY OF A DEVONIAN BIMODAL VOLCANIC ZONE: THE COMERONG VOLCANICS, SOUTHEASTERN N.S.W., AUSTRALIA

DADD, K.A., Department of Geology, Acadia University, Wolfville, N.S., B0P 1X0, Canada.

The mid-Late Devonian Comerong Volcanics of southeastern N.S.W. form the central part of an elongate belt of continental, bimodal volcanic rocks and minor interbedded sedimentary rocks, known as the Eden - Comerong - Yalwal volcanic zone.

The Comerong Volcanics crop out in two parallel belts on the limbs of the north-south trending Budawang Synclinorium and in a small outlier further to the west. Steep dips on the limbs of the synclinorium provide access to the volcanic sequence from the base, an unconformity with multiply deformed Ordovician sedimentary rocks, to the overlying Merrimbula Group. The area provides an excellent opportunity to review the geologic and geochemical evolution of a continental, bimodal volcanic sequence.

Two extensive rhyolite units, up to 350 m thick x 50 km long and interpreted as a series of overlapping lava flows, dominate the stratigraphy of the eastern limb. These units are interstratified with three horizons of mafic lavas and interbedded lacustrine sedimentary rocks. In contrast, there is a thick, up to 1500 m, mafic section on the western limb, overlying minor rhyolite and fluvial sedimentary rocks. The geologic history of the area is dominated by volcanic activity with a paucity of preserved sedimentary rocks.

The basaltic rocks occur typically as pahoehoe lava flows with minor fine to coarse tuff and lapilli tuff. The mafic tuff units display plane to low-angle cross-lamination, contain accidental, angular lithics of rhyolite and essential scoriaceous basaltic clasts suggesting emplacement by base surge. Geochemically the mafic units form three distinct groups which lie along a single trend from extremely fractionated tholeiitic basaltic andesite to moderately fractionated, tholeiitic to transitional basalt. The lowermost unit is the least voluminous and most fractionated with low MgO, Ni and Cr and high incompatible trace element abundances. The uppermost unit is the most voluminous and least fractionated. Olivine and clinopyroxene were probably efficiently fractionated from all geochemical types and in addition ilmenite and calcic plagioclase were fractionating phases for the lowermost unit. The volume increase and change to less evolved compositions upward in the sequence may reflect an increase in the rate of extension in the volcanic zone with time.

The majority of the rhyolitic units consist of cohesive lava flows and domes with some flows up to 350 m thick and 18 km long. Felsic pyroclastic rocks are rare. The flows are high-Si and alkalic, with high Zr and Y abundances and a high Ga/Al_2O_3 ratio typical of the A-type granitoids of southeastern Australia with which they are thought to be comagmatic.

The present outcrop of the entire volcanic belt is structurally controlled (5 - 20 km x 300 km) and the original belt was probably both much wider (up to 70 km) and longer in the Devonian. The Yellowstone - Snake River Plain region in the U.S.A. may be an appropriate modern analogue. Similarities include; geochemistry and eruptive style of basaltic units, geochemistry of the rhyolitic rocks and the presence of extensive lava flows, and the elongate, bimodal nature of the two volcanic belts.

CRUSTAL GROWTH VERSUS RECYCLING AT SUBDUCTION ZONES; EVIDENCE FROM THE CENTRAL ANDES

DAVIDSON,J.P., Dept. Earth and Space Sciences, UCLA, Los Angeles, CA 90024, McMILLAN,N.J., Dept Geology & Geography, University of Eastern Illinois, Charleston, IL 61920, MOORBATH,S.,Dept. Earth Sciences, University of Oxford, Parks Road, Oxford, OX13PR, U.K., HARMON,R.S., N.E.R.C. Isotope Geology Unit, Grays Inn Rd, London, U.K.and WORNER,G.Inst. fur Geowissenschaften, Johannes Gutenberg Universitat, Postfach 3980, D6500 Mainz, F.R.G.

The role of subduction-related volcanism in generation of the continental crust through time has long been debated. Most estimates for the composition of the bulk crust suggest it to be tonalite to diorite, depending on the still poorly known nature of the lower crust. At island arcs, the net flux of material is *basaltic* in composition and the prolific volume of andesites which have long been considered to characterize arc volcanism are shown to be the result of differentiation. This cannot be reconciled with a model in which mantle-crust differentiation at subduction zones generates a tonalite/diorite continental crust.

Arc volcanism in the central Andes over the last 20Ma has generated basaltic andesite to andesite magmas with isotopic and chemical characteristics comparable with estimates of the continental crust. No primitive basalts are encountered in the region. "Baseline" lavas (i.e. the most primitive observed) in the central Andes are enriched in incompatible trace elements. Sr and Nd isotopic ratios further indicate that Rb/Sr and Nd/Sr ratios are enriched in a time integrated sense. This has led to the suggestion that magmas are derived from an enriched subcontinental mantle lithosphere (Rogers and Hawkesworth, 1989). The alternative explanation for the enriched "crust-like" characteristics of the magmas is that primitive basalts (similar to those encountered at island arcs) have simply been contaminated in passing through the thick, old crust of the central Andes.

Consideration of chemical and tracc element data from the Nevados de Payachata volcanic complex and others in N.Chile enables us to assess these two possibilities. We consider the following observations to be pertinent;

1. $\delta^{18}O$ values for whole rocks and mineral separates, in common with other Cenozoic rocks from the central Andes, are high (+6.8 to +11.7 per mil) and inconsistent with closed system differentiation from mantle-derived magmas.
2. Pb isotope compositions vary sympathetically with the composition of the underlying basement; at Nevados de Payachata and the Arequipa - Barroso volcanic suites to the north, low $^{206}Pb/^{204}Pb$ ratios correlate with the presence of unradiogenic Precambrian crust, whereas further south Pb isotope ratios are higher, reflecting the presence of younger, more radiogenic basement.
3. Studies of volcanic rocks in south Chile have shown the strong influence of contamination on magma compositions, varying according to crustal thickness (Hildreth and Moorbath; 1988). Chemical characteristics of magmas from the central Andes form a natural extension of this interpretation; even greater crustal influence is observed in these rocks in keeping with the greater crustal thickness in the central Andes.

We consider that the strong influence of the crust in volcanism over the last 20Ma results from tectonic thickening of the central Andean crust (Isaacs, 1988). The net flux of material from the mantle is probably basaltic, similar in composition to island arc magmas. Baseline magmas in the CVZ are the result of very efficient mixing and homogenization of primitive arc basalts with crustal melts at deep levels. These magmas commonly undergo further differentiation at higher levels in the crust, but may be sufficiently enriched in incompatible trace elements by this stage to be insensitive to the chemical effects of further contamination. The nature of primary mantle-crust differentiation is therefore still unresolved.

Hildreth and Moorbath (1988) Contrib. Mineral. Petrol. 98, 455-489
Isacks (1988) J. Geophys. Res., 93, 3211-3231
Rogers and Hawkesworth (1989) Earth Planet. Sci. Lett. 91, 271-285

OLIGOCENE TO MIOCENE MAGMATIC TRANSITIONS , IN THE MOGOLLON-DATIL VOLCANIC FIELD ,NEW MEXICO, USA.

DAVIS, J.M., HAWKESWORTH, C.J. Dept. of Earth Sciences, Open University, Milton Keynes, MK7 6AA. England.
ELSTON, W.E. Dept of Geology, Univ. of New Mexico, Alburquerque, NM87131.

The late Oligocene and early Miocene of the Colorado Plateau-Basin & Range transition is characterised by voluminous basaltic andesites and andesites. The Mogollon-Datil volcanic field ,S.W. New Mexico, straddles this zone and was active between 38-20Ma. The rocks are high-K and calcalkaline but they occur over a broad zone rather than an arc some 800-1000km from the plate margin, with activity extending some 2-12Ma after the end of subduction.

Stratigraphically, three andesitic lavas sequences are separated by two periods of extensive ignimbrite eruption. This study focusses on the andesitic sequences, whose range in ages from 37-32Ma, to 31-27Ma, to 25-20Ma allow us to investigate changes in magmatic style as Oligocene compressional tectonics gave way to a pre Basin & Range ductile extension . The early units are characterised by highly porphyritic andesites and dacites, with hydrous phenocryst assemblages of plag+cpx+hbl$\pm$opx(+ rare biotite) in a trachytic groundmass. Then there is a shift to aphanitic, fine-grained and dominantly basaltic andesites with anhydrous interstitial microphenocrysts of plag+cpx$\pm$ol. Basalt is rare before 28Ma but relatively common afterwards, consistent with an overall trend to more basic compositions and a more restricted compositional range with time. The middle units are transitional and their earlier andesites and dacites exhibit distinctive reaction coronas and resorbed qtz & sanidine xenocrysts.

All three sequences exhibit high LIL/HFS ratios (Ba/Nb= 50-125) and LREE enrichment (La[n]/Yb[n]=7-10). However, HFS and REE concentrations increase in the younger rocks with relatively little change in LIL elemental abundances. Thus in rocks with MgO>4%, TiO2 increases from <1% (early) to 1.7-2.0% (late), and this is accompanied by a small decrease in K/Ti, but more noticeably Rb/Nb decreases from 7-8 (early) to 2-3 (late). The change to anhydrous conditions around 28Ma is accompanied by a change in $^{87}Sr/^{86}Sr$ ratios, from 0.7055-0.7065 in the early and lower middle units, to 0.7075-0.7085 in the upper middle rocks.The later units then trend back to lower values, 0.7070-0.7065. $^{87}Sr/^{86}Sr$ does not increase with increasing SiO2, but the ratios are consistent with a strong lithospheric component. The high TiO2, low LIL/HFS of the later rocks may indicate the growing influence of a further asthenospheric component. Similar isotope and trace element trends in late Cenozoic, high LIL/HFS basalts from the Western Great Basin were attributed to lateral changes in the age of the mantle lithosphere (Ormerod D.S et al. *Nature* 333 349-353 [1988]).In the Mogollon-Datil field, however, the changes occur in a more restricted area and may therefore reflect vertical stratification of mantle source regions.

ACTIVITY AT THE NATROCARBONATITE VOLCANO OF OLDOINYO LENGAI, NOVEMBER 1988.

DAWSON, J.B., Dept. of Geology, Sheffield University, S1 3JD;
PYLE, D.M., Dept. of Earth Sciences, Cambridge University, CB2 3EQ;
PINKERTON, H., and NORTON, G., Dept. of Environmental Sciences, Lancaster University, LA1 4YW, England.

The sodium carbonatite volcano of Oldoinyo Lengai has been in continuous eruption for the past six years. Since the explosive vulcanian phase of early 1983, activity has been restricted to the eruption of small volume lava flows on to the floor of the pit crater. Between May 1984 and November 1988, the crater has been filling at an average rate of 500m³ of carbonatite per day.

The volcano was monitored for four days during November 1988. During this period, the locus of activity shifted between three centres on the 200m diameter crater floor: the most active being a 10m wide lava lake within a partially collapsed scoria cone. Frequent explosions (every 1-2 seconds) of small volume bubbles (radius<2m) within the centre of the lake ejected material 5-15 m in height, and were accompanied by gas flaring. During the first day, lava flows were almost continuously fed from this centre, which disgorged material at velocities of 1-2m/s through a deeply cut series of lava channels. Approximately 20000m³ of lava were erupted from this centre.

The effusion rate-eruptive style relationship seen in basaltic provinces was confirmed: in general the higher effusion rate flows (20-60m³/minute) were characterised by the formation of large clinkery aa flows, up to 50cm thick, while lower effusion rates (<0.05-0.2m³/minute) were typical of pahoehoe flows. Small amounts of "toothpaste" lava were observed forming, within flows which had ceased flowing but which continued to expand by vesiculation during cooling. The carbonatite lavas exhibited a wide range of vesicle contents: from extremely gas and crystal-rich, relatively viscous material that tended to build constructional 'hornitos' to essentially bubble-free pahoehoe which formed low ratio flows. A feature of great interest was the ability of the lavas to thermally erode. This resulted in most of the flows being restricted to leveed channels of 2-100 cm width for much of their length. Cold blocks of lava immersed in active flows were measured to erode at up to 0.1mm/s.

Field measurements on the channelised flows suggest maximum viscosities for carbonatite in the range 2-100 Pa s (using Jeffries equation), which will augment the measurements made using a portable shear vane viscometer. In addition, over twenty calibrated temperatures of between 575 and 593°C were recorded with a NiCr-NiAl thermocouple. The cooling rate of a pahoehoe lobe was measured to be ~0.1°C/s, corresponding to a thermal diffusivity of ~4*10E-8 m²/s.

Chemically, the products are remarkably similar to the products of the 1960-1966 activity (Dawson 1962), with Na_2O:CaO:K_2O of ~3.7:1.6:1, and 1000*Rb/Sr from 15-19. Minor differences in major and trace elements are due to varying proportions of crystals (from 30%-70% gregoryite+nyereite). Fuller analyses of these new samples, along with radiochemical data on short-lived isotopes of Th, U and Ra will be presented at the meeting.

The Royal Society are acknowledged for providing financial assistance.

RANDOM PATTERNS OF EXPLOSIVE ERUPTIONS

DE LA CRUZ-REYNA, S. Instituto de Geofisica UNAM, C. Universitaria, México 04510 D.F.

Presently, no single statistical distribution of volcanic eruption occurrences appears to fit observed data. The elucidation of the actual patterns of eruption occurrences could help in having a better understanding of the physics behind the volcanic processes.

The analysis of both, the global data and the available data of an individual volcano shows that, if the magnitudes of eruptions are properly accounted above certain "noise level", the stochastic process whose realization consist of point events in time, i.e. the explosive eruptions, can be rather well represented by a simple Poisson point process.

The clue of the problem is to define the adequate "noise level", problem which in turn is directly related with the origin of the different types of eruptions, and to what extent those different types are the result of the same category of physical processes. Many of the previous attempts to describe patterns of eruption occurrences were hampered by counting both explosive and non explosive events as in the same category.

When eruptions are separated in explosive and non explosive categories, the pattern of the explosive category becomes very clearly Poissonian, both in the global scale and for a single volcano. However, when low explosivity or effusive eruptions are considered, the distribution of occurrences is different for each magnitude category and often multimodal. It is thus of primary importance to classify eruptions to this respect, and a suitable parameter to do that has been found to be the Volcanic Explosivity Index (Newhall and Self, 1982).

The analysis of global data, as published in the same above mentioned paper, shows that the number of eruptions per decade (or any other appropriate time interval) in each VEI category equal or greater than 4, follows a simple Poisson distribution. A similar analysis performed on a single volcano (Colima) which, having a good historical record permitted an accurate assignment of VEI magnitudes, yields equivalent results, except that a good adjustment to a simple Poisson distribution can be made to the number of eruptions per decade with a VEI magnitude as low as 2.

The difference in levels of magnitude between the single volcano and the global data, at which occurrence patterns becomes clearly Poissonian, may be attributed to the difficulties in assigning accurate magnitude values to the abundant global activity in the magnitude range around 3.

These results indicates that moderate to large explosive eruptions behaves as random events with no memory of their past history, (at least for times in excess of the sampling period), while low explosivity eruptions may not be considered point events and may be causally related to each other or to the major activity.

Newhall C G, Self S. *J. Geophys. Res.* 87 1982.

PETROLOGY AND PETROGENESIS OF IGNIMBRITES FROM THE CENTRAL ANDES

S.L de Silva, Lunar & Planetary Institute, 3303 NASA Rd. 1, Houston, Tx 77058

The Central Volcanic Zone (CVZ) of the Andes is one of the largest provinces of Late Cenozoic ignimbrite volcanism in the world. Between 21° and 24°S, ~10,000 km^3 of ignimbrite has been erupted onto the high Andes of N. Chile, Bolivia and N.W. Argentina since the beginning of the Late Miocene. This intense phase of ignimbrite volcanism developed in response to tectonic thickening of the Central Andean crust just prior to the late Miocene (Isacks, 1988) and has resulted in a major volcano-tectonic province - the Altiplano-Puna Volcanic Complex.

The typical products of this volcanism are large volume (>500 km^3), crystal-rich (50% phenocrysts) dacitic ignimbrites which in N. Chile dominate the volcanic stratigraphy and account for ~95% (by volume) of the silicic volcanics. These large ignimbrites are calc-alkaline, high-K dacites, with a phenocryst assemblage of plagioclase (An_{28-57}), quartz, biotite, hornblende, Fe-Ti oxides pyroxene, sanidine, and accessory phases. Volumetrically minor high-Si rhyolites are also present which contain plagioclase (An_{15-27}) biotite, pyroxene, Fe-Ti oxides and accesories. The mineralogy and mineral chemistry are unremarkable and are broadly similar to other orogenic silicic volcanic rocks. Phase equilibria suggest that the dacitic magmas equilibrated at temperatures of 673°-878° C with relatively high fO_2 of -11.68 to -17.02. Water contents of the magmas were high; 7.5 -10%. The ignimbrites are LREE enriched with Ce/Yb varying from 7.1 -15.3. Initial $^{87}Sr/^{86}Sr$ ratios of all the silicic rocks (65 - 76% SiO_2) vary from 0.708 - 0.711 but show no systematic variation with SiO_2 or the high Rb/Sr; $^{143}Nd/^{144}Nd$ range from 0.51209 - 0.51226 with constant Sm/Nd (0.17-0.21).

These characteristics convey the remarkable similarity of the huge volumes of silicic magma which have been produced since the Late Miocene, and suggest that the petrogenetic processes have been constant throughout this time. The high $^{87}Sr/^{86}Sr$ and Rb/Sr, the low Sr, $^{143}Nd/^{144}Nd$ and Sm/Nd, as well as the lack of any systematic change in $^{87}Sr/^{86}Sr$ with differentiation, are interpreted as reflecting the "crustal" nature of the ignimbrite magmas. An origin by large scale crustal melting is preferred and the following scenario is envisaged. Elevated geotherms produced by crustal thickening combined with the thermal input from subduction derived magmas results in partial melting of the lower crust. At a critical level of partial melting, ~ 35-40%, this partially molten zone overturns to produce a huge zone of anatexis. This anatectic zone is maintained by thermal input from the subduction process. Diapiric uprise of large volumes of homogeneous dacite melt from this zone results in the formation of high level magma chambers where fractionation produces the small volume of rhyolites and minor compositional heterogeneities.

Huppert & Sparks (1988) show that anatexis maybe accompanied by crystallization, resulting in crystal-rich magmas, and that further evolution of the magmas may occur after emplacement in higher level magma chambers. This may explain the contrasting evidence from two feldspar and Fe-Ti oxide equilibria which indicate that some of the ignimbrite magmas developed at depths of about 35-45 km (10-13 kbars), whereas the glass compositions (when compared with the system $CaAl_2Si_2O_8$ - $NaAlSi_3O_8$ - $KAlSi_3O_8$ - SiO_2 - H_2O) indicate equilibration at about 7 - 15 km (2 - 5 kbars) in the crust. Furthermore, the extent of compositional heterogeneity in individual ignimbrites maybe largely a function of residence time in high level magma chambers; homogeneous magmas reflect little or no evolution at high level, while heterogeneous magmas reflect significant evolution at high levels.

DYNAMICS OF MAGMA ASCENT AND ERUPTION AT KILUAEA VERSUS MOUNT ST. HELENS VOLCANOES

Robert W. Decker, University of Hawaii at Hilo, Hilo, HI 96720, USA

Comparison of geophysical and eruptive activity of Kilauea to that of Mount St. Helens (MSH) leads to interesting conclusions about long-term monitoring of subduction-type volcanoes. Eruptions of Kilauea are frequent, often long-lasting, and normally not explosive; at MSH clusters of brief, often explosive eruptions are separated by repose periods of centuries. Seismicity is high at Kilauea and nearly continuous on a yearly basis; at MSH many years of low seismicity were interrupted by an 8-week, very energetic earthquake swarm. Surface deformation in the summit region of Kilauea is quasi-elastic and nearly continuous; at MSH episodes of non-elastic deformation precede eruptions. Magma ascent from 60 km to a shallow reservoir system at 4 km beneath Kilauea involves about 0.1 km^3 of magma per year and is continuous over decades; at MSH magma ascent from depth to shallow levels is intermittent, rapid over brief periods but averaging much less than at Kilauea.

Ongoing action at 4 km beneath Kilauea is relatively easy to monitor with conventional seismometers and geodetic surveys. The ongoing action at most subduction-type volcanoes is inferred to be deeper (25 km?) and less vigorous. This suggests that different monitoring tactics -- perhaps borehole seismometers and more accurate far-field deformation surveys (GPS?) -- need to be developed to study subduction-type volcanoes during their long repose periods. Obtaining baseline data surveys -- seismic, deformation, electromagnetic, thermal, etcetera -- and repeating these surveys at intervals of several years may also reveal subtle but important changes.

THE TOBA ASH AND OLDER TEPHRA LAYERS OF THE NORTH EASTERN INDIAN OCEAN ODP LEG 121

Jonathan Dehn, Hans-Ulrich Schmincke, and Leg 121 Shipboard Party, Institut für Mineralogie, Ruhr-Universität Bochum, Postfach 102148, D-4630 BOCHUM 1, F.R.Germany

During Leg 121 of the Ocean Drilling Program, three Sites were drilled on the Ninetyeast Ridge. The sediments recovered at these Sites record a history of shallow water- (< 100 m) to phreatic- basaltic volcanism.

At Site 757, 157 m of volcaniclastics were recovered. The tuffs are characterized by interbedded basalt pebbles, shell fragments, lapilli, scoured basal contacts, and graded bedding, suggesting an explosive, shallow water environment. Scattered accretionary lapilli, possibly formed during Surtseyan eruptions, occur in several tens of layers over less than 50 m at the base of this section. They are well preserved by post-depositional carbonate cementation common throughout the volcaniclastic section. This sequence represents approximately 10 million years of Paleocene shallow water basaltic volcanism which kept pace with the slow subsidence of the Ninetyeast Ridge.

At Site 758 ca. 100 m of Campanian coarse grained (lapilli size) basaltic tuffs are typically graded and occur in beds less than 30 cm thick. This sequence again represents more than 5 million years of local basaltic volcanism.

The uppermost tephra layer in Site 758 (approx. 2 mbsf) is 30 cm thick, well graded, with two distinct layers. The age of this layer is 75ka (from sedimentation rate and paleomagnetics). This age and the characteristics of this layer suggest that it is the Toba ash from the last caldera-forming eruption of the Toba caldera in northern Sumatra approximately 800 km distant. The location of this Site falls within the distribution of the Toba, and the thickness of the layer correlates with other cores taken nearby. The Toba ash consists of two distinct depositional phases. The lower Toba is coarse-grained (md 50 μm), relatively crystal rich (3 to 5%), with abundant glass shards. The glass in this layer consists of equal portions of platy/bubble wall shards and blocky shards (40% each), the remainder being bubble-rich pumice fragments (20%). The upper Toba layer contains more fossil material (15%) is fine-grained relative to the lower Toba (md 30 μm) and well-graded. Concentration of pumice fragments in this layer are less than 10% and blocky shards average 10% in the sample. The remaining glass (80%) is composed of exclusively platy and bubble wall shards. The ash is compositionally (XRF of major and trace elements) similar to other Toba ash layers in the north eastern Indian Ocean.

Similar tephra layers have been noted deeper in the stratigraphic section, and could represent older eruptive episodes at Toba or other Indonesian volcanoes though correlations are still uncertain.

SINGLE-CRYSTAL $^{40}Ar/^{39}Ar$ DATING AS AN AIDE IN CORREALTION OF ASH FLOWS: EXAMPLES FROM THE CHIMNEY SPRING/NEW PASS TUFFS AND THE NINE HILL/BATES MOUNTAIN TUFFS OF CALIFORNIA AND NEVADA

DEINO, A.L., Berkeley Geochronology Center, 2453 Ridge Rd., Berkeley, CA 94709.

Single-crystal $^{40}Ar/^{39}Ar$ ages obtained using a fully automated, continuous-laser extraction system demonstrate that phenocrysts of sanidine from mid-Tertiary ash flows of the Great Basin present simple, geologically homogeneous isotopic systems ideally suited to high-precision stratigraphic studies. Review of dated stratigraphic sections in Nevada suggest that the time interval between emplacement of ash-flow sheets in any one part of the mid-Tertiary ignimbrite field averages roughly 0.5 Ma. Through the use of a rapid, precise analytical system it is possible to consistently obtain standard errors of the mean for sanidine samples of 0.1-0.2%, or 20,000 to 60,000 years, more than adequate to distinguish 'average' emplacement events. Precise dating is a necessary element of definitive correlations supported by petrologic, geochemical, and paleomagnetic data. Two examples of correlation of widely separated ash-flow sheets follows.

Similarities in petrology, trace-element chemistry, and radioisotopic ages indicate that the New Pass Tuff (NPT), exposed in the vicinity of the New Pass Range in central Nevada, extends into western Nevada, where it is known as the tuff of Chimney Spring (TCS). Immediately overlying the TCS in western Nevada, the Nine Hill Tuff (NHT) of western Nevada and eastern California is likewise correlative with Unit "D" of the Bates Mountain Tuff (BMT) of central and eastern Nevada.

The main body of both the NPT and the TCS is a vitric-crystal, moderately welded, devitrified, white to red ash-flow tuff with phenocrysts predominantly of chatoyant sanidine and subhedral, bipyramidal smokey quartz. Preliminary trace-element data suggests that both units are compositionally zoned, with strong enrichment of Pb, Th, and other incompatible elements toward the base. Both tuffs have relatively high average Nb (29 ppm for the NPT, 35 ppm for the TCS) and Zr (220, 260 ppm) compared to most other ash flows in western Nevada. Paleomagnetic studies are under way to test correlation of the TCS with the NPT.

Laser-fusion, single-crystal $^{40}Ar/^{39}Ar$ dating of three samples of the TCS/NPT encompassing the east-west extent of the tuff (Seven Lakes Mtn., Stillwater R., New Pass R.) gave a preliminary overall mean age (subject to further calibration of the monitor) of 25.07 ± 0.038 (.022 s.e.m.) with a total spread of 60,000 years. This spread is consistent with analytical error, and these dates are considered supportive of correlation of these exposures.

The NHT is abruptly zoned upward from rhyolite to rhyodacite. The rhyolite is much more widely distributed in western Nevada/eastern California than is the rhyodacite, and is very similar to the rhyolitic Unit "D" of the BMT. Both are thin (generally 10-40 m), densely welded, red-brown to white, sodic sanidine-dominant crystal-poor ash-flow sheets with distinctly high Zr (406 ppm for the BMT, 399 for the NHT) and Nb content (30.5, 29.9 ppm). These tuffs have overlapping normal NRM directions, close to that of the late Oligocene/early Miocene mean.

Laser-fusion, single-crystal $^{40}Ar/^{39}Ar$ dating of five samples of the NHT/BMT across the width of the tuff (Mokelumne Hill; Seven Lakes Mtn.; Stillwater R.; Clipper Gap; Hot Creek R.) yielded a preliminary overall mean age of 25.11 ± 0.017 Ma (8,000 years s.e.m.!) with a total spread of mean ages of only 40,000 years. Although the age data alone may not be conclusive, the very narrow range obtained for NHT/BMT support the hypothesis that all five samples belong to the same eruptive unit. In addition, the $^{37}Ar/^{39}Ar$ ratios of these feldspar samples, a direct measure of the Ca/K atomic ratio, are about 0.03 to 0.05, approximately 3-10 times greater than other K-feldspars from mid-Tertiary tuffs so far analyzed in the Great Basin.

Although the age difference between the NHT/BMT and the TCS/NPT is only 40,000 years, these two tuffs are so markedly different in mineralogy and chemistry that they are easily distinguished in the field, and probably originated from unrelated magma systems.

SEISMIC QUALITY FACTOR IN VOLCANIC AREAS OF SICILY

DEL PEZZO, E., Instituto di Scienze della Terra. Universita' di Catania, Italy, MERI, G. Patane',D. PRIVITERA, E., Instituto Internazionale di Vulcanologia del CMR. Catania

Seismic data from local earthquakes at Mt. Etna and Aeolian islands were analyzed in order to estimate the seismic quality factor in the frequency range 1-20 Hz.

Direct methods for Q evaluation were applied to P and S waves of some aftershocks that occurred a few km south of the Vulcano Island, an active volcano of the Aeolian arc.

A wider set of data was used to estimate the quality factor Qc (coda Q) for coda waves at four station of the Aeolian Islands network.

Results show a high attenuation, with Qc dependent on frequency and ranging from 100 (at 1 Hz) to 400 (at 16 Hz).

A very small zone with high absorbtion of S waves is located beneath Vulcano Island.

Digital data of shallow volcanic earthquakes that occurred in a short time interval near the crater of Vulcano were used to refine Q estimates at a shorter scale. Low Q was found in the uppermost layers.

Coda method was also applied to Etna local earthquakes for estimating Qc. Data show a strong frequency dependence, similar to what was found for Aeolian Islands. Moreover, a depth dependence of attenuation can be inferred from the analysis of coda Q pattern versus lapse time from origin.

Q of volcanic tremor evaluated for Etna area ranges from 12 (at 1 Hz) to 90 (at 5 Hz).

CONTINUOUS RIFTING AND SUBSIDENCE OF KILAUEA VOLCANO'S SUMMIT AND RIFT ZONES, AND UPLIFT OF ITS SOUTH FLANK SINCE THE 1975 M_L7.2 EARTHQUAKE

P. T. DELANEY, A. MIKLIUS, A. T. OKAMURA, and M. K. SAKO, U. S. Geological Survey, Hawaiian Volcano Observatory, Hawaii National Park, HI 96718; and R. S. FISKE, Smithsonian Institution, NHB-119, Washington, DC 20560

A M_L7.2 earthquake originated at 9–10 km depth beneath the south flank of Kilauea Volcano, Hawaii, about 25 km southeast of its summit, on November 29, 1975. This earthquake triggered a brief summit eruption and caused ~1.0–1.5 m of summit subsidence. Concurrently, there was ~0.5–0.8 m of rift-zone subsidence and up to ~1 m or more of rift-zone extension. Most of Kilauea's south flank subsided ~1–3.5 m and moved seaward ~3–8 m, causing a moderate local tsunami. Although there was up to 1.5 m of normal-fault ground rupture along a 25 km zone, the earthquake probably originated from thrust motion on the shallowly dipping contact between the volcanic pile and the underlying oceanic sediments. The focal depth and widespread deformation associated with this earthquake demonstrated that some of Kilauea's fundamental tectonic structures are deeper and more extensive than had been envisioned on the basis of observed shallow magmatic events.

Geodetic data spanning the 13 years following the earthquake confirm this finding. Since 1975, the summit and rift zones of Kilauea Volcano have been extending and subsiding, establishing a pattern that began with the co-seismic deformation. Total extension across the summit has been ~2.25 m, averaging 26 cm/yr until 1983 and 5 cm/yr since. Post-1975 summit subsidence locally exceeds 1.5 m. Subsidence of the middle southwest rift zone has been in excess of 0.75 m and the upper east rift near Mauna Ulu has subsided more than 0.5 m. The lower east rift has subsided ~0.2 m, even at the farthest landward extent of Kilauea, more than 50 km from the summit. Concurrently, distances measured northward from cinder cones in the lower east rift show extensions along the length of the rift zone that average from 3.0 cm/yr to 1.5 cm/yr. Distances measured southward show contractions that are typically ~0.5 cm/yr. For the past 13 years, Kilauea's south flank has been rising, reversing the abrupt co-seismic subsidence of 1975. A tide gauge situated south of Kilauea's summit reveals more than 0.5 m of uplift; a water well situated over the epicenter of the 1975 event reveals an uplift of ~0.4 m. Leveling from the Hilo tidal datum to benchmarks south of Kilauea's summit reveals an uplift of more the 0.6 m. The greatest south-flank uplift is south of the region of geodetic control. Although the summit and south flank deformations have been decelerating since the 1975 earthquake, deformation of the lower east rift continues unabated.

The motions reported here are only partly caused by the frequent but sporadic intrusions that originate at the shallow magma-reservoir system beneath Kilauea's summit and often propagate along its rifts. The most frequently measured data sets are well-characterized by least-squares fits to first- and second-order polynomial functions, implying that the motions result from a relatively continuous, and partially aseismic, deformation of the volcanic pile. These motions affect about 1000 km^2, spanning most of the subaerial exposure of Kilauea; the extent of motions of its submarine surface are unknown but probably appreciable. Thus, Kilauea appears to possess a deformation source deep within the rift zones and/or along the base of the volcanic pile. ·Although Kilauea deformation is typically interpreted on the basis of known shallow magmatic events, much, if not most, of the post-1975 motions are attributable to this deeper source. Based upon these results, the total magma supply rate to Kilauea is probably greater than has been estimated on the basis of observed shallow magmatic activity.

WET SURGE DEPOSITS AT LA FOSSA DI VULCANO: DEPOSITIONAL AND ERUPTIVE MECHANISMS

DELLINO, P., Dip. Geomineralogico, Università Campus,Trav.200 Re David 4,70124 Bari, Italy
FRAZZETTA, G, CNR,Istituto Internazionale di Vulcanologia, Viale Regina Margherita 6, 95126 Catania, Italy
LA VOLPE, L., Dip.Geomineralogico, Università Campus,Trav.200 Re David 4, 70124 Bari, Italy

Wet surge deposits of different volcanic cycles of the recent Fossa activity at Vulcano have been measured on a bed-by-bed basis, with data recorded to millimetre detail.The wet surge layers are varicoloured with variable thickness, with the most recurrent thickness being about 1 cm.The beds consist of fine ash without internal structures.Textural features include:i) accre- tionary lapilli, of maximum size of 0.5 cm, dispersed in the layer or forming continuous layers of submillimetric size; ii) vesiculated layers which represent from 10% to 65% of the total deposit; vescicles have different shapes and smooth walls, varying in volume from 1% to 15-20%; iii) soft-sediment types of bedding deformation, such as gravity flowage ripples, load cast and slumps. The slope angle has not influenced either the concentrations and size of the accretionary lapilli or the shape,size, and distribution of vescicles. Only the thickness of the layers decreases with distance from the vent.

Grain size analyses reveal that the layers are not graded and most of the samples are finer than 50 µm. The grain size distributions are frequently polimodal, suggesting more than one fragmentation event.

SEM investigations have shown several features indicating the hydromagmatic origin of the deposits and stressing the role of the fluids. Noteworthy is the presence of vesiculated grains,produced by magmatic exsolution,which present chilling effects and hydration cracks on the inner walls of the broken bubbles.

The same depositional mechanism must be invoked for all the depositional units. The process must be interpreted in terms of defluidization of a fluidized system formed by fine particles, water and gas. The surge cloud moves on the ground as a visco-plastic system forming a bed, even on the internal walls of the crater. The induration of the bed occurs immediately after deposition , preserving the soft syndepositional textures from destruction and avoiding the loss of the intrapped gas.

The eruptions are of a hydromagmatic type and occur where ascending magma,at least partially fragmented,comes into effective contact with sub-superficial water.The process follows the model suggested by Wohletz (1983-1986), developing in more than one fragmentation act.In the turbulent surge cloud both the development of severe hydration of glassy grains and the formation of the textural features observed in the wet surge deposits of Vulcano occur.

VOLCANO OBSERVERS PROGRAM:A TOOL FOR MONITORING VOLCANIC AND SEISMIC EVENTS IN THE PHILIPPINES

DELOS REYES, P.J. Philippine Institute of Volcanology and Seismology,5th Flr. Hizon Bldg. Quezon Ave.Quezon City, Philippines

The Philippine Archipelago is one of the most tectonically active regions in the world. As such, the frequent occurrences of volcanic eruptions and destructive tectonic earthquakes are to be expected. One of the main objectives in the creation of the Philippine Institute of Volcanology and Seismology (PHIVOLCS) is the mitigation of the effects of volcanic eruptions and earthquake occurrences through prediction and prompt warning.

The Philippines lacks the sophistication in terms of technology needed for volcanic and earthquake prediction, as well as the manpower to perform monitoring procedures. To offset this need, the Institute began harnessing the help of volcano dwellers and residents living in earthquake-prone areas in a program called "Volunteer Observers for Volcanic and Seismic Events in the Philippines". The local volunteers shall pave the way for PHIVOLCS to widen its source area for acquisition of volcano and earthquake-related data as well as increase the frequency of report gathering without too much additional expense. Questionnaires containing queries on observable manifestations of a volcano or seismic event were created and translated into local dialects and distributed to areas in the vicinity of volcanoes presently being monitored by PHIVOLCS. The collection of these questionnaires have been designed to fit set schedules. The ultimate aim of the program is to encourage local residents to participate actively and in doing so, we could awaken the public's awareness by increasing their knowledge of the dangers and risks posed by volcanic eruptions and earthquake occurrences.

Preliminary and partial implementation have shown that this program is indeed useful and could be adapted by other developing countries like the Philippines. Development of this scheme in geologically active areas could eventually lead to the proper implementation of an effective warning and disaster preparedness program.

U-Th-Ra RADIOACTIVE DISEQUILIBRIA AND Sr AND O ISOTOPES IN PITON DES NEIGES AND PITON DE LA FOURNAISE LAVAS (REUNION ISLAND)

DENIEL C., CONDOMINES M., KIEFFER G., UA 10 CNRS et CRV. 5 rue Kessler 63038 Clermont-Ferrand France.

BACHELERY P., Laboratoire de Géologie, Université de la Réunion. 97490 Ste Clotilde.

HARMON R.S., NERC Isotope Geology Centre, 64 Grays Inn Road, London WC 1 X 8 NG United Kingdom.

Ages were determined by the ^{230}Th-^{238}U radioactive disequilibrium method (internal isochrons on whole rock and magnetite). For Piton des Neiges differentiated lavas, these ages range from 160,000 to 12,000 a B.P. and for Piton de la Fournaise lavas, from approximately 300,000 a B.P. to present, yielding a precise picture of the chronology and of the successive calderas development (caldera 1 : 170,000 a ; caldera 2 : <40,000 a : caldera 3 : <7,000 a).

The evolution of the $(^{230}Th/^{232}Th)_0$ of the lavas through the magmatic history of these two volcanoes was also studied to characterize the processes of magma generation and transfer. All samples from both volcanoes show an enrichment in ^{230}Th relative to ^{238}U. In each volcano, the $(^{238}U/^{232}Th)$ ratios are rather homogeneous (0.60 to 0.76 for Piton des Neiges and 0.67 to 0.81 for Piton de la Fournaise). This small dispersion also exists for $(^{230}Th/^{232}Th)_0$ ratios which only vary between 0.81 and 1 for Piton des Neiges and between 0.91 and 1.05 for Piton de la Fournaise. U and Th contents in Piton des Neiges lavas are well correlated with a mean Th/U ratio of 4.2. This ratio is about 4.0 in Piton de la Fournaise lavas.

The absence of obvious correlations between $(^{230}Th/^{232}Th)_0$ and time, $(^{230}Th/^{232}Th)_0$ and Th contents as well as the degree of differentiation and time for Piton des Neiges lavas indicates that there is not only one series of differentiation evolving by crystal fractionation, but different series.

The same samples were also analyzed for Sr isotopes. The $^{87}Sr/^{86}Sr$ ratios vary in a restricted range (0.70413 to 0.70429 for Piton des Neiges lavas and 0.7041 to 0.7044 for Piton de la Fournaise lavas). These small variations probably reflect small isotopic heterogeneities in the magma sources of both volcanoes.

The relative homogeneity of the $(^{230}Th/^{232}Th)_0$ in Piton de la Fournaise lavas, the absence of correlation between this ratio and time, and the position of the samples inside the "mantle-array" in the Th-Sr correlation diagram indicate that the magma transfer time from the zone of partial melting to the surface has always been short (<10 000 a) and that there is no deep reservoir. This transfer time can be better constrained by shorter-lived isotope measurements on modern lavas. One sample from the 1986 eruption shows an excess of 30% of ^{226}Ra over ^{230}Th whereas ^{228}Ra is in equilibrium with ^{232}Th. It indicates that the magma transfer time is in the range 30 to 8,000 a.

The range of $(^{230}Th/^{232}Th)_0$ variation for Piton des Neiges lavas is similar to that for Piton de la Fournaise lavas. However, there are lower values than for Piton de la Fournaise lavas and many data plot below the Th-Sr correlation. Therefore, these variations may also be related to a non-negligible residence time of the magma at depth, resulting in a decrease of the $(^{230}Th/^{232}Th)$ activity ratio by radioactive decay.

Preliminary oxygen isotope measurements were also carried out on some differentiated lavas from Piton des Neiges. For the more primitive lavas (SiO_2<50%), $\delta^{18}O$ values are quite low (5.5 to 5.9‰), very similar to that of MORB. For the more evolved lavas (51%<SiO_2<67%), the range of $\delta^{18}O$ values is wider (5.7 to 6.4‰) and consistent with development of these lavas through a closed system crystal fractionation process. According to these first results, it does not seem possible to better identify the different differentiation series with the aid of O isotopes, as the small observed variations on $\delta^{18}O$ appear to be unrelated to those observed with the Th and Sr isotopes.

PHYSICS RELEVANT TO THE ELUTRIATION OF ASH FROM A PYROCLASTIC FLOW

ROGER P. DENLINGER, U.S.G.S., School of Oceanography, WB-10, Univ. of WA, Seattle, WA, 98195.

The physically violent conditions that characterize pyroclastic flows make direct sampling of flows impractical. Currently flow processes must be inferred from flow deposits and theoretical modeling using laboratory experiments and field observations of velocity and flow behavior. Here I have refined a previous model for the turbulent elutriation of ash from a pyroclastic flow to include the change in air viscosity with temperature, the dependence of elutriation and particle settling velocity on density stratification within the ash cloud, and cloud expansion associated with particle deposition from the cloud. An empirical expression for the settling velocity of irregularly shaped particles is assumed. The refined model is tested with the fully turbulent flow of a density current of fine powder in a submerged flume, where mixture velocity and particle density are measured independently. The laboratory flows segregate to form a dense basal flow and a dilute turbulent cloud, and the model explains the continued generation of the cloud as well as the general decreases of mixture velocity and particle density with height above the dense basal flow. What is not explicitly modeled, but is theoretically expected, are boils of fluid containing high concentrations of powder that burst from the dense basal flow and carry particles high into the cloud. The cloud density then tries to return to some stratified equilibrium through expansion and particle deposition, and equilibrium is achieved in a time averaged sense. These bursts temporarily upset the stable density stratification of the cloud and, if large enough, cause the cloud to surge ahead of the flow. The laboratory experiments were all done at room temperature, and the variation of air viscosity and density with temperature as well as fall velocity relationships are used to infer similar processes occurring within pyroclastic flows.

CHANGES IN THE MAGNETIC ANOMALY AND THERMAL STRUCTURE OF MOUNT ST. HELENS LAVA DOME, WASHINGTON.

ROGER P. DENLINGER, U.S.G.S., Univ. of WA, WB-10, Seattle, WA, 98195.
DANIEL DZURISIN, Cascades Volcano Observatory, 5400 MacArthur Blvd., Vancouver, WA, 98660.

Field, laboratory, and theoretical studies of Mount St. Helens active lava dome suggest that the dome consists of a hot non-magnetized core enclosed in a cool, magnetized carapace. This carapace does not include the talus apron, which is randomly magnetized and does not contribute to the total field magnetic anomaly of the dome. Lab analyses of samples from lobe interiors show that the magnetic properties of dacite within the dome are very uniform when the rock cooled at depths greater than several meters below the surface, and that the induced magnetization is negligible relative to the remanent magnetization. Our studies strongly suggest that the magnetic minerals within the dome are completely oxidized while they are still above their blocking temperature.

Analysis of the growth of the magnetic anomaly over the dome shows that the magnetic carapace thickened at a seasonally variable rate between 2mm and 4 cm per day between 1984 and 1986. This is interpreted to be the average rate of movement of the 500^{o}C isotherm towards the interior of the dome. Study of the magnetic structure and joint structure of the September 1984 lobe, that subsequently was ruptured during a later eruption, provides the following insight into the cooling processes. Newly extruded material cools rapidly for a short period as heat is conducted outward in response to convective cooling of its surface. The cooling rate declines for a few weeks as heat is transferred by conduction to the surface. Thermal stresses due to cooling open fractures that propagate inward from the surface, and once these fractures are large enough the lava cools at a relatively constant rate by convective heat loss from these growing fractures, forming a blocky jointing of the flow. The rate of internal convective heat loss through fractures varies with precipitation and with large scale fracturing during eruptions. The thermally induced fractures propagate incrementally through the flow at a constant average rate by repeated cycles of cooling and fracturing. If the dome remains inactive, the time scale for its complete magnetization is estimated to be 18 to 36 years. This forecast can be improved by drilling into the dome and with continued monitoring of its magnetic field.

THE REDUCTION OF SYSTEMATIC ERROR IN LOCATIONS OF EMERGENT LOW-FREQUENCY EARTHQUAKES AT EREBUS VOLCANO, ANTARCTICA, BY STACKING THE WAVEFORMS OF EARTHQUAKE FAMILIES

DIBBLE, R.R., Victoria University of Wellington, New Zealand
IGUCHI, M., Sakurajima Volcano Observatory, Kagoshima, Japan 891-14

TV monitoring of explosions in the Erebus lava lake has revealed that explosion earthquakes originated at the surface, rather than at several kilometres depth, and at 0.5 second earlier origin times than were determined by computer location program, using a 9 station seismic net on the volcano.

Similar explosions had similar seismic waveforms, as in earthquake families, and digital stacking of families improved the signal to noise ratio, enabling onset times to be read much more reliably. To be independance of video recordings, earthquake families were defined as having cross correlation coefficients exceeding 0.75 between the different members, recorded on the same seismometer. The stacked waveform was subtracted from each original one to show residual differences. When available, the TV explosion times were also stacked, (averaged) and adopted as the family origin time.

Graphs of stacked arrival times against slant distances (0.7 to 11km) from the exploding vent showed an apparent velocity of 4070+/-90 m/s, instead of the 2100 m/s found previously by least squares adjustment in the location program. This was due to onset times of the emergent low-frequency events having been read systematically later and later at increasing distances from the source. Also on occasions, to weak forerunning vibrations which were readable only at the near stations.

Because it was systematic, the error did not cause appreciable RMS residuals in epicentre determinations, and can't be elliminated by increasing the number of seismograph stations. It may well be present in volcano-seismic studies dealing with emergent low-frequency events at other volcanoes. At Erebus, it results in an apparent pipe-like distribution of foci extending to 4km below the vent, with both depth and apparent velocity increasing with earthquake magnitude. That these are artifacts of an erroneously low velocity, late readings of weak onsets, and weak forerunning vibration which correlate with an upbulging of the lava surface in preparation for a surface explosion, is supported by the stacked time-distance graph being linear, rather than hyperbolic as for earthquakes at depth.

The error is proven only for explosions recorded on video, and the new apparent velocity may only be correct in the carapace of the volcanc. It is not yet known what (if any) error is present in truly deep foci, or those under the flanks of the volcano.

CONTRASTING CHEMICAL AND ISOTOPIC VARIATIONS IN THE SOUTH ATLANTIC RIDGE BASALTS: EVIDENCE FOR A DEEP MANTLE PLUME

DIETRICH, V.J. and KOEPPEL, V., Department of Earth Sciences, ETH-Zentrum, CH-8092 Zürich, Switzerland, and CARMAN, M.F., Department of Geosciences, University of Houston, 4800 Calhoun Rd, Houston, Texas 77004

During Deep Sea Drilling Project Leg 73 (South Atlantic), oceanic basement was encountered in Holes 519A, 520, 522B and 524 (26- 29°S latitude and 11°W-3°30'E longitude. The major- and trace (including rare earth-) element characteristics proved that these pillow lavas, flows, and sills are typical normal-type mid- ocean-ridge basalts (N-type MORB). Both the spectra of incompatible elements, such as Ti, V, Y, Zr and Nb and the REE abundances indicate that these basalts are the result of a low- pressure fractionation of olivine, spinel and plagioclase prior to eruption.

The basalts in Hole 524, which was drilled on the southeastern flank of the Walvis Ridge, are more complex: pillows and a sill, both trachybasaltic in composition, appeared in an upper sequence, and a slightly enriched tholeiitic basalt appeared in a lower multiple sill. The chemical characteristics of these alkali basalts are very similar to the characteristics of trachybasaltic and trachyandesitic lavas of the Walris ridge dredged from various locations along the ridge system and from Holes 525A, 527 and 528 (DSDP Leg 74) and the Tristan da Cunha group volcanoes.

Lead isotopes from basalts of Holes 519 and 520 lay consistently in the typical range of N-type MORB from the Mid Atlantic ridge, whereas Pb, Nd and Sr isotopes of the Hole 524 alkali basalts show typical plume characteristics (ε_{Nd}= -2.5 to -3.3 and ε_{Sr}= +17.9 to +13.9), similar to that from the Walvis Ridge, Tristan da Cunha and Gough Islands. However, the Pb, Nd and Sr isotopic signatures of the lower slightly enriched tholeiitic sill in Hole 524 still fall into the MORB array (ε_{Nd}= +5.5 and ε_{Sr}= -8.9), indicating isotopic mixing processes.

Richardson et al. (1982) examined the question of whether Leg 74 Walvis Ridge basalts were derived a) by a "simple two-component model of magma mixing, as might result from the rise of a lower mantle plume through the upper mantle" or b) by "partial melting of mantle similar to an enriched (E-type) MORB source which had become heterogeneous on a small scale due to introduction of small-volume melts and metasomatic fluids". They favour the second hypothesis.

The additional data from Leg 73 basalts, however, show that a mixing process between alkalic melts derived from a deep mantle plume and upwelling asthenosphere is a more plausible interpretation, taking into account that the trachybasaltic and trachyandesitic magmas were generated by complex magmatic processes such as hybridization of kaersutite- and plagioclase-rich cumulates in various proportions and mixing with evolved trachytic melts.

The question of origin for the parental magmas forming the Walvis Ridge is not fully resolved, but according to experimental results and stability field of phlogopite and deep mantle kaersutite (Ulmer et al., this conference), basanitic melts may originate or segregate and equilibrate with a fertile garnet lherzolite at depths ranging between 80 to 100km. According to Nd, Sr and Pb isotope variations, a deeper mantle source appears to be involved, which may have been contaminated by old subducted continental crustal material.

Richardson, S.H., Erlank, A.J., Duncan, A.R. and Reid, D.L. (1982): Earth Planet. Sci. Lett. 59, 327-342.

GEOLOGIC MAP OF MEDICINE LAKE VOLCANO, NORTHERN CALIFORNIA

DONNELLY-NOLAN, J.M., U.S. Geological Survey, Mail Stop 910, 345 Middlefield Rd.,Menlo Park CA 94025, USA

Medicine Lake volcano (MLV) is a Pleistocene and Holocene shield volcano located in the Cascade Range, E of the main arc and NE of Mt. Shasta. Lavas from MLV cover about 2000 km^2. They range in composition from basalt through rhyolite and include both tholeiitic and calc-alkaline types. Basalt and basaltic andesite dominate the lower flanks of MLV. Higher on the volcano, basaltic lavas are mostly absent, andesite dominates, and high-silica lavas are present, including the spectacular late Holocene rhyolites of Glass Mountain and Little Glass Mountain. Volume of the volcano is estimated at 600 km^3, larger than Mt. Shasta which is the largest of the Cascade stratocones. The low shield shape, central caldera, and dominance of mafic lavas are similar to Newberry Volcano of central Oregon, also located in an extensional tectonic environment east of the main Cascade arc.

A preliminary version of the geologic map of MLV covers about 1800 km^2. Scale is 1:50,000. The map includes approximately 230 units and 350 vents. The youngest eruption occurred at Glass Mountain about 900 yrs ago. Wherever possible, individual lava flows were mapped. Some units include multiple flows from the same vent or from several closely spaced vents. Age spans of such units are thought to be short, not exceeding a few tens of years. Only one widespread marker bed is present, an andesitic ash-flow tuff of late Pleistocene age, and even this is not present or not exposed on the S and NE sides of the volcano. Potassium-argon age data are limited for MLV, but based on existing K/Ar and radiocarbon dates, stratigraphic relations and geomorphology, ages of the lavas at MLV were estimated and grouped into 5 time periods. Approximate percentages of the map area covered by lavas of the 5 periods are 0-12 ka, 15%; 12-25 ka, 17%; 25-120 ka, 40%; 120-700 ka, 23%; >700 ka, 5%. The 5% of lavas older than 700 ka may be pre-MLV in age. Most of these older lavas lie on the far W side of MLV and may be part of earlier centers that form a highland of volcanic vents connecting MLV with Mt. Shasta.

Approximate percentages of map area by rock type are 55% basalt (47.2-52.9% SiO_2), 19% basaltic andesite (53.0-56.9%), 21% andesite (57.0-62.9%), 2% dacite (63.0-69.9%), and 3% rhyolite (>69.9%). Some lava flows are compositionally zoned, e.g. Glass Mountain, 65-74% SiO_2, the Callahan flow, 51-58%, Burnt Lava flow, 56.0-57.8%, and Giant Crater lava, 47.2-52.7%.

An area on the NE flank of MLV, covering about 10% of the volcano, has already been published at a scale of 1:24,000: J.M. Donnelly-Nolan and D.E. Champion, 1987, Geologic map of Lava Beds National Monument, northern California, U.S. Geological Survey Map I-1804.

EMPLACEMENT OF THE MAY 18, 1980, LATERAL BLAST NORTHEAST OF MOUNT ST. HELENS, WASHINGTON.

DRUITT, T.H. Department of Geology, University of Wales, Cardiff CF1 3YE, U.K.

Northeast of Mount St. Helens the lateral blast began as a sediment gravity current resembling a high-energy pyroclastic flow, but became more surge-like away from source. Proximal ($\lesssim$8 km from vent) layer A1 gravel resembles an ignimbrite ground layer. It is clast-supported, fines-poor, and lacks hydraulic equivalence (MD/ML, the size ratio of the largest vesicular dacite clast to the largest lithic, is less than one). A1 is overlain erosively by the relatively fines-rich, massive to wavy and cross-laminated layer A2. The massive facies of A2 is up to ~1 m thick, drapes hills, and displays matrix support and coarse-tail grading typical of high-concentration flow. With increasing distance (R) from vent: (1) the average thickness of the deposit (an approximate measure of sedimentation rate in the transient blast) decreases by a factor of ~10^3; (2) distinction between A1 and A2 diminishes; (3) the massive A2 facies becomes rare; (4) ripple cross lamination extends, with increasing frequency, through the entire thickness of the deposit; (5) internal stratigraphy becomes highly variable on a horizontal scale of tens of cm due to interaction of the blast with surface roughness; (6) MD/ML increases from ~0.6 at R=4 km to ~1.5 (approximate hydraulic equivalence) near the edge of the blowdown zone (R=17 km). The blast deposit also becomes richer in dacite with increasing R (from 30 to 80 wt% in the 16-32 mm fraction) because dense lithics were fractionated into the deposit faster than they were replenished by ground erosion. Viewed on a kilometre scale, the radial transition from a flow- to surge-like deposit appears entirely gradational.

The blast was a highly turbulent current, but the character of the deposit was strongly influenced by processes operating in the final moments of deposition. Close to source, rapid suspension fallout immediately behind the blast front generated a concentrated traction carpet in which intense fluidization (due to upward escape of gas from the compacting gravel) caused buoyant removal of large dacite clasts, producing low-MD/ML, fines-poor A1. A thick, massive deposit banked up against Windy Ridge is rich in coarse blocks of frothy dacite, and is a 'scum' of light components derived from proximal A1. A2 was laid down on top of A1 as the blast waned. At greater R, lower initial sedimentation rates behind the blast front resulted in layer-by-layer deposition of poorly or non-fluidized material from bedload and from dilute suspension. Dune and ripple forms generated between 6 and 17 km from vent commonly migrated upstream where the blast was accelerating, and downstream where it was decelerating. Decay of the initial 'pyroclastic flow' occurred because there was insufficient ash component in the trailing body to feed and maintain the flow head. The head thus became progressively more dilute due to sedimentation, decompression, and air entrainment, until it became buoyant and lofted. The paucity of ash in the blast can be attributed to the low water content and weak fragmentation of the dacitic magma.

AGE, STRUCTURAL HISTORY, AND CHEMICAL EVOLUTION OF THE TURKEY CREEK CALDERA, SOUTHEAST ARIZONA

DU BRAY, Edward A., PALLISTER, John S., and SNEE, Lawrence W., U.S. Geological Survey, Denver, CO 80225

Erosion and basin-and-range faulting in the Chiricahua Mountains expose multiple levels through the Turkey Creek caldera, which formed in late Oligocene time in response to eruption of high-silica (77% SiO_2) Rhyolite Canyon Formation ash-flow tuff. Field relations and age data indicate that a hypabyssal (65% SiO_2) porphyry was emplaced shortly after the Rhyolite Canyon Formation was erupted. The porphyry formed a 20-km-diameter ring intrusion (monzonite porphyry, Tmpr; see table below), which locally vented to form alkali-rich dacite lava flows. The porphyry also formed a resurgent hypabyssal core intrusion (Tmpc). The caldera moat was then filled by high-silica rhyolite lava flows (Tmrl, Tmru). New $^{40}Ar/^{39}Ar$ data indicate that ages of the ash-flow tuff (26.93 Ma), monzonite porphyry (26.84 Ma), and moat rhyolites (26.93 Ma) are indistinguishable within analytical uncertainty (±0.11 Ma).

The age equivalence and spatial association of these rocks, and the rarity of compositions intermediate between those of the rhyolite tuff (77% SiO_2) and the porphyry (65% SiO_2) indicate that magmas represented by these two units coexisted across an abrupt compositional interface in a magma chamber. The interface was apparently drawn up into ring conduits for the tuff and was disrupted, which resulted in local mingling of the two magmas. Subsequently, monzonite porphyry (from beneath the interface) intruded and was erupted from the ring conduits that previously fed rhyolite-tuff eruptions.

Field relations, chemistry, and radiometric ages indicate that the outflow tuff was emplaced in three pulses, to form a compound cooling unit. The first (Trc1) and second (Trc2) pulses formed chemically similar rocks, whereas the third (Trc3) pulse is chemically distinct, but volumetrically minor, relative to the first two. Intracaldera tuff (Trci) correlates in composition with tuff of the youngest outflow pulse (Trc3); the first two pulses are not observed in exposed intracaldera tuff.

A breccia zone (~50m thick) occurs along the contact between the central porphyry intrusion and overlying intracaldera tuff. Rock above the contact is monolithologic breccia of recrystallized tuff; that below is monolithologic breccia of granophyric porphyry. The breccias lack evidence of megascopic shear but do display characteristics of low-pressure shock metamorphism.

The magma body responsible for the caldera consisted of a less evolved lower part (monzonite porphyry) overlain by a more evolved rhyolite cap. Tapping this magma body first produced high-silica ash-flow tuff, which led to caldera subsidence, and then produced monzonite-porphyry intrusions and equivalent lavas. The near absence of precaldera floor rocks within the caldera (despite deep erosion) and the apparent absence of intracaldera equivalents for Trc1 and Trc2 outflow tuff suggest that the central intrusion represents a >1-km-thick laccolith that was intruded at or above the base of the intracaldera equivalent of Trc3 tuff immediately following caldera collapse. Intracaldera equivalents of outflow units Trc1 and Trc2 were either not deposited in the caldera or are concealed beneath the laccolith. The breccia zone may represent volume increase (hydrofracturing) that occurred in response to volatile exsolution from the monzonite-porphyry laccolith. Moat lavas (Trml, Trmu) record a return to high-silica magmatism within less than 0.1 Ma of porphyry intrusion.

Unit(n)	SiO_2(%)	Rb(ppm)	Sr(ppm)	Zr(ppm)	Ba(ppm)	Ce(ppm)
Tmru(8)	77.44±0.62	455±114	25±23	193± 8	10± 4	84±15
Tmrl(7)	76.79±1.18	404± 98	39±19	211±22	77±10	136±30
Tmpr(9)	64.86±0.92	203± 49	227±28	526±57	709±66	150±11
Tmpc(5)	65.78±3.42	211± 58	222±56	481±20	712±90	164±18
Trci(15)	76.45±1.08	336±115	34±11	407±72	70±25	204±43
Trc3(4)	75.85±0.35	294± 3	36± 6	381±43	68± 9	206±25
Trc2(14)	77.52±0.26	381± 34	23± 7	279± 9	28±18	136±17
Trc1(12)	77.41±0.31	425± 14	20± 5	291±11	17± 9	131±20

FOUNTAIN-FED SILICIC LAVA FLOWS

DUFFIELD, W. A., U.S. Geological Survey, 2255 North Gemini Drive, Flagstaff, AZ 86001

Descriptions of silicic lava flows recognized as fountain-fed are almost non-existent in the geological literature, whereas many examples of their mafic counterparts are documented in detail. Part of this apparent composition-related difference in mode of emplacement may be an artifact of observations; historic examples of fountain-fed mafic flows are common, but eruptions of silicic magmas are infrequent relative to the human lifespan and therefore rarely observed. In addition, characteristic properties that collectively tend to result in high viscosity also inhibit the occurrence of silicic fallback hot enough to thoroughly weld and rehomogenize into a melt subsequently able to feed lava flows. As a result, generations of geologists trying to accurately decipher the geologic record have concluded that silicic magma either is extruded quietly to form lava flows or is erupted violently to feed columns whose fallback becomes a variably welded mantle or a pyroclastic flow.

Some silicic volcanic masses, however, seem to defy unambiguous interpretation of their emplacement mechanism. Notable examples in the North American Cordillera include Tertiary rocks in southwestern Idaho, in the Trans-Pecos area of Texas, and in southwestern New Mexico. These volcanics show evidence of both welded-particulate and lava-flow origin within individual eruptive units. The coexisting textures generally have been interpreted as the result of a pyroclastic flow so hot that part of it was remobilized as a lava flow after the main eruptive mass came to rest, or alternatively as the result of a lava flow that locally collapsed to feed a welded pyroclastic phase. I speculate that these and perhaps many other silicic volcanic rocks having similarly mixed textures are the products of fountains of silicic lava whose fallback was mostly hot enough to form homogeneous melt that fed lava flows, but was in part cool enough to preserve a welded-particle texture. High volumetric rates of eruption, high eruption temperature (relative to solidus temperature), relatively short trajectories for erupting lava clots and any other conditions (for example, high fluorine or chlorine) that promote relatively low-viscosity fallback, should favor the formation of fountain-fed flows. Minor fluctuations in eruptive conditions could result in local preservation of a welded-particle texture within an otherwise normal-looking lava flow. Without such fluctuations, fountain-fed silicic lavas might totally lack textural evidence of an early particulate history, as is commonly true of their mafic counterparts.

VOLATILE CONTENTS OF OBSIDIAN FROM THE TAUPO VOLCANIC ZONE, NEW ZEALAND, AND IMPLICATIONS FOR ERUPTION PROCESSES.

DUNBAR, N.W., Geoscience Department, New Mexico Institute of Mining and Technology, Socorro, N.M., 87801

KYLE, P.R., same affiliation.

Obsidian in 0.01 to 20 ka rhyolitic tephra deposits from the Taupo Volcanic Zone, New Zealand, contains elevated and variable H_2O (0.2 to 2.5 wt.%) and Cl (0.12 to 0.18 wt.%) contents compared to rhyolitic dome obsidians which quenched at surface pressures (~0.1 wt.% H_2O, ~0.1 wt.% Cl). Major and trace element analyses of the obsidian in the tephra are similar to their associated tephra, suggesting that they are co-genetic. The clear, glassy appearance of the obsidian, their high release temperature of H_2O, and oxygen isotopic composition of +7 permil indicate that the water contained in the obsidian is magmatic, rather than meteoric water introduced after the tephra was deposited. However, the obsidian contains less H_2O and Cl than the primary non-degassed Taupo Volcanic Center magmas, which are determined to be ~4.3 to 5.9 wt.% H_2O and ~0.18 to 0.24 wt.% Cl based on ion and electron microprobe analyses of melt inclusions. Therefore, the obsidian in the tephra deposits is thought to represent partially degassed, quenched primary magma.

There is a rough correlation between the H_2O and Cl contents of obsidian which suggests that the magmatic Cl partitioned into an H_2O-rich fluid phase during eruptive degassing. This correlation can be projected to include the H_2O and Cl contents of melt inclusion, and can be used to determine a partitioning coefficient for Cl between the vapor and the melt of ~5.5.

Using a pre-eruptive H_2O contents for Taupo magma of 4.3 wt.%, and Burnham's (1979) water solubility model, the pressure and depth of initial vesiculation of the magma can be calculated, and occurs at about 0.9 kb or ~3.5 km depth. Initial fragmentation (assumed to occur at a vapor:melt ratio of 3 to 1) will begin at 0.1 kb or ~500 m depth. Obsidian in most of the tephra deposits contains less than 1 wt.% H_2O, and based on this, the pressures and depths of obsidian formation were calculated, and were determined to be generally less than 0.1 kb or 500 m. Therefore, the obsidian in these tephra deposits collapsed and quenched from expanded, fragmented magma. Hydrogen isotopic analyses of H_2O in the obsidian suggest open-system degassing, which supports formation of obsidian from fragmented melt. The variable water contents of obsidian fragments in a single deposit indicates that quenching occurred over a range of depths. This, and the strong alignment of microphenocrysts in obsidian, suggests that fragmented magma was welded onto the conduit walls during eruption, cooled to form obsidian, then incorporated into the tephra.

A tephra with a strongly phreatomagmatic character, the Hatepe phreatoplinian tephra, erupted from the Taupo Volcanic Center approximately 2 ka B.P., contains many individual obsidian fragments with high water contents. Many obsidian fragments contain greater than 2.0 wt.% H_2O, and some fragments up to 2.5 wt.%. The highest water content corresponds to a quench pressure of 0.35 kb or a depth of 1.5 km. The anomalously high magmatic water of obsidian in the Hatepe phreatoplinian tephra as compared to obsidian in plinian tephras from the Taupo Volcanic Center suggests that the meteoric water responsible for the phreatomagmatic nature of this eruption may have also influenced the deep quenching of obsidian. This implies that meteoric water may have interacted with the magma at depths of up to 1.5 km to cause this phreatomagmatic eruption.

MANTLE AND CRUSTAL COMPONENTS IN MAFIC TO INTERMEDIATE LAVAS OF THE CERROS DEL RIO VOLCANIC FIELD, RIO GRANDE RIFT, NEW MEXICO

DUNCKER, K.E., Smithsonian Institution, NHB MRC 129, Washington, DC 20560, WOLFF, J.A., Box 19049, Univ. Texas, Arlington, Texas 76019, HARMON, R.S., NERC Isotope Geology Centre, 64 Gray's Inn Road, London WC1X 8NG, U.K., LEAT, P.T. and Thompson, R.N., Univ. Durham, Durham DH1 3LE, U.K. and DICKIN, A.P., McMaster Univ., Hamilton, Ontario L8S 4M1, Canada

The northernmost part of the Pliocene Cerros del Rio (CdR) volcanic field consists of hawaiites, olivine tholeiites, and a range of mildly alkaline, mostly Q-normative intermediate lavas with up to 63% SiO_2. Several hawaiites contain crustally-derived quartz xenocrysts in O-isotope disequilibrium with their host lavas. Whole-rock $\delta^{18}O$ for all lavas ranges from +6.1 to +7.4 per mil, with considerable overlap between quartz-bearing and quartz-free lavas.

Tholeiites, vents for which appear to be restricted to the flanks of the Jemez Mountains in the western part of the CdR, have trace-element patterns and Sr-Nd isotope characteristics suggestive of asthenospherically derived magmas, resembling OIB tholeiite or E-type MORB, contaminated with a small proportion of upper crust. The volumetrically dominant hawaiites and Q-normative lavas cannot be related to the tholeiites by any process of crystal-liquid fractionation or crustal contamination. Hawaiites possess distinctive and unusual trace element patterns, with depletions in K, Rb, Nb and Ta relative to Th and LREE. Q-normative lavas have higher $\delta^{18}O$, similar $^{87}Sr/^{86}Sr$ and lower $^{143}Nd/^{144}Nd$ compared to hawaiites, and similar trace-element patterns with the exception of generally higher K/Ta and K/Th. They can be modelled as hawaiites strongly contaminated with continental lower crust, most likely by simple mixing with crustal melts rather than via AFC.

Although the hawaiites themselves appear to have interacted with lower crust to some extent, their distinctive trace-element characteristics are a reflection of mantle source composition and not of contamination. This source material also appears to underlie the Colorado section of the Rio Grande Rift (1). It may be modified "mantle wedge" material ultimately related to the early Tertiary subduction of the Farallon Plate beneath western North America. If so, the material became depleted in K and Rb prior to CdR magmagenesis, possibly by dehydration of local mantle during the onset of tectonic extension in the mid-Tertiary.

(1) Leat et al., J. Pet. Lithosphere Issue pp. 351-377 (1988)

A COMPARISON OF DOMINANTLY ANDESITIC PRE-RIFT VOLCANISM TO DOMINANTLY BASALTIC RIFT VOLCANISM, NORTHERN RIO GRANDE RIFT AREA: INSIGHTS INTO THE RELATIONSHIPS AMONG TECTONIC SETTING, CRUST-MAGMA INTERACTION, AND MAGMATIC DIFFERENTIATION

M.A. DUNGAN, M.T. COLUCCI, K.M. FERGUSON, S.D. BALSLEY, Dept. Geological Sciences, Southern Methodist Univ., Dallas, TX 75275; S. MOORBATH, Univ. of Oxford, Parks Road OX1 3PR, Oxford, UK; P.W. LIPMAN, U.S.G.S., MS903, Denver, CO 80225

The Oligocene (33-26.5 Ma) SE San Juan (SESJ) volcanic field and the adjacent Pliocene (4.5-2 Ma) Taos Plateau (TP) volcanic field are representative of two contrasting stages in the volcanic history of the northern Rio Grande rift region. Although the SESJ volcanic field predates the first eruption of basaltic rocks associated with crustal extension in the Rio Grande rift (26 Ma), San Juan magmatism was integral to the long term evolution of crust and mantle source regions for younger rift-related magmas. SESJ volcanic rocks are high-K calc alkalic andesite to silicic dacite (no basalt) erupted from stratocones and calderas, and comprise an early phase of development of the San Juan field. The TP assemblage of tholeiitic flood basalts plus minor high-K andesite and dacite represents volcanism associated with the mature rift. The differences between these magmatic associations are the result of crustal differentiation histories related to contrasting tectonic settings: parent magma diversity played a minor role in comparison to stress regimes and magma supply rates. The presence of andesite and dacite in both fields provides a means for direct comparison of magmas at similar stages of differentiation.

Evolved TP magmas differentiated by AFC in multiple chambers open to repeated mafic recharge. A strong negative correlation between elemental indices of differentiation and Pb isotope ratios indicates assimilation of low U/Pb Proterozoic lower or middle crust. Sr and Nd isotopic data record lateral lithologic heterogeneity among zones of crust-magma interaction. Early SESJ basaltic andesites have combined isotopic characteristics comparable to Taos dacites. We infer that the first stage of SESJ magma evolution occurred in deep crustal reservoirs by the MASH process (Hildreth and Moorbath, 1988). Hybrid basaltic andesites subsequently rose to shallower levels where they evolved further (andesite to dacite) by AFC through interaction with heterogeneous upper crust. Isotopic compositions of younger tuffs and diverse lavas (basaltic andesite to dacite) are generally more radiogenic for Pb and Sr, less radiogenic for Nd, and exhibit strong geographic provinciality. These are also the products of magma evolution in deep chambers plus later shallow evolution in the upper crust. The temporal shift reflects long term hybridization of the crust, and an increasing role of magma stagnation at subcaldera levels, where marked lateral lithologic diversity imparted variable isotopic signatures.

Large, long-lived continental volcanic fields are likely to evolve with crust-magma interaction as a major factor, regardless of tectonic setting. Where there are isotopic and elemental contrasts between old, compositionally diverse crust and mantle-derived magma, spatial and temporal variations in assimilated crustal lithologies provide important information about mechanisms and loci of magma differentiation, and contribute to the recognition and documentation of assimilation.

HIGH-PRECISION GEODETIC MEASUREMENTS ON HAWAIIAN VOLCANOES USING SATELLITE GEODESY

DVORAK, J., P.T. DELANEY, and A.T. OKAMURA, U.S. Geological Survey, Hawaiian Volcano Observatory, Hawaii Volcanoes National Park, Hawaii 96718; W.H. PRESCOTT, U.S. Geological Survey, Mail Stop 977, 345 Middlefield Road, Menlo Park, California 94025

The Global Positioning System (GPS), a new geodetic technique to measure crustal movement using a network of satellites and mobile ground-based radio receivers, is being evaluated on the island of Hawaii. This technique is especially well-suited to the study of ground movement associated with active volcanoes because

- a survey can be completed within a few days to a few weeks.
- measurements are less restricted by weather conditions than other geodetic techniques.
- three-dimensional displacements can be determined to within a few tens of millimeters over distances of up to 100-km.
- ground stations do not have to be intervisible or traversable, so that, surveys can be done in rugged and remote terrain.

GPS surveys were conducted on the island of Hawaii in April 1987 and in August 1988. Approximately 40 ground stations were occupied during each survey. TI4100 radio receivers, which simultaneously receive the time code and two radio signals from four different satellites, were used during both surveys. This allows us to make empirical corrections for the drift of each receiver-clock and for the propagation delays caused by the atmosphere and the ionosphere.

As the first step in processing, we have used satellite positions broadcast by each satellite as a survey was conducted. Our results suggest that these broadcast satellite positions are probably accurate to within a few tens of meters. Because many ground stations were occupied more than once during the 1987 survey, we are able to make a comparison of the variation in station locations determined for the reoccupations. Shown in the figure below is the variation in measured baseline distance (commonly called the mark-to-mark distance in trilateration surveys) for the re-occupation of about two dozen stations during the 1987 survey. This variation is plotted as a function of baseline distance. This graph shows that the variation in baseline distances was less than 30-mm for all but two lines and less than 1-ppm for all but the shortest line. Most of this variation is probably caused by uncertainties in satellite positions.

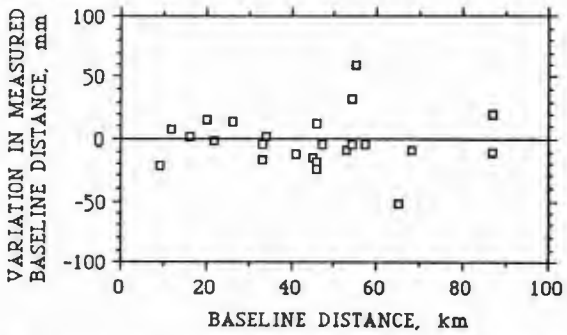

By using data collected at several worldwide stations--whose locations have been determined by other techniques, such as radio interferometry (VLBI) and satellite laser ranging--that track the GPS satellites during our surveys, we will be able to compute a better position for each satellite. Our first attempts in using these tracking data suggest that we can determine *relative* locations to an accuracy of at least 0.2-ppm. This means that we can determine three-dimensional displacements between *any* two stations on the 150-km-wide island of Hawaii to an accuracy of 30-mm.

GPS is a new tool that can be used to monitor active volcanoes. Because of its advantages over other surveying techniques, the use of GPS as a high-precision geodetic technique represents the opportunity to make very accurate measurements of crustal movement over wide areas. We can now address the possible relation that may exist between regional strain and volcanic eruptions and record an earlier stage of small ground movement that may occur during the initial buildup to a volcanic eruption.

PROCESSES BENEATH YELLOWSTONE CALDERA, WYOMING, INFERRED FROM RECENT CRUSTAL MOVEMENTS

DZURISIN, D., U.S. Geological Survey, 5400 MacArthur Blvd., Vancouver, WA 98661, HOLDAHL, S., National Geodetic Survey, NOAA, Rockville, MD 20852, FOURNIER, R.O., U.S. Geological Survey, 345 Middlefield Road, Menlo Park, CA 94025, and SAVAGE, J.C., U.S. Geological Survey, 345 Middlefield Road, Menlo Park, CA 94025

The Yellowstone region has been geologically restless since it was first described by explorers more than a century ago. The most notable symptoms of unrest are vigorous hydrothermal activity, persistent earthquakes, and rapid vertical crustal movements. From 1923 to 1976, the central part of the caldera rose at a maximum average rate of 14 ± 1 mm/yr; from 1976 to 1984, the average uplift rate increased to 22 ± 1 mm/yr. Following a period of relative stability during 1984-85, the caldera floor subsided 25 ± 7 mm during 1985-86, 35 ± 7 mm during 1986-87, and 10 ± 7 mm during 1987-88. For the period from 1984 to 1987, the average horizontal strain rates in the northeast part of the caldera were: $\dot{\epsilon}_1$ = 0.10 ± 0.09 μstrain/yr oriented N33°E ± 9° and $\dot{\epsilon}_2$ = -0.20 ± 0.09 μstrain/yr oriented N57°W ± 9° (extension reckoned positive). A best-fit elastic model of the 1985-87 vertical and horizontal displacements involves depressurization or deflation of a horizontal tabular body, centered 10 ± 5 km beneath Le Hardys Rapids, within a deep hydrothermal system or an underlying body of partly molten(?) rhyolite. The east and west margins of the body are not well determined by the 1985-87 observations, but the pattern of vertical displacements from 1923 to 1976 suggests that the deforming body extends beneath most of the caldera.

Two end-member models each explain most aspects of historical vertical crustal movements at Yellowstone, including the recent reversal from uplift to subsidence. Both models involve crystallization of an amount of rhyolitic magma that is compatible with the thermal energy requirements of the hydrothermal system. In the first model, injection of basalt near the base of the rhyolitic system is the primary cause of uplift. Higher in this system, rhyolite crystallizes and releases all of its magmatic volatiles into the shallow hydrothermal system. Uplift stops and subsidence starts whenever the supply rate of basalt is less than the subsidence rate associated with crystallization of rhyolite and fluid loss. In the second model, uplift is caused primarily by pressurization of the deep hydrothermal system by magmatic gas and brine released during crystallization of rhyolite and trapped at lithostatic pressure within the deep hydrothermal system. Subsidence occurs during episodic hydrofracturing and injection of pore fluid from the deep lithostatic-pressure zone into a shallow hydrostatic-pressure zone. The resulting pressure surge in the shallow zone is accommodated by an increase in the rate of flow of thermal water from the system, a decrease in the rate of recharge of cold meteoric water into the system, or condensation of a small amount of steam and a slight rise in the level of the interface between liquid and steam. Heat input from basaltic intrusions is required to maintain Yellowstone's silicic magmatic system and shallow hydrothermal system over time scales longer than about 10^5 years, but for the historical time period, crystallization of rhyolite can account for most aspects of unrest at Yellowstone, including seismicity, uplift, subsidence, and minor changes in the intensity or location of hydrothermal activity.

VOLCANISM IN AN ACTIVE CARBONATE BASIN: AN EXAMPLE FROM THE GRENVILLE PROVINCE, ONTARIO

EASTON, R.M., Precambrian Geology Section, Ontario Geological Survey, 77 Grenville Street, Toronto, Ontario CANADA M7A 1W4

The relationship of carbonate sedimentation and volcanism in active tectonic environments is poorly understood. The western Central Metasedimentary Belt of the Grenville Structural Province in Ontario, despite the presence of greenschist facies and locally higher metamorphic conditions, provides an opportunity to study these relationships.

The Central Metasedimentary Belt is divided into four lithotectonic domains having broadly similar stratigraphic and magmatic histories. The volcanic sequence in the better studied Elzevir Terrane consists of a lower, tholeiitic shield volcano stage followed by one or two mafic-intermediate-felsic volcanic cycles of calc-alkalic affinity that locally contain small caldera complexes and related pyroclastic flow deposits. The volcanic and sedimentary rocks were deposited between 1285 and 1250 Ma, and were metamorphosed and deformed at roughly 1240-1120 Ma and 1070 Ma. Although these rocks have undergone lower greenschist to upper amphibolite facies metamorphism, in the lower grade areas textures and geological relationships are well preserved. Carbonate depositional environments present with the volcanic complexes (probably volcanic islands) include: (1) In the proximal volcanic environment, stromatolitic dolomite reefs developed adjacent to the island volcanoes. These dolomite reefs and associated marly and black shales serve as hosts for Zn mineralization in the region. (2) In the proximal to distal volcanic environment, deposition of carbonate turbidites derived from an adjacent carbonate platform occurred basinward of the volcanic islands. The carbonate turbidites interfinger with, or are buried by, prograding pyroclastic fans of both volcanic and sedimentary provenance. Rhythmically layered couplets of ash and calc-silicate/impure marble with 2-10 cm scale bedding are common in the turbidite fans of pyroclastic-volcaniclastic origin, and indicate simultaneous carbonate sedimentation and volcanic ash deposition. (3) In the distal volcanic environment, carbonate deposition occurred as turbidites in deep basins and as shelf and platform deposits in shallower areas. "Feather amphibolite" beds present interbedded with these carbonate deposits are interpreted as mafic tuffs and indicate that distal volcanism occurred during carbonate sedimentation. The other three terranes represent variations on this theme with the Bancroft Terrane to the east containing platform carbonates and rift volcanics, the Sharbot Lake Terrane containing only the lower mafic volcanic sequence, and the Frontenac Terrane consisting mainly of platform metasediments.

Zones of pervasive carbonatization are common in the volcanic rocks, and in some cases are related to the incorporation of carbonate during volcanic deposition. The chemistry of many of the volcanic rocks is difficult to interpret because CO_2 mobilizes many of the "immobile" trace elements and the rare-earth elements, making it difficult to apply standard geochemical discrimination schemes to these rocks.

In summary, the presence of abundant carbonate is diagnostic of a marine depositional setting, and features preserved in the carbonates (e.g. stromatolites and sedimentary textures) provide paleoenvironmental controls on the deposition of both the carbonate and intercalated volcanic rocks. This aids in determining the depositional setting of many massive, textureless volcanic rocks and the study of the products of subaqueous pyroclastic volcanism.

GEOPHYSICAL CONSTRAINTS ON MAGMATISM AND CRUSTAL STRUCTURE

EATON, G.P., Iowa State University, Ames, Iowa 50011

Applications of geophysical measurements in the study of molten or partially molten bodies of magma, as well as of cooler masses of in situ magmatic rocks, of complex subvolcano systems, and of the crustal structure of regions of active magmatism have increased significantly in the past 25 years. A brief review of the successes and failures of such efforts is presented, based on published case studies, on theoretical considerations of the geophysical properties of magma and magmatic rocks (in terms both of the absolute values of such properties and relative to those of the country rocks in which the magma was emplaced), and on the viability of different geophysical techniques applied in attempts to answer specific questions raised by geologists engaged in the study of volcanoes or magmatic systems.

The ultimate success of geophysical interpretation in such studies is dependent on the ability to detect, sort and correctly interpret signals arising from, or affected by, a variety of phenomena: the actual presence of magma, itself; the geometric configuration of the magma body; properties of the magma owing to its physical state (e.g., cooling, thermally stable, or warming; moving, or at rest; convecting or non-convecting; etc.); the presence or absence of vigorous hydrothermal circulation in the region around and above the magma mass; the presence or absence of a rock alteration shroud around the body, which may be present whether the body is hot or has cooled to an ambient regional temperature; and the presence or absence of emplacement-related, localized fracture systems in the country rock nearby or deformation in the region of the body arising from the added effect of far-field stresses.

Much of what can be detected geophysically at the surface is thus significantly influenced by processes and phenomena in the shallow crust. These phenomena have the potential to screen, distort, mimic or reinforce signals deriving from a magma body or from the lower crust. In the case of those magmatic systems in which a constructional volcanic edifice is present at the surface, part of the difficulty of interpretation relates to the ability to effect a proper separation of surface or near-surface geologic signals from those arising at the depth of interest and target of relevance. In most cases, the task is not a simple one and the certainty of interpretation is sometimes a function of the availability of a variety of other information bearing on the specific problem that is to be solved. Some convincing case histories are presented in which the viability of the use of geophysical data is demonstrated and its interpretation, independently confirmed.

Studies examined here include gravity investigations, magnetics, active and passive seismic studies and seismic signal delays, electrical methods, thermal gradient measurements and heat flow calculations, and surface deformation studies.

Example sites include the Cascade Range of western North America; Hawaii Volcanoes National Park, Hawaii; Long Valley, California; San Juan Mountains, Colorado; Rio Grande Valley, New Mexico; Yellowstone National Park, Wyoming; as well as several active volcanoes in Japan and ancient magmatic complexes in the British Isles.

GEOCHEMICAL VARIATIONS OF PRIMITIVE BASALTIC ROCKS ALONG THE WESTERN SHOULDER OF THE KENYA RIFT.

EBERZ, G.W., VOLKER, F. AND ALTHERR R. (Institut für Petrographie und Geochemie, Universität Karlsruhe, Karlsruhe, F.R.G.).

Major and trace element data for a wide range of Tertiary basaltic rocks (alkaline to mildly alkaline basalts, basanites, tephrites and nephelinites) from the western shoulder of the Kenya Rift reveal substantial compositional variations parallel to the rift axis from $3^{o}40'N$ to 2^{o} S. In particular, $(Ce/Yb)_N$ ratios < 13 dominate in the northern and central part of the western shoulder, whereas highly fractionated REE abundance patterns with $(Ce/Yb)_N$ up to 25 are found in the southern section of the western shoulder (including the Nyanza Rift area).

The degree of MREE/HREE fractionation follows a similar pattern. Zr/Nb ratios are highly variable in the northern and central sectors (Zr/Nb = 1.7 - 5.6). With the exception of two samples Zr/Nb ratios are less than 3.5 in the south. Therefore, the degree of mantle melting must have been quite variable in the north but more uniformly low in the south.

On primordial mantle-normalized spidergrams (MORB and OIB incompatibility sequence) all samples display maxima within the Nb-La range. Consequently, all basaltic rocks are considered to be derived from a depleted mantle source. However, many samples display negative K-(Th-U), Zr-Hf and Ti anomalies. These may indicate the stability of minor phases during the melting event or a geochemically unusual lithospheric mantle beneath the western shoulder of the Kenya Rift.

Geochemical studies from the eastern Rift shoulder have shown that the volcanic rocks east of Lake Turkana derived their geochemical fingersprints through the Mesozoic Anza Trough event, which modified the lithospheric structure beneath that area. It is therefore possible that the main differences between the northernmost (Lake Turkana) area and further south on the western shoulder may equally be related to different basement lithologies and ages.

THE ORIGIN OF POTASSIC VOLCANISM : IMPLICATIONS OF SOURCES FROM MURIAH, INDONESIA.

EDWARDS, Caroline, Geology Dept. Royal Holloway and Bedford New College, University of London, Egham Hill, Egham, Surrey, TW20 0EX, England , and
MENZIES, Martin, Geology Dept. R.H.B.N.C., University of London, Egham Hill, Egham, Surrey, TW20 0EX, England.

Comparison is made between a high K alkaline volcano (Muriah) situated in an intra-oceanic arc setting and a number of examples of continental alkaline volcanic centres.

Muriah has erupted two compositional lava series, an older K series and a younger high K series.The HK series have: higher K2O for a given MgO content; greater silica undersaturation; and greater enrichment in LIL,LREE and HFSE, than the K series. Incompatible element patterns are similar to those of both island arc and ocean island basalts. Petrography, trace element and isotope data indicate mixing between at least two end members, whilst quantitative modelling constrains these end members and suggests two models for the magma genesis of the two series.

The first model involves three end members: a MORB like mantle wedge; a subduction zone component; and a within-plate component. The second model involves two end members: a mantle wedge which has Dupal anomaly characteristics and a within-plate component. The within-plate component has greater influence during the magma genesis of the high K series. It is believed that the influx of the within-plate component to the level of magma production is controlled by extension in the Bawean trough,in which Muriah is located.

It is apparent from comparison of the geochemical data and tectonic setting of Muriah with that of other alkaline centres, (namely Stromboli, Aeolian islands; NSW leucitites, Australia; Gaussberg leucitites, Antarctica; and the Leucite Hills, Wyoming) that the potassic volcanic rocks from both oceanic and continental settings share similar source components in terms of their trace elements. The LIL and LREE enrichments in these lavas are explained by the presence of a subduction zone component residing either in the oceanic mantle wedge or in the subcontinental lithosphere. As was implied for Muriah, the subduction zone component for the NSW and Gaussberg leucitites may be represented by the Dupal anomaly (i.e. EM2) in the continental lithosphere. The enrichment in HFSE in these lavas is satisfied by the presence of a within-plate component. In the case of Muriah, Stromboli and the NSW leucitites the presence of the within-plate component is related to the superimposition of an extensional environment on a subduction regime. The within-plate component of the Gaussberg leucitites may be directly related to hotspot activity (e.g. Kerguelen-Heard island hotspot). The origin of the HFSE enrichment in the Leucite Hills remains problematical.

The Sr, Nd and Pb isotopes of the alkaline lavas show a considerable variation. Muriah and the NSW leucitites have Sr and Nd isotope ratios similar to bulk earth, whereas Stromboli and the Leucite Hills have higher $^{87}Sr/^{86}Sr$ (0.7050-0.7075). The Leucite Hills have less radiogenic $^{143}Nd/^{144}Nd$ (0.5121-0.5117) and the Gaussberg leucitites have elevated $^{87}Sr/^{86}Sr$ (0.7095) and low $^{143}Nd/^{144}Nd$ (0.5119). Muriah, Stromboli, NSW leucitites and to some extent the Gaussberg leucitites have Pb isotopes similar to the Dupal anomaly (i.e. EM2), however the Leucite Hills have lower $^{206}Pb/^{204}Pb$ and $^{208}Pb/^{204}Pb$.The variation in the Sr, Nd, and Pb isotopes in the potassic volcanics can be explained by the differing tectonic settings of the lavas, i.e. the age of basement or enrichment events, for example the Archean basement or Proterozoic subduction zone enrichment may be the source of the radiogenic Sr and unradiogenic Nd seen in the Leucite Hills lavas and the Sr and Nd isotope ratios of the Gaussberg leucitites must be derived from the Proterozoic basement, since it is unlikely that these are associated with the Dupal anomaly.

Although the isotopes may vary according to their tectonic setting, the trace element chemistry of both oceanic and continental alkaline lavas can be explained by mixing of 2 source components: a subduction zone/Dupal anomaly component(wedge or lithosphere) and a within-plate component.

SILICIC AND BASALTIC VOLCANISM OF JURASSIC AGE ASSOCIATED WITH THE EARLY STAGES OF GONDWANA RIFTING IN ANTARCTICA

ELLIOT, D.H., Byrd Polar Research Center and Dept. of Geology and Mineralogy, Ohio State Univ., Columbus, OH 43210, and LARSEN, D., Dept. of Geology, Univ. of New Mexico, Albuquerque, NM 87131.

The non-marine Permian to Triassic part of the Gondwana sequence in the Transantarctic Mtns. (TAM) was deposited in a retro-arc (foreland) basin related to an active plate margin along the paleo-Pacific margin of the continent. The sequence contains a large, arc-derived, detrital, silicic volcanic component. In the Beardmore area (TAM) clastic sedimentation virtually ceased in Late Triassic to Early Jurassic time, and was replaced by deposition of Lower to Middle Jurassic volcaniclastic beds (upper part of the Falla Fm. and the Prebble Fm.). These beds are overlain disconformably by up to 520 m of flood basalts (Middle Jurassic Ferrar Group).

Stratigraphic, petrographic, and geochemical data indicate that two distinct volcaniclastic sequences are present. The lower one (up to 156 m thick) consists of fluvial sandstone and rhyolitic to high-silica rhyolitic airfall tuff which increases in abundance upward. The tuffs are interpreted to be Plinian airfall deposits from distal volcanoes. The upper sequence is up to 375 m thick and consists of one or more of the following: dacitic to rhyolitic proximal airfall tuff, volcanic-sedimentary debris flow breccia, coarse basaltic tuff and pyroclastic breccia, and fine to coarse volcaniclastic sedimentary rocks. These deposits, related to proximal centers, possibly include products of phreatomagmatic eruptions. The rhyolitic to high silica rhyolitic tuffs in the lower sequence, and the dacitic to rhyolitic tuffs in the upper, have typical calc-alkaline chemistry; tuffs in the upper sequence differ from those in the lower in having markedly higher transition metal contents. The basaltic pyroclastic rocks have geochemical characteristics similar to the overlying flood basalts. Basaltic and silicic volcanism overlapped in Prebble time. Characteristics of the volcaniclastic sequence and field relations suggest tectonism, normal faulting and topographic relief at the time of deposition. Tectonism, however, is best displayed in S. Victoria Land (TAM) where basaltic breccias rest on an erosion surface cut down at least 500 m through Triassic beds into Permian strata. The breccias contain silicic tuff clasts though outcrops of such rocks are not known. In N. Victoria Land (TAM) abundant silicic shards occur in a thin Triassic sandstone sequence; basaltic breccias containing silicic tuff clasts overlie the sandstones and are overlain by flood basalts. The silicic volcanics (and middle Jurassic S-type granites in W. Antarctica) are interpreted to be the result of anatexis associated with emplacement of tholeiitic magmas into the crust. This early phase was accompanied by faulting, rift formation and erosion, and was followed by a short period of bimodal volcanism and then by flood basalt eruption. These events are the expression of a major magmato tectonic rift system of Early to Middle Jurassic age. The rift system, located within the Permian to Triassic foreland basin, represents a major change in tectonic setting and is associated with Gondwana breakup.

REGIONAL SETTING AND TEMPORAL EVOLUTION OF THE MOGOLLON-DATIL VOLCANIC FIELD, SOUTHWESTERN NEW MEXICO

ELSTON, W.E., and ABITZ, R.J., Department of Geology, University of New Mexico, Albuquerque, NM 87131, USA

The mid-Tertiary ignimbrite province of southwestern North America (> 1 million km^2) can be divided into three subprovinces: (1) low-K, Peacock index ~62.5 (calcic), located on the accreted Guerrero terrane of western Mexico (no known sialic basement); (2) medium-K, Peacock index ~54 (alkali-calcic), occupying the Basin and Range province (Proterozoic sialic basement thinned by syn-volcanic ductile extension); and (3) high-K, Peacock index ~47 (alkalic), overlapping the margins of the Colorado Plateau and Great Plains (cratonic Proterozoic sialic basement). The Mogollon-Datil volcanic field overlaps the transition between the Basin and Range and Colorado Plateau provinces.

Early (38-30 Ma) Mogollon-Datil volcanism began with eruption of andesite from central volcanoes, joined ~36 Ma by increasing volumes of quartz latitic ignimbrite from caldera complexes. This resulted in a mildly bimodal assemblage (andesite mode 58% SiO_2, quartz latite mode 71%). Between 30 and 18 Ma, bimodalism became more pronounced, as the siliceous mode shifted to 76% SiO_2 (high-silica rhyolite). The mode for andesite remained at 58% SiO_2 but skewness shifted to lower SiO_2 (basaltic andesite). A cpx-opx-ol assemblage displaced hbl-cpx, as rocks assumed "basaltic" appearance. True basalt became abundant only during Basin and Range block faulting, after 15 Ma.

On Rb vs Yb+Ta and Ta vs Yb plots, all siliceous rocks from the northern part of the Mogollon-Datil volcanic field (overlapping the Colorado Plateau) fall into the field of "within-plate granite," as classified by Pearce et al. (1984). South of the Colorado Plateau, pre-30 Ma siliceous rocks plot as "volcanic-arc granite;" post-30 Ma siliceous rocks plot as "within-plate granite."

Lherzolite and granulite-facies quartzofeldspathic (qf) gneiss xenoliths in Quaternary alkali basalt from Kilbourne Hole (from lithospheric upper mantle and lower crust, respectively) provide data for petrogenetic models of mid-Tertiary volcanic rocks. Continuous evolution of pre-30 Ma andesitic and siliceous rocks can be explained by an AFC model of partial melting of mantle lherzolite, fractionation of plag, cpx, and ol, and assimilation of qf gneiss. Normalized trace-element (including REE) patterns are similar for volcanic rocks and qf gneiss. Fe-Ti oxide and two-feldspar thermobarometry indicate T=750-850°C, P=4-8 kb for a quartz latitic magma chamber (Kneeling Nun Tuff), concordant with P=7-9 kb for qf gneiss. After 30 Ma, andesitic and rhyolitic trends diverged. As ductile extension reached a peak (following the end of subduction on the western plate margin), isotherms rose, due to rise of diapirs at near-solidus temperatures from lower, more mafic, "drier," and less depleted mantle. Partial melts yielded basaltic andesite higher in Fe and incompatible elements. Rhyolitic melts decreased in Ca, Mg, Sr, Ba and increased in SiO_2, REE (except Eu) and other incompatible elements, and maximum $^{87}Sr/^{86}Sr$ to 0.735 (from 0.709 in pre-30 Ma quartz latite), indicating increasing degrees of crustal melting buffered by plagioclase. Crustal contributions are confirmed by an errorchron of 102 Ma for 38-28 Ma rocks.

We conclude that spatial variations in mid-Tertiary volcanic rocks can be attributed to lateral differences in composition, thickness, and state of stress of the continental lithosphere, and temporal variations to rising isotherms in an extending orogen. Contributions from subducted oceanic lithosphere are neither ruled out nor required.

LOW-TEMPERATURE VOLCANICLASTIC FLOWS GENERATED DURING THE 1983 MIYAKEJIMA ERUPTION

ENDO, K., SUMITA, M., INABA, H., KANEMAKI, M., SAKAI, Y., KORE-EDA, W., Department of Earth Sciences, Nihon University, Sakurajousui 3-25-40, Setagaya-ku, Tokyo, 156 Japan, and MIYAJI, N., Hokkaido Agricultural and Experimental Station

During the 1983 Activities of Miyakejima, a volcanic island 180 km south of Tokyo, phreatomagmatic eruptions occurred from P, Q and S craters around the coast, which align on the southern extension of the main fissure.

These craters erupted various types of pyroclastic fall and flow deposits which are different in degree of interaction between basaltic magma and water (Endo et al., 1984b). From P and Q craters, situated beside a lake, scoria fall, base surge, ballistic fall and water-saturated volcaniclastic deposits were erupted. Base surge deposits from S crater in the sea, produced a tuff ring(Sumita, 1985). On the other hand, R crater on the coast near the S crater continued Strombolian eruptions.

These eruptions were recorded by photoes and video. Stratigraphical data surveyed after the eruptions were correlated with these records. Among them, water-saturated volcaniclastic deposits are called PQ-4 (Endo et al., 1984b). Unsorted, breccia-rich deposits of PQ-4 contain essential, poorly-vesiculated scoria. Their horizontal distribution shows very complicated pattern of a lot of lobes (Fig. 1). Each lobe shows a peculiar tongue-shaped microtopography, composed of flat surface having 6 m x 15 m in avarage size, and in front, a bank including abundant large blocks, tree trunks and standing trees (Fig. 2). According to the observation of the relevant eruption, a number of cock's tail jets fell pulsatingly from the Q crater to this area.

From these, characteristics and the forming process of PQ-4 are summarized as follows.

Lithology of PQ-4, being unsorted and massive, and ranging in grainsize from lava blocks to fine ash, resembles that of debris flows. PQ-4 made very flat surface. It suggests that PQ-4 was saturated with water, when it deposited,. PQ-4 moved laterally under water-saturated condition, to form peculiar micro-topography after their ballistic transport by cock's tail jets.

Consequently, it is deduced that PQ-4 is a low-temperature type of volcaniclastic flows, induced by cock's tail jets, but it is not epiclastic origin, though it shows lithology like debris flows.

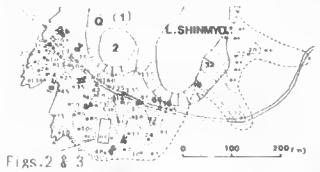

Figs.2 & 3

Fig.1 Thickness of PQ-4 (unit:cm)

Fig.3 Flow direction of PQ-4

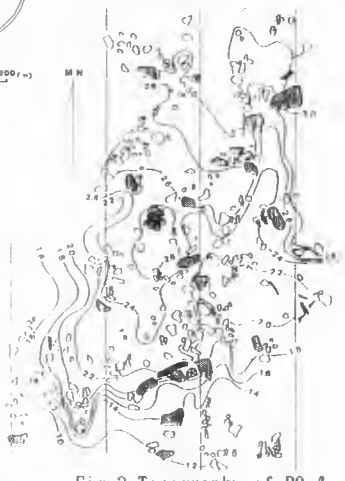

Fig.2 Topography of PQ-4 (contour interval:0.2m)

SPECIFIC TYPE OF VOLCANO-TECTONIC DEPRESSIONS SURROUNDING GREAT GROUPS OF VOLCANOES

ERLICH, E. I., Geol. Dept., University of Colorado, Denver, 595 S. Forest, #311, Denver, CO 80222

Around series of volcanic groups (Medicine Lake, California, volcanic groups of Tolbachik, Ichinsky, Bol'shoy Semiachik, Karymsky, Kamchatka, Fudji and Hakone, Japan, Etna, Italy, Veniaminoff, Alaska) are described topographically expressed volcano-tectonic depressions.

Depressions of this type are usually present within volcanic belts with well-developed continental crust. No major eruptions are associated with creation of these structures. However, there are direct indications of their generation in process of slow subsidence in parallel to the volcanic development within the groups.

Volcanism inside such depressions is usually represented by bimodal series, in more rare cases--by basalts. No significant gravity anomalies are known in association with these structures. Explosive silicic volcanism inside these structures generate series of silicic calderas surrounded by ignimbrite sheets and/or pumice covers. With basaltic volcanoes Hawaiian-type calderas sometimes are associated.

Two different ways of origin are considered for these structures--subsidence in process of crystallization of underlying batholith (magma chamber) and decreasing pressure within the magma generation zone in process of consequently supplying magma to the surface.

The origin of these structures and the necessity of international efforts for their study is emphasized.

SPATIAL AND TEMPORAL EVOLUTION OF THE VOLCANISM OF THE MARTINIQUE ISLAND (LESSER ANTILLES). PETROGENETIC IMPLICATIONS.

ESCALANT, M., COULON C., Laboratoire de Pétrologie Magmatique URA 1277, Faculté des Sciences St-Jérôme, Marseille, France, WESTERCAMP, D., B.R.G.M. Orléans, France, DUPUY, C., Centre Géologique et Géophysique, U.S.T.L., Montpellier, France and DOSTAL, J., Department of Geology, Halifax, N.S., Canada.

The island of Martinique records the most complete geological history within the island-arc of the Lesser Antilles ; the different dated units range from Oligocene to Recent. A detailed study of the products of each of the different volcanic phases represented on the island has been performed.

Three main groups of lavas have been recognized. The first shows mineralogical and geochemical affinities with the island-arc tholeiites. The main chemical characteristics of the second group are typically calc-alkaline although mineralogically it presents a tholeiitic affinity. The third group is mainly calc-alkaline. The calc-alkaline lavas of the second group can be distinguished from those of the third by their high contents of some major elements (Ti, Fe, Mn, P) of the high-charge incompatible elements, of LREE and HREE (Sm, Eu, Tb, Yb, Lu) and also of most of transitional metal elements (Sc, V, Cu, Zn).

The magmatic evolution of the four different sectors of the island from which it has been built has been defined on the basis of a newly established detailed chronostratigraphy covering the last 22 Ma. The first (Miocene ; 19 - 6,5 Ma) and second (Plio-Pleistocene septentrional ; 5,5 - 0,8 Ma) segments evolved in a similar fashion, from an essentially basic submarine, tholeiitic, volcanism to a rather explosive sub-aerial and acid calc-alkaline volcanism. This change coincides with an east to west migration of the volcanic front and with an associated decrease in the volume of lavas. In contrast, the activity of the third segment (Plio-Pleistocene south-occidental ; 3,5 - 0,6 Ma) evolved differently as reflected in the varied but exclusively calc-alkaline magmatism of group 3. The complex mineralogy of the latter indicates a significant degree of magma mixing, analogous to that observed in the terminal phases of segments I and II. The fourth segment (Recent ; 1,2 Ma - Present), is still active and is characterized by the emission of group 3 calc-alkaline lavas.

No apparent chemical evolution with time is observed within the tholeiitic lavas of the first group. On the other hand, within the calc-alkaline lavas (groups 2 and 3) two evolutionary cycles have been established during the volcanic history of the first and second segments. They become progressively enriched with time in incompatible elements (K, Rb, Ba, Li, La, Ce, Pb) and in radiogenic Sr, Pb and O. In the second segment, the enrichment in these elements ceased about 2 Ma ago and low concentrations were also maintained in the subsequent volcanic rocks of segments III and IV.

A model for the origin of the Martinique magmas has been proposed taking into consideration the multiple geological, geodynamical, geochemical and petrogenetic constraints. Assuming that the mantle is the main source of the magmas, subducted sediments are considered to be responsible for triggering magma generation. Tholeiitic lavas are regarded as having been derived by partial melting of the peridotitic mantle enriched by fluids derived from the dehydratation of sediments. Calc-alkaline magmas probably originated from upper mantle metasomatised by the products of partial melting of subducted sediments.

SOME ASPECTS OF THE SEISMIC ACTIVITY OF EL CHICHON VOLCANO (CHIAPAS, MEXICO) DURING THE ERUPTIONS OF MARCH AND APRIL, 1982

ESPINDOLA, J.M., JIMENEZ, Z., ESPINDOLA, V.H., YAMAMOTO, J., and MEDINA, F., Instituto de Geofisica, UNAM, Mexico 04510 D.F.

El Chichon volcano in the state of Chiapas in southern Mexico (17.36°N, 93.23°W) erupted explosively during the months of March and April, 1982. The seismic activity previous to the eruptions was registered by the seismic network of the Chicoasen dam system with stations at distances ranging between 35 and 62 km from the crater. The analysis of these information was reported by Havskov *et al* (1983).

In addition, after the first major eruption on March 29, a network of portable smoked paper seismographs was installed in the area at distances ranging between 12 and 20 km. A preliminary analysis of this data has been made by Medina *et al* (1988). In the present work we present additional data based in the information registered by this last network.

We located the focii of several events of types 1 and 2 which are predominant during the period from March 1st to April 4th. These events ocurr mostly at depths of up to 2 km. After the last eruption, the activity consists almost exclusivly of type 4 (tectono-volcanic) with depths of the focii mostly in the range between 5 and 20 km. There is, no apparent migration in the depths of the hypocenters and and their vertical distribution occurrs in an area some 15 km to the SE of the volcano and the said 20 km in depth. After April 15 the activity decreased abruptly—to only a few events per day but this frequency was still high for the region. The level of the activity previous to the eruptions was reached only in 1983.

Signals of type 3 were registered as continuous tremor in the close range seismograms. Several periods of tremor with durations of tens of minutes to a few hours were detected in the records between March 31 and April 4. Some of them accompany the eruptions themselves but others occur with no apparent simultaneous superficial activity. A conspicuous feature is the presence, in occasions, of two periods of tremor separated by brief periods of almost complete quiescence. The typical frequencies of the tremor in the seismograms fall in the interval 1 to 2 Hz.

Preliminary focal mechanisms of some of the post erution mechanisms are similar to the one reported by Havskov *et al.*, i. e. a thrust fault solution.

References.

Havskov *et al.*,(1983) *GRL*, V.10, No.4, p.293
Medina *et al.* (1988) *Pageoph*, to be published

GEOLOGY OF THE CASCADE VOLCANIC ARC NEAR MOUNT ST HELENS, SOUTHWESTERN WASHINGTON

EVARTS, Russell C., and ASHLEY, Roger P., U. S. Geological Survey, 345 Middlefield Road, Menlo Park, CA 94025

The southern Washington Cascade Range consists of folded subaerial volcanic and shallow-level plutonic rocks, generated during a more or less continuous Eocene to early Miocene period of activity, unconformably overlain by undeformed Pliocene to Holocene extrusive rocks. In the area north of Mount St. Helens, deforested by the 1980 eruption and now exceptionally well exposed, a more than 4-km-thick section of gently E-dipping middle Tertiary volcanogenic rocks crop out on the limb of a broad NW-trending regional syncline. These rocks are largely proximal in character: vent areas and flanks of mafic shields, andesitic cones, silicic flow-dome complexes, and a possible downsag caldera have been recognized. K-Ar and ^{40}Ar-^{39}Ar determinations from this area range from about 35 to 20 Ma, but suggest a hiatus in activity sometime between 30 and 25 Ma.

Available radiometric ages from throughout southern Washington indicate that the volcanic production rate declined markedly after about 17 Ma and remained low until 5 Ma. Following regional folding, uplift, and erosion, volcanic activity increased in the Pliocene and Quaternary but has been less voluminous, more localized, and more sporadic than that which characterized the Eocene to early Miocene period.

Intrusions ranging from diorite to granite were emplaced in a broad NNE-trending belt inferred to represent the roots of the Cascade volcanic front during much of Tertiary time. Three large Quaternary stratovolcanoes (Mount St. Helens, Mount Rainier, and Glacier Peak) also lie along this trend, which may reflect a deep crustal structure that has controlled the loci of felsic magmatic activity in southern Washington throughout Cascade arc history.

Minor faulting and shearing are widespread, but no major structural discontinuities have been recognized, nor has surface breakage been detected along the active St. Helens seismic zone.

The compositions of magmas in the Mount St. Helens area generally became more silicic with time: Eocene rocks exposed west of Mount St. Helens are dominantly olivine+plagioclase-phyric low-potassium tholeiite (K_2O=0.1-0.3%); Oligocene volcanics are chiefly tholeiitic and calc-alkaline basalt and basaltic andesite; and early Miocene rocks are mostly two-pyroxene andesite and dacite and their plutonic equivalents. Pliocene to Holocene volcanic rocks near and at Mount St. Helens range from medium-K basalt to dacite; they crystallized from magmas richer in K_2O and H_2O than did the older rocks. These petrologic variations suggest increasing involvement of the crust in Cascade magmagenesis with time.

ASKJA VOLCANO, ICELAND: A REAPRAISAL OF CALDERA EVOLUTION

S.P.EVERETT and H.RYMER, Dept. Earth Science, Open University, Milton Keynes, MK7 6AA. England

Askja volcano is a large, multiple caldera composed of sub-glacial hyaloclastite/pillow lava formations and post-glacial basaltic scoria and flows. The dimensions of the largest post-glacial caldera appear to be constrained by bifurcation of the associated fissure into eastern and western swarms. A detailed potential field survey has been undertaken to address the relationship between sub-surface fissuring, ring fracture propagation and the mechanics of caldera development at this mature central volcano on the active Icelandic rift. The gravity data produce a net negative Bouguer anomaly over the edifice, reflecting the massive volume of low density hyaloclastite present. Gravity is weakest over and beyond the hyaloclastite ridges of the main caldera margins and is 4-6 mGal higher over most of the caldera floor: due to intra-caldera post-glacial lavas and a possible lesser thickness of hyaloclastite. In the east a strong positive anomaly (c. 8 mGal) characterises eastern Oskjuvatn (small 1875 caldera). It is highly probable that this anomaly is due to relatively high densities associated with the eastern fissure swarm which is presently active. The wide range of densities, 1.6-2.45 Mg m^{-3} ,for hyaloclastite and, 2.6-2.8 Mg m^{-3} , for subaerial and pillow lavas were obtained by surface sampling and Nettleton analysis. 2.5-D and 3-D gravity models have been generated.

The conventional view that the main caldera formed by downfaulting and ring fracture collapse at the centre of a large pre-exisisting stratovolcano (model 1) is evaluated against the alternative possibility that the "caldera walls" grew instead as laterally-confined hyaloclastite ridges and mountains produced by sub-glacial fracture controlled eruptions (model 2). These two models, both consistent with the geophysical data, place upper and lower bounds on the volumes of the intra-caldera lavas, the underlying hyaloclastites and the extent of downthrow on the caldera boundry faults. Model 1 requires downfaulting of 650 m: however; the summit would have become subaerial (for this there is no geological evidence); and there are insufficient voluminous (ca. 30 km^3, the caldera volume) post-glacial fissure eruptions along the Askja fissure swarm. Thus model 2, depicted geologically below, is preferred and it is further proposed that the eastern and western mountains evolved with morphological differences. The western system representing a series of NNE-SSW erupting fissures, producing a repeated series of sub-glacial pillow lavas and hyaloclastite, and inter-glacial subaerial lavas. The eastern mountains were formed entirely during the last glaciation as a massive sub-glacial, hyaloclastite-pillow lava mountain, which never became subaerial. In post-glacial times the topographic depression between the two edifices has filled with basalt lavas. Exposure along the northern rim, shows faulting in the post-glacial lavas of 40-60 m which could be attributed to downsagging, compaction and subsidence. Magnetically the susceptibility of subaerial/pillow lavas is greater than that of hyaloclastite by two orders of magnitude. This difference is reflected in the aeromagnetic data which shows an elongate positive anomaly over the western side of Askja, reflecting the greater proportion of high susceptibility inter-glacial and post-glacial lavas; and a more circular negative area of magnetism over the voluminous, hyaloclastite volume of the eastern mountains. Given that most mature Icelandic central volcanoes are positive topographical features built largely from glacial volcanics and that many possess central caldera-like depressions, the conclusions reached here may have wider relevance to Icelandic volcanism.

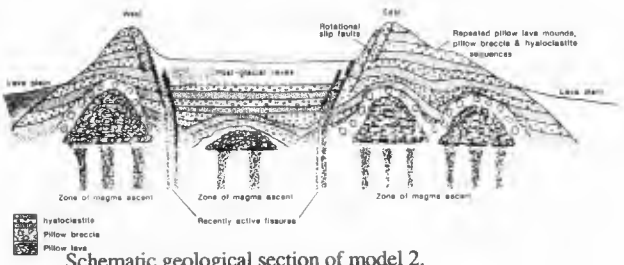

Schematic geological section of model 2. (vertical scale expanded by a factor of 5)

VOLUMINOUS QUARTZ LATITE RHEOIGNIMBRITES IN THE GOBOBOSEB MOUNTAINS AND THEIR RELATIONSHIP TO THE MESSUM COMPLEX (NAMIBIA).

EWART, A., Department of Geology and Mineralogy, University of Queensland, St. Lucia, Queensland, Australia 4067.
MILNER, S.C., Department of Geochemistry, University of Cape Town, Rondebosch 7700 South Africa.

A sequence of quartz latites and basalts forming the Goboboseb Mountains are a southerly remnant of the Etendeka Formation volcanics (130-135 Ma) and crop out over an area of 1000 km^2. The deposits partially enclose Messum, a complex multistage gabbro - granite - syenite ring structure with an exposed diameter of 18 km. The outcrop distribution suggests a northward directed eruption from the northern part of the Messum Complex. The stratigraphy of the lava sequence and the thickness of the principle units can be summarised as follows: Lower Basalts (250 m), quartz latite (QL) unit-I (50-60 m), QL unit-II (30-50 m), QL unit-III (20 m), Upper Basalts (130 m) and QL unit-IV (>60 m).

The quartz latite units are each interpreted as the proximal facies of single cooling units of high-temperature rheoignimbrites, being massive and intensely welded, with original shard textures characteristically destroyed by recrystallisation. Each unit exhibits a thin, extremely fine grained, almost glassy, basal zone, merging into a banded, fiamme-rich zone (up to 10 m thick), individual fiamme are 0.5 to 5.0 cm thick and up to a metre in length (i.e. stretching ratios >20); this is overlain by a massive zone often containing recrystallised groundmass textures; the topmost zone of each unit, where preserved, is pumiceous but still strongly welded. QL unit-I is also characterised by the development of coarse breccias, with individual blocks locally up to 3 m in diameter. Mineralogically, all four units contain sparse phenocrysts of labradorite, titanomagnetite and pigeonite, while QL unit-I contains additional augite. Major and trace element data show a remarkable uniformity within and between different units.

The chemical data show that the Goboboseb quartz latites correlate closely with quartz latites which crop out along the southern margin of the main Etendeka lava field, indicating that the deposits reached at least 100 km north from the Messum complex, further implying a probable minimum outcrop area of ca. 6000 km^2.

The Messum ring structure is thought to have a complex history of intrusion, collapse, extrusion and uplift. The overall structure of the volcanic units, however, also shows a pronounced sag structure resembling a shallow valley trending NNE from Messum. An estimated 300 m of sagging has occurred at the axis of this structure. Aeromagnetic data suggest the existence of a hidden northern margin to the Messum ring structure. It is postulated that this could represent an early caldera developed during eruption of quartz latite units-I to -III, now infilled by these and later volcanics.

No extrusive quartz latites have so far been identified within the Messum Complex, while intrusive equivalents are known only from an eastern outer ring-dyke segment, and a small quartz monzonite plug cutting the quartz latite units north of Messum.

A TRIGONOMETRIC METHOD FOR MEASURING GROUND TILT ON COMPOSITE VOLCANOES

EWERT, J.W., U.S. Geological Survey, Cascades Volcano Observatory, 5400 MacArthur Blvd. Vancouver, WA 98661

Spirit-level tilt (SLT) has been used to measure and detect changes in ground tilt on volcanoes since the technique was developed in the 1960's at the U.S. Geological Survey's Hawaiian Volcano Observatory. The single-setup SLT method requires use of one to three Invar leveling rods, whose lengths (max. 3 m) limit site choices to areas approximately 40 m on a side and with less than 3 m topographic relief. Areas with these specifications are not easily found on steep-sided composite volcanoes. Even if such sites exist, they may not be suitable for monitoring purposes. In addition, small-aperture arrays are particularly susceptible to spurious noise caused by minor bench mark instability.

Except for the inconvenience of transporting leveling rods, the limitations of single-setup SLT can be avoided by leveling traverses around larger-aperture arrays. This procedure can be time consuming, however, particularly in steep terrain, and results in decreased coverage of the volcano by tilt monitors.

These limitations prompted the U.S. Geological Survey's Volcano Crisis Assistance Team (VCAT) to look for a more flexible, alternative method capable of measuring at least moderate-size arrays (100-200 m). A trigonometric leveling system was devised that uses a theodolite and electronic distance meter (EDM) to measure angles and distances between three or more target/prism sets mounted on plumb poles and leveled over bench marks. Elevation differences between the marks are calculated trigonometrically rather than read directly, as with SLT.

Analysis of random errors in such a system shows that if the theodolite is capable of measuring vertical angles to +/- 1 second of arc or less and the EDM is accurate to +/-3 mm or less, ground tilts can be measured with an accuracy comparable to that of SLT (e.g., +/- 5-10 microradians). Accuracy of the EDM has the greatest influence on how small a tilt array can be because the effect of a constant EDM offset error is greatest when measuring short distances and diminishes as the sighting distance increases. Pointing errors increase with distance and place an upper limit on optimal sighting distances.

The system currently in use by VCAT consists of an electronic theodolite capable of measuring zenith angles to +/- 0.5 second of arc (standard error), an EDM with an accuracy of +/-3 mm, and three tiltable free-standing target/prism sets supported by light weight tripods. Field use of this system indicates that optimum sighting distances range from 60 to 100 m (i.e. equilateral triangular arrays ranging from 100 to 175 m on a side), with allowable topographic relief of 12 to 38 m between pairs of bench marks. The less stringent topographic requirement relative to that of SLT greatly increases monitoring flexibility on composite volcanoes, and the larger aperture lessens the effect of minor bench mark instability.

VCAT has used this system to establish tilt arrays on Mount St. Helens, U.S.A., Fuego and Santa Maria Volcanoes, Guatemala, and Cotopaxi and Guagua Pichincha Volcanoes, Ecuador.

Alkaline volcanics from Christmas Island and nearby seamounts: magmatism of the northeast Indian Ocean.

FALLOON, T.J., Geology Department, The University of Tasmania, G.P.O.Box 252C, Hobart 7001, Tasmania, Australia,
VARNE, R., Geology Department, The University of Tasmania, G.P.O. Box 252C, Hobart 7001, Tasmania, Australia,
MORRIS, J.D., Department of Terrestrial Magnetism, Carnegie Institution of Washington, 5241 Broad Branch Road, N.W., Washington, DC 20015, U.S.A., and
HART, S.R., Department of Earth, Atmospheric and Planetary Sciences, Massachusetts Institute of Technology, 77 Massachusetts Avenue, Cambridge, MA 02139, U.S.A.

Christmas Island is located (Lat 10º Long 105º 40' E) south of the Java Trench, in the northeast Indian Ocean, approximately 300 km south of the island of Java and 1440 km from the NW coast of Australia. Volcanism represented by the volcanic rocks on Christmas Island occurred in the Eocene (Lower volcanic series, LVS) and the Miocene or pre-Miocene (Upper volcanic series, UVS) based on palaeontological and stratigraphic evidence from interbedded limestones, and K-Ar dating of three lavas. The exposed sequence is at least 100 metres thick and field evidence suggests a significant time break between the two periods of volcanism.

The LVS consists of dykes, lavas and hyaloclastite breccia. The LVS forms a sodic (Na_2O/K_2O~>2) alkaline series (Mg# 67-15) similar to alkaline volcanics from the Kerguelen (high Na/K group) and southeast Australian sodic alkaline volcanics. The LVS consist of three petrographic groups; ol+cpx-phyric basalts, ol+cpx+plag-phyric basalts and aphyric trachyte. The ol+cpx-phyric basalts contain abundant cumulate and mantle xenoliths. One dyke yielded a suite of nodules consisting of websterite, wehrlite, harzburgite and lherzolite.

The UVS forms a primitive potassic (Na_2O/K_2O~<0.9) alkaline series (Mg# 71-63) similar to other eastern Indian Ocean island suites (Kerguelen low Na/K group; Heard Island). The Christmas Island suite however differs in having significantly higher Ba (>1200ppm, as opposed to <800ppm) and CaO contents and lower FeO contents. Petrographically the high-K Christmas Island rocks are limburgites consisting of olivine (Mg# 86-90) and clinopyroxene (Mg# 81-86) phenocrysts set in a groundmass of fresh to altered glass and augite microlaths.

Altered alkaline volcanic rocks, similar to those from Christmas Island and DSDP site 211, have also been dredged from the Shcherbakov Seamount, and an unnamed seamount of the Vening Meinesz Seamounts.

The LVS of Christmas Island, although compositionally similar to other eastern Indian Ocean island volcanics, has "Dupal"- like isotopic characteristics ($^{87}Sr/^{86}Sr$= 0.70394-0.70399; $^{143}Nd/^{144}Nd$= 0.51276-0.51279; $^{206}Pb/^{204}Pb$ =18.869-19.123; Δ 7/4Pb = 5.5-8.3; Δ 8/4Pb = 39.5-54.0) which are also strikingly similar to those of Quaternary eastern Sunda arc volcanics, indicating isotopically similar mantle sources.

SEISMIC PATTERNS AT MT. ETNA VOLCANO

FALSAPERLA, S., Inst. Internazionale di Vulcanologia - C.N.R., Catania, Italy, LOMBARDO, G., Inst. Scienze della Terra, Universita di Catania, Italy

Records collected at Mt. Etna since 1968 through the seismic network operating on the volcano, have been analyzed in order to characterize the different seismic signals recorded and to look for their time evolution. The station MVT-SLN, which is located at a distance of about seven kilometers from the summit area, has been chosen as a reference one because it was operating without any significant break throughout all the considered period.

Time intervals of moderate quietness of the volcano, characterized by low level of tremor amplitude and a small number of low frequency events, appear to be followed by periods with earthquake swarms and/or rare low magnitude shocks (M<2) which often may evolve towards an increase in the number of low frequency events and to an increment of both the number and the duration of some periodic transient phenomena characterized by a strong enhancement of the tremor amplitude. Significant changes in both the amplitude and the frequency content of volcanic tremor also occur in the time intervals shortly preceding some eruptive activities.

These different stages of volcanic and seismic activities seem to occur not randomly in time and the observed evolution of seismic phenomena recorded, in many cases, has shown to precede the occurrence of either summit or flank eruptions.

At present, the preliminary results described are founded on the analysis of a reduced number on data (1977-1983) compared to the size of the complete data set (1968-1987). It is therefore important to check such preliminary findings for the whole set of data available, as the final goal of this study is to describe a pattern of the volcano Etna which points out the different steps in the evolution of seismic phenomena leading to the various eruptive activities taking place on the volcano.

ERUPTIONS OF THE NORTHERN GROUP VOLCANOES, SHEVELUCH, KLYUCHEVSKOY AND BEZYMIANNY DURING 1980-1989

FEDOTOV, S.A., KHRENOV, A.P., ZHARINOV, N.A., and DVIGALO, V.N., Institute of Volcanology, Petropavlovsk-Kamchatsky, 683006, USSR

The most intense volcanic activity is observed at the northern termination of the Kuril-Kamchatka volcanic belt where the Northern volcanic group is located. Twenty largest eruptions of the age occurred here: the 1956 directed blast at Bezymianny, the 1964 eruption at Sheveluch, the large Tolbachik fissure eruption in 1975-1976, etc. The total weight of juvenile basalts ejected at Klyuchevskoy from 1932 reached 2.8 billion tons.

Bezymianny is in the stage of extrusive eruption since 1956. Growth of the extrusive dome is accompanied by issue of andesites of different viscosity as lava plugs and flows, as well as by the directed blasts of different power. The volume of the dome in 1960 was 0.363 km^3, and it was 550 m high. During the last decade one could observe some changes in the dome formation. Since 1977 eruptions occur every year. A certain regularity is marked in the course of eruptions: squeezing out of rigid andesitic blocks, formation of avalanches; short, occasionally strong explosive episodes; and pouring out of viscous lava flows. The paroxysmal stage was accompanied by explosions and lava flows from 2 to 12 km long and 0.005-0.015 km^3 in volume. After the catastrophic eruption in 1956 the most powerful eruption occurred in 1985 (volume 0.05 km^3). In products of the 1985 eruption the abundance of hornblende increased compared to that of 1984. Outpouring of lava flows of two-pyroxene andesites points to the beginning of the long stage of formation of the stratovolcano with the extrusive core. Eruptions of effusive-explosive style and of different power will apparently occur during this stage.

Sheveluch is the northernmost active volcano in Kamchatka. The volcano is notable for formation of extrusive domes and for their further destruction in the course of explosive eruptions. The most recent eruption of this type occurred on November 12, 1964. After a 16-year period of repose in August 1980 an andesitic dome started to grow in the crater. The largest increase in the volume of the dome was observed during the first three months, when the average production rate was $0.15\text{-}0.20 \cdot 10^6$ m^3/day and the velocity of growth reached 2.5 m/day. At the end of the eruption the dome had a height of 180 m and volume of 0.021 km^3. The growth of the dome ceased at the end of 1981. Single explosions with bomb and pyroclastics ejections started to occur at the dome and at its foot in 1984. As a result, several explosive funnels 25-30 m deep formed at the dome. Great amounts of xenoliths of basic and ultrabasic composition are presented in explosive deposits.

Klyuchevskoy is the most active volcano of the Kuril-Kamchatka belt. Since 1932 2.4 billion tons of lava and 0.4 billion tons of ash have been ejected during its eruptions. During the last decade the activity of the volcano increases. Eight flank eruptions occurred since 1980, six of them in 1987-1988. Eruptions were predominantly of effusive character. There is a tendency of increasing elevations of the flank breakthroughs. The volume of lava issued since 1980 was equal to 90 million tons. Since 1984 the eruptions of the summit crater occur almost continuously. The average production rate increased four times compared to the previous decade; the volume of lava issued from the summit crater since 1980 was equal to 110 million tons. Owing to growth of the intracrater cinder cone the height of the volcano reached ≈4900 m. Calc-alkali alumina subaphyric basalts of constant chemical composition issued to the surface.

OLANGA IGNEOUS EVENT IN NORTH KARELIA 2.4 GA: LAYERED COMPLEXES, MAFIC DYKES SWARM AND VOLCANICS

S.Felitsyn, Yu.Amelin, O.Levchenkov, V.Semenov, N.Sotchevanov, S.Turchenko (IGGP Ac.Sci. USSR, 199034 Leningrad, USSR), A.Ein (Inst.of Geology, Karelian Branch Ac.Sci.USSR, 185610 Petrozavodsk, USSR), Eu.Koptev-Dvornikov (Department of Geology, Moscow University, 109000 Moscow, USSR)

Early Proterozoic igneous suites of N.Karelia are represented by: (1) a bimodal volcanic pile (up to 1500 m think) in the Panajarvi Structural Zone (PSZ); (2) layered complexes of the Olanga group (Kivakka, Tsipringa and Lukullaisvaara massifs) which mark the southerm margin of PSZ; (3) NW-trending dolerite dykes and NEE-trending dykes of highmagnesian gabbro and Pl-porphyrites to form a local, North Karelian swarm closely spaced to the layered massifs.

The gabbro dykes show a genetic link with the Kivakka and Lukullaisvaara complexes as evidenced by petrochemical data. Primary composition of the layered intrusions is that of komatiite-basalt series; computer simulation suggests that their solidification occurred at P = 7 - 8 kb. The calculated primary composition of the Tsipringa complex corresponds to tholeiitic basalt; its emplacement took place at P = 2 - 3 kb. Available data suggest that the Tsipringa complex and the N.Karelian dolerite and plagioclase porphirite dykes are derived from a single magmatic source.

Sm-Nd dating of the Kivakka and Tsipringa complexes, and gabbro dykes from the N.Karelian swarm combined with U-Pb zircon ages of rhyolites from the upper portion of PSZ sequence provide evedence for an igneous event that occurred circa 2.4 Ga ago. This is consistent with the 2.35 - 2.40 Ga episode recorded in the south-western part of in Finland (Koilismaa Structure).

ϵ_{Nd} value (ranging from -0.5 to -2.0) for the Olanga intrusions and N.Karelian dykes is fairly consistent with a single magmatic source. The constant ϵ_{Nd} values and variation of Nd abundance (0.8 - 1.0 to 12 - 15 ppm) suggest that ϵ_{Nd} values are caused by a single magmatic source, but no by contamination of the melt during solidification.

The Olanga igneous event seems to be related to crustal extension in the Karelian craton circa 2.4 Ga ago. General structural pattern, petrochemistry of the volcanics from PSZ and their mineralization (Cu = 150 - 300 ppm in basalts and 350 - 400 ppm in dolerite dykes from the N.Karelian swarm) of the Olanga event are similar to the 1.2 Ga Mackenzie igneous event of Canada.

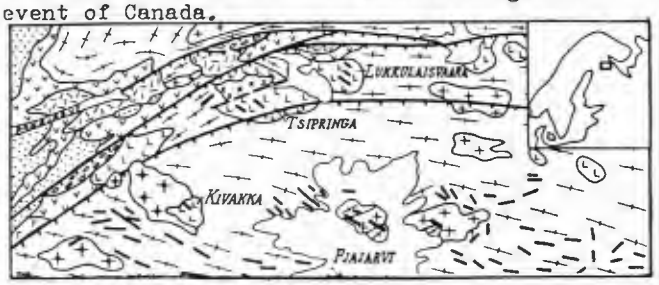

POSTCOLLAPSE LAVAS OF THE PLATORO CALDERA COMPLEX, SOUTHEASTERN SAN JUAN MOUNTAINS, CO: TEMPORAL AND SPATIAL VARIATIONS IN A CHEMICALLY DIVERSE SUITE OF MAGMAS

FERGUSON, K., DUNGAN, M.,Dept. Geol. Sci., Southern Methodist Univ., Dallas, TX 75275; MOORBATH, S.,Univ. of Oxford, Parks Road OX1 3PR, Oxford, UK; LIPMAN, P. W., U.S. G.S., MS903, Denver, CO 80225

Postcollapse units (29.1 to <26.5 Ma; lavas post-dating the La Jara Canyon Tuff) of the Platoro caldera complex comprise high-K, calcalkaline lavas erupted from centers within (Summitville Andesites), or outside but adjacent to (Green Ridge Volcanics, Summit Peak Andesite, Park Creek Dacite), the Platoro-Summitville calderas. Compositional variations, among and within the postcollapse units, record the complex interaction of variations in parent magma compositions, fractionation assemblages, differentiation processes, crustal assimilants, and degrees of assimilation. Compared to the precollapse Conejos Fm. (Colucci et al., this volume), postcollapse lavas generally have more radiogenic isotopic ratios. Most postcollapse units show a general progression from early plag +aug±opx±ol±hb andesites to later plag + aug + bio and/or hb ± sanidine dacites. This progression parallels changes in the relative abundances of andesite to dacite in the postcollapse sequence; andesites dominate in early units (Summitville Andesites) and dacites in later units (Green Ridge Volcanics, Park Creek Dacite).

Incompatible element and isotopic differences among the postcollapse lavas, and between postcollapse lavas and the precollapse Conejos Fm., may reflect spatial and temporal variations in the composition of crustal assimilants. Green Ridge lavas from the NE Platoro caldera, adjacent to the Rock Ck. drainage, have distinctive normalized incompatible element patterns similar to Rock Ck. Member lavas of the Conejos Fm., but at lower abundance levels and with more radiogenic isotope ratios. The differences in abundance levels and isotope ratios may reflect assimilation of crust previously hybridized by interaction with Rock Ck. magmas, or AFC involving the earlier emplaced, Rock Ck. type magmas. Large scale crustal heterogeneiity is reflected in the diagram below. The $^{206}Pb/^{204}Pb$ ratios of postcollapse lavas are plotted versus sample location projected onto an west-east cross-section; they show a pronounced west (18.8) to east (17.7) decrease in $^{206}Pb/^{204}Pb$, with Summitville Andesites (circles), and younger lavas (stars) having similar relative isotopic trends. This trend in isotopic compositions may result from lateral crustal variations and/or progressively greater depths of fractionation to the east. Also reflected in the diagram is the smaller range in isotopes of intracaldera Platoro/Summitville lavas relative to extracaldera lavas. The smaller range in isotope ratios of intracaldera lavas may reflect the hybridization of the subcaldera crust over 7 m.y. of focused magmatism.

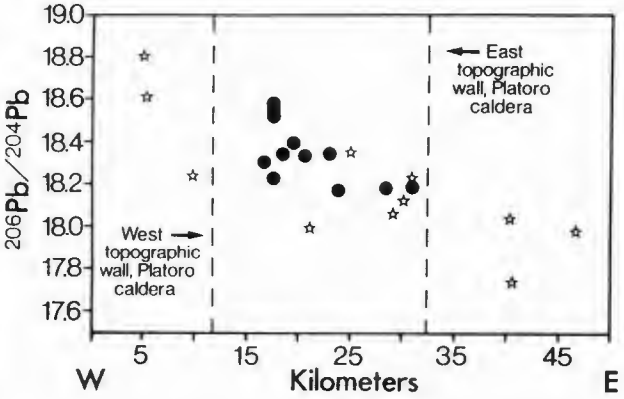

CRUSTAL CONTAMINATION OF SOMALI BASALTS AND CONSEQUENCES ON K/Ar DATING

G.Ferrara, O.Giuliani, S.Tonarini, I.M.Villa, G.Vita
(Istituto di Geocronologia e Geochimica Isotopica CNR, Pisa,Italy)

Basalts from the Gedo region and the Shebely valley (southern Somalia) have been studied from a petrological, geochemical and isotopic point of view by Ali Kassim et al (Geosom 87 Conference, Mogadishu). A slight interaction with the continental crust (Somali basement) has been inferred using some correlations diagrams as $^{87}Sr/^{86}Sr$ vs Rb, $^{87}Sr/^{86}Sr$ vs Sr, REE contents etc.

Field evidences demonstrate the almost contemporaneity of the studied basalts floods (absence of paleosoils, morphology etc.).

Numerous convenctional K-Ar determinations have been carried out on total rock samples; the scatter of the obtained results (12-33 Ma) suggests the presence of excess argon, probably scavenged by the hot basalt en route to the surface through the crystalline Somali basement (radiometric biotite age: 520 - 540 Ma). No relationship between "crustal" parameters (Rb and Sr concentrations, $^{87}Sr/^{86}Sr$) and apparent ages has been found, suggesting the possibility of the existence of a selective Ar contamination of the basalts by a specific component of the Somali crystalline basement (Kfeldspar?).

So far, $^{40}Ar/^{39}Ar$ age determinations have been performed on the samples having the oldest K/Ar apparent ages, around 30 Ma. All three show saddle spectra, demonstrating that excess Ar is indeed present. The minima of the saddles, which represent *maximum* eruption ages, range between 17 and 23 Ma. This reinforces our hypothesis that the scatter of the K/Ar apparent ages is *entirely* due to variable concentrations of excess Ar.

Further Ar-Ar dating on the samples with lowest K/Ar ages, i.e. presumably smallest excess Ar concentrations, is in progress.

These findings demonstrate the necessity of **great** caution in attempting geodynamic reconstructions basing on K/Ar dates of continental basalts.

GLOBAL SEISMIC APPROACH TO THE STRUCTURE OF VULCANO (EOLIAN ISLANDS, ITALY): CASE HISTORY.

FERRUCCI, F. and G. LUONGO , Osservatorio Vesuviano; 249, Via Manzoni 80123 Naples (Italy).
NERCESSIAN, A., Institut de Physique du Globe, 4, Pl. Jussieu 75252 Paris cedex05 (France).

Three field surveys, carried out from 1986 to late 1988, allow to draw a general seismic model of Vulcano, the southernmost active volcanic center of the Eolian Islands (Southern Italy).

As obtained by gaussian-beams direct modeling of five linear seismic profiles, the Moho boundary uprises from Northern Sicily towards the central Tyrrhenian Basin through a major upheaval, equally affecting the intra-crustal layers; the feature is confirmed by observation of teleseismic delays in the islands of Vulcano and Lipari.

Three constant-offset profiles, spaced in azimuth around the island and recorded at 84 stations, with average spacing between two recording-points ranging from 0.2 to 0.5 km, first revealed an unexpected P-arrivals advance at the Fossa Grande crater, Vulcano.

This feature, unresolvable by DSS data, was confirmed and evaluated by means of seismic tomography: the inversion of 1500 P-traveltimes from local earthquakes supplied the seismic signature of a shallow and high-velocity intrusive body, spatially correspondent to a monzogabbro intrusion formerly penetrated by a geothermal drill-hole.

The bulk of the seismicity, monitored by temporary, three component digital arrays and located with a fully 3-D location routine, appears to be almost recursively confined in the crater area and within the intrusive body at shallow to very-shallow depths.

A very high occurrency rate of linearly polarized wavetrains observed in three-component records of such events, randomly chosen, allows to assume that the typical "non-tectonic" aspect of the local seismicity could be largely due to sustained vibration induced by fluid transients.

From such a broad-band seismic data gather, and taking into account interdisciplinary data and interpretations, a general model of the volcanic field is thus proposed.

EJECTA DISPERSAL AND DYNAMICS OF THE 1912 ERUPTIONS AT NOVARUPTA AND THE PLINIAN-IGNIMBRITE TRANSITION, KATMAI, ALASKA

FIERSTEIN, Judy, and HILDRETH, Wes, USGS, Menlo Park, California 94025, USA

The 3-day compositionally-zoned eruptive sequence began with plinian dispersal of ~12 km^3 of rhyolitic fallout (Layer A) along a narrow ESE axis, concurrent with high-energy flows and small valley-filling ash flows that originated from the base of the rhyolitic plinian column. These flows formed the only purely rhyolitic deposits within 8 km of source, as Layer A fell only farther to the S and E, well beyond the limits of the flows. A transition from plinian fall to ignimbrite followed, during which compositionally heterogeneous fallout Layers B_1 and B_2 were deposited along a narrow ESE axis while zoned ash flows began filling the Valley of Ten Thousand Smokes (VTTS). As ash flows filled valleys both N and S, subplinian Layer B_3 was deposited concurrently; it is preserved only beyond the flow margins, to the S and SE. In addition to rhyolite, Layers B_{1-3} contain dacitic and andesitic pumice that increases progressively from 10 to 50 vol%, reflecting the zonation in contemporaneous ash flows. Andesite-rich flow units that cap the flow sequence have no fallout equivalent, indicating that ignimbrite emplacement outlasted the plinian phase.

Ignimbrite volume is >10km^3. The sheet is probably >100 m thick in the upper VTTS and is ~10 m at its eroded terminus 23 km downvalley. Proximal high-energy flow veneers, commonly 1-3 m thick, but as thick as 13 m on Falling Mountain, were deposited by the passing flows on most near-vent ridges. They are a proximal facies of the ignimbrite, sharing the compositional zonation of their valley-filling equivalents. Although most of the ignimbrite is structureless, internal stratification defined by alternating coarse and fine pumice-clast concentrations several meters to a few cm thick developed near flow margins in response to vertical velocity gradients that developed as the flows slowed down.

After a break of a few hours, several pulses of plinian dacite were ejected from an inner, more restricted vent <500 m wide, into which the rhyolitic lava dome, Novarupta, was still later extruded. Coarse dacite fallout accumulated to an unknown depth (>50 m) near vent and to >10 m where its base is exposed 4 km to the E; it thickly mantles the earlier and wider source of the main pyroclastic flows. Intercalated with the dacite fallout are 3 thin intraplinian ignimbrites that flowed as far as 3 km from Novarupta and several andesite-rich fall layers, only 2 of which extend as far as 1 km before pinching out. Two plinian dacite sequences (Layers C-D and F-G) have been traced to Kodiak Island, as far as 110 km downwind where they are each 3 cm thick, resting atop 18 cm of Layers A + B.

Tephra volumes are ~4 km^3 for Layer C-D and ~8 km^3 for F-G. Microprobe analyses show that regional dustfall that accumulated during the break between them and after the entire eruption sequence was over added as much as 1 km^3 of rhyolitic glass shards to each of C-D and F-G; volumes have been adjusted accordingly. The decoupling of a fraction of the fine ash from the rest of the fallout from an eruption column can add significant volumes of ash to later fallout layers.

Lithic isopleths suggest column heights of 30, 25, and 23-26 km for A, C-D, and F-G, with SE-directed wind speeds up to 30 m s^{-1} for A and C-D, and 0-10 m s^{-1} for more symmetrically distributed F-G. Lithic blocks 1-5 m across within 900 m of the vent in Layer F-G are used to calculate exit velocities of 404 m s^{-1} to 764 m s^{-1} and a maximum mass eruption rate, assuming 3% water, of 9×10^8 kg s^{-1}. Lithics in the initial rhyolitic eruptive phase are largely Jurassic siltstones, in place here at depths of 0 to 1500 m. The subsequent dacite fallout units contain lithics dominated by a distinctive dacite vitrophyre, apparently the result of fragmentation of densely welded intravent tuff and perhaps a shallow glassy intrusion. The lithic data thus imply that the vent was excavated no deeper than ~1500 m and that most vent-widening occurred during the initial rhyolitic stage.

MORPHOLOGIC CHARACTERISTICS OF SILICIC LAVA FLOWS

FINK, J.H., Geology Dept., Arizona State University, Tempe, AZ 85287 USA

Distinguishing between the products of explosive and effusive volcanism is usually a straightforward exercise. However, for the largest-scale silicic extrusions, the sharp boundaries that separate lava flows from pyroclastic deposits become less well-defined. The purpose of this presentation is to outline some of the characteristic features that typify silicic lava flows, in order to provide a frame of reference for the interpretation of very large flows.

Most morphologic criteria that can be used to identify silicic lavas arise from their high viscosities. Evidence of vent geometry may be preserved as alignments of domes fed from individual dikes, as elongate ridges or depressions on the flow surface, or as paired fractures with outwardly convex surfaces which develop as an extrusion ceases. Patterns of flow banding may be inherited from vertical movement within the conduit, or imposed by basal shear as the lava advances. In both cases, the uppermost 10-30% of a flow tends to have vertical flow foliations, whereas the lower portion tends to be horizontal. Magmatic volatiles retained in the lava may be prevented from exsolving, leading to a range of vesiculation textures. These textures are typically arranged in sub-horizontal layers, with a light-colored pumiceous zone at the surface underlain by darker glassy and crystalline zones. In some flows, volatile migration may form internal pumice layers, capable of rising as buoyant diapirs to the flow surface. These diapirs appear as regularly-spaced dark outcrops, elongate perpendicular to the down-slope direction. In cross section, they are defined by distortions of flow foliations and have amplitudes which decrease upward, in contrast to compressional surface folds which die out at depth. Internal pumice zones may be associated with anomalously large gas cavities, able to generate explosions that reach the flow surface, and with local zones of internal breccia. Surface folds, which are widespread products of compressional instabilities in lavas, form only in materials whose viscosities or strengths decrease with depth. In contrast to lavas, rheo-ignimbrites, which originate as fragmental pyroclastic deposits, generally have rheologic properties that increase with depth.

Although thoroughly welded tuffs may become fully mobilized and develop many characteristics of lava flows, several of the features described above are not likely to form in flows that originate explosively. Vertical flow banding, coherent internal pumice zones, preserved vent structures, and surface folds are probably all diagnostic of effusive origins.

LARGE VOLUME, HOT PYROCLASTIC FLOWS: IF THEY CAN WELD, HOW CAN THEY FLOW?

FISHER, R. V., Department of Geological Sciences, University of California, Santa Barbara, California 93106

Early workers thought that welded tuffs were lava flows with unique fragmental-like textures and were puzzled by their high silica content relative to high-aspect ratio shapes (area/thickness). Highly viscous silica-rich lavas do not flow very far and they form thick, low-aspect ratio bodies. Realization that welded tuffs are one type of ignimbrite facies produced by deposition from initially fragmental pyroclastic flows allows the interpretation that highly welded tuffs of any composition--basaltic to rhyolitic--move as gas-fluidized or partially fluidized bodies. The flows move long distances covering hundreds of km^2, and therefore behave as a very fluid mass, seemingly unaffected by probable high viscosity of materials with high silica content. Until the mid-1960's, most research on ignimbrite was with thermal and petrologic aspects. Since then, considerable research on ignimbrites has focused upon flow processes. Small-volume pyroclastic flows and surges have been used as the primary analogues for interpreting mechanisms of emplacement for large-volume pyroclastic flows. The outstanding feature of both the small- and large-volume deposits is the ability to flow long distances, resulting in high aspect ratio deposits. This suggests that at all scales they are likely transported as hot, gas-fluidized flows containing abundant particles. The outstanding difference between small-volume and large-volume ignimbrites is that of welding, with large-volume deposits commonly welded and small-volume deposits rarely if ever welded. This suggests a direct relationship between volume and thermal factors. Thus, considerations of emplacement mechanisms need to take high temperatures into account and a question to be asked is, "If particles are hot enough to stick together and weld after deposition, how can they move as a mass flow for 10's of kilometers without particles sticking together to cause the collapse of the flow?" With high concentration, it is expected that in addition to upward moving gases, particle support would also be by grain-to-grain interactions and numerous collisions. Because gas, the fluidizing agent, has a low thermal conductivity, with silicate glass particles having a much higher conductivity, a possible answer to the question is that the particles do not come into contact very often. Thus, it can be postulated that highly welded, large-volume ignimbrites were transported as highly expanded, low-concentration turbulent flows where the number of particle impacts were greatly minimized. Only after collapse of the flow were sufficient numbers of particles brought close enough, long enough to sinter or weld.

MOVEMENT AND DEPOSITION OF A PYROCLASTIC SURGE ACROSS RUGGED TOPOGRAPHY: 18 MAY 1980 ERUPTION OF MOUNT ST. HELENS, WASHINGTON

FISHER, R.V., Department of Geological Sciences, University of California, Santa Barbara, California 93106

The 08:32 PDT 18 May 1980 Mount St. Helens eruption began as a single explosion to produce a blast surge that moved outward in a 180° arc at supersonic speeds, then slowed to subsonic, as is shown by erosional and depositional patterns. The blast surge moved across rugged topography in an expanded state several hundred meters higher than the mountains. The lowest unit is a ground layer (formerly, layer A0), formed by interaction of the surge with the ground; it is overlain by deposits from the blast surge.

Deposition of the blast surge layers is partitioned into a **transport system** and a **depositional system**. The blast surge (transport system) carried the fragments; the depositional system developed from the basal zone of the transport system as two continuously and sequentially formed gas-fluidized sediment gravity flows. Each sediment gravity flow moved downhill according to gravity, independently of the overriding blast surge and each other. The lower layer (A1) sedimented from the strongly turbulent, gas-rich flowhead of the waxing blast surge. The layer above (A2) is from the body of the blast surge as it began to wane. Topographically induced divergent and overlapping surge lobes resulted in thinner and noncontinuous units between layers A1 and A2. Above layers A1 and A2 are locally ponded massive deposits in valleys and depressions formed from gas-rich pyroclastic flows originating by (1) topographic **blocking** of the lower, high-density part of the blast surge that could not surmount ridges and (2) **flowback** and mixing of layers A1 and A2 from slopes $\geq\sim 30°$-35° that drained into separate valleys.

Distances travelled by the blast surge and rates at which coarsest fragments decrease laterally is related to the topographic "grain." The surge runout was farther where topography parallels flow direction, and was least where topography is at right angles to flow. Hazard maps need to take such regional surface roughness into account.

A granulometric feature of the deposits caused by topographic roughness is that the spread in median diameter values is nearly as great in local areas near the volcano as it is over the width of the devastated region. The wide scatter of points produces a **dispersion curve**, which may be characteristic of pyroclastic deposits in other areas.

Pyroclastic flow deposits that occur in separate valley bottoms across high mountain ranges elsewhere, many of which are several orders of magnitude larger than the flows and surges at Mount St. Helens, may have been deposited by mechanisms similar to the blast surge deposits at Mount St. Helens.

SUBMARINE FALLOUT DEPOSIT IN THE SHIRAHAMA GROUP (MIO-PLIOCENE), JAPAN

FISKE, R. S., Smithsonian Institution, Washington, DC 20560, and CASHMAN, K.V., Dept. of Geol. and Geophys. Sciences, Princeton University, Princeton, NJ 08544

A 5-m deposit of massive lapillistone and lapilli tuff, remarkably depleted in fine and medium ash and overlying a pyroclastic debris flow in the shallow submarine Shirahama Group, is interpreted to have formed by the fallout of freshly erupted particles through a column of sea water. Three lines of evidence bear on this interpretation:

Theoretical- The calculated curves below show that lithic spheres (s.g. = 2.4-2.0) falling through sea water have the same terminal velocity (V_T) as water-saturated pumices (s.g. = 1.2-1.1) an order of magnitude larger (see lower stippled area). In air, the same lithic spheres would tend to be associated with dry pumices only 2-3 times as large.

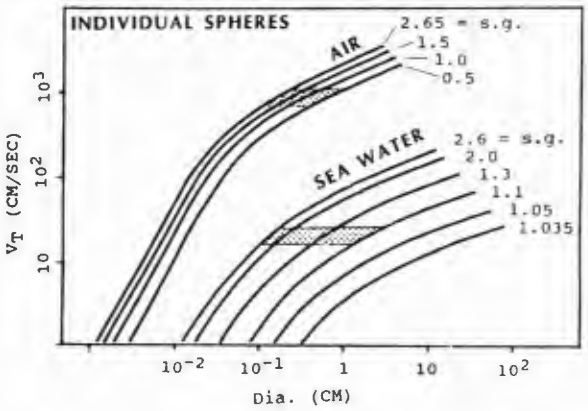

Experimental- To evaluate the effects of particle shape and mutual interaction ("swarm flow"), we are employing a large separation tube, 35 cm in diameter and 3-6 m high. Batches of nonsorted, water-saturated tephra are allowed to settle through the water-filled tube, and sequential samples having prescribed ranges of V_T are collected at the bottom. Preliminary results show that pumice/lithic diameters approach 8-10 to 1 for V_T intervals in the range 28-18 cm/sec.

Field- Outcrop measurements document that pumice and lithics are strongly bimodal, with maxima of pumice diameters 8-10 times larger than those of associated lithics. In addition, the overall grain size diminishes upward through the massive deposit.

We infer that this deposit represents the fallout facies of pyroclastic material erupted from a nearby shallow submarine volcano, and that assemblages of particles having the same V_T's tended to approach hydraulic equilibrium as they settled to the sea floor. Independent confirmation of a contemporaneous eruption comes from TRM studies of the underlying debris flow, which show that it was deposited hot (see TAMURA et al., this Abstract Volume).

MAFIC VOLCANISM ASSOCIATED WITH LATE CENOZOIC EXTENSION IN THE WESTERN US — GEOCHEMICAL VARIATION IN SPACE AND TIME

FITTON, J.G., JAMES, D., Grant Institute of Geology, Edinburgh University, West Mains Road, Edinburgh EH9 3JW, UK and LEEMAN, W.P., National Science Foundation, Washington DC 20550, USA.

The establishment of widespread mafic volcanism across much of the western US in the late Cenozoic followed the cessation of subduction along the Pacific coast. This volcanism accompanied lithospheric extension and block faulting in the Basin & Range (BR) and the Transition Zone (TZ) between the BR and the Colorado Plateau (CP). A transition zone between the Great Basin section of the BR and the Sierra Nevada is represented by the Sierran Province (SP). In an attempt to assess the relative role of asthenosphere- and mantle lithosphere-derived magmas across the western US we have analysed, for major and trace elements, a suite of 440 basic (>4% MgO) lava samples collected from all the major volcanic fields in the region. The data base was divided into four subsets representing the tectono-magmatic provinces (BR, TZ, SP and CP). It was further divided into relatively recent (<5Ma) and older (>5Ma) subsets on the basis of field relations and K-Ar data where available.

The <5Ma subset shows striking chemical differences between the four provinces. The BR lavas are indistinguishable from OIB and therefore appear to have a source within the asthenosphere. In contrast, the TZ and SP basic lavas generally have high La/Nb and Ba/Nb and low Rb/Sr compared with the BR samples. The CP lavas (Hopi Buttes) are similar to other continental nephelinites except for a slight deficiency in Nb. Published isotopic data suggest that the TZ and SP lavas have higher $^{87}Sr/^{86}Sr$ and lower $^{143}Nd/^{144}Nd$ than do the BR basalts. Since many of these lavas are undersaturated and highly magnesian, crustal contamination cannot provide an explanation for the chemical and isotopic differences. The TZ and SP mantle source must have been depleted in Nb and Rb (both highly incompatible elements) and yet enriched in Ba and ^{87}Sr. Since Ba is also highly incompatible in mantle phases, this enrichment must have been superimposed on a previously depleted mantle. The most likely explanation for these chemical and isotopic characteristics is that the TZ and SP magmas had a lithospheric mantle source which was enriched by fluids expelled from a subducted slab. Pelagic sediment, returned to the mantle during subduction, is a possible agent for fluids rich in Ba, radiogenic Sr and unradiogenic Nd, but very poor in Nb. These fluids appear to have metasomatised the base of the sub-continental lithosphere which was subsequently involved in magma generation during later extension. The metasomatism could have occurred between 60 and 40Ma ago when a shallow subducted slab may have extended beneath the whole region. We cannot, however, rule out the possibility that the metasomatism occurred much earlier, during the formation of the crust.

The older (>5Ma) data set, by contrast, shows no differences between BR and TZ and SP lavas. The older BR lavas have high La/Nb and Ba/Nb comparable with the younger TZ and SP magmas. It appears, therefore, that subduction-enriched lithospheric mantle was involved in the generation of all the extension-related basic magmas across the western US until relatively recently. Only over the past 5Ma or so has asthenosphere-derived magma been able to reach the surface essentially uncontaminated by lithosphere, and then only in the centre of the Great Basin and southern BR. This may reflect lithospheric erosion in those regions undergoing the greatest degree of extension (BR). Since magmatism is migrating into the CP, the TZ is still in the early stages of extension whereas the central parts of the BR are now at an advanced stage. Hence the more recent BR magmas are generated from the asthenosphere alone whereas the TZ and SP magmas (and the earlier BR magmas) have interacted with enriched lithospheric mantle.

THOLEIITIC ROCKS OF THE KIRKPATRICK BASALT, CENTRAL TRANSANTARCTIC MOUNTAINS, ANTARCTICA

FLEMING, T.H. and ELLIOT, D.H., Byrd Polar Research Center and Dept. Geol. & Min., Ohio State Univ., Columbus, OH 43210

Jurassic tholeiites of the Ferrar Group crop out in a linear belt which extends over 2500 km along the Transantarctic Mts. This magmatic province which includes lavas, pyroclastics, sills and a large layered basic intrusion, is characterized by initial strontium isotope ratios which are anomalously high for basaltic rocks (average $(^{87}Sr/^{86}Sr)_i$=0.7115) and by trace element ratios more typical of crustal rocks. Detailed geochemical study of the lava sequence exposed in northern Victoria Land (NVL) has identified two distinct chemical compositions referred to as high-Ti (TiO_2= 2.0%) and low-Ti (TiO_2=0.4-0.8%) units (Siders and Elliot, 1985). The high-Ti lavas which cap the sequence in NVL are highly evolved rocks which are extremely homogeneous (SiO_2= 57.0%, FeOT=15.0%, MgO=2.4%, CaO=6.9%). Chemical variation diagrams show that their composition does not lie on chemical trends defined by the underlying low-Ti rocks (SiO_2=52.0-57.0%, FeOT=7.8-10.4%, MgO=4.5-7.5%) and major and trace element models relating the two groups have been unsuccessful.

We have recently conducted a detailed geochemical survey of the lavas exposed in the central Transantarctic Mountains (CTM), located 1300 km south of the lava sequence in NVL. In CTM, lavas are exposed in the Queen Alexandra Range and the Grosvenor Mts. which are separated by 100 km. In both these regions the uppermost lava flow has a distinctive major and trace element chemistry which is remarkably similar to the high-Ti rocks in NVL. The underlying lavas in CTM, however, are generally more evolved than the lavas found below the high-Ti unit in NVL (SiO_2=52.6 -58.6%, FeOT=9.2-12.8%, MgO=2.5-7.7%).

The major difference between the iron-rich lavas in NVL and CTM is their texture and field appearance. In NVL the high-Ti rocks are extremely fine-grained and glassy and form several flows which include pillow lavas. In CTM, the iron-rich rocks are found in a single thick flow (up to 66 m) which has a diabasic texture. Despite the thickness of this flow the chemistry remains extremely homogeneous. In both regions the iron-rich rocks are separated from the underlying lavas by a thin interbed or paleosol (<1 m thick).

The distinctive chemistry of these iron-rich rocks has proved to be a useful marker for correlating local stratigraphic sequences. The presence of lavas separated by 1300 km with such a unique and uniform chemistry and in the same stratigraphic position is remarkable. The similar chemistry is likely to reflect a parallel petrogenetic history. Within constraints of K/Ar age determinations, the iron-rich rocks in NVL and CTM are temporally equivalent and are not significantly younger than the underlying lavas.

The major and trace element composition of the lavas underlying the iron-rich rocks in CTM, while being generally more evolved than the low-Ti lavas in NVL, appear to extend the chemical trends displayed by the NVL rocks, suggesting that these two units may also have a parallel petrogenetic history.

THE FOURTH ACTIVITY CYCLE OF COLIMA VOLCANO, MEXICO

FLORES, D.J., Instituto de Geografía y Estadística, Universidad de Guadalajara, Apdo. Postal 2-98, Guadalajara, Jalisco, 44280 México.

Colima Volcano (19°30' N; 103°37' W) is considered as the most active volcano in Mexico, and one of the most active volcanoes in the world. Its eruptive history has been recorded since more than 400 years ago, and it shows that Colima is a volcano with particular activity in México, because no one other has presented regular activity. The eruptive history began to be considered when near the end of the last century Mariano Bárcena (1887) wrote the most complete report up to then. From him, many others have written about its eruptions, and some scientists have introduced the idea about Colima Volcano has experienced three cycles of eruptive activity and now is in the fourth one.

In accord with Luhr (1981) the cycles should be as follow:

1576 The first eruption recorded after the spaniards in Mexico marks the begining of the first cycle.

1611 Strong ash and scoria emition considered as the end of the first cycle after 35 years.

1749 Without more information is reported an eruption; because the long time with not reports of activity is considered the begining of the second cycle.

1818 Major ash and scoria eruption wich is the end of the second cycle.

1869 After 51 years of no eruptive activity lava and blocks flowed from a parasitic cone named "El Volcancito" on the E side. Began the third cycle.

1913 Pelean eruption and ash flows moved down major canyons. A 300 m deep crater was formed. The third cycle finished.

1961 Lava blocks flowed through the low point in the N crater rim, marking the begining of the fourth cycle.

Each activity cycle alternates wich a period of apparent no eruptive activity. The cycle begins with flows of lava or blocks and finishes with an impetous eruption. Then the"quiet" period, untill the volcanic materials flow again from cone.

The 1913 (January 20) pelean eruption represents the end of the third cycle, followed by 44 years withouth important volcanic events. In the 300 m deep crater there was lava described as a "boiling lake" covered by steam and gases. Some years later it was described as black lava blocks and in 1931, the "plug" formed had come up, because it was 50-60 m deep from the lowest point on the N rim. In 1957 strong steam eruptions were noted and underground noises were listened while weak earthquakes could be felt near the crater. The plug kept moving and during 1961-62 flowed through the lowest point on the N of the crater rim. In 1975-76 the crater dome spilled over the NE rim, reaching "El Volcancito" and following to "El Playón" and almost reaching San Marcos village. Piroclástic flows were reported in 1982 in the SW side of dome and in 1987 an important phreatic explosion at summit caused an avalanche from dome.

Important changes have been reported on dome wich grows and then collapses in the last two years. It is expected that the fourth cycle ends just before or short after the present century finishes. It could be a big explosion from dome at least as in 1913.

RADIATIVE TEMPERATURE MEASUREMENTS AT KILAUEA VOLCANO, HAWAII

Flynn, L.P., Mouginis-Mark, P.J. and Gradie, J.C. Hawaii Institute of Geophysics, University of Hawaii, Honolulu, Hawaii 96822

Recent advances in the remote satellite investigations of active volcanoes, most notably with the Landsat Thematic Mapper (TM) (Rothery *et al.*, 1988), have demonstrated the ability of near-infrared sensors to measure surface temperatures of lava lakes and lava flows. While regional views of a lava lake have been provided by these satellite observations, one of the basic and critical "yardsticks" of the remote sensing era remains unmeasured: what is the temperature (i.e., radiative flux) of recently erupted magma, and how does the radiative temperature of a volcanic area behave with time? Satellite observations provide estimates of lava temperatures and the percentage of the image pixel that is filled by material at this temperature, but lack the temporal context or spatial variability of dynamic lakes. The field method that we describe here provides this high-resolution (~2 m^2) and frequent resampling (~1 minute intervals) data on lava temperatures using spectral measurements made at the wavelengths necessary to measure the blackbody curve.

Radiometric measurements of the Kupaianaha lake (located ~20 km along the East Rift Zone of Kilauea Volcano, Hawaii) were made on October 12, 1987. We used a commercially available (Geophysical and Environmental Research, Inc.) dual-beam infrared imaging field spectrometer, were made in 1000 narrow ($\lambda/\Delta\lambda$ ~ 200 to 600) spectral channels between 0.4 and 3.0 μm. Instrumental counts were converted to absolute fluxes by fitting blackbody curves to data in those portions of the spectrum not significantly affected by atmospheric absorptions. The spectral emissivity was assumed to be constant over the wavelength region observed. The significant outgassing and high absolute humidity of the atmosphere above the lake, combined with the long optical path (~15 - 20 m) between the instrument and the surface, precluded reliable relative or absolute fluxes in the atmospheric absorption bands at 1.5, 2.0, and 2.5 μm.

Visual analysis of video tape recorded over a period of hours concurrent with our spectral measurements shows that the lava lake exhibits three stages of activity. The most typical state of the surface (Stage 1), which can last more than 30 minutes at a time, is one of eerie quiescence where the lake surface is covered by a slow-moving glassy crust. Stage 2 occurs when the surface begins to "rift" forming long (many meters), but narrow (0.5-2 meters), fissures as the crust slowly pulls apart. During Stage 2, the surface is punctuated by several opening rifts (from visual estimation ~5 - 10 cm deep) which expose hotter material that quickly forms a crust. The final stage (Stage 3), which lasts only a few minutes, is dominated by active and rapid rifting (up to 5 meters in width) punctuated by the effervesence of large gas bubbles and small (< 5 m high) fountaining events as segments of the lake surface are subducted. The lake surface is in the Stage 1 quiescent state about 90% of the time.

The most surprising result is the relatively low temperature (~260 - 370°C) of the surface during the quiescent Stage 1. The blackbody fits show that the surface of the lake has at least two thermal components from which radiating areas can be determined. In the quiescent state of the lake, these thermal components probably correspond to the crust (T = 225 - 425°C) and to cracks in the surface (T = 725 - 1025°C). The higher temperature component corresponds to only 0.05% to 0.1% of the surface area. In the second state of activity, the temperature of the crust increases to 525 - 725°C with the higher temperature (825 - 1175°C) material, representing the 1-3% of the area exposed by rifting.

REFERENCE: D.A. Rothery, P.W. Francis and C.A. Wood (1988). *J. Geophys. Res.* **93**, 7993.

THE MARANHÃO, NORTHERN BRAZIL, MESOZOIC BASALT PROVINCE: GEOCHEMISTRY, ISOTOPE CHARACTERISTICS, PETROLOGY, AND PLACE IN THE 'DUPAL' ANOMALY

FODOR, R.V., North Carolina State University, Raleigh, NC 27695, USA; SIAL, A.N., Universidade Federal de Pernambuco, Recife, PE, Brazil; and MUKASA, S.B., University of Florida, Gainesville, FL 32611, USA

The northern Brazil states of Piaui, Maranhão, and Goias contain remnants of Mesozoic flood basalts and hypabyssal rocks that were apparently emplaced during tectonism associated with the opening of the Atlantic Ocean. Analyses and new dates (K-Ar by E.H. McKee, USGS) reveal that this ~700x250 km Maranhão province (5°-8°S) has low-Ti basalts (~1.1 wt.% TiO_2) in the western part that are about 150-190 Ma, and high-Ti basalts (3.4-4.4 wt.% TiO_2) in the eastern part about 115-122 Ma. The low-Ti basalts have a smaller compositional range and are less evolved, Mg# 62-56 and FeO*/MgO 1.2-1.6, than the high-Ti basalt group, Mg# 44-33 and FeO*/MgO 2.5-4. In the high-Ti group, incompatible elements increase as TiO_2 decreases from 4.4-3.4 wt.%. General characteristics of the least evolved members of low- and high-Ti groups include, respectively, Zr 100 and 225 ppm, Sr 225 and 500 ppm, Ba 200 and 600 ppm, Nb 10 and 24 ppm, Y 28 and 35 ppm, $La/Yb_{(n)}$=4.2 and 6.2, where $La_{(n)}$ is 30 and 90. Overall compositions of Maranhão basalts resemble the low- and high-Ti basalts of the Mesozoic Serra Geral (Paraná) province in southern Brazil.

Isotope compositional ranges for low-Ti and high-Ti groups are, respectively: ϵ_{Nd} is -1.6 to -3.8, and -2.2 to -3; ϵ_{Sr} is 26 to 69, and 15 to 18; Pb 206/204= 18.2 to 18.8, and 18.23; Pb 207/204= 15.61 to 15.70, and 15.51 to 15.58; Pb 208/204= 38.66 to 38.80, and 38.38 to 38.55; $\delta^{18}O$ = +8.9 to +12.6, and +6.5 to +8.6.

Ages, compositions, and isotopes suggest that low- and high-Ti groups had independent origins from enriched sub-continental mantle. If high-Ti basalts closely reflect their source composition, and low-Ti basalts underwent crustal contamination (more radiogenic Sr and Pb; higher $\delta^{18}O$), both groups can be modeled from the same source composition. This requires parental picritic liquids for each group, whereby high (e.g. 25%) and low (~12%) percentages of melting respectively yielded low- and high-Ti groups, followed by about, respectively, 60% and 80% gabbroic crystallization during their times from zones of melting to shallow reservoirs. Larger, replenished low-Ti magma systems were more susceptible to crustal contamination (e.g., more radiogenic; less Sr) than high-Ti magmas. While isotopes model as one essentially homogeneous Maranhão mantle source for both groups, trace elements, such as Y, point to small modal variations across the northern Brazil mantle-sources.

Both Maranhão basalt types have isotope compositions like those of low-Ti Serra Geral basalts. When comparing Pb isotopes of Maranhão and Serra Geral high-Ti basalts (uncontaminated) to evaluate DUPAL anomaly, Maranhão has Pb Δ7/4 4.6 to 11, and Pb Δ8/4 72 to 87; Serra Geral has Pb Δ7/4 10 to 13, and Pb Δ8/4 95-125. The small difference is not enough to conform to DUPAL contours as defined by oceanic basalts. Pb 6/4, 7/4, and 8/4 ratios are more consistent with little isotopic difference across mantle beneath Brazil from north to south prior to rifting for Atlantic opening. If DUPAL characteristics existed deep in the mantle before the opening of the Atlantic (Hart, 1988), it was perhaps prevented from manifesting itself by the high-pressure regime, or barrier, imposed by continental lithosphere. Rifting, however, removed lithosphere to enable DUPAL participation in oceanic magmatism. Maranhão low-Ti magmas are probably related to opening of the North Atlantic, and high-Ti magmas to opening of the South Atlantic. Differences in the percentages of melting proposed may relate to a Triassic-Jurassic hotspot origin for low-Ti basalts, and decompression for Cretaceous high-Ti magmas.

A CO_2- AND O_2-RICH VOLATILE PHASE AS THE AGENT FOR RISING VOLCANOGENIC MAGNETITITE

FÖRSTER, Hansgeorg, Institut für Mineralogie und Lagerstättenlehre RWTH, Aachen, Germany

Several 100 Mt massive magnetite fill a pipe in a rhyolite volcano at Chador Malu/Central Iran. The ore contains 59% Fe, 5% REE-rich F-apatite, 3% ankerite-bearing dolomite, traces of quartz, calcite, talc, phlogopite, chlorite, albite, actinolite, melanite, sphene, natrolite, pyrite, and anhydrite.

The sulfur content decreases from 0.36% (1000m level) to 0.05% (1600m level), proving strong degassing within the vent in an O_2-rich environment. In parts, the ore shows fluidal and comb-layering texture. Associated rocks are apatitite (exploitable), carbonatite dikes with pyrochlore, mesocratic trachyte (alkali feldspar + biotite + hornblende), and mega-breccia (rhyolite fragments cemented by magnetite + calcite). The iron oxide melt caused sodium-metasomatism (fenitization) in the country rock (mica schist or rhyolite converted to albitite). The connection to a highly alkaline carbonatite magma is indicated. Chador Malu may be compared with Kovdor, Korshunovsk (SU), Kiruna (Sweden), Iron Springs (Utah), Durango (Mexico), and El Laco (Chile).

Problems for the concept of volcanogenic magnetitite are the high melting point of iron oxide, and the high density of such a melt. Experiments were run with mixtures of sodium carbonate and hematite at 600, 1000, and 1365°C in air at 1 bar to generate sodium ferrite ($NaFeO_2$), and $Na_3Fe_5O_9$. EL BALKHI et al. synthesized sodic magnetite ($Na_2Fe_6O_9$) at low oxygen fugacity. Sodium ferrite lowers the melting temperature of hematite considerably (from 1555 to 1135°C).

The iron ore magma is envisaged to have been silica-poor, iron oxide-rich, sulphide bearing, and sodium-rich (as Na_2CO_3, $NaFeO_2$, $NaFeSi_2O_6$ or $Na_2Si_2O_5$) with a substantial fluid phase (H_2O, CO_2, P, F, SO_3, O_2). When rising to the surface, this magma will foam up:

$$Na_2CO_3\,(l) + Fe_2O_3\,(l) = 2\ NaFeO_2\,(l) + CO_2\,(g)$$

$$2\ NaFeO_2\,(l) + 2\ Fe_2O_3\,(l) = 2\ Fe_3O_4\,(l) + Na_2O(l) + {}^1/_2\ O_2\,(g)$$

The density of the foamy melt is low enough to allow the ascent, the viscosity of iron oxide melt is very low, and the melt may be undercooled (comb layering). The melt solidifies in the vent as magnetitite; parts of the melt may even reach the surface and form magnetite lava or tuff.

THE SYN-DENUDATIONAL EMPLACEMENT OF A GRANITOID BATHOLITH, OLD WOMAN-PIUTE MOUNTAINS, SOUTH-EASTERN CALIFORNIA

FOSTER, David A., HARRISON, T. Mark, Dept. Geological Sci., SUNY at Albany, NY 12222, MILLER, Calvin F., CARL, Brian C., Dept. of Geology, Vanderbilt Univ., Nashville, TN 37235, and FLORENCE, Frank, Dept. of Geology, RPI, Troy, NY, 12181 (COWPIE contribution)

Mesozoic granitoids in the Old Woman (OW) and Piute Mountains area are exposed over ~350 km^2, and are dominated by 74 ± 3 Ma (U-Pb) members of the Old Woman-Piute batholith (OWPB). The batholith consists of two plutonic series, the metaluminous OW granodiorite (MG) and peraluminous two-mica ± garnet granites (PG), both of which were derived by partial melting of continental crust ranging in age from 1.4 to >1.8 Ga as determined from inherited zircon ages, and Sr, Nd, O, and Pb isotopic compositions. Previous studies indicate that the OWBP was emplaced syn-to-post kinematic with an episode of crustal shortening over a period from 85-74 Ma.

Geobarometry on Mesozoic granitoids in the OW indicates a middle crustal level of emplacement with peak pressures occurring during the Mid-Mesozoic shortly after crustal thickening. Al-hb barometry on Jurassic (~150 Ma) tabular intrusions of K-rich granitoid yields Al_T = 2.2 ± 0.1 cations per formula unit for unzoned calcic amphiboles corresponding to a pressure of 7.1 ± 1 kbar for rims in contact with quartz. The MG contains unzoned to mildly zoned hornblendes with a mean Al_T = 1.90 ± 0.06 (5.6 ± 1 kbar); highest pressures are located in the west-central OW (6.2 ± 1 kbar) and southern OW (5.9 ± 1 kbar); lower pressures occur in the east-central and southwestern OW (5.4 ± 1 kbar). The uniform pressure across the OW granodiorite indicates a tabular shape for this pluton and suggests that this range has not experienced major tilting since 74 Ma. Application of the plagioclase-garnet-biotite-muscovite barometer (PGBM) to PG in the OW reveals a pressure of 5.6 ± 1 kbar for the Sweetwater Wash granite, and 5.5 ± 1.5 kbar for the Painted Rock granite (using a temperature of ~700 °C from zircon saturation). Geothermobarometry estimates from twelve recrystallized Proterozoic pelitic schists around the OWPB yield pressures of 5-7 kbars at temperatures of 575-650 °C.

$^{40}Ar/^{39}Ar$ cooling ages from the OWPB and country rocks are nearly concordant; ten hornblende analyses reveal ages of 73 ± 1 Ma, seventeen biotites and muscovites yield ages of 70 ± 2 Ma. and sixteen K-feldspars have age gradients from ~65 Ma in low temperature steps to 70-71 Ma in high temperature steps. The narrow age range from all minerals requires cooling rates of ~100 °C/Ma between 74 and 70 Ma and ~10 °C/Ma between 70 and 60 Ma, which constrain uplift rates of ~4mm/yr between 74 and 70 Ma using geothermal gradients obtained from thermal modeling. This unroofing rate is high enough to cause nearly isothermal uplift due to advection of geotherms and is consistent with the late growth of andalusite and cordierite at the expense of kyanite, staurolite, and garnet in pelitic rocks.

The 74 Ma batholith was emplaced synkinematic with an extensive top-to-the-west shear zone, greater than 1 km thick, exposed in the northwestern OW. This shear zone deforms older compressional structures and remained active until ~68 Ma. Rapid denudation of the OWBP indicated by the barometric and thermochronological data occurred for the most part along this structure coincident with the emplacement of the batholith suggesting a cause and effect relationship between magmatism and extensional unroofing (i.e., core complex formation) in this area. Questions remain; did ca. 75 Ma unroofing generate the OWPB magmas either by pressure release melting, mafic magma input into the lower crust or mantle upwelling; or was unroofing related to emplacement of the OWPB magmas which reduced the strength of the crust causing extensional failure.

VOLCANIC ASH WARNINGS FOR CIVIL AVIATION

FOX, T., International Civil Aviation Organization (ICAO), 1000 Sherbrooke St. West, Montreal, Quebec, Canada H3A 2R2
HEIKEN, G., Los Alamos National Laboratory, MS D462, Los Alamos, NM 87545
SIGVALDASON, G., University of Iceland, Nordic Volcanological Institute, 101 Reykjavik, Iceland
TILLING, R., U.S. Geological Survey, 345 Middlefield Rd., Menlo Park, CA 94025

Volcanic eruption clouds, even in a dilute, dispersed form, are a continuing hazard to airline traffic, especially around the perimeter of the Pacific Basin. Beginning in 1986, the International Civil Aviation Organization (ICAO) established a study group to recommend safety procedures for aircraft operating downwind from explosive eruptions, to evaluate means of warning pilots of such hazards, and to prepare information on volcanic hazards for pilots and aviation meteorologists. Changes have been made to ICAO regulatory documents, establishing the hazardous nature of dilute eruption plumes and procedures to be followed should an aircraft encounter such a plume. Pilots now have formal procedures to follow in describing eruptions that they can see, with the information being passed on to flight controllers, observatories, and the Scientific Event Alert Network.

At this time, the World Organization of Volcano Observatories is attempting to establish an *International Airways Volcano Watch*. This effort now consists of circulating names, phone numbers, and telex numbers of volcano observatories, flight controllers, and aviation meteorological stations within regions. We encourage the staff at the observatories to initiate regional meetings with their counterparts in the aviation industry. We feel that preventing encounters between aircraft and volcanoes can be done within these regions and solicit your help and cooperation to prevent such accidents.

PETROLOGICAL AND GEOCHEMICAL VARIATIONS ACROSS THE CALC-ALKALINE ROCKS OF AEOLIAN ARC (SOUTHERN TYRRHENIAN SEA)

FRANCALANCI L., TAYLOR S.R., McCULLOCH M.T. and WOODHEAD J., Research School of Earth Sciences, Australian National University, Canberra, Australia.

Aeolian Arc lie on 20 Km thick continental crust. A Benioff zone is still active under the arc, with a NW dipping. The aeolian magma composition range from tholeiitic, calc-alkaline (CA), shoshonic, up to potassic. These different types of magmas were erupted in less than one million years, but there is not any overall correlation between magmatic affinity and time or geographic position of the magmas in the arc.

The studied CA rocks include mainly basaltic-andesites from Salina, Lipari and Stromboli and basalts from Alicudi, Filicudi and Panarea islands.

The Filicudi and Salina samples show the highest contents in Al_2O_3, whereas the rocks from Alicudi, Lipari and Stromboli have the highest abundances in MgO. Volcanics from Panarea, Salina and Lipari contain the least amounts in TiO_2, P_2O_5 and Na_2O.

Incompatible trace elements form positive correlation with silica among basaltic - andesites, but not among basalts. At a same silica level, Salina and Lipari rocks are the most depleted in incompatible trace elements, whereas Filicudi and Alicudi magmas are the most enriched. The Alicudi volcanics have also the lowest La/Nb, Th/Nb, Ba/La, Rb/Ba and Rb/Sr ratios and the highest La/Sm and K/Rb ratios.

Nd and Sr isotope ratios vary from 0.512886 to 0.512557 and from 0.70353 to 0.70538, respectively. They are well correlated and each island generally occupies specific region on Sr versus Nd diagram. Sr isotope values define rough positive correlations with Rb/Sr, Th/Nb and alkali and poorly defined negative correlations with Eu/Eu^*, K/Rb and Sr contents. Moreover, $^{87}Sr/^{86}Sr$ are negatively correlated with silica in basalts and positively in basaltic-andesites.

Lead isotope ratios are quite high ($^{206}Pb/^{204}Pb$ = 19.15-19.54; $^{207}Pb/^{204}Pb$ = 15.61 - 15.71; $^{208}Pb/^{204}Pb$ = 38.87-39.36) and, in spite of the fairly large variations in Sr and Nd isotope ratios, they show small differences among the different islands.

The chemical and isotopic variations observed in the rocks of the single islands generally result from due to crystal fractionation, associated to assimilation of crustal material, during the path of magmas to the surface. Neverthless, the general variations in incompatible element contents and ratios, allow us to consider that significant and complex processes of contamination from subducted crustal material also occur in the mantle source (probably MORB-type) of the Aeolian magmas. Moreover, it is possible to suppose a major role of fluids in the genesis of Salina, Panarea and Lipari magmas. These fluids should have increased the values of La/Nb, Ba/La and Rb/Ba ratios of mantle source and allowed higher degrees of partial melting of source. This hypothesis explains the minor amounts in incompatible elements and the higher La/Nb, Ba/La and Rb/Ba ratios of Salina, Panarea and Lipari magmas, in respect to magmas from the other islands.

THE MANTLE SOURCES FOR QUATERNARY ALKALINE VOLCANISM IN THE NORTHERN CANADIAN CORDILLERA

FRANCIS, D., Department of Geological Sciences, McGill University, Montréal, Québec, Canada H3A 2A7 and
LUDDEN, J., Département de Géologie, Université de Montréal, Montréal, Québec, Canada H3C 3J7.

The Stikine volcanic belt comprises a series of Recent alkaline volcanic centers which extends along the northern Canadian Cordillera from north central British Columbia to the central Yukon. Our studies of 5 centers along this belt (Mount Edziza, Mount Llangorse, Alligator Lake, Minto Landing, and Fort Selkirk-see figure) show that the mafic lavas of these complexes range in composition from olivine nephelinites through basanites to transitional alkaline basalts in order of increasing volumetric importance. These mafic lavas represent three distinct alkaline magma series evolving along diverging paths. They cannot be related by low-pressure crystal-liquid fractionation and systematic isotopic differences make it difficult to derive them by variable degrees of melting of a homogeneous mantle source. Field evidence requires, however, that they are intimately interrelated in time and space; at Mount Llangorse and Fort Selkirk, for example, both olivine nephelinites and transitional alkaline basalts have erupted from the same vents. In addition, all three alkaline magma types share a number of anomalous chemical characteristics, including low Ca contents, with respect to other terrestrial equivalents. When corrected for low pressure crystal fractionation, the compositional spectra of individual volcanic centers approximate binary mixing arrays between olivine nephelinite and hypersthene-normative basalt. At centers where all three magma types are present (Fort Selkirk and Mount Llangorse), population gaps along these mixing arrays between the compositions of olivine nephelinite and basanite coincide with the compositions of mantle amphibole and the amphibole-garnet-clinopyroxene plane. This compositional gap appears to represent a thermal divide which separates highly silica undersaturated melts from mildly alkaline melts. A comparison of the glass compositions observed within amphibole pyroxenite versus lherzolite xenoliths in alkaline lavas suggests that the hypersthene-normative end member at the smaller volcanic centers may have been derived from the melting of lherzolite lithosphere, while the olivine nephelinite end member is associated with amphibole pyroxenite veins which cut the lithosphere. The olivine nephelinite magmas may either have formed by the preferential melting of amphibole pyroxenite veins or have produced such veins in the lithosphere. In either case, the rise of highly silica undersaturated melts from an asthenosphere source was a precursor to magmatism in the overlying lithosphere.

MULTI-TEMPORAL RADIANT THERMAL ENERGY MEASUREMENTS OF ACTIVE VOLCANOES: A NEW SATELLITE TECHNIQUE

FRANCIS, P.W., GLAZE, L.S., Lunar and Planetary Institute, Houston, Texas 77058, ROTHERY, D.A., Open University, Milton Keynes, United Kingdom MK7 6AA

Volcanoes are sites at which both heat and magmatic materials are transferred to the surface of the earth. The thermal budgets of active volcanoes are more difficult to monitor directly than the effusion rates of lavas and pyroclastic rocks, or even of volatile species such as SO_2. Few published data are available. The short-wavelength infra-red data of the Landsat Thematic Mapper (TM) provide both a measure of the radiant thermal energy flux, Q, from active volcanoes, and a guide to the nature of the activity.

To calculate Q the two band method developed by Rothery et al.[1] has been modified to take account of background radiation. Using the relationship $Q=sT^4$, the total energy flux can be determined for the background as well as the anomalous heat source[2].

At Lascar volcano, north Chile, radiated thermal energy has shown marked changes through time. TM measurements of Q at Lascar for December 1984 of 6.7×10^7 Watts are consistent with an earlier suggestion that a lava lake was the source of the anomaly, but values for 1985-1986 are so much lower (between 0.9 and 3.8×10^7 Watts) that fumarolic activity was a more likely heat source then. The figure below shows the change in the total flux radiated by Lascar over time. The volcano with plume represents an explosive eruption at Lascar which took place on September 16, 1986. The airplane represents an aircraft observation overflight of the volcano made on January 12, 1987.

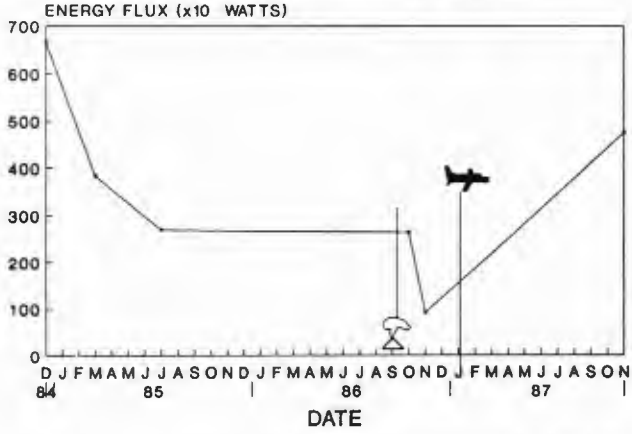

There are many pitfalls in deriving radiant thermal energy budgets for volcanoes by satellite remote sensing techniques, but our work shows that these techniques provide a means of quantitatively monitoring the activity of a volcano in a way which cannot be accomplished by conventional ground studies and may provide a method for predicting eruptions.

1.Rothery, D.A.,et al., J. Geophys. Res. 93, 7993-8008 (1988).
2. Colwell, R.N. Manual of Remote Sensing, The Sheridan Press (1983).

MULTICOMPONENT MIXING OF ZONED MAGMA BODIES AT THE TRANSITION FROM OCEANIC BASALTIC SHIELD TO CALDERA-FORMING SILICIC VOLCANISM: P1, GRAN CANARIA

FREUNDT, A. Schmincke H-U, Institut für Mineralogie, Ruhr-Universität Bochum, D-4630 Bochum, F.R.G.

The abrupt change from Miocene ocean island basaltic shield volcanism (ca. $20*10^3$ km^3) to emplacement of ca. 15 trachytic to rhyolitic ignimbrite cooling units (total volume ca. $5*10^2$ km^3) and formation of a 15 km diameter caldera on Gran Canaria (Canary Islands) is marked by the ca. 50 km^3 composite ignimbrite cooling unit P1, which is zoned from a lower silicic welded tuff (subunits R1-R4) through a mixed rock (subunits M1 and M2) to basalt at the top (subunits B1-B3). A wide spectrum of plastically deformed inclusions and disequilibrium mineral parageneses illustrate thorough magma mixing. The major magmatic components are (1) rhyolite, (2) trachyte, and (3) basalt, all of which were zoned prior to mixing. Additional but minor components are (4) andesitic magma and (5) partial melts from the wall rocks. Rhyolite comprises (a) an initially erupted high-silica crystal-poor variety of minute volume (R1) and (h) a main porphyritic body continuously zoned, with crystal size and abundance increasing downwards in the magma column. Trachyte inclusions in P1 form an independent continuous magma series from evolved trachyte to mafic trachyandesite. Olivine content of basalt increased downwards in the magma column. Compositional gaps exist between all component magmas, with a tiny gap even between the main trachybasalt body (B1 and B2) and the slightly more mafic basalt at the top (B3). Trachyte and basalt inclusions present throughout the rhyolitic lower part of P1 are rare near the base (R1). Trachyte inclusions increase in abundance through R2 and reach a maximum of 70 wt% in trachyte-rhyolite mixed unit R3. The basalt component rises very gradually but jumps to 30-40 wt% from R3 to R4, where trachyte drops to 20 wt% in M1 and approaches zero in M2 and B1. The fraction of basalt continues to rise from R4 through the mixed rock units M1 and M2 to submit B1 (basalt with only 10-20 wt% rhyolite) and ultimately reaches B2 with nearly uncontaminated trachybasalt. Rhyolite input briefly increases back to ca. 10 wt% at the end of the eruption, probably being incorporated via magma erosion along the walls of the conduit and collapse of the chilled envelope of cumulate germane to the resident magma in the silicic chamber. Trachyte, trachyandesite, and rhyolite magmas resided in a common reservoir (with rhyolite next to and trachyandesite most distant from the eruptive conduit) for a substantial period before eruption, forming minor evolved trachyte-rhyolite hybrid magma at the interface. Approaching eruption, trachyte-rhyolite mixing intensified and culminated during reservoir evacuation (forming inclusions with homogeneous matrix and bimodal phenocryst associations, and banded inclusions). The penetration of basalt magma into the evolved magma reservoir--which may have triggered the eruption--was accompanied by a concentrated discharge of partially molten plutonic wall rock fragments (representing older, non-eruptive gabbro, diorite and syenite intru-sions) which probably originated from reaming of a conduit connecting a lower basalt reservoir with the high-level silicic chamber. The zoned trachyte magma can be derived from P1 trachybasalt by fractional crystallization allowing for minor assimilation of sodic partial wall rock melts. Rhyolite cannot be fractionated from trachyte but could have evolved from trachybasalt via andesite, again allowing for selective contaminations.

FLUID PHASE EVOLUTION IN THE M.GENIS LEOCOGRANITIC INTRUSION (SE SARDINIA, ITALY)

FREZZOTTI, M.L, GHEZZO, C.
Dipartimento Scienze della Terra, Siena,
Via delle Cerchia n.3, 53100 Siena, Italy.

The M.Genis leucogranite is one of the post-tectonic shallow Hercynian intrusives in Sardinia. Silicate melt and fluid inclusions have been observed in rock forming quartz and in quartz crystals from the miarolitic cavities. The silicate melt inclusions consist of partially devetrified glass plus a bubble which is often highly distorted. The fluid inclusions cover a great range of temperatures and salinities, but two main groups can be recognized: (1) highly saline (40-65 NaCl wt.%) aqueous inclusions and (2) high density, low salinity H_2O inclusions.

Mixed silicate and salt melt inclusions have been observed during high temperature microthermometric runs ($T \approx 800$ °C). This suggests that the magma became enriched in alkali-chlorides during the late stages of crystallization and that a hydrosaline melt coexisted with silicate melt.

A magmatic origin is strongly indicated for the saline fluids which however are likely to have circulated in subsolidus conditions. Qualitative and quantitative studies suggest that no fluid immiscibility episodes (i.e. boiling) occurred. Highly saline fluids are likely to result by direct magmatic immiscibility.

At a later stage, during the hydrothermal low Temperature evolution, the pluton is invaded by homogeneous low salinity fluids (dilution with meteoric waters).

The comprehensive evolution of the hydrothermal circulation is linked to: (a) presence of widespread systems of joints and microfractures related to brittle deformation; (b) the cooling pattern of the pluton which controlled the whole convective system.

DETERMINATION OF FLOW DIRECTION AND VENT POSITIONS IN WHAKAMARU IGNIMBRITE USING ANISOTROPY OF MAGNETIC SUSCEPTIBILITY

FROGGATT, P.C. and LAMARCHE, G. Research School of Earth Sciences, Victoria University, P.O. Box 600, Wellington New Zealand

Whakamaru Ignimbrite is one of the largest volume (>1000km^3) ignimbrites in Taupo Volcanic Zone, New Zealand. It is young (250-300ka) and itself provides few clues to the location of the source area, being thick, finegrained and often deeply buried by younger pyroclastics. Lake Taupo has traditionally been assumed as the source, being caldera-like and central to the distribution of the ignimbrite. The geothermal area of Wairakei, north of the lake contains a very thick sequence of the ignimbrite and has also been postulated as a source area.

As part of a study of the magnetic remnance of this ignimbrite, the magnetic fabric was measured as a proxy indicator of flow direction and hence vent position. Over 35 sites of Whakamaru Ignimbrite have been sampled to provide a good areal coverage of the formation. Total susceptibility is in the range of $5x10^{-3}$ to 10^{-2} SI and is due to magnetite, as shown by IRM acquisition and thermal demagnetisation. The degree of anisotropy is weak (<5%) and the shape of the ellipsoid of suscepibility ranges from weakly prolate to weakly oblate according to the site, although the results are consistent within one site. It is assumed that the AMS is principally due to the alignment of magnetite grains exhibiting shape anisotropy so that the ellipsoid maximum (K1) axis indicates flow direction.

The minimum (K3) axis is near vertical for all the sites, suggesting minimal rotation of the ellipsoid during compaction. The K1 axis orientations do not indicate a single point source for the ignimbrite. Rather, directions of flow suggest at least 3 well constrained sites, one near Wairakei, one in the northern part and one in the southern part of Lake Taupo defining a SSW - NNE line through the centre of the lake. This may be interpreted as either discrete vents along a line or eruption from a 35km long fissure. Lack of critical exposure currently limits finer resolution. Vertical height of samples above the base of the ignimbrite could not be determined to check if vent locations progressed along the line with time, but with more northerly sites generally indicating the northern source and southerly sites the southern source a continuous fissure seems plausible.

MINERALOGIC, CHEMICAL, AND ISOTOPIC EQUILIBRATION BETWEEN MAGMAS: IMPLICATIONS FOR MAGMATIC INCLUSIONS IN PLUTONIC SYSTEMS

FROST, Thomas P., USGS, MS 938, 345 Middlefield Road, Menlo Park, CA 94025

Mafic to intermediate magmatic inclusions in granitoids commonly are in mineralogic and Sr and Nd isotopic equilibrium with their hosts. Inclusion textures, along with major- and trace-element compositions, however, suggest that most inclusions represent either undercooled magmas not genetically related to the host or cumulus material which may or may not represent early crystallization of the host.

Sr contents of inclusions in single plutons vary widely; Rb and Ba are 2-5 times lower than in host plutons. Many inclusions have REE, Y, Zr, Nb, and Zn abundances higher than those of their host but 2-5 times lower than schlieren of demonstrable cumulus origin from the host felsic magma. Cumulus schlieren also have distinct textures (euhedral mafic phases and interstitial plagioclase) when compared to inclusions (acicular apatite, plagioclase phenocrysts and euhedral groundmass plagioclase, euhedral or poikilitic sphene, fine grained anhedral and/or prismatic hornblende, quartz xenocrysts rimmed by hornblende).

Mineralogic equilibration between inclusions and host magmas in water-rich, slowly cooled plutons is predicted by phase relations. Sphene, hornblende, and biotite in place of the Fe-Ti oxides and anhydrous mafic silicates that might otherwise form in mafic magmas provides a sink for REE, Nb, Y, Zr, and Zn. Diffusion of these elements from the host through the residual liquid of undercooled inclusions may result in abundances of these elements greater than in the host. Volatile exsolution or filter pressing of residual felsic liquids from partially crystallized inclusions also may result in inclusion compositions with cumulate-like characteristics. Mechanical disaggregation of inclusions may occur if the crystallinity is low following incorporation.

Sr and Nd isotopic tracer diffusion between liquids is rapid but chemical diffusion of these elements is much slower (Baker 1988; Lesher 1988; Van der Laan and Wyllie 1988). Isotopic diffusion between the residual liquid in partially crystallized inclusions and the host magma affords a mechanism by which initially distinct magmas may be in or approach isotopic equilibrium without being in chemical equilibrium. Plagioclase phenocrysts may record initial isotopic ratios in inclusions that represent incorporated mafic magmas.

With high degrees of undercooling, inclusions may remain relatively pristine in terms of their isotopic and chemical compositions prior to incorporation in the host. With decreasing differences in heat content between host and inclusion (and increasing residual liquid proportions in the resulting inclusion) at the time of inclusion incorporation, the greater the likelyhood of isotopic, chemical, and mechanical exchange between inclusion and host. Cumulus origins from the magmas which crystallized to form the host are also permitted by some of the available evidence. Post-incorporation modifications may complicate interpretation of the origins of inclusions.

PLIOCENE THOLEIITIC BASALT FROM JAPAN SEA SIDE, SOUTHWEST JAPAN

FURUYAMA, K., Department of Geoscience, Faculty of Science, Osaka City University, Sugimotocho, Sumiyoshiku, Osaka 558 JAPAN.

Volcanic activity on the Japan Sea side in Southwest Japan during late Neogene is characterized by alkali rock series which range basalt to rhyolite. However, a newly discovered basalt lava in the area belong to low- or middle-K_2O tholeiite, and has interesting petrographical and petrochemical features. The basalt named TGBS, 2.8Ma K-Ar dating, is exposed in the upper part of the Pliocene Teragi Group, which consists of voluminous rhyolite tuff, conglomerate, mud stone and andestic volcanic rocks in ascending order. It flowed down slope and filled up the valley consisted of the older volcanic rocks in the group. It is composed of an accumulation of numerous flow units, each of which is several tens centimeters to several meters thick. The lowest part of a flow unit is massive and other part has the appearance of autobrecciated lava. Blocks sometimes have radiating cracks which seem to be the effect of water cooling. Phenocrysts are of olivine and euhedral-elongated plagioclase. The groundmass texture in each block shows various degrees of cooling. It ranges complete glass through matrix composed of dendritic augite and swallow-tail or belt-buckle of plagioclase to holocrystalline matrix. Matrix part of the autobrecciated lava is essentially composed of fragments with various cooling textures. Above rapid cooling texture resemble to abyssal basalt though the TGBS effused on a land.

Chemical compositions of the TGBS is characterized by low SiO_2(49.8-53.6 %), low K_2O(0.2-0.9 %) and high MgO(7-9.6 %), T-FeO (9.2-11.6 %), Ni(150-320ppm), Cr(230-340ppm) contents. The TGBS is rich in Na_2O comparative to the Quaternary low alkali tholeiite in Northeast Japan. Against lower contents of HFSEs such as Ti,Zr and Nb are common characteristics in island arc tholeiites, those of HFSEs in TGBS is high (TiO2>1 %, Zr;95-140ppm, Nb;5-12 ppm). Ni and Cr contents of island arc tholeiites are usually low than those in TGBS. TGBS has high contents of LREEs comparative to those in Quaternary Northeast Japan tholeiites, and shows gently LREE enriched chondrite-normalized REE pattern. Thus in spite of low K_2O content in both TGBS and NE Japan tholeiite, other chemical characteristics are different to each other. It is suggested that chemical compositions of TGBS has not suffered from a downgoing slab. It contrasts with late Neogene-Quaternary tholeiitic rocks in the Northeast Japan which is characterized by island-arc tectonic setting. TGBS may have originated from a dirpir of enriched mantle which should took place during the Japan Sea opening.

PETROGENETIC IMPLICATIONS OF RB-SR AND SM-ND ISOTOPES RELATED TO POST-CALDERA VOLCANISM IN THE WESTERN MOGOLLON-DATIL VOLCANIC FIELD, NEW MEXICO

FUTA, Kiyoto and RATTE, James C., U.S. Geological Survey, Box 25046, Denver, CO 80225

Two distinct groups of post-caldera volcanic rocks have been identified in the western part of the Mogollon-Datil volcanic field (M-D) on the basis of age, volume, major/trace element and isotope geochemistry, and structural setting. Both groups largely postdate the ~36-28 Ma voluminous (on the order of 1000 km^3) silicic ignimbrites and lavas that dominate M-D.

Group I comprises hypersthene normative andesites (23-27 Ma) with an original volume on the order of 100 km^3. These were erupted from structurally controlled, regional dike systems and from small (1-10 km^3) shield volcanoes. Samples for analysis were collected from one set of shield volcanoes, aligned along the ENE Morenci lineament (ML). Sr initial ratios of Group I andesites range from 0.7062 to 0.7098 and ε_{Nd} values, from -5.3 to -7.5, which suggests assimilation of crustal material by the magma. Sr initial ratios of three volcanic vents decrease from NE to SW along the ML with little change in ε_{Nd}. A change in source is suggested by those samples on the ML near its intersection with the NNE Morenci-Reserve fault zone (MRFZ) that have Sr and Nd isotope values that trend towards the Group II isotope characteristics.

The less voluminous Group II rocks (21-<1 Ma) are essentially bimodal basalt and rhyolite. Eruptive centers in the western M-D are mainly within the NNE MRFZ. The basaltic rocks of Group II on the MRFZ have a range of Sr initial ratios from 0.7031 to 0.7052 and ε_{Nd} values from +9.2 to +1.7. The spread in Sr and Nd isotopic ratios suggests crustal contamination of a magma derived from a depleted mantle reservoir. Group II lavas, derived from vents that are localized along a major fault zone between the Colorado Plateau and the Mogollon plateau, show less contamination by upper crustal materials than the Group I lavas. This may indicate that the fault zone facilitated ascent of the magma with less opportunity for assimilation.

Several samples, placed in Group II on the basis of age, have characteristics that are transitional between Groups I and II. They are located between Groups I and II and are intermediate in Rb-Sr and Sm-Nd isotope data. These samples may represent different degrees of crustal contamination between Groups I and II magmas as extension continued in this transition area between the Rio Grande rift and the Colorado Plateau.

BASALTS FROM THE KERMADEC ARC-HAVRE TROUGH AND THE TAUPO VOLCANIC ZONE : PETROLOGY AND GEOCHEMISTRY OF BASALTS IN A TRANSECT FROM AN OCEANIC TO ENSIALIC TECTONIC SETTING

GAMBLE, J.A., Department of Geology, Victoria University of Wellington, New Zealand,
SMITH, I.E.M., Department of Geology, University of Auckland, New Zealand, and
GRAHAM, I.J., Institute of Nuclear Sciences, DSIR, Lower Hutt, New Zealand.

In the western Pacific, the Tonga-Kermadec-Hikurangi subduction system is more or less continuous over 3000 km comprising a series of paired volcanic arcs and extensional back-arc marginal basins. Towards the southern end of the system the Kermadec arc and Havre Trough (KAHT) segment is oceanic whilst the Taupo Volcanic Zone (TVZ) is ensialic. While they differ markedly in relative abundance, basalts are the only magma type common to arc and back-arc in each segment. In KAHT basalts and basaltic andesites predominate whereas in TVZ basalt is subsidiary to andesite and rhyolite.

Primitive basalts (Mg#>65, Ni ~100 ppm) from KAHT and TVZ contain phenocrysts of olivine ± plagioclase. Clinopyroxene appears in more evolved specimens and orthopyroxene in the most evolved specimens. A single dredge sample from the floor of the Havre Trough is mildly alkaline (normative nepheline ~.27%), all other samples are hypersthene normative ranging from olivine to quartz tholeiite. Basalt tetrahedral projections delineate an array parallel to but distinct from the 1 atmosphere MORB cotectic, confirming the evolutionary path inferred from petrography. Scatter about this inferred "arc basalt cotectic" can be explained in terms of accumulation of phenocryst phases. This scatter is more pronounced for rocks from the volcanic arcs than the back-arcs and we interpret this to indicate the ease of passage of mafic magmas through the extensional lithosphere of the back-arc setting in contrast to the complexities of magma chambers beneath the volcanic arcs.

Basalt from the Havre Trough resembles MORB with low LIL and HFS elements, a flat (~25 x chondrite) REE pattern and $^{87}Sr/^{86}Sr$ = .702556 and ΣNd = +9.3. Basalts from the Kermadec arc show variable REE patterns from LREE depleted (Ce/Yb_N ~.4) to LREE enriched (Ce/Yb_N ~3). Multielement spidergrams of these basalts are strongly depleted in HFS and HREE relative to MORB and the Havre Trough specimen, but enriched in LIL. Isotopic ratios are more radiogenic than MORB with $^{87}Sr/^{86}Sr$ = .7033 - .7041 and ΣNd = +7.5 - +5.2. Basalts from TVZ show parallel LREE enriched patterns (Ce/Yb_N ~2). Spidergrams show similar but less marked HFS depletions than the Kermadec arc rocks and stronger enrichments of the LIL elements. Isotopically the TVZ data define an array overlapping data from the Kermadecs (range $^{87}Sr/^{86}Sr$ = .703878 - .705200 and ΣNd = +5.2 - +2.2).

Melting of MORB depleted mantle wedge, enriched by LIL bearing fluids from the slab can supply primary magmas of appropriate composition. These magmas will register depleted HFS and HREE geochemistry inherited from previous extraction of melt and elevated isotopic ratios reflecting the mobility of LIL and LREE. There is no need to appeal to retention of Nb (Ta) bearing phases in the source region. Variable fluxing and mixing of LREE and LIL from the slab may account for the isotopic variations in the KAHT lavas while interaction with subarc continental crust probably accounts for the spread of the TVZ data. Quantification of the relative contributions of slab and crust are being evaluated.

THE INTERPLAY BETWEEN CENOZOIC EXTENSION AND MAGMATISM IN THE BASIN AND RANGE PROVINCE

GANS, Phillip B., and MAHOOD, Gail A., Dept. of Geology, Stanford University, Stanford, CA 94305

Cenozoic magmatism and extensional tectonism in the Basin and Range province of the western United States are intimately related on a local scale, but their regional progression across the province is difficult to explain solely in the context of North American-Pacific plate interactions. For example, during the Eocene to Miocene, both extension and magmatism generally swept southward across the northern part of the province and simultaneously swept northwestward across the southern part of the province, converging at the latitude of Las Vegas at about 10 Ma. In any given area, volcanism and extensional faulting commonly exhibit a characteristic, short-lived, 3-stage history that appears to reflect rapid changes in the thermal and mechanical state of the underlying lithosphere.

Phase 1: Precursor, relatively small volume, eruptions of compositionally diverse (basalt to rhyolite, predominantly andesite) lavas and tuffs occur over a period of several Ma prior to the onset of appreciable extension. Petrologic data from these magmas document the influx of enriched(?) mantle-derived basalt into the crust and extensive hybridization with crustal partial melts.

Phase 2: Culminating eruptions of dacite-rhyolite coincide with the onset of rapid, large-magnitude extension within relatively narrow supracrustal corridors. Outpourings of 100's to 1000's of km^3 of magma in less than 1 Ma record the existence of mid-crustal magma chambers of batholithic dimensions beneath the extending areas. Petrologic data suggest these silicic magmas evolved largely by fractionation of andesitic hybrids and, as such, may contain relatively large (50%) mantle contribution. Initial strain rates on the order of 10^{-14}/sec. are suggested by the rapid tilting of syntectonic volcanic and sedimentary successions and the abrupt decompression and cooling of mid-crustal metamorphic/plutonic rocks in the footwalls of major normal faults.

Phase 3: A greatly reduced extensional strain rate (e.g., 10^{-16}/sec.) is accompanied by volumetrically minor eruptions of basalt +/- rhyolite. This late history of slow, broadly distributed faulting and widely scattered bimodal volcanism is often cited as classic "Basin and Range" tectonism, but accounts for only a fraction of the total strain and volume of erupted magma within the province.

These closely linked but regionally diachronous volcanic and tectonic histories are best explained by an "active" rifting model. Asthenospheric upwelling, partial melting in the upper mantle, and an influx of basaltic magma into the crust thermally weakened the lithosphere during Phase 1. Plausible explanations for the cause of this mantle instability and its regional migration include convective loss of a thickened thermal boundary layer (Houseman et al, 1981, JGR v. 86, p.6115-6132) and foundering of underplated oceanic lithosphere (Bird, 1979, JGR, v. 84, p.7561-7571). The crust had been previously thickened in the Mesozoic and, after sufficient heating, began to spread, thereby decompressing mid-crustal magma chambers during Phase 2 syntectonic eruptions. Despite large variations in the magnitudes of upper crustal strain during this phase, the crust thinned uniformly, suggesting that the lower crust was capable of large-scale lateral flow - an inference supported by petrologic observations of extensive crustal melting. Extensional strain rates decreased and magmatism waned during Phase 3 in response to the loss of gravitational potential and the cooling and depletion of the lower crust and upper mantle. The present crustal thickness of 30 km, after having been stretched by an average factor of 2.0, argues that up to 5 km of the crustal column in the Basin and Range represents new basaltic material added to the crust during stretching.

PETROLOGIC EVOLUTION OF LAVA FROM THE PUU OO ERUPTION OF KILAUEA VOLCANO, HAWAII

GARCIA, Michael O., Hawaii Institute of Geophysics, University of Hawaii, Honolulu, HI 96822
RHODES, J. M., Geology-Geography Dept., University of Massachusetts, Amherst, MA 01003
WOLFE, E. W., U.S. Geological Survey, Cascades Volcano Observatory, Vancouver, WA 98661

The continuing eruption of Kilauea Volcano, 1983 to present, provides an excellent opportunity for a detailed petrologic examination of magmatic processes. Lavas from the early episodes (1, 2 and part of 3) are hybrids produced by mixing a differentiated rift-zone-store magma (~5.6 wt. % MgO) with a more mafic magma. These hybrid lavas were erupted along a discontinuous, 7.5 km long fissure. Fissure eruptions were replaced by central vent eruptions following episode 1. During episode 3, a central vent, Puu Oo, formed that became the principal site of eruptive activity for episodes 4-47. Lava erupted from the Puu Oo vent during episodes 3-47 is geochemically distinct from the lava erupted during the early episodes. It has a complex geochemical pattern that may result from the interplay of two processes. The lava became progressively more mafic through episode 31. This variation is probably due to magma mixing, with the proportion of the evolved component decreasing with time. The evolved component is a mixture of the hybrids erupted during episode one. The mafic component is probably a magma intruded from the summit reservoir and has a high MgO content (>9.5 wt. % MgO). The composition of this component is similar to that erupted at the summit of Kilauea in September, 1982.

Superimposed on the long-term compositional variation is a short-term variation that occurred during repose periods between the episodic eruptions of Puu Oo. Over periods of 8 to 36 days, 3 x 10^6 m^3 or more of fractionated magma formed. Lava erupted during the early part of some episodes is 5 to 6% more fractionated than later lava. For most episodes (especially episodes 11-29), more mafic lava was not erupted, indicating that the volume of fractionated lava in the Puu Oo reservoir prior to those eruptions was greater than that erupted.

At the beginning of episode 48 (July, 1986), the locus of eruptive activity to shift 3 km downrift. The composition of lava erupted at this new vent is identical to that erupted at Puu Oo in 1985 and 1986. The lava at the new vent has been erupted nearly continuously and has been sampled once a week. A low amplitude (~1.2 wt. % MgO) temporal variation in the composition of the lava has been noted. This MgO variation follows by roughly 35 days changes in summit tilt. For example, an increase in tilt is followed by increase in MgO content of the lava. An increase in tilt may reflect an increase in magma supply from the mantle, which causes greater pressure in the summit to vent plumbing system. This may force the magma through the rift zone faster causing the magma to be less fractionated when it is erupted. The apparent 35-day lapse between a summit tilt change and the succeeding compositional change of the lava erupted at the vent yields a magma velocity of ~22 m/hr through the conduit system from the summit to vent.

THE TUMISA VOLCANO: A PYROCLASTIC FLOW AND DOME COMPLEX IN THE ANDES OF NORTHERN CHILE

GARDEWEG, Moyra C., Servicio Nacional de Geología y Minería, Casilla 10465, Santiago , Chile.
JONES, Adrian P., School of Geological Sciences, Kingston Polytechnic, Penryhn Road, Kingston upon Thames, KT1 2EE, U.K.

The Quaternary Tumisa Volcanic Complex (2.1 to <0.4 Ma), located in the western margin of the Main Cordillera of the Chilean Andes around 23° 30' S and 67°50' W, is a composite of three local and partially overlapping units of lavas and domes built on extensive pyroclastic flows (300 m2) found mainly west of the cones and, surrounded by later parasitic flank-domes. Later hydrotermal alteration has produced a small economic sulphur deposit. The pyroclastic flows correspond to monolithologic lithic and pumiceous block-rich flows (1-60m thick), characteristically unwelded, unsorted, chaotic and topographically controlled. These originated in the explosive collapse and/or disruption of growing domes in an initial explosive phase in the evolution of the volcano. The blocks, of juvenile material, show wide ranges in vesicularity (s.g. 2.6 to 0.7 gm/cm3) and, ocassionaly prismatic jointing, this late blocks commonly more than a meter in size reaching up to 10 m near the vent.

The lavas of the cones and blocks of the pyroclastic flows are calc-alkalinés andesites and dacites with common (up to 10% in volume) dark, fine grained basic inclusions of basaltic to andesitic-basaltic composition in sharp contact with the host lavas. The andesites and dacites are highly porphyritic (10-40%) with large (cm-scale) plagioclase, hornblende and orthopyroxene phenocrysts. Partially resorbed quartz and biotite coexist with mantled olivine containing Cr-spinel. The basic inclusions comprise acicular, sometimes skeletal hornblende, elongate plagioclase and varius xenocrysts derived from the host rock set in brownish, vesicular rhyolitic glass to give a hyalodoleritic texture. They are interpreted as a basaltic liquids which quenched on intrusion into a dacitic or andesitic magma chamber. The intrusion induced physical changes in the chamber and mixing of the two magmas, which involved the mechanical transfer of phenocrysts between both liquids and chemical exchanges. The basic inclusions have chemical trends continuous with the host lavas, with no overlap or gap between them. Some of the characteristics of this suite of rocks can be explained by fractional crystallization, but their mineral assemblages and textural features indicate that the dominant process was late stage magma mixing between two magmas of contrasting composition, in a high level crustal chamber. It appears that such a mixing process has been important in the generation of the Upper Cenozoic calc-alkaline suites of the Central Andes.

CHEMICAL DIVERSITY OF MAFIC LAVAS FROM THE MOUNT BACHELOR VOLCANIC CHAIN, OREGON

GARDNER, C. A., U.S. Geological Survey, Cascades Volcano Obs., 5400 MacArthur Blvd., Vancouver, WA. 98661

The 26-km-long, N-S-trending chain of cinder cones, lava flows, and shield volcanoes that compose the 18-8-ka-old Mount Bachelor volcanic chain (MBVC) in central Oregon records a history of petrologically diverse mafic volcanism. About 40 km^3 of basalt and basaltic andesite (49-57 wt% SiO_2) was erupted during two major pulses of activity that are subdivided into four eruptive episodes.

Most MBVC lava flows are olivine- and plagioclase-phyric and contain plagioclase, olivine, Fe-Ti oxides, and, in some samples, clinopyroxene in the groundmass. Lava flows from the summit cone of Mount Bachelor, which have the highest SiO_2 contents, are petrologically distinct, in that they contain augite as a phenocryst phase and pigeonite supplants olivine as a groundmass phase. Olivine and most plagioclase phenocrysts are normally zoned, but plagioclase phenocrysts also exhibit oscillatory and reversed zonation. In most thin sections, both clean and sieve-textured plagioclase phenocrysts occur. In two thin sections, two groundmass plagioclase compositions coexist.

A total of ten geochemical groups were distinguished within the MBVC suite on the basis of major- and minor-element whole-rock geochemistry. On silica-variation diagrams, these groups fall into two distinct assemblages (PM1 and PM2), both of which contain basalt and basaltic andesite. Basalt of the more voluminous PM1 assemblage is less evolved (Mg#=66-62, FeO*=8.07-7.3, TiO_2=1.5-1 wt%, Cr=295 ppm) than that of the PM2 assemblage (Mg#=59-54, FeO*=10.7-10, TiO_2=1.95-1.75 wt%, Cr=215 ppm). Also, rare-earth-element (REE) contents for PM1 geochemical groups (which include Mount Bachelor) are lower than those for PM2 groups. A third assemblage (PM3), containing only basaltic andesite, was noted on the basis of relatively low REE contents (the lowest of the MBVC suite) and high Al_2O_3 and Sr contents.

Petrologic models support mineral-fractionation trends, basalt-normalization patterns, and incompatible trace-element ratios in suggesting that basaltic andesite within both the PM1 and PM2 assemblages, was derived from basalt by crystal fractionation of the observed mineral assemblage. Petrologic models and petrography, however, suggest that replenishment and minor amounts of magma mixing also probably occurred. The data further suggest that none of the PM1 or PM2 basalt is parental to the REE-depleted PM3 basaltic andesite and that the source area for the PM3 magma differs from that of either the PM1 or PM2 magma.

The vents of the more voluminous PM1 lava flows lie along the central axis of the chain, whereas those for the volumetrically much smaller PM2 and PM3 lava flows occur off the axis. Temporal relations show that several geochemical groups comprising two to three assemblages were erupted, apparently concurrently, during the two most voluminous eruptive episodes. These relations suggest that the MBVC was underlain by more than one magma chamber.

MAGMA WITHDRAWAL AND ERUPTION DYNAMICS DURING THE PLINIAN PHASE OF THE LONG VALLEY CALDERA ERUPTION, CALIFORNIA

GARDNER, J.E., SIGURDSSON, H., and S.N. CAREY University of Rhode Island, Graduate School of Oceanography, Narragansett, R.I. 02882

The climactic eruption of Long Valley Caldera (~0.74 Ma) began with a plinian phase, followed by emplacement of ashflows comprising the Bishop Tuff. Isopachs based on minimum thicknesses at several distal localities give a volume for the plinian phase of about 260 km^3 (120 km^3 D.R.E.), in good agreement with previous estimates of between 100 and 300 km^3 (Bailey et al., 1976). Pumice and lithic isopleths for seven levels of the plinian deposit show that eruption column height and mass eruption rate (MER) increased during the first 60% of the plinian phase from 24 to 42 km and $7x10^7$ to $4.5x10^8$ kg/s, respectively. Column height and MER remained relatively constant during the rest of the plinian phase with a possible peak at the end, coinciding with the initiation of ashflow emplacement. The duration of the plinian phase, based on an average MER of $3.5x10^8$ kg/s, was 8.5 days. With a constant viscosity of $3.5x10^6$ P and assuming a slight magma density gradient the initial magma withdrawal layer thickness is estimated on the order of 160 m, increasing by 60 to 80% at the end of the plinian phase.

Concentrations of both incompatible (≥85% in the glass) and compatible trace elements increase slightly in the lower half of the plinian deposit and then decrease markedly in the upper half. Preliminary results suggest that most of this trend reflects variations in melt composition and is thus unrelated to crystal content. Pumice density, ranging from 0.51 to 0.81 g/cm^3, correlates negatively with these trace element trends and may record a slight volatile gradient within the magma chamber.

Covariation of incompatible and compatible elements cannot be attributed to fractionation by the crystal assemblage found in the pumice, but may reflect inherent heterogeneities within the magma chamber. As withdrawal layer thickness increased during the first half of the eruption, concentrations of most trace elements slightly increased. The withdrawal layer then tapped less "enriched" magma which became dominant by the end of the plinian phase. These trends cannot be produced by simple two-endmember mixing, thus, they represent the tapping of one or more heterogeneous layers. Renewed eruption of the more "enriched" magma in the first pyroclastic flow (Hildreth, 1977) may have resulted from vent widening by initial ring fracturing.

SCIENTIFIC DRILLING IN THE VALLES-TOLEDO CALDERA COMPLEX AND ITS HIGH TEMPERATURE GEOTHERMAL SYSTEMS

GARDNER, J.N. (Los Alamos National Laboratory, Los Alamos, NM, 87545); HULEN, J.B. (University of Utah Research Institute, Salt Lake City, UT 84108); GOFF, F. (Los Alamos National Laboratory, Los Alamos, NM, 87545); NIELSON, D.L. (University of Utah Research Institute, Salt Lake City, UT 84108); ADAMS, A., CRISWELL, C.W., GRIBBLE, R., MEEKER, K., MUSGRAVE, J.A., SHEVENELL, L., SMITH, T., SNOW, M.G., AND WILSON, D. (all of Los Alamos National Laboratory, Los Alamos, NM 87545)

Research bore Valles Caldera #1 (VC-1) was continuously cored to 856 meters in the southwestern moat zone of the 1.12 Ma Valles caldera, and penetrated 333 meters of post-caldera volcanic and volcaniclastic rocks. The base of the VC-1 volcanic sequence is a breccia of South Mountain Rhyolite (0.507 Ma), which lies beneath 35 meters of volcaniclastic conglomerate. Over the conglomerate is a sequence of ignimbrites and interbedded rhyolites, which form a group of moat volcanic products that are chemically and petrogenetically distinct from other post-caldera rhyolitic rocks. VC-1 also penetrated an active hydrothermal outflow plume from the caldera. Deep geothermal fluids from the caldera breach the ring fracture and leak along the northeast-trending Jemez fault zone, mixing with meteoric fluids along the way. Active for about 1 million years, the outflow plume gives rise to the fluids that emerge today as the well known hot springs of the Jemez Springs-Soda Dam area.

VC-2a and VC-2b were continuously cored to 528 meters and 1.762 kilometers, respectively, on the western flank of the Valles caldera's resurgent dome. Each hole sampled interbedded sequences of caldera-fill volcaniclastic rocks and densely welded intracauldron Bandelier Tuff. The sequence in VC-2a is: 0-22 m landslide, volcaniclastic sandstone, and accretionary lapilli tuff; 22-65 m upper tuffs; 65-80 m debris flow and volcaniclastic sandstone; 80-356 m Tshirege Member tuffs; 356-362 m volcaniclastic rocks; 362-477 m Otowi Member tuffs; and 477-528 m (T.D.) lower tuffs. The sequence in VC-2b is: 0-174 m landslide, debris flows, volcaniclastic sandstones, accretionary lapilli tuffs, and an intermediate (?) composition, subvolcanic intrusion; 174-366 m Tshirege Member tuffs; 366-372 m volcaniclastic sandstone; 372-599 m Otowi Member tuffs; 599-742 m lower tuffs; 742-798 m Santa Fe Group sandstone and Cochiti Formation debris flows; 798-1558 m Paleozoic sedimentary rocks; and 1558-1762 m (T.D.), quartz monzonite. Stratigraphy and extremely lithic-rich (up to 90%) zones in the tuffs suggest that the VC-2a and -b drill sites may be proximal to vents. The Tshirege (?) tuffs also show intrusive, or possibly invasive, relations with the underlying volcaniclastic rocks. Structural correlations between the core holes indicate the earlier Toledo caldera (1.45 Ma; Otowi Member tuffs) experienced no structural resurgence similar to the Valles caldera. The hydrothermal system penetrated by these bores consists of a shallow vapor-rich cap, which has evolved from an earlier 200°C liquid-dominated system, stratigraphically separated from underlying, stacked, liquid dominated reservoirs up to at least 300°C.

PALEOMAGNETIC AND ROCK MAGNETIC INVESTIGATIONS IN VALLES CALDERA CSDP EXPERIMENTS: IMPLICATIONS FOR THERMOCHEMICAL PROCESSES ATTENDING CALDERA DEVELOPMENT

GEISSMAN, J.W., Dept. of Geology, University of New Mexico, Albuquerque, NM 87131; GARNDER, J., GOFF, F., ESS-1, Los Alamos National Laboratory, Los Alamos, NM 87545

CSDP Experiments VC-1, VC-2A, and VC-2B have provided an unprecidented opportunity for detailed study of the response of the magnetization signal in a wide range of lithologies to complex igneous and subsequent, thermochemical processes, largely of Quaternary age. In the VC-1 core hole, paleomagnetic data prompted a revision in the volcanic stratigraphy and indicated that the moat volcanic sequence intersected is less than 730 ka, consistent with isotopic age data. Late Paleozoic strata contain up to three components of remanent magnetization (RM): (1) a first removed moderate positive indication RM (I=+58°, α_{95}=2.8°, N=105 samples), unblocked by 350°C when in magnetite and 550°C when in hematite; (2) an RM of opposite declination and moderate negative inclination (D=173°, I=-47°, α_{95}=5.5°, N=47, assuming the positive inclination RM is north-seeking), thought to have been acquired during an elevated thermal flux attending Valles Caldera development; (3) a shallower negative inclination, RM (D=160°, I=-11°, α_{95}=4.4°, N=28) removed over the highest ranges of unblocking temperatures, of late Paleozoic age. The first two RM's are viscous partial thermoremanent magnetizations (VPTRMs); one was activated at moderate (~300°C) temperatures between 1.47 and 0.97 Ma, attending caldera development during the Matuyama chron, the other at near present downhole temperatures (~100-180+°C) during the Brunhes normal polarity chron (past 730 ka) and perhaps within the past 10 ka.

In the VC-2A experiment, the upper 450 m of section, including rocks with weak MOS_2 mineralization, is characterized by RM's, carried by magnetite, of moderate negative inclination, acquired prior to the Brunhes, in agreement with preliminary interpretations of the volcanic stratigraphy. Quartz poor welded tuffs below 460 m exhibit only positive inclination RM's, again in magnetite. A possible explanation is that the lowermost part of the section is pre-Bandelier in age, erupted during the Olduvai subchron or Gauss chron. Alternatively, these units could have been remagnetized at near-present thermal conditions during the past 730 ka. Based on thermal activation theories for assemblages of magnetized particles, the presence of a reverse polarity RM requires that temperatures in the upper portion of the VC-2A section during the Brunhes did not exceed 300-350°C.

Representative samples from the complete VC-2B section, the most recent experiment, are presently being measured. Hematite clastic strata, inferred to be the Permian Yeso and Abo Formations, from over 500 m of section, yield only moderate to steep positive inclination magnetizations; no vestige of a shallow inclination late Paleozoic magnetization can be isolated in these units, unlike the VC-1 experiment. Assuming a correct interpretation of the stratigraphy, these red beds appear to have been pervasively thermochemically remagnetized, possibly at temperatures approaching 400°C, during a normal polarity chron (i.e., Brunhes or earlier). The quartz monzonite pluton at the base of the section contains only low coercivity magnetizations; a constraint on the age of this unit from paleomagnetic data is doubtful.

THE EVOLUTION OF BININTIANG MALAKI AND BALANTOC CRATERS, TAAL VOLCANO ISLAND

GERONIMO,S.G., Philippine Institute of Volcanology & Seismology, 5th & 6th Flrs, Hizon Bldg., Quezon Ave., Quezon City, Philippines

On the northwestern limb of Taal Volcano Island, Batangas Province lies a basaltic volcanic field composed of several coalescing tuff rings and a tuff cone with contrasting morphology, stratigraphy and deposit types. These centers are parasitic cones of Taal Volcano. The formation of Binintiang Malaki and the Balantoc craters were apparently controlled by a NW-SE trending fracture system which runs across the volcano island.

Binintiang Malaki, a tuff cone, is relatively young and is characterized by a steep edifice. It has produced a wide spectrum of deposits ranging from very wet pyroclastic surges to lava extrusions. The Balantoc Craters, however, are monogenetic centers that show low-angle vent forms. Deposits produced are mostly of pyroclastic tuffs. These centers are proximally positioned but exibit contrasting land forms and eruption styles.

Based on the vent morphology, stratigraphy and textural characteristics of the deposits, Binintiang Malaki has erupted lavas and pyroclastics with extremely low to very high degree of lake water involvement, in contrast to the Balantoc Craters deposits which are predominated by relatively dry pyroclastic tuffs. The strong shift from very dry eruptions to phreatic type for Binintiang Malaki cone, is due to the 'open and seal' process which took place in successive cycles during the cone build-up. The Balantoc Craters, however, possess a 'tight' vent system which limited the access of water into their conduits. These factors are primarily controlled by hydrologic conditions within area. It is believed that the dike that feeds the Balantoc craters has completely recrystallized and reactivation of these craters may unlikely occur in the future. The conduit of Binintiang Malaki probably stems from a branch dike, similar to that of the Balantoc Craters, but accessible to the deeper magma reservoir of Taal Volcano Island.

MAGMA MIXING AND TEXTURAL DEVELOPMENT OF RHYOLITES FROM THE INYO VOLCANIC CHAIN, EAST-CENTRAL CALIFORNIA, USA

R. G. Gibson and M. T. Naney, Chemistry Division, Oak Ridge National Laboratory, P. O. Box 2008, Oak Ridge, TN 37831-6110

Detailed petrographic and electron microprobe analysis of silicic lavas from the Inyo volcanic chain, east-central California, supports the hypothesis that magma mixing was the primary process responsible for the bimodal mineral chemistry and banded texture typical of these rocks. Twenty-three surface and drill hole samples examined in detail may be subdivided into three groups: I) non-banded tephra and dike samples from the Inyo Craters containing andesine phenocrysts, Mg-rich opx [Fe/(Fe+Mg)=0.12-0.35], and abundant ilmenite; II) non-banded samples from the upper part of the Obsidian Dome tephra and the dike near Obsidian Dome containing oligoclase+alkali feldspar phenocrysts, Fe-rich opx+cpx+bt+amph [Fe/(Fe+Mg)= 0.5-0.8], and no ilmenite; and III) banded samples from the early Obsidian Dome tephra, the conduit beneath Obsidian Dome, and the body of the Glass Creek, South Deadman, and Obsidian Domes. Banding is defined either by variations in glass color and chemistry or variable microlite abundance. Compositions of all minerals in group III are bimodal and compositional groups can be correlated with textural features; grains with compositions similar to group I minerals occur in brown glass or microlite-rich bands whereas grains with compositions like their counterparts in group II occur in microlite-poor bands of colorless glass.

Features of the group III samples are best explained by mechanical mixing between two crystal-bearing siliceous magmas similar to groups I and II. On the basis of phenocryst compositions and glass chemistry, the mixing end members are interpreted to have been of rhyolitic (T=775°C, log fO_2=-15.0, fH_2O=30-175 bars) and dacitic (T=870°C, log fO_2=-11.9, fH_2O=100-600 bars) compositions. Because all of the dike samples are unmixed, mixing probably occurred while the two end-members were being drawn simultaneously through the subvolcanic conduits. Banding in the group III samples formed either as 1) samples of the comingled magmas were immediately vented to the surface and quenched, preserving bands of two distinct glass compositions (e.g. early Obsidian Dome tephra) or 2) bands of the hotter dacitic magma crystallized microlites in order to attain thermal and chemical equilibrium with the cooler rhyolitic magma.

Research sponsored by the Division of Engineering and Geosciences, Office of Basic Energy Sciences, U. S. Department of Energy under contract DE-AC05-84OR21400 with Martin Marietta Energy Systems, Inc. RGG participated in the Laboratory Cooperative Postgraduate Research Training Program administered by Oak Ridge Associated Universities.

THE EL RUIZ MAGMATIC-HYDROTHERMAL SYSTEM

GIGGENBACH, W. F., Chemistry Division, DSIR, Private Bag, Petone, New Zealand

Before and after the 13 November 1985 catastrophic eruption, the volcano Nevado del Ruiz in Colombia received considerable geological, geophysical and geochemical attention. In attempts to assemble the resulting information into an internally consistent model, it soon became apparent that many of the phenomena associated with the eruption could not be explained in terms of magmatic processes alone.

The lack of cumulative deformation and of deep earthquakes suggested that no major magma movements were associated with the eruptive period. The amount of 'new' magmatic material produced during the eruption was also much too small to account for the large amounts of SO_2 released then and during subsequent periods. The stratigraphy of the eruption deposit corresponds essentially to the ejection of volcanic debris followed by eventual prodution of very minor amounts of pyroclastic material hot enough to form a welded tuff. Hornblende and biotite in this high temperature material are marginally decomposed suggesting that the pumice ejected was derived from a highly degassed, 'aged', high viscosity magma body. The enigmatic occurrence of 'banded' tremor also is not readily explained in terms of purely magmatic processes.

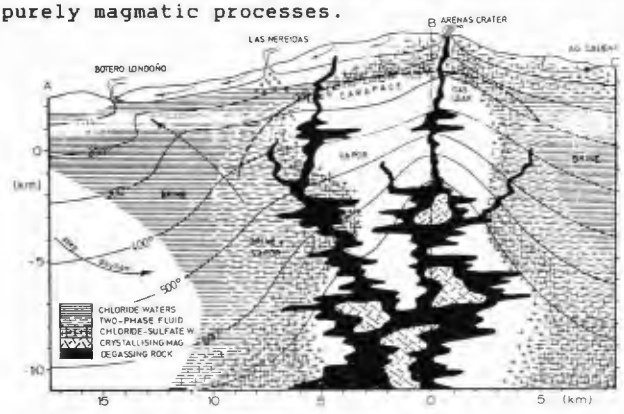

The quite common discharge of thermal waters, acid chloride-sulfate at elevations >3000m, neutral chloride-bicarbonate at lower altitudes, and of fumarolic steam over the flanks of the volcano suggets that the El Ruiz structure houses an extensive hydrothermal system. The acid-sulfate waters are likely to be produced by direct absorption of magmatic vapors into shallow groundwater, their occurrence over wide areas indicates that high temperature, SO_2 containing gases are present at very shallow levels within the upper parts of the volcanic structure. The large amounts of originally magmatic gases having accumulated within this reservoir may play an important part in the eruptive process and may explain the absence of detectable magma movement and the large amounts of SO_2 produced. Injection of stored vapors into overlying shallow groundwater and associated acoustic phenomena may be responsible for 'banded' tremor and other seismic signals. The model above is compatible with geological, geophysical and, especially, isotopic and chemical evidence.

CALK-ALKALINE POST-OROGENIC VOLCANISM OF THE PYRENEES

GILBERT, J.S, BICKLE, M.J. & CHAPMAN, H.J., Department of Earth Sciences, University of Cambridge, Cambridge, CB2 3EQ, England.

The Hercynian orogenic belt of NW Europe originally extended from the Gulf of Mexico to eastern Europe. It formed between Devonian and Permian times probably as a result of the interaction between the African (Gondwana) plate in the S and the Laurasian plate in the N. Hercynian age rocks of the Pyrenean chain have been interpreted as having formed through processes on the Iberian "microplate" which was situated between the colliding plates prior to, and during, the Hercynian orogenic event.

Many evolution models of the Hercynian belt invoke both subduction related processes as well as continent-continent collision. However, the high temperature-low pressure Hercynian metamorphism in the Pyrenees has recently been re-interpreted in terms of a purely extensional setting (Wickham & Oxburgh 1987, Phil. Trans. R. Soc. Lond. A321, 219-243).

This study presents new chemical and isotopic data for the post-orogenic Permo-Carboniferous volcanic and plutonic rocks of the Pyrenees which were erupted either during or just post the metamorphism. These calc-alkaline igneous rocks have previously been interpreted as subduction or collision related, although the possibility remains of them having been the result of extensional tectonic processes where basalt interacted with crust. The volcanic rocks crop out in an E-W trending strip along the southern margin of the Axial zone of the Pyrenees and dip towards the S at approximately 80°. The poorly exposed and weathered nature of the rocks places restrictions on the interpretation of chemical data and in turn interpretation of the tectonic setting. The rocks range in composition from rhyolitic to basaltic, with the bulk being peraluminous rhyolitic ignimbrites.

Trace and REE data for the most basic rocks confirm their calc-alkaline nature but is unable to discriminate between a directly subduction related origin or an origin involving mixing with crust. The Nd-isotopic values for all the volcanic rocks are consistent with incorporation of a substantial Mid-Proterozoic crustal component and depleted mantle model ages range from 1400 to 2180 Ma. These data therefore do not preclude a rift-related setting with eruption of mainly crustally derived melts. The nature of the mantle derived melt component is therefore poorly constrained in the Pyrenees as it is elsewhere in the Hercynian orogen.

TH ISOTOPES AND U-SERIES DISEQUILIBRIA IN SUBDUCTION-RELATED VOLCANIC ROCKS

GILL, J. and WILLIAMS, R., Earth Sciences, UCSC, Santa Cruz, CA 95064

We have measured the activities of 5-6 radionuclides in samples from more than 60 volcanoes at 12 continental margins or island arcs: Cascades, Costa Rica, Aleutians, Sunda, Banda, Sangihe, Marianas, Izu-Bonin, Tonga, Antilles, and especially Japan and Papua New Guinea. In about half the samples from continental margins, both ^{238}U and ^{226}Ra are in radioactive equilibrium with ^{230}Th. In the other half there is excess ^{230}Th or ^{226}Ra or both, typically by 5-20% and 10-50%, respectively. These characteristics are similar to those of intra-plate alkali basalts. They can result from 1-2% batch melting of lherzolite, or from larger degrees of open-system dynamic melting.

In contrast, Th-enrichment is rare in island arcs, occurring only in some volcanoes behind volcanic fronts. Virtually all arc magmas have excess ^{226}Ra (but not ^{228}Ra), which decrease from maxima of about 300% with differentiation. There is ^{238}Th equilibrium in about half of these, and excess U in the other half. The greater Ra-enrichment in arc than continental margin magmas is attributed either to differences in the processes of melt extraction beneath continents, or to crustal residence times several thousand years longer at continental margins. The U-enrichment may reflect recent preferential exhalation of U during slab dehydration, or the stability of accessory phases such as perovskite or rutile which preferentially retain Th, or slower or more fractional melt extraction. The greater likelihood of excess U in arcs requires that these differences are more pronounced there.

Just as $(^{238}U)/(^{230}Th)$ ratios provide uniquely quantitative measurements of incompatible element fractionation during magma genesis, so $^{230}Th/^{232}Th$ ratios also uniquely constrain a modern-day versus time-averaged parent-daughter trace element ratio in the source: the Th/U ratio. Th isotope ratios can be normalized to those in chondrites, with B_{Th} values ranging from -2 to +28 in sources of arc magmas. This range is similar to that of Sr isotopes, and greater than that of Nd or Hf isotopes with which B_{Th} values correlate positively.

About half the subduction-related samples lie within the Th-Sr-Nd-Pb mantle arrays defined by oceanic basalts. Because the difference in Th/Sr between sediments and the MORB source is greater than the difference between their Nd/Sr ratios, this isotopic similarity is a better test of sediment-subduction models, and limits sediment to <1% in most cases.

Th isotope ratios are atypically high in the other half of subduction-related samples. Indeed, Th isotopes differ from Sr-Nd-Pb in that arcs, not MORB, are the most depleted global reservoir for Th. These high Th isotope ratios may be caused bv: recent source depletion via partial melting which would preferentially extract Th (e.g., at ridge crests or in backarc basins); recent source metasomatism by U-enriched slab-derived fluids; or slow melt formation or ascent rates. Source-depletion is suggested because the highest Th isotope ratios are in rocks with very low Th+REE+HFSE concentrations, but all three processes may contribute. U-enrichment of arc sources as well as magmas contributes to the secular decrease in the Th/U ratio of the mantle.

THE PICRITIC TERTIARY LAVAS OF W. GREENLAND: CONTRIBUTIONS FROM 'ICELANDIC' AND OTHER SOURCES.

GILL, R.C.O., *RHBNC, University of London, Egham TW20 0EX, UK*, HOLM, P.M., PEDERSEN, A.K, and HALD, N., *University of Copenhagen, Denmark*, LARSEN, J.G., and NIELSEN, T.F.D., *Geological Survey of Greenland, Copenhagen, Denmark* and THIRLWALL, M.F., *RHBNC, London, UK.*

The Tertiary volcanic region of West Greenland is notable among CFB provinces for the unusually high proportion of primitive picritic magmas erupted. The picrite basalts, forming a sequence of lavas and hyaloclastites up to 1 km thick near the base of the volcanic succession, show a wide range of composition (MgO 14-29 wt%, Mg number 70-85 and Ni 400-1400 ppm), largely consistent with olivine control. Chondrite-normalised incompatible-element patterns show relative depletion in the most incompatible elements, but have $(Ce/Y)_N$ ratios slightly above 1.00, the overall enrichment being around 10x chondrite. Zr/Nb ratios range from 14 to 33 similar to T- and N-type MORB.

$^{87}Sr/^{86}Sr$ and $^{143}Nd/^{144}Nd$ ratios of nearly all samples coincide with the oceanic mantle array (the ranges are 0.7029-0.7035 and 0.51316-0.51301 respectively). The distribution of compositions lies close to PREMA, similar to present-day Iceland but distinct from picrites of other CFB provinces.

Slight differences in elemental and isotopic composition can be distinguished between stratigraphic and geographic sub-groups. For example the 'Older Disko' picrite basalts have the least fractionated REE patterns ($[Ce/Y]_N$ = 0.9-1.4), the 'Younger Disko' picrite basalts have $[Ce/Y]_N$ = 1.2-1.9, while those from Lower Svartenhuk and Ubekendt Ejland are more enriched in LREE ($[Ce/Y]_N$ = 1.4-3.0). These sub-groups define a series of fields distributed perpendicular to the mantle array in $^{143}Nd/^{144}Nd$-$^{87}Sr/^{86}Sr$ space. The coupling of elemental differences with both Sr and Nd isotopic composition suggests that old enrichment/depletion processes have contributed, albeit subtly, to compositional variation among the picritic lavas.

The covariance of incompatible element ratios and radiogenic isotopes can be interpreted in terms of three main source components: a depleted source similar to that of North Atlantic N-type MORB, a more enriched OIB (Iceland-like) source, and a component depleted in radiogenic Sr relative to $^{143}Nd/^{144}Nd$. The overall similarity of isotopic and trace element patterns to those of modern Icelandic values may reflect the influence on asthenospheric melts of a mantle jet rising beneath the evolving intra-continental rift into which the lavas were erupted. The chemical and isotopic characteristics of the West Greenland lavas contrast with the early picritic/ankaramitic equivalent lava in the East Greenland Tertiary volcanic province, in which the contribution of an enriched source domain is much more apparent.

CALCITIC CARBONATITE LAVAS REINTERPRETED; THEIR SIGNIFICANCE FOR MAGMA GENESIS

GITTINS, J. & JAGO, B., Department of Geology, University of Toronto, Toronto, Ontario, Canada M5S 1A1

Calcitic lavas, as opposed to the highly alkalic Oldoinyo Lengai type, are often alleged to be calcitized alkalic types in which nyerereite is pseudomorphed by calcite. Criteria have been published purporting to distinguish "calcitized" nyereriete from primary igneous calcite that crystallized at elevated pressure prior to eruption. Such an interpretation of calcitic carbonaite lavas substantially increases the incidence of alkalic carbonatite magma and makes them much less a rarity than the single active volcano Oldoinyo Lengai suggests. This, in turn, affects ideas about the course of carbonatite magma evolution and the evaluation of candidates for primitive carbonatite magmas.

Studies of Oldoinyo Lengai lavas erupted during the past year show far higher F and Cl contents than were previously recognized and indicate how F, Cl, Sr, Ba, and REE are distributed mineralogically. These studies confirm that F and Cl are concentrated in the quenched liquid surrounding the phenocrysts, and experimental work confirms that F and Cl partition preferentially into water-saturated calcite liquids that lack Na, but that when Na is present Cl is lost to the aqueous fluid leaving F in the carbonate liquid.

Further studies of the role of F in carbonatite magma evolution show that 5 wt.% of F lowers liuidus temperatures in the system Na_2CO_3-$CaCO_3$ by 170°-200°C at 1 kbar and increases liquid density causing flotation of calcite and nyerereite. Melting experiments show that the composition $Na_2Co_3$25-$CaCo_3$75 with 5% F crystallizes calcite at one atmosphere pressure making it clear that highly calcitic magmas containing F can erupt to form Cl-bearing lavas with almost no trace of nyereriete.

Since most calcitic carbonatite magmas are, therefore, not metasomatised or diagenetically altered alkalic carbonatites there is less reason to accord the highly alkalic magma a primary role in carbonatite magma evolution but rather to consider it a product of fractional crystallization under rather special conditions. The role of F now seems to be incontrovertible. We believe that F at least equals and probably exceeds the importance of water in carbonatite magma evolution. It enables fractional crystallization to develop Oldoinyo Lengai type magma from a more primitive, dry, modestly alkalic, calcite-dolomite magma, and together with Cl controls the crystallization of the Nb ore mineral pyrochlore. Because of crystal flotation consequent upon the effect of F on magma density the lavas of Oldoinyo Lengai do not always represent the composition of the magma from which they crystallized.

QUANTITATIVE ANALYSIS OF THE TRANSPORT AND DEPOSITION OF VOLCANIC ASH FALLS

GLAZE, L.S., SELF, S., University of Texas at Arlington, Arlington, Texas 76019

An essential tool for volcanologists, particularly those involved in hazard awareness, is a predictive capability for ash fallout. This is important both in regions proximal to the source volcano and in distal areas. While there are models available to enable prediction of clast sizes and thickness of tephra fall from the eruption column in the near-source areas, there have been few attempts to quantitatively model the fallout of ash from downwind plumes.

The Suzuki model incorporates turbulent atmospheric diffusion to predict the dispersal and fallout of ash, giving the mass distribution of tephra on the ground. Parmaters controlling this process are the average vertical emplacement velocity, column height, grain size distribution, and atmospheric conditions. Suzuki's model assumes a single mean wind velocity at all altitudes and can predict ash fall for simple atmospheric conditions, as in the August 17, 1980, eruption of Hekla, accurately. An improvement to the model has been made incorporating varying wind velocities with altitude, and tested on the July 22, 1980, ash fall from Mount St. Helens. Results show an encouraging ability to duplicate an ash deposit resulting from dispersal in varying winds.

This model has also been applied to the September 16, 1986, eruption of Lascar in north Chile. Almost everything that is known of this eruption was learned from remote sensing data. Ash fall was recorded at only one point downwind from the volcano. Complicated wind conditions at the time of the eruption, with strong winds blowing to the southeast and to the east at even higher altitudes. This complex wind structure explains the dispersal pattern predicted by the model which has two distinct local maxima, one along an easterly axis and one along a south-easterly axis. The model also predicts that the proximal isomass contours close well short of the vent as was predicted in an earlier study of this eruption. In the Lascar case remote data provided all parameters needed for the dispersal model except the atmospheric wind profile which was taken from a radiosonde ascent downwind of the volcano. With little ground truth it is possible to predict ash falls from volcanoes given volumes of ash, eruption column heights, typical grain size parameters, and weather patterns. With further detailed documentation of eruptions such models can be refined and ash fall predictions improved.

SOURCE OF POTASSIUM IN POTASSIUM-METASOMATIZED, EXTENDED TERTIARY ROCKS OF THE MOJAVE DESERT

GLAZNER, ALLEN F., Dept. of Geology, CB#3315, University of North Carolina, Chapel Hill, NC 27599, and **BARTLEY, JOHN M.**, Dept. of Geology and Geophysics, University of Utah, Salt Lake City, UT 84112

Highly potassic, metasomatized volcanic and sedimentary rocks are common in extended terranes of the southwestern U.S. Although these rocks have been mistaken in some cases for primary ultrapotassic rocks, several lines of textural, field, and geochemical evidence demonstrate their metasomatic origin. K-metasomatic rocks are characterized by (1) partial to complete replacement of plagioclase by Or_{95-100} adularia; (2) exceedingly high K_2O contents which commonly surpass 12 wt%, coupled with strong enrichment in Rb and strong depletion in Ca, Mg, and Sr; (3) oxidation of mafic minerals, with local stability of biotite; and (4) association with strongly tilted rocks and low-angle normal faulting. In general, K-metasomatized rocks are found in the hanging walls of low-angle normal fault complexes.

Two models have been proposed for the source of the potassium in K-metasomatized rocks. In the first, K is derived from below, from hydrogen-metasomatized lower-plate rocks; in the second, K is derived from above, from circulating brines in a saline lake above fractured volcanic rocks. Our studies of K-metasomatism in three areas of the Mojave Desert (Cady Mountains, Rodman Mountains, and Waterman Hills) support the lower-plate model and conflict with the brine model. Evidence against the brine model includes: (1) lack of lacustrine sedimentary rocks of the proper age, and (2) control of metasomatism by upward-terminating, dike-like, jasper-filled breccia zones, which clearly served as conduits for K- and Si-rich fluids from below. The brine model cannot account for the jasper-filled breccia zones.

We have studied biotite granodiorite in the lower plate of the Waterman Hills detachment fault (WHDF) in an effort to learn the source of the potassium. Three textural variants occur; (1) lineated biotite granodiorite, far from the WHDF; (2) strongly mylonitic granodiorite, close to the WHDF; and (3) cataclastic granodiorite, in steep, deeply penetrating, anastomosing shear zones that cut the granodiorite. Preliminary geochemical data (Figure 1) indicate that cataclastic and mylonitic granodiorite are significantly depleted in K_2O relative to fresh granodiorite, as would be expected from their greenschist mineralogies. In addition, mylonitic granodiorite is strongly depleted and cataclastic granodiorite is mildly depleted in SiO_2 relative to fresh granodiorite (Figure 1). Silica liberated by these reactions could supply the matrix of the jasper-filled breccia zones. Other elements follow enrichment/ depletion patterns that are complementary to upper-plate rocks; for example, Rb is strongly depleted and Sr is mildly enriched in cataclastic and mylonitic granodiorite. Thus, lower- and upper-plate rocks could represent complementary parts of a hydrothermal system.

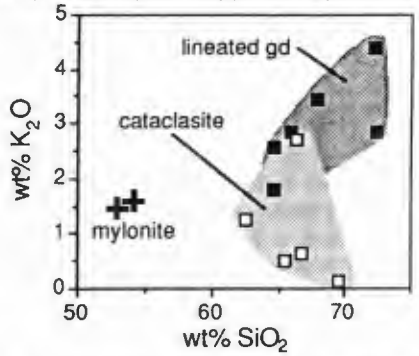

Figure 1. Plot showing depletion of K in mylonitic and cataclastic granodiorite relative to fresh granodiorite.

An argument against derivation of potassium from lower-plate rocks is that the amount of chloritic mylonite in the lower plate is generally insufficient to account for all the potassium added to the upper plate. However, steep cataclastic zones in the Waterman Hills make up about 25 vol% of the granodiorite and penetrate deeply into the lower plate. These zones may tap a large enough volume of the lower plate to account for the added potassium.

In summary, derivation of potassium from saline lakes cannot explain Mojave Desert occurrences of K-metasomatized Tertiary rocks. Derivation from altered lower-plate rocks satisfies current geochemical and field data. Although this model need not apply to all occurrences of K-metasomatized rocks in the southwestern United States, the strong association of K-metasomatized rocks with low-angle normal faulting and chloritic lower-plate alteration suggests a genetic link.

THE VOLCANO IN THE LAKE IN THE PLAIN ABOVE THE HOTLINE: THE SINKER BUTTE STORY

GODCHAUX, M.M., Department of Geology, Mount Holyoke Coll., So. Hadley, MA 01075
BONNICHSEN, Bill, and JENKS, M.D., Idaho Geological Survey, Moscow, ID, 83843

Sinker Butte is a complex and majestic mid-Pleistocene hydroclastic volcanic edifice which topographically and aesthetically dominates the surrounding countryside. It is the most prominent in a line of about 20 spatter-frosted tuff cones which extends for 120 km from southeast of Bruneau, Idaho, northwestward to Marsing, Idaho. This line is near the SW margin of the western Snake River Plain graben, coinciding with the present course of the Snake River. Basalt magmas rose repeatedly to the surface, encountering a wide variety of eruptive environments around and within a large lake. Earlier eruptions produced sheet flows which had subaerial portions and also developed a variety of water-affected deposits the particular type depending upon flow rate and morphology, lake level and bottom topography, etc. These deposits included (1) columnar flows in which portions of the columns are hydrated, (2) palagonitized pillow deltas, and (3) littoral deposits composed of hyaloclastite and debris flows derived from them. Later eruptions were dominated by the explosive interaction of rising batches of basalt magma with the water-soaked deposits. The explosions produced bedded to massive, fresh to palagonitized, and block-laden to accretionary lapilli-bearing hydroclastic tuffs and blast and/or surge and pyroclastic flow deposits carrying up to Volkswagen-sized blocks. At most vents, the explosive phase "died with a whimper" as subsurface water was depleted and/or the edifices were built up above lake level, so that the final ejecta formed welded-spatter rims or caps on the tuff cones.

At Sinker Butte the first 100-foot layer is a complex package of tongues of massive grey-green to black, cindery-to muddy matrix debris-flow (?) deposits, cross-bedded black sand beach (?) or deltaic (?) deposits, and thin white silt (loess?) lenses containing sparse basaltic cinders. Above this layer is a discontinuous layer (50 feet thick or less) of spectacular base-surge deposits exhibiting low-angle cross-bedding, accretionary lapilli, and cut-and-fill structures. The third layer up from the bottom is the thickest (about 600 feet) and most extensive; it contains at least two angular unconformities, and consists mostly of bedded yellow to red palagonite tuff with large block and bomb sags whose asymmetries indicate ballistic trajectories centered within the tuff cone. Pillow-rind fragments generally become more numerous and larger upward, as the proportion of lake-sediment chips diminishes, suggesting a progressive deepening of the explosion focus. The uppermost 100 feet of Sinker Butte is a flat-topped sheet of welded spatter and cinders, with a small centrally-located spatter vent about 20 feet high Large flows issued from a well-exposed radial dike on the east side, and probably from now-obscured flank vents on the southwest and/or west sides. One of these flows entered water and built a pillow delta more than 6 miles away from Sinker Butte.

DATING OF HYDROTHERMAL EVENTS IN ACTIVE GEOTHERMAL SYSTEMS: EXAMPLE FROM THE VALLES CALDERA, NEW MEXICO, USA

GOFF, F., GARDNER, J., and WOLDEGABRIEL, G., Los Alamos National Laboratory, Los Alamos, NM 87545
GEISSMAN, J. W., University of New Mexico, Albuquerque, NM 87131
HULEN, J. B., University of Utah Research Institute, Salt Lake City, UT 84108
SASADA, M., Geological Survey of Japan, Tsukuba, Ibaraki, 305 Japan
SHEVENELL, L., Desert Research Institute, P.O. Box 60220, Reno, NV 89506
STURCHIO, N. C., Argonne National Laboratory, CMT 205, Argonne, IL 60439
TRAINER, F. W., P.O. Box 1735, Corrales, NM 87048

Several dating techniques are now available to unravel the complex evolutionary history of active geothermal systems. These include K-Ar (K-rich hydrothermal minerals), U-Th, and U-U disequilibrium (hot springs deposits; Qtz, Cc, and Fluor veins), electron spin resonance of cold or near-surface hydrothermal minerals, paleomagnetic analysis of hydrothermally altered rock, and thermal transient analysis of temperature gradients. When combined with geologic mapping, stratigraphy, dates on fresh volcanic products, and other scientific studies, the relation of hydrothermal events to volcanic and geomorphic processes can be evaluated. Using these techniques, an informative hydrothermal history has been developed for the Valles caldera, NM (see Table 4, field excursion 17B of this meeting).

Earlier work revealed that the Valles caldera formed 1.12 Ma, that resurgence occurred approximately within 0.1 m.y. of caldera formation, that ring-fracture volcanism was essentially continuous from 1.05 to 0.13 Ma, and that a large, intracaldera lake was drained ≥0.5 Ma. Recent work shows that the Valles liquid-dominated system (Tmax=300°C) first formed ~1 Ma (U-U, K-Ar, paleomag.) and that it has been continuously active to the present day (U-U, U-Th). A sub-ore-grade Mo deposit was formed from liquid water at shallow levels beneath Sulphur Springs ~0.66 Ma (K-Ar). The SW caldera wall was breached by the ancestral Jemez River between 0.5 and 0.48 Ma which cut a canyon 335 m deep into the SW moat (U-U, K-Ar, paleomag.). Because the Mo deposit now resides in a vapor zone above the liquid-dominated reservoir, the vapor zone formed after 0.66 Ma. Fluid inclusion evidence from Sulphur Springs indicates that the top of the liquid-dominated reservoir descended rapidly. It is our belief that this rapid descent is linked to sudden drainage of the intracaldera lake ~0.5 Ma.

After draining of the lake, the SW moat was progressively filled with rhyolitic flows and tuffs (~0.4 to 0.13 Ma) that are chemically and isotopically distinct from other post-caldera rhyolites and the Bandelier Tuff. We suggest that this more recent batch of shallow, silicic magma is partly responsible for the relatively long life of the Valles geothermal system. This shallow magma may be entirely responsible for renewed hot spring activity in San Diego Canyon (≤110 Ka, U-Th) and the "reheating" event observed in deep Precambrian rocks beneath the western caldera margin. The reheating is best expressed as an increase from 60°C/km at 3000 m to 90°C/km at 4400 m. Thermal transient analysis and $^{40}Ar/^{39}Ar$ suggest this event is ≤60 Ka whereas fluid inclusion data indicate a post-caldera age.

A COMPARISON OF LATE PROTEROZOIC AND MESOZOIC BASALTIC DIKES ALONG THE EASTERN MARGIN OF NORTH AMERICA

GOLDBERG, STEVEN A., and BUTLER, J. Robert, Department of Geology, University of North Carolina, Chapel Hill, NC 27599-3315

Late Proterozoic metadiabase dike swarms are exposed within Precambrian basement massifs dispersed along the Appalachian orogen, and are among the best-preserved records of Late Proterozoic rifting related to the opening of Iapetus. These dikes exhibit similar field and age relations, and occur from northwestern North Carolina to southeastern Labrador within the Globe, Elk River, Watauga River, Pedlar, Lovingston, Honey Brook-Mine Ridge, Avondale-West Chester, Reading Prong, Lincoln, and Long Range massifs. Although dikes in some massifs show a wide range of orientations, the mean for individual massifs varies from N30E to N63E, with a mean of N44E for the entire Appalachians. The dominant NE trends could be attributed to a consistent NW-SE tensional regime controlled by mantle stresses rather than crustal anisotropies that existed during the separation of Laurentia. These trends contrast sharply with the NW to NNW trends of Mesozoic diabase dikes from the southern and central Appalachians, which are associated with the opening of the Atlantic Ocean. In this area, reactivation along structural fabric from the Late Proterozoic rift zone was apparently not a controlling factor in the break-up of Pangea.

Average major element abundances for different Late Proterozoic swarms (Bakersville, Skyline, Hudson Highlands) show relatively minor variation. Likewise, enrichments of light rare earth, incompatible, and high field strength element abundances are similar (Figure below), and suggest a common or similar petrogenesis. Dikes are enriched in TiO_2, K_2O, P_2O_5, Zr, light REE, and depleted in Ni and Cr relative to MORB and Mesozoic dikes. Arguments based on trace element and Sr and Nd isotopic data within the southernmost swarm indicate that the enrichments could not result from assimilation or mixing of typical crustal material. Compositions reflect significant olivine, plagioclase, and clinopyroxene fractionation in proportions of approximately 1:9:10. ϵNd values of -1.6 to +3.5 and ϵSr values of +10.3 to +12.4 for an age of 734 Ma are consistent with derivation from a non-MORB mantle source depleted with respect to Nd/Sm, but enriched with respect to Rb/Sr. A comparison of the most primitive Late Proterozoic and Mesozoic dike compositions suggests distinct source characteristics.

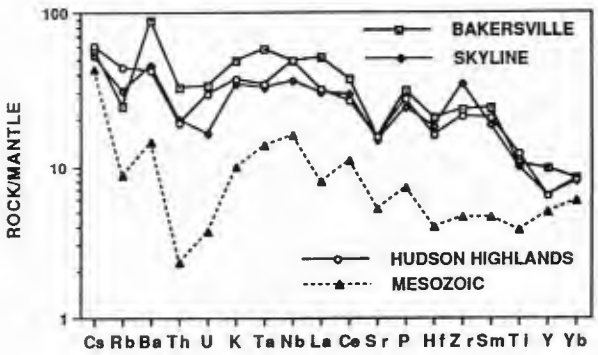

PETROLOGY AND GEOCHEMISTRY OF THE THIRTYNINE MILE VOLCANIC FIELD, COLORADO: An Intracontinental Shoshonitic Suite

GOLDMAN, D.S., Dept. of Geology, University of Florida, Gainesville, Fl., 32611,
PERFIT M.R., Dept. of Geology, University of Florida, Gainesville, Fl., 32611,
RIDLEY, W.I., Branch of Geochemistry, U.S. Geological Survey, Denver, Co.

The Thirtynine Mile volcanic field (TMVF), located in central Colorado, covers an area of approximately 1000 Km2 and is composed of basaltic to rhyolitic lavas of Oligocene age. The northeastern part of the TMVF is dominated by volcanic breccias and lahars which are interbedded with shoshonitic basaltic flows. A felsic suite of rocks comprised of latites, trachytes and quartz-trachytes is locally abundant. The shoshonitic basalts are characterized by the presence of cpx, plagioclase, magnetite, and olivine. The felsic suite is mineralogically dominated by plagioclase, hornblende, biotite, and large (up to 1mm) euhedral phenocrysts of apatite.

The samples are moderately to highly fractionated and with increasing SiO2 contents and decreasing Mg#s, there are fairly systematic increases in Rb, Ba, Zr, Nb, and La whereas Sr, P, and Ni exhibit decreasing concentrations. The TMVF rocks are characterized by high K2O contents (2.5 to 5.5wt.%) and high LIL element abundances; Ba = 1140 to 2740 ppm and Sr = 488 to 1330 ppm. Although LIL concentrations are high, Rb/Sr ratios are low (.032 to .32). The shoshonitic basalts and felsic rocks have similar steeply fractionated (La/Yb = 9 to 22 Chon), and LREE enriched (100 to 200 x chrondrites), REE patterns with no significant Eu anomalies.

Major and trace element modeling suggests that the felsic rock suite could not have been derived by simple fractional crystallization of a parental shoshonitic magma. However, calculations indicate that the felsic rocks could be related to each other by fractional crystallization. Isotopically the TMVF have low radiogenic lead values; 206/204 17.40 to 17.76, 207/204 15.45 and 15.47, 208/204 37.32 to 38.99 and relatively unradiogenic initial 87Sr/86Sr ratios; .704740 to .705401. The isotopic data in conjunction with trace element ratios suggest the influence of a lower crustal component during the petrogenesis of the TMVF magmas. Available 87/86 Sr and trace element data for regional upper crustal rocks suggest that the TMVF magmas did not assimilate a significant amount of upper crustal material. Evidence suggests the relative enrichment of LILs and LREE reflects an enriched mantle component in the petrogenesis of primary magmas. The spatial and temporal association between the basalts and felsic suite and evolution of the TMVF cannot be explained by simple crystal fractionation processes or melting within the crust, yet the two suites form relatively continuous chemical variation trends and exhibit only slight isotopic differences. This suggests magma mixing or AFC type processes between mantle-derived magmas and lower crustal material occurred during the petrogenesis of the TMVF.

SUBAQUEOUS VOLCANICLASTIC ROCKS OF THE CONFEDERATION LAKE AREA, ONTARIO, CANADA: DISCRIMINATION BETWEEN PYROCLASTIC AND EPICLASTIC EMPLACEMENT

GORTON, M.P., & STIX, J., Department of Geology, University of Toronto, Toronto M5S 1A1, Canada

A sequence of Archean-age subaqueous volcaniclastic rocks crop out in Lost Bay of Confederation Lake, Ontario. The rocks consist dominantly of intermediate-felsic composition lapilli tuffs, tuff breccias, tuffs and fine grained epiclastic rocks that have a strong turbidite association, as well as minor lavas.

The coarse grained rocks are volcaniclastic mass flow deposits that are massive, matrix-supported, and consist of light colored clasts set in a darker matrix rich in crystals, juvenile and lithic fragments. The deposits frequently are capped by fine-grained debris. Individual clasts may be ungraded, normally graded, and/or inversely graded. Juvenile clasts consist of andesitic pumiceous and dense fragments that exhibit a range of vesicularities and may represent a continuum. Quartz feldspar porphyry fragments with highly enriched trace element compositions are found within lapilli tuffs and tuff breccias near the top of the Cycle II stratigraphy. It is difficult to determine whether these fragments are juvenile or lithic, and whether they represent eruption from new source volcanic domes and/or unroofing of hypabyssal intrusions. There is insufficient evidence to show the coarse units are direct products, without reworking, of explosive eruptions. The andesitic composition, abundant unvesiculated and pumiceous clasts, and relatively thin flow deposits characteristic of the coarse rocks imply dome growth and fragmentation. Dome growth and eruptions may have been subaqueous as well.

Turbiditic fine grained rocks crop out in much of Lost Bay. The rocks range from very fine grained cherty tuffs to coarse grained clastic deposits. Many of the very fine grained units lack quartz, while coarser grained volcaniclastic rocks may contain as much as 15% detrital quartz. The deposits are both massive and bedded. Normal grading, Bouma sequences, convoluted bedding, ripup clasts, and flame structures are common. The units lack sedimentary structures indicative of deposition above wave base.

Near the base of the Lost Bay stratigraphy very fine grained clastics crop out that generally lack quartz and have relatively low trace element concentrations with steep REE patterns. Stratigraphically above, these deposits give way to coarser clastics that contain abundant detrital quartz, have much higher trace element contents, and generally flat REE patterns. This change occurs at approximately the same stratigraphic level as the first appearance of abundant quartz feldspar porphyry fragments, with similarly high trace element concentrations, in the lapilli tuffs and tuff breccias. These observations indicate that detrital quartz within the fine grained deposits may have been derived from the reworking of quartz feldspar porphyry fragments. These quartz-rich fine grained units thus appear epiclastic, not pyroclastic.

EVOLUTION OF MAGMA MIXING IN AN ALKALINE SUITE : THE GRANDE CASCADE SEQUENCE (MONTS DORE, FRENCH MASSIF CENTRAL)

Alain GOURGAUD, Université Blaise Pascal et UA n°10, Centre de Recherches Volcanologiques, 5 rue Kessler, 63038 Clermont-Ferrand, France.
Benoit VILLEMANT, Université Pierre et Marie Curie, Laboratoire de Géochimie comparé et systématique, 4 place Jussieu, 75230 Paris Cedex 05, France.

The Monts Dore area is an alkaline volcanic district where the youngest part, Sancy volcano, has been built up by successive trachyandesitic eruptive cycles. One of these cycles is represented by the Grande Cascade sequence (about 0.40 m.y. old). The exposed sequence begins with hydromagmatic pyroclasts followed by a thick lava flow. These units exhibit spectacular mechanical mixing features (basic cognate inclusions, globules and strip-like bands) between coexisting and contrasted magmas. At the summit of the sequence, basic trachyandesitic lava flows are texturally homogeneous. Their hybrid origin is postulated.

The mineralogical data indicate the transfer of phenocrysts from the basic component to the felsic one and vice versa : strong mineralogical disequilibrium features (Mg - olivine in the felsic component and sanidine in the basic one), strong zoning (normal or reverse) of most phenocrysts, polymodal distribution of the plagioclase compositions.

Major and trace elements systematics applied to the sequence indicate :

- linear correlations between major elements (correlation coefficients close to 1), between hygromagmaphile elements, and between transition and hygromagmaphile elements. The representative points of basic trachyandesites plot on the linear trends, which is compatible with their assumed hybrid origin.
- the end-members are highly contrasted : primary basalt and evolved trachyte.

Magma mixing has been modelled using major and trace elements together and calculating a "best mixing line" (Provost and Allègre, 1979). The results of the calculations suggest that magma mixing, involving basaltic and trachytic endmembers, was a major process in the evolution of the Grande Cascade sequence and confirms that the trachyandesite are considered hybrids.

MAGMATIC EVOLUTION OF LATE CENOZOIC VOLCANIC ROCKS OF THE LAU RIDGE, FIJI

GRAHAM, I.J., Institute of Nuclear Sciences, DSIR, P.O. Box 31-312, Lower Hutt, New Zealand, COLE, J.W., Department of Geology, University of Canterbury, Private Bag, Christchurch, New Zealand, GIBSON, I.L., Department of Earth Sciences, University of Waterloo, Waterloo, Ontario, Canada.

There are three groups of lavas exposed on islands of the Lau Ridge: the Lau Volcanic Group (LVG), erupted between 13.95 and 5.40 Ma are predominantly andesite; Korobasaga Volcanic Group (KVG), 4.39-2.44 Ma old are predominantly basalt and Mago Volcanic Group (MVG), 2.03-0.28 Ma old, are basalt-hawaiite. LVG and KVG lavas are medium-K tholeiitic rocks with high LILE/HFSE ratios and negative Ta anomaly, characteristic of island arcs, while MVG lavas are ne-normative alkalic rocks with high LILE and HFSE, and slightly positive Ta anomaly, all characteristic of ocean island basalts. $^{87}Sr/^{86}Sr$ ratios for LVG and KVG lavas range from 0.70280-0.70400 and for MVG from 0.70347-0.70366, while $^{143}Nd/^{144}Nd$ ratios for LVG and KVG range from 0.513033-0.513081, and for MVG from 0.512887-0.512900.

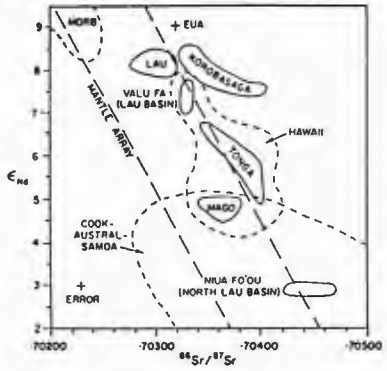

LVG lavas are interpreted as having been erupted in a primary island arc (Vitiaz arc) during the Miocene. Basaltic lavas were derived by approximately 19% partial melting of peridotite in the mantle wedge with only minor LILE enrichment from the subduction zone. Andesites and dacites are products of low-pressure plagioclase-pyroxene-titanomagnetite dominated crystal fractionation. KVG lavas are considered to have been erupted during the initial stages of rifting in the Lau Basin. There are chemical differences between KVG lavas in the northern and southern ends of the Lau Ridge - those at the northern end appear to have been derived from a more depleted source than LVG but with a greater amount of subduction component; those at the southern end probably came from a slightly enriched source with less suduction component. MVG basalts and hawaiites appear to have been derived from an enriched mantle with little or no subduction input. The hawaiites cannot have been derived from the basalts, and the two magma types must have come from different sources, indicating mantle heterogeneity. Differences in the basalts on the island of Mago are consistent with some olivine + augite fractionation. The lack of subduction influence indicates the MVG lavas are tectonically unrelated to the present-day Tonga arc, and the lack of depletion indicators suggests they are tapping a different part of the mantle wedge.

THE GEOCHEMICAL EVOLUTION OF TAMBORA VOLCANO, INDONESIA

GRALL-JOHNSON, H.M., SIGURDSSON, H., and CAREY, S., Graduate School of Oceanography, University of Rhode Island, Kingston, R.I. 02881, USA

Volcanic stratigraphy of Tambora has been studied from exposures in the 1815 caldera walls and evidence from sediment cores in adjacent ocean basins. Following a long period of strato-cone construction, Tambora developed its first caldera prior to 43,000 y.b.p. During this period about twenty adventive cones erupted on the flanks of the volcano, including the island of Satonda to the north. The early caldera was largely filled by a 400 m thick Caldera Lava formation between 43,000 and 10,700 y.b.p. Subsequent phreato-magmatic activity in the early caldera produced the 100 m thick Black Sands tephra formation between 10,700 and 5,900 y.b.p. Sub-plinian activity and pyroclastic flow events produced the Brown Tuff formation between 5,900 and 1,210 y.b.p. Thus a period of dormancy of about 1,100 years occurred before the cataclysmic eruption of 1815, resulting in formation of the second caldera. Post-1815 activity has produced two lava flows on the floor of the new caldera.

The geochemistry and petrology of 42 samples from all the above formations has been studied. Tambora products range from moderately potassic trachybasalts (Na_2O 3.6, K_2O 2.8, SiO_2 49.7%) characterising the strato-volcano, to trachyandesites (Na_2O 4.7, K_2O 5.2, SiO_2 59%) in the 1815 products. All products of the Tambora volcanic system define very coherent geochemical trends, and in general the magmas become increasingly more evolved and incompatible-element enriched with time. At the most primitive end of the trends is basalt from the adventive crater of Satonda (MgO 10.2%). Incompatible element content of Tambora products ranges from 530 to 1150 ppm for Ba and 60 to 220 ppm for Rb. The temporal trend of enrichment in incompatible elements is displayed by the major stratigraphic succession: strato-volcano formation, Caldera Lavas and 1815 products, but Black Sands and Brown Tuff formations and parasitic vents on the flanks of Tambora do not conform to this relationship. Preliminary calculations show that the principal geochemical trends can be attributed to shallow-level fractional crystallization processes.

LARGE RHYOLITES IN THE KEWEENAWAN MIDCONTINENT RIFT PLATEAU VOLCANICS OF MINNESOTA - LAVAS OR RHEOIGNIMBRITES?

GREEN, J. C., Geology Dept., University of Minnesota-Duluth, Duluth, MN 55812 and
FITZ, T. J., Dept. of Geology, University of Delaware, Newark, DE 19711

Rhyolite and icelandite eruptive units make up 10-25% of the bimodal, gently tilted 1.1 Ga North Shore Volcanics. Along with numerous smaller units which are evidently mostly lavas are about 18 large flows (50-400 m thick) that have ambiguous physical characteristics common to both typical lavas and rheoignimbrites. Airfall ash and pumice are rare. The icelandites contain 58-68% SiO_2 (ave. 63.9, n=17) and 6.51-8.80% Na_2O+K_2O (ave. 7.67); rhyolites contain 69.0-76% SiO_2 (ave. 72.6, n=29) and 7.1-10.0% Na_2O+K_2O (ave. 8.42). Most are aphyric or sparsely porphyritic, with Fe-augite, magnetite, ± fayalite as mafic phenocrysts. Three of the largest can be traced for 25-40 km along strike, and were probably originally much larger with volumes of 100-300 km^3. Crucial exposures of top and basal contacts are typically lacking. Several units which show highly vesicular, flow-folded top zones and/or flow-folded and breccia bases are interpreted as lavas; one, perhaps 1 km thick, is a large dome. One unit may be an agglutinate, and others, which show relict fiamme at the top or base, are probably rheoignimbrites. One, in Duluth, was emplaced as two cooling units: a low-T unwelded unit followed by a high-T unit which underwent secondary flowage. A few, including the largest, were probably very high-T (>1000°C), flowing en masse and crystallizing directly (not devitrifying) to phaneritic tridymite + feldspar from this hot, dry, rapidly emplaced "reconstituted lava" (see Fig. 1). No caldera-related structures have been found, despite the large volumes of some of these units, and they are thought to have been erupted through fissures from deep crustal chambers.

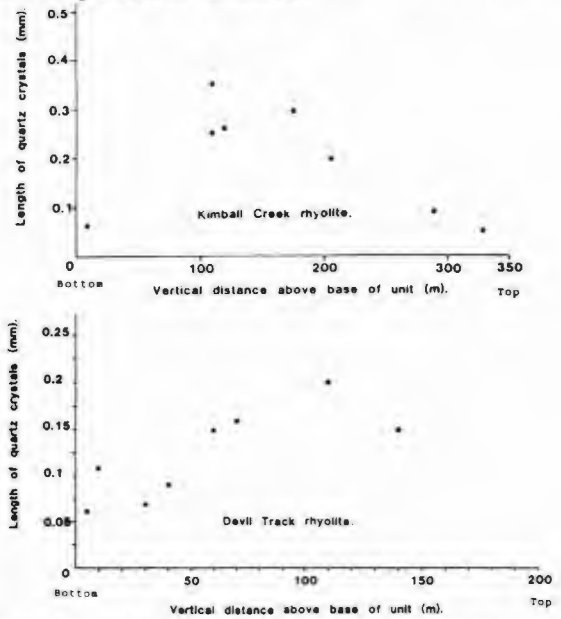

Fig. 1 Two large rheoignimbrites crystallized as simple cooling units, as shown by grain size maximum of groundmass tridymite paramorphs near the center.

GEOLOGY AND PETROLOGY OF THE MOUNT GARIBALDI VOLCANIC FIELD, GARIBALDI VOLCANIC BELT, SOUTHWESTERN BRITISH COLUMBIA, CANADA

GREEN, Nathan L., Department of Geology, University of Alabama, Tuscaloosa, AL 35487-0338.

At least six Pleistocene-Holocene volcanic complexes are located within the Mount Garibaldi volcanic field. The oldest eruptive products occupy paleovalleys along the western and southern margins of the field and consist of: (i) 0.46-0.51 Ma dacite lavas and (ii) a possibly contemporaneous succession of highly altered andesitic pyroclastic and laharic breccia with minor basaltic andesite, andesite, and dacite lavas. The overlying Mount Garibaldi edifice was constructed during at least two distinct periods of activity. Initial (0.22-0.26 Ma) eruptions produced a predominantly dacitic composite cone and a series of domes on its southern and northern flanks. Holocene activity involved (i) Pelean eruptions that constructed a supraglacial dacitic tuff breccia cone, and (ii) summit extrusion of dacite lava after melting of the underlying continental ice sheet led to collapse of the western flank of the cone. Younger basaltic andesite and dacite lavas were extruded on the southern margin of the volcanic field.

Mount Garibaldi dacites are characterized by ferromagnesian phenocryst assemblages which indicate varied crystallization conditions: (i) Cpx+Opx+Mt±Ilm; (ii) Hbl+Cpx+Opx+Mt±Ilm; (iii) Hbl+Opx±Cpx+Bt+Mt; and (iv) Hbl±Bt+Mt+Ilm. Some dacites contain fused granodiorite xenoliths. Associated andesites have similar phenocrysts, but also locally contain plagioclase-two pyroxene crystal clots cored by corroded olivine (Fo_{80-74}) with orthopyroxene (En_{76-71}) and vermicular magnetite overgrowths. Basaltic andesite phenocryst assemblages include olivine (Fo_{83-78}), plagioclase (An_{73-43}), clinopyroxene, orthopyroxene (En_{80-73}), and titanomagnetite; one lava contains resorbed pargasitic hornblende. Observed mineralogical relations, coupled with Fe-Ti oxide/pyroxene thermometry and thermodynamic calculations, suggest that the andesitic and dacitic magmas underwent extensive crystallization at 949-1069°C and ln fO_2 of about -21 within upper crustal (2-5 kb) reservoirs.

Mount Garibaldi lavas are generally characterized by low Rb and TiO_2; low to moderately high Nb, Ta, Hf, Zr, Ni, Cr, Th/U (2.48-3.70), and La/Yb_N (4.07-16.63); high Sr, Ba, and K/Rb (544-843); and variable $\delta^{18}O$ (5.7-7.7) and $^{87}Sr/^{86}Sr$ (0.7031-0.7036) contents. Major and trace element variations are compatible with open-system evolution of discrete magma batches involving assimilation-fractional crystallization (AFC) accompanied by varied degrees of magma mixing. Lack of correlation between isotopic compositions and incompatible element abundances probably reflects variations in both source composition and AFC processes. Upper-crustal contamination of individual magmas was heterogeneous, involving incorporation of both xenocrysts and rhyolitic melts derived from underlying Cretaceous granodiorites.

THERMAL HISTORIES OF VICTORIAN PERIDOTITE XENOLITHS

GREIG, A. AND NICHOLLS, I.A., Dept. Earth Sciences, Monash University, Clayton, Victoria, Australia, 3168.

At the Anakie cone, SP peridotite xenoliths may be classified into three textural types: granuloblastic tabular (GT), granuloblastic equant (GE) and coarse. GT xenoliths are unusually fertile containing abundant Al-rich enstatite and Cr-diopside with OL Mg87-89. Foliations are defined by tabular OL neoblasts and stringers of SP and PX. Porphyroclasts are mainly OPX with rare strained OL, illustrating the recrystallized nature of these rocks. Both porphyroclast and neoblast OPX have homogeneous cores, but show marked compositional gradients 100-200μm from their rims, with core to rim increases in CaO (0.6-1.2%), Al_2O_3 (4.5-6%) and TiO_2 (0-0.3%) and a decrease in MgO (32.5-31.5%). Thermometry based on the Ca contents of neoblasts and most porphyroclasts of OPX (Sachtleben & Seck, 1981) suggest these xenoliths had equilibrated to temperatures of 1000°C (core values) before being heated to 1150°C (rim values). However, a few OPX porphyroclasts with rare, thick CPX exsolution lamellae show evidence of rehomogenization in CaO and Al_2O_3. This indicates the heating event followed prior cooling to 1000°C. CPX also preserve a history of heating with rims depleted in CaO and enriched in MgO and Al_2O_3.

Granuloblastic equant xenoliths consist of neoblasts of OL, OPX, CPX and porphyroclasts of OPX. Foliation is well defined by pyroxene rich layers. OPX porphyroclasts have cores with abundant fine CPX lamellae and unexsolved rims. OPX neoblasts are also unexsolved.

OPX zoning is opposite to that in GT xenoliths. Al_2O_3 decreases from core to rim (5-2.5%), MgO increases (32.5-33.5%), while CaO remains constant. Temperatures for neoblasts based on Al exchange between OPX and SP (Sachtleben & Seck, 1981) are 1000°C for cores, decreasing to 800°C at rims. CaO contents of neoblasts give temperatures of 900°C, which probably represent blocking temperatures, but porphyroclasts give temperatures of up to 1300°C when CPX lamellae are integrated into the analysis. CPX also show cooling, with rims enriched in CaO and depleted in Al_2O_3 relative to cores. Thus in contrast to GT xenoliths, GE xenoliths have had an extensive cooling history.

Coarse xenoliths have a similar thermal history to GE xenoliths.

Two contrasting thermal regimes in the mantle have clearly been sampled. The reheating experienced by GT xenoliths is most likely due to proximity to basaltic magma (represented by cumulate xenoliths at this locality?). The homogeneous cores of OPX neoblasts in some GE xenoliths show appreciable variation in Al_2O_3 contents (4.5-5.3%) at levels lower than those of porphyroclasts (5.5%, reconstructed composition). This suggests that recrystallization has occurred at progressively lower temperatures and that once formed the neoblasts have continued to cool, leading to marginal zoning. Thus cooling and deformation were probably contemporaneous and may be related to mantle upwelling.

IDENTIFYING SEISMOLOGICAL PRECURSORS FOR MT.ETNA ERUPTIONS.

GRESTA, S., Istituto di Scienze della Terra, Catania University, Italy, and LONGO, V., Istituto Internazionale di Vulcanologia - CNR - Catania, Italy.

A rewiev of seismological studies at Mount Etna during the period 1978-1987 has been performed in order to identify possible eruptive precursors.

The eruptive activity of Etna volcano, during the considered time interval,was very high (9 flank eruptions and many explosions and eruptive episodes at the summit craters).

Some case-histories have been considered by focusing the analyses on both earthquakes and volcanic tremor. Time variations of the following parameters were investigated:

- Earthquake daily number
- Seismic energy release
- Hypocentral locations
- b value of the frequency-magnitude law
- Tremor energy
- Tremor spectral contents

Objective criteria to define as "precursor" a time change of a certain parameter have been proposed, too. The variation of a parameter at the time t can be defined as "precursor" when the difference between its value V(t) and its previous average value V_a is greater than the standard deviation of V_a:

$$|V(t) - V_a| > \sigma_{Va}$$

Nevertheless, by considering a single precursor only, even in this way, the number of "correct predictions" resulted less than the "false alerts".

The correlation among the most promising parameters (earthquake number and energy, and tremor spectra shapes) seems a better tool for the "prediction" of lateral eruption by using seismic data.

It seems more difficult the "prediction" for both terminal and subterminal eruptions, that seem start without any appreciable change for the considered seismological parameters.

EVIDENCE FOR THE GENERATION OF CALC-ALKALINE ANDESITES FROM COMPOSITIONALLY ZONED LAVA AT MEDICINE LAKE VOLCANO, N. CALIFORNIA

GROVE, T.L., BAKER, M.B., KINZLER, R.J., Department of Earth, Atmospheric and Planetary Sciences, Mass. Inst. Tech., Cambridge, Ma., 02139, USA. and DONNELLY-NOLAN, J.M., U.S. Geological Survey, 345 Middlefield Road, Menlo Park, CA 94025

Several well exposed, compositionally zoned high-alumina basalt (HAB) - andesite eruptions provide evidence of the magmatic processes which lead to the generation of andesite at Medicine Lake Volcano. These andesites are compositionally similar to typical medium-K orogenic andesites, and the basalts are similar to HABs found throughout the Cascade volcanic province. Three flows have been studied in detail: Burnt Lava, Giant Crater - Chimney Crater (GC-CC) lava field and the Callahan Flow. At Burnt Lava, quenched magmatic inclusions of HAB are found along with xenoliths of melted granitic crust in a compositionally uniform andesite. At the GC-CC lava field and the Callahan flow there exists a one to one correlation between age and chemistry; the oldest lavas are compositionally most evolved (andesite), and the youngest lavas are the most primitive (basalt). The evolved lavas are aphyric and contain 1-4 % phenocrysts and inclusions which record the existence of at least 3 magmatic components. One component is primitive mantle-derived basalt. The second is a highly evolved ferroandesite or ferrobasalt which was produced by extensive fractionation of the basalt parent. The third is an upper crustal component which has been melted with the heat generated from the HAB to andesite fractionation process.

Simple geochemical models of the assimilation process don't work. Models which assume that assimilation of crust occurred simultaneously with fractionation of the HAB parent estimate unrealistically large amounts of assimilation, and estimate a ratio of assimilation to fractional crystallization (R) >1 for both GC-CC and the Callahan. Such a large amount of assimilation is inconsistent with thermal models estimated for the melting of crust by crystallization of basalt at shallow crustal levels (R = 0.3). Therefore, the process of assimilation at GC-CC and the Callahan did not involve continuous addition of crust as fractionation occurred. Instead, heat and mass transfer were decoupled. The fractionation of basalt to ferroandesite occurred without extensive contamination of basalt by crust, but supplied heat to melt surrounding crust. Subsequent injections of primitive HAB into the magmatic system triggered mixing of compositionally distinct and spatially isolated reservoirs to produce the compositionally zoned flows.

EVIDENCE FOR CRUSTAL AND MANTLE SOURCES OF TERTIARY, EXTENSION-RELATED VOLCANISM IN EAST-CENTRAL NEVADA

GRUNDER, A. L., and FEELEY, T. C., Department of Geology, Oregon State University, Corvallis OR 97331

Hundreds of cubic kilometers of two-pyroxene andesites and dacites, biotite-hornblende dacites, and biotite rhyolites were erupted during early stages of extension (∿39 to 34 Ma) in east-central Nevada. These lavas and tuffs were accompanied by minor volumes of basaltic andesite, containing olivine, pyroxene, and xenocrystic quartz, hornblende-pyroxene andesites, and high-silica biotite rhyolite. The volcanic section is preserved in fault blocks and slices in a ∿100 km-wide belt of extreme crustal extension, bounded to the west by the Butte Mountains and to the east by the Confusion Range. The Tertiary section disconformably overlies the upper units of the Paleozoic miogeoclinal section.

The lower part of the volcanic section, the Early Suite, crops out mainly on the periphery of the area, is characterized by disequilibrium mineral textures and assemblages in basaltic andesites to dacites, virtually lacks rhyodacites to rhyolites (Fig. 1), and includes the only high-silica rhyolites. The most abundant magma type in the area is represented by lavas of the Middle Suite, which includes the voluminous Kalamazoo tuff and the tuff of Cooper Summit (both zoned from dacite to rhyolite). The base of the Late Suite is marked by the tuff of North Creek and associated lavas; these units bear biotite and clinopyroxene. Overlying biotite-hornblende lavas are more biotite-rich than similar units of the Middle Suite.

Lavas of the Early Suite can be modeled as mixtures between a basaltic andesite ($\delta^{18}O$ ∿7.5‰), itself a crustally contaminated mantle melt (low SiO_2, high Sr_i), and rhyodacite representing a crustal melt. Only very minor fractionation of clinopyroxene is required. Most of the compositions (silicic andesites, $\delta^{18}O$ ∿8‰) require ∿60% of the mafic end member. The high-silica rhyolites ($\delta^{18}O$ ∿11‰) are fractionated relative to the model crustal melt, possibly reflecting differentiation in isolated magma chambers. The Middle Suite ($\delta^{18}O$ ∿8-10) fills the chemical gap in the Early Suite, suggesting a larger proportion of crustal contamination. The crustal contaminant for the Middle Suite, however, has higher Sr_i and lower εNd than that for the Early Suite (Fig. 2), suggesting that the locus of crustal melting moved to deeper (older) levels.

The Late Suite is chemically nearly identical to lavas of the Middle Suite, except that K, Rb, and Zr are somewhat elevated at comparable SiO_2; the Kalamazoo tuff is similarly enriched relative to associated lavas. This suggests that the alkalic signature is of crustal or fluid origin and does not reflect input from a different mantle source.

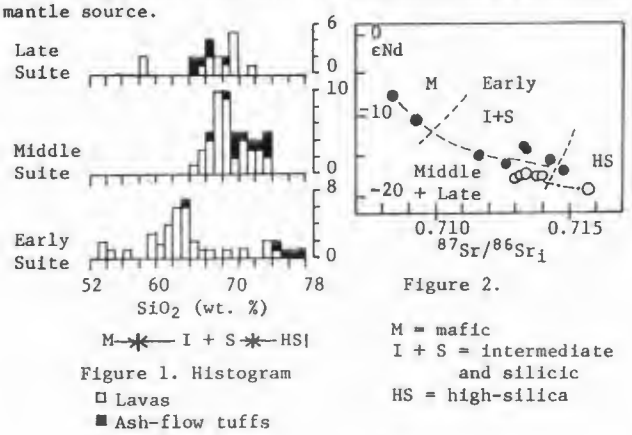

Figure 1. Histogram
□ Lavas
■ Ash-flow tuffs

Figure 2.
M = mafic
I + S = intermediate and silicic
HS = high-silica

PHYSICAL FEATURES AND CONTROLS OF ANDEAN PLEISTOCENE PYROCLASTIC FLOW DEPOSITS (34°00' 34° 20'S)

GUERSTEIN, P. G., Centro de Investigaciones Geologicas (CIG), Calle 1 n° 644, 1900 La Plata, Argentina

Physical features, composition, and controls of the Associacion Piroclastica Pumicea (APP), an extensive Pleistocene pyroclastic formation in the eastern flank of the Andes, Argentina, are here analyzed. APP is composed of air fall (AFD) and pyroclastic flow (PFD) deposits of rhyolitic composition (72-76% SiO_2). Equivalents of these accumulations appear in the central region of Chile, where only PFD have been identified. Observed variations in the AFD grain size and thickness and of the PFD spreading support the hypothesis that the effusive center was located in the Diamante caldera, where the Maipo volcano has been emplaced.

The AFD crop out sporadically in a small piedmont area. In some places they are covered by reworked pyroclastics, fluvial sediments and/or by PFD. They may be also completely eroded. These deposits are composed by four sheets of concordant lapillitic ash, produced by several effusive stages which probably correspond to a unique plinian eruption.

PFD are well exposed in the Main Cordillera, along the W-E flowing streams Del Rosario, Yaucha and Los Papagayos, and their respective tributaries. They constitute a simple cooling unit originated by a unique flow episode. North-south variations of the physical characteristics--welding degree, lithic-pumice content and size--are clearly displayed in the stream valleys where they were deposited. However, they do not show large petrographic and chemical changes.

Regional N-S variations within PFD in the main bed valleys of Del Rosario (a), Yaucha (b), and Los Papagayos (c), are the following: 1) welding intensity (a: moderate, b: low to null, c: low to null); 2) average thickness (a: 150 m, b: 150 m, c: 100 m); 3) maximum pumice size (a: 20 cm, b: 45 cm, c: 45 cm). 4) Pumice percentage (a: 5-10%, b: 15-20%, c: 20-25%; 5) maximum lithic size (a: 8 cm, b: 20 cm, c: 20 cm); 6) lithic percentage (a: 5%, b: 5-10%, c: 10%).

These evidences suggest that the main control on the physical features of APP could have been the migration of vents along ring fractures combined with physiographic controls like depth and amplitude of the valleys. It is inferred that volcanic activity started at the northeastern sector of the Diamante caldera and migrated progressively to the South. This change in vent position occurred together with rapid diminution of P, T and volatile amount in the magma chamber.

REGIONAL VOLCANIC TRENDS IN THE LASSEN AREA OF NE CALIFORNIA, SOUTHERNMOST CASCADE RANGE

GUFFANTI, Marianne, US Geological Survey 922 National Center, Reston, VA 22092, USA, CLYNNE, Michael A., MUFFLER, L. J. P., and SMITH, James G., US Geological Survey, MS 910, Menlo Park, CA 94025, USA

Hundreds of short-lived, small- to moderate-volume, mostly mafic volcanoes occur throughout the Lassen area (120°30' to 122°10' W; 40°15' to 41° N) and surround a few larger, generally more silicic, polygenetic volcanic centers. Within the area, we identified 521 volcanic vents younger than 7 Ma; we classified these into five age intervals and five compositional categories based mainly on SiO_2 content. The Lassen volcanic region is associated with subduction of the Gorda North plate beneath the North American plate. Beneath the locus of vents, depth to the subducting plate is estimated to range from 85 km on the west to 130 km on the east. Five large polygenetic volcanic centers younger than 3 Ma occur in the western part of the volcanic region, where the subducting plate is 85 to 110 km deep. Normal faults and linear groups of vents are evidence of widespread crustal extension. NNW alignments of these features indicate NNW orientation of maximum horizontal stress in the Quaternary.

Volcanism older than late Miocene is not common in the Lassen region, making the volcanic record there much shorter than that of the range to the north. During the past 7 m.y., the locus of volcanic activity shifted westward and contracted. Most mafic volcanism is calcalkaline; however, lesser volumes of low-K high-alumina olivine tholeiite (HAOT) also have erupted throughout the Lassen region since late Miocene. Lassen HAOT is chemically similar to HAOT found east of the Lassen region in the NW Basin and Range province.

The meager volcanic record prior to the late Miocene and the westward shift and contraction of the locus of volcanism during late Miocene could be related to changes in convergence angle, slab dip, or spreading-ridge position. However, since the middle Miocene, basaltic volcanism and faulting in the northern Basin and Range province have become restricted successively outward into narrower marginal zones. Impingement of an extensional stress regime on the Lassen region during the late Miocene perhaps initiated widespread volcanism in the region. Prior to the middle Miocene, a compressive crustal stress regime may have inhibited the surface expression of arc magmatism, even though subduction was occurring.

The occurrence of HAOT within the Lassen region implies tectonic control of magma generation. We suggest that Lassen HAOT is generated in the same manner as HAOT in the extensional Basin and Range province behind the arc. Calcalkaline basalt, on the other hand, likely is derived from melting of mantle metasomatized by introduction of slab-derived fluids. Thus, different domains of magma generation in the mantle, one related to extension and the other to the presence of a subducting slab, appear to overlap in the Lassen region.

EOCENE VOLCANISM IN CENTRAL IDAHO, U.S.A.: RESEARCH SUMMARY OF THE SOUTHEASTERN CHALLIS VOLCANIC FIELD

HACKETT, William R., MOYE, Falma J., and SNIDER, Larry G., Department of Geology, Idaho State University, Pocatello, ID 83209

In this report, we synthesize our data on the regional stratigraphy, volcanic facies, petrography, bulk-rock major- and trace-element geochemistry, and geochronology from the southeastern Challis volcanic field, in the northwestern part of the Idaho Falls 1-by-2-degree quadrangle, Idaho. Four new $^{40}Ar/^{39}Ar$ age dates are given.

The Challis volcanic field of central Idaho is one of several compositionally diverse Eocene volcanic fields that occur over a wide area in the northwestern U.S. and southeastern British Columbia. The tectonic setting of this volcanism is poorly understood. The most voluminous volcanism in the Challis field occurred from about 50 to 44 Ma, and was focused along the trans-Challis fault system, a northeast-trending volcano-tectonic depression. Our 2,000-square-kilometer study area lies to the southeast of the Trans-Challis fault system, where silicic tuffs are less voluminous, and the underlying andesitic, hypabyssal, and prevolcanic basement rocks are therefore well exposed.

The Challis Volcanics were emplaced onto a high-relief terrain of Paleozoic and Mesozoic sedimentary rocks, and extensional faulting was synchronous with volcanism. Hence, the distribution and thickness of volcanics was controlled by both pre-Tertiary topographic and Eocene (synvolcanic) structural relief. From oldest to youngest, the volcanic units include: (1) up to 700m of andesitic lavas and tuff breccias, deposited between 49.3±0.7 Ma and 48.25±0.20 Ma [new $^{40}Ar/^{39}Ar$ date (hbd)]; (2) up to 230m of the dacitic ash-flow tuff of Antelope Creek; (3) up to 470m of dacite lava flows and tuff breccias [new $^{40}Ar/^{39}Ar$ date of 49.03±0.21 Ma (bio)]; (4) 250-300m of the andesitic to dacitic ash-flow tuff of Cliff Creek; (5) up to 200m of the dacitic-to-rhyolitic, ash-flow tuff of Cherry Creek, erupted from the Lehman Basin cauldron complex, and concurrent deposition of the tuff of Stoddard Gulch; (6) up to 300m of dacitic lava flows, domes and tuff breccias, exposed over most of the area; (7) volcanism ended with local rhyolitic and rhyodacitic intrusions, domes and lava flows [new $^{40}Ar/^{39}Ar$ dates: 47.39±0.20 (san), 47.78±0.20 (bio)].

Most andesite lavas probably erupted from fissures, and volcanic facies do not indicate major central-vent complexes. Dacitic volcanism is characterized by the emplacement of fissure-controlled, dome-flow complexes with associated pyroclastic aprons. Most ash-flow sheets contain abundant lithics, some decimeter-sized. The three cooling units of the voluminous tuff of Cherry Creek were probably emplaced during catastrophic roof failure of the Boon Creek stock in the Lehman Basin area; the stock later intruded its own ejecta. The tuffs of Antelope Creek, Cliff Creek and Stoddard Gulch consist of numerous small-volume ash-flow tuffs that issued in places from volcanic domes and small collapse structures.

Volcanic rocks of the southeastern Challis field comprise a K-rich, calcalkaline suite, and range from absarokite to rhyolite in composition. The most voluminous magma types are high-K andesites and dacites. Silicic rocks (dacites to rhyolites) are crustal melts, which are separated from a mafic-to-intermediate rock series by a 60-63 wt % silica compositional gap. Petrographic and geochemical data from mafic-to-intermediate rocks suggest that the parental magmas of this magma series are high-K basic andesites and shoshonites. Polybaric fractionation of predominantly ferromagnesian minerals from such parental magmas produced more evolved shoshonites, latites and high-K andesites. Absarokites and high-K basalts are picrites with cumulophyric textures and very high concentrations of the compatible elements Mg, Cr and Ni. These primitive rocks do not represent liquid compositions, but are intermediate liquids that have accumulated olivine and chrome spinel ± clinopyroxene crystals.

Epithermal precious-metal deposits are associated with shallow, intermediate-to-felsic intrusions, and include both hot-spring and vein mineralization.

[This research is supported by NSF EAR8618629-RUI, with REU supplementals; by the Idaho State Board of Education; and by the U.S. Geological Survey Hailey 1-by-2-degree CUSMAP project. We gratefully acknowledge the following U.S.G.S. staff: Betty Skipp for unpublished field data, Ron Worl for logistical support, and Larry Snee for use of $^{40}Ar/^{39}Ar$ analytical facilities. Stan Mertzman of F&M College performed the bulk-rock x-ray fluorescence analyses.]

THE 1985 NEVADO DEL RUIZ ERUPTION: SCIENTIFIC, SOCIAL AND GOVERNMENTAL INTERACTION PRIOR TO ERUPTION

M. Hall and CERESIS Group
Escuela Politécnica Nacional
Quito, Ecuador

A study involving South American scientists, sociologists, and engineers evaluated the responsabilities and actions of the different groups that played important roles leading up to the 13 November 1985 eruption of Nevado del Ruiz, Colombia, which resulted in 23,000 deaths. The study is based upon interviews of all leading government, scientific, media, and civil defense participants and the detailed perusal of all reports, publications, and newspapers during the 11 months prior to the eruption.

A few of the conclusions are:

1- The small phreatic eruption of 11 Sept. was a catalyst for mobilizing national government interest. Had it not occurred, a greater catastrophe might have resulted.
2- Scepticism was widespread, in and out of government, concerning a possible eruption, moreso a catastrophe, as well as what the government was doing about it.
3- Differences in culture and tradition of the two affected provinces played important contrasting roles in the pre-eruption preparation and response. This influenced the way that the media covered the crisis which in turn affected public awareness.
4- A possible tragedy was foreseen by the government and the informed community with the publication of the hazards map on 7 Oct. and the prediction that Armero ran a 100% chance of being seriously affected if lahars were generated. The map met with hostile opposition by economic interests.
5- Limited distribution and short lead-time of the hazard map greatly hindered civil defense's ability to prepare for the catastrophe.
6- Limited scientific data from a marginal monitoring program, no baseline data, and greatly delayed processing, precluded a realistic attempt to understand or predict an eruptive event.
7- The lack of systematic and sustained preparation of the threatened communities was the major defect. Most civil defense groups are simply not organized (nor funded) to prepare for possible impending disasters.

ADVANCES IN VOLCANO HAZARD EVALUATION IN ECUADOR

-M. Hall, C. von Hillebrandt, B. Beate
Instituto Geofísico, Escuela Politécnica Nacional, Quito, Ecuador

South America's Andes are inhabited by a significant urban and rural population as well as being crowned by a large percentage of the world's active volcanoes. Many of these cones have high relief, often 3000m above their bases, and support large glacier caps. Eruptions of almost any one of the many hundred active volcanoes threaten nearby communities with primary flows as well as others located tens and hundreds of kilometers downstrean with devastating mud-flows. Avalanche deposits produced by large scale collapse of the cone are now being recognized in many areas.

Following the Nevado del Ruiz tragedy, it became inperative to accelerate the evaluation of hazards associated with Ecuador's large stratocones that loom over the Inter Andean Valley, home to more than 3 million people.

Seven hazard maps (scale 1:50,000), published in 1988 by the Instituto Geofísico, include Cotopaxi, Guagua Pichincha, Tungurahua, Pululagua, Cuicocha and Antisana volcanoes. The Instituto's program, supported by a USAID-UNDRO project has also hosted four workshop-courses with LatinAmerican participants aimed at improving our response to volcanic activity. Eight volcanoes are presently being monitored for seismicity and deformation, through USAID-UNDRO, USGS-VCAT, and UNESCO-WOVO support.

MAGNETIC POLARITY DOMAINS, STRUCTURAL DOMAINS, PETROGRAPHY AND PALEOMAGNETISM: THEIR BEARING ON THE ORIGIN AND DEFORMATION OF THE EARLY PROTEROZOIC MATACHEWAN DYKE SWARM, CANADA.

HALLS, H.C. and BATES, M.P. Dept. Geology, University of Toronto, Erindale Campus, Mississauga, Ontario, Canada L5L 1C6
PALMER, H.C., Dept. Geophysics, U. Western Ontario, London, Ontario, Canada N6A 5B7

The Matachewan dykes form a large radiating swarm that covers an area of more than 250,000 km² of the Archean Superior Province in Canada. The dykes are 2.45 Ga old (Heaman,1988) and are iron-rich tholeiites often characterized by pale green, anhedral plagioclase phenocrysts. They fan northwards from a broad focus in the Lake Huron region, and are deflected in trend on crossing the Kapuskasing Structural Zone (KSZ) where deep crustal rocks of amphibolite to granulite metamorphic grade have been brought to the surface (Percival,1983). The dykes possess one of two directions of remanent magnetization (D=20°/210°,I= +/-20°) referred to respectively as of normal(N) and reversed (R) magnetic polarity.

Within the KSZ, Matachewan dykes are found only in the lower grade rocks and differ in several important respects from their counterparts outside the Zone. They are relatively fresh having only a few local patches of hydrous alteration of the feldspars; they contain a blue-green amphibole and a plagioclase that has a tea-coloured cloudiness under plain light (Halls and Palmer, 1988a,b). The amphibole occurs as rims around clinopyroxene but also as discrete crystals and is highly aluminous (Palmer and Barnett, this volume). The dykes are generally non-porphyritic and all have N polarity.

Outside the KSZ on its south side where host rocks have greenschist to amphibolite metamorphic grades, the dykes are often strongly altered (Halls and Shaw, 1988; Bates and Halls,1988a; Halls and Palmer,1988a). Feldspars are heavily speckled with hydrous alteration products; pyroxene may be almost completely replaced by chlorite and a green, relatively fibrous amphibole with low Al content (Palmer and Barnett,this volume).

North of the KSZ, where the regional metamorphic grade may be slightly higher than to the south, Matachewan dykes also contain the blue-green amphibole, are generally more hydrously altered than dykes within the KSZ but are much fresher than those south of the KSZ.

All dykes lying outside the KSZ have clear plagioclase as opposed to the tea-coloured cloudiness within; many contain the green plagioclase phenocrysts and R polarity types outnumber those of N polarity about 4 to 1 (Halls and Palmer,1988a,b; Bates and Halls,1988b).

A most unusual feature of the Matachewan swarm is that the N dykes within the KSZ pass along strike to both the north and south into populations having dominantly R polarity which lie outside the main KSZ boundary faults (Bates and Halls, 1988b;Halls and Palmer,1988a). Along Hwy 101 to the west of Chapleau, alternate domains of N and R polarity dykes are found, and the boundaries between these domains also appear to be faults (Halls and Palmer,1988b).

The above differences in petrology and magnetic polarity of dykes within and outside the KSZ can be explained as a consequence of differential crustal uplift, the N dykes within representing a generally deeper expression of the Matachewan swarm. Cross-cutting relations show that N dykes are younger than the R set (Halls,1989).

A model is presented whereby dykes are emplaced laterally northwards from magma chambers lying in the focal region, with basaltic magma being injected at progressively deeper levels within the crust of the Superior Province, down to a maximum depth of about 30 km.

Using our paleomagnetic data and the structural domain concept of Freund (1974) we show that the change in trend of the Matachewan swarm across the KSZ may be due to differential horizontal rotations of the crust of up to 30° that occurred several hundred million years after cratonization of the Superior Province, in response to a WNW-ESE compression associated with the Hudsonian orogeny (Halls and Bates,1989).

References: Halls and Palmer, 1988a,b; Bates and Halls, 1988a,b: Proceedings of Lithoprobe Workshop on KSZ Transect,U. Toronto; Heaman, 1988: GAC 1988 Abstract Volume; Halls, 1989; Halls and Bates, 1989: GAC 1989 Abstract Volume; Halls and Shaw 1988: Can. J. Earth Sciences; Freund,1974: Tectonophysics.

TERTIARY EXTENSIONAL VOLCANISM ON THE CANADIAN-PACIFIC MARGIN: QUEEN CHARLOTTE BASIN

HAMILTON, T.S., Geological Survey of Canada, Pacific Geoscience Centre, P.O. Box 6000, Sidney, B.C., V8L 4B2, Canada, and DOSTAL, J., Department of Geology, St. Mary's University, Halifax, N.S., B3H 3C3, Canada

Extensional volcanism of the Masset Formation characterized the long-lived initial phase of Tertiary basin development in the Queen Charlotte portion of the Canadian-Pacific continent-ocean margin. Magmatism, which dominated from Late Eocene to Early Miocene across the width of the Insular Belt from 51 to 54 N.Lat., was succeeded by regional subsidence and sedimentation (Skonun Fm). Late Neogene uplift in the Queen Charlotte Islands generally greatest in the south and west, differentially stripped the sedimentary and volcanic basin fill, exposing denuded blocks of Mesozoic basement with extensive and highly directional Masset-age dyke swarms and coeval mesozonal and epizonal plutons. The extent of contiguous fault-bounded blocks of similar facies, attitude and degree of uplift is less than a few kilometers on a side, obscuring correlations and confounding the subdivision of the Masset into regionally significant members.

The Queen Charlotte's succession comprises diachronous graben-fill accumulations dominated by aphyric to sparsely porphyritic flows, with many bimodal sections. The least evolved are within-plate calc alkaline volcanics and I-type plutonics early in the local succession and transitional morbs later on. Progressive rifting is evident in: the change from high- to low-pressure fractionates, increased melt % inferred from trace element inversion of cogenetic packages and several extensive sequences that culminate in thick dacite or rhyolite ignimbrites. The longevity of magmatism, the tholeiitic parentage and the rifting of the thick crustal section on the North American side of this transtensile margin derive from interaction with tectonic elements in the Northeast Pacific. The extensional volcanism of the Masset Formation marks the transition from N.Am.-Farallon to N.Am.-Pacific plate boundaries and the northwards transit of the Kula-Farallon and Farallon-Pacific Rises. Similarities in the geology of this mixed calc alkaline-tholeiitic assemblage to ancient volcanic belts of the continental shields suggests that the extensional volcanism of the Queen Charlotte marginal basin could provide an instructive model.

RECOGNIZING COMAGMATIC BASALTIC DIKES WHEN THEY ALL LOOK ALIKE

HAMMOND, Janet G., Pasadena City College, Pasadena, CA 91106

Within Proterozoic magmatic provinces, basaltic dikes and sills of very similar composition occur over extremely wide areas. It is often difficult to identify which intrusions belong to a single magmatic event, especially if they display varying amounts of alteration.

Conserved element ratios (Pearce ratios) used recently to identify comagmatic basalts are also useful for dikes. Perfectly conserved elements do not enter into differentiation processes, so their ratios remain constant. Ideally, comagmatic rocks plot as a single point on a bivariate diagram constructed with conserved element ratios which have different numerators but the same denominator.

In hypabyssal basaltic rocks, K, P, Zr, and Ba approximate conserved elements, and comagmatic rocks cluster closely on ratio plots using these elements. Alteration may produce some spread in the clusters, but they are still useful. For example, two sets of similar mildly alkaline basaltic dikes are recognized in the Nain anorthosite complex (Labrador) on the basis of different orientation and high versus low P_2O_5 (Weibe, 1985). As expected, these form two very distinctive clusters on a K/Zr versus P/Zr diagram. The high P_2O_5 group shows distinctly greater variation in P/Zr which corresponds with textural evidence that apatite crystallized early. Under these circumstances P behaves less like a conserved element.

A second example is the division of middle Proterozoic diabase dikes and sills in the southwestern U.S.A. into two comagmatic suites (below). There is no a priori field evidence for two groups, and they are not distinguishable on traditional geochemical plots. Fresh and altered samples are present in both groups.

The recognition of comagmatic intrusions should aid geochronological studies aimed at determining the timing of magmatism in a province. This method may also prove useful in matching basalt flows with feeder dikes in areas where only remnants remain.

Other types of conserved element ratio plots are designed to assess the role of specific minerals in differentiation processes. They are also interpreted as indicators of comagmatic relationships if all points fall on a line with a very high correlation coefficient. The differences between similar, but obviously not comagmatic, Proterozic diabases are so subtle on these diagrams, that it is hazardous to use them to test for comagmatic relationships.

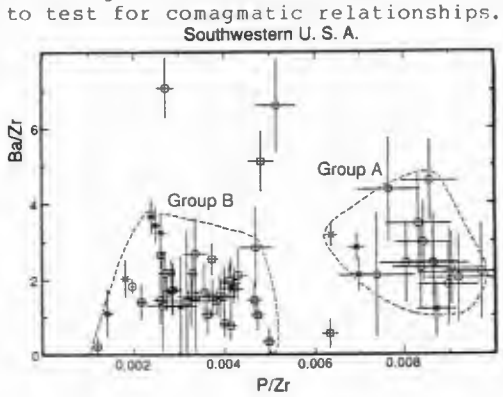

EOCENE MAGMATISM, CHALLIS VOLCANIC FIELD, CENTRAL IDAHO

HARDYMAN, R. F., U.S. Geological Survey, Reno Field Office, Mackay School of Mines, Reno, Nevada 89557

The Challis volcanic field is the largest and perhaps most diverse of the volcanic fields that constitute one part of an extensive belt of volcanic and plutonic rocks of Eocene age that occurs throughout the northwestern United States. Eocene volcanism in the Challis field began about 51 Ma, culminated in large-volume explosive eruptions between about 49 and 45 Ma, and was essentially over by about 40 Ma. The volcanic field consists of a lower sequence of mafic and intermediate volcanic rocks (51-49 Ma) and an upper sequence of felsic pyroclastic rocks (49-45 Ma). These volcanic rocks are cut by mafic to felsic intrusions as young as 40 Ma and a major granitic pluton, the Casto pluton, was emplaced into the volcanic pile about 47-44 Ma.

The lower sequence of mafic to intermediate volcanics locally exceed 1000 meters in thickness, was erupted from numerous small strato- and shield volcanos and dome complexes and was deposited on an erosional surface of more than 300 meters of structural and topographic relief carved on Precambrian and Paleozoic sedimentary rocks. The lower sequence rocks include K-rich andesite, andesite, latite, and minor volumes of Mg-rich and K-rich basalt.

Large-volume silicic pyroclastic eruptions dominated volcanic activity in the Challis volcanic field for about 4 million years. Initial eruptions of rhyodacitic magma evolved through rhyolite and terminated with eruption of high-silica, alkali-rhyolite magma. The older rhyodacitic volcanism initiated development of a huge cauldron complex (Van Horn Peak-Thunder Mountain cauldron complex) with dimensions of approximately 110 by 65 km. The younger rhyolite and alkali-rhyolite pyroclastic eruptions formed smaller calderas (Twin Peaks and Thunder Mountain calderas) superimposed "cookie-cutter" fashion on this cauldron terrane. Products of the explosive phase of volcanism exceed 6000 meters in composite thickness within the eroded cauldron terrane. Although intermediate to mafic magmatic activity had significantly waned by the onset of silicic pyroclastic volcanism, eruptions of mafic and intermediate magma continued well into the period of silicic volcanism and intermediate intrusions locally post-date the silicic volcanic rocks.

Individual cupolas of silicic magma may have risen diapirically from a batholith-sized source to sufficiently shallow levels of the crust to give rise to the Twin Peaks and Thunder Mountain calderas. Contemporaneously, a third body of silicic magma rose to a level necessary to invade the lower and thickest part of the intracauldron volcanic pile and cooled to form the Casto pluton.

PALEOMAGNETISM OF PROTEROZOIC MAFIC DIKES, SOUTHWEST MONTANA FORELAND, USA

HARLAN, S.S., Geissman, J.W. Both of Department of Geology, University of New Mexico, Albuquerque, New Mexico 87131, Snee, L.W. U.S. Geological Survey, Denver, CO., Schmidt, C.J., Western Michigan University.

The Archean crystalline basement of the SW Montana foreland is cut by greater than 30 regularly spaced NW-trending faults of presumed or demonstrable Precambrian ancestry. Intruded along or parallel to many of these faults are swarms of Proterozoic mafic dikes. Development of the faults and emplacement of the dikes is thought to have accompanied extensional deformation related to formation of the Proterzoic Belt Basin and rifting of the northwestern margin of the North American craton. Exposures of these dikes are limited to the Tobacco Root, Ruby, and Highland Ranges. Field, geochemical, and isotopic data indicate the presence of three distinct dike sets which represent two distinct periods of dike injection at about 1450 Ma and 1120-1130 Ma.

Paleomagnetic results from southern Tobacco Root dikes indicate two distinct periods of RM acquisition. Group A dikes (1450 Ma, Rb-Sr) yield a moderately well-defined dual-polarity remanent magnetization (RM) of northeast (SW) and moderate negative (positive) inclination (D = 49.5°, I = -66.8°, κ = 30.15, α_{95} = 12.4°, n = 6 sites) with a pole at 13.7°N, 153.3° E (δp = 16.9°, δm = 20.5°). This pole is similar to that of age equivalent units elsewhere in North America, but is clearly distinct from those of Belt units believed to be of similar age. Group B and C dikes (Rb-Sr = 1120-1130 Ma) display a complex RM dominated by Tertiary or PDF affinity; this overprint is usually incompletely removed during AF or thermal demagnetization. A resultant mean direction based on principal component analysis of planar and linear data is: D = 302.3,° I = -20.7° (n = 95 samples, k_1 = -12.9 k_2 = -3.1, $\alpha_{95}3\text{-}1$ = 3.35° $\alpha_{95}3\text{-}2$ = 8.3°). A pole can be calculated at either 14.8°N, 127.6°E or 14.0°S, 307.3°E. Either pole is displaced significantly from poles of either the Belt Supergroup or Keeweenawan or Grenvillian igneous units. The first pole plots relatively close to that of ca. 900 Ma Little Dal volcanics and Uinta Mtns. Supergroup, whereas the second pole plots near the 670-700 Ma end of the Hadrynian track. In either case, RM acquisition may be significantly younger than previously assumed on the basis of existing isotopic age determinations. $^{40}Ar/^{39}Ar$ dating is currently underway to investigate this possibility.

Highland Range dikes are characterized by a well-defined reverse polarity RM of D = 191.1°, I = - 61.7° (κ = 45.9, α_{95} = 7.7°, n = 9 sites). This direction is distinct from Proterozoic dikes elsewhere in Southwest Montana and is similar to reverse polarity expected directions for Late Cretaceous or Early Tertiary time. These dikes have probably been remagnetized due to intrusion of nearby Late Cretaceous plutons. Discordance between observed and expected directions is probably due to subsequent Laramide or Neogene tectonism.

THE MESOZOIC IGNEOUS ROCKS OF WESTERN DRONNING MAUD LAND, ANTARCTICA

HARRIS, Chris, Dept. of Geochemistry, University of Cape Town, South Africa

Contemporaneous continental flood basalts and alkaline plutons are exposed in Dronning Maud Land, close to the 0° meridian. The 420 m thick Kirwan basalts (172 Ma., Faure et al., Chem. Geol., 1979) are typical continental tholeiites. Straumsvola (170 $\pm$4 Ma., Grantham et al., S.A. J. Antarctic Res., 1988) is a nepheline syenite pluton which is associated with a suite of dykes of wide ranging compositions, from pyroxenite and lamprophyre to phonolite and peralkaline granite. Tvora is a syenite pluton of unknown age which is exposed some 10 km south east of Straumsvola, which appears on the basis of field evidence to be of similar age. Sistenabben is a quartz syenite pluton of probable Mesozoic age. The Kirwan basalts are exposed in the south west Kirwanveggen (73°S, 6°W) while Straumsvola and Tvora (72°10′, 0°15′), and Sistenabben (73°20′S, 0°40′W) occur on either side of the Jutulstraumen, a major rift system which divides the high-grade metamorphic terrain in the east from essentially undeformed rocks of similar age, to the west.

The Kirwan basalts show a restricted range in major element composition (e.g. SiO_2 50.1-52.1; MgO 5.1-6.6) which can be explained by 30% fractionation of an assemblage of plag, cpx, olivine and Ti-mgt in the proportions 51:35:11:3. Some incompatible elements (e.g. Zr) show variations of > x2 which may indicate that these basalts were derived from parent magmas which were extracted from a common source by slightly different degrees of partial melting. Sr-, Nd- and O-isotope data suggest that crustal contamination was not important in their petrogenesis.

The Straumsvola complex is thoroughly alkaline; in addition to the nepheline syenite plutonic rocks, a suite of comenditic dykes, which cut the syenite, are present which have up to 4 % normative ns and accessory minerals such as dalyite and vlasovite which are characteristic of strongly peralkaline granites. The Tvora and Sistenabben syenites show no strong alkaline affinities. Oxygen isotope data for minerals and whole rocks from all three plutons do not suggest much (if any) crustal component and this along with the comenditic composition of some of the dykes is typical of rift environments.

Of the Karoo basalt types of southern Africa, the Kirwan basalts are geochemically most similar to the southern Lebombo variety of the Sabie River Basalt Formation. The position of this part of Dronning Maud Land adjacent to the southern Lebombo in Gondwanaland reconstructions is consistent with recent models (e.g. Martin and Hartnady, J.G.R., 1987). The association of alkaline magmas with rifting is well established in the East African rift but not in the Karoo province. Nephelinite lavas are found at the base of the Karoo lava pile in the northern Lebombo and it may be that the relative proximity of these nephelinites to the Straumsvola alkaline complex in predrift Gondwanaland is significant.

DYNAMICS OF THE 1986 ERUPTION OF AUGUSTINE VOLCANO, ALASKA: PETROLOGY AND SEISMICITY

HARRIS, G., Department of Geology and Geophysics and Geophysical Institute, University of Alaska, Fairbanks, AK 99775, POWER, J., Alaska Volcano Observatory and U.S. Geological Survey, Fairbanks, AK 99775, and SWANSON, S.E., and KIENLE, J., Department of Geology and Geophysics and Geophysical Institute, University of Alaska, Fairbanks, AK 99775

Precursory seismic activity began 9 months before Augustine erupted in March of 1986. Hypocenter migration from 0.5 km below sea level to 1.0 km above sea level during this 9 month precursory phase may be related to upward migration of a rejuvenated hydrothermal system. Influx of a basic andesite into a magma chamber containing silicic andesite at a depth of about 2 km and subsequent mixing-induced crystallization could have provided the heat necessary to drive such a rejunvenation.

Pumice flows of silicic andesite (SiO_2 61-62 wt%) represent the first eruptive phase in late March and early April of 1986. Compositionally (major oxides in groundmass glass) and petrographically (low phenocryst: groundmass ratios, clear groundmass glass) these lavas are very similar to the 1976 dome lavas and probably represent residual magma left in the magma chamber after the 1976 eruption. At the onset of the first eruptive phase, seismicity gradually changed from earthquake to explosive activity over an 18 hour period beginning approximately on March 26, 1986.

A lava flow of relatively heterogeneous andesite (SiO_2 58-62 wt%) was extruded from the summit region of the volcano in late April, 1986. Variable to high modal skeletal olivine, mixed groundmass textures (mixing of clear and microlite rich groundmass), and bimodal distribution of plagioclase rim compositions suggest that the magma of the lava flow is the product of mixing the basic andesite and the residual silicic andesite from the 1976 eruption. During the same time period a homogeneous silicic andesite (SiO_2 60-62 wt%) dome was extruded. The change from explosive to extrusive activity is probably due to volatile loss. The change from the flow to the dome activity appears to be related to a viscosity increase due to the higher crystallinity of dome magmas. Seismically these two extrusive events are characterized by periods of repetitious microearthquake activity.

A second dome-building episode from August 10 to September 10 produced a spine of silicic andesite (SiO_2 61-63 wt%) and more pyroclastic flows. The spine-building event was accompanied by litmited earthquake activity, suggesting that the magma involved came from shallow depth in a hot environment.

The K_2O content of groundmass glass in the silicic andesite dome and spine is elevated relative to other 1986 glasses. This may be due to contamination of magma along the sidewalls of the chamber prior to extrusion in the waning stages of the 1986 eruption. High phenocryst:groundmass and microlitic groundmass:clear glass groundmass ratios in the dome and spine samples also suggest a more complex history for this magma. Textural and compositional dissimilarities between the 1976 and 1986 domes indicate that the sidewall magma was extruded during the 1986 eruption only. The relative frequency of recent eruptions (3 in the past 25 years) may have facilitated the extrusion of the sidewall magma through an increase in the heat flux to the magma chamber.

MANTLE AND BASALTIC MAGMA EVOLUTION IN A CONTINENTAL RIFT: EVIDENCE FROM THE ETHIOPIAN VOLCANIC PROVINCE

HART, W.K., Geology Dept., Miami Univ., Oxford, OH 45056, **WOLDEGABRIEL, G.**, ESS-1/D462, Los Alamos Natl. Lab., Los Alamos, NM 87545, **WALTER, R.C.**, Berkeley Geochron. Center, 2453 Ridge Rd., Berkeley, CA 94709, and **MERTZMAN, S.A.**, Geology Dept., Franklin & Marshall College, Lancaster, PA 17604

Middle to late Cenozoic mafic lavas from Ethiopia exhibit chemical and isotopic diversity that is linked to eruption age and location. Trace element and Sr, Nd, and Pb isotopic data are interpreted to indicate involvement of two depleted and two enriched mantle reservoirs throughout Cenozoic Ethiopian rift development. The characteristics imparted by varying degrees of melting of these reservoirs have been modified by crystal fractionation, and in some cases, crustal contamination.

Initial Oligocene rifting and volcanism, as manifested by the rift-bounding plateau flood basalts, is attributed to asthenospheric upwelling and melting of heterogeneous, enriched subcontinental lithospheric mantle. Mildly alkaline lavas were derived from a LoNd array source similar to that inferred for other mantle derived lavas and xenoliths from East Africa and for numerous oceanic islands (eg. Sr$_I$=0.7036, Nd$_I$=0.5127). Contemporaneous tholeiitic lavas were derived from a source similar to that producing oceanic basalts from Samoa and the Society Islands. As lithospheric thinning and rifting continued into the Miocene, upwelling depleted OIB-type asthenosphere interacted with the lithospheric sources producing hybrid melts (eg. Sr$_I$=0.7035, Nd$_I$=0.5128). Crustal contamination is most evident in the Oligocene to Miocene plateau basalts and is suggested to have taken place primarily at mid- to lower crustal levels. By 4-5 Ma bp continental break-up had begun in Afar leading to production of basaltic magmas derived almost entirely from a depleted OIB-type reservoir (eg. Sr$_I$=0.7035, Nd$_I$=0.51285-0.5129). In the Main Ethiopian Rift, where continental break-up is less advanced, young rift basalts retain a geochemical signature consistent with enriched - depleted mantle hybridization. During the Holocene, proto-oceanic crust characterizes the Afar, and input from a depleted MORB source first becomes apparent (eg. Sr$_I$=0.7030, Nd$_I$=0.5130-0.5131). This evolutionary sequence is further highlighted by trace element ratios of least-fractionated basalts from the Main Ethiopian Rift (MER), west-central Afar (WCA), and northern Afar as presented in the table below.

Chronologic and tectonic control on mantle melting, mantle reservoir interactions, and crust-mantle interactions is a theme common to many extensional regions, as is the apparent role of a depleted OIB-type reservoir. Input from enriched mantle during continental extension is also prevalent, but the geochemical signature of this component varies from region to region suggesting a strong link to local crust formation history and local enrichment events such as subduction driven lithospheric recycling.

Group	Ba/La	Ba/Th	Ba/Ta	Th/Ta	La/Th
MER >17Ma	16.5	154	239	1.55	9.3
MER 11-8Ma	16.1	220	285	1.29	13.7
MER 6-4Ma	17.7	237	241	1.02	13.4
MER <3Ma	9.0	105	111	1.06	11.7
WCA 11-6Ma	9.0	89	128	1.44	9.9
WCA 5-4Ma	7.8	75	90	1.20	9.7
WCA 4-3Ma	9.6	97	124	1.28	10.1
WCA <3Ma	8.6	89	53	0.60	10.4
N. Afar	5.3	77	84	1.07	14.5
N-MORB	4.2	63	57	0.91	14.9
Iceland	7.6	84	79	0.93	11.1
Gough/Walvis	16.6	154	226	1.47	9.1

AN EXTENSIVE, HOT, VAPOR-CHARGED RHYODACITE FLOW,BAJA CALIFORNIA, MEXICO

HAUSBACK, Brian P., Geology Department, California State University, Sacramento, 6000 J Street, Sacramento, California, 95819

The Providencia rhyodacite lava flow of southern Baja California is an unusually extensive salic extrusion. Remnants of the flow overlie lower to middle Miocene volcanic rocks and occur in a 27 km long belt near the city of La Paz. Isopachs of the flow show a maximum thickness of 120 m and indicate a minimum volume of 8.6 km^3. Persistent flow bands are closely spaced and parallel the base of the flow. These flow bands are thin, planar lithophysal cavities that give the rock a distinct parting. In the upper part of the flow the banding is strongly deformed into isoclinal to open folds. Flow directions, developed from fold axial information, together with the isopach data suggest that the rhyodacite flowed at least 23 km north-northwest from its source south of La Paz.

The Providencia rhyodacite (68-72.5% SiO_2, 3.8% Na_2O, and 4.5% K_2O) contains about 5% phenocrysts (plag > opx > Fe-Ti oxides) set in a devitrified groundmass of fine-grained alkali feldspar (and tridymite?). Lithophysal planar cavities are lined with large (as long as 3 mm) vapor phase crystals whose paragenetic relationships define a crystallization order from oldest to youngest: 1) fayalite + thick laths of brown hornblende, 2) α-quartz, 3) hematite, and 4) tridymite + apatite + rare biotite + rare fibrous green hornblende.

Field evidence suggests, but does not prove, that the Providencia rhyodacite is a primary lava flow rather than a remobilized pyroclastic flow. A high volatile content together with a high eruption temperature acted in concert to maintain a low viscosity, a fact that probably facilitated flow of the lava to great distances.

TIMING OF ALKALINE AND ULTRAMAFIC-ALKALINE VOLCANISM WITHIN THE RUSSIAN, THE SIBERIAN, AND THE NORTH AMERICAN ANCIENT PLATFORMS

HAUSEL, W. Dan, Geol. Survey of Wyoming, P.O. Box 3008, Laramie, WY 82071, ERLICH, E.I., Geol. Dept., Univ. of Colorado, Denver, 595 S. Forest, #311, Denver, CO 80222, and Sutherland, W.M., Geol. Survey of Wyoming, Box 3008, Laramie, WY 82071

Comparisons of radiometric ages show alkaline and ultramafic-alkaline magmatism within three major platforms of the northern hemisphere occur in the form of short synchronous pulses which coincide with major stages of tectonic reconstructions. Such pulses are of interplate nature and show a tendency to coincide with major stratigraphic boundaries and reversals of magnetic polarity. This leads to the conclusion that they reflect activity on a level deeper than the Upper Mantle possibly on the Core-Mantle boundary.

Discussions on the effects of volcanism on climate, biological extinctions, etc., have to consider that great eruptions of flood basalts usually occurred only within a single platform - on all others the same time span is characterized by intensification of tectonic movements.

Comparisons for the last 40 Ma for the northern Circum-Pacific show that such pulses have durations of about 5 m.y. Intensive eruptions of alkaline basalts in one type of structure corresponds to intensification of subalkaline silicic explosive volcanism in other types of structures. Both types of activities reflect intensification of volatile flows.

Radiometric ages for each Province constantly range from 250 to 400 m.y. These figures reflect time of exhaustion of heat reserves in the magma-feeding zones in the roots of each Province.

GEOCHEMISTRY OF PERALUMINOUS LEUCOGRANITES, SOUTH-CENTRAL ARIZONA

HAXEL, Gordon B., USGS, Flagstaff, AZ 86001, USA

Early Tertiary syntectonic plutons of peraluminous leucogranite in the region from the Baboquivari and Coyote Mountains west to the Sonoyta Mountains are geochemically distinctive.

The plutons typically comprise older phases of leucocratic medium-grained granite intruded by younger phases of highly leucocratic granite and pegmatite. These two phases are intermingled on outcrop to hillside scales, and apparently were widely and repeatedly produced during crystallization of the plutons.

Most samples of the peraluminous leucogranites have 73-77 wt.% SiO_2, molar $Al_2O_3/(CaO+Na_2O+K_2O)=1.05-1.25$, and $Fe^{+3}/Fe=0.4-0.8$. Accessory minerals include various combinations of biotite, muscovite, and garnet. Halogen contents are low: F≤800 ppm, Cl<100 ppm.

The least-evolved of the older-phase granites have the highest Fe, Co, Ba, Ba/Rb, and Eu/Eu*. Relative to average upper continental crust (Fig. 1), most first-transition-period elements (FTPE, Sc-Zn), Mo, and W are markedly depleted, but Mn and Sn are less depleted. LILE, HREE, and U are slightly enriched.

The most-evolved of the younger-phase granites manifest strong depletion in the feldspar-compatible elements Ba, Sr, and Eu; FTPE; and LREE (Fig. 1). Nb and Ta increase strongly in abundance with evolution, but W, Sn, Hf, and Th do not. Ta and Th are negatively correlated. The most highly evolved granites have unusually low Nb/Ta, 4-8, and K/Rb, 70-150. Mn and HREE are erratic and largely controlled by garnet, though HREE do tend to increase with evolution. In two plutons, Cs is relatively depleted in the more evolved rocks.

Because the more-evolved and less-evolved granites are intermingled, geochemical fractionation by uni- or bidirectional element migration or transport on a magma-chamber or pluton scale is unlikely. Rather, the younger-phase granites apparently were generated by widespread *in situ* or nearby fractional crystallization of the older-phase granites (as proposed by P.J. Michael: Contrib. Mineral. Petrol., *87*, 179). Separation of crystals and residual fluids may have been facilitated by deformation.

The upper-crustal geochemical evolution of the peraluminous leucogranite plutons evidently was dominated by crystallization of feldspars, ferromagnesian minerals, and LREE-bearing trace minerals. During crystallization, only Nb and Ta remained generally and strongly incompatible.

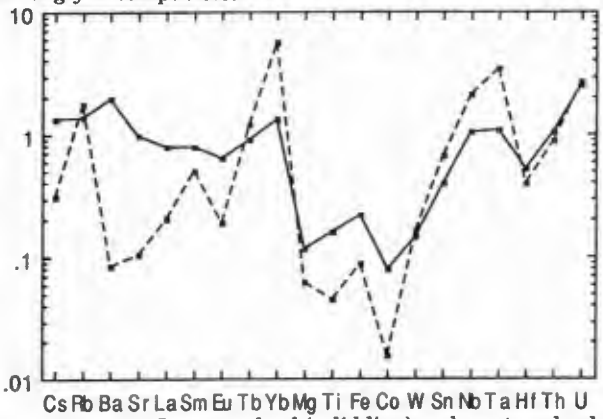

Figure 1. Least-evolved (solid line) and most-evolved (dashed line) Pan Tak Granite (Coyote Mountains) normalized to average upper continental crust.

DISPERSAL AND GRINESIZE CHARACTERISTICS OF THE AIRA-TN ASH, EXTENSIVE TEPHRA BLANKET ASSOCIATED WITH THE ITO IGNIMBRITE, JAPAN

HAYAKAWA, Y., Department of Geography, Tokyo Metropolitan University, Setagaya-ku, Tokyo 158, Japan

The Aira-Tn ash is considered as an air-fall part of the Ito pyroclastic flow, extremely large eruption occured in southern Kyusyu about 22,000 yBP. The dispersal of the ash is exceptionally wide in and around Japan (Fig. 1). Along the dispersal axis, it reaches as far as 1,350km from source, where the thickness is less than 1cm. It is measured 8cm at eastern flank of the Fuji volcano, 870km from source. At Sukumo 240km from source, it is 37cm thick resting on the preceding Osumi plinian tephra. More proximal area, however, it is hardly identified on the Osumi tephra or Ito ignimbrite in southern Kyushu. Toward the windward side it again appears 200-500km away from source. The ash is also found as far as 1,000km across the dispersal axis. Overall distribution of the Aira-Tn ash can be enclosed with a circle, the center 500km ENE of source and a radius of 1,000km.

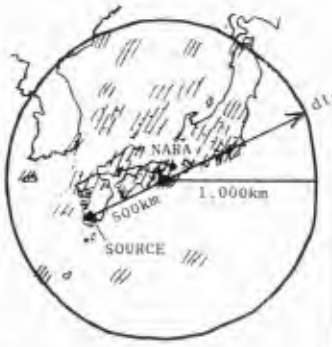

Fig. 1 Dispersion circle of the Aira-Tn ash. Data source: Machida & Arai (1983, Quat. Res. Japan, 22, 133-148)

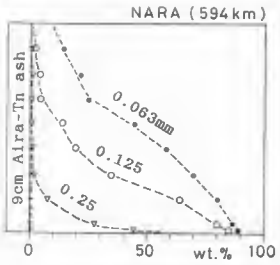

Fig. 2 Grainsize profile of the Aira-Tn ash at Nara.

Constituents of the Aira-Tn ash are almost entirely fine vitric materials: bubble-wall glass shards and micropumice. With distance from source, the median diameter of the ash deposit gradually decreases from 0.088mm at 240km to 0.053mm at 1,160km. However, the most conspicuous grainsize variance is found in vertical profile of a given section. The grainsize becomes progressively finer upward. Fig. 2 is a section example at Nara 590km from source. The median diameter is about 0.25mm at the base and smaller than 0.06mm at the top.

This normal size-grading characteristic of the Aira-Tn ash strongly suggests that the style of the eruption was instantaneous rather than steady state, the duration of culminating phase was not longer than the travel time for ash particles from source to the most proximal outcrop showing a normal size-grading. Time sequence of eruption and deposition of the Aira-Tn ash is considered on some reasonable assumptions. If wind velocity is taken at 20-40m/s, the culminating phase of the eruption is calculated less than 1 hour and deposition of ash about 10 hours.

U-Pb DATING OF MAFIC DYKE SWARMS: WHAT ARE THE OPTIONS?

Heaman, L.M., Department of Geology, Royal Ontario Museum, 100 Queen's Park, Toronto, Ontario, Canada, M5S 2C6.

Precise emplacement ages for mafic dyke swarms are a pre-requisite for global correlation of mafic magmatic events, accurate calibration of Apparent Polar Wander Paths and for understanding mechanisms of dyke emplacement. Recent advances in U-Pb geochronology and the discovery that certain mafic dyke samples contain trace amounts of U-bearing minerals, such as baddeleyite and zircon, have been instrumental in establishing emplacement ages for some of the worlds largest dyke swarms to a precision of +2 Myr. One of the more profound discoveries from this precise dating is that huge volumes of mafic magma, sometimes in excess of 100,000 km^3, have been emplaced over large distances (in excess of 2000 km) in geologically short periods of time (<5 Myr). This is well illustrated by the identical ages obtained for four widely spaced dyke samples from the Mackenzie swarm (1267+2 Myr) and three samples from the Hearst-Matachewan swarm (2452+3/-2 Myr), including dykes from the latter swarm that have both normal and reversed paleomagnetic polarities. In addition, both the primary emplacement age and the time of metamorphism can been obtained from a U-Pb study of some metamorphosed mafic dyke samples.

Baddeleyite (ZrO_2) is an ideal mineral for U-Pb age determinations because it is most often concordant, contains abundant uranium (>300 ppm) with virtually no common lead, is rare in most crustal rocks so is unlikely to occur as xenocrysts and is not known to form during metamorphism. Baddeleyite commonly occurs in the coarser-grained central portions of large dykes (more than 20m wide) but in some swarms baddeleyite can be found in almost every sample. Despite these advantages, obtaining U-Pb ages from baddeleyite can prove difficult because it often forms tiny crystals (<50 microns in the longest dimensions) requiring special sample handling procedures.

Zircon, whenever present as a primary phase, can also be an excellent mineral for U-Pb age determinations in mafic dykes. However, some caution is necessary because zircon xenocrysts may also be present. Primary zircon in mafic rocks commonly forms anhedral, skeletal grains that are often more magnetic than coexisting zircon xenocrysts. In metamorphosed mafic dyke samples, metamorphic zircon can be used to establish the time of metamorphism. Metamorphic zircon commonly occurs either as overgrowths on baddeleyite or as tiny, discrete, multi-faceted, soccer ball-shaped grains. Metamorphic rutile occurs in some samples but is less desirable than metamorphic zircon when both minerals are present because rutile usually contains abundant common lead. Examples of metamorphosed mafic dyke samples where both the time of emplacement and metamorphism have been obtained will be presented.

MANTLE-CRUSTAL LITHOSPHERE OF NORTH-CENTRAL MONTANA, USA: EVIDENCE FROM XENOLITHS

HEARN, B.C., JR., USGS, Reston, VA 22092 USA; COLLERSON, K.D., Univ. Calif., Santa Cruz CA 95064 USA; MACDONALD, R.A., Univ. Lancaster, Lancaster, UK; and UPTON, B.G.J., Univ. Edinburgh, Edinburgh, UK

Rocks of the exposed and concealed Precambrian crystalline basement are part of the Archean Wyoming craton or Wyoming Province, 2.5-2.8 Ga or older, and have been extensively overprinted by 1.7-1.9 Ga metamorphic and intrusive activity. Seismic data indicate 45 to 50 km crustal thicknesses. Eocene alkalic subsilicic to silicic magmas contain xenoliths derived from upper crustal to upper mantle depths.

In the Bearpaw Mountains (BPM), rocks of the shonkinite -- mafic phonolite series (SMP), especially pyroclastic deposits, contain biotite/phlogopite pyroxenites, abundant crustal granulites and amphibolites, rare garnet pyroxenites (Collerson et al., 1989) and locally, spinel peridotites of two textural groups, cumulate and porphyroclastic. Only a few Missouri Breaks (MB) alnöite and kimberlite diatremes contain deep-source xenoliths: crustal granulites; rare upper-mantle spinel, garnet-spinel, and garnet peridotites; and rare phl + cpx ± calcite glimmerites from unknown depths.

MB granulites are felsic, intermediate, and mafic; assemblages are mainly cpx + grt + pl + rt ± hbl ± sulfide. Densities range from 2.67 to 3.44 g/cm^3; most are 3.0 to 3.2. Rb/Sr from 0.03 to 0.14 suggests that this lower crust is less depleted in LIL elements than exposed deep-crustal granulite terranes elsewhere.

BPM bi/phl pyroxenites contain cpx + bi(phl) ± ol, and have cumulate or hypidiomorphic-granular textures; many probably crystallized from SMP magmas at shallow depths (1-10 km). Cumulate spinel peridotites (wehrlites and dunites) contain cumulus phases ol (Fo_{87-92}) + Cr-cpx and intercumulus phases Cr-sp + poikilitic Cr-phl + Cr-cpx + opx, and probably crystallized in the upper mantle from SMP magmas or precursor melts. A subgroup of cumulate peridotites, richer in phl and cpx of lower Mg and Cr contents, may be from the lower crust or upper mantle. Upper-mantle porphyroclastic spinel peridotites contain ol (Fo_{88-92}) + Cr-cpx + opx + Cr-sp ± Cr-phl; half contain phlogopite as disseminated grains or as elongate to equant clots around Cr-spinel.

MB peridotites are coarse granular and porphyroclastic dunites, harzburgites, and lherzolites that have low cpx contents. A lower P-T group (2-pyroxene and gar-cpx methods) indicates a normal shield geotherm, whereas a higher P-T group is above that geotherm. Phlogopite is present in many lower P-T peridotites; only a few lower P-T spinel peridotites contain pargasitic amphibole, with equilibrium texture.

Mean densities of 3.0 to 3.25 g/cm^3 for BPM and MB high-P granulites and BPM garnet pyroxenites imply lower-crustal P-wave velocities of 7.2 to 7.9 km/s, equal to or significantly higher than measured lower-crustal velocities in nearby U.S. and Canadian refraction profiles. The presence of underplated or within-crust phlogopite-bearing cumulate peridotites near the crust-mantle boundary is consistent with the diffuse character of BPM-area Moho reflections; phlogopite markedly lowers P-wave velocity (from 8.3 to 7.4 km/s for 30% phlogopite).

The presence of phlogopite in pyroxene-depleted peridotites suggests an early depletion event and a younger metasomatic enrichment event. This sequence is in accord with isotopic and geochemical evidence elsewhere in the Montana portion of the Wyoming Province, which shows mantle depletion at 2.5-2.6 Ga, enrichment at 1.7-1.9 Ga, and much younger enrichment in the late Mesozoic or early Tertiary. Phlogopite in the upper mantle may be both a source and a product of widespread potassic magmatism in this region.

INTERACTION OF VOLCANOGENIC FLUIDS WITH HOST ROCKS AND METEORIC WATERS, AND THEIR RELATIONSHIP TO MINERALIZATION

HEDENQUIST, J.W., Mineral Deposits Dept, Geological Survey of Japan, 1-1-3 Higashi, Tsukuba 305, Japan.

The generation and evolution of volcanogenic hydrothermal fluids from a parent magma has been the goal of recent studies on fumarolic gases (e.g. Giggenbach, 1987), related hydrothermal fluids (e.g. Kiyosu and Kurahashi, 1984; Sturchio et al., 1988; Giggenbach and Sheppard, 1989) and trace metals in volcanic discharges (e.g. Buat-Menard and Arnold, 1978; Symonds et al., 1987, 1988). In order to interpret the relation of these volcanic fluids to ore deposition, their interaction with the host rocks and adjacent meteoric system must also be considered. Alteration and stable isotope studies of active and fossil systems have been conducted for this purpose.

Wall rock fragments ejected from White Island volcano, New Zealand, consist of veined andesitic flows and tuffs (Simmons and Hedenquist, in prep.). The veins are largely alunite (natroalunite) and anhydrite, with narrow leached haloes containing pyrite in the otherwise fresh rock. The sulfur isotopic composition of the coexisting alunite and pyrite indicate formation at ~400°C. At this temperature, the condensed magmatic brine adjacent to the volcanic vent will be comprised largely of the associated chloride species KCl, NaCl, $CaCl_2$, $FeCl_2$ and HCl, as well as H_2SO_4 (the latter from SO_2 disproportionation). Relatively little wallrock alteration will take place as this fluid flows through fractures. Rather, reaction between the chloride species and sulfuric acid will precipitate the observed sulfates and pyrite, generating HCl in the process (e.g. Burnham and Ohmoto, 1980). Once the brine ascends and cools to <300°C, dissociation of HCl will cause extreme hydrolytic leaching and congruent dissolution of the rock, as noted by Giggenbach and Glasby (1977) from analyses of surficial brine precipitates; deposition of metals, particularly copper as enargite, may accompany this dissolution (copper is depleted in the surface precipitates).

Gold and copper mineralization can form in this high sulfidation environment (Stoffregen, 1987; Hedenquist, 1987), often associated with siliceous residue and an advanced argillic alteration assemblage of alunite, alunite, pyrophyllite and enargite. Several examples occur in the Nansatsu district of Kyushu (Hedenquist et al., 1988). Leaching of the host andesites occurred at 200-250°C by meteoric-dominated water in which the sulfate was derived from SO_2 disproportionation; however, much of the necessary acidity (pH ≤2) of the dilute fluid would have been due to HCl. This is consistent with the interaction of volcanic gases and meteoric waters observed near Japanese volcanoes, which results in acid brine production (Mizutani and Sugiura, 1982; Kiyosu, 1985). Such interaction of volcanogenic gases with a meteoric convection cell at Nansatsu (extinct volcanic vents are ~2 km distant) would have generated the necessary acidity, with the volcanic component presumably supplying the majority of the metals. In order to form an ore deposit in such a situation, interaction of a meteoric system with the volcanogenic fluid may be necessary to assist in condensing the volatile gases (including metals), which otherwise may dominantly discharge to the surface.

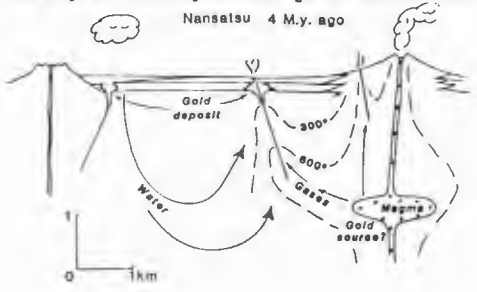

TEXTURAL DISTINCTION OF SILICIC LAVAS AND WELDED TUFFS USING PROCESSED SCANNING ELECTRON MICROSCOPE IMAGES

HEIKEN, G., Earth and Space Sciences Division, Los Alamos National Laboratory, Los Alamos, NM 87545
SHERIDAN, M., Arizona State University, Department of Geology, Tempe, AZ 85281
WOHLETZ, K., Earth and Space Sciences Division, Los Alamos National Laboratory, Los Alamos, NM 87545, and
DUFFIELD, W., U.S. Geological Survey, 2255 N. Gemini Drive, Flagstaff, AZ 86001

The pyroclastic or lava-flow origin of some widespread rhyolite sheets is controversial because of their textural similarities. Distinction among glassy silicic lavas, rheomorphic ignimbrites, and densely welded tuffs of similar composition by conventional field and petrographic methods often leads to ambiguous interpretations. A new method using processed scanning electron microscope (SEM) image data from ion-etched, polished thin sections reveals diagnostic hidden textures.

Part of this method's success depends upon etching of thin sections by chemical or ion techniques. The etching enhances subtle textural and mineralogical features by producing a microtopography related to material hardness. Even after etching, SEM micrographs of secondary or backscattered electrons might not show textural features. Digital image processing is effective in enhancing subtle textural variations not easily distinguished in the original image. Processing includes edge enhancement, gray level filtering, and binary digitization. In some cases, x-ray maps of key elements complement the processed images.

Samples from lava flows, welded tuffs, and rheomorphic tuffs that have been examined include: (1) lava flows at Inyo-Mono domes of California, the widespread Miocene flows of the central Snake River Plain of Idaho, and Taylor Creek lavas of New Mexico; (2) welded tuffs from the Bishop Tuff of California and the latite ignimbrite of Bodie Hills in California; and (3) rheomorphic ignimbrites, including the Green Tuff of Pantelleria, tuffs of the Montana Mountain sequence of northern Nevada, and tuffs from the Trans-Pecos volcanic field of Texas.

Textural features of lavas, revealed by this technique, are various types of cracks (most notably perlitic ones), flow foliations, microfolds, and unfractured crystals. Hidden textures in welded tuffs include individual shard boundaries of annealed pyroclasts, collapsed vesicles, areas of welded fine ash, fractured crystals, and thermally modified xenocrysts and xenoliths. Size distributions and shape factors of clasts in tuffs can be extracted from a binary image data set and are useful for identifying rheomorphic deformation.

DISTINGUISHING STRONGLY RHEOMORPHIC TUFFS FROM EXTENSIVE SILICIC LAVAS: IMPLICATIONS FROM TRANS-PECOS TEXAS

HENRY, Christopher D., PRICE, Jonathan G., RUBIN, Jeffrey N., Bureau of Economic Geology, The University of Texas at Austin, Austin, Texas 78713

Both pyroclastic-flow deposits that have undergone such extensive secondary flow that they closely resemble lavas and true extensive, large-volume silicic lavas occur in the Trans-Pecos volcanic field. Their characteristics suggest some useful, although not always diagnostic, methods for distinguishing the two.

Pyroclastic flow features, such as flattened pumice and vertical gas-escape pipes, in the most strongly rheomorphic tuff are preserved only in a 5-m-thick base of a 100-m-thick flow. Overlying rheomorphic tuff is strongly foliated and lacks pyroclastic features except for sparse lithics. Upward, the foliation defines broad, open folds. The upper half of the flow is intensely brecciated; the breccia contains a variety of textural types and is identical to breccias developed in silicic lavas by viscous flow.

The best example of an extensive silicic lava is a single flow (maximum thickness = 110 m; volume = 50 km^3) that crops out over 1000 km^2. A probable source in the north-central part of its outcrop indicates a minimum flow distance of 40 km. Outcrop- and microscope-scale evidence of lava-flow origin includes abundant flow bands and folds, elongate vesicles, trachytic texture, and autobreccias and vitrophyres at the base and top of the flow. In contrast to the rheomorphic tuff, the base consists of either massive, flow-banded rock or breccia of massive to vesicular blocks. Despite extensive search, no pyroclastic features were found.

Basal breccias, which were not found in any rheomorphic tuffs, may be unique to lavas. In contrast, upper breccias occur in both lavas and rheomorphic tuffs. Lavas are typically chemically and mineralogically homogeneous, whereas even rheomorphic tuffs appear to be zoned. Aspect ratios of Texas lavas, although low by conventional standards, are much higher than those of unequivocal tuffs in the region. Lavas erupted from fissures and are not ponded within source calderas, unlike tuffs. Pumice and lithic fragments or inclusions can occur in either tuffs or lavas and are not diagnostic.

AN OVERVIEW OF THE LOW P-Ti MESOZOIC CFB OF GONDWANA

HERGT, J.M., HAWKESWORTH, C.J., The Open University, Walton Hall, Milton Keynes, MK7 6AA and BREWER, T.S., The University of Nottingham, Nottingham, NG7 2RD.

Continental flood basalts (CFB) with unusually low P and Ti contents (LPT) extend from Brazil, through southern Africa, across Antarctica and into southeastern Australia and appear to have been associated with the breakup of the Gondwana supercontinent. New elemental and isotopic data from Australian and Ferrar Group Antarctic tholeiites show remarkable similarity confirming the shared petrogenesis of these magmas. Critical trace element and isotopic signatures are best explained as being inherited from a lithospheric mantle source. The unusual chemistry is believed to have been imposed on the source (depleted by previous basalt extraction) during subduction. This source contamination and the subsequent partial melting episode appear to have been very reproducible over distances of thousands of kilometres.

This uniformity in CFB magma-types is replaced by a variety of tholeiites in the Theron Mountains (which lie between the Transantarctic Mountains and Queen Maud Land) and includes different HPT and LPT members. For example, the LPT rocks have higher TiO_2 contents (generally 0.8-0.9 wt % or more) but extend down to values of 0.6 wt % typical of the Australia-Ferrar group. This type of variation is more consistent with the enormous volume of data now available for rocks of the Karoo and Paraná tholeiites. Most would now agree that the chemistries of these tholeiites also reflect their lithospheric mantle source regions, so that it is now possible to map out different magmatic provinces within the LPT-zone.

The most abundant LPT tholeiite in southern Africa is the Lesotho-type and its trace element signature is shown below with a representative Australian-Ferrar pattern (normalised to primitive mantle). The latter is significantly more depleted in Sr, P, Ti and enriched in Rb, Ba, Th, U and Pb compared with the Karoo tholeiite. Interestingly, in the Theron Mountains, tholeiites exhibit characteristics which can be correlated with both of the types illustrated. This is also holds for the Sr and Nd isotopic signatures (as shown), and the implications for the stabilization of the sub-continental lithospheric mantle source will be explored.

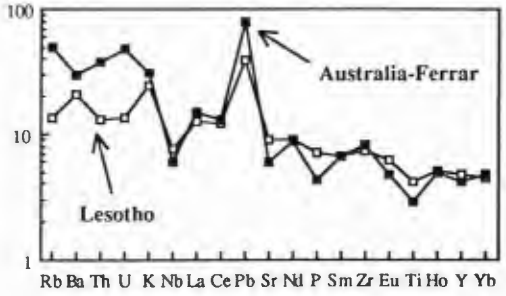

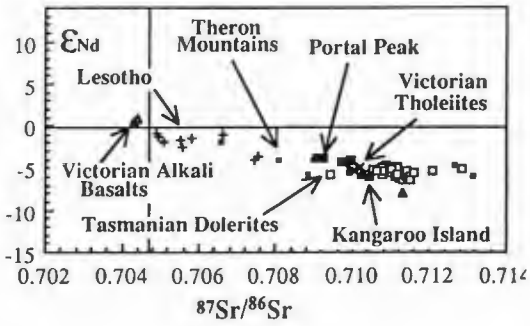

THE COUPLING OF SHALLOW INTRUSIONS TO DEEP MAGMATIC SOURCES: NEW ELECTROMAGNETIC CONSTRAINTS FROM SOCORRO, NEW MEXICO

HERMANCE, J.F., Department of Geological Sciences, Brown University, Providence, RI 02912, and
NEUMANN, G.A., Department of Geological Sciences, Brown University, Providence, RI 02912

The Socorro "magma body" beneath the Rio Grande Rift in Central New Mexico represents a control case which the geoscience community has come to accept as one of the prime examples of an intrusive magma body beneath a continental rift. To further study this feature, in particular its relation to large-scale features delineated elsewhere beneath the rift, we operated a sequence of densely spaced (5-10 km), wideband (10-4000 s) remote referenced, three component magnetic variation measurements along an E-W line which transected the southern margin of the magma body. Our profile was deployed so as to cross precisely above the center of the most seismically active portion of the structure mapped by Sanford and his colleagues southwest of Socorro.

Of a wide variety of models that were assessed using a generalized 2-D inversion algorithm, we conclude that no plane layered model for the crustal structure beneath the surface basins is able to account for our observations -- we absolutely require an asymmetric structure in the crustal basement, with the crust being more conductive to the east than to the west. In addition, the data absolutely require a more conductive core directly beneath the middle of our profile. These attributes place important constraints on geophysical and tectonomagmatic models for this region:

First, the resistivity structure beneath the western end of our profile, which is physiographically adjacent to the Colorado Plateau, has properties which are remarkably similar to those reported for interior regions of the Plateau.

Second, the intracrustal conductor subtending the area to the east of the profile has a conductance (depth integrated conductivity) which is remarkably similar to that proposed for elsewhere along the rift.

Third, the conductive core at shallow levels in the crust appears to be associated with the zone of microseismicity described by Sanford and his colleagues, and might be a zone of diffuse magmatic intrusions, enhanced hydrothermal circulation, or a combination of both.

Thus, while certain details of our model need further evaluation, there should be little doubt that fundamental physiotectonic processes are mapped into the electrical properties of the lithosphere over a wide range of scale-sizes.

PETROLOGY OF A SEAWARD EXTENSION OF THE EAST AFRICAN RIFT IN THE NORTHERN MOZAMBIQUE CONTINENTAL MARGIN.

HERNANDEZ J., U.P.M.C., Lab. Petrologie Mineralogique, 4, place Jussieu, 75252 Paris Cedex 5, (France) and
MOUGENOT D., U.P.M.C., Lab. Geodynamique sous marine, 06230 Villefranche sur mer (France).

Two North-South extensional structures, the Kerimbas graben and Lacerda basin, occur in the Tertiary and Cretaceous sediments of the Northern Mozambique continental margin. The Kerimbas graben has been previously interpreted as a submarine extension of the East African rift. The MD40/MACAMO I cruise sismic experiments demonstrated that its eastern limit corresponds to a preexisting fault extending down to the Moho. Along the western limit tilted blocks separated by recent normal faults are observed. The volcanic basement has been dredged, east of the graben, on Grandidier seamount, in a transform zone extending along the ocean- continent boundary, with distensive opening in Senonian time. The age of the seamount (based on Globotruncana determinations) is Coniacian to Campanian. The lavas and breccias have hawaiitic compositions. The other seamounts intruded in neogene sediments are comprised of nephelinites and basanites. The chemical characteristics of the lavas are identical to that of the alkaline lavas of the eastern rift, notably the Kenya nephelinites.

All the lavas are highly vesicular and their fluid content estimated based on Cl content of the glasses and the vesicles volume is ≈ 2% H_2O. Measurements of inert gases, N_2, H_2, O_2, CH_4, etc. are in progress.

Mineralogy of the lavas attests to their strong alkaline character (nepheline, perovskite, Al-Ti-Cpx). The recent lavas contain frequent xenocrysts of olivine, ortho- and clinopyroxene. Cr and Na content in some pyroxene xenocrysts are similar to pyroxene Cr-poor suite encountered in alkali basalts and more frequently in kimberlites. Other xenocryst more closely resemble disaggregated peridotite or pyroxenite xenocrysts.

It appears that the Kerimbas graben is a post-Middle Miocene continental graben which remains active. All the lavas related to the first stages of its opening are strongly alkaline and fluid-rich. Phenocryst and xenocryst mineralogy implies an inhomogeneous and partly metasomatized mantle under the rift.

The Macamo II cruise (January-February 1989) should provide detailed information on the northern termination of the Kerimbas graben and its southern articulation with the Mozambique channel. Preliminary results on the volcanics dredged during the 1989 cruise will be also presented.

DIRECT DETERMINATIONS OF VOLATILE GRADIENTS IN THE BANDELIER TUFF THROUGH ANALYSIS OF MELT INCLUSIONS

HERVIG, R.L., Center for Solid State Science, Arizona State University, Tempe, AZ, 85287-1704

DUNBAR, N.W., Dep't of Geoscience, New Mexico Institute of Mining and Technology, Socorro, N.M., 87801

The Lower Bandelier Tuff and precursor plinian tephra, which erupted at 1.45 Ma in northwestern New Mexico, are thought to be the product of a zoned magma chamber. We have attempted to directly determine the pre-eruptive volatile gradient of this magmatic system using ion and electron microprobe analyses of melt inclusions in magmatic phenocrysts. Large melt inclusions (up to 400 microns in diameter) are abundant in quartz crystals from the Lower Bandelier ignimbrite and associated plinian tephra. Melt inclusions in phenocrysts from the plinian tephra are generally composed of clear glass and contain few shrinkage bubbles. Most inclusions appear to be primary, but some fill pockets where the host crystal had been resorbed, or had incompletely grown. Inclusions in crystals from the ignimbrite samples generally contain shrinkage bubbles, and the size and number of bubbles varies between inclusions. Some inclusions appear altered, but pristine inclusions can be found.

Major element composition of pristine melt inclusions closely resembles bulk rock composition, which suggests that no extensive post-entrapment crystallization has taken place, and no zone of compositionally altered melt developed around the growing crystal. In cases where inclusions appeared altered, patchy remobilization of K and Na can be detected by electron microprobe analysis. Some pocket-filling inclusions from the plinian tephra appear pristine but have a uniformly high K_2O content, and correspondingly low Na_2O. This does not appear to be due to alteration, and may represent a localized high-K zone in the upper portion of the magma chamber.

Mean water contents of melt inclusions from 2 bulk pumice samples from the Lower Bandelier plinian tephra are 4.7 wt.% (n=4, base of plinian) and 4.3 wt.% (n=10, top of plinian). Melt inclusions from a bulk sample of the transition zone between the plinian tephra and the Lower Bandelier ignimbrite have a mean H_2O content of 4.3 wt.% (n=12), and melt inclusions from three samples of the Lower Bandelier ignimbrite contain 1.7, 2.1, and 2.2 wt.% H_2O (n=14, 21, and 14 respectively). The three samples of the ignimbrite are from different stratigraphic heights, but due to the eruptive style of the ignimbrite, these cannot be directly correlated to the original depth in the chamber. Trace element chemistry determinations by neutron activation analyses of bulk samples (1 pumice lump each) will allow determination of the relative positions of ignimbrite samples. Other analysed elements which are known to be compatible in a magmatic volatile phase include F, Cl, B and P. The mean contents from melt inclusions in the two plinian samples and the transition sample are: F 0.22, 0.24, and 0.14 wt.%; Cl 0.24, 0.29 and 0.20 wt.%; B 47, 46 and 41 ppm; and P 186, 283 and 154 ppm (n=4, 10 and 12 respectively for F, B and P; n=6, 18, and 19 for Cl). The mean contents of the ignimbrite melt inclusions, in the order given above, are: F 0.08, 0.14 and 0.07 wt.%; Cl 0.17, 0.21 and 0.16 wt.%; B 26, 28 and 18 ppm; and P 174, 183 and 170 ppm (n=14, 21 and 14 respectively for F, B and P; n= 23, 28 and 26 for Cl). These data suggest that a volatile gradient was present in the magma which produced the Lower Bandelier plinian and ignimbrite, and that the degree of gradient present varied between elements. The highest water content observed in a plinian inclusion was ~5 wt.%, and the lowest in an ignimbrite inclusion was ~1.0 wt.%, which define the range of the H_2O gradient with the data we now have available. The calculated density contrast between a Bandelier melt with 1 and 5 wt.% H_2O is approximately 0.16 g/cm^3

Certain trace elements were also analysed by ion microprobe in Bandelier melt inclusions. The trace elements in the large set of inclusions cover the approximate range of trace elements seen in the Lower Bandelier plinian and ignimbrite, and show a rough inverse correlation with the volatile contents of the inclusions.

THE MAFIC, ALKALIC WELLS GRAY-CLEARWATER VOLCANIC FIELD -- EVIDENCE OF CRUSTAL EXTENSION?

HICKSON, C.J., Geological Survey of Canada, 100 West Pender Street, Vancouver, B.C. CANADA V6B 1R8

Basaltic volcanism in the form of small-volume, subaerial and subaqueous eruptions has occurred in the Wells Gray-Clearwater area of east-central British Columbia. These eruptions have been dated by the K-Ar method and by relationship to known glacial periods. The oldest known eruption may be as old as 3.2 Ma, but is more likely 2 Ma or less. The youngest eruptions are less than 7560 $\pm$ 110 radiocarbon years. The most extensive basalts are valley-filling and plateau-capping flows of the Clearwater unit. The deposition of these flows has overlapped at least three periods of glaciation, recorded in the form of tuyas, ice ponded valley deposits and subglacial mounds (SUGM).

Flows of the Wells Gray-Clearwater suite appear to have erupted from vents that are both spatially and temporally separated. The individual eruptions were of low volume ($<1 km^3$) and chemically distinct from one another. Major element compositions are variable, but the lavas are predominantly alkalic. Olivine is the predominant phenocryst phase; plagioclase and augitic clinopyroxene are rare, but both minerals are ubiquitous in the groundmass. Orthopyroxene was not seen in any of the samples. Flows appear to have erupted with minimal crystal fractionation or crustal contamination. The range of compositions seen in the suite is best explained by a process of partial melting and progressive depletion of the mantle source by earlier melting events. Isotope analyses of $^{87}Sr/^{86}$, $^{143}Nd/^{144}$ and whole-rock Pb indicate that the mantle source may be derived from a remnant of subducted oceanic lithosphere which has been variously depleted by the prior generation of basaltic melts.

The alkali olivine basalts of the Wells Gray-Clearwater area have erupted onto a tectonically active surface. A peneplain (erosion surface), formed in Eocene-Miocene time has been uplifted since the Miocene and uplift may be continuing. This uplift is in response to an elevated geothermal gradient, possibly due to crustal extension. The elevated geothermal gradient and reduced pressures attendant with recent uplift and erosion may have initiated basaltic volcanism in the region, rather than a fixed mantle hot spot as proposed in earlier work.

PRELIMINARY GEOLOGIC MAP OF THE MOUNT ADAMS VOLCANIC FIELD, CASCADE RANGE OF SOUTHERN WASHINGTON

HILDRETH, Wes, and FIERSTEIN, Judy, USGS, Menlo Park, California 94025, USA

Ice-capped Mount Adams towers atop the Cascade crest some 50 km due E of Mount St. Helens. The 3743-m andesite-dacite stratocone stands at the focus of a basalt-to-rhyodacite volcanic field containing >60 Quaternary vents. The main cone today exceeds 200 km^3, and at least half as much more was eroded during late Pleistocene time from earlier high-standing components of the compound edifice; peripheral basalts add another ~ 70 km^3. Nearly all of the high cone above 2300 m was constructed during latest Pleistocene time, probably between 20 and 10 ka, explaining the abundance of late-glacial till and the scarcity of older till. Products of this eruptive episode on the main cone range from 54 to 62% SiO_2. Contemporaneous and younger peripheral vents yielded lavas and scoriae in the range 48-57% SiO_2, and, along with Mount Adams, they define a recently active N-S eruptive alignment 40 km long and only 5 km wide. If we include vents as old as 0.3 Ma, this zone lengthens to 55 km, trending N 10° W, attesting to modest E-W extension in the upper crust. Basalts within this zone are extremely varied compositionally, ranging from quartz- to nepheline-normative and from 0.16 to 1.60 wt % K_2O (at 48-49% SiO_2). Andesites also reflect this heterogeneous ancestry, ranging from 0.9 to 2.1 wt % K_2O at 57.5 % SiO_2.

Beneath the young edifice, eroded stumps of at least two earlier andesite-dacite cones are as old as 0.5 Ma, representing several eruptive episodes and a spectrum of rock compositions that extends continuously from 52 to 69% SiO_2. Coalescing shields of basalt (48-53% SiO_2) peripheral to the stratocone complex interleave with the andesite-dacite lavas erupted focally, demonstrating persistent contemporaneity and absence of systematic secular petrochemical evolution. Adams is the most potassic, petrochemically most "intra-continental", stratocone in the Cascades. Its products contain 2.0-2.6 wt % K_2O at 60% SiO_2 (and 4% at 69% SiO_2), double that of Mount St. Helens.

There have been no recorded eruptions of Mount Adams, and, of the 11 Holocene vents, none are known to have erupted products younger than 3500 years. Seven of the Holocene eruptions took place at flank vents 2000-2500 m in elevation and produced a wide range of compositions (49-61% SiO_2); the other four vents are peripheral to the main cone at 1100-1600 m and 48-54% SiO_2.

Dacitic lavas and a few block-and-ash flows (63-69% SiO_2) erupted several times from the focal area and rarely on the periphery, but none are younger than 0.1 Ma. A single rhyodacite (72% SiO_2) is undated but also old. The antiquity of all known silicic units, in conjunction with the heterogeneous mafic compositions of the late Pleistocene summit cone and of Holocene lavas erupted around that cone, make it appear unlikely that Mount Adams is now underlain by an upper-crustal magma reservoir.

Weak H_2S-bearing fumaroles still rise from crevasses in the summit icecap. Subjected to this solfataric flux, the breccia-and-scoria core of the stratocone has suffered severe acid-sulfate leaching and deposition of alunite, kaolinite, silica, gypsum, sulfur, and Fe-oxides. Where exposed in glacial headwalls, the 4-km^2 rotten core is a persistent source of avalanches and debris flows, the largest of which travelled as far as 60 km after breaking loose about 5100 years ago, creating the southwest notch and shelf for the perched White Salmon Glacier.

SIGNIFICANCE OF DISTINCT RHYODACITIC PROVINCES WITHIN THE THREE SISTERS REGION OF THE OREGON CENTRAL HIGH CASCADES.

HILL, Brittain E., Department of Geology, Oregon State University, Corvallis, OR 97331-5506.

The Three Sisters region of the Oregon central High Cascades (OCHC) has been a locus of silicic (SiO_2 > 60%) volcanism from the late Miocene to the Holocene. While the Three Sisters stratovolcanos are the most prominent silicic vents in this area, the largest silicic vent in the OCHC lies 10-15 km east of the Three Sisters at the Tumalo Volcanic Center (Hill, 1988, G.S.A. Abstr. 20-7:398). Silicic volcanism has also occurred at Broken Top volcano 5 km east of the Three Sisters. This work involves the study of over 140 OCHC units, including all the major silicic units of the 5 volcanic centers.

Analysis of rhyodacitic (SiO_2 > 68%, K_2O < 4%) units defines two distinct magmatic provinces within the OCHC. Rhyodacites associated with the Three Sisters stratovolcanos are characterized by 72-76% SiO_2, with 4-5 $(La/Sm)_n$, 0.6-0.7 Eu/Eu^* and flat HREE's at about 10X Chondritic. From 5 to 20 km east of the Three Sisters, rhyodacites associated with Broken Top and the Tumalo Volcanic Center (BT-TVC) range from 68-75% SiO_2, with 2.5-3.5 $(La/Sm)_n$, 0.4-0.6 Eu/Eu^*, and flat HREE's at 20-30X Chondritic.

Major and trace element variations are nearly continuous between BT-TVC rhyodacites and more mafic (SiO_2 < 68%) BT-TVC units, with the exception of a small but significant compositional gap from 72-74% SiO_2. Observed elemental variations between 60-72% SiO_2 are consistent with Plagioclase+Pyroxene-dominated fractional crystallization, with subordinate amounts of magma mixing. Preliminary models for rhyodacites with 74-75% SiO_2, which are the largest volume OCHC silicic units, suggest these magmas were produced through partial melting of a presumedly intermediate composition(?) crust; crystal fractionation would involve unusually large volumes (>500 km^3) of a mafic parent within a closed system. P_2O_5 <0.03 % and flat $HREE_n$ patterns indicate a lack of residual apatite, garnet, or zircon in the source rock.

Geochemical variations for Three Sisters rhyodacites are discontinuous with more mafic Three Sisters units, having a major compositional gap from 66-72% SiO_2. Observed elemental variations between 60-66% SiO_2 are also consistent with Plag+Px-dominated fractionation, with minor amounts of magma mixing. Three Sisters rhyodacites cannot be produced through any reasonable model of crystal fractionation. A preliminary model for Three Sisters rhyodacites involves partial melting of a HREE-depleted source (graywacke?) with no residual apatite, garnet, or zircon.

The distinct spatial restrictions on the rhyodacite types, and the similarities between Three Sisters and BT-TVC magmas with SiO_2 < 66%, indicates that the observed variations in rhyodacitic magma are probably controlled by pronounced changes in the composition of shallow (<10 km) crust between the Three Sisters and BT-TVC volcanic centers.

EXPERIMENTAL STUDY OF AMPHIBOLE BREAKDOWN IN MOUNT ST. HELENS DACITE WITH APPLICATIONS TO MAGMATIC ASCENT RATE DETERMINATIONS

HILL, P.M.
RUTHERFORD, M.J. (*Both at: Department of Geological Sciences, Brown University, Providence, RI. 02912*)

Post May 18, 1980 Mount St. Helens dacites show partial breakdown of amphibole to small (<50μm) plagioclase, pyroxene and Fe-Ti oxide crystals. The product crystals form a breakdown rim mantling the remaining amphibole. Isothermal experiments were conducted relating breakdown of amphibole to pressure decrease with time, in order to determine magma ascent rates (from a 7km deep magma chamber to the surface) which could result in the breakdown of amphibole. The experiments were also conducted to quantify the extent of breakdown (rim width) as a function of ascent rate. Two types of experiments were performed using samples of May 18, 1980 pumice containing pristine amphibole. Samples were initially equilibrated for ~20hr under H_2O saturated conditions at 920°C and 2kb. In the first type of experiment, the pressure was then lowered at a constant depressurization rate to simulate steady magma ascent. The second type of experiment involved a fast (1-2hr) drop to final pressure which was then held, simulating magma quickly rising to and residing in near-vent magma reservoirs (<1km). The experiments were conducted over 9hr and 2,3,4, and 9.5 day periods to a final pressure of 200-300 bars.

Amphibole breakdown rims first appear in both types of 4 day runs. Rim widths average 10-12μm and the product crystals are <1-4μm in size. The 9.5 day, constant depressurization run was difficult to interpret because of the similarity in grain size between possible rim crystals and groundmass. Some amphiboles, however, are observed to have a breakdown rim 30μm wide with product crystals 4-40μm in size. Slower depressurization rates, therefore, produce wider breakdown rims and larger product crystals.

Amphiboles from dacite of the Oct. 31, 1981 dome forming event possess two distinct sets of breakdown rim widths and product crystal sizes that occur in roughly equal proportions. The two sets have average rim widths of 10μm (set A) and 45μm (set B), and average product crystal sizes of 1-4μm and 4-50μm, respectively. Rim widths and product crystal sizes are independent of initial amphibole crystal size (100-450μm).

The rapid depressurization runs produced an almost fully crystallized assemblage of radial growth plagioclases and many small Fe-Ti oxide crystals, totally unlike the texture of the dome dacite. The runs performed at a constant depressurization rate contain roughly 30% glass and more closely reproduce the texture of the natural sample. The close correlation between the rim sizes of the 4 day experiments and those of set A in the natural sample indicate that a portion of the magma forming the Oct. 31, 1981 lobe rose at a rate of 65-70m/hr from a magma chamber at 7km depth.

EVIDENCE FOR TWO EXPLOSIONS IN THE MAY 18, 1980 LATERAL BLAST AT MOUNT ST. HELENS, WASHINGTON

Hoblitt, R.P., U.S. Geological Survey
David A. Johnston Cascades Volcano Observatory
5400 MacArthur Blvd., Vancouver, WA 98661

The deposit produced by the May 18, 1980, lateral blast at Mount St. Helens, Washington, has been interpreted as the product of a single extended explosion. Models to explain the deposit's stratigraphy have accordingly invoked one density current and attributed the various stratigraphic units to flow dynamics. Yet satellite data (Moore and Rice, 1984), photographs (Pierson, 1985), seismic data (Kamamori and others, 1984), and eyewitness accounts provide permissive evidence of two explosions within 2.5 min of the triggering earthquake. These independent data suggest that certain features of the blast deposit may be due to a discontinuous eruption rather than to flow dynamics.

Consider how the second of two closely spaced and highly energetic density currents might have affected the deposit of the first, which had only been on the ground for 10 to 100 s and was still hot, inflated, and friable. The deposit of the first would be partly or entirely eroded away in exposed locations by the second density current, but would be preserved in sheltered environments, such as in the lee of obstacles. However, the deposit from the second density current would be found in both sheltered and exposed locations.

In sheltered settings, the May 18 blast deposit's lower, coarse-grained unit (variously called by previous workers the "basal unit", the "coarse basal unit", the "basal gravel layer A1," or "A1 and A0") is locally divisible into two coarse-grained subunits separated by a finer grained subunit. The lower of these two coarse-grained subunits contains a larger proportion of cryptodome dacite and a smaller proportion of hydrothermally altered nonjuvenile clasts than does the upper coarse-grained subunit. The finer grained subunit consists of sheared comminuted soil and (or) structureless to faintly bedded silt- to sand-sized ash.

These three subunits can be interpreted as evidence of two depositional events separated by a brief repose. In this scheme, the two coarse-grained subunits reflect deposition from two density currents during their waxing stages. The finer grained subunit reflects two processes: (1) shearing at the base of the second density current, and (2) ash accumulation during the waning stage of the first density current, before the arrival of the second. The relative proportions of cryptodome dacite and hydrothermally altered clasts suggest that the first explosion was dominantly magmatic and the second had an appreciable phreatomagmatic component.

Explanations based wholly on flow dynamics can also be devised; for instance, the three subunits and clast-populations differences could be attributed to local topographic effects. These alternatives, however, must either dismiss the independent data sets that suggest two explosions or assume that one explosion produced little or no deposit. As is evident from the widely cited photographs of Rosenquist (Voight, 1981), the initial explosion was huge, and satellite imagery (Moore and Rice, 1984) indicates that the second explosion was an even larger. Thus, either explosion was apparently of sufficient magnitude to have produced substantial deposits by itself.

Kanamori, H. et al., 1984, JGR, 89, 1856-1866.
Moore, J.G., and Rice, C.J., 1984, in Explosive Volcanism: Inception, evolution, hazards: Washington, D.C., National Academy Press, 133-142.
Pierson, T.C., 1985, GSA Bull., 96, 1056-1069.
Voight, Barry, 1981, USGS Prof. Paper 1250, 69-86.

CONTINENTAL VOLCANISM ASSOCIATED WITH A DESTRUCTIVE PLATE BOUNDARY: NEW ZEALAND

HODDER, A.P.W., Department of Earth Sciences, University of Waikato, Hamilton, New Zealand.

Much of the Recent volcanic history of New Zealand has been successfully interpreted as a consequence of its straddling the Indo-Australian-Pacific plate boundary, but the volumetrically small basalts of northern New Zealand are not readily accommodated in such a model. Furthermore, many of these basalts have geochemical signatures more akin to those of intraplate or extensional settings. However, such age data as are available for these volcanics are not consistent with their being a consequence of the plate's passage over a stationary hotspot; rather a more diffuse mantle source must be required. Rather similar age-distance problems have been described for Eocene-Recent intraplate volcanism on the Campbell Plateau to the southeast of New Zealand, and for the volcanics of eastern Australia. All these rocks have sufficient geochemical similarities to propose as their common source a mantle heterogeneity which transcends the presently active plate boundary. Seismic tomography also suggests a mantle heterogeneity in this region.

If subduction related volcanism is superimposed on and is itself followed by continental volcanism, it is possible that the heterogeneity may be locally contaminated by the downgoing slab, or equivalently that uprising magma from the mantle wedge may have continental/intraplate rather than subducting geochemical characteristics. In addition it may be that the magma ascent routes established during a subduction regime may be re-used by subsequent continental volcanism (as may have occurred in northernmost New Zealand) or vice versa (as may have occurred in Taranaki, western North Island). These possibilities become even more likely when it is considered how the relative importance of extension and subduction and the location of this destructive plate boundary have varied during the Cenozoic.

ASSIMILATION OF CONTINENTAL SEDIMENTS OR SUBCONTINETAL LITHOSPHERE DURING DIFFERENTIATION OF OCEAN ISLAND MAGMAS (GRAN CANARIA, CANARY ISLANDS)

K. Hoernle and G Tilton (Dept. of Geology; University of California; Santa Barbara, CA 93106)
H-U Schmincke (Arbeitgruppe Vulkanologie; Insitut für Mineralogie; Ruhr Universität; D4630 Bochum; FRG)

The late-stage Roque Nublo volcanics (4.4-3.4 Ma) on Gran Canaria, Canary Islands show extreme chemical diversity. The range of compositions includes minor tholeiites, a complete suite of alkali basalts, hawaiites, mugearites, benmoreites and trachytes, and a complete suite of basanites, tephrites, ne-mugearites, ne-benmoreites and phonolites. Mass balance calculations are consistent with a genetic relationship, via crystal fractionation, for rocks within a given suite. Crystal fractionation cannot relate samples in different suites. Most of the trace element data further supports the crystal fractionation model.

Thirty whole-rock samples for the basalts (Differentiation Index < 35) and the evolved volcanics (DI > 35) were also analyzed for Sr, Nd and Pb isotopes. The evolved volcanics are distinct in all isotope ratios from the basalts but do fall on extensions of the trends formed by the basalt data. The evolved volcanics, which in most cases have high Sr, Nd and Pb concentrations, have more radiogenic 87/86 Sr and 208/204 Pb ratios, but less radiogenic 143/144 Nd, 206/204 Pb and 207/204 Pb than the basalts. The low 207/204 Pb ratios, for a given 206/204 Pb ratio, are lower than any yet observed for ocean island volcanics and suggest mixing with a source which had a very low U/Pb ratio for > 2 Gyrs. The correspondingly high 208/204 Pb ratios suggest a high Th/U ratio, whereas the Sr and Nd isotopes suggest high Rb/Sr and low Sm/Nd ratios of this source. Three phonolite samples from the late Shield, Fataga Formation (13-9 Ma), which have higher Nd and Pb but significantly lower Sr concentrations than the Roque Nublo evolved volcanics, have Pb and Nd isotopes similar to the shield basalts but have extremely radiogenic Sr isotope ratios ranging from .75 to .83.

If we accept that the basalts and the evolved rocks are genetically related, then the distinct isotopic characteristics between them must have resulted from assimilation during storage and fractionation within the upper mantle or crust beneath Gran Canaria. The isotopic and inferred trace element characteristics of the contaminant are consistent with assimilation of small amounts (probably < 1%) of either >2 Gyr (1) continental metasediments and/or metagranitoids, or (2) recycled subcontinental lithosphere metasomatically altered by subduction processes. Since Gran Canaria is underlain by several kilometers of sediments shed from the >2 Gyr West African Craton, we prefer crustal contamination to explain the observed isotopic differences. Nevertheless, recycled subcontinental lithosphere cannot be ruled out until the composition of the lithosphere beneath the Canaries has been determined through mantle xenolith studies.

GEOCHEMISTRY OF LATE CENOZOIC MAFIC LAVAS FROM SOUTHERN NEW MEXICO

HOFFER, J.M. and ANTHONY, E.Y. Department of Geological Sciences, University of Texas at El Paso, El Paso, TX 79968-0555

Late Cenozoic lavas from southern New Mexico may be divided into two groups: older lavas (approximately 10 to 3 Ma) are predominantly tholeiites and have low values of TiO_2,, whereas younger lavas (3 Ma and younger) have lower SiO_2, higher TiO_2, and variable compositions from tholeiite through basanite. Many of the young alkaline flows, e.g. the Potrillos, Afton/Aden, Black Mountain, and Elephant Butte, are found in valleys formed by recent faulting in the Rio Grande Rift, whereas tholeiites, e.g. Animas, Hachita, and Deming, are found on the rift flanks.

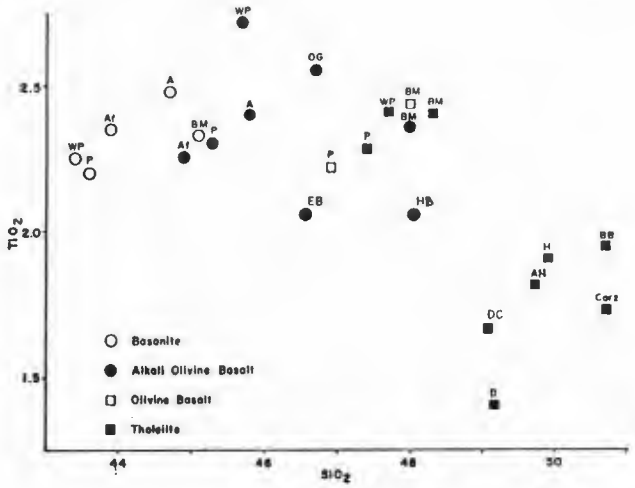

(WP West Potrillo (1-2 Ma), Af/A Afton/Aden (0.2-1.2 Ma), BM Black Mountain (0.2-0.6 Ma), EB Elephant Butte (2.1 Ma), P Palomas (3.0-5.2 Ma), HB Hillsboro (4.2 Ma), D Deming, DC Deming - Cook's Peak, AN Animas (0.5 Ma), H Hachita (11.8 Ma), Carz/BB Carrizozo/BrokenBack

These observations are in contrast to the northern New Mexico portion of the Rift, in which alkaline compositions are often found on the flanks and along the Jemez Lineament, and tholeiites are axial. Our observations are in agreement with those of Kempton and others (1987) for the Geronimo field. They find that flank lavas are older (9 to 3 Ma) and less alkalic than valley lavas (3.5 to 0.3 Ma).

Normative classification shows good correspondence with geochemical indices. Nepheline normative rocks generally have higher Sr ($\bar{x}$ = 666 ppm), Ba ($\bar{x}$ = 476 ppm), and Nb ($\bar{x}$ = 60 ppm) than less alkaline rocks (Sr = 475, Ba = 330, Nb = 37), making ratios such as Zr/Nb and Zr/Ba useful in distinguishing between the two groups.

Kempton, P.D., Dungan, M.A., and Blanchard, D.P. (1987) Geol. Soc. Amer. Spec. Paper 215, 347-370.

DEMONSTRATION OF USE OF DIGITAL SATELLITE AVHRR IMAGES FOR ERUPTION CLOUD MAPPING

Holasek, Rick E. and **Rose, W. I.**, Dept. of Geol. Engrg., Geology & Geophysics, Michigan Technological University, Houghton, MI 49931 USA

This poster presentation will be a display of digitally processed weathered satellite images of eruption clouds from recent eruptions of Augustine (1986), El Chichon (1982), Mount St. Helens (1980) and Lonquimay (1988-89).

Carried aboard NOAA weather satellites, the advanced very high resolution radiometer (AVHRR) collects imagery with 4 and 1 km resolution in 5 spectral bands (0.58-0.68; 0.73-1.1, 3.55-3.93; 10.5-11.3; 11.5-12.5 microns). The imagery can map eruption clouds in three dimensions using thermal bands and atmospheric temperature profiles as has been demonstrated by M. Matson (eg. 1984, JVGR, 23: 1-10) and Y. Sawada (1987, Tech. Rep. Met. Res. Inst. [Japan], No. 22). In our work we used multispectral techniques to distinguish meteorological clouds from eruption clouds. This is possible when two thermal IR bands are collected, as is the case for NOAA 9 and NOAA 11. The two thermal bands are ratioed and displayed along with other bands, allowing mapping of eruption clouds even in partly cloudy conditions. We can show some examples of detection of ash plumes below some thin meteorological clouds.

We have also begun to explore plume dispersion and opacity by studying images where we have some ground truth including local weather conditions, upper air temperatures and winds, eruption cloud particle concentrations, eruption cloud heights, ash fallout times and ash compositions (Rose et al., JVGR, 93: 4485-4499). If the grain size distribution of particles in the cloud can be estimated, the minimum particle concentration of an opaque plume can be calculated. We examined how to recognize and outline opaque parts of plumes, a difficult problem which is aided when multispectral images are available. All thick opaque plumes eventually disperse and become transparent to the sensor. We present examples of transparency maps of dispersing plumes. If transparency of the plume can be accurately mapped, it may be possible to quantify plume dispersion patterns.

We hope that our work can eventually help lead to real time use of weather satellites for volcanic eruption monitoring.

INVESTIGATION OF MAGMATIC PROCESSES: SMALL-SCALE SAMPLING OF MAFIC ENCLAVES AND DACITE HOSTS

HOLDEN,P., DAVIDSON,J.P., HALLIDAY, A.N. Dept. Geological Sciences, University of Michigan, Ann Arbor, MI 48109, and DESILVA, S.L., Lunar and Planetary Institute, 3303 NASA Rd 1, Houston, TX 77058.

Mafic inclusions (enclaves) in granitoids and their volcanic equivalents occur commonly in orogenic rock suites. Textural evidence indicates that the inclusions have been injected into the host in a liquid or plastic state. However, isotopic differences betweeen enclave and host preclude a direct relationship through closed system differentiation. We have examined the isotopic variations encountered on a small scale in passing from inclusion to host, in order to assess the degree of elemental and isotopic exchange.

Samples were selected from the Purico-Chascon volcanic suite (<1.5Ma) of the central Andes, for which an isotopic difference between bulk dacite and inclusions has been shown to exist. A detailed traverse was made by cutting 7 chips over a distance of 5-7 cm perpendicular to the enclave - host interface (Chips labelled A to G in the diagrams below; chip D has not been analyzed at this time). In addition, five sites were sampled with a microdrill (c. 1 mg of sample) to determine Sr isotopic variation on the smallest scale. On a gross scale, there is a trend of decreasing $^{143}Nd/^{144}Nd$ and increasing $^{87}Sr/^{86}Sr$ in passing from enclave to host, but the most extreme isotopic compositions and the highest Sr and Nd concentrations are actually encountered within a few mm of the enclave/dacite interface. The microdrill samples confirm this trend but also indicate that heterogeneity exists on a finer scale. A plagioclase xenocryst sampled by microdrilling gave $^{87}Sr/^{86}Sr = 0.708191 \pm 20$.

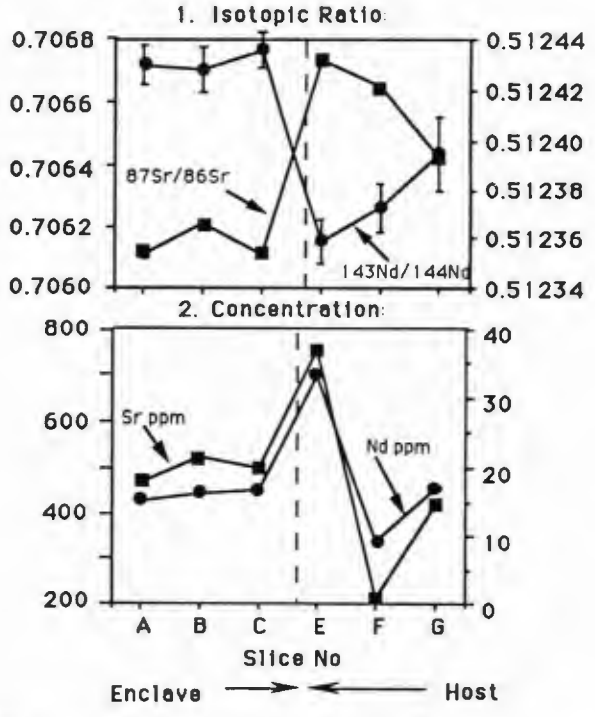

The systematics may be explained by interaction between three components; mafic liquid (enclaves) crustal material (represented by plagioclase xenocryst) and dacite (itself probably the result of crustal contamination of more mafic magmas). The occurrence of extreme isotopic compositions at the margin rather than well into the dacite is enigmatic, but may reflect greater elemental mobility at the interface and concentration of low melting fraction crustal melts. The high elemental *concentrations* at the margin may record a diffusion profile.

ALKALINE VOLCANISM FOLLOWING THE CESSATION OF SUBDUCTION ALONG THE ANTARCTIC PENINSULA

HOLE, M.J., British Antarctic Survey, High Cross, Madingley Road, Cambridge CB3 0ET U.K.

Following more than 200 Ma of subduction of Pacific oceanic crust beneath the west coast of the Antarctic Peninsula, subduction ceased by a series of ridge crest-trench collisions. However, magmatism continued after the cessation of subduction with basaltic rocks of the intraplate alkaline association being erupted from centres scattered along the whole length of the peninsula.

In the southwest, on Alexander Island, a suite of Miocene-Pleistocene (7-<1 Ma) olivine and alkali basalts, tephrites and basanites were erupted between 18 and 48 Ma after the cessation of subduction.

In the northeast, at Seal Nunataks, tholeiites, olivine and alkali basalts were erupted less than 4 Ma ago, almost synchronously with the cessation of subduction in that area (4-6 Ma). Correlated trace element-isotope variations can be explained by a model involving mixing of a LILE-, ^{87}Sr-depleted end-member, similar to the source for non-Dupal OIB and N-type MORB, with isotopically enriched mantle material with high LILE/HFSE ratios. This enriched mantle component may have been generated during the previous 200 Ma of subduction related magmatism within the Antarctic Peninsula.

Post-subduction high-Mg andesites ('bajaites'), which are associated with the cessation of subduction along other continental margins (e.g. Baja California, southern Chile), are apparently absent within the Antarctic Peninsula. This is likely to be a result of differences between the plate configurations prior to and during the cessation of subduction along different continental margins.

Off Baja California, the inactive spreading ridge is preserved, and the continued presence of the foundered slab beneath the continental margin was probably a prerequisite for the generation of bajaites in that area. By contrast, along the west coast of the Antarctic Peninsula, ridge crest-trench collision took place and the leading oceanic plate probably continued to subduct. Under these circumstances, uprise of alkalic magmas from asthenospheric sources could have been permitted through the resulting 'no-slab window' and/or via subducted oceanic fracture zones. The latter case seems attractive for the occurrences of alkalic basalts at Seal Nunataks as they form a linear chain coincident with the landward trace of two major oceanic fracture zones, which are known to have been subducted for c.20 Ma.

RECURRENT VOLCANISM AND MAGMATIC CYCLES AT SAN FRANCISCO MOUNTAIN, COLORADO PLATEAU, ARIZONA

HOLM, R. F., Department of Geology, Northern Arizona University, Flagstaff, AZ, 86011

San Francisco Mountain is an andesitic volcano within an intraplate basaltic volcanic field. The composite volcano, composed of about 110 km^3 of andesite (87%), dacite (12%), and rhyolite (1%), is at the center of a volcanic system that contains nearly 11 km^3 of mostly dacite in 5 peripheral silicic centers. The andesitic to silicic lavas of the volcanic system contributed over 24% of the erupted products of the San Francisco volcanic field during a period that spans over 40% of the time in the late Miocene to Holocene when the field developed. A long lifetime and low average growth rate that was 1 to 2 orders of magnitude lower than the rates of composite volcanoes in volcanic arcs indicates that San Francisco Mountain was supplied by a long-lived source, and probably had long repose periods.

Volcanic stratigraphy and geochronology document recurrent volcanism in 5 growth stages each beginning with the eruption of silicic lavas. The first 2 stages ended with voluminous andesite that constructed stratocones, but the volume and proportion of andesite declined in the 3rd stratocone. Andesite is a minor component of the last growth stage, which was dominated by parasitic domes and lava flows of dacite and rhyolite. The progression from silicic to andesitic lavas during a growth stage may record the tapping of a chemically zoned magma chamber from the top down.

The growth stages were supplied by at least 4 magma cycles, which probably were driven by basalt from the mantle. Episodic resupply of parental basalt to a differentiating crustal magma chamber can account for the availability of low to highly evolved lava in each of the magma cycles, and is compatible with concurrent basaltic volcanism in the field. Repeated influx of basalt will also add heat to produce anatectic magmas that may compose all, or parts of, the peripheral silicic centers. Declining erupted volumes and declining proportions of andesite to silicic lavas since about 0.67 Ma suggest diminished resupply of basalt.

Major- and trace-element geochemistry, petrography, and field data indicate multiple processes of magma genesis. Coherent curvilinear trends on variation diagrams and simple phenocryst assemblages suggest that most of the andesites and some of the silicic lavas are derivatives from generally similar basaltic parents in the different magma cycles; highly fractionated rhyolite is characterized by peralkaline chemistry, enrichment in Rb and Zr, and depletion in Ba. Many of the dacites and some of the andesites are hybrid lavas; they contain complex phenocryst assemblages and cognate inclusions. The origin of the silicic liquids in the mixes is not readily determined in all the lavas, but the mafic liquids appear to have been basalt and andesite. Strong depletion of Zr and enrichment in Rb may identify some silicic lavas as crustal anatectic melts. Rare metamorphic xenoliths display anatectic textures. Anatectic and mixed liquids appear to have made greater contributions to the parasitic domes and peripheral silicic centers than to the central stratocones. Thus, a complex magmatic system is indicated.

HOW CALDERAS RESURGE

HON, Ken, USGS, Hawaiian Volcano Observatory, Hawaii National Park, HI, 96718, and
FRIDRICH, Chris, Department of Energy, Box 98518, MS 523, Las Vegas, NV, 89193

The resurgence of large ash-flow calderas was first recognized by Smith and Bailey (1968), who proposed that renewed pressure arched the roof of the main magma chamber. The deeply eroded Lake City and Grizzly Peak calderas in Colorado provide strong evidence that the resurgent intrusions rise above basement rocks and are emplaced within ash-flow tuffs of the caldera fill. Probable resurgent intrusions identified in remnants of other deeply eroded calderas (Questa, Turkey Creek, Mt. Aetna, Salma) also intrude intracaldera tuff. Excellent exposures and preservation of complete stratigraphic sections within the Lake City and Grizzly Peak calderas allow reconstruction of the top of the resurgent intrusions and the resurgent domes; areas of maximum uplift of the domes are centered directly over the main part of the resurgent plutons. The interface between fractured caldera floor and the coherent block of intracaldera tuff serves to localize the upwardly migrating magma.

Multiple pulses of intrusion can be documented at both calderas. At Lake City, early radially oriented intrusions, which are reversely zoned, were later truncated by the main resurgent intrusive body; geophysical data indicate that the final form of the intrusion was stock-like and extends at least 4-5 km below the present surface. Two main intrusive pulses were a principle cause of resurgence within the Grizzly Peaks caldera, and the shapes of these reversely zoned plutons define a resurgent intrusion of laccolithic form. Initially, most resurgent intrusions probably spread as sill-like bodies near the base of the intracaldera fill. Increased loading by the growing intrusion, which may downwarp the underlying caldera floor rocks, and stoping of the conduit during emplacement of succesive intrusive phases eventually produce intrusions with stock-like shapes (e.g., the central intrusions of ring complexes).

Laccolithic models for resurgent domes differ in two respects from those developed in sedimentary rocks. First, slip parallel to bedding planes that accompanies flexure of sedimentary strata does not appear to occur in the relatively massive intracaldera tuff units. The absence of weak bedding-plane layers causes an increase in the effective thickness of caldera fill in comparison to a similar thickness of sediments and requires development of brittle fractures to account for extension of units during doming. Radial, and possibly concentric, fractures appear to form early and allow lava to extrude in the center of resurgent domes, whereas greater extension during later stages of resurgence is accommodated by the formation of a keystone graben structure, which inhibits the rise of magma. The number and size of all fractures diminishes with depth in the domed caldera fill. Second, the ring fault--and other subsidence-related faults--act as detachment surfaces surrounding the growing dome. During advanced stages of doming, the intracaldera block may pull away from wall rocks outside of the ring fault; this dislocation can result in large upward displacements along the ring fault (>1 km) and provide pathways for magma to reach the surface as ring domes.

Regional detumescence and renewed magmatic pressure due to vesiculation were suggested by Marsh (1984) as the most likely causes of resurgence. Evidence for regional detumescence is difficult to establish from field observations and, furthermore, the effectiveness of this model is dependent on viscous rather than elastic behavior of the upper crust. Increased pressure due to volatile exsolution seems improbable because of the relatively nonvesiculated condition of most resurgent intrusions. Instead, we favor a simpler alternative of continued magmatic input. Most resurgent domes have volumes ranging from 50-150 km^3; published eruptive rates for large silicic calderas range from 10^{-2} to 10^{-3} km^3/yr. Thus, reasonable times for resurgence due to continued magmatic input within the system generally fall between 10^4-10^5 years, in agreement with radiometric dates bracketing the formation of resurgent domes in young calderas.

RHYOLITIC ASH-FLOWS AND LAVA FLOWS OF THE WEST-CENTRAL SNAKE RIVER PLAIN (SRP): DISTRIBUTION, STRATIGRAPHY, AND PETROGENESIS

HONJO, N., LEEMAN, W.P., Keith-Wiess Geological Laboratories, Rice University, Houston, TX 77251, and BONNICHSEN, B., Idaho Geological Survey, University of Idaho, Moscow, ID 83843

Voluminous mid-Miocene (8-13 Ma) ignimbrites and rhyolitic lava flows (Idavada volcanics) are exposed along the northern and the southern margins of the west-central Snake River Plain. These rhyolites unconformably rest on Cretaceous to Tertiary granitic rocks and Eocene Challis volcanics and are locally capped (or intercalated with) by minor Tertiary basalt flows and fluvial and lacustrine sediments. At both margins, the rhyolites dip gently and thicken toward the SRP. NW- to EW-trending faults drop the western SRP forming a graben-like structure where the inferred sources of the rhyolites are buried by younger basalt flows and sediments. Idavada volcanics range in composition from quartz latite (68% SiO_2; 4.5% Fe_2O_3; 130 ppm Sr) to high-silica rhyolite (75% SiO_2; <2% Fe_2O_3; <20 ppm Sr) and are characterized by anhydrous mineral assemblages (Plagioclase $\pm$ Sanidine $\pm$ Quartz + Augite + Pigeonite $\pm$ Hypersthene + Fe-Ti oxides $\pm$ Fayalite). Pyroxene temperatures of Lindsley (1983) range from 800°C (high-silica rhyolites) to 1000°C (quartz latites). Sanidines occur in lower temperature (<900°C) samples. The differences in mineral compositions and modal proportions between units are useful for stratigraphic correlation.

Along the northern margin of the west-central SRP (ie., Mount Bennett Hills), eastward migration of volcanism is inferred from the stratigraphic relationships and is consistent with a simple model that the ignimbrites were erupted from a series of eastwardly migrating eruptive centers.

Although some units exposed along the southern margin of the west-central SRP (ie., Bruneau-Jarbidge eruptive center) may be widely dispersed, the limited areal distribution of many of these units suggests that they have been derived from distinct local sources. In addition, many of the units on the southern margin differ in composition (higher Si and Rb, lower Fe, Mg, Ba, Sr, and Zr) from the rhyolites exposed in the northern margin of the west-central SRP.

On the basis of anhydrous mineral assemblages, high magmatic temperatures, and crustal isotope ratios ($^{87}Sr/^{86}Sr$ = 0.709-0.713; $^{143}Nd/^{144}Nd$ = 0.51219-0.51230), we have inferred that west-central SRP rhyolites formed by fusion of dry crustal rocks due to heating by basaltic intrusions. In each local eruptive center, successive silicic magmas became less evolved chemically and their temperatures increased. These trends are inconsistent with progressive fractional crystallization and, instead, suggest that the rhyolites were produced by increasing degrees of partial melting as time progressed (ie., fractional melting).

THE RELATIONS BETWEEN CRUSTAL EXTENSION AND FLOOD BASALT VOLCANISM IN THE COLUMBIA RIVER AND DECCAN PROVINCES

HOOPER, P. R. Department of Geology, Washington State University, Pullman, WA 99164

The typical sheet flows of tholeiitic flood basalt of the Columbia River Basalt Group (CRBG) were erupted through crust which was undergoing mild WSW extension (M1%) and NNW compression, but no crustal thinning. The magma followed NNW planes of tensional strain that were developed by the stress regime at the base of the crust and propagated to the surface by the magma. At the end of the Grande Ronde Basalt eruption that part of the Columbia Plateau lying south of the Olympic Wallowa Lineament (OWL) underwent much greater degrees of extension (~20%), by the development of grabens and by crustal thinning. The change in strain was accompanied by a change in the nature of the volcanicity. Typical tholeiitic flood eruptions ceased. They were replaced by more varied volcanic material (alkalic to calc-alkalic) extruded in small volumes along the graben faults which resemble those associated with the Basin and Range and Rio Grande extensional provinces.

On the Deccan Plateau of India, the main tholeiitic eruptions were fed through feeder dikes without a preferred orientation, which implies a lack of horizontal extensional strain at that time (66-67 Ma). This was followed by significant E-W extension along the western edge of the province (parallel to the present Bombay coastline) as indicated by the Panvel monocline and N-S trending normal faults which form grabens offshore. This slightly younger tectonic activity (62-64 Ma) was accompanied by small volume eruptions of alkalic (lamprophyric) and intermediate composition in the Bombay area extruded through highly oriented N-S dikes.

These observations lead to the following conclusions: (1) that the widely remarked relationship between continental flood basalt volcanism and crustal extension is a real one; (2) that because the large volume tholeiitic eruptions precede the crustal extension, they are associated with the cause, not the result, of extension; and (3) that the crustal extension and thinning which typically follow continental flood basalt eruptions are accompanied by a distinctive phase of volcanicity of relatively small volume and diverse intermediate to alkaline composition. The sequence of events observed in the Columbia River and Deccan provinces can also be recognized in the Karoo and Parana provinces. On the Columbia Plateau the implication is that the eruptions of flood basalt were accompanied by, but were not caused by, the active back-arc spreading. Like the Deccan, the sudden eruption of the CRBG probably requires an additional (hot spot) component.

THE ROLE OF MAGMATIC VOLATILES DURING PHREATOMAGMATIC VOLCANISM

HOUGHTON, B.F., New Zealand Geological Survey, Rotorua, New Zealand, and

WILSON, C.J.N., Department of Earth Sciences, University of Cambridge, Cambridge, United Kingdom.

The relative role of magmatic volatiles and external water in phreatomagmatic volcanism has never been properly assessed. Many 'wet' eruptions show abundant evidence for strong vesiculation immediately prior to or during magma:water interaction and fragmentation. Evidence for the role of vesiculation is 'frozen' into juvenile clasts by quenching and can be quantified by measuring clast vesicularities. The vesiculation histories of magmas are frequently complex but can be simplistically considered thus.

During 'dry' explosive eruptions with high discharge rates a distinctive uniform assemblage of highly to extremely vesicular clasts is generated, as each portion of magma fragments at a critical threshold of vesicularity. If discharge rates are lower, opportunities arise (particularly with fluid magmas) for volatiles and magma to decouple, and broader clast vesicularity populations are generated with highly vesicular new magma being ejected with earlier degassed, less vesicular material.

During wet explosive eruptions, magma is quenched and fragmented regardless of its vesiculation state by interaction with water. There is thus a contrast between endmember dry and wet eruptions where fragmentation occurs at "constant" vesicularity and "constant" time respectively.

Combining field evidence and clast vesicularity data gives models for the relative timing of vesiculation and fragmentation by magma:water interaction. We demonstrate this from case studies of both fluid (basaltic) and viscous (rhyolite) magmas from Germany and New Zealand.

ROCK AVALANCHES IN THE CALDERAS OF FERNANDINA AND VOLCAN WOLF, GALAPAGOS ISLANDS, AND THEIR BEARING ON THE ORIGIN OF CALDERA-FILL BRECCIAS

HOWARD, Keith A. and CHADWICK, William W., U.S. Geological Survey, Menlo Park, CA 94025, U.S.A.

Catastrophic rockfall avalanches swept off the walls of Fernandina caldera in 1968 and 1988 and Volcan Wolf caldera sometime before 1946. Caldera collapse triggered the 1968 event and collapse influenced the others. The debris spread into the calderas at high energy and high speed. The resulting debris sheets provide modern analogs of breccia deposits that occupy many older calderas.

Table 1. Preliminary comparisons of avalanches.

Debris-forming event	Thickness (m)	Volume (10^6m)	Max. fall H (m)	Max. travel D (m)	H/D	Potential energy (ergs)
Wolf lobe	60	20	580	1350	0.42	$2x10^{21}$
Wolf kipuka	–	–	600	>2500	<0.24	–
Fernandina '68	>15	150	850	>1600	<0.53	10^{22}
Fernandina '88	300	1000	1050	4500	0.26	10^{23}

Avalanche debris in Volcan Wolf caldera forms a stubby lobate mass 60 m thick and 700 m long. The debris fell more than 500 m from its source: thick, massive, cliff-forming basalt flows. Failure was along a sloping buttress unconformity, on which the thick flows overlay thin clinkery flows from lava cascades into an earlier caldera. Marginal ridges and transverse structures mark the lobe. The debris consists of angular coarse rubble, in which the largest blocks are 3.5 m wide and few are smaller than fist size. The farboschung (H/D, Table 1), commonly thought of as the angle of friction, is higher than for some other avalanches of comparable size and potential energy, such as the Elm, Little Tahoma Peak, and Silver Reef events. The coarse grain size, lack of matrix, and 60-m-high snout are consistent with high strength.

Two km from the Wolf caldera wall a small central kipuka of rubble surrounded by caldera-floor basalt appears to represent an older, nearly buried, much more extensive debris sheet.

The 1968 Fernandina avalanche occurred during caldera collapse and is attributed to oversteepening of the wall combined with seismic shaking from the accompanying swarm of magnitude-5 earthquakes. During this collapse, the floor of the 800-m-deep caldera deepened another 350 m. Following collapse, a new caldera lake hid most of the avalanche debris sheet. The exposed margin of the debris, before it was buried by the 1988 event, was 10-15 m thick and represented 2% of the total volume as estimated from the size of the scar. The exposed debris extended 650 m beyond the caldera wall and up 85 m onto a pre-existing tuff cone. This amount of runup indicates a minimum velocity of 40 m/sec. At maximum runup the snout of the deposit was only 0.5 m high, and the thickness was less than the diameter of the larger clasts, suggesting that some drainback may have occurred. Tranverse ridges and troughs as deep as several meters and spaced about 20 m apart marked the surface of the sheet. The deposit consisted of poorly sorted basaltic rubble, including blocks as large as 2 m in diameter in a matrix of pebble- and sand-size debris. Blocks were abraded surprisingly little; delicate spiney lava surfaces were preserved.

The massive 1988 Fernandina avalanche was probably also triggered by magnitude-5 earthquakes. A scallop-shaped segment of the wall 250-300 m wide and 2-3 km long fell 1 km into the caldera near its deepest part. The debris spread 4 km across and up most of the sloping caldera floor, filling and leveling it in a tapering wedge as thick as 250 m. The force of the avalanche displaced the pre-existing caldera lake across and nearly 150 m higher up the sloping caldera floor. Monolithologic hummocks on the debris sheet indicate that nearly coherent blocks were carried with little disruption from the source. A following basaltic eruption that vented from the base of the avalanche scar invites comparison to the slope-failure triggering of the 1980 Mount St. Helens eruption.

BASALTIC ROCKS AND RELATED XENOLITHS FROM THE TRANS-DANUBIAN VOLCANIC REGION OF SE AUSTRIA AND W HUNGARY.

HUEMER, H., Institute of Petrology, University of Vienna,Dr.Karl Lueger-Ring 1,A-1010 Wien, Austria.
EMBEY-ISZTIN, A., Dep. of Mineralogy and Petrology, Hungarian Natural History Museum, Muzeum krt. 14-16, H-1088 Budapest, Hungary.
SCHARBERT, H.G., Institute of Petrology, University of Vienna,Dr.Karl Lueger-Ring 1,A-1010 Wien,Austria.

The Tertiary-Quarternary volcanic activity in Transdanubia (Pannonian Basin) extends from the Graz-Basin (SE Austria) to the Central Range (W Hungary) and includes some volcanic activity in Yougoslavia and CSSR.

The partial melting and genesis of magmas of the Pannonian Basin are linked to the evolution of this basin which is caused by an upwelling of the upper mantle and, as a consequence, extension of the basement with fault blocks and recent sinking. Crustal under-plating by mafic magmatic rocks has been considered to be the main force in epirogenic uplift.

The lavas change their character in space and time: A Miocene phase, the earliest rocks of which occur in the W, within the Alpine region, produced trachytic, trachyandesitic and quartz-trachytic lavas whereas a Pliocene/Pleistocene phase generated alkali basalts, basanites, nephelinites, olivin basalts and olivin tholeiites. The youngest rocks spread into N Hungary and Slovakia (CSSR).

The most important basaltic region is that of the Central Range where different types of xenoliths can be found both in basaltic tuffs (Szigliget, Szentbekalla, Gerce) and basaltic flows (Bondorohegy).

By means of mineralogical and geochemical data we tell mantle-derived ultramafic xenoliths from granulite facies xenoliths and clinopyroxene-rich cumulates from the lower crust.

Upper mantle xenoliths have been defined mainly as spinel lherzolites and harzburgites. Pressure calculations vary between 10 and 20kb, increasing from E to W, at not unusually high temperatures of about 1100°C.

Xenoliths from lower crust are mainly plagioclase-bearing one or two pyroxene granulites and,more rarely, garnet granulites.

The protolith of the granulite facies xenoliths was a tholeiitic gabbro. Geobarometric estimates yielded only 4.5-6.5kb for these xenoliths whereas two-pyroxene geothermometry yielded high temperatures of equilibration (>900°C). This is in concordance with a high positive geothermal anomaly of this region. At Bondorohegy only garnet-free granulite facies xenoliths occur whereas at Szigliget both garnet-free and garnet-bearing granulite facies nodules occur. This may be connected with differing thermal conditions below this region.

Less frequently clinopyroxene-rich nodules are found. The clinopyroxene-rich cumulate nodules derived from an alkali basaltic liquid, essentially not different from the host lava. These Xenoliths are clearly younger than the granulites, since they are virtually undeformed.

Concluding our observations we suggest a petrologically heterogeneous upper mantle beneath the Pannonian Basin. Furthermore a transitional mantle-crust boundary zone beneath the Central Range as postulated by seismic and geothermal data is attributed to numerous veins of clinopyroxenites.

Finally the occurence of garnet in granulite facies xenoliths depends on the P-T-conditions in lower crustal levels which are influenced by different geothermal gradients.

RELATIONS BETWEEN ERUPTIVE CONDITIONS AND THE HIGH LEVEL PLUMBING OF MOUNT ETNA BETWEEN 1700 AND THE PRESENT

HUGHES, J.W. and GUEST, J.E., University of London Observatory, Mill Hill Park, London, NW7 2QS, and
DUNCAN, A.M., School of Earth Sciences, Luton College of Higher Education, Park Square, Luton, LU1 3JU.

Etnean lava flow-fields erupted since 1700 AD display a marked sectorial distribution around the volcano in terms of their morphology. On the western flank the lava flow-fields are typically long and narrow and characterised by short eruption durations (<32 days) and high average effusion rates whilst flow-fields to the east are generally broad and complex in nature, of long durations (>32 days) and low average effusion rates.

Variation in magma effusion rate is recognised as being a major factor in influencing the morphology of lava flow-fields. In the eastern sector the initial phase of an eruption may have a relatively high effusion rate which is followed by a longer phase of much reduced magma output during which time a complex flow-field evolves. In this eastern sector it is suggested that the reduced lithostatic load due to the Valle del Bove sector collapse depression and the general lack of support on this seaward side of the volcano allows fissures to remain agape for long durations enabling magma to rise from depth as the eruption proceeds. However, in the western sector which is buttressed by mountains' the lithostatic load is distributed more uniformly and the erupting fissures close once the magma pressure falls below a critical level. This terminates eruptions before complex flow-fields can develop.

In conclusion, the sectorial distribution and variable lava flow-field morphology observed since 1700 is interpreted as a reflection of an asymmetrical stress field within the volcanic pile and its influence on the high-level plumbing system. This asymmetry is a result of the lack of buttressing of the seaward flanks and the departure from conical shape of the volcanic construct. Before 1700, in a period of higher magma output and differing magma petrography, a plumbing system with a greater high level storage capacity may have operated. The absence of any preferred sectorial distribution of flank eruption flow-fields in this period may indicate that a local stress field, induced by the high level plumbing system, was suppressing the effects of the asymmetrical lithostatic stress field which is currently important in controlling eruptive conditions.

AN OVERVIEW OF HYDROTHERMAL ALTERATION AND VEIN MINERALIZATION IN CONTINENTAL SCIENTIFIC DRILLING PROGRAM CORE HOLE VC-2B, VALLES CALDERA, NEW MEXICO

HULEN, J.B.[1], GARDNER, J.N.[2], GOFF, F.[2], NIELSON, D.[1], LEMIEUX, M.[1], SNOW, P.[2], MEEKER, K.[2], MUSGRAVE, J.[2], and MOORE, J.[1]

1. University of Utah Research Institute, Salt Lake City, Utah 84108
2. Los Alamos National Laboratory, Los Alamos, New Mexico 87545

Completed in the west-central Valles caldera, core hole VC-2B penetrated 1762 m through Plio-Pleistocene intracaldera ignimbrites and Miocene to Pennsylvanian sedimentary rocks into Precambrian quartz monzonite (Fig. 1). Rocks in the upper 800 m and lower 250 m of the hole are extensively altered and veined; intervening Paleozoic siliciclastic and carbonate rocks are essentially unaltered and only sparsely veined. Sericitic alteration, with near-surface kaolin, predominates to 300 m; chlorite-sericite alteration prevails between that depth and 800 m. Deep alteration is primarily propylitic. Identified vein minerals comprise quartz, calcite, ankerite, fluorite, anhydrite, barite, epidote, wairakite, sericite, chlorite, hematite and pyrite, as well as rare rhodochrosite, chalcopyrite, chalcocite, sphalerite, galena, tetradymite(?), stibnite (?), and pyrargyrite. Fluid-inclusion homogenization temperatures (T_h) for deeper veins closely match current temperatures (Fig. 1), suggesting recent entrapment of the contained fluids. Shallow T_h's, however, are higher than current temperatures, indicating a high-level cooling trend. Shallow inclusion fluids are dilute (<0.7 equiv. wt.% NaCl--similar to contemporary Valles geothermal reservoir fluid), but deep ones are apparently more saline (up to 2.9%). Therefore, VC-2B may have penetrated "stacked" hydrothermal cells separated by nearly impermeable Paleozoic strata.

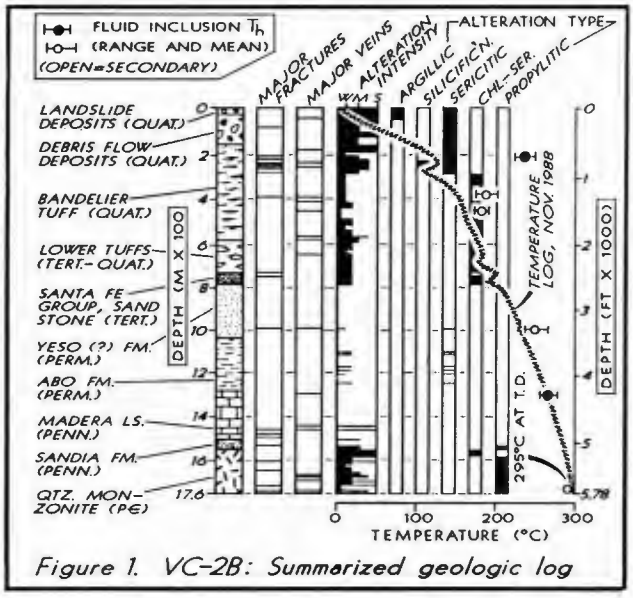

Figure 1. VC-2B: Summarized geologic log

MESOZOIC CONTINENTAL VOLCANISM IN EASTERN CHINA

HUO Yuhua, Institute of Geochemistry, Academia Sinica, Guiyang, Guizhou Province, P.R. China

Mesozoic volcanism is very strong in the coast areas of Eastern China. The volcanism started from Late Triassic and finished at the end of Cretaceous Period, followed by the Cenozoic volcanism. In direction from inland to coast, i.e. from west to east, the Mesozoic volcanism tends to be younger and stronger. The strongest volcanism occurred in the Late Jurassic.

Some authors suggested that the Mesozoic volcanic rocks in this area would be resulted from the subduction of the West Pacific Plate toward the Asian continent, belonging to the island arc series. In contrast, the author suggests that they were formed in a continental environment. The evidences are as follows: 1) There is no Mesozoic subduction zone in the coast areas; 2) Volcanic rocks in this area predominantly consist of rhyolitic rocks, and the ignimbrites are abundant while andesites and basalts are rare. Obviously, it is distinct from the rock association of island arc; 3) Andesites in this area mostly belong to the alkali-calcic series ($CaO<Na_2O+K_2O$), being typical of a continental tectonic environment; 4) Their geochemical characteristics are dissimilar to those of island arc rocks. The SiO_2 contents vary greatly from 47 to 81%, $FeO+Fe_2O_3/MgO>2$, $K_2O/Na_2O>0.8$, and contents of Rb, Sr, Th, U and Zr are higher than those of island arc calc-alkaline rocks; 5) It is not in agreement with the characteristics of plate subduction in the west coast of America; 6) Geotectonic studies have shown that ancient Eurasian continental margin in Mesozoic times was located to the east of the line linking Japan and Taiwan, and the present location of Mesozoic volcanic rocks is not an island arc area.

Most of Mesozoic volcanic rocks in this area may have been derived from the different levels of crust. The evidences can be summarized as follows: 1) The rhyolitic rocks comprised about 70-86% of volcanic rocks in the whole area. It means that these rocks may have not been produced by differentiation of basaltic magma derived from upper mantle; 2) Many petrological sections show the evolutional tendency varying from acidic to intermediate; 3) There is a close relationship between the compositions of volcanic rocks and that of an ancient acidic basement(1700-1800Ma) in this area; 4) The volcanic rocks are characterized by REE geochemical features of crust(high REE contents, larger LREE/HREE and lower δEu); 5) Initial $^{87}Sr/^{86}Sr$ ratios are high(0.7045-0.7145); 6) In this area the crust is thick(about 30 Km); 7) Volcanic rocks would be formed under a compression-stress condition.

MONTANA POTASSIC VOLCANISM: GEOCHEMICAL EVIDENCE FOR INTERACTION OF ASTHENOSPHERIC MELTS AND METASOMATICALLY-VEINED PRECAMBRIAN SUBCONTINENTAL MANTLE LITHOSPHERE

IRVING, Anthony J., O'BRIEN, Hugh E. and McCALLUM, I. S., Dept. of Geological Sciences, University of Washington, Seattle, WA 98195

Magmatic rocks from several of the Eocene-Oligocene potassic to sodic alkalic subprovinces of central Montana possess isotopic and trace element features clearly indicative of interaction of ascending melts with ancient mantle lithosphere related to the Wyoming craton. Furthermore, mantle xenoliths from several of the alkalic subprovinces appear to be samples of depleted lithosphere, and contain mineralogic and geochemical evidence for an ancient metasomatic enrichment event.

Sr-Nd isotopic systematics for alkalic rocks from Haystack Butte, Crazy Mountains, Yogo Peak, Leucite Hills (Wyoming) and Smoky Butte define an array extending from Bulk Earth to ϵ_{Nd} of -25 (Figure 1), which we interpret as a mixing line between an asthenospheric component and ancient light-REE enriched mantle lithosphere. The Ba enrichment in these rocks, which is also a feature of exposed Archean crustal rocks of the Wyoming craton (eg., Mueller and Wooden, 1988), is correlated with $-\epsilon_{Nd}$, implying that most of the Ba resides in an ancient component. Pb isotopic compositions are also consistent with a mixed source melting model (Figure 2), and for the Highwood Mountains rocks define a 1.87 Ga pseudoisochron which may date the enrichment.

Ultramafic xenoliths within the Highwood Mountains minettes comprise glimmerite-veined harzburgites and phlogopite dunites, which most likely represent ancient depleted residual mantle lithosphere that has undergone metasomatic enrichment by mica-saturated fluids. One glimmerite vein is relatively enriched in Ba, Rb (Rb/Sr 0.41) and light REE (Sm/Nd 0.13), and has $^{87}Sr/^{86}Sr$ of 0.743615 and $^{143}Nd/^{144}Nd$ of 0.510893 (ie., ϵ_{Nd} of -33 at 52 Ma). We interpret this vein to be a Precambrian metasome, and calculated model ages relative to average depleted mantle are 2.6 Ga for both Sr and Nd isotopic systems.

Rocks from the Highwood and Bearpaw Mountains have elevated $^{87}Sr/^{86}Sr$ compared with the other alkalic subprovinces (Figure 1), which may in part be explained by a range in Sr isotopic composition within the subcontinental lithosphere or a greater degree of assimilation of vein material by asthenospheric melts. Differences in Pb isotopic composition between the Highwood and Smoky Butte samples also argue for variability of isotopic compositions within the ancient lithosphere. However, an important observation for *all* of the Montana-Wyoming alkalic provinces is the lack of correlation of $^{87}Sr/^{86}Sr$ with Rb/Sr, which implies that the Rb/Sr variation is a young feature and therefore not related to the ancient lithospheric component. We believe by analogy with Recent potassic volcanics from Italy, Sunda-Banda and Mexico that a third Rb-enriched component may have been added to the asthenospheric wedge during the regional Eocene-Oligocene subduction event. Similarly we ascribe the relative depletions in Nb, Ta and Ti shown by all the Montana potassic rocks largely to young subduction processes, although we cannot rule out a contribution from ancient lithosphere. These conclusions are consistent with tectonic models implying very shallow subduction of the Farallon Plate beneath Washington, Idaho and Montana in the early Tertiary (eg., Bird, 1984).

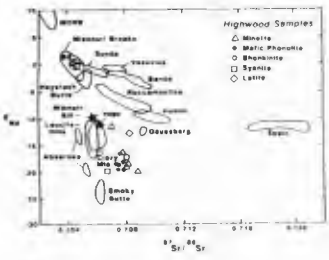

Figure 1

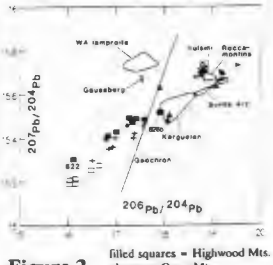

Figure 2

filled squares = Highwood Mts.
plusses = Crazy Mts.
open squares = Smoky Butte
dots = Leucite Hills
crosses = Spain
open triangles = Haystack Butte
filled triangles = Navajo

EARTHQUAKE SWARMS ON THE INTRUSION-EXTRUSION PROCESS OF ANDESITIC MAGMA AT SAKURAJIMA VOLCANO, JAPAN

ISHIHARA, K., Sakurajima Volcanological Observatory, Disaster Prevention Research Institute, Kyoto University, Sakurajima, Kagoshima 891-14 Japan

The swarms of volcanic micro-earthquakes called as B-type earthquakes are the most common and typical forerunner for explosive activity at the summit crater of the Sakurajima volcano. However, the physical meanings of B-type earthquakes have not made clear, because it was difficult to determine the hypocenters precisely and B-type earthquakes have wide variations in their wave forms and predominant frequencies. The new networks of borehole seismometers made it possible to determine the location of B-type earthquakes. The physical meanings of the swarms of B-type earthquake are discussed in relation to the eruptive activity and the ground deformation of the volcano.

B-type earthquakes are categorized into two types, BL (1-3 Hz) and BH (4-8 Hz), by the predominant frequency. Both BL-type and BH-type erathquakes originate just beneath the summit crater as explosion-quakes do. The range of focal depth of BL-type earthquakes is shallower ($d < 2$ km) than that of BH-type ($d < 3$ km).

The swarms of BH-type earthquakes were observed mainly during inflation-stages with no significant changes of eruptive activity. On the contrary, the swarms of BL-type earthquakes originated during the period of sudden deflation of the summit with ash emission. The BL-type activity were sometimes accompanied with the intermittent ejection of volcanic blocks similar to Strombolian eruptions, and weak air-shocks were often observed simultaneously with the occurrence of BL-type earthquakes.

These results suggest that BH-type earthquakes might reflect the intrusion of magma into the magma conduit, and BL-type earthquakes are generated in the conduit closely related with the degassing of magma extruded up to the crater bottom.

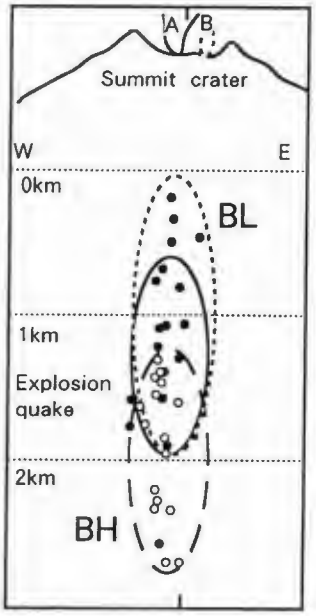

The hypocenters of BL-type earthquakes, BH-type earthquakes and explosion-quakes

HOW TO INDUCE CALC-ALKALI ANDESITE FROM ISLAND ARC THOLEIITE: FRACTIONATION MODEL OF HYDROUS THOLEIITIC MAGMA IN HAKONE, HOTAKA AND AKAGI VOLCANOES, JAPAN

ISHII, Teruaki, Centre for Marine Geology, Dalhousie University, Halifax, N.S., Canada B3H 3J5 (after 1 June 1989, c/o Dr. R. Fiske, NHB-119, Smithsonian Inst., Washington, D.C. 20560, USA), and YAMAGUCHI, Takashi, Mitsubishi Mining & Cement Co., Ltd., 2270 Yokoze, Chichibu, Saitama 368, Japan.

In pyroxene crystallization sequences, pigeonite (Pig) is common in the later stage of tholeiitic intrusions (Fig. 1) as well as in the groundmass stage of tholeiitic lavas (Fig. 2), but Pig seldom appears as a phenocryst in those lavas (Fig. 3).

During fractional crystallization of anhydrous minerals from relatively wet tholeiitic magma in the magma reservoir, water content in the residual liquid increases, and liquidus-solidus of Ca-poor pyroxene fall gradually (Fig. 3), resulting in the crystallization of magnesian phenocryst orthopyroxene (Opx). The crystallization trend delineated through these Opx can represent that of a Ca-poor pyroxene in the magma reservoir (named phenocryst trend or reservoir trend), which never contain Pig, because it has steeper slope (Fig. 3) than that of the PER-(=pigeonite eutectoid reaction) line which is the lower stability limit of pigeonite.

Alternatively, if relatively wet magma of each stage erupted from the magma reservoir through vents to the surface as a lava-flow, its water content decreases due to degassing as the magma ascended, and the liquidus-solidus of the ascending magma rise quickly (not temperature of magma), crystallizing rapidly phenocrysts of pyroxene (Opx) through microphenocryst to the groundmass (Pig) generations with a small temperature decrease (Fig. 2). The crystallization sequence in each lava (named lava-flow trend) always contains pigeonite in the groundmass, because the trends have less-steep slope than that of the PER-line.

The above model can well interpret two different trends observed for the reservoir and lava-flows in the Hakone, Hotaka and Akagi volcanoes. The water content of tholeiitic magmas in those volcanoes are suggested to become higher in this order.

The degree of iron-concentration has an inverse relation to that of water concentration in magma during differentiation. The same source magma can produce low iron-enrichment trends such as the calc-alkali rock series, through higher water concentration (Fig. 4). Calc-alkali andesites in Hakone, Hotaka and Akagi volcanoes may be derived from the hydrous tholeiitic magmas.

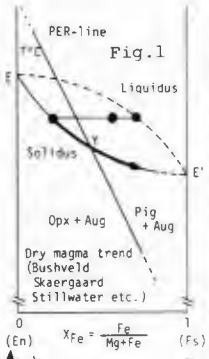

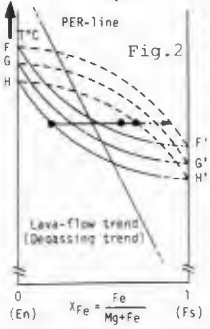

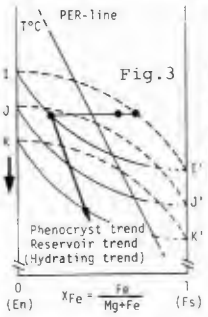

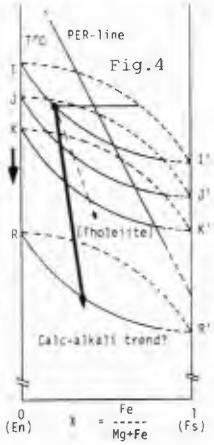

Note
←:Moving direction of liquidus and solidus.

A MECHANICAL MODEL FOR LAVA DOMES THAT INCLUDES A MECHANISM FOR ERUPTIVE GROWTH

IVERSON, R.M., USGS, Cascades Volcano Observatory, 5400 MacArthur Blvd., Vancouver, WA
DENLINGER, R.P., USGS, c/o Oceanography Dept., University of Washington, Seattle, WA

The shape, size, and growth mechanisms of lava domes can be modeled mathematically by considering force equilibria in static, brittle shells that enclose pressurized magma and gas. The thickness (t) and tensile strength (σ) of the dome's solid, outer shell and the unit weight (γ) and excess pressure head (h) of the enclosed magma and gas determine the equilibrium force balance (figure 1). Assumptions of axial dome symmetry, shell homogeneity, and membrane forces render the shell-magma system statically determinate. Assumptions about lava-dome rheology therefore are unnecessary.

Equations that describe permissible equilibrium dome shapes yield an orderly family of solutions, the members of which are distinguished by the value of a single dimensionless parameter, $D = \sqrt{\sigma t/\gamma}/h$. A physically reasonable value of D produces an excellent fit to post-May 1981 morpohologic data for the Mount St. Helens dome, assuming that the dome's talus apron contributes cosmetically, but not mechanically, to its shape (figure 1).

During transient disequilibrium states, gradual tensile failure of the brittle shell permits eruptive dome growth. In our model, accelerating, endogenous dome growth results from accelerating, subcritical crack growth in the shell and culminates in tensile rupture and lava extrusion. On the basis of the rate of magma pressure increase and the fracture-mechanical properties of the shell, the model also predicts the time interval between eruptions. At Mount St. Helens long periods of dome equilibrium have been disrupted by explosions or extrusions that attend eruptive growth. A combination of seismic and geodetic data for each eruption in 1981 and 1982 supports the hypothesis that the dome's outer shell provided the main impediment to extrusion. Analysis of the May 1982 eruptive episode also shows that other causes of creep-rupture behavior, such as a nonlinear pressure increase in the magma conduit, are inconsistent with available data.

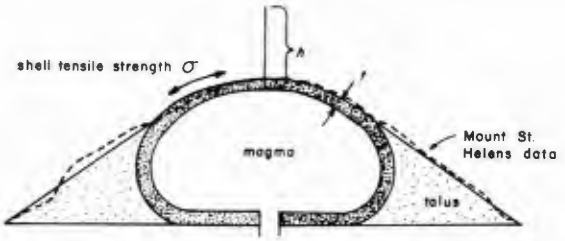

Fig. 1. Dome cross section for D = 1 and 35° talus slopes

GEOCHEMICAL AND THERMAL STRUCTURES OF THE PLIOCENE GEOTHERMAL SYSTEM IN THE KUSHIKINO GOLD MINE AREA, SOUTHERN KYUSHU, JAPAN

IZAWA, E., Department of Mining, Kyushu University 36, Hakozaki, Higashi-ku, Fukuoka 812, Japan

Pliocene gold mineralization in the Kushikino area consists of epithermal quartz-adularia-calcite veins. Regional geologic and gravity data indicate a following succession of events: (1) regional subsidence and andesitic volcanism with a minor quartz diorite porphyry intrusion (8 Ma to 4 Ma), (2) a later silicic intrusion at depth and following uplifting of the area, and (3) major fracturing, formation of the geothermal system and gold mineralization (4Ma).

Studies of hydrothermal alteration and fluid inclusions reveal the three dimensional thermal structure of the fossil geothermal system and suggest that the present ground surface represents a horizontal section at a depth of about 400 m below the paleosurface. Propylitically altered andesites, which host gold bearing quartz veins, occur in the central high temperature zone (>200°C) that extends 8 km east to west and 4 km north to south. The propylitic zone is surrounded by weakly altered andesites of the smectite-zeolite zone which grades outward into unaltered andesites. In altered andesites of these alteration zones igneous plagioclase, sometimes albitized, is persistent. Quartz veins and silicified zones are enveloped by a narrow zone of intense alteration with little or no plagioclase persisting. Three types of the alteration envelope are the mica-chlorite zone in the deeper part, and the intermediate argillic and the kaolinite-mica zones in the shallower part of the vein system.

As volcanic rocks in the study area consist primarily of andesitic lava flows and tuff breccias and hence their original chemical compositions are assumed to have been rather homogeneous throughout the area, data of major and minor element analysis for rocks from various alteration zones reveal the geochemical structure of the geothermal system and provide information on the fluid associated with mineralization at the Kushikino deposit. Compositions of original andesite, except H_2O, remain unchanged in altered rocks of the widespread propylitic and the smectite-zeolite zones. However, Au, As and S increase slightly in altered rocks of both alteration zones. This suggests that some ingredients were probably fed to heated ground water by deeper mineralizing fluid.

High ferrous/total iron ratios in altered andesites in the central part of the propylitic zone compared with unaltered andesites indicate that deep mineralizing fluid was relatively reduced. In contrast, ferrous/total iron ratios are markedly low in intensely altered rocks which envelope veins in the upper level. This implies that reduced fluid became oxidized in the upper part of the geothermal system. Oxidation would occur as a result of mixing of deep mineralizing fluid with shallow meteoric ground water and/or boiling of high temperature ascending fluid. Both mixing and boiling would provide a favorable environment for gold deposition in the Kushikino geothermal system.

HIGH-LEVEL WATER TABLES ON HAWAIIAN TYPE VOLCANOES AND INTERMEDIATE DEPTH GEOELECTRIC STRUCTURES, KILAUEA VOLCANO, HAWAII and PITON DE LA FOURNAISE VOLCANO, ISLE DE LA REUNION

JACKSON, D.B., U.S. Geological Survey, Hawaiian Volcano Observatory, Hawaii National Park, HI 96718 and LENAT, J-F., Univ. Clermont 2, 5 rue Kessler, 63038 Clermont-Fd, France

Intermediate-depth Schlumberger resistivity soundings on Kilauea and Fournaise volcanoes show that both have low resistivity regions which underlie their calderas at a few hundred meters depth and which deepen stepwise away from the summit areas. On Kilauea electric logs from a deep drill hole (1262 m) at the summit show that the top of the low resistivity zone defined by soundings coincides with the water table. We infer that the pervasive low resistivity zone beneath Fournaise's caldera is also related to a high-level ground-water body. Porosities of these volcanic edifices are too great to support large (>20 m/km) hydraulic gradients; thus lateral boundaries, probably composed of nearly impervious high-angle dikes and cone sheets, confine the ground-water bodies. Resistivities of the ground-water zones on Kilauea and Fournaise are about 10 ohm-m and about 200 ohm-m respectively. This difference of resistivity is probably related to the depths of the shallow magma reservoirs of the two volcanoes. The reservoir at Fournaise is within the volcanic edifice above sea level and thus convected ground water is probably of low salinity. The reservoir at Kilauea is also within the volcanic edifice but about 2 km below sea level and thus upwardly convected ground water has a higher salinity and a lower resistivity than the ground water beneath Fournaise.

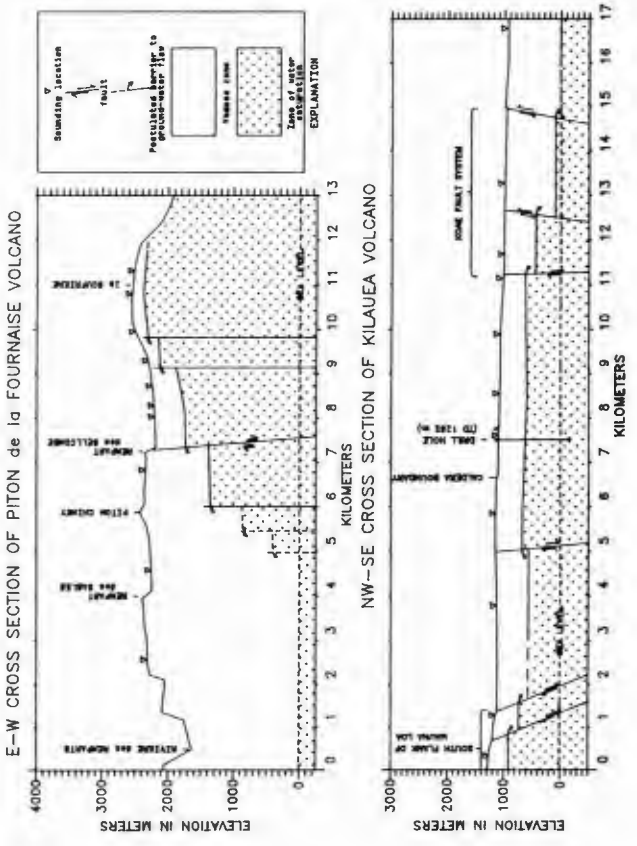

CHEMICAL EVOLUTION OF ARCHEAN MAGMATISM IN A CONTINENTAL RIFT ENVIRONMENT: THE STEEP ROCK VOLCANIC SERIES, ATIKOKAN, ONTARIO, CANADA

JACKSON, M.C., Hawaii Institute of Geophysics, University of Hawaii, Honolulu, Hawaii, U.S.A.; STONE, D., Ontario Geological Survey, 77 Grenville St., Toronto, Ontario, Canada; and KAMINENI, D.C., Atomic Energy of Canada Ltd., Ottawa, Ontario, Canada.

In the Atikokan area of northwestern Ontario, Canada, metavolcanic and metasedimentary rocks overlie an Archean unconformity on 2.9 Ga tonalitic basement. The sequence above the unconformity consists in ascending order of: (1) a basal conglomerate/sandstone, (2) stromatolitic limestone, (3) ultramafic pyroclastics, (4) mafic pillow lavas, and (5) intermediate to felsic volcanics as flows, tuffs and breccias. This sequence probably was deposited in an intracontinental rift zone. The replacement of shallow water sediments and ultramafic pyroclastics by deep water pillow lavas is evidence of deepening water depth with time. This was followed by progressive shoaling of a more centralized volcanic center during production of the more evolved intermediate to felsic volcanics. The early ultramafics have LREE-enriched chondrite-normalized REE patterns and unusual enrichments in other incompatible trace elements. The younger mafic volcanics are typical Archean tholeiites with flat REE patterns. The trace element composition of the upper intermediate to felsic volcanics indicates that they can not be related directly to the mafic volcanics by closed-system fractionation processes and their petrogenesis probably involved magma mixing and/or assimilation along with fractional crystallization (AFC). The chemical evolution of extrusive magmas in this Archean rift zone can be interpreted as indicating either: (a) a decreasing amount of deep level crustal contamination with time as the magma plumbing system became better established, or (b) progressive tapping of a more depleted mantle source, followed by shallow level AFC processes in a central volcano to produce the intermediate to felsic volcanics. The Atikokan volcanic series exhibits an unusually complete cycle of the volcano-tectonic evolution of an Archean continental rift.

THE WEST AUSTRALIAN LAMPROITES: MULTIPLE TAPPING OF OLD ENRICHED SUB-CONTINENTAL LITHOSPHERE

A.L. JAQUES, Bureau of Mineral Resources, GPO Box 378, Canberra, ACT, Australia.

Diamondiferous olivine lamproites of mid-Proterozoic (1180 Ma) age at Argyle (AK1 pipe) in the East Kimberley and Miocene (20 Ma) age at Ellendale in the West Kimberley lie within Proterozoic mobile belts surrounding the Precambrian (Archaean ?) Kimberley block of Western Australia. The Ellendale diamond pipes form part of the West Kimberley (Fitzroy) lamproite province which comprises more than 100 intrusions, all of Miocene age, ranging from olivine-rich (~29% MgO) to leucite-rich (<5% MgO, ~12% K_2O) lamproite.

The Argyle and Ellendale lamproites have high MgO, Ni and Cr contents, and are highly enriched in Rb, Sr, Ba, Th, U, K, Nb, Ta, LREE, P, Zr, Hf, and Ti but depleted in Al, Fe, Ca, Na, Sc, and HREE. The Miocene lamproites are more strongly enriched in Rb, Ba, Th and LREE, and have higher Ba/Rb, Ba/La and La/Nb, and lower K/Rb and K/Ba. Both suites have strongly radiogenic Sr and unradiogenic Nd isotopic compositions, indicating derivation from similar enriched sources. Both lamproite suites have crustal Pb isotopic signatures: the Argyle initial Pb isotopic compositions (at 1180 Ma) fall on the average crustal growth curve, whereas the Ellendale lamproites have very high initial $^{207}Pb/^{204}Pb$ (Nelson et al, 1986; Sun et al, 1986). The lamproites are interpreted as low-percentage melts of ancient, refractory sub-continental lithosphere which has undergone long-term (>2 Ga) geochemical enrichment (high Rb/Sr, low Sm/Nd). The isotopic and trace element data for the lamproites show that the mantle enrichment is heterogeneous, even on a small scale.

Early cratonization (~1.8 Ga) of the Proterozoic mobile belts (Halls Creek Province) surrounding the Kimberley Block has resulted in craton-type (up to 220 km) lithospheric thicknesses. Rare xenoliths, xenocrysts and inclusions in diamond indicate that both eclogite and reduced refractory peridotite, mostly lherzolite, were stabilized within the diamond field in the source regions of the West Australian lamproites prior to the early-mid Proterozoic (>1.5 Ga). The peridotite is the source of peridotitic suite diamonds at Argyle and may be the residue from early Precambrian tholeiitic basalt magmatism. Most of the Argyle diamonds are of eclogitic paragenesis and are strongly depleted in $\delta^{13}C$ (-5 to -16 /oo PDB (Jaques et al, 1989). Both the peridotite and eclogite have been geochemically enriched (K and Rb-rich pyroxene, LIL titanate etc) but to varying extents. Part of the enrichment appears to be associated with recycling of early Proterozoic crust. This may explain the very high Ba, high Ba/La and Pb/La, low K/Ba and Sr/Nd, negative Eu anomalies, and the high U/Pb required in the early evolution history by the Pb isotopic compositions of the lamproites. The eclogitic inclusions and the strongly ^{13}C-depleted carbon isotopic compositions of the eclogitic diamonds also appear to be derived from recycled oceanic crust. Lamproite magmatism in the mid-Proterozoic and mid-Miocene resulted from reactivation of this geochemically enriched lithosphere.

PRESSURE, GAS CONTENT AND ERUPTION PERIODICITY OF A SHALLOW, CRYSTALLISING MAGMA CHAMBER

JAUPART, C., TAIT, S.R. and VERGNIOLLE, S.,
Laboratoire de dynamique des systèmes géologiques,
Institut de Physique du Globe de Paris, Université
Paris VII, 4, Place Jussieu, 75252 Paris Cédex 05

In volcanic eruptions magmatic systems are sampled as they undergo chemical differentiation. The question of how eruptions are triggered must be addressed if the bias inherent in this sampling process is to be correctly interpreted. Fractional crystallisation in magma chambers provides both a means of differentiation and a triggering mechanism as it can cause oversaturation of volatile species. We calculate the overpressure in the chamber and consequent increase in its volume by deformation of the surrounding rocks as crystallisation proceeds and gas bubbles are formed. When the overpressure reaches a value of twice the effective tensile strength of the volcanic edifice, an eruption occurs. We show the quantitative effects on the pressure history of the form of the solubility law (depending on the volatile species present), the crystallisation contraction and the presence of some initial mass of gas at t = 0. The most important of these is the solubility law. We show that, once saturated, the more soluble is the volatile species, the more important it is for the development of overpressure in the chamber. Only a few per cent fractional crystallization are required to cause overpressures equal to the fracture criterion for a pure H_2O gas phase. A pure CO_2 gas phase cannot cause important overpressures because of its low solubility. We calculate the volumetric deformation of the surroundings and the erupted volume of lava as a fraction of the chamber volume. In the cases of Kilauea and Krafla volcanoes where the volume of the magma chamber is known approximately, our results are close to observations of both the amounts of tumescence and volumes of melt ejected from the chamber. In this model the repose time between eruptions is determined by the rate of crystallisation. Estimates for the time required to reach overpressures equal to the fracture criterion are on the order of a few years for basaltic melts and a few hundred years for more viscous sytems. Over the course of many eruptions this model predicts an approximately constant output rate of lava. If the chamber is a closed system, after an eruption, the amount of magma ejected is replaced by an equivalent volume of gas. The amount of gas builds up with each successive eruption and eventually the magma chamber roof can become unstable causing caldera collapse.

LARGE SCALE CRUST FORMATION BENEATH CALDERA COMPLEXES

JOHNSON, C.M., Department of Geology and Geophysics, University of Wisconsin, Madison, WI 53706

The combination of sustained (up to 15-20 Ma) eruption of magmas with generally low crystal contents and recurrent caldera-forming eruptions of highly evolved magma in relatively short time intervals (< 1-2 Ma) at some magmatic centers, suggests that a common requirement to developing caldera complexes is a large flux of mantle-derived basalt into the lower parts of the system. Recent Nd isotope data obtained from several Cenozoic calderas in the western U.S., including Grizzly Peak, Kane Springs, McDermitt, Questa, the San Juan Mtns, Valles, Woods Mtn., and Yellowstone, indicate that the silicic rocks contain large, perhaps dominant, mantle components, as marked by Epsilon Nd values that are > 5 units above those of the pre-Cenozoic basement.

Nd isotope ratios determined on mafic rocks of several complexes (premonitory mafic lavas or samples from strongly zoned tuffs) range from mantle values to those that overlap the silicic rocks, indicating that the primary mechanism for producing the silicic tuffs is assimilation/fractional crystallization of basalt. Conservative calculations for several centers suggest that the crust may be thickened by up to 5-10 km through basalt injection and crystallization and accumulation of mafic minerals. The volume of crust that is hybridized (assimilated basement + new basalt) may exceed 50 % of the original crust volume. These processes can profoundly modify the chemical and O, Sr, and Nd isotopic compositions of the lower crust, although Pb isotope variations in the pre-existing crust will be largely preserved because of the relatively low Pb flux from the mantle. Later silicic magmas that may be generated largely by crustal melting, in addition to late mafic magmas that undergo assimilation as they pass through the hybridized crust, will appear substantially more primitive in their O, Sr, and Nd isotope ratios, although Pb isotope ratios will still identify crust assimilation.

Granitic plutons that can be confidently tied to large-volume volcanic fields have similar Nd and Pb isotope ratios, suggesting that such bodies represent the waning stages of the caldera-related magmatism. Epsilon Nd values of some isolated Cenozoic plutons that were emplaced in the western U.S. are 2-12 units lower than those of the silicic tuffs, suggesting that some plutons formed largely by crustal melting that was accompanied by low basalt fluxes. Such plutons probably were not associated with large volcanic fields and therefore represent a fundamentally different type of crustal magmatism than caldera complexes. Evaluation of the extent of new crust formation in the continental interior based solely on analyses of isolated plutons may underestimate the volume of primitive components that have been added to the crust.

CONTINENTAL CAINOZOIC MAGMATISM OF EASTERN AUSTRALIA: MODELS FOR RIFT-SHOULDER VOLCANISM

JOHNSON, R.W.,
KNUTSON, J., and
SUN, S.-S., all of Bureau of Mineral Resources, G.P.O. Box 378, Canberra, A.C.T. 2601, Australia

Cainozoic volcanism in eastern Australia appears to represent a response to the break-up of eastern Gondwanaland, and particularly to the development of the Tasman Sea and Coral Sea marginal basins 80-50 Ma ago. The nature and origin of the intraplate Cainozoic volcanoes of eastern Australia (and New Zealand) are considered in detail in a new compilation of data and interpretations (Johnson et al., 1989).

The fundamental distinction between lava-field, central-volcano, and minor leucititic eruptive centres in eastern Australia, first proposed by P. Wellman and I. McDougall, forms the basis of the compilation. These volcanoes form a narrow swath that follows the eastern coastline for more than 4000 km, swinging out and back through more than 12° of longitude, and roughly following the axis of the passive-margin mountains representing the 'highlands' of eastern Australia.

The central volcanoes and leucititic centres have an age range of 34-6 Ma, and they young southwards at a rate of 65 mm/yr. These centres do not define a straight trace, perhaps because their source is two or more hotspots, or a hotline, rather than a single hotspot. The irregular trace is more or less coincident with the lava-field volcanoes (mainly 50-30 Ma) which, in contrast, are neither age-progressive nor obviously hotspot/hotline related.

The origin of the lava-field volcanism, and how this volcanism relates to the hotspot/hotline volcanoes, are discussed in the compilation, in part using analogies from other regions of the world. However, time-space relationships in eastern Australia appear to be unique: nowhere else is there a continental age-progressive trace of such length, and only in a few places does analagous continental volcanism of 'lava-field' type exist along passive margins (for example: Red Sea and Gulf of Aden; possibly Marie Byrd Land, Antarctica).

One interpretation is that the lava-field volcanism relates to intraplate stresses in the Indo-Australian plate caused by its interaction with surrounding plates. Another concept is that the lava-field volcanism results from shallow-asthenospheric partial melting below an 'upper plate', induced by detachment faulting at the time of continental extension and seafloor spreading. However, the coincidence of the hotspot/hotline volcanoes with the swath of lava-field volcanism is not accounted for satisfactorily by either of these shallow-asthenosphere models. The coincidence therefore may be indicative that some of the lava-field volcanism at least is a consequence of regional upwellings of hot and deep asthenospheric mantle. However, the tectonic cause of these upwellings remains unclear - especially, how the east-Australian upwellings relate to the upwelling that presumably underlay the Tasman and Coral seas spreading system 80-50 Ma ago.

Johnson, R.W., J. Knutson, & S.R. Taylor, (Editors) 1989. Intraplate volcanism in eastern Australia and New Zealand. Australian Academy of Science and Cambridge University Press.

PITON DE LA FOURNAISE, REUNION: TRACE ELEMENT CONSTRAINTS ON THE MAGMA PLUMBING SYSTEM

Jean-Louis JORON and Michel P. SEMET, LPS/GST, 91190 Gif/Yvette, LGCS/UPMC, 75252 Paris, France and Institut de Physique du Globe de Paris, CNRS UA 04196

In recent years, Piton de la Fournaise (PdF) has erupted 1-2 times/yr, mostly from locations near the summit crater (2632 m high) or from flank fissures generally located inside the Enclos Fouqué (EF). EF is a large arcuate collapse structure that contains the summit crater (Bachelery, 1981).

For the eruptions considered, the integrated magma production rate has been on the order of 0.4 m³/s, a figure about three times higher than the average computed from the entire volume of the volcano (1,600 km³) since the beginning of its activity (380 ka).

INAA trace element analysis of prehistoric and recent lavas has provided a data base for the interpretation of magmatic processes that puts constraints on the deep (from differentiation) and superficial (from chemical patterns vs. eruptive location) plumbing systems.

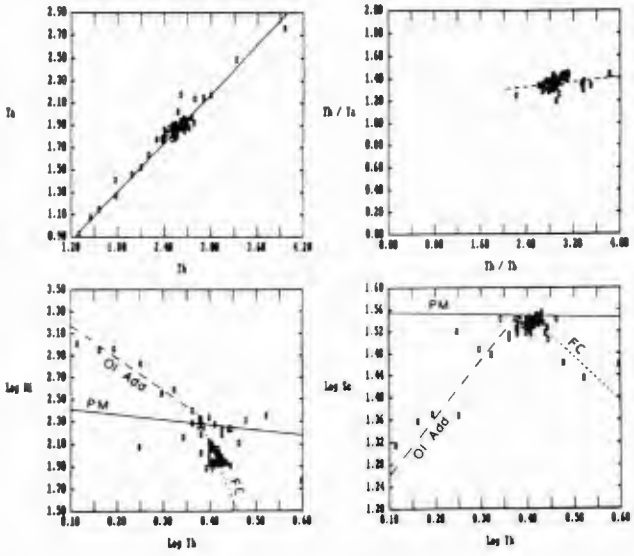

We conclude that: (1) "Normal" basaltic to mugearitic products, generally restricted to elevated eruptive points, are the result of variable but minor amounts of crystal fractionation from primary magmas issuing from partial melting of a relatively homogeneous source at possibly slightly variable degrees; (2) "Oceanites" (Lacroix, 1936), emitted during spasms of high production rates (e.g. 1977), along semi-continuous fissures extending from the summit to sea level, are the result of entrainment of the high density Ol ± Cr spinel crystals accumulated in crustal reservoirs during a protracted history of feeding and eruptive discharge.

PdF therefore stands out as a volcano where magmas are rapidly transferred from their source to the surface (see U/Th results of Condomines, 1988). However, at variance with Albarède and Tamagnan (1989) we do not attribute most entrained olivines to a xenocrystic ss. origin. The term "pricrite" should be banned from the Piton magmatology.

REMARKABLE UNREST AT IWO-JIMA CALDERA, VOLCANO ISLANDS, JAPAN

KAIZUKA, Sohei, Dept. of Geography, Tokyo Metropolitan University, Fukazawa 2-1-1, Setagaya-ku, Tokyo, 158 JAPAN
NEWHALL, Christopher, MS 905, U.S. Geological Survey, Reston, Virginia 22092 USA
OYAGI, Norio, National Research Center for Disaster Prevention, Tennodai 3-1, Tsukuba-shi, 305 JAPAN
YAGI, Hiroshi, Inst. of Earth Sciences, Dept. of Mathematics and Physics, National Defense Academy, 1-10-20 Hashirimizu, Yokosuka, Kanagawa Prefecture, 239 JAPAN

The floor of the largely submarine Iwo-jima Caldera has been updomed to form the main body of Iwo-jima (Sulfur Island). Uplift is reflected by raised wave-cut terraces and a change from submarine to littoral to subaerial deposition of volcanic tuffs. Uplift near the center of the caldera has occurred at an average rate of 15-20 cm/y since the caldera floor rose above sea level about 500-700 years ago. Episodes of faster and slower uplift are suggested by the terraces themselves and variations in the rate and pattern of historically measured uplift. Uplift is accompanied by seismic swarms, measurable displacement along numerous faults, and hydrothermal activity beneath much if not all of the island.

Uplift and accompanying unrest can be explained as injection of magma into a 3 to 4 km deep, subcaldera reservoir. The volume of postcaldera uplift above and below sea level is more than 10 km^3 and thus a similar volume of magma is inferred to have accumulated since the caldera formed. The total volume of magma beneath Iwo-jima may be considerably larger. We refer here only to magma that has accumulated since caldera formation, augmenting any magma that remained immediately after caldera formation. The volume of uplift above sea level during the past 500-700 years is roughly 5 km^3, suggesting an average injection rate of 7-11 x 10^6 m^3 of magma per year. Magma is supplied to other circum-Pacific volcanoes at similar rates or faster but usually erupts within a few years or decades. In contrast, magma at Iwo-jima has accumulated for centuries or millennia without magmatic eruption.

Nothing in existing data from Iwo-jima suggests that a magmatic eruption is imminent. However, such an accumulation of magma cannot continue forever. We suggest that an eruption of up to 10 km^3 of magma is more likely from Iwo-jima than from any other volcano with which we are familiar. Continued monitoring of Iwo-jima may eventually capture information about the precursors to large eruptions, not presently known, that will be vital for forecasting such eruptions in more densely populated areas.

STRATIGRAPHY, CHRONOLOGY, AND STYLE OF THE 1976 PYROCLASTIC ERUPTION OF AUGUSTINE VOLCANO, ALASKA

KAMATA, Hiroki and WAITT, Richard B., Cascades Volcano Observatory, U.S.G.S., 5400 MacArthur Blvd., Vancouver, WA 98661, U.S.A.

An eruption of Augustine Volcano between January and April 1976 produced pyroclastic falls, flows, and lava domes. We have determined the chronology of these events by comparing the stratigraphy with published records of seismicity, infrasonics, and plume observations. From explosions on January 23, 1976 (all times in G.m.t.), three thin air-fall-ash beds are identified: a pale-brown fine ash (unit A1) (1611), a gray fine ash (unit A2) (1658), and a brown ash (unit A3) (2008). On January 24 (0217), a pale-yellow, small-volume ash-flow deposit (unit F1) was emplaced over much of Augustine Island. On January 24 (~0600-~1440), a series of lobate pumice-flow deposits (unit F2) were emplaced on the northeast flank of the volcano. Unit F2 locally melted the snowpack to cause small pumiceous floods (unit L). On January 24 (1840), a pink ash bed (unit A4) accumulated atop an eolian deposit on the surface of the unit F2 pumice flows. The main plinian eruption (unit P) that occurred on January 25 (1457) deposited white pumice and ash over most of the island and as far away as Anchorage, 300 km northeastward. On February 5-8, block-and-ash flows (unit B) were erupted. On February 8-18 and again in mid-April, lava domes were extruded. Early in the 1976 eruption, windows of a hut at Burr Point, near the north coast of the island 6 km from the vent, were broken out, and the metal roof was penetrated by pumice and lithic fragments. J. Kienle and R.B. Forbes in 1976 inferred that the destruction was caused by turbulent clouds of hot gas and dust which detached from eastward-turning unit F2 pumice flows and traveled directly northward to the hut. Our stratigraphic evidence indicates that the hut was damaged instead by the unit F1 ash-flow (0217 January 24), before the eruption of unit F2, and that the roof was dented by lithic fragments of the plinian fall of January 25. The unit F1 ash-flow deposit is as thick as 20 cm in topographic lows but thins to nil on adjacent hummocks. Although unit F1 had a small volume and left a thin deposit, it is distributed radially about the island. Unit F1 was hot enough to char wood, but its abundant vesicles suggest that it was saturated with water vapor. Altogether, our observations suggest that unit F1 was deposited by a high-velocity pyroclastic surge erupted before the slower and more restricted unit F2 pumice flow. At Augustine, pyroclastic surges such as unit F1 are important hazards, as are infrequent debris avalanches and attendant tsunamis.

VOLCANISM AT A BACK-ARC BASIN -AGE AND Sr ISOTOPE CHARACTERISTICS OF THE JAPAN SEA AREA

KANEOKA, I., Earthquake Research Institute, University of Tokyo, Bunkyo-ku, Tokyo 113, Japan.
NOTSU, K., Faculty of Science, University of Tokyo, Bunkyo-ku, Tokyo 113, Japan.
TAKIGAMI, Y., Kanto-Gakuen College, Tatebayashi, Gunma Prefecture 374, Japan.
FUJIOKA, K. and SAKAI, H., Ocean Research Institute, University of Tokyo, Nakano-ku, Tokyo 164, Japan.

The Japan Sea is regarded as one of the typical back-arc basins, which developed between the Japanese Islands and the Asian Continent. It is classified into a mature basin, which has an evidence of past spreading(Toksöz and Bird,1977). It has typical oceanic structures in the northern and eastern parts(Japan Basin and Yamato Basin), but still keeps continental structures in the central part(Yamato Ridge) and the southern area(e.g.,Korea Plateau)(Ludwig et al.,1975). The estimate for the formation age of the Japan Sea has been of much debate,which ranges from 10Ma to more than 30Ma.

With the aim to characterize the evolution mode of the Japan Sea, we have performed K-Ar, Ar-40/Ar-39 and Sr isotope analyses for volcanic rocks dredged from the seamounts in the Yamato Basin and some related areas. Investigated rocks include basalts and trachyandesites and mostly of alkalic character. Present results together with reported data indicate that most dredged rocks from the basin areas show radiometric ages of less than 20Ma, whereas rocks recovered from the areas where continental crusts are observed show radiometric ages of more than 20Ma. K-Ar ages exceeding 100Ma have been reported for some igneous and metamorphic rocks from the latter areas (e.g., Lelikov and Bersenev,1975). Based on such data, it is inferred that the Yamato Basin would have formed prior to 17Ma and probably later than around 25Ma. The Japan Basin might have formed in a similar period or a little earlier.

The Sr-87/Sr-86 ratios observed for dredged rocks from the Yamato Seamount Chain show values ranging from 0.70357 to 0.70388, suggesting incorporation of some time-integrated components enriched in incompatible elements such as continental crustal materials. This seems to be quite different from the Mariana Trough region, where Sr-87/Sr-86 ratios of N-type MORB values have been reported for dredged rocks. Some volcanic rocks dredged from the Yamato Ridge and the continental shelves show Sr-87/Sr-86 ratios of more than 0.7045(Ueno et al.,1974), which also suggests the contamination effect by the continental crustal components. Hence it might be conjectured that the opening of the Japan Sea have not developed sufficiently enough to show the characteristics of typical N-type MORB source materials without being affected by the preexisting continental crustal materials. Such situation might have occurred due to the suppression effect to the extensional field in the basin areas caused by the existence of the Eurasian plate and the moving Pacific plate against it.

DEEP STRUCTURE AND EVOLUTION OF THE AVACHINSKY VOLCANO, KAMCHATKA

KARGOPOLTSEV, A.A., Institute of Volcanology, Petropavlovsk-Kamchatsky, 683006, USSR

As shown by geophysical data the Avachinsky volcanic group in Kamchatka has a contrasting block structure down to the depths of 10-12 km.

In general, one can distinguish the south-west, central and north-east blocks in the seismic section. They differ significantly in velocity and density properties of rocks.

This is particularly characteristic of the central and south-west blocks. Within these blocks there occurs a sharp change of signs of gravitational field. Against a background of this field within the Avachinsky volcano there occur local anomalies. Here in the seismic section one can also distinguish the zones with velocity inversion.

The block to the east of the Avachinsky volcano is characterized by consistent positive gravity anomaly. It merges with the vast positive field of the Nalachevsky uplift. In general,high velocities are characteristic of this block.

It is possible that in the historic time the uplift of the NE block occurred along with formation of numerous andesitic extrusions.

During this period the Avachinsky volcano-tectonic depression is formed. It is well expressed in the roof of the Cretaceous basement rocks.

The depression 24 km wide is complicated by a system of faults and by a local trough which is located under the SW flank, asymmetrically with respect to the center of the volcano. Here occurs a sharp submergence of rocks of the Cretaceous basement from a depth of 0.5-0.8 km to 5.0-5.5 km.

Such an amplitude of the fault, which is expressed in isolines of the actual velocity of 5 km/s,cannot be explained only by submergence of the central part of the depression because the Avachinsky volcano-tectonic depression is in general expressed by gradual subsidence of isolines of actual velocity from NE to beneath the volcano, and in the SW side it has an amplitude of about 2 km.

Apparently we have here the uplifted block with the anomalous properties in the upper part ($\bar{V}$=5.5 km/s, σ = 2.75-2.77 g/cm³) which allow us to relate it to subvolcanic intrusion. This intrusion, presumedly connected genetically with the feeding zone of the volcano, was the reason for tectonic deformations which formed the local trough. A zone of absorption of P-wave high-frequency components (up to 6-7 Hz) has been detected within the uplifted block between depths of 1.5 and 3 km. The velocity inversion is well expressed in its lower part. These data point to significant warming up of enclosing rocks within this block.

Analysis of geophysical (the existence of asymmetrical depression and active seismic zone) and geological data on morphology of the Avachinsky volcano indicates that in its history there was a stage of great failure of the ancient edifice and growth of a new cone.

ALEUTIAN MAGMATIC SYSTEMS: AN INTEGRATED VIEW

KAY, R. W. and KAY, S. Mahlburg, Institute for the Study of the Continents, Snee Hall, Cornell University, Ithaca, NY, 14853, USA.

Magmatic and tectonic processes, inferred from the mineralogy and the chemical and isotopic compositions of igneous rocks, operate within the Aleutian subduction system. The system functions sequentially: outputs of one stage are inputs of the next. The magmatic stage begins in the mantle, under the Aleutian volcanic line. Transfer of a melt or solute-rich fluid, which includes components from sediment and hydrothermally altered oceanic crust, from the subducted plate into the overlying mantle peridotite causes the mantle to partially melt and rise as a broad convective limb in regions under active volcanoes. The melt percolates continuously through the rising peridotite over a depth range from 100 to perhaps 30 km, where it segregates as basalt and ponds under the lithosphere, which is largely crust. Residual mantle largely descends both away from the trench and between volcanic centers. Evidence for subducted sediment and hydrothermally altered oceanic crust in the source region of Aleutian magmas comes from trace elements, radiogenic isotopes and ^{10}Be. However, oxygen isotopic values of Aleutian arc lavas are near those of MORB, indicating that the bulk of the Aleutian magmas comes from the mantle. Regional variations in incompatible trace element and isotopic abundances in Aleutian arc volcanoes, (examples: Buldir, Moffett, Great Sitkin, Okmok) as well as some of the heterogeneity within single centers, probably result from variability in the subducted component. In major element composition (except K_2O), the most mafic Aleutian basalts are similar to MORB, and our hypothesis is similar to hypotheses for magma generation and migration at the mid-oceanic ridges. The observation that volcano spacing along both arcs and at mid-oceanic ridges is about the same supports our speculation that both result from transverse convective rolls. The crust-mantle boundary is magmatic, and coincides with a series of short-lived magma ponds whose bases are formed by the accumulation of olivine and clinopyroxene. Crystallized high-Al basalts and their accumulated liquidus phases, constitute the lowermost crust. Some of the original oceanic crustal basement probably remains in large, coherent (about 500 km.) arc crustal segments. Pieces of this oceanic crust metasomatized by arc intrusive bodies occur as xenoliths in Tertiary dikes on Kanaga Island. The hydrated upper layers of this oceanic crust, as well as sediments on top of it, should undergo dehydration and melting in response to heating that accompanies magmatic intrusion, and can be recycled upward within the arc crust. These magma chambers probably did not exist until the arc crust was built to some minimum thickness in the Tertiary. In the regions between coherent crustal blocks, large volcanoes are attributed to extensional stress regimes. Here the arc crust probably consists of a larger proportion of arc-derived magmas. High-temperature Mg-rich magmas can reach the surface in these regions.

THE PATAGONIAN PLATEAU BASALTIC PROVINCE

KAY, S. Mahlburg, Institute for the Study of the Continents, Snee Hall, Cornell University, Ithaca, New York 14853, USA, and RAMOS, V.A., Servicio Geológico Nacional, Avda. Santa Fe 1528, 1060 Buenos Aires, Argentina.

The Patagonian Plateau province in southern South America is one of the earth's largest continental basaltic provinces. Mafic volcanism has occurred discontinuously in different parts of the province from the late Cretaceous until the Recent. Despite the voluminous volcanism, evidence for large amounts of related extension is lacking. Instead, the volcanism appears to be loaded on top of the plateau. Volcanism correlates with subduction of young ocean crust and oceanic ridges along this part of South America throughout the Tertiary. Geochemical work on this province is in the initial stages.

Some regional generalizations can be made. First, periods of extensive plateau volcanism are accompanied by minimal activity in the arc. In the south, major periods of plateau volcanism and hiatuses of arc activity in the Eocene and late Miocene correlate with periods of ridge subduction. Although ridges are not subducted intact, preliminary data on the timing and character of the plateau magmatism suggest a correlation with a mantle anomaly associated with the demise of the ridges. Lesser amounts of plateau volcanism can be nearly contemporaneous with arc volcanism. Second, Tertiary arc magmatism was more persistent in the north than in the south. Existing geochemical data on the plateau rocks appear to reflect this difference as basalts from the north show a persistent enrichment in the alkalis and alkaline earths relative to the light rare earths (i.e., Ba/Nb > 15) that is not seen in the southern basalts suggesting that this enrichment is due to a mantle component related to the more extensive arc magmatism in the north. Limited isotopic data is inconsistent with this contrast reflecting differences in degree or type of crustal contamination between the two regions.

Geochemical variations in basalts throughout the plateau suggest different amounts of melting of variably enriched mantle control the geochemical nature of the basalts and that crustal contamination is minor. The most extensive melting event probably occurred in the Oligocene to early Miocene in the Somuncura plateau region (39°-42°S). Although preliminary geochemical results show wide variations in the Somuncura lavas, some of them are like Hawaiian tholeiites in that they have low incompatible element concentrations (La - ppm), flat light and steep heavy REE patterns, and $^{87}Sr/^{86}Sr$ initial ratios near 0.705. These lavas may represent extensive melts of primitive mantle. In contrast, overlying Pliocene basalts have steep light and heavy REE patterns and lower $^{87}Sr/^{86}Sr$ initial ratios and suggest lesser amounts of melting of a more depleted mantle that has seen a recent enrichment event associated with arc magmatism. The cause of the Somuncura event is unclear although it correlates with a period of slow relative convergence along the entire coast of South America and a hiatus of arc volcanism in this region.

DEGASSING AND CONVECTION PROCESSES OF BASALTIC MAGMA : A CASE STUDY ON IZU-OSHIMA VOLCANO

KAZAHAYA,K., TAKAHASHI,M. Environmental geol. Sect., Geol. Surv. Japan, Higashi, Tsukuba, Ibaraki 305, Japan.
AND SHINOHARA,H. Dept. of Chem., Tokyo Inst. Tech., 2-12 -1 O-okayama, Meguro, Tokyo 152, Japan.

Active volcanoes degas to a greater or less extent whether the volcanoes are erupting or not. High rate of degassing except for the eruption tends to occur in the post-eruption stage. To degas the amounts of magmatic volatiles, it is necessary to transport the comparable amounts of melt to the vesiculation level at shallower depth. We attempt to estimate the transportation rate of magma to the vesiculation level for Izu-Oshima volcano with the method shown in the following flow chart and discuss about the magma convection.

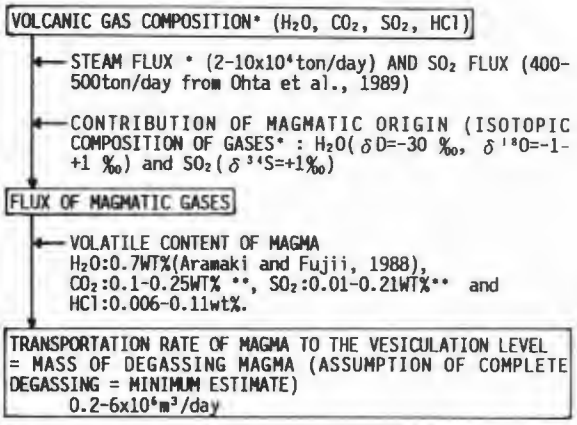

*:measured in this study.
**:estimated from the data of oceanic pillow lava given by Garcia et al., (1979).

Izu-Oshima volcano erupted in 1986. The high degassing activity is continued over a year duration since Nov., 1987, the latest explosion with the formation of pit crater. The mass (minimum) of degassing melt of Izu-Oshima volcano is estimated in the range from 0.2 - 6 x 10^6 m^3/day. The acummurated mass of degassing melt until Feb., 1989 is 0.7 - 24 x 10^8 m^3 which is 6 - 170 times larger than the product of 1986 eruption. The intense convection in the conduit is necessary to explain the above estimation.

The driving force of enormous amounts of melt transportation should be the buoyancy caused by the density difference between the degassed melt and non-degassed melt in the conduit. For example, the degassed melt is denser by about 0.1g/cm^3 than the non-degassed one with the water content of about 1wt%. A simple Poiseuille flow model is used to calculate the parameter sets satisfying the estimated mass of degassing melt. The condition needed is obtained as follows: conduit diameter of 10 - 30 m, density defference between ascending and descending melt of 10^{-3} - 10^{-2} g/cm^3, viscosity of 10^3 - 10^4, asending velosity in the conduit of 5 - 50 cm/sec and Rayleigh number of 10 - 100, which are thought to be possible conditions.

The volume of conduit (<10^7 m^3) is comparable to that of degassing melt in a day. The result, that the enormous amount of melt is degassing, implies that the volatile contents in magma chamber should be reduced by magma convection and the density becomes increased. The density increase enhanced in the magma chamber could give rise to the injection of new magma by buoyancy. In some volcanoes, several times excess of magmatic volatile emissions, as compared with the emissions estimated from the products of eruption, have already found by privious workers. These facts suggest that the degassing process including magma chamber is a fundamental process of less viscous magma.

TRANSPORT OF SILICIC MAGMAS THROUGH DIKES: COUPLING OF HYDRODYNAMICS AND SOLID MECHANICS

KELKAR, S., and VALENTINE, G.A.
Earth and Space Sciences Division, Los Alamos National Laboratory, Los Alamos, NM 87545 U.S.A.

The flow of silicic magmas through dikes and conduits in the upper crust is governed by the interplay between fluid dynamics and solid mechanics. The strong temperature and strain-rate dependence of viscosity in silicic magmas may lead to very complex flow processes. Dimensional analysis of the Navier- Stokes equations for nonlinear-viscous flow leads to the following important parameters: Gz, the ratio of convective heat transfer to heat diffusion; G, the ratio of viscous heat generation to heat conduction; Pr, the ratio of momentum diffusion to heat diffusion; and Re, the ratio of inertial forces to viscous forces. For dike widths of 1 m and flow speeds ranging from 0.1 to 10 m/s a rhyolitic magma has Gz = 10^2 to 10^4, G = 10^2 to 10^5, Pr = 10^7, and Re = 10^{-3} to 10^{-1}. The high values of G indicate that dissipative heating will be very important in the flows, producing appreciable temperature/viscosity changes along a dike.

The flow of magma in dikes is also strongly dependent upon the solid mechanics of the country rock. It is well known that the orientation of dikes is generally perpendicular to the local least principal stress. Significant dike widths, on the order of meters, are necessary to permit the observed flow rates. This can occur only through tensile fracture opening, hence the pressure within the dike must exceed the least principal stress. Since the pressure is partly determined by the hydrodynamics, it is important to understand the coupled fluid/energy transfer and deformation processes for the dike. Due to the inherent nonlinearity of the processes, different initial and boundary conditions lead to a wide variety of possible scenarios. For example, if a rhyolitic magma heats up due to viscous dissipation, its viscosity will decrease. Decreasing viscosity will lead to increased flow speed (assuming a constant volumetric flow rate) and possibly to a decrease in pressure which in turn will allow the dike width to decrease. Eventually, unless some balance is achieved between these coupled effects, a runaway situation may result leading to surface eruption. On the other hand, if magma does not have sufficient mechanical energy, heat loss to the crustal rocks may dominate, eventually leading to solidification and dike emplacement. An additional factor that may affect flow in dikes is that the compliance of a host fracture is generally much larger towards its center than at the crack edges. Thus the flow may be increasingly concentrated toward the middle of a dike during a magmatic event; the result may be a gradual evolution from a dike geometry to that of a circular conduit.

Because of the strong coupling (nonlinearity) of the hydrodynamics and solid mechanics of dike flow, especially for silicic magmas, the most promising approach to the theoretical study of the process is by numerical simulation, where all important terms in the governing equations can be retained. We will present results of hydrodynamics modeling of flow within dikes with nonlinear-viscous effects included. Preliminary considerations of the solid mechanics effects will also be presented.

MAGMATIC CHARACTER OF ALKALINE VOLCANIC ROCKS FROM A CONTINENTAL RIFT ENVIRONMENT: CRUSTAL CONTAMINATION VERSUS ENRICHED SUBCONTINENTAL MANTLE. A SR ISOTOPIC CASE STUDY FROM THE KAISERSTUHL (FED. REP. GERMANY)

KELLER, J. and SCHLEICHER, H., Mineralogisch-petrographisches Institut, D-78 Freiburg (Fed. Rep. Germany).

The Kaiserstuhl is composed by a great variety of alkaline volcanic and subvolcanic rocks from the tephritic, phonolitic and carbonatitic families. Rocks of tephritic composition hold the greatest volume and hence represent the most important type of magma of the Minocene volcanism in the southern part of the Upper Rhine Rift Valley.

The geochemical variation in the tephrites shows a rather uniform fractionation series (KIM 1985). Fractionation took place under low pressure conditions and hence definitely within a crustal environment. The tephritic rocks are enriched in potassium with a primary K_2O/Na_2O ratio of about 1, Mg-values between 45 and 55, and SiO_2 contents of 43-51 %.

$^{87}Sr/^{86}Sr$ data obtained from mineral phases show evidence of contamination of the tephritic magma with crustal-derived Sr during fractional crystallization. For the tephritic rocks an originally K-basanitic source magma is postulated (KELLER 1984). This is thought to be represented by some rare basanitic rocks. As possible contaminants crystalline rocks of the adjacent Schwarzwald basement are being taken into account. AFC-curves between an olivinbasanitic source magma and different contaminants were calculated. The diagrams point towards the following conclusions:

- The tephritic rocks show contamination by crustal material (usually < 10 %). The degree of contamination, however, differs from element to element. This point suggests selective assimilation of crustal material rather than bulk rock assimilation.
- The alkaline character of the tephritic magma series cannot exclusively be explained by crustal contamination. The development of potassium-pronounced magmas must already have taken place in a subcontinental enriched mantle environment.
- Isotopic data from the tephritic rocks point to a magmatic development within several subsystems, i.e. seperate magma chambers.

RINCON DE LA VIEJA VOLCANO, NORTHWESTERN COSTA RICA: EVOLUTION OF A COMPOUND STRATOVOLCANO

KEMPTER, K.A., Department of Geology and Geophysics, Louisiana State University, Baton Rouge, LA, 70803, and BENNER, Shawn, G., Geology Department, Colorado College, Colorado Springs, CO, 80903

Geologic mapping of the summit region and deeply dissected southwestern flank of Rincon de la Vieja volcanic massif has documented a complex stratigraphic sequence dominated by plinian/sub-plinian tephra deposits and two-pyroxene andesitic lavas. The preserved volcanic succession has been subdivided into four phases, characterized in ascending stratigraphic order as follows:

1) a voluminous sequence of porphyritic, pilotaxitic lavas intercalated with less voluminous tephra and debris flow deposits,

2) a thick sequence of alternating tephras and lava flows with minor pyroclastic flows and surge deposits,

3) plinian and sub-plinian tephras with minor interbedded lava flows, and

4) an inversely graded plinian tephra deposit (dated at approximately 4000 ybp (Melson et al., l985)) and subsequent strombolian and phreatic deposits.

Petrographically, the andesitic lavas exhibit little change through time with respect to phenocryst composition and percentage. The lavas typically contain 30 to 45% phenocrysts of plagioclase, augite, hypersthene, and magnetite, with augite > hypersthene by approximately 2:1.

A tephra isopach map has been constructed for the 4000 ybp tephra deposit, showing an asymmetric dispersal pattern with a west-trending, curvilinear dispersal axis. Two atmospheric wind components at the time of the eruption are suggested by the dispersal axis: a lower wind component prevailing from the east-northeast, and an upper wind component trending due west. Two eruption pulses are recognized in the tephra deposit, yielding a combined estimated volume of 0.38 km^3.

Although seven identifiable cones have coalesced to produce the volcanic massif, only one eruptive center has been active since the last plinian eruption. North-northeast migration of volcanism is suggested by relative cone and crater age relationships, accounting for younger, steeper, and less eroded flanks to the north. Reconnaissance geologic mapping of deposits on the north flank indicate that tephra deposits are exponentially thinner than those to the southwest, suggesting that prevailing east-northeasterly winds have influenced tephra deposition for much of Rincon de la Vieja's eruptive history.

Geochemical data on selected lavas throughout the documented stratigraphic sequence demonstrate moderate variations in major element composition, with SiO_2 values ranging from 54 - 62%. K_2O values and Rb, Zr, and Ba trace element concentrations exhibit behavior sympathetic to silica content. Chondrite normalized REE data are well constrained and suggest a single magmatic source. When placed in a stratigraphic context, these data argue that punctuated influxes of mafic magma caused digressions in magmatic evolution, contradicting a simple open or closed magmatic system model.

EVOLUTION OF THE CONTINENTAL LITHOSPHERE: ISOTOPIC AND TRACE ELEMENT EVIDENCE FROM RECENT CENOZOIC BASALTS FROM THE SOUTHWESTERN U.S.A.

KEMPTON, P.D., ORMEROD, D.S., HAWKESWORTH, C.J., The Open Univ., Milton Keynes, UK MK76AA; and FITTON, J.G., Univ. of Edinburgh, Edinburgh, UK EH93JW

Isotopic and trace element analyses of Cenozoic (<17 Ma) alkalic basalts from the Basin and Range (BR) and its tectonic boundaries to the west (Sierran Province, SP) and east (Colorado Plateau–BR transition zone, ETZ) record the effects of subduction on the composition and evolution of the sub-continental lithosphere beneath the southwestern U.S.

BR alkalic basalts are chemically similar to OIB, having high ϵNd (+4.2 to +0.8) and TiO_2 (2–3 wt%) with low Ba (300–550 ppm), Ba/Nb (< 15) and $^{87}Sr/^{86}Sr$ (0.7029–0.7039), suggesting an asthenospheric mantle origin. Both ETZ and SP lavas have higher Ba contents (200–2673 ppm), coupled with higher Ba/Nb (15–250) and lower TiO_2 (< 2.5 wt%) than BR basalts, characteristics typically associated with subduction zone magmas. In addition, SP lavas have generally higher Ba/Nb, K/Ti and Sr isotope values than ETZ basalts. Lavas from the northern portion of the ETZ (N. Arizona–central Utah) have unusual low $^{87}Sr/^{86}Sr$ combined with low $^{143}Nd/^{144}Nd$ and plot below and to the left of the mantle array, indicating low time-integrated Rb/Sr ratios.

Pb-isotopic values are distinct for each area. BR exhibits only a small isotopic range, while ETZ and SP have overlapping to lower $^{206}Pb/^{204}Pb$ with northern ETZ and SP at higher $^{207}Pb/^{204}Pb$ (Fig. 1a). Linear distributions on Pb–Pb plots for both ETZ and SP yield source ages of 1.5 Ga, but the southern ETZ array is displaced to lower $^{207}Pb/^{204}Pb$, indicating a lower U/Pb ratio (μ_1) than for northern ETZ or SP.

The Sr, Nd and Pb isotopic trends cannot be attributed to magma–crust interaction since (1) no correlation between $^{87}Sr/^{86}Sr$ and 1/Sr is observed, and (2) analyzed lower to mid-crustal xenolith suites from the area do not form reasonable mixing end members (Fig. 1b). The high Ba/Nb, Rb/Sr, K/Ti and U/Pb ratios in the transition zone basalts indicate that subduction processes have enriched the subcontinental lithosphere beneath the southwestern United States. The range in isotopic and trace element ratios suggest that enrichment processes ranged from fluid-dominated (SP and Colorado Plateau) to melt-dominated (northern and southern ETZ) (Figure 1b). Although the effects of recent subduction cannot be dismissed, isotopic evidence suggests that these characteristics were largely imposed upon the lithosphere about 1.5 Ga ago. Chemical differences in magmas derived from lithospheric sources reflect ancient, rather than recent, subduction processes in the western US; geochemical boundaries in the lithosphere correspond to domains established during the Proterozoic which were ultimately assembled into western North America between Proterozoic and late Paleozoic times.

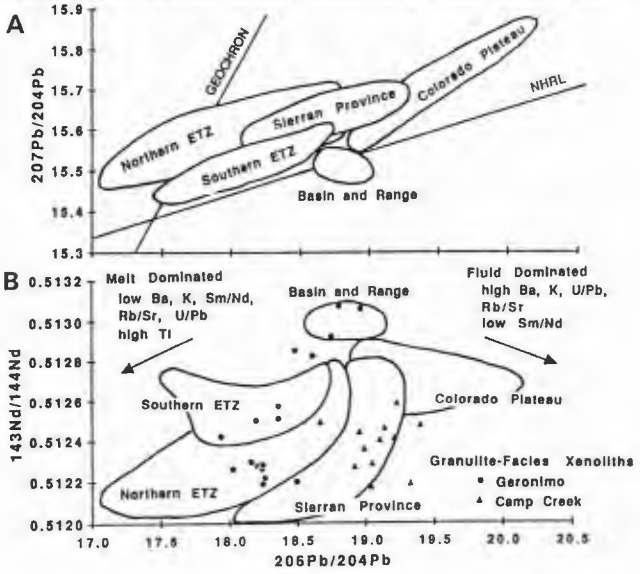

SUBVOLCANIC HYDROTHERMAL SYSTEMS IN THE CONTINENTAL CRUST

KESLER, Stephen E., Department of Geological Sciences, University of Michigan, Ann Arbor, MI 48109

Hydrothermal systems are associated with most subvolcanic environments in the upper 5 km of the continental crust. According to the fluid inclusion record found in ore deposits that were formed by these systems, they can be divided into two groups. Simple systems consist essentially of low to moderate salinity, chloride-bearing water with a low K/Na ratio, which boils as it rises, releasing vapors that condense in the top of the system. These systems rarely exceed 300 C, occupy tens to hundreds of cubic km, and appear to consist dominantly of meteoric water. Low salinity (>1% NaCl) waters in these systems form Au-Ag-As-Sb or W-Sn veins (depending on relative abundances of H_2S and CO_2), higher salinity (up to 30% NaCl) waters form Pb-Zn-Cu-Ag veins, and the vapors mix with overlying groundwater to form Hg-Sb deposits. Complex systems include highly saline, chloride-rich brine with a high K/Na ratio and coexisting vapor. These systems have temperatures in the 300 to 800 C range, occupy volumes of only a few cubic km, and appear to have been derived largely from cogenetic magma. The saline brines form porphyry Cu-Mo-Au and skarn Cu-Pb-Zn-Ag deposits, whereas the vapors mix with groundwater to form acid-sulfate Au-Ag deposits. Complex systems are commonly enclosed within a larger, peripheral simple system, although all simple systems are not known to be cored by complex systems.

Although deeper parts of all systems are hotter than shallower parts, both types of hydrothermal systems can form at similar crustal depths, depending on the position and crystallization history of genetically related magma. Granitic batholiths that are confined to larger, deeper chambers, commonly serve as sources of heat to drive long-lived simple systems. Granodioritic stocks, which reach higher levels in the crust and release water and gases more rapidly and violently, create shorter-lived complex systems that form chemical and thermal perturbations in the larger scale, simple systems. Systems of both types tend to remove their upper parts explosively, with hydrothermal explosions associated with simple systems extending to shallower depths than magmatic(?) explosions associated with complex systems. The main uncertainty in the overall evolution of continental hydrothermal systems is the chemical contribution made to these systems by magmas.

GEOLOGICAL EFFECT OF KLYUCHEVSKOY ERUPTIONS IN 1932-1988

KIRENOV,A.P. and DVIGALO V.N., Institute of Volcanology, Petropavlovsk-Kamchatsky, 683006, USSR

Klyuchevskoy is one of the most active volcanoes of the world. During the last 56 years 5 summit and 15 flank eruptions occurred with the total volume of erupted material of about 1 km³. During the last decade the average production rate of the material erupted through the summit crater increased 4.25 times compared to the previous decade.

As a result of summit eruptions the morphology of the crater changed essentially. Sinks about 384 m deep (eruption of 1968) emerging when the activity waned, filled up gradually with lava and cinder cones. After filling the crater, the lava poured out down the slopes (eruptions of 1937, 1945, 1978, 1984-1988) which led to formation of mudflows, failures, and phreatic explosions. A cinder cone continued to grow, rose above the crater, increasing the height of the volcano by 150-170 m (193 m in 1988). As a result, the volcano reached the height of about 3850 m. Flank eruptions occur more frequently on the eastern slope of the volcano. In the historic time the first flank eruption was observed in 1932. In 1987 and 1988 there occurred simultaneous lava outpouring from the summit crater and from the radial fissures on the slope. The length of the fissures varied from a few hundreds of meters to 3-4 km. The fissuring on the slope in 1988 proceeded from below upwards. Eruptive centers on the fissures acted as effusive and explosive-effusive craters. In recent years the activity of Klyuchevskoy increased: the sustained summit crater eruption goes on along with flank breakthroughs.

The dynamics of the summit eruption is characterized by a low explosivity index, changing lava flow rate of 0.4-25 m³/s, viscosity of 10^2-10^6 poise, lava temperature of 1080°C. The character of the eruption in the years discussed does not depend on the period of volcano repose, volume of erupted material, hypsometric level of lava issue to the surface.

The solid products of eruptions are mostly lavas and a small amount of pyroclastics. The products are high-alumina calc-alkali basalts; in lavas of the 1932 and 1938 eruptions magnesian basalts were found. In synchronously collected samples of lava from the summit crater and in lavas produced by flank eruptions different amounts of pyroxene and olivine have been found, they are more abundant in the latter. From 1945 the chemical composition of rocks is invariable.

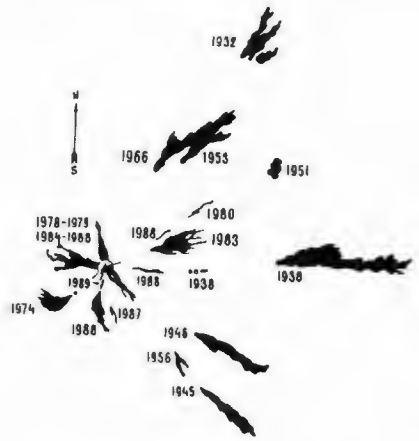

Lava flows of the 1932-1989 Klyuchevskoy eruptions

THE MORPHOLOGICAL AND DYNAMICAL EVOLUTION OF LAVA FLOWS AND FLOW-FIELDS

CHRISTOPHER KILBURN, Osservatorio Vesuviano, Centro Sorveglianza, Via Manzoni 249, 80123 Napoli, Italy.

Lava flows and flow-fields pass through a range of morphological and dynamical states during emplacement. Nevertheless, recurring patterns have been recognised among the final dimensions, shapes and time-averaged characteristics (e.g., average effusion rate) of lavas from several volcanoes. The existence of such patterns suggests systematic behaviour in either or both (a) how a lava is brought to the surface, and (b) how it is distributed during emplacement.

Although eruption rates vary during the course of an effusion, the essential morphological and dynamical features of flow and flow-field growth can be explored using steady discharge-rate models. In addition, provided that the mutually opposing interaction between the forces due to flow thickening and those due to crustal growth leads to simple dynamic or static equilibrium, qualitative analysis can be further simplified by treating separately the emplacement of homogeneous lava and the effects of crustal cooling.

At a steady discharge-rate, the advance of an unconfined, homogeneous lava settles to an equilibrium state such that the gravitational force pulling the lava is balanced by its rheological resistance to motion. For a non-Newtonian lava with an effective yield strength, the flow assumes in cross-section an approximately parabolic profile, its specific geometry depending on the lava's physical properties and gravity. The balance between gravitational and rheological forces can then be expressed in terms of flow depth, lava density and rheology, gravity and ground slope. This force balance shows that larger flows (in cross-section) and higher velocities, imposed stresses and shear rates are all favoured by increasing lava density and rheological resistance, gravity, slope and discharge-rate. The combined increase in stress and shear rate also favours surface disruption and, thus, channel flow and a'a and blocky surfaces.

Simple radiation and conduction cooling models of crustal growth show that the time t(c) to reach a particular state of cooling (expressed in terms of the ratio of crustal resistance to net driving force) increases with the size of a flow in cross-section. New flows are generated when effusion continues beyond a critical value of t(c). Hence, the complexity of a flow-field, which increases with the number of flows it contains, increases with T/t(c), where T is the duration of eruption.

Among effusions of comparable duration, therefore, the conditions favouring larger flows also favour simpler flow-fields (smaller T/t(c)). In agreement with field observations, this association suggests that increases in eruption rate, lava viscosity and yield strength will promote changes in flow-field morphology from compound flow-fields of tube-fed pahoehoe to simple flow-fields of channel-fed a'a.

DISTRIBUTION OF RARE AND TRACE ELEMENTS IN KAMCHATKAN VOLCANIC ASHES BASED ON DATA OF INSTRUMENTAL NEUTRON ACTIVATION ANALYSIS

KIRIANOV, V.Yu., Institute of Volcanology, Petropavlovsk-Kamchatsky, 683006, USSR,
FELITSYN, S.B., Institute of Pre-Cambrian Geology and Geochronology, Makarov Embankment,2, Leningrad, 199164, USSR, and
VAGANOV, P.A., State University, Naberezhnaya 7/9, Leningrad, 199164, USSR

The study presents the data on elemental composition of 38 samples of volcanic ashes from the Holocene eruptions of Sheveluch (eruptions 1500 and 2000 years ago), Khangar (eruption 6900 years ago), Opala (1500 years ago), and from recent eruptions of Bezymianny (in 1981 and 1985) and Klyuchevskoy (February 1987) volcanoes.

Elemental composition of volcanic ashes from various volcanoes generally corresponds to petrochemical zonation of Holocene acid volcanism of Kamchatka manifested in increased alkalinity of volcanites from east to west within each volcanic zone and for the overall Kamchatka.

Differences in abundance of rare and trace elements in the samples of volcanic ash from one and the same eruption collected at different distances from the volcano are due to eolian gravitational differentiation.

The results of instrumental neutron activation analysis (INAA) can be regarded as an indicator of the trace form of occurrence of some elements (Au, in particular) in volcanic ashes.

The formation of elemental composition of ashes is greatly due to processes of interaction between volcanic gases and ash particles in the eruptive cloud. Data on composition of volcanic gases and aerosols in the regions of volcanic activity point to the enrichment of volcanic gases and aerosols in Hf, As, Sb, Cs, Rb, Au, Ag, and F. The listed elements are characterized by high values of enrichment coefficients in volcanic gases and aerosols as compared to their contents in lavas, which results from their high mobility in the melt-gas system. The distribution of the elements in ash fractions confirms the conclusion about sorbing volcanic gases by the porous fragments of pumice and about coagulation of aerosol particles on the surface of ash as the ash cloud cools down.

Volcanic ashes from the studied eruptions of Kamchatkan volcanoes have higher abundances of As, Au, Ag, Sb, Cs, Rb, and Ba as compared to the average composition of the earth's crust.

Based on the distribution of element abundances in volcanic ashes of Kamchatka we obtained the following estimates of element ejection together with the ashes of Sheveluch (2000 and 1500 years ago), Opala (1500 years ago) and Khangar 6900 years ago: gold $2 \cdot 10^8$ g, uranium $5 \cdot 10^{10}$ g, and silver $1.2 \cdot 10^{10}$ g; the density of tephra was accepted to be 1.0-1.7 g/cm³.

Quantitative estimates of element ejection in volcanic ash are understated because the amounts of submicronic ash particles in the erupted products were not taken into account. The scales of explosive volcanism manifestations allow us to regard it as an important source of supply of the enumerated elements to the Earth's surface.

IDENTIFICATION OF HIGH-TEMPERATURE FLUID FLOWS IN THE MUTNOVSKY HYDROTHERMAL SYSTEM

KIRYUKHIN, A.V., Institute of Volcanology, Petropavlovsk-Kamchatsky, 683006, USSR

The high-temperature fluid flows have a composite structure and it is difficult to identify them even when the hydrothermal systems are penetrated by drill holes. It is almost impossible to assess the fluid discharge by direct methods on the basis of pressure-permeability data (Darcy's formula) because of low reliability of data used in calculations.

Among the "indirect" methods of high-temperature fluid flow identification in the Mutnovsky geothermal system the most efficient are:

1. The method of three-dimensional temperature field reconstruction which is based on the modelling the temperature logging data (in drill holes). Analysis of temperature distribution within the "Dachny" Site of the Mutnovsky geothermal field points to the existence of at least two ascending high-temperature fluid flows, (a) the "Main" flow, which is ascending at an angle of 45° from the south in the region of well 01; the cross section area of this flow is 1 km², the temperatures are 270-280°C, and (b) the "South-East" flow, which ascends subvertically in the region of well 013.

2. Tracer experiments. NaCl and sulphanol were employed as the tracers. It has been determined that the natural velocity of the "Main" high-temperature fluid flow is up to 40 m/day.

3. Study of secondary hydrothermal mineralization (Slovtsov, 1988). This method is very efficient in identifying on the basis of characteristic mineral associations the zones with different phase state of the fluid: (a) high-temperature chloride-sodium waters, (b) steam, and (c) condensate waters. It has been determined by this method that the volume of the vapor-dominated reservoir is about 1 km³.

4. Hydrochemical methods. They are used for obtaining information on phase state and temperature of fluid in geothermal reservoirs (the temperature obtained from Na-Kgeothermometer is 310-315°C, wells 01 and 013). The ascending high-temperature fluid flows are also characterized by high abundance of gold (up to 0.1 ppb, compared to the background value of 0.01 ppb).

CHEMOSTRATIGRAPHY OF THE KEWEENAWAN MAMAINSE POINT VOLCANICS, ONTARIO: MANTLE SOURCES AND CONTINENTAL-RIFT EVOLUTION

KLEWIN, K.W. and BERG, J.H., Dept. of Geology Northern Illinois Univ., DeKalb, IL 60115 USA

The Keweenawan Mamainse Point volcanics of the eastern shore of Lake Superior in Ontario are related to the Mid-Continent Rift of North America. They are unique among the several Keweenawan volcanic sections because of the nearly complete section spanning almost the entire period of volcanism. We have analyzed over 350 consecutive flows representing the entire section. The flows have been subjected to burial metamorphism and are variably altered, although many elements (eg. HFSE and REE) are not affected. Variations of chemistry with stratigraphy reveal that the section consists of several chemically distinct, stratigraphically constrained groups. Crustal contamination appears to be limited to a small group of flows near the middle of the section.

Two general trends are apparent in the major element data: a trend of increasing alumina with decreasing Mg# whose most primitive flows are high-MgO picrites and basalts, and a second trend of decreasing alumina with decreasing Mg# whose most primitive flows are high-Al olivine tholeiites. Flows of the first trend form the lower part of the section while second trend flows form the upper part. Variation in the first trend is due to fractionation of ol+cpx+spl followed by ol+cpx+plag, while the second trend is due to two stages of ol+cpx+plg fractionation at different pressures. The main trends begin at about the same Mg# (72-74) and comparison to experimental studies indicates a change in the depth of melt generation from 20-30 kb to 8-12 kb.

The distinct character of the groups is emphasized on incompatible element plots. When plotted versus stratigraphy, ratios such as Zr/Y and Zr/Nb vary significantly over the section and change abruptly between groups. The observed variations cannot be accounted for by fractional crystallization or partial melting processes and are instead most likely inherited from their mantle sources (i.e., heterogeneity). The picrites and basalts of the lower part are enriched in incompatible elements which indicates derivation from variably enriched subcontinental lithosphere. Later tholeiitic flows were probably derived largely from upwelling asthenosphere. In addition, there are scattered flows and dikes geochemically very similar to OIB and P-MORB. The chemistry of the tholeiites can be modelled as mixing between depleted asthenospheric and plume-derived melts.

The change of depth of melt generation and the chemostratigraphy of the section suggest that upwelling asthenosphere, probably initiated by a lower mantle plume, began to thermally thin the subcontinental lithosphere. The first melts were generated at depth in the lithosphere by this influence. As the lithosphere thinned, melting took place at lower pressures. Eventually, the former lithosphere was parted and upwelling asthenosphere was melted and mixed with melts derived from the lower mantle plume. The vertical structure of the subcontinental mantle indicated by the chemostratigraphy is, with increasing depth: variably enriched lithosphere, depleted asthenosphere, and undepleted lower mantle.

MID-TERTIARY POTASSIC MAGMATISM IN NORTHERN LUZON (PHILIPPINES): SIMILARITIES TO CONTINENTAL RIFT VOLCANISM

KNITTEL, U., Department of Geology, University of Melbourne, Parkville, Victoria 3052, Australia

ALBRECHT, A., Department of Geology, University of New Mexico, Albuquerque, N.Mexico 87131, USA

The central part of northern Luzon started to subside rapidly at the end of the Oligocene and formed the asymmetric Cagayan Basin. The formation of the initial graben structure followed the end of westward directed subduction along a trench east of Luzon (paleo-Quezon Trench) and is interpreted as failed attempt of back-arc basin formation (instead the South China Sea opened).

Subsidence was accompanied by potassic alkaline magmatism. Two suites have been studied in detail: The Palali Intrusion and the Cordon Syenite Complex. The former consists exclusively of salic phonolites, nepheline syenites and nepheline monzonites (MgO<3 wt.%) while the latter is composed a differentiated suite ranging from tephritic phonolite (6 % MgO) to monzonite (2 % MgO). Similar assemblages (exclusively salic rocks and differentiated suites) occur in intra-plate rift systems (e.g. in the East African Rift in Kenya).

Trace element signatures of the potassic rocks from Luzon, on the contrary, are typical of arc rocks (low Ti, Nb, Ta, Zr, Hf). $^{87}Sr/^{86}Sr$ ratios are lower than commonly observed for potassic rocks (~0.7037) and $^{143}Nd/^{144}Nd$ ratios are high (0.51290-0.51296) and are within the range observed for the slightly older calc-alkaline suites in the same area.

The generation of alkaline magma is related to the thinning of the crust during a period of crustal extension (possibly caused by trench retreat) and the resulting uplift of the underlying mantle. With regard to its trace element and isotopic composition the mantle has retained the characteristics that were aquired during the preceeding subduction episode. The potassic magmas share these characteristics.

These data show that geochemical data can not unambiquously be used to assign magmatism to tectonic settings on the basis of trace element signatures. The potassic rocks erupted in the Late Oligocene in Luzon have the characteristics of arc volcanics but were generated in a rift environment.

INFLUENCES OF CRUSTAL STRUCTURE, EXTENSION, AND VOLCANISM ON THE NATURE OF SEDIMENTATION IN THE ORDOVICIAN MARGINAL BASIN OF WALES

KOKELAAR, PETER. Earth Sciences Department, Liverpool University, PO Box 147, LIVERPOOL, L69 3BX, UK.

Steep structural discontinuities which penetrated the lithosphere profoundly influenced the location, composition, and styles of volcanism in the Welsh Ordovician ensialic arc and superimposed marginal basin. In the basin, intense bimodal volcanism occurred along complex and relatively narrow graben systems, reflecting exploitation by magmas of upper crustal splay faults rooted on the deeper discontinuities. Contemporary marine basin-fill sediments were dominantly intruded by concordant magma bodies, with transgressions and eruptions mostly developing along normal faults which propagated into this cover. Extrusive magmas commonly were ponded against contemporary fault-scarps or related flexures. In a basin-scale regime of sinistral transtension, extension across the oblique-trending grabens was commonly more or less orthogonal, and subsidence was generally persistent. However, at the site of the Snowdon Caldera, in N Wales, uplift due to rhyolite resurgence repeatedly interrupted the general subsidence, and in contrast to elsewhere the volcaniclastic successions about the caldera site contain numerous unconformities. The volcaniclastic record of basaltic volcanism and attendant sedimentation, following caldera collapse and rhyolitic ash-flow eruption, shows the alternating developments of submarine and emergent-island volcanoes. During submarine phases, hyaloclastite and lava piles prograded from both fissures and central vents, and during subaerial phases Strombolian volcanoes supplied volcaniclastics to littoral-zone fans and aprons where storm- and tidal-current reworking occurred and cliffs were rapidly formed. Relative changes of sealevel in the order of 100 to 200 m were common, and the volcaniclastic successions clearly reflect both the vertical movements and the nature and duration of contemporary eruptions.

It is clear from the work in Wales that shallow-marine volcanogenic sediment successions may be used to elucidate a crude volcanic and related tectonic history. However, before detailed histories can be determined, further research is needed to analyse and quantify the influences of sedimentary processes on the primary volcanic record. Particular attention should be paid to the modifications of primary clast populations by processes such as, for example, weathering and hydrothermal alteration, and mechanical segregation, mixing, and grain-form changes resulting from transport.

QUANTITATIVE TEXTURAL STUDIES OF MAGMATIC AND HYDROMAGMATIC TEPHRA USING THE SCANNING ELECTRON MICROSCOPE (SEM): AD 79, 1631, AND 1906 DEPOSITS OF VESUVIUS.

KOMOROWSKI J-C. and SHERIDAN M.F. (Both at: Arizona State University, Department of Geology, Tempe, AZ, 85287; 602-965-3760; BITNET: ATM3S @ ASUACAD)

The surfaces of pyroclastic grains exhibit numerous markings. They record the mechanical and chemical signature of a diversity of processes which have affected the particles throughout their evolution from genesis through transport, deposition and diagenesis. SEM textural analysis of pyroclasts can thus significantly contribute to a better understanding of explosive volcanic phenomena (melt vesiculation, rheology, role of water during fragmentation, transport and deposition of tephra). Multivariate statistical techniques (cluster, principal component, and discriminant analysis) can be applied to morphological data in order to investigate variations between textural abundance and: (1) stratigraphy; (2) eruptive style; and (3) the nature of tephra produced. We present the results from a detailed analysis of surficial and internal textures of 780 juvenile vitric clasts (250-500 μm in size) from the AD 79, 1631, and 1906 eruptions of Vesuvius.

Samples collected from each eruptive suite include those from pumice fall, fine ash, pyroclastic-surge, pyroclastic-flow, and pisolitic ash deposits. Fragments were cleaned and individually observed in the SEM using secondary electrons for surface analysis. Polished sections of pyroclasts were observed with backscattered electrons for characterization of internal textures. Chemical analyses of surficial and internal features were obtained using energy dispersive spectra (EDS) X-ray techniques.

Juvenile vitric tephra of magmatic origin is characterized by: (1) an abundance of surface and internal features diagnostic of vesiculation and melt fragmentation by violent exsolution of juvenile volatiles; and (2) an absence or minor development of syn-eruptive secondary alteration minerals. A variety of textural criteria are diagnostic of hydromagmatic origin. Our studies of Vesuvius tephra show that pyroclast morphology as a result of water-melt interactions is strongly dependent upon: (1) the amount and source of water; (2) the depth of interaction; and (3) the degree of vesiculation.

Interaction of a vesiculated magma with the near-surface hydrologic system results in brittle deformation of the melt. Vitric pyroclasts will be moderately to prominently vesiculated with fracture surfaces. Depending on the amount of water involved hydrated cracked surfaces, pitting, etching, and secondary alteration minerals will develop to some degree. Tephra from several explosive phases of the AD 1906 eruption and from the initial vent-clearing event of the AD 79 eruption are examples of this type of water-melt interactions.

When magma interacts with the hydrologic system at greater depth (≥ 2 km aquifer at Vesuvius) viscous melt deformation will occur. Poorly vesiculated dense globular vitric clasts rich in microlites form. These clasts have a marked quenched (congealed) and diktytaxitic morphology. They result from (1) rapid quenching of hot fluid melt at depth prior to pervasive vesiculation; and (2) violent distortion and melt rupture due to fluid instability at the vapor-melt interface. Abundant hydration cracks and alteration minerals develop on pitted and etched surfaces.

Textural data from the AD 79 tephra indicate that pyroclastic surge, pyroclastic flow, and accretionary lapilli-rich ash deposits of the last 8 hours of the eruption resulted from interaction of magma with the aquifer at a depth ≥ 2 kms. The hydromagmatic character of the eruption increased with time as vesiculated tuff, mud hurricane deposits, and phreatic breccias were emplaced in the wanning phases of the eruption.

Future textural studies of tephra will investigate: (1) the relationship between clast size and textural development; (2) criteria for discriminating juvenile versus non-juvenile tephra, products from wet versus dry hydromagmatic activity; and (3) parameters controlling the development of quench textures (surface tension, viscosity, density).

FRACTURE MECHANISMS OF POLYGONAL AND CIRCULAR CAULDRONS

KOMURO, H., Department of Geology, Faculty of Science, Shimane University, Matsue, Japan

Japanese Cenozoic cauldrons are classified into circular and polygonal types.

The polygonal cauldron shows an irregular outline and is bordered with steeply dipping unconformity surfaces which originate in intersecting normal to vertical faults. It is characterized by caldera collapse before the main eruption. The mean diameter of cauldrons is 10 km, and the vertical displacement of the collapse is about 400 – 500 m. Ascent of a magma chamber produced the initial doming of the earth's crust prior to the caldera collapse. The dome is estimated to have been about 30 km in diameter.

The circular cauldron is delimited by ring fractures, and cauldron fills show basin structure. The scale of this type cauldron is equal to that of the polygonal type, but the collapse displacement is more than 800 – 1,000 m. Circular cauldron was formed by contraction or collapse of the magma chamber, because the floor of this type cauldron subsided after the large eruption.

Transitional type cauldrons from the polygonal to the circular is also known. This type cauldron is characterized by a small circular collapse nested in a larger polygonal cauldron.

Model experiments and three-dimensional plastic finite element analyses revealed following points.

1. Radial fractures are initially produced near the center of the dome and grow outward, which is followed by vertical short concentric fractures. These concentric fractures intersect the radial fractures like a letter T, but continuous ring fractures do not develop during the doming. Accordingly, the collapse caldera show a polygonal outline, because its margin is bounded by intersecting radial and concentric fractures.
2. Fractures which produce a polygonal caldera diminish downward.
3. In case of cohesive model material, radial fractures only develop, and any cauldron is not produced. Subsidence of the polygonal cauldron is accommodated with the horizontal extension on the dome apex.
4. Concentric shear fractures develop around the magma chamber. They extend upward and link with the surface fractures. Eruption may begin at the time of this fracture linkage, when the surface caldera should been formed already.
5. The collapse of the magma chamber, which is caused after the large eruption, yields horizontal compressive stresses near the surface and tensile stresses around the chamber. Outward dipping ring fractures and a circular cauldron are formed, but radial fractures are not produced at all. The collapse displacement is larger than that of the polygonal cauldron.

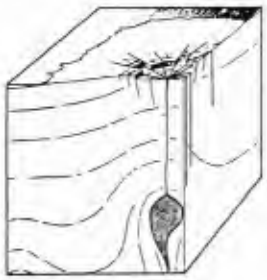

Idealized polygonal cauldron.
Note the crustal doming, shallow concentric and radial fractures.

VOLATILE CONTENTS OF PANTELLERITE

KOVALENKO, V. I. (Institute of Geology of Ore Deposits, USSR Academy of Science, Staromonetny 35, Moscow 109017), **HERVIG, R. L.** (Center for Solid State Science, Arizona State University, Tempe, AZ 85287-1704) and **SCHAUER, S.** (Dept. of Chemistry, Arizona State University, Tempe, AZ 85287-1604)

In an ongoing project to understand the origin of peralkaline rocks, we have been studying the volatile and trace element chemistry of trapped melt inclusions in phenocrysts from pantellerite and related rocks from Pantelleria. For this work we used the ion microprobe because of its high spatial resolution and good sensitivity for many elements from H to U. A preliminary study (Kovalenko et al., 1988) of a very trace element-enriched pantellerite showed that trapped melt inclusions in quartz and anorthoclase phenocrysts were also rich in water, F and Cl (4 wt.% H_2O, 0.5 wt.% F, 1 wt.% Cl). Analyses of the pantellerite matrix glass showed similar F, slightly lower Cl, but much lower water ($\leq$0.5 wt.%). They concluded that when this pantellerite erupted, water was lost but carried with it only small amounts of Na and Cl. Recent analyses of a trapped melt inclusion in an anorthoclase phenocryst from the Green Tuff has shown much less H_2O (1.5 wt.%) but the same F (0.5 wt.%). Analyses of inclusions in phenocrysts from more basic compositions on Pantelleria (hawaiite, aluminous trachyte, agpaitic trachyte) have not shown more than 0.2 wt.% H_2O, but their F contents are surprisingly high (0.2, 0.3, and $\geq$1 wt.%, respectively). Electron probe analyses for F give lower values and we are working on resolving this discrepancy. However, the relative changes in F are consistent for both techniques.

The physical properties of silicate liquids are generally related to their chemical composition. Dissolved volatile components, in particular, can be extremely important in determining melting points, crystallization sequence and viscosity. Degassing of water is expected upon eruption, but the pantellerites we have studied do not show a loss of F and only small depletion of Cl during this event. Scarfe (1977) measured the viscosity of a pantellerite, finding only a small decrease in fluidity (less than an order of magnitude) compared to metaluminous rhyolite. However, Dingwell et al. (1985) found that the viscosity of peralkaline melts could be greatly reduced when F was added (Cl also reduces viscosity but with less efficiency). Depending on the relation between halogen contents and viscosity, even though water must be lost upon eruption, halogen-rich pantellerites may remain somewhat fluid. A complicating factor is the rapid crystallization of pantellerite upon loss of water (Bailey and Macdonald, 1987) although this should be checked on halogen-rich compositions.

Bailey, D. K., Macdonald, R. (1987) In, Magmatic processes: Physicochemical principles, B. Mysen, Ed. Geochemical Society Special Pub. 1, 91-105.
Dingwell, D. B., Scarfe, C. M., Cronin, D. J. (1985) American Mineralogist, 70, 80-87.
Kovalenko, V. I., Hervig, R. L., Sheridan, M. F. (1988) American Mineralogist, 73, 1038-1045.
Scarfe, C. M. (1977) Canadian Mineralogist, 15, 185-189.

A ROLE OF SOUTH-HANGAI "HOT SPOT" IN THE GEODYNAMICS OF THE LATE-CENOZOIC VOLCANISM OF THE CENTRAL ASIA (C.A.)

KOVALENKO V.I., YARMOLYUK V.V. Institute of Ore Deposite Geology, Petrology & Geochemistry USSR Academy of Sciences, Staromonetny, 35, Moscow, 109017, USSR; SAMOILOV V.S. Institute Geochemistry, Favorsky, 1, Irkutsk, 664033, USSR; BOGATIKOV O.A., IGEM.

In the late Cenozoic in the C.A. (south of Siberia in the USSR, Mongolia, China) the huge mountains, depressions (for examples - Baikal lake), areas of basaltic volcanism were formed. Such processes are active at present, becouse this region is area with high seismity.

The new tectonical picture of the C.A. is explained by collision of Indian and Euro-Asian lithospheric plates (Molnar,Tapponie, 1975) and connected passive rifting or by active rifting under uprising of the astenospheric diapirs independent of from collizion (Zorin et al., 1980).

Our new geological materials from Mongolia and compilation of geological & geophysical data for all C.A. showed that there was active "hot spot" (h.s.) beneath South Hangai (Central Mongolia), begining from late Mezozoic upto Cenozoic. Magmatism in the area of h.s. took place about 100 millions years, had specifical composition (alkaline rocks with carbonatites, ongorhyolites, alkaline basaltoids), spase limitation, huge volume. We believe that the geodynamics of the late-cenozoic volcanism of C.A. was result of complicate set of collision of the Indian & Euro-Asian plates and of activity of South-Hangai h.s. (fig.1). In this case there was formed the

1. basaltic areas, 2. the anomal mantle with the depth less than 100km, 3. South-Hangai hot spot, 4.plates and blocks boundaries, 5. Dzunbain graben, 6. vectors of t the plates movement, 7. the direction of Amur plate rotation. Plates and blocks: E-A - Europe-Asian;I-Indian; T-Tibet;T-D-Tarim-Djunggar; C-Chinese,Al-Alashan,Or-Ordos.

C.A. collision's belt with a number of mobile microplates. The formation of the west boundary of Amur microplate took place under the action of h.s. but the rotation of Amur microplate counter-clockwise during the collision was favorable for opening of the riftogeneous depressions(for example - Baikal lake) & for intensive volcanism in Mongolia. The processes of the extension between the microplates are connected with activity of the basaltic volcanism of another regions of C.A. (Ma Xingyuan, 1988). The generation of anomal mantle beneath such tectonical structures and connected basaltic volcanism were result of both passive riftogeneous extension and preservation of anomal mantle in the South-Hangai h.s.

THE EFFECT OF PARTICLE SETTLING ON CONVECTION AT HIGH RAYLEIGH NUMBERS

KOYAGUCHI, T.*, HALLWORTH, M.A.**, HUPPERT, H.E.**, SPARKS, R.S.J.*, *Department of Earth Sciences, University of Cambridge, Downing Street, Cambridge CB2 3EQ, U.K., **Department of Applied Mathematics and Theoretical Physics, University of Cambridge, Silver Street, Cambridge CB3 9EW, U.K.

The settling of particles in a convecting fluid is a common phenomenon in many volcanic and magmatic situations. We have investigated experimentally the settling behaviour of particles in a fluid heated from below and/or cooled from above. We have found that the convective motion or pattern changes depending on the initial particle concentration.

Experiments were carried out in a tank 20x20x20 cm deep using water and well-sorted silicon carbide powder (~15 μm in diameter, ρ=3.2 g/cm^3). The temperature difference between the initial fluid temperature and the heated base (or cooled top) is typically more than 10°C, which implies Rayleigh Number > 10^9.

The particles were initially uniformly distributed throughout the tank by vigorous stirring, and then left to settle. Temperature and particle concentration profiles were measured at various levels using thermistors and a light extinction device built especially for this study.

In the experiments with extremely low initial particle concentrations (<0.01 wt.%), the particles gradually settle out, while being homogenised throughout the tank by vigorous convection. The concentration decreases with time exponentially (cf. Martin and Nokes, 1988; Nature, 332: 534-536).

In the experiments with higher initial particle concetrations (e.g. several different initial particle concentrations from 0.3 to 1.2 wt.%), the overall turbulent convection is surpressed. Particles settle out leaving clear layer above the suspension layer in the early stages (Fig.A-C). Within the suspension, temperature and particle concentration are uniform due to convection; the temperature increases and the particle concentration slightly decreases with time due to sedimentation at the base. The temperature of the clear layer, insulated from the suspension layer by the stagnant interface, increases only slightly during this stage. As the stagnant interface descends leaving hot fluid above it, the density stratification becomes unstable. Eventually the whole system overturns (in our experiments several minutes after initiation), and particle concentration becomes uniform (Fig.D), and more dilute (about 0.05 wt.%) than the initial one. After several small-scale overturns (Fig.E-F), the particles settle in the same way as when the initial particle concentration is extremely small.

The result shows that the convective pattern in magma chambers could be greatly modified by the presence of even a small quantity of phenocrysts.

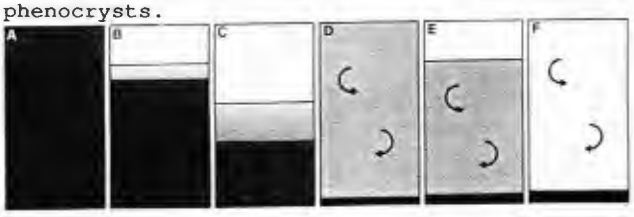

FAILED ARM SETTING OF THE GRENVILLE DIKE SWARM IN THE LIGHT OF ITS GEOCHEMISTRY

KUMARAPELI, STEPHEN and ST. SEYMOUR, KAREN, Geology Department, Concordia University, Montreal, Canada H4B 1R6 and FOWLER, A., Department of Geology, University of Ottawa, Ottawa, Ontario, Canada K1N 6N5

The approximately 700-km long Grenville diabase dike swarm in the Southeastern part of the Canadian Shield is a clear example of a continental mafic dike swarm injected into a failed-arm setting. The failed arm is the Ottawa graben, an Iapetan aulacogen which extends into the continental interior for a prominent salient-the Sutton Mountains salient - of the Appalachian foldbelt. The salient itself seems to have been inherited from an Iapetan triple junction - the Sutton Mountains triple junction. The products of synrift volcanism at the triple junction are represented by metabasaltic rocks of the Tibbit Hill formation.

A commonly accepted view of the emplacement of continental dike swarms is that the magma moved in the crust largely laterally and away from the associated "hot-spot" which in the case of the Grenville dike swarm is the Sutton Mountains triple junction. Although the dike swarm cannot be traced east of the shield margin (northwest of Montreal) because of the Cambro-Ordovician platformal cover, it probably continues further eastwards as a basement feature. The dike swarm shows a tendency to converge eastwards and if this tendency continues in the direction of the Sutton Mountains salient, it will converge on Tibbit Hill Formation. These geometric relations have led to the speculation that the dikes emanate from the eruptive centre of the Tibbit Hill volcanics and that the dike rocks and the volcanics are genetically related. One way to investigate this problem is to compare the ages of the two magmatic products. This, however, is not possible with the available geochronological data. Although the age (U-Pb, zircon) of the Tibbit Hill Formation is known as approximately 555 Ma, the age of the dikes is not known with any precision. Another way to approach the problem is through a comparative study of the chemistry of the dikes and the volcanics. The dikes are tholeiites with plagioclase-augite-olivine-titaniferous magnetite assemblages indicative of low pressure equilibration. On the Zr-Ti-Y petrotectonic space they show a continuous spectrum of compositions which straddle the field of intraplate basalts and into the field of oceanic tholeiites. Similarly, K,Ti,Zr,Sr and Nb contents increase from MORB-like values to those characteristic of continental tholeiites. Increased "Within-Plate" affinity is also indicated by increased LREE fractionation and Zr/Y and Ti/Y ratios. Nb/Y ratios (<0.5), however, indicate a tholeiitic character. In contrast, the Tibbit Hill volcanics are predominantly "Within-Plate" transitional basalts. Thus, the chemical data negate the hypothesis that the Grenville dike swarm and the Tibbit Hill volcanics are genetically related. However, the possibility that the dikes were injected laterally from triple junction cannot still be ruled out. For example, a decreased depth of mantle melting during the initiation of seafloor spreading at the triple junction may have led to the generation of the tholeiitic dike magma which did not penetrate through the already consolidated Tibbit Hill volcanics but became injected laterally into fault zones including those associated with the failed arm. Alternatively, the dikes may have been derived from a mantle source beneath the rift zone.

AUTOMATION OF A CORRELATION SPECTROMETER FOR MEASURING VOLCANIC SO_2 EMISSIONS

KYLE, P.R., Geoscience, N.M. Tech., Socorro, N.M. 87801
MCINTOSH, W.C.

The Barringer correlation spectrometer (COSPEC) is widely used to measure emission rates of SO_2 in volcanic plumes. Measurement are made by traversing under the volcanic plume in a vehicle, aircraft, boat or by using stationary ground based scans. Ground-based measurements are usually made by manually scanning the tripod mounted COSPEC across the plume. Typically data are recorded in analog form on a chart recorder and peak areas determined by counting squares or by digitizing the data.

In an attempt to obtain detailed records of short-termed emission rates we have mounted the COSPEC on a motorized variable speed pan and tilt drive. The drive automatically traverses from 0.2°/sec to over 2°/s in either scan (horizontal) or tilt (vertical) mode.

The COSPEC has been interfaced to a laptop computer via an analog to digital converter board. Inputs into the computer include the COSPEC SO_2 signal, automatic gain control, 2 supplemental gain signals, and digital inputs indicating the position of the COSPEC calibration cells, and microswitches on the scanning drive which indicate scanning direction. Computer programs have been developed to collect and store input data. Given stable plume conditions the COSPEC can be left automatically scanning and collecting data for many hours. It is necessary to manually insert the SO_2 calibration cells at the beginning and end of automated runs.

SO_2 fluxes are easily and rapidly calculated using a computer program which retrieves data from files, searches for the appropriate calibration measurements and then looks at individual peaks. The SO_2 peak associated with an individual scan is displayed and baseline positions selected using a mouse. Calculated SO_2 fluxes are stored in a data file and output to a printer. The ability to manually select the baseline is important when the plume is doubling back on itself or is asymmetrical.

We have successfully operated the system under extreme conditions of altitude (11,000 ft) and temperature (-20° C) at Mt. Erebus, Antarctica. Future tests will be made at Kilauea volcano in March. The instrument will be on display and available for hands-on demonstrations.

SUNSET CRATER, SOUTHERN COLORADO PLATEAU, ARIZONA - NEW PETROLOGICAL AND GEOCHEMICAL RESULTS INDICATING MULTIPLE MAGMA SOURCES FOR THE 1065-1180 ERUPTION

LARSEN, G., Institut für Mineralogie und Lagerstättenlehre, RWTH Aachen, 5100 Aachen, FRG
HOLM, R.F., Geology Department, Northern Arizona University, Flagstaff, Arizona 86011, USA

Sunset Crater, a cinder cone, is situated in the eastern part of the San Francisco Volcanic Field. The volcanic deposits include the Kana-a and the Bonito lava flows and related vents southeast of Sunset Crater as well (e. g. Gyp Crater, Vent 512). Several agglutinate mounds and rootless lava flows are situated on top of the Bonito lava flow, resulting from older material that collapsed onto the emerging lava flow and was rafted away. Eruption history started in 1064/1065 with the construction of an early cinder cone followed by the early Kana-a lava flow (from the eastern base) and the eruptions of Vent 512 and Gyp Crater. The early cinder cone was breached by the eruption of Bonito flow stage 1 material in 1180 and restored by following, and subsequently waning, Strombolian phases. The activity continued with Bonito flow stages 2 and 3 and the late Kana-a flow eruptions. The major amount of the Bonito flow deposits apparantly originated at a vent now concealed beneath Sunset Crater.

Samples from the different localities (Bonito lava flow, Kana-a lava flow, Gyp Crater, Vent 512) are very similar in composition, representing alkali basaltic characteristics. According to several diagrams they can be identified as Within Plate Basalts (WPB). This coincides with their geotectonic position on the southern margin of the Colorado Plateau, and the vents being controlled by a major fracture zone.

Petrographic observations reveal similar texture for all units. The intersertal to intergranular (sometimes hyalocrystalline) matrix of plagioclase, olivine, clinopyroxene, and magnetite contains phenocrysts of olivine and a few sieve textured xenocrysts of clinopyroxene. Only Vent 512 samples are free of clinopyroxene xenocrysts.

Major element patterns allow the discrimination between two distinct groups, i.e. Bonito + Kana-a lava flows and Vent 512 + Gyp Crater. In comparison Bonito and Kana-a basalts tend to be higher in SiO_2, Al_2O_3, and Na_2O and lower in TiO_2, FeO*, CaO, MgO, and K_2O. Bonito agglutinate mound (from the top of Bonito stage 1, see above) cannot be related to either of these groups, but seems to be the least evolved material. Interpretation of trace element distribution suggests that Sunset Crater and associated vents were supplied by several batches of magma, which - corresponding to the localities - can be defined as Bonito, Kana-a, Gyp Crater, Vent 512, and Bonito agglutinate mound.

Referring to major and trace element patterns of all Bonito flow units a differentiation with time from a common parent magma can be concluded. Some inconsistent abundances of trace elements may be due to multiple eruption cycles (stages 1, 2, and 3) fed by episodic resupply of the parent magma. Slightly different compositions of the resupplying batches could explain the trace element distribution observed. Mass balance calculations support this model of cogenesis by differentiation from a common parent magma with at least two cycles. Cogenetic relationships between Vent 512 agglutinate (parent) and Vent 512 lava can also be derived. Olivine (subordinately spinel) fractionation appears to be the controlling factor in both cases.

Further mass balance calculations indicate the lack of cogenesis between Bonito flow, Kana-a flow, Gyp Crater, Vent 512, and Bonito agglutinate mound. Thus the idea of separate batches of magma - and perhaps separate sources - supplying Sunset Crater eruptions is supported.

EVOLUTIONARY HISTORY OF A QUATERNARY ALKALINE STRATO-VOLCANO : VICO, ITALY.

M.A. Laurenzi[1], A.Bertagnini[2], A.Sbrana[2], I.M.Villa[1]
[1]Ist. di Geocronologia CNR,Pisa [2]Dip.Scienze della Terra, Pisa, Italy

We present a detailed volcanological, petrochemical and geochronological investigation on a strato-volcano belonging to the Quaternary potassic Roman Comagmatic Province (Italy). Our aim is to reconstruct its history by quantifying the parameters of its evolution.

Volcanic stratigraphy was redefined in great detail. Tephrostratigraphy and facies analyses of pyroclastic deposits allowed a consistent reconstruction of the eruptive sequences of most pyroclastic units. These data led us to a refinement of the pre-existing subdivision into 4 activity periods. The first one was characterized by plinian eruptions and minor lavas; lavas built up the volcano in the second phase ; caldera-forming ignimbritic eruptions predominated in the third one; the fourth period consists of hydromagmatic pyroclastics , correlated to an intracalderic lake, and of final lavas (Monte Venere). In all activity periods, magmas belong to the High-K Series and display a rather high degree of evolution (compositions range from phonolitic tephrites to trachites, the majority of samples being trachiphonolites); the primitive magmas common in other nearby centers (e.g. Vulsini, Sabatini) are absent here. The dominant petrogenetic process at Vico is low-P fractional crystallization. A shallow magmatic chamber/chambers were active in the four periods. Input of heterogeneous types of HKS magmas led to at least three different evolutive "sub-series" in the 2nd, 3rd and 4th periods.

In order to constrain a volcanological model, we need reliable estimates for duration and time-separation of the eruptive periods. Available K/Ar ages not always agree with stratigraphy; this may be due to the presence of very small amounts of excess ^{40}Ar (≈1 ppb). The a priori possibility that samples from Vico are affected by Ar excesses of the same order of magnitude as the other well-known instances in the Roman Province made it necessary to use the $^{40}Ar/^{39}Ar$ stepwise heating technique, which allows a self-consistency check on the presence, and goodness, of an age plateau. A total of seventeen samples were irradiated. Our effort was both to representatively sample all formations and to bracket onset and termination of the activity periods; some limitations came from alteration and/or lack of suitable K-rich minerals.

The lowermost plinian pyroclastite has a plateau age of 418±5 ka. Isochron treatment of the data confirms this age value, with an atmospheric intercept. This unit is the largest of the first activity phase; other minor altered pyroclastites conclude phase 1, but the volcanological evidence (paleosoils,erosions,etc) favors a relatively short activity interval. For the outcropping basis of phase 2, the Acquaforte flow, a K/Ar age of 300 ka was obtained by two laboratories. Despite the uncertainty on the exact boundaries, it is apparent that the average activity during the 420 - 300 ka period was significantly lower than that immediately preceding and following it.

The uppermost lava of Phase 2 (258±2 ka) is directly overlain by pyroclastites of Phase 3: the 3 largest formations (Ignimbrites B, C, D) yield plateau ages of 157±3, 151±3, 138±2 ka, respectively; the only coexisting sanidine-leucite pair gives concordant plateau and isochron ages. The final phonolitic-tephritic lavas of Phase 4 are about 60 ka younger than the pyroclastite climax. Thus, during the 330 ka life-span of Vico volcano, activity was concentrated in 4 rather short activity bursts.

IDENTIFICATION OF MAGMA SOURCES IN CONTINENTAL MAFIC MAGMATISM: THE RIO GRANDE RIFT.

LEAT, P.T., THOMPSON, R.N. Dept. of Geol. Sciences, University of Durham, Durham DH1 3LE, England; MORRISON, M.A., HENDRY, G.L., Department of Geol. Sciences, University of Birmingham, Box 363, Birmingham, B15 2TT, England, and DICKIN, A.P., Department of Geology, McMaster University, 1280 Main Street West, Hamilton, Ontario L8S 4M1 Canada

The Rio Grande rift runs N-S from southern New Mexico to the Colorado-Wyoming State line. From north to south asthenospheric mantle potential temperature decreases (corresponding to distance from the Yellowstone plume), amount of extension increases, and the thickness and age of the crust and mechanical boundary layer of the lithospheric mantle (MBL) decreases. These factors controlled the composition of volcanic systems in the rift. But there are no simple progressive changes in erupted volume or chemical composition of magma from north to south, because: (i) the trade-off between amount of extension and mantle potential temperature generated sub-constant volumes of mafic magma along the rift and (ii) mafic magmas were generated by partial melting of both lithospheric and asthenospheric mantle; homegenization of "end-member" melts ranged from near-perfect to virtually non-existent. In larger volume systems (>10km^3 erupted magma), extensive lower-crustal or sub-crustal magma chambers trapped and homogenized different mantle melts, and mafic magma tended to experience fractionation and assimilation of crust. In smaller volume systems, batches of mantle-derived melt equilibriated in sub-crustal magma chambers but tended not to mix with other batches, or be contaminated significantly by crust.

Mafic magmas erupted during early Miocene extension had a broadly calcalkaline character, with little variation in composition along the length of the rift. The proportion of melts from asthenospheric and lithospheric mantle sources which contributed to individual magma systems can be surmised in favourable cases: (1) The melts of the MBL mantle can be identified by their high abundances of K and related trace elements, and low $^{143}Nd/^{144}Nd$. (2) There is sufficient knowledge of certain systems to be fairly sure that asthenospheric melts had a "back-arc" chemical character, derived from mantle modified by Cenozoic subduction of oceanic lithosphere.

There was a mid-Miocene relative lull in extension and volcanism, when a fundamental change occurred in the mantle, as the early Miocene "back-arc" asthenosphere was replaced by hot OIB-source asthenosphere from the Yellowstone plume. Subsequent mafic magmatism associated with late Miocene-Recent extension was chemically complex. Only in the extreme south did pure OIB-type magmas erupt in large volumes. In most of the rift, late Miocene-Recent melts from three mantle sources: (i) OIB source asthenosphere, (2) the MBL and (3) a thermal boundary layer (TBL) of "back-arc" mantle trapped below the MBL all contributed to erupted mafic magmas. Most mafic magmas were cryptic mixtures of melts from two or three of these sources, but magmas approaching "end-members" were erupted locally.

HOTSPOT ORIGIN FOR GIANT RADIATING DYKE SWARMS: EVIDENCE FROM THE MACKENZIE IGNEOUS EVENTS, CANADA

LeCheminant, A.N., Continental Geoscience and Mineral Resources Branch, Geological Survey of Canada, Ottawa, Ontario, Canada, K1A 0E4, and Heaman, L.M., Department of Geology, Royal Ontario Museum, Toronto, Ontario, Canada, M5S 2C6.

The Mackenzie dyke swarm is one of the worlds most widespread episodes of mafic magmatism, extending for more than 2400 km along strike with a width of more than 1800 km. The dykes fan out in a radial array and converge towards a focal point north of the Coppermine Homocline. Precise U-Pb baddeleyite dating of four widely-spaced dyke samples indicates that the entire swarm was emplaced in a geologically short period of time at 1267+2 Myr and overlap within analytical uncertainty a U-Pb zircon/baddeleyite age for the Muskox intrusion (1270+4 Myr). The Mackenzie dykes are considered to be feeders to the Coppermine River flood basalts so these lavas were also extruded at this time and together with the dyke swarm represent an estimated volume of mafic magma in excess of 200,000 km^3.

The geological record preserved in the Coppermine Homocline suggests that prior to the outpouring of the Coppermine River flood basalts, the northwestern part of the Canadian shield was developing as an epicontinental basin that experienced uplift and subaerial exposure with the regional development of a karst topography followed by a short interval of subsidence. The location and regional extent of the karst topography combined with the radial pattern of the Mackenzie dyke swarm imply that uplift in the form of a broad dome centered north of the Coppermine Homocline occurred prior to Mackenzie magmatism. Previous investigations have linked Mackenzie magmatism to an underlying region of hot asthenosphere and we extend this view to suggest that the Mackenzie hotspot was caused by the presence of a large mantle plume at the base of the lithosphere. This plume produced the domal uplift (diameter in excess of 1000 km) that preceded Mackenzie magmatism.

VOLCANIC EMISSION OF SO2 AND TRACE METALS: A NEW APPROACH

Le Cloarec M.F., Lambert G., Centre des Faibles Radioactivités, CNRS/CEA, 91198 GIF/Yvette CEDEX, FRANCE.

Mean values of SO_2 fluxes coming from volcanoes are usually calculated from direct measurements in volcanics plumes. Fluxes of other components are then evaluated by normalisation to this SO_2 flux. Therefore it is of great interest to get an accurate evaluation of the SO_2 global output from active volcanoes. As the volcanic source represents only a few percent of the total atmospheric source of SO_2, it cannot be confirmed from a knowledge of the global sulfur cycle.

The situation is quite different in the case of the volcanic source of 210-Po, last radioactive nuclide of the 238-U/226-Ra series: Lambert et al(1982) showed, through the evaluation of the global atmospheric budget of 222-Rn and its decay products, that volcanoes represent about 50% of the source of 210-Po in the atmosphere. This is why we propose to normalise volcanic emissions of SO_2 and trace metals to 210-Po.

The volcanic flux of 210-Po was estimated to $5*10^4$Ci/year; it is worthy of note that this evaluation is made through an atmospheric model(Lambert et al,1982), without taking into account any measurements in volcanic plumes. Then measurements of SO_2/210-Po ratios in volcanic gases were conducted on several active volcanoes, giving a mean value of the order of 1mCi of 210-Po/ton of SO_2. Relating this value to the flux of 210-Po gives a global flux of volcanic SO_2 of $50*10^6$ tons/year.This estimation is about three times higher than that proposed by Berresheim and Jaeschke in 1983, from direct measurements in volcanic plumes.

Fluxes of trace metals emitted by degassing magmas where calculated on the basis of emanation coefficients(ε) defined in a model of radium daughters emission from Mount Etna(Lambert et al, 1985/86): such coefficients show the partition of each element between gaseous and magmatic phases. The model allowed the determination of ε_{Po} (=1), ε_{Bi} (=0.5)and ε_{Pb} ($=10^{-2}$). Therefore a budget of $5*10^4$Ci/year of 210-Po corresponds to $5*10^2$Ci/year of 210-Pb.

The volcanic output of common lead is then evaluated from a mean value of the specific activity of 210-Pb per mg of common lead: we measured 210-Pb/Pb ratios in several lava samples from various volcanoes and used an intermediate value of 0.4dpm of 210-Pb/mg of Pb which agrees well with values given by Condomines et al(1987); this yields a global volcanic lead output of 2500 tons/year.

The volcanic fluxes of other metals are related to the flux of lead by the equation: $\Phi_X = \Phi_{Pb}*(\varepsilon_X C_X/\varepsilon_{Pb} C_{Pb})$, where Φ is the flux of a given metal, C its concentration in basalts. The emanation coefficients were estimated in Mount Etna aerosols(Pennisi et al,1987) for 8 metals. Results are shown in the following table:

Φ_{Bi}= 1500 T/year Φ_{Al}= 8800T/year
Φ_{Cd}= 1000T/year Φ_{Mg}= 45000T/year
Φ_{Cu}= 15000T/year Φ_{Na}= 194000T/year
Φ_{Zn}= 5000T/year Φ_{K}= 250000T/year

Our fluxes evaluations fall in the range of those of Nriagu(1979), obtained using a different approach, and agree, for Bi and Pb, with the values proposed by Patterson and Settle(1987).

This measurements correspond to metals emitted as vapours and condensed in the cold plume as aerosols; the high values found for very low volatile metals are due to their very high concentrations in basalts, the part of volcanic dusts in plume being negligible(Lambert et al,1987).

In spite of difficulties such as a precise estimation of 210-Pb/Pb ratios and, may be, of a global mean value of the ε coefficients- here determined in Mount Etna plume- it seems that the main feature of the method described here to estimate volcanic fluxes is the possibility to extend it to a large number of chemical species.

BASALTIC VOLCANISM OF THE SNAKE RIVER PLAIN, IDAHO: MAGMA SOURCES AND MANTLE-CRUST EVOLUTION

LEEMAN, W.P., Earth Sciences Division, National Science Foundation, Washington, DC 20550, and Rice University, Houston, TX 77251, U.S.A.

The Snake River Plain (SRP) bimodal basalt-rhyolite volcanic province of southern Idaho comprises two structurally distinct regions. The main NE-trending magmatic axis is defined by the locus of known and inferred silicic eruptive centers that decrease in age from SW Idaho (ca. 14 Ma) to Yellowstone Park (<2 Ma). As silicic activity at each of these centers waned, volcanism shifted to mainly basaltic activity. Because of the northeasterly age progression of the eruptive centers, the absence of crustal thinning, and the presence of $^3He/^4He$ and lithosphere-scale thermal anomalies at YP, it is widely believed that the province is related to passage of N. America over a hot spot presently located beneath Yellowstone. In contrast, the NW-trending western SRP is a graben structure related to NE-SW regional extension since late Miocene time; it is subsidiary to the main axis in terms of magma production, has intermittently produced basaltic magmas throughout much of its history, and does not conform to the age patterns for the main SRP axis.

Isotopically, SRP basalts are distinct from most ocean island basalts (OIB) associated with mantle plumes. Most SRP basaltic magmas are olivine tholeiites (SROT) characterized by relative contents of incompatible elements similar to those of E-MORB and some OIB, but they differ from OIB in having high $^{87}Sr/^{86}Sr$ (0.705-0.707), low ε_{Nd} (-2 to -4), and Pb isotopic compositions that define a steep $^{207}Pb/^{204}Pb$ - $^{206}Pb/^{204}Pb$ array which is interpreted as a 2.5 Ga secondary isochron for the basalt source. Oxygen isotope and trace element data provide strong arguments that isotopic compositions of Sr, Nd, and Pb in SROTs do not reflect contamination of OIB-like magmas by crustal material. Thus, a *lithospheric* vs. deeper mantle source is inferred for these magmas.

This raises the question of how lithospheric melting is triggered. Conductive heat transfer is too slow to induce large volume melting of a moving lithospheric plate, whereas the non-OIB geochemistry of SROT implies that there cannot be significant convective heat transfer via ascent of *magmas* from sub-lithospheric depths. Some process is seemingly required that either transfers heat into the lithosphere or lowers its solidus, neither of which result in significant mass transfer. It is proposed that lithospheric melting may be triggered by upward transfer of reduced volatiles (e.g., H_2, CH_4) in combination with a process such as redox-melting. Rather than requiring dramatic heating of the lithosphere over a relatively short time frame, its melting point may be reduced by oxidation of ascending volatiles to form H_2O, which in turn promotes H_2O-undersaturated melting. In the absence of significant mass transfer via silicate melts, chemical and isotopic budgets are buffered by the lithospheric mantle, which differs compositionally from the asthenosphere (i.e., OIB-source) because of its different history and long separation (at least since 2.8 Ga) from convecting sub-lithospheric mantle.

Once formed, SROT magmas play a significant role in modifying the deep crustal and possibly upper mantle composition. Based on phase equilibria studies and the plagioclase+olivine phyric nature of most SROT, it appears that they most commonly tap magma reservoirs at pressures less than 8-10 kbar (middle to lower crustal depths). Assuming hydrostatic equilibrium, normal continental crust is not sufficiently dense to sustain basaltic eruptions from such shallow depths. It is proposed that SROT parental magmas ascend to Moho or lower crustal depths where they attain neutral bouyancy, form sill-like intrusive bodies, and differentiate. Periodic intrusions gradually modify the lower crust by adding gabbroic-ultramafic cumulates, and provide heat to partially melt pre-existing crust to form rhyolitic magmas (which erupt first owing to their greater bouyancy). Only after low density silicic magmatism wanes (as the crust becomes more refractory) and average crustal density increases (due to solidification of mafic sills and extraction of silicic anatectic melts) can voluminous basaltic volcanism be sustained from crustal level reservoirs. These effects are time dependent and become more pronounced with distance from the Yellowstone hot spot. This scenario is consistent with observed eruptive history of the main SRP axis as well as the anomalous high density, normal thickness crustal structure of the province. Persistent basaltic volcanism in the western SRP apparently reflects continuing lithospheric extension that is unrelated to the hot spot.

VOLCANOES OF THE ANTARCTIC PLATE AND SOUTHERN OCEANS

W. E. LEMASURIER, University of Colorado at Denver, Denver, CO 80204 USA, and J.W. THOMSON, British Antarctic Survey, Cambridge CB3 0ET UK

The IAVCEI Working Group on Antarctic Volcanology has completed a volume entitled "Volcanoes of the Antarctic Plate and Southern Oceans," which describes the status of knowledge of all known Neogene volcanoes in the south polar and subpolar regions. It represents an update and expansion of the Catalogue of Active Volcanoes for Antarctica (Berninghausen & Neumann van Padang, 1960), and is being published by the American Geophysical Union as part of its Antarctic Research Series. The volume attempts to present both an overview of south polar volcanic provinces and summary data for each volcano or volcano group. Descriptions of over 100 volcanoes, contributed by 31 authors, are included. These are grouped into seven chapters, each introduced by a summary that describes major regional characteristics. The majority of volcanoes described are younger then 10 Ma, and 8 have been historically active. Holocene activity has been inferred for 30 others, based on ash layers on or within glacial ice, fumarolic activity, and other criteria.

Most south polar volcanoes are intraplate and alkaline. The dominant rock types nearly everywhere are basaltic, but alkaline and peralkaline felsic rocks are locally abundant in Marie Byrd Land (MBL) and the western Ross Embayment (WRE). The continental rocks do not seem to be very different from those found on intraplate oceanic islands, except perhaps in the complexity and abundance of felsic rocks found in some continental localities. Highly potassic rocks have been found only at Gaussberg and its environs. The most common pyroclastic rocks are hydroclastic, related to subglacial and periglacial environments of eruption. No large silicic ignimbrite fields have been found anywhere in Antarctica.

The distribution of most volcanoes on the continent and in the surrounding oceans seems closely related to rift features. The MBL and WRE volcanoes lie on opposite flanks of a major rift system, and the Antarctic Peninsula (AP) volcanoes are believed to be related to post-subduction extension along a relict convergent plate boundary. Oceanic volcanoes that occur on or near a mid-ocean ridge are composed of saturated or oversaturated rocks; undersaturated rocks are found well off the ridge crests. Subduction related volcanoes are found only in the South Sandwich arc and among the Miocene volcanoes of the AP. Linear volcanic features are found in both oceanic and continental environments, but none can be convincingly described as hot spot traces. This is consistent with evidence that the plate has not moved significantly during the past 30 m.y. or more. The dominant tectonic environment in Neogene time appears to have been one of broad extensional stress within a stationary plate, that led to local attenuation of the lithosphere, accompanied by alkaline volcanism.

LARGE LANDSLIDES ON THE SUBMARINE EAST FLANK OF PITON DE LA FOURNAISE VOLCANO : NEW RESULTS FROM HIGH-RESOLUTION SONAR IMAGING AND ROCK SAMPLING.

J.V. Lénat *, P. Cochonat**, P. Bachelery***, P. Boivin *, B. Cornaglia****, C. Deniel*, P. Labazuy*, E. Le Drezen**, P.W. Lipman*****, G. Ollier**, B. Savoye**, P. Vincent*, M. Voisset**

* OPGC (CRV-CNRS), UNIV. CLERMONT II, 5 rue kessler, 63038 CLERMONT-FERRAND, FRANCE. Tel : 73 34 67 00. ** IFREMER, CENTRE DE BREST, BREST, FRANCE. *** LAB. GEOL., UNIV. REUNION, FRANCE. **** LAB. GEOPHYS. MAR. IPG PARIS, PARIS, FRANCE ***** USGS, DENVER, USA.

Previous studies of the submarine parts of Piton de la Fournaise (Seabeam, magnetic and gravity surveys) have revealed the main features of this area (visible on the 3-D topographic diagram below) : (a) terminations of the two active volcanic rift zones near the coast, (b) evidence that the subaerial Grand-Brûlé slide has a large submarine continuation, and (c) presence of a large topographic bulge with a softly chaotic surface that suggested material from one or more landslide(s).

A new cruise, in August 1988, has provided additional data : 1500 km^2 of high-resolution side-scan sonar images, dredging at 13 sites, coring at 10 sites, and seafloor photography at 16 sites. The sonar was the SAR, from IFREMER, a deep-towed sonar which has the capability to scan over a 1500 m wide swath, with a resolution of 0.30m.

The acoustic profiles have been processed to build a mosaic, which along with the Seabeam map, provides a detailed picture of the surveyed zone. Most of the acoustic facies can be precisely identified using the rock samples and the seafloor photographs. The surface lithology exhibits various rock types. The young lava flows near the coast are apparently the only massive or non-disturbed formations. All the rest is composed of sediments derived from the erosion and fragmentation of the recent lava flows, and of material from major slides.

The slumped material of the Grand Brûlé slide (~25km^3) forms hummocky topography, typical of a debris avalanche. The model of formation of the large bulge (~600km^3) is not yet established. At the surface, it is almost entirely composed of material of subaerial origin, even in its most distal part, at least 40 km offshore and 2500m deep.

Detailed analysis of the various data now available will probably allow a precise reconstruction of the dramatic history of this area, and derived models should be useful for similar areas.

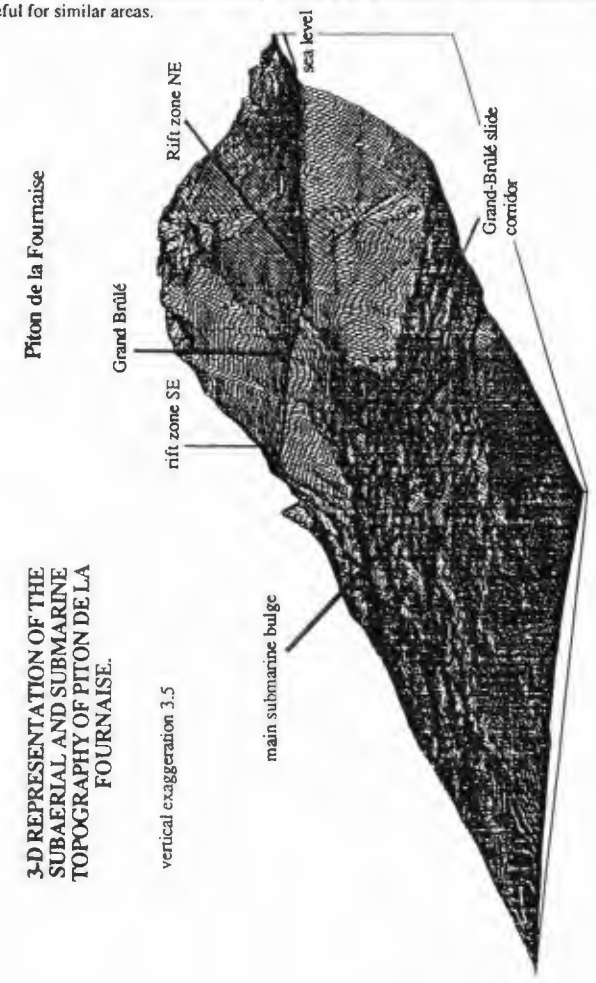

3-D REPRESENTATION OF THE SUBAERIAL AND SUBMARINE TOPOGRAPHY OF PITON DE LA FOURNAISE.

GEOLOGY AND DYNAMICS OF RECENT EPISODIC ERUPTIVE ACTIVITY AT CERRO BRAVO VOLCANO, COLOMBIA

LESCINSKY, David T. and WILLIAMS, Stanley N., Department of Geology and Geophysics, Louisiana State University, Baton Rouge, LA 70803 USA

The northernmost active Andean volcano, Cerro Bravo, is a small, two-pyroxene andesitic stratovolcano. It is located amongst Tertiary volcanics that locally compose the crest of the Central Cordillera. Sitting within an older caldera 3 km in diameter, Cerro Bravo reaches an elevation of 4000 m, covers 35 km^2 and has a volume of 11.5 km^3. Tephra deposits mantle the countryside more than 30 km away and grade into pumiceous pyroclastic flows and voluminous block and ash flows at the base of the volcano. The summit is a mosaic of high-aspect ratio lava flows, domes, and craters that have been intersected by faults and horseshoe-shaped craters. At present, Cerro Bravo is in a period of quiescence with no visible activity or thermal manifestations.

There have been six major eruptive episodes (CB6-CB1) during the past 6,000 years (Herd, 1974) with the most recent (CB1) 500 ybp (CHEC, 1983). These episodes are characterized in tephra deposits as multiple pulses of coarse and fine pumice with major separations of well-developed paleosols. Pulses within episodes are often separated by layers of clay that may represent a time hiatus and possibly distinguish distinct eruptions. However, the absence of organic matter, root casts, etc. that often identify paleosols suggest that these clays represent thick ash layers with local accumulations, that have been altered by the abundant precipitation. It is likely that the episodes of activity represent a period of days to a few years during which there were a number of distinct eruptions and numerous ash emissions.

Column heights and volumes were calculated using isopach and isopleth maps constructed from field data. The major pulses of CB1, CB2, CB3, and CB5 all had column heights of approximately 21 km. The wide variation in total volume for these episodes: CB1-0.18 km^3, CB2-0.30 km^3, CB3-0.56 km^3, and CB5-0.66 km^3, reflects the duration and/or the number of individual pulses during the episode. Much less intense, CB4 had three pulses of activity with column heights of 8 km or less but a total volume of 0.27 km^3. It should be noted that the estimates of volumes do not include the pyroclastic flows that accompanied all of the episodes except for CB1.

An interesting feature of Cerro Bravo is the block and ash flows which cover a large portion of the northern and eastern sides of the volcano. Although these flows have hummocky topography and large boulders present, they can be distinguished from avalanches by the presence of pumice, their monolithologic nature, and their hot emplacement. No blast deposits were identified. The paucity of outcrops makes it impossible to determine whether the flows are the result of gravitational instability, faulting, or eruption.

An examination of the stratigraphic relationships of the deposits suggests the following sequence of events has been repeated several times:

1. episode initiated by an explosive plinian eruption with accompanying or precursory pyroclastic flows,
2. waning of the eruption often followed by pulses of increased magnitude,
3. cessation of plinian style eruption and initiation of dome building,
4. a collapse of the dome creating block and ash flows, and
5. a period of quiescence and soil formation.

Examination of pumice clasts and geochemical analyses indicate that magma mixing takes place at the start of the eruptive sequence, probably acting as the trigger mechanism initiating an episode of activity.

The potential hazards of Cerro Bravo are large. Pyroclastic flows and avalanches would have significant impact by cutting the major land route from Bogotá west and destroying large coffee stockpiles, but would cause little loss of life. Ash-fall would likely be the greatest hazard. Two episodes, CB5 and CB6, each account for more than one meter of tephra underlying the city of Manizales, 20 km to the west.

RHEOLOGICAL AND KINEMATIC CHARACTERISTICS OF THE 1986 PYROCLASTIC FLOWS AT MT. ST. AUGUSTINE, ALASKA

LINKE, ANTHONY J., Dept. Geology/Geophysics, University of Alaska, Fairbanks, AK, 99775, and
BEGET, JAMES E., Dept. Geology/Geophysics, University of Alaska, Fairbanks, AK, 99775

Pyroclastic flows from the 1986 eruptions of Mt. St. Augustine are modeled as simple Bingham materials possessing both a yield strength and an apparent viscosity. Yield strength of the flows can be determined from the thickness and downhill slope of lateral levee deposits and from flow competence. Deposit density was estimated from a buoyancy analysis of an incidentally entrained "hydrometer" transported in the flow. Apparent Bingham viscosity is estimated from a relationship between yield strength, critical thickness (ie. levee thickness), total depth of flow, and mean flow velocity. Velocities are reconstructed from the superelevation of levee deposits formed as flows experienced centripetal acceleration.

Morphometric data were collected from pumiceous pyroclastic flow units and from block and ash flow units. Results for the data set at Mt. St. Augustine suggest that yield strength and apparent Bingham viscosity decrease as distance from the vent increases; yield strength decreased from 8 to 2-3 kPa and Bingham viscosity decreased from $6*10^3$ to $1.8*10^3$ P, (fig. 1) as flows travelled 5 km down the pyroclastic fan. Grain size analyses show that mean clast size decreased from 18 to 11 cm within 5 km of runout.

These data suggest a relationship between particle size and rheological parameters: bulk strength and flow resistance tend to decrease as large clasts are progressively removed from the flow through deposition and fragmentation. Therefore, rheological properties of pyroclastic flows can be quite variable and may change and evolve during flow and emplacement.

A two-dimensional kinematic model which includes changing viscous resistance has been developed for the Mt. St. Augustine flow units. Predicted velocities are consistent with observations and field-derived reconstructions of flow velocities. We use this model to evaluate the effects of variations in depositional rate, total flow depth, and flow viscosity on flow velocity.

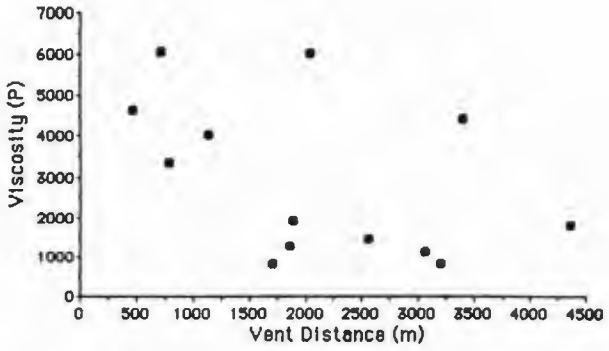

Figure 1. Relationship between Bingham viscosity and flow distance. Variation reflects differing initial masses of flow units.

INTRACONTINENTAL RIFT COMPARISONS: BAIKAL AND RIO GRANDE SYSTEMS

LIPMAN, P.W. (USGS, Denver, CO) for the USA-USSR Cooperative Study Group (US Nat. Acad. Sci., USSR Acad. Sci., US Geol. Survey)

The Rio Grande rift (RGR) in SW USA and the Baikal rift (BR) in Siberia are major intracontinental extensional structures of Cenozoic age that affect regions about 1500 km long and several hundred km wide. In 1988, these two systems were compared by study groups of 8 US and 8 Soviet geoscientists during cooperative field workshops in each rift. Despite contrasts in tectonic framework, both rift systems have generally similar timing, extensional styles, and geophysical signatures.

Both rifts have been active since late Oligocene time and have generally similar histories of initial extension and sedimentation in broad basins, followed by late Neogene uplift and block faulting, with deposition of sediments in axial basins. Axial parts of both rifts are multiple asymmetrical grabens, linked by structurally complex transverse accomodation zones. Both rifts are characterized by dominantly basaltic Neogene volcanism, especially along rift flanks; axial volcanism has been more voluminous in the RGR and includes some silicic magmas. The voluminous calc-alkaline mid-Tertiary volcanism that immediately preceded rifting in RGR has no counterpart in the Baikal region, which was magmatically and tectonically quiescent for 150 m.y. prior to inception of Tertiary rifting. Neither rift merges with an oceanic spreading center. Both rifts occupy the crests of broad topographic swells that developed during rifting. The average elevation for RGR is about 1.5 km higher than BR. Geophysical expression of both rifts includes (1) broad gravity lows related to regional thinning of the lithosphere, along which are centered axial highs related to crustal thinning along the rift crest and even narrower axial lows related to sedimentary fill; (2) high axial heat flow--higher in RGR than BR; (3) active seismicity and prominent seismotectonic structures--now especially active in BR; (4) only limited expression of rift features in aeromagnetic trends that mostly show older cratonic structures.

Both rifts are near boundaries of stable cratonic blocks with broad tectonically active regions characterized by complex Phanerozic orogenic histories. Both rifts follow older structural trends: BR along the boundary between Archean crust of the Siberian platform and mobile belts in Trans-Baikal and Mongolia, RGR along the crest of the Late Cretaceous-early Tertiary Laramide compressional belt of the eastern Cordillera but largely truncating the dominant grain of Precambrian structures. Many of the differences between the two rifts appear to reflect initial conditions of extension: within a hot recently active magmatotectonic belt for RGR, versus within relatively cold stabilized crust for BR. Gross structures of the two regions have become more similar as the rift systems matured. Controversy continues for both rifts, between advocates of active rifting driven by asthenospheric upwelling within continental areas, and proponents of broadly distributed deformation related to distant plate-boundary interactions--Indo-Asian collisional tectonics for BR and Pacific-American plate interactions for RGR.

IMPLICATIONS OF AN UNUSUAL INTRACALDERA CLASTIC DEPOSIT FOR CREATION OF FRACTURE PERMEABILITY IN THE VALLES HYDROTHERMAL SYSTEM, NEW MEXICO

LITTLE, T.M., Terra Tek Core Services, Salt Lake City, Utah 84108
HULEN, J.B., NIELSON, D.L., Univ. of Utah Research Institute, Salt Lake City, Utah 84108

The intracaldera Otowi (1.45 Ma) and Tshirege (1.12 Ma) Members of the Bandelier Tuff are commonly separated by clastic strata designated the S_3 by Nielson and Hulen (1984). Megascopically, these rocks appear typically to be fine-grained, epiclastic sandstones with little vertical or lateral variation. Detailed petrographic analysis, however, reveals that they are locally of pyroclastic origin. In Continental Scientific Drilling Program core hole VC-2A (Fig. 1), for example, the S_3 is massive to vaguely contorted, contains accretionary and armored lapilli as well as blocky shards, and invades the overlying Tshirege Member as thin clastic stringers; here, the S_3 may have been deposited en masse from a wet pyroclastic surge. The unit thickens toward the center of the Valles caldera (Fig. 1), where (1) Self et al. (1986) infer a Plinian vent for initial eruptions of the Tshirege Member, and (2) geothermal drilling has defined a major upflow zone in the Valles hydrothermal system. We suggest that in part the S_3 may represent early, phreatic and phreatomagmatic eruptions from this vent. Inevitably associated hydraulic fracturing may be a key control on thermal fluid upflow.

REFERENCES

Nielson, D.L., and Hulen, J.B., 1984, J. Geophys. Res., 89, 8695-8711.
Self, S., et al., 1986, J. Geophys. Res., 91, 1779-1799.

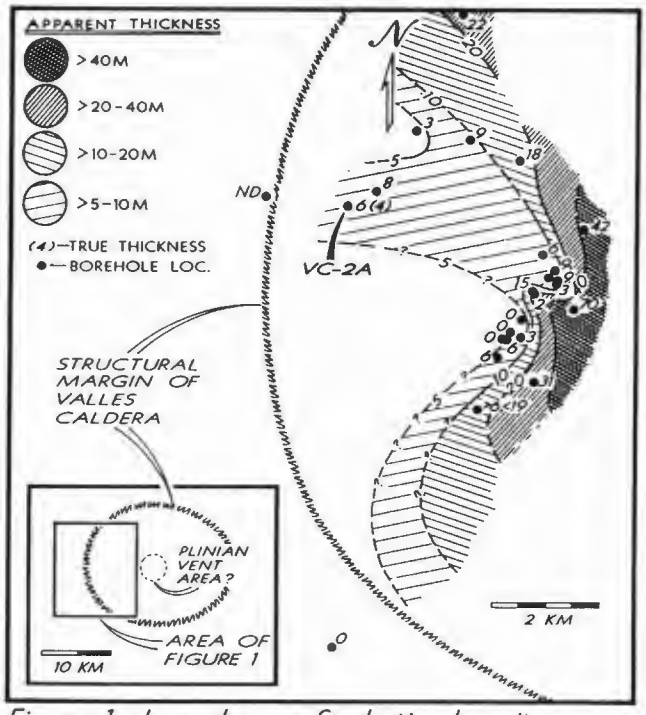

Figure 1. Isopach map, S_3 clastic deposits

GEOCHEMISTRY OF AMPHIBOLITES AND METADOLERITES FROM THE TUNGKILLO-PALMER-COOKE HILL AREA, MT LOFTY RANGES METAMORPHIC BELT, SOUTH AUSTRALIA

LIU, S. F. & FLEMING, P. D., Department of Geology, La Trobe University, Bundoora, Victoria, Australia 3083

Numerous small amphibolites and metadolerites intruded the Cambrian Kanmantoo Group metasandstones in the Tungkillo-Palmer-Cooke Hill area, which lies in the highest metamorphic grade region (sillimanite-K-feldspar-bearing grade) of the Mt Lofty Ranges metamorphic belt, South Australia. They intruded at various stages throughout the deformation history (Liu 1988); some of them intruded pre- to syn-D1, while others intruded post-D1 and pre-D2, and post-D2. However, these mafic rocks are all tholeiitic in composition and geochemically indistinguishable.

The analyzed 23 samples of amphibolites and metadolerites have an average SiO2 content of 49.77% and 49.59% respectively and show little variation in contents of major and trace elements, which is characteristic for ocean-floor basalts. The 'immobile' incompatible elements Zr, Y, Ti, P and Nb define a clear linear relationship between Zr and the other elements, indicating that these elements maintain their igneous relationships during metamorphism reaching grades up to those corresponding to upper amphibolite facies metamorphism for the studied rocks. The 'mobile' elements such as K, Rb have been slightly enriched during metamorphism. Such an enrichment will bring an increase in the variation in chemical compositions. However, the present major and trace element contents of the analysed amphibolites and metadolerites are still close to those for MORBs, esp. E-MORBs.

Average Zr/Nb ratios for the amphibolites and the metadolerites are 14.7 and 15.8 respectively. These ratios are within the range of those for MORBs. In spidergrams including elements of Sr, K, Rb, Ba, Nb, P, Zr, Ti and Y, the analyzed rocks define fairly flat patterns which are close to those for an average E-MORB (Sun et al 1988) and MORBs from the America-Antarctica Ridge (le Roex et al 1987).

The average $(La/Y)_{ch}$ ratios are 1.50 and 1.28 for amphibolites and metadolerites respectively. Analyzed samples of amphibolites and metadolerites give chondrite-normalized values of 20-40 for REE and define flat REE patterns which resemble that for E-MORBs (Sun et al 1988).

On Pearce's (1980) Zr-Ti tectonomagmatic discriminating diagram these data fall into the MORB field and define a typical MORB trend. On the Ti-K-P diagram of Pearce et al (1975), most of the data plot into the oceanic field even though metamorphism is most likely to bring the plots towards the non-oceanic field. On Pearce & Cann's (1973) Ti-Zr-Y and Ti-Zr-Sr diagrams the analyses fall into the field for ocean floor basalts. Finally, on a Nb-Zr-Y diagram of Mechede (1986) they mainly plot into a field for MORBs.

It is suggested that the amphibolites and metadolerites in the Tungkillo-Palmer-Cooke Hill area were derived from a similar mantle source to that for MORBs in a possible continent-ocean boundary/extensional tectonic environment.

PRIMARY AND SECONDARY CRYSTALLIZATION TEXTURES IN SILICIC VOLCANIC ROCKS

LOFGREN, G.E., SN-2 NASA Johnson Space Center, Houston, TX 77058

Textures are one of the primary tools for determining the cooling history of a rock. Certain textural features are more characteristic of crystallization from a melt and others are more characteristic of devitrification of glassy rocks. Many textures, however, are not unique to one environment. When a melt crystallizes at a given temperature, it may not matter how it arrived at that temperature, i.e. whether it was cooled directly from high temperature or was first quenched to a glass and then reheated. In general uniform textures crystallize directly from the melt while nonuniform textures such as those related to fracture surfaces crystallize during devitrification. Crystallization experiments and recent advances in the understanding of crystal growth can help to relate textural features to particular growth conditions.

Distinguishing primary from secondary crystallization textures in silicic volcanic rocks requires the evaluation of the microscopic textural elements, the macroscopic features, and the field setting. Certain petrographic elements such as dendrites and coarse, open spherulites, which necessarily crystallize from an amorphous medium, usually crystallize from a silicic melt upon the initial cooling. Such crystals could be the result of secondary devitrification of a quenched glass, but for the reheated glass to crystallize in such a manner, it would have to be reheated quickly to near the solidus temperature of the rock; mostly likely a rare event. Orb texture and hydration and crystal fronts are more characteristically devitrification phenomena. Micropoikilitic quartz or snowflake texture can occur as a result of either process.

Nucleation is an another important variable when attempting to distinguish primary from secondary textures. The more variable the spatial nucleation pattern, the more likely the process is to be secondary. Magmas that crystallize during their primary cooling tend to have more uniform nucleation patterns than magmas quenched to glass and subjected to secondary processes. But if two melts reach the same temperature uncrystallized and with the same propensity to nucleate (including number, kind, and spatial distribution of nuclei) one by primary cooling and one by reheating, the subsequent crystallization would be very similar and it is doubtful that the two could be distinguished without use of other factors.

Often the field setting and spatial crystallization pattern are more useful to uniquely determine the cooling history than the textural features alone. In the obvious case of a glass that is reheated slowly, crystallization would most likely occur from fracture surfaces or other imperfections inward. Crystallization would tend to be at lower temperatures (very high degrees of supercooling) and have appropriate crystal forms i.e. very-fine, closed, usually spherical, spherulites. Thus textures which appear to be related to fracture (or other secondary) surfaces most assuredly are devitrification.

A much more subtle case of secondary crystallization could be in a collapsed pumice fragment which has been reheated to form a glass blob or even a larger mass of glass. The distribution of heterogeneous nuclei which would most likely be related to previous surfaces, e.g. in the vesiculated pumice, should dominate the crystallization pattern. The difficulty would be to properly interpret the crystallization pattern, to identify previous surfaces and how they affect nucleation and subsequent crystallization.

Using textures to divine rock cooling histories has always been a highly interpretative science. And while the increased knowledge of crystal growth and the few experimental studies that have been completed have clarified how some textures form, set limits on others, and indicated new features to examine, their are still few if any unique sign posts.

LOCATION OF ETNEAN SEISMIC EVENTS AND RELATIVE PROBLEMS

LOMBARDO, G., Ist. Scienze della Terra, Università di Catania.
PRIVITERA, E., Ist. Internazionale di Vulcanologia - C.N.R. Catania.

Results concerning the study of problems related to the location of local earthquakes in the etnean area, are briefly reported.

A series of tests have been made using different seismic phases, as well as several location algorithms and crustal velocity models. Both the original Geiger algorithm and the one implemented on the Basic Hypo earthquake location program (Mendoza & Morgan, 1985), have been in particular tested, as well as the EVM algorithm (Caccamo & Neri, 1984).

Moreover, either single or multilayer crustal velocity models have been used.

The seismic events available were about 200, recorded in the time interval 1984-1986, by a total number of eleven vertical component stations and two three components ones. Nevertheless, it was possible to use only a number of stations ranging between 5 and 10 for the localization of each earthquake.

The hypocenter locations were obtained using alternatively either only the P phase onsets or several combinations of S phases readings detected either by vertical or horizontal seismometers.

The quality of locations has been tested through the analysis of residuals and by comparison with some macroseismic epicenters of etnean earthquakes, the location of which is particularly reliable as they are very shallow and have a mesoseismal area with an average radius of a couple of kilometers.

The results set into evidence that the location of the hypocenters is not significantly dependent on the algorithm used, even if the location through the program Basic Hypo is strongly affected by the choice of the starting hypocenter. Moreover, a strong influence is observed if the S phase arrivals are introduced or not in the calculation. In particular, the quality of the location improves significantly when S phase readings, obtained through the horizontal seismometers, are used. Reliable earthquake locations were also obtained using only P phase onsets but only when the number of recording stations is not less than six-eight.

The use of S phase onsets therefore appears to be of foundamental importance in the location of seismic events taking place in volcanic areas, as it showed to produce significant qualitative improvements in the accuracy. This study made also possible the evaluation of station residuals, in order to optimize the location procedure, allowing at the same time to express some interpretative hypothesis on the internal structure of Mt. Etna.

INTERACTION OF BASALT FLOWS WITH WATER DURING EMPLACEMENT AND SOLIDIFICATION

LONG, Philip E., Geophysics Section, K6-84, Pacific Northwest Laboratory, Richland, WA 99352

Subaerial continental flood basalt flows exhibit features associated with interaction with water during both emplacement and solidification. Features resulting from interaction between basalt magma and surface water are generally well known and include pillows, hyaloclastite, quench breccia, spiracles, explosion structures, and rootless cinder cones.

The result of interaction between basalt flows and surface water during solidification is the highly fractured central parts of basalt flows known as entablature. Samples of entablature show petrographic textures indicative of quenching; fracture propagation direction indicators on the surfaces of basalt columns of flows with well-developed entablatures demonstrate that typically 80% or more of the heat was lost from these flows through their upper surface. When coupled with thermal modelling, these observations imply that convective removal of heat occurred by circulation of large amounts of water from the surface of the flow down cooling joints to the 100° C isotherm. This conclusion has been controversial for Columbia River Basalt (CRB) flows in part because of the large amount of water required to produce the entablature in single flows as large as 2,000 km^3. Entablatures make up a wide range of proportions of individual flows, ranging from flows that lack entablatures entirely, to those in which the entablature follows a restricted meandering trend representing drainage blocked by the flow itself, to voluminous entablatures which may occupy as much as 80% of a flow and extend over 1/4 to 1/3 of the Columbia Plateau (total original areal extent = 164,000 km^2). The amount of water required to account for the extensive entablatures can be shown to be reasonable by estimating the amount of water required to quench a unit volume of basalt and by considering the rate of application of water used to quench the 1973 Heimaey flow, Iceland. A simple calculation suggests that the flood-stage flow rate of the present-day Columbia River could quench an appropriately large area of a CRB flow due to the extremely low relief maintained by the relatively high rate of eruption during Grande Ronde time. The greater rainfall and runoff associated with the subtropical climate of the mid-Miocene make it even more likely that sufficient water was available to produce the observed quenching.

A common objection to the quenching hypothesis is that cooling joints in entablature show no evidence of palagonitic alteration typically associated with pillow zones or hyaloclastite. The explanation for this is that water and steam are always separated from magma by a dry conduction zone ranging in thickness from a few centimeters to a few meters depending on quenching rate. Because of convective flow of water in cooling joints, solidified basalt that falls below the 100°C isotherm is rapidly cooled to ambient temperature. Consequently, the window of time for temperatures at which basalt can be rapidly altered is very narrow, and reaction kinetics prevent observable alteration from actually occurring. This interpretation is supported by examination of cores from areas of the 1973 Heimaey flow that were intentionally flooded with copious amounts of seawater. Cooling joints in these cores show no alteration rinds even under high magnification in spite of the known quenching history and the occurrence of quench textures similar to those observed in entablatures world-wide.

Supportive evidence for abundant water on the evolving Columbia Plateau is provided by common occurrence of features associated with interaction of water and magma during flow emplacement. Extensive pillow zones along the plateau margin are the most common, but interpretation of thick (>40 m) breccia zones in the upper half of the Umtanum flow provide a remarkable example of the result of hydromagmatic explosive activity. The basis for this interpretation is that the angular breccia clasts show glassy quench rinds that range in thickness from ~2 cm to 0 cm depending on the side of the clast observed. Apparently, the process of brecciation was occurring simultaneously with quenching, suggesting a situation analogous to the flow of tube-fed pahoehoe into the ocean along the south flank of Kilauea (e.g., the recent Puu O'o eruptions illustrated on the cover of the May 1988 issue of *Geology*). The essential requirement for creating such breccias is that magma at near-liquidus temperatures come in direct contact with sufficient quantities of water to sustain continuous quenching in which brecciation occurs by explosions which, in turn, exposes more magma which then brecciates and so on. In order for this process to create the thick breccia of the Umtanum, either the flow was emplaced in water deeper than the flow's ultimate thickness or large quantities of water would have to over top the flow prior to the formation of significant crust. This work was supported by the U. S. Department of Energy under Contract DE-ACO6-76RLO 1830.

GROWTH OF LAVA FLOW-FIELDS ON EARTH AND MARS

LOPES, R.M.C. and KILBURN, C.R.J., Osservatorio Vesuviano, Centro Sorveglianza, Via A. Manzoni 249, 80123 Naples, Italy. (Also at University of London Observatory, London NW7 2QS, U.K.).

Flow-field growth can be described in two stages, before and after cooling-controlled flow propagation becomes significant. These two stages are generally represented by distinct planimetric forms, which are best characterised by the ratio of their maximum width to length (Wm/Lm). Stage I is dominated by lengthening (Wm/Lm decreasing with time). Stage II begins when the flow reaches a critical cooling time (tc) and new flows are formed by breaching or overflow of the cooled margins. The flow-field enters a widening phase, where Wm/Lm increases with time. Although this growth pattern was determined for Etnean lavas (1), it should be applicable to all lavas because of its dependence on cooling. Local factors, however, will also affect Wm/Lm and tc, and so it is necessary to use normalised geometrical and time factors in order to determine a general growth pattern.

A measure of the thermal age of the flow-field (duration/tc) is used as the normalised duration. tc is related to the average thickness of the flow-field using a radiative cooling model. A measure of how crustal growth changes the initial (uncooled) w/l is used to normalise Wm/Lm, assuming a simple Bingham model. The scatter introduced by ignoring rheological terms is assessed.

Data for Etna, Pu'u O'o, Vesuvius and a range of more silicic lavas yield a plot in which Stage I and Stage II flow-fields show a significant positive trend between normalised Wm/Lm and duration, with both stages clearly defined. The scatter is acceptable in view of the possible variation in rheological terms. The trend is also followed by martian lavas from Alba Patera, for which durations have been calculated using a radiative cooling model (2) and measurements of flow thicknesses obtained directly from Viking images. These lavas are an order of magnitude larger than the terrestrial lavas analysed and were emplaced over shallower slopes than is typical for Earth and under a lower gravity. It is therefore suggested that:
(i) the approximate measures used in the normalisation of Wm/Lm and duration are acceptable and can be used to define a general flow-field growth trend;
(ii) Alba Patera lavas followed a similar planimetric growth pattern to lavas on Earth.

References:
(1) Kilburn, C.R.J. and Lopes, R.M.C., J. Geophys. Res., vol 93, no. B12, 1988.
(2) Pieri, D.C. and Baloga, S., J. Volcanol. Geotherm. Res., 30, 29-45, 1986.

THREE-DIMENSIONAL COLUMN MODEL FOR FISSURE ERUPTIONS

LOPEZ, Dina L. and WILLIAMS, Stanley N., Department of Geology and Geophysics, Louisiana State University, Baton Rouge, LA 70803, USA

A three-dimensional eruption column model has been derived for fissure eruptions produced by linear sources in a uniformly stratified atmosphere. The assumptions of Morton's (1956) model for turbulent gravitational convection from maintained sources are taken into consideration: uniform density gradient in the atmosphere, volume rate of entrained air at the sides of the plume proportional to the vertical velocity within the plume at each height, small density variations inside the plume in comparison with the density of the ambient fluid at the level of the source, and no change in the volume of the source fluid when it mixes with the ambient fluid. The governing equations are derived from the laws of conservation of mass, momentum and bouyancy rather than heat. The solution of that system of equations leads to the relationship $H = 5.2(Q/L)^{1/3}$, where H is the column height in meters, Q is the heat flow rate in Joules/sec, and L is the length of the fissure in meters. The heights predicted by the application of this equation are lower than those predicted by Stothers et al.'s (1986) two-dimensional model.

When our column height equation was applied to the 1783 Laki eruption and the Roza flow of the Columbia River Basalts, we found values of 2 and 8 km, respectively. The Laki value is too small in comparison with the 9-10 km maximum column height contemporary report for this eruption (Thorarinsson, 1970). This value was calculated with the average volumetric eruption rate which must be much smaller than the actual instantaneous eruption rate, especially because the entire 13 km-long fissure was not wholly or simultaneously active during the eruption. If the maximum eruption rate was at least an order of magnitude higher than the average eruption rate, then the calculated height of the column would be about 5 km. According to this result, the Laki eruption could only have injected aerosols into the troposphere and did not penetrate the stratosphere. However, the observed haze and atmospheric effects in Europe, as well as the Greenland ice record of sulfuric acid deposition during that year (Hammer et al, 1980) indicate a more pronounced effect in the atmosphere. A strong effect in the atmosphere and darkness for a time as long as one year have been already proposed (Stothers et al, 1986) for the Roza Flow.

The small values of H found with this model suggest that it can predict the correct order of magnitude of the column height but lacks accuracy because linear sources are not truly continuous but rather closely spaced point-sources with non-uniform rates of eruption, the uncertainties in heat flow rate calculations, and also because of the deviation of the real cases from the assumptions of the model. Although Sparks's (1986) thermodynamical model predicts that non-uniformity of the atmospheric density gradient and deviation from the other assumptions of the Morton's model do not affect significantly the predictions of column heights for point sources, this has not been proved yet for fissure eruptions.

GEOLOGIC AND CHEMICAL EVOLUTION OF QUATERNARY VOLCANISM: THE 37–42 S CHILEAN SECTOR OF THE SOUTHERN ANDES

LOPEZ-ESCOBAR, L. and MORENO, H.R., Department of Geology and Geophysics, University of Chile, Casilla 13518 Correo 21 Santiago, Chile

K-Ar age determinations (25 samples) from volcanoes along the 37-42 S segment of the southern volcanic zone of the Andes demonstrate volcanism throughout the Quaternary, but three main morphostratigraphic units have been recognized at most centers on the basis of relative erosion. The oldest consists of subhorizontal sequences of lavas, 1.5 to 0.4 Ma, which represent remnants of Pleistocene cones (previously mapped as Cola de Zorro Fm. between 37-38 S). The second (0.6-0.3 Ma) includes highly eroded edifices on top of, or interfingered with the upper parts of the earlier sequences. The youngest comprises well preserved composite stratocones, most of them active, whose ages are less than 0.25 Ma. The volcanic front is located west of the N10 E Liquine-Ofqui regional fault zone. Vent alignments are either parallel to it or strike along conjugate SW-NE or NW-SE trends. Historic eruptions have occurred along all three fracture patterns.

Basalt and basaltic andesite, with phenocrysts of plagioclase + clinopyroxene + Mg-olivine +/- orthopyroxene +/- opaques, are volumetrically dominant. Andesites, silicic andesites, dacites, and rhyolites are less abundant and have phenocrysts of plagioclase + clinopyroxene + orthopyroxene + Fe-olivine +/- quartz +/- opaques. Extensive ignimbrite sheets, varying in composition from basaltic andesite to rhyolite, fill the Central Depression. They are mainly related to volcanic sequences older than 0.9 Ma. Local ignimbrites, related to young composite stratovolcanoes have been recognized in Lliama, Villarica, and Puyehue volcanoes. Volcanic debris avalanches have been documented at Antuco (basalt to basaltic andesite in composition) and Calbuco (andesitic composition) volcanoes. Smaller peripheral cones on the flanks of large edifices vary in number from 0 to 40. They may be parasitic or independent. Minor centers are located mainly along the Liquine fault zone. Most of them are more primitive in composition than nearby stratovolcanoes. These volcanoes have grown rapidly (Antuco has grown 1000 m in 10000 a), but Quaternary glaciation has eroded them at high rates, which increase southward. Historic eruptions have been hawaiian, strombolian, vulcanian, phreatomagmatic, and sub-plinian: large plinian and peleean eruptions are suggested by prehistoric deposits.

Significant geochemical trends are observed in time and space. In some volcanic complexes, older units tend to be more silicic. There are also N-S and W-E variations in major and trace elements and isotopic compositions. In some aspects (K/Ba, $^{87}Sr/^{86}Sr$, and $^{143}Nd/^{144}Nd$) the 37-42 basalts are similar to OIB, but in others (K/La, Ba/La, Sr/Nb) they are more like IAB. Evaluation of these trends suggests that the mantle, contaminated with aqueous fluids from subducted oceanic crust, played an important role in establishing the geochemical characteristics of these rocks. Critical elemental ratios, more than Sr and Nd isotopic ratios, also suggest continental crustal contributions.

ON THE RELEVANCE OF SEDIMENTARY MAAS DEPOSITS IN MAAR-DIATREMES

LORENZ, V., Institut für Geologie, Universität Würzburg, Pleicherwall 1, 8700 Würzburg, FRG.

Maar volcanoes are the result of hundreds to thousands of explosive interactions of magma and groundwater. The tephra ejected by this explosive activity is predominantly deposited in thin-bedded base surge deposits in a tephra ring surrounding the maar crater. Because of large amounts of condensated steam these tephra beds are moist to wet and tend to form lahars in areas of high relief.

Maar-diatreme volcanoes are active only for days, weeks, months or up to a few years. The longer the explosive activity of a maar-diatreme volcano lasts the more the diatreme grows in diameter and depth and its rock content subsides. Growth of the diatreme leads to instability and failure of the country-rocks exposed in the oversteepened crater walls as well as to destabilization of the overlying wet tephra beds. Wallrocks and tephra ring slices collapse and slump, fall or flow onto the crater floor depending on slope angle, cohesiveness and water content of rocks and tephra beds. Thus, several different sediment types such as slope debris, rock falls, and many wet-tephra-derived lahars form.

Because of continued growth of the maar crater mass movements of crater wall rocks and overlying tephra lead to formation of many thick-bedded sediments which are interbedded with the primary pyroclastic base surge deposits on the crater floor.

Early in the evolution of a maar-diatreme volcano, when its diameter is still rather small, the diatreme will contain a very high proportion of such mass deposits. With continued explosive activity, however, the crater floor becomes larger in depositional area and, therefore, more and more base surge tephra beds get deposited on the floor. Consequently the ratio between thin-bedded base surge deposits and thick-bedded mass deposits increases from small to large diatremes as well as from the lower structural levels to higher structural levels within large diatremes. The more the crater enlarges the higher also the ratio of lahars derived from the growing tephra ring and reaching towards the centre of the crater floor in respect to the country-rock derived slope debris and rock-falls.

In most diatremes, especially in badly exposed diatremes, these subsided sediments of mass movement origin usually have been interpreted as being directly related to the explosive activity: diatreme breccias, deposits derived from fluidized (pyroclastic) systems, TKB (tuffisitic kimberlite breccia) etc.

Lorenz, V., 1986: Bull.volc., 48, 265-274.

THE WEST MAGEIK LAKES SILL: ANALOGUE FOR THE FEEDER OF THE 1912 ERUPTION AT THE VALLEY OF TEN THOUSAND SMOKES?

LOWENSTERN, Jacob B. and WALLMANN, Peter C., Dept. of Geology, Stanford University, Stanford, California, U.S.A. 94305

Within one hundred meters of the ignimbrite deposited by the 1912 eruption at the Valley of Ten Thousand Smokes (VTTS), a rhyolitic sill complex crops out in a glacially scoured valley on the slopes of Mt. Mageik, an active Aleutian stratocone. Because both the sill and VTTS suite intrude the Jurassic Naknek siltstone and comprise two of the few systems known to contain high-silica rhyolite on the Alaska Peninsula, this Tertiary(?) sill complex may provide an analogue for the feeder of the more recent eruption.

Emplacement of the sill complex is roughly perpendicular to the valley walls (which trend N35°E) and sub-parallel to the strike of the host siltstone (which strikes N75°W and dips 15°NE). The propagation direction is locally indicated by flow lineations and lobe cusps (Pollard et al., 1975). Three separate sills have been identified: two of them (Sills 1 and 2) may represent an en echelon front for the same intrusion. The other (Sill 3) may have emanated from a different part of the parent system, or could be an earlier pulse of less differentiated magma (see table). Sill 1 reaches a maximum thickness of 5 m before pinching out to the SW. The other two sills have thicknesses that increase from 1 to 10 m toward their SW end, where they are truncated by the vertical contact of an intrusive hornblende dacite porphyry. This stock has caused significant brecciation of the rhyolite and disseminated sulfide mineralization within the rhyolite and particularly within its own brecciated carapace. Because it cross-cuts the sill complex and has Sr concentrations lower than Sill 3 (see table), the dacite porphyry and rhyolite sill complex are not likely to be petrogenetically linked.

Sill/Naknek contacts are generally parallel to sedimentary bedding and can be either smooth and straight or highly jagged and irregular on the centimeter scale. Fractured areas at sill borders typically have small zones of autobreccia that include disrupted Naknek fragments. Stoped blocks are dislodged along prominent joint sets, resulting in sharp, locally discordant contacts. If the sills were to have erupted, they would probably have followed one of these joint sets. Hildreth (1987) and Wallmann and Pollard (1988) have suggested that the 1912 VTTS rhyolite propagated from Mt. Trident toward the Novarupta area along one of the major through-going fractures in the Naknek that trend N20°W, perpendicular to the Aleutian Trench. The West Mageik Lake sill complex shows that magmas can also move concordant to bedding in the Naknek, demonstrating the possibility that sill-like intrusion may have played a role in the transportation of magma in 1912.

Two of the sills (1 and 2) have similar high-silica rhyolite compositions and the other is a more plagioclase-rich rhyolite (Sill 3). Phenocrysts in the sill complex consist almost entirely of plagioclase (now partially sericitized) with a few small (<0.5 mm) grains of Fe-Ti oxides. This mineralogy contrasts with the VTTS rhyolite, which contains phenocrysts of quartz, plagioclase, orthopyroxene, and magnetite phenocrysts. Additionally, the two high-silica rhyolite lobes have lower Fe concentrations than VTTS rhyolite and contain 3% normative corundum. These characteristics, combined with abnormally high Sr values, point toward a significant crustal component in the sill magmas. Because the rhyolite of Sill 3 contains even higher Sr concentrations than the Naknek, the contaminant is probably not the siltstone, but some deeper horizon.

Numerical modeling shows that greater than 5% Naknek assimilation relative to crystal fractionation of the VTTS dacite would have resulted in concentrations of Sr that are higher and concentrations of Rb and Na that are lower than those observed for the VTTS high-silica rhyolite. This is consistent with the small ε_{Sr} shift reported by Hildreth (1987) from VTTS dacite to rhyolite. In this respect, the VTTS suite appears similar to the sill complex, as neither has assimilated appreciable amounts of shallow (<1.5 km) country rock.

Hildreth W (1983) J Volcanol Geotherm Res 18:1-56

Hildreth W (1987) Bull Volcanol 49:680-693

Pollard DD, Muller OH, Dockstader DR (1975) Geol Soc Am Bull 86:351-363

Wallmann PC and Pollard DD (1988) Eos, Transactions AGU 69:1472

	Sill 1	Sill 2	Sill 3	VTTS Rhyo.	Naknek Siltst.	Dacite Porph.	VTTS Dacite
SiO_2	77.2	77.2	72.2	76.9	64.9	64.5	64.6
TiO_2	0.15	0.15	0.29	0.17	0.51	0.54	0.71
Al_2O_3	14.1	14.3	15.2	12.5	15.5	16.0	15.7
Fe_2O_3	0.73	0.89	2.50	1.39	6.07	5.57	5.21
MgO	0.00	0.44	0.61	0.02	2.56	1.93	2.14
CaO	0.70	1.28	2.56	0.95	4.39	4.53	4.97
Na_2O	4.63	4.68	4.35	4.36	2.36	3.98	4.20
K_2O	2.12	2.01	1.72	3.22	1.59	1.58	1.74
Zr	116	126	114	157	96	131	151
Sr	238	332	502	52	387	417	237
Rb	51	46	41	~70	45	34	38
Ba	918	--	--	960	778	722	600

VTTS analyses from Hildreth (1983).

GEOCHEMICAL EVIDENCE FOR ASTHENOSPHERE-LITHOSPHERE INTERACTION IN THE GENESIS OF QUATERNARY ALKALINE MAGMAS IN THE NORTHERN CANADIAN CORDILLLERA

LUDDEN, J.N. Département de Géologie, Université de Montréal, Montréal, Quebec, Canada H3C 3J7,
FRANCIS, D., Department of Geological Sciences,McGill University, Montréal, Quebec, Canada H3A 2A7, and
ZINDLER, A., Lamont Doherty Geological Observatory, Palisades, NY, 10964, USA.

The Quaternary alkaline volcanic centres, of the Stikine volcanic belt of the northern Canadian cordillera, extends from north-central British Columbia to central Yukon. Mt Edziza, the southernmost and the largest of these centres, comprises four volcanic formations of Miocene to Recent age, ranging in composition from transitional alkaline basalt to hawaiite and pantellerite. Sr- and Nd-isotope compositions of the most primitive lavas in this centre are comparable to those of MORB (Figure 1). The Mt Edziza lavas are considered to be related to upwelling of asthenosphere in central BC as a result of overriding of the Kula rise by the North American plate in the Miocene.

The more northerly centres of the Stikine belt display a range in composition from olivine nephelinite to transitional alkaline basalt. Both field and petrographic evidence indicate an intimate spatial and temporal relationship between these two magma types. In the Fort Selkirk centre the olivine nephelinite magmas display isotope characteristics comparable to MORB, whilst the alkaline basalts of this centre and the Alligator Lake centre define more radiogenic isotope compositions (Figure 1).

The olivine nephelinite end-member of the magma spectrum represents small volumes of non-radiogenic, strongly Si-undersaturated melts, which have infiltrated the more radiogenic sub-Cordilleran lithosphere. Francis and Ludden (this vol.) suggest that these melts are represented by amphibole-pyroxenite veins in an anhydrous lherzolite lithosphere.

This model differs from other models of nephelinite genesis in that the nephelinitic melts are the precursor to more extensive melting of the lithosphere to produce more Si-saturated mafic lavas.

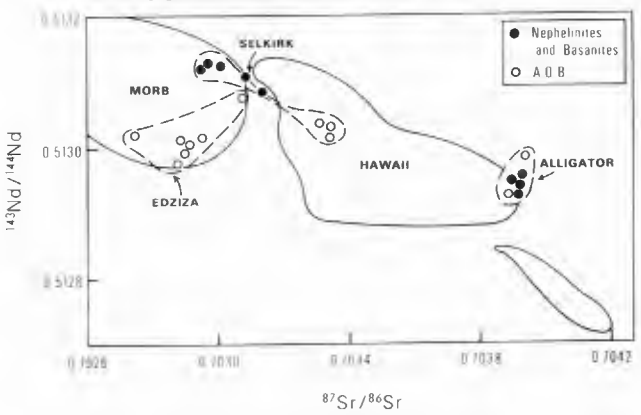

PRIMARY VOLCANIC FEATURES IN THE PROTEROZOIC "LEPTITE FORMATION" - A METAMORPHIC CASE STUDY.

LUNDSTRÖM, I., Geological Survey of Sweden, Box 670, S-751 28 Uppsala, Sweden.

The Southern Svecokarelian Volcanic Belt consists of ca 1.9 Ga old metavolcanites and metasediments, which were intruded by different granitoids at about 1.9 and 1.8 Ga. The volcanites were erupted in some kind of a continental margin situation. The belt was regionally deformed and metamorphosed up to high amphibolite facies of low-P type after ca 1845 Ma.

Within the Swedish part of the belt, it is possible to discern two fundamentally different settings or facies types for the volcanites. These are here called the SE:ern and NW:ern facies types,respectively.

The SE:ern facies type.

Stratigraphy The SE facies type is characterized by a ca 1 km thick interval of mostly limestone-interbedded tuffites, within a thick sequence of frequently turbidite-like metasediments.

Volcanic facies, modes of eruption and deposition No features indicating proximal volcanic facies such as possible lavas, volcanic breccias, subvolcanic intrusions or synvolcanic alterations have been identified so far. However, the scarcity of volcanites, their calm depositional environments (limestone interbeds), and the dominance of metasediments seem to indicate a more distal and subaqeous depositional situation.

The NW:ern facies type

Stratigraphy Here volcanites instead predominate the stratigraphic column, while sediments are rare. The sediments are mostly coeval or younger than the volcanites. The volcanic part of the succesision is probably 5-10 km thick

In the lower part of the stratigraphy, voluminous, massive, homogeneous, finegrained quartz-keratophyric rocks with very little bedding predominate. They contain 10-30 vol.-% quartz and albite phenocrysts in an quartz-albite matrix. The phenocrysts are frequently subhedral, but fragmented forms are also common, indicating explosive eruption. Occasional welding- or compaction-like structures as well as corroded phenocrysts and structures resembling gas segregation pipes indicate a hot state of deposition. Therefore, this pyroclastic association (sense of Schmid 1981) certainly contains ash flow tuffs, although clear eutaxitic textures and shards are rare. Possible and sparse accretionary lapilli and the homogeneity of the association seem most compatible with subaereal eruption and deposition, although deposition may locally have been shallowly subaqeous as shown by occasional limestone and siltstone interbeds.

Upwards these sedimentary layers increase and the phenocryst frequency decreases. Therefore the pyroclastic association grades into a more tuffitic (sense of Schmid 1981) one, where the discrimination of tuffaceous silt- and mudstones from fine ash-tuffs becomes almost impossible.

In several areas then follows a volcanic greywacke formation, which in turn is superposed by a siltstone formation.

Volcanic facies, modes of eruption and deposition The stratigraphic sequence thus records a transition from explosive subaereal volcanism to subaqeous reworking of the volcanites. Thus a regional transgression is implied. Naturally, a good appreciation of the amount of reworking throughout the stratigraphic column would be very worthwhile, although it seems very difficult to carry out.

Within the more or less reworked pyroclastic formations, several indications of a rather proximal volcanic facies can be found. Within the generalized stratigraphy, described above, quick changes in depositional environments implying rough topography are not uncommon. Shallow intrusive plugs, dykes and possible lavas all indicate that a volcanic centre was nearby. Likewise sub-seafloor hydrothermal alterations demand good access to volcanic heat.

Correlations

Although the structural relations are not fully clear, radiometric ages indicate that the volcanites of the two areas are of the same general age. Furthermore, transitional relations between the two types of stratigraphies can be found in intervening areas. It is therefore possible that the volcanites of the SE:ern facies type are the distal equivalents of the NW:ern volcanites.

SEISMIC EVIDENCE OF A CLOSE RELATIONSHIP BETWEEN LOCAL TECTONICS AND VOLCANISM IN THE CAMPANIA REGION (NAPLES, SOUTHERN ITALY).

LUONGO G. and F. FERRUCCI, Osservatorio Vesuviano; 249, Via Manzoni, 80123 Naples (Italy).

HIRN, A., Institut de Physique du Globe; 4, Place Jussieu, 75252 Paris Cedex05 (France).

A multi-method seismic experiment,carried out in the neapolitan area of quaternary volcanism in the years 1985-1987, allows to detect some major structural features of the crust and to interpret them in terms of local tectonics and related volcanic behaviour.

i) the seismic signature of the top of a very-low rigidity body, interpreted as the shallow magma chamber of Campi Flegrei Caldera, is obtained at the center of the volcanic area by P-SV converted waves from distant shots, recorded at a very dense local array.

The boundary is slightly deeper than the bulk of the seismicity of the 1982-1984 seismo-volcanic crisis.

On the contray, no geophysical evidence of magma chamber has been obtained at Mt. Vesuvius, the other main active volcanic center of the area

ii) a strong upheaval of the Moho (z = 20 km) is detected in correspondence of Campi Flegrei, where the PmP reflection ranges of four linear and two constant-offset DSS profiles intersect at depth.

Mt. Vesuvius, although distant less than 30 km from Campi Flegrei, is emplaced in a very different crustal environment.

In fact the crustal thicknesses abruptly increase (by as much as 6-10 km) from Campi Flegrei towards the outer limits of the volcanic area, accompanied by thickening of a high-velocity (7.0 - 7.2 km/s) lower-crust layer and by strong increase of the shallow layers velocities .

The very different structural context in which the two volcanoes are found to be emplaced and to have developed, supplies a possible first explaination of the substantial difference of their erupted products, volcanic behaviours and histories.

THE GEOCHEMISTRY AND VOLCANOLOGY OF THE TERTIARY BASALTS OF THE GIANT'S CAUSEWAY AREA, COUNTY ANTRIM, NORTHERN IRELAND.

LYLE, P., Environmental Studies Department, University of Ulster, Jordanstown, Northern Ireland, BT37 OQB.
PRESTON, J., Department of Geology, Queen's University, Belfast, Northern Ireland.

The spectacular columnar-jointed Tertiary tholeiitic basalts of the Giant's Causeway district are a localized sequence of flows, the Causeway Tholeiite Member (CTM), within the Antrim Lava Group of northeast Ireland. Tertiary volcanism in Ireland occurred in two cycles, producing the mostly hy-normative olivine tholeiites of the Lower (LBF) and Upper (UBF) Basalt Formations, separated by a thick laterite horizon, the Inter-basaltic Formation. The Causeway lavas erupted on to this Interbasaltic lateritic surface and are olivine-poor, quartz-normative tholeiites.

Apparent differences in fractionation trends between the LBF and the CTM argue against the CTM being the fractionation products of Lower Basalt magma. Geochemical evidence, including REE data, is presented to show that they are part of the second cycle of eruption, which produced the Upper Basalts, and are derived principally by high-level fractional crystallization of a low alkali tholeiite magma with MORB characteristics. Similar compositions are common in the overlying Upper Basalts.

Enrichment of some CTM flows in elements such as K,Rb,Ba,P and Si is attributed to selective crustal assimilation in a frequently replenished magma chamber. Microprobe analysis of mesostatial glasses in the CTM suggests that residual liquids may also have played a role in Si,K and P enrichment.

Major areas of lavas in the British and Irish Tertiary Volcanic Province appear to be closely coincident with Mesozoic sedimentary basins. The structural pattern of the north Antrim area is one of ridges and basins controlled by fault systems on a Caledonoid trend, all of which have undergone Mesozoic and Tertiary reactivation. The CTM comprises thick ponded flows erupted into such a basin, possibly a half-graben in form, with maximum sediment and lava thickness near the fault. It is proposed that the Causeway flows resulted from tectonically controlled decompression melting of previously depleted mantle, with the magma equilibrating in the crust before erupting as sheet floods contained within the margins of the basin.

The Causeway basalts characteristically show well developed colonnade and entablature structures. Pillow lavas and hyaloclastite breccia horizons occur frequently at the base of flows, along with interbasaltic horizons of fluvial or lacustrine sediments. Eruption of the basalts resulted in disruption of the contemporaneous drainage pattern leading to the formation of shallow lakes and the probable inundation of flow surfaces. This flooding must have modified the cooling regime of flows, initially by the entry of water along major joint planes that are seen in the upper parts of the lava, and led to the formation of two-tiered columnar flows.

VOLCANIC FLOW: AXES AND SOURCES INFERRED FROM MAGNETIC DATA

MACDONALD, W.D., Department of Geological Sciences, State University of New York, Binghamton, N.Y. 13901, and
PALMER, H.C., Department of Geophysics, University of Western Ontario, London, Ontario, Canada, N6A 5B7

The precise measurement of volcanic flow lines from clasts or phenocrysts is time-consuming because of the need to measure the orientations of many grains individually. By determining the ellipsoid of anisotropy of magnetic susceptibility (AMS) the contributions of all Fe-bearing minerals of a sample are integrated quickly and simultaneously. Typically the axis of elongation of the AMS ellipsoid is aligned with the axis of flow determined by other means. Also, for distal areas of ash-flow sheets, the plane of flattening of the AMS ellipsoid is tilted consistently towards the source (imbrication effect). Thus in optimal circumstances the AMS technique can be used to decipher efficiently the source region of pyroclastic rocks. The method promises to be particularly useful in old and dissected volcanic fields. Complications can arise owing to contributions to the AMS signature from fabric components such as vesicles, extension cracks, intersecting fabric surfaces, and related phenomena. We describe AMS results from the Bandelier tuff of the Valles caldera and our attempts to decipher source areas for several regions of dissected mid-Tertiary pyroclastic rocks of NE Nevada.

TEPHRA FALLOUT HAZARD MAP OF VESUVIUS

MACEDONIO, G., CNR - Centro Studi Geologia Strutturale e Dinamica dell'Appennino, 56100 Pisa, Italy; PARESCHI, M.T., Centro di Ricerca IBM, 56100, Pisa and SANTACROCE, R., Dip.to di Scienze della Terra, University of Pisa and Istituto Internazionale di Vulcanologia, CNR, Catania, Italy.

Recent papers allowed the preliminary assessment of the volcanic hazard related to the future explosive renewal of Vesuvius activity by numerically simulating the tephra fallout of a "maximum expected event" whose features (mass, settling velocity distribution of particles, column height, particles diffusion coefficient, etc.) were fixed on the base of historical and geological data as well as of empirical and theoretical considerations. This paper provides a hazard map for tephra fallout of such a maximum expected event based upon a statistical study of the wind regime in South Italy during a 15 years period (1962-1976). By assuming discrete values of the horizontal wind components along a vertical grid and a negligible vertical component, $n_z \cdot m_x \cdot m_y$ wind profiles are possible, where n_z is the number of step intervals in the z direction, and m_x and m_y are the number of wind intensity values in the x and y directions. The analysis of wind regime during the considered period reveals that only a subset N of the possible profiles actually occurred ($N \ll n_z \cdot m_x \cdot m_y$), allowing the computation of the corresponding frequence of occurrence. For each of these wind profiles, isomass lines on ground are computed (50, 100 and 200 Kg/m2, involving serious expected damages) and, for each point enclosed in areas defined by these curves, a probability of occurrence equal to that of the corresponding wind profile is assigned. The hazard map, for each fixed mass concentration on ground, is obtained by summing in each point the probability of occurrence calculated for all the different wind profiles. These data combined with remote sensing information (Landsat TM bands with pixel resolution of 30 m) inherent to urban and agricultural areas allow the first establishment of actual volcanic risk maps of the Vesuvian area.

THE FEATHERBED VOLCANICS, QUEENSLAND, AUSTRALIA: ORIGIN AND EVOLUTION OF A COMPOSITE CAULDRON

MACKENZIE, D.E., Bureau of Mineral Resources, GPO Box 378, Canberra A.C.T., 2601, Australia.

The Featherbed Volcanics constitute the largest caldera-related volcanic field in the 1100 x 300 km Permo-Carboniferous NE Queensland felsic igneous province. They are mostly confined to a 3000 km^2 volcano-tectonic depression made up of eight subsidence structures. The volcanics and related granitoids form two distinct groups: I-types (315-300Ma) and A-types (290-280 Ma).

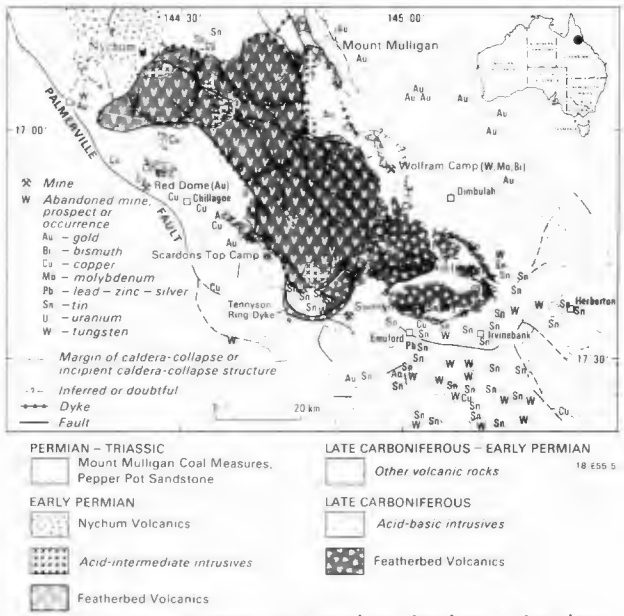

Most of the I-type volcanics define a basin-like sag structure intruded by granite porphyries, but lacking other features of a cauldron. Other I-type volcanic sequences occur in caldera and outflow sheet remnants around the younger cauldron. Each succession ranges from rhyolitic to less abundant, generally younger, dacitic or andesitic ignimbrite; lava is rare.

The A-type volcanics, predominantly rhyolitic ignimbrite with rare andesite and dacite, are preserved in four nested calderas and intruded by resurgent granitoids and microgranite ring dikes. Domes, flows, and plugs of rhyolite crop out around the cauldron margin. Caldera-wall collapse breccias and moat sediments are absent, and resurgent structures are poorly developed.

These observations, along with geochemical and isotopic data indicate that: (1) intermediate I-type magma was derived from a hydrous igneous source and felsic, A-type magma from a relatively dry, F-rich (high-grade metamorphic?) source; (2) I-type magma was too small in volume, and/or was emplaced too deep (due to its composition), to generate cauldron collapse in the SE sag; (3) A-type magma, due to its composition and large volume(s), was emplaced at very shallow levels, resulting in large-volume ignimbrite eruptions and caldera collapse; (4) infilling kept pace with subsidence, impeding caldera-wall collapse.

Abundant W-Sn, W-Mo-Bi, base-metal, and Au mineralisation related to the I-types reflects extended fractionation of hydrous compositions. Sparse base-metal, Sn, Au, U, Sb, and W mineralisation related to the A-types reflects limited fractionation, shallow emplacement, and substantial fluid loss of dry, F- and metal-rich magma.

A COMPARATIVE STUDY OF THE 1984 MAYON ERUPTIVE PRODUCTS

MAGALIT, C. T., Philippine Institute of Volcanology and Seismology, 5th Flr., Hizon Bldg., Quezon Blvd., Quezon City, Philippines 3008, MELSON, W., Smithsonian Institution, Washington, D.C., U.S.A., and DEL MUNDO, E. T., Philippine Institute of Volcanology and Seismology, 5th Flr., Hizon Bldg., Quezon Blvd., Quezon City, Philippines 3008

The two-phase eruptive activity of Mayon Volcano which started on September 9 and ended on October 6, 1984, was characterized by different eruptive styles and varying explosivities. The activity was initiated by short lava effusion on the night of September 10 which was subsequently followed by pyroclastic ejection depositing lithic-rich pyroclastic flow deposits along Buang gulley on the NW-side of the volcano. A quiet effusion of lava flow on the western side of the volcano occurred on September 14-18 after which a five-day lull ensued. The second phase of the eruption which started on September 23 was characterized by violent ejection of pyroclastic flows on the south, southeast and eastern sector of the volcano, and strong strombolian activity decreasing in intensity as the eruption progressed, culminating in a weak ejection of pyroclastic flow on October 6 along the western flank of the volcano.

This paper attempts to offer possible petrologic explanations for the different eruptive styles thru time of the volcano. Bulk chemical and petrographic analyses, mineralogical, bulk, matrix scan and glass analyses by microprobe were done on the juvenile pyroclastic flow bombs from Buang gulley and the Camalig lava flow representing the explosive and quiet eruptive styles, respectively, from the first phase of the eruption, and juvenile bombs from the Bonga pyroclastic flow representing the second phase. Bulk chemical analysis showed that there was not much inhomogeneity in the magma. Bulk SiO_2 content ranged from 52-54%. The volatile content of the magma could not have played a significant role either, since estimates of the volatile content ranged from 2-4% among the deposits. Petrographic analysis, however, showed that different viscosities due to different crystal content must have been the single most important determining factor in the explosivity of the eruption. Average percent phenocryst was highest in the Buang pyroclastic flow with 55.2%, followed by Bonga pyroclastic flow with 54.4% and lowest in the Camalig lava flow with 51.5%. Analysis of the matrix glass representing the pre-eruption composition of the residual melt yielded SiO_2 of about 60% among the deposits, higher than the bulk silica content by about 6 to 8%. The relatively evolved residual melt could have increased the viscosity of the magma thereby increasing its explosive potential to produce pyroclastic flows.

NOBLE GAS EVOLUTION IN MEDIUM-TEMPERATURE FUMAROLES (VULCANO, ITALY)

MAGRO G. and PENNISI M., Istituto di Geocronologia e Geochimica Isotopica, Via Maffi, 36, Pisa, Italy

The evolution of noble gases (He, Ne, Ar), some of their isotopes (^4He, ^{36}Ar, ^{38}Ar, ^{40}Ar), and N_2, measured in medium - temperature fumaroles from the crater of Vulcano (Aeolian islands, Italy), has been followed since 1979.

Until 1986 the He, Ar and N_2 excesses pinpoint the presence of a deep component in the fluids (He / Ne = 300, $^{40}Ar/^{36}Ar$ = 3000, N_2 / Ar = 1500, max. values). Some important changes were evident in 1987-1988: the He / Ne, $^{40}Ar/^{36}Ar$ and N_2 / Ar ratios began to decrease in 1987 and they fell towards atmospheric values in 1988. Such a trend can be explained by a change in the mixing ratio between a deep component and a shallow "atmospheric" component.

An input of non-degassed and air-satured groundwater is the likely reason for the increase of the shallow component, as pointed out by the Ne / Ar ratio close to the value typical of air-satured water. This is confirmed by the negative correlation between the $^{40}Ar/^{36}Ar$ and N_2 / Ar ratios and the water concentration in fumarolic fluids: a sharp decrease of these ratios corresponds to a vapour increase.

SNOW AND ICE PERTURBATION DURING ERUPTIONS -- HISTORICAL PERSPECTIVE ON A SIGNIFICANT VOLCANIC-HYDROLOGIC HAZARD

MAJOR, Jon J., U.S. Geological Survey, Cascades Volcano Observatory, Vancouver, Washington, 98661, and **NEWHALL**, Christopher G., U.S. Geological Survey, National Center, Reston, Virginia, 22092

Some of the most voluminous and catastrophic lahars and floods result from eruptions of volcanoes mantled by a substantial cover of snow and ice. The 1985 eruption of Nevado del Ruiz, which generated lahars that claimed thousands of lives and damaged property valued at millions of dollars (US), underscores the observation that the effects of eruptions, even those considered relatively minor, can be exacerbated when volcanic products interact with snow and ice. Fundamental questions regarding the processes that perturb snow and ice during eruptions and the relative importance of each process can be addressed in part by a comprehensive review of the historical record. In this analysis, we have reviewed more than 100 volcanic events on snow-and-ice covered volcanoes.

The literature provides examples of more than 40 snow-clad volcanoes worldwide that have erupted in historical time and produced lahars or floods. Most of these volcanoes are located at latitudes higher than 35°; those at lower latitudes reach altitudes generally above 4,000 meters.

At least five types of volcanic events can perturb mantles of snow and ice and result in the formation of lahars and floods: (1) Pyroclastic flows, pyroclastic surges, blasts of hot gases and pyroclastic debris, and hot-rock avalanches interact with snow and ice through erosion, mixing, and melting; (2) Surficial lava flows may override or burrow into snow and ice; (3) Melting at the base of a glacier or snowpack may occur during subglacial pyroclastic eruption, lava extrusion, or by fumarolic activity from a geothermal field; (4) Ejection of (hot) water from a crater lake onto the flanks of a snow-clad volcano may melt snow and add water to that from the ejected lake; (5) Tephra falls may blanket large areas mantled by snow and ice.

Historical records of volcanic eruptions at snow-clad volcanoes show: (1) Flowing pyroclastic debris and blasts of hot gases and rock debris appear to be the most common volcanic events that generate lahars and floods. These processes account for about 40 percent of the reported lahars or floods caused by melting of snow and ice. (2) Heating the base of a glacier or snowpack by subglacial eruptions or by geothermal activity may induce basal melting and ponding of water that can lead to sudden outpourings of water or sediment-rich debris flows. (3) Flowing pyroclastic debris, blasts of hot gases and rock debris, and subglacial melting commonly generate lahars and floods having volumes that exceed 10^5 m^3. (4) Surficial lava flows generally cannot melt snow and ice rapidly enough to form large lahars or floods owing to the sluggishness of heat transfer by conduction. Meltwater produced by surficial lava flows commonly is converted into steam. (5) Tephra falls usually alter ablation rates of snow and ice but generally do not produce sufficient meltwater to form lahars and floods.

COOLING, DEVITRIFICATION, AND FLOW OF LARGE HOT RHYOLITE LAVA FLOWS: NUMERICAL MODELING RESULTS

MANLEY, Curtis R., Dept. of Geology, Stanford University, Stanford, CA, 94305. [bitnet: manley@denali.stanford.edu].

A finite-difference method was used to model the cooling and crystallization of large-volume high-temperature rhyolite lava flows. Such flows are known or suspected in the Snake River Plain - Yellowstone Park region, Trans-Pecos Texas, and the Bushveld. The present model is most applicable to rhyolite lavas of calcalkaline affinity such as those of the Bruneau-Jarbidge eruptive center [BJEC] (Bonnichsen,Idaho BMG Bull 26,1982), SW Idaho. These flows have individual minimum volumes from 10 to 200 km^3 and can be followed from 8 to 42 km along drainage canyons.

The thermal model (see Long & Wood,GSA Bull,1986) was developed and calibrated using drill core data from the Inyo Obsidian Dome (~73% SiO_2; 55 m thick) near Long Valley Caldera, E CA, and is able to match that flow's crystallization zoning. The model accounts for the temperature and composition dependence of both thermal conductivity and heat capacity, and uses a realistic density zonation in the flow (Manley & Fink,Geology,1987). Cooling is by conduction. Latent heat generated by crystal growth is added; rain/snowfall is modeled by subtracting average annual heat used to transform snow at 0°C to steam at 300°C below the flow surface.

Using an eruption temperature of 850°C, solidification of Obsidian Dome was found to occur in ~7.5 years. Although erupted undercooled by 100-200°C, crystallization (growth of spherulitic devitrification material) lagged extrusion by 4-5 years. During this period, cooling at the upper and lower margins of the flow produced quenched obsidian largely free of spherulites. This effective 'delay' in crystallization results from the very low diffusion rates in these high viscosity rhyolitic melts.

The cooling model was then applied to one of the BJEC lava flows (~74% SiO_2; 150 m thick). Pyroxene geothermometry indicates equilibration temperatures between 900 and 1020°C for BJEC lavas (Honjo *et al.*,GSA Abs,1987). For modeling, eruption temperature was taken as 930°C and solidus as 700°C. Results imply that formation of vitrophyre lasted up to 4 to 6 years after extrusion, at which time spherulite growth became dominant in the interior. Cooling of the flow center to the solidus took ~60 years.

In these lavas, devitrified blocks commonly found in basal crumble breccias (Bonnichsen and Kauffman,GSA SP 212,1987) imply that flow advance continued into the early stages of crystallization. This brackets movement of the flow as lasting from ~6 to 10 years after extrusion began. Even if these units vented as ignimbrites, secondary viscous flowage continued this long after welding.

As an added check of the model, the relation between flow velocity and viscosity (Nichols,J Geol,1939) was evaluated for these lavas. Assuming a 10 to 25 km advance of the flow front during 10 years of flowage over generally flat terrain (0.5-1.0° slope), effective viscosities (reflecting melt viscosity plus the restraining effect of crumble breccia around the entire flow front) for the moving flows range from 1.9E11 to 1.7E12 poise. These values are reasonable for rhyolite lava flows (Blake,IAVCEI Proc Volc 2,1989).

Given large flow volume and high volume-eruption rate, high viscosities are not an impediment to silicic lava flows being able to travel distances comparable to flow-out lengths of ignimbrite-forming pyroclastic flows. Emplacement of thoroughly-welded silicic units of wide areal extent does not necessitate an ash-flow origin.

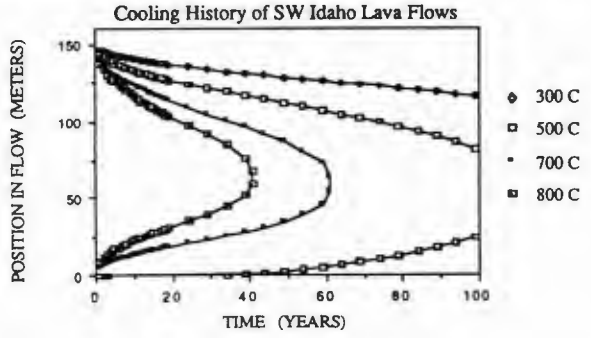

ASSIMILATION - FRACTIONAL CRYSTALLISATION PROCESSES INVERTED

MANTOVANI, M.S.M., Departamento de Geofísica, Instituto Astronomica e Geofísico, Universidade de São Paulo, Av. Miguel Stefano 4200, Caixa Postal 30627, São Paulo, Brazil, HAWKESWORTH, C.J. and WRIGHT, D., Department of Earth Sciences, The Open University, Milton Keynes, MK7 6AA, U.K.

In many areas mantle derived magmas are contaminated with crustal material in shallow level magma chambers or in conduits en route to the surface. Such contamination may be greatest in the higher temperature, more primitive magmas, or it may be linked with open system differentiation such that the more evolved rocks are more contaminated. Theoretical models suggest that some contamination is likely, but it remains extremely difficult to evaluate how much contamination has taken place in any particular magmatic suite. Thus an inversion program has been developed to evaluate assimilation fractional crystallisation (AFC) processes from selected minor, trace element and isotope analyses on suites of related rocks.

The program has been designed to calculate either the open system conditions and the nature of the contaminant consistent with the observed chemical changes between more primitive and more evolved rock types, or with prior knowledge of the contaminant to evaluate the composition of likely parental magmas. However, since inversion is a non-linear problem a large number of solutions are possible mathematically and these have to be constrained by good geological control. The results of AFC calculations are presented for two very different rock suites. Cerro Galan is a caldera complex in NW Argentina. Rocks range from basaltic andesite to dacite and good correlations are observed between $^{87}Sr/^{86}Sr$ (0.7055-0.7155) and both major and trace element abundances. Geological considerations suggest that the dacites are crustal melts, and given that they are likely contaminants the parental magmas had $^{87}Sr/^{86}Sr \approx 0.51258$. The second example is from the continental flood basalts in the southern province of the Paraná basin. Once again there are acid rocks which are likely crustal melts, but the variations between isotope and major trace and trace elements are less well defined than at Cerro Galan. The estimated parental magmas have $^{87}Sr/^{86}Sr \approx 0.709$ and $^{143}Nd/^{144}Nd \approx 0.51231$.

In detail the chemical trends suggest that different mechanisms of open system differentiation may have persisted in Cerro Galan and the southern Paraná. Cerro Galan samples fall into two groups; one has compositions consistent with up to 50% *closed system* fractional crystallisation, whereas the other scatters to relatively high SiO_2. Of particular interest is that the shift to high SiO_2 in the Cerro Galan rocks is more scattered, i.e. there is less of a relationship between mg* and SiO_2, and hence between the amount of crust added and the amount of fractional crystallisation, than in the southern Paraná suite. Moreover, that is despite the fact that the isotope-element, and isotope-isotope arrays are more tightly defined for Cerro Galan than for the southern Paraná. It would appear that the AFC processes as modelled here offer a better approximation of the processes responsible for the observed chemical variation in the southern Paraná, than at Cerro Galan. The reasons for this are still a matter for speculation, but it may be that individual magma batches are more likely to be displaced to high SiO_2 by magma mixing processes in a discrete centre with a high level magma chamber like Cerro Galan, than in the plumbling system for continental flood basalts.

GEOCHEMICAL VARIATIONS IN THE LATE-ARCHAEAN KLIPRIVIERSBERG BASALTIC PLAIN-TYPE SUITE, SOUTH AFRICA, AND THEIR CONSTRAINTS ON MAGMA CHAMBER DYNAMICS AND MAGMA SUPPLY SYSTEMS.

MARSH, J.S., BOWEN, M.P., BOWEN, T.B. Department of Geology, Rhodes University, Grahamstown, South Africa.

ROGERS, N.W. Department of Earth Sciences, The Open University, Milton Keynes, England.

The Klipriviersberg Group is a small continental flood- or plain-type tholeiitic suite forming the basal unit of the Ventersdorp Supergroup, an undeformed supracrustal suite covering an area of 200 000 km^2. The volcanic rocks were erupted during a phase of lithospheric thining leading to rifting of the Kaapvaal cratonic block in the late Archaean (2.7 Ga).

From the base up the Klipriviersberg Group comprises the Westonaria, Alberton, Orkney, Jeannette, Loraine, and Edenville Formations with a maximum combined thickness of 1.8 km. Samples were obtained from several cores drilled in the Klerksdorp goldfield close to the type area of the Klipriviersberg Group. The Westonaria and Jeannette formations are not represented in the cores but from other studies the Jeannette lavas are known to be compositionally very similar to those of the Loraine F., and the Westonaria F. is discontinuous and has Komatiitic affinities. A particularly well developed sequence through 1.4 Km of subaerially erupted lavas from the remaining formations was sampled in detail.

Compositionally the lavas range from siliceous picritic basalts to tholeiitic andesites. The Loraine and Edenville lavas are geochemically indistinguishable. Despite mild greenschist facies metamorphism igneous textures are well preserved. The Alberton lavas are sparsely feldspar-phyric but aphyric lavas predominate in the other formations.

The Alberton (Mg#=53-43; Zr=108-137ppm) and Orkney (Mg# =50-430; Zr=90-110ppm) lavas have a narrow range in composition and are more differentiated than the compositionally variable Loraine/Edenville lavas (Mg# =75-47; Zr=34-97ppm). Ratios of incompatible elements with similar D are the same in all three groups, but ratios such as Zr/Y, LREE/HREE vary between groups in a manner which is consistent with crystal/liquid equilibrium. In the Alberton and Orkney lavas Co, Cr, Ni correlate positively with Zr . On the other hand within Loraine/Edenville lavas variation of Zr, etc., with compatible elements is typical of that generated by fractional crystallization. Moreover, the least evolved (in terms of Zr) Alberton and Orkney lavas plot on the projection of the Loraine/Edenville fractional crystallization trend. Vertical composition profiles reveal the following: In the basal Alberton Formation both Zr and Ni increase erratically with height, but in the suceeding Orkney Formation Zr and Ni decrease with height. The Loraine/Edenville sequence has an overall trend towards more primitive compositions at the top punctuated by a number of inflections suggesting a cyclical operation of petrogenetic processes.

These features suggest that the dynamics of the Alberton and Orkney magma chambers were dominated by magma mixing. For the Loraine/Edenville lavas the upward trend to more primitive lavas contrasts with upward trends to more differentiated basalts observed in the Karoo and in the Deccan. Either this requires eruption from a density and compositionally zoned magma chamber, or magma was supplied from a network of chambers, or feeder channels, with degree of fractionation controlled by respose time or ascent rate.

HYDROMAGMATIC ERUPTIONS IN THE QUATERNARY VOLCANISM OF THE NE OF SPAIN

MARTI, J., Instituto de Geología Jaime Almera CSIC. c/Martí y Franqués s/n 08028 Barcelona (Spain)

The Quaternary volcanism of the NE of Spain is of intraplate alkaline type and it is only represented by olivine basalts and basanites. The origin of this volcanism is related to extensional tectonics which produced mantle derived magmas. Trace element contents suggest that these volcanic rocks derived from poorly differentiated primary magmas which were originated in a homogeneous mantle enriched in incompatible elements. A low volcanicity rift model without lithospheric thining may be applied to explain this volcanism which seems to be related to the last extensive period of the European rifts system. The uniformity in the geochemical composition of these volcanic rocks and the occurrence of peridotite xenoliths in some cinder cones suggest that the magma transport from source to eruption site took place without storage in sallow magma chambers. The location of the main volcanic vents is related to the post-alpine normal faults system which produced a horst-and-graben distribution in this area. The volcanic activity was nearly continuous from 350.000 to 11.000 years ago.

Forty well preserved volcanic cones have been recognised and a typical strombolian eruption style has been considered for many of them in the previous works. Nevertheless, the cartography and detailled study of these cones have revealed that, at least, fourteen of them have undergone some phreatomagmatic or phreatic explosive phases during their evolution. This hydromagmatic activity is responsible of a wide diversity of pyroclastic deposits, whose study has enabled to distinguish several eruptive sequences amoung these volcanoes. In all, seven main eruptive sequences characterized each one by a different succession of strombolian, phreatic or phreatomagmatic phases have been identified:

..(1) phreatomagmatic -- (2) strombolian (Plaça Ribera volcano)
..(1) strombolian -- (2) phreatomagmatic (or phreatic)-- (3) strombolian (Racó, Puig de les Medes, Llacunagra and Puig Redó volcanos)
..(1) phreatomagmatic -- (2) strombolian -- (3) phreatomagmatic -- (4) strombolian (Puig de Banya de Bòc, Puig Granollers and Can Simó volcanos)
..(1) phreatic (Clot de l´Omera volcano)
..(1) phreatic -- (2) phreatomagmatic -- (3) strombolian -- (4) phreatomagmatic (Closa de Sant Dalmai volcano)
..(1) strombolian -- (2) phreatomagmatic -- (3) strombolian -- (4) phreatomagmatic -- (5) strombolian (Puig d´Adri volcano).

These differences in the explosive activity of these volcanoes are due, essentially, to the different ways of magma/water interaction in each volcano, which are determined by the geological structure of this area and, especially, by the hydrological features of the ground.

RISK EVALUATION AT COLIMA VOLCANO, MEXICO

MARTIN-DEL POZZO, A.L., Instituto de Geofísica, UNAM, D. Coyoacan 04510 D.F. Mexico and Soler-Arechalde, A.M., same address.

Colima Volcano, 19°30'44"N and 103°37'02", Mexico's most active volcano has been cyclic in its historical activity. Following an explosive tefra and pyroclastic flow producing eruption, lava level is lowered several hundred meters and slowly begins its ascent (50 yrs), finally fills the crater as a dome and breaches it to form thick lava flows every six years. Afterwards freatomagmatic eruptions begin and tefra producing eruptions dominate. At the end of the 100 yr cycle another explosive tefra and pyroclastic flow producing eruption clears the dome and lava level is again lowered.

Pre-historic debris avalanche eruptions formed the older horseshoe caldera so cone colapse to the south must also be considered as a longer term hazard. Since 76 years have passed since the last explosive eruption, and lava flows have erupted in 1961-2, 1975-6, 1981-2 it is possible that the tefra-magmatofreatic phase is near. In 1987, part of the dome subsided probable related to freato-magmatic activity. Pyroclastic fall would affect Cd. Guzman, Venustiano Carranza, Zapotiltlan, Huescalapa, Tuxpan, Zapoltiltic and other cities besides the main highway, railroad and communications. Atenquique lumber center, since it is located in the river to the NE of the volcano could be subject to lahars. In the most explosive phase several towns: La Yerbabuena, Becerrera, San Antonio, el Fresnal and San Marcos may well be in the path of pyroclastic block and ash flows. Although lavas have flowed in all directions, the only populated area is to the south, where in 1976 a suburb of Queseria was abandoned because of the advance of the lava flow. If structural collapse of the volcano were to occur the hazardous area would be broadened to include the state capitol, Colima City and more than 200,000 people.

DIFFERENT ROLES OF WATER IN VOLCANIC PHENOMENA, AS DERIVED BY THE CHANGING CHEMICAL COMPOSITIONS OF FUMAROLIC GASES.

Martini, M. and Giannini, L.
Department of Earth Sciences
University of Florence
Via La Pira 4, 50121 Florence, Italy

Water vapor is normally the most abundant component of volcanic fumaroles, and its concentrations are often considered as due to sources external to the magma itself. Different possibilities have been suggested on the basis of isotopic studies, which successfully differentiated primary magmatic, meteoric, and metamorphic contributions. For a given system, however, the extent of such different contributions can change in time, according to different activity stages.

The results obtained during a significant period of time for the concentrations of water vapor, carbon and sulfur species in fumaroles characterized by different temperatures and chemical compositions, are here presented with the aim of distinguishing specific variations in response to the changing influence of water on volcanic activity.

The strong increase in temperatures, as well as in concentrations of "magmatic" components, observed at Momotombo (Nicaragua) from 1973 to 1985, is interpreted as mainly due to the depletion of a "buffering" shallow water body, possibly induced by the exploitation of the nearby geothermal field.

At Phlegrean Fields (Italy), the data referring to the period 1980-1988 clearly indicate a feeding water reservoir at intermediate depth, and the changing vapor concentrations are considered as the consequence of changing thermal input from the low-lying magma body.

Two stages of activity can be derived from the data collected at Vulcano (Italy) from 1977 to 1988. A first period, up to 1985, during which water of probable recent meteoric origin acted mainly as a diluting component of magmatic species arising from the magma chamber; subsequently, an increased heatflow from depth appears responsible for the observed chemical changes.

The possibility of obtaining some evidence on the different influence of water on volcanic systems appears of not negligible importance for forecasting purposes. According to the above mentioned interpretation of compositional changes observed in volcanic fumaroles, a low probability for a resumed activity can be estimated at Momotombo and, prior to 1985, at Vulcano; this probability appears as moderate for Phlegrean Fields and, since 1985, slightly higher for Vulcano.

THE VESUVIUS ERUPTION OF 1906.

MASTROLORENZO G. Osservatorio Vesuviano
Via Manzoni, 249. 80123 Napoli, Italy.
D'ALESSIO G., Dip. Geofisica e Vulcanologia, Napoli.
MUNNO R., Dip. Geofisica e Vulcanologia, Napoli.
ROLANDI G., Dip. Geofisica e Vulcanologia,
Largo S. Marcellino, 10. 80138 Napoli, Italy.

The explosive paroxism of 1906 ended a 30 year eruptive cycle of Vesuvius (Southern Italy).

The paroxysm started during a period of subterminal effusive activity and can be divided into three major phases . The first phase was characterized by violent strombolian activity and the generation of high lava fauntains,which formed a wide scoria deposit with a volume of about 1.2×10^7 cu. m. This phase was followed by an intense vulcanian explosion (phase 2) that produced a fall deposit with a volume of about 5×10^7 cu. m. The third and last phase was phreatomagmatic and erupted fine ash.

The distribution,granulometry and morphology of the products sugest that column hight and eruption rate varied, respectively , from 550 to 3000 cu. m/s and from 5 to about 10 Km.

The evolution of the eruption was accompanied by a change in the chemistry of the products to more basic composition. This chemical change represents the last stage of an unidirectional trend which had continued for the whole of the preceding 30 year cycle and which may reflect the gradual drainage of a common magma reservoir.

MONITORING VOLCANIC ERUPTIONS USING METEOROLOGICAL SATELLITE DATA.

Michael MATSON, National Oceanic and Atmospheric Administration, Washington, D.C. 20233

Meteorological satellite data have been used to detect volcanic eruptions since the eruption of Augustine volcano in Alaska in 1976. The satellites provide daily global coverage. Imagery and digital data can be used with radiosonde data to determine the altitude of an eruption, the size, speed and position of the plume, and in which direction the plume is moving. In remote areas, satellite data is often the only information available about an eruption. Examples of eruptions detected by meteorological satellite data are shown for Mt. St. Helens, Alaid, El Chichon, Galunggung, Una Una, and Mt. Etna. With the advent of PC-based image processing systems, it is possible for volcanologists to process and analyze this satellite data quickly and relatively inexpensively.

GEOCHEMISTRY AND TECTONISM OF LAVAS ERUPTED DURING THE TRANSITION FROM COMPRESSION TO EXTENSION, SOUTHERN MARYSVALE COMPLEX, SOUTHWESTERN UTAH

MATTOX, S.R., and WALKER, J.A., Department of Geology, Northern Illinois University, DeKalb, IL 60115

Cenozoic lavas of the southern Tushar mountains and the northern Markagunt Plateau record compositional variations associated with the change from late Oligocene - early Miocene compression to early Miocene - Quaternary extension. The early event produced stratocones of the Mt. Dutton formation (age=26-23 Ma) with near vent lava flows and flow breccias flanked by laterally extensive lahars. These calc-alkaline lavas have relatively low, but variable, K_2O and range from basaltic andesite to andesite (+,*). The Mafic Lava Flows of Circleville Mountain and correlative units (age=23-21 Ma) overlie the Mt. Dutton as widespread flows of sheet geometry. This change in eruptive style is accompanied by a shift to silica-undersaturated to -oversaturated absarokites, shoshonites, and banakites (△). After a 7 Ma hiatus and continuing into the Quaternary, basalts, high-K andesites and dacites, and rhyolites were erupted from scattered volcanic centers (⊡). The field defined by this last stage of volcanism is intermediate to those of the calc-alkaline and K-rich suites on the K_2O-SiO_2 plot of Peccerillo and Taylor (1976).

Previous investigators (Rowley and others, 1988) have inferred the main phase of structural differentiation between the Colorado Plateau and the Basin and Range to be coincident with the change to more potassium-rich volcanism 23 Ma ago; therefore, in their interpretation, the K-rich suite marks the inception of bimodal volcanism. An alternative interpretation, following ideas presented for the Aeolian Islands by Keller (1974) and Ellam and others (1988), relates potassic volcanism to the detachment and demise of the subducted slab. Besides their close temporal relationship, the calc-alkaline and K-rich suites also share similar trace element characteristics. For example, ratios of LILEs and HFSEs clearly separate calc-alkaline and K-rich lavas (K/Ba=25.5, Zr/Nb=17.5) from those of the youngest suite (K/Ba=11.9, Zr/Nb=7.9). Further, two individual stratocone complexes have geochemical characteristics transitional from the calc-alkaline to K-rich suite (*).

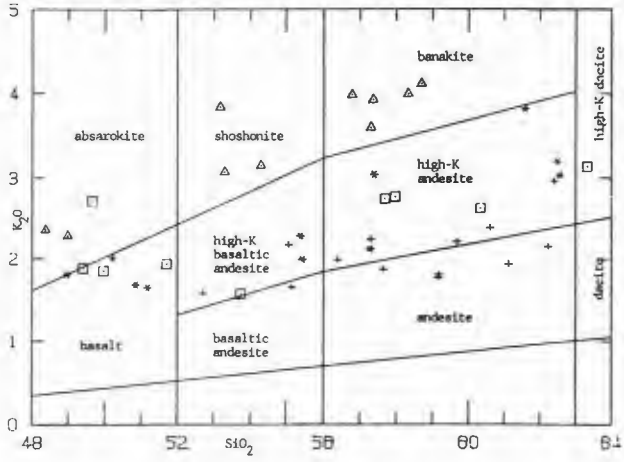

TERTIARY VOLCANIC ROCKS OF THE TINAJA LISA-NIDO AREA, NORTH-CENTRAL CHIHUAHUA, MEXICO

MAUGER, Richard L., Dept. of Geology, East Carolina University, Greenville, NC 27858 USA

Ash-flow, dike, and phaneritic intrusive rhyolites with abundant mafic clots define the Tinaja Lisa caldera (30km X 20km; mid to late Eocene). Small mafic intrusions cut the intrusive rhyolites. Large peripheral rhyolite flow-domes erupted after localized uplift and erosion of the caldera rocks. Next (37-39 Ma) Agate andesite lavas from widely scattered vents and a massive lower Gallego pyroclastic-flow rhyolite were emplaced. Both rocks have 40-50% coarse, seive-textured K-andesine glomerocrysts with intact andesine-labradorite cores. The Gallego glomerocrysts, with anorthoclase and sanidine overgrowths, are embedded in a "rhyolitic" matrix. Later smaller-volume Gallego units include glomerocrystic rhyolite flows, pyroclastic-flow rhyolites with cpx-plag-ilm glomerocrysts and quenched more-mafic vesciculated blobs, and flow and intrusive andesite with very coarse seive-textured K-andesine glomerocrysts (50% xtals). The Agate-Gallego units may exceed 1000 cukm of rock. Contemporaneously, the Espinazo pyroclastic-flow rhyolites erupted from linear vents in western Gallego Canyon, filling a smaller caldera (10km X 10km) near to the center of the Agate-Gallego outcrop area. Aphyric basaltic lavas are interbedded with basal Espinazo units. After a 5 Ma hiatus, "transitional" basalts (Milagro-type) were erupted over much of north-central Chihuahua. Ash-flow rhyolite interbedded with these basalts was erupted from a major caldera near Rincon de Alamo, and small-volume rhyolites (surge, air-fall and pyroclastic-flow) were erupted from a small caldera at the north-west tip of Cordon el Gato. Volcanism ended after large-volume peralkaline rhyolites were erupted from a shallow caldera complex farther south. These rhyolites, 300+m thick in S. del Nido, are not recognized north of the Nido fault, a younger feature that separates the Nido and Tinaja Lisa blocks.

Volcanism was driven by basalt injected at the base of the crust. A "stacked sill" complex extended upward as fresh magma infusions displaced more evolved magmas (leucogabbro and anorthosite) to higher, mid crustal (?) levels. Residual sill liquids and crustal-rock partial melts coalesced as dry rhyolite magmas. These moved to the upper crust or spread laterally, causing nearly crystallized sill plagioclase to disaggregate and react to sieve-textured K-rich andesine glomerocrysts. The Agate-Gallego magma probably formed this way; some was erupted soon after the "mixing" event (Agate) and some remained at depth long enough for alkali feldspars to overgrow the glomerocrysts. Though voluminous, these eruptives lack centralized caldera sources but rose from widely distributed small vents, suggesting a sill-like magma chamber. Opx and cpx (no biotite nor hornblende) might suggest that the chamber was too deep to interact with surface-derived water. Elsewhere anorthositic terranes with associated "dry" granitic rocks may represent rocks formed in other such "stacked sill" complexes.

DISTAL PANIZOS IGNIMBRITES (NORTH WESTERN ARGENTINA), MASS WASTING PROCESSES AND STRUCTURES.

Mario M. Mazzoni. Centro de Inv. Geol. (CIG) Calle 1 nº 644. La Plata, Argentina.

Lateral correlation of cooling units and flows in the eastern border of Panizos volcano (22º15'S, 66º45'W) and mesas is highly constrained by lateral variation of flows, by the exposure of different stratigraphic sections, by other local or regional still undetermined ignimbrites, and by mass-wasting processes, particularly obscuring their basal relationships with underlying volcaniclastics. In relation to the last problem, which is here focused, it was found that our field criterion of identifying the ignimbrites at distance through the grayish castelleted aspect of outcrops -in contrast to smoother surfaces of older volcaniclastics- was decieving. For example, at Ciénago, detailed inspection of erosion pillars attests reworked ignimbritic and volcaniclastic layers dipping up to 50°, highly contrasted with the regional horizontality of tertiary units. Other complex relations, with participation of primary pyroclastics, though not fully understood, may be explained in terms of alternating episodes of mass-wasting (specially slumping) and aggradation. Pedestal pinnacles are frequent at Ciénago, and specially at Cerro Urusmayo. The pillars are mainly volcaniclastic in the former and ignimbritic in the latter, but both have protective roofs of tabular pinkish slightly welded ignimbrites - up to many meters long, lying above an inclined smooth and conspicuous erosive plane. Largest dimensions of blocks and interspersed finer grained debris parallel this plane. Nearby face-cliffs and pillars show concave and also smooth planes, dipping between 4° and 50°, with similar ignimbritic material in both sides.

Through dynamic evaluation of present slopes in this desertic area, we interpret that pedestals and unconformities described above are the result of different mass wasting processes, specially debris slides. In present slopes, cliff debris is coming down from the upper ledges of mesas, generally composed by more welded ignimbrites. The blocks fall, roll or slide, and stop at different points above the pediment, where they potentially can protect from future erosion, either the underlying less resistant material, -generally unwelded crystal-rich ignimbrites-, and the slope plane. It is remarkable that though the pedestal hiatus may be several Ma long (youngest age found for Panizos ignimbrites is 9 Ma), the unconformity is only local. Otherwise, the ignimbritic material above the plane may have formed slightly afterwards than the one beneath, and either simultaneously if thick cooling units are affected. Consequently, it may not separate different cooling units. We believe these features can be preserved if subsequent episodes of valley ponding bury ignimbritic slopes, as it may happen in desertic regions affected by recurrent explosive volcanism.

DEPLETED SOURCES FOR VOLCANIC ARC BASALTS: CONSTRAINTS FROM BASALTS OF THE KERMADEC-TAUPO VOLCANIC ZONE BASED ON TRACE ELEMENTS, ISOTOPES AND SUBDUCTION CHEMICAL GEODYNAMICS

McCULLOCH, M.T., Research School of Earth Sciences, Australian National University, Canberra, Australia,
GAMBLE, J.A., Department of Geology, Victoria University of Wellington, Wellington, New Zealand.

Primary MORB are generally agreed to have originated by partial melting of mantle peridotite distinguished by a time integrated depletion of LREE and LIL which register as high $^{143}Nd/^{144}Nd$ and low $^{87}Sr/^{86}Sr$ isotopic ratios. In these rocks the absolute abundances of incompatible trace elements are controlled largely by melting parameters. Volcanic arc basalts are distinctive, revealing relative enrichments in LIL and depletions in HFS elements which are not compatible with a simple melting hypothesis such as that applicable to MORB. Moreover, isotopic ratios of Sr and Nd in arc basalts are distinctive although depleted relative to bulk earth values.

To account for the differences between MORB and arc basalts and particularly the apparent decoupling of LIL and HFS elements, multicomponent models involving MORB depleted mantle, subducted sediment and metasomatic fluids derived from the slab have evolved. Furthermore, to explain apparent depletions of HFS elements (e.g. Nb and Ta) relative to MORB, mineral assemblages unique to inferred high redox conditions in the mantle wedge have been invoked, often with scant or uncritical consideration of analytical parameters such as detection limits, analytical precision, etc. An example of particular relevance concerns the use of Nb and its (uncritical) use in multielement spidergram type diagrams. How often are high LIL/Nb (e.g. Ba/Nb) ratios and Nb depletions relative to MORB quoted as distinguishing features of arc basalts? We have made a careful study of Nb abundances in N-MORB and arc basalts using data from spark source mass spectrometry (which gives detection limits down to <1 ppm) and high precision X-Ray fluorescence (where long counting times and full correction procedures have been used). From this study we conclude that the abundances of Nb in MORB (2.0 ± 1.0) and oceanic arc basalts (1.5 ± 1.0) are indistinguishable. Moreover, we would also suggest that commonly used MORB normalisation values for Nb (3.5 ppm) are too large, by a factor of two.

Applying the principle of Occam's Razor, we maintain that there is no need for retention of HFS buffering assemblages in the mantle wedge and that HFS depletion is a consequence of the depleted nature of the arc basalt source. The high LIL, LREE and the radiogenic isotopes are slab derived features whereas HREE and HFS elements remain fixed in the slab and hence depleted in the arc magma source. Consideration of the chemical features in terms of subduction rates, ba -arc spreading rates and flow and porosity in the mantle wedge (e.g. Spiegelman and McKenzie, 1987) leads us to conclude that subduction rates are sufficiently high relative to extension in the back arc to ensure a net surfeit of slab transfer to the wedge. Problems of mass conservation can be accommodated by the phenomena of roll-back.

PROXIMAL FACIES OF THE WILD HORSE MESA TUFF, CALIFORNIA: IMPLICATIONS FOR NEAR VENT PROCESSES DURING ASH FLOW ERUPTIONS

MCCURRY, M., Department of Earth Sciences, New Mexico State University, Las Cruces, N.M. 88003

Excellent exposures of proximal to distal parts of the 15.8 Ma Wild Horse Mesa Tuff (WHMT) allow for an unusually unambiguous interpretation of their eruption and emplacement processes. The tuff is metaluminous to mildly peralkaline in composition and was erupted in three major pulses with volumes of approximately 40, 20, and 20 km^3, respectively. The second and third eruptions produced mixed magma pumices that only occur at the tops of the respective members. Each eruption produced multiple flow units that cumulatively covered an area of about 600 km^2 to a maximum thickness of at least 320 m.

Proximal facies of the WHMT are identified by coarse lag deposits at the base of many flow units, and by an exponential increase in the maximum size of dense lithics within individual units toward the inferred vent zone. Only the outflow parts of the tuff are exposed. Both intracauldron tuff and vents are covered by younger lava flows and caldera-scarp breccia. However, some flow units are apparently exposed to within a few hundred meters of the source vents based on extrapolations of maximum lithic size. The largest lithics are of angular to well rounded Mesozoic quartz monzonite and quartz monzonite breccia, and accessory rhyolite breccia with maximum dimensions of at least 14, and possibly as high as 20 m across. These are apparently among the largest lithic sizes that have been documented in the outflow portion of an ash flow unit.

The second and third members of the WHMT exhibit rapid horizontal variations within their proximal facies that are highly uncharacteristic of the rest of the flow units. For example, both thin rapidly, over an originally horizontal surface, while maximum lithic size increases toward the inferred vents. The thinning is not a result of erosion because mixed-magma pumices, and layer-3 surge and fallout deposits are well preserved. These features may be explained by either drain-back over a caldera scarp or, as predicted by some numerical models of explosive eruptions, to column collapse at some distance from the vent.

The uppermost member of the WHMT is underlain in most areas by tuff and lapilli tuff of apparent fallout origin. These deposits are generally well sorted and stratified, increase in grain size and thickness towards the inferred vent zone, and are comagmatic with and gradational upwards into the overlying ash flow tuff. However, within the proximal facies of the tuff, they also exhibit anomalous features. These included distinctive bed forms that are characteristic of pyroclastic surges such as low angle dunes. They also exhibit a sharp decrease in thickness near the inferred vent zone, that parallels that of the overlying ash flow unit. These features would seem to support the idea that many of the anomalous features seen in the proximal facies of the tuffs are a result of column collapse at some distance from the source vents.

CENOZOIC HOTSPOT TRACKS IN THE EASTERN PART OF THE AUSTRALIAN PLATE

McDOUGALL, Ian, Research School of Earth Sciences, The Australian National University, Canberra ACT 2601, Australia.

Three essentially linear, subparallel chains of Cenozoic volcanoes are recognized in the eastern part of the Australian plate, remote from plate margins. Each chain has a northerly strike and extends over more than 1000 km. Each chain is developed in a different crustal setting, but all are interpreted to be hotspot tracks.

In eastern continental Australia, Cenozoic volcanism is confined to a zone averaging about 400 km wide, subparallel to the coast, within and adjacent to the highlands. Two major types of volcanic provinces are recognized. The central volcano provinces comprise large volumes of basaltic lava with some felsic flows or intrusives, generally building a substantial volcano. These central volcanoes are distributed over a relatively broad zone southward from 21°S, and exhibit a systematic younging to the south, with the rate of migration of the volcanism averaging 65 ± 3 mm/year over the last 35 Ma.

The Tasmantid Seamounts form a well-defined linear chain of large, flat-topped, submarine volcanoes built upon oceanic crust of the Tasman Basin, which lies immediately to the east of the Australian continent. Dating of basalts recovered by dredging shows that there is a progressive and systematic younging southward along the chain at an average rate of 67 ± 5 mm/year.

The Lord Howe Seamount chain is about 300 km east of the Tasmantid chain, and is built adjacent to the western flanks of the Lord Howe Rise, which is continental in structure. Recent dredging of some of the seamounts confirm their volcanic origin, but the only ages available are from Lord Howe Island, active about 7 Ma ago.

The congruency of strike of the three volcanic chains in settings ranging from oceanic to continental, together with the indistinguishable rates of propagation of the volcanism in two of the chains, is strong evidence that these hotspot traces are effectively recording northward motion of the Australian plate away from Antarctica across sublithospheric mantle source regions for the volcanism over the last 35 Ma. The results reinforce the view that hotspots provide a useful frame of reference for plate motions and that hotspots are fixed relative to one another in the mantle to within the uncertainties.

GEOCHRONOLOGY OF CRETACEOUS - TERTIARY MAGMATIC ACTIVITY IN CENTRAL CHIHUAHUA, MEXICO

MCDOWELL,F.W.,Dept. of Geological Sciences, Univ. of Texas, Austin, Texas 78713, MAUGER, R.L.,Dept. of Geology, East Carolina Univ.,Greenville, North Carolina 27858, and WALKER, N.W.,Dept. of Geological Sciences, Univ. of Texas, Austin,Texas 78713

Exposures of igneous rocks extend westward from Chihuahua City (CC) nearly continuously across the states of Chihuahua and Sonora to the mainland coast of western Mexico. To the west in the Sierra Madre Occidental, a thick cover of mid-Tertiary volcanic units conceals all but small and disconnected exposures of older rocks. Near CC, uplifted Basin and Range blocks and effects of paleo-topography developed upon Laramide folds, have preserved composite sections that represent at least 40 Ma of magmatic activity.

Even in the CC area, correlation and isotopic dating of the older portions of most sections are restricted by extensive mid-Tertiary and younger cover and by effects of alteration. Among the oldest units are the Penas Azules Volcanics, a 3 km-thick (minimum) sequence of dominantly intermediate flows and lahars dipping 30° to 60° east. This unit is exposed only in the Majalca Canyon area, about 40 km NNW of CC, where a single K-Ar age of 68 Ma has been obtained for it. Approximately 30 km N of CC, undated and altered rhyolitic flows, breccias, and pyroclastic units rest upon middle Cretaceous limestones and are overlain by a well-dated mid-Eocene to Oligocene section. Igneous activity during the Paleocene-early Eocene was widespread but is represented mainly by numerous small intrusive bodies with K-Ar ages ranging from 58 to 53 Ma. Some of these intrude undated volcanic units. The 58 Ma (fission-track) Chivato tuff is the oldest igneous unit in the Palomas area, 50 km SW of CC. Elsewhere in the region there is no definitive evidence for igneous activity before middle to upper Eocene.

Beginning at about 45 Ma, the region was inundated with a sequence of felsic pyroclastic eruptives, interspersed with locally thick rhyolite flows and glomerocrystic intermediate lavas. Particularly productive intervals appear to have been from 45 to 41 Ma, 38 to 35 Ma, and 33 to 28 Ma. Though selected areas are dominated by products of only one of these periods, activity on a regional scale was probably continuous. Several calderas have been recognized as sources for major ash-flow units, including a partially exposed large caldera in Majalca Canyon that contains a thick sequence of altered intracaldera tuffs (Majalca Canyon sequence). Based on their alteration and low structural position, these tuffs were once thought to be the oldest igneous rocks in the region, but reinterpretation of field data has demonstrated their caldera association. A $^{206}Pb/^{238}U$ zircon age of 42 Ma establishes time equivalence to part of a sequence of K-Ar-dated outflow-facies units in surrounding ranges. The upper portions of the mid-Tertiary sequence contain abundant basaltic andesite lavas with interlayered rhyolitic tuffs, some of which have peralkaline tendencies, including distinctive trace-element enrichments and phenocryst mineralogies, in contrast to the more typical calc-alkaline units common to the lower parts of the section.

The Cretaceous - Tertiary magmatic history of the CC area has two distinct components, for which dated intervals are 68 to 53 Ma, overlapping the time of regional Laramide compression, and 45 to 28 Ma, which pre-dates the onset of Basin-and Range faulting in the region. A stratigraphic break between these two components is evident, but dating control is not yet sufficient to establish the presence and duration of a time break. The younger and more voluminous interval began at least by 45 Ma, progressing gradationally through partly overlapping stages. Earliest activity (ca. 45-38 Ma) produced a mingling of both felsic and intermediate effusives, and gave way to an interval (38-30 Ma) in which calc-alkaline felsic tuffs predominated. The final stage, in which basaltic andesite lavas predominate with subordinate rhyolitic tuffs, began in some areas by 33 Ma and was widespread between 30 and 28 Ma. Unlike neighboring volcanic fields where a dominantly andesitic section is present at the base, felsic ash-flow tuffs are prominent during the entire mid-Tertiary magmatic record at CC. They represent the earliest inception and longest time interval yet found in any area of southwestern North America affected by the mid-Tertiary ignimbrite flare-up.

TIMING AND DISTRIBUTION OF OLIGOCENE IGNIMBRITE ACTIVITY IN THE MOGOLLON-DATIL VOLCANIC FIELD, S.W. NEW MEXICO

McINTOSH, William C., CHAPIN, Charles E., New Mexico Bureau of Mines and Mineral Resources, Socorro, N.M. 87801, and SUTTER, John F., U.S. Geological Survey, National Center, Reston, Va., 20292

$^{40}Ar/^{39}Ar$ age spectra and paleomagnetic analyses tightly constrain the history of ignimbrite volcanism in the 36-24 Ma Mogollon-Datil volcanic field. High-precision (±0.15 Ma) sanidine plateau ages have been obtained from most of the 25+ voluminous (100-1200 km^3) regional ignimbrites. Age and paleomagnetic data allow reliable correlation of ignimbrites among isolated ranges, providing an integrated time-stratigraphic framework for the entire field.

Mogollon-Datil ignimbrite activity was strongly episodic, being confined to 4 brief (<2.6 Ma) eruptive episodes separated by 1-3 Ma gaps during which no caldera-forming eruptions occurred. Ignimbrite activity generally tended to migrate from the southeast towards the north and west.

Episode 1 (36.1-33.5 Ma): Rhyolitic ignimbrite activity, dominantly low-silica, commenced at the southeast edge of the field with eruption of the Organ Mountains caldera and associated outflow sheets at 36.1 and 35.6 Ma, closely followed by eruption of the nearby Doña Ana caldera at 35.4 Ma. Activity shifted 100 km northwest with eruption of the Kneeling Nun Tuff (>900 km^3) at 34.8 Ma, followed by several less voluminous ignimbrite eruptions from 34.8 to 33.5 Ma.

Episode 2 (32.0-31.3 Ma): After a 1.5 Ma hiatus, low-silica rhyolitic ignimbrite activity shifted north and west, producing the Hells Mesa (32.0 Ma, 1200 km^3), Caballo Blanco (31.6 Ma, a.k.a. Fall Canyon), and Tadpole Ridge (31.3 Ma) Tuffs.

Episode 3 (28.9-27.3 Ma): Following a 2.4 Ma hiatus, the "ignimbrite flare-up" occurred, producing within a span of 1.6 Ma more than 12 regional units, primarily high-silica rhyolites, totalling >6000 km^3. Well-dated units within this interval include Davis Canyon (29.0 Ma), La Jencia (28.8 Ma), Vicks Peak (28.5 Ma), Bloodgood Canyon (28.0 Ma), Lemitar (28.0), and South Canyon (27.3 Ma) Tuffs. Calderas for these units were located near the western and northern margins of the volcanic field.

Episode 4 (24.3 Ma): After a 3.0 Ma hiatus, Mogollon-Datil ignimbrite activity ended near the northern edge of the field with the eruption of the high-silica rhyolite tuff of Turkey Springs at 24.3 Ma.

Mogollon-Datil ignimbrite episodes 1,3, and 4 closely parallel the timing of ignimbrite activity in the San Juan volcanic field of Colorado, indicating regional tectonic control of caldera-forming rhyolitic eruptions.

Paleomagnetic data and $^{40}Ar/^{39}Ar$ plateau ages precisely constrain 7 geomagnetic polarity reversals which occurred during Mogollon-Datil activity. This polarity record can be confidently correlated with the polarity record of well-dated San Juan units, and furthermore has potential to aid in radiometric calibration of the worldwide Magnetic Polarity Time Scale determined from marine magnetic anomalies.

ASSESSMENT OF VOLCANIC HAZARDS ON BOUGAINVILLE ISLAND, PAPUA NEW GUINEA

McKEE, C., Rabaul Volcano Observatory, Papua New Guinea.
JOHNSON, R.W., Bureau of Minerals Resources, Australia.
PATIA, H., Rabaul Volcano Observatory, Papua New Guinea.

Bougainville Island, which is 200 km long and up to 60 km wide, is the largest member of the Solomon island arc. Late Pliocene - Quaternary andesitic stratovolcanoes dominate the skyline along most of the island. Prior to this study, only reconnaissance geological mapping and infrequent surveillance had been carried out on these volcanoes, and no assessment had been made of volcanic hazards. Our work, involving detailed geological mapping, tephrastratigraphic studies and analysis of the historical record of volcanic activity, has revealed that there are four active or potentially active volcanoes on the island. These are Billy Mitchell, Loloru, Balbi and Bagana. Previously, Billy Mitchell was regarded as extinct, but it is now known to have produced two large volume (c. 10 km^3) explosive eruptions in the past one thousand years and earlier explosive eruptions are also indicated. Eruptions at Loloru have also been predominantly explosive. In the past 13,000 years, Loloru has produced at least five large explosive eruptions, the most-recent about 3,000 years ago. Eruptions at Balbi have been a mixture of mild explosive and effusive activity, while Bagana's activity is predominantly effusive but infrequently punctuated by explosive or collapse events.

The main volcanic hazards identified on Bougainville are:-

- ignimbrites and pyroclastic surges (Loloru, Billy Mitchell).
- block and ash flows and debris avalanches (Bagana, Balbi).
- lava flows (Bagana, Balbi, Loloru).
- floods (Billy Mitchell, Loloru).
- lahars (Balbi).
- ash falls (Billy Mitchell, Loloru, Balbi).
- gas emissions (Bagana).
- limnic gas bursts (Billy Mitchell, Loloru).

These hazards could affect large parts of Bougainville and large numbers of its inhabitants (current population 165,000), as communities are developing rapidly in areas quite close to the volcanoes. Of particular concern is the fact that this development is taking place in a province where there have been no historical volcanic disasters and where there is no great perception of volcanic hazards.

VOLCANIC TREMOR FROM AROUND THE WORLD

McNUTT, S.R., California Department of Conservation, Division of Mines and Geology, 630 Bercut Drive, Sacramento, CA 95814

Volcanic tremor or related phenomena have been recorded at more than 120 volcanic areas worldwide. A comprehensive literature search of over 560 references covering 105 volcanoes was made to determine quantitative relationships between different tremor parameters. Unpublished data from 15 volcanoes were added to the compilation.

Preliminary results show that more than 240,000 episodes of tremor are reported in the literature. Analyses of subsets of these data show that approximately 65% of tremor episodes accompany eruptions of gases or lava, and 35% occurred with no eruption. Volcanic tremor preceded eruptions on a time scale of minutes to hours in approximately 20% of the cases studied, and followed eruptions in about 15% of the cases. Durations of individual tremor episodes range from minutes to years: 62% from 1-59 minutes; 17% from 1-23 hours; 10% from 1-6 days; and 3% weeks or longer. No data on durations were given for 8% of the episodes. Continuous tremor episodes with durations longer than one year have occurred at Etna, Stromboli, Arenal, Kilauea, and Oshima volcanoes.

Based on data from 55 volcanoes for which it was reported, the mean frequency of volcanic tremor is 3.8 Hz, and the median value is 3.2 Hz (Figure 1 below). The range of frequencies reported for tremor extends from 0.12 Hz to 15 Hz. The higher values are typical of station distances of less than 1 km and active geothermal systems, while the lower values are typical of distances on the order of 5-10 km and magmatic activity.

Observations of tremor depend critically on seismic stations, and data on seismic stations are readily available for 78 volcanoes. Of these, 25 volcanoes have at least one seismic station within 1 km of the vent, while the most distant station to record tremor is 430 km away. (Hydrophones have recorded T-phases from submarine eruptions up to 8,600 km away.) Detection thresholds, normalized to reduced displacement, could be calculated for 43 volcanoes. Twelve volcanoes have detection thresholds less than 1.0 cm^2; the lowest thresholds are 0.02 cm^2 at Kilauea and 0.05 cm^2 at Ruiz. Estimates of the maximum amplitude of tremor, again normalized to reduced displacement, were calculated for 22 volcanoes. These range from 0.56 cm^2 to approximately 100,000 cm^2, the latter value accompanying the great Vesuvius eruption of 1906. All of the values over 100 cm^2 except one occurred when large eruptions were in progress. The dynamic range of tremor at individual volcanoes varies from 14 to 75 dB, with a mean of 38 dB and a median of 37 dB (Figure 2 below).

Felt tremor has been reported at 10 volcanoes: Paricutin, Lamington, Etna, Api Siau, Sierra Negra, Vesuvius, Ruiz, Pacaya, Surtsey, and Kilauea. Deep (>10 km) tremor or low-frequency events have occurred at 3 volcanoes: Kilauea, Oshima, and Lassen. Banded tremor -- periodic episodes separated in time at regular intervals -- has occurred at 6 volcanoes: Karkar, Ruiz, Pavlof, Suwanose-jima, Ulawun, Klyuchevskoy, and at Old Faithful geyser. Spasmodic tremor has occurred at Kilauea, Mount St. Helens, Fuego, Klyuchevskoy, Long Valley, and Vesuvius. At 17 (82%) of the 22 volcanoes where wave types are known or could be inferred, tremor is composed mainly of surface waves, while tremor at the other 5 (18%) is composed mainly of body waves. This reflects the fact that most tremor sources occur at shallow depths where several modes of surface waves are efficiently generated.

Based on synthesis of all the information highlighted above, it is concluded that the occurrence of tremor at active volcanoes is nearly ubiquitous. The observations themselves, plus the theoretical work of many authors, clearly show that several different source mechanisms are required to explain the many varied observations. Because most tremor occurs at shallow depths when eruptive activity also is occurring, the present author concludes that pressure fluctuations caused by degassing processes are likely to be the most common source mechanisms.

Figure 1. Tremor Frequency

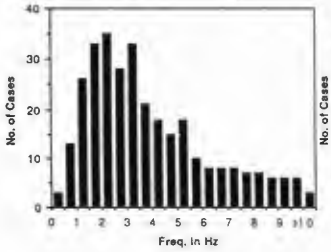

Figure 2. Tremor Dynamic Range

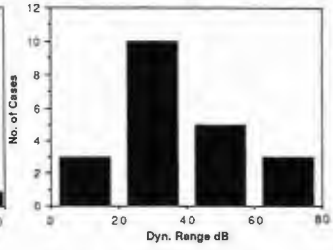

DISTAL FACIES OF ACTIVE CONTINENTAL MARGIN VOLCANIC ARCS : A LATE CARBONIFEROUS EXAMPLE AND MODERN ANALOGUE

McPHIE, J., BMR, Canberra, Australia

During the Late Carboniferous, the New England Orogen of eastern Australia consisted of a continental margin volcanic arc in the west, a central subaerial and marine shelf, and an eastern open ocean. The southern portion of the volcanic arc in NSW is no longer exposed. However, sedimentary and volcanic rocks derived from it (the Currabubula Formation) provide a record of the processes and environments along its eastern flank, and strongly reflect the character of source volcanoes. The present eastern limit of the formation is erosional and its western limit is a major fault. There are two principal lithofacies : the volcanic facies is mainly composed of sheets of welded rhyolitic ignimbrite, accompanied by minor non-welded ignimbrite and ashfall tuff; the epiclastic facies comprises cobble orthoconglomerate, with lesser cross-bedded sandstone, paraconglomerate, and laminated mudstone.

Conglomerate and sandstone were deposited in an extensive fluvial braidplain. Pyroclastic flows periodically spread across the braidplain, leaving ignimbrite tens of metres thick in topographic depressions, and covering low-lying interfluves. Laminated mudstone possibly accumulated in restricted lakes and/or abandoned braidplain channels. Some paraconglomerate has been interpreted as tillite which originated as ablation moraine. Laminated pebbly mudstone containing ice-rafted dropstones also implies proximity to alpine glaciers. The clastic components of the epiclastic facies include pumice, shards and crystals, abundant volcanic and less abundant non-volcanic lithic (notably granitoid and metasedimentary) fragments. Erosion surfaces are commonly evident at outcrop scale, and the ignimbrite sheets delineate some major disconformities interpreted as palaeovalleys. The ignimbrites in turn were partly excavated by incision of drainage channels and thinned by removal of the non-welded topmost layers. Airfall ash was probably generated with the pyroclastic flows though reworked soon after deposition and dispersed within the epiclastic facies, or else preserved in waterlain tuffaceous mudstone intervals. At least one large magnitude, phreatomagmatic eruption occurred, generating debris flows and floods which accompanied emplacement of widespread primary pyroclastic deposits.

The facies association, facies geometry and setting of the Currabubula Formation are comparable to part of the western flank of the modern Andean volcanic arc in northern Chile. The analogy has guided reconstruction of the now concealed or eroded proximal part of the Late Carboniferous volcanic arc. Source area uplift, alpine glaciation and explosive volcanic eruptions are the principal factors that control the facies associations and geometry of such arc flank sequences. Welded ignimbrite sheets dominate the volcanic facies of both the modern and Late Carboniferous flank sequences because they have superior resistance to erosion compared with other pyroclastic deposits, and they extend further than silicic or intermediate lavas. Primary volcanics that are easily eroded or source-restricted are, however, represented in the distal association as clasts in the accompanying epiclastic facies.

KEANAKAKOI ASH : DEPOSITS FROM EXPLOSIVE ERUPTIONS OF KILAUEA ~1790AD.

McPHIE, J., BMR, Canberra, Australia; WALKER, G.P.L., HIG, Honolulu, Hawaii, and CHRISTIANSEN, R.L., USGS, Menlo Park, California

Kilauea caldera is surrounded by well bedded ash and lapilli deposits of the Keanakakoi Ash Member. The deposits are 5 to 12 m thick along the southern rim of the caldera and comprise more than a dozen separate layers. Part of the member was produced by an explosive eruption in the caldera around 1790AD. The event features in Hawaiian oral history because warriors close to the caldera at the time were killed, apparently by the effects of the explosions.

The historic record refers to the culmination of a prolonged explosive eruption that had three main phases. The first phase was phreatomagmatic and generated well bedded airfall ash rich in glassy, variably vesiculated, juvenile magmatic and dense, lithic pyroclasts. The second phase produced a strombolian scoria fall deposit, followed by phreatomagmatic ash similar to that of the first phase. The third and culminating phase was phreatic, and deposited lithic-rich lapilli and block fall layers, interbedded with cross-bedded surge deposits, and accretionary lapilli-rich, fine ash beds. This final phase comprised at least four explosive pulses, one of which may have been responsible for the deaths of the warriors. The three phases were separated by quiescent spells during which primary ash was redeposited downwind in dunes migrating southwestward, and locally eroded by fluvial runoff close to the rim.

Explosive hydrovolcanic eruptions from Kilauea's summit are rare. The special circumstance promoting such behaviour over more typical lava effusion appears, in this case, to have been exceptionally deep withdrawal of magma in the summit conduit. The ash deposits indicate that magma was held near the level of groundwater aquifers, which at present are almost 500 m below the southern rim. Also, the explosive activity at Kilauea's summit coincided with lava effusion from vent(s) on the East Rift Zone at an elevation between 300 m and 400 m asl. The rift zone eruption probably drained magma from the summit storage and lowered the magma column there to a level perhaps as much as several hundred metres below the rim. A discontinuous layer of reticulite at the base of the Keanakakoi Ash close to the caldera rim indicates that fire fountaining took place from summit vents prior to the hydrovolcanic activity. The deposition of reticulite close to its source without other proximal deposits (such as denser scoria, block or bomb beds), suggests that the eruptions originated from a deep crater, with only the lightest pyroclasts from the top of the fire fountains being blown clear of the crater rim. Heavier pyroclasts presumably fell back into the crater. Finally, during the early decades of the nineteenth century the floor of Kilauea was much lower than at present (some 300 m to 500 m below the rim).

The change from phreatomagmatic to phreatic phases in the Keanakakoi eruption may reflect the progressive degassing and cooling of the magma during deep withdrawal, so that magma vesiculation no longer contributed to the explosive interaction with water by initiating the fragmentation process. Thereafter, the main role of the subsiding magma column was to supply heat for the steam production that drove phreatic explosions of the final phase.

CHLORINE AND TRACE ELEMENT EMISSIONS FROM MOUNT EREBUS, ANTARCTICA

MEEKER, K. A., ESS-1, MS D462, Los Alamos National Laboratory, Los Alamos, NM 87545 USA

KYLE, P. R., Geosciences Department, New Mexico Institute of Mining and Technology, Socorro, NM 87801 USA

FINNEGAN, D., INC-7, MS J514, Los Alamos National Laboratory, Los Alamos, NM 87545 USA

CHUAN, R., Brunswick Corporation, Costa Mesa, CA 92626 USA

Ozone is depleted in the Antarctic stratosphere during spring due to reactions mainly with Cl compounds. Mt. Erebus, an active volcano on Ross Island, Antarctica, has contained a permanent anorthoclase phonolite lava lake since 1972 and may be a significant source of HCl to the Antarctic atmosphere and thus could have a role in the ozone destruction.

During December 1986 we measured in the Erebus plume SO_2 emissions by correlation spectrometer (COSPEC), particle sizes and emission rates using a quartz crystal microbalance cascade impactor (QCM) and collected acidic volatiles and trace metals on particle and ^{7}LiOH-treated filters. The filters were analyzed by instrumental neutron activation and ion chromatography. QCM samples were examined by energy dispersive x-ray analysis and scanning electron microscope.

Enrichment factors in the Erebus plume for volatile elements Cl, F, As, S, and Au were between 10^3 and 10^5. The enrichment factor (EF) is a measure of the degree of fractionation of a volatile element versus a nonvolatile element between the gas and the magma. Elemental Au and a Au-Cl compound were seen as particles in the QCM samples. Cl was also associated with As and Sb on particle and treated filters. These findings indicate that Cl may be important in vapor-phase transport.

Atmospheric element fluxes were determined using the average measured SO_2 flux of 20 tonnes/day (t/d) and element/S ratios. HCl dominated with a flux of 104 t/d, although HF was also substantial at 40 t/d. Fluxes for Na, K, Zn, and As were 7, 6, 0.2, and 0.1 t/d, respectively. Preliminary results suggest Sb and Au emission rates of 2 and 0.1 kg/day, respectively.

The measured HCl emission rate for Erebus is about 2% of the estimated global volcanic flux, suggesting that global estimates are probably low. In 1983, Erebus was emitting 230 t/d of SO_2, and assuming a Cl/S ratio of 10, as previously measured, Erebus could have been emitting as much as 1000 t/d of HCl. Under normal conditions HCl has a short residence time in the troposphere, which prevents it from reaching the stratosphere. This may not be the case in the dry Antarctic atmosphere, especially during the winter months when HCl from Erebus could potentially reach the stratosphere and be involved in the ozone depletion process.

CRYPTIC METASOMATISM AND CREATION OF MELTS WITH DEPLETED CONTENTS OF THE HIGH-FIELD-STRENGTH ELEMENTS: COUPLED EFFECTS DUE TO INFILTRATION OF MELT INTO HARZBURGITE

MEEN, James K., Dept. Geology, University of North Carolina, Chapel Hill, NC 27599, and AYERS, John C., Dept. Geology, Rensselaer Polytechnic Institute, Troy NY 12180

Many magmas derived from metasomatized mantle above subducted slabs and some magmas from continental mantle have variably depleted high-field-strength element (HFSE) contents compared with their contents of large-ion-lithophile elements (LILE). This may not reflect similar depletions in original metasomatizing liquids nor result from retention of HFSE-concentrating phases in residues of melting of metasomatic mantle. In fact, melts of experimentally-modelled metasomatites are comparably enriched in both HFSE and LILE.

Most subduction-related magmas and many continental alkaline magmas probably have source regions composed of complicated stockworks in which enriched dikes and veins are distributed within an older matrix of refractory harzburgite that was residual to extraction of basaltic liquids. Low-degree partial melts of such a mantle will be unevenly distributed and may not be able to separate from their sources. In this case, surface-energy considerations suggest that the liquids will infiltrate the harzburgitic matrix, resulting in exchange of minor and trace elements between the liquid and the solids. This may result in profound alterations of trace-element enrichments in both end-members.

Olivine and orthopyroxene preferentially extract Ti, Nb, Zr, and Ta from the liquid, resulting in HFSE-depletion in the latter, but reaction with harzburgite does not similarly reduce contents of LILE. The extent of relative depletion depends on the effective value of liquid:solid and on the mineral constitution of the solid. (For example, HFSE are more readily extracted by orthopyroxene than by olivine.)

In cases in which the matrix contains clinopyroxene, liquid-solid interaction results in the enrichment of clinopyroxenes in Sr, LREE, and some other LILE. This is not accompanied by significant changes in the major-element chemistry of the solid or liquid, and is a mechanism of causing cryptic metasomatism of the wall-rocks to the stockwork.

Sr-Nd-Pb isotopic compositions of both liquids and solids may undergo significant linear shifts due to the exchange, although the liquids experience only limited change in major- and trace-element compositions during such reactions. Examples of such decoupling of elemental and isotopic compositions in some suites of magmatic rocks believed to have been derived from metasomatized continental mantle systems will be described.

If, following infiltration of the wall-rock, the temperature of the stockwork is elevated further, the liquid may be extracted from the system because of the greater amount of liquids present, because the matrix becomes more deformable, or by a combination of both effects. Alternatively, liquids may crystallize *in situ*, resulting in modal metasomatism of the mantle over a relatively wide area.

Effects discussed above are pronounced only where extensive interactions between liquid and depleted peridotite occur. This particular type of zone-refining may occur where liquids derived from asthenospheric sources must pass through thick cold lithosphere to reach the surface. Passage requires advective heating of the lithosphere by multiple magma batches and results in development of extensive stockworks along preferred pathways. As these stockworks are, presumably, the source of the majority of continental mantle xenoliths, our sample of the continental lithosphere is biased towards one that dominantly records the complex solid-liquid interactions in such a system.

Sources of many subduction-related magmas and continental alkaline magmas may reside in stockworks, and extraction of the liquids can result in intense peridotite-liquid interaction. Liquids depleted in HFSE and xenoliths exhibiting complex metasomatic features may, thus, be reflections of processes that occur during passage of fertile material through overlying mantle. Depletion of HFSE in igneous rocks in continental settings is, therefore, not necessarily an indication that a subduction-related component was involved in their source.

EVOLUTION STAGES OF THE SOUTHWEST CHINA TRAP AND THEIR CHEMICAL FEATURES

MEI, Hou-Jun, Institute of Geochemistry, Academia Sinica, P.O. Box 91, Guiyang 550002, Guizhou Prov., China

The Southwest China Trap, occurring in Sichuan, Yunnan, Guangxi, and Guizhou provinces, can be divided into three stages of basaltic magmatism.

Stage I, Preparatory Trap (Late Proterozoic--Carboniferous) includes Precambrian norite intrusions in Yanbian county and dolerite dykes in Dongchuan county, Ordovician--Carboniferous Panzihua layered intrusion swarm with V-Ti-Fe ore in Xichang prefecture and Dukou municipality.

Stage II, Ortho-trap (Permian) includes the Emeishan Basalt Formation of flood basalt, covering an area about 260,000 km^2, dolerite dyke swarms in Qiaojia county and in Dali county, and the Hongshijin intrusion swarm of ultramafic-mafic rocks in Huili-Yuanmo area (274.7 Ma). The average of chemical composition of the Emeishan flood basalt (109 samples, in wt.%) is as follows: 48.29% SiO_2, 3.21% TiO_2, 13.60% Al_2O_3, 5.37% Fe_2O_3, 8.48% FeO, 0.18% MnO, 4.86% MgO, 8.35% CaO, 2.58% Na_2O, 1.25% K_2O and 0.36% P_2O_5. Most of the flood basalt is richer in Ti, K and Na than other trap areas on the world. However, it seems as if the Emeishan basalt should belong to tholeiite suite, because the flood basalt has high F value in F-A-M diagram and has few nepheline norm of C.I.P.W. method, and most of the flood basalt has quartz norm. The REE patterns of the flood basalt are between that of continental tholeiite and continental alkali basalt.

Stage III, Para-trap (Triassic-Jurassic) includes Triassic Banwa dyke swarm of titanaugite dolerite in Wenshan and Bose prefecture, covering about 120,000 km^2, the Anding swarm of norite in Wenshan prefecture, and the Longkang necks of andesite-basalt in Funing and Napo county, and Jurassic Shiping dyke swarm of dolerite (165.3 Ma) in Shiping and Jianshui county, covering about 10,000 km^2. The titanaugite dolerite of Banwa swarm may be the product of an inner-plate basaltic magma according to the Th-Hf-Ta diagram of Wood. What characterizes the rocks of the Banwa and Anding swarm is similar to the rocks of the trap of Noril'sk area in Siberia, U.S.S.R.

THE GEOCHEMISTRY AND PETROGENESIS OF TERTIARY ANOROGENIC RHYOLITES FROM N.E. IRELAND

MEIGHAN, I. G., Department of Geology, The Queen's University, Belfast, N. Ireland, U.K., GAMBLE, J. A., Department of Geology, Victoria University of Wellington, New Zealand, and MCCORMICK, A. G., Department of Geology, The Queen's University, Belfast, N. Ireland, U.K.

In N.E. Ireland Tertiary rhyolites are associated spatially and temporally with the Interbasaltic Formation, a horizon which marks a period of quiescence in the eruption of the early Tertiary flood basalts. They include a localized lava dome complex and intrusive members: ash-flow deposits are also known. Volumetrically they provide the best opportunity to study subaerial silicic volcanism in the British Tertiary Volcanic Province (BTVP). In comparison with the Scottish centers their setting ranges from "Highland" (H), i.e. N of Highland Boundary Fault through "Midland Valley" (MV) to "Southern Uplands" (SU).

Phenocryst phases include quartz, plagioclase (Ab85-Ab66), alkali feldspar (Or46-Or63) and rare biotite (Fe/Fe + Mg = .98) and fayalitic olivine; allanite, zircon and apatite and Fe-Ti oxides are accessories.

LIL and HFS elements have been determined for specimens from all known localities together with REE and O, H, Sr and Nd isotopes on representative samples. Data encompassing the compositional range are presented.

Setting	D.I.	Rb/Sr	Ce_N/Yb_N	Eu/Eu*	εNd^{60Ma}	$\partial^{18}O_{w.r.}$	$\partial D_{w.r.}$
H	95.5	228.5	0.54	0.029	-4.1	+9.4	-103
MV	95.4	82.2	1.04	0.052	-6.2	+8.3	-103
MV	96.6	467.0	0.47	0.013	-2.2	+6.6	-107
MV	94.6	3.67	5.24	0.30	-3.4	+10.2	-89
SU	92.4	14.82	-	-	-1.5	+9.5	-

Other pertinent geochemical parameters include negative correlations between Rb and Sr, Rb and Ba and high abundances of U, Th and Cs and Sn. Zr decreases with increasing Rb but Nb increases. The REE patterns have strong negative Eu-anomalies, Eu and Eu/Eu* decreasing with >Rb and with >Differentiation Index (D.I.) values. Furthermore, total REE abundances actually decrease with >D.I., the patterns evolving from LREE enriched ($Ce_N/Yb_N \leq 6.4$) to LREE depleted ($Ce_N/Yb_N < 0.5$).

The chemical trends are explained by extensive fractionation of feldspars plus accessory phases. However, despite overall geochemical similarities (e.g. low Sr), it is apparent that the rhyolites do not constitute a single comagmatic suite and clearly simple fractional crystallization cannot account for the spread in isotopic data. Essentially the latter is interpreted as reflecting interaction of the parental magmas with the lithosphere. Regression of all the available Rb-Sr data yields a 60 Ma "age" which is within error of independent determinations by the K-Ar and $^{40}Ar/^{39}Ar$ methods. The initial ratio, $0.707 \pm 9(2)$, is comparable to other crustally contaminated differentiates from BTVP. The coherence of these Rb-Sr data suggest that extensive magma fractionation followed bulk and selective contamination of the parental magmas. The Nd isotopic values are significantly more radiogenic than those for acid rocks in the Hebridean sector of BTVP and are consistent with a model involving contamination of mantle-derived magmas in the upper crust.

Interpretation of the oxygen isotope data is complicated by: (1) the d values, which indicate some interaction with meteoric water, and (2) a porphyritic obsidian with a high ^{18}O value (+13.1‰) which perhaps is the result of low temperature hydration. Nevertheless, some of the oxygen values may reflect interaction with lithosphere at the magmatic stage. Thus the rhyolites are envisaged as end products of the extreme crystal fractionation of mantle derived mafic magmas which interacted with crust.

STRUCTURE AND FORMATION OF LA PRIMAVERA, CALDERA, JALISCO, MEXICO

MENA, M. and YOKOYAMA, I., Instituto de Geofisica, Universidad Nacional Autónoma de Mexico, Ciudad Universitaria, 04510 Mexico, D.F.

La Primavera caldera was formed about 95,000' years B.P., accompanying ash flows representing about 20 km^3 of magmas. It measures about 13 km in diameter but the boundary is not always clear due to extrusion of post-caldera domes. It is classified as a "resurgent caldera" by geologists. Since 1980, many drillings exploring for geothermal energy reached depths of 2 to 3 kilometers at the center of the caldera. The results of the drillings, together with those of geophysical explorations, provide information about the subsurface structure of the caldera and, consequently, bases for discussion about its formation process.

REGIONAL STRUCTURE Bouguer gravity anomalies in the region along a north-south line reaching about 60 km long from La primavera caldera to San Marcos have been obtained by the Japan International Cooperation Agency (1986). At both end points drillings by the Comision Federal de Electricidad have reached the granitic basement at depths of about 2.8 km. This proves that regional gravity anomalies can be interpreted in terms of the depths of the granitic basements.

CALDERA STRUCTURE The local gravity anomalies show two lows within the caldera, reflecting the configuration of andesitic basements for which an average depth of 700 m has been determined by drillings. The anomalies suggest that there were two explosion centers during the caldera-forming eruptions and that each explosion center formed a funnel-shaped depression as has been found for many other calderas. The mass deficiency within the caldera is estimated by Gauss's theorem at 1.3×10^{10} ton. The relationship between the mass deficiency [delta] M (ton) and caldera diameter D (km) agree with the relationship

$$[\text{delta}]M = 2.0 \times 10^{6} D^{3.3}$$

which was previously deduced by Yokoyama (1987) from the data from various low gravity anomaly type calderas. This relationship means that the caldera structure is approximately three-dimensional: the larger in diameter, the deeper in depression. If calderas were formed by pistonlike collapses producing an equivalent vertical depression (around 100 m), the structure would be two dimensional.

Drilling results reveal that surface topographies such as post-caldera domes scarcely disturb the subsurface strata. The two explosion centers assumed to be within the caldera from the gravity anomalies produced explosion funnels of about 700 m depth in the andesitic basement, but the granitic basement at a depth of about 2.8 km, remained unbrecciated. Such a subsurface structure means that caldera formation does not need "collapse into magma reservoirs", and that no particular "resurgences" are necessary to interpret uplifts of the caldera surface after its formation.

ASTHENOSPHERE-LITHOSPHERE INTERACTION BENEATH THE ZUNI- BANDERA VOLCANIC FIELD, NEW MEXICO.

MENZIES, Martin A. Department of Geology, (RHBNC), University of London, Egham, Surrey, TW20 OEX, England.
KYLE, P., Department of Geosciences, (NMIMT), Socorro, New Mexico, U.S.A.

The Zuni-Bandera volcanic field is located in the "transition zone" between the Colorado Plateau & the Basin & Range and throughout the Quaternary alkaline and tholeiitic lavas were erupted concurrently. To what extent this can be related to lithospheric extension and increasing amounts of melting can be assessed with geochemical data.

High level crustal input : The overall linearity of the ZBVF data on a $^{87}Sr/^{86}Sr$ vs. Sr diagram has traditionally been interpreted to mean that the volcanic rocks in question have mixed with variable quantities of crustal material, but the highest concentrations of K, SiO_2 [Rb, Th, La, Ce, Sm, Zr, Hf] occur in the basaltic rock with the lowest strontium isotopic ratio & the highest MgO content. Also concentrations of these elements *decrease* systematically from alkaline to tholeiitic compositions with a concomitant increase in $^{87}Sr/^{86}Sr$.

Low level crustal input: In general the high Zr/Ba (or high Ta/Sr, low La/Nb) ratios of the ZB volcanic rocks are not compatible with supra-subduction enrichment processes, & are more akin to intra-plate enrichment processes. Furthermore the variation in Th/Ta ratio is similar to that observed in intra-plate oceanic and continental volcanic rocks & attests to the lack of any enrichment in Th relative to Ta as might be expected if crustal material had been recycled into the source during subduction. Finally, none of the ZB volcanic rocks have the elevated Ba/Ta ratios associated with classic arc magmas. The only hint of possible crustal involvement - the highest La/Nb & Ba/Ta ratios are associated with the most radiogenic isotopic ratios. This may imply that a Proterozoic or Archaean component was involved in magmagenesis but that its contribution is minor having been swamped by trace element enrichments associated with intra-plate processes.

Mantle processes : The use of a partial melting diagram can help constrain the character of mantle components & the possible mechanisms involved in their origin. The ZBVF data have a greater variation in Zr/Y and Zr/Nb ratio than most oceanic volcanic rocks & the data define an hyperbola between two compositionally distinct components similar to that defined by P-T-N MORB's from the Southern Oceans. Within the ZBVF, however, the $^{87}Sr/^{86}Sr$ ratio *increases* towards the field of MORB such that the rock with the highest Zr/Y ratio (small degree melt) has the lowest $^{87}Sr/^{86}Sr$ ratio & the rock with the lowest Zr/Y ratio (large degree melt) has the highest $^{87}Sr/^{86}Sr$ ratio.

Interpretation : In general the basaltic rocks exhibit considerable diversity in their trace element and isotopic ratios due primarily to mixing of magmas from distinct asthenospheric (mantle) & lithospheric (crust or mantle) sources. Since the Zuni-Bandera enriched component has some similarities to other southern Basin & Range alkaline magmas it is proposed that it has a similar source in the MORB asthenosphere. The greater enrichments in trace element ratios, particularly La/Yb and Zr/Y, suggest that the alkaline magma at Zuni-Bandera is a very small degree melt of the asthenosphere (e.g.Ta/Yb=6.0; $(La/Yb)_N$=60; Zr/Y = 19; $^{87}Sr/^{86}Sr$ < 0.703). The most chemically depleted tholeiitic magma is believed to be a larger degree melt of the lithospheric mantle (e.g. Ta/Yb < 0.5; $(La/Yb)_N$ < 15.0; Zr/Y = 4-5; $^{87}Sr/^{86}Sr$ > 0.706) as the amount of extension increased and the thickness of the melt column increased. The petrology and chemistry of basalt-borne xenoliths from the ZBVF would permit extraction of such tholeiitic melts at appropriate degrees of melting.

VOLCANIC HAZARD ASSESSMENT OF SANTIAGUITO DOME, GUATEMALA

MERCADO, R. and ROSE, W.I., both at Michigan Technological University, Houghton, MI 49931,
MATIAS, O. and GIRON, J., both at Seccion de Vulcanologia, INSIVUMEH, 7a Avenida 14-57, Zona 13, Guatemala, Central America

Santiaguito is a 350 m high dacitic dome located in the 1902 eruption crater of Santa Maria Volcano. It has been continuously active since its birth in 1922, and its dacitic character was verified with 18 new XRF analyses (63-67% SiO2). Present activity is centered at Caliente vent, and is characterized by 1-5 small phreatic (?) ash eruptions per hour, and constant avalanching from a 5 km long lava flow. Small accumulations of ash (1 mm) occur as far away as 14 km from the dome.

Ten weeks of field work in the spring of 1988 resulted in the preparation of hazard maps for Santiaguito. Considerable hazards are associated with the dome. Hazard zonation is strongly controlled by the assymetrical southwatd slope of basement topography, parallel drainages and very high rainfall (3-6 m/yr). The 1902 crater geometry, which bounds the dome to the north, east, and west also directs hazards southward. Ashfall hazards are controlled by the prevailing wind directions, which will tend to carry ash to the west from June to November, and to the east from December to May. Two main hazards are of special concern: (1) the possibility of dome collapse and associated pyroclastic flows, and (2) lahars and flooding. Ashfall and lava flow hazards to inhabited areas are minimal.

The most hazardous event in Santiaguito's continuous 67 years activity occurred in 1929 when a collapse of the dome generated pyroclastic flows, killing as many as 5000 people. Two smaller collapses occurred in 1973, and small nuees ardentes of a variety of scales have been generated by collapse of active lava flow fronts.

Lahars and flooding have been the most serious hazard over the past 15 years. The town of El Palmar has been severely affected by aggradations in rivers draining the dome, and the situation is worsening as the only remaining barrier between River Nima II and the town is laharic deposits which are likely to shift with the incoming rains. The Guatemalan government is in the process of moving the town, but there are still about 1000 families in the town and inmediate countryside. Several other towns and major highways south of El Palmar are also potentially threatened.

PETROGENESIS OF RECENT ALKALI BASALTS IN WELLS GRAY PROVINCIAL PARK, BRITISH COLUMBIA

P. Metcalfe, Skyline Explorations Ltd., 301-675 W. Hastings St., Vancouver, B.C., Canada

Basaltic volcanism in the area of Wells Gray Provincial Park, east-central British Columbia, represents some of the youngest volcanic material in the Canadian Cordillera. Basalts from the eleven centres studied range in age from 0.3 Ma to as recent as 300 a. The centres are polygenetic and, with one exception, of central type. The maximum erupted volume for any centre is 0.3 km^3, suggesting that centres separated by greater than 10 km derive magma from separate source regions.

Lavas erupted from the centres are alkaline, with Mg numbers ranging from 60 to 66. The lavas are olivine and clinopyroxene phyric and contain abundant xenocrysts of olivine and clinopyroxene with moderately abundant xenoliths of spinel lherzolite, spinel clinopyroxenite and websterite. Incognate clinopyroxene compositions are of four distinct types. Occurrences of kaersutitic amphibole in clinopyroxenite and one occurrence of primary apatite in ferroan websterite indicate the presence of volatile phases within the subcordilleran mantle.

Major and trace element concentrations in the Wells Gray lavas indicate that significant crystal fractionation has not occurred and that the lavas are derived from source regions which are slightly enriched in Fe. Incompatible element concentrations in lavas erupted from the same centre indicate that later lavas are more refractory in composition. It is probable that later lavas erupted from each centre were derived, in part, from a volume of that source region depleted by extraction of the earlier lavas.

Incompatible element concentrations and Sr and Nd isotopic ratios define two major magma types, Type 1 being enriched in Ba and $^{87}Sr/^{86}Sr$ and depleted in Zr and $^{143}Nd/^{144}Nd$ relative to Type 2 lavas. Isotopic variation between these lava types lies subparallel to the trend observed in data from ocean island basalts. Isotopic variation is also observed between earlier and later eruptive events within discrete centres; a correlation is observed with P_2O_5, suggesting that this variation is controlled by melting of or equilibration with a phosphate phase in the source region.

The chemical, mineralogical and isotopic heterogeneity of the Wells Gray lavas is interpreted as evidence of equivalent heterogeneity present in the source regions, caused by mixing of source material with MORB and alkali basalt isotopic signatures. The mixing event is interpreted as mantle metasomatism; the metasomatic event was sufficiently recent as to preclude equilibration of Nd isotopic compositions before generation of the lavas.

ROLE OF CO_2 AS CARRER GAS IN DEGASSING OF SULFUR DURING THE 1783 LAKAGIGAR ERUPTION (ICELAND).

METRICH, N., Laboratoire P. Sue, CEN-Saclay, 91191, Gif-sur-Yvette, France, and SIGURDSSON, H., Graduate School of Oceanography, University of Rhode Island, Narragansett, R.I. 02882, USA.

12.3 km³ of basaltic magma were produced during the 50-day Lakagigar eruption, which may have been derived from a high-level reservoir of the Grimsvotn central volcano. Whole-rock composition is Fe-Ti basalt (Mg# 0.45). However, melt inclusions trapped in anorthitic plagioclase and Fo_{86} to Fo_{75} olivines show a large range of compositions, from rare olivine-tholeiite (Mg# 0.64, K_2O 0.10 wt %) to Fe-Ti basalt (Mg# 0.59-0.42 ; K_2O 0.3-0.4 wt %). Most matrix glasses are Fe-Ti basalts, with Mg# from 0.47 to 0.37. The most differentiated liquids (Mg# 0.34) are rich in TiO_2 and FeO and are trapped as rare melt inclusions in clinopyroxenes. The observed range of chemical compositions indicates that the magma chamber was vertically zoned before eruption, with Fe-Ti basalt as dominant type and with highly evolved Fe-Ti rich basalt confined at the top. Occurence of olivine-tholeiite magma is consistent with periodic refilling of the magmatic system. Major element variations in Fe-Ti basalt are also considered as the result of both magma-mixing and fractional crystallization processes.

Chlorine content increases from 50 ±50 ppm in primitive tholeiite up to 230±100 ppm in Fe-Ti basalts, without clear evidence of degassing. Melt inclusions show that sulfur varies from 1000 ±200 ppm to 2020 ±100 ppm, for Mg# between 0.64 and 0.41. Sulfur degassing correlates both with vesicularity and magma composition. Thus in matrix glasses sulfur decreases from 1490 ±160 ppm to 500 ±150 ppm, as Mg# decreases (0.47 to 0.37) and vesicularity of the magma (~1 to 65 vol %) strongly increases. These results imply that at least 75 % of the initial sulfur content has been lost during the eruption. Low sulfur content of matrix glasses can be regarded as the effect of efficient degassing in relation to the vesicularity of the magma. The high vesicularity of some tephra indicates the presence of a major volatile phase. There is no evidence for high water content in this magma, but the most probable major volatile phase is CO_2.

Our model is consistent with the hypothesis of CO_2 degassing of primitive tholeiite magma at depth, inducing a quasi-permanent CO_2 flux to the shallow-level magmatic reservoir, and accumulation of a CO_2-rich free volatile phase in the upper part of the system. Vertical gradients in CO_2-induced vesicularity and major element magma composition were established in the reservoir. During magma withdrawal from the reservoir and eruption, sulfur degassing was controlled by inherent CO_2-induced vesicularity of the magma. These results have important implications for degassing of basic and CO_2-rich magmas during volcanic eruptions, as they indicate that the efficiency of sulfur degassing is largely controlled by the vesicularity and abundance of a free CO_2-rich volatile phase.

INTRACALDERA FACIES OF THE AMALIA TUFF: INSIGHTS INTO COLLAPSE AND ERUPTION PROCESSES

MEYER, J.M., University of California, Santa Barbara, Santa Barbara, California 93106

Extreme post-collapse extensional tilting of the Questa caldera due to early Rio Grande rift extension has resulted in 3 cross-sectional views of the intracaldera Amalia Tuff near the south caldera wall. These exposures allow investigation of the lateral variation of the intracaldera megabreccia unit both along and at right angles to the caldera margin. Additionally, a unique? "basal broken crystal" intracaldera unit has been identified.

The megabreccia facies changes outward at right angles to the south caldera margin. Nearest to the south caldera wall, the megabreccia zone thickens and welding and devitrification in the Amalia tuff are less developed. With increasing distance from the caldera wall breccia blocks become smaller and more rounded and a greater range of the available pre-caldera stratigraphy is found in the blocks.

Parallel to the south caldera margin, the megabreccia is spatially and compositionally variable. In the southwest portion of the caldera, the blocks are dominantly of andesite flows and the megabreccia facies occurs near the base of the caldera fill. In the southeast portion of the caldera, the blocks are dominantly of quartz latite flows and intrusions, the megabreccia facies is stratigraph-ically higher in the intracaldera tuff, and blocks are large and coherent. A pre-collapse volcanic center is interpreted near the southeast caldera wall. Units in that center are more massive, would have resisted slumpage until later in the caldera fill cycle, and would have slumped in larger, more coherent blocks.

Locally, on the top of megabreccia blocks, there is a unit of the Amalia Tuff that is massive to poorly bedded and has distinctly more broken phenocrysts than the normal ashflow unit. This broken unit contains variable amounts of lithic fragments that appear to be intrusive equivalents of the Amalia Tuff. Examples exist of both sharp and gradational contacts with the overlying tuff. This unit is termed the basal broken crystal zone, and is interpreted as representing the initial vent clearing phases of intracaldera tuff following short-term pauses in the eruptive cycle. These deposits may be only preserved very near to the vents in the caldera fill, where eruption and flow-transport process have not incorporated them into the main body of the ashflow.

The occurrence of megabreccia blocks at different stratigraphic horizons suggests piecemeal failure of the oversteepened structural caldera margin during collapse. The appearance of basal broken crystal horizons on top of megabreccia blocks suggests that caldera wall slumpage occurred during short-term pauses in the caldera fill cycle and that the initiation of the next pulse of eruption (be it from the same or different vents) was highly explosive. Similar basal broken crystal units should occur in other deposits.

INTRUSION OF BASALTIC MAGMA INTO A CRYSTALLIZING GRANITIC MAGMA CHAMBER: CORDILLERA DEL PAINE IN THE SOUTHERNMOST ANDES, CHILE

MICHAEL, P.J., Department of Geosciences, The University of Tulsa, Tulsa, OK 74104

The 12 m.y. Cordillera del Paine pluton intrudes unmetamorphosed Cretaceous turbidites and occupies an elliptical area of 150 km^2. It is located 30 km east of the eastern margin of the Patagonian batholith and 25 km west of 2 m.y. old, tholeiitic-alkaline Patagonian flood basalts, and is in a tectonic province that is transitional between the active arc and the back-arc. The well-exposed pluton is composed predominantly of a homogeneous biotite granite, the Paine Granite (PG), which intruded to a shallow level.

At lower exposures near the margins of the pluton, there are gabbros, monzodiorites and quartz monzodiorites: the Paine Mafic Complex (PMC). The contact of the PMC with the PG is at a remarkably constant elevation throughout the pluton. Mafic inclusions are extremely rare above 1000 meters a.s.l, whereas mafic rocks dominate exposures at lower levels. Near the margins of the pluton, contacts between the PMC and PG are parallell with sidewall contacts of PG and country rock. Mafic magma may have ascended to a level that was governed by the degree of solidification of the PG. Alternatively, the intrusion of mafic magma may have been directed by a local stress regime that was generated by the PG.

The PMC is highly disrupted by the PG at the core of the pluton, and consists of zones of monzodiorites separated by zones of PG that are charged with mafic inclusions. At both the margin and core of the pluton, mafic rocks are frequently chilled against the PG or against intermediate rocks and they have crenulate, convex-inward margins. Fragments of solid, chilled mafic rock were swept up by the PG near contacts indicating that basaltic and granitic magmas have comingled. The extent of physical stirring was greater in the core of the pluton, suggesting that at the time of mafic intrusion, the PG was cooler, more crystallized and less mobile at its margins, and thus inhibited magma mixing. High-level mixing was inhibited in all parts of the pluton by the strong thermal contrast between mafic and granitic magmas, and by the chilled basalt at the interface. Rocks having 60-68% SiO_2 are rare within the pluton.

Layered gabbros at the pluton's margins grade irregularly upward into monzodiorites and quartz monzodiorites. Crystals in gabbros are strongly zoned, and frequently have reaction rims. The gabbros have cumulate textures and disequilibrium mineral assemblages including forsteritic olivine (rimmed by orthopyroxene) and quartz. The cumulate nature of the gabbros and the geochemical variations within the PMC suggest that monzodiorites and quartz monzodiorites were derived mostly by fractional crystallization of mafic magma: high-level mixing between mafic and granitic magmas did not occur. However, there is evidence for localized, volumetrically insignificant mixing between granitic magma and evolved mafic (i.e., intermediate) magma.

Although high-level mixing was inhibited for thermal reasons, it is possible that granitic and intermediate-composition magmas contaminated each other at lower levels. The disequilibrium assemblages in dikes and gabbros suggest that mafic magma was slightly contaminated by granitic magma at lower levels, before it was intruded to its current high level. Similarly, a late phase of the PG in the core of the pluton is slightly more mafic than the rest of the PG, and may have resulted from contamination of granitic magma by intermediate magma at depth.

Mafic dikes which have intruded the upper levels of the PG have essentially the same mineralogy and reactions as the PMC. Their chemistry and petrography suggests that the mafic magmas were fairly primitive and were transitional between alkali olivine and tholeiitic basalts. Their estimated compositions are remarkably similar to those of the Patagonian flood basalts to the east.

The Fitz Roy massif, located 200 km north of Cordillera del Paine in Argentina, is a bimodal granite-gabbro pluton that is structurally and petrographically similar to Paine. It is 18 m.y. old and is in a similar tectonic position as Cordillera del Paine. Compared to the PMC, the Fitz Roy mafic rocks have higher CaO and Zr/Nb, and lower Na_2O, TiO_2, Sr and Nb. Comparison of the granitic rocks from the two plutons reveals the same differences: the Fitz Roy granite has higher CaO and Zr/Nb and lower Na_2O, TiO_2, Sr and Nb at a particular SiO_2 content, than the PG. The consistent characteristics between granites and mafic rocks within each pluton, despite marked differences between the plutons, suggests that the granites have formed by extended fractional crystallization of mafic magmas which were similar to the ones emplaced contemporaneously with the granite. .

PETROGENESIS OF THE MT WELD CARBONATITE COMPLEX

MIDDLEMOST, Eric, Dept. Geology & Geophysics, University of Sydney, 2006, NSW, Australia.

The circa 2.06 Ga Mt Weld carbonatite complex of Western Australia intrudes an Archean greenstone sequence. Carbonatites form the core of the complex and they are surrounded by phlogopite glimmerites. The dominant carbonatite is sövite. It is intruded by rauhaugites and carbonate-rich veins. The rauhaugites are essentially composed of ankerites, ferroan dolomites, micas, magnetite and apatite, with accessory amounts of pyrrochlore, ilmenite, sphalerite, baddeleyite, pyrite, galena, and REE-rich phases. The micas consisted of titan-phlogopites, low-Ti phlogopites and tetraferriphlogopites. Overall the rocks of the complex are strongly enriched in C, F, P, S, K, Ca, Rb, Sr, Y, Zr, Nb, Cs, Ba, La, Hf, LREE, Ta, Pb, Th and U.

A potassic, peralkaline, silica undersaturated, aillikitic lamprophyric magma was parental to the complex, and it segregated from a fertile harzbugite source rock at approximately 1150^{o}C and 3.0 GPa. When the magma was about 2.5 km below the surface it expanded explosively, and brecciated and reacted with the country rocks. Fractional crystallization, aided by wall-rock reaction, generated the sövite, together with a residual magma enriched in Mg, Fe, and the incompatible elements. Part of this residual magma reacted with the Mg-rich, but relatively Si- and Al-poor, country rocks to produce the phlogopite glimmerites. Later the mechanical mixing of fragments, and rheomorphic lenses, of glimmerite with the residual magma generated the rauhaugites. It is postulated that the Mt Weld complex was emplaced into a rift that developed at the edge of an earlier lithospheric dome.

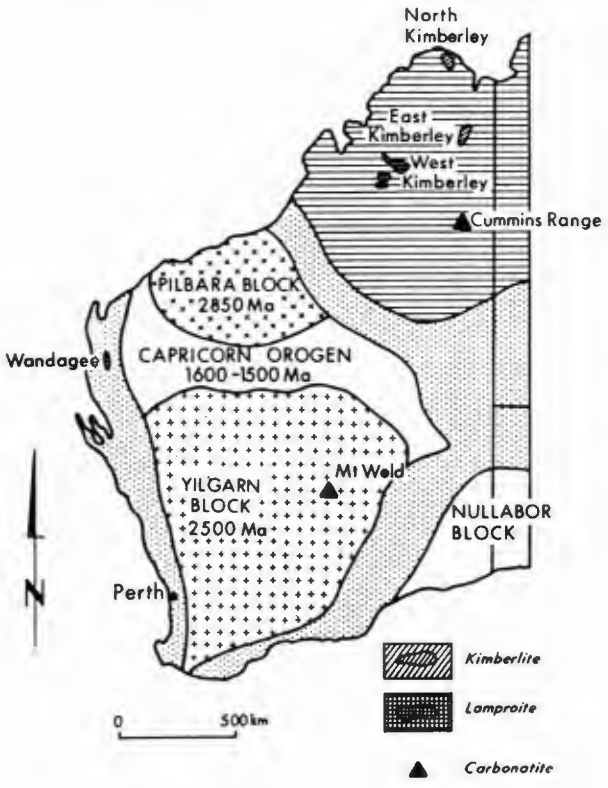

DSS PROFILING ACROSS THE EOLIAN ISLANDS VOLCANIC REGION (TYRRHENIAN SEA, ITALY).

MILANO, G., Osservatorio Vesuviano; 249, Via Manzoni 80123 Naples (Italy).
GUERRA, I., Dip.to Scienze della Terra, Univ. di Cosenza; Rende (Cosenza) ITALY.

The experiment, carried out in 1986, focused the crustal structure of the two southernmost of the seven Eolian Islands, as well as the transition towards the Central Tyrrhenian Basin (at North) and the Northern Sicily Peloritani chain (at South).

Five linear and three constant-offset profiles, modeled by gaussian-beam dynamic ray-tracing, supply the picture of a very rough topography of the crust-mantle interface in the South-North direction (normal to the chain and towards the center of the young, pseudo-oceanic basin).

In particular, the presence of short-wavelength upheavals of the lower-crust interfaces is remarked, as already observed elsewhere in the same basin by OBS refraction profiling.

A major upheaval is emplaced beneath the Southern Eolian active volcanic area, in correspondence of the island of Vulcano, where the whole crust appears to be affected by a general uprise of the equal-velocity boundaries.

This evidence is directly confirmed by passive seismics: teleseismic recording at a dense seismic array shows sharp P-waves advances in the Vulcano area, fully fitting the intermediate-lower crust structure constrained by two, short-range, reversed profiles.

Forward-modeling of two overlapping linear profiles in northern Sicily, retrieval and critical re-interpretation of a 200 km long West-East and of a 550 km long NW-SE traverses of the Tyrrhenian basin, allow to draw a general map of the Moho topography in the area.

A closer view of the shallow-intermediate structure of the active volcanic area is also supplied by merge of active and passive seismics data.

PHYSICAL VOLCANOLOGY AND COMPOSITIONAL CHARACTERISTICS OF THE EASTERN ALEUTIAN ARC AND THEIR CONSTRAINTS ON RHEOLOGIC, TECTONIC, AND PETROGENETIC MODELS

MILLER, T.P., U.S. Geological Survey, 4200 University Dr., Anchorage, Alaska, 99508, USA

The eastern Aleutian arc (EAA) is defined by >35 Quaternary volcanic centers built entirely on continental crust along a segmented 1200-km-long volcanic front extending from near Unimak Pass in the Aleutians to within 130 km of Anchorage. Previous attempts to correlate the spacing, size, composition, and tectonic setting of these volcanic centers have been hampered by a lack of data. Recent geologic mapping and topical studies have identified the principal volcanic centers in the region and significantly expanded our understanding of their eruptive history, composition, and geologic setting.

The Quaternary centers, 19 of which remain active, began to form about 1 Ma in the EAA and have been the sites of 120 historic eruptions. At least 30 centers have been active in Holocene time and 8, scattered over 700 km of the arc, have been sites of 9 major caldera-forming eruptions in latest Pleistocene and Holocene time. The caldera-forming eruptions have bulk ejecta volumes estimated at 10 to >50 km^3 and represent 20-30% of known Holocene eruptions of this magnitude worldwide.

Aleutian arc volcanoes have been considered to have a rather regular spacing of 60-70 km but spacing between centers actually varies greatly. Some "segments" of the arc consisting of 3-4 volcanic centers have a very regular spacing between volcanoes but spacing of different "segments" ranges from 18 to 54 km. Distances between centers elsewhere in the EAA are much less regular and in some cases quite small. A 75-km-long segment in the Katmai area, for example, contains 9 closely-spaced centers. An "average" spacing distance for the EAA (and for the entire arc) appears to be relatively meaningless. It is more significant for modeling purposes that (a) various "segments" have quite different volcano spacings and that (b) the longest volcano-free segment in the entire EAA is 100 km.

Most centers have volumes of <100 km^3; individual centers, however, vary in size from samll central vent volcanoes with volumes of 5-20 km^3 to large long- lived stratocone-caldera complexes with volumes of 300-400 km^3. Volcanic centers do not decrease in size from east to west as some have suggested; instead the largest centers occur in the western 400 km of the EAA, perhaps in response to a complex relationship between convergence angles and rates, crustal thickness and composition, and nature of the subducted material.

EAA cone-building volcanic rocks (based on~1000 analyses) consist predominantly of andesite and low SiO_2 dacite (SiO_2 55-64%); basalts are relatively uncommon. Andesites are medium-K and average 1.27% K_2O at the 57.5% SiO_2 reference level. Rhyolite occurs in ash-flow tuffs and post-caldera domes at several calderas, but high-SiO_2 (>75%) rhyolite is found only in ejecta from the 1912 Valley of 10,000 Smokes eruption and at the associated Novarupta dome.

A change from interspersed tholeiitic and calc-alkaline centers (typical of volcanoes in the oceanic part of the arc) to solely calc-alkaline volcanism occurs 500 km east of the continental shelf edge between Veniaminof and Black Peak calderas, coincident with a change from mafic to silicic post-caldera volcanism and with a trend towards smaller volcanic centers. The 770 km of EAA east of this point (30% of the entire Aleutian arc) is characterized solely by calc-alkaline volcanic centers. Although crustal models are poorly constrained, the abrupt change in several distinct compositional and physical characteristics may be related to the nature and thickness of the crust. Continental crust east of this point may be sufficiently thick and extensive to inhibit the rapid upward passage of magma, resulting in fractionation, mixing, assimilation, and a calc-alkaline differentiation trend. The formation of large high-level magma chambers, as indicated by the unusually large number of calderas along the whole EAA, is apparently not governed by crustal thickness or whatever other factors control the spacing, size, and compositional trends.

QUARTZ LATITES OF THE ETENDEKA FORMATION, NAMIBIA - THE PRODUCTS OF MAJOR HIGH-TEMPERATURE RHEOIGNIMBRITE ERUPTIONS.

MILNER, S.C., & DUNCAN, A.R., Department of Geochemistry, University of Cape Town, Rondebosch 7700 South Africa.

The Etendeka Formation Volcanics (130-135 Ma) of northwestern Namibia form part of the Karoo Igneous Province of southern Africa and consist of a series of basalts interbedded with quartz latites. The quartz latites make up a significant proportion of the succession (>25 %) and constitute as much as 60 % of the outcrop in the southern Etendeka region. They occur as voluminous (80-800 km^3), widespread (up to 4500 km^2) sheet-like units typically between 40 and 300 m thick. Three main groups of quartz latite, the Springbok, Tafelberg and Interbedded coastal groups have been identified. The Upper Springbok unit covers the largest continuous area (ca. 2700 km^2) and has a maximum thickness of 300 m. Individual units consist of basal, main and upper zones. The main zone usually constitutes over 70 % of the unit thickness and typically consists of featureless devitrified quartz latite. In contrast the basal and upper zones of the flow, commonly 5-6 m and 7-10 m thick respectively, are characterised by flow banding, pitchstone lenses and breccias which occasionally contain rare pyroclastic textures. The pyroclastic textures include fiamme (stretching ratios >20), pumice lapilli and glass shards. The quartz latites are sparsely porphyritic (<10 %) with glassy or devitrified groundmass textures. The phenocrysts consist of plagioclase, pyroxene, titanomagnetite and rare ilmenite. Pyroxene and plagioclase geothermometry indicate high (1000-1100 ^oC) temperatures of crystallisation which coupled with an absence of primary hydrous phases, indicate that the quartz latites were relatively hot, H_2O-undersaturated magmas. Major element compositions are very similar in different groups of quartz latites but individual units have extremely uniform compositions both vertically and laterally, which has enabled minor and trace element chemistry to be used as a primary criterion for the correlation of individual quartz latite units across the Southern Etendeka region.

The quartz latites display features common to both rhyolite lavas and ignimbrites and are clearly the products of an unusual eruption style. Despite the flow banding, flow folding and brecciation, more commonly associated with rhyolite lavas, the local preservation of pyroclastic textures and the broad areal extent of these units have led to the conclusion that the quartz latites were erupted as dense, high-temperature ash-flows which underwent en masse lava-like flowage prior to their final emplacement (i.e. they are rheoignimbrites). A combination of high eruption temperatures and calculated viscosities of 10^5 Poise (comparatively low for magmas involved in pyroclastic eruptions) help to explain the completely welded and homogeneous textures encountered at most outcrops. The apparent mobility of the quartz latite ash flows (in excess of 130 km from possible vent areas), coupled with their high eruption temperatures and strongly welded nature require high volume rates of magma eruption and/or descent from very high eruption columns (~10-13 km high).

Volcanic events during the breaking up of the continental crust at Shimane Peninsula, Japan Sea-side of SW Japan

Miyake,Y. and Yamauchi,S.,Dept.of Geology, Shimane University, Matsue, 690,Japan.

Japan Sea opened in the Miocene age as the back arc basin of the Southwest Japan Arc. In the Shimane Peninsula facing the Japan Sea (Fig.1), volcanigenic rocks and sedimentary rocks of middle Miocene are widely distributed and the volcanic events are divided into three stages (Stage I,II,III). The mode of volcanism and the petrochemistry of this area changed form the Stage I to III. It can be attributed to the gradual change of the stress field of SW Japan arc trench system.

Stage I (extensional); Numerous sills and sheets intruded into the marine sediments. These rocks intruded into the wet unconsolidated sediments, marginal part of intrusives beeing suffered shattering fragmentation and intrusion of clastic dikes. The chemical compositions of the intrusives vary from basalt to dacite, and the more fractionated magma intruded into the upper horizon. It is concluded that magma, gradually changing the chemical composition, intermittantly intruded during the sedimentation.

Stage II(neutral);Several submarine volcanoes were formed simultaneously, and plutonic bodies were formed under each corresponding volcano. One of these volcanoes consists of dacitic central lava dome,basaltic lava, and ring dikes (2km in diameter).

Stage III(neutral - compressional); Basaltic lavas erupted in the shallow marine or subaerial circumstances. Many dikes trending north crop out.

Chemical compositions of these magmas changes gradually. In the stage I, basaltic rocks are tholeiitic, very low in K_2O (0.1wt%) and plotted in the MORB field of Ti-Fe/Mg diagram, although Nb is depleted compared to REEs. K,Rb,Ba and LREEs increase toward Stage III (K_2O 1-2% in Stage III). And following the Stage III, the eruption of alkaline basalt (late Miocene-Quarternary) bagan.

Fig.1 Locality map.

PRELIMINARY Sr, Nd, AND Pb ISOTOPIC EVIDENCE FOR MAGMA SOURCES IN SOUTHWESTERN ALASKA

Moll-Stalcup, E.J., Wooden, J.L., Box, S.E., and T.P. Frost, U.S. Geological Survey, Menlo Park, CA, 94025

New Sr, Nd, and Pb whole-rock isotopic data for latest Cretaceous and Cenozoic volcanic and plutonic rocks from the Kuskokwim Mountains in southwestern Alaska define at least three compositional groups on isotope diagrams. Group A is represented by young (<6 Ma) tholeiitic basalts that have primitive Sr, Nd, and Pb isotopic compositions which plot within the field for MORB on Pb-Pb and Sr-Nd isotope diagrams. Group B is represented by latest Cretaceous to Paleocene plutons that are intermediate to felsic (58-68% SiO_2), have moderate $^{87}Sr/^{86}Sr$ and $^{143}Nd/^{144}Nd$ ratios, and have Pb isotopic ratios which plot within the field for MORB, but at more radiogenic compositions than the young basalts. Group C comprises latest Cretaceous to Paleocene volcanic rocks and one of the plutonic rock samples; these rocks have intermediate SiO_2 contents (58-64%) similar to contemporaneous plutonic rocks (Group B), but lower K_2O contents and higher $^{87}Sr/^{86}Sr$, lower $^{143}Nd/^{144}Nd$, and higher $^{208}Pb/^{204}Pb$ and $^{207}Pb/^{204}Pb$. Although Pb isotopic compositions vary widely, all the data plot within the fields for MORB defined by Zindler and Hart (1986), precluding any significant contribution of old continental crust in the formation of these rocks. Limited data suggest that $^{87}Sr/^{86}Sr$ decreases and $^{143}Nd/^{144}Nd$ increases with increasing SiO_2 contents for the latest Cretaceous and Paleocene rocks, possibly indicating that the parental magmas which formed in old lithosphere or mafic crust were contaminated by more isotopically primitive crustal rocks--such as the Mesozoic island-arc basement of the area. Differences in isotopic composition between the plutonic and volcanic rocks require different mantle source compositions and may also indicate different crustal residence level in an isotopically stratified crust. The young basalts formed in asthenospheric mantle, which is clearly unrelated to that of the older rocks.

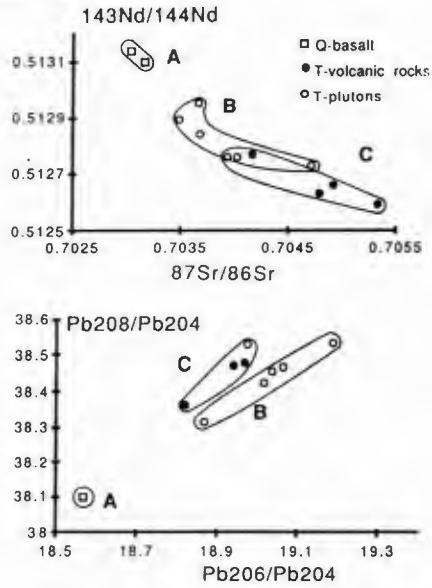

PURACE VOLCANO COLOMBIA

MONSALVE, M.L., INGEOMINAS, AA 695, Popayan, Colombia
CERG, Dpt of mineralogy, University of Geneva, CH-1211 Genève 4, Switzerland

Purace volcano (altitude 4650 m) is part of the central volcanic range of Colombia, it is located 30 km. Southeast from Popayan, capital of the Department of Cauca. It is at the western extremity of a 15 km volcanic chain called Sierra de los Coconucos. It consists of two imbricated craters, the inner one having a diameter of 500 m and a depth of 80 m. Recent activity indicates that it poses a threat for the region; a hazard assesment program is being carried out (Cooperation between INGEOMINAS and CERG, University of Geneva).

The geological history of the volcano can be divided into three major stages: "Chagarton", "Pre-Purace" and "Actual-Purace". As regards the volcanic hazard, it is the latter stage which has been analysed in detail: its products are andesitic lavas, ash and scoria flows, ash and block flows, and pyroclastic falls. The petrographical study shows that these products have a common assemblage of labradorite, hypersthene, augite, hornblende and magnetite, however preliminary geochemical analyses indicate a slight shift towards a more acidic composition with time.

An investigation of the historical documents indicate that the Purace was at least active since the beginning of the last century. During this period, its more common products were ash falls, blocks and bombs, and sometimes lahars. The last eruption took place in March 1977, and it consisted of a minor ash emission.

Actually Purace shows two principal groups of fumaroles, the outer one located in the northern flank, and the inner one related to an east-west explosive fracture in the deep crater. Their temperatures range between 90 and 155°C.

The evolution of the volcanic activity is monitored by a seismic station from the GERSCO Project (regional seismic hazard assesment) as well as periodic visits to the crater where the fumaroles and fractures are controlled.

THE ANDEAN Nd-Sr ISOTOPIC ARRAY: AN EXPRESSION OF CRUST-MANTLE MIXING.

MOORBATH, S. & TAYLOR, P.N., University of Oxford, Department of Earth Sciences, Parks Road, Oxford OX1 3PR, U.K.

We present an updated compilation of the Andean Nd-Sr isotopic array for Recent volcanics (Fig.1) based on c.150 samples, covering a broad compositional range, from the Austral and Southern Volcanic Zones (AVZ, SVZ, 52° - 33°S) and the Central Volcanic Zone (CVZ 27° - 18°S) (published data and Oxford unpublished analyses). The hyperbolic array extends without break from within the steep so-called "mantle array" (top left) to the shallow "crustal array" (bottom right) conventionally interpreted as either progressive involvement of crustal components or of sub-crustal, enriched lithospheric mantle, or both.

The diagram does not suggest any evidence for isotopic discontinuity between different sectors of the sub-Andean mantle, or indicate any fundamental variation in petrogenesis between different centres. The entire Nd-Sr array can be modelled by mixing isotopically homogeneous mantle-derived melts of oceanic island arc or depleted-mantle character with progressively older (Phanerozoic to Proterozoic) and thicker (c.30 to c.70 km) crust northwards from the SVZ to the CVZ. The MASH (melting, assimilation, storage, homogenisation) model of Hildreth and Moorbath (1988), involving mixing of melts derived from a normal-mantle wedge and from lower crust, explains the narrow and characteristic isotopic base range for each volcanic centre. Some centres also exhibit superimposed AFC trends. The overall trend of the array is towards contamination with Middle Crust (MC, Fig.1) - or average undifferentiated crust - rather than Lower Crust (LC). This can be explained as the result of recent (<20 Ma) thickening of undepleted Phanerozoic and Proterozoic crust, with the process of geochemical and isotopic differentiation of the crust not yet completed.

It is questionable whether any Recent volcanic centres along the Andean arc include geochemically and isotopically pristine mantle-derived magmas uncontaminated by continental crust.

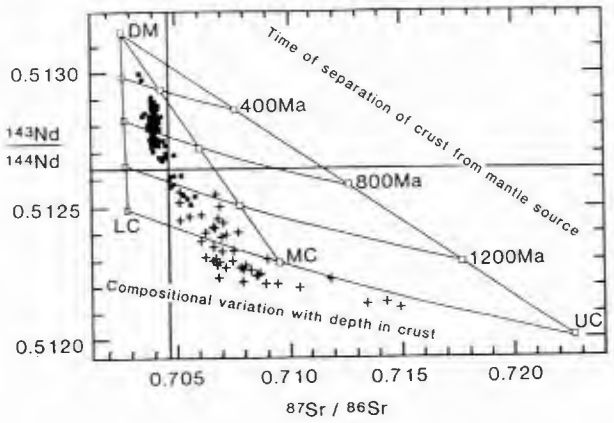

Fig.1 Andean Nd-Sr isotopic array modelled as mixing between mantle and older crust, using crustal averages of Taylor & McLennan (1985). Symbols: ▪ AVZ & SVZ; + CVZ.

VOLCANIC GEOLOGY OF SAO MIGUEL, AZORES

MOORE, R.B., USGS, Box 25046, MS 903 DFC, Denver, CO 80225

The island of Sao Miguel, Azores, about 62 km long and 14 km wide, consists of four trachytic stratovolcanoes and surrounding basaltic lavas. A new geologic map of Sao Miguel, based on field work on the entire island during 1980-1983 and 1988-1989, portrays in detail the distribution of all vents, flows, domes, pumice rings, caldera-outflow sheets, and other pyroclastic deposits. The major volcanic features of this island, from west to east, are: 1) the Quaternary trachytic stratovolcano of Sete Cidades; 2) a zone of alkali basaltic cinder cones and lava flows, with minor trachyte, of Quaternary age (zone 2); 3) the Quaternary trachytic stratovolcano of Agua de Pau; 4) a zone of alkali basaltic cinder cones and lava flows, with minor trachyte, of Quaternary age (zone 4); 5) the Quaternary trachytic stratovolcano of Furnas; 6) the Pliocene and Pleistocene trachytic stratovolcano of Povoacao; and 7) the Pliocene and Pleistocene Nordeste volcanic complex, mostly alkali basalt with minor trachyte.

Seventy new radiocarbon and 7 new K-Ar ages augment the stratigraphic data. Average eruptive recurrence intervals for the past 3,000 years in the areas active during latest Holocene time are about 400 years for Sete Cidades, 1,150 for Agua de Pau, 370 for Furnas, and 155 for zone 2. However, the interval at Sete Cidades increased to about 680 years for the past three eruptions (the most recent was about 500 years ago), and the interval at Furnas decreased to about 195 years for the past five eruptions (the most recent occurred in A.D. 1630). Mafic eruptions in zone 4 occurred about every 1,000 years during latest Pleistocene and early Holocene time; none has occurred there since eruption of the Fogo A trachyte pumice about 5,000 years ago.

The subaerial volume of trachyte extruded during latest Holocene time (0.12-0.13 km^3/century) is about double that of cogenetic basalt (0.06 km^3/century). Submarine eruptions, such as that of A.D. 1811 off the western coast of Sao Miguel, and mafic intrusions of unknown volume (whose existence is indicated by locally-abundant xenoliths of mafic and ultramafic plutonic rocks) would increase the above value for basalt. Radiocarbon ages and stratigraphic data indicate that a basaltic eruption in zone 2 and a trachytic pyroclastic eruption of Furnas Volcano are long overdue.

A TYPE-SECTION FOR THE LEVANT VOLCANIC PROVINCE (LVP) - BASED ON K/Ar DATING AND MAPPING OF THE VOLCANISM IN THE GOLAN HEIGHTS, ISRAEL.

D. Mor, G. Steinitz
The Geological Survey of Israel, Jerusalem

The Levant Volcanic Province (LVP, Schulman, 1981) extends through northeastern Jordan and southern Syria to the Golan Heights. Minor volcanic fields also developed in the Galilee (northern Israel), around the Hula Valley and in southern Lebanon.

The LVP is part of an extensive volcanic field developed during the Cenozoic on the northwestern part of the Arabian Plate. This field is aligned roughly in a northwestern direction, subparallel to the Red Sea. As such it constitutes part of the Tertiary tectonic and magmatic pattern of the plate development in the Middle East.

The location of this volcanism in the Golan Heights is important due to its proximity to the northern part of the Dead Sea Rift (DSR) Valley, which is assumed to be a transform fault on the Red Sea spreading system.

The volcanism of the Golan Heights is presented in three maps at a scale of 1:50,000. The stratigraphic criteria for the subdivision of the volcanics were based both on morphologic criteria and on extensive K/Ar dating of more than 230 samples from 76 sites.

The volcanic sequence overlying the Early Pliocene regional erosional unconformity, the "Bashan Group", is subdivided into five formations which differ in their morphologic attributes, their distribution as well as in their K/Ar ages:

Formation	Distribution	Age (m.y.)
Leja	Southwestern Syria	n.d.
Golan	Northern-central Golan	0.4-0.1
Ortal	Central-southern Golan, Hula Valley and southern Lebanon	1.6-0.7
Mechki	Southern Lebanon, northern Galilee and Korazim area	2.9-1.7
Cover Basalt	Southern Golan, southern Syria, eastern Galilee, Korazim area and northern Jordan	5.0-3.7

In the area investigated the Cover Basalt, which originated from broad lava-cones with gentle slopes, builds an extensive plateau, probably extending over the present DSR. The Mechki Basalt consists of a long lava-flow, which flowed southward along the Rift Valley and several cones in the Galilee. Ortal Formation basalts are developed as lava-cones in the Central Golan, as a lava-field in the Hula Valley and as a long lava-flow in the Yarmouk gorge. The Golan Formation forms elongated lava-cones with which some 70 cinder-cones are associated - all arranged in two parallel NNW trending lineaments; The Leja Formation is represented by one cinder-cone and several lava flows.

This new detailed chronostratigraphy set up for the volcanism of the LVP clarifies the stratigraphic relations between the various volcanic units and the associated continental sequences. It can serve as a basis for: a) detailed studies on the structural development and relations between the LVP and the DSR; b) studies on the petrological development of a young volcanic province on the Arabian Shield, probably not unrelated to the Red Sea system.

EVOLUTION OF THE KILGORE CALDERA: A MODEL FOR CALDERA FORMATION ON THE SNAKE RIVER PLAIN-YELLOWSTONE PLATEAU VOLCANIC PROVINCE

MORGAN, L.A., U.S. Geological Survey, Denver, CO 80225; DOHERTY, D.J., Arco Alaska, Inc., Box 100360, Anchorage, AK 99510; BONNICHSEN, B., Idaho Geol. Survey, Moscow, ID 83843

Eruption of the densely welded 4.3-Ma tuff of Kilgore and subsequent formation of the now-buried Kilgore caldera mark the last major caldera-forming events on the Snake River Plain. Exposures of the tuff of Kilgore on either margin of the plain suggest an areal extent of more than 25,000 km^2 and a volume exceeding 1000 km^3. The Kilgore caldera spans the 90-km width of the plain and covers a roughly circular area of more than 6500 km^2. Its position has been inferred from structures and facies in the tuff of Kilgore and associated deposits and from flow direction indicators (magnetic fabric and flow-lineation marks) and granulometric and component (free-crystal, lithic, and pumice clasts) data. Part of the topographic rim of the caldera, exposed on the north, is marked by rheomorphic folds and a zone of arcuate normal faults dropping down toward the plain. At least two major source areas are associated with the tuff of Kilgore. A volumetrically minor eruption from a vent located on the southern margin of the caldera may have triggered the climactic eruption from one or possibly two major vents on the northern margin. Eruptive vents appear to be restricted to the margins of the caldera along possible fissures marking the edges of a large grabenlike depression. Eruption of the tuff of Kilgore was preceded and followed by emplacement of rhyolitic lava flows along the perimeter of the caldera. Juniper Buttes, near the center of the caldera, is inferred to be a dome associated with the resurgence of the Kilgore caldera.

The tuff of Kilgore and its caldera have been compared with other large-volume ignimbrites and calderas in the Snake River Plain-Yellowstone Plateau in order to model caldera formation in this province. These include the McDermitt, Owyhee-Humboldt, Bruneau-Jarbridge, Oakley Valley, Heise, and Yellowstone Plateau volcanic fields. The comparisons suggest that (1) most of the ignimbrites had high magmatic (>800°C) and emplacement temperatures, as is evident from the dense welding and thin (most <30 m thick, many <15 m thick) nature of the units, as well as anhydrous phenocryst assemblages and low crystal contents; (2) the thin, large-volume, high-temperature, densely welded, areally extensive ignimbrite identified as the major caldera-forming product may actually represent several separate ignimbrites which erupted nearly simultaneously from multiple vents; (3) these multiple vents or small (<20 km diameter) source calderas are aligned along the perimeter of larger (60-90 km diameter) collapsed structural calderas; (4) some pyroclastic flows apparently originated from low eruptive columns, as is evident from the apparent lack of extensive pre-ignimbrite plinian fall deposits, the general small size of enclosed lithics, the dense welding, and the restricted distribution of individual ignimbrite members to their particular source; and (5) caldera collapse occurred late in the eruptions of large-volume ignimbrites and many calderas now span the width of the Snake River Plain (45-90 km). The present-day topography of the Snake River Plain is a direct result of the size of calderas or volcanic fields in which they are located and later thermal contraction. Calderas in this northeast-younging Cenozoic volcanic province may be uniquely different from most other calderas in these respects.

GEOMORPHOLOGY AND EVOLUTION OF THE QUATERNARY STRATOVOLCANOES IN THE HIGH CASCADES AND JAPAN

MORIYA, I., Dept. Geography, Kanazawa Univ., Kanazawa 920 JAPAN

Japanese Islands, with ca. 200 Quaternary volcanoes including ca. 70 active ones, are located in a subduction zone composed of 5 arcs. Seventy percent of the volcanoes are strato-volcanoes. They develope in 4 definite stages: 1) Formation of a large cone composed of a pile of basaltic-andesitic lava flows and scoriaceous pyroclastics (mainly by Strombolian eruptions); 2) Further growth of the large cone by thick andesite lava flows and lithic pyroclastics (mainly by Vulcanian eruptions). Partial destruction of volcanoes, such as Bandai-san in 1888, occurs sometimes in this stage due to the steepness; 3) Destruction of the summit by predominantly explosive eruptions and extension of the lower slopes by deposition of dacitic pyroclastic flows (mainly by Pelean and Plinian eruptions); and 4) Formation of a small summit caldera with dacite lava domes. This evolutionary sequence suggests that the development of stratovolcanoes in Japan can be explained by Bowen's theory that basalt magmas differentiate in a chamber in the crust closed to continuous resupply of magma from the upper mantle.

The High Cascades volcanic chain, occurring in a subduction zone, has ca. 10 large and ca. 50 small to medium stratovolcanoes of andesite. Most of the volcanoes are composed of piles of basalt to andesite lava flows and scoriaceous pyroclastics similar to the Japanese stratovolcanoes in the first stage. An exception is Mt. St. Helens. Most of the stratovolcanoes south of Mt. Adams inclusive are cut by N-S trending normal faults and/or open fractures through the summits. In some volcanoes extrusions of rhyolite domes in alignment and/or effusion of basalt flows occurs closely in time and space in the lower slopes. Hence it is likely that the stratovolcanoes in the High Cascades are growing by continuous feeding of magma into shallow chambers from the upper mantle, because magma can easily rise up in the High Cascades, which is in a tensional stress field.

In Japan the Quaternary stratovolcanoes often rise above plateaus of Plio-Pleistocene dacite-rhyolite ash flow deposits. On the other hand the strato-volcanoes in the High Cascades stand on platforms of basalt flows. This difference in evolution between the two regions could be interpreted as follows: In the High Cascades, where tension cracks commonly developed, magma generated in the upper mantle could easily penetrate through the crust. As tension cracks increased, they gradually united in to form magma chambers to build up the stratovolcanoes. In Japan basalt magmas could not easily rise through the crust due to compressional field stress but fused part of the crust, which erupted first to form voluminous dacite-rhyolite ash flows and later andesite cones. According to Landsat Images, many normal fault scarps are found in most of the volcanoes in the subduction zones in the world, indicating that they stand in tensional stress fields. The Japanese arcs and volcanoes are possibly special or minor ones in the world. These features of the stratovolcanoes in Japan are consistent with a hypothesis by K. Nakamura and Y. Kobayashi that the Japanese Islands (Tohoku, Kanto and Chubu districts) are sandwiched between two subducting slabs of the Pacific and Eurasian plates.

The volcanic evolutions of the two regions suggest that volcanoes in subductionzones do not continuously form during ongoing subduction but rather that magma generates only as a result of some special event, such as changes of speed or trend of plate motions.

BERYLLIUM ISOTOPES, BORON-BERYLLIUM SYSTEMATICS AND URANIUM SERIES DISEQUILIBRIA IN THE NEW BRITAIN ARC

MORRIS, J.D. and TERA, F., Department of Terrestrial Magnetism, Carnegie Institution of Washington, 5241 Broad Branch Rd. N.W., Washington, DC, 20015
GILL, J.B., Earth Sciences Board, University of California, SantaCruz, CA, 95064
LEEMAN, W.P., Earth Science Division, National Science Foundation, Washington, D.C., 20550
JOHNSON, R.W., Bureau of Mineral Resources, GPO Box 378, Canberra ACT 2601, Australia

^{10}Be is a cosmogenic and radioactive ($T_{1/2}$ = 1.5 Ma) nuclide which is strongly enriched in oceanic sediments and depleted in mantle reservoirs. Ratioed to the stable isotope ^{9}Be, ^{10}Be/Be atom ratios are $<5 \times 10^{-11}$ in the mantle, and average 5000×10^{-11} in surface pelagic sediments. The ^{10}Be/Be ratio in sediments decreases as a function of age, and sediments older than 8-10 Ma have negligible concentrations of ^{10}Be. Lavas from volcanic arcs have ^{10}Be/Be atom ratios in the range $1 - 100 \times 10^{-11}$; values in excess of those of the mantle require addition of a young sediment component to the arc source region. Boron is also strongly enriched in oceanic sediments, as well as in the altered part of the subducting oceanic crust. B/Be ratios in arc lavas vary from 5 to 190, relative to typical mantle values (<10).

^{10}Be, Be and B abundances and U-series activity ratios have been determined for 12 lavas from historic eruptions at 9 volcanoes in the New Britain (NB) arc. ^{10}Be/Be ratios vary from 3 to 50 while B/Be ratios range from 12 to 190; the two ratios are well correlated ($r^2 = 0.86$) and independent of SiO_2 or MgO content. (^{230}Th/^{232}Th) ratios are high, 1.2-3.0, implying a Th-depleted or U-enriched source. (^{238}U/^{230}Th) ratios are 0.96-1.14 and (^{210}Po/^{230}Th) ratios are in the range 1.4-3.5. The highest ^{10}Be/Be and B/Be ratios are seen in lavas with the highest (^{230}Th/^{232}Th) ratios. Lavas from a region of arc-continent collision at the westernmost end of the arc show no ^{10}Be or U excess, although Ra excess is present. Lavas from behind the volcanic front are characterized by low B/Be (Makalia and Garove) and low (^{238}U/^{230}Th) (Garove) ratios. For lavas from the volcanic front, as ^{10}Be/Be ratios increase from 10 to 50, Ba/La increases from 20 to 45, La/Th from 5 to 15, K/La from 1000 to 1700, and Ba/Rb from 5 to 15. The highest ^{10}Be/Be and B/Be ratios are seen in lavas with the lowest abundances of the incompatible elements K, Rb, Ba, La.

The ^{10}Be/Be and B/Be ratios of the NB arc array extend to higher values than those seen in the mantle or continental crust, and require the addition of a subducted component. Similar mixing trends are seen in other arcs. The slope for the NB array on a plot of ^{10}Be/Be *vs* B/Be is shallower than those of most other arcs, implying a lower ^{10}Be/B ratio in the subducted component. The subducted and recycled component may be either B-enriched fluids derived from young sediments, or a mixture of high-^{10}Be young sediments and high-B altered MORB. The high K/La and B/Be ratios in the lavas, relative to sediments, argue against bulk incorporation of sediments. The low ^{10}Be/B for the NB arc could mean either recycling of somewhat older sediments in NB, or of a subducted component which is more nearly slab dominated. The extremely high B/Be ratios seen in the NB arc indicate relatively larger proportions (but still less than 10% in any model) of a recycled component here than seen elsewhere.

^{10}Be/Be, B/Be and (^{230}Th/^{232}Th) ratios are highest in the eastern NB arc and decrease to the west. The good two component mixing behavior seen in the Be-B systematics suggests that the subducted component is well homogenized, and does not vary significantly along the length of the arc. The observed variation along strike may thus reflect either larger slab contributions in the east, or a more depleted, and thus more easily modified, mantle source in the eastern arc.

THE MATTABI ASH FLOW TUFF AND ITS RELATIONSHIP TO THE MATTABI MASSIVE SULPHIDE DEPOSIT

MORTON, R. L., and HUDAK, G. J., Dept. of Geology, University of Minnesota-Duluth, Duluth, Minnesota, 55812; FRANKLIN, J. M., Geological Survey of Canada, Ottawa, Ontario, K1E 0I8

The South Sturgeon Lake area of northwestern Ontario is underlain by an Archean submarine caldera which is host to 5 massive sulphide deposits. The caldera is 30km in strike length and is partly filled by mesobreccia, subaqueous debris flows and other epiclastic rocks and three distinct ash flow tuff units. The most voluminous of these is the Mattabi ash flow tuff which varies from 200 to more than 1400m in thickness and can be traced across the entire length of the caldera.

Based on flow morphology and composition the Mattabi ash flow tuff is divisible into three distinct units: a lower mixed debris and ash flow unit (50-200m thick) which occurs only near caldera margins, b) a bedded quartz crystal-pumice-rich unit (175-1050m thick) and c) an upper massive ash unit (50-300m thick). The bedded unit is host to the Mattabi massive sulfide deposit, as well as numerous other massive sulfide occurrences, and exhibits a pronounced stratigraphic and geochemical cyclicity. Individual beds can be subdivided into basal quartz-and pumice-rich lower sections overlain by bedded ash tops; thicknesses of individual beds vary from 15 to 170m. Each bed also exhibits a pronounced zonation of trace elements with high contents of Zr, Y and Nb at and/or near the base gradually decreasing upwards into the ash tops. The overlying massive ash unit contains no known massive sulfide mineralization and lacks any pronounced geochemical zoning.

The bedded nature and geochemical zonation of individual beds (flow units) can be explained by periodic eruptions from a zoned or layered, recharged siliceous magma chamber. The difference in flow morphology between this unit and the overlying massive ash flow tuff most likely reflects the deep submarine nature of the eruptive vents associated with the bedded deposits. The periodic and submarine nature of the Mattabi eruptions is indicated by the presence of massive sulphide lenses and bedded debris flow deposits between flow units. The ore lenses, which comprise the Mattabi deposit, formed between eruptive events from high temperature fluids whose origin may be related to processes within the magma chamber; these processes also controlled and triggered the periodic eruptions.

HAZARD AND RISK EVALUATION OF LAHARS, COTOPAXI VOLCANO, ECUADOR.

Patricia Mothes, Instituto Geofisico,
Escuela Politecnica Nacional, Quito, Ecuador

Lahars from future eruptions of glacier-clad Cotopaxi volcano in northern Ecuador represent the greatest risk to the population and infrastructure concentrated along the three drainages that head on its 6000 meter high peak. During many of its 35 historic eruptive periods lahars have overrun or severely affected local populations, their economy and livestock.

The Los Chillos Valley, a suburb of Quito, Ecuador's capital, as well as the Latacunga Valley, have frequently faced ruin by lahars. While to the east of Cotopaxi, on the Amazonian plain, lahars have swept through riverine towns such as Puerto Napo on only three known occasions since 1534. Laharic deposits of the 1877 eruption, the last major event, comprise the foundation for 6500 homes, hundreds of businesses, vital national infrastructure and agricultural activities.

In Latacunga Valley, the building boom has established 3500 new home lots upon these 112 year old deposits, while some of the provinces largest industries and the PanAm highway are also located in this broad risk zone. In the Chillos Valley 1500 new home lots, the trans-Ecuadorian pipeline, the source for 40% of Quito's potable water and a hydroelectric plant are located in the high risk lahar zone. Presently, in both valleys 30,000 people reside in the maximum risk zone and 133,000 people live in the zone of lesser risk.

A hazards map (USGS #1-1072) published in 1978 provided the first modern evaluation of the potential lahar problem, however national Civil Defense made few advances in educating the public about the potential hazards. In 1988 a second hazards map was published as part of the Instituto's USAID-UNDRO program. Based upon substantially more fieldwork, the map denotes a larger threatened area than was shown in the earlier version.

In recognition of the potential high risk to the socio-economic structure from future lahars, the author prepared a series of risk maps emphasizing the population and infrastructure in the two risk zones. These maps are compiled using a 1:25,000 topographic base upon which are superimposed the most recent population data and locations of schools, hospitals, pipelines, main arteries, bridges, industries, and other sites of human congregation.

Perhaps the first of their kind made in Latinamerica, the risk maps have multiple purposes; providing Civil Defense with a base for planning and preparedness, with data to create an emergency evacuation plan, to educate the public, besides serving as the map base for an eruption scenario used in a recent desk-top simulation of an hypothetical Cotopaxi eruption. The full social and economic impact of the wide distribution of these risk maps is yet unknown.

NASA'S EARTH OBSERVING SYSTEM - A NEW REMOTE SENSING TOOL FOR MONITORING ACTIVE VOLCANISM AROUND THE WORLD

Mouginis-Mark, P.J., Hawaii Institute of Geophysics, University of Hawaii, Honolulu, Hawaii 96822, U.S.A.

Early in 1989, NASA selected a remote sensing investigation of active volcanism as one of 20 inter-disciplinary investigations that will utilize a planned series of unmanned polar orbiting satellites that collectively will form the Earth Observing System (EOS). EOS will comprise at least two polar-orbiting spacecraft that will observe the Earth's surface at a variety of wavelengths and resolutions. The spacecraft have intended lifespans of ~15 years, so that data will be obtained between ~1995 - 2010. EOS will permit the analysis of active volcanoes, their inputs into the atmosphere, and the assessment of volcanological hazards. This paper reviews the EOS volcanology project goals.

EOS will provide synoptic daily coverage of the Earth's land surface and atmosphere. The following instruments will be flown: an imaging radar (3, 8 and 24-cm wavelength, quad-pol, 15-55° incidence angle, 15 - 55 m/pixel resolution); a moderate resolution (500 - 1,000 m/pixel) imaging spectrometer that operates between 0.470 - 14.235 μm (called MODIS); a high resolution (~30 m/pixel) imaging spectrometer that operates between 0.4 - 2.5 μm (called HIRIS); a thermal infrared spectrometer (called TIGER); a laser ranging device (called LASA); and a global ozone mounting radiometer with 1 km resolution (called GOMR) that has the ability to measure the mass flux of sulfur dioxide due to unique spectral features at 0.3 - 0.335 μm.

A series of automatic eruption alerts (using the automatic detection of thermal or sulfur dioxide spikes in the global synoptic MODIS and GOMR data sets) will be built into the EOS software to provide near-real time (within 90 minutes) notification of a volcanic eruption (or precursive thermal activity in a summit lake) occuring anywhere in the world. Targeting and acquisition of data from the high spatial resolution sensors will take place within 2 days and will permit the following objectives to be addressed:

1) The identification and quantitative measurement of thermal anomalies associated with active volcanoes, including the production of temperature maps of active lava flows and the measurement of the thermal profile of eruption clouds.

2) The determination of the mass flux rate of sulfur dioxide injected into the stratosphere by explosive volcanism. It will also be possible to conduct the tracking of such clouds as a function of space and time, to infer the rate of dispersal of the gas within these clouds, and assess the rate of SO_2 conversion into sulphates.

3) The derivation of meter-scale topographic difference-maps of entire lava flows or volcanic cones using radar interferometry. This method will permit quantitative estimates of both the mass eruption rate and the rate of volcano inflation/deflation to be determined. Radar data will also provide all-weather day/night mapping capabilities in order to track advancing lava flow fronts and the modification of summit areas during activity.

4) Lithologic mapping of volcanic provinces on a regional scale will be possible using uniform quality data sets at a variety of wavelengths. Radar will permit the estimation of the percent surface cover of aa and pahoehoe lava types (as well as more subtle textural variations due to rheological properties of the flows) for an entire volcano, while visible/near-infrared data will enable the rate of vegetation recovery of an eruption site to be estimated. It should also be possible to determine the rate of fall-out of solids from an eruption plume using spectral mixing models.

EOS will provide the volcanological community with an unprecidented opportunity to study on-going eruptions. Aspects of this project are expected to include interactions with national and international geological programs (such as the International Decade for Natural Hazard Reduction, and the International Space Year). As the project evolves, interested volcanologists are encouraged to contact the author for current information on the volcanology goals and the general capabilities of the EOS spacecraft.

PETROLOGIC AND GEOCHEMICAL VARIATIONS IN BASALTS ASSOCIATED WITH BIMODAL VOLCANISM IN THE ARIZONA TRANSITION ZONE: PRELIMINARY RESULTS FROM KAISER SPRING

MOYER, Thomas C., Department of Geology, Vanderbilt University, Nashville, TN 37235, ESPERANÇA, Sonia, Department of Geosciences, Old Dominion University, Norfolk, VA 23529

Basaltic lavas associated with the Kaiser Spring (KS) bimodal center in western Arizona span an age range of approximately 4.5 m.y., with the first eruptions beginning at about 12.5 Ma. Preliminary geochemical studies of these lavas have identified at least 3 types of basalt: (1) early-erupted tholeiitic basalts (TB), (2) late-erupted alkali-olivine basalts (AOB), and (3) quartz-bearing mafic andesite (QMA). These lavas have distinctive isotopic compositions: TB= ϵ Nd of -6 to -8 and $^{87}Sr/^{86}Sr$ of 0.707 to 0.708; AOB= ϵ Nd of +1.2 and $^{87}Sr/^{86}Sr$ of 0.7042; QMA= ϵ Nd of -2 and $^{87}Sr/^{86}Sr$ of 0.7048. In addition, TB and QMA lavas have more radiogenic $^{207}Pb/^{204}Pb$ and $^{208}Pb/^{204}Pb$ for their $^{206}Pb/^{204}Pb$ composition than the AOB. QMA is distinct from both TB and AOB in its unradiogenic $^{206}Pb/^{204}Pb$ composition. Despite these isotopic variations, the AOB and TB lavas have similar major and trace element compositions (e.g. the REE pattern for an AOB plots between two similarly shaped patterns for TB). QMA can be distinguished by higher Ba and K. When normalized to primitive mantle values, the KS basalts show relative depletion in Ti and Hf, positive Ba, Nb, and P, and variable Rb, K, and Ta. In general, the KS basalts have lower concentrations of incompatible elements (including LREE) than the alkali-olivine and feldspathic basalts associated with recent Colorado Plateau and Basin and Range volcanism.

The trace element similarity but isotopic disparity between the KS-AOB and TB lavas precludes a process involving significant contamination of primary AOB by radiogenic and incompatible element enriched upper crust. Possible explanations for the isotopic compositions of the AOB and TB lavas include assimilation/anatexis of mafic lower crust as exemplified by xenoliths from Chino Valley and Camp Creek in central Arizona or derivation of all basaltic melts from a heterogeneous subcontinental mantle. Available isotopic data for mantle xenoliths from the SW US show no evidence for an enriched subcontinental mantle with ϵNd less than "Bulk Earth". Because lower crustal xenoliths show a much larger range of isotopic composition, we prefer an explanation involving lower crustal contamination of AOB magma. Although variable, the compositions of mafic, lower crustal amphibolites, granulites and eclogites are more depleted in incompatible elements than the mantle-derived melts which percolate through them. Thus, significant contamination could occur before it is detected with "standard" geochemical criteria. The unradiogenic $^{206}Pb/^{204}Pb$ composition of the QMA and relative enrichment in Ba and K may reflect small amounts of upper crustal contamination. The elevated $^{207}Pb/^{204}Pb$ and $^{208}Pb/^{204}Pb$ of the TB and QMA may indicate that the Pb contaminant is from an older or less disturbed crustal province than the one identified from the xenoliths of central Arizona.

The trace element patterns for the KS-AOB are essentially similar to the younger AOB lavas of the San Francisco volcanic field on the Colorado Plateau; their lower incompatible element abundances may reflect differences in the degree of partial melting of the source. The isotopic composition of the AOB from both localities (close to "BE") is similar to that of mafic pyroxenite and some lherzolite xenoliths from several localities in the SW US. They are probably representative of melts from the subcontinental mantle.

THE DEVELOPMENT OF AN ARCHEAN MAFIC-FELSIC VOLCANIC CENTRE: LAC DES VENTS COMPLEX, NORTHERN ABITIBI BELT, QUEBEC

MUELLER, W. and CHOWN, E.H., Centre d'Études sur les Ressources Minérales, Université du Québec à Chicoutimi, Québec, G7H 2B1, Canada.

The 2-2.5 km thick Lac des Vents complex developed on an extensive, primitive submarine basalt plateau. Stratigraphically, the edifice occupies the middle section of a 6 km thick volcano-sedimentary sequence. The volcanic complex is divided into five distinct felsic units (FV 1-5) which are separated by massive to pillowed or brecciated basalt flows and gabbro sills. Abundant vesicles in the basalts suggest shallow water depths. Two felsic feeder dykes are observed, one displaying a succession of chilled margins indicating multiple felsic magma pulses.

Felsic volcanic units FV 1-4, and interstratified basalt flows and gabbro sills document the construction of the volcanic edifice, whereas FV-5 shows its emergence and destruction. The first felsic unit is characterized by well-preserved pumice flows up to several metres thick and massive to brecciated rhyodacitic lava flows. Pyroclastic turbidites and reworked pyroclastic debris are subordinate. The FV-2 unit is dominated by heterolithic pyroclastic flows which are composed of vesicular juvenile pyroclasts, basalt and non-vesicular felsic fragments originating from the consolidated edifice and, locally, abundant accidental rip-up clasts of argillite/shale up to 1 m in diametre, deriving from the underlying background sediments. The abundant sedimentary clasts and heterolithic character is suggestive of redeposition of non-lithified pyroclastic flows. The matrix of these deposits contains flattened pumice fragments and bubble wall shards proving a pyroclastic origin. The third unit represents the major constructional episode. Massive to brecciated lava flows and metre thick sequences of graded or massive bedded pyroclastic flows prevail. Intercalated volcaniclastic turbidites, and argillite and shale beds indicate that deposition continued in a subaqueous environment. The FV-4 unit is composed of massive to brecciated felsic lava flows, in part resedimented as indicated by volcaniclastic sandstone between angular blocks. Volcanogenic sediments of an epiclastic origin constitute the summital FV-5 unit. The basal portion of this unit is characterized by framework-supported amalgamated conglomerates solely composed of volcanic material. Higher-up in the section volcaniclastic sandstone dominates. Wavy and plane-bedded sandstones interstratified with argillite and fine-grained sandstone indicate wave-induced structures typical of the shallow marine association.

The Lac des Vents complex represents the gradual shoaling of a volcanic edifice and its emergence. Paroxysmal volcanism is indicated by the abundance of pyroclastic flows where constituents are derived from phreato-magmatic and/or plinian-type eruptions.

GEOLOGIC MAP OF THE LASSEN REGION, CASCADE RANGE, USA

MUFFLER, L.J.P., and CLYNNE, M.A., U.S. Geological Survey, Menlo Park, CA 94025, USA

A preliminary geologic map of the Lassen region of the southernmost Cascade Range, northeastern California, by M.A. Clynne and L.J.P. Muffler, will be displayed at the IAVCEI General Assembly. The map, at a scale of 1:50,000, encompasses 1400 km^2 centered on Lassen Volcanic National Park. Field work for the final map, encompassing 2000 km^2, will be completed by 1991. The purpose of the geologic mapping is to provide the basis for a variety of petrologic, volcano-hazards, geothermal, tectonic, geochronologic, and glacial studies.

The map displays three major late Pliocene and Quaternary volcanic centers, each of which represents focusing of regional calc-alkaline mafic volcanism and was maintained throughout its life by continuing input of basalt from depth. Each center was built in three stages: (I) early cone-building basaltic andesite and andesite lava flows and pyroclastics, (II) subsequent thick, cone-building lava flows of andesite and silicic andesite, and (III) late silicic domes and flows flanking the composite cone of stages I and II. The Maidu volcanic center (2.0-0.8 Ma) and the Dittmar volcanic center (> 2.0-1.4 Ma) are extinct; the Lassen volcanic center (< 600 ka) is still active.

The map presents significant new detail on the silicic rocks that comprise Stage III of the Lassen volcanic center. Stage III began at 400 ka with the emplacement of silicic domes, the eruption of at least 50 km^3 (DRE) of rhyolite pumice, and the development of a 30 km^2 caldera located north of the Stage-I and Stage-II andesite cone (Brokeoff volcano). This caldera subsequently was completely filled by dacite and rhyodacite domes erupted in two groups (240-200 ka and < 100 ka). Prominent in the younger group are the domes of Lassen Peak (erupted between 29 and 18 ka) and Chaos Crags (1 ka), as well as the products of the 1914-1917 eruptions from the summit of Lassen Peak. Throughout most of Stage III, andesites produced by the mixing of mafic and silicic magma were erupted primarily on the Central Plateau, just northeast of the silicic domefield.

Surrounding the three main volcanic centers are numerous volcanic edifices related to the regional calc-alkaline volcanism of the southernmost Cascade Range. Discrete basaltic andesite to andesite shield volcanoes occur near the Cascade crest. In contrast, much of the eastern part of the map area is a plateau of coalescing small volcanoes of basaltic andesite.

Low-K_2O olivine tholeiite occurs sporadically throughout the map area and is probably related to impingement of Basin and Range extensional tectonics on the Cascade Range.

Glacial deposits, primarily related to advances of ice at ~ 18 ka and 70 ka (?), cover much of the higher terrain. Prior to the emplacement of the Lassen Peak dome, a thick cover of ice on the Central Plateau fed glaciers that extended radially outward.

Hot springs, fumaroles, and hydrothermally altered areas are manifestations of the Lassen geothermal system, a parasitic vapor-dominated system centered along the contact between Brokeoff volcano and the silicic dome field.

EVOLUTION OF PLIOCENE AND QUATERNARY VOLCANISM IN THE SEGMENT OF THE SOUTHERN ANDES BETWEEN 34° AND 39° S.

MUÑOZ, J.O., Servicio Nacional de Geología y Minería, Casilla 10465, Santiago, Chile.
STERN, C.R., University of Colorado, Department of Geological Sciences, Boulder, CO. 80309, U.S.A.

Quaternary intra-arc extension and associated alkaline basaltic volcanism has occurred in the section of the southern Andean volcanic belt between 34° and 39°S. South of 39°S intra-arc extension is absent. In the region between 34° and 39°S, the Quaternary orogenic volcanic belt is divided in: 1) a north-northeastern trending volcanic front located in the Main Cordillera, currently active and 2) arc centers located to the east along north-northwestern trending precordilleran uplifts. Intra-arc alkaline basalts have been erupted along the valleys flanking these precordilleran uplifts.

Magmatism in the present-day volcanic belt between 34° and 39°S began in the Pliocene, when the volcanic front developed east of the Main Cordillera, along the precordilleran uplifts. These Pliocene centers erupted subalkaline magmas similar chemically to those currently being erupted along the Main Cordillera. During the Early Pleistocene a few centers on the precordilleran uplifts erupted magmas of progressively more alkaline affinity but with arc-type mineralogic and chemical characteristics. By the Late Pleistocene, magmatic activity in these centers had diminished, the volcanic front had migrated westward to its current location and changed to a north-northeastern orientation. Alkaline intra-arc and back-arc basaltic volcanism had been initiated in the valleys flanking the precordilleran uplifts, and subalkaline volcanism continuous to be erupted along the precordilleran uplifts.

The Early Pleistocene alkaline arc-type lavas erupted along the precordilleran uplifts, as well as the Quaternary alkaline basalts erupted in the valleys flanking these uplifts, have higher La/Yb, La/Sm and Ce/Yb ratios than, but Ba/La and 87Sr/86Sr ratios similar to, the subalkaline magmas erupted along both the Pliocene and late Quaternary volcanic fronts. Their TiO2 contents, La/Nb ratios and Ta and Nb negative anomaly are intermediate between subalkaline arc magmas in the same region and alkaline lavas of the Patagonian plateau basalts south of 39°S. Alkaline arc, intra-arc and back-arc lavas could be formed by lower degrees of partial melting of a mantle source similar to that for the subalkaline magmas erupted along the Pliocene and present-day volcanic fronts.

MAPPING REMOTE VOLCANOES WITH SATELLITE IMAGES: ISLA FERNANDINA, THE GALAPAGOS ISLANDS

Munro, D.C. and Mouginis-Mark, P.J. Hawaii Institute of Geophysics, University of Hawaii, Honolulu, Hawaii 96822

Many volcanoes are difficult to study due to their remote locations. We are developing satellite data interpretation techniques that permit us to perform large-area (10^3 - 10^4 km^2) mapping of such volcanoes. We report here on our preliminary interpretations of Isla Fernandina, which is formed by the subaerial segment of a single polygenetic volcano centered at 0°37'S, 91°55'W. Volcanological studies of the Galapagos Islands have been hampered due to their isolated location and delicate ecology. Since the comprehensive overview by Nordlie (1973), no detailed study of these volcanoes has been published.

Two data sets of Isla Fernandina have enabled us to map the distribution of vents and lava flows. During the Space Shuttle Challenger mission STS 41-G (Oct. 1984), the Large Format Camera (LFC) collected ~7 m resolution stereo b/w photographs. A SPOT-1 panchromatic scene (10 m/pixel) was also collected on April 27th 1988. When combined these data provide a synoptic view of the whole of Isla Fernandina. Supplementing these data, we also utilized a variety of color hand-held photographs obtained from the Space Shuttle on mission 51-J in October 1985. The color images were used to help discriminate between aa and pahoehoe lava flows on the volcano on the basis of their albedo (aa was assumed to be dark, pahoehoe to be bright) at off-nadir viewing geometries.

Our analysis has permitted the investigation of the distribution of eruption sites and structure of Isla Fernandina. A total of 83 lava flows and 671 cones have been identified (Fig.1a, b). A predominance of small flows originates at high elevations, and large surface area flows appear to have sources at lower elevations, suggesting that a two-level internal structure of the volcano may exist. At lower elevations 25% of eruptions appear to have occurred from well defined radial fissures, and the remainder from localized vents. At higher elevations the activity is controlled by circumferential fissures (Fig.1c). Apparently there is an absence of eruption sites between 820 m and 1000 m elevation. Our study indicates a change in orientation of minimum principal stress between the summit region and the flanks of the shield, but no preferential azimuthal distribution of large volume eruptions.

Reference: Nordlie, B.E. (1973), Geol. Soc. Amer. Bull., v. 84, p. 2931-2956.

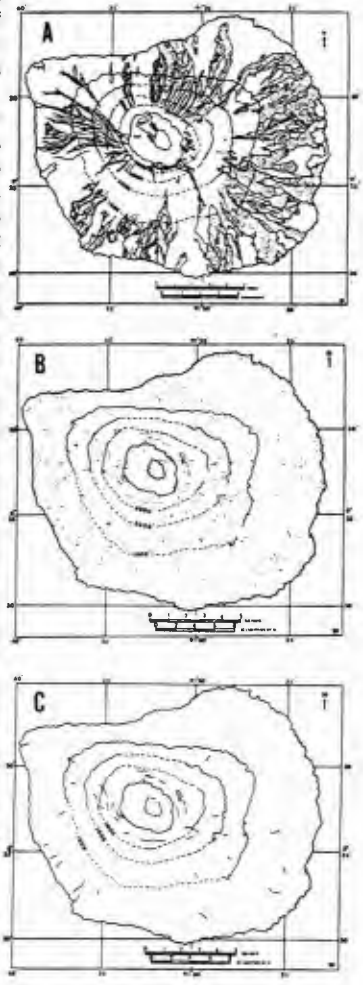

Fig. 1: A) Lava flows; B) Cones; C) fissures, identified from satellite images of Isla Fernandina, Galapagos.

THE PATH-DEPENDENT CRYSTALLIZATION OF INTERMEDIATE-COMPOSITION MAGMA

MURPHY, Mark Thomas and Marsh, Bruce D., Dept. of Earth & Planetary Sciences, the Johns Hopkins University, Baltimore, MD, 21218

The emplacement history of magma results from its path-dependent cooling and transport. The transport is coupled to the cooling rate through the production of solids (crystals) which greatly elevates the viscosity. Suspension theory can approximate the viscosity of magma as a continuous function of crystallinity. A simple (duct flow) mechanical and thermal model, suggests that an andesitic magma will stagnate due to its viscosity after 18% crystallinity, a dacite after about 12%. The width of the active zone (where the local velocity is less than 1/10 of the center-line velocity) is strongly dependent upon water content of the initial melt. Water strongly affects the melt liquidus, decreasing the crystallization interval and allowing a faster build-up of crystals.

Field relations at intermediate composition, dome/shallow-plutonic complexes can mimic this behavior. Detailed mapping of the Tatoosh igneous complex, western WA reveals a dynamically similar system, evolving from lava flows, through dome-building flows and plugs, to a sill-like pluton. Mineral compositions and textures suggest that the magma arrived at the subsurface at about 1.5 wt. % water and less than 10 vol. % crystallinity, subsequently developing a volatile-rich cap of about 4.5 wt. % water. Granitic rocks evolved under large undercoolings while the dome lavas crystallized close to their liquidus.

It is suggested that water acts in a disequilibrium fashion to buffer groundmass crystallinity. Mass-balance modeling indicates that at moderate water contents (4.5 wt %) liquidus suppression and groundmass resorption keeps undercooling at a low level. Drier melts (1.5 wt. %) do not build up water as quickly and crystallize at higher undercoolings. Textures of the Tatoosh lavas and plutons can be explained with these mechanisms. These results suggest that the crystallization path and resultant volcanic/plutonic evolution of magma is primarily dependent upon the initial crystallinity, water content, and groundmass mineralogy of the magma at depth.

A MICROCOMPUTER-BASED SYSTEM FOR COLLECTION AND ANALYSIS OF TIME-SERIES DATA FROM RESTLESS VOLCANOES

MURRAY, T.L., LAHUSEN, R.G., EWERT, J.W., LOCKHART, A.B., Cascades Volcano Observatory, U.S. Geological Survey, 5400 MacArthur Blvd.,Vancouver, Wa., 98661.

The U.S. Geological Survey's Cascades Volcano Observatory (CVO) has developed a microcomputer-based system for the collection and analysis of low-sampling-rate digital data (i.e., data sampled at intervals greater or equal to 1 minute, such as data from electronic tiltmeters or strainmeters). Either 8-bit or 16-bit laptop computers collect telemetered data or digitize analog signals. These data are then transferred to an IBM PC-compatible host computer via an RS-232 serial port. Aperiodically collected data, such as from electronic distance meter (EDM), spirit-level tilt, or geochemical measurements, are entered into the host computer by hand, utilizing either word processors or BASIC programs. The primary function of the host computer is for data storage and analysis. Comparisons between the various data sets can be quickly done on the host with the program BOB, originally developed for this purpose on a VAX minicomputer.

Laptop computers are used as collection devices because they have built-in modems and are able to operate on internal batteries during power failures. A simple circuit allows as many as 4 laptops to share a single serial port of the host.

Utilizing commercially available software that gives the host computer multitasking capabilities, the host can collect the data from the laptops in background mode while the user simultaneously runs analysis or plotting programs or other application software (such as word processing) in the foreground. Plots can be generated or aperiodic data entered without interfering with the automatic data-collection process.

This system provides the user with the flexibility to choose among different telemetry and computer-based data-acquisition systems, the only requirement being their ability to transfer data through an RS-232 serial port. Simple BASIC programs running on the host computer can translate the data formats into those compatible with BOB. The system can be initially configured to use only data entered by hand, and expanded later to include telemetered data.

Parts of the system are currently being used at several volcanoes, including Mount St. Helens and Kilauea, U.S.A., and Fuego, Guatamala. A complete system is installed in Ecuador to assist in monitoring Pichincha Volcano.

TEMPORAL CHANGE IN CHEMISTRY OF MAGMA SOURCE IN CENTRAL KYUSHU, SOUTHWEST JAPAN: PROGRESSIVE CONTAMINATION OF MANTLE-WEDGE

NAKADA, S., Dept.Geol., Fac.Sci., Kyushu University, Fukuoka 812, Japan, and KAMATA, H., U.S.Geol.Surv., Cascades Volcano Observ., 5400 MacArthur Blvd., Vancouver, WA 98661, U.S.A.

The volcanism related to the subduction of the Philippine Sea (PHS) plate began in central Kyushu at 5 Ma after a 10 m.y. pause of igneous activity. It formed a large volcano-tectonic depression, the Hohi volcanic zone (HVZ; Kamata, 1989), and has continued to the present with decreasing magma production rate. The products are largely medium-K, calc-alkaline andesite and dacite, which become enriched in K with time. The proportion of tholeiitic rocks also increases with time. Calc-alkaline high-Mg basaltic andesite (YbB) was erupted in the early stage of the HVZ activity (5-4 Ma), and differentiated high-alumina basalt (KjB) was erupted in the late stage (after 2 Ma). These compositional changes may reflect melting of hydrous mantle owing to resumption of PHS plate subduction at about 6 Ma, as well as an easier mode of magma ascent in the early stages of volcanism.

In contrast to the basalt in HVZ, the northwestern Kyushu basalt (NWKB) has erupted extensively but sporadically on the back-arc side of the HVZ since 11 Ma, and hence is not related to PHS plate subduction. The products are mainly transitional and alkali basalt with minor amount of high-alkali tholeiitic basalt, which show no notable chemical change with time.

NWKB, YbB and KjB show MORB-normalized incompatible-element spectra different from each other, as well expressed in both Nb and Sr anomalies. The patterns of KjB and NWKB are typical of island-arc basalt and of within-plate basalt, respectively. YbB shows a pattern intermediate between the two others. The three incompatible-element patterns can also fit those of their primary magmas and magma sources, even if the effects of fractionation and partial melting are considered. We suggest that the magma source under central Kyushu changed in composition from a within-plate-type fertile mantle to an island arc-type depleted mantle as the subduction of PHS plate advanced, but it remains fertile under northwest Kyushu.

In order to explain the temporal change of source mantle in central Kyushu, we propose a model of progressive contamination on mantle-wedge composition, in which both processes of contamination by a subduction component (eclogite melt is assumed) and subtraction of partial melts from the mantle are repeated as the subduction continues. We conclude that 1) progressive contamination of the mantle-wedge could continue for a few million years, so long as the subduction of oceanic plate continues, and 2) the composition of mantle-wedge has converged to the value which does not depend on the initial composition of the mantle-wedge, but on the composition of subduction component, if the processes of magma production and convection in the mantle-wedge are uniform.

PLAGIOCLASE-RESORPTION TEXTURES AS A CONSEQUENCE OF THE RAPID ISOTHERMAL DECOMPRESSION OF MAGMAS

NELSON, S. T., Department of Earth and Space Sciences, UCLA, Los Angeles, CA 90024, MONTANA, A., Department of Earth and Space Sciences and Institute of Geophysics and Planetary Physics, UCLA, Los Angeles, CA 90024

Magma mixing is considered to be a major cause for sieve and embayed volcanic plagioclase phenocrysts. We propose a simpler isochemical model for plagioclase resorption--rapid magmatic decompression. The composition of plagioclase is pressure dependent; decompression causes plagioclase in equilibrium with liquid to become more calcic and results in a greater proportion of liquid, conceivably causing the dissolution of relatively sodic plagioclase commonly observed in volcanic rocks.

We performed two sets of high-pressure experiments on a basaltic andesite. The first set involved crystallization at 1150°C at 1 atm, 6, 8, 10, and 12 Kbar to establish the equilibrium composition of each phase as a function of pressure. As expected, the plagioclase becomes more sodic with increasing pressure, ranging from $Ab_{38}An_{58}Or_4$ at 1 atm to $Ab_{52}An_{39}Or_8$ at 12 Kbar. In the second set, the 1150°C/12Kbar phase assemblage was crystallized for 24 hr., pressure was rapidly dropped ($dP/dt \geq 0.2$ Kbar/min) isothermally in 2, 4, and 6 Kbar increments, for successive experiments, and held for several hours. The extent of resorption depends on the pressure drop and on the post-decompression run duration. A 6 Kbar pressure drop results in nearly complete resorption of all crystalline phases, whereas a 2 Kbar drop produces limited resorption.

The latter set of experiments produced sieve and embayed textures in plagioclase that mimic those in natural assemblages. They provide experimental verification that such textures in volcanic rocks may result from rapid magmatic transport toward the surface, eliminating the necessity of proposing magma mixing in some cases. Further studies of this type may help constrain magma ascent rates on the basis of phenocrystic disequilibrium textures.

NEW EVIDENCE FOR A CONCEALED, PRE-BANDELIER-AGE CALDERA IN THE WESTERN VALLES CALDERA COMPLEX, NEW MEXICO

NIELSON, D.L., HULEN, J.B., University of Utah Research Institute, Salt Lake City, Utah 84108
GARDNER, J.N., Los Alamos National Laboratory, Los Alamos, New Mexico 87545

Continental Scientific Drilling Program core holes VC-2A and VC-2B (Fig. 1) furnish new evidence for the origin of the pre-Bandelier-age (>1.45 Ma) Lower Tuffs of Nielson and Hulen (1984). In both core holes, this unit is a non- to densely welded, rhyolite ash-flow tuff, petrographically affiliated with the overlying Bandelier Tuff. By contrast with the Bandelier, however, it is dominantly lithic-rich (commonly 20 vol. %, locally >70 vol. %), probably indicating proximity to source vents. The complete Lower Tuffs section penetrated in core hole VC-2B can be correlated with units "A" and "B" of the San Diego Canyon ignimbrites (Turbeville and Self, 1988), a 2.8 m.y.-old unit exposed beneath the Bandelier Tuff a few km to the southwest.

An isopach map of the Lower Tuffs (Fig. 1) shows that the unit attains apparent thicknesses of up to 652 m in the west-central Valles caldera. Outside the caldera, its maximum thickness is about 80 m (Turbeville and Self, 1988). This relationship, together with the unit's lithic-rich character, suggests that its eruption may have resulted in creation of one or more small and now concealed pre-Valles calderas.

REFERENCES

Nielson, D.L., and Hulen, J.B., 1984, J. Geophys. Res., 89, 8695-8711.
Turbeville, B.N., and Self, S., 1988, J. Geophys. Res., 93, 6148-6156.

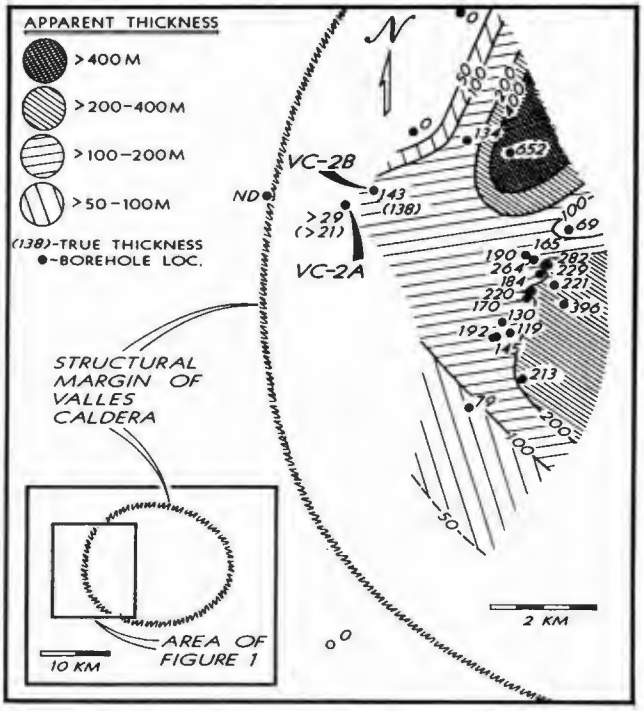

Figure 1. Isopach map of the Lower Tuffs

EYEWITNESS ACCOUNTS AND PHOTOGRAPHS OF THE 18 MAY 1980 ERUPTION OF MOUNT ST. HELENS, WASH.

NIELSEN, Elizabeth A., WAITT, Richard B., U.S. Geological Survey, 5400 MacArthur Blvd., Vancouver, WA 98661, and MALONE, Stephen D., Geophysics Program AK-50, Univ. of Washington, Seattle, WA 98195.

The 18 May 1980 eruption of Mount St. Helens is the best documented and most intensely studied volcanic eruption in historical time. Eyewitness observations and photographs are critical to this documentation. Only partly published, the eyewitness accounts have been integral to certain interpretations of the sequence and timing of the initial eruptive phenomena[1,2] and the resultant deposits.

Although thousands of individuals in the region observed distal effects (sounds, ashfall, mudflows, or floods), only about 150 persons witnessed details of the eruptive phenomena during the first few hours, either from aircraft or ground viewpoints within 75 km of the volcano. About 50 observers photographed the eruption; more than 150 images were taken during the first 5 min. Most eyewitnesses observed the eruption under stressful if not life-threatening conditions, and many had to interrupt their observations to evacuate; nonetheless, only a few inconsistencies occur within and among their accounts, and thus most data seem reliable.

The initial events--massive failure of the bulging N slope, debris avalanche, and directed blast--were recorded in several now-famous sequences of photographs from ground viewpoints NE and W of the volcano and from an aircraft nearly over the summit. But topography and rapid development of the eruption cloud obscured these viewpoints after only a few tens of sec. Eyewitnesses to the S and those farther E, NE, N, and NW observed continued advance of the directed blast, perhaps the subsequent failure of the summit, and development of a vertical plume. Campers at the N extent of the devastated area experienced the directed blast and ashfall.

Many eyewitnesses recorded their observations within a few days of the eruption; 32 parties were interviewed in 1980.[3] Additional eyewitnesses are being interviewed, detailed accounts of their observations and experiences prepared, and a comprehensive photographic reference set documenting the first few hours of the eruption assembled.

Evidence of relative timing of events during the first few hours is recorded on films and video and audio tapes made from the air and from ground viewpoints W and NW of the volcano. Seismograms and satellite data provide the absolute times of certain events, including the magnitude 5.1 earthquake, destruction of a seismometer NE of the volcano by the directed blast, development of the vertical column, and movement of the eruption plume to the NE. Eyewitness accounts and photographs are being coordinated with these data to reconstruct the relative and absolute timing of events to within a few sec during the first 5 min--resulting in a comprehensive synthesis of the first few hours of eruptive activity.

[1]Moore, J.G., and Rice, C.J., 1984, in Explosive volcanism: Wash. D.C., Nat. Acad. Press, p. 133-142.
[2]Voight, B., 1981, USGS Prof. Paper 1250, p. 69-86.
[3]Rosenbaum, J.G., and Waitt, R.B., 1981, USGS Prof. Paper 1250, p. 53-67.

THE EFFECTS OF RANDOMIZATION OF PERIODIC PROCESSES ON PATTERNS OF MAGMA COMPOSITION.

NIELSEN, R.L., College of Oceanography, Oregon State University, Corvallis, Oregon 97331-5503

Natural igneous systems are characterized by irregular, periodic activity. If viewed on a short term basis, the relative roles of fractionation, magma mixing and eruption all vary, apparently at random. This variation in the activity of processes is usually the cause cited to explain the scatter we usually see in the geochemical signature of natural systems.

Quantitative modeling is often done by chosing two points and defining a process or set of processes that describes their relationship. That linkage is hypothetical in that we do not know that we actually have examples of parent and daughter magmas. However, we can reasonably justify this approach by assuming we are dealing with an environment where the same set of processes were active over a long time period.

Existing differentiation models that involve a combination of processes have all taken the approach of fixing the relative roles of the processes that generate the calculated trends. Even in cases where the processes are interacting periodically, the periodicity is fixed. It is intuitive that random processes will create random patterns. However chaos theory states that in some cases where randomization is applied to a set of fixed conditions or constraints, a pattern can emerge that is diagnostic of those constrains.

The approach I have taken is to apply randomization to the results of a phase equilibria constrained open magma system model. This model calculates the effects of fractional crystallization, recharge, assimilation and eruption on the calculated liquid lines of descent of natural mafic magmas. Several parameters were randomized independently, sampling, recharge rate, eruption rate, assimilation rate and the periodicity of mixing. Each of these was randomized about a fixed value and the effect was evaluated by running a set of calculations covering the possible, realistic combinations.

The results indicate that if fractional crystallization is active, the distribution of major elements is bounded by the fractional crystallization liquid line of descent (FC LLD) and a line linking the parent magma and the assimilant or the most evolved magma composition. Scatter is generally constrained to that envelope, the size of which is greatest for element pairs with strongly inflected FC LLD. The pattern of scatter is a complex function of the mixing and phase equilibria constraints and the endmember compositions. Randomization has the effect of changing the distribution of calculated magmas within the envelope. If we are going to be able to apply these results or other similar calculations to natural systems, we first need more information about the characteristics of natural systems, particularly, eruption volumes, magma chamber size, pattern of long term vs. short term periodicity etc.

THE SOUTHERN CORDILLERAN BASALTIC ANDESITE SUITE, SOUTHERN CHIHUAHUA, MEXICO: A LINK BETWEEN TERTIARY CONTINENTAL ARC AND FLOOD BASALT MAGMATISM IN NORTH AMERICA

NIMZ, G.J. (1,2), CAMERON, K.L. (1), KUENTZ, D. (1), NIEMEYER, S. (2); (1) Earth Sciences, University of California, Santa Cruz, CA, 95064; (2) Lawrence Livermore National Laboratory, Livermore, CA, 94550

Mid-Cenozoic orogenic andesites and ignimbrites of western Mexico, southwestern New Mexico, and Arizona are commonly capped by basaltic andesites, most 29-20 Ma. We refer to these mafic lavas as the Southern Cordilleran Basaltic Andesite (SCORBA) suite, and they may constitute the most extensive Cenozoic basaltic suite in North America. The SCORBA suite has trace-element and isotopic characteristics of orogenic (arc) rocks (e.g. Ba/Nb > 40), and silica content (53-56% SiO2) like the Grande Ronde Basalt, which represents about 80% of the volume of the Columbia River Group.

SCORBA lavas and rare mafic lavas (PRE-SCORBA) interlayered with older ignimbrites were studied from a 700 km-long NE-SW transect of southern Chihuahua, Mexico. SCORBA and PRE-SCORBA lavas with relatively low K/P (<7) and differing Ba/Nb (50 vs 18) have similar isotopic compositions, arguing against their isotopic signatures being controlled by crustal assimilation. Along the entire length of the transect, the basaltic rocks have ϵNd and 87Sr/86Sr near Bulk Earth and 206Pb/204Pb and 207Pb/204Pb ratios that lie along a 1.7 Ga pseudoisochron. The Pb isotopic variation is geographically controlled, becoming more radiogenic from east to west, reflecting mixing in mantle source regions. The eastern mantle source has low 206Pb/204Pb and is a mixture of an intra-plate component with relatively high Nb/Y (>0.8) and a second component with low Nb/Y. The latter could be oceanic mantle-like (e.g. Nb/Y≈0.1) or Bulk Earth-like (Nb/Y≈0.2). The western mantle source is also mixed but contains less of the intra-plate component. Overprinting both the eastern and western sources is a Cenozoic subduction component that is responsible for the western radiogenic Pb. The subduction component fades out to the east (inland).

This transect crosses the inferred position of the Mojave-Sonora megashear, previously proposed to be a major lithospheric boundary, separating Proterozoic basement to the east from Phanerozoic basement to the west at the latitude of the transect. Most chemical changes near the inferred position of the megashear are subtle, and they may be gradational rather than abrupt. The uniformity of Sr and Nd isotopic compositions across the inferred position of the megashear indicates that one or more of the following statements is true: (1) Phanerozoic and Proterozoic sub-continental lithosphere are indistinguishable in Sr and Nd compositions in southern Chihuahua, (2) the megashear is not a lithospheric boundary separating Phanerozoic and Proterozoic crust in the vicinity of the transect, or (3) the isotopic signatures were acquired in the asthenosphere rather than in sub-continental lithosphere.

The principal difference between the SCORBA suite and the earlier mid-Cenozoic andesite to rhyolite orogenic suite is average SiO2 content. This difference reflects regional stress regimes at the time of eruption and magmatic plumbing. SCORBA was erupted in a more extensional tectonic environment than the orogenic suite. SCORBA magmas reached the surface more quickly and directly than most PRE-SCORBA basaltic magmas, and the suite experienced less differentiation. Although the tectonic setting of SCORBA was more extensional than the orogenic suite, it was less extensional than that of true flood basalts because SCORBA was erupted from central vents rather than major fissures.

The SCORBA suite closely resembles the Grande Ronde Basalt in average SiO2 content, LIL/Nb ratios, voluminous nature, and Sr and Nd isotopic compositions. Furthermore, SCORBA west of the megashear and the Grande Ronde have similar Pb isotopic ratios. Voluminous continental basalts include a spectrum of compositions from intra-plate tholeiites to rocks with more orogenic affinities. The common feature they share is eruption in an extensional tectonic environment, be it intra-plate, back arc, or perhaps intra-arc. The Grande Ronde is intermediate in the compositional spectrum but SCORBA is at or near the orogenic extreme.

DYNAMIC FRACTIONAL CRYSTALLIZATION AND MIXING IN CALC-ALKALINE MAGMA CHAMBERS: PHASE EQUILIBRIA AND MASS BALANCE CONSTRAINTS, IZTACCÍHUATL VOLCANO, MEXICO

NIXON, G.T., *Geological Survey Branch, Ministry of Energy, Mines, and Petroleum Resources, 756 Fort St., Victoria, B.C., Canada V8W 3A3*

The combined effects of magma mixing and dynamic fractional crystallization (MFC) during hybridization of primitive basaltic and evolved dacitic magmas at Iztaccíhuatl have been modelled using EQUIL.FOR (Nielsen, 1985) modified so as to reproduce experimentally determined low pressure liquidus relations for a typical end-member basalt. In addition, phase equilibria for hydrous conditions (P_{H2O} = 1kb) that are likely more appropriate for Iztaccíhuatl magma chambers have been derived from experimental data and natural glass and whole rock compositions. The results of the phase equilibria calculations indicate that 1) *anhydrous* mineral compositions closely match observed phenocryst compositions; 2) under hydrous conditions or at high mixing rates, pyroxenes and olivine play a more important role than plagioclase in controlling the liquid line of descent; and 3) MFC paths plotted in pseudoquaternary projections explain many of the phenocryst reaction textures observed in the hybrid lavas of Iztaccíhuatl.

Mass balance calculations place constraints on the relative rates of mixing versus dynamic fractional crystallization. Closed system crystal-liquid fractionation of primitive end-member basalt produces too great an enrichment of incompatible elements (e.g. K, Rb), and too strong a depletion of compatible elements (e.g. Mg, Ni, Cr) to explain abundances observed in dacites. Instead, these magmas can only be related by more complex processes in which liquid state mixing appears to dominate over dynamic fractional crystallization.

Ref: Nielsen, R.L., (1985). EQUIL.FOR: A program for the modeling of low-pressure differentiation processes in natural mafic magma bodies. Computers and Geosciences, v. 11, p. 531-546.

CHEMICAL COMPARISON OF THE OCEANIC AND CONTINENTAL PORTIONS OF THE ALEUTIAN ARC

NYE, C.J., Geophysical Institute, University of Alaska, Fairbanks, Alaska 99775

The Aleutian Island - Alaska Peninsula volcanic arc spans 2,500 km from west to east. There are about 80 volcanoes on the volcanic front and only a few behind the front. The western half of the arc is built on oceanic crust and the eastern half is built on Mesozoic and younger continental crust. With the exception of the nature of the overlying crust, subduction parameters are fairly constant throughout the arc. This affords a relatively straightforward opportunity to evaluate the effect of overlying crust on arc magmas by comparing the composition of magmas from the different halves of the arc.

The published database, on which the following discussion is based, contains about 900 samples. These have major and trace element and isotopic compositions broadly typical of relatively mature arcs built on oceanic or thin continental crust. They are dominantly medium-K calcalkaline and tholeiitic basalts through dacites. Magmas from the two halves of the arc are broadly similar, and fields on Harker variation diagrams overlap substantially. The following subtle differences are noteworthy: 1) The oceanic portion of the arc is dominated by basalt and basaltic andesite, while the continental portion of the arc is dominantly andesite; 2) At SiO_2 contents above 55%, magmas from the continental half of the arc usually have lower TiO_2 and higher MgO (and thereby lower FeO/MgO) than oceanic magmas; 3) During magma evolution CaO, and thereby CaO/Al_2O_3, do not decrease as fast in continental as in oceanic magmas; 4) At moderate SiO_2 contents, continental magmas have lower concentrations of some incompatible elements (Zr, Y, and to a lesser extent K, Rb, and Ba) and higher concentrations of Cr and Ni. Lack of arc-wide data on many other trace elements precludes their meaningful comparison. There is little, if any, systematic difference in radiogenic isotope ratios between the two halves of the arc. Compositional differences outlined above demonstrate that continental magmas are not simply more fractionated than oceanic magmas.

Volcanoes built on oceanic crust range from extremely calcalkaline to extremely tholeiitic, although most lavas lie on the tholeiitic side of the dividing line of Miyashiro (1974). In contrast, most, but not all, volcanoes built on continental crust are calcalkaline. Thus a discussion of chemical differences between the two portions of the arc is similar to the ongoing discussion of the origin of calcalkaline vs tholeiitic suites. Much of the data summarized here can be explained by existing theories emphasizing alternate fractionation assemblages. Some of the data, such as low concentrations of some incompatible trace elements in siliceous lavas, also require more assimilation or partial melting of upper-plate continental crust in the continental half of the arc.

THE SUBMARINE, VOLCANICLASTIC SEQUENCE "RIO PECOL LUNGO (RPL)" - SOUTHERN ALPS, ITALY

OBENHOLZNER, J.H., Inst.f.Geosciences, MUL, A-8700 Leoben, Austria
PFEIFFER, J., Inst.f.Geology, ETH CH-8092 Zurich, Switzerland.

At the upper Anisian/lower Ladinian in a basin environment a nearly tectonically undisturbed section of volcaniclastic rocks is exposed. From base to top the following layers are observable: 5,5 m sandstone shale facies (proximal turbidite):intercalations of marls and carbonate-arenite with quartz- and feldspar-fragments; 21 m graded conglomerate (BCL, VC1): rounded platform carbonate boulders(dia.max.80 cm) at the base, increase of volcanic pebbles up to the top; 7 m intercalations of crystal- and clast- rich layers (VC2-VC4, TVC); 38 m poorly bedded, crystal-rich layers (VC5): crystal-content more than 60%; 11 m massive, clast-rich layer (VC6); 6 m intercalations of crystal- and clast-rich layers (VC7-VC12);30 m massive, crystal- and shard-rich layer (VC13): well sorted; and 15 m bedded, graded ash turbidites.

Volcanic clasts (1-3 cm) and fragments (1-5 mm) are of rhyolitic and intermediate composition. The rhyolitic lava clasts are non-vesiculated,type 1 is phenocryst-poor an other (2) phenocryst-rich, often biotite bearing. They occur from the basal conglomerate up to VC12. Very fresh biotite, quartz, plagioclase and K-feldspar crystals are abundant in all layers, indicating the pyroclastic fragmentation of a dacitic to rhyolitic magma as the origin of the volcaniclastic detritus.Type 2 clasts and free crystals can be correlated to the same event. Time equivalent ignimbrites or lavas are not documented in the area, although the features of sedimentation indicate a near source deposit.

The clast-rich layers constitute of angular basin-carbonates, in minor amounts volcanic clasts (dia. max. 3 cm), embedded in a matrix of chlorite-cemented crystals. Sorting is very poor. Single larger clasts (15-20 cm) are floating in a finer groundmass.

The intercalations of crystal- and clast-rich layers interrupt the general normal gradation in the exposed section. All cited units show discrete boundaries, so a multi-stage event for deposition is assumed with the sandstone shale facies deposit as a precursor. The mode of transportation changed significantly during the deposition of the epiclastic RPL-sequence,which do not show any interlayers of nonclastic basin sediments. The basal conglomerate represents a channelized sediment with debris-flow characteristics. Others are interpreted as deposits of turbidity currents of different concentrations and grain flows, partially laminated.

In this basin sequence the platform- carbonate boulders from BCL are rather exotical.The limited occurrence is more indicative for an earthquake respectively rockfall controlled input than for a subaerial source of the volcaniclastic detritus. A brief description of these carbonates refers to wacke-, grain-, rudstones and Olangocoelia bafflestones. Beginning dolomitisation, channels and vugs in some carbonates filled with vadose silt indicate vadose diagenesis before redeposition took place.

GEOCHEMISTRY OF THE OLIGOCENE VOLCANIC ROCKS FROM OKUSHIRI ISLAND, NORTHEASTERN MARGIN OF THE JAPAN SEA

OKAMURA, S., Institute of Earth Science, Sapporo College, Hokkaido University of Education, Sapporo, 002 Japan

The Japan Basin is believed to have been formed by the rifting of a Tertiary convergent margin. Okushiri Island, situated on the northeastern border of the Japan Sea, forms the northern extension of the Northeast Honshu Arc. This Island was the site of intensive volcanism from Oligocene to late Pliocene time. The Oligocene volcanic rocks, which represent a precursory volcanism of initial rifting of the Japan Basin(back arc basin), consist of terrestrial lava flows composed of High-Mg andesites (HMA) and High-Ti basalt to andesite (HTV), and rhyolitic pyroclastic rocks.

The rocks of HMA group show high contents of MgO(7.3-10.7%), Cr(426-770ppm) and Ni(209-250ppm), and have low Ti/Zr ratios(60-64), and thus are similar to boninites and sanukites. However, their plagioclase-phyric nature(14-22% phenocryst) distinguishes the Okushiri HMA from other HMA, and shows similarity to the bronzite andesites from Bonin Islands. This suggests that Okushiri HMA are likely to have undergone slight modification by crystal fractionation whithin the continental crust prior the eruption.

HTV group rocks are characterized by high concentrations of the incompatible elements, but they exhibit lower contents of the compatible element such as Mg, Cr, Co and Ni compared with HMA. According to the Major and trace element geochemistry of HMA and HTV rocks, the order of increasing partial melting must be HTV < HMA, provided that both of the rocks were derived from similar source peridotite. The MORB-normalized geochemical patterns show that HMA are enriched in LIL elements such as Sr, Rb, Ba and Th, but depleted in HFS elements such as Nb, Zr, Hf and Ti compared with HTV. This implies that the HMA magma was pre-enriched with LIL elements.

According to isotopic composition,HMA rocks are characterized by a narrow range of initial $^{87}Sr/^{86}Sr$ from 0.70346 to 0.70352 and ϵNd from +4.2 to 4.7. On the contrary, the HTV rocks show a relatively broad range of initial $^{87}Sr/^{86}Sr$ from 0.70390 to 0.70444 and ϵNd from +3.3 to 4.6. Such a broad $^{87}Sr/^{86}Sr$ range suggests that assimilation might have occured for HTV rocks. The $^{87}Sr/^{86}Sr$ ratio increases linearly with increase in SiO2 and Rb/Sr, and vice-versa. It is believed that such a linear relationship can result owing to the combined process of fractional crystallization and assimilation.

Finally, it is suggested that in order to account for the major, trace elements and isotopic covariations, complex models involving combined fractional crystallization, assimilation and partial melting of source peridotite are required.

COMPOSITION AND TEXTURAL VARIATIONS IN LAVA FROM GLASS MOUNTAIN, CALIF.: EVIDENCE FROM THERMAL SPECTROSCOPY.

ONDRUSEK, J., CHRISTENSEN, P., and FINK, J.H., Dept. of Geology, Arizona State University, Tempe, AZ 85287
Bitnet: AGJXO@ASUACAD

Glass Mountain, in the Medicine Lake Highland of California, is a large silicic lava flow which appears to be the product of magma mixing. A map of the distribution of various compositions on the flow surface would be useful in the interpretation of the dynamics of this eruption. The Thermal Infrared Multispectral Scanner (TIMS) instrument generates images containing compositional information, and may have use in creating composition distribution maps. However, textural variations on lava flows also strongly influence TIMS imagery, and proper interpretation requires separation of textural and compositional components. Glass Mtn. is an excellent locality to test these effects on TIMS data. It is young (ca. 1100 yrs.), has little weathering, and virtually no vegetative cover.

Samples representing three textures in each of two compositions (rhyolite, ca. 73% SiO_2; and dacite, ca. 62% SiO_2) were collected. The textures are characterized as 1) coarsely vesicular pumice (CVP), with vesicles typically 0.5 cm in size; 2) finely vesicular pumice (FVP), with 1 mm vesicles; and 3) glassy obsidian. High-resolution thermal infrared emission spectra of these samples were obtained in the laboratory with a Mattson Cygnus FTIR spectrometer.

In the non-vesicular rhyolite samples, a broad spectral feature was observed centered at 1080 wavenumbers; non-vesicular dacite samples showed the same feature centered at 1120 wavenumbers. This shift in wavelength is consistent with compositional variations affecting the degree of polymerization and the bond strength of the Si-O tetrahedron. The depth of this absorption feature progressively decreases with increasing vesicularity, and is barely evident in samples with 0.5 cm vesicles. These changes due to texture are independent of composition and do not alter the absorption band location.

The implication for the interpretation of TIMS imagery is that glassy lavas of similar composition, such as dacite and rhyolite (about 10% SiO_2 difference) may be distinguishable. Such separation is difficult to achieve over large areas by other methods. However, this discernibility diminishes with increasing vesicularity, due to the decrease in absorption band depth. Vesicles as small as a few millimeters have a profound effect on thermal IR spectra, and such vesicular lavas are quite common on silicic lava flows. Given sufficient spectral (and spatial) resolution, it may be possible to determine both compositional and textural variations. Based on these lab results, TIMS imagery from the non-vesicular portions of Glass Mtn. will be used to measure the areas of the various compositional zones; these data will then be inserted into various eruption models in order to test the models' applicability to Glass Mtn.

INFRARED REMOTE SENSING AND FIELD TECHNIQUES FOR VOLCANO MONITORING

OPPENHEIMER, C.M.M. and ROTHERY, D.A., Department of Earth Sciences, The Open University, Milton Keynes, MK7 6AA, England.

Fieldwork at active volcanoes using infrared thermometers is being undertaken to help understand satellite infrared data. Complementary Landsat TM and NOAA AVHRR imagery is being acquired. So far, we have examined the temporal and spatial characteristics of the surface (radiant) temperature distributions associated with magmatic features and moderate temperature fumaroles at Stromboli and Vulcano, respectively.

Preliminary interpretation of our field observations indicates that in the case of incandescent vents at Stromboli, rapid and significant fluctuation of temperature (see figure), is attributable to: (i) variation in the amount of volcanogenic fumes, coming between the radiometer and the hot target, and (ii) the activity of the magma within the vent.

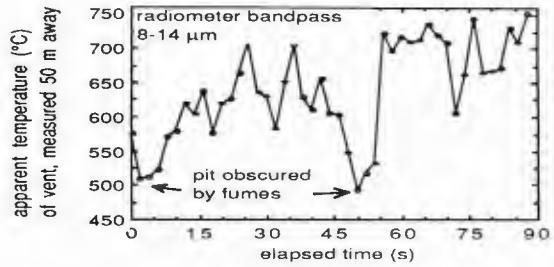

A further effect results from the nature of strombolian activity itself: the frequent, mildly explosive eruptions cover areas of the crater floor with incandescent scoria (see figure). The spectral exitance of (infrared) radiation from affected regions, particularly at wavelengths near the peak of the Planck function, increases abruptly following such an episode, then decreases exponentially as the material cools. Such superimposed effects may be expected to complicate significantly the interpretability of the satellite 'snapshot'.

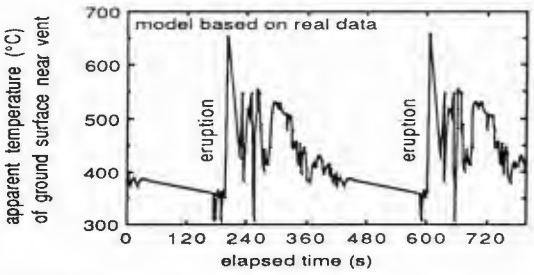

The fumarole system on Vulcano (gas temperatures about 100 - 400°C) would almost certainly not be recognisable on currently available spaceborne imagery, as insufficient areas of the ground have high radiant temperatures. This brackets the kinds of volcanic phenomena which can be monitored from space.

Future work will focus on high temperature fumaroles, and the feasibity of distinguishing between fumarolic and magmatic causes of remotely sensed volcano hotspots.

ELECTRON MICROPROBE ANALYSIS OF HYDROTHERMAL MONAZITE: EVIDENCE OF REE MOBILITY AT WAIRAKEI AND OLYMPIC DAM

ORESKES, N., Geology Dept., Stanford Univ., Stanford, Ca., 94305, U.S.A., MITCHELL, P.A., Geology Dept., Univ. of Canterbury, Christchurch 1, N.Z., and PAQUE, J.M., Geology Dept. and Center for Materials Research, Stanford Univ., Stanford, Ca., 94305, U.S.A.

At the Wairakei geothermal field, New Zealand, 75 samples of drill core and cuttings and 17 samples of siliceous precipitates from wellhead production equipment, were collected and analyzed for REEs and Y by bulk rock neutron activation analysis (NAA). The results suggest that all REEs except Eu are being transported by and deposited from the low salinity, near neutral pH geothermal fluids at $T \leq 265^{o}C$. Regardless of lithology, hydrothermally altered rocks have very similar REE patterns, with La values ~10^2x chondrite, and very similar La/Sm and Tb/Lu ratios, suggesting possible REE homogenization due to hydrothermal alteration. Compared with rock data, siliceous precipitate has an order of magnitude lower REE content, with slight depletion of light REEs relative to heavy REEs. Extreme negative Eu anomalies suggest that, except for trace amounts, Eu is either not transported in or not deposited by the fluid within the production equipment.

At the Olympic Dam Cu-U-(REE) deposit, South Australia, 100 samples of hematite-rich hydrothermal breccias and of altered granite wall-rock were taken from drill core and underground development, and analyzed by NAA. The breccias are strongly enriched in LREE compared to unaltered and weakly altered wall-rock. The most REE-rich breccias occur in the geographic center of the deposit, are associated with extreme hematite metasomatism and intense brecciation, and contain La up to 10^5 x chondrite, with La/Lu up to 100. Many of these breccias display positive Eu anomalies.

In order to quantify the extent of REE mobility and to evaluate the partitioning of REEs between fluids and hydrothermal minerals, we have analyzed hydrothermal REE phases from Waraikei and Olympic Dam. Since alteration phases are typically very fine-grained (<10μ) and therefore not amenable to mineral separation for bulk analysis, the electron microprobe is the most logical analytical alternative. However, quantitative analysis of the REEs is difficult due to extensive peak overlap of the REE X-ray spectra. Since most REE-bearing minerals contain varying concentrations of the majority of REEs, an accurate analysis requires correction for peak overlap. In addition, background subtractions must be made manually based on spectrometer scans over the area of interest, and background intensities vary depending on the host mineralogy. Failure to make these corrections will lead to incorrect REE abundances and ratios.

We have calculated overlap and background corrections for microprobe analysis of hydrothermal monazite from Wairakei and Olympic Dam. Preliminary data indicate that the Olympic Dam monazite is Th-free, but contains significant La, Nd, Sm, Pr, and Eu, in addition to Ce. In contrast, the Wairakei monazite contains several per cent Th, 5-10% each La and Nd, minor Sm, Y, and Ca, but no Eu. Both monazites contain several weight % Si. The absence of Th in the Olympic dam monazite, presence of significant Sm, and bulk rock positive Eu anomalies, suggest that REEs were probably derived from a mafic source at depth, rather than from the surrounding granite, whereas the Wairakei data are consistent with mobilization of REEs from the local, dominantly rhyolitic, volcanics.

THE GREEN TUFF OF PANTELLERIA : AN EXEMPLE OF INTENSELY WELDED PYROCLASTIC DEPOSIT

ORSI, G., Department of Geofisica e Vulcanologia, University of Naples, Italy, and SHERIDAN, M.F., Dept. of Geology, Arizona State University, Arizona 85287

The island of Pantelleria, located in the Sicily Channel, is the type locality for peralkaline magmatism. Many intensely welded pyroclastic deposits occur on the island. The Green Tuff, which is the youngest among these tuffs, was erupted 50 Ka b.p. and its emplacement was followed by a caldera collapse. The chemical composition of this tuff ranges from the base upwards from pantellerite to trachyte. Although the total volume is difficult to calculate as part of it was deposited into the sea and a caldera collapsed after its eruption, an estimate of 1.5 Km has been proposed.

The origin of the Green Tuff has been debated by various authors being considered as an ignimbrite, as a welded fall or as a combination of welded blast and ignimbrite. The authors have suggested that it was mainly emplaced by pyroclastic flow mechanism with minor fall and surge products. The different nature of the single beds is testified either by textural characters or by particle-size distribution. Pyroclastic-flow deposits are ponded in valleys having an even upper surface dispite deposition onto an irregular topography. In some cases they are easily recognizable due to the presence of degassing pipes and embrication of clasts. Lithic fragments in these members are well rounded.

The pyroclastic nature of the deposit, dispite the intense welding of most of the succession, is clearly evidenced by lateral and vertical variations from welded to non-welded facies in the same depositional units. Furthermore the different members have different areal distribution on the island according to eruption mechanism and explosivity. The air-fall beds are dispersed toward E-NE. The distribution of the surge and flow beds is controlled by the paleomorphology. Only toward the end of the eruption, due to an increase of the explosivity, the hot and sticky member g was erupted and covered the whole island. Density profiles also evidence the presence of different depositional units and their pyroclastic origin.

ERUPTIVE BEHAVIOR, VENT LOCATIONS, AND CALDERA DEVELOPMENT OF CERRO PANIZOS, CENTRAL ANDES

Ort, M.H., Dept. of Geological Sciences, University of California, Santa Barbara, 93106, USA, Coira, B.L., Universidad Nacional de Jujuy, Casilla de Correo No. 258, (4600) S.S. de Jujuy, Argentina, and Mazzoni, M.M., Centro de Investigaciones Geologicas, Calle 1, No. 644, (1900) La Plata, Argentina

Cerro Panizos, a 20km diameter ignimbrite center on the Argentina-Bolivia border in the central Andes, was the source for at least four ignimbrite cooling units totaling >500km^3 in volume. Baker (1981) identified it as an "ignimbrite shield", an ignimbrite center that underwent little syn- or post-eruptive subsidence, based on satellite imagery. Field and paleomagetic work suggest the ignimbrite center had several vents and is either a collapse caldera, filled by late-stage ignimbrites and post-caldera lava flows, or a nested caldera.

Original distribution and thicknesses of the various cooling units vary. The lowermost ignimbrites are generally confined to eastern valleys. The middle ignimbrites, which form 200+m thick extracaldera deposits, are distributed radially. Pre-existing lava domes channeled and ponded the pyroclastic flows in the south. Welding and thicknesses of flow units are greatest toward the northern parts of the ignimbrite center. The uppermost units are restricted to the eastern half of the ignimbrite center, with greatest thicknesses and degree of welding in the southern sectors. Pumice clasts in the upper units are up to 1.2m in diameter in the south, but are 0.5m maximum in the north.

Identification of lithic fragment types shows ignimbrites lower in the stratigraphy contain predominantly Ordovician sedimentary fragments, while Tertiary lava fragments are most common in the upper ignimbrites. Ordovician sediments are at the surface or underlie Tertiary rocks throughout the area. Pre-ignimbrite Tertiary lavas have been found near Cerro Panizos in the southern part of the center. Sources for the middle ignimbrites lie toward the north and middle of the center, while later pyroclastic flows issued from more southerly vents.

Anisotropy of magnetic susceptibility studies, which can indicate flow directions, suggest a central to northern vent for the lower and middle flows and a southern vent location for the upper flows.

Ventward dipping (5^o-8^o) middle and upper ignimbrites and surge deposits are found close to the southern vent. This may be due to "downsagging" (Walker, 1984), or to ponding of pyroclastic flows in the center of a developing caldera, resulting in greater welding and subsidence of a central depression. This depression is morphologically similar to a downsag caldera, but without involvement of substrate. The latter is preferred, as the depression size can account for only a small fraction of the erupted material. It is proposed that Cerro Panizos is a collapse caldera, possibly nested, with ring vents covered by later ignimbrites and lava flows. Similar models may explain "ignimbrite shield" morphologies elsewhere.

DISINTEGRATION OF ORDOVICIAN PYROCLASTIC FLOWS UPON ENTRY INTO THE SEA, NORTH WALES, U.K.; IMPLICATIONS FOR SUBAQUEOUS WELDING

ORTON, G.J., Department of Earth Sciences, Monash University, Clayton, Victoria, 3168, Australia.

The large ash flow sheets from the Ordovician marginal basin of Snowdonia, North Wales have been cited previously as the best documented examples of subaqueous welded pyroclastic flows. The Garth Tuff of the Capel Curig Volcanic Fm. and the lower outflow sheet of the Pitts Head Tuff in particular provide notable case studies of ash flow tuffs which although erupted and deposited subaerially can be traced into marine settings. However, more detailed analysis of sedimentary facies within intercalated epiclastic successions, as well as identification of more distal unwelded representatives of the Pitts Head Tuff, illustrate that both pyroclastic flows disintegrated shortly after entering the sea.

The Garth pyroclastic flow entered the sea from a wide, low gradient braidplain and persisted as a continuous sheet for 5 km past the coastline. Thereafter, its only distinct expression consists of isolated pods of welded tuff which are thought to represent the dense unmixed centres of flow lobes stemming from preferential incorporation of water along the clefts of a polylobate flow front. The Pitts Head pyroclastic flow, in contrast, descended from an intensively-faulted basin margin and small, high gradient alluvial fans directly into marine environments. Along coastlines, evidence for vigorous interaction of the pyroclastic flow with basin baters includes: 1) development of a thick, disorganised, collage of various admixtures of unwelded tuff and sandstone along the flow base, 2) extensive rheomorphic folding of primary flow foliation ascribed to upward streaming of water vapour generated at the tuff/sediment interface, and 3) intrusion of large, sand dikes into centre of tuffs during later stages of flow emplacement. Continued ingestion of sediment/water mixtures quickly transformed the entire flow into a series of thinner, unwelded pumiceous or crystal rich debris flows. Locally developed perlitic fractures are the only evidence that some of this pyroclastic debris was once hot.

The contrasting patterns of disruption for the two pyroclastic flows across the critical air-water interface are related to distance of coastline from source vents and the topography or hydrodynamic roughness of subjacent landscapes. These would control flow velocities, amounts of fluidisation, thickness of the turbulentbasal boundary layer, and the related 3-dimensional morphology of the flow front. Successful penetration into the sea was most favourable with fully deflated flows and linear low gradient, near-shore profiles.

The failure of both pyroclastic flows, however, to either remain intact whilst accomplishing this feat, or retain sufficient heat to weld in depths of water greater than deflated flow thicknesses implies that development of subaqueous welding from hot pyroclastic flows entering the sea is highly improbable.

INTERACTION BETWEEN SURFACE WATER AND BASALT FLOWS OF THE GRANDE RONDE FORMATION, COLUMBIA RIVER BASALT GROUP: SECONDARY HYDROEXPLOSION STRUCTURES

ORZOL, L. L., 3107 N.E. 53rd Ave.,Portland, Oregon 97213, and CUMMINGS, M. L., Department of Geology, Portland State University, Portland, Oregon 97207

Secondary hydroexplosion structures occur within flows of the Grande Ronde Basalt of the Columbia River Basalt Group in the Troy basin of northeastern Oregon. Data from nineteen stratigraphic sites in the canyons of the Grande Ronde and Wenaha Rivers and their tributaries indicate that the maximum number of flows that contain explosion structures at any one site is six.

The textures and features within the explosion structures indicate two main processes; mixing and fragmentation. The formation of a hydroexplosion structure involves mixing of basalt from either adjacent or subjacent portions of the flow. Neighboring, closely-spaced bands and layers of differently textured basalt indicate that the mixing occurred after initial crystallization of the flows. Ripple-like joint surfaces and aligned microphenocrysts and microlites within textural bands indicate upward movement of the lava during formation of the structure. Fragmentation occurs by shearing and brittle fracture resulting in block-size to mm-size breccia clasts. Shearing occurs primarily between textural types and does not produce extensive breakage. Brittle fracture produces distinct clasts. The mechanism for mixing and fragmentation is explosive vaporization of water, violent upward movement of steam through still molten lava, and entrainment of molten lava from areas adjacent to the developing structure.

Areas of distinct jointing patterns, breccia bodies within the flow, and overthickened flow-top breccias characterize the outcrop-scale relations. The entablature and colonnade jointing described by Long and Wood (1986) occur in the flows where explosion structures are not present. The jointing patterns within the structure differ from those where the structures are absent. Flow zones based on jointing characteristics within the structures include a lower zone where platey-jointing predominates and a zone in the upper 1/3 to 1/2 of the flow where arch-shaped joints are dominant. Within the upper part of the zone with arch-shaped joints, the arches are truncated by a central spine of breccia. In the lower part of this zone, bodies of breccia are trapped beneath continuous arches.

The breccias of the central spine and the trapped breccia bodies differ from flow-top breccias in that clasts are predominantly non-vesicular and microscopic textures are indicative of mixing of lava of distinctly different cooling textures. Multiple-generation clasts occur within the central spine and trapped breccia bodies. Non-vesicular clasts coated by a thin layer of finely brecciated clasts occur in the central spine. Clast color indicates varying degrees of oxidation as determined by mossbauer spectroscopy; red is associated with hematite as the oxide phase and black with magnetite. Clasts with more well-developed intergranular textures are commonly oxidized; vitrophyric textures are commonly black.

The trapped breccia bodies, central spine, and the flow-top breccia zone average 42% and range from 23 to 84% of total flow thickness. The flow-top breccias contain abundant scoriaceous clasts.

Long, P. E., and Wood, B. J., 1986, Structures, textures, and cooling histories of Columbia River Basalt flows: Geological Society of America Bulletin, v. 97, p. 1144-1155.

GEOCHEMICAL EVOLUTION OF CONTINENTAL FLOOD BASALTS DURING PROTEROZOIC MIDCONTINENT RIFT

PACES, J.B.†, Dept. of Geol. Engnrg, Geology and Geophysics, Michigan Technological University, Houghton, Michigan 49931

The 1.1 Ga Midcontinent Rift of North America represents a major episode of continental break-up and flood basalt accumulation (>20 km of rift volcanics). Chemical, isotopic and stratigraphic data from lavas exposed in the Lake Superior region are used to model magmatic processes active during the late-stages of rift evolution.

The Portage Lake Volcanics (PLV) consist of a 5 km thick section of more than 220 flood basalt flows and represent the youngest exposed lava succession within the main rift graben. Mg- to Fe-rich olivine tholeiites predominate, although more evolved lavas exist throughout the pile. PLV lavas are relatively high in MgO (0.55-0.75) and Ni (190-360 ppm), however, even the least evolved tholeiites are preferentially enriched in LIL elements (e.g. slightly LREE-enriched patterns with La/Yb_N ~3). The pile exhibits a complex, non-random (albeit noisy) pattern of compositional variation with stratigraphy. Over the entire section, tholeiites show a crude trend of successively less evolved compositions with height (mg' <0.6 at the base of the section and >0.7 at the top). Superimposed on this overall trend are cyclic variations including several, voluminous cycles of progressively less evolved tholeiites (major cycle trends) disrupted, in turn, by less voluminous cycles of increasingly more evolved lavas (minor cycle trends).

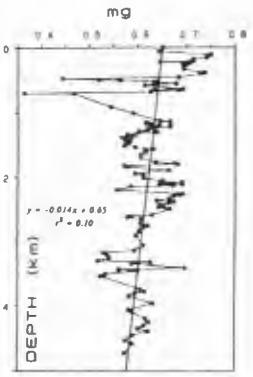

Initial Nd-Sr isotopes show little variation, lying near bulk Earth values. However, $\epsilon_{Nd}(T)$ increases slightly with stratigraphic height to values of +0.5 to +0.8 in the youngest, least evolved tholeiites.

Compositions of less evolved, olivine tholeiitic magmas indicate multiple-saturation at moderate pressures (7-9 kbar), whereas more evolved magmas fall closer to 1 bar cotectics. Variations in major elements can be modeled by up to 80% olivine gabbro crystallization from a least evolved PLV parent, however, trace element compositions are not consistent with closed system crystal fractionation. In particular, both the observed Ni contents and the range in incompatible element ratios (i.e. La/Yb) are greater than values predicted by closed system fractionation models. Data are best modeled by evolution within an open system where magma chambers experience continuous fractional crystallization with episodic replenishment and mixing of parental magma followed by occasional tapping of hybrid magmas. Geochemical and isotopic modeling suggests that additional processes (e.g. crustal assimilation, variable partial melting, high pressure fractionation) were negligible or second order compared to crystallization-replenishment-tapping processes.

Strato-geochemical variations are related to a model of polybaric crystallization in the evolving rift. Open-system crystallization occurred in large, quasi-steady state magma chambers located near the base of the crust. The degree of magmatic evolution depends on variable rates of parental magma influx, lava extrusion and plate spreading (higher rates yield less evolved magmas). Hybrid magmas were either erupted directly to the surface as less evolved, major cycle lavas, or were injected into intra-crustal magma chambers where further crystallization produced more evolved, minor cycle magmas. The overall compositional trend may have been related to progressive decreases in magma chamber residence times caused by gradual crustal thinning and establishment of efficient conduits. Strato-isotopic variations suggest that tholeiitic magmas were eventually isolated from interaction with old continental crust, implying the development of juvenile mafic crust in the axial region of the rift. Trace element and isotopic evidence indicate that the source had a time-averaged LIL-enriched signature. Cumulative geological, geochemical, and geophysical evidence favor upwelling of a fertile mantle plume as the rift mechanism.

†presently at Dept. of Geol. Sciences, Univ. of Tenn., Knoxville, TN 37996-1410

AMPHIBOLE CHEMISTRY OF DIABASE DIKES AS AN INDICATOR OF THE TIMING OF BASEMENT UPLIFTS

H.C. Palmer, and R.L. Barnett, Department of Geophysics, University of Western Ontario, London, Ontario, Canada N6A 5B7.

The continuity of east-west-trending subprovinces of the central Superior province of the Canadian Shield is interrupted by a northeast-trending zone of granulite grade rocks of the Kapuskasing structural zone (KSZ). The eastern margin of the KSZ is a zone of cataclasis, the Ivanhoe Lake cataclastic zone, which juxtaposes the high grade rocks against greenschist facies rocks of the Abitibi subprovince. An older limit can be placed on the timing of differential uplift from the amphibole chemistry of diabase dikes that cut the country rocks.

Matachewan dikes form the oldest and most areally extensive of the dike swarms in the Precambrian of Ontario. Kapuskasing dikes of ENE trend have a much more limited distribution being confined to the Chapleau block of the KSZ and the Wawa Domal Gneiss terrain. Matachewan dikes are apparently absent from the highest grade part of the Chapleau block of the KSZ but to the west, Kapuskasing dikes are seen to cut Matachewan dikes establishing the age relationship between them. Kapuskasing dikes, like Matachewan dikes, contain amphibole except at one locality on the footwall side of the Ivanhoe Lake Cataclastic Zone (ILCZ). Amphiboles from Matachewan dikes in the low grade country rocks of the Abitibi Subprovince are ferro-edenites carrying ∿4% Al_2O_3; this fact, together with the presence of well developed crystal faces of amphibole against plagioclase suggests that the amphiboles are igneous products. To the northwest of the KSZ Al_2O_3 contents are ∿5%. Beginning in the Wawa Gneiss Terrain, Al_2O_3 content in amphibole from both Matachewan and Kapuskasing dikes rises from these regional values to ∿10% in proximity to the ILCZ. The Al contents indicate that both dike swarms were emplaced at a deeper crustal level in the KSZ and by implication the differential uplift along the ILCZ postdates Kapuskasing dike emplacement.

PETROGENESIS OF RHEOMORPHIC TUFFS AND SILICIC LAVAS, DAVIS MOUNTAINS VOLCANIC FIELD, TEXAS

PARKER, D.F., Dept. Geology, Baylor University, Waco, TX 76798, USA

Rheomorphic tuffs and unusually extensive silicic lava flows are associated with four major volcanic centers and formations (Paisano Volcano = PV; Buckhorn Caldera = BC; Paradise Mountain Caldera = PMC; Star Mountain Formation = SMF) of the Davis Mountains volcanic field (DMVF). Major element plots of 97 analyses show no "Daly Gap" between mafic and silicic magmas. Silicic magmas, dominated by anhydrous phenocryst assemblages (af,cpx,±mt,il), evolved from basaltic parents, many of which are quartz normative. Intermediate rocks are trachyte porphyries. Most rhyolites are peralkaline (PV,BC,SMF) and others are borderline metaluminous (PMC). Nepheline trachyte, present in minor late intrusions, is absent from the main volcanic series, and forms separate trends on major and trace element variation diagrams.

Trace element plots of Rb,Sr,Y,Zr, and Ba versus Nb illustrate differentiation trends. Sr was strongly depleted in all centers by plagioclase fractionation. After early enrichment in basalts, Ba was similarly depleted in trachyte by alkali feldspar fractionation, but shows late enrichment in some rhyolites (PV,PMC). Rb and Y form linear enrichment trends with Nb, but with different slopes. Zr forms linear enrichment trends with Nb in two systems (BC,SMF), but was buffered in two others by zircon fractionation (PV, SMC). The oldest silicic unit (SMF) exhibits anomalously low incompatible trace element concentrations similar to those in mafic rocks.

Major and trace element fractionation modelling of each system is compatible with differentiation dominated by fractional crystallization of observed phenocryst phases. Models requiring assimilation of Ba and Sr rich crustal rocks by silicic magma are not required because partition coefficients for Ba and Sr between alkali feldspar and melt are highly variable and depend upon the CaO contents of melt and feldspar. Calculated D values for Ba in rhyolite range from 25 to 0.7 and for Sr from 18 to ~1; extreme fractionation of some rhyolite resulted in low, but stable Sr and Ba contents and even slight increases of Ba in some systems.

Despite the variety of silicic magmas, each center yielded rheomorphic tuff or unusually extensive lava. The development of fluidal textures in tuff and large flow distances in silicic lava was more strongly controlled by high eruption rates, moderately high temperatures (~900 °C based upon pyroxene and FeTi oxide data), and low volatile contents (creating denser ash flows), than peralkaline chemistry.

Crustal assimilation by basalt may have created quartz normative mafic magmas that could differentiate to rhyolite. Minor differences in amount and type of assimilant, or in the chemistry of assimilating basalt could have been exaggerated during differentiation, yielding the variety of silicic magmas observed. Late nepheline trachyte probably evolved from silica-undersaturated alkalic basalt.

LAMPROITIC TO ROMAN-TYPE ULTRAPOTASSIC MAGMATISM IN CENTRAL ITALY: PETROLOGICAL GEOCHEMICAL AND ISOTOPIC VARIATIONS

PECCERILLO Angelo and CONTICELLI Sandro

Istituto di Scienze della Terra, University of Messina (Italy), and Dipartimento di Scienze della Terra, University of Florence (Italy)

The Roman Comagmatic Province is the site of extensive recent ultrapotassic volcanism. In its northern end, the Roman Province overlaps with the Tuscan Province where, together with crustal anatectic rocks, several small outcrops of highly primitive, mafic ultrapotassic rocks occur.These range in age from 4.0 to less than 1.0 ma and differ from typical mafic roman volcanics in that they display higher K_2O, K_2O/Na_2O, K_2O/Al_2O_3 and lower Al_2O_3, Na_2O and CaO. Overall, these rocks have petrochemical characteristics close to those of lamproites. A continuum in the variation of petrological, geochemical and isotopic characteristics exists between roman volcanics and South Tuscany lamproites. K_2O, K_2O/Na_2O, TiO_2, high-field strength elements (HFSE) and large ion elements (LILE) and Sr isotope ratios decrease more or less regularly from lamproites to roman volcanics. $^{87}Sr/^{86}Sr$ ranges from 0.710 to 0.717 and is negatively correlated with Sr and Sr/Rb ratio. Preliminary Nd isotopic determinations gave values around 0.51209 for lamproites;these are lower than ratios of both roman and tuscan anatectic rocks. LILE/HFSE ratios are higher in roman than in lamproitic rocks, though the latter have still much higher values than lamproites from intracratonic areas.

Although processes of interaction between mantle-derived magmas and crustal material are commonly found in South Tuscany, mass balance calculations rule out that the compositional variations from roman-type to lamproitic magmatism are the product of crustal assimilation by roman mafic liquids. Petrological, geochemical and isotopic data are best explained by assuming for all the mafic magmas under investigation a genesis in a heterogeneous upper mantle.These heterogeneities can be explained by assuming for the lamproitic and roman-province magma sources a contamination by distinct types and abundances of fluids or melts, both of subduction origin, during the Tertiary tectonic evolution of Apennines. A more complex model invokes an interaction between two enriched mantle reservoirs, one of lamproitic and one of roman-type composition. Two components, one of intraplate and one of subductive nature, are believed to be involved in the contamination of the lamproitic source, whereas a subduction-related contaminant was responsible for the roman magma source anomaly.According to the model, the two contamination events occurred at different stages of the evolution of Apennines.

EVOLUTION OF MAGMAS DURING CONTINENTAL EXTENSION: THE MOUNT TAYLOR VOLCANIC FIELD, NEW MEXICO

PERRY, Frank V., Department of Geology, University of New Mexico, Albuquerque, NM 87131
BALDRIDGE, W. Scott, Earth and Space Sciences Division, Los Alamos National Laboratory, Los Alamos, NM 87545
DEPAOLO, Donald J., Department of Geology and Geophysics, University of California, Berkeley, CA 94720, and
SHAFIQULLAH, M., Laboratory of Isotope Geochemistry, Department of Geosciences, University of Arizona, Tuscon, AZ 85721

The Mount Taylor volcanic field (MTVF) lies in an extensional setting on the present tectonic boundary between the Basin and Range province and the southeastern Colorado Plateau and is dominated by Mount Taylor, a composite volcano active from >3 to 1.5 m.y. ago. Growth of the volcano began with eruption of rhyolite, followed by quartz latite and finally latite. The early eruptions of quartz latite formed the major volume of the volcano. A variety of alkalic basalts were erupted throughout the lifetime of the volcano.

The compositional variations of MTVF rocks resulted primarily from fractional crystallization of mildly alkaline hy-hawaiite magmas. Differentiation of magmas occurred in multiple, short-lived magma chambers, a result of a low magma flux from the mantle that could not support a single, long-lived chamber.

A small number of intermediate magmas were produced by mixing of evolved hy-hawaiite and rhyolite, primarily in the early history of the field. Mixing may have occurred when rhyolite magmas formed in lower crustal magma chambers, ascended to upper crustal levels, and were injected into the base of mafic magma chambers.

Nd, Sr, and O isotopes indicate that small amounts of crustal assimilation accompanied fractional crystallization and affected all of the evolved MTVF rocks. Assimilation/fractional crystallization occurred primarily in the lower crust as hy-hawaiite differentiated to evolved hy-hawaiite or latite.

Our physical model is that, early in the history of the field, evolved lower crustal magmas ascended into the upper crust, where density filtering (possibly aided by a relatively large magma flux that locally heated the crust and raised the depth of the brittle-ductile transition) and a reduced extensional stress field inhibited further ascent until magmas evolved to rhyolite or quartz latite. Later in the history of the field, latite magmas ascended directly from the lower crust and erupted without further significant differentiation, probably because of increased crustal extension.

THE MECHANISMS OF PERIODIC EXPLOSIONS FROM LABORATORY MODELING EXPERIMENTS

PERSIKOV E.S. and STEINBERG G.S., Institute of Marine Geology and Geophysics, Far Eastern Branch of the Acadmey of Sciences of the USSR, Yuzhno-Sakhalinsk 693002, USSR

Explosions at some andesitic volcanoes occur with periods of hours to days between explosions. These episodic explosions indicate that a volcanic conduit has a cap that impedes free outflow of gases. The time necessary for a significant lava cap to form due to cooling and crystallization exceeds the explosion period by several orders of magnitude. The mechanism of formation of a lava cap has been considered based on experiments for modeling periodic vesiculation of andesitic melts. Modeling was performed by step-wise decompression of water-saturated andesitic melts. For and initial T=1000°C, P_{H2O}=2 kb ($T_{solidus}$=830°C, $T_{liquidus}$ 1060°C) an isothermal decompression of a water -saturated andesitic melt leads to loss of volatiles and an attendant rise in the solidus temperature. As a result, the melt, without temperature change, overcools, turns glass-like, and becomes a cap for gases rising from below ($T_{solidus}$ 1000°), closing the vent opened by the explosion. In experiments with T=1150°, no lava cap forms during decompression ($T_{solidus}$ 1150°). In successive explosions, an inverse relation arises in a volcanic system: degassing of magma under conditions of a closed system results high pressure which destroy the lava cap, and "reopens" the system. Subsequent rapid vesiculation of the magma and explosion, i.e. degassing under open system conditions, results in eruption of degassed magma (ash, ejecta, pyroclastic flows) and overcooling of the remaining magma which becomes a glass-like lava cap and "closes" the system. This process is cyclic. The lava cap that forms after large explosive eruptions is degasses magmatic material; loss of volatiles increases its viscosity sharply and can lose its ability to flow (T T_{sol}), causing it to be squeezed out as a solid body (dome) or shattered by a renewed explosion.

LAVA TUBES AT MAUNA ULU, KILAUEA VOLCANO, 1972-1974

PETERSON, Donald W., U. S. Geological Survey, MS-910, Menlo Park, California 94025, and
HOLCOMB, Robin T., U. S. Geological Survey, WB-10, University of Washington, Seattle, Washington 98195

Extensive systems of lava tubes formed several times during the eruption of Mauna Ulu from 1969 to 1974, and the general origin and behavior of the tubes through 1971 were described in previous papers by various authors. Tubes that developed from 1972 to 1974 confirmed the earlier observations and provided further insights into the development of lava tubes and their role and significance in the growth of basaltic shield volcanoes.

Lava tubes at Mauna Ulu developed by at least four different processes: (1) accretion of flat, rooted crusts across streams within confined channels; (2) accretion of overflows and spatter to levees, which built arched roofs across streams; (3) jamming together and fusing of plates of floating crust; and (4) progressive extension of pahoehoe lobes by molten distributaries beneath a solidified crust. By these various processes, tubes can develop in different parts of lava flows under a variety of flow regimes. Tubes can therefore become ubiquitous within pahoehoe flows and distribute a large fraction of the lava delivered to the surface during a sustained eruption.

Tubes transport lava efficiently. Once formed, the roofs of tubes insulate the streams within, allowing the lava to retain its fluidity for a longer time than if exposed directly to ambient air temperature. This enables the flows to travel for greater distances and spread over wider areas. Even though supply rates were moderate at Mauna Ulu, generally about 1 to 5 m^3/s, the principal tubes conducted lava as far as the coast (13 km distant) where it fed extensive pahoehoe fields on the coastal flats and added new land to the island. The largest and most efficient tubes developed during periods of sustained extrusion when new lava was being supplied at nearly constant rates.

Because of their ubiquity and efficiency, lava tubes exert significant control upon the shapes of shield volcanoes. Traditionally the low aspect ratio (height/diameter) of shield volcanoes has been attributed chiefly to the fluidity of basaltic lava. However, fluidity alone is not an adequate control because it depends so strongly on the temperature of the lava, and when lava is exposed to the air its temperature, and thereby its fluidity, decline rapidly. Lava tubes provide a means of insulating the lava, thereby preserving its fluidity, while they also serve as conduits that allow lava to travel for great distances across the surface. The process enables basaltic volcanoes to attain diameters that are very large relative to their heights.

At Mauna Ulu, during the episodes when surface overflows were brief and few tubes formed, a tendency was noticed for the angles of slope (and thereby the aspect ratio) of the lava shields growing around the vents to increase appreciably. In contrast, during sustained episodes when many tubes developed and much of the new lava traveled through them for longer distances, the slope angles of the shields tended to increase only slightly. The highly variable character of the eruptive activity prevented the relations among the volumes of surface flow vs. tube flow and the resulting rate of change of the slope angle from being rigorously documented. However, future eruptions at basaltic shield volcanoes may provide opportunities to test these relations.

HIGH TEMPERATURE FLOOD SILICIC LAVAS (?) FROM THE PARANA' BASIN (BRASIL)

PETRINI, R., Institute of Geocronologia e Geochimica Isotopica, C.N.R., Pisa, Italy
CIVETTA, L., Department of Geofisica e Vulcanologia, University of Naples, Italy
IACUMIN, P., Institute of Mineralogia e Petrografia, University of Trieste, Italy
LONGINELLI, A., Institute of Mineralogia e Petrografia, University of Trieste, Italy
BELLIENI, G., Institute of Mineralogia e Petrografia, University of Padova, Italy
COMIN-CHIARAMONTE, P., Institute of Mineralogia e Petrografia, University of Palermo, Italy
ERNESTO, N., MARQUES, L. S., MELFI, A., PACCA, I, Institute Astronomico e Geofisico, University of Sao Paulo, Brazil, and
PICCIRILLO, E.M., Institute of Mineralogia e Petrografia, University of Trieste, Italy.

The Lower Cretaceous flood volcanism in the Paranà basin is represented by dominant tholeiite (c. 96 vol. %) and ryolite (c. 4 vol. %; 30,000 Km^3). The acid volcanics overlain the tholeiites and are concentrated towards the continental margin where theiy attain the maximum thickness (c. 400 m). Individual sheets (c. 10 -70 m thick) may be traced in the field for over 20 -30 Km. They are characterized by a thin (4-5 m) glassy basal zone, a dominant (over 90%) massive and crystalline main zone and a thin brecciated and/or vesiculated upper zone. Oxygen isotope data show that rhyolites suffered significant post-eruptive fluid interaction more pronounced in the basal zone [$\delta^{18}O$(%): obsidian = + 16 to + 19, and crystalline type = +12 to +15].

In southern Paranà the ryolites and the basalts are "poor" in incompatible elements (I.E.) relative to the analogues of northern Paranà. Chemistry reveals that both the I.E. - poor and - enriched rhyolites are compositionally homogeneous also at single sheet scale.

Petrology and isotope geochemistry support for the rhyolites an origin by partial melting of " basic-intermediate" lower-crust material. The high temperature of eruption (> 1000 °C), the chemical homogeneity and paleomagnetic data suggest very high rate of ascent from unzoned magma reservoirs.

Small but systematic chemical differences may be found between single sections, suggesting distinct magma systems, and a maximum extent of homogeneous product between 20 to 100 Km, consistently with paleomagnetic data.

The important extensional regime during the acid volcanism suggests that magma outpouring probably benifited of various feeding fissures. In this case the extent of a single flow probably did not exceed 10 - 20 Km. The extensive sheet form would be the result of effusive eruptions of low-viscosity (10^5 - 10^6 poise) high-temperature magmas from subcontemporaneously active fissures.

The effusive character of the eruption is consistent with a genesis of rhyolite (melts) at "quasi-anhydrous" condition as required by the high temperature of Paranà acid volcanics.

LEAD ISOTOPES IN SPINEL-LHERZOLITE-BEARING ALKALIC BASALTS, SAN LUIS POTOSI, MEXICO.

Pier, J.G., Podosek, F.A., and Luhr, J.F., Department of Earth and Planetary Sciences, and McDonnell Center for Space Sciences, Washington University, St. Louis, Mo., 63130
Aranda-Gomez, J.J., Instituto de Geologia, Universidad Nacional Automoma de Mexico, Guanajuato, GTO, 36000, Mexico

Lead isotopic compositions were determined for 19 alkalic basalts and 4 kaersutites from two Quaternary volcanic fields (Santo Domingo and Ventura) in the state of San Luis Potosi, Mexico. These samples have similar $^{207}Pb/^{204}Pb$ values, ranging from 15.56 to 15.64. Greater variability is found in the other two Pb ratios; $^{206}Pb/^{204}Pb$ ranges from 18.80 to 19.30 and $^{208}Pb/^{204}Pb$ ranges from 38.22 to 38.98. Most samples plot within the field defined by MORB-OIB on Pb isotopic diagrams, but have less radiogenic $^{206}Pb/^{204}Pb$ than that measured for similar volcanic rocks from the Cameroon line and Ahaggar. With the exception of samples from the eastern margin of the province, $^{207}Pb/^{204}Pb$ is highly correlated with $^{208}Pb/^{204}Pb$; however, $^{206}Pb/^{204}Pb$ is uncorrelated with both $^{208}Pb/^{204}Pb$ and $^{207}Pb/^{204}Pb$. $^{206}Pb/^{204}Pb$ is highly variable across the province but is relatively homogeneous for samples erupted in close geographic proximity. $^{208}Pb/^{204}Pb$ is highly correlated with $^{87}Sr/^{86}Sr$ and with incompatible trace element abundances, whereas such correlations are not observed for $^{206}Pb/^{204}Pb$ or Epsilon Nd. $^{208}Pb/^{204}Pb$ and $^{87}Sr/^{86}Sr$ are both displaced to higher values in samples from Santo Domingo, which lies to the east of Ventura.

Previous investigations of Sr and Nd isotopic systematics in these samples suggested a three-component model; the Pb data support such a model. Excluding the 4 easternmost volcanic samples, the SLP Pb data describe a plane (a reduced Chi squared of 1.04 is calculated for this model). Reasonable candidate-endmembers are the MORB reservoir, the St. Helena source, and a component with the Pb signature of pelagic sediments. The third component has the same Pb composition as Mexican ore deposits (Cumming et al., 1979); thus, it could be argued that crustal contamination is the source of this component and the local homogeneity of $^{206}Pb/^{204}Pb$. There is minimal petrographic evidence for contamination, however, and this process is unlikely to generate isotopic-elemental correlations. The isotopic and elemental correlations of these samples are inferred to arise within the mantle in response to correlated mixing-partial melting processes, with little modification occurring during passage through the crust.

AIRBORNE REMOTE SENSING OF ACTIVE VOLCANOES

PIERI, D.C.,and A.B. KAHLE, Jet Propulsion Laboratory, Pasadena, CA 91109

Recent advances in technology have permitted the deployment of a variety of remote sensing devices to take advantage of airborne and orbital perspectives of volcanic activity at a wide variety of wavelengths (1,2). In addition, rugged new devices for recording ground observations on video tape in the near- and thermal-infrared are also available (3,4). This instrumentation provides the volcanologist with a whole new arsenal of tools with which to attack problems associated with active volcanic processes, as well as extending the wavelength range over which emplaced features can be studied.

Since 1986 we have carried out a series of observations on the thermal infrared signatures of a number of active volcanic features with the Thermal Infrared Multispectral Scanner (TIMS) aboard the NASA C-130 Land Survey research aircraft, deployed from the NASA Ames Research Center, Palo Alto, California. Our library of data includes observations of volcanic activity at Mauna Loa and Kilauea in Hawaii (with USGS/HVO), Mt. Etna, Vesuvius, the Aeolian Islands, and Campi Flegrei in Italy (with CNR, Vesuvius and Catania Observatories), and at Mt. St. Helens (with USGS/CVO). Of particular recent interest has been September 1988 infrared radiometric observations of the active lava pond and tube system at the C-Vent of the PuuOo shield on Kilauea, in collaboration with colleagues of the USGS Hawaii Volcanoes Observatory. During daytime and nightime sorties, we were able to observe the dynamics and heat source distribution within the active lava pond, as well as to map the surface thermal trace of the lava flowing about 1-2 meters below the surface in a closed tube system. Observations were carried out in a variety of bandpasses from mid-visible through 12 microns in the thermal IR. In addition, we were able to map the dimensions and morphology of the hot water plume emanating from the point of lava entry into the ocean at the mouth of the active tube. It has become clear from our initial experiments at applying remote sensing techniques from an airborne perspective, as well as from pioneering work by others (e.g., 2,5) from orbit, that these techniques will be essential in future attempts to provide comprehensive physical data and boundary constraints for well-posed physical models of volcanic activity now being developed (e.g., 6,7).

This work represents research carried out at the Jet Propulsion Laboratory of the California Institute of Technology under contract to the NASA Land Processes Program.

REFERENCES: (1) Kahle, A.B., et al., 1988, JGR., 93, 15239-15251; (2) Rothery, D.A., et al., 1987, JGR., 93, 7993-8008; (3) Pieri, D.C., et al., 1984, Abst. with Prog. 97th Ann. GSA Mtg., 16, 623; (4) Gradie, J., et al., 1988, Proc. Lunar Planet. Sci. XIX, 407-408; (5) Glaze, L., and P. Francis, 1989, Nature, in press; (6) Baloga, S.M., 1987, JGR., 92, 9271-9279; (7) Baloga, S.M., and D.C. Pieri, 1986, JGR., 91, 9543-9552.

SEISMIC REFRACTION PROSPECTING ACROSS THE NEAPOLITAN AREA OF VOLCANISM (SOUTHERN ITALY).

PINO, N. A., Dipart. Geofisica e Vulcanologia, University of Naples; 10, Lg. S.Marcellino 80134 Naples (Italy).
FERRUCCI, F and C. GODANO, Osservatorio Vesuviano; 249, Via Manzoni 80123 Naples (Italy).

Five linear profiles and two regional-scale fan-profiles, carried out in the years 1985-1987 and intersecting each other within the volcanic area of Naples (which accounts for three volcanoes active at present or in historical times), allow to draw an accurate picture of crustal and upper mantle major interfaces.

Forward-modeling by gaussian-beam dynamic ray-tracing, both for linear and constant-offset profiles, constrains a relative Moho high at a depth of 20 km beneath the center of the volcanic area, corresponding to the Campi Flegrei Caldera and the Ischia volcanic Island at surface.

On the contrary, a much thicker crust (even more than 30 km) is symetrically found beneath the carbonate complexes bordering the volcanic area (Mts. Lattari at South-East and Mt. Massico at North-West): a Moho depth of 35-40 km had already been obtained under the Apennines chain (at its immediate East), accordingly with a Bouguer gravity low of -30 to -40 mgal.

The abrupt Moho deepening (the diameter of the whole area does not exceed 150 km) is accompanied by strong lateral changes of the crust structure, with outwards thickening of the lower-crust (7.0-7.2 km/s) layers and increase of the average crustal velocities (from <6.0 km/s to >6.2 km/s).

A critical reinterpretation of three OBS lines, performed in the early eighties, allows to infer that major structural changes should also separate the volcanic area from the young (10 to 4 My) pseudo-oceanic Tyrrhenian basin at West.

In comparison with former, multi-disciplinary geophysical results, the recent dynamic behaviour of the area is modeled as essentially driven by dual(NW-SE and SW-NE) tensile tectonic mechanisms.

AN OVERVIEW OF TWO CONTINENTAL ALKALINE IGNEOUS PROVINCES IN NAMIBIA.

By

F.PIRAJNO, R.H.SMITHIES AND J.S.MARSH.

Geology Dept, Rhodes University, Grahamstown, S.Africa.

Products of intracontinental alkaline magmatism are widespread in the SW region of Africa (Angola, Namibia and South Africa). These are represented by a series of igneous complexes including saturated and under-saturated mafic and felsic rocks, carbonatites and kimberlites. The majority form groups that are arranged along NE-trending lineaments, others have northerly alignments. The NE trends are probably old structures re-activated during the Pan-African and Gondwana tectonic events. In this paper we discuss and compare the general characteristics of two NE-trending major groups of intracontinental igneous rocks in Namibia. The Kuboos-Bremen Line is a series of alkaline intrusive complexes, extending across the Orange River (NW South Africa and Southern Namibia) for about 270 km. The complexes were emplaced during the late phases of the Pan-African tectongenetic event at about 550 Ma. Alkali granites form the most southerly intrusive, whereas small carbonatite-bearing stocks occur at the NE end of the Line. One of these intrusions is the Tatasberg Complex consisting of discrete intrusions of alkali-granite, syenite, feldspathoidal syenite and carbonatite. Known mineralisation includes porphyry type Mo-Cu and Pb-Ag associated with Si-oversaturated rocks. High concentrations of REE are present in the carbonatites. The Mesozoic Damara alkaline igneous province comprises at least 15 volcanic-plutonic complexes, two of which are currently being investigated by us in detail (Erongo Volcanic Complex and Paresis Volcanic Complex). The province extends for about 350 km in a NE trending zone in the central part of the Damara Orogen. The complexes were emplaced between 145 and 120 Ma during the late phases of the Gondwana break up, following voluminous outpourings of basaltic lavas and ash flow tuffs of the Etendeka Group. The complexes include mafic and felsic under-to oversaturated rocks with carbonatite plugs in the northeast, and they represent deeply eroded remnants of volcanic centres, characterised by dominant pyroclastic activity (ignimbrites and rheomorphic ash flow tuffs). Mineralisation includes greisen-related W-Sn-F, REE in dry alkali granites, Fe ore, F, Nb and REE in carbonatites.

These two provinces represent two distinct ages and are presently exposed at different levels. Moreover, the overall lack of mafic material within the exclusively plutonic Kuboos-Bremen Line may reflect a greater component of crustally derived magma, compared to the series of volcano-plutonic complexes of the Damara Province. The linearity of the two provinces may be related to localisation of magma generation along zones of crustal weakness. The magma source region consequently controls the resulting mineralisation. Granitic magmas in particular may inherit certain crustal characteristics such as base metal enrichments in the case of the Kuboos-Bremen Line, and Sn-W in the Damara alkaline igneous province.

COMPLEX EVOLUTION AND CRYSTALLIZATION HISTORY IN BASIC AND ACID INTRUSIONS: THE CASE STUDY OF PUNTA FALCONE (NORTHERN SARDINIA ITALY)

POLI, G.E., TOMMASINI, S., Department of Earth Sciences, P.za Università, 06100 Perugia, Italy.

A group of small stocks consisting of acid and mafic intrusive rocks outcrop in an area of ca. 3.5 km² at Punta Falcone (Northern Sardinia, Italy). The stocks, belonging to the Sardinia-Corsica Batholith, emplaced in a late tectonic phase, after the last deformative event of the Hercynian orogenesis. Structural features among and within the stocks are quite complex. The granitic stocks (GR I, GR II, GR III hereafter) intrude each others with sharp contacts; GR II and GR III are unzoned whereas GR I is zoned and includes a stratiphied gabbroic mass of about 0.2 km². Moreover a narrow interaction zone (IZ), max. 2 mt. width, develops along the contact between the GR I and the mafic body.

This paper presents field, mineral chemistry and geochemical data on Punta Falcone rocks, with the aim to study the genesis and the evolution of these acid and basic systems, and better understand the relative physico-chemical interactions.

The acid system is composed by Granodiorites, Monzogranites and Leucogranites (GR I), Monzogranites (GR II) and Granodiorites (GR III). The three stocks show different evolutive processes. GR I formed in the context of a single magmatic batch. The parental magma underwent an in situ c/f process; then, during emplacement, the proportion of solid and liquid fractions were modified by filter pressing and/or flow differentiation. Therefore each sample represents various percentages of early crystallized minerals and evolute residual liquid. On the contrary, GR II and GR III stocks exhibit only a slight evolution by a simple c/f process.

Clarified the role played by differentiation processes, it was possible to constraint the chemical composition of the parental magmas of each stock and then their origin. These magmas, infact, may be formed by different degrees of partial melting of the same crustal igneous source, intermediate in composition. Their geochemical features are also due to different amounts of residual mineralogical phases retained after segregation of melts.

The mafic system consists of massive and cumulate horneblende-bearing gabbros, which display a stratiphied structure. Geobarometric data on horneblendes and trace elements geochemistry suggest that at least two c/f processes, occurred at different pressure, were responsible for the stratiphied structure of the gabbroic mass.

Basic-acid interactions developed as an attempt to requilibrate the system to the new physico-chemical conditions when the basic magma intruded the GR I anatectic magma. Significative transformations occurred in the mafic system both during crystallization and sub-solidus phases. Furthermore a tested AFC process is able to explain the genesis and composition of the narrow contact zone (IZ), even if some difficulties arise to define the geochemistry of the basic end member.

PETROLOGY OF PETER I ISLAND, ANTARCTICA

PRESTVIK, T., Department of Geology & Mineral Resources Engineering, University of Trondheim, Norway, BARNES, C.G., Department of Geosciences, Texas Tech University, Lubbock, Texas, USA, and SUNDVOLL, B., Mineralogical-geological Museum, University of Oslo, Norway

Peter I Island is located in the Bellinghausen Sea 400 km NE of Thurston Island, West Antarctica. It is an Upper Miocene-Pliocene volcanic island situated adjacent to a former transform fault on the upper continental rise of the presently passive margin between the Pacific and Antarctica. The Peter I Island volcanism took place at the same time as post-subduction, rift-related volcanism occured in the nearby Marie Byrd Land, Eights Coast, and Alexander Island; and it is possible that Peter I Island activity was related to these examples of well-defined continental magmatism.

The present study is mainly based on a collection of rocks resulting from the Norwegian Aurora expedition to the island in 1987, comprising alkaline basalt, hawaiite, benmoreite, and trachyte. The basic rocks typically contain phenocrysts of olivine (Fo 61-84), diopsidic augite, and plagioclase (ca An 60). Small xenoliths comprise mantle-type spinel lherzolite, cumulate clinopyroxenite and gabbro and felsic inclusions that consist of medium-grained strained quartz, placioclase, and abundant colorless glass. Chemically, the basic rocks are characterized by rather high MgO (7.8-10.2) and TiO_2 (3.1-3.7) and relatively low CaO (8.4-9.5) contents. They have steep REE patterns, (La/Yb)N =20 with HREE only 5x chondrite. Y and Sc are almost constant at relatively low levels. Compatible trace elements such as Ni and Cr show considerable variation (190-300 and 150-470 ppm resp.), whereas V shows only little variation. Sr and Nd isotope ratios are rahter constant with $^{87}Sr/^{86}Sr$ averaging 0.70388 and $^{143}Nd/^{144}Nd$ 0.51277, both typical for oceanic island volcanism, and slightly below the mantle "array". Preliminary oxygen isotope analyses average $\delta^{18}O$ = +6.0°/oo. Incompatible trace elements vary by a factor of 1.5-2.0 within the range of the basic rocks.

Various kinds of "process identification" diagrams suggest that the incompatible trace element variations represent different degrees (7-15%) of partial melting. These melts were later modified by 10-15% ol + cpx ± sp fractionation. The source, which is isotopically rather homogeneous, is characterized as "enriched" as is typical for both ocean island and continental basalts. The very small variation in Y (and Sc?) and the very fractionated REE pattern indicate that the source had an Y and HREE-rich residual phase, most probably garnet.

The benmoreite and trachyte formed by multiphase fractionation from the basic rocks. The fractionating assemblage included iron-titanium oxides, and apatite as demonstrated by an extremely fractionated REE pattern of the trachytes [(La/Yb)N > 100].

VARYING SCALES OF MANTLE HETEROGENEITY IN SOUTH-EASTERN AUSTRALIAN CONTINENTAL LITHOSPHERE: DATA FROM CAINOZOIC INTRAPLATE BASALTS OF WESTERN VICTORIA.

PRICE, R.C.& GRAY, C.M., Geology Department, LaTrobe University, Bundoora, Vic., Australia, 3088.
FREY, F.A., Massachusetts Institute of Technology,Cambridge,Mass.,U.S.A. 02139.

In the western districts of Victoria, southeastern Australia, basaltic volcanism has occurred almost continuously through the Cainozoic with volumetric peaks at 42-57 and 0-5 Ma. On the basis of geomorphology and composition volcanics with ages less than 5 Ma can be subdivided into *plains basalts* that form a thin (<50m) but extensive veneer of tholeiitic to transitional basalt, and younger alkalic *cones basalts*.

The plains basalts range in age from 4.5 Ma to virtually the present day with a peak in the number of ages at 2.2 Ma. 450 new major element, trace element, and Sr isotopic analyses show that in contrast to the cones, tholeiitic and transitional basalts dominate the plains. 52% of the analysed rocks are tholeiitic (>10% Hy in the norm.), 33% are transitional (0-10% Hy), and alkalic (0-5% Ne). Less than 2% of the plains samples are moderately and strongly alkalic rock types.

Initial $^{87}Sr/^{86}Sr$ ratios vary greatly (.7037-.7058 in 450 samples) and there is a general decrease in isotopic ratio with degree of silica undersaturation whereby hawaiites show the lowest and basaltic icelandites the highest ratios. All the radiogenic tholeiitic rocks are 2 Ma or older and the less radiogenic hawaiites are younger than 2 Ma. With time the eruptives became progressively more alkalic and showed less scattered $^{87}Sr/^{86}Sr$ isotopic ratios.

Regionally a north-south boundary within the province separates an eastern, relatively radiogenic sector ($^{87}Sr/^{86}Sr$=.7040-.7058; mean=.7047) dominated by tholeiitic rocks from a western sector ($^{87}Sr/^{86}Sr$=.7037-.7048; mean=.7042) where transitional types are more significant. This east-west separation is considered to reflect a major lithospheric boundary within the province. Locally, isotopic mapping, coupled with geochronological and geochemical data has identified domains generally less than 15 km. in length that represent either single flows or groups of related flows.

The bulk of the plains basalts represent derivative magmas that have undergone crystal fractionation involving principally olivine. $^{87}Sr/^{86}Sr$ ratios do not correlate with abundances of elements normally expected to have high concentrations in crustal rocks (eg. K, Na, Al) and this feature, together with Pb isotopic data, and the coherence of the isotopic domains precludes crustal contamination as an important process affecting geochemical variations. The geochemistry of the post-5 Ma basalts reflects mixing of multiple, heterogeneous, mantle sources and subsequent crystal fractionation at various levels in the crust and upper mantle. Primary plains basalts were produced by partial melting of a complex, lithospheric mantle source characterized by extensive and variable short range heterogeneity. The alkalic rocks that make up the cones could be derived from a more homogeneous, deeper mantle source.

ARCHIVES AND DATA BASE FOR ITALIAN ACTIVE VOLCANOES: ADSVI AND BaDSVI

PRINCIPE, C., Istituto di Geocronologia e Geochimica Isotopica - C.N.R., Pisa and Gruppo Nazionale per la Vulcanologia - C.N.R., Roma, Italy
ROMANO, G.A., Istituto CNUCE - C.N.R., Pisa, Italy

The data base BaDSVI and connected archives ADSVI concern all "historic"-type data on italian active volcanoes: e.g. fenomenological, geochemical, bibliographical.

ADSVI consist in a collection of microfilms and microfiches (also transferred on optical disks) of the historical documents that describe, since XVI century, the status and the volcanic activity of the italian volcanoes such Vesuvius, Etna, Aeolian Islands, etc. .. In addition we recorded all "recent" bibliography containing analitical data on fumarolic and from soils and on thermal springs inside volcanic areas (e.g. Ischia, Phlegraean Field, ...).

A computerized index connect archives and data base.

The goals of BaDSVI are:

i) to give a service in the volcanological reconstruction of the historic eruptions, and in statistical - type researches on volcanic activity;

ii) to organize analitical data on thermal waters and volcanic gases for immediate use by peoples who work in the active volcanic areas surveillance.

Friendly interfaces are studied to simplify the system access, in addition are disposable some interfaces with the more usual utility programs (printing tabs, diagrams, selected list of records, etc. ...).

The system is running on the IBM 3081 computer installed at the C.N.R. Institute and will be accessible in BITNET network, using network services.

PC version of data base, for limited data blocks will be also disposable.

LARDERELLO REVISITED: NEW DATA UPHOLD THE 4 Ma AGE

M.Puxeddu[1], I.M. Villa[2] ([1] IIRG-CNR, Pisa; [2] IGGI-CNR, Pisa)

Seven years ago, Del Moro et al (Contrib.Min.Petr. 81(1982)340) proposed a history of the Larderello geothermal field: after the intrusion of a granitic body at 5-8 km depth about 4 Ma ago, which totally reset wall-rock biotites, the field cooled monotonically up to the present day. Numerical modelling predicts that the field could sustain its long life if continuously resupplied with heat from below. This model was challenged by Cliff (J.Geol.Soc.Lond. 142(1985)97) who asserted that the field had to be very young because biotites had not been reset despite being at 350 - 380° C.

New recoveries were made since, including the long-sought granite.

The biotite from well San Pompeo 2962 m (T ≈ 460°C; 1.61±.12 Ma by K/Ar) completely recrystallized during an early peak phase of the hydrothermal activity; a biotite from well VC11 (2946 m, T = 300° C), contact-metamorphosed by an aplitic dykelet, yielded 2.9 ±0.03 Ma; a biotite from the granite itself (well MV7, 3485 m, 320-350° C) yielded 3.8 ± 0.1 Ma. An Ar-Ar spectrum on the K-feldspar from MV7-3485 shows pervasive contamination with excess Ar (contrasting with the fact that all biotites had coincident K/Ar and Rb/Sr ages) and a saddle minimum of 2 Ma. This spectrum is rather ambiguous: it could represent a totally reset, zero age with an excess Ar concentration of 3.0 ppb, or a partly reset staircase spectrum with superimposed 2.2 ppb excess Ar. The latter case would support Cliff's two-pulse model. However, if the stepwise heating data are used to derive diffusion parameters ("thermochronometry"), one can obtain at most 227°C as closure temperature for the K-feldspar, which would achieve the observed 16% loss in 12 years or less at 350°, and in 56 years at 320°C. This irreal figure would require a rise by at least 150°C since 1933-77.

Petrography of over 500 drill core recoveries never shows the typical retrogression of the cold, fossil geothermal fields (e.g. Boccheggiano). In these cases, typical high-T assemblages (Kf+Ep+Chl+Sphe) are cut by low-T veins (Cc+Qz+Mu+Chl+Py). On the contrary, in the *center* of the Larderello field the high-T (250° -350°C) assemblages are sporadically replaced by lower T assemblages (150° - 250°C) only in the uppermost 1.5 - 2 km; in the periphery of the field, local replacements are more frequent. Most importantly, we ***never*** observe high-T assemblages cutting or substituting low-T ones: that is, no large-scale pulsations occurred. We do observe cross-cutting veins (i.e. intermittent hydrothermal activity), but all of the same temperature range.

Fluid inclusion microthermometry shows that the trapped hydrothermal fluid had a higher temperature than the present in-hole T (Belkin et al, Geothermics 14 (1985) 59) by 50°- 100°C; the T_h data indicate *no* hot-cold-hot history. New data from the San Pompeo well (Marignac et al, in prep.) indicate that an old fluid (400° -600°C, lithostatic P, salinity up to 50 - 60 wt%) was present in that well below 1.5 km , and is now confined to depths exceeding 3 km. The more superficial fluid (250° - 350°C, hydrostatic P, low salinity) resembles that seen by Belkin et al .

In conclusion, all the new evidence supports the single pulse model and rules out a history of two discrete pulses separated by a cold episode. The long life of the field can only be sustained if heat is steadily supplied from below; this is tantalizingly corroborated by teleseismic data (Foley,Toksoz,Batini,1989) who see an anomalous body extending into the upper mantle and broadening with increasing depth.

DECAY OF THICKNESS AND GRAINSIZE OF TEPHRA FALL DEPOSITS.

PYLE, D.M., Dept. of Earth Sciences, Downing St., Cambridge, CB2 3EQ, England.

The thickness and grainsize parameters of tephra fall and ash fall deposits provide one means by which volcanologists may analyse quantitatively the products of explosive eruptions. From such data, the dynamics and dimensions of eruptions may be assessed by applying the available models of pyroclast dispersal.

Field data, in the form of thickness isopachs or grainsize isopleths are commonly plotted on log-log thickness-area plots, where most data fall along curves. This simply implies that the decay of these parameters is exponential. The interpretation of these data is greatly simplified by plotting them instead on log(thickness)-square root(area) diagrams where exponentially dependent data will fall along straight lines.

The decay of the thickness and grainsize is best quantified by reference to the respective decay "half-lives": b_t, the thickness half-distance and b_c, the clast-size half-distance. The thickness half-distance is a measure of the dispersal of the deposit. It ranges from ~0.5km for small "cone building" eruptions, to 15-20km for the most widely dispersed plinian-style fall deposits. The clast half-distance is related principally to the column height, and ranges between <1 for eruptions with column heights lower than 10km, and 3-15 for plinian-style eruptions.

The value of this new scheme is that data can be linearly extrapolated to provide an estimate of the maximum thickness T_o of the deposit, and hence the volume from the Cole/Stevenson formula: $V=13.08T_o b_t^2$. A second feature is that the two half-distances need not be equal. The half-distance ratio is a measure of the "fragmentation", or inital grainsize population, of the deposit and ranges between 0.2 (fine skewed population) and 2.5, for most deposits. This further implies that widely-dispersed fall deposits need not be the products of high eruption columns.

A revised classification scheme for tephra fall deposits is proposed, in which the thickness half-distance ("dispersal") is plotted against the half-distance ratio ("fragmentation"). This can be simply contoured in terms of the clast half-distance and column heights derived from the models of tephra dispersal.

This analysis may also be applied to widely dispersed co-ignimbrite ashes, which typically have b_t ~60-100km. This simplifies the determination of the volumes of these ash falls and, combined with an improved mass-balance calculation, may be used to assess the partitioning of eruptive products between tephra fall, ash fall and ignimbrite.

GEOLOGICAL SETTING AND METALLOGENETIC MECHANISM OF GOLD DEPOSITS RELATED TO VOLCANIC-SUBVOLCANIC ACTIVITY IN EAST CHINA

QIJIANG, Ren, ZHAOWEN, Xu, and RONGYONG, Yang, Department of Geosciences, Nanjing University, People's Republic of China

The gold deposits related to volcanic-subvolcanic activity in East China can be divided into three major types: (1) vein deposits: this type can be further divided into three subtypes, namely (a) gold telluride deposits, such as Jmjushan; (b) low-sulfur deposits, such as Tongjing; (c) high-sulfur deposits, such as Jingquasi; (2) breccia-pipe deposits, such as Qiyugou, and (3) porphyry deposits, such as Shaxi.

In comparison to metallogeny of Circum-Pacific countries, the characteristics of this kind of hydrothermal gold deposits in East China are as follows:

(1) The metallogenic ages, predominantly from 90 to 170 Ma, are greater than those in most other countries.

(2) The economic values of the gold deposits of porphyry and breccia-pipe types are more important that those of vein types.

(3) Major deposits are mostly located on the edge of a volcanic basin of "superimposition type", in which the basement consists dominantly of Precambrian metamorphic rocks.

(4) Although the host rocks of orebodies belong to calc-alkalic, alkalic-calcic, alkalic igneous rocks, the dominant ones are calc-alkaline series.

(5) The high-sulfur vein-type gold deposits have been seldom found so far.

The volcanics and subvolcanic intrusives related to gold deposits in East China are located in three kinds of tectonic setting, namely: (1) Cenozoic island arc, (2) Mesozoic continental arc, (3) continental rift belt, associated with crustal extension, such as the Mesozoic volcanic basin along Tanchen-Lujiang deep fault. The most important gold deposits occur chiefly in the Mesozoic continental arc. According to mineral paragenesis, alteration and O-H isotopic composition of ore-bearing fluids and physical-chemical parameters of ore-bearing hydrothermal solution (especially their temperature, salinities, and chemical composition), the gold-bearing hydrothermal systems related to volcanic-subvolcanic activity can be classified as follows:

1. Meteoric-water-dominated system. 2. Mixing hydrothermal system. 3. Auriferous porphyry copper system. Most of gold deposits are the product of the first hydrothermal system; the gold in this kind of system is mainly extracted from country rocks by the vadose solution at depth. For the formation of the gold deposits related to the second and third hydrothermal systems, the volcanic magma played a more important role; at least part of the gold is derived from the magma.

The main mechanism in controlling the concentration and precipitation of gold in the three hydrothermal systems are boiling, mixing, and dilatancy.

Based on the characteristics of hydrothermal systems related to volcanic-subvolcanic activity, the prospecting method for this type of gold deposits in eastern China will be discussed by the authors.

CENOZOIC ISLAND ARC VOLCANIC ROCK SERIES AND SPACIO-TERMPORAL EVOLUTION ON FILDES PENINSULA, KING GEORGE ISLAND

QINGMIN, Jin, NANGUI, Shun, and FUXIANG, Kuang, Nanjing Institute of Geology and Mineral Resources

Cenozoic island arc volcanic rocks spreading in NE-SW widely distribute over Fildes Peninsula where locate at the southwestern end of King George Island. These rocks formed in Paleocene to Oligocene, which are composed of two rock series: low-K and high-aluminium tholeiites and calc-alkali basalts.

Low-K and high-aluminium tholeiites predominate in the area, which consists of tholeiites, alkaline olivine basalts, andesitic trachy-basalts, and basaltic-andesitic breccia, agglomerates and tuff. REE concentration (35.49 to 167 ppm) and La/Yb ratios (5.35 to 9.35) show that these rocks relatively enrich in LREE and slightly differ from oceanic tholeiites.

During Paleocene, early volcanic activity is restricted to southwestern part of the peninsula. The eruption centers lies to the southwestern coast, and Flat Top Hill and Horatio Stump are the main composite craters. Volcanism was predominant of extrusive flow and the volcanic rocks formed the Jasper Hill Member which consist of high aluminium basalts, basaltic andesites, and minor agglomerates and volcanic breccia at bottom. To associate with strong rifting in later stage of the volcanic activity, volcanism was enhanced and volcanic centers migrated northward. Eruptive style is still predominant of central type. The lava formed a broad basalt plateau in central and north part of the peninsula. The basalt plateau is composed of high aluminium basalts, andesitic basalts and pyroclastic rocks. This is period of the most intensive volcanic activity in the area.

In last Paleocene, the extensive area were uplifted until above sea level by differential block movement, and result in forming "red top" at the top of the Agate Beach Member basalts, and the "red top" reflect oxidation-erosion environment.

In Eocene, eruption centers of the south peninsula migrated eastward to the southeastern coast. At the beginning, volcanic activity was predominant of explosion, agglomerates and tuff were deposited in addition to volcanic breccia in caldera; and deposited alkaline basaltic and/or tholeiitic pyroclastic rocks in volcanic collapses or caldera basin; and volcanic-sedimentary rocks which contain plant fossil in the center of the basin, which formed Fossil Hill Member. Soon afterwards, eruptive activity took place in the southeastern and northeastern peninsula, the volcanism deposited basaltic-basaltic andesitic agglomerate and breccia lava of the Block Hill Member.

The scale of the last volcanism is relatively small in the area, and mainly overflow of calc-alkaline basaltic-andesitic lava. Andesites, andesitic trachybasalts, dacites and pyroclastic rocks distributed in the Fildes Cape of the north part and the northeastern Uruguay Station, which compose Block Hill Member. Eruption centers located in Norma Cove and Rocky Cove, and the flow direction of the volcanic products is from southeast to northwest. It belongs to volcanic cycle III in the area.

The composition of calc-alkali basaltic-andesitic lava is similar to the low-K high aluminium tholeiites, but the total abundance of REE is higher than the tholeiites and increase with alkalinity.

From Paleocene to Eocene, as time goes on, the spaciotemporal evolution of the island arc volcanism of the Fildes Peninsula as follows: eruption activity migrated from south to north. During the early stage, the scope of volcanism is relatively small and restricted to the southern part of the peninsula; up to the middle stage, the scale of volcanism extended into the whole area; in the later stage, the eruption center transferred to the northeastern part, and the scope of volcanism was reduced. Overflow of lava predominated in the northern part, while subvolcanic intrusion predominated in the southern and central part of the peninsula. The magma evoluted from tholeiitic to calc-alkaline rocks. During magma ascending, aluminium and abundance of K, Ba, Sr in the magma were increased by contamination of crust material.

CRETACEOUS-TERTIARY MAFIC DYKE INTRUSIONS IN KOTTAYAM REGION, SOUTHWESTERN INDIA: GEOCHEMICAL IMPLICATIONS FOR CONTINENTAL MAGMATISM AND LITHOSPHERIC PROCESSES

RADHAKRISHNA, T. and THAMPI, P.K., Centre For Earth Science Studies, Trivandrum 695 031, India, MITCHELL, J.G., School of Physics, University of Newcastle Upon Tyne, UK, NE1 7RU and BALARAM, V., National Geophysical Research Institute, Hyderabad 500 007, India

The post Archaean continental magmatism in Southwestern Indian Shield is largely manifested in the form of dyke intrusions. They are generally regarded as Mesozoic magmatic responses related to the rifting along the west coast. Exact ages of these intrusions or their petrogenetic history are not yet clearly understood. We reported elsewhere the Proterozoic ages (2030 $\pm$ 65 m.y; K-Ar isotope ages)along with petrogenetic interpretations for an ENE-WSW dolerite dyke swarm. In this paper we are presenting new K-Ar isotope results, geochemistry and petrogenetic aspects of the dyke intrusions occurring within the charnockite and other related high grade country rocks around Kottayam.

The dyke intrusions in Kottayam region are broadly grouped into NW-SE trending dolerites and NNW-SSE trending leucogabbros . The field observation that the dolerite cutting through leucogabbro is significant. The relative chronology thus inferred is confirmed by K-Ar isotope age data. The isotope data are compatible with 85 $\pm$ 5 m.y age for the leucogabbro swarm and 65$\pm$ 1 m.y for the dolerite swarm suggesting magmatism at different stages of crustal extension. The results coupled with precise palaeomagnetic vectors would be of interest to understand rifting and the northward drift of India.

Petrographically the dyke swarms contain plag+cpx+opaques+oliv+opx+biot+ap; however, the leucogabbros are always devoid of olivine and orthopyroxene. Geochemical data on several representative samples show that leucogabbros and dolerites are conspicuously distinct in their compositions. The leucogabbros have enhanced levels of incompatible elements, 60-100 x chondrite REE abundances and higher levels of REE pattern. The leucogabbros are transitional in chemistry between tholeiite and alkali basalt having more affinity towards alkaline type whereas the dolerites are transitional between MORB and continental tholeiites with affinity towards the former. There are no significant differences in Mg-values of both swarms. The incompatible element abundances and their ratios, in comparison to the MORB, upper crustal averages and country rock geochemistry would suggest that the affects of crustal contamination are negligible and the compositions are controlled by petrogenetic processes. The different and consistent REE and trace element features in both rock units precludes them being related to each other by crystal fractionation. The incompatible trace element chemistry could be explained by different degrees of melting and/or minor variations of incompatible elements in the source region.

PETROLOGY AND GEOCHEMISTRY OF THOLEIITIC DIKES IN THE EASTERN FENNOSCANDIAN SHIELD : EVOLUTION OF A MIDDLE PROTEROZOIC CONTINENTAL RIFT

RÄMÖ, O.T., University of Helsinki, Department of Geology, P.O.Box 115, SF-00171, Helsinki, Finland

In southern Finland, several sets of mainly WNW trending Subjotnian (1.65 Ga) diabase dikes intruded the Early Proterozoic Svecofennian (1.9-1.8 Ga) crust in an extensional anorogenic tectonic setting. The dikes were emplaced concurrently with voluminous epizonal silicic intrusions (rapakivi granites) and associated felsic dike rocks, and probably represent feeders to continental volcanics. At a later stage, Jotnian (1.27 Ga) diabase dikes were emplaced in a NW trending sandstone-filled graben in southwestern Finland. No silicic magmatism is known to be associated with the younger Jotnian diabases.

The Subjotnian (SD) and Jotnian (JD) diabases show many of the geochemical characteristics of the Phanerozoic continental flood basalts. SD are olivine-normative to quartz-normative (from Ol 11% to q 17%), quite evolved (Mg# 33 to 54, Ni<50 ppm), high Ti (av. TiO_2 2.5%) tholeiites that occasionally exhibit high-Al characteristics (up to 18.5% Al_2O_3). JD are less evolved olivine tholeiites (Mg# 39 to 56, Ni 50 to 100 ppm, Ol 9 to 21%) with high Ti (av. TiO_2 2.2%) and Al_2O_3 ranging from 13.7 to 17.2%. Mg# correlates positively with Al and negatively with Ti in both SD and JD. Abundances of incompatible trace elements are up to three times higher in SD relative to JD, e.g., averages (in ppm) for SD are Rb (49), Ba (625), Nb (21), and Zr (248); for JD the values are Rb (21), Ba (480), Nb (7), and Zr (113). Also REE compositions of SD and JD differ markedly: SD have more LREE-enriched patterns with La 90 to 175 times chondritic, $(La/Yb)_N$ 5.9, and no Eu anomaly, while JD show La 25 times chondritic, $(La/Yb)_N$ 3.6, and a slight positive Eu anomaly. Primordial mantle normalised incompatible element patterns of SD resemble those of continental tholeiites (CT), whereas JD show patterns closer to initial rifting tholeiites (IRT).

$\epsilon_{Nd}(T)$ values of the diabases (Fig. 1) exhibit clearly that a LREE-depleted mantle existed beneath the Fennoscandian Shield during Middle Proterozoic time. ϵ_{Nd} values correlate positively with Mg# and negatively with K_2O (Fig. 1), Rb, Zr, and Ce. This suggests that the magmas have inherited their enriched character by processes involving crustal contamination coupled with fractional crystallisation. The 1.65 Ga SD dikes intruded in a bimodal association in which large volumes of silicic magmas were produced in the cratonised Svecofennian crust. In such a melt-loaded crust mafic melts passing through could easily be contaminated, especially with incompatible elements. The 1.27 Ga JD dikes were probably emplaced into a more mature rift with thinned continental lithosphere, and thus were less affected during their passage through the crust.

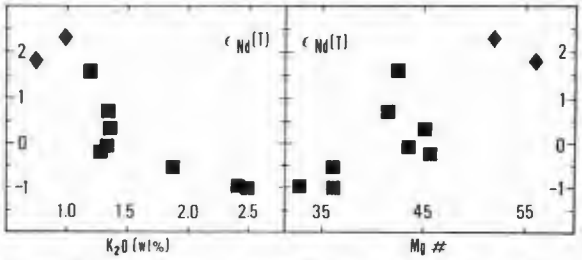

Figure 1. $\epsilon_{Nd}(T)$ values versus K_2O(wt%) and Mg# of the Subjotnian (■) and Jotnian (♦) diabase dikes.

ERUPTIVE HISTORY OF MAYON VOLCANO, PHILIPPINES

RAMOS-VILLARTA, S.C., University of the Philippines, UPCCAB Office, Diliman, Quezon City, Philippines.
CORPUZ, E.G., Philippine Institute of Volcanology and Seismology, Hizon Bldg, Quezon Blvd, Quezon City, Phil.
NEWHALL, C.G., U.S. Geological Survey National Center, MS 905 Reston, Virginia 22092 U.S.A.

Mayon Volcano is an active andesitic volcano in the eastern (Bicol) volcanic chain, and has erupted 44 times over approximately 400 years of recorded history. Of these eruptions, more than half caused loss of life or serious damage to property. In addition, lahars unrelated to volcanic activity have occurred at least 7 times.

The volcano consists of basaltic to andesitic lava flows, pyroclastic flow and debris flow deposits, and tephra fall deposits. Except for the 1814 Plinian eruption, all other historical eruptions have been Vulcanian or Strombolian. Two common eruptive sequences are recognized: some eruptions begin with mild explosions and light tephra fall, intensify to include puroclastic flows and end with lava extrusion (e.g., the 1968 eruption), whereas other eruptions begin with quiet emission of lava and end with explosive ejection of pyroclastic materials (e.g., the 1984 eruption).

The volcano's near-perfect symmetry implies that most of its eruptions have been from a central vent, that pyroclastic ejecta are distributed more or less uniformly around all sectors of the volcano, and that no recent eruptions have been large enough to destroy that symmetry.

FLOOD BASALT VOLCANISM IN SPACE AND TIME

RAMPINO, M.R., Earth Systems Group, Dept. of Applied Science, New York University, New York, NY 10003, and
STOTHERS, R.B., NASA, Goddard Space Flight Center, Institute for Space Studies. New York, NY 10025

We have established a chronology of the dates of major continental flood basalts using a compilation of published potassium-argon, argon-argon, and other ages of basaltic rocks and related intrusions. These data have been augmented by additional information regarding stratigraphy, paleomagnetism, geochemistry, and other properties of flood basalts. Eleven distinct episodes of flood basalt volcanism have occurred over the past 250 million years. They are listed here with their start date in Myr BP: The Siberian Traps (250±10), Eastern North American Basalts (200±5), South African (Karoo) (190±5), Antarctic (170±5), South-west African (135±5), Serra Geral (130±5), Rajmahal Traps (110±5), Deccan Traps (66±2), Brito-Arctic (62±3), Ethiopian (35±2), and Columbia River (17±1). The main eruptive stages of these flood basalts were relatively brief (< 2-3 Myr).

Flood basalt episodes have occurred quasi-periodically, with a mean cycle time of 32±1 Myr (error of the mean). Initiation dates of the basaltic eruptions are close to times of mass extinctions of life, and dated large impact craters. The Deccan Traps of India, for example, correlate well with the K/T mass extinctions, and worldwide physical evidence of a large impact. The mass extinctions and impact craters also occur with a similar period of about 30 Myr. An impact-related cause for the flood basalt volcanism is indicated, and recent modeling of impactor penetration suggests that basaltic volcanism could be initiated by large asteroids or comets hitting continental crust . Continental flood basalts mark the initiation of subcontinental hotspots. The possibility that mantle plume activity, and subsequent hotspots and rifts could be triggered by large impacts is worthy of further study and geophysical modeling.

The flood basalt eruptions may have considerable effects on the environment, as they are capable of releasing large amounts of sulfur volatiles into the atmosphere. It is possible that periods of massive basaltic volcanism can prolong the conditions adverse to life, and contribute to the extended "Strangelove Ocean" of low productivity that persists for >500,000 years after some major mass extinction events.

Table 1. Ages of flood basalt initiations and mass extinctions.

Flood basalts		Mass extinctions	
Episode	Age (10^6 years)	Stage	Age (10^6 years)
Columbia River (U.S.)	17 ± 1	Lower to middle Miocene	14 ± 3
Ethiopian	35 ± 2	Upper Eocene	36 ± 2
Brito-Arctic	62 ± 3	Maastrichtian	65 ± 1
Deccan (India)	66 ± 2		
		Cenomanian	91 ± 0
Rajmahal (India)	110 ± 5	Aptian	110 ± 3
Serra Geral (S. America)	130 ± 5	Tithonian	137 ± 7
South-West African	135 ± 5		
Antarctic	170 ± 5	Bajocian	173 ± 3
South African	190 ± 5	Pliensbachian	191 ± 3
Eastern North American	200 ± 5	Rhaetian/Norian	211 ± 8
Siberian	250 ± 10	Dzulfian/Guadalupian	249 ± 4

Compositional dependence of Pb isotopic signatures in the lower crust exhibited by xenoliths from Kilbourne Hole, New Mexico.

REID, M.R., Dept. of Earth and Space Sciences, UCLA, Los Angeles, CA 90024

Pb isotope analyses of lower crustal xenoliths from Kilbourne Hole, New Mexico, exhibit the unradiogenic Pb isotope signatures typically ascribed to the lower crust but also reveal systematic variations in Pb isotopic signatures with composition. Three groups of lower crustal xenoliths are considered here: gabbro-norite-anorthosite *mafic orthogneisses (MO)*; charnockitic *silicic orthogneisses (SO)*; and both pelitic and psammitic *paragneisses (P)*. Of these, at least the SO and P are inferred to have been emplaced during formation of the crust at ~1.7 Ga.

Pb concentrations in the xenoliths increase in the order: MO (0.4-0.9 ppm) →SO (4.1-8.7 ppm) →P (10.8-18.0 ppm). Leaching experiments show that <4 wt% caliche (locally present in the samples) may account for up to 27% of the Pb of the untreated MO samples and has a significant effect on the Pb isotope characteristics (Figure 1). After leaching, all of the Kilbourne Hole xenoliths fall to the left of the geochron on a $^{207}Pb/^{204}Pb$-$^{206}Pb/^{204}Pb$ diagram (Figure 1). Both the $^{206}Pb/^{204}Pb$ ratios and μ's of the MO are consistently higher than the SO and P (μ=2.3-5.3 vs <2 in the SO and P). Nevertheless, the initial ratios of the MO are difficult to explain by formation at ~1.7 Ga and are more consistent with the underplating of magmas like those erupted in the rift between 40 and 10 Ma ago. In $^{208}Pb/^{204}Pb$-$^{206}Pb/^{204}Pb$ space (Figure 1), the fields of SO and P overlap and yield time-integrated Th/U ratios of ~15. Time-integrated Th/U ratios for the MO are considerably lower (~3) which also may be attributable to relatively recent extraction from the mantle.

The Pb isotope characteristics of the SO and P are consistent with an early-middle Proterozoic origin. Moreover, their high Th/U ratios and Pb contents show that silicic materials can more readily account for the high Th/U reservoir required by global Pb systematics than can mafic materials. On the other hand, the Pb isotope characteristics of the MO are most easily explained by relatively recent mafic intrusion of the lower crust. This inference is only strengthened if crustal assimilation was involved in the origin of the MO. Textural evidence of their intrusion has apparently been erased by subsequent recrystallization related to continued rift activity.

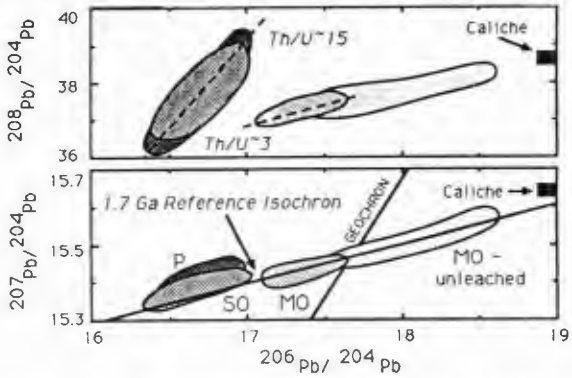

Figure 1. Pb isotope characteristics of Kilbourne Hole xenoliths

FLOOD BASALTS AND HOTSPOT TRACKS: PLUME HEADS AND TAILS

RICHARDS, Mark A., Department of Geological Sciences, University of Oregon, Eugene, Oregon 97403,
DUNCAN, Robert A., College of Oceanography, Oregon State University, Corvallis, Oregon 97331,
COURTILLOT, Vincent E., Institut de Physique du Globe de Paris, Place Jussieu, 75005 Paris

Massive accumulations of basaltic lavas of tholeiitic composition occur worldwide. These provinces are variable in age (predominantly Mesozoic and younger) and may cover areas as large as 2 million km^2 with as much as 2 km-thick sequences of lava flows. Volcanic eruptions appear to have been mainly non-explosive, from fissures, and single large-volume, low-viscosity flows covered enormous areas extremely rapidly, leading to the descriptive term "flood basalts." In general, field, magnetostratigraphic and age data indicate that the predominant portion of these provinces accumulated in a few million years at most.

These enigmatic events are not satisfactorily explained by any known plate tectonic process. Although many flood basalt provinces occur along continental margins and are associated with initiation and early development of rifting, there are notable exceptions, e.g., the Columbia River Basalts, the Siberian Traps, and the Deccan Traps. An association of flood basalts with hotspots was noted by Morgan (1972, 1981), who suggested that flood basalts occurred at the initiation of mantle plume activity following entrapment of plume material beneath an insulating continent. We have re-examined the spatial and temporal links between hotspots and the three largest flood basalt events of the last 200 Myr, and we find that the relative volumes of melt and eruption rates can be quantitatively explained by a simple model of mantle plume initiation. Continental lithosphere and rift tectonics are not required and we may expect to find flood basalt provinces as a natural consequence of the initiation of hotspot activity, in ocean basins as well as on continents.

The Deccan basalts of India (67 Ma), the Parana-Etendeka basalts of Brazil and Namibia (125 Ma), and the Karroo basalts of southern Africa (190 Ma) have each been traced to presently active hotspots: Reunion, Tristan da Cunha, and Marion, respectively. A continuous record of volcanic activity connects the flood basalt provinces with the hotspots, and the flood basalts are the earliest manifestation of the hotspot volcanism. From estimates of the original volumes of flood basalts and precise radiometric dating of the duration of volcanism at each province we find that eruption rates were approximately 30 times greater than those observed at the active hotspots. We seek to explain this basic observation.

Following Whitehead and Luther (1975) we consider a low viscosity plume being fed at a constant rate at the base of the mantle (CMB). If the plume remains connected to its source, it forms a very large "head" followed by a feeder "tail." When the plume head reaches the base of the lithosphere it produces melting, doming, and often continental rifting. The tail causes reduced but continuous activity following the initial flood basalt event, and forms a hotspot track due to motion of the lithospheric plate. Using reasonable plume buoyancy and mantle viscosity values and using observed eruption rates at hotspots to estimate plume supply rate, our simple quantitative model shows, for example, that the Deccan Plateau could have been formed by a blob of material ~240 km in diameter which initiated the Reunion hotspot. This model is also successful for the Parana and Karroo events.

Other continental flood basalts have been linked to active hotspots: the Columbia River Basalts to Yellowstone, the Brito-Arctic basalts to Iceland, and the Rajmahal basalts to Kerguelen. Large, submerged oceanic plateaus may also be flood basalts formed during the initial activity of hotspots, such as the Ontong Java Plateau, associated with the hotspot that formed the Louisville Ridge (south Pacific Ocean). Much of the anomalously shallow Caribbean plate is thought to be a thick accumulation of basalt flows, which has been linked to the initiation of the Galapagos hotspot.

We note two logical consequences of our model:

(1) A deep-mantle origin for flood basalts is consistent with the observation that they often have enriched geochemical signatures more similar to ocean island (hotspot) basalts or continental crust than to mid-ocean ridge basalts (MORB) derived from the shallow sub-oceanic mantle.

(2) Rampino and Stothers (1988) have proposed that flood basalt eruptions coincide with mass extinction events, both of which they suggest are caused by periodic meteor impacts. However, this appears implausible if hotspots and flood basalts are closely related: Meteors would not coincidentally land on mantle plumes, and they could not be buried deeply enough upon impact to result in hotspot sources which remain relatively stationary with respect to plate motions for periods of ~100 Myr. Rather, we suggest that if the flood basalt-extinction relationship holds, both are the result of plume initiation and, perhaps, core-mantle boundary instability.

RELATIONS BETWEEN ASH-FLOW MAGMATISM AND CRUST MODIFICATION IN THE SAN JUAN VOLCANIC FIELD, COLORADO

RICIPUTI, L.R. & JOHNSON, C.M.,
Department of Geology & Geophysics,
University of Wisconsin, Madison,
WI, USA, 53706.

Epsilon Nd values of mineral separates from the large volume ash-flow tuffs of the San Juan volcanic field in south central Colorado range from -9.7 to -6.5. Nd isotope ratios generally increase as the ash-flow tuffs become younger, suggesting an increase in mantle component with evolution of the magmatic system through time.

This trend can be modelled as an ongoing interaction between an influx of mantle-derived basalts and lower crustal Proterozoic country rock during the development of the magmatic system. The San Juan tuffs have epsilon Nd values midway between those of Proterozoic granitic rocks (-10 to -14) and local mantle values (+2 to -1), as indicated by basaltic lavas erupted in the nearby northern Rio Grande rift. The low epsilon Nd values of the oldest ash-flow tuffs (Sapinero Mesa and Fish Canyon) may indicate that a large amount of crustal assimilation occurred during the early stages of evolution of the magmatic system. Continued injection of mantle-derived basalt extensively hybridizes the crust, driving the bulk epsilon Nd value closer to that of the mantle. Subsequent magmatism, as reflected in the Bachelor and younger tuffs, will contain substantially larger mantle components.

Unit	Age (Ma)	Volume (km^3)	ε_{Nd}
Nelson Mtn	26.15	>500	-7.0
Wason Park	27.15	100-500	-7.0
Mammoth Mtn	27.60	100-500	-6.5
Bachelor	27.60	>1500	-7.4
Fish Canyon	27.80	>3000	-7.9
Sapinero Mesa	29	>1500	-9.7

MAFIC JUVENILE FRAGMENTS FROM PYROCLASTIC SURGE DEPOSITS ASSOCIATED WITH DEBRIS AVALANCHE DEPOSITS AT NEVADO AND FUEGO DE COLIMA VOLCANOES, MEXICO

ROBIN C (Université Blaise Pascal and CNRS, 5 rue Kessler, 63038 Clermont-Ferrand Cedex, FRANCE)
KOMOROWSKI J-C. (Arizona State University, Department of Geology, Tempe, AZ, 85287; 602-965-3760; BITNET: ATM3S @ ASUACAD)

The transition between the terminal cones and the ancestral edifices of Nevado and Fuego de Colima is marked by the deposits of gigantic volcanic debris avalanches of the Mount St. Helens type. Pyroclastic surge-like deposits (here interpreted as a blast deposit) were discovered in association with these avalanche deposits.

At **Nevado de Colima** the outcrops studied are directly on the debris avalanche deposit near the mouth of the avalanche caldera. The tephra consist of a 3 to 5 m thick sequence of gray poorly-sorted coarse-grained lenticular layers 1 to 2 m long and a few cm to 40 cm thick. These layers are interbedded with poorly-sorted ash- and pebble-size dune bedded layers with abundant gray to brown pumice and lithic fragments of andesite which are analogous in composition and mineralogy to andesite lavas visible in the caldera wall. The dune-bedded coarse-grained layers are separated by very fine-grained white ash layers containing white pumice fragments. **An unusual characteristic of the dune-bedded deposits is the abundance of unbroken black poorly-vesiculated cauliflower bombs up to 10 cm in diameter.** Scanning electron microscope textural data on the major vesiculated fraction reveal well-developed and fresh vesiculation features and non-altered glassy surfaces all compatible with an explosive magmatic origin. The mafic juvenile fragments represent the most primitive magma ever erupted by the volcano (SiO_2 = 52.50 %). The lavas directly preceding and following the debris avalanche event are silicic andesites (SiO_2 = 59 %).

At Fuego de Colima deposits similar to those described above for Nevado were observed directly overlying the debris avalanche deposit near the crest of hummocks on sides facing the volcano. Vesiculated dark fragments and centimetric bombs composed of black mafic magma interpreted as juvenile in origin are common throughout these pyroclastic deposits. The juvenile mafic fragments have 56 % SiO_2. The lavas from the upper parts of the caldera wall are dacites (65 % SiO_2) whereas the terminal cone is composed of silicic andesites.

At Nevado, several petrologic data are unequivocally compatible with a model for interaction of mafic magma from depth with residual andesitic or dacitic magma from the superficial magma chamber just prior to the eruption of pyroclastic blast-like deposits associated with cone collapse. This evidence includes: (1) banded juvenile bombs of intermediate composition; (2) the range of composition of these bombs from SiO_2 52.50 % to 58 %; (3) inverse zoning in clinopyroxene with strong Mg enrichmnent towards the rim; (4) mineral destabilization in plagioclase; and (5) significant compositional variations for the vitric phase within the same sample. Volcanic debris avalanche events at Nevado and Fuego de Colima may thus correspond with major breaks in the petrological evolution of the volcanoes and the start of a new magmatic cycle. **Consequently, major injection of mafic magma within the presently perched viscous dome of the active Fuego cone could clearly enhance the likelyhood of southward flank collapse in this already unstable edifice.** Such a scenario must be considered in future hazard assessment of the active Fuego cone. Risk to life and property for the entire Colima region associated with such catastrophic phenomena would be immeasurably greater in comparison with hazards related to the last explosive outburst in 1913 which resulted in the emplacement of pyroclastic flows over uninhabited regions of the upper flanks of the volcano.

COMPOSITION OF CONTINENTAL LITHOSPHERE BENEATH THE COLORADO PLATEAU AND ITS ROLE IN THE GENESIS OF ALKALINE MAGMAS

RODEN, M. F. Dept. of Geology, Univ. Georgia, Athens GA 30602, SMITH, D., Dept. Geological Sci., Univ. Texas, Austin TX 78713, and SHIMIZU, N., Earth Atmosph. & Planet. Sci., MIT, Cambridge MA 02139

We developed a model for the composition of the continental lithosphere based on isotopic and trace element[1] analyses of xenoliths from the Oligocene Navajo diatremes. These xenoliths include garnet peridotites derived from near the base of the Oligocene lithosphere and spinel peridotites, eclogites and disaggregated garnet peridotities derived from shallower depths. The shallow lithosphere is commonly hydrated, depleted in a major (ave. Fo = 91) and trace element sense (typically LREE/HREE < chondrites; Ti to < 100 ppm and Sr to < 1 ppm in cpx) and is isotopically similar to Proterozoic oceanic lithosphere. Present-day highly radiogenic Nd isotopic compositions of some minerals probably reflects long-term (>1Ga) isolation from mantle convection; low Nd (0.97 ppm) and high Sr/Nd (160) and moderate 87Sr/86Sr (0.705) of separated amphibole suggest that seawater may have been important in the hydration event. Olivines (typically Fo 92) derived from disaggregated garnet peridotites suggest that the lithosphere becomes increasingly depleted with depth, however, garnet peridotites from the greatest depths have chondritic or LREE-enriched REE patterns and are isotopically similar to OIB although displaced slightly below the mantle array. A most intriguing feature is an inverse correlation between 87Sr/86Sr and calculated temperature in garnet peridotites; we interpret this correlation to reflect the intrusion of low 87Sr/86Sr magmas into the base of the continental lithosphere. These intrusions may be related to the warming of the Plateau lithosphere as deduced from present-day heat flow measurements. The garnet peridotites from The Thumb are isotopically similar or identical to the Hopi Buttes lavas: these alkaline magmas may have formed by melting near or at the base of the lithosphere where repeated intrusions of incompatible element-rich, low 87Sr/86Sr, high 143Nd/144Nd magmas produced a "steady-state" peridotite enriched in incompatible trace elements and isotopically similar to OIB. Warming during the late Tertiary produced melting in this region and ultimately, the Pliocene Hopi Buttes monchiquites.

[1] Including, in addition to our data, data from Ehrenberg (1982) and Menzies and Hawkesworth (1987)

COMPOSITIONAL GRADIENTS IN THE BANDELIER TUFF (PLEISTOCENE), PAJARITO PLATEAU, LOS ALAMOS AND SANTA FE COUNTIES, NORTHCENTRAL NEW MEXICO

ROGERS, Margaret Anne, MARA, Inc., 1753 Camino Redondo, Los Alamos, New Mexico 87544

The Pajarito Plateau, which flanks the eastern side of the Jemez Mountains, has extensive exposures of the Bandelier Tuff which were mapped at a scale of 2.54 cm = 122 m for the Los Alamos National Laboratory. The mapping project required the establishment of new stratigraphic units within the most extensively exposed member, the Tshirege. The mapping units, A, B, C, D, E, and F, have lateral continuity, depositional boundaries, topographic expression, and differences in coloration, crystallization, and welding. No unit appears to represent a single event and some units are obviously composed of several.

In order to find a means of correlating subsurface information with outcrop, 142 whole-rock samples (primarily Tshirege, but including Otowi, Cerro Toledo Tuffs, and El Cajete) from 56 locations were analyzed for Na, K, Rb, Cs, Mg, Ca, Sr, Ba, Al, Si, Sn, Pb, Ti, Zr, Hf, As, Sb, Bi, V, Nb, Ta, Se, Mo, W, Cl, Mn, Fe, Co, Cu, Au, Zn, Sc, La, Ce, Sm, Eu, Tb, Dy, Yb, Lu, Th, and U. Discriminant analysis showed that U was the most important element in identifying the Tshirege subunits and 82.7% of known samples were correctly classified using U, Fe, Th, and Cs values.

Geochemical trends for the Otowi, Cerro Toledo Tuffs and Tshirege are remarkably similar. The Cerro Toledo Tuffs lie unconformably between the lower and upper members of the Bandelier, the Otowi and Tshirege respectively. Available data shows differences for Al, Si, K, Zr, Sb, Hf, and Ce between the Otowi and Tshirege and for Mo and Ta between the Cerro Toledo Tuffs and the Bandelier. For Sb the Cerro Toledo Tuffs and Otowi trends are alike. V was found only in the Otowi ash flows. Ti was found only in the Tshirege. No Eu was found in the Cerro Toledo Tuffs and no Mg, Sr, Cr, or Au was found in any unit.

Early/late enrichment factors show the Bandelier enriched in Cl, Mn, Zn, As, Rb, Nb, Cs, Ta, W, Pb, Sm, Dy, Yb, Lu, Th, and U and depleted in Na, Sc, Ti, Fe, Co, Cu, Mo, Ba, La, Eu, and Tb. The Otowi is more enriched than the Tshirege in Al, K, Ca, Mn, As, Zr, Nb, Sb, Hf, Ce, Sm, Dy, Yb, Lu, and Th and the Tshirege is more enriched than the Otowi in Si, Cl, Zn, Rb, Cs, Ta, W, Pb, Yb, and U. The Otowi is more depleted than the Tshirege in Ti, Co, Mo, Eu, and Tb and the Tshirege is more depleted than the Otowi in Na, Sc, Fe, Cu, Ba, and La. The Cerro Toledo Tuffs are less enriched than the Bandelier in Zn, Cs, W, Th and U and less depleted than the Bandelier in Co. For As, Mo, Sb, Ba, Ta the Cerro Toledo Tuffs show other differences with the Bandelier.

Geochemical trends within the Tshirege rarely show either consistent enrichment or depletion from subunit to subunit. The various patterns of enrichment or depletion for elements as well as elemental ratios are repeated in most cases. There is a strong suggestion that within a subunit (also, within an outcrop) that the early/late enrichment factor trends of the Tshirege are repeated. This is true for Units A and B.

POTASSIC MAFIC ROCKS FROM THE VIRUNGA AND THE KAROO AND THE COMPOSITION OF THE SUBCONTINENTAL MANTLE

ROGERS N.W., [1]ELLAM, R.M., PEATE, D.W. and HAWKESWORTH, C.J. Dept. of Earth Sciences, Open University, Milton Keynes, MK6 7AA , U.K. and [1]Dept. of Earth Sciences, University of Oxford, Parks Rd., Oxford OX3 0BP, U.K.

The parental basanites of the potassic lavas of the Virunga Province, W. Rift, Central Africa are shown to be hybrid magmas which result from interaction between an asthenospheric component, represented by local melilitites, and lithosphere-derived ankaramites. The latter occur in monogenetic cones scattered throughout the province and are considered to have been derived directly from the lithospheric mantle and to have suffered insignificant crustal contamination en route to the surface. Their $^{87}Sr/^{86}Sr$ values range from .7057 up to .7072 and $^{143}Nd/^{144}Nd$ from .51258 down to .51243, reflecting their trace element enriched (high Rb/Sr, low Sm/Nd) source. Pb isotopes in the ankaramites show little variation with $^{206}Pb/^{204}Pb$ varying from 19.16 - 19.29, $^{207}Pb/^{204}Pb$ from 15.73 - 15.78 and $^{208}Pb/^{204}Pb$ from 40.45 - 40.70. The latter two ratios however are particularly extreme for mantle-derived magmas and result from both the antiquity of the source region and its high time-integrated Th/Pb ratio. High values of $^{208}Pb^*/^{206}Pb^*$ also indicate a high Th/U ratio and this is reflected in the measured values in the rocks which may be as high as 6. Some key element ratios, such as Th/Ta, are also slightly anomalous compared with non-potassic intra-plate basalts, but the ankaramites have high concentrations of both HFS and LIL elements and thus differ significantly from the subduction-related potassic rocks of the Italian Province. Age constraints are difficult to place on the source enrichment event. Model Nd ages suggest that it occurred during the late Proterozoic while the high $^{207}Pb/^{204}Pb$ ratios imply a complex evolution with U/Pb fractionation much earlier in Earth history.

Similar trace element features are seen in other mafic magmas of lithospheric origin, notably the Nuanetsi picrites from the Karoo Province and the high-Ti flood basalts from the Parana. Nd isotope variations in the Nuanetsi samples suggest a source age of ~1.0 Ga, while Pb isotopes imply low U/Pb but high Th/U. Th/Ta ratios again tend to be slightly high. However, in contrast to the Virunga, the picrites define a vertical trend on the Nd-Sr isotope diagram, although $^{87}Sr/^{86}Sr$ values are no greater than those in the Virunga ankaramites. Similarly, Pb isotope data from the Parana basalts suggest a source age of 1-2Ga while the high-Ti rocks again have low $^{87}Sr/^{86}Sr$ coupled with high $^{208}Pb^*/^{206}Pb^*$.

These three examples of basaltic volcanism thus show a number of common features that appear to be characteristic of their lithospheric source regions. These include low time-integrated Sm/Nd, high Th/U, low to moderate Rb/Sr but a complex U/Pb fractionation history. In addition all three examples are characterised by high TiO_2 and HFS element abundances and while ratios such as Th/Ta are slightly anomalous, there is not the marked preferential enrichment of the LIL over the HFS elements as seen in subduction-related magmatism. Trace element enrichment is thus attributed to the migration of small volume melts into the continental lithospheric mantle at various times since the Archaean, with Sr isotopes in particular reflecting stabilisation of discrete potassic (and hence Rb-bearing) phases such as amphibole and phlogopite. Comparison with OIB from the DUPAL anomaly again reveals similar geochemical features and it is suggested that such anomalous OIB sources reflect interaction with delaminated subcontinental lithosphere.

REGIONAL VARIATIONS IN Sr AND Nd ISOTOPIC COMPOSITION OF SHIELD VOLCANOES, CENTRAL MEXICO

ROGGENSACK, K., and BARREIRO, Barbara, Department of Earth Sciences, Dartmouth College, Hanover, NH 03755

The Central Mexican Volcanic Belt (MVB) is chraracterized by 139 shield volcanoes interspersed with more than 1,000 cinder cones. This volcanism is Plio-Quaternary in age and largely calc-alkaline in composition. The shields range between 50 and 63 wt.% silica with common plagioclase, olivine, and pyroxene phenocrysts and glomerocrysts. Hornblende phenocrysts are very rare. Major element chemistry of the shields is very similar to that of the cinder cones (Hasenaka and Carmichael, 1987). The major difference is that titanium and phosphorous are higher in the shield volcanoes and are high compared to other calc-alkaline arcs. One-third of the shields have TiO2 >1.3 wt.% (as high as 1.7 wt. %) and one-half have P_2O_5 >0.3 wt.% (as high as 0.6 wt. %).

Cluster analysis (two-stage density fusion) has previously been used (Connor,1987; Roggensack, 1988) to show that the cinder cones and shield volcanoes have non-uniform geographic distributions. Each of these volcanic forms occur in distinct geographic groups or clusters which overlap locally. The geographic clusters of shields are related to chemical composition. Student t-tests show that the oxides TiO_2, P_2O_5, SiO_2, and MgO are significantly different between shield clusters at the 90% confidence interval. Also, REE concentrations have different relative levels of total REE enrichment between clusters. Since the REE concentrations correlate negatively with silica, calc-alkaline (POAM) fractionation can not be the main control of their enrichment level. A Sr and O isotope study by McBirney et. al. (1987) found that crustal contamination had a negligible effect on REE concentrations at Paricutin cinder cone. The inter-cluster major and trace element differences, negative REE and silica correlation, and the Paricutin data all suggest that distinct geographic shield clusters have distinct chemistry due to source heterogeneity.

Preliminary Sr-Nd isotopic data on the shield volcanoes indicates that there is a relationship between isotopic composition and geographic location. $^{87}Sr/^{86}Sr$ ratios from 12 samples vary between 0.70324 to 0.70432 falling exactly within the range established by Verma and Hasenaka (1987) for cinder cone samples and some shield samples. Several $^{143}Nd/^{144}Nd$ values (ca. 0.5128) are also within the range previously reported by these authors (0.51271-0.51295). The Sr isotopic compositions from the shields are correlated with silica content and 1/Sr implying assimilation of crustal material (AFC). These correlations are only apparent between volcano samples from the same geographic cluster, and separate distinct clusters seem to form distinct mixing trends, indicating that the different shield clusters have distinct mixing end-members. On the diagram three regression lines are plotted through data points from three distinct clusters (r^2 values : 0.97,0.94, and 0.69). This preliminary isotopic data is in good agreement with inter-cluster major and trace element variation, suggesting that distinct geographic shield clusters have distinct chemical histories involving different source compositions and variable crustal interaction.

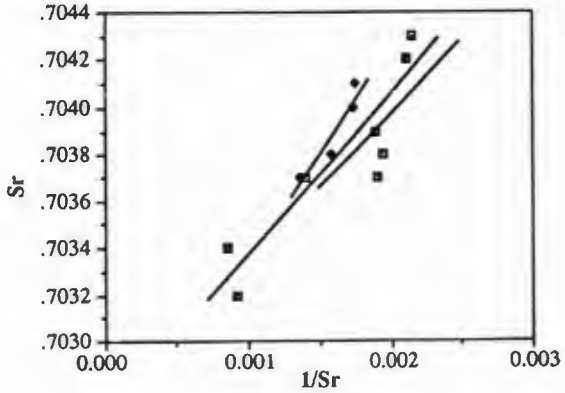

THE MOST POWERFUL PLINIAN ERUPTIONS IN CAMPANIAN AREA (SOUTH ITALY).

ROLANDI G., Dip. Geofisica e Vulcanologia,
Largo S. Marcellino, 10. 80138 Napoli, Italy.
MASTROLORENZO G., Osservatorio Vesuviano,
Via Manzoni, 249. 80123 Napoli, Italy.
D'ALESSIO G., Dip. Geofisica e Vulcanologia.
Napoli, Italy.

For the last 25,000 years, activity in the Campanian Volcanic District (Southern Italy) has been dominated by violent explosive events from Campi Flegrei and Somma-Vesuvius. We have present new data on some of the most powerful plinian eruptions from these two centres.

Only a few plinian events have occurred during the last 10,000 years in Campi Flegrei. Among the deposits related to these events the Pomici Principali and the M. S. Angelo formation have been studied.

The Pomici Principali formation, which was generated between 11,000 and 8,000 yr. B. P., is a sequence of seven single pumice layers interbedded by cinder beds. The total volume of this deposit is about 0.14 cu. Km (DRE), and volcanological analisys indicates that the single pumice layers range from sub plinian to plinian type.

The M.S.Angelo formation,which has been dated at 5.000 yrB. P. ,(C14), has the same composition (trachyte) as, but smaller volume than, Pomici Principali.

The Sarno plinian eruption of Somma -Vesuvius , which occurred 22,000 yr. B.P. is the largest plinian deposit in the Campanian area with a volume of about 6 cu. Km and a maximum inferred thickness at the source of about 5 metres .

The Ottaviano phonolitic pumice formation, generated about 8,000 yr B. P., has a maximum inferred thickness of about 5 metres. The geometry of these and other prehistoric deposits indicates that the distribution of the products was controlled by westerly winds, similar to those which have governed the distribution of most of Vesuvius' historical plinian and sub plinian airfall deposits (e.g. paroxismal events of 1906 and 1944).

A NEW LOCALITY OF TWO MICA GRANITES AND PEGMATITES IN EAST CENTRAL SONORA, MEXICO

ROLDAN-Q.,J., Estación Regional del Noroeste, Instituto de Geología, UNAM, Apartado Postal 1039, Hermosillo, Sonora 83000, México

In the Sierra de Aconchi, two-mica granites and associated pegmatites are exposed in an area covering about 200 km^2. This assembly has been named the Aconchi Batholith, and is located 100 km NE of Hermosillo, Sonora and about 200 km SE of Douglas, Arizona.

Pegmatites are an important constituent of this batholith. In places quartz and microcline crystals can be as large as 20 cm. In the past, beryl was mined from pegmatites in few localities. The main strike of the pegmatites is N15°-30°W, their shape is tabular to lenticular, few are oval or circular. Common dimensions are less than 1 to 30 m wide and 20 to 200 m long. They consist of quartz, microcline, albite, muscovite, almandine and scarce beryl and muscovite.

The Aconchi Batholith intrudes older biotite-hornblende-bearing granites to the south, and Precambrian gneisses and metasediments to the north. Contacts to the east and west of the batholith are faults against Tertiary clastic sediments or Cretaceous rocks.

The granites vary from fine grain to porphyritic or pegmatitic; graphic textures were observed megascopically and microscopically. Muscovite generally predominates over biotite, microcline, orthoclase, albite and quartz are the essential constituents. The most common secondary minerals are sericite, chlorite and epidote. Primary muscovite and almandine are characteristic minerals, of the granites of the Aconchi Batholith. In Arroyo Peñasco, pegmatitic lenses grade laterally into the alkali granite with abundant garnet.

Only a few chemical analyses of major elements for the two-mica granites are available. Their SiO_2 content varies from 71.59-74.63% ; Al_2O_3, 11.90-14.88% ; CaO, 0.63-1.63% ; Na_2O, 3.67-4.30% and K_2O, 3.57-4.48%.

There is only one K/Ar isotopic age of 35.96 $\pm$ 0.70 Ma for the Aconchi Batholith, by Damon et. al. (1983) using muscovite.

The muscovite-bearing alkali granite of the Aconchi Batholith is of the type described by Miller and Bradfish (1980) in Arizona, eastern California and Nevada. In northern Sonora muscovite-bearing granites have been reported in Sierras Pozo Verde, Magdalena, La Madera and Mazatán. Sierra de Aconchi is located along this trend of expossures of two mica granites.

VOLCANIC GAS RELEASES TO THE EARTH'S ATMOSPHERE: SOME IMPORTANT PROBLEMS AND IDEAS FOR SOLUTIONS

ROSE, W.I., SYMONDS, R.B., BERNARD, A.*, CHESNER, C.A., ANDRES, R.J., Michigan Technological University, Houghton, MI 49931 and **REED, M.**, University of Oregon, Eugene, OR 97403

Direct data on the emission rates and concentrations of gases and associated materials released by volcanoes have increased greatly, but our understanding of this data is limited because of a number of diffcult problems. Some of the problems that have concerned our group are: 1) It is difficult to obtain direct measurements or samples of high temperature volcanic gas. In spite of a growing commitment to field work at volcanoes, there are relatively few mesurements of emission rates and most of these have been obtained with an instrument which measures SO_2 only. Direct gas sampling of high temperature vents is only very rarely possible and only a fraction of these samples are close to pristine. 2) We need to have a better understanding of how to scale up eruptions. Currently we are only able to make educated guesses about upscaling measured emission rates of gases from low-level conditions to full scale eruptions where conditions are certainly very different and much harder to measure. 3) We need to understand more fully the species and reactions which occur in volcanic clouds, plumes and fumaroles. The chemistry of volcanic gas is extraordinarily complex, involving species which contain much of the periodic table. The number of possible reactions is enormous. 4) There is a paucity of direct data on the volcanic gas compositions associated with some magma types (eg. rhyolites, potassic alkaline magmas). This is a particular problem if we are to assess the possible global effects of megaeruptions (>40 km^3 dense rock equivalent magma), which are usually rhyolitic.

We are hopeful that current research is beginning to address the problems outlined. 1) Multiple simultaneous measurement and sampling techniques now allow for more complete descriptions of active gas emissions. One particularly promising area is the probability of remote sensing of emission rates of several gas species using raman spectroscopy. The goal of remotely measuring two or more species in real time at an active vent is especially desirable. 2) Satellite sensors and digital imagery may provide previously unobtainable data to aid in scaling up emission rates and compositions. The possibilities for development in this area are limited only by our imagination and the future may hold real time volcano monitoring by satellites. 3) Thermodynamic modelling of volcanic gas chemical systems with 40+ components is now progressing rapidly and our understanding of speciation and reactions is now really tangible. Diverse sampling techniques allow us to constrain and check the thermodynamic predictions, and evaluate applicability. This allows us to forecast reactions beyond the range of our own data. 4) The possible worldwide effects of megaeruptions must be addressed by a diverse group of scientists, including volcanologists, atmospheric physicists and atmospheric chemists. If volcanologists can provide an accurate estimate of the source signal of such an event, then atmospheric scientists can perhaps develop an wholistic model of worldwide atmospheric effects. If records of one or more megaeruptions can be found in strata such as contained in the Vostok core, then such models can perhaps be tested and refined.

*Present address:
Laboratoire de Geochimie, Universite Libre de Bruxelles

EVOLUTION OF VOLATILES IN THE MAGMATIC SYSTEM OF THE CAMPI FLEGREI CALDERA, ITALY

ROSI, M., Instituto di Mineralogia e Petrografia, University of Pisa, Pisa 56100, Italy, and SIGURDSSON, H., Graduate School of Oceanography, University of Rhode Island, Kingston, R.I. 02881, USA

The active Campi Flegrei volcanic complex belongs to the alkali-potassic province of western Italy. The complex is dominated by a 12 km diameter caldera formed during the eruption of the Campanian ignimbrite 35,000 y.b.p. After the main collapse, the caldera was progressively filled by products of successive eruptions which have continued to historical time. Post-35,000 yr. activity has occurred at several vents scattered inside the caldera, showing a steady decline in eruptive intensity with time. Significant periods of activity were 5,000 and 3,700 y.b.p. and the Monte Nuovo event of 1538 AD. Four explosive eruptions which have produced widely dispersed tephra fallout in the last 5,000 years have been studied in detail in terms of eruption dynamics and petrology. These are the eruptions of Agnano (4,300 ybp), Astroni and Averno (both 3,700 ybp), and Monte Nuovo 1538 AD.

Isopleths of lithic and pumice clasts in the tephra fallout have been mapped in order to constrain comun height and mass discharge rates of magmas during these events. Eruption column heights range from a few km for the weak Monte Nuovo event, to as high as 25 km for the plinian eruption of Agnano. Thus in general, the Campi Flegrei magmatic system shows a systematic decrease in both intensity and magnitude of eruptions with time.

Electron microprobe analyses of the composition of glass inclusions trapped in phenocrysts from the tephra provide information on pre-eruption volatile content and evolution of the magmas. Host mineral crystallization has little affected the inclusion composition. Results show that liquid compositions of magmas erupted in the successive eruptions are remarkably similar, and that the observed whole-rock compositional trends with time are dominantly related to modal crystal content. Results indicate a progressive compositional evolution of the Campi Flegrei magmatic system tapped in these eruptions. Thus a systematic increase in Na_2O and decrease in MgO is observed in trapped glass inclusions with time. Total volatile content, as determined from inclusion analysis, shows a range from 3 to 4.5 wt.%, with a general correlation between inferred water content and the observed eruption intensity. The magmas are exceptionally chlorine-rich, judging from glass inclusion analyses (7,000 to 10,000 ppm Cl), whereas sulfur content is modest (200 to 350 ppm S) but in accord with the low iron content of these magmas.

SENSOR REQUIREMENTS FOR REMOTE SENSING OF HOT VOLCANOES

ROTHERY, D.A. and OPPENHEIMER, C.M.M.,
Department of Earth Sciences, The Open University, Milton Keynes, MK7 6AA, England

Recent work shows that Landsat TM sensors in the short wavelength infrared (SWIR) part of the spectrum are capable of measuring radiant temperatures and radiant thermal budgets of magmatic features and hot fumaroles. The availability of data in two wavebands is vital in that it allows the size and temperature of radiant areas smaller than a pixel to be measured, if the background radiance is known, or can be assumed.

The types of volcanic phenomena whose size and temperature make them amenable to measurement using TM SWIR measurements are moving lava flows, lava lakes more than about 10m across in any level of activity, incandescent vents and fumaroles above about 400 °C and covering more than a few percent of a pixel. Drawbacks include the wavebands used, the instantaneous field of view of the sensors, fumes and other atmospheric effects, repeat frequency and timeliness data distribution. This study outlines the spectral and spatial characteristics required of future remote sensing systems to fullfil a quantitative observational role for hot surface phenomena on active volcanoes.

Absorption by the atmosphere limits visible and infrared remote sensing to a few "windows": 0.4-1.3μm, 1.5-1.8μm, 2.0-2.5μm, 3-5μm, and 8-12μm.In order to take advantage of radiance measured at two or more wavelengths to derive accurate temperature and area information on the sub-pixel scale it is necessary to make measurements at wavelengths for which the spectral radiance properties are greatly different at different temperatures. The lower sensitivity limit (governed by instrumental, atmospheric and surface constraints) is about 0.1 to 1.0 mW cm^{-2} sr^{-1} μm^{-1}. There is no upper limit; until now this has been dictated by the other, non-volcanic, uses envisaged for the sensor. Given the uncertainties involved it there is no merit in trying to achieve either precision or accuracy smaller than 10°. For all-purpose volcanic uses, a useful band-pass sensor system capable of recording radiance on an 8-bit logarithimic scale would comprise:

1 or 2 bands in the 1.5-1.8μm window (0.1-300 mW cm^{-2} sr^{-1} μm^{-1}), bandwidths 0.1μm.
1 or 2 bands in the 2.0-2.5μm window (0.1-300 mW cm^{-2} sr^{-1} μm^{-1}), bandwidths 0.1μm.
1 or 2 bands in the 3-5μm window (0.1-300 mW cm^{-2} sr^{-1} μm^{-1}), bandwidths 0.5μm.
1 or 2 bands in the 8-12μm window (0.8-100 mW cm^{-2} sr^{-1} μm^{-1}), bandwidths 2μm.

This could measure temperatures in the range 50 °C to 1100 °C occupying between .01% and 100% of a pixel, having at least two sensors which were operating below saturation level. There would sometimes be three or more sensors returning data, which would enable background temperatures on bimodal surfaces to be measured rather than assumed, and would allow scope for determination of polymodal temperature distributions. The system would remain useful if it had only one band within each window, though it would be highly desirable to retain two bands in the 3-5μm window. An imaging spectrometer across the whole spectral range could prove even more versatile. A realistic yet useful spatial resolution would be in the range 50-200m.

TOPOGRAPHIC CONTROL OF HAZARD DISTRIBUTION AT SOUFRIERE VOLCANO, ST. VINCENT, LESSER ANTILLES

ROWLEY, K.C., U.W.I., St. Augustine, Trinidad, W.I.

Soufriere, St. Vincent has been the most active sub-aerial volcano in the Lesser Antilles island arc, during the historic period of the last three centuries. Field mapping, stratigraphic exercises and the use of C14-dating of clastic flow deposits point to a high frequency of explosive activity extending back to approximately 4000 years B.P. Almost all of the flow products of these eruptions are located on the southern side of the volcano.

The southern sector of the volcano is composed predominantly of pyroclastic units which appear to have been deposited during a Post-Pleistocene reconstructive phase which contrasts with an earlier less explosive phase when effusive products, found mainly in the northern two-thirds of the mountain, contributed more significantly to the creation of this strato-volcano. This difference in eruptive style is believed to be partly related, among other things, to the development of a crater lake and its role in influencing the consistent production of clastic deposits from large-scale phreato-magmatic activity.

There are also indications of an early Post-Pleistocene collapsed southern sector of the main structure resulting in the establishment of a significantly lowered southern lip on the volcano. A relatively prolonged period of consistent topographic control of the clastic as well as other magmatic deposits may be largely responsible for the present configuration of the volcano and it continues to be a major influence on the distribution of hazard which are to be associated with eruptions at the Soufriere.

Most of the deposits are indicative of Vulcanian to Plinian eruptions originating from summit craters with or without associated intra-crater dome lavas. Whereas the pre-historic deposits provide valuable data on the scale and distribution of probable hazards the historic eruptions have offered clearer insights into the mechanism of the most recent outbursts. Wide variations of magnitude and dispersive power are observed or inferred from the major historic events and their earlier counterparts.

Notwithstanding the inferred consistent role of the process of column collapse of vertical eruption clouds in the generation of clastic flows, the distribution of flow deposits appears to have been directionally consistent over the last 4000 years. The areal distribution patterns of flow units and other associated hazards though closely dependent on the scale of the event appears to be strongly influenced by a) summit topography and b) flank configuration.

The interesting physiographic features displayed at the Soufriere volcano include significant altitude differentials at sections of the summit, a Somma wall to the north, an upper flank escarpment to the north-west and two east-west trending gorges in the lower southern flanks. These observations coupled with the relatively consistent summit crater activity make this volcano an ideal case for modelling the behaviour of explosive eruptions of different scales of violence and magnitude. The findings of such studies could be useful in the assessment of hazards at other Antillean volcanoes.

ERUPTIVE MECHANISMS ON PITON DE LA FOURNAISE VOLCANO ASSOCIATED WITH DECEMBER 4, 1983, AND JANUARY 18, 1984 ERUPTIONS FROM GROUND DEFORMATION MONITORING AND PHOTOGRAMMETRIC SURVEYS.

J.C. RUEGG (1), J. ZLOTNICKI (1) AND P. BACHELERY (2)

(1) I.P.G. Observatoires Volcanologiques, tour 24, 2e étage 4 Place Jussieu 75252 Paris cedex 05 (France)
(2) Univ. Réunion, Géologie, B.P. 5, 97690 Ste Clotilde (France)

Two photogrammetric aerial surveys have been carried out over the summit area of the shield basaltic volcano Piton de la Fournaise (Indian Ocean), one survey in 1981 and the second one in 1984. During this time, only two eruptions occurred; both December 4, 1983, and January 18, 1984, eruptions opened fissures more or less radial on the South-West part of the summit. Because of the slight and erratic ground deformations measured on the dry-tilt, continuous tilt stations and, on the geodetic network between 1981 and November 1983, and between February 1984 and the second survey in June 1984, ground deformations revealed by the two photogrammetric surveys are essentially associated with the two eruptions. The photogrammetric surveys are able to give a general view of the displacement field induced by volcanic activity.

Horizontal and vertical displacements reach 40cm of amplitude while the accuracy of the method is about 3cm. Horizontal displacement vectors indicate a North-East ground deformation of the South-West part of the cone where the effusive vents opened. A more diffuse uplift along the main fractures zones which cut the volcanic edifice is observed, while towards the East of these fractures, only slight - less than 10cm - and opposite displacements are noticed. This displacement field pattern can be associated with the main geological structures of the dome of Piton de la Fournaise volcano (main fractures zones, unwelded blocks of the summital area). Some consequences of the observed displacement field may be outlined for the volcanic observational ground deformation networks.

To estimate the displacement field revealed by the photogrammetric surveys, a simple model of dyke intrusion has been computed. This latter is based on a model of dislocations and take into account the main fractures zones. Good agreement is observed between computed and observed data in the area of the effusive vents. Some disagreement remain in the North-West part of the survey where horizontal deformations are small and erratic and, in the North part where an uplift was observed but which can be associated with the North active fracture zone.

The model points out three results. Firstly dykes are issued from a superficial magma reservoir composed of dykes and sills complexes located at a depth less than 3.5 km beneath the summit. Secondly, an Eastern dipping normal fault, associated with the main fractures zones, is to introduce in the model geometry so as to uncouple the East flank of the cone from the more stable West flank, which is in good agreement with the observed geological structures. Thirdly, for these December, 1983, and January, 1984 eruptions, a radial intrusion cannot explain the photogrammetric data. It seems that the intrusion was issued from a sill or from the upper part of the magmatic reservoir and was bending as the intrusion moves away from the summit area just before the eruptions.

EVOLUTION AND SOURCES OF MAGMAS IN THE SIERRA MADRE OCCIDENTAL CONTINENTAL ARC, MEXICO

RUIZ, JOAQUIN, Department of Geosciences, University of Arizona, Tucson, Arizona 85721

The Sierra Madre Occidental (SMO) volcanic province forms the largest continuous silicic continental arc in the world. Mid-Tertiary, silicic caldera-derived ignimbrites overlie older (> 50 Ma) batholitic and intermediate volcanic rocks and extend more than 1400 km, from the United States border to south of the Trans Mexican Volcanic Belt. Lavas and ash flow tuffs cover an area greater than 250,000 km2 and may have an average thickness approaching 1 km. Silicic volcanism was confined to an interval between about 40 to 27 Ma and is coincident in time with the subduction of the Farallon Plate of the west coast of North America. The volcanism is thought to be related to subduction processes. Generally, there is an increase in the alkalic nature of the rocks with distance from west coast. Calc-alkalic volcanics form the main portions of the SMO. High silica, topaz and tin bearing rhyolites occur on the eastern part of the SMO and are associated with high K calc-alkalic rocks.

The silicic ignimbrites and lavas of the SMO have Sr initial ratios between 0.7044 and 0.7078 and epsilon Nd values between -5.8 and +1. Most analyzed rocks, however, including high-silica, topaz-bearing rhyolites, have epsilon values between -2 and +1. Similar high silica rhyolites in New Mexico have Nd epsilon values around -6 and in Utah around -10 indicating large amounts of old and isotopically evolved crustal material in the original melts. The Mexican lower crust, however, seems to be relatively young and isotopically unevolved. Lower crustal xenoliths from maars throughout northern and central Mexico have isotopic compositions similar to those of the silicic volcanics. Xenolith and geologic considerations also indicate that the lower crust underlying most of the SMO is isotopically and lithologically similar. Seismic and gravity data also indicate that the crust under is not very different in thickness (ca. 35 km) anywhere under the SMO. Inasmuch as the lower crust underneath the SMO is not very radiogenic, large amounts of crustal material can be incorporated by mantle derived magmas without significant altering their original isotopic compositions. Thus the relative constancy in the isotopic ratios of the silicic volcanics should not be interpreted as produced by uncontaminated mantle-derived magmas. This is evident in central Mexico (San Luis Potosi), where andesites shown to be derived from mixing basaltic and rhyolitic magmas show little change in Sr and Nd isotopic ratios. In addition negative isostatically compensated Bouguer anomalies argue against large amounts of underplating needed to produce the silicic volcanics solely from crystal fractionation of mantle derived basalt. On the contrary the gravity data suggest that light density material such as batholitic rocks underlie the SMO. The isotopic, geologic and geophysical data indicate that the only plausible model for the source of the melts of the SMO involves interactions between crust and mantle materials. The melts that ultimately produced the silicic volcanics had to have a large crustal component. Trace element modelling show that intracrustal AFC of these melts occurred at most of the studied volcanic centers to produce the final volcanic products.

LAYERED COMPLEXES - DYKE SWARM - VOLCANICS: A SINGLE IGNEOUS EVENT

RUNDQVIST,D.V., SEMENOV V.S., TURCHENKO,S.I. FELITSYN, S.B. Institute of Precambrian Geology & Geochronology, the USSR Academy of Sciences, 199034, nab.Makarova 2, Leningrad, USSR

Regional Precambrian mafic dyke swarms often show spatial and genetic relationships with the coeval layered complexes and subaerial volcanics. Geochemical and geochronological evidence permits a magmatic "triad": layered complex - dyke swarm - subaerial volcanics related to a single igneous event to be revealed. All the units of the triad are known to occur, e.g. in North Karelia (Panajarvi structure, 2.4 Ga), South Karelia (Burakov structure, 2.4 Ga) and Kola Peninsula (Pechenga structure, 2.1 Ga).

The study of geochemistry combined with the analysis of the geological relationships within the triad in question provides information on geodynamics of the igneous suite generation. The emergence of such triads marks a definite stage of crustal development, i.e. the transition to an epi-cratonic regime followed by rifting and activation of mantle volcanism. Such processes are most intense in the ranges: 2.4 - 2.1, 1.7 - 1.6 and 1.2 - 1.1 Ga.

The revealed genetic linkage between the units of triads enables to assess the composition and potential mineralization of the comagmatic intrusions based on the dyke composition; a dyke swarm pattern and compositional variations along its strike suggest the site of layered complexes (magma chambers).

The gabbro-noritic dykes of North Karelian swarm are connected with the Kivakka and Lukullajsvaa a layered complexes showing a primary basalt-komatiitic composition and higher contents of PGE. The Qu-normative tholeiitic dykes of the Karelian swarm are associated with the Tsipringa layered complex, and their comagmatic subaerial volcanics contain high Cu-concentration.

ORIGINS OF THE 1954-1960 LAVAS OF KILAUEA VOLCANO: Constraints on Shallow Reservoir Magmatic Processes

J.K. RUSSELL, Dept. of Geological Sciences, University of British Columbia, Vancouver, B.C., V6T 2B4, and

C.R. STANLEY, Dept. of Geology and Geophysics, University of Calgary, Calgary, Alberta, T2N-1N4

Between 1954 and 1960 Kilauea Volcano, Hawaii erupted four times. Kilauea summit eruptions occurred in 1954 at Halemaumau and in 1959 at Kilauea Iki. In 1955 and 1960 large volumes of basalt lava erupted from the east rift zone of Kilauea Volcano. Our analysis demonstrates that the 1954-1960 Kilauea lavas can be related solely through fractionation and sorting of the observed phenocryst assemblage from a single batch of magma. Specifically, we have used Pearce element ratio diagrams to make the following observations and inferences:

1) The conserved element ratio P/K for each eruption has less variance than is expected from analytical uncertainty. We cannot reject the hypothesis: ***The analyses of each eruptive period represent a comagmatic suite of rock compositions.***

2) Each of the 4 groups of lavas has the same mean P/K ratio. We cannot reject the hypothesis: ***The 1954-1960 lavas originated from a single magma or a series of magmas with identical P/K and Ti/K values.***

3) Where each set of lava analyses is plotted in the Pearce element ratio diagram X=Si/K and Y= 0.5(Mg+Fe) + 1.5Ca + 2.75Na + .25Al/K, the data fit a slope of 1.0. We cannot reject the hypothesis: ***The chemical variation in each data set is consistent with sorting of OL +/- PL +/- AU.***

4) The differentiation trend defined by the 1959 lavas overlaps some of the 1954, 1955 and 1960 lava compositions. We cannot reject the hypothesis: ***Fractionation and sorting of OL, PL and AU has generated the 1954-1960 Kilauea lavas from a single batch of magma.***

Finally, using the most Mg-rich glass analysis in the Kilauea Iki data (SG-05) we have modelled the fractional crystallization path with thermodynamic-based calculations. The thermodynamic calculations predict a liquid line of descent which is consistent with the path inferred from rock and glass analyses. Therefore, the simulations provide an additional test of our hypotheses and corroborate the postulated differentiation model. Additionally, the thermodynamic calculations suggest that differentiation took place at pressures of approximately 0.3 GPa and over a range of 100°C.

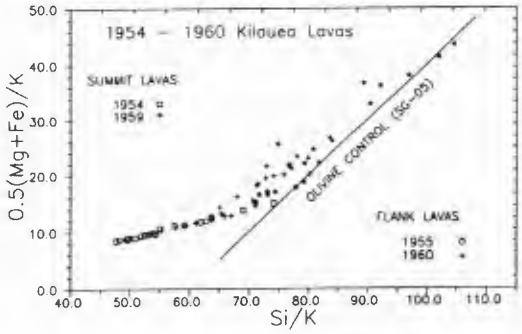

An FM Pearce element ratio diagram illustrating the chemical diversity of the 1954, 1955, 1959 and 1960 Kilauea lavas. Solid line is forced through the most Mg-rich Kilauea Iki glass analysis (SG-05) and defines olivine control with respect to that composition. The pronounced deviation marked by the 1954 lavas is consistent with the effects of cotectic precipitation of plagioclase and augite.

EXPERIMENTAL INVESTIGATION OF CONDITIONS IN SUBVOLCANIC MAGMA CHAMBERS

RUTHERFORD, Malcolm J.,
JOHNSON, Marie C.,
FOGEL, Robert F. *All at: Department of Geological Sciences, Brown University, Providence, R.I., 02912*

Using experimental phase equilibrium studies done with controlled P, T, fO_2, and $X(H_2O)$, it is possible to constrain depth and intensive parameters including volatile fugacities in subvolcanic silicic magma chambers. The information needed from the natural rock is phenocryst and matrix glass compositions, and, if possible, the composition of phenocryst melt inclusions. The volatile content of the melt inclusions is useful but not essential if the phenocryst assemblage is extensive. Melt inclusion volatile contents obtained by the electron microprobe difference method and by F.T.I.R. spectroscopy have both been used successfully. F.T.I.R. spectroscopic analyses have great potential because they give both concentration and melt speciation (i.e., H_2O and OH) information.

Basic phase equilibrium studies have now been done for a range of compositions including a dacite with 64 wt. % SiO_2, a quartz latite (67% SiO_2) and a high SiO_2 (75 wt. %) rhyolite. The important data derived from these studies includes the following: (1) a relationship between $X(H_2O)$ in the coexisting fluid and amphibole stability for a range of P and T. (2) A similiar relationship for biotite stability. (3) Data showing the change of plagioclase composition with $X(H_2O)$ in the melt for a range of P and T. (4) An experimental calibration of total Al in hornblende vs. pressure, a sensitive and widely applicable geobarometer. In addition, the solubility and speciation of CO_2 in rhyolitic magmas has been experimentally calibrated as a function of fCO_2 and T over the pressure range 500 to 6500 bars.

Using the experimental phase equilibria and analyses of natural minerals and glasses, conditions have been derived for a number of silicic volcanic magma chambers. The Mt. St. Helens, May 18, 1980 dacitic magma chamber was at 920°C, 7 $\pm$1 km and in equilibrium with a $X(H_2O)$ = 0.67 fluid. The Fish Canyon Tuff quartz latite magma was at 760°C, 8 $\pm$1.5 km, and contained a fluid phase with $X(H_2O)$ = 0.5 just prior to eruption. In contrast, the post-Bishop Tuff Long Valley Caldera volcanic rocks represent an essentially H_2O-saturated magma derived from 5 to 6 km.

ERUPTION PREDICTION FROM MICROGRAVITY

RYMER Hazel and BROWN Geoff
Department of Earth Sciences,
The Open University,Walton Hall,
Milton Keynes, MK7 6AA, UK

Changes in gravity (Δg) and elevation (Δh), are related by the Bouguer corrected free-air gradient (BCFAG). By assuming that observations are made on a flat plane of at least 2 km radius, the numerical value of the BCFAG can be calculated simply for any given density (ρ) since

$$\frac{\Delta g\ (\mu Gal)}{\Delta h\ (m)} = -(308.6 - 41.91\ \rho\ (Mg\ m^{-3}))$$

In the volcanic context, departures from the BCFAG are interpreted in terms of sub-surface magma movements or density changes. Any data plotting on the RHS of the Figure represents overall inflation, and data plotting above the predicted BCFAG (areas 2 and 3) represent overall sub-surface mass increase. The interpretation of departures from the BCFAG (see Figure) depends in which region data fall. For example, deflation and mass decrease at a volcano (area 1) would probably be due to downwards magma drainage, leaving partially hollow dykes. However deflation with mass increase (area 2) would accompany local magma intrusion into relatively low density surroundings. Similarly, inflation with mass increase (area 3) normally is associated with magma intrusion into pre-existing voids and dyke formation. Finally, inflation and mass decrease (area 4) results from magma vesiculation or incomplete collapse of voids after inflation.

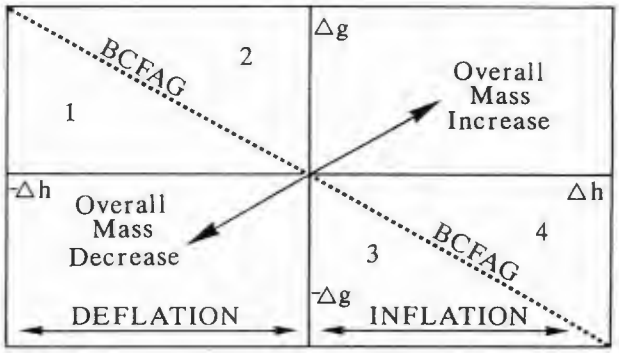

Poas is a complex stratovolcano in Costa Rica, supporting a hot acidic meteoric water lake. The last eruption of juvenile material was in 1953 and was followed in the later 1970s by intermittent phreatic activity. Since then, the crater lake has apparently buffered any fluctuations in energy from the cooling magma below (see Brown et al. this volume). By early 1988, the lake level had fallen 40 m and by Dec. 1988 by a further 10 m. Microgravity/elevation data obtained for the period Feb. 1987-March 1988 show significant departures from the BCFAG (max. 200 µGal and -33 cm) at crater bottom stations. Crater rim stations plot on the predicted BCFAG and stations on the volcano flank plot on the origin (cf. Figure). An overall mass increase of ca. 2 x 10^8 kg with deflation is calculated from crater bottom data. This mass increase probably represents a magma intrusion into pyroclastic debris and unconsolidated ashes. Such an intrusion would have caused the disappearance of the crater lake by excess evaporation. The depth to the intrusion is estimated from the aerial extent of the gravity change to be <<500 m.

A.A. Eggers showed that precusory mass deficiencies seen as departures from the BCFAG correlate with eruption magnitude. Here we recognise a further effect: mass increase during enhanced thermal output which, similarly, may be an eruption precursor. Monitoring microgravity may therefore provide important constraints on both physical changes in volcanic systems and assessment of potential hazard.

EFFECT OF FLOW VELOCITY ON TEMPERATURE AND CHEMICAL COMPOSITION OF FUMAROLIC GASES

Saito, G*, Shinohara, H. and Matsuo,S**
Department of Chemistry, Tokyo Inst. Tech. O-okayama, Meguro-ku, Tokyo 152, Japan
*Research Center for Earth's Interior, Okayama Univ., Misasa, Tottori-Pref.682-02
**Department of Chemistry, The University of Electro-communications, Chofu-city 182

Flow velocity measurements of fumarolic gases using a Pitot tube at the I-crater fumarolic area of My. Usu, Hokkaido, Japan were carried out. At the same time, temperature measurement of gas vents and the sampling of fumarolic gases were also made.

When the flow velocity is low, the outlet temperature is low. However, even when the flow velocity is low, there are fumaroles with high outlet temperature as seen in the figure.

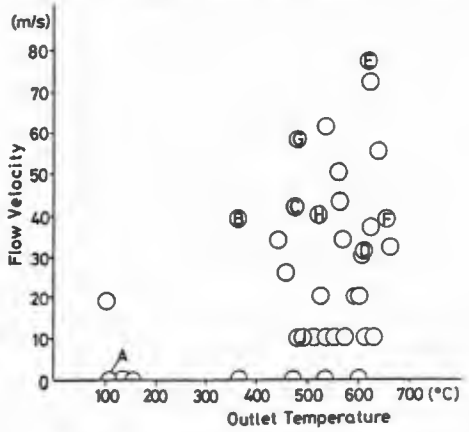

Hence the flow velocity of gas is not the sole factor that controls the outlet temperature. The apparent equilibrium temperature (AET) of the reaction, $3H_2 + SO_2 = H_2S + 2H_2O$, is always higher than the outlet temperature. The relationship between AET - outlet temperature - flow velocity is as follows: 1) when the flow velocity is the same, the difference between AET and outlet temperature is larger for lower temperature fumarolic gases, and 2) when the outlet temperature is the same, AET is lower for fumarolic gases with higher flow velocity. An interpretation for the above two facts is given on the basis of the rate of temperature and pressure drops associated with the flow velocity.

Based on the measured activity ratio of ^{232}Th and ^{238}U in the ejecta, the activity ratio of ^{220}Rn and ^{222}Rn in the magma is estimated to be 0.75. The measured activity ratio at the vent of a fumarole with the flow velocity of 39m/s is less than 0.5. This result indicates that the time elapsed after the gas leaves from the magma top is at least 32.5 seconds. Then, the minimum depth of the magma top is calculated to be 1.3km. Although the above calculation is oversimplified, a continuos measurement of $^{220}Rn/^{222}Rn$ will be one of the candidates which can monitor the fluctuation of the depth of magma top.

ACCRETED ISLAND ARCS AND CROSS-CUTTING BATHOLITHIC BELTS OF THE NORTH AMERCIAN CORDILLERA

SALEEBY, J.B., Division of Geological and Planetary Sciences, Caltech 170-25, Pasadena, CA 91125

The basement framework of the western Cordillera consists in large part of tectonically accreted island arc terranes and cross-cutting batholithic belts. The arc terranes are diverse in terms of magmatic history, tectonic disruption and basement relations, and represent several distinct systems. Terranes of the two oldest systems occur in inner and outer belt positions. The inner belt runs from central Alaska to the northern Sierra Nevada. It was in its major developmental phases by the Devonian, and was constructed on imbricated North American continental rise strata outboard of a passive margin. The outer belt includes the Alexander Terrane (AT) of SE Alaska and younger amalgamated arc terranes of the Alaska Peninsula and Queen Charlotte-Vancouver Islands. The AT contains a tremendous volume of primitive arc volcanic and plutonic material formed between ~550 and 410 Ma. This early Paleozoic arc was rifted during the Devonian, and appears to have drifted for a substantial part of the late Paleozoic as a Panthalassa oceanic plateau. It was amalgamated to additional arc terranes in the late Paleozoic to early Mesozoic and then accreted to North America during an active arc phase in the Early Cretaceous. In Alaska to northern Washington latitudes the AT system bounds major fragments of an east-Pacific fringing arc system of mid-Paleozoic to mid-Jurassic age (McCloud arc), as well as belts of collapsed open ocean and marginal basin terranes. This arc-ocean basin mosaic was accreted against the inner continental rise system in several stages ending in the Middle Jurassic. In Oregon and California remnants of the major arc systems present to the north are missing or are highly fragmented. In this region the analogous belt of accretionary terranes is composed of composite ophiolites which record a late Paleozoic to early Mesozoic boundary transform system with superposed forearc igneous complexes, and a Middle and Late Jurassic interarc basin system with local vestiges of an outer fringing arc. The AT system and perhaps parts of the McCloud system migrated along the outer edge of the composite ophiolite belt, although detailed kinematic histories are poorly known.

The Cordilleran-wide belt of accreted arcs and ophiolites began major collapse against North America in the Middle Jurassic with final accretion occurring in the Early Cretaceous. The Middle Jurassic Omineca crystalline belt of British Columbia represents a plutonic-metamorphic welt formed along the inner suture of the McCloud system. The southern extension of this belt widens southward into the Nevada-California region where it diverges from the suture trend and cuts into every pre-Late Jurassic accretionary terrane of the region as well as Proterozoic North America. The Cretaceous Sierra Nevada batholith cuts obliquely across the Jurassic plutonic belt and lies along the suture produced by the boundary transform. Interarc basin ophiolite which formed along the transform system constitutes basement for the Cretaceous Great Valley forearc basin. To the north the Idaho batholith and Coast Plutonic belt formed along the suture between the McCloud system and the AT system. Major phases of magmatism commenced here in the mid-Cretaceous and ceased in the Eocene. The Sierran-Idaho-Coast batholithic belt represents a continent edge magmatic arc developed above an east-dipping subduction zone which established itself beneath the hanging wall of the accreted island arc and ophiolite terranes. Subduction zone magmas preferentially intruded major crustal sutures, and in the process transformed the sutures and the juxtaposed ensimatic terranes into new North American sialic crust.

MAGMA MIXING AND CONVECTIVE COMPOSITIONAL LAYERING WITHIN THE VESUVIUS MAGMA CHAMBER

SANTACROCE, R., Department of Scienze della Terra, University of Pisa, and CNR - Istituto Internazionale di Vulcanologia, Catania, Italy, and
CIVETTA Lucia, Department of Geofisica e Vulcanolgia, University of Naples, Naples, Italy, and
GALATI Rita, Department of Geofisica e Vulcanologia, University of Naples, Italy.

A chemical and isotopic study was made on the pyroclastic deposits of the last two plinian eruptions of Vesuvius: A.D.79 "Pompei" and 3,800 B.P. "Avellino". Both Pompei and Avellino pumice-fall deposits are characterized by marked compositional variations from white phonolite at the base to grey tephritic phonolite at the top. The pumice separated from flows and surges of the last phases of the Pompei eruption return to phonolitic composition. In both Avellino and Pompei sequences a strong compositional gap separates white from grey pumice. Gray pumice has distinct nearly homogeneous isotopic composition ($^{87}Sr/^{86}Sr$ = 0.70749-54, $^{144}Nd/^{143}Nd$ = 0.512507 for Pompei; 0.70760-69, 0.512504 for Avellino). Kfeldspar separated from both grey and white pumice has, in all cases, "white" $^{87}Sr/^{86}Sr$ ratio (0.70767-79 for Pompei, 0.70728-33 for Avellino). The observed variations are interpreted as reflecting a pre-eruptive zonation of the magma chamber in which at least two (Avellino) or three (Pompei) different convective layers can be recognized; it is however likely that the chamber has been more intricately zoned. Although mineralogical evidence exists in both eruptions of interaction between magma and calcareous country rocks, crustal contamination does not significantly modified the isotopic signature of erupted products. Evidence of syneruptive magma mingling occurs in Pompei grey pumice as well as in Avellino both white and grey pumice. In the case of Pompei the proportions of white pumice intermingled with the grey one (5-20%) could have induced a moderate increase of the $^{87}Sr/^{86}Sr$ ratio (estimated original "grey value": 0.70748-50). No reliable valuation of the phenomenon is possible for Avellino deposits.

The correspondence of the $^{87}Sr/^{86}Sr$ range of Avellino and Pompei products with that recorded in the lava flows erupted during the most recent period of activity of the volcano (1631-1944) suggests that the isotopic variations occurring in Avellino and Pompei deposits be mainly the result of the history of the Vesuvius shallow magma-chamber: they should reflect: 1) repeated pulses of new magma entering the chamber and mixing with the grey portion of the resident magma, 2) fractionation of this mixed magma, 3) formation of a differentiated light cap that increases the white layered portion chamber by adjoining a new layer having the isotopic inprint of the last mixing episode. It has finally to remark that preliminary $^{87}Sr/^{86}Sr$ ratios from other plinian and subplinian eruptions indicate a repetitive behaviour of the Somma-Vesuvius volcanic complex in the last 20-25,000 years, hence suggesting substantial unicity of its magma chamber and continuity of its feeding system.

SIMULTANEOUS OBSERVATIONS OF ERUPTION CLOUD OF THE NOVEMBER 21, 1986 IZU-OSHIMA ERUPTION WITH IMAGES OF GMS AND NOAA, AND WEATHER RADAR

SAWADA, Y., Seismol. and Volcanol. Dept., Japan Meteorological Agency, 1-3-4 Ote-machi, Chiyoda-ku, Tokyo 100 Japan

The highest altitude of the eruption cloud at Izu-Oshima, in the evening on November 21, 1986, was estimated as 14 - 16 km based on ground observations and analyses of picture data. At around 1730 JST, extent of the cloud was well and almost simultaneously detected by GMS image, and the weather radar settled at the summit of Mt. Fuji (wave length; 10.4 cm), and also, the eruption cloud was seen at 1906 JST, in both images of GMS and NOAA (see the upper and lower in Figure).

The highest altitude of the eruption cloud obtained at around 1730 JST in GMS image was estimated as 7 - 9 km, from GMS data using air sounding data at Tateno and Hachijo-jima stations. However, the radar data showed the height of 10 - 12 km. The highest altitudes of the cloud taken at 1906 JST, estimated from GMS and NOAA data, using air sounding data were 4 - 6 km in the both cases.

By considering the parallax of GMS image over Izu-Oshima, the corrected top altitude ranging from 10 to 16 km was obtained for the 1730 JST eruption cloud, that well coincides with the radar data. Thermal energy release of the eruption cloud, estimated using Briggs's method was an order of 10^{23} ergs. During these analyses, it was experienced that radar data can well observe the densest portion and its top altitude of eruption cloud, and GMS image can monitor widely dispersed cloud, and NOAA image can well detect thin edge of extent of dispersed eruption cloud.

The low value of the top altitude, estimated from GMS data and air sounding data is due to GMS temperature of the top surface of erution cloud higher than the ambient air temperature. According to inspections of picture data, it was not noticed that the highest portion of the eruption cloud at around 1730 JST was thin, and it is unlikely that the internal heat could radiate outside to the top surface of the cloud. Therefore, it is most likely that there were active heat emissions on the top surface of the eruption cloud, even during its ascendings.

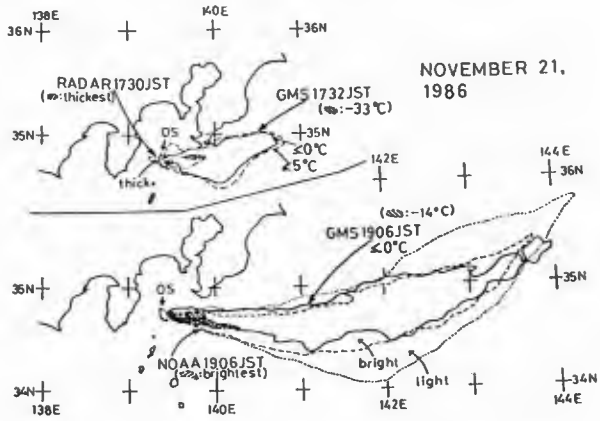

Fig. Extent of the eruption cloud, detected by images of GMS and NOAA, and radar.

POTASSIUM METASOMATISM IN THE CREEDE MINING DISTRICT, SAN JUAN VOLCANIC FIELD, COLORADO

SAWYER, D.A., SWEETKIND, D., RYE, R.O., SIEMS, D.F., REYNOLDS, R.L., ROSENBAUM, J.G., LIPMAN, P.W., BOYLAN, J.A., U.S. Geological Survey, Denver, CO 80225; and BARTON, P.B., BETHKE, P.M., and CURTIN, G.C., U.S. Geological Survey, Reston, VA 22092

Pervasive K metasomatism of Bachelor intracaldera tuff in the Creede Mining District was recognized by Ratté and Steven in the middle 1960's as having formed by a hydrothermal alteration process. The K-metasomatic alteration is characterized by enrichment of potassium coupled with strong depletion of sodium. In Bachelor rhyolite, K_2O concentrations are increased, from a normal range of 4.5-5.5 to 7.5-14 wt.%. Sodium contents decrease from 3-4 wt.% Na_2O to 0.1-2%. CaO also decreases from about 1.5 wt.% down to less than 0.20 wt.%. Rb increases (from 150 to 225-460 ppm) and Sr decreases (140-170 to 40-80 ppm) with increased K/Na. Immobile elements include Ti and Zr; other major elements vary only slightly. The main mineralogical changes are conversion of plagioclase phenocrysts and groundmass alkali feldspar to nearly pure K-feldspar (Or_{97}).

The alteration boundary of the K metasomatism occurs within the Bachelor caldera fill, not at its upper depositional contact with younger units. K metasomatism is pervasive in the central part of the Creede district, particularly between the Amethyst and Bulldog veins, and decreases on the flanks of the Bachelor caldera resurgent dome. Gradual increases in the K/Na ratio to peak values adjacent to the mineralized vein structures suggest that these structures may have served as metasomatic fluid pathways.

The pervasive K metasomatism of Bachelor caldera fill was thought by earlier workers to have occurred at about 27.5 Ma, and thus would have significantly preceded Ag-Pb-Zn ore mineralization at 25.1 Ma. However, K metasomatism affects both the San Luis caldera fill (26.1 Ma Nelson Mt. Tuff) and clasts and matrix of conglomerates in the Creede Formation, the moat filling sediments of the Creede caldera (age 26.9 Ma). In a vertical transect (Equity mine) rhyolitic Nelson Mountain Tuff shows a progressive increase in the degree of K metasomatism downward, from relatively unaltered rocks near the surface to rocks at depth having mol. K_20/Na_20 from 18-19, the highest yet measured. Therefore, at least some of the K metasomatism is younger than 26.1 Ma. Minimum age of the K metasomatism is 25.1 Ma; main-stage epithermal veins of this age cross-cut K metasomatized rocks.

Primary magnetite is progressively oxidized to hematite and then to rutile during K metasomatism, thereby producing an order of magnitude decrease in magnetic susceptibility and intensity of remanent magnetization. Magnetic mineralogy is modified much more than by the late argillic alteration associated with the mineralized veins. Wide variability of initial magnetic properties of the Bachelor caldera rocks makes difficult the use of magnetic susceptibility as an indicator of hydrothermal alteration.

The $\delta^{18}O$ values of K metasomatized rocks in the district range from 2.7 to 11.7 ‰. Regionally most rocks show a depletion in $\delta^{18}O$ relative to original values in unaltered rhyolitic tuff (8+/-0.5 ‰). In detail, $\delta^{18}O$ and K_2O/Na_2O relationships are complex and local trends differ in the northern and southern parts of the district. K-metasomatized rocks show a wide range of $\delta^{18}O$ values in some areas and a narrow range in others. Locally some rocks show a pattern of enrichment in $\delta^{18}O$. The general pattern of depletion in $\delta^{18}O$ with increasing K_2O/Na_2O is different than that observed in the Rio Grande rift and Basin and Range (mostly associated with basins formed by extensional faulting), where patterns of $\delta^{18}O$ enrichment have been interpreted as evidence of low-temperature hydrothermal alteration by alkaline brines.

The observed depletion of $\delta^{18}O$ in most K metasomatized rocks, coupled with local enrichments in $\delta^{18}O$, requires that at least two fluids were involved. The wide range of $\delta^{18}O$versus K_2O/Na_2O may reflect mixing of fluids and/or overlapping stages of alteration, fluid isotopic evolution due to water/rock interactions, temperature variations, and permeability-controlled variations in the degree of alteration. The major K-metasomatic fluids appear to have had isotopic signatures similar to those of the ore-forming hydrothermal system, and although their age is constrained to be pre-ore, these new data suggest that the K-metasomatic alteration may be an early stage in the evolution of the ore-forming hydrothermal system.

REAL-TIME SEISMIC MONITORING OF MT. ETNA, ITALY

SCARPA, R., Dip.to di Fisica, Universita' dell'Aquila, L'Aquila, Italy, NERI, G., PATANE', D., PRIVITERA, E., Istituto Internazionale di Vulcanologia, C.N.R., Catania, Italy.

Mt. Etna is a polygenic volcanic system characterized by a significant seismic activity (volcanic tremor, low-frequency earthquakes, seismic swarms) often associated with eruptive episodes. Since early 1989 a new seismic network is operating in this densely populated volcanic area and provides a real-time monitoring of local seismicity. This is a part of a more general hazard mitigation program aimed to reduce risks related to eruptive phases and the largest intensity earthquakes. Presently, 10 stations, including 2 digital three-component seismometers, are linked, via cable and telemetry, to a recording center located at the Istituto Internazionale di Vulcanologia, in Catania. The final configuration will consist of 25 stations, five of them with three-component broand-band digital seismometers and the remaining 20 equipped with vertical transducers.

The automatic data acquisition system is able to process up to 70 signals, sampled at 125 Hz and divided into two subsets, each one not exceeding 48 channels. This system operates in master/slave configuration, performs the event recognition and supplies a real-time analysis of hypocenter locations, magnitudes, fault-plane solutions and basic source parameters. Computer storage is 254 Mb, allowing to record episodes of volcanic tremor and seismic swarms lasting several hours. In addition, magnetic tape recording of triggering events allows an off-line analysis trough a distinct unit of the monitoring system. Some examples are illustrated.

GEOCHEMICAL CHANGES ASSOCIATED WITH CRYSTAL FRACTIONATION, DIFFERENTIATION, AND ALTERATION OF THE EOCENE SORREL SPRING SYENITIC COMPLEX, CUSTER COUNTY, IDAHO

SCHALCK, D. K., Department of Geology, Washington State University, Pullman, WA 99164

The Sorrel Spring syenitic complex (SSS) is associated with the high-K volcanic rocks in the southeast portion of the Eocene Challis volcanic field in central Idaho. SSS has an irregular, sheet-like shape and intrudes Devonian dolostones and Eocene volcaniclastic rocks. The major feldspars are sanidine and anorthoclase and all phases have miarolitic cavities, which suggest SSS was intruded into a subvolcanic environment.

SSS is composed of a lower olivine syenite (shonkinite), a middle pyroxene syenite, and an upper biotite syenite. Cumulates are found in the lower portion of the intrusion and the latest differentiates are found above the central portion of the intrusion in the "sandwich horizon". Silicified, potassic, carbonate, and zeolitic alteration zones are found in the intrusion, and the dolostones and volcanic rocks near the most altered portions of the intrusion are also silicified.

Chemical trends with differentiation include an increase in SiO_2, Na_2O, Zr, and Nb, a decrease in MgO, Ni and Cr, and first an increase and then a decrease in K_2O, P_2O_5, TiO_2, and V. The olivine syenite is spacially associated with the dolostones and always has olivine phenocrysts. Chemically, the olivine syenite is characterized by SiO_2 that ranges from 48.4-52.3 wt % and elevated MgO values that range from 2.7 to as high as 23.3 wt %. Ni and Cr are also high and range from 257-862 and 607-1380 ppm, respectively. The pyroxene syenite has SiO_2 that ranges from 52.4-59.0 wt %, and elevated P_2O_5 and TiO_2 values as compared to the olivine syenite. SiO_2 in the biotite syenite ranges from 58.9-62.8 wt %, and Nb and Zr reach the highest levels in the biotite syenite and the associated aplitic dikes.

Quartz, carbonate, and K-feldspar, occur as alteration minerals in veins and veinlets and as selective replacement of other minerals in the olivine and pyroxene syenites. These same minerals, plus sphene and baddeleyite, occur in miarolitic cavities in the biotite syenite. This relationship suggests that these minerals are hydrothermal in the lower portion of the intrusion and may be deuteric or magmatic in the central part of the intrusion.

K_2O is elevated in olivine syenite that has K-feldspar veinlets visible in hand specimen. K_2O reaches its highest values, >9.0 wt %, in pyroxene syenite that is found as isolated dikes, in the border zones of the intrusion, and in associated aplitic dikes. K_2O also attains these high values in biotite syenite found in the "sandwich horizon". These relationships suggest that high K_2O is a function of several processes. K_2O is low in the cumulate phases and increases with differentiation. K_2O also increases toward the border zones of the intrusion. K_2O is higher when potassic alteration, as indicated by K-feldspar veinlets, is seen in hand speciman. The changes in K_2O in SSS are related to K_2O supplied by the source of the magma, K_2O from crustal interaction, and K_2O from a hydrothermal source.

SR, ND AND PB ISOTOPE STUDIES ON ALKALINE VOLCANICS AND CARBONATITES FROM THE KAISERSTUHL, FED. REP. GERMANY

SCHLEICHER, H., KELLER, J., Mineralogisch-petrographisches Institut, D-78 Freiburg, and KRAMM, U., Mineralogisches Institut, D-44 Münster, Fed. Rep. Germany.

The Miocene alkaline volcanoe of the Kaiserstuhl belongs to the Cenocoic volcanic province of Central Europe and is situated in the southern part of the Rhinegraben rift valley. Geophysical evidence reveales updoming of the crust-mantle boundary in this region, possibly as the result of a mantle plume.

The volcanic and subvolcanic rocks of the Kaiserstuhl complex include a great variety of rocks from the tephritic and phonolitic families (e.g. leucite tephrites, essexites, shonkinites, theralites, phonolites, ledmorites, tinguaites, hauynophyres). Olivine nephelinites and melilitites as well as basanites (limburgites) are also of importance. In the subvolcanic centre carbonatites occur in form of stocks (sövites) and numerous dikes (alvikites). Also extrusive carbonatitic volcanism (lapilli tuffs) is reported.

In geochemical terms a subdivision in K- resp. Na-dominant series seems to be possible. The Sr isotopic data strongly support these results. $^{87}Sr/^{86}Sr$ ratios of primary mantle melts (olivine nephelinites, melilitites and nepheline-basanites, the main representatives of the Na-series) range from 0.7032 to 0.7040 ($^{143}Nd/^{144}Nd$ = 0.5129-0.51285), supporting the concept of a metasomatic event > 100 Ma ago. On the other hand, different degrees of crustal contamination can be shown for rocks of the tephritic-essexitic as well as the phonlithic families ($^{87}Sr/^{86}Sr$ = 0.7039 - 0.7051; $^{143}Nd/^{144}Nd$ = 0.51274 - 0.51284). The detailed interpretation gives evidence for a further metasomatic overprinting, related to the upwelling of the mantle diapir beneath the Kaiserstuhl.

The carbonatitic rocks of the Kaiserstuhl are characterized by a very uniform Sr isotopic composition (mean = 0.70365 ± 2). A genetic linkage between carbonatites and ultramafic diatreme breccias as well as melts from the turjaitic magma family (bergalites) is supported by both Nd and Sr isotopic data.

THE RELATIONSHIP BETWEEN METAMORPHOSED VOLCANITES OF THOLEIITIC AFFINITY (KOERIS FORMATION) AND SULPHIDE-BEARING METASEDIMENTS (GAMS MEMBER, HOTSON FORMATION), IN THE PROTEROZOIC BUSHMANLAND GROUP, NAMAQUA MOBILE BELT, SOUTH AFRICA

Aylva E. Schoch, Hermann E. Praekelt and Wayne P. Colliston
(Dept. of Geology, Univ. Orange Free State, Bloemfontein 9300, South Africa)

The Namaqua mobile belt consists of at least eleven tectonostratigraphic terranes. Geological complexities were investigated in detail in the vicinity of Aggeneys (Fig.).

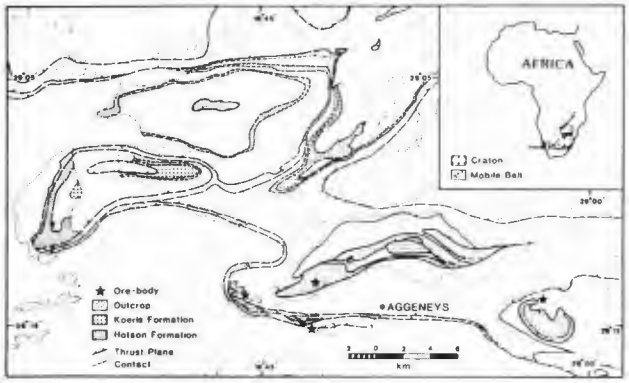

Sequence mapping and stratigraphic synthesis of the Aggeneys Terrane (Colliston et al. 1989) provided a copmprehensive tectonostratigraphic model of an ancient deformed region and also the correct position of statabound ore deposits (sphalerite, galena, chalcopyrite) in the uppermost 200 m of the Hotson Formation. The most likely source of the sulphides is indicated by the superjacent Koeris Formation, which provides abundant evidence of Proterozoic volcanicity. The ore was probably derived from contiguous cryptovolcanic sites which acted as precursors for the thick succession of mafic lavas. The fumerolic action created coeval major ore bodies identified by stars in Fig. 1. These are, from left to right: Black Mountain, Broken Hill, Big Syn, Gams. The major deposits under discussion represent the more proximal facies while the less well mineralized banded iron formation towards the north is interpreted as the more distal facies. The extent of the relevant Koeris volcanites corroborates this conclusion; the amphibolites beneath a metarhyolite marker at Gams are 330 m thick while the comparable metalavas northwest of Aggeneys are only 80 m thick.

REFERENCE: Colliston, W.P., Praekelt, H.E. and Schoch, A.E., 1989. A broad perspective (Haramoep) of geological relations established by sequence mapping in the Proterozoic Aggeneys terrane, Bushmanland. S. Afr. J. Geol.

CHARACTERIZATION OF ACCRETIONARY LAPILLI

SCHUMACHER, ROLF, Institut für Mineralogie, Ruhr-Universität, D-4630 Bochum, FRGermany.

Accretionary lapilli are concentric ash aggregates, which consist either of a coarse-grained core surrounded by a fine-grained rim (Rim or R-type), or which consist only of the core (Core or C-type). They are common in fine-grained ash deposits of various origin around explosive volcanoes. Accretionary lapilli from fallout deposits, ignimbrites, and surge deposits are distinctly different in (a) field relationships, (b) internal structures, and (c) grain-size characteristics of accreted ash, as summarized below.

R and C-type lapilli in ash layers from elutriation clouds

(a) They are enriched at the bottom of the fallout dust layer (due to their high settling velocity). Maximum size and relative amount of the aggregates decreases as distance from vent increases.
(b) The ash particles form an open framework with point contacts (at least in parts of individual lapilli; average density $\simeq$1200 kg/m^3). The outer fine-grained rim is either internally graded or consists of $\pm$ discontinuous laminae of fine and very fine ash (multiple rims).
(c) Maximum grain-size of accreted ash is 0.25 - 0.35 mm; Md 20 - 30 μm; $\sigma\phi$ 1.6 - 1.9. Maximum grain-size decreases with increasing distance from source.

C-type lapilli in fallout deposits from eruption clouds

Only C-lapilli were discribed from (phreatomagmatic) eruption clouds. Internal structures and grain-size distribution of these aggregates are similar to those of C-lapilli found in surges, so a grain-size analysis of the ash matrix is necessary to confirm an eruption plume origin.
(a) C-lapilli are enriched at the bottom of the fallout ash.
(b) Ash particles are densely packed and have planar contacts; large central graines acted as accretion nuclei.
(c) Maximum grain-size of accreted ash is up to 4 mm; Md $\pm$ 63 μm. Maximum grain-size decreases with increasing distance from vent.

R and C-type lapilli from ignimbrites

(a) They occur only in thin-bedded ash flow deposits; R-type is found only in proximal facies, C-type in distal facies (or in proximal facies of ignimbrites that had a large proportion of entrapped water). Aggregates are enriched in the upper part of discrete, proximal ash layers; in distal facies they are irregularly distributed in individual layers. Maximum lapilli-size decreases with increasing distance from source, but the relative amount increases.
(b) Cores of R and C-lapilli are roller-shaped. The accreted ash is densely packed with planar particle contacts (average density $\simeq$1600 kg/m^3); vesicles are common. The outer rim of R-lapilli is internally graded.
(c) Cores of R-type and C-type are similar in the grain-size distribution of accreted ash. Maximum grain-size is 0.35 - 0.5 mm; Md 30 - 50 μm; $\sigma\phi$ 1.5 - 1.9; It rarely changes with distance from vent.

R and C-type lapilli from surge deposits

(a) They occur in the upper part of thin-bedded surge deposits that are rich in fine ash; R-type in proximal, C-type in distal facies (or in proximal facies of surges that had a large proportion of entrapped water).
(b) Ash particles > 0.4 mm in the center acted as accretion nuclei. The ash is densely packed, but vesicles are rare. The outer rim of R-lapilli is thinner than the rim of ignimbrite-related R-lapilli.
(c) Cores of proximal R-lapilli are finer grained (due to smaller amounts of fraction 0.35 - 0.125 mm) than distal C-lapilli. Maximum grain-size of accreted ash is $\pm$ 2 mm; Md $\pm$ 63 μm; $\sigma\phi$ 2.0 - 2.4.

MAGMA MINGLING DURING ERUPTION OF A LAYERED MAGMA BODY: THE TOPOPAH SPRING TUFF, SOUTHERN NEVADA

Schuraytz, B. C., Lunar and Planetary Institute, 3303 NASA Road One, Houston, TX 77058
Vogel, T. A., Department of Geological Sciences, Michigan State University, East Lansing, MI 48824
Younker, L. W., Earth Sciences Department, Lawrence Livermore National Laboratory, Livermore, CA 94550

The 13.2 Ma Topopah Spring Member (Tpt) of the Paintbrush Tuff provides a record of the continuous withdrawal of ~1200 km^3 of magma from a stratified reservoir. The ash-flow sheet consists predominantly of crystal-poor high-silica rhyolite (HSR) that grades upward into crystal-rich quartz latite (QL) near the top of the sheet. Major and trace element chemical analyses of glassy pumice lumps and microprobe analyses of their silicate and oxide phenocrysts have been used to reconstruct the compositional and thermal gradients within the pre-eruptive magma body.

Pumice lumps from the base of the ash-flow sheet are all HSR and show variations of 75.8-79.3% SiO_2, 30-45 ppm La, and Fe-Ti oxide temperatures of 686°-785°C. The top of the ash-flow sheet contains both QL and HSR pumice lumps with variations of 67.7-79.1% SiO_2, 30-224 ppm La, and 650°-985°C; thus the full range of magmatic variation is represented by ejecta from the uppermost level. However, the variation in pumice lump compositions at this uppermost level is not continuous, but rather shows gaps within the intervals of 71.8-75.8% SiO_2 and 35-152 ppm La, and a paucity of intermediate Fe-Ti oxide temperatures. Only two out of 50 pumice lumps have intermediate compositions (INT) with ~73% SiO_2 and 93-111 ppm La.

The Mg# of biotite phenocrysts show strong correlations with bulk pumice composition, resulting in a bimodal distribution with modes at 0.44 and 0.65 for HSR and QL, respectively. Biotites with $50 < Mg\# < 60$ although present within the HSR from the lower portions of the ash-flow sheet, are not volumetrically significant, consistent with the interpretation of a gap in magmatic composition. However, several pumice lumps from the top of the ash-flow sheet, including HSR, INT, and QL contain a heterogeneous assemblage of biotites with Mg# of both 0.44 and 0.65. In these samples the dominant biotite Mg# always correlates with the bulk pumice composition and biotites with intermediate Mg# do not occur.

The figure below shows the variations in Ti and Al determined by microprobe analyses of glass bubble walls in pumice lumps (frequency increments represent 5 analyses; open circle represents bulk pumice). Glass within HSR is relatively homogeneous whereas glass within INT and QL record variable degrees of magma interaction, generally consistent with the extent of biotite heterogeneity. These features suggest that magma mixing was not efficient and that interaction occurred late in the eruptive episode.

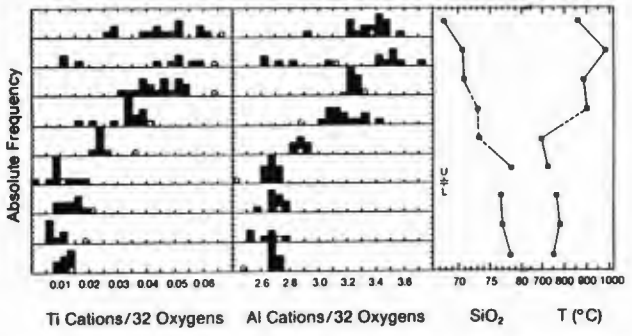

We interpret these results to indicate that (1) the reservoir comprised two magma layers with HSR overlying QL, (2) the compositional interface was ultimately breached during eruption resulting in simultaneous withdrawal of both magma layers, and (3) limited magma mingling occurred during flow through the eruptive vents.

HORIZONTAL DEFORMATION OF KILAUEA VOLCANO

SEGALL, Paul U.S. Geological Survey, Menlo Park, CA, & Geophysics Dept, Stanford University, Stanford, CA,
DELANEY, Paul T. Hawaiian Volcano Observatory, Hawaii

The Hawaiian Volcano Obs. has operated an EDM network on Kilauea Volcano since 1970. We computed horizontal displacements for three epochs: 1970-4, 1974-6, and 1976-82. The 1974-6 epoch spans the M 7.2 Kalapana earthquake. We estimate measurement errors from the network misclosures. Assuming the variance is $\sigma^2 = a^2 + b^2L^2$, where L is line length, we estimate a and b by maximum likliehood, extending the methods of *Segall and Matthews, J.G.R., 1988*. For the 1970-4 epoch $a \sim 5$ mm, and $b \sim 1 \times 10^{-6}$. The misclosures in the 1974-6 and 1976-82 data are larger, possibly due to unmodeled vertical deformation or rapid postseismic deformation during the 1976 survey. Minimum vector norm solutions, which hold the networks center of mass fixed, are shown for the three epochs below, with 95 % confidence ellipses. Notice the large displacement gradients at 155° and 155°20′ which bound Kilauea's south flank. The south flank has moved SE relative to the distal parts of Kilauea's rift zones during all three epochs. This region corresponds to the Kalapana aftershock zone and flanks the most active part of the rift system.

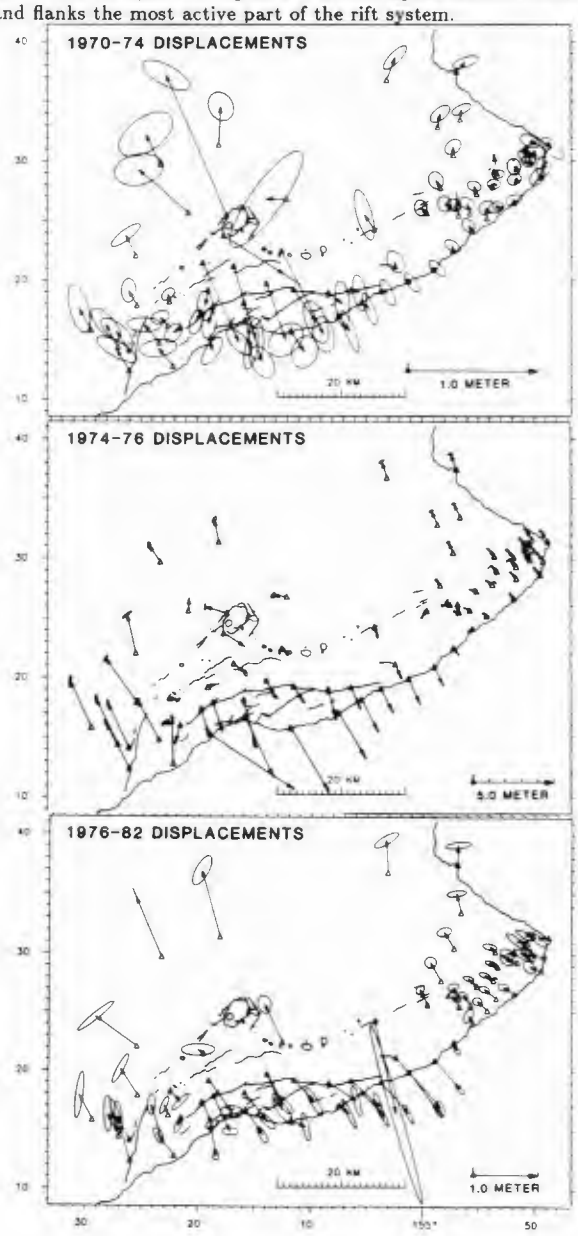

LARGE-SCALE DACITE EFFUSIVE VOLCANISM, CHAO VOLCANO, NORTH CHILE

SELF, S., Dept. of Geology, Univ. of Texas at Arlington, Arlington, Texas 76019 and DE SILVA, S.L., and FRANCIS, P.W., Lunar and Planetary Institute, 3303 NASA Rd. 1, Houston, Texas 77058

Chao is one of the largest volume Quaternary dacite lava flows yet documented (Guest and Sanchez, 1968), and one of the longest. An estimated 26 km^3 has been erupted from a vent system between two andesitic composite volcanoes in the main chain of northern Chile. Recent work suggests that Chao is not a monogenetic feature but a dacite volcano that has produced at least three closely spaced eruptions approximately past 0.5 million years ago.

The earliest Chao products found so far are coarse, non-welded pumice flow deposits that form an apron in front of the main lava flow. They cover about 20 km^2 and are up to 15 m thick. The pumice and dense juvenile clasts have typical Chao dacite mineralogy but lower phenocryst contents than later pumice and lavas, about 15 vol% (vesicle-free). No lava flow corresponding to this eruptive event has been recognized. These pumice flows are truncated by an erosion surface above which andesitic fluvial gravel and debris flow deposits from neighbouring Paniri volcano occur.

The second eruptive event was the most voluminous. An early explosive phase is recorded by up to 5 m of coarse, non-welded pumice flows, containing clasts 2-3 m in diameter. Pumice is typical Chao high-K dacite (phenocrysts = plag + qtz + hbl + biot + sphene + oxides) and phenocryst contents are 20 -30 vol%. This phase was followed by effusion of 22 km^3 of lava in two large, superposed coulees (Chao I and II). The lava has up to 60 vol% crystals in a glassy groundmass. The lower, larger flow unit is 14 km long and has 350 m-high flow fronts. Three K/Ar determinations on Chao I lava indicate that it is 0.427 $\pm$ 0.123 Ma.

The third phase of activity began with a small pyroclastic eruption forming a pumice cone of dense clasts around the vent and a fall deposit of scattered pumice dispersed to the SE. This was followed by effusion of coulee III, which is 3 km^3 in volume.

The aspect ratio (V/H) of Chao is about 1:30, similar to other rhyolite lava bodies and it is therefore not exceptional in this regard, just large. However, very high internal viscosities of between 10^{14}-10^{23} Pa s are implied by the petrological characteristics. We suggest that the exceptionally large volume, the local slope (3-6°) and a high eruption rate, caused long coulees to form rather than domes. This observation is consistent with the characteristics of other large extrusive dacite lava bodies in the region.

PETROLOGICAL EVOLUTION OF MIOCENE CONTINENTAL INTRAPLATE VOLCANICS OF BANKS PENINSULA, NEW ZEALAND.

SEWELL, R.J., New Zealand Geological Survey, Department of Scientific and Industrial, Research, Christchurch, New Zealand.
WEAVER, S.D., Department of Geology, University of Canterbury, Christchurch, New Zealand.

Banks Peninsula, on the east coast of the South Island, New Zealand, includes a minimum of 2000 km^3 of Late Miocene (11-5.8 Ma) volcanic rocks of alkalic to transitional intraplate affinity. The province comprises the eroded remnants of two large differentiated composite volcanoes, Lyttelton (350 km^3 and originally 35 km diameter) and Akaroa (1200 km^3 and originally 50 km diameter), and a host of minor volcanic centres. Systematic field mapping has established a detailed volcanic stratigraphy which is illustrated in recently published 1:50 000 geological maps.

We have identified an early subalkaline potassic series from basaltic andesite to peraluminous high-silica rhyolite which was followed by construction of the two central volcanoes. In the volcanoes, mafic rocks predominate and there are evolutionary sodic series from alkalic and transitional basalt to ne and qz normative trachytes. The youngest phase of volcanism consists of basanite lavas and rare nephelinites, fed from monogenetic vents, corresponding to an overall trend to more mafic and more undersaturated, compositions.

Rocks of the main sodic series have (Ce/Yb)n ratios from 7.0 in mafic compositions to 11.0 in trachytes which have moderate Eu anomalies (Eu/Eu* 0.30). Sr and Nd initial isotopic ratios in the mafic rocks are in the ranges 0.7029 to 0.7038 and +6.7 to +3.0, whereas felsic rocks have ratios of 0.7029 to 0.7052 and +6.3 to +0.8. These data reflect the susceptibility of felsic magmas to crustal contamination and overall are compatible with models of combined assimilation/fractional crystallisation and minor mantle source heterogeneity. The potassic subalkaline series has (Ce/Yb)n ratios of 6.0 to 8.6, declining to 1.3 in high-silica rhyolites which have extreme Eu anomalies (Eu/Eu* 0.027 - 0.070). Sr and Nd isotopic ratios in the rhyolites are 0.7041 to 0.7059 and +4.0 to +2.4, and these were most likely to have been derived by protracted fractional crystallisation of associated intermediate compositions accompanied by crustal contamination, rather than by pure crustal melting. The relationship between mafic potassic subalkaline rocks and overlying Lyttelton rocks is unclear but the former probably represent initial mantle-derived magmas that were contaminated significantly as they reamed their way through continental crust.

Comparison with other Late Cenozoic intraplate provinces of the South Island and Sub-Antarctic islands indicates limited mantle heterogeneity beneath the New Zealand region. All mafic volcanic rocks have time-integrated light-REE depleted and low Rb/Sr mantle source characteristics giving rise to low initial Sr isotopic values (generally <0.7032) and high positive epsilon Nd values (generally 5-7).

The history of southern New Zealand is one of widespread continental intraplate volcanism associated with extensional tectonics from mid-Cretaceous to mid-Tertiary times when the change to compressional tectonics corresponded to the propogation of the present day plate boundary through the region. When volcanically active, Banks Peninsula lay just outside the margin of the zone of compressional deformation. The subsequent broadening of this tectonic zone appears to have "turned off" the alkaline intraplate volcanism of Banks Peninsula and other South Island centres.

MIDDLE PROTEROZOIC ALKALINE GRANITES FRANKLIN MOUNTAINS, EL PASO, TEXAS

SHANNON WM, Department of Geosciences, Texas Tech University, Lubbock, Texas, USA

A suite of middle Proterozoic alkaline granites and associated volcanics are exposed for a distance of 25 km along a westward tilting Basin and Range fault block that comprises the Franklin mountains near El Paso, Texas. These granites intruded a Proterozoic continental shelf sequence comprising marble, volcaniclastic breccia, and quartzite. They also intrude coeval porphyritic trachytes and rhyolitic ignimbrites of the Thunderbird Formation. A thick sequence of Paleozoic strata unconformably overlies the Proterozoic rocks.

The Franklin Mountains plutons and volcanics are ≈ 1100 Ma old. The sequence of intrusion is as follows.

oldest

1) melanocratic ferroedenite-bearing alkali-feldspar granite
1b) alkali-feldspar granite porphry
2) fluorite-bearing biotite granite
3) hornblende aegirine quartz syenite
4) fluorite-bearing hornblende-biotite granite
5) leucocratic alkali-feldspar granite
5b) topaz-bearing biotite granite
6) albite-microcline riebeckite granite

youngest

All the granitoid intrusions (except 5b) are alkaline as is shown by high Zr (200-1200 ppm). The group (1, 1b) granites intrude only the Proterozoic shelf sequence. The biotite granite (2) is by far the most voluminous intrusive phase (>90%). The group (3) syenites are volumetrically small but chemically resemble group (1, 1b). The REE contents of all phases are unusually high (e.g. average Ce content): (1, 1b) = 275, (2, 4, 5) = 265, (3) = 245, (6) = 700 (ppm). The REE Ce/Yb slopes for all the rock groups are subparallel: (1, 1b) = 17.5, (2, 4, 5) = 15.9, (3) = 15.8, (6) = 17.1. Groups (1, 1b) and (3) have high Fe = 2.9-6.6%, Sc = 8-15, Zr = 300-1200, Yb = 12-18, and Ba = 900-1100 and low Rb = 90-200, Zn = 75-200, and Sr <= 200 (ppm). Group (2, 4, 5) ranges are: Fe = 1-4%, Rb = 185-275, Sc = 1-4, Zn = 15-120, Zr = 200-500, Ce = 150-450, Yb = 10-20, and Ba = 300-600 (ppm). The group (6) ranges are: Fe = 2.3-8.4%, Rb = 390-630, Zn = 300-1200, Zr = 300-1200, Ce = 200-1400, and Yb = 20-50 (ppm) all of which increase with differentiation.

Quartz $\delta^{18}O$ values are: (1) = +8.9, (2) = +7.7, (3) = +8.8 and +8.9, (4) = +8.0, (5b) = +7.7, (6) = +8.3, +8.6, and +8.8 (+/- 0.1 per mil). The corresponding whole-rock $\delta^{18}O$ are lower by +0.4 to +1.1 per mil.

These geochemical and isotopic data do not support an origin in a convergent margin setting (Norman et al, 1987, Can J Earth Sci) but are typical of anorogenic granites.

THE EARLY PRECAMBRIAN PECHENGA-VARZUGA RIFT ZONE IN THE BALTIC SHIELD

SHARKOV E.V. Institute of Ore Deposit Geology, Petrology, Mineralogy & Geochemistry, USSR Academy of Sciences, Staromonetny, 35, Moscow, 109017, USSR; SMOLKIN V.F., Geological Institute Kola Branch of the USSR Academy of Sciences, Fersmana, 14, Apatites, 184200, USSR

Pechenga-Varzuga rift zone consists of two large, asymmetric graben-syncline structures made of petrographically similar volcanic and sedimentary rocks. Both structures are characterized by very thick sequences of rocks (7.5-11.5 km) volcanic material predominating over sedimentary. Basaltic andesites are dominant near the base of the sequence. They are followed by subaeral alkaline basalts and picrites intercalating with red sandstones and gritstones. Two uppermost volcanic units are formed in deep submarine conditions. They include pillow-lavas and gialoclastites; these units are divided by a thick (1 km) turbidite-like black-shist unit, made of fillites, silicites, phosphorites.

Pillow-lavas are represented by tholeiitic basalts with REE pattern close to MORB, and high-Ti ferropicrites with REE pattern close to intraplate volcanics (continental rifts and oceanic islands). During the final stage Pechenga-Varzuga zone has experienced powerful stress deformation, accompanied by appearance of rocks of calc-alkaline (andesites, dacites) and in the end - K-subalkaline (K-granites, alkaline granites) affinities. All these features are uncommon for usual type of evolution of a rift zone but rather common for back-arc spreading zone.

In this relation it is important to note that Pechenga-Varzuga zone is located in the rear of a deep-seated Laplandsky trust which could be traced by exposures of high-pressure granulites; magmatic rocks here are represented by sinkinematic intrusions of anorthosites (calc-alkaline affinity) and high K-granites (subalkaline affinity); magmatic series are just the same, as on final stages of evolution of Pechenga-Varzuga zone. The trust is traced for about 700 km and extends from the Northern Norway, Central Finland and South-Western part of Kola Peninsula (USSR) to the White Sea (Kolvitsky massif). But it is only part of its primary length - its northern ending is covered by caledonian napples, and southern ending - beneath the White Sea. We believe this trust to be suture of the collizion zone, while Belomorsky megablock was subducted beneath Kola megablock.

The evolution of Laplandsky trust and Pechenga-Varzuga zone took place within rather narrow limit - 2,0±0,1 ga. We think that they both are elements of the system volcanic arc - back - arc basin in the collision zone of continental plates. Similar back-arc systems are now known in Alpian - Himalayan fold belt (Western Mediterranean, the Black and Caspian seas) and in the Western Part of the USA (Rio Grande rift). This idea is supported by high thickness of volcanic and sedimentary sequence, submarine type of the upper lavas, existence of strong tangential deformation during the final stages of the rift evolution, accompanied by typical subduction-type magmatic series.

SIZE AND SHAPE CHARACTERISTICS OF HYDROVOLCANIC TEPHRA

SHERIDAN, M.F., Department of Geology, Arizona State University, Tempe, AZ 85287

The size characteristics of tephra from deposits of hydrovolcanic origin are a function of many factors: (1) the nature and frequency of the explosions,(2) the pre-eruptive condition of the initial material at the moment of rupture, (3) the incorporation of external material into the moving flow, (4) aggregation or rupture of particles during movement, (5) the efficiency of size segregation of clasts during transport away from the source, and (6) the selective deposition of tephra from the pyroclastic flow or surge. Hydrovolcanic eruptions are highly variable in the number and energy of explosions, the degree of initial fragmentation of clasts, the ratio of juvenile to non-juvenile components, and the temperature and condition of entrained water. The process of fragmentation may range from essentially a single pulse to a complicated sequence of rupture and annealing of semi-solid grains produced by a cascade of compression and decompression events. Size populations of clasts produced by such processes can best be described by a model of sequential fragmentation. The maturity of such size distributions is indicated by the gamma exponent of the sequential fragmentation model. The size distribution of the very-coarse and very-fine sized tephra in hydromagmatic deposits are difficult to accurately specify for various reasons. Multiple size-modes commonly are present. Therefore, characterization of these deposits by the mean and standard deviation of a single Gaussian are misleading and inaccurate. The identification and characterization of multiple populations from selected portions of the size spectra is critical because these size modes show consistent values within samples from the same deposit and between samples from similar deposits, they must have an important genetic significance. However, more detailed analysis is needed before interpretation of the various modes is firmly established.

Several methods are currently used for shape analysis of pyroclasts from hydrovolcanic deposits. Essential for quantitative interpretation of grain morphology is the observation of key textures from a statistically significant number of individual clasts using SEM images. The general shape of clasts, indicated by their aspect ratio, and the degree of vesiculation of glassy tephra could provide information on the fragmentation and quenching of the magma. More sophisticated shape characterization such as fractal interpretation of grain perimeters or Fourier analysis of grain boundaries may provide much new information about the origin of the tephra, but these methods have not been widely used. In the future, shape analysis will probably be done by automated methods. One promising technique is to view polished grain mounts that have been thinned in an ion beam. Data from the SEM, transferred to an image processing system as grey-scale images of morphology or as element maps, reveals hidden features that allow interpretations not possible otherwise.

PARTITION OF CHLORINE COMPOUNDS BETWEEN SILICATE MELT AND HYDROTHERMAL SOLUTIONS

SHINOHARA H.,(Tokyo Institute of Technology, Department of Chemistry, Meguro-ku, Tokyo 152, Japan) MATSUO S., Department of Chemistry, University of Electro-Communication, Chofu 182, Japan) IIYAMA J.T.,(Department of Earth Sciences, Chiba University, Chiba 260, Japan)

Experimental partition equilibrium study of chlorine compounds between silicate melt and chlorine containing aqueous solutions was carried out at 810°C and in the pressure range from 0.6 to 6.0 kb. Synthesized glass with normative compositions ranging from Ab50,Or23,Q27wt% to Ab40,Or17,Q40,C3wt% was used as starting materials for silicate melts.

The relationship between chloride concentrations in the melt and in the aqueous phase varies with pressure, as shown in the figure. At 0.6 and 1.2kb, the chloride concentration in the melt was constant in certain ranges of chloride concentration in the aqueous phase, which indicates the presence of vapor-liquid immiscibility of the aqueous solution. The relationship at 2.2kb, which can be represented by a convex curve, may indicate non-ideal behavior of chlorides in the aqueous phase.

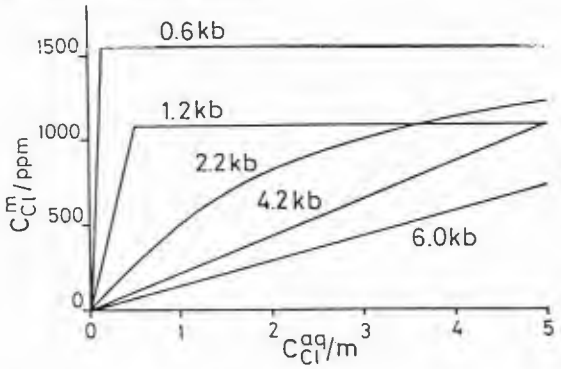

Partition ratio (D) of chlorides (NaCl+KCl) at infinite dilution (C in melt/C in aq, C:mol/kg) exhibits a strong negative pressure dependence (D=0.30 at 0.6kb and D=0.004 at 6.0kb), which is attributed to large negative partial molar volumes of alkali chlorides in the aqueous phase.

The ratio of HCl/(NaCl+KCl) in the aqueous phase is strongly controlled by the atomic ratio of Al/(Na+K) in the melt. For example, at 0.6kb, the ratio HCl/(NaCl+KCl)=0.003 was obtained in the aqueous phase equilibrated with the melt whose Al/(Na+K) ratio was unity, and HCl/(NaCl+KCl) was 10 in the aqueous phase equilibrated with the melt whose Al/(Na+K)=1.1. When the ratio of Al/(Na+K) in the melt was fixed at 1.1, the HCl/(NaCl+KCl) ratio in the aqueous phase exhibits a strong negative pressure dependence (10 at 0.6kb and 0.005 at 6.0kb).

LATE PRECAMBRIAN VOLCANIC COMPLEXES AND DYKE SWARMS OF THE SIBERIAN PLATFORM

Shpount B.R., Institute of Geology, Yakut Branch, Siberian Department, USSR Academy of Sciences, 39 Lenin pr., Yakutsk, USSR

In the late Precambrian the Siberian platform was the locus of recurrent magmatic activity that manifested itself mostly in volcanic form with high explosive index (about 98%) and predominant potassic spezialization. Such petrochemical characteristics were consistent with a rifting geotectonic regime dominating the evolution of the Siberian paleocontinent in Riphean and Vendian times.

Late Precambrian magmatic bodies are represented by dikes, near-surface thin sills and, occasionally, series of lava flows up to first hundreds of meters thick and up to 20 km long. There are hardly any ash deposits left in the vicinity of volcanic vents which bear resemblance to central-type volcanoes and reach 0.5 km in diameter. The bulk of pyroclastic material was involved in sedimentation processes and redeposited into numerous horizons of tephroids, volcanoterrigenous and volcanocarbonate rocks.

Dyke swarms make up the roots of ancient volcanic complexes. In the Riphean volcanogenic-sedimentary sequences, they form elongated,on echelon chains oriented along the axes of their paleorifts and their branches. Down section,in the Archean crystalline basement,the dykes dichotomically branch,decrease in thickness with the orientation controlled by the direction of shear joints in zones of shearing and pulling apart of metamorphic rocks.

Noteworthy is a similarity in petrochemical characteristics between contemporaneous dyke bodies and volcanogenic rocks.On the other hand there is a gradual increase in potassic alkalinity and cilica content from dykes to subalkalic sills,lava and pyroclastic formations,which was related to emanation redistribution of volatile and alkaly metal components during melts crystallization in the near-surface crustal horizons.

Study of compositions of magmatic complexes of different ages formed in the Siberian platform during the Riphean and Vendian has shown that their maximum basicity was restricted to periods dating back to about 1400,1240,700 m.y. whereas higher potassic alkalinity was restricted to about 1650,1500,1350,1200,1050,910,680, 550 m.y.The revealed periodicity for the alternation of the complexes probably reflects the rhythms of the fluid breath of the mantle with which a metamagmatic transformation of initial melts was associated.

GEODYNAMIC REGIME FOR THE FORMATION OF RIPHEAN DYKE SWARMS IN THE ANABAR MASSIF, SIBERIAN PLATFORM

Shpount B.R., Oleynikov B.V., Shakhotko L.J., Smirnov D.L., Institute of Geology, Yakut Branch, Siberian Department, USSR Academy of Sciences, Yakutsk, 677981, USSR

Basic dykes of late Precambrian age are wildely distributed in the Anabar massif of Early Archean metamorphic rocks thrown into sharp isoclinal folds of northwesterly strike (320°-340°). The dykes vary from a few cm to first tens of m in thickness, from tens of m to 10-15 km in length, they are disposed vertically and at high angles (80°-85°) with northward and northwestward dips.

Dyke bodies of each block were represented in rose diagrams according to variable strikes and taking into account their lengths. Then the dyke "peaks" in the rose diagrams were compared with the strikes os rupture dislocations in Archean sequences. Approximately 3500 dykes were treated in such a statistical way in order to determine tectonic stress fields. Consideration of the data obtained suggests that in Riphean times the Anabar massif experienced pulsating, bilateral compression determined by three directions of major horizontal stress: 60°NE, 300°NW, and 90°. The compression resulted in shear fractures and faults, the latter being filled with a pressurized basaltic magma from the mantle. The strike azimuths of these basic bodies formed during several stages of tectonomagmatic activity were determined by their proximity paleorifts fringing in arcuate fashion, the Anabar high of the Archean crystalline basement to the east and west. The marginal southeast and southwest blocks of the Anabar massif are characterized by the most branched dyke net with strike azimuths 275°,290°,40-45°, 60-80°, 90°. The block stripe in the central part of the massif is dominated by dyke concentrations along small-scale strike-slip faults with azimuths 60° and 80-90°. The dykes located in the intermediate zones between the axis and peripheral blocks of the massif have predominant 60° and 85-90° trends and subordinate 275° and 290° trends. Standing apart are the dykes of 310-330° trend located along a ramp zone on the east slope of the massif. These bodies were formed under compression-tension regime, which caused magma retardation in the intermediate magma chambers and appearance of plagiophyric facies of basic bodies.

The model for the formation of branched dyke swarms is characteristic of interrift areas of the Siberian platform basement that separate late Precambrian paleorift structures.

CERRO JOCOTITLAN, A NEW ACTIVE VOLCANO IN THE CENTRAL PART OF THE TRANS-MEXICAN-VOLCANIC-BELT.

SIEBE C., KOMOROWSKI J-C., and SHERIDAN M.F. (All at: Arizona State University, Department of Geology, Tempe, AZ, 85287; 602-965-3760; BITNET: ATM3S @ ASUACAD)

Cerro Jocotitlán (19°43'25",99°45'50") is an isolated composite volcano located 70 km NW of Mexico city and 50 km N of the city of Toluca. A large scattered population strongly dependent on agriculture and several important towns with light industry are located within a radius of 10 km from the volcano. Considered extinct, this volcano has not been studied previously.

Radiocarbon dating of the youngest pyroclastic deposits from the summit region give an age of 680 ± 80 years B.P. Cerro Jocotitlán should therefore be considered an active volcano presently in a state of repose. The proximity of this active volcano to the most densely populated area of Mexico warrants a more detailed assessment of hazards due to a potential renewal of activity.

Cerro Jocotitlán (3,952 m) rises more than 1,300 m above the flat lacustrine and fluvial sequences of the Toluca basin. The morphology of Cerro Jocotitlán is intermediate between that of a typical stratovolcano and a dome. The entire edifice rests on an older Tertiary bimodal complex of rhyolite domes and basaltic scoria cones. The first constructional stage of the volcano was characterized by major outpouring of dacitic lavas creating an edifice with shallow dips and a concave-upward profile. This stage culminated with a catastrophic explosive eruption which lead to the deposition of a regional obsidian-rich dacitic Plinian fall and pumice-rich pyroclastic surge sequence with a minimum thickness of 10 meters. This highly destructive event was followed by the construction of an enormous dacite dome with a steep convex-upward profile within the former crater. This stage was accompanied by the effusion of several extensive lava flows and minor Plinian fall and pyroclastic surge activity.

A major Quaternary flank collapse abruptly ended this second constructional stage and resulted in the emplacement of a 1.5-2 km^3 volcanic debris-avalanche deposit which spread as far as 12 km N-NE of the volcano over an area of 80 km^2. Field studies indicate that this catastrophic event was primarily a rockslide as evidenced by minor breakage, disruption, and flowage of avalanche material during its emplacement. Flank failure was most likely triggered by a major earthquake related to faults of the southern block of the Acambay graben 10 km to the north. The avalanche deposit is characterized by an H/L ratio of 0.11, and more than 100 hummocks, several perfectly conical and reaching more than 100 m in height. Hummocks are composed mostly of large blocks (0.5-100 m in size) set in coarse gravel to pebble-size matrix with little evidence of pervasive hydrothermal alteration. Blocks from the avalanche deposit show a remarkable homogeneity in chemical composition (dacites, 60-64 % SiO^2) but significant heterogeneity in rock texture and clast size. Minor explosive activity contemporaneous with flank failure was characterized by emplacement of pumice and obsidian-rich pyroclastic surges and Plinian falls directly above and between large boulders of the debris avalanche deposit. Thick soils developed from this debris avalanche deposit suggest an age of several thousands of years.

Post-flank collapse activity was characterized by the extrusion of a small dome with associated small lava flows within the avalanche crater. Field evidence suggest a long repose time between this dome activity and the recent 680 ± 80 y. B. P. explosive event which produced thick hydromagmatic rim breccias, obsidian and pumice-rich block-and-ash flow deposits and pyroclastic surge deposits which were confined to steep barrancas west and south of the present summit.

VOLCANIC VOLATILE MASS YIELD ESTIMATES TO THE ATMOSPHERE AND CLIMATE EFFECTS

SIGURDSSON, H., Graduate School of Oceanography, University of Rhode Island, Kingston, R.I. 02881, USA, and METRICH, N., Laboratoire Pierre Sue, CEN/Saclay, 91191 Gif- sur-Yvette, France.

The dominant global impact of volcanic activity is related to the effects of volcanic gases on Earth's atmosphere. These include the climatological impact caused by increase in the aerosol optical thickness of the stratosphere due to injection of sulfur compounds, leading to tropospheric cooling and the effects of volcanic chlorine, other halogens and OH^- radicals from dissociation of magmatic water on the Earth's stratospheric ozone layer. Erupted silicate particles do not play an important role as agents of atmospheric impact. Their optical properties are distinct from those of volcanic aerosols such as sulfuric acid, and the atmopsheric residence time of volcanic ash is short due to particle aggregation. The yield to the atmosphere of sulfur and halogens varies greatly with magma composition and degassing is largely controlled by the amount of carrier gases such as water and carbon dioxide. Because of these effects, the climatic impact of a volcanic eruption is not primarily governed by the degree of explosivity or the volume of erupted magma, but more importantly by the chemical composition of the magma. Atmospheric impact is dependent on the rate of volcanic volatile input, as the stratospheric half-life of a large volcanic aerosol such as from the 1815 Tambora eruption is of the order of two years.

Source rates of volcanic volatiles in past eruptions have been determined by petrologic studies of glass inclusions in phenocrysts in tephra. The average atmospheric yield of sulfur from basaltic, intermediate and silicic eruptions is 600, 560 and 70 ppm, respectively; 65, 920 and 135 ppm for chlorine and 100, 500 and 160 ppm for fluorine. A petrologic data base of volcanic volatile output from Recent and late Quaternary eruptions reveals that sulfur yield in individual events may reach 10^{10} to 10^{11} kg, such as in the Laki 1783 basaltic fissure eruption in Iceland and the 1815 explosive trachytic eruption of Tambora in Indonesia. In Laki tephra matrix glass, sulfur concentration correlates negatively with vesicularity, indicating that degassing of sulfur is controlled by the amount of other carrier gases such as CO_2 and H_2O.

Degassing of chlorine may exceed sulfur output and in the case of Tambora the yield of chlorine is estimated as 6.2×10^{10} kg, or about two orders of magnitude higher than the current annual release of chlorofluorocarbons. The same eruption emitted 4.3×10^{10} kg fluorine, judging from petrologic evidence. HCl and HF gases are not known to form aerosols in the atmosphere and are generally believed to fall out rapidly as adsorbed components on tephra, but the consequences on atmospheric chemistry of such large halogen injections have not yet been studied. Although HCl is inert toward ozone, reactions of HCl with OH^- radicals can lead to formation of atomic chlorine, followed by catalvtic decomposition of ozone.

Data on sulfur output for several historic eruptions shows a correlation with the observed mean decrease in Northern Hemisphere surface temperature associated with the eruption. Volcanic gas emissions from individual volcanic arc eruptions are likely to cause increases in the stratospheric optical depth that result in surface landmass temperature decline of 1 to 3 ^oK for less than a decade. Trachytic and intermediate magmas are much more effective in this regard than high-silica magmas, and may also lead to extensive ozone depletion due to effect of halogens and magmatic water. Hotspot related basaltic fissure eruptions in the subaerial environment have a higher mass yield of sulfur, but lofting of the volcanic aerosol to levels above the tropopause is required for a climate impact. High-latitude events, such as the Laki 1783 eruption can easily penetrate the tropopause and enter the stratosphere, but formation of a stratospheric volcanic aerosol form low-latitude effusive basaltic eruptions is problematical, due to the elevated low-latitude tropopause. Due to the high sulfur content of hotspot-derived basaltic magmas, their very high mass eruption rates and the episodic behaviour, hotspots must be regarded as potentially major modifiers of Earth's climate.

EVOLUTION OF BRINES OF MAGMATIC (?) AND METEORIC ORIGIN IN ARC-RELATED GEOTHERMAL SYST EMS: EXAMPLES FROM THE FRESNILLO AG-PB-ZN DISTRICT, MEXICO, AND BROADLANDS, NEW ZEALAND.

SIMMONS, Stuart F., Geology Dept., Auckland Unversity, Private Bag, Auckland, NEW ZEALAND

Brine fluids occur in active and fossil magmatic-related geothermal systems of arc setting; they play a prominant role in the formation of epi- and meso-thermal Ag-Pb-Zn deposits whereas their presence in Au-Ag epithermal deposits, and analogous geothermal systems, appears ephemeral. Two contrasting evolutionary paths for brine fluids are exemplified in detailed fluid inclusion studies of the Fresnillo district and the Broadlands geothermal system. Importantly, these systems formed in a strikingly similar geologic and tectonic settings, during felsic magmatism.

At Fresnillo, evidence from early mineralization at the center of the district indicates the coexistence of two compositionally distinct fluids (Fig. 1) of (a) 10 eq. wt. % NaCl and (b) <4 eq. wt. % NaCl, which cooled from 300° C to <250° C, and boiled intermittently, while fluctuating from lithostatic to hydrostatic conditions (80 to 30 bars) at an estimated paleodepth of 325 m. A third more saline brine was also present (Fig. 1). Late mineralizing fluids identified in epithermal veins from the periphery of the district also indicate the presence of two distinct fluids of essentially similar compositions at 180°-260° C; here brine fluids were injected into veins in cyclic pulses which specifically relate to periods of Ag-Pb-Zn sulfide deposition. Regionally, the water table appears to have lowered by as much as 400 m between these early and late mineralizing events. These data, plus absence of evidence for fluid mixing, imply density stratification between a deep brine resevoir and shallow, dilute meteoric fluids within an extremely dynamic geothermal system. Geologic, tectonic and isotopic evidence support a magmatic origin for brines; hence by inference, injection of brine pulses is thought to have been triggered by release of fluids during crystallization, or by recurring intrusion of magmas at depth. However, based on conceptual models of magmatic brine evolution (Fournier, 1985, USGS PP 1350), it is apparent that P-T paths of cooling magmatic vapors would generate a diversity of salinities in liquid condensates; such diversity has yet to be observed, and generation of the Fresnillo brines with relatively constant compositions remains ambiguous.

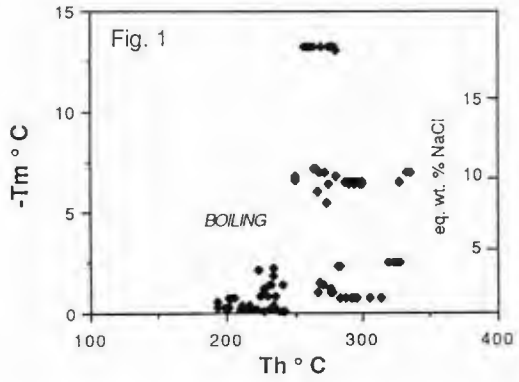

At Broadlands, brines identified in secondary inclusions (9 total) from a single sphalerite crystal (DH-16, 300 m depth) range from 1 to > 20 eq. wt. NaCl, but differ significantly from present day fluid salinities of ~ 0.2 wt. % NaCl and other inclusions within the same sample. Most brine hosted fluid inclusions homogenize at ~ 240° C, and most likely originate from the continuous boiling of a single pulse of dilute meteoric fluid. This requires at least 99% vaporization of the parent liquid, which could be accomplished where cooler fluids encountered much hotter rock, resulting very locally in a fluid boiling to virtual dryness. Conversely, isothermal boiling to dryness may result from a pressure decrease where the temperature was buffered by a sufficiently large rock mass.

DEVONIAN SHALLOW MARINE VOLCANICLASTICS IN EASTERN AUSTRALIA: MASS FLOW OR SUBAQUEOUS PYROCLASTIC FLOW DEPOSITS?

SIMPSON, C., Department of Geology, University of Wollongong, P.O. Box 1144, Wollongong, 2500, Australia

Debate continues in the literature as to whether subaerial pyroclastic flows can make a smooth transition into water and continue to move as gas-supported subaqueous flows. Evidence for ingestion of water into a flow indicates that the gas-driven mechanism of the pyroclastic flow has been reduced or lost and as such a mass flow depositional origin should be proposed.

The Early Devonian Tangerang Formation is a continental graben-fill sequence, up to 2000 m thick, which includes silicic subaerial pyroclastics, shallow marine volcaniclastics and epiclastics. Shallow marine volcaniclastics of the Devils Pulpit Member (DPM) are up to 200 m thick and have been emplaced primarily by mass flow processes. A shallow marine depositional setting is indicated by sparse broken but unabraded fossil fragments in both the DPM and the enclosing tuffaceous epiclastic sequence, which consists of mass flow and cross-bedded, tidal-dominated shelf deposits.

The volcaniclastics of the DPM consist of ash-, lapilli- and block-sized aggregates of unbroken and fragmented crystals, glassy and accidental lithics, abundant relict shards, fine ash and minor pumice, indicating a freshly erupted pyroclastic mode of fragmentation for the detritus. Location of source volcanoes is unknown but is presumed to be in a large area of contemporaneous subaerial volcanism north of the DPM exposures.

A variety of facies can be recognised within the DPM, ranging from volumetrically minor primary pyroclastics to extensive epiclastics involving slight to moderate degrees of reworking. Primary deposits are restricted to a small part of the sequence where high density, pumice-poor portions of pyroclastic flows entered the sea without explosive fragmentation. The resultant deposits are massive and poorly sorted, characterised by abundant, large glassy lithic fragments, a large vitric component of ash and shards and relatively few crystals. Rapid vertical and lateral grading from these primary pyroclastics into crystal-rich volcaniclastics reflects elutriation of the vitric component during injestion of water and transformation into high particle concentration mass flows. Finer grained, massive to normally graded vitric-rich horizons up to 10 m thick are interpreted as redeposited ash-fall material, derived either from continuous subaerial eruptions or from secondary explosions where pyroclastic flows entered the sea.

Features of the DPM such as thick massive beds, vitric depletion, sparsely distributed fossil fragments and the scarcity of large pumice clasts, attest to the importance of mass flow epiclastic processes in the deposition of the DPM sequence.

MAFIC INCLUSIONS IN THE TSCHICOMA FORMATION, JEMEZ VOLCANIC FIELD, NEW MEXICO

SIMS, K.W., Institute of Meteoritics, Department of Geology, University of New Mexico, Albuquerque, NM 87131, LOEFFLER, B.M., Department of Geology, Colorado College, Colorado Springs, CO 80903, LINDEMAN, T.G., Department of Chemistry, Colorado College, NOBLETT, J.B., Department of Geology, Colorado College, and FUTA, K., U.S.G.S., Denver Federal Center, Denver, CO 80225

The Tschicoma dacites of the Polvadera Group, Jemez Volcanic Field, contain abundant inclusions of basaltic andesite. These inclusions commonly range in diameter from 1 to 12 cm and consist of acicular plagioclase, acicular oxyhornblende, vesicles (20%, enough to make the inclusions buoyant in their dacite host) and glass. Mafic inclusions such as these are now widely attributed to magma mixing. Two mechanisms have been proposed: a decrease in density as crystallization and volatile exsolution take place in a mafic magma cooling beneath a felsic magma reservoir; and forceful injection of a mafic magma into a felsic reservoir. In the latter mechanism, both magmas are fully liquid on mixing, whereas in the former, the mafic magma must be partially crystallized before mixing.

For the inclusions in the Tschicoma dacite, we can demonstrate not only that they were produced by magma mixing between the host Tschicoma dacite and an associated basaltic magma, but that the mechanism had to be forceful injection. Our evidence: 1) Major- and trace-element, as well as isotopic, data allow a least squares mixing calculation between the Tschicoma dacite and the associated Lobato basalt, which reproduces the chemistry of the inclusions. 2) Glomeroporphyritic clots of the host Tschicoma dacite, consisting of glass-charged (sieve texture) plagioclase (An37-48), hornblende and biotite, are found within the inclusions. The plagioclase in these clots, both in the inclusions and in the host Tschicoma, has reversely-zoned rims (An50-52), which reflect the higher An content of the inclusions (An49-56). This rim post-dates the resorption indicated by sieve texture. Thus, these plagioclases seem to record a thermal and chemical reequilibration in response to the injection of a higher-temperature, more-mafic magma into the dacite. 3) Statistical analysis of grain size (length x width), grain acicularity (length/width) and coefficient of variance of grain size (size variability) shows a systematic variation both with inclusion size and with position within an inclusion. Grain size and the coefficient of variance of grain size increase with inclusion size, indicating a longer period of crystal nucleation and slower cooling. Acicularity decreases in larger inclusions, indicating smaller degrees of undercooling. Within one inclusion, grain size decreases, and acicularity increases, towards the boundary of the inclusion, reflecting more rapid cooling at the boundary. These observed variations in texture indicate that the inclusions were incorporated while in a liquid state. This supports forceful injection. 4) Modelling of heat flow for a spherical molten inclusion solidifying within a viscous liquid host suggests that outer boundaries cool roughly ten times more rapidly than the inclusion interiors and that smaller inclusions cool more quickly than the larger ones, roughly in inverse proportion to the square of the inclusion radius. This model qualitatively agrees with our observation of cooling rate based on statistical analysis of grain size and acicularity. Again, this supports forceful injection, since there would be no such systematic variation in texture if the mafic magma were partially crystallized before mixing.

SOME ASPECT OF IRON ORE AND MANGANESE ORE DEPOSITS IN RELATION TO MAGMATISM: A CASE STUDY FROM IRON ORE GROUP, NORTH ORISSA, INDIA

SINGH, P.P., Department of Geology, Utkal University, Bhubaneswar, India 751 004

Geologic mapping in parts of the Iron Ore Basin, north Orissa has documented critical genetic relationships between the rocks of Iron Ore Group, and iron and manganese ore mineralization. Iron Ore Basin is composed of volcanic-sedimentary rocks belonging to youngest Iron Ore Group of Proterozoic age. The lithostratigraphic packages contain pillow lava, tuffs-shale, banded iron formation and associated ore mineralization. The granitic massif to the east of the basin are extremely intersected by dolerite dyke swarms, possibly as feeders, pouring basic volcanics on which rocks of the sedimentary cycle of the basin rest. The pillowed basic volcanics have tholeiitic affinity and tuffites are clastic products of rhyodacitic volcanism. The basic lava is interlayered with tuffites and grading upward/laterally into ore rich tuffaceous sediments. The spartically close and consistent distribution of the iron and manganese concentration have a broad space-time relation with the basic volcanism in the basin. The basin owed its origin to strike-slip motion subjected to period of transtensile regime. A source of pyroclastic and exhalative (volcanic-hydrothermal) model to account for the genesis of the iron ore and manganese ore distribution is inferred.

PRE-ERUPTIVE H_2O AND CO_2 IN PLINIAN AND EARLY ASH-FLOW MAGMA OF THE BISHOP TUFF

SKIRIUS, C. M., Department of the Geophysical Sciences, University of Chicago, Chicago, IL 60637

Glass inclusions in quartz phenocrysts from individual lumps of pumice collected from stratigraphic levels within the plinian air fall deposit and three overlying early ash-flow units of the Bishop Tuff were analysed by Fourier transform infrared (FT-IR) spectroscopy for their H_2O and CO_2 contents. Most of the plinian inclusions (70%) yielded 5 - 6 wt.% H_2O and $\leq$ 0.01 wt.% CO_2. Inclusions from lumps of pumice from the same plinian stratigraphic levels have comparable ranges in H_2O and CO_2. Ash-flow inclusions yielded approximately the same range in water concentrations with ~50% of the inclusions having higher (0.01 - 0.02 wt.%) CO_2 concentrations. Anderson, et al (in press) reported lower water (~4.3 wt.%) and higher CO_2 (up to 0.066 wt.%) for inclusions analysed by FT-IR from the latest and hottest Mono Lobe ash-flow. Assuming that the magma was gas-saturated prior to eruption as put forth by Anderson, et al, then the plinian and ash-flow crystals grew at H_2O-CO_2 saturation pressures of approximately 1500 to 2400 bars, in accord with their findings. A few plinian inclusions have up to 7 wt.% H_2O and 0.024 wt.% CO_2 and evidently formed at greater depth.

A group of devitrified plinian and ash-flow inclusions were heated in an internally-heated gas pressure vessel at 800°C and 2 kbar for approximately 20 hrs. and quenched at pressure prior to spectroscopic analysis. This procedure dissolved the devitrification products (crystals $\pm$ vapor bubbles) and produced clear, glassy, unfractured samples which yielded 5.0 to 5.8 wt.% H_2O and $\leq$0.02 wt.% CO_2, values similar to the majority of unheated inclusions, and allows the initial volatile content of previously unsuitable devitrified samples to be determined. The overlap in H_2O and CO_2 concentrations between plinian and early ash-flow inclusions suggests that both plinian and early ash-flow material sampled similar depths within the pre-eruptive magma body.

TRACE ELEMENT AND RADIOGENIC ISOTOPE CONSTRAINTS ON THE GENESIS AND EVOLUTION OF RHYOLITIC MAGMAS BENEATH VALLES CALDERA

SKUBA, C.E., WOLFF, J.A., Department of Geology, Univ. of Texas at Arlington, Arlington, TX 76019

Rhyolitic volcanism within the Jemez Mountains became dominant by 3 Ma, climaxing with the eruption of the Otowi and Tshirege Members of the Bandelier Tuff from the Valles caldera at 1.45 Ma and 1.12 Ma respectively. Prior to the eruption of the Otowi, minor rhyolitic activity produced the San Diego Canyon ignimbrites (SDC) in the southern part of the present-day caldera at approximately 2.8 Ma. Domes and tuffs of the Cerro Toledo Rhyolite (CT) erupted between the Otowi and Tshirege Members, while post`Tshirege activity produced the Valles Rhyolite (VR) ring domes.

Trace element variations within the rhyolite units generally reflect the fractionation of the observed phenocryst assemblage. However, the behavior of elements such as Rb, Th, Yb, and Ta, which remain incompatible throughout rhyolite fractionation, suggest a mixing relationship between high-Th/Yb,Rb/Yb and low-Th/Yb,Rb/Yb compositions. Th and Rb depletion relative to Yb is progressive from SDC through Otowi and CT to Tshirege, with an abrupt return to high-Th/Yb,Rb/Yb compositions in the VR. Preliminary Pb, Sr and Nd isotopic data indicate the presence of both mantle and crustal components in the rhyolites. Asthenospherically-derived tholeiites erupted at ca. 2 Ma in the adjacent Cerros del Rio lava field may represent the mantle component. Pb isotopes show very little variation despite considerable heterogeneity of Pb in local crustal rocks, suggesting that a dominant volume of rhyolite (that ultimately erupted to form the Bandelier Tuffs) was produced by a single melting event at 2-3 Ma, in response to the emplacement of basaltic magma in the crust. The trend to low-Rb/Yb,Th/Yb compositions up to and including the Tshirege appears to result from the continued addition of smaller quantities of more mafic (dacitic?) lower crustal melt to the established rhyolitic magma body, during fractionation to a highly evolved, zoned system. Contrasting trace-element signatures in the components of individual banded pumices from the Otowi Member indicate that one such addition may have triggered its eruption.

ORIGIN OF ALKALINE, TRANSITIONAL AND CALC-ALKALINE MAGMAS, WRANGELL VOLCANIC BELT (WVB)

SKULSKI, T., FRANCIS, D., Dept. of Geol. Sci. McGill University, Montreal, PQ, Canada H3A 2A7, and **LUDDEN, J.**, Dept. de Geologie, Universite de Montreal, PQ, Canada H3C 3J7.

The mid- to late-Cenozoic, NW-trending WVB has formed over the obliquely convergent North American continental margin. In SE Alaska, the WVB comprises 26 Ma to Recent (eg. Wrangell Volcano, see fig.) calc-alkaline lavas that overlie a N-dipping Benioff zone. In SW Yukon and NW British Columbia, the WVB comprises Miocene transitional and minor alkaline and calc-alkaline lavas that overlie a splay in the Queen Charlotte-Denali strike-slip system (Duke River fault). Alkaline lavas (alkaline olivine basalt AOB, hawaiite HAW, and mugearite MUG, see fig.) precede transitional lavas (basalt BAS, basaltic trachyandesite BTA, trachy-andesite TRA, trachyte TRY, and rhyolite RHY) and are followed by calc-alkaline lavas (basaltic andesite BAD, andesite AND, and dacite DAC, eg. Lava Creek, 60° 35'N 138°W) in the SE WVB. In the St. Clare volcanic field (61°25'N 140°15'W), there is a complete chemical progression from least-evolved, AOB to younger BAS that is characterized by decreasing Ba/Nb, La/Sm, La/Yb, Zr/Y and $^{87}Sr/^{86}Sr$. The BAS and AOB magmas differ from their calc-alkaline counterparts in the NW WVB in that the former do not have high Ba/K, Ba/La and Ba/Nb ratios. Crustal contamination cannot explain the chemical features of the primitive basaltic magmas. The correlation between Ba/Nb, $^{87}Sr/^{86}Sr$ and major elements in evolved alkaline, young transitional (Count Creek), and calc-alkaline (Lava creek) lavas requires crustal assimilation. However, the chemical variations in the primitive basalts are best explained by mixing between OIB-like and T-MORB-like mantle sources. Subduction must have been coeval with the transitional magmatic stage since hybrid calc-alkaline - transitional lavas are found in the St. Clare field (see fig.). The hybrid lavas have lower Ba/Nb and Ba/La than their Alaskan counterparts. These features can be explained by mixing of slab-derived LIL-rich fluids with the BAS source.

The magmatic relationships in the WVB can be reconciled with a model in which a leaky transform fault initially tapped a heterogenous OIB and T-MORB-like mantle source. Subsequent metasomatism of this source produced arc magmas.

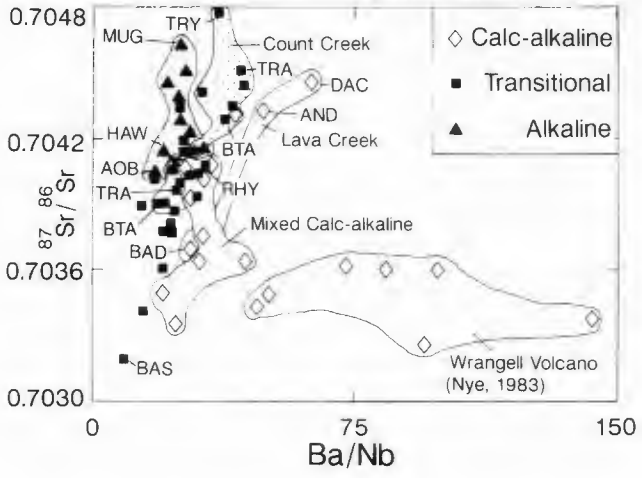

THE RELATIONSHIP BETWEEN LATE CENOZOIC ALKALINE VOLCANISM AND GLACIATION IN THE ANTARCTIC PENINSULA

SMELLIE[1], J.L., HOLE[1], M.J., SYKES[2], M. A., AND SKILLING[1], I.P.

[1] British Antarctic Survey, Natural Environment Research Council, High Cross, Madingley Road, CAMBRIDGE CB3 0ET, UK.

[2] ESSO Expro UK Ltd., Biwater House, Portsmouth Road, Esher, Surrey UK.

The terrestrial Cenozoic history of Antarctica is the poorest known of all the continents. However, within Marie Byrd Land and the Antarctic Peninsula, there are widespread, substantial sequences of Miocene-Recent alkaline volcanic rocks. Together, they represent the best-preserved Late Cenozoic terrestrial record in Antarctica.

Within the Antarctic Peninsula volcanic outcrops, analysis of the lithofacies assemblages can be used to interpret the eruptive environment. Lithofacies association 1 (N Alexander Island; 7.7-3.9 Ma) consists of thin units of fluvial sediments and till-like conglomerates interbedded with columnar-jointed lavas and hyaloclastites. Abundant striated clasts in the sediments, and polished and striated pavements with ice-molded landforms beneath some sequences suggest that the lithofacies were formed during subglacial eruptions beneath wet-based ice. Lithofacies association 2 (SW Alexander Island; Rothschild Island; Seal Nunataks; 5.4-<0.1 Ma) mainly comprises thick piles of pillow lavas and/or well-stratified monomict tuffs and lapillistones formed of highly vesicular, palagonitized vitric scoria, with abundant sedimentary structures including large-scale channel bedforms and slumps. These lithofacies probably represent fissure-erupted tindars formed in either a submarine or (perhaps more plausibly) subglacial setting. Lithofacies association 3 (James Ross Island Volcanic Group; 7.1-0.3 Ma) is a distinctive assocation of multiple superimposed lava:hyaloclastite couplets. Lenses of conglomerate interpreted as tillite occur frequently at the basal unconformity and more rarely within the volcanic sequence. Although there is evidence for a marine influence and fluctuating sea-levels, the bulk of the succession probably formed as hyaloclastite deltas during subglacial eruptions through a relatively thin (< 200 m) ice cover. Lithofacies association 4 (Hornpipe Heights; 2.5 Ma) is a distinctive sequence of oxidized Strombolian airfall tephra, agglutinates and clastogenic lavas which are draped against a steep pre-volcanic surface. There is no evidence for interaction with either ice or water and the source vent is beneath the present ice surface, signifying significantly lower local ice levels during late Pliocene time.

These interpretations of the outcrops provide convincing evidence for significant glaciation affecting the Antarctic Peninsula during much of the last 7 Ma. At least one period of reduced ice levels occurred during the Pliocene.

SOUTHERN WASHINGTON CASCADE MAGMATISM: FOCUS ON THE INDIAN HEAVEN LAVA FIELD

SMITH, D. R., Dept. of Geology, Trinity Univ., San Antonio, TX 78284, and LEEMAN, W. P., Earth Sciences Division, Natl. Science Foundation, Washington, D.C. 20550

A geochemical survey of southern Washington High Cascade stratovolcanoes and lava fields has revealed the existence of several mafic magma types, most of which occur in the Indian Heaven (IH) lava field located between Mts. St. Helens and Adams. More then 20 vents define a ~30 km, north-south trend within this field. Intermittent eruptions at these multiple vents began <730,000 yrs. ago, the most recent occurring <10,000 yrs. ago (Hammond and Korosec, 1983). The IH lavas are dominantly mafic and include 4 main types: [plag+oliv]-phyric tholeiitic basalts (TH), [oliv±plag± rare cpx]-phyric calcalkaline basalts and basaltic andesites (CA), [oliv±plag]-phyric basalts transitional between these two (TR), and [cpx+oliv±relict amphibole]-phyric, high-K_2O calcalkaline basaltic andesites (KBA). Andesite is volumetrically minor and felsic rocks are absent. Stratigraphic relations do not reveal any strong relationships among magma type, vent, and time of extrusion, but the KBAs appear to be low in relative abundance and may be among the oldest IH eruptive products.

The geochemistry of IH mafic lavas reveals several notable features:

(1) They are characterized by relatively high Mg#'s (0.56-0.68) and MgO contents (~6.5-8.7 wt.%). Compatible elements (e.g., Ni, Cr, Co) show considerable overlap among the mafic lava types.

(2) Normalized incompatible element patterns for the THs exhibit fairly smooth, convex upward patterns. In contrast, KBAs exhibit elevated abundances (relative to THs) and strong HFSE (e.g., Nb, Ta) depletions. TR and CA lavas have abundances intermediate to THs and KBAs; some exhibit HFSE depletions of lower magnitude than the KBAs. Plots of some element ratios (e.g., Ta/Yb vs. Th/Yb, Ba/Zr vs. Nb/Zr) reveal two linear trends. The first lies within a mantle array defined by MORBs and OIBs, with CAs lying towards OIBs and THs lying within the MORB field. The second trend, defined largely by KBAs, lies at a steep angle from the first trend, extending from the MORB field towards ratios typical of volcanic arc magmas and/or pelagic sediments. TRs are distributed between both trends. The lavas conforming to the mantle array also have low boron contents (1-4 ppm), and low Ba/La (<18)and K/Cs (<32,000) relative to typical arc basalts. LILE ratios show wide variations (e.g., Ba/Rb=11-43, K/Rb=415-839, K/La=276-665) that do not correspond with magma type.

(3) Isotopic variations are small but significant ($^{87/86}Sr$= 0.70304-0.70385, $\delta^{18}O$=+5.5-6.1 permil, $^{207/204}Pb$=15.550-15.634, $^{206/204}Pb$=18.8320-18.974, $^{208/204}Pb$=38.398-38.790). Lead and oxygen isotopic ratios do not correlate with mafic magma compositions, but there is a slight positive correlation between $^{87/86}Sr$ and some element ratios (e.g., Ba/Nb), with the KBAs being the most radiogenic. Lead-lead diagrams show that the IH lavas fall within the field for OIBs, along a trend lying above MORB and extending into fields for sediments/ores.

The available data suggest that the diverse IH mafic magmas were not produced by crystal fractionation of observed phenocryst phases or by differing degrees of partial melting of a homogeneous source. Furthermore, the data (perhaps with exception of Pb isotopes) indicate that most IH magmas apparently ascended without significant interaction with crustal material. If a crustal component was involved in their petrogenesis, it was distinct from crust involved in the generation of other southern Washington Cascades magmas (e.g., Mt. St. Helens). The generation of the mafic magmas probably involved mixing of different chemical reservoirs within the mantle wedge, including sources similar to those producing MORBs and OIBs. In general, a subducted slab/ sediment component was not as important in affecting these sources as for most other volcanic arcs. The wide variety of IH lavas erupted close in space and time implies the existence of a complex mantle with small-scale heterogeneities beneath this portion of the Cascades.

OBSERVATIONS ON THE RECORD OF CENOZOIC PYROCLASTIC VOLCANISM IN NONMARINE SEDIMENTS, NORTHWEST AND SOUTHWEST UNITED STATES

SMITH, Gary A., Dept. of Geology, Univ. of New Mexico, Albuquerque, NM 87131, U.S.A.

Volcaniclastic sedimentation adjacent to the Cascade Range, Oregon and Washington, and within extensional basins of Arizona and New Mexico record volcanism by 1) the composition of the sediments and 2) the geometry of the deposits.

Pyroclastic (±autoclastic) fragments dominate over epiclasts in the sedimentary deposits. Contrary to recent efforts to redefine these terms, emphasis should be retained on fragmentation, rather than deposition, mechanisms. Volcaniclastics are unique clastic sediments because most grains are produced by volcanic processes without the intervening weathering necessary to produce epiclasts. Neogene sedimentary aprons and basin fills adjacent to the Cascades principally contain reworked pyroclasts initially emplaced as pyroclastic flows and falls. Where source areas are preserved it is apparent that silicic eruptives are overrepresented in sediments because of the greater reservoir of pyroclastic sediment associated with silicic magmas.

Varying pyroclast:epiclast ratio of sediments may record episodes of volcanic activity. Miocene sediments in central Washington alternate between monomictic pumiceous, dacitic pebbly sands (syneruption), and polymictic epiclast-rich gravels (intereruption). Alluvial fans flanking rhyolite domes in New Mexico coarsen upward from conglomeratic sandstones dominated by pyroclasts and glassy rhyolite to sandy conglomerates with more abundant devitrified rhyolite epiclasts; this trend records diminished stripping of tephras and increased erosion of domes that corresponds to an upward decrease in primary pyroclastic units and spacing of paleosols.

Volcaniclastic sedimentary sequences may show geometric features that reflect the episodic nature of aggradation under eruption impacted conditions. In the Northwest, pyroclast-rich sediments, often associated with primary pyroclastic units, form broad syneruption sheets that are incised during intereruption periods. Resultant paleovalleys may fill with coarser, epiclast-rich sediment if there is subsidence to drive aggradation in the absence of excessive eruption generated sediment loads. Distinct syneruption and intereruption sediments are not recognized in alluvial-fan successions in the Southwest; perhaps because arid-climate depositional style is controlled by the episodicity of storms to provide runoff rather than episodicity of eruptions to provide sediment.

The sedimentary record of volcanism and the impact of volcanism on terrestrial deposition take on variable forms in different areas in response to style and frequency of eruptive events, tectonic setting and subsidence history of the depositional site, and climate.

MAGMA CHAMBER PROCESSES BENEATH LARGE RHYOLITE VOLCANOES OF THE TAUPO VOLCANIC ZONE, NEW ZEALAND.

SMITH, Ian E. M., Department of Geology, University of Auckland, Private Bag, Auckland, New Zealand.

The Taupo Volcanic Zone (TVZ), central North Island, New Zealand is dominated by the presence of large caldera-type rhyolite volcanoes. Two are considered active, the others range back in age to about 1.5Ma before the present. All have produced moderate to large scale eruptions of predominantly rhyolitic material as pryoclastic fall and flow deposits together with subordinate lava; basaltic magmas are a rare but important component of the TVZ volcanoes.

Chemical data show that, for the most part, the eruptives have very uniform compositions although among the older deposits (Mangakino Volcano) there is variation from dacitic to rhyolitic compositions and one of the young volcanoes (Okataina Volcano) shows a discrete dacitic eruptive sequence.

Detailed studies of the young eruptive sequence from Taupo Volcano (less than 2.2Ka) indicates that identifiable magma batches have existed for periods of the order of 1.0Ka during which time they have been tapped in successive eruptive events. Deposits from individual eruptions may display considerable physical diversity but chemical compositions of individual pumice clasts are remarkably homogeneous. Further, mineral assemblages and mineral compositions show no significant variation other that that related to temperature dependent equilibria. Deposits produced by eruptions separated by periods of greater than 1.0Ka may also be identical in terms of their chemical compositions and mineral assemblages.

These observations suggest that moderately large homogeneous magma chambers (of the order of hundreds of cubic kilometres) have existed at relatively shallow crustal levels for periods of the order of thousands to tens of thousands of years and during this time have fed multiple eruptions. This suggests that the magmas were continuously homogenised by active convection.

The rare basalt magmas which originate beneath the TVZ play a significant role in the physical processes of the rhyolite volcanoes and also as an end member in a spectrum of mixed materials which include rare andesitic together with dacitic compositions. The evidence from mixed pyroclastic deposits, mixed pumice clasts and hybrid clasts indicates a variety of types of interaction in shallow crustal chambers between basalt and rhyolite magmas. At one and of the spectrum there is physical mixing with no chemical mixing while at the other, virtually complete chemical mixing produces a liquid whose hybrid origin is evidenced only by dual crystal populations.

THE YELLOWSTONE-SNAKE RIVER PLAIN VOLCANIC SYSTEM: KINEMATICS, CONTEMPORARY DEFORMATION AND MAGMA SOURCES

SMITH, R.B., NAGY, W.C. Department of Geology and Geophysics, University of Utah, Salt Lake City, Utah 84112, VASCO, D.W., Air Force Geophysical Laboratory, Hanscom AFB, Ma. 01731

Quaternary caldera-forming volcanism, active resurgent domes, extensive hydrothermal activity, heat flow >1500 mWm^{-2}, and widespread earthquake activity reflect the dynamics of the Yellowstone Plateau; the active element of the Y-SRP system. The topograhically high Plateau coincides with a 300 km-wide mantle bulge that rises more than 400 m above the surrounding topography. Whereas, a systematic topographic decrease southwesterly, parallel and normal to the axis of the 800 km Snake River Plain, and a "V" shaped shoulder of seismicity extending laterally away from the aseismic SRP volcanics suggests thermal subsidence and a lack of significant seismogenic-deviatoric stresses of the SRP crust.

Widespread earthquakes, the largest M_L7.5, have occurred on the perimeters of the Yellowstone Plateau. Whereas, shallow swarms and smaller events, M<6.5, characterize the caldera and it's hydrothermal systems. Rheological models suggest that maximum earthquake focal depths are restricted to depths less than ≈ 5 km beneath the caldera by temperatures exceeding 350°C, defining a very thin seismogenic layer, relative to maximum focal depths of ≈ 20 km outside the caldera but still within the mantle bulge. Regional strain rates from cumulative seismic moments of 10^{-13}/s are accommodated by N-S extension of up to 4.7 mm/yr in the adjacent Hebgen Lake fault zone; rates as large as along the San Andreas fault.

Unprecedented uplift, revealed by leveling, of as much as 75 cm over the Yellowstone caldera occurred between 1923 and the mid-1970's. Extremal inversion of these height changes suggests two shallow volumetric sources for the uplift at depths of 2 to 4 km: 1) a 10^{-4} km^3 increase in the northeast caldera, near the Sour Creek resurgent dome and close to a body of anomalously low seismic P-wave velocity, and 2) a 10^{-4} km^3 increase in the southern caldera on the east flank of the Mallard Lake dome. From 1977 to 1987, cumulative height increases of 12 cm and a 60 microgal gravity decrease, were observed along a profile that crosses the northern caldera. Inversion of these data infer that the causative anomaly was in the same northern caldera location as the 1923-1976 anomaly and was not deeper than 9.0 km. It involved a density increase of more than 0.002 gm/cm^3.

The P-wave upper-crustal velocity structure beneath the Yellowstone Plateau, revealed by earthquake tomography and refraction profiles, shows a heterogeneous structure with a caldera-wide 10% low-velocity body to depths of ≈15 km that is thought to reflect a remnant magma reservoir. A pronounced 20% P-wave decrease occurs in a restricted volume of the upper crust beneath the northern caldera where P-wave attenuation increases by 70%. The anomalous velocity-density-attenuation anomalies in the northern caldera are consistent with a range of plausible physical models for the upper-crust ranging from 10%-40% partial melts to a vapor-dominated systems. The lower crust of the Yellowstone Plateau is however, seismically indistinct from that of the surrounding thermal undisturbed Rocky Mountains. This suggests the ascent of magmas to upper-crustal reservoirs at rates that did not allow significant seismic velocity perturbations of the lower crust. The Yellowstone velocity model is consistent with the SRP crustal structure where the near-surface basaltic layer thins from 2 km in SW Idaho to zero at Yellowstone while the silicic layer is 2 km thick and extends to the Yellowstone caldera. An unusually high velocity, 6.5 km/s layer, cores the mid-crust and is interpreted as a mafic, solidified remnant of the SRP magma reservoir.

The contemporary height and gravity changes of the Yellowstone Plateau, when interpreted with the youthful volcanic history, the heterogeneous seismic velocity structure, and extremely high heat flow are consistent with models of shallow magma transport, unusual hydrothermal activity or accelerated episodes of tectonisim.

MAFIC INTRUSIVES IN PRECAMBRIAN ROCKS OF THE WYOMING PROVINCE AND BELT BASIN

SNYDER, G.L., U.S. Geological Survey, Federal Center MS 913, Denver, CO 80225, USA,
HALL, R.P., Department of Geology, Portsmouth Polytechnic, Portsmouth PO1 3QL, UK,
HUGHES, D.J., Department of Geology, Portsmouth Polytechnic, Portsmouth PO1 3QL, UK, and
LUDWIG, K.R., U.S. Geological Survey, Federal Center MS 963, Denver, CO 80225, USA

Precambrian mafic and ultramafic intrusives occur in nearly all the fault-block mountain ranges of the Archean Wyoming Province. They range from large, complex layered intrusives to simple dikes and sills in swarms that inflate the country rock from 5 to 30 percent. Although most individual tabular intrusives are only meters wide and one to several km long, at least one dike is mappable for 130 km. Most mountain ranges and the adjacent Belt basin contain intrusives of three or more ages; some, but never all, times of intrusion are repeated from range to range. Times of least intrusive activity are about 1.0, 1.6, and 2.3 Ga throughout the Wyoming Province as well as the Canadian shield. Archean and Early Proterozoic intrusives, most of which are metamorphosed, trend mainly northeasterly parallel to the edge of the Wyoming Province in the southeastern half of the province; orientations are more diverse in the northwestern half. Middle and Late Proterozoic intrusives, most of which are not metamorphosed, trend northwesterly along the southeastern and northwestern margins of the Wyoming Province but are unrecognized in the interior.

Precambrian mafic magmas generated mostly Proterozoic clinopyroxene-dominant tholeiites with lesser plagioclase-phyric ("leopard rock") diabases, orthopyroxene-dominant norites, or olivine-dominant troctolites. The immobile-element chemistry of a majority of these rocks in southeastern Wyoming is consistent with an island arc environment. The generally Archean ultramafic rocks, which occur in much smaller quantities, have been postulated to have been emplaced as extrusive oceanic basement, as entire liquid or semisolid intrusives, or as cumulate portions of other intrusives. Mafic and ultramafic magmas derived from different mantle sources succeeded each other, either as crosscutting components of sheeted swarms or as successive liquid components of large inhomogeneous plutons. Middle and Late Proterozoic intrusives include differentiated varieties such as quartz dolerites, alkalic olivine dolerites, or even quartz porphyry rhyolites. Recently studied intrusive sequences from southeastern Wyoming include many of the above compositions in complex field relationships.

VOLCANOLOGY OF POPOCATEPETL VOLCANO, MEXICO

SOLER-ARECHALDE, A.M. Instituto de Geofísica UNAM, D.Coyoacán 04510 D.F. Mexico and Martin-Del Pozzo, A.L., same address.

A historical revision was made of Popocatepet's activity since 1500 in order to verify the kind of activity and the eruption dates. Popocatepetl (19°01'N, 98°37'W) was formed over the old Nexpayantla volcano wich destruction produced a debris avalanche. Afterwards the Popocatepetl cone was formed by andesitic air fall pumice, ash flows, lapilli tephra and lava flows. The descriptions of activity at "Popo" previous to the Spanish Conquest speak only of ash and sand air falls. Diego de Ordaz in 1519 climbed the volcano and described ash fall, "burnt stones" and fire inside the crater. There is a report of ash fall in 1530 and in 1539 ash reached Huehotzingo, Cholula and Tlaxcala. Strong ash fall was described in 1633 and in 1665 ash fell in Puebla for four days. There were four ash fall eruptions from 1665 to 1720 (1664, 1667, 1697, 1720). The last activity period in 1920 was an eruption provoked by a dynamite explosion on the volcano to obtain sulphur. At present, "Popo" is in a fumarolic state. After reviewing the historical documents and scientific publications on Popocatepetl we undertook preliminary fieldwork. Complementary correlation techniques were used on some of the products.

THE GEOCHEMISTRY OF BASALTS AND MANTLE XENOLITHS FROM THE HANNOUBA REGION, EASTERN CHINA; IMPLICATIONS FOR THEIR PETROGENESIS AND THE COMPOSITION OF SUBCONTINENTAL MANTLE

Song, Y., Zhi, X. and Frey, F.A., Department of Earth, Atmospheric and Planetary Sciences, Mass. Inst. Tech., Cambridge, Ma., 02139, USA.

Northwest of Beijing there are large (~20,000km^2) plateaus of Cenozoic basalt. The Hannouba region, 200 km NW of Beijing, is important because of the intercalated tholeiitic and alkali basalt flows and the abundant mantle xenoliths in the alkalic basalts. The alkalic basalts range in MgO from 5.7 to 10.6%, and most of the compositional variations require segregation of a clinopyroxene-rich assemblage containing significant amounts of garnet and Fe-Ti oxides. Incompatible element abundances and isotopic ratios ($^{87}Sr/^{86}Sr$ = 0.70379 to 0.70399, $^{143}Nd/^{144}Nd$ = 0.51287 to 0.51298, $^{206}Pb/^{204}Pb$ = 17.78 to 17.92, $^{207}Pb/^{204}Pb$ = 15.46 to 15.52 and $^{208}Pb/^{204}Pb$ = 37.82 to 38.05) in these continental alkalic basalts overlap with those of oceanic island basalts; therefore, the mantle source of these continental and oceanic alkalic basalts was compositionally and isotopically similar.

In contrast, to the small isotopic range of the alkalic basalts, spinel peridotite xenoliths in these basalts are isotopically diverse; clinopyroxenes from six samples have Sr and Nd isotopic ratios ranging from near MORB-like to bulk earth estimates. Two samples with $^{143}Nd/^{144}Nd$ > 0.51348 have relatively high CaO and Al_2O_3 (1.8 to 2.7%), low Mg number ~90, and relative depletion in LREE. In contrast harzburgites have lower $^{143}Nd/^{144}Nd$, higher $^{87}Sr/^{86}Sr$ and relative enrichment in LREE. There is no simple genetic relationship of the alkalic basalts to these xenoliths. The isotopic diversity of mantle xenoliths relative to their host basalts is typical.

Relative to alkalic basalts, the tholeiitic basalts have lower abundances of incompatible elements, different incompatible element abundance ratios and a much wider isotopic range ($^{87}Sr/^{86}Sr$ = 0.70418 to 0.70479, $^{143}Nd/^{144}Nd$ = 0.51268 to 0.51283, $^{206}Pb/^{204}Pb$ = 17.10 to 17.56, $^{207}Pb/^{204}Pb$ = 15.36 to 15.47 and $^{208}Pb/^{204}Pb$ = 37.20 to 37.93). The isotopic ratios and incompatible element abundance trends defined by Hannouba lavas are consistent with mixing of isotopically and compositionally distinct components. The low $^{206}Pb/^{204}Pb$ ratios in the tholeiites and an inverse $^{87}Sr/^{86}Sr$ - $^{206}Pb/^{204}Pb$ trend are characteristic of other continental lavas. A possible explanation is a lower crustal component in the tholeiites. However, the $^{143}Nd/^{144}Nd$, Sm/Nd and $^{87}Sr/^{86}Sr$ ratios of Archean granulites in eastern China and granulites from other localities do not lie on the mixing trends defined by Hannouba lavas. The isotopic data of the tholeiites trend towards the EM-1 oceanic mantle component (Hart, 1988). We propose that melting within upwelling asthenosphere created the Hannouba alkalic lavas whereas the tholeiitic lavas resulted in large part from partial melting of continental lithosphere that was heated by the ascending asthenosphere.

STRUCTURE AND PETROLOGY OF THE CENOZOIC VOLCANICS OF THE BOLIVIAN LAKE TITICACA AREA.

SORIA-ESCALANTE, E.and BARREIRO, Barbara, Earth Sciences Dept., Dartmouth College, Hanover NH 03755

The Lake Titicaca (LT) volcanics are located in the NW end of the Altiplano domain, between the Eastern and Western Cordillera of the Central Andes of Peru-Bolivia. Detailed mapping of the volcanics in Bolivia provided evidence that volcanism was closely related to the tectonic evolution of the LT trough. The two main volcanic areas are:

The **Condor-Jipiña volcanics** (CJ) of Upper Miocene age, emplaced in the Tiquina Peninsula, covers app.150 km^2, overlies the "Puna" erosion paleosurface and Devonian sediments. The succession displays 2 phases of activity, from base to top: 1) Santiago pyroclastics: at least two units of poorly welded, crystal rich, andesitic to latitic ash-flow tuffs [sn-qz-bt-hb-cpx (aug)], interbedded with abundant breccia tuffs and mud- flows. This first phase ends with andesite lava flows [pl-hb-cpx(aug)-bt-qz]. 2) Condor-Jipiña composite volcano: basalt-andesitic to andesitic [pl-hb-cpx(aug)- bt-sn-qz] lava flows, tephra and mudflows. Several eruptive sites were controlled by a small subsidence caldera . This phase ends with the extrusion of the Torreni rhyodacitic, tuffaceous dome and flows.

The **Copacabana ash-flow tuffs** (CP), cover 50km^2 of Upper Paleozoic sediments in the western shore of LT (Copacabana peninsula). They consist of mildly welded, crystal rich [sn-qz-bt-hb] tuffs and breccias of rhyolitic composition, usually as extrusions of domes and plugs. A Plio-Qt age is tentatively assigned in basis of geomorphology.

Major elements geochemistry shows that both CJ and CP are silica saturated, high-K calcalkaline and shoshonitic (K2O/Na2O>1) suites, with strong peraluminous character (Al/K+Na+Ca=1.06 to 1.56). By comparing with published data from the E and W Cordillera volcanic arcs (n=250), LT volcanics appear highly enriched in Fe(T) and P2O5.

Preliminary Pb, Nd, Sr isotopic data revealed strong variations in isotopic ratios suggesting an isotopically heterogeneous magma source and a variable role of crustal contamination through time. Pb isotopic ratios between CP and CJ volcanics are significatively distinct despite of their geographical proximity. These variations suggest that CP magma suffered contamination from the 2 Ga. granulites of the Arequipa Massif.In contrast, the CJ volcanism seems to be emplaced over an area with no Arequipa Massif-like rocks. Both LT volcanics are interpreted as magma batches with variable degrees of crustal contamination moving upward through the NW-SE faulting system that controls the trough. New data of petrology,isotopes and K/Ar age determinations currently in progress, will provide additional information to define the geodynamic and petrologic evolution of the region.

PROTEROZOIC DYKE SWARMS IN MINNESOTA - A RECORD OF INTRAPLATE EXTENSION AND MAGMATISM BETWEEN 2150 AND 1100 MA.

SOUTHWICK, D.L., and CHANDLER, V.W., Minnesota Geological Survey, 2642 University Ave., St. Paul, MN 55114, USA

Although it has been known for many years that mafic dykes of several different orientations, ages, and compositional characteristics occur in the Precambrian terranes of Minnesota, the definitions and regional dimensions of discrete dyke swarms were not well established before the availability of a state-wide, high-resolution aeromagnetic survey. The following Proterozoic dyke swarms are now recognized.

1. Kenora-Kabetogama swarm (approx. 2125 Ma): Trends NW across varied Archean terranes in northwestern and west-central Minnesota and fans from trends of about 340° at its eastern edge to about 300° at its southwestern edge. The swarm is about 400 km long, and contains many hundreds to several thousands of dykes over a width in excess of 300 km. The frequency of dykes is greatest near the radial midpoint of the swarm, where geophysical modeling indicates that dyke material locally makes up about 25 percent of the shallow crust and some master dykes are as thick as 200 m. This is the largest Proterozoic dyke swarm in the USA.
2. Southwestern Minnesota swarm (approx. 1760 Ma): Trends WNW (az 290°) across varied Archean and Early Proterozoic terranes; intersects western part of Kenora-Kabetogama swarm. Contains many tens to a few hundreds of dykes within a poorly defined swarm width of about 100 km. Some dyke-related aeromagnetic anomalies are negative, and thus imply reversed polarity.
3. East-Central Minnesota swarm (age unknown but bracketed between 1770 and 1100 Ma): Trends ENE (az 080°) across Early Proterozoic terrane; consists of several very long and straight master dykes and an unknown number of short, thin dykes. This swarm has not been studied in detail.
4. Keweenawan swarm (about 1100 Ma): Trends NE (az 030°-060°) across a varied Precambrian terrane, parallel to the axis of the Midcontinent rift system. Most dykes are 75 km or less from the rift axis, and a great many of them are of reversed polarity, implying that they are an early manifestation of rift magmatism.

The Kenora-Kabetogama swarm records a dispersed style of crustal extension that was obscurely related to the development of the Early Proterozoic Penokean orogen. In contrast, the Keweenawan swarm records a more focused style of extension that led ultimately to the development of a narrow continental rift in the Middle Proterozoic. The Minnesota dyke swarms of intermediate age cannot be correlated with specific tectonic events.

This work was supported by the Minnesota Future Resources Commission of the Minnesota Legislature.

GEOCHEMISTRY AND Sr ISOTOPIC COMPOSITIONS OF POST-BANDELIER TUFF RHYOLITES, VALLES CALDERA, NEW MEXICO: EVIDENCE FOR MULTIPLE MAGMA SYSTEMS IN THE JEMEZ MOUNTAINS VOLCANIC FIELD

SPELL, T.L.*, KYLE, P.R., Dept. of Geosciences, New Mexico Tech, Socorro, New Mexico, and THIRWELL, M., Department of Geology, Royal Holloway & Bedford New College, Egham, U.K. *present address: Dept. of Geological Sciences, State Univ. of New York at Albany, Albany, New York, 12222.

The Jemez Mountains Volcanic Field in north-central New Mexico is a major site of Pleistocene silicic volcanism. Eruption of the upper Bandelier Tuff at ~1.12 Ma led to caldera collapse and formation of Valles Caldera. Post caldera volcanism has continued intermittently until ~0.15 Ma and has been entirely rhyolitic. These eruptives constitute the members of the Valles Rhyolite Formation which is dominated both volumetrically and temporally by the Valle Grande Member (VGM), ranging in age from ~1.12-0.45 Ma. Other members of the Valles Rhyolite Formation were erupted before (Deer Canyon, Redondo Creek) or after (VC-1 rhyolite, El Cajete, Battleship Rock, Banco Bonito) the VGM.

Rhyolites of the VGM are lithologically heterogeneous, ranging from aphyric obsidians characteristic of the oldest dome to coarsely porphyritic rocks (total phenocrysts ≈ 25-35%) characteristic of the younger domes. Typical phenocryst assemblages include sanidine (Or_{41-61}) + quartz + plagioclase (An_{7-20}) + biotite + hornblende + Fe-Ti oxides ± zircon ± allanite ± apatite ± clinopyroxene ± orthopyroxene. VGM rhyolites are high-silica (SiO_2 >75% anhydrous), high-K, and are depleted in Fe, Mg, Mn, Ti, and Ca. Although major element compositions are relatively constant, trace elements show well defined variations (increasing or decreasing 2-3 fold) with decreasing age. Whole rock chemistry, phenocryst chemistry, and isotopic dating indicate that VGM rhyolites can be divided into 2 main groups; group 1 ranging from ~1.12-0.71 Ma and group 2 from 0.55-0.51 Ma. Within the groups incompatible trace elements (e.g., Rb, Cs, Y, Nb, HREE, Ta) increase, whereas compatible elements (e.g., Sr, Ba, Zr, LREE, Eu) decrease. These changes in chemistry are consistent with Rayleigh fractionation models involving modal phenocryst phases. Group 1 rhyolites are characterized by variable $^{87}Sr/^{86}Sr_i$ values of 0.70544-0.71102 suggesting assimilation - fractional crystallization processes may have occured. In contrast, group 2 rhyolites are characterized by more uniform $^{87}Sr/^{86}Sr_i$ values of 0.70512-0.70553.

Limited geochemical data on rhyolites erupted prior to the VGM (Redondo Creek Member) suggest they may be parental to group 1 VGM magmas. Analyses of the younger members of the Valles Rhyolite Formation (VC1 rhyolite, El Cajete, Battleship Rock, Banco Bonito) show them to be chemically distinct from VGM rhyolites. These rocks are much less evolved, having low-silica (SiO_2 <75%), low-K, low abundances of incompatible trace elements, and high abundances of compatible trace elements (e.g., Sr ≈ 120-170 versus <45 for VGM rhyolites). They are also distinct isotopically, having lower $^{87}Sr/^{86}Sr_i$ values of 0.70464-0.70478.

These data suggest that rhyolites erupted in the Jemez Mountains since the formation of Valles Caldera at ~1.12 Ma are the products of at least 3 separate magmatic events and were not derived from one large long-lived magma chamber.

JURASSIC SILICIC VOLCANISM IN SOUTHERN PATAGONIA (47° 30′ S LATITUDE)

SRUOGA, P., Consejo Nacional de Investigaciones Cientificas y Tecnicas (CONICET), Secretaria de Mineria, Santa Fe 1548, Piso 12, Capital Federal, 1060, Republica Argentina

Ignimbrites of the Deseado Massif, known as Bahia Laura Group, represent local expression of a vast silicic extension-related volcanism that erupted during Middle Jurassic times (160 m.y.) in the southwestern margin of Gondwanaland.

Outcrops of these units are recognized in extra-Andean Patagonia (Somuncura and Deseado Massives), Patagonian Chilean-Argentinian Cordillera, Tierra del Fuego and Antartida, covering an estimated area of 1,000,000 km^2 including subsurface and continental-platform equivalent units.

Jurassic volcanics at 47° 30′ S latitude are remarkably homogeneous in composition. This persistent ignimbritic type eruptive event includes a monotonous pile of volcaniclastic products (ash-flow tuffs, air-fall tuffs, breccias, lacustrine epiclastic sediments), minor interbeddeddacitic and andesitic lava flows, and final rhyolitic domes.

Crystal-poor ignimbrites contain sanidine sodic plagioclase, quartz, and minor biotite, titanomagnetite, ilmenite, zircon, apatite, and monacite. Dacites and andesites contain an intermediate to calcic plagioclase as the main phenocryst accompanied by altered amphibole, titanomagnetite, and apatite.

They appear to have equilibrated at shallow depth, under low temperatures (~800°C) and relatively high fO_2 conditions, in high-level magma chambers,though evidence for caldera forming eruptions is insufficient.

The ignimbrites are high-silica, potassium-rich, slightly peraluminous rhyolites. They are enriched in incompatible elements and depleted in feldspar-controlled trace elements (Sr, Ba, Eu^{+2}). Typical values for a 77o/o SiO_2 ignimbrite are: K_2O/Na_2O=1.34, FeO^t/MgO=12.78, CaO=0.44o/o, Rb=236 ppm, Sr=23 ppm, Ba=273 ppm, U=6 ppm, Th-29 ppm, Ta=1 ppm, Sc=4.69 ppm, Hf=5.42 ppm, REE=162 ppm, Ba/La=6.41, La/Yb=8.52, Eu/Eu =0.29.

The geochemical comparison between the coastal area of Puerto Deseado and the Andean region of Sierra Colorada shows some minor but important differences that reflect the influence in source of subduction-related magmatism westwards, located presumably in present Chilean coast where Jurassic plutonics have been recognized recently.

Although poorly studied, the Andean Jurassic volcanic units show variations in composition along its strike, being the segment considered here the most acidic, suggesting a particular geodynamic configuration far yet from being understood.

DERIVATION OF AXIS COEFFICIENTS FOR PEARCE ELEMENT RATIO DIAGRAMS

C.R. STANLEY, Dept. of Geology and Geophysics, University of Calgary, Calgary, Alberta, T2N 1N4, and
J.K. RUSSELL, Dept. of Geological Sciences, University of British Columbia, Vancouver, B.C., V6T 2B4

In igneous petrology, Pearce element ratio (PER) diagrams have been used : i) to determine whether members of a rock suite are co-genetic, ii) to identify the minerals involved in differentiation processes, and iii) to evaluate the extent of fractional vs. equilibrium crystallization. The approach required to test these and other hypotheses with PER diagrams has recently been summarized by Nicholls (1988) and Russell and Nicholls (1988) [Contribs. Miner. Petr., Vol. 99]. In order to effectively test specific petrologic hypotheses, axis coefficients for the PER diagrams are determined so that trends defined by rock compositions can be easily interpreted in terms of specific minerals. For example, a PER diagram with abcissa; Si/K and ordinate; 0.5(Mg+Fe)/K can be used to monitor the effects of accumulation or loss of a variety of silicate minerals (Figure below). In this diagram, olivine separation causes trends with slopes of 1.0 while orthopyroxene controlled trends have slopes of 0.5.

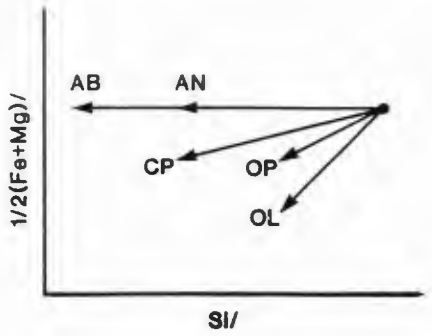

Unfortunately, selection of the optimal combination of axis coefficients is a non-trivial task, especially where the system being investigated has a large number of phases or complicated mineral solid solution . Our work has established a formal set of rules and matrix operations which facilitate the determination of PER diagram axis coefficients. These rules and operations can be used to i) determine the vector displacements associated with the addition or subtraction of a mole of a specific mineral, given a set of axis coefficients; or ii) to determine axis coefficients which produce unique vector displacements for specific minerals. Using the second procedure, two types of PER diagrams can be designed. By designating all vector displacements to be parallel, the axis coefficients for ***Hypothesis Test Diagrams*** can be determined to test whether the addition or removal of a specific set of phases to or from a system can explain the observed 1compositional variations. Alternatively, by desig-nating all mineral vector displacements to be mutually perpendicular, axis coefficients can be calculated for ***Discrimination Diagrams***. Discrimination diagrams can test whether the observed chemical variations ***require*** that a specific phase be involved and can be used to estimate the extent of that involvement. The combination of Hypothesis Test and Discrimination Diagrams provide a means to test most petrologic hypotheses.

LOWER PROTEROZOIC VOLCANISM IN THE TRANS-HUDSON OROGEN, CENTRAL CANADA

Mel R. STAUFFER, Department Geological Sciences, University of Saskatchewan, Saskatoon, Canada, S7N 0W0

Although unrecognized until less than a decade ago, the Trans-Hudson orogen in the Churchill Province of the Canadian Shield is a belt of metamorphosed and deformed rocks on the scale of the North American Cordillera. This orogen is composed of thick sequences of metavolcanic and metasedimentary rocks along with a large number of intrusive bodies, one of which, the Wathaman batholith, is the largest known Precambrian batholith.

Volcanic rocks occur primarily in two belts within the juvenile portion (Reindeer Lake Zone) of the orogen: the Flin Flon domain and the La Ronge domain, separated by over 200 km of predominantly metasedimentary gneisses.

Recent U-Pb dating of zircons by several workers indicates that volcanism in these two domains was more-or-less coeval and took place during the time span between 1910-1870 Ma, but may have begun earlier. Major and trace-element geochemical studies indicate that volcanism probably took place in subduction-related, volcanic arcs of both oceanic and continental environments. Nd isotopic data suggest that the volcanic magma was derived from the mantle at about 1900 Ma.

In some of the less-deformed parts of these two volcanic belts, especially in the Flin Flon domain, numerous primary volcanic structures are well-preserved, including: pillow lavas, massive flows, flow breccias, pillow breccias, hydroclastites, columnar jointing, ropy structure, crystal-settling zonation, a variety of vesicle (amygdule) arrangements, laminated tuffs, tuff breccias, welded tuffs, pumice-bearing pyroclastic flows, and primary deformational features such as flow rolls, rip-up clasts, and load casting.

In the Flin Flon domain there is a sequence of at least 10 km of subaqueous flows locally overlain by over 2 km of subaerial material. Here also, a number of volcanic-event stories can be deduced, ranging from individual flow and cooling histories to dome and blast sequences that occur in rhyolitic parts of the volcanic pile.

FLUID MECHANISM OF PRESSURE GROWTH IN VOLCANIC (MAGMATIC) SYSTEMS

STEINBERG A.S. and MERZHANOV A.G., Institute of Structural Macrokinetics, Academy of Sciences of the USSR, Chernogolovka, 142432. USSR,

STEINBERG G.S., Institute of Marine Geology and Geophysics, Far Eastern Branch of the Academy of Sciences of the USSR, Yuzhno-Sakhalinsk 693002, USSR

A mechanism of pressure rising in a closed system with constant volume (isochorous system) saturated with volatiles is considered.

It is shown that rising of gas bubbles in such a system to a height is accompanied by pressure rising to $\Delta P = \rho gh$ value (ρ -magma density; g - the acceleration to gravity). Analysis of values for isothermic processes without mass exchange between rising gas and magma is made. It has been shown that poorly dissolved gases (CO_2, N_2 etc.) can play an important role in raising pressure in the system and initiating eruption.

FLUID MECHANISM OF PRESSURE GROWTH AND SEISMIC REGIME OF VOLCANOES BEFORE ERUPTIONS

STEINBERG G.S., Institute of Marine Geology and Geophysics, Far Eastern Branch of the Academy of Sciences of the USSR, Yuzhno-Sakhalinsk 693002, USSR,

STEINBERG A.S., MERZHANOV A.G., Institute of Structural Macrokinetics, Academy of Sciences of the USSR, Chernogolovka, 142432, USSR

Variation of seismic regime of volcanoes before eruptions is treated based on fluid mechanism of pressure growth. Pressure growth in a volcanic conduit before an eruption is associated with rise of gas bubbles during degassing of magma. Relations have been derived that describe pressure change into the stage of preparation of an eruption. It is shown that accumulation of conditional deformations ε is in a linear relation with relationship U that describes gas bubble rise velocity: $\varepsilon = k(U-1)$, where k is ratio coefficient. This relationship approximates better than the exponential and hyperbolic relationships used before. It seems suitable to approximate accumulation of conditional deformations by means of the proposed function since it reflects a theoretically proved and experimentally supported mechanism of pressure growth during degassing under conditions of a closed isochoric system.

Estimation of increase in number of earthquakes before an eruption based on the proposed mechanism yields a good agreement with the observed one.

TRACE-ELEMENT AND Sr, Nd, and Pb ISOTOPIC COMPOSITION OF PLIOCENE AND QUATERNARY ALKALI BASALTS OF THE PATAGONIAN PLATEAU LAVAS OF SOUTHERNMOST SOUTH AMERICA

STERN, C.R., Department of Geological Sciences, University of Colorado, Boulder, Colorado 80309 USA

FREY, F.A., Department of Earth, Atmosphere & Planetary Sciences, Massachusetts Institute of Technology, Cambridge, Massachusetts 02139 USA

FUTA, K., and ZARTMAN, R.E., Isotope Branch, United States Geological Survey, Denver Federal Center MS963, Denver, Colorado 80255 USA.

The Pliocene and Quaternary Patagonian plateau alkali basalts of southernmost South America can be divided into two groups. The "cratonic" group, erupted in areas of Cenozoic plateau volcanism and continental sedimentation, shows considerable isotopic variation, with $^{87}Sr/^{86}Sr$ = 0.70316 to 0.70512, $^{143}Nd/^{144}Nd$ = 0.51292 to 0.51264, and $^{206}Pb/^{204}Pb$, $^{207}Pb/^{204}Pb$ and $^{208}Pb/^{204}Pb$ = 18.26 to 19.38, 15.53 to 15.68, and 38.30 to 39.23 respectively. These values are within the range of oceanic island basalts, as are the Ba/La, Ba/Nb, La/Nb, K/Rb, and Cs/Rb of the "cratonic" plateau basalts In contrast, the "transitional" group of alkali basalts, erupted along the western edge of the outcrop belt of the Pliocene and Quaternary plateau lavas in areas that were the locus of earlier Andean orogenic arc volcanism, have a much more restricted range of isotopic composition, given approximately by $^{87}Sr/^{86}Sr$ = 0.7039, $^{143}Nd/^{144}Nd$ = 0.51284, $^{206}Pb/^{204}Pb$ = 18.60, $^{207}Pb/^{204}Pb$ = 15.60, and $^{208}Pb/^{204}Pb$ = 38.50, which is very similar to the isotopic composition of Andean orogenic basalts from the southern Andes. Also in contrast to the "cratonic" group, both the "transitional" and Andean orogenic basalts are displaced to high $^{87}Sr/^{86}Sr$ at a given $^{143}Nd/^{144}Nd$ and to high $^{207}Pb/^{204}Pb$ at a given $^{208}Pb/^{204}Pb$. The "transitional" alkali basalts have Ba/La, Ba/Nb, La/Nb, and Cs/Rb higher than the "cratonic" and oceanic island alkali basalts, although not as high as Andean orogenic arc basalts.

The trace element and isotopic data suggest that the "cratonic" alkali plateau basalts do not contain the subducted slab-derived components that impart the high Ba/La, Ba/Nb, La/Nb, Cs/Rb, $^{87}Sr/^{86}Sr$ at a given $^{143}Nd/^{144}Nd$, and $^{207}Pb/^{204}Pb$ at a given $^{208}Pb/^{204}Pb$ to Andean arc basalts. Instead these basalts formed by relatively low degrees of partial melting of heterogeneous lower continental lithosphere and/or asthenosphere, probably due to thermal and mechanical pertubation of the mantle in responce to subduction of oceanic lithosphere below the western margin of the continent. The"transitional" alkali basalts do contain components added to their source region by either (1) input of smaller amounts of slab derived volatile rich fluids than below the arc and/or input of fluids with lower Ba/La, Ba/Nb, La/Nb, and Cs/Rb than below the arc due to progressive downdip dehydration of the subducted slab, or (2) previously active subarc source region contamination processes, which affected the mantle source of the "transitional" alkali plateau basalts earlier in the Cenozoic.

Thus, decreasing degree of partial melting in association with lessened significance of slab-derived components, and presumably volatiles, is a fundamental factor in the change from arc to back-arc volcanism in southern South America.

THE EMPLACEMENT HISTORY AND VISCOSITY OF TWO RHYOLITES

Richard J. Stevenson. Department of Earth Sciences, University of Waikato, Private Bag, Hamilton, New Zealand.

In New Zealand, rhyolite lavas have not been observed to erupt in historical times. However, the measurement of fabric parameters from lava flow unit profiles provides an insight into the physical properties and emplacement history of rhyolite lavas.

Two contrasting Cenozoic rhyolites from the North Island, New Zealand, were examined: a calc-alkaline rhyolite obsidian flow (~100ka age, 3 km length) from Ben Lomond, Taupo Volcanic Centre; and a pantelleritic flow sequence of Quaternary age from Mayor Island.

Generally, the lava flow stratigraphy comprises: a finely vesicular pumice carapace; upper obsidian; central devitrified rhyolite; basal obsidian and/or basal breccia. The Ben Lomond lavas include a pumiceous explosion breccia that occurs both above the central rhyolite core and cross-cuts the upper two fabric units. Extensive secondary spherulitisation occurs in the upper obsidian layer of the Ben Lomond flow, particularly above the central rhyolite core and below the pumiceous explosion breccia pod.

In contrast, Mayor Island lavas have no explosion breccia and no significant secondary lithophysae within the upper obsidian layer, indicating a contrasting emplacement history.

Fabric profile measurements include density, proportions of primary and secondary voids, microlite size, void and autoclast aspect ratios.

The porosity profile provides information on the distribution of volatiles in the emplacing lava and the spherulites, on post emplacement volatile migration also shown by trace element profiles (particularly Sr,Y,Rb).

From this data, together with petrographic and field structural observations, an emplacement history for both rhyolites is presented.

Major element chemistry, estimates of flow temperature and volatile proportion may be used to calculate emplacement viscosity. Pantelleritic lavas have significantly lower viscosity ($\eta=10^7$-10^8poise) and were emplaced from a spatter fed hawaiian-type eruptive column. In contrast the Ben Lomond calc-alkaline lava was emplaced as a deflated foam ($\eta=10^{10}$ poise, flow centre) forming lobate flows.

PETROLOGY OF LAVAS AND TEPHRAS FROM EGMONT VOLCANO, NORTH ISLAND, NEW ZEALAND

STEWART, R.B., Department of Soil Science, Massey University, Palmerston North, New Zealand

Egmont Volcano is a medium to high-K andesite stratovolcano located on the western margin of North Island. The typically porphyritic lavas contain xenocrysts and glomerocrysts (cumulates) which reflect the multi-stage evolution of the Egmont eruptives. The xenocryst assemblage comprises plagioclase, clinopyroxene, titanomagnetite, amphibole, olivine and rare orthopyroxene and biotite. Large Mg-rich olivines in one group of lavas contain Cr-spinels and are the only high Cr phases found so far in otherwise predominantly low Cr lavas.

The cumulate clots comprise:

cpx + tm ± pl ± ol
cpx + pl + tm + opx
cpx + pl + tm + amph ± ol

where cpx = clinopyroxene, opx = orthopyroxene, amph = amphibole, ol = olivine, pl = plagioclase and tm = titanomagnetite.

Amphibole in Egmont lavas is a reddish-brown magnesiohastingsitic hornblende, often resorbed or exhibiting opacite rims. It contrasts with the olive-green pargasitic hornblende of the tephras, the difference reflecting changes in P_{H_2O} during an eruption. Pumiceous eruptives contain up to 4.5% H_2O, which stabilizes amphibole, in contrast to the <2% H_2O in the degassed lavas where amphibole is breaking down.

Late stage phases include plagioclase, a second generation of titanomagnetite accompanied by rare ilmenite, orthopyroxene, clinopyroxene and olivine. Some acicular, more Fe-rich orthopyroxene appears to coexist with cristobalite/tridymite in vesicles in lavas, indicating probable post-extrusion crystallization. Temperature estimates from crystal chemistry indicate minimum temperatures of 1000°C for xenocryst phases while rare titanomagnetite-ilmenite pairs from late-stage crystallization indicate temperatures of about 850°C.

The evidence from crystal chemistry thus far demonstrates the complex history of Egmont Volcano, with crystallization occurring over a range of temperatures, water contents and depths. The resultant lavas and tephras are therefore hybrids and any bulk rock chemistry will reflect this derivation from heterogeneous sources.

DISRUPTION OF SILICIC MELT STRUCTURE BETWEEN THE TWO BANDELIER CALDERA-FORMING ERUPTIONS, NEW MEXICO, USA

STIX, J., and GORTON, M.P., Department of Geology, University of Toronto, Toronto M5S 1A1, Canada

The Cerro Toledo Rhyolite is a group of high silica rhyolite domes and tephras which was erupted during the time between the Lower Bandelier Tuff (LBT) at 1.45 Ma and Upper Bandelier Tuff (UBT) at 1.12 Ma. Due to the exceptionally good time-stratigraphic control on the Cerro Toledo Rhyolite tephra sequence, the tephras allow us to track the evolution of silicic magma over a period of 0.33 Ma between the two caldera-forming eruptions. The Cerro Toledo Rhyolite tephras represent the changing composition of the most fractionated liquids at the top of the magma chamber due to crystallization during this 0.33 Ma period. Three independent estimates, based on major and trace element modelling, indicate 70% crystallization (mainly sanidine and quartz) during this time. Highly incompatible elements such as Cs generally increase in concentration upsection through the tephra sequence, whereas elements such as Zr and LREE exhibit different behavior. Zr steps down upsection from 312 ppm at the base of the tephra sequence to 134-178 ppm in the bulk of the tephras. Zr then increases abruptly upward to 320 ppm in the most evolved Cerro Toledo Rhyolites. The Hf/Cs ratio initially declines upsection, then becomes nearly constant. The dramatic rise in Zr to 320 ppm, coupled with the nearly constant Hf/Cs ratio, suggests that zircon crystallization was suppressed with time. LREE show broadly similar relations, except that the La/Cs ratio continually declines upsection through the Cerro Toledo Rhyolite tephras. This implies that a LREE-rich accessory mineral (allanite and/or chevkinite) continued to crystallize, but at a progressively slower rate.

We have examined three parameters - temperature, bulk composition, and volatile content of the magma - which may have controlled the crystallization behavior of zircon and the LREE-rich phase(s). Changes in temperature cannot account for many of the observed Zr, Hf, and LREE trends. However, the dramatic increase in these trace elements in the most evolved Cerro Toledo Rhyolites and basal UBT plinian tephras is accompanied by a similar increase in iron and halogen contents. If changes in halogen contents are indicative of changes in overall volatile levels at the top of the magma chamber, the increase in volatiles and iron may have disrupted the structural state of the magma, increased the solubilities of zircon and the LREE-rich phase(s), and raised the saturation levels of Zr and LREE. Disruption of the melt structure may have resulted from (1) Fe as a network modifier or quasi-molecular complex, (2) formation of non-bridging oxygens, and (3) complexing of Al and alkalies by OH, F, and/or Cl.

RELATIONSHIP BETWEEN MAGMATIC AND HYDROTHERMAL PROCESSES IN THE SUMMITVILLE, COLORADO GOLD DEPOSIT

STOFFREGEN, ROGER E., Dept. of Geol. Sciences, S.M.U., Dallas, Texas, 75275, RYE, ROBERT O., M.S. 963, U.S. Geological Survey, Denver, Colorado, 80225, and BETHKE, PHILIP M., M.S. 959, U.S. Geological Survey, Reston, Virginia, 22092.

The Summitville gold deposit is an excellent example of a mixed magmatic-meteoric hydrothermal ore deposit in a relatively near surface (<1 km) environment. Summitville is located on the margin of the Platoro-Summitville Caldera complex and occurs within the South Mountain quartz latite porphyry. Intense acid-leaching along fractures in the quartz latite has produced irregular pipes and lenticular pods of vuggy silica which are developed vertically over 300 m and reach thicknesses of up to 70 m. The vuggy silica is enclosed sequentially by alteration zones of quartz-alunite, quartz-kaolinite and clay. Gold mineralization formed primarily within the vuggy silica subsequent to the acid-sulfate alteration and was accompanied by covellite, enargite, and luzonite along with minor kaolinite.

The $\delta^{34}S$ values of alunite range from 18.2 to 24.5‰, while those of coexisting pyrite range from -8.1 to -2.2‰. The sulfur isotope systematics indicate that the sulfate was derived from the disproportionation of magmatically derived SO_2. If $\delta^{34}S_{\Sigma S} = 0$‰ and if the system was in both isotopic and chemical equilibrium, the sulfate and sulfide $\delta^{34}S$ values indicate redox conditions slightly below the H_2S/SO_4 boundary. The $\delta^{18}O$ values of sulfate in alunite range from 10.5 to 16.3‰, and correlate with δD values which range from -70 to -38‰. These data indicate that the disproportionation of the SO_2 occurred in fluids which ranged from nearly purely magmatic water to mixtures of magmatic and meteoric water. The $\delta^{18}O$ of surrounding kaolinites range from 5.3 to 12.3‰ and correlate with δD values of -81 to -103‰. These data indicate that the aggressive acid-leaching in the core of the alteration zones was produced by fluids of predominanly magmatic origin and that the kaolinite formed in the outer zone where the magmatic waters were progressively diluted with meteoric water.

The $\Delta^{34}S$ values between coexisting alunite and pyrite range from about 25 to 30‰, indicating depositional temperatures of about 250° to 200°C. These temperatures are consistent with filling temperatures of secondary fluid inclusions in quartz phenocrysts from the vuggy silica and quartz-alunite zones. $\delta^{18}O$ values of quartz in the vuggy silica and quartz-alunite zones range from 11.0 to 15.0‰ and generally increase with elevation, indicating a general decrease in temperature at higher levels of the deposit for a given zone of alteration.

The ore assemblage of sulfides + kaolinite occurs in voids or in veinlets crosscutting the vuggy silica alteration. δD values for these kaolinites are -98 to -122‰ and $\delta^{18}O$ values are 7.3 to 9.7‰. These data suggest that exchanged meteoric water was dominant during ore deposition, in contrast to the earlier magmatic water dominant acid-leaching event. However, the H_2S/SO_4 ratio of the system appears to have remained relatively constant between the two stages, as evidenced by $\delta^{34}S$ values for ore stage sulfides that are similar to those for pyrite from the acid-leaching stage. Relatively low pH conditions were apparently maintained during ore deposition, as indicated by the presence of kaolinite, but not sericite, in the ore sulfide assemblage.

The paragenesis and stable isotope data from the deposit thus indicate an early acid-leaching stage dominated by magmatic H_2O, H_2S and SO_2, and a later ore stage dominated by exchanged meteoric H_2O but by the same magmatically derived sulfur species. The early magmatic components are believed to have been introduced in a vapor plume that rose to the upper portions of the volcanic edifice. This vapor plume condensed near its interface with meteoric water to produce highly acid sulfur-rich but metal-poor fluids responsible for acid-sulfate alteration. Although details of the ore forming system are poorly understood, it is thought to have resulted from the collapse of the vapor plume and consequent replacement of the vapor by a mixed magmatic-meteoric water system that became progressively more meteoric dominated.

EXPERIMENTAL AND ANALYTICAL CONSTRAINTS ON THE DEGASSING OF BASALTIC AND RHYOLITIC MAGMAS

STOLPER, E., Div. Geol. Planet. Sci., Caltech, Pasadena, California, 91125, USA

I will report on the results of experiments conducted by me and my colleagues to determine (1) the solubilities of CO_2 and H_2O in basaltic and rhyolitic melts at pressures up to several kilobars; (2) the speciation of CO_2 and H_2O in glasses quenched from basaltic and rhyolitic melts; (3) isotopic fractionations between vapor and C- and H-bearing species in rhyolitic melts; and (4) the diffusivities of C- and H-bearing species in rhyolitic melts and glasses.

These experimental results will be compared with results of analyses of the concentrations and isotopic compositions of water and carbon dioxide in volcanic glasses from a variety of settings to set constraints on the behavior of volatiles in high-level magmatic systems. Some important conclusions include: (1) Dissolved CO_2 and H_2O in obsidian from pyroclastic rocks and lava flows from the ca. 1340 A.D. eruption of the Mono Craters, CA, generally decreased as the eruption proceeded. Results for obsidian clasts from the pyroclastic deposits suggest that the parent magma was relatively rich in CO_2 (perhaps from degassing of basaltic magmas underplating the silicic magmatic system) and that degassing during this early phase of the eruptive sequence approached closed system behavior. Hydrogen isotopic data suggest a transition to open system degassing late in the eruptive sequence, perhaps coinciding with a transition from explosive to quiescent eruptions. (2) Analyses of glass inclusions from phenocrysts from the plinian and ash-flow deposits of the Bishop Tuff, CA, indicate that H_2O was enriched and CO_2 was depleted upwards in the preeruptive magma. This is most easily understood if the magma was saturated with a CO_2-H_2O vapor throughout. Crystallization of a vapor-saturated parent liquid similar to the ash-flow inclusions would generate residual liquids enriched in H_2O and depleted in CO_2 similar to the plinian inclusions. Assuming vapor saturation, pressures of entrapment of the inclusions are typically 1.5-2.5 kbar. (3) Submarine basaltic glasses are often supersaturated with respect to CO_2 at their eruption depths, suggesting that magma transport from depth can be so rapid that degassing is incomplete and kinetically limited. In such cases, vesicle gases may be enriched preferentially in rapidly diffusing components (e.g., light rare gases) and concentration profiles in slower diffusing components (e.g., water and CO_2) are to be expected adjacent to vesicles and may be used to set constraints on time scales of magma ascent.

MAGMATISM FROM AN ARC-CONTINENT COLLISION ZONE: VOLCANIC ROCKS FROM THE FLORES-LEMBATA ARC SECTOR, SUNDA ARC, INDONESIA.

STOLZ, A.J., Geology Department, University of Tasmania, G.P.O. Box 252C, Hobart, Tasmania 7001, Australia.
VARNE, R., Geology Department, University of Tasmania, G.P.O. Box 252C, Hobart, Tasmania 7001, Australia.
DAVIES, G.R., Department of Earth Sciences, The University of Leeds, LS2 9JT, United Kingdom.
WHELLER, G.E., CSIRO Division of Exploration Geoscience, P.O. Box 136, North Ryde, NSW 2113, Australia.
FODEN, J.D., Department of Geology, University of Adelaide, Adelaide, SA 5000, Australia.

Twelve active or recently active volcanoes on the Indonesian islands of Flores, Adonara, Lembata and Batu Tara in the eastern Sunda arc, are built of volcanic materials ranging in composition from low-K tholeiite, through medium- and high-K calcalkaline types to K-rich leucite basanite. Compared with MORB and OIB, all Flores-Lembata rocks have low contents of TiO_2 and Nb (HFSE), and high Ba/Nb, La/Nb and Ba/La values. The transition from tholeiites poor in K, Rb, Ba, and Sr (LILE) to LILE-rich leucititic varieties is also marked by increasing Nb and LREE contents. The rocks exhibit a broad range of $^{87}Sr/^{86}Sr$ (0.70468-0.70706) and $^{143}Nd/^{144}Nd$ (0.512946-0.512447) values, and a moderate range of $^{206}Pb/^{204}Pb$ (18.825-19.143), $^{207}Pb/^{204}Pb$ (15.643-15.760) and $^{208}Pb/^{204}Pb$ (38.67-39.51) values.

As would be anticipated from the tectonic setting, these trace element and isotopic data suggest that volcanic source materials beneath this part of the Sunda arc may be a mixture of four or five main components: MORB- source or depleted MORB- source mantle, OIB- source mantle, old-enriched subcontinental lithosphere, and perhaps subducted Indian Ocean sediments. The low-K tholeiites could have been formed by relatively small degrees of partial melting of MORB- source mantle which has been modified by subduction-related fluids, but the K-rich volcanics have trace element and isotopic characteristics which indicate the involvement of subcontinental lithosphere in their source regions, rather than subducted sediment or slab-derived fluid/melt. The source components of the calcalkaline rocks are more difficult to distinguish; they may include MORB- and OIB-source mantles, and a melt/fluid derived from subcontinental lithosphere or subducted sediment.

It is difficult to reconcile the minor and trace element data with popular models which derive all mafic arc volcanics, from K-poor to K-rich, from depleted MORB-source mantle that has been later enriched in LILE. However, the modelling of arc volcanics as melts of OIB-source mantle requires that HFSE in primary arc magmas are somehow buffered to relatively low concentrations, perhaps by a residual Ti-rich phase.

GIANT HOLOCENE DEBRIS AVALANCHE FROM VOLCAN COLIMA, MEXICO

STOOPES, G. R., and SHERIDAN, M.F., Dept. of Geology Arizona State University Tempe, AZ. 85287

New field work has added information about the distribution, character, and mode of emplacement of the large Holocene volcanic debris avalanche from Volcan Colima. This new information is essential for hazard assessment of Volcan Colima, one of the most active and potentially dangerous volcanoes in North America.

4,300 years ago, sector collaspe of a postulated 4000 m high ancestral andesitic cone produced a caldera that is now mostly buried by the present Volcan Colima. The huge debris avalanche deposit from this event covers an area greater than 2,000 km^2 with an estimated average thickness of 10-15 m, yielding a volume between 20-30 km^3. The avalanche first filled proximal topography and then flowed down two drainages: the Rio Salado to the south and the Rio Naranjo to the southeast. The avalanche ponded momentarily where these two drainages meet 80 km south of the old volcano. Here it surmounted a 80 m topographic barrier and rushed westward through a gap in the surrounding hills near the pueblo of San Miguel, and also continued down the main drainage to the southwest. The two avalanche lobes then converged to the south and entered the ocean along a 20 km swath, over 100 km from the source. Hummocks 20 m high are evident 3 km from present ocean shore. The debris avalanche also moved down the Rio Armeria drainage to the southwest, but here it only traveled 30-40 km down drainage and did not reach the ocean.

The debris avalanche has hummocky topography, closed depressions, and a boulder strewn surface. Abundant charcoal from incorporated trees at one location will be used to confirm the date of the event. The avalanche consists of brecciated and pulverized andesitic clasts and broken up, but more or less coherent blocks from the old mountain that are suspended in the pulverized matrix. Both block facies and mixed facies are common in outcrops. Vesiculated andesitic material is present in the avalanche and probably represents juvenile material. Meter-size andesite boulders exhibiting breadcrust texture occur in the avalanche at distal locations. Limestone and red sandstone clasts ripped up from the underlying bedrock are also incorporated, even in very distal locations, indicating the powerful and turbulent nature of the avalanche.

There is a difference in morphology between the eastern and western portions of the avalanche deposit near the present cone. The western portion consists of large, steep hummocks and coherent debris avalanche blocks that may represent discrete slabs that moved only a short distance. In contrast, the smaller, rounder hummocks toward the south and southeast probably resulted from movement of a more disaggregated avalanche. This is consistent with the increased travel distance down the southeastern drainages.

Portions of the debris avalanche near the old caldera are covered by lava flows and pyroclastic material from the new cone. Where exposed, the surface of the avalanche has a 0.5-1 m soil. Near the city of Colima (32 km south of the present cone) and directly to the east, the avalanche is overlain by a younger lahar which has smoothed out the hummocky topography. To the west and south of Colima the avalanche is covered by a thick (5-25 m) layer of reworked avalanche material that also forms terraces and chokes the Rio Armeria drainage. This deposit masks any evidence of lahars or other deposits. Only in a few locations close to the present cone is the base of the avalanche evident, where pyroclastic flow, surge, and ashfall deposits underlie the avalanche in places; at greater distances lahars or bedrock underlie the avalanche.

The debris avalanche from Volcan Colima traveled over100 km before entering the ocean near the town of Cerro de Ortega. The great mobility of the avalanche results in an extremely low H/L ratio (0.04). Topography around a cone greatly influences the distribution of avalanche material. Volcanoes like Colima, with relief of 3000 m or more, have an increased probability for highly mobile avalanches. These are all important parameters for hazard evaluation of Volcan Colima.

PETROLOGICAL COMPARISON OF AXIS TO FLANK VOLCANISM IN THE NORTHERN RIO GRANDE RIFT, NEW MEXICO AND COLORADO, U.S.A.

STORMER, J. C., Jr., Geology & Geophysics, Rice University, POB 1892, Houston TX 77251, and DUNGAN, M. A., Department of Geological Sciences, Southern Methodist University, Dallas TX 75275

Magmas from the flanks of this rift have been known to be generally more alkalic than those from the axis. However, recent studies show that several similar magma suites developed simultaneously in the Taos Plateau volcanic field (TPVF), within the rift, as well as in the Ocate volcanic field (OVF), on the immediate flank, and Raton-Clayton volcanic field (RCVF), 100-200 km east of the rift axis.

The earliest volcanic products of both the TPVF and RCVF are porphyritic hornblende (±biotite) bearing dacite domes (8-10 Ma). The trace element characteristics of these magmas are consistent with melting of a lower crustal source with garnet in the residuum, probably by mafic magma injection during the inception of this cycle of magmatism. They cannot have been produced by differentiation of any mafic magma in these volcanic fields. In contrast, the monolithologic andesitic and dacitic shields which accompany later basalts in all three fields show evidence for complex AFC processes with the basalts as one endmember. Although the silicic assimilant in the AFC process appears to be be similar in composition to the early porphyritic dacites, the hydrous mineralogy is unique to the early dacites.

The most voluminous and least alkalic magmas in all three fields are basalts with distinctive ophitic-diktytaxitic textures. These are essentially contemporaneous in the interval 2-4.5 Ma. In the TPVF these basalts are distinctly lower in alkali and incompatible trace elements (i.t.e.'s) than the equivalent rocks of the other fields. The TPVF basalts also show a strong positive correlation between SiO_2 (49-54%), alkalies, and i.t.e's as the result of mixing with AFC-derived andesitic magmas. The OVF and RCVF diktytaxitic basalts cluster near 49% SiO_2, and do not show evidence for extensive crustal mixing. The higher i.t.e. abundances in the OVF and RCVF in comparison to the TPVF may be the result of variable partial melting of a similar mantle source, with the flank experiencing a lower percentage of melting.

Alkali olivine basalts are absent from the TPVF but are dominant components of the early OVF and RCVF. They have higher trace element abundances but similar patterns to the diktytaxitic basalts. Basanite and nephelinite with distinctive mineralogy and extreme composition,were erupted only in the later stages (~2 Ma) of the RCVF (distal flank).

The youngest rocks in all three fields are monogenetic cones of trachybasalt and basaltic trachyandesite. These often contain xenocrysts of probable crustal origin, and appear to have been generated by complex AFC processes operating on mildly alkalic parental basalts. The production of these magmas continued longer on the flanks (RCVF<10 Ka, OVF<0.8 Ma) than the axis (TPVF<1.8 Ma).

These petrological observations suggest extensive interaction between basalt magma and the lower crust throughout a period 0-10Ma both in the rift axis and on the flanks. Volcanism within the rift was concentrated in the middle of the cycle and generally less alkalic. This may be a function of prior, mid-Cenozoic volcanism and higher magma production rates in the rift. However, the available sources and magmatic processes must have been similar throughout.

FRACTIONATION AND CONTAMINATION PROCESSES, CRATERS OF THE MOON LAVA FIELD, IDAHO, 2000-2500 YEARS BP

STOUT, M.Z., Dept. of Geology and Geophysics, University of Calgary, Calgary, Alberta, Canada T2N 1N4
NICHOLLS, J., Dept. of Geology and Geophysics, University of Calgary, Calgary, Alberta, Canada T2N 1N4
KUNTZ, M.A., U.S. Geological Survey, MS 913, Box 25046, Federal Center, Denver, CO, USA 80225

The Craters of the Moon lava field, Idaho, was the site for eruption of approximately 4 km^3 of basaltic lava flows in the late Holocene (2000-2500 yr BP). On the basis of 52 whole-rock analyses, the flows fall into two distinct compositional groups: basalts with 44-52% $SiO_2$and trachyandesites with 55-64% SiO_2. The two groups can also be distinguished with Si/K ratios: basalts have a range of 17-21 and trachyandesites have a range of 9-15. None of the available analyses have SiO_2 contents or Si/K values between the ranges cited.

The basalts contain olivine (∿Fo50), plagioclase (∿An45), rare augite, and minor ulvöspinel (∿Usp65) phenocrysts in a groundmass of olivine (∿Fo30), plagioclase (∿An30), augite, and Fe-Ti oxides. The trachyandesites contain microphenocrysts of olivine (∿Fo35-10), plagioclase (∿An30), Fe-Ti oxides (∿Usp70), rare augite, and alkali feldspar (∿Or45-20) in a groundmass of olivine (∿Fo10), plagioclase (∿An15), augite, minor alkali feldspar, and Fe-Ti oxides (∿Usp55); in addition, zircon and apatite occur as minor phases in the groundmass and as larger crystals in glomerocrysts with olivine and Fe-Ti oxides.

Xenocrysts of olivine, plagioclase, rare augite, and alkali feldspar and xenoliths consisting of olivine (Fo30-7), plagioclase (An38-10), hypersthene, Fe-Ti oxides, zircon, apatite, and baddeleyite in a pumiceous matrix occur in trachyandesite flows. Inclusions of pumiceous rhyolite, ranging from meter- to microscopic-size, are present in several cinder cone vents for the trachyandesite flows. Microscopic pumice inclusions are present in trachyandesite flows, but meter-size pumice inclusions have not been recognized in these flows. Geophysical evidence suggests that the inclusions represent Tertiary rhyolitic rocks that form the upper crust through which basaltic magmas rose to the surface.

Derivation of trachyandesite from basalt by crystal fractionation, overprinted by contamination of basalt by pumiceous rhyolite, is suggested by coherent trends and nonzero intercepts on Pearce element ratio plots. The chemical variations cannot be explained by fractionation of olivine and plagioclase alone but must include augite and Fe-Ti oxide accumulation/fractionation as well.

Thermodynamic modelling suggests that olivine and plagioclase phenocrysts and microphenocrysts were not in equilibrium with the enclosing melts at surface pressures. In order to have cotectic crystallization of olivine and plagioclase, pressures in excess of 0.5 GPa are required. A high pressure fractionation/accumulation stage is consistent with indications from the chemical data that augite and Fe-Ti oxide phases participated in the derivation of trachyandesite from basalt. The modelling also shows that augite would appear on the liquidus with olivine and plagioclase at high pressures.

GEOTHERMAL SYSTEM GEOCHRONOLOGY BY U-SERIES METHODS: PROGRESS AND PROSPECTS

STURCHIO, N.C., Argonne National Laboratory, CMT-205, Argonne, Illinois 60439

The U-series dating methods have been exploited widely in Quaternary geochronology (e.g., for corals, tufas, travertines, speleothems, sediments, magmas). However, relatively little attention has been given to the geochronology of geothermal systems. The practical application of these dating methods has recently been investigated using α-counting techniques for a variety of materials from active geothermal systems at Yellowstone (Wyoming), Long Valley (California), Valles (New Mexico), and other sites. The results of these studies indicate that some valid generalizations may now be made regarding the utility and limitations of U-series methods for geothermal system geochronology.

The ratio of ^{230}Th ($t_{1/2}$=75,200 yr) to its parent ^{234}U ($t_{1/2}$=248,000 yr) provides the most useful and direct dating tool for the range ~1000 to ~350,000 yr. The $^{230}Th/^{234}U$ ratio has been used for dating hot spring deposits of travertine and sinter, and vein deposits of calcite and silica. The principal limitations of this method are: the low U/Th ratios in hot spring deposits and vein minerals (mostly <1.5) require multiple analyses and the use of $^{230}Th/^{232}Th$ vs. $^{234}U/^{232}Th$ isochron plots for dating; many samples may not be dated unless an initial value for $^{230}Th/^{232}Th$ is assumed; secondary deposition or mobilization of U may occur in porous or fractured material, obscuring its age; and amounts of available material in veins or vugs may be very small (<1g), requiring mass spectrometry techniques for analysis. Best results are derived from relatively pure, unfractured, nonporous material; replicate analyses should always be performed for verification. Ages obtained should either satisfy the constraints of field relations or be rejected.

Changes in whole rock U/Th caused by geothermal fluid-rock interaction may be dated in favorable situations (e.g., U accumulations on aquifer surfaces produced where low-Eh geothermal waters mix with high-Eh shallow groundwaters, or U depletions in acid-altered rocks), using whole rock drill core analyses plotted on a $^{230}Th/^{232}Th$ vs. $^{234}U/^{232}Th$ isochron diagram. This method has been used to date the initiation of post-glacial thermal water discharge through rhyolite at a site in Biscuit Basin (Yellowstone). Similar applications may be found in aquifers having initially high permeability and homogeneous U/Th (e.g., unzoned flow breccias or unwelded tuffs) where significant changes in U/Th have been imposed by geothermal processes on a time scale that is short relative to the $t_{1/2}$ of ^{230}Th.

The $^{234}U/^{238}U$ ratio can, in principle, be used to date material up to ~1 Ma using an assumed value for the initial ratio. However, at several of the investigated localities, initial $^{234}U/^{238}U$ has varied considerably with time. Therefore, this method should not be considered accurate unless the initial ratio can be verified independently.

The excess ^{226}Ra method can be used to date travertine ≤10,000 yr old, if the initial activity of ^{226}Ra ($t_{1/2}$=1602 yr) is known. Modern travertine at Mammoth Hot Springs (Yellowstone) has excess ^{226}Ra activity that ranges from 6 to 15 pCi/g. The accuracy of this method is limited by the uncertainty of the initial ^{226}Ra activity, but travertine deposition rates may be obtained from a plot of excess ^{226}Ra vs. stratigraphic position.

Further efforts in the application of U-series methods (especially $^{230}Th/^{234}U$) to the geochronology of geothermal systems are encouraged. Mass spectrometry techniques are preferable when sample quantities are limited and/or when maximum precision is required.

VOLCANIC RISK AT COLIMA VOLCANO: ECONOMIC AND GEOGRAPHIC ASPECTS.

SUAREZ-PLASCENCIA, C., Instituto de Geofísica,UNAM,D. Coyoacan 04510 D.F. Mexico and Martin-Del Pozzo, A.L., same address

Colima (19°30'44"N,103°37'02"W) is presently Mexico's most active volcano and although the last eruptions 1962, 1976 and 1982 have produced only small lava flows and accompanying Merapi type avalanches from the summit dome, explosive eruptions have been documented in the past. Pyroclastic flows and widely-dispersed pyroclastic fall deposits caused devastation in the 1616, 1818 and 1913 eruptions. An older debris avalanche covers more than 1200 km^2 to the south of the volcano where 462,000 people live including the 103000 that live in Colima, the State Capitol. The area to the south of the Volcano has an annual population growth rate of 3.5%. The main highway and railroad pass less than 20 km from the crater and are built on the avalanche, pyroclastic flow and lahar deposits from the volcano. More than 33% of Guadalajara's, Mexico's second largest city's electric supply comes from the Manzanillo thermoelectric plant and passes 7 km from the crater. The area has 353 manufacturing industries although main economic activities are sugar cane and lumber industry. There are sugar cane refineries at Queseria and Tamazula and a large lumber plant at Atenquique, which has been affected by large floods in the past. To the north of the volcano the area would be affected mainly by fall deposits reaching Cd. Guzman, Tamazula and Zapoltitic (Wich have gypsum and cement plants besides a population of 101,000). Open pit mining at Peña Colorada and Las Encinas would also be affected.

ERUPTIVE HISTORY OF KUTCHARO CALDERA IN THE NORTHEAST HOKKAIDO, JAPAN.--especially on the post-Kutcharo caldera activities--

SUMITA, M., Department of Earth Sciences, Nihon University, 3-25-40 Sakurajousui, Setagaya-ku, Tokyo 156, Japan.

Kutcharo caldera, in the northeast Hokkaido, Japan, located in the southwest part of the Shiretoko-Akan volcanic chain, belonging to the Kurile volcanic zone. It is one of the largest caldera in Japan and its size is 26X20km. Three post-Kutcharo caldera volcanoes(Nakajima, Atosanupuri and Mashu) exist in the caldera and at the rim of the caldera. The Kutcharo volcand erupted 9 large scale ignimbrites(Katsui & Satoh, 1963) and numerous plinian pumice falls in the middle to late Pleistocene. Those ignimbrites named Furume welded tuff(0.34Ma;FT, Koshimizu & Ikushima, 1989), Kpfl-VIII, Kpfl-VII, Kpfl-VI, Kpfl-V, Ksfl, Kpfl-IV(0.13Ma;FT, Okumura for personal communication), Kpfl-III, Kpfl-II and Kpfl-I(0.03Ma;^{14}C,Satoh, 1969), from older to younger respectively. Most of all ignimbrite are non welded except for Furume welded tuff and a part of Kpfl-IV.

Original form of Kutcharo caldera formed during the stage of the large scale ignimbrite of Ksfl & Kpfl-IV. Subsequently, Kpfl-III, II and a large scale pyroclastic flow of Kpfl-I were ejected and the original form of the caldera was modified(Kpfl-I deposits cover the inner wall of the caldera).

Two more pyroclastic flows and surge deposits were ejected after the Kpfl-I from three post-Kutcharo caldera volcanoes, Atosanupuri(ATNfl), Mashu volcanoes(Ma-f fl) and Nakajima volcano. Atosanupuri and Mashu volcanoes formed calderas by ejecting those pyroclastic flows.

Tephra stratigraphy and distribution indicate their vent positions and eruptive history in the post-Kutcharo caldera stage.

Outlines of the development of Kutcharo volcano, especially those of the activities in the post-Kutcharo caldera stage are summarized as in Table 1.

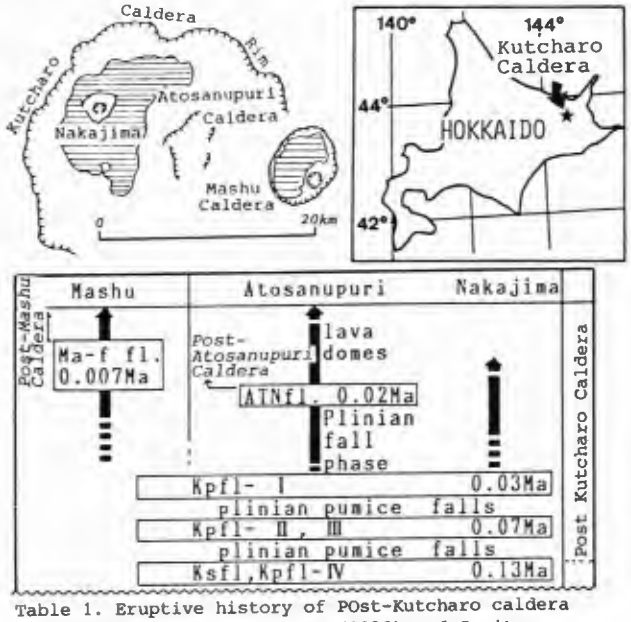

Table 1. Eruptive history of POst-Kutcharo caldera (modified after Katsui et al.(1986) and Sumita (1987)).

NEW STYLES OF HOT SPOT VOLCANISM, AUSTRALIA - IMPLICATIONS FOR GLOBAL PROCESSES

SUTHERLAND, F.L., Division of Earth Sciences, The Australian Museum, Sydney, NSW, 2000

Hot spots form simpler to more complex upwellings, giving different styles of volcanic traces (eg Hawaiian plume cf Galapagos toroidal diapir). Australian-Antarctic and SW Pacific traces show unusual large scale features.

'Boomerang' like chains seem to emanate from old triple point systems. The main 'boomerang' system trends towards the 65 Ma Coral Sea rift. The simplest interpretation is hot spot flares that diminish in time. Boomerangs in eastern Australian-Antarctic Victoria Land are convex WNW to NW, but New Zealand-Campbell Plateau ones point N to NE, i.e. either dextral or sinistral to directions of plate motion. This favours a mantle flow control.

Boomerang chains propagate from rift structures 500-1000 km across, but from 96 Ma Tasman rifting possibly over 3000-3500 km. A reconstruction correlates Tasman triple points (North Tasman, Gippsland, South Tasman and Australian-Antarctic-New Zealand) with the Australia-Antarctic Ridge and Balleny Island, Mt. Melbourne and Mt. Erebus hot spots.

Such 'superstring' hot spot systems would generate extensive basalt belts (east Aust.) and produce important global effects.

Major activity for Australian systems (96, 65, 35, 4-5 Ma) correspond with a suggested 31 ±1 Ma flood basalt cycle. Significant hot spot rifting at 65 Ma, added to Deccan basalts, better match Ir values at the Cretaceous-Tertiary boundary (volcanic versus meteoritic catastrophic extinction debate). Extended hot spot lines potentially test Earth expansion.

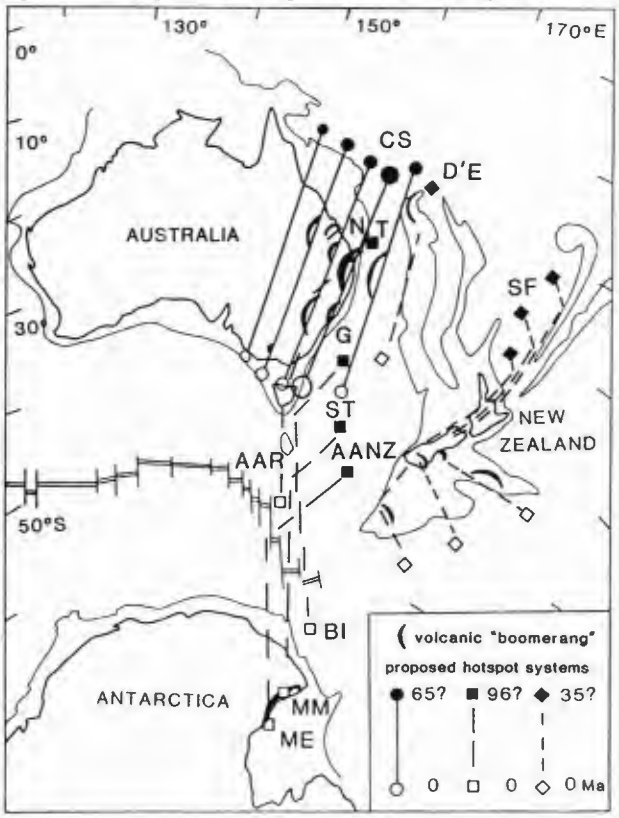

DUPLICATED COLLAPSE OF THE OLD-TAMAGAWA CALDERA WAS SHOWN BY DRILLINGS IN THE SENGAN GEOTHERMAL AREA, NORTHEAST JAPAN

SUTO, Shigeru, Geological Survey of Japan 1-1-3, Higashi, Tsukuba, Ibaraki, 305 Japan.

Geological outline of the Old-Tamagawa caldera was shown by 29 drillings, which depth were ranging from 200 meters to 2486 meters, in the Sengan geothermal area, northeast Japan. The caldera is 10 kilometers in diameter and the maximum total thickness of the Old-Tamagawa Welded Tuffs which is the intracaldera welded tuff is more than 2700 meters. The Old-Tamagawa Welded Tuffs are divided into the Rhyolite Welded Tuff A, 1, 2 and 3 (RA, R1, R2 and R3) in ascending order, and the distribution of all of the tuff members are restricted in the Old-Tamagawa Caldera. No outflow deposit was found around the caldera region because of the long time denudation. The Old-Tamagawa Welded Tuffs is overlain by the Tamagawa Welded Tuffs and the Young Volcanic Rocks. The Tamagawa Welded Tuffs are divided into the Rhyolite Welded Tuff 4 (R4, 2Ma) and the Dacite Welded Tuff (D, 1Ma) in ascending order and both of these two units distributed widely.

All of the intracaldera tuffs are characterized by large amount of large quartz and plagioclase phenocryst and densely welding. The correlation of each tuff units from bore holes were carried out by petrographical, paleomagnetic and physical studies of the rock samples. The rocks in the unit RA are characterized by slightly larger size of the phenocryst and the reversed magnetic polarity, and those of R2 by slightly smaller size of the phenocryst and the normal magnetic polarity. The porosities of each units decreasing with depth through different trend each other. At the lower part of the unit RA near the caldera rim, the tuff intercalated with the layers of accidental lithic fragments, ranging up to 63 meters in thickness. There is no difference between the overlying and the underlying tuffs both lithologically and physically. So the thick lithic layers are thought to be the caldera collapsed breccia which is formed at the deposition of the tuff. The distribution area of the unit R2 is narrower than those of RA. And the geological structure shows the duplicate collapse of the Old-Tamagawa Caldera.

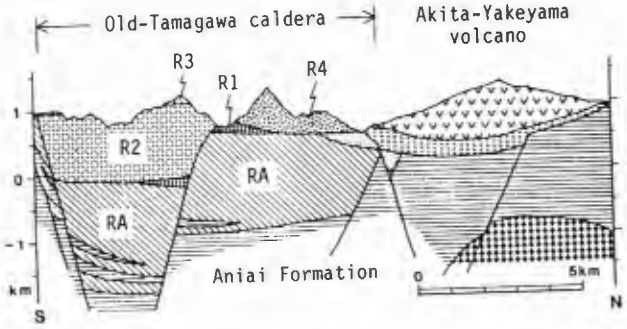

Geological cross section from the north (right) to the south (left).

A MULTIPLE-SPECIES VOLCANIC GAS SENSOR -- TESTING AND APPLICATIONS

SUTTON, A. Jefferson, U.S. Geological Survey, Mailstop 959 National Center, Reston VA. 22092, and MCGEE, Kenneth A. U.S. Geological Survey, Cascades Volcano Observatory, 5400 MacArthur Boulevard, Vancouver WA. 98661.

Comprehensive environmental testing of chemical sensors provides a firm basis for making and interpreting in-situ geochemical measurements in volcanic environments. With this objective, we have evaluated an electrochemical sensing technique initially developed by the U.S. Geological Survey (Sato, M., and McGee, K.A., 1981, USGS Professional Paper 1250.) Sensor evaluation included more than 100 systematic laboratory tests and a rigorous field experiment at Long Valley, California, beginning in 1985. The sensing technique is based on a variant of fuel cell technology. The analyte gas species acts as a fuel, and an oxidizing agent such as oxygen combines with the fuel to produce a chemical product and an electrical current proportional to the analyte concentration. The sensor's small size (less than 125 cubic cm), negligible power consumption, and rugged construction make it a good candidate for continuous in-situ gas measurements in volcanic and geothermal areas at temperatures up to 150 C. It has been used successfully at several volcanic systems in the United States, for example, Kilauea and Mauna Loa, Hawaii.

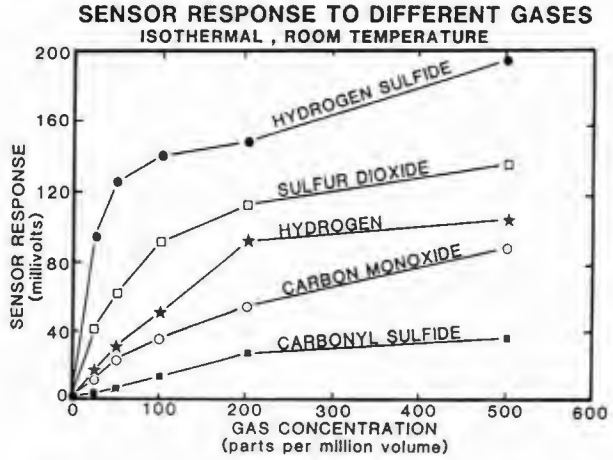

Electrochemical sensors typically are sensitive to several gas species that are chemically and/or physically similar. Furthermore, these sensors are often affected by variations in temperature, pressure, and other parameters that affect diffusion and reaction rates at the sensor. The sensor under study shows a systematic response to several common volcanic gases, including H2, SO2, H2S, CO, HCl, HF, COS (see figure). Parameters such as temperature, pressure, load resistance, and internal resistance have complex effects on the sensor; however, the effects can be minimized by measuring or controlling their variation. The sensitivity of the sensor to multiple volcanic gas species enhances its value as a monitoring tool.

PROXIMAL FACIES OF A LOW-ASPECT-RATIO IGNIMBRITE—THE TOSU PYROCLASTIC-FLOW DEPOSIT FROM ASO CALDERA, JAPAN

SUZUKI-KAMATA, Keiko and KAMATA, Hiroki, Cascades Volcano Observatory, U.S.G.S., 5400 MacArthur Blvd., Vancouver, WA 98661, U.S.A.

The Tosu pyroclastic-flow deposit is a low-aspect-ratio ignimbrite (LARI) erupted 70,000 years ago from Aso caldera in Kyushu, Japan. It averages less than 2 m thick, is distributed as remarkably far as 155 km from the source, and contains low-density rhyolitic pumice (Watanabe, 1978). Near the caldera rim, the Tosu has abundant accidental lithic fragments. In the proximal area (9-34 km from source), the Tosu is >5-4 m thick and heterogeneous in lithofacies that varies sharply among adjacent outcrops. It shows 3 different lithofacies from bottom to top: (1) abundant lithic fragments and depleted in fine ash (FD; fines depletion), (2) abundant in lithic fragments with fine-ash matrix (LI; lithics), (3) abundant in fine ash and relatively poor in lithic fragments (NI; normal ignimbrite). In the proximal area, NI overlies LI and FD and is less than 1 m thick, but in the distal area (34-155 km) the Tosu is mostly NI and less than 1.5 m thick. Because NI is the dominant facies in the distal area and corresponds to the uppermost facies in the proximal area, we interpret NI as the deposit from the "flow body" of a pyroclastic flow. LI commonly overlies FD and underlies NI. LI is 0.7-3.3 m thick near the caldera rim, pinches and swells laterally among adjacent outcrops, and commonly grades upward into NI. The "layer 2a" facies, composed mostly of fine ash, in places lies between LI and FD. These observations suggest that LI is a lensoid variation of NI in which lithic fragments are selectively concentrated. FD lies at the base of NI and LI commonly with a sharp contact. FD is >3 m thick at the caldera rim, is thicker beyond topographic ridges, and in places shows dune structure that resemble structure in pyroclastic-surge deposits. Three largest maximum-lithic size (ML) from the Tosu deposit decreases steadily with distance from the source. Three largest maximum-pumice size (MP) decreases less regularly than ML. ML exceeds MP within 35 km of the source, while MP exceeds ML beyond 35 km. Thus ML exceeds MP in the zone where the proximal lithofacies of LI and FD occur. ML vs distance diagram shows the inflection of the decrease rate of ML at 20 km. The distance of the inflection point from the source tends to increase as volume of a pyrolastic flow deposit increases. The distance of the inflection point of a LARI is generally larger than that of a high-aspect-ratio ignimbrite (HARI), which suggest that the eruption of the first is more violent than is the latter.

COMPOSITIONAL CONVECTION IN VISCOUS MELTS

TAIT, S.R. and JAUPART, C.,
Laboratoire de Dynamique des Systèmes Géologiques
Université Paris 7 et Institut de Physique du Globe
4 place Jussieu, 75252 Paris Cedex 05, France

During fractional crystallization of magma, gradients in temperature and composition develop on different scales because of the large difference between their respective coefficients of diffusivity. The varied convective phenomena which can result are likely to play a central role in the crystallization and chemical evolution of magma chambers, producing such features as compositional zonation. So far, experiments to study these processes have mainly been carried out with aqueous solutions of inorganic salts in which the solution viscosity is low (10^{-3} Pas). Hence, it is not clear to what extent these experiments accurately represent the dynamics of more viscous melts such as silicate magmas. Here, we describe the characteristics of compositional convection during the solidification of a viscous melt using an original experimental technique. A small amount of an organic compound is added to an aqueous solution of a simple salt which allows the viscosity of the solution to be varied independently of its chemical composition and liquidus temperature whilst retaining other merits of aqueous solutions such as a simple binary phase diagram, convenient liquidus temperatures and a transparent working solution. We study supereutectic melts in which fractional crystallization produces less dense residual liquid. To simulate the crystallization of magma at the floor of an intrusion, the solution is cooled through the bottom of the experimental tank causing the growth of a horizontal layer of crystals. Eventually, convective instability is observed and compositional plumes rise from the crystallizing region. We find that the critical time for the onset of convection scales with viscosity to the power two thirds and that the faster the solution is cooled, the longer it takes for convection to start. Instability begins when a critical solutal Rayleigh number (Ra_c) for the boundary layer developing ahead of the advancing crystallization front reaches a value of approximately ten. This parameter is defined as:

$$Ra_c = \frac{\Delta\rho\, g}{\mu D}\left(\frac{D}{V}\right)^3$$

where $\Delta\rho$ is the compositional density difference across the boundary layer, g the acceleration due to gravity, μ the viscosity, D the compositional diffusivity and V the instantaneous velocity of advance of the crystallisation front. Thus, compositional convection involves two time scales; that characteristic of crystal growth and that characteristic of boundary layer instability. Under the rapid cooling conditions which obtain near the margins of a magmatic intrusion shortly after its emplacement into cold country rocks, the time scale of crystal growth is likely to be too rapid for convection to occur. However, crystallisation slows with time, and after a certain thickness of rock has crystallised (a few tens to hundreds of metres for basaltic magma) compositional instability will occur. This implies that in a magma chamber much thicker than this compositional convection can be a major process of magmatic differentiation.

EXPERIMENTAL STUDY OF LIQUID-FILLED CRACKS IN GELATIN ---- VELOCITY AND SHAPE ----

TAKADA, A., Geological Survey of Japan
1-1-3 Higashi, Tsukuba, Ibaraki Pref., 305, Japan

A three-dimensional crack propagation mechanism is important for understanding magma transport, but it remains unknown. This study treats the propagation of an isolated crack as an elementary process. In gelatin experiments, physical properties of gelatin (elastic constants, density, strength), those of injected liquid (density, viscosity), injected volume, injection rate, and the stress field of gelatin can be controlled quantitatively. We can observe crack propagations in a laboratory. Maaløe (1987) studied the shape of a crack in gelatin. Takada (1989) reported the direction of crack growth and propagation on the hydrostatic condition.

The shape, size (h, l, w), velocity of a propagating isolated crack on the hydrostatic condition were measured on photographs or pictures of video. h, l, w, are the crack vertical height, the crack horizontal length (the major axis), the crack horizontal width (the minor axis) respectively. In the following experiments, the physical properties of gelatin were constant (density: 1007Kg/m^3, Young's modulus: about 10^3Pa). The stress condition of gelatin was hydrostatic, because the Poisson's ratio is 0.5.

(exp1) The liquids with various densities and viscosities (air, silicon oil) were injected slowly (low injection rate) from the bottom of a gelatin container (30cml long, 30cm wide, 50cm high) by a syringe, so that the vertical cracks were formed. The trend of a crack can be controlled by the tip of a syringe needle. If the injected volume of liquid exceeds the critical value, the vertical crack started to ascend spontaneously as an isolated crack.

(exp2) Unlike exp1, before injection of a liquid, a vertical fracture was formed in gelatin. The various liquids were injected slowly along this pre-existing fractures in gelatin.

(1) The velocity of a crack which is propagating upward depends on the crack size, density difference, viscosity of a liquid, etc. For example, the velocity is in proportion to h^4.

(2) The crack shape is reported. The ratios w/h, l/h also depend on the crack size and some of the physical properties. For example, the ratio w/h is in proportion to h.

(3) The shape of a crack tip is reported.

Maaløe, S.(1987) Contrib Mineral Petrol 96:47-55.
Takada, A.(1989) Kagoshima International conference on Volcanoes 1988, Proceedings p.99-102

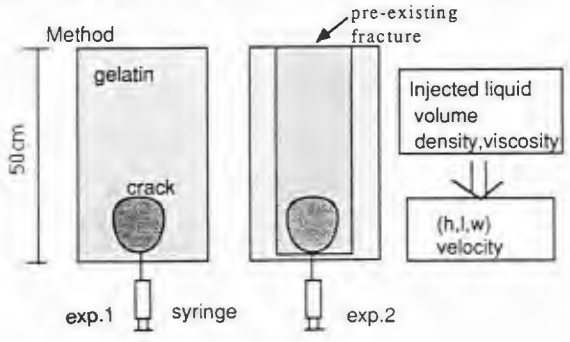

VOLCANO MONITORING IN PAPUA NEW GUINEA

TALAI, B., Rabaul Volcano Observatory, Papua New Guinea.

Rabaul Volcanological Observatory is responsible for monitoring the activity of 14 active and 23 dormant volcanoes in Papua New Guinea (PNG). These volcanoes are a danger to the lives of over 200,000 people living in a total area of 16,000 km² - that is 6.8% of the total population over 3.8% of the total land area of the country.

Regular volcano monitoring in Papua New Guinea started in late-1937 after the disastrous Rabaul eruptions in May 1937 which resulted in over 500 deaths. Temporary observatories operated at Rabaul between 1940 and 1945. Since the establishment of a permanent observatory at Rabaul in 1950, extensive nation-wide volcano surveillance operations have been developed and 7 additional out station observatories have been established on some of the active and dormant volcanoes within the country. The result is that in 1989, 13 out of 36 of Papua New Guinea's active and dormant volcanoes are being monitored to some degree.

Volcano surveillance at Rabaul comprises the maintenance of 13 seismic stations, 37 tilt stations, 30 EDM lines, 40 km of levelling lines, 5 tide gauges, 47 strandline stations, 43 gravity stations, 5 magnetometer stations, 5 thermal water sampling points, and 50 temperature points. The 7 outstation observatories are manned by part-time observers who are responsible for operating a seismograph and in some cases a tiltmeter. Regular investigations at active volcanoes within PNG involves aerial inspections, dry tilt measurements, levelling, EDM, gravity and temperature measurements which are carried out on an annual or bi-annual basis.

GRAIN MORPHOLOGY AND GRAIN SIZE STUDIES OF THE FINE ASH DEPOSITS FROM THE 180 A.D. TAUPO ERUPTION, CENTRAL NORTH ISLAND, NEW ZEALAND

TALBOT, J., and SELF, S., Dept. of Geology, University of Texas at Arlington, UTA Box 19049, Arlington, TX, 76019.

The rhyolitic 180 A.D. Taupo eruption, which took place from a vent in proto-Lake Taupo, contains several different types of fine ash fall deposits. These include a basal unit, the Initial ash, containing a lower section produced by hydromagmatic explosions which was subsequently deposited by normal ash fall, and an upper section in which the process of fragmentation fluctuated between hydromagmatic activity and dry vent processes and deposition occurred through rainflushing of fine ash from the eruption cloud. The Initial ash is overlain by the essentially "dry-vent" Hatepe plinian pumice fall deposit within which are interbedded rainflushed ash beds and two thin, small scale, pyroclastic flow deposits which are found up to 45 km from the vent. Overlying the Hatepe plinian deposit is the Hatepe ash deposit which was mainly formed by water-aided deposition of material from the Hatepe plinian eruption column.

The Hatepe phase was followed by a short break in the eruption (probably a few hours or less) after which renewed activity produced the Rotongaio ash deposit. This deposit is formed largely of non-vesicular juvenile clasts and was produced through explosive interaction between degassed magma, perhaps a cryptodome, and lake water. The proximal Rotongaio Ash overlies an erosion surface produced by intense pluvial action. There are several internal erosional surfaces within the proximal Rotongaio Ash indicating that much water was being deposited along with ash fall. Following this, there was a return to essentially dry plinian activity producing the Taupo plinian deposit which contains minor rainflush horizons and this was succeeded by eruption of the Taupo Ignimbrite. After all eruptive activity ceased, a final fine ash bed, the co-ignimbrite ash, was deposited.

Information that lead to interpretations of eruptive and depositional mechanisms will be presented. This includes field evidence , granulometric data, component studies, and clast morphology studies. It was found that a combination of these methods was effective in determining the different origins of the Taupo fine ash deposits. A preliminary quantitative study of grain shape was also conducted on grains from the three major ash deposits, Initial, Hatepe, and Rotongaio ashes. Less than half of the grains studied were suitable for Fourier analysis, thus, investigation of results was confined to the fractal method. This was found to be useful in distinguishing clasts of the three major fine ash deposits.

HOT PYROCLASTIC DEBRIS FLOW IN THE SHALLOW SUBMARINE SHIRAHAMA GROUP (MIO-PLIOCENE), JAPAN

TAMURA, Y., Geological Institute, University of Tokyo, Tokyo 113, Japan; KOYAMA, M., Institute of Geosciences, Shizuoka University, Shizuoka 422, Japan; and FISKE, R.S., Smithsonian Institution, Washington, D.C. 20560

A coarse, proximal volcanic breccia forms the lower 5 m of a 10-15 m submarine pyroclastic deposit exposed near Dogashima, Izu Peninsula, Japan. This breccia, consisting of fresh two-pyroxene andesite (SiO_2 = 60%), contains numerous blocks (≤ 5 m) that have chilled glassy rinds and cooling cracks suggesting that they were essential products of a nearby eruption. We have studied the thermoremanent magnetization (TRM) of these blocks to determine whether they retained significant heat while being deposited in the shallow marine environment.

6-13 oriented cores were obtained from six representative blocks. All samples were subjected to progressive thermal demagnetization at 50°C intervals from 100°C to 600°C. Secondary unstable magnetization parallel to the present geomagnetic field was removed after demagnetization at 200-250°C. The resulting orientations of stable TRM in the six blocks can be seen to cluster tightly in the upper hemisphere projection shown below (circles = 95% confidence limits).

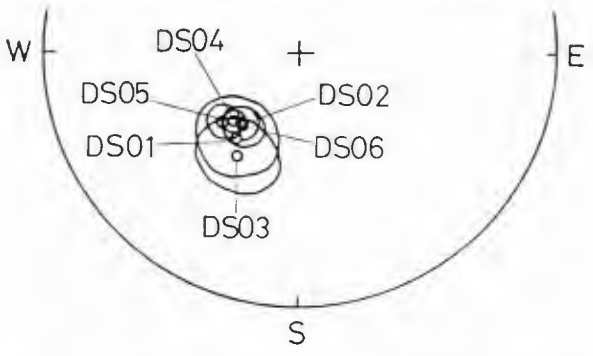

Most samples show random TRM orientations above 450-500°C. Since Curie temperatures of Fe-Ti oxides are >450°C, and oxidation of titanomagnetite to titanomaghemite does not seem to break the stable TRM, each sample is interpreted to have two partial TRM's, one dominant (<450°C) and the other between 450°C and the Curie temperature.

We conclude that the studied blocks were hot (about 450°C) when deposited, and therefore that the pyroclastic debris flow in which they are contained was the direct product of a contemporaneous eruption. This conclusion is supported by the cogenetic submarine fallout deposit that overlies this debris flow (see Fiske and Cashman, 1989, this Abstract Volume). It is probable that this pyroclastic debris flow, when moving downslope, was a 3-phase mixture of volcanic clasts, entrained sea water, and steam.

DEGASSING OF MAGMATIC VOLATILES DURING ERUPTION OF TAMBORA: STABLE ISOTOPE, VOLATILE, AND HALOGEN TRACERS

TAYLOR, B. E., CORNELL, W. C., Geological Survey of Canada, 601 Booth Street, Ottawa, Ontario, Canada K1A 0E8, and SIGURDSSON, H., and CAREY, S., School of Oceanography, University of Rhode Island, Narragansett, Rhode Island, 02882-1197, U.S.A.

Hydrogen and oxygen isotope composition, and H_2O, Cl, F, and S contents of dense glass, scoria and pumice from tephra fall and pyroclastic flow deposits of the 1815 eruption of Tambora volcano, Sunda arc segment, Indonesia archipelago, record extreme degassing and alteration. Two distinct phases of activity are represented: four initial tephra falls, followed by pyroclastic flows and a major co-ignimbrite ash fall. Principal units were sampled in vertical section near the caldera rim, and at two distal locales (Boha and Gambah; 20 and 25 km, respectively, from the vent). Welded pyroclastic flow and lag breccia was also obtained from the caldera-rim section. Comparison of major and trace element compositions of whole-clasts and glass, specifically, indicates that the magma erupted during the 1815 eruption was a homogeneous nepheline-normative trachyandesite. In contrast, hydrogen isotopes, and H_2O, Cl, F, and S contents show considerable diversity.

Hydrogen isotope composition and water content of dense glassy clasts from tephra fall and welded pyroclastic flow and lag breccia indicate a marked decrease in δD (from -88 to -158) with a decrease in water content (from 0.23 to 0.12 wt. % H_2O). This co-variance is similar to trends found for continental rhyolites in the western U.S. and is ascribed to progressive magmatic degassing. The low water content (< 0.23 wt. % H_2O) of all dense glass clasts suggests, however, that the magma represented by these clasts experienced surface, or near-surface open-system degassing. Dense glass clasts found in the tephra may therefore represent fragments of slightly older dome, or shallow conduit-quenched magma.

Dense glasses from welded pyroclastic flow and lag breccia have the lowest primary δD values (-158 and -141) yet reported. Local meteoric water has δD ≈ -10, and the $\delta^{18}O$ of both samples is 6.2. Thus, these samples represent rewelding of extremely degassed (at surface) melt which has not been subsequently altered. In contrast, high water contents (up to 1.04 wt. % H_2O) of scoria from pyroclastic flows are correlated with lower oxygen isotope ratios (5.0 to 5.6 °/oo), and non-systematic variations in δD suggest post-eruption alteration.

F, Cl, and S contents of dense glass are much lower than those in glass inclusions analyzed by Devine et al. (1984). Welded pyroclastic flow and lag breccia glasses have the lowest δD and F of all clasts, and among the lowest Cl contents. For all other clasts, Cl, F, and S are poorly correlated with δD. Thus, whereas our data suggest some surface degassing of the halogens, most were apparently lost from the uprising magma during earlier stages of degassing.

CHEMICAL AND ISOTOPIC INVESTIGATIONS OF FUMAROLIC FLUIDS FROM CAMPI FLEGREI CALDERA.

TEDESCO, D., Osservatorio Vesuviano, Via Manzoni 249, 80123 Napoli, Italy.

Chemical and isotopic investigations have been carried out on volcanic gases sampled from the Campi Flegrei caldera during and after the 1982-1984 bradyseismic crisis (ground uplift and seismic activity). The results provide further insights into the source mechanisms of the geophysical events and into the nature of the accompanying geochemical response of fumarolic fluids.
Intensive survey of the hottest fumarole (Bocca Grande, 155°±5°C) at Solfatara, at the center of the Campi Flegrei caldera between 1983 and 1988 shows that the chemistry of the gases changed significantly with the evolution of the geophysical events. In particular, an increase of the gas/vapour ratio and a decrease of the S/C and Cl/C ratios preceded and accompanied the decline in intensity of the bradyseismic crisis. Thermodynamic calculations on gas analyses suggest that the Bocca Grande fluids were fed by a steam reservoir at about 300m depth, the temperature of which dropped from about 250°±15°C in 1983-1985 to 220°±15°C in 1987. The end of the crisis (1984) was thus associated with an apparent decrease in the thermal input to this reservoir beneath Solfatara from hotter, deeper reservoirs. Helium and carbon isotope ratios measured during the crisis show no significant deviations with respect to their pre and post crisis values; this suggests a low contribution from mantle derived fluids. In addition the compositional trends among the Campi Flegrei fluids do not provide any evidence that trend supporting a shallow intrusion of magma beneath the caldera was responsible for the ground uplift and seismic activity observed in 1982-1984.

Solfatara crater, Bocca Grande fumarole. October 1983-January 1989

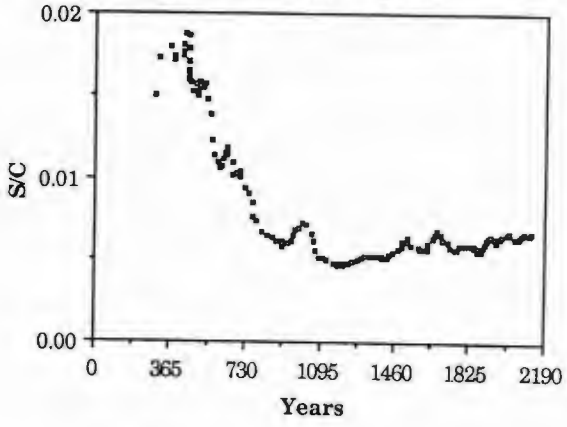

ISOTOPIC EVIDENCE FOR THE ORIGIN OF LATE TERTIARY METALUMINOUS AND PERALKALINE RHYOLITES FROM THE GREAT BASIN, WESTERN U.S.

TEGTMEYER, K., FARMER, G.L., Dept. of Geological Sciences and CIRES, University of Colorado, Boulder, CO 80309; and BROXTON, D.E., Los Alamos National Laboratory, Los Alamos, NM 87545

The Nd isotopic compositions have been determined for a set of Late Tertiary rhyolites from the SW Nevada and McDermitt volcanic fields to characterize the source regions of these extension related, high-silica rhyolites. In SW Nevada, pumice samples from large volume metaluminous ash-flow tuffs reveal that each silicic magma had developed weak Nd isotopic zonation prior to eruption, with high-silica rhyolites having lower ε_{Nd} values than trachytes at deeper levels in the chamber. These isotopic differences correlate directly with Nd concentration ([Nd]) variations, the high-Si rhyolites having the lowest [Nd] (30 ppm) and the trachytes the highest (100 ppm). At any given [Nd] the ε_{Nd} values for the major ash-flows increase through time with trachyte pumices varying (see figure below) from ε_{Nd} = -11.3 (Topopah Spring member; 13.4 Ma) to -9.6 (Ammonia Tanks; 11.2 Ma) .

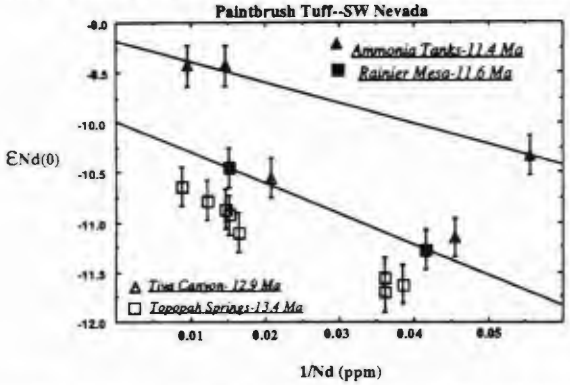

Identical patterns of correlated Nd isotopic compositions and [Nd] variations are observed in peralkaline rhyolites from both the SW Nevada and McDermitt volcanic fields. Two peralkaline ash-flow tuffs from the McDermitt volcanic field show particularly strong Nd isotopic gradients but, in contrast to the metaluminous rhyolites, highest ε_{Nd} values and [Nd] occur in high-silica samples with decreasing ε_{Nd} and [Nd] values in low-silica rhyolites (Double-H Mtns Tuff ε_{Nd} = +6.4 to +2.0, [Nd] = 90-54 ppm; Long Ridge Tuff members 2 & 3 ε_{Nd} = +3.1 to +2.4, [Nd] = 50-30 ppm). The Nd isotopic compositions within peralkaline rhyolites from the Silent Canyon (14.5 - 13.4 Ma) and Black Mtn. (6 Ma) volcanic centers in SW Nevada are also correlated with [Nd] (Grouse Canyon Tuff, ε_{Nd} = -5.4 to -6.3, [Nd] = 50 - 30 ppm; Pahute Mesa member of the Thirsty Canyon Tuff, ε_{Nd} = -6.9 to -8.1), but their ε_{Nd} values are distinctly higher than the values for metaluminous rhyolites in the same region.

The consistent positive correlation between ε_{Nd} values and [Nd] in each of the ash-flow tuffs, regardless of the sense of vertical Nd zonation in their parent magma chambers, provides strong evidence for *in situ*, open system additions of wall rock material to silicic magmas during their residence in the upper crust. However, the proportion of incorporated wall rock required to produce the range of isotopic compositions in the metaluminous and peralkaline rhyolites is small (< 10% crustal Nd) and need not have influenced the bulk chemical evolution of these magmas. Estimates of the ε_{Nd} values for magma originally feeding the upper crustal magma chambers are in every case similar to values for principally mantle-derived basaltic rocks erupted in the same area (-9 to -10 in SW Nevada; +8 to +6 at McDermitt). This correspondence suggests that rhyolites could have differentiated directly from mantle-derived magmas with little crustal interaction. Even though the bulk compositional differences between the metaluminous and peralkaline rhyolites cannot be accounted for on the basis of isotopic data alone, it may be significant that magmas parental to the metaluminous rhyolites were derived from an ancient, "enriched" continental mantle source, whereas the magmas parental to the peralkaline rhyolites in southern Nevada could have been dominantly derived from oceanic (OIB-type) mantle.

BERYLLIUM-BORON SYSTEMATICS OF ISLAND ARC LAVAS

TERA, F. and MORRIS, J.D., Department of Terrestrial Magnetism, Carnegie Institution of Washington, 5241 Broad Branch Rd. N.W., Washington, D.C., 20015
LEEMAN, W.P., Earth Science Division, National Science Foundation, Washington, D.C., 20550

In the hope of shedding some light on the process of subduction at convergent margins and the chemical process by which elements from the subducted plate are transferred to the overriding mantle, we have determined B and Be concentrations and abundances of the radioactive isotope ^{10}Be ($T_{1/2}$ = 1.5 Ma) in 70 lavas from volcanic arcs. By virtue of its atmospheric origin via spallation reactions on O and N and its tendency to hydrolize in sea water, ^{10}Be is enriched in oceanic sediments ($\sim 5000 \times 10^6$ atoms/gram, a/g). In contrast ^{10}Be concentration in mantle derived magmas from mid-ocean ridges, ocean islands and continental rifts is below detection limits ($< 1 \times 10^6$ a/g). Stable ^{9}Be in these magmas and in sediments shows a narrow concentration range (0.2 to $\sim$ 2 ppm); thus the wide range in $^{10}Be/^{9}Be$ isotopic composition (5×10^{-11} to 5000×10^{-11}) is primarily controlled by the variability in ^{10}Be.

Boron is present in high concentration in sea water (4.6 ppm) and is strongly enriched in oceanic sediments (50 to 150 ppm) relative to MORB and OIB (1 and 2–3 ppm, respectively). B is also strongly enriched in the altered portion of the subducted oceanic crust (10 to 300 ppm depending on degree of alteration). Like ^{10}Be, the Boron budget in arc lavas (2–100 ppm) is nearly completely controlled by a recycled subduction component. Consequently these two tracers are largely insensitive to variations in the chemistry of the sub-arc mantle and to crustal contribution. The $^{10}Be/^{9}Be$ ratio in island arcs ranges from a low mantle value of $< 5 \times 10^{-11}$ up to 60×10^{-11}. The B/Be ratio also extends from a mantle value of $\sim$ 10 to 185. These ratios are not correlated with indices of fractionations (SiO_2, MgO) and reflect the ratios of the magmas source.

Plotted on $^{10}Be/Be$ vs B/Be diagram the data from five arcs define well correlated ($r^2 \geq 0.85$) mixing arrays of positive but variable slopes. These linear trends are consistent with being mixing lines of two well defined end-members, a circumstance that requires that the subducted component involved in arc magmatism be nearly homogeneous along the length of each arc (650–1900 km). Bulk sediments, however, cannot be the high ^{10}Be, high B end member as they do not fall on the extrapolated arc trends. B enriched fluids derived from young sediments or a mixture of ^{10}Be-rich sediment plus B-rich altered basaltic slab are suitable end members.

The mixing trends of the five arcs studied converge on the low $^{10}Be/Be$ and B/Be ratio characteristics of "pristine" mantle as an end member. These results suggest that B does not accumulate in the mantle wedge during ongoing metasomatism and magmatism. Either B is extremely fugitive and is quickly transferred through the mantle to the earth's surface, or the metasomatised B-rich mantle created above subduction zones is swept out by convection at about the rate at which it is formed.

Although far from being exhaustive and fall short of complete characterization of the mixing lines' end members, the Be-B systematics appear to provide a framework within which a broader geochemical database may lead to quantitative identification of the end members and their relative contributions.

VOLCANIC AND SEISMIC HAZARDS WITHIN THE EAST AFRICAN RIFT IN TANZANIA AND RECOMMENDATIONS FOR HAZARD REDUCTION

TESHA, A.L., Ministry of Energy and Minerals, PO Box 903, Dodoma, Tanzania
EBINGER, C.J., Geodynamics Branch, NASA/Goddard Space Flight Center, Greenbelt, MD 20771

Tanzania is bordered on the north by a southern extension of the magmatically "wet" Kenya rift (Eastern rift) and on its western margin by the magmatically "dry" Western rift (see Figure). Along the length of both the Western and Eastern rifts, active eruptive centers generally are located within the fault-bounded rift valleys. Fault-bounded basins in both the Western and Eastern rifts contain several kilometers of clastic and volcaniclastic sediments that record a Miocene-Recent history of explosive and effusive volcanicity. In the Eastern rift near Arusha, volcanic activity began approximately at 5 Ma, or 10-15 m.y. after initial volcanic activity within the northern Eastern (Kenya) rift. Flows and airfall ash deposits from the isolated volcanic province near Mbeya (Rungwe province) in the Western rift have been dated at 7.2 Ma-11 Ka by $^{40}K/^{40}Ar$ methods. Within the Mbeya region, the number of pyroclastic flows and ignimbrites is much greater in Plio-Pleistocene time than during Miocene time, and trachytic ash blankets regions over 300 km away from eruptive centers.

The fault-bounded rift valleys and uplifted regions flanking both rift zones in Tanzania are seismically active. Earthquakes have been reported throughout the depth range 0-30 km in the Western rift, but no data are available to determine the depth extent of seismicity in the Eastern rift. Based on field and seismic evidence, high-angle normal and strike-slip faults bounding and linking rift basins may penetrate to deep crustal levels.

The historic record documents catastrophic events related to seismic and volcanic activity in the rift valleys. Large landslides have occurred along the flanks of shield volcanoes with loss of life in these densely-populated, high rainfall areas. Rumbling noises and active CO_2 venting are common the Mbeya region (Western rift) and in the Arusha region (Eastern rift). Thick sedimentary sequences interbedded or underlying basalts deposited in rift valleys would tend to amplify ground motions caused by earthquakes. Internal waves generated by sediment flows beneath deep anoxic lakes could overturn parts of the anoxic lakes, leading to mass fish kills and loss of a major protein source for villagers.

Considering the recent seismic and volcanic activity in the southern East African rift system, a monitoring network of seismic stations/volcanological observatories is needed in Tanzania. Considering the distribution of earthquake epicenters, the location of major faults and sedimentary basins, the population distribution, and future national development plans, a main station located at Dodoma and telemetering stations at Arusha, Mbeya, and Kigoma could mitigate casualties and damage. In addition, data collected from these seismic networks will improve our understanding of the geometry of major faults systems bordering the rift valleys and the evolution of magmatic processes within this active continental rift.

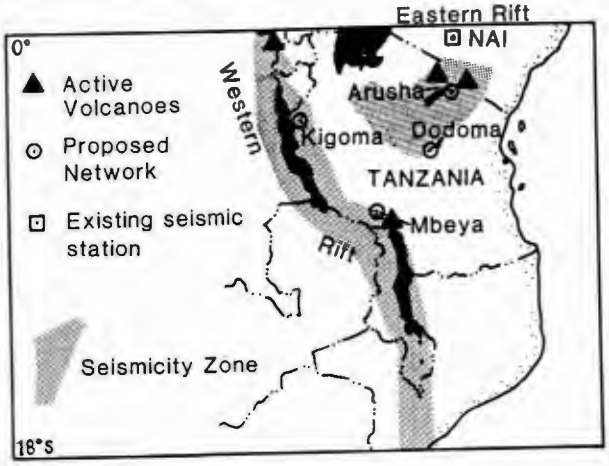

EARLY-RIFT BASALTIC VOLCANISM OF THE NORTHERN RIO GRANDE RIFT

THOMPSON, R.A., U.S. Geological Survey, Denver Federal Center, Denver, CO 80225, and JOHNSON, C.M., Department of Geology and Geophysics, University of Wisconsin-Madison, Madison, WI 53706

Basaltic volcanism concomitant with rifting in the San Luis Valley segment of the northern Rio Grande rift ranges in age from 27 to <4 Ma. Pliocene basalts of the Taos Plateau volcanic field occupy the present axial rift depression, whereas Oligocene to Miocene basalts of the Hinsdale Formation are restricted to the uplifted rift margins and mesa-capping lavas of an intrarift, axial horst that form the San Luis Hills.

Oligocene (~26 Ma) volcanic rocks of the Hinsdale Formation in the San Luis Hills range from 49% to 57% SiO_2 and include both nepheline and hypersthene normative lavas. A mildly alkalic series consisting of trachybasalt, basaltic trachyandesite, and trachyandesite is volumetrically dominant, tholeiites are subordinate, and xenocrystic trachyandesites containing abundant quartz and plagioclase xenocryts occur only locally. In contrast, basalts of the Pliocene Taos Plateau volcanic field are dominated by tholeiites; trachybasalts to trachyandesites are minor.

Relative to the San Luis Hills tholeiites (La/Sm_n=2), the more alkaline series are enriched in LREE and have La/Sm ratios that increase in the trachybasalt-basaltic trachyandesite suite (La/Sm_n=3) to xenocrystic trachyandesites that are the most enriched (La/Sm_n=4). Chondrite-normalized, extended REE patterns for the San Luis Hill lavas are similar in shape within the series; they have characteristic Nb and Ta depletions and high K and Th relative to Ta, Nb and LREE and are more characteristic of subduction-related magmas of continental margins. Major- and trace-element constraints support a petrogenetic model of fractionation plus assimilation for sub-groups within the suite, although the model cannot relate lavas for the entire suite.

Initial $^{87}Sr/^{86}Sr$ ratios for the San Luis Hills suite (0.7044-0.7056) and ϵ_{Nd} values (-1.1 to -7.4) correlate negatively; the most evolved compositions have the lowest ϵ_{Nd} values and highest $^{87}Sr/^{86}Sr$ ratios, suggesting significant contribution from the continental crust. The $^{87}Sr/^{86}Sr$ and ϵ_{Nd} values for the San Luis Hills suite overlap the range observed for the Pliocene Taos Plateau lavas but extend to lower ϵ_{Nd} and higher $^{87}Sr/^{86}Sr$. Unlike the Taos Plateau lavas, Pb isotopic signatures in the San Luis Hills lavas ($^{206}Pb/^{204}Pb$, 17.580-18.133; $^{207}Pb/^{204}Pb$, 15.447-15.526; $^{208}Pb/^{204}Pb$, 36.986-37.682) demonstrate no systematic correlation with whole-rock chemistry, suggesting domination by crustal Pb of variable isotopic compositions.

The lack of systematic variation in isotopic signatures in the most primitive members of both the Oligocene and Pliocene basalts are interpreted to reflect broadly similar mantle sources. Wide variation in chemical compositions of these lavas suggest extraction from sources that were at variable depths, had differing residual mineralogy, and underwent variable degrees of partial melting.

WHAT IS THE INFLUENCE OF THE YELLOWSTONE MANTLE PLUME ON PLIOCENE-RECENT WESTERN U.S.A. MAGMATISM?

THOMPSON, R.N., LEAT, P.T., Department of Geological Sciences, University of Durham, Durham DH1 3LE, England, and EUGENE HUMPHREYS University of Oregon, Eugene OR 97403, U.S.A.

Although the Yellowstone plume has previously been considered to be only a relatively-local phenomenon, causing magmatism during the last 10Ma along the Snake River Plain and adjoining regions, recent numerical modelling has emphasised that hot mantle upwelling within the comparatively narrow neck of a plume feeds an outflow zone of at least 1000 km radius immediately beneath the overlying lithospheric plate. Both westward movement of the N American plate, and the obstruction caused by deep cratonic roots to the NE of Yellowstone, force outflow of relatively-hot upper mantle from the plume beneath the entire extended region of west and southwest U.S.A. We emphasise that only one plume, centered on the Yellowstone area, is sufficient to feed a hotter-than-average upper mantle beneath the whole region. Local variability in Pliocene-Recent magmatism results from: (1) variable lithospheric thickness; inherited from the pre-mid-Miocene, post-Laramide, Himalayan-style phase of western U.S.A. extension; (2) variable contemporaneous extension; (3) progressive elevation of potential temperatures in the sub-continental convecting mantle along radii from the Yellowstone area; (4) variable inputs to the asthenosphere-source magmatic systems from locally-fusible lithospheric mantle and crust.

The behaviour of lithospheric mantle of a given thickness during extension may vary greatly in response to the potential temperature of the underlying convecting mantle. To take extreme cases: (1) When the potential temperature of the underlying mantle is low enough for considerable extension to take place (whatever specific model) before anhydrous asthenospheric decompression melting begins, post-extension re-thickening of the sub-continental lithospheric mantle is probable. We consider that this model does not apply, for the most part, in the western U.S.A. because of the asthenospheric heating related to the Yellowstone plume. (2) When the potential temperature of the underlying mantle is high enough to yield anhydrous magmas by decompression melting at the onset of extension, the upwelling liquids will form dyke swarms in the overlying lithosphere, feeding sill swarms concentrated in the uppermost lithospheric mantle. The thermal effect of these dyke swarms will be to create steep-sided domains of lithospheric mantle. Finite-element calculations predict that these will be convectively unstable and downwell ("drip") into the underlying asthenosphere, except where they are inherently buoyant as a result of previous extreme geochemical evolution. The sideways propagation of the "drips" leads to wholesale delamination of lithospheric mantle. Lateral and vertical variations in the seismic velocity structure of the upper mantle beneath the western USA is consistent with the view that this process is currently widespread throughout that region.

THE SKAFTAR FIRES FISSURE BASALT ERUPTION IN 1783-85

THORDARSON, T., and SELF, S., Dept. of Geology, University of Texas at Arlington, Arlington, Texas 76019

The Skaftár Fires (Lakagígar) eruption from the Grímsvötn volcanic system in S. Iceland in 1783-85 produced one of the largest lava flows in historic times (14.7 ± 1.0 km3). Although the devastating effects of this eruption are well documented, surprisingly little is known about the eruptive behavior in 1783-85, including the distribution of tephra.

The 27 km long crater-row is composed of 10 en echelon fissures distributed on both sides of the much older Laki hyaloclastite mountain, from which the eruption takes its more common name. Each fissure is a continuous crater-row. Three crater types occur: scoria cones, spatter cones, and tuff cones. Scoria cones are always the largest crater type on each fissure.

Although there is some evidence to suggest that Grímsvötn may have been active in the spring of 1783, the Skaftá Fires eruption started on June 8 with a short-lived explosive event on a 1.8 km long fissure. Shortly thereafter lava began to flow from the fissure into the Skaftá River gorge, reaching the lowlands four days later. Analysis of the tephra stratigraphy around the crater row, along with contemporary descriptions, make it possible to identify 10 rifting and eruptive phases. Each phase began with a seismic swarm, which led to the formation of a new fissure. The opening of new fissures was followed by short-lived phreatomagmatic activity, caused by the high water table around the eruption site. Activity usually changed to violent strombolian and then effusive, as draw-down of the water table around the fissure proceeded.

Contemporary descriptions of the characteristics and location of the explosive activity make it possible to relate tephra stratigraphy to the progress of the eruption on a week-by-week basis. Due to extensive erosion of the tephra sheet near the crater-row only six tephra units have been positively identified. Two of the units (P1 & P2) are completely composed of phreatomagmatic tephra and were largely derived from two tuff cones. The volume of tephra produced, including the widespread, thin ash fall in mainland Europe, is 0.45 km^3 DRE, or 2.9% of the total volume erupted.

Maximum effusion rates occurred in the first two phases. These are estimated to be 8.5 to 8.7 x 103 m^3 s^{-1} from fissures totaling 2.2 km in length, equating to average mass eruption rates of 4.5 to 5.6 x 10^3 kg s^{-1} per meter length of fissure. Eruption rates gradually decreased over the 8 months of activity on the Skaftár Fires crater row. Fire fountain heights estimated from observations and model calculations are 800-1400 m and altitudes attained by the convecting plumes above the crater row were up to 12 km a.s.l. The release of gases and tephra produced a haze which led to a famine that decimated the population of Iceland by 21.6%.

THE RELATIVE ROLES OF SOURCE COMPOSITION AND FRACTIONAL CRYSTALLIZATION IN THE PETROGENESIS OF CONTRASTED PLIOCENE-RECENT VOLCANIC ASSOCIATIONS OF THE MESETA CENTRAL OF COSTA RICA

THORPE, R.S., Department of Earth Sciences, The Open University, Milton Keynes,MK7 6AA, KUSSMAUL, S., Universidad de Costa Rica, Ciudad Universitaria, San Pedro, Costa Rica, Central America.

The volcanic associations of Central America are derived from parental basaltic magmas formed by varying degrees of partial melting of mineralogically heterogeneous mantle, variably enriched by components derived by dehydration of subducted oceanic lithosphere (± sediment). Such magmas experience polybaric fractional crystallization during crustal ascent and crystal sorting during magma storage prior to and during eruption. The relative role of these factors through time has been evaluated by study of volcanic products erupted during a short time interval (less than ca. 1 Ma)within a limited area in central Costa Rica.

The volcanic rocks of the Meseta Central of Costa Rica are divided into the Pliocene and/or Pleistocene 'intracanyon lavas' (the 'Colima Formation'), and the younger Pleistocene-Recent lavas of the active volcanoes of the Cordillera Central, termed the 'post-avalanche lavas'. These include products of the active volcanoes Poas, Barba, Irazu and Turrialba. The intra-canyon lavas and pyroclastic flow deposits form a high-K andesite-dacite association while the post-avalanche lavas belong to a basalt-basaltic andesite-andesite association. The earlier volcanic groups include porphyritic rocks with aphyric equivalents, while the post-avalanche lavas are all porphyritic and contain gabbro xenoliths. At a given SiO_2 concentration the intracanyon lavas/pyroclastic flow deposits have higher concentrations of TiO_2, K_2O, P_2O_5 and other large-ion lithophile (LIL) elements in comparison with the post-avalanche lavas. These volcanic rocks have essentially identical $^{87}Sr/^{86}Sr$ ratios of ca. 0.7036-0.7037.

These contrasted volcanic associations are derived from basaltic parent magmas formed by different relatively low degrees of partial melting of recently LIL-enriched mantle containing residual Ti-bearing phases. Variable degrees of fractional crystallization of olivine gabbro mineral assemblages occur at varied crustal depths. For the (cogenetic) intracanyon lavas/pyroclastic flow deposits, fractionation of large magma batches occurred in the lower crust prior to rapid uprise and eruption. By contrast the post-avalanche lavas rose as small magma batches to small sub-volcanic chambers before experiencing fractional crystallization of observed pheno-cryst phases prior to eruption. The contrasted parental magmas of the intracanyon lavas/ pyroclastic flow deposits in comparison with that of the post-avalanche lavas indicates that a change in mantle partial melting conditions and/or source composition occurred during a relatively short time interval (ca. 1 Ma) with-in the Pliocene and/or Pleistocene.

GEOMORPHOLOGY, STRATIGRAPHY, AND HAZARD MAPPING AT NEVADO DEL TOLIMA, CORDILLERA CENTRAL, COLOMBIA

THOURET Jean-Claude, Laboratoire de la Montagne Alpine, Université de Grenoble I J.Fourier ; CANTAGREL Jean-Marie, Centre de Recherches Volcano logiques, Université de Clermont-Ferrand II ; CEPEDA Hector, MURCIA Armando, Ingeominas, Ibagué, Colombia.

Ice-clad and fumarolic Nevado del Tolima volcano (4° 40'N, 75°20'W, 5000m, south of Ruiz) includes four units: (1) a plateau-like basement of 1.4 to 1 Ma andesite lava flows; (2) an upper Pleistocene caldera; (3) a dissected upper Pleistocene stratovolcano; (4) a cone-shaped, summit volcano made of recent, composite domes.

The stratovolcano is built by thick andesite lava flow and pyroclastic-flow deposits (1 to 0.3Ma), mostly emplaced towards the south, which cover an old N50W tectonic scarp of the Central Cordillera. Tolima volcano is displaced towards the SE of the major quaternary volcanic axis by normal faults that strike N30W and cross the major N20E strike-slip Palestina fault.

A caldera was created during the upper Pleistocene (about 0.3-0.2Ma). Evidence are: a high arcuate wall-like ridge on the SW; thick co-ignimbrite breccias, scoria or pumice or lithic-rich pyroclastic-flow deposits emplaced towards the south, SE and east, as far as the 150-200m thick volcaniclastic fan of Ibagué at 35km.

The andesitic and dacitic summit volcano was createdwithin a 2km wide crater opened around 14,000 BP; welded pumice and scoria-rich flow deposits were emplaced towards the SE (Rio Combeima) and NE (Rio Totare). A cluster of domes was intruded during the Late Glacial and Holocene. Their formation is witnessed by thick block-lava flows towards south and east, pumice or scoria-rich pyroclastic-flow deposits towards east and NE, especially between 14,000-13,000, 11,500-9500, and around 4700 BP, as well as by tephra-fall deposits towards the west and NW. Interactions with the icecap probably triggered debris flows which filled in part the Combeima and Totare valleys, and formed the Holocene terraces incised in the volcaniclastic fans of Ibagué and Venadillo (40-50km). The latest major activity was a plinian explosion which deposited a pumice-fall layer at about 3600 BP (1cm at 30km) towards the west and NW. Minor tephra-fall and lahars occurred through the history, until the 1918 and 1943 small events.

Three hazard maps are presented: tephra-fall and lahars, pyroclastic flows, surges and debris avalanches, lava flows and volcanic-glacial flows. Mapping was based on the stratigraphical record, mostly since 14,000 BP and on historical accounts. 300,000 people live within a 35km distance around this volcano that had a more explosive behavior than Ruiz. In spite of the small icecap (5km2), lahars are the most probable hazard, even if any given eruption were weak, because of the steep slope gradient, and because of probable interactions with the icecap. Besides, scoria flows and debris avalanches can be triggered towards the SE, and transformed in lahars that would destroy the populated Combeima valley and the lower suburbs of Ibagué (50,000 people).

EARLY JURASSIC QUARTZ NORMATIVE MAGMATISM OF THE EASTERN NORTH AMERICAN PROVINCE: EVIDENCE FOR INDEPENDENT MAGMAS AND DISTINCT SOURCES

TOLLO, R.P., Department of Geology, George Washington University, Washington, DC 20052 and GOTTFRIED, D., U.S. Geological Survey, Reston, VA 22092

Compositions of diabase dikes, basalt lava flows, and the chilled margins of intrusive diabase sheets from Virginia to Massachusetts define a suite of at least four quartz normative magma types associated with the Early Mesozoic rifting of eastern North America. These quartz normative magmas, all of which have been recognized previously, include 1) high titanium (HTQ: TiO_2 > 1.0 wt.%), 2) low titanium (LTQ: TiO_2 = 0.7-0.8 wt.%), 3) high iron (HFQ: Fe_2O_3T = 13-15 wt.%), and 4) high iron-titanium (HFTQ: Fe_2O_3T > 15 wt.%, TiO_2 > 1.3 wt.%) types. New trace element data, summarized below, indicate that the four magma types are distinguished by different combinations of the elemental ratios 100Nb/Ti, Th/Hf, Hf/Ta, and La/Yb (chondrite normalized).

Trace Element Ratios (averages-basalts)

Magma Type	100Nb/Ti	Th/Hf	Hf/Ta	La/Yb(n)
HTQ	0.10	0.85	4.72	3.21
LTQ	0.07	0.95	6.08	1.68
HFQ	0.07	0.94	6.67	2.07
HFTQ	0.05	0.78	7.98	1.44

Th/Hf and 100Nb/Ti are not effective discriminants between the LTQ and HFQ types. Detailed traverses through closed system diabase sheets indicate that all of the above ratios remain essentially constant throughout an extended range (3-12 wt.% MgO) of fractionation. As a result, these new trace element data provide strong evidence that the regionally extensive quartz normative magma types are not related by differentiation, as proposed by previous investigators. In addition, models invoking an LTQ to HFQ lineage involving pyroxene fractionation are inconsistent with observed higher Sc values in the HFQ type. Furthermore, proposed HTQ to HFTQ lineages are not supported by the observed lack of significant enrichment in the light rare earth elements (notably La), Zr, Ta, and Th. The stratigraphy of the basalt sequences, which can be broadly correlated between basins, indicates that the different magma types were erupted cyclically and may have been penecontemporaneous. However, the differences in incompatible trace element ratios negate possible derivation from a single zoned magma chamber. The observed consistency of selected trace element ratios with fractionation suggests that these data may be characteristic of the magmatic source materials. We propose that these regional magma types were derived from heterogeneous source materials and remained largely independent during ascent, shallow-level emplacement, and eventual eruption. The data demonstrate that interpretations based on trace element concentrations must involve a combination of elements with a range of geochemical properties in order to distinguish subtle magmatic variations. In this case, the data further underscore the need for distinguishing the effects of source area heterogeneity from complex melting processes in order to understand the origin of the diverse magmas that characterized the early stages of the Mesozoic rifting of eastern North America.

SOURCE DYNAMICS OF THE "VOLCANIC" QUAKES CONNECTED TO THE FOSSA GRANDE CRATER ACTIVITY AT VULCANO (EOLIAN ISLANDS, ITALY).

TONANI, F., Dip. Geofisica dei Fluidi, Univ. di Palermo; 12, Via Archirafi 90100 Palermo (Italy).
GODANO, C. and FERRUCCI F., Osservatorio Vesuviano; 249, Via Manzoni 80123 Naples (Italy)

The occurrence of monochromatic microevents at the crater of Vulcano had already been observed in the late sixties: qualitative interpretations attributed them to fluid transients in a two-phase geothermal system connected to the crater itself.

Throughout the whole 1988, a dramatic rise of the volcanic gases temperatures (over 450°C in August) brought the central system to a condition, characterized by massive presence of magma-originated gases.

Two micro-seismicity field surveys, carried out in 1987 and 1988 by use of dense, digital three-component arrays, allowed to state that number, relative magnitude and frequency of occurrence of typical quakes did not vary before and during the temperature-increase event.

Furthermore, the surveys allowed to obtain a reliable 3-D model of the Vp heterogeneity in the area and to state that almost all the relocated events were contained in a dome-shaped, shallow and small high-velocity intrusive body.

Although similar in shape, the "volcanic" events are spread in depth between 3 km b.s.l. and the surface: the shallowest are better recognized by early development of Rayleigh surface-waves.

Frequency-domain observation of some seismic sequences , characterized by presence of both "volcanic" and "tectonic"-like events, allows to assume a similar origin for both.

The statement is confirmed by particle-motions and polarization coefficients computed on 200, randomly chosen three-component records, recorded at four sample-stations symetrically emplaced with respect to the crater.

A high rate of occurrence of linearly polarized wavetrains (over several seconds of the seismic signal, filtered around the dominant frequencies of its velocity spectrum) suggests that sustained excitation of body waves at assigned frequencies could mark the whole seismicity of the crater area; the time-frequency domains behaviour of the events could be therefore expressed in terms of gas-flow velocity through one or more resonators.

An hypothesis of trigger of the sustained source is also sketched.

THE PYROCLASTIC ERUPTION OF AIRA CALDERA, 22,000 YEARS AGO -REMARKABLY HOMOGENEOUS HIGH-SILICA RHYOLITE ERUPTION-

TSUKUI, M., Department of Earth Sciences, Faculty of Science, Chiba University, Chiba 260, JAPAN, and ARAMAKI, S., Earthquake Research Institute, University of Tokyo, Bunkyo-ku, Tokyo 113, JAPAN

22,000 years ago, about 100km^3 of magma erupted from northern end of the Kagoshima Bay in southern Kyushu, Japan. It produced 5 units of pyroclastics; (1) 98km^3 of airfall pumice (Osumi pumice fall; OS), (2) 13km^3 of oxidized, fine-grained Tsumaya pyroclastic flow (TSU), (3) Kamewarizaka breccia (KM) of the new vent opening and enlargement stage, (4) 250km^3 of Ito pyroclastic flow (ITO) at the climactic stage, (5) >50km^3 of co-ignimbrite ash fall (AT ash). The series of eruption was systematically examined.

Phenocrystic minerals of the whole sequences are ubiquitously plag+qtz+opx(X_{Mg}45-60)+mt+il. One exceptional sample (Ito 11c) carries Fe-rich oliv (Fo26-28) and cpx beside other phases. Fifty-five new XRF analyses of 10 major and 15 trace elements show that the majority of the erupted magma consists of a remarkably homogeneous high-silica rhyolite with SiO_2 74-76.5 wt%(H_2O free and 100% normalized). The maximum fluctuation found both in major and trace elements is ±40%. These variations can be explained by the mechanical separation of phenocryst phases (mainly of plag) or by crystal-liquid separation near the roof of the magma chamber.

Mt-il temperatures and opx-mt-qtz pressures show narrow ranges i.e. 770±20°C and 3-5kb, respectively. Although, the sample ITO 11c shows similar temperature, its calculated pressure is closed to 0kb.

These bulk and mineral chemistry and temperature-pressure estimation suggest that the magma chamber was not zoned but was very homogeneous throughout.

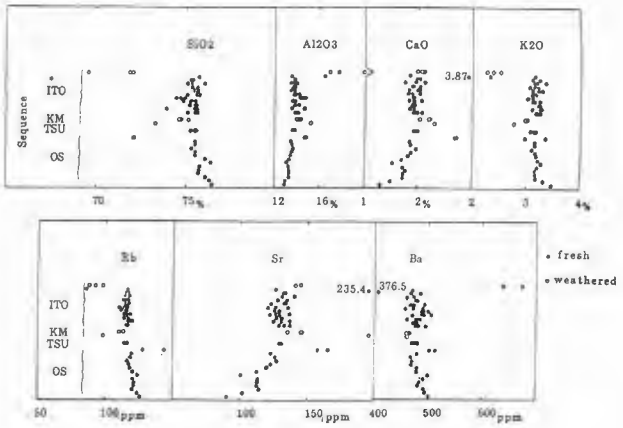

VOLCANISM OF TRANSCAUCASIAN RISE--CENOZOIC RIFT ZONE IN THE CAUCASUS, USSR

TSVETKOV, A. A., Institute of Ore Deposit Geology, Petrology, Mineralogy & Geochemistry, USSR Academy of Sciences, Staromonetny 35, Moscow, 109017, USSR

Caucasus is a geologically complex fold belt where exposed rocks range from the Precambrian to Quaternary. It consists of several structural zones many of which are interpreted now as ancient island arcs which collided with each other and with Euro-Asian continent in course of evolution of the Thetis during Mesozoic and Cenozoic. The area of recent volcanism in the caucasian segment of the Alpine-Himalayan orogen is restricted to the intersection of two Neogene-Quaternary calc-alkaline-shoshonitic island arcs: Caucasian-Anatolian and Caucasian-Elbursian framed on the north by deep basins of the Black and the Caspian seas and on the south by thick thrust zones marked by ophiolites. Within the limits of the USSR, recent volcanism is restricted to Transcaucasian Rise. This deep-seated structure is expressed by a set of sublongitudinal faults, transects all previously formed tectonic zones, and continues southward into Iran and Turkey.

Transcaucasian Rise is characterized by a high heat flow (>80 mw/m^2), north-south trending regional maximum of isostatic anomalies, and relatively low density mantle, which leads to the conclusion that beneath this region, considered by some scientists as northern ending of Afro-Arabian rift system, we have mantle astenolith. Within Greater Caucasus, in the vicinity of Elbrus volcano composed mainly of rhyolites and dacites, available geophysical data show at depth several low-velocity layers --probably due to occurrence of magmatic melts mostly anatextic in nature. Such layers are distinguished also in the Lesser Caucasus (Aragats volcano), where rhyolitic ignimbrites are widespread. In Akhalkalaki Plateau and Erevan area, late Pliocene deep fissures cutting the whole thickness of the crust were used as pathways for ascent of voluminous undifferentiated basaltic melts. According to geophysical and geological data, horizontal extension within Transcaucasian Rise definitely played a role subordinate to compression caused by tectonic collision of Euro-Asian and Arabian plates.

Pliocene-Quaternary volcanic rocks of the Transcaucasian Rise are represented by mildly alkaline and K-subalkaline magmatic series. Low-K rocks are found only in few centers (Kazbek, Ararat, Kelskoye Plateau). Mean composition of caucasian neovolcanics is close to that of high-K calc-alkaline series of Phanerozoic continental foldbelts. These series differ from those of continental rifts in lack of bimodal patterns, relatively low concentrations of Ti, Fe, P, LREE, Zr, and Nb, and high Al. However, all Transcaucasian rocks from basalt to rhyolite are characterized by relatively high concentrations of LREE and low concentrations of HREE and Y. Moreover, even basic rocks are enriched in P, LREE, Nb, Zr, Hf. These features closely resemble those of continental-rift rocks, while low abundances of Ti and Fe, and high concentrations of Al, correspond to orogenic rock series.

MAGMATIC ZONATION OF KURILE ISLAND ARC--EVIDENCE FROM $^{143}Nd/^{144}Nd$, $^{87}Sr/^{86}Sr$ AND REE IN RECENT VOLCANICS

TSVETKOV, A. A., INstitute of Ore Deposit Geology, Petrology, Mineralogy & Geochemistry, USSR Academy of Sciences, Staromonetny, 35, Moscow, 109017, USSR

The isotopic composition of Nd, Sr, and REE abundances were measured in Quaternary lavas from the whole length of Kurile arc (Atlasova, Paramushir, Chirinkotat, Makanrushi, Aves, Lovushki, Brouton, Chirpoy, Iturup and Kunashir islands and some submarine volcanoes). To investigate patterns of transverse zonation, four profiles were made in the northern, central, and southern segments of the arc. Twenty-seven samples were analyzed: nine from the Frontal and 18 from the Back-Arc zone (seven basalts, nine basaltic andesites, nine andesites, one dacite, one rhyolite). The results are presented on Fig. 1.

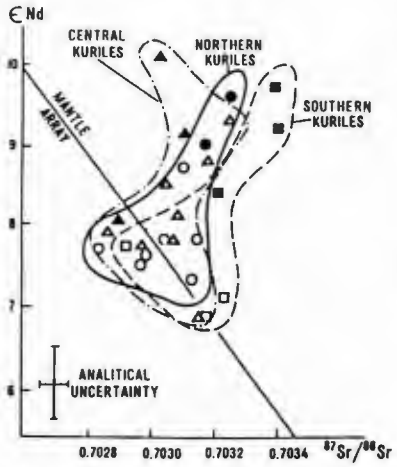

Fig. 1. Patterns of Kurile Island Arc isotopic zonation

A fundamentally new type of transverse isotopic zonation was determined: a decrease of both $^{87}Sr/^{86}Sr$ and $^{143}Nd/^{144}Nd$ ratios from the volcanic front of the arc towards its rear side, i.e. from the Pacific Ocean towards the marginal sea of Okhotsk. The changes in isotopic parameters correlate well with corresponding changes of petro-geochemical features of the volcanic rocks. The most significant pattern is the increase in incompatible LIL element concentrations in the back-arc volcanics as compared to coeval and petrographically similar rocks of the frontal zone.

The analysis of theoretically appropriate models of arc magmatism shows that the cause of the isotopic and most probably geochemical zonation is the compositional heterogeneity of the upper mantle beneath the Kuriles. Of minor importance seems to be contamination of magmatic melts in the frontal zone of the arc by seawater Sr. We believe that the origin of the compositional heterogeneity of the mantle in the Kurile region is directly related to differences in the duration of magmatism in the frontal and back-arc structural zones. The involvement of oceanic sediments and basement material--other theoretically possible components of arc magma-generating process--is considered to have occurred on a very small scale.

TRANSITION FROM RHEOMORPHIC-WELDED AIRFALL TO SPATTER FLOW: EVIDENCE OF ASH FOUNTAINING IN THE LATE PLINIAN PHASE OF THE LATERA CALDERA, CENTRAL ITALY

TURBEVILLE, B. N., and BARKER, D. S., Department of Geological Sciences, University of Texas at Austin, Austin, TX 78713-7909

Toward the end of the main ash-flow phase (ca. 0.16 Ma) of the Latera caldera, central Italy, Plinian eruptions near the NW caldera rim produced coarse-grained tephra, proximally exposed in > 30 m high faces of the Toscopomice (Casa Colima) quarry. The stratigraphy exposed in a narrow SW-NE paleovalley records continuous eruption of compositionally zoned magma (Landi, 1987) and consists of the following progression: white phonolitic pumice abruptly grades upward to, and partly intrudes, black spatter-like pumice of phonolite composition, in turn overlain by densely welded tuff, which grades upward to tephriphonolitic scoria and ash. The upper, welded, part of this sequence - informally referred to as the "Pitigliano Complex Vulcanite" - has long been among the more enigmatic deposits in the Latera area. This sequence displays evidence for both fall and flow emplacement, and is here interpreted as an ash fountain-fed deposit that proximally welded as spatter but became sufficiently fluidized in parts to behave as a pyroclastic (spatter) flow. This mechanism requires that the eruption underwent abrupt transition from a vigorously convecting Plinian column to a weakly convecting ash fountain (c.f. Horn and Moore,1986), and suggests that this period of explosive activity culminated with unusually high accumulation rates. The rapidly emplaced tephra must have retained sufficient heat to weld by compaction in the lower parts, yet contained sufficiently high proportions of fluidized fines to have flowed outward along the northern caldera rim and eventually weld by vapor-phase sintering.

The densely welded unit grades upward and laterally to a partly lava-like sequence of agglutinated scoria and ash, interpreted here as the proximal rheomorphic facies of a spatter-flow deposit. Evidence of rheomorphism in the welded sequence includes: (1) pronounced elongation and contortion of welded pumice clasts, (2) well developed secondary vesiculation of welded clasts, (3) differential shearing and associated minor folding developed between welded spatter clasts and less competent ash matrix, (4) > 75-fold upward increase in the compaction of individual clasts, from non-welded to completely compacted and rheomorphic, commonly in less than 2.0 m, and (5) localized zones where the welded facies was apparently autobrecciated under its own lateral momentum, after compaction and sintering processes were essentially complete.

These unusually abrupt transitions in eruptive behavior and deposit characteristics are attributed to: (1) rapid draw-down and highly efficient fragmentation, as evidenced by numerous, coarse-grained plutonic lithics and abundance of fines, (2) large-scale eruption column instability due to a brief phreatomagmatic episode, (3) marked volatile and rheological contrasts during tapping of this zoned system, and (4) rapid, proximal emplacement of tephra into a narrow paleovalley, that favored retention of heat and dominantly upward expulsion of escaping gas and fluidized fines.

References:

Horn, M. and Moore, J.M., 1986, Numerical simulation of ash fountaining on Venus, Earth, and Mars; EOS (abst.), v. 67, p. 1246.

Landi, P., 1987, Un esempio di zonatura composizionale in camere magmatiche superficiali: l'eruzione piroclastica alcalino potassica di Pitigliano (Volcano di Latera); Rend. Soc. Ital. Mineral. Petrol., v. 42, p. 123-140.

HIGH-TEMPERATURE FLOW BANDED ASH-FLOW TUFFS : A REVIEW OF OCCURRENCES IN SOUTHERN AFRICA

TWIST, D., Bushveld Research Institute, University of Pretoria, Rep. of South Africa., BRISTOW, J.W., DBCM Geology Dept, Box 47, Kimberley, RSA, VAN DER WESTHUIZEN, W., Geology Dept, UOFS, Bloemfontein, RSA

In recent years field studies have lead to the recognition of dacitic to rhyolitic flow units which show characteristics of both ignimbrites and lavas. In particular these rocks show laminar flow structures and have been referred to as rheo-ignimbrites or high temperature ash flows (HTAF's). Previously, viscous flow structures were recognised in locally developed peralkaline volcanic complexes leading to the term rheo-ignimbrite.

Dacitic to rhyolitic rocks with laminar flow structures show (i) extensive lateral extent (substantially greater than rhyolite lava flows), (ii) low aspect ratios, (iii) fiamme and eutaxitic textures (generally rare), (iv) broken phenocrysts, (v) a high degree of welding, (vi) flow banding and folding, (vii) ramp structures, (viii) vesicular zones and lithophysae, (ix) autobreccias in the upper zone or surface and (x) a paucity of air-fall deposits: i-iv are typical of ash-flows, whereas v-ix most commonly occur in lavas.

HTAF's have now been recognised on at least four continents, in associations dating from the Archaean to the Tertiary, but this style of volcanism is particularly characteristic of southern Africa. Examples include the provinces of Etendeka, Erongo and Sinclair (Namibia), Lebombo, Soutpansberg, Rooiberg (Bushveld Complex , RSA) and Ventersdorp (RSA) and Nuanetsi (Zimbabwe). The Lebombo and Rooiberg, are among the greatest accumulations of siliceous volcanic rocks on Earth. Similar rocks occur in Australia (Springs Well Tuff), Brazil (Parana), USA (Trans Pecos, Snake River), Ethiopia and elsewhere.

The associations range from dominantly basaltic to dominantly rhyolitic, though bimodalism is present in most cases. All the provinces were emplaced in continental settings and all apparently formed during periods of crustal extension. Two compositional end members are defined, one peralkalic ("Erongo-type") and one sub-alkalic or mildly alkalic ("Lebombo-type"). The flows apparently represent the eruptive equivalents of both I- and A-type granitic magmas.

Where available, temperature estimates are always unusually high and indicate a range from 850degC to perhaps >1100degC. As temperatures increase, the eruption mechanics become increasingly obscure. The Rooiberg Province is regarded as the high-temperature end-member of a continuous spectrum: it was partly emplaced at super-liquidus temperatures and is the most enigmatic member of the suite. In general, associated mafic magmatism is considered as the heat source and driving mechanism for this style of volcanism.

In the field, the greatest difficulty lies in distinguishing HTAF's from rhyolitic agglutinate. We favour emplacement by outwelling or boiling over (rather than column collapse) of a minimum-volatile pyroclastic medium. Plinian cloud eruption and column collapse would have lead to excessive heat loss and development of air-fall deposits which are rarely found in the rocks described here.

THE ROOIBERG FELSITE (BUSHVELD COMPLEX): TEXTURAL EVIDENCE PERTAINING TO EMPLACEMENT MECHANISMS FOR HIGH-TEMPERATURE SILICEOUS FLOWS

TWIST, D., Institute for Geological Research on the Bushveld Complex, University of Pretoria, Pretoria 0002, South Africa, and ELSTON, W.E., Department of Geology, University of New Mexico, Albuquerque, NM 87131

Considerable debate has recently focussed on the nature and origin of extensive siliceous flows that show the characteristics of both lavas and ignimbrites. One of the most spectacular and perplexing manifestations of this style of volcanism, the Rooiberg Felsite, is an integral part of the ca. 2.05 b.y. old Bushveld igneous province.

The Rooiberg is the later and more voluminous component of a bimodal volcanic suite erupted prior to the high-level emplacement of the Bushveld plutonic phases. The earlier eruptives comprise mainly basaltic andesites, whereas the 5 km thick Rooiberg succession is composed principally of dacites and rhyolites.

Like similarly enigmatic eruptives described in southern Africa (e.g., Lebombo) and North America (e.g., Snake River), the Rooiberg flows form extensive sheets, only rarely contain lithics and fiamme-like structures, and are often flow-banded. Some units exhibit distinctive, highly vesicular flow-top zones. Autobrecciation is seen at flow tops but never at the bases. High fluidity is evidenced by the intimate mixing of sandy and basal flow materials in areas where the flows crossed unconsolidated sediments.

Phenocrysts rarely exceed a few percent of the mode and are sometimes completely absent. The phenocrysts are often highly resorbed. Some, perhaps many, may have grown in the melt after eruption.

Matrices are variable, but often only weakly devitrified. They sometimes contain a bewildering variety of extremely thin, elongate crystal forms (dendrites), which may be straight or curved, simple or branching. Swallow-tailed crystallites are also common. Using Lofgren's experimental observation base, it is inferred that: 1. Flows with these textures crystallized at high degrees of supercooling from superheated melts (i.e., melts in which all the crystallization nuclei had been previously destroyed, probably at temperatures >1100 degrees C); and 2. Certain crystallites could only have grown during the initial phase of liquid-state cooling, and not during a later solid-state devitrification.

These observations suggest that the flows must either represent true lavas and the fiamme-like structures are not collapsed pumices, but rather flattened agglutinate material; or, the felsites were emplaced as extremely hot particulate ash-flows, in which the particles themselves were essentially composed of (? supercooled) liquid. The eruption mechanics must then have enabled this material to spread across vast tracts of landscape with minimal temperature loss, eventually compacting well above the softening temperature of glass.

THE GENESIS OF CRETACEOUS BASANITES FROM THE CALCAREOUS ALPS (AUSTRIA): EXPERIMENTAL, GEOCHEMICAL AND FIELD CONSTRAINTS

ULMER P., TROMMSDORFF V., and DIETRICH, V.J., Department of Earth Sciences, ETH-Zentrum, CH-8092 Zürich, Switzerland

Basanite dikes (local name: Ehrwaldite) of Mid-Cretaceous age occur over a distance of at least fifty kilometers in a narrow, east-west trending zone within the Austroalpine Mesozoic cover nappes of the Northern Calcareous Alps (NCA). The dikes intruded when the NCA were still part of the Austroalpine continental basement far away from a possible Penninic subduction zone. After emplacement the dikes were subjected to "non-metamporphic" conditions of $\leq$120C and $\leq$1kbar as a consequence of nappe transport. A Horst-Graben-system, possibly related to transform fault zones, is proposed to account for the ascent of the basanitic melts. .

The dikes vary in mineral content from olivine (fo_{91-87}, Ni 2000 - 3300ppm) + Ti-cpx basanites to slightly more evolved basanites which also contain kaersutite and Ti-biotite. Minor phases are picotite (only as inclusions in olivines and their pseudomorphs), Ti-magnetite, ilmenite, apatite, carbonates, and sulfides. Primitive ne-normative (ne = 11 - 17, x_{Mg} = 0.74) bulk compositions of the rocks are demonstrated by: (in wt%) SiO_2=39, TiO_2=3.2, Al_2O_3=12, FeO_{tot}=10.5, MgO=12.5, CaO=12.5, Na_2O=2.2, K_2O=0.9, P_2O_5=0.8 and by trace elements (in ppm) Nb=90, Zr=300, Y=20, Sr=1000, Ba=650, Rb=20, La=75, Ce=125, Yb=1.45, Lu=0.18, Ni=325, Cr=440, F=1000. ($^{87}Sr/^{86}Sr$), average 0.7034 and ($^{143}Nd/^{144}Nd$), average 0.51280, corresponding to εNd=+4.5.

Mantle inclusions within the dikes are common but do not exceed 5vol%. They comprise olivine, sodium bearing clinopyroxene (Na_2O = 1.1 - 1.4wt%, Al_2O_3 = 3.5 - 9wt%, x_{Mg} = 0.867), Cr-spinel, and minor orthopyroxene (Al_2O_3 = 2.6wt%, x_{Mg} = 0.873). Inclusions of garnet-pseudomorphs occur within some of the clinopyroxene xenocrysts. Minimum P-T conditions of 25kbar and 1250C are inferred from the xenolith assemblage.

Piston cylinder experiments were performed on powders of the natural basanites containing 4.2 wt% H_2O at 15 - 25kbar and 1000 - 1400C in sealed graphite-containers. Phase relations and mineral compositions obtained from these experiments indicate the same minimal P-T conditions for mantle-melt equilibration as those inferred from the xenocryst assemblage. Kaersutite was observed as a stable phase up to temperatures between 1150C and 1200C at all pressures investigated to date. The presence of kaersutite may play an important role in the differentiation of basanitic melts. High temperature kaersutites are K-rich (K_2O = 1.68 - 1.95) and have higher K_2O-contents than their coexisting melt phase (K_2O = 1.2 - 1.4 at 1150C), thus increasing the Na/K-ratio in the differentiated liquids.

Comparison of the obtained geochemical data with those of other basanites to olivine nephelinites from Europe and worldwide shows striking uniformity. The data demonstrate similarities in the mantle source rocks and in the melting characteristics with European alkaline rocks of different age and from different localities.

MAGMATIC EVOLUTION OF A MID-PROTEROZOIC CONTINENTAL RIFT: GIANT DYKES, DYKES AND RING-COMPLEXES OF THE TUGTUTOQ LINEAMENT, S. GREENLAND

UPTON, B.G.J., Geology Department, University of Edinburgh, Edinburgh, EH9 3JW, Scotland.

Genesis and emplacement of a remarkable suite of alkaline rocks accompanied trans-tensional tectonism in southern Greenland during the mid- Proterozoic. The Tugtutoq lineament, inferred to be a deeply eroded continental rift, is defined by faulting, an elongate gravity high and alkaline intrusions composing a dyke-swarm and 'central type' intrusive complexes.

An evolutionary sequence of intrusions ranging from early (transitional) olivine basalts and hawaiite, to late trachytes and comendites, is ascribed to crystal fractionation of a deep (or sub-) crustal mafic magma reservoir. A crude correlation between decreasing dyke widths (c. 500m to <5m), increasing degree of fractionation (basaltic to comendite) and time is related to progressive fractionation of the parent magma body at depth and to diminishing extensional stress. The latest intrusions (of quartz trachyte and comendite) were by ring-faulting and stoping, producing a high-level (sub-volcanic?) ring complex.

Two major intrusive events involving basaltic/hawaiitic magmas initiated the rifting and gave rise to the Older and Younger Giant Dyke Complexes (OGDC and YGDC) respectively. These underwent closed-system fractionation to produce peralkaline salic differentiates.

Sidewall crystallisation in the OGDC produced a stratified residual magma that yielded a suite of syenites grading up into sodalite foyaite. Congelation of the YGDC involved formation of convecting cells several hundred m wide, by up to 3 Km length and of unknown vertical extent, with concomitant production of series of layered cumulates. Of these, the most primitive have the cumulus assemblage ol + plag: more evolved cumulates have ol + plag + FeTi ox + ap assemblages, with later acquisition of cpx. The overall evolution is from gabbroic through ferro-syenogabbroic to syenitic cumulates. Unlike the OGDC, LT residues from the YGDC involved both silica over- and silica under-saturated peralkaline rocks.

THE IMPORTANCE OF MULTIPHASE, COMPRESSIBLE, AND TURBULENT FLOW IN ERUPTION COLUMNS, PYROCLASTIC FLOWS AND SURGES

VALENTINE, G. A. and WOHLETZ, K. H., Earth and Space Sciences Division, Los Alamos National Laboratory, Los Alamos, NM 87545

Because explosive eruptions generally involve the high speed flow of a mixture of solid, liquid, and gaseous materials, the effects of compressibility, interphase coupling, and turbulence are of fundamental importance for interpreting field data. Without an appreciation of these effects, unnecessary explanations for observations may arise that overlook the basic physics.

The bulk density, effective viscosity, and sound speed of pyroclastic flows are in general functions of the proportion of gas to solids. For example, the sound speed for such mixtures may be in the range of several hundred meters per second for very dense (solid volume fraction, $G > 0.4$) or very lean flows ($G < 1 \times 10^{-4}$), but for intermediate solid volume fractions, the sound speed is expected to approximately range from 10 to 100 meters per second. Hence eruption columns, pyroclastic flows, and surges are likely to be internally supersonic even at modest flow speeds. Entrainment of air along flow margins decreases with increasing Mach numbers and may be insignificant for numbers greater than one. Because dusty gas flows are optically opaque for dust concentrations greater than about 1×10^{-6}, observations cannot reveal the bulk flow regime of most pyroclastic flows and surges.

Turbulence increases effective viscosity along with diffusion of heat and mass. Sources of turbulence in high-speed, multiphase flow include: Kelvin-Helmholtz shear instability, Raylelgh-Taylor instabilities caused by body forces, buoyancy effects, differential accelerations, Richtmyer-Meshkov instabilities of shock interactions with interfaces, shock interactions with suspended particles, and interphase drag. Accordingly, it is not appropriate to classify pyroclastic flows as laminar and surges as turbulent. In general, turbulent transport is mathematically expressed by the Reynold's stress tensor, a fundamental term in the equations of motion. Because there is currently no general solution technique for Reynold's stress transport for multiphase flows, it is necessary to simplify the stress tensor by using empirical relationships.

An important aspect of deposition from multiphase flows is the concept of flow relaxation, the time it takes particles and gas to reach thermal and velocity equilibration. For particles in the range of 1 to 10 mm in diameter, flow relaxation time can be greater than several tens of seconds, during which a flow or surge can move over 1 km. Sound signals that permit a flow to react to topography are attenuated greatest in flows that have small relaxation times, are supersonic, or condense water vapor.

Based upon these physical considerations, deposit character must be considered in order to judge the turbulence of flows and surges. The massive depositional character of pyroclastic flows is thought to represent a flow regime buffered between laminar and turbulent, whereas the thinly bedded and heterogeneous nature of surge beds likely results from bulk density and velocity fluctuations over a wide range of flow regimes from relatively dense laminar to turbulent and dispersed flow.

EXPERIMENTAL PYROCLASTIC DENSITY CURRENTS

Vallance, J.W. and Rose, W.I. Jr, Department of Geology, Michigan Technological University, Houghton, MI 49931

Experimental pyroclastic density currents are produced by pouring 1 liter of 600°C ash down an inclined surface (1.8 m long) moistened with water. The objective of the experiments is to simulate natural pyroclastic flows. Flows generated by pouring hot ash on dry surfaces do not behave like pyroclastic flows. Although a thin film of water where the hot ash first contacts the inclined surface is needed to fluidize the ash, the flows subsequently move with equal facility across wet or dry surfaces. These flows are much more mobile than flows generated by pouring either hot or cold ash on dry surfaces. The ash is from a crystal-rich, pumiceous pyroclastic flow, which occurred at Mount St. Helens on 18 May 1980. All particles coarser than granule-size are removed. High frequency temperature and pressure measurements are made with a high speed data acquision system.

The experiments duplicate characteristics typical of pyroclastic flows. Pulsate flow results from unsteady supply of sediment. The first pulses move down slope, gradually become more dilute by incorporating air, then slow and lift off the surface. Because later more sediment-rich pulses overtake earlier pulses as they begin to slow, the flow front exhibits sudden velocity jumps. Unchannelized flows with low aspect ratios exhibit more acute pulsating behavior than channelized flows. Within individual pulses, higher frequency velocity fluctuations could result from gravity instabilities or complex interactions between the basal avalanche and the ash cloud. Pressure measurements show larger fluctuations with frequencies similar to those of major velocity pulses and smaller fluctuations with frequencies similar to those of high frequency velocity pulses. Flow fronts develop cleft and lobe structures like those observed at Mount St. Helens on 22 July and 7 August 1980. The flow fronts of unchannelized flow and to a lesser extent channelized flow exhibit piecemeal ejection of coarser, lower density particles. We observe three parts to a moving flow: a sediment-rich, basal avalanche, a low density, overriding ash cloud surge, and a convecting plume of fine ash and gas. The basal avalanche develops by gravity segregation of coarser and denser particles from the inflated mixture of gas, vapor, and ash in the source area. As the flow moves down slope, the boundary between the basal avalanche and the ash cloud above sharpens. Concurrently a strong thermal gradient between the avalanche and the overriding parts of the flow develops. At 60 cm from source the temperatures 0.5 and 3.5 cm above the inclined surface are 400°C and 250°C, whereas at 112 cm the temperatures are 400°C and 100°C. Away from source where the flow is fully segregated, the front of the basal avalanche forms a bulbous head, and fine-grained ash streams behind in its wake. The interface between the avalanche and the ash cloud is more diffuse near the flow head because of elutriation and better defined in the trailing parts of the flow. When accelerating forces are reduced (decreased slope) or retarding forces increased, the basal avalanche may slow so that the ash cloud surge detaches from and outruns it.

The overlapping, lobate deposits of the flows have digitate distal margins, commonly with concentrations of coarse particles. Despite their unsteady nature, the flows produce a layer-2 analogue: crystal-rich at the base, coarse lithics most common in the basal half, and coarse pumice most common at the top of the deposit. The ash cloud surge probably forms the very fine grained, glassy layer at the top of the deposit that may be analogous to layer 3. A thin veneer of very fine grained glass and sparsely scattered coarse particles is deposited when the ash cloud surge outruns the avalanche. An exact analogue to a fines-depleted layer 1 is not observed. Nevertheless, observations suggest piecemeal ejection of coarser particles from the flow front as a process that could produce both fines-depleted deposits and lateral levees in natural pyroclastic flows. High energy flows with low aspect ratios may form extensive blankets of fines-depleted deposits in front of the main body of the flow by means of this process, whereas lower energy channelized pyroclastic flows may simply drop coarser particles at their margins.

CYCLIC, BIMODAL VOLCANISM IN A CONTINENTAL VOLCANIC ZONE, SOUTHWESTERN NEW BRUNSWICK, CANADA

VAN WAGONER, N.A., DADD, K.A., BALDWIN, D.K. and McNEIL, W., Department of Geology, Acadia University, Wolfville, N.S., B0P 1X0, Canada.

The coastal volcanic belt of the northeastern United States and New Brunswick comprises a bimodal sequence of marine to subaerial Silurian and Early Devonian volcanic rocks. We determined the physical and chemical volcanology and interpreted the tectonic setting of the northern extension of this belt, exposed along the coast of Passamaquoddy Bay, southwestern New Brunswick. This belt comprises about 180 km^2 of intercalated littoral to subaerial bimodal volcanic and sedimentary rocks, forming a 4 km thick section that is intruded by the St. George Batholith and overlain unconformably by the coarse alluvial deposits of the Late Devonian Perry Formation.

Bimodal, mafic-felsic volcanism occurs in four cycles. Mafic volcanism accompanies felsic volcanism in each cycle with felsic units being most voluminous in all but the final cycle where mafic flows dominate over small felsic intrusions. Sedimentary rocks are interbedded with the volcanic rocks throughout the sequence but predominate in the final cycle which likely represents waning stages of volcanism.

Hawaiian, Strombolian, Plinian and Vulcanian eruptive systems are represented. The mafic units form flow, scoria cone, phreatomagmatic tuff cone, and peperitic breccia deposits. The felsic units were emplaced as welded and nonwelded air fall, ash cloud, ground and base surge, and pyroclastic flow deposits, as well as lava flows and domes. Facies analysis and unit morphology indicates eruptions from multiple small volcanic centres. The basaltic flows, however, consistently flowed from the N and NE to the S suggesting eruption from a single rift system.

The sedimentary rocks are mainly red siltstone and sandstone with plane and cross-bedding and lamination, mudcracks, raindrop imprints, vertical to inclined burrows and a faunal fossil assemblage typical of intertidal conditions. Reworked volcanic rocks are rare. All sedimentary units contain well preserved cuspate and scoriaceous shards, indicating deposition in a low energy environment with rapid sedimentation rates.

The extrusive volcanic rocks display a compositional gap between 58 and 69% SiO_2. The mafic rocks are tholeiitic and both mafic and felsic rocks have a within plate tectonic affinity. Major elements plots of the felsic rocks suggests they are calcalkalic, but the abundances of the immobile elements Y, Nb and Zr, are comparable to those of alkalic to peralkalic rhyolites. The three lower mafic units plot as distinct groups for most immobile trace elements but lie along a single trend with incompatible elements (Y, Nb, Zr) and SiO_2 decreasing upward in the section, and compatible elements (Ni, Cr) increasing upward.

Considering the constraints based on 1) composition of the volcanic rocks, 2) nature of volcanic cycles, 3) thickness of the sequence and the subsidence history, 4) rates of sedimentation, 5) facies relationships, and 6) synvolcanic structures, the most likely setting is a volcanic plain lacking large calderas located within a continental rift.

EVALUATION OF MAGMATIC PROCESSES FOR THE PRODUCTS OF THE NEVADO DEL RUIZ VOLCANO, COLOMBIA FROM GEOCHEMICAL AND PETROLOGICAL DATA

Nicole VATIN-PERIGNON, Pierre GOEMANS, University Joseph-Fourier, Lab. of Geology, URA 69, 15, rue Maurice Gignoux, 38031 Grenoble Cedex, France and Richard A. OLIVER, ILL, 156 X, 38042, Grenoble Cedex, France

The Ruiz eruptive products form a series varying from basaltic andesites to dacites that display the characteristic features of subduction-related calc-alkaline volcanism. Minor and trace element concentrations show pronounced differences separating the Old Lavas (O.L.>1Ma) from the Young Lavas (Y.L. <0,5Ma) and from Pleistocene, Historic and the November, 1985 heterogeneous pumices. Many trace elements vary systematically in concen tration from basaltic andesites to dacites. It is noticed the enrichment of the LILE, Rb, Ba, Th and K and the HFSE, Nb, Zr and Hf. In contrast, P, Ti and Tb decrease regularly whereas LREE remain relatively constant. The highest concentrations of Zr, Hf and Nb in acid andesites and dacites are consistent with small amounts of zircon as accessory mineral phase. dacites tend to be most depleted in P and Ti suggesting apatite, titanomagnetite and ilmenite fractionation. Th is chosen as the most convenient differentiation index as it gives the higest Th max/Th min ratio for the immobile Highly Hygromagmaphile (H.HYG) ele ments. The flattening of the La-Th and Ce-Th correlations indicate that differentiation is accompagnied by incorporation of these ele ments in crystallizing phases. The excellent Hf/Zr linear correlation yields a Zr/Hf ratio of 33.8, close to the chondritic value of 34 (Shima 1979). A fractionation models has been tested using the least squares method of Wright and Doherty (1970). The least diffe rentiated lava in the Ruiz series was chosen as parent magma (Th=2.66 ppm). Results show low least-squares residuals. Modeling for the O.L. support fractional crystallization of 31.6 % Pl + 17.9 % Opx + 3.4 % Mt + 2.5 % Cpx + .9 % Ol + .8 % Ilm to from andesites. For Y.L., modeling utilized pumices from the March, 1595 and the November, 1985 eruptions and mineral compositions derived by electron microprobe analyses. Good results are provided with low residuals to evolve from andesites (Th = 6.2 ppm) to dacites (Th = 10.7 to 16.6 ppm). The degree of crystallization required is around 20 % and the crystallizing minerals are considerate to be Pl + Cpx + Opx + Mt (+ Ilm + accessory phases). The distribution coef ficients of Th for these minerals are estimated to be less than 0.01. Bulk distri bution coefficients (D) have been calculated by slopes of least-square regression lines on logarithmic diagrams and the highly incompati ble element (Th) taken as a reference (Treuil and Varet, 1973 ; Allègre et al., 1977 ; Villemant et al., 1981). The evolution of O.L. and Y.L. indicates that the fractional crys tallization process is dominant. The contami nation is not likely to be an important process in the series.

GROUND DEFORMATION STUDIES IN THE AEOLIAN ISLANDS (SOUTHERN TYRRHENIAN SEA, ITALY): THE LIPARI-VULCANO ERUPTIVE COMPLEX

VELARDITA R., C.N.R., International Institute of Volcanology, V.le Regina Margherita, 6, 95123, Catania, Italy
FALZONE G., C.N.R., International Institute of Volcanology, V.le Regina Margherita, 6, 95123, Catania, Italy
PUGLISI B., C.N.R., International Institute of Volcanology, V.le Regina Margherita, 6, 95123, Catania, Italy
VILLARI L., Earth Sciences Institute, University of Messina, Contrada Papardo, 98166 Messina-S.Agata, Italy

The Aeolian Islands Volcanic Arc is characterized by an high level of risk due to the presence of the active volcanoes Stromboli and Vulcano. This condition is aggravated by the considerable population increase close to these volcanoes. For this reason a monitoring program of the volcanic activity in the area has been developed through the study of both geophysical and geochemical parameters. Among the monitored geophysical parameters the ground deformation studies have revealed to be one of the most valuable tool to control volcanic activity. Interesting informations have been collected since 1975 both on the horizontal and vertical component of ground deformations by means of periodical EDM (Eleptrooptical Distance Measurements) surveys on two trilateration networks located on the islands of Lipari and Vulcano, and by means of continuously recording bore-hole tiltmeters.

Two seismic sequences of some importance, the Gulf of Patti seismic crisis in 1978 and the 1985 seismic swarm in the island of Vulcano, took place in the considered time lapse. Variations of the deformation parameters have been observed in good correlation with the seismic events and the geochemical parameter variations.

Recently important modifications of the temperature and gas composition of fumaroles at Vulcano have been recorded, which have not been accompanied by strong modifications of the monitored geophysical parameters (seismicity, ground deformation, gravity) except for the tilt signal correlated with the increase of local seismic activity. Furthermore a dilatation of the volcanic edifice of "La Fossa" (Vulcano) was observed from December 1987 to April 1988.

In the light of the past observations an analysis of the more recent data is proposed giving particular consideration to the "Special Surveillance Plan" on Vulcano during the Summer 1988 which has been prompted by the geochemical parameters variations observed since the end of 1987.

STABILITY OF VOLCANIC BUBBLY FLOWS : IMPLICATIONS FOR BASALTIC ERUPTIONS

Sylvie VERGNIOLLE and Claude JAUPART
Laboratoire de Dynamique des Systèmes Géologiques
Université Paris 7 et Institut de Physique du Globe
4 place Jussieu
75252 Paris Cedex 05 FRANCE

Fluid dynamical models of volcanic eruptions are usually made in the homogeneous approximation where gas and liquid are constrained to move at the same velocity. Basaltic eruptions exhibit the characteristics of separated flow, where the gas phase moves with respect to the liquid phase. We use the two-phase flow equations to investigate the behaviour and stability of basaltic bubbly flows, such as those observed during effusive flank eruptions at Kilauea volcano.

The behaviour of the system is determined by the sign of $E=\rho_1 v_1^2 - \rho_2 v_2^2$, which is a measure of the difference between the kinetic energies of the liquid and gas phases respectively. In bubbly flows, the gas phase velocity is the sum of the liquid phase velocity and the bubble rise velocity which depends on the bubble size. If E is positive, the energy is in the liquid phase, which corresponds to small bubbles. If E is negative, the energy is in the gas phase, which corresponds to large bubbles. During the ascent in the volcanic conduit, the velocity of the gas phase increases more rapidly than that of the liquid phase, due to pressure release which acts to enlarge bubbles. Thus, if E is initially negative, it stays negative. If it is positive at depth, it may become negative during ascent. In this event, a movement with kinetic energy initially in the liquid phase changes to a movement with kinetic energy in the gas phase. This transition is highly unstable and is accompanied by very large variations in the flow parameters (velocity, bubble size, pressure gradient) for small variations in conditions at the conduit entry. Such unstable behaviour is not observed in volcanic bubbly flows, which provides constraints on the flow conditions and parameters at depth. For a given liquid velocity, it is possible to calculate the range of bubble diameters, which leads to unstable behaviour. For example, bubble sizes in the approximate range of 1-10 cm, are not allowed in a Hawaiian effusive phase. Conversely, knowing the bubble size in an erupted sample, it is possible to calculate a lower bound for the liquid phase velocity.

LATE PRECAMBRIAN MAFIC DYKE SWARMS OF THE ALDAN SHIELD.

VERKHALO-UZKY,V.N. Institute of Precambrian Geology & Geochronology, the USSR Academy of Sciences, 199034, nab. Makarova 2, Leningrad, USSR.

The dyke sets of the Aldan shield ranging in age from the Archaean to Mesozoic are dominated by Late Precambrian mafic dykes. They define major swarms up to 600 km long and circa 100 km wide with the predominant NE- and NW-trending sets in the western and eastern Aldan shield respectively (Fig.1). Individual dykes reach 12-15 km in length and 0.1-0.3 km in width, most abundant being 0.1-2.0 km long and 0.5-20m wide. Vertical and subvertical dykes are common to mark the faults in Archaean-Proterozoic metamorphic terrains; the sills cutting unmetamorphosed Proterozoic rocks and rapakivi-like granites (1860 Ma) occur only in the south-eastern and western shield.

The dykes and sills are dolerites, gabbro-dolerites, quartz and microgranophyre dolerites. The major dykes show zoning either with middle-grained gabbro-dolerites in the central and fine-grained dolerites in the outer parts, or dolerites and doleritic porphyrites respectively. Chilled margins up to 1-10 cm thick composed of vitrophyric dolerites occur. They also constitute thin dykes and apophyses. The rocks are fresh and show ophitic, gabbro-ophitic, doleritic and micropegmatitic textures and contain Cpx and Pl, often Qu, rarely Opx; microgranophyres contain KFsp. Accessory minerals are apatite, sphene, zircon, magnetite, Ti-magnetite, pyrite. The diabase dykes with relict ophitic texture and primary minerals totaly replaced by amphibole, epidote, chlorite, albite, calcite form an independent, probably an earlier age group.

Petrochemistry shows compositional differences in the near-contact and central parts of major dykes, the absence of essential compositional differences in the dykes from the NW- and NE-trending swarms at significant chemical variations within single fault structures.

The age of dykes is defined by their cross-cutting relations with sedimentary and igneous rocks dated at 2.0-1.65 Ga. K-Ar dates available range from 1400 to 850 Ma.

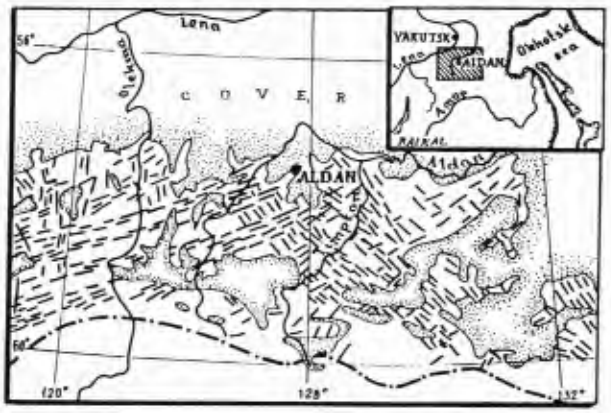

ORIGIN AND EVOLUTION OF THE EASTERN PART OF THE MEXICAN VOLCANIC BELT, MEXICO

VERMA, S.P., Max-Planck-Institut für Chemie, Abt. Geochemie, D6500 Mainz, F.R. Germany and (present address) Depto. de Geotermia, Div. Fuentes de Energía, Instituto de Investigaciones Eléctricas, Apdo. Postal 475, Cuernavaca, Mor., 62000, Mexico.

The Mexican Volcanic Belt (MVB) and the Middle-America Trench (MAT) are not parallel to each other. In fact, the distance between them increases from west to east. The volcanism in the Eastern part of the belt is located at more than 400 km from the trench. Concerning the origin of the MVB most workers associate it with the subduction of the Cocos plate along the MAT. However, other researchers have proposed that strike-slip faulting and rifting along the MVB actually control the associated volcanism.

One of the most conspicuous features of the Eastern MVB is the basin of Serdán-Oriental which is bounded on the east by Pico de Orizaba and Cofre de Perote and on the west by Volcán La Malinche. Two prominent structures are located in this basin: in the north the well-studied Los Humeros caldera and in the center at about 50 km S of the former, the Las Derrumbadas rhyolitic twin domes. The latter are surrounded by numerous cinder cones, lava flows and maars. The style of volcanism in these two parts of the basin is different, namely, while in Los Humeros all rock-types from basalt to rhyolite are present, in Las Derrumbadas clear compositional gaps persist.

New major and trace element and Sr, Nd and Pb isotope data are obtained from both areas in the Serdán-Oriental basin. Furthermore, geochemical data have also been published on several other volcanic centers in the Eastern MVB.

Models of fractional and equilibrium melting on possible mantle mineralogies, on mantle and lower crustal xenoliths from Mexico as well as Morb-sediment sequence (DSDP Sites 487 and 488) from Cocos plate near the MAT are developed in order to understand the genesis of parental magmas in the MVB. These are complemented by models of fractional crystallization with or without crustal assimilation (using new geochemical data on granitic-granodioritic Teziutlán Formation, limestone and other sedimentary outcrops in the MVB) to further constrain the origin and genetic relationships of mafic and evolved magmas in the Eastern MVB.

In the Los Humeros area, published and new $^{87}Sr/^{86}Sr$ ratios range from 0.7034-0.7040 for basalts (n=6), 0.7040-0.7044 for basaltic andesites (n=12), 07040-0.7046 for andesites (n=8), 0.7041-0.7043 for dacites (n=5), to 0.7040-0.7048 for rhyodacites and rhyolites (n=7). On the other hand, in the Las Derrumbadas area, the $^{87}Sr/^{86}Sr$ ratios vary from 0.7040-0.7046 for basalts (n=5), 0.7043 for basaltic andesite (n=1), 0.7047-0.7050 for andesites (n=4), to 0.7045-0.7053 for rhyolites and obsidians (n=11). For comparison, the published Sr isotope ratios for basalts to dacites from the Pico de Orizaba range from 0.7039-0.7050 (n=18).

On a Sr-Nd isotope diagram, the samples from the basin of Serdán-Oriental plot on the mantle array, except for one andesite (older than the rhyolitic twin domes) that falls considerably on the left of the negative correlation shown by the other samples. This may indicate the presence of a new source-component sampled for the first time from the Eastern MVB. Furthermore, this andesitic magma shows Pb isotope ratios that are significantly lower than for all other samples studied from this basin.

SALPETERKOP, SOUTH AFRICA: A STRUCTURAL DOME PIERCED BY A CARBONATITE VOLCANO

VERWOERD, W.J. and L. CHEVALLIER, Department of Geology, University of Stellenbosch 7600, South Africa.

Domal uplift as a precursor to volcanism is a well-known phenomenon in the case of basaltic shields, acid to intermediate calderas and carbonatite-nephelinite volcanoes, but kimberlites and diatremes show no such doming. In East Africa doming is mainly evidenced by the attitude of the pre-volcanic granitoid erosion surface. In Brazil, on the other hand, plutonic carbonatite complexes have been emplaced in sedimentary formations and show strong doming of adjacent beds. However, comparatively few examples of carbonatites exposed at the volcanic level are known where a clear relationship with a structural dome in otherwise horizontally bedded strata can be demonstrated.

The Salpeterkop dome, situated 270km NE of Cape Town, is 5,5km in diameter and the vertical displacement is approximately 900m. It has been eroded to form concentric ridges of sandstone and shale dipping 20^{o}-40^{o} outward, whilst steeper dips are encountered towards the middle. The sedimentary rocks are of Permian (Karoo) age and the deformation, on geomorphological grounds, is late Cretaceous or early Tertiary. At the center of the dome is a small caldera, 1,5km across, filled with tuffaceous sediments. The caldera rim consists partly of silicified breccia containing some fragments from the deep-seated basement, and partly of intrusive carbonatite. Carbonatite also intruded radial and tangential fractures as well as bedding planes; the radial fracturing extends to at least 16km from the center. Cone-sheets are not prominent. Other intrusive rocks are minor plugs of olivine melilitite and numerous irregular bodies of clast-rich "K-trachyte", considered to be mobilised potassic fenite.

A two-stage model is proposed in which the doming is ascribed to a subjacent body of carbonatite and its carapace of fenite, followed by central uplift and explosive eruption. The cause of the deformation may be pressure due to the ascent of the magma, thermal expansion, volatile build-up or some combination of these factors. In order to arrive at reasonable assumptions about the shape and depth of the magmatic body, numerical modeling of stress and strain has been carried out, using the finite element method, for three kinds of evenly pressurized sources: a laccolith, a sphere and a columnar diapir. The results are compared with the deformation pattern observed in the field and found to support the two-stage model.

The dome of Gross Brukkaros volcano (10km) and the Hatzium dome (2,4km) in Namibia have several features in common with Salpeterkop. The Richat dome, Mauritania, though much larger (38km), also resembles the Salpeterkop dome. They represent a special category of carbonatites with or without volcanism, in which the cap rocks have been preserved. Doming ahead of intrusion and eruption may well be an essential structural feature of carbonatite emplacement, analogous to the diapiric emplacement of salt domes.

RELOCATION OF THE SEISMIC ACTIVITY AT VULCANO (EOLIAN ISLANDS, ITALY) IN A THREE-DIMENSIONALLY HETEROGENEOUS MEDIUM.

VILARDO, G., Osservatorio Vesuviano; 249, Via Manzoni, 80123 Naples (Italy).
PINO, N. A., Dip.to Geofisica e Vulcanologia, University of Naples; 10, Largo S. Marcellino 80134 Naples (Italy).

P-waves seismic tomography, performed on 1500 first-arrival pickings obtained at a dense (2 stations/sq.Km) digital seismic array, allowed to draw shape and extent of a shallow, high-velocity body beneath the Fossa Grande active volcano in the Vulcano Island (Southern Italy).

The seismicity of the area is relocated in such a very heterogeneous structure (abrupt lateral Vp variations even larger than 1.0 km/s are detected at the same depth, only few kilometers apart) by means of a fully three-dimensional location routine.

Spatial clustering of the events is observed in correspondence of the crater, while use of S-waves by three-component seismographs allows to put stronger constraints on the focal depths of the deeper events, all offset with respect to the volcanic field. An attempt is also made for evaluating the energy release associated to the typical events of the area, in comparison with truly tectonic events occuring close to the island.

In figure are shown the Vulcano Island (A) and the geometry of the top of a 3.0 km/s layer (B), as obtained by the P-traveltimes inversion.

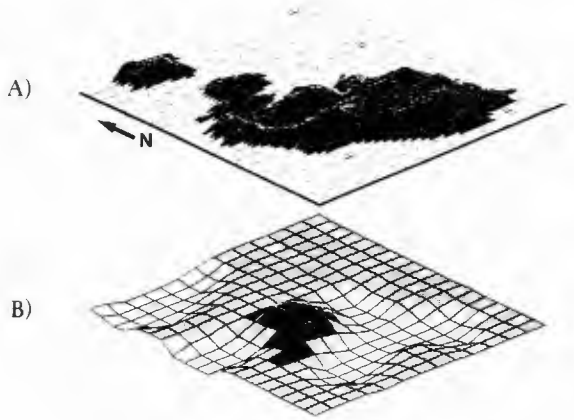

PUNCTUATED EQUILIBRIA : POTASSIC VOLCANOES SHOW 100 ka CLIMAX-GAP-CLIMAX ACTIVITY CYCLES

Igor M. Villa (Istituto di Geocronologia CNR, via Maffi 36, Pisa, Italy)

High-resolution $^{39}Ar/^{40}Ar$ chronostratigraphic data have been obtained for four volcanic centers of the potassic Roman Volcanic Province. The geochemical implications of the ubiquitous presence of excess Ar are discussed elsewhere (Villa 1987). We shall concentrate here on the geochronological results. The ages transcend local interest because they reveal a common pattern, which is seen here for the first time owing to two very favorable circumstances: the presence of K-rich minerals, such as sanidine and leucite, which make possible Ar-Ar dating of Quaternary lavas with a precision of 1% or better, i.e. allow to resolve events 10 - 20 ka apart over the last Ma; and the existence af a detailed stratigraphical,volcanological and geochemical framework to insert the dates into.

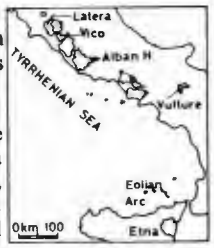

Vùlture. The lowermost outcropping unit consists of phonolitic-trachytic ignimbrites, on which a sanidine plateau age of 740 ± 15 ka was obtained by Villa (1986). They are *immediately* overlain by a pyroclastite having transitional chemistry (phonolitic-tephritic), whose saddle spectrum requires an age < 640 ka, and by a 500 m - thick pile of tephritic to foiditic lavas, lahars and pyroclastites. A dozen leucites & sanidines yield plateaus or saddles; all ages fall in the range 590 - 630 ka (Villa,1986).

Alban Hills. The Villa Senni leucite-tephritic marker tuff (351±15 ka, recalculated after Radicati et al, 1981) covers most of the area, and the formation immediately underlying it has not been recognized beyond doubt. Immediately above it, about 20 mostly leucititic major fissural lava flows are known; out of 10 that were dated, nine are 260-280 ka old, and one 170 ka (Funiciello &Villa, in prep.).

Làtera. Seven or eight ignimbritic units were erupted successively (Sparks, 1975). The lowermost one ("A") is a trachite yielding a plateau age of 248 ± 2 ka (Villa, 1988). Two further Ar-Ar age spectra on ignimbrites ("E" and a small one between "A" & "B") have yielded two indistinguishable plateaus at 250 ka (Landi & Villa, in prep.) while the last one, phonolite "G", has a consensus K/Ar age of 160 ± 5 ka (Barberi et al, 1984). Cinder cones and lava flows overlying "G" have unchecked K/Ar ages; their compositions range from olivin-latites to tephritic leucitites.

Vico. As described in detail by Laurenzi et al (this volume), four activity phases are easily discriminated; each phase lasts 20-30 ka at most and is followed by a 100 ka gap. A very important finding is that one 80 cm thick paleosoil formed in less than 7 ka, under the then prevailing climatic conditions.

Conclusions. In those instances where sampling was frequent enough, potassic volcanoes appear to erupt climactically, with activity phases of 20 - 40 ka alternating with quiescence periods of 80 - 100 ka. During a climax, the chemistry of the erupted rocks appears to follow one single evolutionary trend. After the climax, activity plummets for a comparatively long period (of the order of 100 ka in four cases out of 4) and resumes with products that may have a different chemistry and a different eruption mechanism. All this suggests that magma chamber recharge may be the dominant phenomenon in determining both the length of the stasis and the chemistry of the subsequent eruptive climax.

GROUND DEFORMATION AT MT. ETNA (SICILY-ITALY) SINCE 1978: CORRELATIONS WITH THE SEISMIC AND VOLCANIC ACTIVITY

VILLARI L., Earth Sciences Institute, University of Messina, Contrada Papardo, 98166 Messina-S. Agata, Italy
FALZONE G., C.N.R., International Institute of Volcanology, V. le Regina Margherita, 6, 95123 Catania, Italy
PUGLISI B, C.N.R., International Institute of Volcanology, V.le Regina Margherita, 6, 95123, Catania, Italy
VELARDITA R., C.N.R., International Institute of Volcanology, V.le Regina Margherita, 6, 95123, Catania, Italy.

Since 1978 the horizontal and vertical component of ground deformation have been sistematically investigated by means of periodical EDM (Eleptrooptical Distance Measurement) surveys and continuously recording bore-hole tiltmeters.
The trilateration networks are located respectively on the southwestern, the southern and the north eastern flanks of the volcano.
The bore-hole tilt stations have experienced destructive episodes due to both volcanic activity and very adverse weather conditions which often characterize the hight altitude at Mt. Etna. Despite these problems the tilt stations have provided valuable informations on the activity state of the volcano. Peculiar frequency components have been investigated in the tilt signal of different stations, which can be correlated with different phases of volcanic activity.
With respect to the horizontal component of ground deformation, the observed pattern deduced from the trilateration data results very complex, clearly due to the very active dynamics that affected the volcanic structure since 1978.
The peculiar observed behaviour of the different sectors of the volcanic edifice, appears to proceed from many interesting factors, namely: i) relative location of the trilateration networks with respect to the structures mobilized by magma intrusion and uprise; ii) injection, uprise and eruption m chanism; iii) presence of preexisting structural discontinuities which constrain stress propagation.
The observed deformation pattern has been then compared with both the eruptive and the seismic activity occurring in the etnean area during the concerning time lapse.
Much emphasis is given to the more recent data, with the aim of contributing to the present state of the volcano knowledge.

U-Th DISEQUILIBRIUM IN K-RICH VOLCANISM SOURCES IN ITALY (LATIUM, CAMPANIA and EOLIAN ISLAND ARC).

VILLEMANT B. and FLEHOC C., Université Pierre et Marie Curie, T26/16 E3
4 pl Jussieu 75256 Paris Cedex 05 France

A Systematic study of trace elements characteristics and Th-U disequilibrium of primary magmas has been performed in the recent potassic volcanism of Latium (Vico, Vulsini, Ernici), Campania (Phlegrean Fields, Somma Vesuvius, Ventotene Island) and Eolian Island Arc (Stromboli). The magma sources are characterized by strong Th-Ta fractionation with increasing Th/Ta ratios from the South(10) to the North (50) of the whole potassic province. The variations of this ratio are correlated to the variations of Sr and Nd isotopic ratios.
Strong variations of the Th/U ratio occur in most of the studied magma series. Many processes may produce these fractionations. Interaction of the magmas with hydrothermal fluids produces U enrichments (Vesuvius, Stromboli) or U depletions (Vico,VentoTene, Stromboli) relative to Th. These U enrichments or depletions depend probably on the fact that interaction occur at surficial or deep levels of the crust and on the oxygen fugacities. In some favourable cases the evolution of the initial $^{230}Th/^{232}Th$ ratios of the magmas can be estimated giving the initial Th/U ratio of the magma source. This is well illustrated by the case of Vico and Vulsini volcanoes showing that a strong U-Th fractionation has occured in the mantle source related to the bulk Th-U enrichment and Th-Ta fractionation of the Latium Province. Conversely, there is no significant Th-U fractionation in the primary magmas of Stromboli. Trace elements systematics indicates a strong variation of the partial melting degree of the mantle source of Stromboli producing the primary melts of the so called H-K, Calk-Alkaline and Shoshonitic series. This shows that partial melting processes are unlikely to produce significant Th-U fractionation in these series. A model of metasomatic enrichment of the Italian magma sources by a silicate melt is proposed to explain the increase of the Th-U and Th-Ta fractionations from the South to the North of the Italian K-rich volcanism.

THE IMPORTANCE OF UPDOMING IN THE FORMATION OF COLLAPSE CALDERAS : SHOULD VON BUCH BE REHABILITATED ?

Pierre M. VINCENT, Université Blaise Pascal, Centre de Recherches Volcanologiques, 5 rue Kessler, 63000 Clermont-Ferrand, France.

Examples from Africa, Corsica and Massif Central (France) show that the ring-fault surrounding the subsided block of a collapse caldera is inward-dipping, becoming vertical with depth. The initial fracture results from an upward pressure (cone-sheet fracture of Anderson), related to a surface doming. The sinking of the funnel-shaped block may begin before any eruption occurs, as a result of the stretching of the roof ("pre-eruptive caldera", or "pre-caldera", Vincent 1963, 1971). After eruption, the collapse takes place because of loss of support - either abruptly (Krakatau type) or step by step, after minor eruptions of which the rythm is controlled by the weight of the truncated cone "stopper", acting as a safety valve (Tibestian type).

The fact of initial up-doming is difficult to ascertain in large resurgent calderas, because of subsequent uplift movements. It is more apparent in some non-resurgent calderas, like in Mont-Dore (France) or in Tarso Voon, Tibesti (Tchad). In this last example, a 80 km large ignimbritic "shield-sheet", the pre-eruptive tumescence is around 800 m high. After caldera collapse, detumescence was prevented - or limited -by "key-stone" sinking, bringing about a lateral compression resulting in concentric folds - a fact long-known from Mull, Scotland.

There is no paradox in caldera geometry if a two-stage mechanism is admitted, the formation of the fracture, related to upward pressure, preceding the subsidence along this fracture at a later stage.

The initial upward pressure may result in multiple fractures, possibly injected by cone-sheet dykes, as in Toon volcano, Tibesti. The stepped fault structure known in some calderas can theorically appear at the pre-caldera stage. This could be the case of the Larderello geothermal field (Italy), with no surface magmatism. Pre-caldera formation offers an alternative explanation for some cases where ignimbrites are thicker on the inside than on the outside of the caldera.

If accepted, this interpretation is a rehabilitation of part of the theory of the "craters of elevation" of von Buch (1819, 1836) and subsequently, Dufrenoy and Elie de Beaumont (1833).

DEVELOPMENT OF GEODETIC MONITORING PROGRAM AT MERAPI VOLCANO, INDONESIA, AND ANALYSIS OF PRECURSORY MONITORING DATA AT MOUNT ST, HELENS VOLCANO, USA: PROGRESS IN TESTING AND APPLYING THE MATERIALS SCIENCE APPROACH TO VOLCANO ERUPTION PREDICTION

VOIGHT, Barry, U.S. Geological Survey and Penn State University, 334 Deike Building, University Park, PA 16802, CASADEVALL, T.J., U.S. Geological Survey, Cascades Volcano Observatory, Vancouver, WA 98661, and CORNELIUS, R., Penn State University, University Park, PA 16802

A central issue in disaster prevention is the prediction of hazardous events through the application of modern science and technology. In a new way of approaching eruption prediction, a mathematical analogy has been drawn between terminal stages of material failure and the precursory behavior of a volcano as it builds toward an eruption (Voight, 1988). Eruption processes may thus be described in terms of a fundamental law that governs material failure (Voight, 1989). Analytical or graphical procedures derived from this law may be used to predict rock "failure", and the attendant eruption, from precursory monitoring data involving geodetic, seismic, and geochemical observations. Despite its promise, the reliability and sensitivity of the method should be further explored for various volcanoes and eruptive styles. Current efforts include (1) the testing of prediction methods against existing monitoring data collections for recorded eruptions; and (2) the design of monitoring systems and baseline networks at specific volcanoes, with the aim to provide a prediction capability for anticipated near-future eruptions and to assist disaster prevention.

In regard to Part 1, prediction reliability is assessed through the detailed analysis of data from Mount St. Helens volcano for 1980 through 1986, involving 19 eruptive events, and carried out with the cooperation of the USGS Cascades Volcano Observatory.

In Part 2 we discuss progress and problems in the establishment in 1988 of a deformation network at Merapi Volcano, Java, accomplished under a cooperative agreement involving USGS, US AID/OFDA, and VSI. As a significant explosive eruption seems likely within the near future (next few years) at Merapi, this site is particularly suitable to test prediction methodology. Current dome volume >5 x $10^6 m^3$ is of concern because hazardous historic eruptions at Merapi have been associated with dome volumes exceeding 3 x $10^6 m^3$. Additional concerns involve signs of potential major slope instability. The monitoring program comprises two parts, an "observatory network" and a "summit network". The summit network was designed to provide details of precursory displacement and strain of the edifice in the near-field of the vent, as well as growth and deformation of the lava dome. An observatory network, using sites at the base of the cone as the principal instrument locations, was designed to assess remotely the movement of a few stations critical to an impending eruption or an unstable slope. Measurement systems considered include theodolites, EDM systems, electronic tilt (currently proposed), and GPS technology. New equipment is needed at Merapi to satisfy requirements for high precision (to detect small strains), and high frequency of observations. Some conventional instruments (e.g. Rangemaster III) appear inadequate due to noise and imprecision. As GPS instruments are unlikely to be dedicated to individual volcanoes, frequency of observation is anticipated as a problem that could hamper the use of GPS for eruption prediction.

Voight, B., 1988, Nature 332(6161):125-130.
Voight, B., 1989, Science 243:200-203.

THE EVOLUTION OF CUICOCHA VOLCANO AND THE VOLCANIC HAZARDS ASSOCIATED WITH IT

VON HILLEBRANDT M., C. G., Instituto Geofísico, Escuela Politécnica Nacional, Casilla 2759, Quito, Ecuador.

Cuicocha Volcano is located approximately 100 km North of Quito in the Western Cordillera of Ecuador. It is the most recent center of emission of the Cuicocha-Cotacachi Volcanic Complex. The activity of this complex extends back into the Pleistocene, while the last eruption of Cuicocha occurred less than 3000 years ago.

Cuicocha Volcano consists of five dacitic domes located in and around a caldera lake whose area is approximately 6 km^2. Four principal phases of activity have been identified:

"D" The first, during which Cuicocha dome was formed occurred more than 3100 years ago. The dome, whose original diameter might have been 1.5 km, consists of oxihornblende dacites.

"C" Huge pyroclastic flow and fall deposits whose volume is calculated at around 4.8 km^3 and the caldera were formed. Dated at around 3100 years before presente.

"B" Consisted primarily of pyroclastic surges and falls. Dated at around 2900 years before present.

"A" Four domes which are located in the interior of the caldera, forming two islands and consisting of hornblende dacites were formed.

Presently the volcano does not demonstrate any signs of reactivation.

Given that the last eruptions of this volcano occurred recently, and that a large population lives in the area of influence, a volcanic hazards map was prepared and published. The following different hazards were evaluated:

1. Pyroclastic flows. They represent the greatest hazard, could affect an area of 200 km^2 determined by combining the limits of the prehistoric flows with those derived from the application of the energy line concept. The resultant risk is great because approximately 50,000 people live in the area of maximum hazard.

2. Lahars. Given the volume of water (.5 km^3) in the caldera, lahars would probably precede and/or accompany the eruption, which could affect the same areas as the pyroclastic flows.

3. Pyroclastic falls. Given that the principal wind direction and the identified fall deposits are westward, the area of maximum hazard from this phenomenom would be in this direction; fortunately very few people live in these areas.

4. Dome formation. This would be an additional danger if they develop on the outside of the caldera, because their collapse and associated pyroclastic flows could also affect the maximum hazard area.

5. Gas emissions. Because the conditions of Cuicocha are similar to those of Nyos and Monoun, Camaroon, there could be an accumulation of toxic gases which could be explosively emitted causing a great catastrophe.

Given this large potential hazard, the Geophysical Institute of the Escuela Politécnica Nacional operates one seismometer and has installed a small EDM net.

FLUORINE GEOCHEMISTRY OF THOLEIITIC TO POTASSIC-ALKALINE ARC VOLCANICS FROM THE BANDA SEA REGION, EASTERN INDONESIA

VROON, P.Z., BERGEN, M.J. van, POORTER, R.P.E., Dept. of Chemical Geology, Univ. of Utrecht, the Netherlands

VAREKAMP, J.C., Dept. of Earth & Environm. Sci., Wesleyan Univ., Middletown (CT), U.S.A.

Fluorine contents of lavas from ten active volcanoes in the Banda Arc (BA) and easternmost Sunda Arc (ESA), including arc-tholeiitic (TH), calcalkaline (CA), high-K calcalkaline (HKCA) and potassic-alkaline (ALK) rock types, largely follow across- and along-arc systematics in potassium levels. Within a NE-SW along-arc chain of six BA centres, dacites from Banda Api (TH) contain 210-370 ppm F, andesites from Manuk and Serua (CA) 80-300 ppm, amphibole-bearing (basaltic) andesites from Nila and Teon (HKCA) 150-610 ppm, and biotite-bearing andesites from Damar (HKCA) 390-490 ppm. Within a S-N across-arc transect of four ESA volcanoes, basaltic andesites from Sirung (TH-HKCA) contain 430-580 ppm, basalts-andesites from Ili Boleng and amph.+-biotite-bearing basalts-andesites from Ili Lewotolo (both HKCA) 400-820 ppm, and tephritic leucitites from Batu Tara (ALK) 1200-2250 ppm. Within-suite variations of F are largely consistent with an incompatible behaviour, but, F often increasing stronger in the absence of hydrous phenocrysts, amphibole destabilization coinciding with a drop in F contents (Nila), and F being strongly enriched in amphibole-rich 'blobs' (Teon), also point to mineral controls during evolution processes (e.g., amphibole and biotite in HKCA rocks contain about 3000 and 5500 ppm F respectively). Despite the evolved character of all rocks, and the possibility of late-stage degassing effects (e.g., medium-temperature fumaroles of Ili Lewotolo contain 0.047 mol% HF), the regional co-variation between F, K and many other incompatible trace elements at similar SiO_2 levels calls for spatial differences in initial F contents of primary magmas. This is particularly evident from the cross-arc systematics in the ESA, culminating in the products of Batu Tara that have by far the highest F and K contents, and at the same time are the most mafic rocks found. Variations in degree of partial-melting of a homogeneous source do not satisfactorily explain our trace-element data, and would not agree with the variations in isotopic ratios known for this region. Our results thus suggest that F reflects spatial variations comparable to other geochemical signatures of the volcanoes around the Banda Sea. Among these, the isotopic data in particular suggest involvement of continent-derived material in magmagenesis. K/F ratios of the hydrous-phenocryst free series are close to those of mantle phlogopites, which may indicate that, if continental material has contributed significantly to F budgets at all, phlogopite has been an intermediate storage medium in source regions.

COMPUTER SIMULATIONS OF LAVA FLOW HAZARDS

WADGE, G.
N.U.T.I.S., Department of Geography, University of Reading, Reading RG6 2AB, U.K.

The path taken by a lava flow depends mainly on the rheology of the magma, the eruption dynamics and the topography over which it flows. A computer program has been written to simulate lava flow using a digital elevation model (DEM) of the topography as the empirical data and the other main factors as interactive variables. The main simplifying assumptions are that the flow can only extend from its distal ends - no proximal overflow or budding is allowed, and the flow boundaries are limited by a minimum thickness (yield strength) criterion. The computational approach is a finite difference initial value type and output is to a computer graphics screen.

Simulations of recent lava flows on Etna have been made using this method. These simulations are reasonably similar to the real flows with two qualifications. Great care must be taken in the construction of the DEM to ensure high precision and accuracy. The simulated results become increasingly inaccurate if the real flow is long-lived with proximal budding of new flows.

The motivation for this work is to seek the ability to predict the path and rate of advance of lava flows so that the hazards it poses can be evaluated. Such an ability could be used in two ways. Firstly, for general forward planning, a number of simulations could be aggregated for a region to estimate the future probabilities of flow coverage. Secondly, the program could be run during an actual eruption to answer questions such as- Given this vent position and current effusion rate, where will the flow front be tomorrow afternoon?

THE GALERAS VOLCANO OF SOUTHWESTERN COLOMBIA. A preliminary paleomagnetic and radiometric study.

WAGNER, J.-J.[1], DELALOYE, M.[1], MONSALVE, M.L.[1,2] and ESPINOSA, A.[2].
1 CERG, Dpt. of Mineralogy, The University, CH-1211 Geneva 4, Switzerland.
2 INGEOMINAS, AA 695, Popayan, Colombia.

This volcano of 4'272 m height is located at a latitude of 1°N and a longitude of 77° 18'W near the town of Pasto in the Department of Nariño. It is a stratovolcano with a horse shoe caldera open towards the west. The central cone, situated near the oriental rim, peaks at 4'180 m and has a diameter of 200 m.

It is one the most alive of Colombia; eruptions are known through documents since the XVI century. The activity was mainly explosive and sometimes effusive. Since January 1988 the fumaroles are more active. A hazard assessment study has been started.

The lavas are of andesitic nature with olivine and two pyroxenes. Some of them are richer in olivine. The amount of SiO_2 varies from 53 to 63%.

The debris avalanches of the occidental area could be related to at least two major events responsible for the collapse which formed the caldera. Products of the blast associated with the most recent event outcrop on the oriental flank. A Carbon 14 age determination of burnt wood indicates an age greater than 40'000 years BP.

Deposits of ash and scoria flows are common around the volcano where one finds also a plinian sequence of ash and pumice. They are cut by many vertical faults witness of a high tectonic activity.

The most recent pyroclastics associated with the central cone correspond to ash fall and breadcrust bombs.

Potassium-Argon dating on the lava flows located on the external flank of the caldera give a general age of about 3.5 Ma. Paleomagnetic directions from the same flows are very stable and are of normal and reversed polarities which is compatible with the age.

RAPID MOBILIZATION OF WINTER-SPRING SNOWPACK DURING ERUPTIONS AT MOUNT ST. HELENS VOLCANO IN 1980-1986 AND AT AUGUSTINE VOLCANO IN 1986

WAITT, R.B., KAMATA, Hiroki, Cascades Volcano Observatory, U.S. Geological Survey, 5400 MacArthur Blvd., Vancouver, WA 98661, and **DENLINGER, R.P.,** U.S. Geological Survey at Department of Oceanography, University of Washington WB-10, Seattle, WA 98195

Between May 1980 and May 1986 several volcanic explosions and related hot mass-wastage events at Mount St. Helens interacted with snowpack to cause huge snow avalanches, snowflows, slushflows, and floods that moved far from the initial sites of interaction. The main causes of snow mobilization are (1) ballistic impacts of explosively impelled dome-dacite projectiles on the steep crater walls and (2) incipient or partial melting of snow by rapidly admixed hot fragmented dome dacite or juvenile pumice.

The cataclysmic pyroclastic surge of May 1980 incipiently melted snow at the turbulent surge base to swiftly form slushflows laden with pyroclastic debris. These flows united downslope into slushy sheetfloods that rapidly melted and transformed into great lahars farther down the volcano flanks.

In March 1982, explosively impelled blocks triggered several simultaneous huge snow avalanches from about a third of the crater walls. These avalanches formed a debris-laden snowflow that traveled 7 km mainly over gentle slopes. Incipient melting transformed the central part of this flow into a fluid slushflow. Meanwhile in the crater, rapid melting by hot juvenile pumice (and erupting gas?) formed a transient lake that overflowed to send a watery pumice-bearing flood downvalley.

In February 1983 and May-June 1984, several separate small explosions and hot domerock avalanches rapidly mixed hot lithic fragments with crater-wall and crater-floor snowpack to rapidly melt snow and form a variety of snow avalanches and flows, slushflows, and watery floods. In April 1982 and May 1986, hot-rock avalanches from the dome interacted with crater-floor snow to form small watery floods. But small pyroclastic flows and surges did not mix with snow and thus melted too-little snow to form secondary slushflows.

Augustine volcano erupted between 27 March and 31 August 1986 and sent scores of pyroclastic flows down its snowclad north and northeast flanks. On the north flank, the highly pumiceous oldest flow merges downslope into a water-scoured surface discontinuously overlain by matrix-free large boulders and bouldery gravel. Thus the first extensive pumiceous flows interacted swiftly with snowpack to form high-discharge relatively clear-water floods. An extensive early pyroclastic flow that barely reached the sea has properties that suggest that it mixed with snow and formed a hybrid between pumiceous pyroclastic flow and lahar. This flow has low-relief (centimeters-high) margins, a low slope and low-relief surface, numerous discontinuous subparallel narrow and shallow surface channels, delicate willow branches charred only at surface resting points, and areas of collapse topography and openwork fumarolic pipes. In a steep gully, the pumice is in the form of waterlaid bars. Such features all together indicate that the flow was relatively thin and cool yet highly mobile. The flow subsided and vented by melting of underlying snow, its surface was rilled and locally reworked by its rapidly expelled water, and this watery flood locally redeposited pumice.

THE PETROGENETIC SIGNIFICANCE OF INTERSTRATIFIED HIGH- AND LOW-TI VOLCANIC ROCKS IN NICARAGUA

WALKER, J.A., Department of Geology, Northern Illinois University, DeKalb, IL 60115, CARR, M.J., Department of Geological Sciences, Rutgers University, New Brunswick, NJ 08903, and FEIGENSON, M.D., Department of Geological Sciences, Rutgers University, New Brunswick, N.J. 08903

Interstratified high- and low-Ti volcanic rocks have been found at a number of volcanoes in Nicaragua, including within a single cinder cone. Low-Ti volcanic rocks have distinctly higher concentrations of K_2O, Ba, Rb, Sr, La, Ce, Nd, and P_2O_5 than high-Ti volcanic rocks. Low-Ti volcanic rocks also have manifestly higher Ba/La and $^{87}Sr/^{86}Sr$ and lower Ti/Zr than their neighbors with higher TiO_2.

These compositional differences cannot be attributed to fractional crystallization from a common parent magma nor to partial melting from a common source region. Instead they indicate enhanced subduction zone or slab contributions to the source region of low-Ti primary magmas via fluids from dehydration of the downgoing plate. On average, however, the middle rare-earth element contents of the low-Ti basalts (Sm through Dy) show less enrichment than expected, while Zr and Nb show more. These averaged "anomalies" suggest the added, but variable petrogenetic involvement of subducted pelagic sediment.

Therefore, geochemical distinctions between the high- and low-Ti basalts are keyed to variable source contributions from subducted Cocos lithosphere, including its sediment cover. At most, about 5% sediment of varying composition is involved in magmagenesis, consistent with ^{10}Be constraints.

The suggested relationship between the sources of the high- and low-Ti basalts implies that the former is closer in composition to "pristine" mantle wedge, if such exists. Interestingly, the high-Ti basalts possess conflicting trace element earmarks of both "depleted" and "enriched" ocean floor basalts. These discordant trace element traits can be reconciled through relatively high degrees of melting of a mantle wedge with a transitional chemistry. It is suggested that this somewhat-enriched mantle foundation extends beneath the entire Central American arc, except central Costa Rica, where magmas are generated in more-enriched mantle.

If generalizations from Nicaragua are apropos, then wide fluctuations in the amount of slab (with sediment) involvement in magmagenesis are possible beneath small portions of volcanic arcs, even under individual volcanoes. The trace element compositions of other Central American basalts, however, suggest that unusually high degrees of melting may be required for such wide fluctuations in slab contributions.

INVESTIGATIONS OF THE MECHANICS OF SURFICIAL DEFORMATION IN THE NOVARUPTA BASIN, VALLEY OF TEN THOUSAND SMOKES, KATMAI NATIONAL PARK, ALASKA

WALLMANN, Peter C. and POLLARD, David D., Department of Geology, Stanford University, Stanford CA 94305-2115

Novarupta Basin is the site of the vent for a compositionally zoned eruption of 15 km^3 of rhyolite to andesite magma which produced the Valley of Ten Thousand Smokes (VTTS) in 1912. Mapping and topographic profiling of fractures in the basin has revealed four regions and styles of deformation: (1) translational block slides and slope-parallel opening fractures (gulls) on the flanks of Trident and Broken Mtn., (2) arcuate grabens between Broken Mtn. and Trident, (3) opening fractures on the flanks of Trident and near Novarupta dome, and (4) grabens on the crest of the Turtle, a large mound of tephra adjacent to Novarupta dome. Some, but not all of these fractures are related to the subsurface vent geometry. For example, the arcuate grabens are an expression of the vent rim at depth. Subparallel bedrock joints and opening fractures in the tephra are compatible with dike propagation along from Trident to Novarupta dome.

Reconstruction of the original fracture geometries, necessary because of the rapid degradation of fracture walls and scarps in the weakly cohesive tephra of the vent region is based on a comparison of modern photographs with those taken by the Griggs' expeditions to the VTTS in 1916, 1917, 1919. Preliminary evaluation of these photographs indicates that degradation of fault scarps on the Turtle has been significant and must be accounted for to determine fracture and fault displacements and orientations. Other early photographs show crosscutting sets of rills on the flank of the Turtle, indicating ongoing deformation of the Turtle concurrent with formation of the rills. Also, orientations of active rills on the flanks of Broken Mtn. and the Turtle are not always parallel to the maximum slope. These data are used to constrain deformation in the vent region and the mechanism of origin of the Turtle.

In order to understand the implications of surficial fractures for the subsurface geometry of the vent, numerical and physical models are being constructed to analyse the observed fracture pattern. These models focus on three principle areas of interest with respect to the surficial deformation: (1) the effect of compaction on large thicknesses of tephra; (2) the effect of primary depositional topography on slide and gull formation; and (3) the effect of subsurface intrusion of magma bodies, such as a laccolith underneath the Turtle and a dike feeding Novarupta dome.

A finite element code which allows thermo-elastic modeling of axisymmetric features will be combined with Riehle's (1974) model for compaction of ash flow sheets to assess the effects of compaction on deformation. Preliminary calculations show that large horizontal strains at the surface can be induced by compaction alone. Results from these models will be compared with topographic profiles over compactional fractures in the western VTTS. To analyse the slides and gulls, gravitational creep of thick sequences on primary depositional slopes of varying attitudes will be modeled. These numerical techniques will also be used to study the effects of dike intrusion and laccolith inflation on the weakly cohesive surficial deposits of the vent region.

Physical models using mixtures of sand and clay to model the weakly cohesive tephra of the vent region complement numerical models of laccolith inflation in inelastic material. Comparison of the results from both modeling techniques should constrain the origin of the Turtle. Other physical models will give insight into the effect of fault movement in vent bedrock units on non-elastic surficial material.

Riehle, J. R., 1974, Calculated compaction profiles of rhyolitic ash-flow tuffs: *Geol. Soc. Am. Bull., v. 84*, p. 2193-2216.

SATELLITE SURVEY OF SULFUR DIOXIDE EMISSIONS DURING EXPLOSIVE ERUPTIONS

WALTER, Louis S.,
KRUEGER, Arlin J.,
SCHNETZLER, Charles C.,
DOIRON, Scott D.,
SULLIVAN, Dan P.
Goddard Space Flight Center, Greenbelt MD, 20771

Explosive volcanism is a significant source of SO_2 in the sulfur cycle and has also been implicated as a possible contributor to the cause of climate change. However, recent emissions of extraordinarily large quantities of SO_2 during the eruptions of El Chicon and Nevado del Ruiz have underscored the great variability in the levels of SO_2 generated by volcanoes. In order to shed some light on the reasons for this, we have initiated a survey of satellite data of volcanic SO_2 emissions.

The Total Ozone Mapping Spectrometer was launched on the Nimbus 7 spacecraft in 1978 and is still operating, observing the entire Earth each day with an average spatial resolution of 66 km. It has demonstrated utility in mapping significant levels of SO_2 concentrations exploiting the UV absorption characteristics of the gas.

We have focused our survey on eruptions reported in the SEAN Bulletin and, thus far, have examined TOMS data acquired in 1979 and 1980. The 1979 eruptions observed are 4/13 Soufflriere(3)[1], 6/6 Ambrym(2) and 11/13 Sierra Negra(3). The following volcanoes have been observed in 1980 TOMS data:

DATE	VOLCANO	VEI	SO_2[2]
1/30	Nyamuragia	3	22
5/1	Makushin	1	1
5/18	St. Helens	5	340
7/6	Pavlof	2	3
7/23	Ambrym	3	5
8/17	Hekla	3	452
10/6	Ulawun	3	95

Detection of the Makushin and Pavlof eruptions is somewhat uncertain.

It is interesting to note that in the 1980 data, seven other eruptions and five additional eruptions of Mt. St. Helens, all of which had VEI values of 3, were not observed. This may be because of low SO_2 abundances or because the SO_2 was not injected high enough into the atmosphere.

[1] Date, name and VEI are given in each case.
[2] Preliminary (probably low) estimates of SO_2 (in kilotons) emitted to the upper atmosphere.

THE ROLE OF ANDESITIC AND MAFIC MAGMAS IN THE GENESIS OF RHYOLITE ASH-FLOW TUFFS, TOMOCHIC VOLCANIC CENTER, SIERRA MADRE OCCIDENTAL

WARK, David A., Department of Geology, Rensselaer Polytechnic Institute, Troy, New York 12180.

Rocks of the Tomochic Volcanic Center (TVC) record the evolution of waning continental arc magmatism, as the rate of Farallon plate subduction beneath western North America decreased. Between ~40 and 30 Ma, volcanism progressed through three overlapping stages, characterized by (I) extrusion of andesitic lavas [~40 to 35 Ma], (II) caldera-forming eruptions of large-volume rhyolite ash-flow tuffs [34 and 31.4 Ma], and (III) extrusion of basaltic andesite lavas [~30 Ma]. Petrologic and geologic data indicate rhyolite genesis by ~closed-system fractionation of andesite, and andesite genesis by mingling of mantle-derived magmas (related to late-stage basaltic andesites?) with melts of the deep crust.

Andesitic lavas are porphyritic with phenocrysts of opx, cpx, and plag; hbld and bio are the dominant ferromagnesian phases in some dacitic rocks. Andesites and dacites exhibit arc-like trace element signatures (depleted Nb and Ta relative to LIL) and have initial Nd and Sr isotope ratios (ε_{Nd} = -2.3 to -5.2 and $^{87}Sr/^{86}Sr$ = .7060 to .7089) that are inversely correlated, trending toward values typical of old continental crust on an ε_{Nd} - $^{87}Sr/^{86}Sr$ diagram.

The two ash-flow tuffs that originated at the TVC have contrasting chemical characteristics which reflect different paths of fractional crystallization; each tuff represents less than 50% the original mass of parental andesite. Isotopic data require no assimilation of crust during fractionation to rhyolite: initial Nd and Sr isotope ratios (ε_{Nd} = +0.5 to -2.7 and $^{87}Sr/^{86}Sr$ = 0.7053 to 0.7066) from TVC rhyolites are inversely correlated and overlap those of andesites and dacites. The Vista tuff (34 Ma) is a crystal-rich high-silica rhyolite with phenocrysts of ksp, plag, qz, hbld, bio, mt, and sph. Among Vista samples, the most evolved are strongly depleted in elements compatible with the phenocryst assemblage (including Ba, Sr, Y, and MREE), and have the highest ratios of ksp to plag, the most sph, and the least hbld and bio. Mineral-pair T estimates are between ~700 and 750 °C; Al contents of hbld indicate equilibration at relatively low pressures (<3 kbar). The four members of the Rio Verde tuff (31.4 Ma) exhibit little chemical variation, but have higher Ba, Sr, Y, and REE contents than Vista. Rio Verde chemistry reflects fractionation of the dominant phenocryst assemblage, which includes plag, cpx, opx, and FeTi oxides. In addition, hbld is present in member III, and bio and ksp in member IV, but trace elements compatible with these phases are not depleted. Rio Verde magmas equilibrated at higher temperatures (>850 °C) than Vista.

Crystal-poor basaltic andesites (BA) are members of a suite of late-stage mafic lavas (SCORBA suite of Cameron and others) found throughout the Sierra Madre Occidental (SMO). Lavas of this suite contain sparse phenocrysts of ol, aug, and plag, are depleted in Ta (and to lesser degree Nb), and have Nd and Sr isotope ratios near bulk earth. Regionally, BA's were extruded during crustal extension *after* ash-flow volcanism had ended. At the TVC, however, BA was also extruded with hybrid intracaldera lavas at ~34 Ma, *providing direct evidence that BA was present at depth during earliest rhyolite ash-flow volcanism*. Hence, BA magmas, although extruded mostly after ash-flow activity had ended, may have been an integral component of earlier magmatism at the TVC and in other parts of the volcanic field. It is proposed that BA's (or more mafic precursors) were trapped by density contrasts in the deep crust, where they interacted with crustal melts to form magmas of intermediate composition. Some of these magmas were extruded during early andesitic volcanism; others evolved by ~closed-system fractionation to generate the voluminous rhyolites of the SMO.

PRECURSOR ERUPTIVE ACTIVITY OF THE LARGE-VOLUME RAINIER MESA TUFF, SOUTHWESTERN NEVADA, U.S.A.

WARREN, R. G. and VALENTINE, G. A., Earth and Space Sciences Division, Los Alamos National Laboratory, Los Alamos, NM 87545

The Rainier Mesa Tuff (RMT) is a widespread welded ignimbrite with an approximate volume of 1000 km^3 that was erupted from the Timber Mountain-Oasis Valley caldera complex in southwestern Nevada 11.6 Ma ago. The RMT is petrologically zoned from high-silica rhyolite at the base to dacite (quartz latite) at the top. Throughout much of the RMT's extent, especially north of its source caldera, the ignimbrite is underlain by a layered sequence that is up to 64 m thick. We interpret this layered sequence to represent precursor eruptive events that culminated in the eruption of the main ignimbrite.

The layered sequence consists of up to 20 cycles; each cycle consists of basal white pumice lapilli and ash beds which grade into an upper brown to gray, massive bed of dominantly ash-sized material. The white basal beds are typically planar-parallel and are typically about 1-5 cm thick. Local low-angle cross bedding is present. Thus the white beds are probably dominantly fallout layers with a pyroclastic surge component, or, alternatively, were slightly windworked during deposition. Clasts and shards within the white beds are generally highly vesicular, with ash particles consisting mainly of bubble walls; nonvesicular glass is very rare. Petrologically the white beds of all the cycles are identical to the basal portion of the RMT.

The massive, fine-grained beds at the top of each cycle show evidence of mass flow such as fragile clasts of underlying white beds in many cases, but in others it is possible that the beds were deposited by fallout. Some of the beds contain possible calcified plant fragments ranging from grasses to tree branches. The most common particle type in the massive beds is blocky, nonvesicular ash. Although the massive beds have some petrologic components of the RMT, their dominant components resemble more closely underlying ignimbrites; dacitic to basaltic-andesitic ashes also are intercalated within the layered sequence.

The thickness of individual cycles is about 0.5 m at the bottom of the sequence; upward in the sequence the cycles become progressively thicker until the uppermost ones are 2.5 - 6.0 m thick. Although the time represented by the sequence is unknown, there is no evidence for a large time break either between cycles or between the sequence and the RMT. Between the topmost cyclic unit and the main ignimbrite are 2 m of planar bedded pumice ash and lapilli containing almost no nonvesicular particles. Included in the unit, which consists mainly of high-silica rhyolite, is a 4 cm thick ash layer that ranges in composition from basaltic andesite to dacite.

We interpret the bedded sequence below the RMT to record a period of alternating small-scale Plinian eruptions of RMT magma and hydrovolcanic eruption of pre-RMT material. The cycles had longer durations as time progressed, and "primed" the vent(s) for the main ignimbrite eruption. The culminating eruption may have been partially triggered by intrusion of basaltic andesite magma into the rhyolitic part of the magma chamber, producing the sustained magmatic eruption of the Rainer Mesa Tuff.

EVOLUTION OF A PROTEROZOIC VOLCANIC ARC AT A CONTINENTAL MARGIN SOUTH OF THE SKELLEFTE ORE PROVINCE, NORTHERN SWEDEN

WASSTROM, Annika, Geologisk-mineralogiska institutionen vid Abo Akademi, Domkyrkotorget 1, 20500 Abo, Finland

The stratigraphy of the investigated Knaften area starts with deposition of subaquatic, mostly basic volcanics intercalated with clastic sediments 1.9-2.0 Ga old. The volcanic rocks consist of different volcaniclastics and lavas. The clastic sediments are represented by graywackes, turbidites and graphite-bearing argillites. Well-preserved primary structures such as pillows, bedding structures, slumping and a Bouma sequence have been found in these supracrustal rocks.

Granitoids intruded the supracrustals partly before the end of the volcanic period at 1.9 Ga. They show some subvolcanic structures. Interpreted as apophyses from these intrusives are partly concordant quartz porphyritic dykes in the volcanics. Some water-deposited, well-preserved rhyodacitic tuffites seem also to have a connection with the granitoids.

In the mafic volcaniclastics and between the mafic lavas and the rhyodacitic tuffites, gabbroic-ultramafic sills have intruded. These indicate a late extension in the area.

At about 1.2 Ga the supracrustal rocks and the granitoids were cut by dolorite dykes.

The investigated area seems to have some resemblance with the oldest supracrustals and granitoids in the Skellefte Ore Province, although it is isolated because of tectonic movements and intrusion of younger granitoids. The Skellefte Ore Province is interpreted as a volcanic arc with the continent to the north.

Geochemically, some of the volcaniclastic material from the Knaften area seems to be of undifferentiated mantle-derived magma, others have a tholeiitic character. The most primitive material has basaltic komatiite composition and indicates initial rifting. The pillow lavas are tholeiitic. They have probably formed in the ocean part of an island arc, in a subduction zone. The material is probably contaminated. Geochemically, the granitoids seem to have intruded in an actively subducting plate-margin volcanic arc.

GEOPHYSICAL CHARACTERISTICS OF THE 1986-1987 ERUPTION OF IZU-OSHIMA VOLCANO, JAPAN

WATANABE, H., Izu-Oshima Volcano Observatory Earthquake Research Institute, University of Tokyo, Yayoi 1-1-1, Bunkyo, Tokyo 113, Japan

A basaltic stratovolcano, Izu-Oshima, located about 100 km SSW of Tokyo, erupted from the summit during November 15-23, 1986 and succesively from flank fissures during 21-23. The fissure vents extended from the caldera floor to the NW slope outside the caldera rim. A minor summit eruption occurred on December 18. Total amount of the products were 60-80 x 10^6 tons.

Before and during the summit eruption, the seismic activity was high at the north and western parts of the Oshima island, but unexpectedly no seismic swarm activity and ground inflation were observed around the summit region. There occurred, however, remarkable precursory phenomena around the central cone Mihara-yama; anomalous secular variations in the geomagnetic total force, rapid decrease in the subterranean electrical resistivity, and thermal anomaly at the crater bottom, all indicating the elevation of temperature / uprise of magma in the conduit beneath the summit crater. Volcanic tremors also started to occur beneath Mihara-yama at the beginning of July 1986. At first, the mode of tremor occurrence was periodic, and then became continuous at the end of October.

In contrast to the summit eruption, the fissure eruptions were accompanied by a very intensive earthquake swarm and remarkable ground deformation. After the beginning of the fissure eruption, the earthquake swarm propagated toward both the NW and SE directions to form a NW-SE seismic zone across the island. Many cracks and remarkable subsidence were observed around the fissures and at the southeastern part of the island. Variations in the gravity and geomagnetic fields also suggested the formation of tensile cracks beneath the island. The NW-SE trends of the fissure vents, the distribution of epicenters, and the subsidence zone, are consistent with the common tectonic stress field around Izu-Oshima island which is situated at the northern border of the subducting Philippine Sea plate.

On November 18, 1987, magma of the lava lake in the Mihara-yama crater was drained through the bottom of the crater. Associated with the drain back of magma, ground inflation was detected by volumetric strainmeters and tiltmeters. The center of inflation was estimated to be 4-5 km deep beneath the northwestern foot of the volcano. Observation by an array of tiltmeters installed over the whole island in 1987, further revealed that the volcanic tremors were accompanied by small subsidence at the same source area as that of inflation that occurred on November 18, 1987. These facts strongly suggest that the volcanic conduit beneath the summit crater became freely connected to the magma reservoir beneath the northwestern foot of the volcano after the fissure eruptions, and that the pressure accumulation and release are repeated in the gas reservoirs at or around the upper part of the conduit where the volcanic tremors are generated associated with the release of gas pressure.

HIGH PRESSURE ASH-FLOW TUFFS FROM THE SOUTHERN SIERRA MADRE OCCIDENTAL, JUCHIPILA, ZACATECAS, MEXICO

WEBBER, K.L., SIMMONS, Wm. B., FERNANDEZ, L.A., and MONTAGUE, K.A., Department of Geology and Geophysics, University of New Orleans, New Orleans, LA 70148

A 1 km thick sequence of Oligocene (26 Ma) volcanics are located at the southern end of the Sierra Madre Occidental (SMO) near Juchipila, Zacatecas, Mexico. This mid-Tertiary volcanic sequence is composed predominantly of rhyolitic ash-flow tuffs (AFT) with lesser amounts of basaltic-andesite and andesite. This series can be characterized as high-K calc alkaline with 2% K_2O at 56% SiO_2 and an alkali-lime index of 58.5. A typical Juchipila AFT with 73% SiO_2 has major element abundances of 5.5% K_2O, 3.5% Na_2O, 0.6% CaO, 0.1% TiO_2, 1.5% FeO*, 0.2% MgO, 13.5% Al_2O_3; and trace element abundances of 800 ppm Ba, 275 ppm Zr, 190 ppm Rb, 50 ppm Sr, 75 ppm Y, and 20 ppm Th. The AFT are LREE enriched with LREE concentrations approximately 150-200 times chondrite and HREE concentrations 25-35 times chondrite.

The Juchipila AFT are phenocryst poor containing no more than 20% phenocrysts, 80% to 90% of which are typically feldspars. The predominate phenocryst is barium-rich alkali feldspar which ranges in composition from sanidine (Or58-Or64) to anorthoclase (Or34-Or43) with 0.5% to 4.0% celsian. However, many of the anorthoclase phenocrysts have corroded hyalophane cores with up to 14% celsian, the highest barium content known for rhyolitic, peraluminous AFT. Plagioclase in AFT ranges from An16 to An43.

The AFT of the SMO were erupted as a result of mid-Tertiary Pacific-margin subduction. In northern Mexico, K. Cameron, et al. (1980) recognized two calk-alkaline facies; a moderate-K facies in the SMO near Batopilas, Chihuahua, and a high-K facies further east in the Basin and Range province of Chihuahua (CBR). This west to east increase in AFT alkalinity across the SMO to the CBR corresponds with increasing distance from the mid-Tertiary Pacific plate margin, and an inferred increase in depth to the subduction zone.

The Juchipila AFT sequence is located approximately on strike with Batopilas in the northern SMO, relative to the inferred position of the mid-Tertiary plate margin. If subduction along the Pacific margin had remained relatively constant, we would expect the chemistry of the Juchipila AFT to be similar to those of Batopilas. However, the Juchipila sequence is geochemically and mineralogically more similar to the high-K facies of the eastern CBR. This suggests fundamental differences in the conditions of magma genesis along the strike of the SMO. Compositional changes in volcanics along strike of the present-day Andes volcanic arc have been correlated with variable angles of dip of the subducting plate and differences in crustal thickness. The high-barium content of anorthoclase phenocrysts in Juchipila AFT suggests that these crystals may have formed at high pressures. Thus our mineralogical and geochemical observations for the Juchipila volcanics suggest that mid-Tertiary subduction was not continuous along strike, and that subduction occurred at a steeper angle beneath the southern SMO than in the northern SMO.

Cameron, K.L., et al. (1980) Geology, 8, 87-91

GEOMORPHIC AND PEDOLOGIC CRITERIA FOR RECOGNIZING POLYCYCLIC VOLCANISM AT SMALL BASALTIC CENTERS IN THE WESTERN U.S.A.

WELLS, S. G., RENAULT, C. E., AND McFADDEN, L. D., Department of Geology, University of New Mexico, Albuquerque, NM 87131

Studies of geomorphic degradation and soil development of volcanic landforms at small (< 1 km^3) basaltic centers in southern Nevada and California indicate that (1) eruptive history is more complicated than previously recognized and (2) multiple basaltic lava and scoria eruptions from single vents are intermittent with periods inactivity lasting 10^3 to 10^5 years. This style of repeated eruptions is classified as polycyclic (Crowe et al., this volume), and the timing of multiple events from a single vent must be deciphered in order to understand the ascent history of individual pulses of magma. We propose four geomorphic and pedologic criteria for recognizing polycyclic volcanism which are based upon detailed studies at the Cima and Crater Flat volcanic fields in California and Nevada, respectively.

1. Pyroclastic-fall units separated by a buried soil indicates that a period of surface stability and concomitant soil development have occurred on the volcanic units prior to a second eruption which buries the soil with tephra.
2. Degradation of scoria cones by small debris-flow and channelized-flow processes produce debris aprons at the base of the cone and require at least 10^3 years to form. When these apron deposits are overlain by pyroclastic-fall deposits, long-term cone erosion and volcanic inactivity has preceded a second eruption.
3. Debris aprons, which only occur below cone slopes showing debris-flow and channel-flow erosion, indicate long-term erosion. Thus the occurrence of debris aprons below cone slopes which show no signs of erosion indicates that a younger pyroclastic-fall unit has buried the older, eroded cone slope.
4. Several morphometric parameters of a scoria cone are sensitive to cone age. Cone slope angle decreases with time as the ratio of apron length to total cone length and apron height to total cone height increase with time. These parameters can be used to recognize polycyclic volcanism where several overlapping cinder cones of significantly differing age occur within a vent area.

The timing between multiple eruptions is provided by the degree of soil development. Soils associated with these volcanic landforms are formed primarily in eolian sands and silts which mantle and fill voids in the scoria and lava. The primary pedogenic horizons of these soils include a strongly developed vesicular A horizon, a thin cambic B or an oxidized C horizon, and a stage I secondary calcium carbonate horizon. Such soil development appears to require 10^3 years. Soils associated with increasingly older ages of volcanic landforms are usually characterized by systematic changes in B horizon thickness and secondary carbonate morphology.

These geomorphic and pedologic criteria not only provide field techniques for recognizing the polycyclic nature of scoria cones but are useful in understanding the complexities of strombolian eruptions and enhancing geologic mapping of volcanic centers where radiogenic dates are unavailable and field relations are unclear. Geomorphic and pedologic studies are ongoing in an attempt to refine the four criteria, improve the accuracy of assessing the time intervals between eruptions, and determine the regional extent of polycyclic volcanism in the western U.S. Preliminary observations suggest polycyclic volcanism has occurred at numerous other centers in California and Nevada as well as centers in New Mexico.

MESOZOIC CONTINENTAL MAGMATISM AND ITS METALLOGENY IN SOUTHEAST CHINA

WENDA LI, Nanjing Institute of Geology and Mineral Resources, 534 East Zhong Shan Road, Nanjing, People's Republic of China

Mesozoic continental magmatism in southeast China was strong and related to the tensile condition of the continental margin during the Pacific plate subducting under the Eurasia. The famous tensional fracture Tancheng-Lujiang rift zone, accompanied with several deep-faults parallel or subparallel to the subduction zone, and a series of nearly E-W trending deep-faults reflecting the activation of the Proterozoic basement faults controlled a series of down-faulted volcanic basins and central or linear volcanic eruptions in this part of Circum-Pacific zone.

Volcanic-plutonic magmatism commenced with weak manifestation of eruption in Late Triassic, became prosperous in Late Jurassic to Early Cretaceous, and wanned in the early Late Cretaceous. Only isolated fissure eruptions of alkali basalt magma occurred toward Cenozoic. The volcanic-plutonic magmatism reveals a zonal migration from west to east both in age and in chemistry, they show more acidic and richer in potassium with elapse of time. Petrochemically they displayed more characteristics of a continental margin rather than that of an island arc.

The metallogeny possesses esential similarity with that of Andes in the types of various metal deposits and in their tendency of distribution pattern from inner (coastal) to outer (hinterland) zone: Fe→Cu,Au,→Sn,W,→Pb,Zn,Ag. Because of zonal migration of magmatism centers therewith their mineralization, distrubution patterns may be overlaped. Erosion made the pattern more complicated. Shallow seated or epithermal Au-Ag deposits, especially those types related to hot-spring sinter deposits in the younger volcanic area are lacking. The common porphyre types are those of Mo, Sn, W and Pb-Zn, the last one was often associated with Ag. Prospecting and exploration practice proved that Pb-Zn and Ag deposits are more common than the Au in this area, implying the deeper dissected and eroded condition than in Andes.

ISOTOPIC AND GEOCHEMICAL STUDIES OF A LITHOSPHERIC COLUMN SAMPLED BY COLORADO PLATEAU XENOLITHS

WENDLANDT, E., Department of Earth and Space Science, University of California, Los Angeles, CA 90024; DE PAOLO, D. J., Berkeley Center for Isotope Geochemistry, University of California-Lawrence Berkeley Laboratory, Berkeley, CA 94720; BALDRIDGE, W. S., ESS-1, Geology/Geochemistry, M.S. D462, Los Alamos National Laboratory, Los Alamos, NM 87545

Xenolith lithologies from Moses Rock Dike and Mule Ear diatremes include peridotites, garnet amphibolites, granulites, eclogite, sillimanite gneisses, schists, and greenstones, and represent a vertical lithospheric column from the central Colorado Plateau. Nd and Sr isotope and trace element compositions were analyzed for the crustal xenoliths and one eclogite xenolith in an attempt to understand initial lithosphere formation and subsequent intra-lithosphere stabilization processes.

Trace element analyses for six samples of eclogite, mafic amphibolite, granulite, and greenstone show significant similarities. REE patterns show relative LREE enrichment (normalized La/Yb = 1.7 - 7.7) with negative Eu anomalies. Sm/Nd ratios of mantle xenoliths have relative HREE enrichment.

Lower crustal garnet amphibolites and granulites have ε_{Nd} = -7 to -9, with restricted $^{87}Sr/^{86}Sr$ of 0.70406-0.70420. An eclogite has ε_{Nd} = -1 and $^{87}Sr/^{86}Sr$ of 0.70676. Low- to mid-crustal gneisses show lower ε_{Nd} (-15 to -17) and more radiogenic Sr (0.71424 to 0.71680). A greenstone xenolith has ε_{Nd} = -4 and $^{87}Sr/^{86}Sr$ = 0.70850. With the exception of the eclogite and one sample of garnet amphibolite, these xenoliths show relatively uniform Sm-Nd model ages in the range 1.66-1.88 Ga. These T_{DM} ages correspond well to published lithosphere formation ages of granitoids for regions bordering the Colorado Plateau (T_{DM} = 1.7-2.0 Ga, Bennett and DePaolo, 1987). The uniformity of the model ages suggests these xenoliths are fragments of lithosphere initially formed during the early Proterozoic. These xenoliths come from a variety of crustal depths, indicating that 1.7-1.8 Ga old material is found throughout the crustal column.

The eclogite xenolith has an Nd model age of 1.24 Ga, and one garnet amphibolite has a model age of 1.54 Ga. The model ages indicate that these mafic rocks were added to the lithosphere more recently than the time of the major crust-building event at ca. 1.7 Ga. There have evidently been some additions to the crust and/or the uppermost mantle lithosphere from the convecting mantle subsequent to 1.7 Ga, so that the granitoid upper crustal model ages are not entirely representative of the crustal column. It should be possible to estimate the extent of later additions from an expanded data set. Colorado Plateau eclogite xenoliths have been interpreted to be remnants of subducted Mesozoic oceanic crust (Helmstaedt and Doig, 1975). However, Mesozoic MORB typically have ε_{Nd} = +8 to +10. Our analysis argues against the interpretation of eclogite as subducted Cretaceous MORB.

OBSIDIAN LAVA: A PERMEABLE FOAM ERUPTION MODEL

Westrich, H. R., and Eichelberger, J. C.,
Geochemistry Division, Sandia National Labs,
Albuquerque, NM 87185

Recent studies of the volatile content of young, volcanic rhyolites has led to a better understanding of the degassing history of hydrous rhyolite magmas and the development of the 'permeable foam' model for the non-explosive eruption of obsidian flows (e.g. Obsidian Dome, CA.). Results indicate that magmatic decompression is rapid and is responsible for the episodic loss of a water-rich fluid from the magma during Plinian eruptions. Degassing continues as the magma ascends, eventually yielding a gas-permeable magmatic foam upon eruption which has equilibrated to a one atmosphere, water vapor content of 0.1 wt.%. After extrusion, increasing lithostatic load within the flow (>0.1 MPa) causes bubble collapse and vapor resorption, producing the dense, dry glassy interior (obsidian) and pumiceous carapace common to rhyolite flows.

Supporting evidence for this model has come from a series of experiments designed to examine the effects of pressure and temperature upon bubble resorption in hydrous rhyolite obsidian. Samples were vesiculated at 900°C for 30 minutes after which they were heated at 900°C for 2 days at 0.1, 0.2, 0.4, and 1.0 MPa. Textural and microscopic examination of these samples indicate that bubbles in a 'magmatic foam' can be completely resorbed at pressures as low as 0.4 MPa; bubble resorption is incomplete at lower pressures. These tests demonstrate that a permeable magmatic foam can collapse to a dense obsidian without preservation of relict vitroclastic textures found in welded tuffs.

Additional bubble resorption tests made with fiamme from a welded tuff indicated that some textural features (e.g. vesicles, Fe-Mg lineations) can be eliminated or obscured after heating at 900°C and 1.0 MPa for 2 days; increasing run duration to 20 days did not appreciably affect textural features. The effect of welding temperature upon bubble resorption was also evaluated using previously vesiculated samples of flow obsidian. These samples were heated at 900, 800, 700, and 600°C at 1.0 MPa, where resorption was found to be nearly complete at temperatures above than 800°C. The results from these bubble resorption tests can be used for interpretation of textural features found in welded ash flow tuffs, especially those of peralkaline compositions, where emplacement temperature, lithostatic loads, water contents, and perhaps eruption mode are similar to those found in obsidian lava flows.

*This work was performed at Sandia National Laboratories, which is operated for the U.S. DOE under contract number DE-AC04-76DP000789.

CRUSTAL ASSIMILATION AND COEXISTING SILICIC AND MAFIC MAGMAS IN THE VANDFALDSDALEN MACRODIKE, EAST GREENLAND

WHITE, C.M., SQUIRES, E., LAWRENCE, D.C., Department of Geology and Geophysics, Boise State University, Boise, ID 83725; and GEIST, D.J., SAWKYA, L., Department of Geology, Hamilton College, Clinton, NY 13323

The Vandfaldsdalen macrodike is a funnel-shaped gabbroic dike, 200m to 500m wide and Eocene in age. A marginal series extends inward from the walls of the intrusion and a subhorizontally layered central series occupies the pluton's interior. The gabbros of the marginal and central series are differentiated in a manner analogous to the Marginal Border Series and Layered Series of the much larger Skaergaard Intrusion.

Of particular interest is a body of granophyre, 500m wide and 130m thick, which overlies iron-rich diorite at the top of the central series (see projected cross section below). Near its margins, where it is chilled against basalt, the granophyre consists of as much as 35% granitic xenoliths derived from gneissic rocks of the Archean basement. The granophyre that hosts xenoliths at these locations is a mafic, fine-grained rock containing pyroxenes similar to those in chilled-margin gabbro of the lower part of the macrodike. Toward the interior of the granophyre body, the proportion of xenoliths decreases and the host rock becomes increasingly felsic. Major-element abundances and Sr and Nd isotopic ratios in granophyre samples (xenoliths removed) define straight-line arrays which are best explained as mixes of an undifferentiated gabbroic liquid and assimilated granitic gneiss.

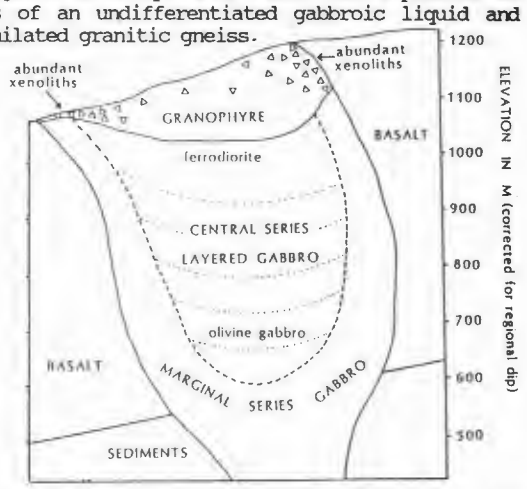

We propose that the macrodike evolved by two different and spatially isolated processes: (a) fractional crystallization in the lower part of the intrusion which led to an iron-enriched dioritic liquid and (b) assimilation of granitic xenoliths near the top of the intrusion which produced the silica-rich granophyre. Judging from the mutually intrusive contacts between granophyre and the adjacent ferrodiorite, the felsic and mafic parts of the macrodike may have coexisted at one time as separate liquids, with the light felsic liquid floating on the denser mafic one. The compositions of juxtaposed granophyre and ferrodiorite indicate transfer of chemical components between the two liquids was very limited; however, heat from the gabbroic part could have diffused across the density boundary, enabling assimilation to proceed nearly to completion in the interior of the felsic layer.

MAAR VOLCANISM AT HOPI BUTTES, ARIZONA: HYDROVOLCANIC ERUPTIONS ROOTED IN UNCONSOLIDATED STRATA

WHITE, J.D.L., & FISHER, R.V., Dept. Geological Sciences, Univ. California, Santa Barbara, CA 93106

Base surge deposits form thin tuff rings around maar craters in the exhumed Mio-Pliocene Hopi Buttes volcanic field of NE Arizona. The surge deposits commonly contain <50% by volume of recognizable juvenile pyroclasts. Large proportions of accidental rock fragments are characteristic of tuff ring deposits, and have been related to thermal/-hydraulic fracturing of the wall rock in the zone of hydrovolcanic interaction. The maars at Hopi Buttes show evidence of a related hydrovolcanic eruptive process dependent upon the availability of unconsolidated, fluidal mud at the site of interaction.

Many detailed techniques used to investigate modern hydrovolcanic deposits (sieve analysis, systematic SEM study, etc.) cannot be consistently applied to the ca. 6 Ma old lithified, altered tuffs at Hopi Buttes. The problem is acute when working with the very-fine grained matrix, which has been altered to bentonitic clays and/or calcite. We cannot consistently distinguish recycled bentonitic clay of the Bidahochi Fm. from fine-grained ash produced during high-energy hydrovolcanic eruptions (& subsequently altered) by petrographic means, so we've used other procedures to decipher the eruptive dynamics of these ancient volcanoes.

In the Hopi Buttes area, magma rose through rocks of the Colorado Plateau sequence, and encountered unconsolidated bentonitic/calcareous mud (the Mio-Pliocene Bidahochi Fm.) approximately 50m below the eruptive surface. Four lines of evidence indicate that most of the non-juvenile component in surge deposits is redeposited Bidahochi mud, and that hydrovolcanic interactions generally occurred within this unconsolidated mud. (1) The non-juvenile component of base surge deposits is composed of dispersed grains of quartzo-feldspathic silt and sand surrounded by a clay matrix of indeterminate origin, with very few fragments of siltstone or sandstone. (2) Meter-size and larger lumps of mudrock occur within near-vent surge deposits. (3) Few clasts of lapilli size or smaller were derived from the Wingate Formation, which directly underlies much of the Bidahochi Fm. in the Hopi Buttes. (4) Maar crater-filling deposits indicate that km-wide craters were formed within the Bidahochi deposits: If all of the clay-size matrix in the surge deposits was formed by alteration of juvenile ash, and does not represent recycled Bidahochi mud, where did the ejected mudrock go?

We propose that in this case hydrovolcanism was rooted within clay-rich sediment of the Bidahochi Fm., and that water-saturated mud, rather than water alone, served as the coolant driving hydrovolcanic fuel-coolant-interactions (FCI's). The permeability of fine mud is negligible, and the settling velocity of clay flakes extremely small: the clay thus cannot be separated from the water involved in hydrovolcanic interactions. Unlithified, water-saturated clay has very high porosity, which permits the mud to liquify when disturbed and can also result in sufficiently high water/magma mass ratios within the interacting slurry to produce explosive eruptions.

As an eruption progressed within the unconsolidated sediments at Hopi Buttes, the weak sediments collapsed between blasts. Magma thus encountered a water-and-sediment slurry many times during the eruption cycle as the crater's mud walls slipped repeatedly into the zone of interaction. The thick, weak sediment pile at the surface resulted in broad, widely-flared funnel-shaped vents, reflecting the sediments' susceptibility to failure. Once the angle of repose was attained along a maar's walls no more mud slipped in. Hydrovolcanic eruptions then ceased, because the wet, collapsing mud had served as the coolant for the FCI's. Cinder deposits may cap the maar, though the continued wetness of mud beyond the vent is attested to by peperitic bases of lava flows that flowed beyond the maars' ejecta rims and onto the surrounding playa.

AN EPISODIC MODEL FOR VOLCANIC ARC ACTIVITY IN CENTRAL AMERICA

White, R.A., U.S. Geological Survey, MS977, 345 Middlefield Rd., Menlo Park, CA 94025
Carr, M.J., Geology Dept., Rutgers University New Brunswick, NJ 08903
Harlow, D.H. U.S. Geological Survey, MS977, 345 Middlefield Rd., Menlo Park, CA 94025

For areas of Central America where the history of major eruptions and earthquakes is relatively complete, arc volcanism is observed to be temporally related to megathrust zone activity offshore - unusually small volumes are erupted during the decade preceeding great thrust earthquakes, while unusually large volumes are erupted during the decade or so following such earthquakes. This dependency of volcanism on megathrust zone activity is predicted by a simple episodic model with the following two important features - 1) the fore-arc sliver transfers stress from the thrust zone to the volcanic axis, and 2) the primary magma chambers are located at the base of the crust beneath the volcanic axis.

Prior to a great thrust earthquake, locking of the thrust zone produces compression at the volcanic axis and constricts conduits above magma chambers. Large eruptions do not occur during this stage, although small eruptions may occur as magma already within conduits is squeezed out. Decoupling during a great thrust earthquake produces tension at the volcanic axis, opening conduits. Large volumes of magma, which may have accumulated in the primary magma chambers during the compressional stage, are now free to ascend. This model predicts normal stresses beneath the volcanic chain that are compressional prior to great thrust earthquakes and tensional afterward. If large enough, these stress fields should produce predominantly strike-slip faulting and normal faulting respectively. Recent volcanic chain data from central Guatemala to Costa Rica indicate that this entire region may currently be in the pre-earthquake stage. Currently, eruptive volumes are low and strike-slip earthquakes predominate. No great thrust earthquakes have occurred along this stretch since before 1916.

GEOLOGICAL FEATURES AND GEOCHEMISTRY OF THE ACIDIC UNITS OF THE SERRA GERAL VOLCANIC FORMATION, SOUTH BRAZIL.

WHITTINGHAM, A.M., Department of Earth Sciences, University of Oxford, Parks Road, Oxford, OX1 3PR, United Kingdom.

The Serra Geral Volcanic Formation of the Paraná Basin, South Brazil, comprises a stack of basalt flows, with a significant proportion of interbedded acidic (67-71 Wt% SiO_2) volcanics towards the top of the succession, mainly in the south of the province. There is a marked scarcity of rocks of intermediate composition. The volcanics have an approximate age of 125 m.y., and this with their proximity to the Atlantic coast links them with the opening of the South Atlantic.

The acidic units form widespread sheet-like deposits, suggesting an ignimbritic emplacement mechanism. However, in outcrop and thin-section features typical of lava flows, including banding, pipe vesicles, breccia and vitrophyres, are locally present at the tops and bases of these units. This indicates they are probably high temperature ash-flow tuffs that underwent rheomorphism after eruption before finally coming to rest.

The acidic rocks have previously been divided into two sets on the basis of differences in the chemistries of the two groups. The Chapeco Acid Volcanics (CAV) are distinctly higher in the incompatible elements and TiO_2 than the Palmas Acid Volcanics (PAV). The CAV occur predomiantly in the northern half of the province, while the more abundant PAV outcrop in the south.

In this study chemistry, mineralogy and outcrop features have been used to further divide the PAV into separate units. Individual units exhibit no significant laterally or vertically variation in composition. This allows regional stratigraphic correlations to be attempted, and thus the construction of maps and cross-sections tracing the individual units throughout the area. From this the temporal variation in chemistry and distribution of the acidic volcanics, and the post-eruptive regional tectonics of the area, have been investigated. The acidic volcanic units are progressively offset north-eastwards up sequence, approximately parallel to the coast, suggesting that through time the centre of volcanism was moving in a north-easterly direction with respect to the present day Brazilian continental margin.

Rare rocks of intermediate composition exist in the province, which have previously been taken to suggest the derivation of the acidic volcanics from the basalts by fractional crystallisation. One acidic unit displays sill-like features, and at its upper and lower contacts it grades compositionally into the surrounding basaltic units. These intermediate rocks are clearly not the product of fractionation processes. A mechanism involving mixing or assimilation of basaltic and acidic end members is suggested. This implies high temperatures of emplacement for the acidic rocks, and has important implications for proposed origins of the acidic magmas.

INCREMENTAL POLYBARIC FRACTIONATION AND THE CHEMO-MECHANICS OF MAFIC DIKE EMPLACEMENT - PHASE RELATIONS, FLUID DYNAMICS AND WATERMELON SEEDS

WHITTINGTON, Dave, Roy F. WESTON Inc. 1635 Pumphrey Ave., Auburn, Alabama 36830

The emplacement of mantle-derived mafic melts into shallow crustal levels is controlled by density variation of inhomogeneous lithosphere in the context of the density, compressibility and polybaric phase relations of a melt ascending through the upper mantle and the overlying continental crust. The theory of incremental polybaric fractionation (IPF) addresses these issues by combination of mechanical and chemical aspects of mafic melts.

The conventional model of the lithosphere-as-density-filter requires two numerical refinements. First, a compressibility correction (in the form of an "effective average overburden density") is generated through an inverted solution of experimental pressure-magma density data. Second, a simple hydrostatic model of magma transport is used to predict that a magma will ascend along a pre-existing fracture whenever the Fracture Tip Dilation (FTD) ratio is greater than 1.0.

$$\text{FTD ratio} = [p_{c1}Z - p_m H]/[p_{c2}(Z-H)]$$

where: p_m, p_{c1} and p_{c2} are the melt density and the effective average overburden density at, respectively, the trailing and the leading edge of the tap of magma (see diagram, below). H and Z are the height of the magma and the depth to the trailing edge of the tap.

The implication of the FTD ratio for dike emplacement is that polybaric fractionation, originally conceived for mantle diapirs in ductile settings, becomes relevant to brittle regimes of the upper mantle and crust. A tap of ascending magma stalls at a balance depth due to the reduction of p_{c1} (i.e. a change in the confining pressure at the trailing edge as the tap ascends through a density barrier) driving FTD to a value that is less than 1.0. Decompression associated with ascent toward this depth promotes saturation of dense SiO_2-poor phases. Fractionation reduces the residual value of p_m and FTD becomes greater than 1.0 as the melt resumes its ascent toward the next balance depth (provided heat loss in excess of the latent heat(s) of fusion is negligible). Iteration through increments of ascent-stalling-fractionation and resumed ascent comprise IPF consistent with present day and Mesozoic examples of continental magmatism.

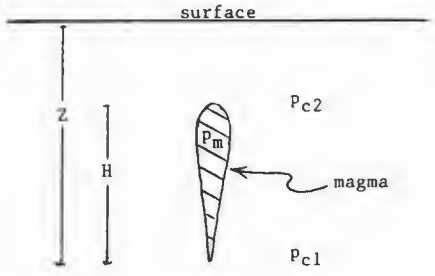

PROCESSES AND TIMESCALES OF SYENITE NODULE FORMATION: IMPLICATIONS FOR MAGMA CHAMBER DYNAMICS

WIDOM, E., GILL, J., Earth Sciences, University of California at Santa Cruz, Santa Cruz, CA., 95064, and SCHMINCKE, H.-U., Institut fur Mineralogie, Ruhr-Universitat Bochum, 4630 Bochum, West Germany.

Ejected syenite nodules are abundant in the 4500 year old trachytic pumice deposit of Fogo A, Sao Miguel, Azores. Most of the nodules were erupted during a high-energy eruptive pulse which marked the transition from light colored pumice lapilli and ash falls to surge deposits of a more mafic, banded pumice.

The syenite nodules are composed predominantly of sanidine crystals (80-90 %), with amphibole, pyroxene, and minor amounts of opaque oxides, biotite, and quartz. Accessory phases include zircon, pyrochlore, and fluorite.

Distinct textural variations exist despite the cumulate texture of interlocking sanidine crystals common to all nodules. Some nodules have only optically homogeneous sanidines, while others have perthitic feldspars or a combination of the two. Void space of several volume percent between sanidine crystals is common in the nodules with optically homogeneous sanidines, but decreases significantly in the nodules with more perthitic feldspars. Accompanying the decrease in void space in the perthite bearing nodules is the development of fine-grained, granulated feldspars.

Four of seven nodules are identical to the Fogo A trachytes in major and trace element composition, except for their U/Th ratios. The similarity of syenite and trachyte Sr concentrations demonstrates that the syenites represent bulk-liquid rather than cumulate compositions, because the high partition coefficient for Sr in sanidine (D=5.5) would require cumulate syenites to have Sr concentrations much higher than their parent liquids. Non-representative sampling of the syenite nodules due to their coarse grain size, or preferential volatilization of U may account for the difference in U/Th ratios between syenite nodules and host trachytes.

Uranium-series disequilibria provides further evidence that some of the syenite nodules are cogenetic with the Fogo A trachytes. Three of the nodules have Th-isotopic compositions identical within 1-sigma errors to the trachytes, which implies that they crystallized in equilibrium with the Fogo A liquid within the past 10,000 years. Assuming initial Th-isotopic ratios of 0.87 for all nodules, two nodules yield model ages of approximately 12,000 years, and the third, which is in radioactive equilibrium, yields a minimum age of 200,000 years.

The three nodules that are in isotopic equilibrium with the Fogo A trachytes are also compositionally equivalent to the trachytes. In contrast, the nodules with older model ages differ compositionally from the trachytes, suggesting that multiple batches of chemically distinct trachytic magmas have been stored below the Fogo volcano for at least 200,000 years.

Nodule age also can be correlated qualitatively with texture. The young nodules (cogenetic with Fogo A trachytes) consist predominantly of homogeneous sanidines with void space between crystals. The >200,000 year old nodule contains only perthitic feldspars with no void space and pervasive granulation. The 12,000 year old nodules are texturally intermediate.

The following model is envisioned for the formation of the syenite nodules:

The chemically zoned Fogo A trachyte evolved by near-eutectic fractional crystallization close to the low temperature minimum on the ab-or join, producing small variations in major element concentrations but large variations in trace element concentrations. However, as sidewall or roof crystallization occurred, trace elements and volatiles in the neighboring boundary layer liquid must have attained sufficiently high concentrations to precipitate incompatible element-rich accessory phases, freezing the incompatible element concentrations of the liquid into the syenite material.

Older syenite, isolated beneath or behind the recently formed Fogo A syenites, became insulated and cooled slowly with time, causing exsolution of the feldspars, while dynamic processes in the magma chamber such as repeated injections of magma and explosive eruptions caused deformation, compaction, and loss of volatiles from void space. The high-energy eruptive pulse sampled variable depths of the syenitic magma chamber boarders which range in age from a few thousand years to >200,000 years old.

PHREATIC ERUPTIONS: A PROPOSAL TO IMPROVE THEIR DEFINITION AND CLARIFY THEIR SIGNIFICANCE

WILLIAMS, Stanley N. and YOUNG, Richard H., Department of Geology and Geophysics, Louisiana State University, Baton Rouge, LA 70803 USA

Volcanologists have long considered the appropriate definition of phreatic eruptions to be based upon the presence or absence of juvenile magmatic materials in the deposits. Phreatic eruptions are generally believed to be the result of interaction between some igneous heat source and groundwater, not necessarily involving actual contact between magma and groundwater. In this context, phreatic eruptions can be seen as a special case of "Fuel-Coolant Interaction" (or FCI) in which magmatic materials are not ejected.

The question of the "phreatic" nature of eruptions is often of considerable importance when experts are called upon to make assessment of the risk posed by volcanic activity. Recently, several eruptions have highlighted the problems associated with making that decision: Mt. Baker (1975); Soufriére Guadeloupe (1976); Mount St. Helens (1980); and Nevado del Ruiz (1985). In the first two instances, these eruption sequences ended without significant "magmatic" activity; while the latter examples proceeded to produce catastrophic magmatic results. Considerable controversy surrounded the nature of the eruptive activity at each center and a review of the evidence suggests that inconsistent criteria were applied from one instance to another.

We propose that the time has arrived for volcanologists to clarify what is meant by the term "phreatic" and to establish some more rigorous basis for making the interpretation that a particular eruption was phreatic. In this effort, we are motivated by our feeling that a careless or uninformed use of the term may (and has) result in a serious underassessment of the threat posed by volcanic activity. We believe that recent conceptual and technical advances in descriptive ash morphology, eruption dynamics, and volatile detection would allow us to more carefully make a determination of the fundamental nature of an eruption. This proposed scheme is parallel in conception to the proposal of Sigurdsson and Carey (1987, IAVCEI at Vancouver) for a quantitative classification of eruptions based on their "intensity".

Our proposed definition would limit the term "phreatic" to eruptions which not only produced no juvenile solid products but also no juvenile gases. The March and April, 1980 eruptions of Mt. St. Helens are an excellent example where appropriate monitoring of the gas phase (using a COSPEC) revealed that the sometimes spectacular eruptions were truly devoid of magmatic products, solid or gaseous. The Sept., 1985 eruption of Nevado del Ruiz provides an example of failure of the traditional definition. There the failure to recognize the very large magmatic gaseous emission of the eruption (80,000 metric tons of SO_2) and the official description of the eruption as phreatic may have contributed significantly to the underassessment of the magnitude and immediacy of the threat posed by that volcano (which two months later erupted to kill approximately 25,000).

We propose to consider truly phreatic eruptions as special cases of the FCI model, in which none of the "fuel" is ejected. These probably represent instances in which the ratio of fuel to coolant is <0.2. Heiken and Wohletz (1985) have used the SEM to examine the details of the morphology and surface features of the ejected grains and can distinguish phreatic ash even from phreatomagmatic ash. We explicitly want to focus increased attention on the role of magmatic gases as a critical part of the system. The COSPEC, TOMS satellite, or much simpler gas analyses can provide remote or direct data on the presence or absence of magmatic gases. Field observation of column dynamics, or later analyses of ash distribution and grain size variations should provide the basis for distinction between phreatic and other eruption type deposits. An integrated approach seems justified when making a decision concerning any eruption.

THE ROLE OF LITHOSPHERIC MANTLE SOURCES IN THE GENERATION OF EXTENSION-RELATED BASIC ALKALINE MAGMATISM IN WESTERN EUROPE.

WILSON, Marjorie, Department of Earth Sciences, Leeds University, Leeds LS2 9JT., U.K., and DOWNES, Hilary, Department of Geology, Birkbeck College, 7/15 Gresse Street, London W1P 1PA, U.K.

Tertiary-Quaternary alkaline magmatism within Western Europe is broadly related to major extensional features (e.g. Rhine graben, Limagne basin) transecting regions of domal uplift (e.g. Massif Central, Rhenish Massif). Primitive basic magmas, ranging in composition from mildly alkaline basalts to basanites and nephelinites, have isotopic and trace element geochemical characteristics which suggest an origin by variable degrees of partial melting of a heterogeneous mantle source. A fundamental problem in understanding their petrogenesis involves the relative roles of lithospheric and asthenospheric mantle source components.

Within the largest central volcanic complex, Cantal in the Massif Central (11.2 - 2.9 Ma), alkali basalts and basanites were erupted more or less contemporaneously throughout the history of the volcano, whereas nephelinites are associated with late-stage flank eruptions Combined Nd-Sr-Pb isotopic data for these basic magmas can be interpreted in terms of mixing between distinct mantle components similar to the sources of Dupal and HIMU oceanic island basalts and MORB. Coherent linear arrays in plots of $^{143}Nd/^{144}Nd$ and $^{87}Sr/^{86}Sr$ versus $^{206}Pb/^{204}Pb$ indicate that the high K_2O/Na_2O magmas (nephelinites) preferentially sample the Dupal-like end-member whereas the low K_2O/Na_2O magmas (alkali basalts and basanites) contain a greater contribution from the HIMU-like end-member. The Cantal nephelinites also have similar trace element characteristics to Dupal OIB whereas the basanites and alkali basalts have more affinity with HIMU OIB, consistent with their isotopic characteristics. Isotopic and trace element data for alkaline basic volcanics from other localities within the region are in general agreement with these observations.

The nature of the shallow upper mantle beneath the Massif Central is well constrained by the occurrence of abundant spinel lherzolite xenoliths within the volcanics. Whilst these are unlikely to represent the actual source of the primary magmas they may provide some constraints on the geochemical characteristics of the upper mantle. In terms of their Sr-Nd isotope geochemistry they span the complete range from MORB to Dupal-OIB. Those with MORB-like isotopic signatures and strong incompatible element depletion are common and provide evidence for the existence of MORB source mantle which may represent upwelling asthenosphere within the major regions of extension. Limited Pb-isotopic data additionally suggests the existence of both HIMU and Dupal-like components. However their location remains more enigmatic. Both could potentially reside within the lithosphere but either could be introduced within a deep mantle plume or hot-spot. The observation that the late stage nephelinites of Cantal have a strong Dupal isotopic and trace element signature strongly suggest that this is a lithospheric component.

VOLCANOSEISMIC STUDY OF MT. KELUT, EAST JAVA, INDONESIA

WIRAKUSUMAH, A.D. Geology Department, Victoria University of Wellington, P.O. Box 600 Wellington, New Zealand

Mt. Kelut is an active andesitic volcano in East Java, Indonesia. It lies within a volcanic belt that is about 150 km above the north-dipping Benioff zone, where the Indian Ocean plate is being subducted beneath Java. The longest period of quiescence of the volcano during the period 1300-1900 AD is 75 years, and the shortest is 9 years. During this century, the volcano erupted in 1901, 1919, 1951, and 1966, killing a total of about 5400 people.

The seismicity at Mt. Kelut in 1985 and 1986 (in its repose condition) has been studied, using 271 volcanic earthquakes all of magnitude less than 3.0. In addition, 2177 regional tectonic earthquakes were recorded at Kelut Volcano Observatory during this period. The statistics of recurrence for the volcanic earthquakes are such that the time interval between successive events shows a poisson distribution (random) with an average interval between earthquakes of 68 hours. The magnitude-frequency relationship for the volcanic earthquakes gives a b-value of 2.2, which is the normal value for volcanic earthquakes.

Four types of volcanic earthquakes at Mt. Kelut have been classified on the basis of their waveforms. Type-1 events have clear P and S waves with S much larger in amplitude than P; type-2 have impulsive P and S waves with their amplitudes about equal; type-3 have emergent P waves and ill-defined S waves, with large amplitudes in the middle of the event; type-4 show emergent P waves and often no apparent S waves, with amplitudes relatively constant throughout the event. About 20% of the earthquakes were type-1, 36% type-2, 37% type-3, and 7% type-4. All these earthquake types are A-type volcanic earthquakes (of Minakami). No low frequency volcanic earthquakes (B-type of Minakami) or volcanic tremor were recorded at Mt. Kelut during the period studied.

The distribution of hypocentres shows that almost all the volcanic earthquakes were located west of Mt. Kelut at a maximum depth about 4.5 km. Of the type-1 events, 70% were located on the southwest flank of the volcano, whereas 80% of the type-2 events were located on the northwest flank. Locations of the type-3 and type-4 events were unreliable because of difficulties in onset reading of those earthquakes.

The hypocentres of the volcanic earthquakes lie close to two active normal faults in the summit area of Mt. Kelut. A west dipping fault strikes N-S and can be traced for about 9 km; it passes about 500 m west of the lake that occupies the summit crater of the volcano. Landslides occur frequently along a zone where an active scarp is exposed, and hydrothermal activity occurs along a zone near the active scarp. The other fault strikes NE-SW and dips NW; it passes about 500m north of the lake and can be traced about 8 km. Several lava domes are cut by this fault, and it is related to zones of local cracking and subsidence.

VAPORIZATION AND CONDENSATION OF WATER DURING HYDROVOLCANIC ERUPTIONS

WOHLETZ, K. H., Earth and Space Science Division, Los Alamos National Laboratory, Los Alamos, NM 87545

Tephra deposits produced by hydrovolcanic eruptions show textural features indicative of the presences of moisture during their emplacement. Cohesivity of moist tephra promotes ash aggregation. In general tephra characteristics have been classified as "dry" or "wet," indicating whether or not abundant liquid water is present during tephra emplacement.

During eruption, decompression and vaporization of water occurs after its initial thermal equilibration with hot magma. The proportion of external water vaporized during decompression depends upon the thermodynamic state of the initial equilibrium, which in turn is generally dependent upon the initial mass ratio of water to magma.

After eruption, expansion and condensation of water vapor occurs during emplacement of tephra in flows and surges. If condensation causes the liquid water content in pyroclastic flows and surges to rise above about 10 volume percent, tephra becomes very cohesive and develop "wet" deposit textures; if the content increases to a range from about 30 to 60 volume percent, tephra are emplaced as lahars.

The amount of condensed water emplaced with tephra can be numerically predicted for eruptions where the initial mass ratio is known. The prediction is based upon a multicomponent thermodynamic calculation that considers the degree to which the expanding fluid behaves isentropically or isothermally. Additionally, solution of a continuity equation for this system requires inclusion of nonlinear contributions: (1) progressive vapor escape during surge or flow deflation with runout; (2) the dependence of solid-gas mass fraction upon degree of deflation; (3) runout distance as a function of deposit volume; and (4) two-phase effects upon the vapor equation of state.

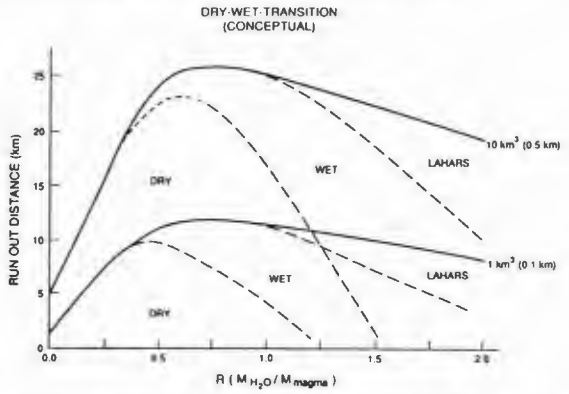

Results of this model show that for small volume eruptions (~1 km^3), initial water/magma mass ratios (R) of 1.00 < R 1.25 can produce deposits that show a facies distribution of near vent dry deposits through medial wet deposits to distal lahars. Lower R values produce dry deposits or dry deposit with distal wet facies; and larger R values produce only wet and laharic facies. However, for larger volume eruptions, larger R values are required to produce a dominantly wet or laharic facies. Considering the lower availability of water to vents erupting large-volume deposits helps to explains why large volume pyroclastic flows generally show only dry facies character where they have a hydrovolcanic origin.

EVIDENCE FOR MULTIPLE HYDROTHERMAL EVENTS AND MINERALIZATIONS IN THE JEMEZ MOUNTAINS, NEW MEXICO

WOLDEGABRIEL, G. and GOFF, F.
ESS-1, Geology/Geochemistry, MS D462
Los Alamos National Laboratory
Los Alamos, NM 87545

K/Ar dates on illitic clays (<2 μm, 2-0.25 μm, and <0.25 μm) separated from subsurface and surface thermally altered samples are used to document hydrothermal episodes in the central Jemez Mountains (Valles caldera), New Mexico. Eleven subsurface samples were obtained from the tectonically and hydrothermally brecciated Paleozoic rocks of the 856-m-deep VC-1 and from thermally altered Plio-Pleistocene volcanic rocks of the 527.6-m-deep VC-2A Continental Scientific Drilling Program core holes. The rest of the samples (11) were collected from altered rocks cropping out along the topographic rim and ring fracture of the Valles caldera and the surrounding late Miocene-Pliocene rocks of the southeast Jemez Mountains. The latter samples provided three whole rock K/Ar dates. The clay separates are illitic (>85%) with K_2O contents of 8.24-10.04% for the core samples and 4.21-9.55% for the outcrops.

Several hydrothermal events are now recognized in the Jemez Mountains region. The earliest event (17-11 m.y., n=4) from altered and illite-rich (>95%), lower most Paleozoic rocks in VC-1 may be correlative with inception of volcanism in the Jemez region (≤16.5 m.y.) provided the five alteration-mineralization stages recognized in these rocks have completely reset older diagenetic clays. Illitic clay separates from altered andesite, dacite, and rhyolite from the topographic rim and flanks of the caldera indicate a hydrothermal event (8.07-6.45 m.y., n=5) associated with waning stages of the Keres Group (13-5.8 m.y.). Slightly altered basalt, andesite, and rhyolite lavas from the topographic rim of the Valles caldera yielded minimum ages of 8.05, 7.07, and 6.1 m.y., respectively, and lie within the age bracket of the Keres Group rocks. Quartz veins intruded Keres Group rocks along shear and breccia zones in the Cochiti mining district of the southeastern Jemez between 6.1 m.y. and 5.6 m.y (n=4). Ages of 1.34 to 1.0 m.y. (n=4) in illite-rich (>90%), hydrothermally altered Paleozoic rocks at a depth of 479 m in VC-1 suggest hydrothermal activity contemporaneous with the formation of Toledo (1.45 m.y.) and Valles (1.12 m.y.) calderas. Ages of 0.83 to 0.66 m.y. (n=4) from illite-rich (>95%), hydrothermally altered Lower Tuffs, Bandelier Tuffs, and post-caldera fill tuff in VC-2A indicate that the Sulphur Springs portion (western ring fracture zone) of the active Valles geothermal system was created soon after caldera formation. The relatively long life of the Sulphur Springs system is probably related to caldera resurgence and the formation of post-caldera rhyolite domes (1.0-0.13 m.y.) along the ring fracture zone.

Major gold and silver mineralization is associated with the emplacement of the Cochiti mining district vein system. Weak sphalerite-chalcopyrite mineralization occurs with the 1.34 to 1.0 m.y. old altered zone in VC-1, whereas galena, chalcopyrite, barite, and molybdenite occur in the very complex, hydrothermally and tectonically brecciated lower zone (800-856-m-depth) of VC-1. Molybdenite (up to 0.56%) associated with 0.66 m.y. old illitic clays occurs with fluorite and trace chalcopyrite, sphalerite, and rhodochrosite in the shallow (40-m-depth) levels of VC-2A. K/Ar results of post-caldera hydrothermal activity are consistent with stratigraphic relations and agree with ages obtained by U/U, U/Th, and paleomagnetic methods.

NEW GEOLOGIC MAP OF THE ISLAND OF HAWAII

WOLFE, E.W., U.S. Geological Survey, David A. Johnston Cascades Volcano Observatory, 5400 MacArthur Blvd., Vancouver, WA 98661, and
MORRIS, Jean, U.S. Geological Survey, P.O. Box 51, Hawaii National Park, HI 96718

Results of recent geologic mapping on the Island of Hawaii are summarized in a new, 1:100,000-scale geologic map, the first comprehensive compilation of Big-Island geology since publication of the classic map of Stearns and Macdonald in 1946. This new compilation incorporates mapping completed during the past decade by more than a dozen contributors. It comprises a detailed geologic base for analysis of patterns and rates of volcano growth, volcano structure, magmatic evolution, and volcanic hazard.

Boundaries of the individual lava flows, vent deposits, and tephra sheets that form the present surface are shown over much of the Island. However, the map is necessarily less detailed in areas of difficult access, particularly the areas of denser rain forest, and limitations of scale have also required some generalization of detail.

The emphasis of the map is strongly chronostratigraphic. The younger lavas, mostly Holocene and latest Pleistocene basalt that comprises most of the surfaces of Kilauea, Mauna Loa, and Hualalai Volcanoes, but also including local postglacial Hawaiitic lava on Mauna Kea Volcano, are assigned to chronostratigraphic units with boundaries at 10,000, 3,000, 1,500, 750, and 200 radiocarbon years. Additional divisions are shown locally at 5,000 and 400 radiocarbon years. Local stratigraphy has been determined from recognition of cross-cutting or overlapping relations that directly indicate superposition and from interpretation of flow-surface modification by weathering or by deposition of mantling deposits. Radiocarbon ages, determined mostly by Meyer Rubin, provide the primary absolute-age control for the chronostratigraphy.

Older lavas, all of late Pleistocene age, are mapped as lithostratigraphic units. The most extensive are the lavas of Mauna Kea and Kohala, which, on each of these volcanoes, consist of an older essentially basaltic section and a younger section ranging from hawaiite to trachyte (Hamakua and Laupahoehoe Volcanics on Mauna Kea; Pololu and Hawi Volcanics on Kohala). Glacial deposits on the upper flanks of Mauna Kea are mapped as members within both the Hamakua and the Laupahoehoe Volcanics. Older units of the other volcanoes include the Hilina Basalt on Kilauea, the Ninole Basalt on Mauna Loa and the Waawaa Trachyte Member on Hualalai.

The map strikingly portrays volcanic patterns such as the summit calderas and rift zones of Kilauea and Mauna Loa, the control of rift-zone structure on the distribution of postshield vents on Hualalai and Kohala, the development of radial vents on the north and northwest flanks of Mauna Loa, the development of extensive flow fields extending from prehistoric summit shields now indented by the summit calderas of Kilauea and Mauna Loa, and the general inward younging of Mauna Kea and Kohala.

ORIGIN OF WIDESPREAD SILICIC LAVAS AND LAVA-LIKE TUFFS

JOHN A. WOLFF, Dept. of Geology, University of Texas at Arlington, UTA Box 19049, Arlington, Tx 76019

It is virtually an axiom in volcanology that silicic ejecta are distributed over large areas of country during explosive eruptions, while effusions of similar compositions invariably form lava domes or short, stubby flows that are restricted to near-vent areas. Recently it has become clear that silicic (ca. 70% SiO_2) lavas covering up to 10^3 km^2, and with aspect ratios in the range 1:500 - 1:1000, exist within the Tertiary volcanic fields of the western U.S.A., notably southwestern Idaho and the Davis Mountains, Texas (1,2). These rocks are <u>not</u> misidentified rheoignimbrites. However, extensive ultrarheomorphic tuffs that closely resemble lavas (lava-like tuffs) typically occur in close association with true extensive lavas (2,3), and distinctions must be made on a case-by-case basis within individual volcanic fields. The nature, extent and relation to underlying topography of flow-unit basal breccias provide the only safe criteria for distinguishing between lavas and lava-like tuffs.

Both rock types form most readily from relatively low-viscosity magmas that experience small degrees of undercooling during eruption. These requirements are fulfilled by silicic magmas with low water contents. Dome-forming silicic lavas consist of initially water-rich, degassed magma (4), and are therefore strongly undercooled, have low temperatures, and high viscosities and yield strengths which inhibit the extrusion rate. In contrast, a dry rhyolite has a liquidus temperature close to 1000°C, is therefore relatively fluid and can attain a high extrusion rate, and experiences little undercooling during eruption. This combination of properties and behaviour allows hot, dry silicic magmas to form widespread lava flow units. Explosive eruption of magma with low volatile contents leads to the formation of dense pyroclastic flows which experience little mixing with the atmosphere and consequent cooling, while high initial temperatures, low viscosities and small degrees of undercooling greatly enhance welding and rheomorphism prior to final groundmass solidification, resulting in a lava-like tuff.

Most described examples are metaluminous to weakly alkaline trachydacites and low-silica rhyolites with moderate phenocryst contents, anhydrous assemblages, and Fe-Ti oxide temperatures in excess of 900°C, fully consistent with low magmatic water contents. These melts perhaps originate by anatexis of volatile-depleted lower crust. The lack of associated calderas in the Idaho and Texas fields, despite volumes in the range 10 - 10^3 km^3, may imply eruption from lower- or mid-crustal depths.

(1) Bonnichsen & Kauffman, GSA Spec. Pap. <u>212</u>, 119-145 (1987).
(2) Franklin et al., GSA abs. w. progs. <u>21</u>, 11 (1989).
(3) Henry et al., Geology <u>16</u>, 509-512 (1988).
(4) Eichelberger et al., Nature <u>323</u>, 598-602 (1986).

ASHFLOW CALDERA FIELDS: EVOLUTIONARY TRENDS

WOOD, Charles A., Johnson Space Center, SN15, Houston Texas 77058, and
DUNCAN, Claire D., Summer Intern, Lunar and Planetary Institute, Houston, TX 77058.

Isolated volcanoes are rare. Where regional tectonic controls are dominant (subduction zones, rifts and island hot spots), volcanoes occur in lines, otherwise they cluster into roughly circular patches which are the surface expressions of magma generation zones. Clustering of basaltic scoria cones and lava flows into *monogenetic volcano fields* is well known (e.g. San Francisco Volcanic Field, Arizona). Silicic calderas also typically occur in *ashflow caldera fields* (ACF), the best studied being the San Juan Volcanic Field of Colorado. We propose that ACFs evolve in systematic patterns, rather than randomly as a collection of independent volcanoes. To test this idea we have compiled the following information for 12 ACFs: area, volume, lifetime, number of calderas, average caldera diameter, nearest neighbor distance, and duration of caldera formation. The ACFs are: Kane Springs, NV; Long Valley, CA; Jemez, NM; Trans-Pecos, TX; Marysvale, UT; McDermitt, NV; Tibesti, Chad; Timber Mt., NV; Yellowstone, WY; San Juan, CO; Younger Granite Province, Nigeria, and Mogollon-Datil, NM. These fields span 3 orders of magnitude in volume, some are long dead and others are still active.

Field area vs. volume: These two measures of field size increase together, with area increasing faster than volume up to ~20,000 km^2; thereafter area changes only by a factor of two, but volume increases by an order of magnitude. The rough maximum area of ACFs (corresponding to circles of diameter ~100 km) may reflect a limiting size of underlying batholiths or magma source regions.

Field volume/area vs. caldera number: Field area and volume are well correlated with the number of calderas in a field. Caldera number triples with each order of magnitude increase in field volume. Thus, ACFs grow not by proportionate increases in number of calderas, but by dramatic increases in the volume of erupted material at each caldera.

Field volume vs. average caldera diameter: The average caldera diameter for all but one of the ACFs is 17.3 ± 4.6 km. This suggests that batholith cupolas - the magma chambers that volcanoes collapse into to form calderas - are approximately equal in size in these ACFs. Note that caldera size does not vary with total field volume. Field volume increases not because of increased numbers of calderas, nor due to bigger calderas, but simply because each caldera is the vent for larger volumes of magmatic material. The average diameter of the three Yellowstone calderas is 54 km! Yellowstone is either a unique ACF, or perhaps its caldera complex results from multiple episodes of caldera collapse that have not been distinguished in the field. Certainly, the two discrete areas of resurgence in the youngest Yellowstone caldera are very unusual.

Caldera number vs. duration: There is only a very general increase in the number of calderas with increasing duration (the interval from the first to the last dated caldera-forming eruption) in the measured ACFs. The observed rate of caldera formation varies from 0.5 to 7.0 calderas/m.y., with an average of 2.3 calderas/m.y. The reciprical of this value (~0.4 m.y./caldera) may indicate the average time required to establish or replenish a magma chamber.

Field volume vs. lifetime and eruption rate: The total duration of activity (lifetime) of ACFs tend to increase with field volume; field volume increases by approximately an order of magnitude as the lifetime doubles. Thus, the average extrusion rate greatly increases with total erupted volume. For field volumes of 10^2, 10^3, 10^4, and 10^5 km^3, the rough eruption rates are 40, 400, 1500, and 3000 km^3/m.y., respectively. This increase in eruption rate with volume is consistent with previous findings for individual lava flows, scoria cones, and monogenetic volcano fields. There are two exceptions to the volume/lifetime trends: both Marysvale and Trans-Pecos had long lifetimes, but small total volumes.

Conclusions: This preliminary study has identified systematic trends in the evolution of ashflow caldera fields, demonstrating that such fields, despite differences in magma compositions and tectonic histories, evolve in generally predictable ways. The single most important factor controlling ACF activity is the total field volume: Given a field volume it is possible to make general estimates of field area, lifetime, caldera number, and eruption rate.

BORON ISOTOPIC SYSTEMATICS IN ISLAND ARC MAGMAS

Woodhead, Jon.D and McCulloch, Malcolm T, Research School of Earth Sciences, A.N.U., Canberra, Australia.

One of the outstanding problems in studies of island-arc magma genesis is quantifying the relative contributions from pristine and altered oceanic crust and subducted sediment to the magma source region. Whilst radiogenic isotope and trace element geochemical studies have generally identified some contribution from one or more of these components, quantitative estimates have remained elusive.

Stable isotope systems which undergo fractionation only in the uppermost portion of the Earth's lithosphere can, in principle, provide an unambiguous means of identifying recycled crustal components. Boron is enriched in marine sediments by factors of $\sim 10^{1-3}$ relative to upper mantle concentrations and it is now well established that the boron isotopic composition of seawater ($\delta^{11}B$=40‰) is much heavier than that of the upper crust. Recent studies (Spivack et.al., 1987) have also shown that the isotopic composition of desorbable boron in marine sediments ($\delta^{11}B$ = 13.9 to 15.8), altered oceanic crust ($\delta^{11}B$ = 0.1 to 9.2) and serpentinized peridotites ($\delta^{11}B$ = 8.3 to 12.5) are all distinct from fresh MORB ($\delta^{11}B$ = -3.7 to -1.7). However ~90% of the boron in marine sediments is not readily desorbable and has been shown to have a composition ($\delta^{11}B$ = -4.3 to 2.8) which overlaps with that of MORB.

On a global scale, the mass flux of subducted altered oceanic crust is ~4.2×10^{16}g/a relative to that of subducted sediments (up to 1.3×10^{16} g/a). Thus, although the concentration of fixed boron in marine sediments is a factor of ~5 times higher than in altered oceanic crust, the overall boron budget of subduction zones magmas may have a significant contribution from altered crust. In addition subduction of seawater derived boron or desorbable sediment boron, could also produce $\delta^{11}B>>0$ signatures in arc basalts. For these reasons we have commenced a study of the $\delta^{11}B$ and B concentrations in island-arc volcanic rocks and associated geothermal systems. Preliminary data are presented for geothermal waters of the Taupo Volcanic Zone, New Zealand and work is currently in progress on volcanic rocks from Mariana island arc.

THE FLUID DYNAMICS AND THERMODYNAMICS OF EXPLOSIVE ERUPTIONS

WOODS, Andrew W., Department of Applied Mathematics and Theoretical Physics, Cambridge University, England, CB3 9EW.

A model for Plinian eruption columns is derived from first principles and investigated numerically. The dynamics particular to the basal 'gas-thrust' region and the upper buoyancy-driven region are treated separately. The thermal interactions in the column are modelled using the steady-flow energy equation. The model accounts for fallout of particles and the resulting loss of the thermal energy source and the decrease in density.

The column is modelled as being in a steady state with a constant continuous supply of material from the vent. The model consists of the equations for the conservation of mass flux and momentum flux, the steady flow energy equation and a further dynamic equation which governs the entrainment of air. In the gas-thrust region we complete the model with an equation representing the drag on the jet due to mixing with the surrounding air, following the results of Prandtl (1954). In the buoyancy-driven region we complete the model with the entrainment assumption (Morton et al., 1956), which states that the horizontal entrainment velocity is proportional to some characteristic column velocity at that height. The bulk properties of the column, including the density, temperature, gas mass fraction and specific heat evolve with height in the column. The atmosphere is modelled with a linearly decreasing temperature in the troposphere, a constant temperature in the tropopause and a linearly increasing temperature in the stratosphere.

The main predictions of the model are that: (1) there is a very rapid expansion of the column in the basal gas-thrust region; (2) the total column height increases with initial temperature, initial velocity and vent radius but decreases with initial gas content of the erupted material; (3) column collapse occurs for initial velocities of the order of 100 m/s, with the precise value increasing as the initial gas content decreases; (4) for large vent radii or low initial gas content of the erupted material the velocity in the column can increase with height in the buoyancy-driven region rather than decaying to zero monotonically; (5) the interaction of the potential energy with the enthalpy is the dominant thermal interaction in the upper region of the column.

The model is investigated for the case in which particles in the column are in thermodynamic equilibrium with the gas and are carried with it (Woods, 1988). The effect of the fallout of particles of different sizes is then incorporated by allowing each particle to remain in the column up to the height at which the mean upward velocity is just sufficient to support its weight. Using this fallout criterion the maximal dispersal radii for particles of various sizes falling out of the column are calculated. Finally, we discuss the influence of non-equilibrium effects arising because large particles retain their thermal energy for a longer time than small particles although they fall out of the column at a lower height thus removing an important source of thermal energy.

Morton BR, Taylor Sir Geoffrey, Turner JS, 1956, Turbulent gravitational convection from maintained and instantaneous sources, Proc. Roy. Soc., A234:1-23.

Prandtl L, 1954, Essentials of fluid dynamics, Blackie, Glasgow.

Woods, AW, 1988, The fluid dynamics and thermodynamics of eruption columns, Bull Volcanol, 50:169-193.

PROTEROZOIC DIABASE DYKE SWARMS IN NORTH CHINA

XIAODE, Chen, Institute of Geology, State Seismological Bureau, Beijing, China

Diabase dyke swarms occupy an area of about 150,000 km^2 in north China, striking NW in the north, NW and WNW in the center, and NW, WNW, and NE in the south. These dykes were dated by K-Ar isochron method, yielding ages of 1.2-1.3 Ga and 1.5-1.6 Ga.

Based on the results of chemical analyses, the rocks are both quartz- and olivine-normative tholeiites. They are somewhat higher in K-Na and lower in Mg. However, these groups do not necessarily coincide with those based on chemical analyses and directions.

The phenocrysts of diabase porphyrite are mainly plagioclase; pyroxene is scarce. In three analyzed plagioclase microphenocrysts where zoning was discernible, the An content gradually changed from 81 in the core to 63 in the rim. This indicates crystal fractionation and contamination of the magma with country rock.

On the basis of strike direction and petrography, at least six groups can be recognized: the NW/4, NE/4, and sublatitudinal-trending diabase containing olivine.

The dykes appear as straight lines on large-scale maps, while small-scale mapping shows them to be curved. In the south, some dykes have more branches than in other areas.

SIGNIFICANT EFFECTS OF VOLCANIC DUSTS ON THE SUMMER CLIMATE OF CHINA

XU QUN, Jiangsu Meteorological Institute
Nanjing, Bei-Ji-Guo,No.2., China

Significant climatic effects in the lower Yangtze have been explored in the case of great volcanic eruptions since 1883. Abnormal cool summers tend to occur just in the years of volcanic eruptions or 2 years following when the solar direct beams were sharply attenuated. The occurrences of such cool summers have been greatly increased recently showing the strengthening of volcanic activities and it also resulted from the upward trend in airborne particulates by anthropogenic effects.

The direct solar radiation in clear skies of China(data of 5 stations) have decreased of about 19% through recent 28 summers(1959-1986). It highly correlates with the cooling trend of mid-China during June-September, especially in July-August and also with the significant decreasing trend of summer rainfall of north China. These correlations show when solar heating on Asia continent is greatly reduced due to volcanic aerosols, summer monsoon of east Asia tends to be weakened with its monsoon rainy belt of high summer(July-August) normally locating at north China retreating southward to mid-China. Hence, the recent cooling of mid-China(Yangtze valley) with more rainfall and the drying trend of north China during high summer have been thus caused by more frequent volcanic eruptions since 1963.

The most influencing volcanic eruption on summer climate of China for recent 70 years is El-Chichon(1982). As for historical times since A.D.1500, China had suffered from a series of "volcanic winter" during summer half years. The most cold summer occured in 1601 when a great northern volcanic eruption just occurred(Lamb, 1970.,Hammer et al 1980), the annal of 4 counties in lower Yangtze recorded following phenomena: "snow flying in heaps and men were clothed with cotton during July". A notable frost ring event also occurred in the western U.S.A. at this summer(LaMarche et al,1984).

LATE PLEISTOCENE TEPHRA ORIGINATED FROM THE CRATER SUBMERGED IN THE SEA BETWEEN HONSHU AND HOKKAIDO, JAPAN

KOTARO YAMAGATA, HIROSHI MACHIDA,
Department of Geography, Tokyo Metropolitan University, Setagaya-ku, Tokyo 158, Japan.
FUSAO ARAI, Department of Geology, Gunma University, Maebashi 371, Japan.

The two late Pleistocene pumice falls and pyroclastic flows were described in the environs of Hakodate, southern Hokkaido, Japan. The sources of them have not yet been determined. A detailed stratigraphic and petrographic studies proved that both tephras were derived from a single eruptive episode. This tephra is named the Zenikame-Menagawa tephra (Z-M). Z-M contains hornblende, orthopyroxene, cummingtonite, biotite, magnetite, plagioclase and quartz as phenocrysts. Mineral assemblage and refractive indices of hornblende and orthopyroxene in this tephra differ from lower to upper, implying the existence of a compositionally-zoned magma chamber.

Isopach map of pumice falls and grain-size characteristics of pumice falls and flows clearly show that the source vent lies in the sea of the Tsugaru Straits close to the present shore (Fig.1). The bathymetry of this area reveals a crater-like depression with a diameter of ca.2km, 2.5km offshore about 50m deep (Fig.2). This is very likely to be regarded as the vent of Z-M. As this tephra has no evidence of phreatomagmatic origin, and also has both radiocarbon and stratigraphical ages of the last glaciation, 33-45ka, the eruption should have occurred on land when sea level was lower than 50m below the present level.

Z-M covers extensive area of southern and eastern Hokkaido (Fig.3). The volume is estimated ca.19km^3 for the pumice falls and ca.9km^3 for the pyroclastic flows.

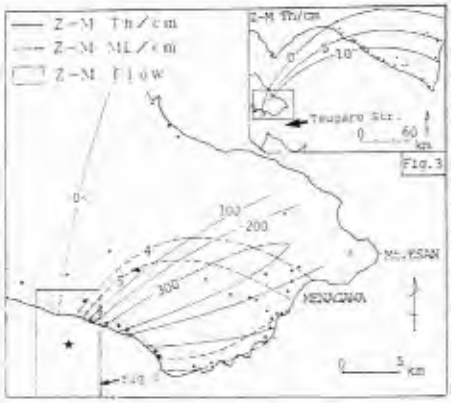

Fig.1 Isopach map and Isograde map of the ML

Fig.2 Bathymetric map

CONTINENTAL RIFT FORMATION IN CENTRAL ASIA IN PHANEROZOIC

YARMOLYUK V.V., KOVALENKO V.I. Institute of Ore Deposit Geology, Petrology, Mineralogy & Geochemistry, USSR Academy of Sciences, Staromonetny, 35, Moscow, 109017, USSR;SAMOILOV V.S. Institut of Geochemistry, Favorsky 1, 664033, Irkutsk, USSR.

In Central Asia continental rift formation took place within southern folded frame of the Siberian platform (NW China, Mongolia, southern Siberia) in Devonian, Permian, Early Mezozoic (T_3-J_1),Late Mezozoic (J_3-K_{1-2}), Late Cenozoic. Each epoch of rift-genesis was characterized by formation of systems of long grabens & normal faults, intensive alkaline, bimodal & basaltic magmatism. Structural position of the rift formation zones is controlled by a few fault systems which are conformable to the southern margin of the Siberian platform.

Rift zones of different age are often spased within a single deep-seated fault system, however their geological development was independent and for each epoch was determined by a concrete geodynamic environment.

In Devonian active continental margin evrironment (ACM) of the Andian type existed in Central Asia that appeared along the border of the paleo-Siberian continent and the Hercinian Paleo-Thetis. A graben system was formed in the back portion of the ACM along the margin of the Siberian platform (Minusa, Rybinsk etc.). Rift zone magmatism was represented by alcaline (basanites, phonolites, comendites, alkali gabbroids, syenites & granites) & subalkaline (olivine basalts, trachites, syenites) rocks.

In Late Paleozoic, a geodynamic environment existed in Central Asia (Californian type ACM) which corresponds to the modern environment in the western USA. As a result, a large rift system was formed within the ACM with overall length exceeding 2000 km. Rift magmatism was represented by bimodal basalt-comendite volcanic associations & alkali granitoids.

The Early and Late Mezozoic epochs correspond to successive stages of development of the Mongol-Okhotsk collision belt. Rift formation zones tend to occur in peripherical parts of the collision belt. In Early Mezozoic, alkali & subalkali (Li-F) granites, bimodal basalt-comendite associations developed in these zones. In Late Mezozoic, more abundant were extrusions of subalkaline olivine basalts as well as of ongorhyolites, ongonites, high-silica trachirhyolites.

The appearance in Cenozoic of the Baikal rift zone is related to the collision of the Indian & Asia continental plates. Magmatism was represented by subalkaline basalts and alkaline basaltoids.

These, continental rift formation with the area under consideration developed repeatedly & in different geodynamic environments. Rift zones of different age were confined to the same deep-seated faults. The latter are viwed as trans lithospheric split-offs preserving this feature during the larger part of the Phanerozoic. Extensional sub-environments pertinent to this or that geodynamic environment brought about rift-genesis processes in the zones of such split-offs. On the whole, the territory of the Central Asia represents a particular structural unit of the Earth which can be identified as a region of polychronous rift formation.

PRECURSORY EARTHQUAKES OF THE 1943 ERUPTION OF PARICUTIN VOLCANO, MICHOACAN, MEXICO

YOKOYAMA, I. and DE LA CRUZ-REYNA, S., Institute de Geofisica, Universidad Nacional Autonoma de Mexico, Ciudad Universitaria, 04510 Mexico, D.F.

Paricutin volcano is a monogenetic volcano of which birth and growth were observed by modern volcanology. At the time of its birth in 1943, the seismic activity in central Mexico was mainly recorded by the Wiechert seismographs at the Tacubaya seismic station in Mexico City about 320 km E of the volcano area. It is interesting to examine the precursory seismic activity of the eruption, though there are some limitations in the available information, such as imprecise location of hypocenters by a single station and lack of earthquake data with magnitudes under 3.4, due to the large epicentral distance and low instrumental magnification. The available data show that the first important precursory earthquake occurred on Jan. 7, 1943, and its magnitude was 4.7. Subsequently 21 earthquakes ranging from 3.5 to 4.8 in magnitude occurred before the outbreak of the eruption on Feb. 20. Though the number of earthquakes is small, it is clear that they do not follow the Gutenberg-Richter's formula and show a predominant magnitude of 4.2.

Except for the first shock, which was one of the largest, the time variation of magnitudes shows an increasing tendency towards the outbreak. The total seismic energy released by the precursory earthquakes amounted to 6×10^{19}erg. Considering that statistically there is a threshold of cumulative seismic energy release ($10^{17\text{-}18}$erg) by precursory earthquakes in polygenetic volcanoes erupting after a long quiescence (Yokoyama, 1988), the above cumulative energy is exceptionally large. This suggests that a monogenetic volcano may need much more energy to clear the way of its magmas to the earth surface than a polygenetic one.

The S-P times of the precursory earthquakes do not show any systematic changes within the observational errors. In almost all the precursory earthquakes, the main wave train were preceded by head P-waves refracted at the Moho-discontinuity. Direct P-waves followed 4-5 sec later. This means that the hypocenters were rather shallow, in the crust and did not migrate significantly.

The predominant period of compressional seismic waves of the precursory erthquakes also shows an increasing tendency towards the outbreak, suggesting that the volume of focal zone had increased with time. However, the predominant period of the precursory earthquakes is smaller than those of tectonic earthquakes occurring off the Pacific coast. This fact helped in the identification of the Paricutin precursory earthquakes.

The present study reveals that a significant movement of magmas beneath Paricutin started in the upper crust 45 days before the outbreak, and that upward migration of the magmas in this type of volcanoes involves much more energy than that in the polygenetic type.

ERUPTION DYNAMICS AND PETROLOGY OF THE NINE MOST RECENT ERUPTIONS OF NEVADO DEL RUIZ VOLCANO, COLOMBIA

YOUNG, Richard H. and WILLIAMS, Stanley N., Department of Geology and Geophysics, Louisiana State University, Baton Rouge, LA 70803 USA

Field measurements and petrographic analyses of pumice lumps from the most recent tephra deposits which mantle the slopes of Nevado del Ruiz volcano have been combined to provide a context in which to view the disastrous eruption of 13 November 1985 (R0). The nine most recent eruptions (R8-R0) have been quantified in terms of volume, grain-size, dispersal pattern and petrographic character. Column heights for these eruptions have been estimated by applying theoretical models of clast dispersal. These results allow direct comparisons of individual eruptions of the recent past, improving hazard assessment at this volcano and increasing the data base for Northern Andean volcanism, in general.

Measurements of the five largest lithic and pumice clasts have been used to produce isopleth maps of tephra distribution for each eruption. These maps have been used to define dispersal axes and estimate theoretical column heights following the method of Carey and Sparks (1986). Isopach maps of deposit thicknesses have been used to estimate total individual volumes. Results indicate that the earlier eruptions have all been less intense events (lower column heights) than R0, but of greater magnitude, producing up to 18 times more volume of material. These deposits have been dispersed along variable axes, up to 180 degrees away from the NE direction of the 1985 deposit. Median grain-size maps indicate that all deposits are fine-grained and not widely dispersed, plotting in the subplinian field on a plot of median grain-size versus area covered. This is interpreted to be a result of the crystal-rich nature of the Ruiz eruptive products (20-60 volume percent phenocrysts).

The pumices are all crystal-rich augite-hypersthene andesites with minor amounts of olivine. Silica concentrations for banded pumices erupted in 1985 range from 62-65.6 percent, with the less abundant, light-colored, high-silica products appearing to be degassed and vesiculating in a brittle manner. A possible temporal trend in magmatic water content exists, with R6 substantially more hydrous (more hornblende) than all other eruptions. R6 may have been largely phreatic in nature; deposits are very fine-grained, lithic-rich and seldom contain juvenile tephra. Preliminary volumes and column heights for each eruption are summarized below.

ERUPTION	VOLUME (Km^3)	COLUMN HEIGHT (Km)
R0	0.016	27.5
R1	0.064	7.5
R2	0.157	25.5
R3	0.001	5.0
R4	0.171	22.0
R5	0.049	20.5
R6	0.079	13.8
R7	0.169	23.5
R8	0.287	24.0

HOLOCENE ERUPTIONS AT MOUNT MAZAMA, OREGON; CHARACTERISTICS AND DISTRIBUTION OF PLINIAN AIRFALL DEPOSITS

YOUNG, Simon R., Volcanology Research Group, Division of Environmental Science, Lancaster University, Lancaster LA1 4YQ, U.K.

The 6845 ±50 yrs. B.P. caldera-forming eruption of Mount Mazama (Crater Lake, Oregon) was preceded within 200 years by 2 plinian eruptions venting from different parts of the climactic magma chamber, producing voluminous airfall deposits followed by lava flows. An ongoing study of the Holocene airfall tephras of Mt. Mazama has confirmed the presence of three widespread tephra blankets, which show different dispersal axes and field characteristics, enabling straightforward correlation of layers over a wide area.

The Llao Rock pumice, erupted less than two hundred years before the climactic eruption, shows the volume and dispersal of a plinian deposit, and is dispersed to the south-east. The less voluminous Cleetwood pumice, which was erupted immediately prior to the climactic event, shows a narrow dispersal pattern towards the east-southeast. The first deposit from the climactic vent is a thin, non-juvenile ash layer formed during vent initiation. This is followed by a complex airfall sequence consisting of three lobes representing at least two phases in the evolution of the climactic plinian column.

The lower pumice unit of the climactic pumice fall consists of northern and eastern lobes generated either from 2 distinct but contemporaneous plinian columns, or by differential wind shear of a single column. The upper pumice unit contains several abrupt grainsize jumps which may represent vent enlargement events or primary fragmentation control related to lowering of magma volatile content due to degassing as the eruption proceeded. Overall reverse grading through this deposit is consistent with an increasing mass flux until column collapse, and final column collapse is preceded by increasing instabilities in the eruption column and generation of numerous pyroclastic flows close to the vent, the final welded ignimbrite being generated from the collapsed column.

Input of new isopleth data to recently published dispersal models suggests a column height in excess of 55 km for the pre-collapse plinian column during the single-vent phase of the climactic eruption, and in excess of 35 km for the pinian column during the Cleetwood eruption. New volume estimates for the Holocene deposits from Mt. Mazama indicate that they represent the most voluminous airfall deposits from the same magma chamber in the Holocene record (plinian airfall volume >20 km^3 tephra), although a significant portion of distal 'Mazama ash' is thought to be of coignimbrite rather than true Plinian airfall origin. The huge dispersal area (1.7 million km^2) and volume (60 km^3 tephra) of the distal ash suggest that it was deposited from a very large ash cloud generated in conjunction with voluminous valley-filling ignimbrites of the ring-vent stage of the climactic eruption.

GEOCHEMICAL AND ISOTOPIC EVIDENCE FOR THE GENESIS OF K-RICH CENOZOIC MAGMATISM IN HEILONGJIANG (THE AMUR RIVER) AREA, N.E. CHINA

ZHANG, M. & SUDDABY, P., Dept. of Geology, Imperial College, London, SW7 2BP, U.K.

Situated between the Songliao graben and Xiaoxingan mountain, the K-rich Cenozoic volcanic rocks in Heilongjiang area (125.54' - 126.36' E., 48.30' - 49.30'N) form a part of the marginal W. Pacific volcanic zone. These rocks come from three groups of volcanoes, Kele, Erkeshan and Wudalianchi and were erupted during three eruptive episodes: Later Neogene, Middle Pleistocene (0.56 - 0.28 m.y.), and the Recent (A.D. 1719 - 1721).

On the basis of their modal composition, these K-rich rocks can be divided into 3 types: 1. ultrabasic olivine leucitites (ol+cpx+lc+ne+phl+oxides), 2. basic leucite basalts (ol+cpx+lc+af+phl+oxides), and 3. basic to intermediate trachytic basalts (ol+cpx+af+phl+oxides).

Geochemically, all these K-rich rocks show strong enrichment of incompatible elements. However, their normalized trace element patterns are dissimilar to subduction-related high-K rocks and to OIBs, thus indicating a possible lithospheric source. Isotopically, these K-rich rocks are moderately enriched in radiogenic Sr and depleted in radiogenic Nd, with $Sr^{87}/Sr86$ = 0.7050 - 0.7057 and Nd^{143}/Nd^{144} = 0.51250 - 0.51232, but strongly depleted in radiogenic Pb, with Pb^{206}/Pb^{204} = 16.84 - 17.31, Pb^{207}/Pb^{204} = 15.33 - 15.43, and Pb^{208}/Pb^{204} = 36.51 - 37.34. These Pb isotope characteristics suggest that the source lithospheric mantle was depleted in U and Th at an early stage of the earth's history. Combining the constraints from isotopic data with those from geochemical data, we can propose two possible models for the genesis of the primitive K-rich magmas: 1, the depleted lithospheric mantle was metasomatized by fluid from the deep asthenosphere before the partial melting which formed the K-rich magma; or 2: the mixing of magmas generated from the partial melting of the depleted mantle with that from an enriched asthenospheric mantle below. Furthermore, the negative correlation of Pb isotope ratio with Sr^{87}/Sr^{86} and SiO_2 implies that the lower crust material may add its contribution to the K-rich magma during its way to the surface.

When the data from all the K-rich rocks is plotted on trace element diagrams (e.g. MgO-Sr or MgO-Ce), considerable scatter is seen. However, systematic variations can be seen when the data from individual volcanoes is separately plotted. This could reflect different assimilation and fractional crystallization processes in shallow chambers.

The heterogeneity of the mantle in N.E. China is well demonstrated by the geochemical differences between these K-rich rocks and alkali basalts from the adjacent area.

ON THE THEORY OF MAGMA ASCENT IN A VISCOUSLY DEFORMABLE CONDUIT

ZHARINOV, S.E., Institute of Volcanology, Petropavlovsk-Kamchatsky, 683006, USSR

Slow magma ascent in a vertical cylindrical conduit imbedded in a denser and more viscous medium is considered, assuming that both magma and country rocks are homogeneous incompressible Newtonian fluids. Recent laboratory experiments by Scott, Stevenson and Whitehead (1986) and Olson and Christensen (1986) have shown that disturbances of the conduit caused by fluctuations in the rate of the buoyant magma supply can propagate upward quasi-stationarily (at a constant speed without changing their waveform). Two types of waves have been observed depending on the regime of magma supply: isolated soliton-like waves, and periodic wavetrains. In spite of the analytical and numerical analysis carried out by several authors (Barcilon and Richter, 1986; Ida. 1987; Takahashi and Satsuma, 1988) the complete theory has not been developed yet.

An approach is suggested to solve the problem within a class of disturbances defined to be non-zero in a finite segment of the conduit. Algorithm and numerical estimates are presented for the propagation speed, length, and amplitude of the waves. In case of small-amplitude disturbances our results are very close to those given by the known soliton-like solution of the problem. For the large disturbances of the conduit the discordance turned out to be rather considerable, specifically, our approach predicts much higher propagation speed which is in satisfactory agreement with the experimental data of Olson and Christensen (1986).

Approximate analytical solutions as well as asymptotic formulae have been derived to estimate the wave parameters. For the case of isolated wave the dimensionless propagation speed c, halflength l, amplitude r, and volume w have been found to be related as follows (in the limit of very large disturbances, $w \to \infty$):

$$c = 0.16w^{2/3}, \quad l = 3.1w^{1/3}, \quad r = 0.9w^{1/3}$$

If the rate of the buoyant magma supply is increased from the background value Q_0 and sustained at a higher level Q_1, the dimensionless propagation speed of the periodic wavetrain is

$$c = (Q_1/Q_0)^{1/2} + 1,$$

and asymptotic solution for the other parameters of the wavetrain (in the case $Q_1/Q_0 = f \to \infty$) are given by

$$w = 15.5f^{3/4}, \quad l = 7.73f^{1/4}, \quad r = 2.26f^{1/4}$$

The mechanism of the intermediate-term deep seismic precursors of the island arc volcanic activity as well as some features of the eruptive process and some other phenomena may be explained by means of the obtained theoretical relationships.

REFERENCES

Barcilon,V.& Richter,F.M. J.Fluid Mech.164,429-448(1986).
Ida,Y. Nagara 6, 150-159 (1987).
Olson,P. & Christensen,U. J.Geophys.Res. 91,6367-6374 (1986).
Scott,D.R., Stevenson,D.J. & Whitehead,J.A. Nature 319, 759-761 (1986).
Takahashi,D. & Satsuma,J. J.Phys.Soc.Jpn.57, 417-421 (1988).

ERUPTIVE DYNAMISM AND VOLCANOMAGNETIC VARIATIONS ON PITON DE LA FOURNAISE VOLCANO

J. ZLOTNICKI AND J.L. LE MOUEL
I.P.G. Observatoires Volcanologiques
Tour 24, 2e étage, 4 Place Jussieu 75252 Paris cedex 05 (France)

Fifteen eruptions occurred during the last three years on the shield basaltic volcano Piton de la Fournaise (Indian Ocean). Most eruptions burst on the North or South flanks of the summital cone while one of them - in March 1986 - opened fissures outside the youngest caldera Enclos Fouqué. During these years up to seven automatic and radioteletransmitted stations have been settled. The magnetic field intensity is simultaneously measured every minute at each station with a 0.25 nT accuracy. All the field differences between the intensities measured at stations P_i and P_j are studied. So, up to 21 differences can contribute to determine the spatio-temporal volcanomagnetic variations and, to evaluate the setting of dykes, and the migration of magma towards the ground surface during the last pre-eruptive seismic swarms.

For all the eruptions or seismic crises without eruptions which are often associated with seismic events of low magnitude (less than 2) and of superficial depth (less than 3.5 km), magnetic variations have been recorded. The amplitude of these variations can reach several nanoteslas during the days or weeks which precede the eruptions, and can even overcome 12 nT during the last pre-eruptive seismic crisis which is followed by the opening of fissures (see the two eruptions on November 1987 on Figure). Variations are observed in the remote stations for crises interesting the whole volcanic massif (for example, March 1986). The time constants are in the range of one minute or less to several weeks. The comparison between volcanomagnetic variations associated with the fifteen eruptions lead to discriminate magnetic signatures according to the features of the eruptions; and the different wavelengths give information about the depth of the stresses sources.

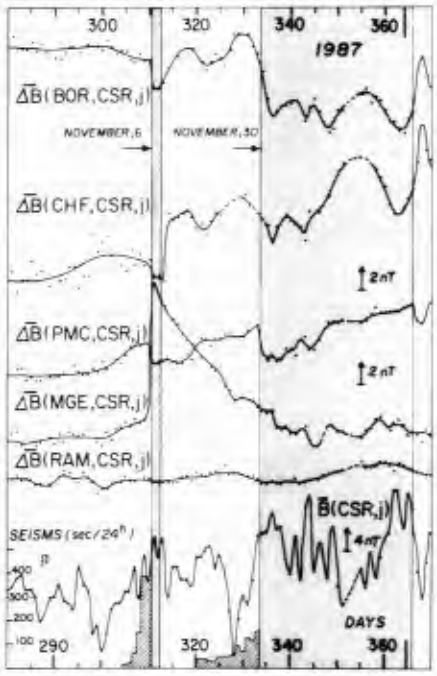

Mean daily values associated with November 6, and December 30, 1987, eruptions.

LATE ARRIVALS

EARLY PROTEROZOIC EXTENSIONAL MAGMATISM IN CENTRAL ARIZONA

DANN, J.C., Department of Earth and Planetary Science, Washington University, St. Louis, MO 63130.

The Early Proterozoic of central Arizona is part of a 1300 km wide orogenic belt of dominantly juvenile crust (ca. 1.6 - 1.8 Ga), interpreted to represent the accretion of diverse tectonostratigraphic terranes. No ophiolites have yet been reported, however, the early tectonostratigraphic history of one, unique, crustal block is dominated by extensional magmatism (ca. 1740 Ma). From bottom to top the system consists of 1) layered gabbro; 2) gabbro to quartz diorite, minor granite, roof pendants of sedimentary and felsic volcanic rocks, all cut by an extensive dike swarm; 3) a sheeted dike complex with locally abundant diorite and granitoid screens; and 4) a stratigraphically continuous, highly silicified unit that marks an abrupt transition from sheeted dikes to submarine volcanic rocks. The mafic rocks are overlain by dacitic volcaniclastic rocks and jasper and then a thick succession of turbidites (ca. 1730 Ma).

Cross cutting relationships suggest the entire mafic system is coeval, and the conspicuous lack of dikes in the layered gabbro interpreted to be a deeper level of the system suggests that the dike swarm represents rifting of the congealed roof above a still molten magma chamber. The abrupt and stratigraphically continuous transition from sheeted dikes to volcanic rocks, as well as the presence of the overlying turbidites, indicate that the extensional magmatic system formed the floor of a marine basin.

Near the southern boundary of the crustal block the extensional magmatism was manifest as a mafic dike swarm in granite, sheeted dikes with granite screens, and a silicified transition to submarine volcanic rocks. The granite is ca. 1760 Ma, possibly 20 my older than the mafic magmatism. The presence of this older granite, the felsic roof pendants, the distinctive silicified unit, and the generally more evolved nature of the magmatic system suggest that earlier arc or continental crust was rifted and fragmented and involved in the mafic extensional system during formation of a marginal marine basin. The basin became emergent during intrusion of high-silica, granite-rhyolite-caldera complexes (ca. 1700 Ma), was buried by quartzite, and then affected by foreland thrust and fold deformation (ca. 1650 Ma) and low greenschist facies

IGNIMBRITES OF WESTERN AND SOUTHWESTERN RAJASTHAN, INDIA : PETROLOGICAL AND GEOCHEMICAL STUDIES.

Vinod Agrawal and Rajani Upadhyaya, Univer. Department of Geology, Udaipur 313 001, INDIA

Vast accumulations of ignimbrites are exposed as scattered outcrops at several localities in western and southwestern Rajasthan, India. These ignimbrites are generally associated with felsic lava and pyroclastic rocks of Precambrian and early Cretaceous (?) age. There is diversity of ignimbrite deposits due to difference in erruptive history, viscosity, volume and mobility of pyroclastic flows, welding and compaction. The present work makes an attempt to study the ignimbrites of three localities of SW Rajasthan.

1. Karara - Tavidar area (24°54' N: 72°05'E) : The Karara - Tavidar volcanic provincve is composed of voluminous ignimbrites and subordinate lava flows and volcanoclastics. The ignimbrites of the area are trachytic to rhyolitic in composition. The rhyolitic ignimbrites can be further classified as (i) normal ignimbrites (ii) sodi-potassic ignimbrites (iii)potassi-sodic ignimbrites. The rocks have middle to highly welded texture and plastic deformation and welding together of glass shards is a common feature. The petrological and field studies are indicative of a definite caldera event in the area.

2. Gurapratap Singh - Diri area (25°35'-25°40' N : 73°-73°10' E): In the area the ignimbrites are associated with intermediate to acid lava. The ignimbrites are dacitic to rhyolitic in composition (64 to 78% SiO_2) Glass shards with varying degrees of distortion due to welding, corroded quartz and collapsed pumice fragments are characteristics of these rocks.

3. Manihari area (25°40' : 73°07') : The Manihari ignimbrites inspite of intense welding show glass shards in varying degree of preservation. These are rhyolitic in composition and can be classified in three main types on the basis of petrochemical characters viz. (i) ignimbrites (ii) high-silica ignimbrites (iii) potassic ignimbrites.

The field, petrological and geochemical studies carried out on these ignimbrites revealed their volcanological origin. The results of the studies have been discussed in the paper alongwith the probable pattern of erruptive mechanism.

PIEZOTHERMOMETRIC MEASUREMENTS ON KILBOURNE HOLE XENOLITHS AND CONSTRAINTS ON THE THERMAL EVOLUTION OF THE SOUTHERN RIO GRANDE RIFT

Gilles Y. Bussod, Geophysics Group, Earth and Space Sciences Division, MS C335, Los Alamos National Laboratory, Los Alamos, NM 87545

A simple thermal conduction model constrained by piezothermometric arrays obtained from coexisting minerals in both crustal and mantle xenoliths from Kilbourne Hole, New Mexico is used to understand the development of rifting and the thermal evolution of the lithosphere in the SRGR. The 1-D finite difference code involves crustal thinning and underplating by dike injection principally into the uppermost mantle (Fig. 1). The model is in good agreement with the thermometric arrays assuming a transient, pre-rift gradient superimposed on a stable geotherm yielding a gradient of 20°C/km in the 40-km-thick crust and 3°C/km in the mantle 30 m.y.a. This is consistent with pre-rift volcanic activity in the area possibly related to Laramide orogenic events. A massive injection of basaltic dikes and sills (20-30 Vol. %) in the uppermost mantle and at the base of the crust probably occurred in the early development of the SRGR, between 20 and 30 m.y.a. The heat contribution due to the injection of dikes is treated as a temperature dependent heat source distributed uniformly throughout the intruded region which extends from 35-55 km depth. Textural observations along with major and trace element chemistries of the mantle and crustal xenoliths indicate intense metasomatism and recrystallization may have occurred during partial melting associated with this event 20 to 30 m.y.a. This is consistent with early rift bimodal volcanism associated with crustal contamination and linked to approximately 30% total NE-SW extension. Dike injection and crustal thinning cease at 20 m.y.a. associated with the mid-Miocene lull in volcanic activity. The total volume of material injected, 100 km^3/km length of rift per m.y., is approximately an order of magnitude less than for a mid-ocean ridge. Conductive cooling of an uppermost mantle (40-45 km depth) from temperatures of over 1200°C (22 m.y.a.) leads to a present day heat flow of 80 mW/m^2 within observed values (Fig. 2). This model suggests that:

1. Crustal thinning may be minor in the SRGR and that magmatic injection is the dominant contributor to rift extension. If correct, the present day MOHO is due to underplating.

2. Rifting may have been associated with pre-San Andreas fault coupling of the Pacific and North American plates (30 m.y.a.) and subduction of the Farallon plate, and is no longer active at present. These conclusions are consistent with the minor extension and volcanic activity since 20 m.y.a. in the SRGR.

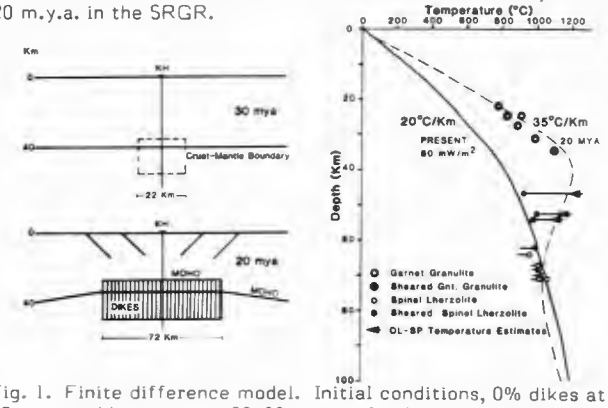

Fig. 1. Finite difference model. Initial conditions, 0% dikes at 30 m.y.a., dike injection 30-20 m.y.a., final configuration 70% dikes (underplating) at 20 m.y.a.

Fig. 2. Kilbourne hole crustal and upper mantle thermometric arrays. Model temperature profiles shown at 20 m.y.a. (dashed line) and present (solid line).

INTRACALDERA DEPOSITS AT "IL PIANO" (VULCANO, AEOLIAN ISLANDS, ITALY).

DE ASTIS G., LA VOLPE L., Dipartimento Geomineralogico, Università, Via Salvemini, 70124 Bari, Italy, and FRAZZETTA G., Istituto Internazionale di Vulcanologia, Viale R. Margherita, 6, 95123 Catania, Italy.

The Piano, that has a maximum elevation of 500 m a.s.l., is a subcircular caldera, 2.5 km in diameter, formed between 107,000 and 99,000 years B.P. Its formation has been connected to the collapse of the upper part of the former composite cone, with its height originally about 1,000m a.s.l.

As a consequence of many cycles of volcanic activity, the caldera was infilled by different volcanic deposits, in a period between 99,000 and <10,000 years B.P.

In the entire volcanic history, two main phases can be distinguished. The first phase, occurring between 99,000 and 78,000 years B.P., was characterized by a quasi-purely magmatic activity, with the formation of a sequence of lava flows, at least 170 m thick, and andesitic in composition.

The second phase, ranging between 78,000 and <10,000 years B.P., shows a more complex history with great variation in the volcanic deposits. Wet surges, dry surges, fall beds, cinder and scoria cones, welded and non welded scoriae deposits, ash flows and lava flows, are the principal types of deposits produced during this period of actvity.

The structural pattern, the dispersal of the deposits and their relationship indicate that the volcanic activity occurred inside the caldera, partially through a ring fault system.

Unconformities and strong erosional surfaces have allowed more than 10 volcano stratigraphic units (V.S.U.) to be distinguished, in which the magmatic components range in composition from basalts to andesites. Some of the recognized V.S.U. show an evolution from hydromagmatic to purely magmatic type of eruption, as observed in the Fossa cone.

Using contour map processing, the landform of the caldera at the time of its formation has been reconstructed. For each V.S.U. the dispersal of the deposits has been calculated, on the basis of field data and of a theoretical models of the emplacement.

The present landform is a combination of many factors in which erosional processes have played an important role.

WET VERSUS DRY VOLCANISM: AN EXAMPLE AT LA FOSSA CONE OF VULCANO (AEOLIAN ISLANDS, ITALY)

DE ROSA R., Dipartimento Scienze della Terra, Università della Calabria, Arcavacata di Rende, 87036 Cosenza, Italy, FRAZZETTA G., Istituto Internazionale di Vulcanologia, Viale R. Margherita, 6 95123 Catania, Italy, and LA VOLPE L., Dipartimento Geomineralogico, Università, Via Salvemini, 70124 Bari, Italy.

On Fossa cone the eruptive cycles show a similar pattern of activity starting with wet-surge beds, followed by dry-surge beds, fall deposits and finally by lava flows. This pattern has been interpreted in terms of a decreasing in the efficiency of water-melt interaction (Frazzetta et al., 1983).

The present study is focused on dry-surge deposits which represent an intermidiate stage between very wet and purely magmatic conditions.

Dry-surge deposits at La Fossa generally consist of unconsolidated fresh sandy laminae, in which planar bedding and large-scale cross-stratification are the main bedforms.

A 70-cm continuous sequence of Palizzi dry-surge deposits, which has hardened in the field, has been removed for detailed laboratory investigation.

Three main types of structures are present, in decreasing order of abundance: i) alternance of sub-millimetric beds formed by a couple of coarse and fine ash laminae; ii) centimetric beds formed by coarse ash showing normal grading overlaied by a fine upper ash layer of uniform thickness.

All the beds consist of juvenile particles with rare lithic fragments, suggesting a high level of magma fragmentation in the conduit.

A different distribution of the crystal-glass ratio has been observed in the three main types of structure, whereas the morphology of the grains is similar in all the beds. Glassy particles are poorly-vesiculated with sub-angular forms and with the presence of hydration cracks, even on the inner part of the broken bubbles. Both glasses and crystals exhibit either a weaklypitted surface or a thiny film of overgrowth and coating of secondary minerals, including vapour-phase crystallization.

The uniformity of the morphological features of the grains suggests that the three types of beds are due to a different modality in the mechanisms of transportation, rather than to different fragmentation processes.

A SUBAQUEOUS CALDERA IN THE ORDOVICIAN (CARADOC) MARGINAL BASIN OF WALES

HOWELLS, M.F., REEDMAN, A.J. and CAMPBELL, S.D.G., British Geological Survey, Aberystwyth, Dyfed, Wales, UK, SY23 4BY.

The Lower Rhyolitic Tuff Formation represents a major episode of caldera-forming, sub-alkaline rhyolitic ash-flow tuff volcanism in the Caradoc sequence of Snowdonia (NW Wales). c.60 km^3 of primary ash-flow tuff was erupted and the thickness variations distinguish an intracaldera and outflow facies. The caldera, with a diameter of c.12 km, developed across a shoreline, with a low coastal plain in the SW and a deepening marine environment to the N and E. The eruptions commenced subaerially in the S but later the centres migrated northwards beyond the shoreline. Caldera development was as follows:

1. Prior to the eruptive cycle, magma movement at depth locally updomed partially lithified sediments at the surface and here the suprajacent intracaldera tuffs are markedly discordant with the substrate.
2. Volcanic arc related basalt magma, locally pillowed, leaked to the surface, about the periphery of the domal structure.
3. The earliest acidic ash-flow tuff eruptions were from fissure vents, in the SW quadrant of the caldera, in a major NE-trending fault zone. Associated movements along active fault scarps caused accumulation of thick wedges of megabreccias.
4. The centre of the main-phase caldera-forming eruptions migrated north-eastwards to lie close to the northern margin of the caldera, resulting in its asymmetric downsag form. Tuff accumulation broadly kept pace with subsidence. Associated outflow tuffs were emplaced in shallow-marine to deep shelf environments.
5. Rhyolite intrusions and extrusions were intimately associated with pre-, syn- and post-caldera development. Five main groups, subalkaline to peralkaline, have been distinguished geochemically and their distribution reflects changes in structural controls in the caldera with time. Trace element ratios of the acidic ash-flow tuffs have discriminated phases of development and relationships with specific rhyolite compositions.
6. A phase of rhyolitic emplacement was associated with caldera resurgence and the resulting pattern of differential uplift largely controlled the shallow-marine reworking of the intracaldera tuffs.
7. The intracaldera tuffs are underlain by shallow-marine sediments and overlain by basaltic sediments derived from shallow-marine reworking of basaltic islands of transitional within-plate tholeiite to ocean island basalt composition. The volcanism of the centre culminated with peralkaline rhyolite and ash-flow tuff emplacement.
8. Late stage extensive hydrothermal alteration of the intracaldera tuffs was associated with sulphide mineralisation.
9. Petrogenetic studies suggest that the rhyolitic groups are derived from a range of basaltic parent magmas, predominantly by fractional crystallisation but with limited assimilation of continental crust.

THE EVOLUTION OF REE IN GARNET AND CLINOPYROXENE MEGACRYSTS IN ALKALI BASALTS FROM CHINA

HUANG WANKANG, WAN JUNWEN, XIE GUANGHONG, Institute of Geochemistry, Academia Sinica, Guiyang, Guizhou Province,P.R.C., and A.R. Basu, Department of Geological Sience, University of Rochester, Rochester, NY 14627 USA

The clinopyroxene and garnet megacrysts occurring in alkali basalts from Kuandian, Liaoning Province and Hanobar, Hebei Province Eastern China have been investigated. The Al-augite megacrysts possess the compositions of Ca/Ca+Mg=0.402-0.495 and Mg/Mg+Fe=0.713-0.846. There is a trend of crystallization differentiation with the increase of CaO content and the decrease of MgO content in Al-augite. The Al_2O_3 contents of all the Al-augites are larger than 8.06%, and a positive correlation between the Al_2O_3 contents and Ca/Ca+Mg values is found, that is,the Al_2O_3 content in clinopyroxene increases at the latter stage of crystallization. Though many experimental results show that the higher the pressure, the more the Al_2O_3 content in clinopyroxenes, it is hard to imagine that the pressure could be higher at latter stage of clinopyroxene crystalization. The garnet megacrysts from Kuandian have the Mg/Mg+Fe values ranging from 0.64 to 0.72, and show a crystallization differentiation trend which appears while the MgO content decreases and the FeO content increases.

The REE contents and their chondrite-normalized patter of Al-augite megacrysts are similar with that of clinopyroxene megacrysts in volcanic rocks in the world. Six REE chondrit-normalized patterns of Al-augites crossed each other. because the latter crystallized one has higher LREE and lower HREE than the former. According to the La,Ce contents in Al-augites and Yb, Lu contents in garnets(Cpx: the former with La 1.5ppm, Ce 7ppm, the latter La 2.4ppm, Ce 9ppm; Gt: the former with Yb 12.2ppm, Lu 1.88ppm, the latter Yb 8.17ppm, Lu 1.05ppm), the calculated values of crystallization index F range from 0.6 to 0.75 for Al-augite megacrysts and from 0.82 to 0.93 for garnet megacrysts. It means that the crystallization process of Al-augites lasted longer than that of garnets, and there was almost half volume of magma left as a residue liquid while crystallization of Al-augite megacrysts had terminated.

The REE evolutions in garnet and Al-augite during crystallization process exhibited the changes of REE contents in primary magma, from which the megacrysts crystallized. That is, the LREE contents were increasing while the HREE were decreasing in primary magma. Whatever the host rocks are thought as the primary or residual magma, the REE contents of calculated primary magma still fall in the REE range of alkali basalts.Because the Pb isotope data are very different between the Al-augite and host rocks,it is reasonable to suppose that the megacrysts had crystallized from alkali basalt magma, but might not be the magma of the host rocks.

This program was supported by NSF U.S.A..

THE RELATION OF FLOW REGIMES TO STRATIGRAPHY

KIEFFER, SUSAN WERNER, U.S. Geol. Survey, Flagstaff, AZ 86001 and Dept. of Geology, Arizona St. Univ., Tempe, AZ 85287

Measured velocities and measured (or inferred) depths of volcanic flows (ranging from low-viscosity lava flows to pyroclastic flows, surges, and blasts) suggest that both gas compressibility and gravity can play important roles in the momentum of the flow. The relative roles of these two effects may vary spatially and temporally. At the present time no theoretical models can account for both gravity and compressibility simultaneously for flows across complex terrain.

Gravity effects can often be isolated and studied in river, lava, or debris flows because compressibility can usually be neglected if the flows do not contain much gas. In a gravity flow, the rheology can vary so substantially that rigid-body sliding can be considered as one end-member, whereas inviscid flow of a fluid in a relatively shallow channel (hydraulics) provides another end-member. In inviscid, incompressible channel flow, transitions in flow regime occur when the Froude number, Fr changes from < 1 to > 1 [$Fr = u/a$, where u, is the flow velocity, and a is a characteristic velocity $(=gD)^{1/2}$; g is the acceleration of gravity and D is depth]. When $Fr<1$, flow is subcritical, we perceive it as "deep and slow", and standing waves do not exist; this flow regime has been called the "lower flow regime" by sedimentologists. When $Fr>1$, flow is supercritical, we perceive it as "shallow and fast", and standing waves (hydraulic jumps) are stable (this is the "upper flow regime" of sedimentologists). Transitions between subcritical and supercritical flow regimes have been observed both in Hawaiian lava rivers, in debris flows, and in high-gradient rivers. Transitions between the two flow regimes can be caused by changes in bed slope, in discharge, or in channel shape, or by flow spreading. Although these transitions can be documented in an active flow by measurements of velocity, depth, and wave structure, it is extremely rare to find field evidence of the flow regimes after the flows have waned because the characteristics of the flow field change with time during both the waxing and waning phases of an event. Thus, it is sometimes difficult to unravel the temporally and spatially variable flow field from the sedimentary record left after a flow.

Compressibility may dominate in the momentum equation if a flow is gassy, but it is much more difficult to isolate and document the effects of compressibility in the field. There are two flow regimes in compressible-gas flow that are semiquantitatively analogous to subcritical and supercritical shallow-channel flow. When the Mach number, M, changes from <1 to >1, the flow regime changes from subsonic to supersonic ($M = u/c$, where c is the sound speed of the fluid). If $M<1$, flow is subsonic and standing waves do not exist within the flow. If $M>1$, flow is supersonic, and standing waves (shock or rarefaction waves) can exist in the flow.

There is an analogy between shallow-channel flow and compressible-gas flow that is useful for flow visualization. If the momentum equations for shallow-channel flow and for compressible-gas flow are nondimensionalized, pressure and depth become equivalent variables. All properties of a compressible-gas flow field and of a shallow-channel flow field become comparable. The transitions between subcritical and supercritical flow that are rather easily documented in gravity-driven flows can be used to understand the transitions between subsonic and supersonic flow regimes that are less easily documented. The problem of relating changes in compressible-gas flow regimes to the sedimentary record (including erosion as well as deposition) is the same as in shallow-channel flow.

Gravity and compressibility may have comparable roles in many volcanic flows, that is $M\sim1$ and $Fr\sim1$. The equations of motion for such flows have not yet been solved. However, the possibility of changes back and forth between subsonic, supersonic, subcritical and supercritical conditions suggests that these flow fields will be extremely complex. Different flow regimes should be expected. They can have dramatically different transport capacities because flow velocity and depth are highly regime-dependent, and the final record of the flow event may be an incomplete record of some of the erosion and sedimentation that occurred throughout a flow field that was very complex spatially and temporally. For example, changes of flow regime may have occurred on scales ranging from kilometers to meters during the waxing and waning phases of the lateral blast of May 18, 1980 at Mount St. Helens, because of lateral spreading of the flow (influencing both the compressibility and hydraulic effects) and the response of the flow on a very local scale to the complex terrain through which it travelled .

FISSURE-VENTS IN THE RING-FRACTURE SYSTEM OF THE HWASAN CALDERA, REPUBLIC OF KOREA

REEDMAN, A.J., British Geological Survey, Aberystwyth, UK, SY23 4BY, PARK, K.H., Korea Institute of Energy and Resources, 219-5 Garibong Dong, Guro-Gu, Seoul, Korea, and MERRIMAN, R.J., British Geological Survey, Keyworth, Nottingham, UK, NG12 5GG.

In southern Korea, late Cretaceous volcanism within a continental volcanic arc bordering the Asian/Pacific margin was characterised by the voluminous eruption of acidic ash-flow tuffs accompanied by caldera-collapse. At the Hwasan caldera, approximately 15 km in diameter, post-Cretaceous erosion has exposed the ring-fracture system and the adjacent caldera floor; the thick (>1.5 km) intra-caldera rhyolitic tuff sequence is partially preserved. The sub-volcanic sequence of well bedded Cretaceous sediments exhibits low dips ($0-20^{o}$) both inside and outside the caldera. The ring-fracture system cuts these sediments and consists of steeply inward dipping ($70-85^{o}$) inner and outer faults, the outer fault being the main caldera-bounding fracture. Between these faults the sediments dip sub-vertically and form a 'steep belt' up to 700 m wide in which sediments of contrasting competence have been subjected to either brittle or ductile deformation. The shortening required to accommodate the relative downward movement, on inward dipping faults, of the central caldera block accounts for the formation and internal deformation of the steep belt and for the small-scale folding and thrusting of strata in the central block adjacent to the inner ring-fault.

A flared fissure-vent system is exposed along a 20 km sector of the inner ring-fault. It consists of a series of tuff dykes, the largest, up to 700 m wide, comprising a multiple intrusion of five contrasting facies. These facies, in order of emplacement, are:

1. Welded rhyolitic tuff, locally brecciated, with a sub-vertical welding foliation.
2. Nonwelded, rhyolitic, crystal-rich lapilli tuffs. This is the most voluminous of the tuff facies in the fissure-vent system and can be traced from the vent into the intra-caldera tuffs.
3. Andesite, in the form of a large plug and associated dykes intruding the tuffs of 1 and 2.
4. Coarse, nonwelded, pyroclastic breccia containing blocks (<2 m) of all previous facies and occurring as an elliptical pipe-like intrusion and dyke system cutting the andesite plug.
5. Nonwelded, heterolithic, crystal tuff and pyroclastic breccia, with delicate, flow-aligned shards in the matrix, occurring in narrow dykes cutting facies 2.

A tuff dyke, up to 20 m wide, comprising pyroclastic breccias similar to either facies 4 or 5 crops out sporadically along the outer ring-fault.

GRANOPHYRIC PORPHYRIES OF THE NYACK SECTION: NEW CONTACTS OLD PROBLEMS

Steiner, J.C., Department of Earth and Planetary Sciences, City College of New York, New York, NY 10031, and Walker, R.J., Radiation Center, Oregon State University, Corvallis, OR 97331

Four basaltic horizons (H1-H4) occur in the Nyack, New York section of the Palisades. At the western limit, coarse two pyroxene basalt porphyries (H1) intrude pigeonite diabases (H2) along a north-south contact and upwarp a veneer of diabase and metashale. The porphyries are defined on the basis of slender (to 5 cm) augite laths and plagioclase phenocrysts set in a weak to moderately altered glassy mesostasis; the mesostasis locally comprises up to eighty volume percent of the rock and is five to ten percent granophyric.

H1 is iron-enriched (12-14% FeO^{*}) and Cr poor (10 ppm) relative to diabases (8-12% FeO^{*} and 100-300 ppm, respectively) and a multiphase intrusion based on a two fold variation in its REE and trace metal abundances. H1 correlates in REE and trace metal patterns to granophyric layers of the southern Palisades.

To the east, H2 diabases are in contact with the iron-enriched (avg 17% FeO^{*}) porphyry H3 having REE and trace metal concentrations similar to H1. Porphyry H3 faces pigeonite diabase H4 on the east. The H3 mesostasis contains unusual microscopic particles of reduced iron (possibly kamacite), native copper, chalcocite and other sulfide species. This assemblage suggests either (1) an extreme diffusive and oxidative disequilibrium during the alteration of the glasses or (2) an iron-enriched source (mantle, meteorite or iron-formation) at stages of magma generation or intrusion.

In general, the mineralogy and geochemistry of the four basaltic horizons are similar to those reported previously from the Palisades. However, there are notable differences: (1) the presence of iron-enrichment trends in all horizons and (2) the absence of modal olivine or orthopyroxene. In particular, the observed iron- and vanadium-enrichment are at variance with a magnetite fractionation theory for the origin of the commonly observed chromium-depletion trends. Similarly, pyroxene fractionation is incompatible with the non-covariant scandium trend. Basaltic liquids in the Nyack section thus differ from their counterparts in other sections in requiring fractionation of, for example, chromium spinel at depth rather than in the Palisades system, or the batch melting of an iron-rich and heterogeneous source. The REE and trace metal systematics favor the fractionation hypothesis.

INDEX

Presenter is the first author except where underlined.
Asterisk denotes invited contributions.

Selected conversion factors*

TO CONVERT	MULTIPLY BY	TO OBTAIN
Length		
inches, in	2.540	centimeters, cm
feet, ft	3.048×10^{-1}	meters, m
yards, yds	9.144×10^{-1}	m
statute miles, mi	1.609	kilometers, km
fathoms	1.829	m
angstroms, Å	1.0×10^{-8}	cm
Å	1.0×10^{-4}	micrometers, μm
Area		
in^2	6.452	cm^2
ft^2	9.29×10^{-2}	m^2
yds^2	8.361×10^{-1}	m^2
mi^2	2.590	km^2
acres	4.047×10^{3}	m^2
acres	4.047×10^{-1}	hectares, ha
Volume (wet and dry)		
in^3	1.639×10^{1}	cm^3
ft^3	2.832×10^{-2}	m^3
yds^3	7.646×10^{-1}	m^3
fluid ounces	2.957×10^{-2}	liters, l *or* L
quarts	9.463×10^{-1}	l
U.S. gallons, gal	3.785	l
U.S. gal	3.785×10^{-3}	m^3
acre-ft	1.234×10^{3}	m^3
barrels (oil), bbl	1.589×10^{-1}	m^3
Weight, mass		
ounces avoirdupois, avdp	2.8349×10^{1}	grams, gr
troy ounces, oz	3.1103×10^{1}	gr
pounds, lb	4.536×10^{-1}	kilograms, kg
long tons	1.016	metric tons, mt
short tons	9.078×10^{-1}	mt
oz mt^{-1}	3.43×10^{1}	parts per million, ppm
Velocity		
ft sec^{-1} (= ft/sec)	3.048×10^{-1}	m sec^{-1} (= m/sec)
mi hr^{-1}	1.6093	km hr^{-1}
mi hr^{-1}	4.470×10^{-1}	m sec^{-1}

TO CONVERT	MULTIPLY BY	TO OBTAIN
Pressure, stress		
lb in^{-2} (= lb/in^2), psi	7.03×10^{-2}	kg cm^{-2} (= kg/cm^2)
lb in^{-2}	6.804×10^{-2}	atmospheres, atm
lb in $^{-2}$	6.895×10^{3}	newtons (N)/m^2, N m^{-2}
atm	1.0333	kg cm^{-2}
atm	7.6×10^{2}	mm of Hg (at 0° C)
inches of Hg (at 0° C)	3.453×10^{-2}	kg cm^{-2}
bars, b	1.020	kg cm^{-2}
b	1.0×10^{6}	dynes cm^{-2}
b	9.869×10^{-1}	atm
b	1.0×10^{-1}	megapascals, MPa
Density		
lb in^{-3} (= lb/in^3)	2.768×10^{1}	gr cm^{-3} (= gr/cm^3)
Viscosity		
poises	1.0	gr cm^{-1} sec^{-1} *or* dynes cm^{-2}
Discharge		
U.S. gal min^{-1}, gpm	6.308×10^{-2}	l sec^{-1}
gpm	6.308×10^{-5}	m^3 sec^{-1}
ft^3 sec^{-1}	2.832×10^{-2}	m^3 sec^{-1}
Hydraulic conductivity		
U.S. gal day^{-1} ft^{-2}	4.720×10^{-7}	m sec^{-1}
Permeability		
darcies	9.870×10^{-13}	m^2
Transmissivity		
U.S. gal day^{-1} ft^{-1}	1.438×10^{-7}	m^2 sec^{-1}
U.S. gal min^{-1} ft^{-1}	2.072×10^{-1}	l sec^{-1} m^{-1}
Magnetic field intensity		
gausses	1.0×10^{5}	gammas
Energy, heat		
British thermal units, BTU	2.52×10^{-1}	calories, cal
BTU	1.0758×10^{2}	kilogram-meters, kgm
BTU lb^{-1}	5.56×10^{-1}	cal kg^{-1}
Temperature		
°C + 273	1.0	°K (Kelvin)
°C + 17.78	1.8	°F (Fahrenheit)
°F − 32	5/9	°C (Celsius)

*_Divide by_ the factor number to reverse conversions.
Exponents: for example 4.047×10^{3} (see acres) = 4,047; 9.29×10^{-2} (see ft^2) = 0.0929.